

TRANSACTIONS

OF THE

AMERICAN INSTITUTE OF MINING AND METALLURGICAL ENGINEERS

(INCORPORATED)

Volume 162

IRON AND STEEL DIVISION 1945

TECHNICAL PAPERS AND DISCUSSIONS AND SYMPOSIUMS PRESENTED BEFORE THE DIVISION AT
MEETINGS HELD AT NEW YORK, FEBRUARY 15-18, 1943, AND FEBRUARY 20-24, 1944,
AND AT CLEVELAND, OCTOBER 16-18, 1944; ALSO PAPERS SCHEDULED FOR
THE MEETING AT NEW YORK, FEBRUARY 19-22, 1945, WHICH WAS
CANCELED

PUBLISHED BY THE INSTITUTE
AT THE OFFICE OF THE SECRETARY
29 WEST 39TH STREET
NEW YORK 18, N. Y.

Notice

This volume is the eighteenth of a series containing papers and discussions presented before the Iron and Steel Division of the American Institute of Mining and Metallurgical Engineers since its organization in 1928; one volume each year, as follows:

1928, Iron and Steel Technology in 1928 (later listed as Volume 80 of the TRANSACTIONS); 1929 (vol. 84), 1930 (vol. 90), 1931 (vol. 95), 1932 (vol. 100), 1933, 1934, 1935, 1936, 1937, 1938, 1939, 1940, 1941, 1942, 1943, 1944 and 1945, TRANSACTIONS of the American Institute of Mining and Metallurgical Engineers, Iron and Steel Division.

This volume contains papers and discussions presented at the meetings at Cleveland, Oct. 16-18, 1944; New York, Feb. 15-18, 1943 and Feb. 20-24, 1944; and papers scheduled for the New York Meeting, February 19-22, 1945, which was canceled.

Papers on iron and steel subjects published by the Institute prior to 1928 are to be found in many volumes of the TRANSACTIONS of the Institute; in Vols. 37 to 45, inclusive; 47, 50 and 51, 53, 56, 58, 62, 67 to 71, inclusive; 73 and 75. Vol. 67 was devoted exclusively to iron and steel.

Iron and steel papers published in the TRANSACTIONS before the year 1936 may be found by consulting the general indexes to Vols. 1 to 35 (1871-1904), Vols. 36 to 55 (1905-1916), Vols. 56 to 72 (1917-1935), and Vols. 73 to 117 (1926-1935).

COPYRIGHT, 1945, BY THE
AMERICAN INSTITUTE OF MINING AND METALLURGICAL ENGINEERS
INCORPORATED

PRINTED IN THE UNITED STATES OF AMERICA

THE MAPLE PRESS COMPANY, YORK, PA.

Chem. Engin.
Direct
4-23-46
23043

FOREWORD

As Chairman of the Iron and Steel Division, I am proud, and justifiably so, to introduce this 162nd volume of the TRANSACTIONS of A.I.M.E., and 18th consecutive annual volume containing the papers and discussion presented at recent meetings of the Division. I feel that it is accurate to state that this is not only the largest volume of iron and steel papers ever published by the Division, but it is also the best, as a glance at the table of contents will show. There are papers and discussion in this volume on every phase of iron and steel production and metallurgy except blast-furnace practice. Since 1941 the Blast Furnace and Raw Materials Committee, one of the most important and active groups in the Division, has had its own separate and excellent PROCEEDINGS, and it is unfortunate that government restrictions on meetings forced this Committee to cancel its annual spring conference, which was to have been held in conjunction with the Open Hearth Conference last April.

I should like to take this opportunity to call the attention of all who read this volume to the separate publications of the two other operating committees of the Division—the National Open Hearth Steel Committee and the Electric Furnace Steel Committee. Both of these groups hold well attended and important conferences each year, and the papers and transcript of discussion at these conferences are published separately in the form of annual PROCEEDINGS, both of which are valuable to anyone desiring up-to-date information on the manufacture and metallurgy of open-hearth and electric-furnace steel.

Coming now to the contents of the 1945 Division TRANSACTIONS, I should like to express my appreciation and the appreciation of the Executive Committee for the splendid job done by the Physical Chemistry of Steelmaking Committee, and especially by its Chairman, T. S. Washburn, in arranging the symposia on deoxidation and segregation, the papers and discussions of which are published in entirety in this volume. I should also mention that the secretary of this Committee, K. L. Fethers, with the able assistance of J. B. Austin, worked up the symposium on the determination of hydrogen in steel.

The Physical Chemistry of Steelmaking Committee, in addition to arranging symposia and special technical sessions at the regular meetings of the Division, and being active in steering many excellent technical papers on steelmaking to the Division Publications Committee, during the last few years, has also taken on the added responsibility of arranging the metallurgical sessions at the Open Hearth conferences, and has summarized and abstracted for the open-hearth group the technical and scientific papers presented at its own meetings.

Other valuable symposia, published in this volume, which should be of interest to specialists, include the symposium on dilatometric analysis, arranged by F. M. Walters, Jr., Chairman of the Division's Metallography Committee, and the symposium on cohesive strength arranged by Maxwell Gensamer. These papers, together with the 15 papers on metallography and on properties of iron-rich alloys and steel, should give the physical metallurgists among our members a varied and wholesome fare.

ERLE G. HILL, *Chairman,*
Iron and Steel Division.

WHEELING, WEST VIRGINIA

September 15, 1945.

CONTENTS

	PAGE
Foreword. By E. G. Hill.	3
A.I.M.E. Officers and Directors.	4
Iron and Steel Division Officers and Committees	8
Howe Lectures and Lecturers.	11

TECHNICAL PAPERS AND DISCUSSION

Steelmaking

An Electrical Analogue of the Flow of Heat in a Regenerator System. By K. HEINDLHOFFER and B. M. LARSEN. (<i>Metals Technology</i> , August 1945) (With discussion)	15
A Completely Automatic Control of Open-hearth Reversal. By B. M. LARSEN and W. E. SHENK. (<i>Metals Technology</i> , June 1945)	37
A Rapid Laboratory Method for Estimating the Basicity of Open-hearth Slags. By W. O. PHILBROOK, A. H. JOLLY, JR. and T. R. HENRY (<i>Metals Technology</i> , August 1945).	49
Application of pH Slag-basicity Measurements to Basic Open-hearth Phosphorus Control. By MICHAEL TENENBAUM and C. C. BROWN. (<i>Metals Technology</i> , August 1945) (With discussion)	60
Effect of Ingot Delivery Time as a Factor in Quality of Bessemer Steel. By HOWARD C. DUNKLE. (<i>Metals Technology</i> , August 1945) (With discussion).	73

Structure and Properties of Iron-rich Alloys

Creep Properties of Some Binary Solid Solutions of Ferrite. By CHARLES R. AUSTIN, C. R. ST. JOHN and R. W. LINDSAY. (<i>Metals Technology</i> , August 1945)	84
Recovery of Cold-worked Aluminum Iron as Detected by Changes in Magnetic Properties. By J. K. STANLEY. (<i>Metals Technology</i> , January 1945)	106
Effect of Variables on the Recrystallization of Silicon Ferrite in Terms of Nucleation and Growth. By JAMES K. STANLEY. (<i>Metals Technology</i> , August 1945) (With discussion)	116
Oxide-metal Layers Formed on Commercial Iron-silicon Alloys Exposed to High Temperatures. By RAYMOND WARD. (<i>Metals Technology</i> , August 1945)	141
The Liquidus-solidus Temperatures and Emissivities of Some Commercial Heat-resistant Alloys. By JAMES T. GOW, ANTON DE S. BRASUNAS and OSCAR E. HARDER. (<i>Metals Technology</i> , August 1945) (With discussion)	156
Ar'' in Chromium Steels. By EUGENE P. Klier and ALEXANDER R. TROIANO. (<i>Metals Technology</i> , February 1945) (With discussion)	175

Transformation of Austenite

Transformation of Austenite in a Steel Containing 3 Per Cent Chromium and 1 Per Cent Carbon. By E. P. Klier. (<i>Metals Technology</i> , September 1945).	186
Isothermal Transformation of Austenite in One Per Cent Carbon, High-chromium Steels. By TAYLOR LYMAN and ALEXANDER R. TROIANO. (<i>Metals Technology</i> , September 1945) (With discussion)	196
Time-temperature Relations in Tempering Steel. By J. H. HOLLOMON and L. D. JAFFE. (<i>Metals Technology</i> , September 1945) (With discussion).	223

- Time-temperature Transformation Curves for Use in the Heat-treatment of Cast Steel. By C. T. EDDY, R. J. MARCOTTE and R. J. SMITH. (*Metals Technology*, September 1945) . 250

Properties and Structure of Steel

- Tensile Deformation. By JOHN H. HOLLOMON. (*Metals Technology*, June 1945) (With discussion) . 268
- Effects of Cold-rolling on the True Stress-strain Properties of a Low-carbon Steel. By F. J. MERINGER and C. W. MACGREGOR. (*Metals Technology*, September 1945) . 291
- Distribution of Carbon between Titanium and Iron in Steels. By W. P. FISHEL and BRISON ROBERTSON. (*Metals Technology*, October 1944) (With discussion) . 310
- Effect of Time of Storage on Ductility of Welded Test Specimens. By CLARENCE E. JACKSON and GEORGE G. LUTHER. (*Metals Technology*, January 1945) (With discussion) . 315
- Metallurgical Factors of Underbead Cracking. By S. L. HOYT, C. E. SIMS and H. M. BANTA. (*Metals Technology*, June 1945) . 326

SYMPOSIA

Symposium on Determination of Hydrogen in Steel

- Introduction By J. B. AUSTIN. . 353
- Methods of Analyzing for Hydrogen in Iron and Iron Alloys. By T. D. YENSEN and R. K. MCGEARY. . 355
- Vacuum-fusion Analysis of Steel for Hydrogen. By G. DERGE, W. PEIFER and B. ALEXANDER . 361
- Determination of Hydrogen in Iron and Steel by Vacuum Extraction at 800°C. By J. G. THOMPSON . 369
- Determination of Hydrogen in Steel Sampling and Analysis by Vacuum Extraction. By R. M. SCAFE. . 375
- A Modified Vacuum Extraction Apparatus. By W. D. BROWN . 381
- Determination of Hydrogen by Vacuum Extraction and Tin Fusion. By JOHN NAUGHTON . 385
- Determining the Hydrogen Content of Molten Steel by Vacuum Extraction. By C. B. POST and D. G. SCHOFFSTALL. . 390
- Determination of Hydrogen in Molten Steel by the Gas-tube Method. By J. G. MRAVEC . 398
- Preliminary Experiments on the Total Combustion Method for the Analysis of Hydrogen in Steel. By GEORGE A. MOORE . 404

Symposium on Segregation (*Metals Technology*, September 1944)

- Fundamental Principles Involved in Segregation in Alloy Castings. By R. M. BRICK. Appears in Volume 161. Not included here:
- Review of Factors Underlying Segregation in Steel Ingots. By B. M. LARSEN. (With discussion) . 414
- Introduction to the Session on Segregation in Steel. By EARLE C. SMITH. . 436
- Relation of Open-hearth Practice to Segregation in Rimmed Steel. By J. W. HALLEY and G. L. PLIMPTON, JR. (With discussion). . 438
- Segregation in a Large Alloy-steel Ingot. By S. W. POOLE and J. A. ROSA. (With discussion) . 459
- An Investigation of the Technical Cohesive Strength of Metals. By D. J. MCADAM, JR. and R. W. MEBS. (*Metals Technology*, August 1943) (With discussion). . 474

Symposium on Cohesive Strength (*Metals Technology*, December 1944)

- Summary of Symposium. By M. GENSAMER . 538
- The Technical Cohesive Strength of Metals in Terms of the Principal Stresses. By D. J. MCADAM, JR. . 549
- Fracture and Flow in Metals. By P. W. BRIDGMAN . 562

- Conditions of Fracture in Steel. By J. H. HOLLOMON and CLARENCE ZENER. Appears in Volume 158. Not repeated here.
- Some Speculations Regarding the Plastic Flow and Rupture of Metals under Complex Stresses. By L. R. JACKSON. (*Metals Technology*, December 1944) 584

Symposium on Recent Developments in Dilatometric Analysis

- A High-speed Dilatometer and the Transformational Behavior of Six Steels in Cooling. By A. L. CHRISTENSON, E. C. NELSON and C. E. JACKSON. (With discussion). . . 606
- Dilatometric Studies of the Graphitization of Cast Iron. By N. A. ZIEGLER. (With discussion) 627
- An Interferometer Type of Dilatometer, and Some Typical Results. By L. A. WILLEY and W. L. FINK. (With discussion). 642

Deoxidation Symposium

- Introduction. By GILBERT SOLER 657
- Deoxidation of Basic Open-hearth Steel. By T. S. WASHBURN. 658
- Slag-metal-oxygen Relationships in the Basic Open-hearth and Electric Processes. By J. S. MARSH. (With discussion). 672
- The Total Oxygen Content of Plain Carbon Open-hearth Steel during Deoxidation and Teeming. By MICHAEL TENENBAUM and C. C. BROWN. (With discussion). . . 685
- The Occurrence of Oxygen in Liquid Open-hearth Steel—Sampling Methods. By T. E. BROWER and B. M. LARSEN 712
- Effect of Deoxidation on the Strain-sensitivity of Low-carbon Steels. By H. K. WORK and G. H. ENZIAN. (With discussion) 723
- The Relation among Aluminum, Sulphur, and Grain Size. By C. E. SIMS. 734

Contents of 1945 Institute of Metals Division Volume. 737

Index 741

A.I.M.E. OFFICERS AND DIRECTORS

For the year ending February 1946

PRESIDENT AND DIRECTOR

HARVEY S. MUDD, Los Angeles, California

PAST PRESIDENTS AND DIRECTORS

C. H. MATHEWSON, New Haven, Connecticut

CHESTER A. FULTON, Baltimore, Maryland

TREASURER AND DIRECTOR

ANDREW FLETCHER, New York, N. Y.

VICE-PRESIDENTS AND DIRECTORS

JOHN L. CHRISTIE, Bridgeport, Conn.

ERLE V. DAVELER, New York, N. Y.

WILBER JUDSON, New York, N. Y.

J. R. VAN PELT, Columbus, Ohio

D. H. McLAUGHLIN, New York, N. Y.

LEO F. REINARTZ, Middletown, Ohio

DIRECTORS

RAYMOND F. BAKER, New York, N. Y.

H. J. BROWN, Boston, Mass.

C. H. BENEDICT, Lake Linden, Mich.

MILTON H. FIES, Birmingham, Ala.

CHARLES H. HERTY, Jr., Bethlehem, Pa.

O. H. JOHNSON, Denver, Colo.

J. C. KINNEAR, New York, N. Y.

ROBERT H. MORRIS, Ansted, W. Va.

J. C. NICHOLLS, Toronto, Ont., Canada

RUSSELL B. PAUL, New York, N. Y.

JOHN R. SUMAN, Houston, Texas

ROBERT W. THOMAS, Ray, Ariz.

F. A. WARDLAW, Jr., Salt Lake City, Utah

CLYDE E. WEED, New York, N. Y.

EUGENE A. WHITE, Tacoma, Wash.

FELIX E. WORMSER, New York, N. Y.

W. E. WRATHER, Washington, D. C.

SECRETARY

A. B. PARSONS, New York, N. Y.

DIVISION CHAIRMEN—Acting as Advisers to the Board

EARLE E. SCHUMACHER (Institute of Metals), Murray Hill, N. J.

M. L. HAIDER (Petroleum), New York, N. Y.

ERLE G. HILL (Iron and Steel), Wheeling, W. Va.

L. A. SHIPMAN (Coal), Knoxville, Tenn.

E. A. HOLBROOK (Education), Pittsburgh, Pa.

B. C. BURGESS (Industrial Minerals), Spruce Pine, N. C.

STAFF IN NEW YORK

Assistant Secretaries

EDWARD H. ROBIE

FRANK T. SISCO

E. J. KENNEDY, JR.

Assistant Treasurer

H. A. MALONEY

Advertising Manager

"Mining and Metallurgy"

WHEELER SPACKMAN

IRON AND STEEL DIVISION

Established as a Division February 22, 1928

(Bylaws published in the 1939 TRANSACTIONS Volume of the Division)

Officers and Committees for Year ending February 1945

E. G. HILL, *Chairman*, Wheeling, W. Va.
W. A. HAVEN, *Past Chairman*, Cleveland, Ohio
GILBERT SOLER, *Vice-Chairman*, Canton, Ohio
T. S. WASHBURN, *Vice-Chairman*, Indiana Harbor, Ind.
FRANK T. SISCO, *Secretary*, 29 West 39th Street, New York 18, N. Y.

PAST CHAIRMEN

RALPH H. SWEETSER, 1928
G. B. WATERHOUSE, 1929
W. J. MACKENZIE, 1930
F. M. BECKET, 1931
F. N. SPELLER, 1932
JOHN JOHNSTON, 1933

L. F. REINARTZ, 1934
A. B. KINZEL, 1935
C. E. WILLIAMS, 1936
FRANCIS B. FOLEY, 1937
J. T. MACKENZIE, 1938

J. HUNTER NEAD, 1939
FRANK T. SISCO, 1940
C. H. HERTY, JR., 1941
E. C. SMITH, 1942
H. W. GRAHAM, 1943
W. A. HAVEN, 1944

Executive Committee

Until 1946
WALTER CRAFTS
C. D. KING
W. J. REAGAN

Until 1947
G. R. BROPHY
H. J. FORSYTH
A. P. MILLER

Until 1948
K. L. FETTERS
J. S. MARSH
C. E. SIMS

Blast Furnace and Raw Materials

W. E. BREWSTER, *Chairman*
T. B. COUNSELMAN, *Vice-Chairman*
B. W. NORTON, *Vice-Chairman*
OWEN R. RICE, *Secretary*

A. J. BOYNTON
P. F. DOLAN
P. G. HARRISON
W. A. HAVEN
G. W. HEWITT

H. W. JOHNSON
T. L. JOSEPH
C. D. KING
R. A. LINDGREN
H. E. McDONNELL
J. C. MURRAY

J. H. SLATER
G. E. STEUDEL
H. A. STRAIN
H. M. STUBBLEFIELD
C. L. WYMAN

Open Hearth Steel

L. F. REINARTZ, *Chairman*
A. P. MILLER, *Vice-Chairman*
FRANK T. SISCO, *Secretary*

G. S. BALDWIN
J. M. CAHILL

CLYDE DENLINGER
C. R. FONDERSMITH

H. M. GRIFFITH
W. C. KITTO

L. A. LAMBING
E. L. RAMSEY
A. E. REINHARD
E. A. SCHWARTZ

GILBERT SOLER
A. H. SOMMER
F. L. TOY

D. N. WATKINS
T. T. WATSON
M. F. YAROTSKY
W. H. YECKLEY

Bessemer Steel

E. C. WRIGHT, *Chairman*

H. C. DUNKLE
J. D. GOLD
H. W. GRAHAM

M. A. JONES
C. D. KING
E. E. MCGINLEY
R. E. PENROD

W. J. REAGAN
G. A. REINHARDT
A. W. THORNTON

Electric Furnace Steel

EXECUTIVE COMMITTEE

H. W. McQUAID, *Chairman*
FRANK T. SISCO, *Secretary*

C. W. BRIGGS
A. L. FEILD
T. J. McLoughlin

T. S. QUINN
W. J. REAGAN

C. A. SCHARSCHU
GILBERT SOLER
E. A. WALCHER

CONFERENCE COMMITTEE

C. W. BRIGGS, *Chairman*
W. J. REAGAN, *Vice-Chairman*

SAMUEL ARNOLD, III
J. B. CAINE
W. M. FARNSWORTH
K. L. FETTERS
R. H. FRANK

R. C. GOOD
R. P. HEUER
JOHN JUPPENLATZ
ANDREW KAUL, III
G. A. LILLIEQVIST

H. E. PHELPS
F. B. RIGGAN
J. F. ROBB
G. E. STOLTZ
N. I. STOTZ

Physical Chemistry of Steelmaking

T. S. WASHBURN, *Chairman*
K. L. FETTERS, *Secretary*

R. S. ARCHER
JOHN CHIPMAN
G. R. FITTERER
J. J. GOLDEN
J. W. HALLEY

C. H. HERTY, JR.
T. L. JOSEPH
B. M. LARSEN
J. S. MARSH

W. O. PHILBROOK
L. F. REINARTZ
C. E. SIMS
GILBERT SOLER
H. K. WORK

Metallography and Heat Treatment

F. M. WALTERS, JR., *Chairman*

WALTER CRAFTS
J. T. EASH
SAMUEL EPSTEIN

J. T. NORTON
HOWARD SCOTT

G. V. SMITH
G. A. TIMMONS
CYRIL WELLS

Membership

W. E. BREWSTER, *Chairman*

E. L. APPLIGATE
O. E. CLARK

P. F. DOLAN
R. M. GARRISON

H. L. GEIGER
J. L. GREGG

J. W. HALLEY
J. E. JACOBS
E. C. MILLER
J. C. MURRAY

R. M. PARKE
H. S. RAWDON
W. E. REMMERS

C. E. SIMS
J. M. STAPLETON
M. J. UDY
E. R. YOUNG

Mining and Metallurgy

A. B. KINZEL, *Chairman*

R. H. ABORN

T. S. FULLER

Howe Memorial Lecture

E. G. HILL, *Chairman*

J. H. HALL

E. C. SMITH

Robert W. Hunt Medal and Prize

E. G. HILL, *Chairman*

F. B. FOLEY

J. H. NEAD

H. A. STRAIN

J. E. Johnson, Jr. Award

R. A. LINDGREN, *Chairman*

O. E. CLARK

T. L. JOSEPH

J. M. STAPLETON

L. F. SATTELLE

Programs

J. S. MARSH, *Chairman*

J. B. AUSTIN
GERHARD DERGE
H. B. EMERICK

W. O. PHILBROOK
GILBERT SOLER

MICHAEL TENENBAUM
F. L. TOY
F. M. WALTERS, JR.

Publications

C. M. LOEB, JR., *Chairman*

L. S. BERGEN
EARNSHAW COOK

F. B. FOLEY
J. L. GREGG

R. K. KULP
B. M. LARSEN

Nominating

W. A. HAVEN, *Chairman*

E. S. DAVENPORT

F. B. FOLEY
H. J. FRENCH

E. C. SMITH

The Howe Memorial Lecture

THE Howe Memorial Lecture was authorized in April 1923, in memory of Henry Marion Howe, as an annual address to be delivered by invitation under the auspices of the Institute by an individual of recognized and outstanding attainment in the science and practice of iron and steel metallurgy or metallography, chosen by the Board of Directors upon recommendation of the Iron and Steel Division.

So far, only American metallurgists have been invited to deliver the Howe lecture. It is believed that this lecture would gain in importance and significance were it possible to include metallurgists from other countries, but the Institute has not yet been able to do this on account of lack of special funds to support this lectureship.

The titles of the lectures and the lecturers are as follows:

- 1924 What is Steel? By Albert Sauveur.
- 1925 Austenite and Austenitic Steels. By John A. Mathews.
- 1926 Twenty-five Years of Metallography. By William Campbell.
- 1927 Alloy Steels. By Bradley Stoughton.
- 1928 Significance of the Simple Steel Analysis. By Henry D. Hibbard.
- 1929 Studies of Hadfield's Manganese Steel with the High-power Microscope. By John Howe Hall.
- 1930 The Future of the American Iron and Steel Industry. By Zay Jeffries.
- 1931 On the Art of Metallography. By Francis F. Lucas.
- 1932 On the Rates of Reactions in Solid Steel. By Edgar C. Bain.
- 1933 Steelmaking Processes. By George B. Waterhouse.
- 1934 The Corrosion Problem with Respect to Iron and Steel. By Frank N. Speller.
- 1935 Problems of Steel Melting. By E. C. Smith.
- 1936 Correlation between Metallography and Mechanical Testing. By H. F. Moore.
- 1937 Progress in Improvement of Cast Iron and Use of Alloys in Iron. By Paul D. Merica.
- 1938 On the Allotropy of Stainless Steels. By Frederick Mark Becket.
- 1939 Some Things We Don't Know about the Creep of Metals. By H. W. Gillett.
- 1940 Slag Control. By C. H. Herty, Jr.
- 1941 Some Complexities of Impact Strength. By Alfred V. de Forest.
- 1942 Time as a Factor in the Making and Treating of Steel. By John Johnston.
- 1943 The Development of Research and Quality Control in the Modern Steel Plant. By Leo F. Reinartz.
- 1944 Gray Iron—Steel Plus Graphite. By J. T. MacKenzie.
- 1945 On the Toughness of Hardened Steels. By Marcus A. Grossmann.

On the General Principles of the Flow of Heat in a Steady-State System

By H. B. G. ...

TECHNICAL PAPERS AND DISCUSSIONS

The general principles of the flow of heat in a steady-state system are discussed in this paper. The author shows that the flow of heat is determined by the temperature difference between the two ends of the system and the thermal conductivity of the material. The flow of heat is proportional to the temperature difference and the thermal conductivity, and inversely proportional to the length of the system.

The author also discusses the flow of heat in a system with a variable thermal conductivity. He shows that the flow of heat is determined by the temperature difference between the two ends of the system and the average thermal conductivity of the material. The flow of heat is proportional to the temperature difference and the average thermal conductivity, and inversely proportional to the length of the system.

According to the discussion in this paper, the flow of heat in a steady-state system is determined by the temperature difference between the two ends of the system and the thermal conductivity of the material. The flow of heat is proportional to the temperature difference and the thermal conductivity, and inversely proportional to the length of the system.

An Electrical Analogue of the Flow of Heat in a Regenerator System

BY K. HEINDLHOFFER* AND B. M. LARSEN,* MEMBER A.I.M.E.

(New York Meeting, February 1945†)

THIS paper describes a relatively simple electrical apparatus that, through the close analogy between the flow of heat and of electricity, enables one to solve quickly and with satisfactory accuracy many complex problems in heat flow. This device, developed in 1935, has proved especially useful in the solution of certain practical problems relating to the design and efficiency of regenerators for an open-hearth furnace or coke oven, yielding within a few hours information that would take weeks or even months to acquire by mathematical^{1,2} or experimental³ methods of comparable accuracy. Its description now is prompted by growing interest in such analogues, as shown by several recent papers.^{4,5}

The analogy between flow of heat and of electricity appears to have been recognized first by Maxwell who, in his famous *Treatise on Electricity and Magnetism* (1881) says:

The analogy between the theory of the conduction of electricity and that of the conduction of heat is at first sight almost complete. If we can take two systems geometrically similar, and such that the conductivity for heat at any part of the first is proportional to the conductivity for electricity at the corresponding part of the second, and if we also make the temperature of any part of the first proportional to the electric potential at the corresponding point of

the second, then the flow of heat across any area of the first will be proportional to the flow of electricity across the corresponding area of the second . . . Thus, in the illustration we have given, in which flow of electricity corresponds to flow of heat, the electric potential to temperature, electricity tends to flow from places of high to places of low potential, exactly as heat tends to flow from places of high to places of low temperature.

He noted, however, that this analogy is restricted:

. . . there is, however, one remarkable difference between the phenomena of electricity and those of heat. Suspend a conducting body within a closed conducting vessel by a silk thread, and charge the vessel with electricity. The potential of the vessel and of all within it will be instantly raised, but however long and however powerfully the vessel be electrified, and whether the body within be allowed to come in contact with the vessel, or not, no signs of electrification will appear within the vessel, nor will the body within show any electrical effect when taken out. But if the vessel is raised to a high temperature, the body within will rise to the same temperature, but only after a considerable time, and if it is then taken out it will be found hot, and will remain so till it has continued to emit heat for some time. The difference between the phenomena consists in the fact that bodies are capable of absorbing and emitting heat, whereas they have no corresponding property with respect to electricity.

According to this statement the application of the analogy would be limited to problems of steady flow that do not involve heat-capacity effects. In spite of this

Manuscript received at the office of the Institute Oct. 13, 1944. Issued as T.P. 1798 in METALS TECHNOLOGY, August 1945.

* Research Laboratory, United States Steel Corporation, Kearny, New Jersey.

† Meeting canceled.

¹ References are at the end of the paper.

restriction, numerous problems could be solved either by mapping out the equipotential surfaces in an electrical counterpart geometrically analogous to the heat flow, or by taking advantage of those cases in which the electrical distribution has already been worked out and applying this result directly to the analogous heat-flow problem.

Maxwell's restriction can be removed, however, and the analogy extended to problems of transient or cyclic flow involving heat storage by giving up the similarity in shape. The heat-conductor system is regarded as dissected into parts, each of which is then reconstructed in terms of electric circuit elements—i.e., condensers and resistors—no self-induction being required, since a magnetic field has no corresponding counterpart in the thermal system. These circuit elements are then connected to form a network in which, though it has no physical resemblance to the original, the electric current flows in a manner precisely corresponding to the flow of heat in the thermal system. It is difficult experimentally to make the network continuous, since the circuit elements (condensers and resistors) are lumped unless cables are used; the analogy therefore is strict only if the degree of subdivision of circuit elements is infinitely great. In practice, however, a moderate degree of subdivision suffices.

FUNCTION OF THE REGENERATOR

A regenerator is any cyclic heat interchanger in which a hot fluid (combustion gases) flows in one direction for a finite period over a network of solid material (checker brick) that absorbs heat, the flow being then reversed, when a cold fluid (air) flows in the opposite direction to reabsorb the heat added to the solid material in the first half of the cycle, the path of flow being the same in both directions. This constitutes a complete period whose duration is usually not less than 15 min. and not

more than one hour. Regenerators are used in many kinds of furnaces, their purpose being to increase the flame temperature of the furnace by returning to the combustion zone part of the heat in the waste gases leaving the furnace; by this means more high-temperature heat is available, with consequent greater economy of fuel.

In considering what goes on in the regenerator, we can neglect the furnace, its sole role being to deliver the hot gases, provided that it is assumed to be operated so that both the composition and temperature of these gases are reasonably constant. On this basis, and on the basis that the temperature of the air entering during the other half of the cycle is sensibly constant, the conditions external to the regenerator are definite. The problem is to ascertain the relations between the temperature of the hot gases, of the heated air, and of the brick, along the whole length of the regenerator at any point in the cycle when the regenerator is in steady operation. The relation of the temperature of the gas entering to that of the air leaving the regenerator is a measure of the efficiency of temperature interchange. As this efficiency increases, for a given ratio of volume of gas to that of air flowing and for a given period of reversal, the maximum brick temperature increases; this, which must ordinarily be kept below some level that depends largely upon the composition of the brick being used, may limit the efficiency or necessitate shortening of the period. The analogue aids us in analyzing this and other regenerator problems so as to choose the optimum conditions of operation or of design.

TEMPERATURE SCALE

On the basis that the temperature T_g of the incoming gas in the first half of the cycle, and that T_a of the incoming air in the second half of the cycle, are both sensibly constant, we may conveniently consider T_a as base and equal to zero and

choose the difference $T_b - T_a$ as the unit or the range of our temperature scale, and express all other temperatures as percentages of $T_b - T_a$. For example, if the temperature T_b of the brick at some point is 1300°F. , and if T_b is 2500° and $T_a = 100^\circ$, on our scale T_b would be $(1300 - 100)/(2500 - 100) = 50$ per cent. The use of this dimensionless scale of temperature simplifies discussion of the problem, and in particular simplifies the translation of temperature in the thermal case into potential in the electrical analogue.

ANALOGY BETWEEN FLOW OF HEAT AND OF ELECTRICITY AS APPLIED TO REGENERATOR PROBLEM

A pair of regenerators reduced to their simplest elements, with a furnace chamber between them, is illustrated diagrammatically in Fig. 1, in which the assembly is compared to an analogous electrical network. Each regenerator is represented as a tube whose wall has a given heat capacity per unit of length; we assume, as a first approximation,* that the material of the wall has infinite conductivity, with zero heat loss from its outer surface, which corresponds to the central plane of the brick, so that heat can flow unobstructed into it. Consider the cycle in one member of a pair of actual regenerators: Air, initially at temperature zero on our scale, flows for a given period in a given direction at a constant rate, hence with constant heat-carrying capacity (this process is illustrated by the left-hand regenerator and left-hand graph in Fig. 1). At the end of the given period the flow is reversed and in the second half of the cycle the gas, initially at temperature 100 per cent, flows in the reverse direction at a constant rate, and with a constant heat-carrying capacity, both of which may be different from, usually

greater than, the corresponding characteristics of the air, because the mass of the gas normally is greater than that of the air. (For ease of illustration the second half of the cycle is shown schematically by the right-hand regenerator and the right-hand graph of Fig. 1.)

The total heat transferred in one cycle is in direct proportion to the relative shift of the temperature-distribution curve in the brick in this cycle, and the heat transfer between gas and brick and between brick and air depends upon the vertical distance between the respective pairs of curves in Fig. 1. Heat transfer takes place by conduction, convection and radiation. The last is very small in the air half cycle but in the gas half cycle it becomes appreciable at the higher temperatures. Convection and conduction through the gas are complex, rendering a rigorous treatment impracticable or even impossible; hence in this type of problem it is usual to assume Newton's law of cooling—namely, that the quantity of heat transferred over unit area in unit time is proportional to the temperature difference between gas or air and solid. This rule is equivalent to the assumption of a virtual "resistance" at the interface, the reciprocal of this resistance being usually known as the "heat-transfer coefficient" of the system. This "resistance" corresponds to the constant of proportionality in Newton's law.

The problem is to find, for the steady state of cyclic operation, the temperature distribution along the gas stream and the air stream, and along the surface of the heat-absorbing and the heat-emitting solid, as these distributions determine the effectiveness of heat interchange. The purpose is to bring up to as near 100 per cent as is feasible the temperature of the air leaving the regenerator and entering the furnace. To solve this problem, we must devise an electrical network in which electric charges flow similarly to heat in the regenerator, and to measure at any point in this net-

* As will be shown later, this is merely a step toward a more accurate account of the temperature distribution within the brick, whose conductivity is far from infinite.

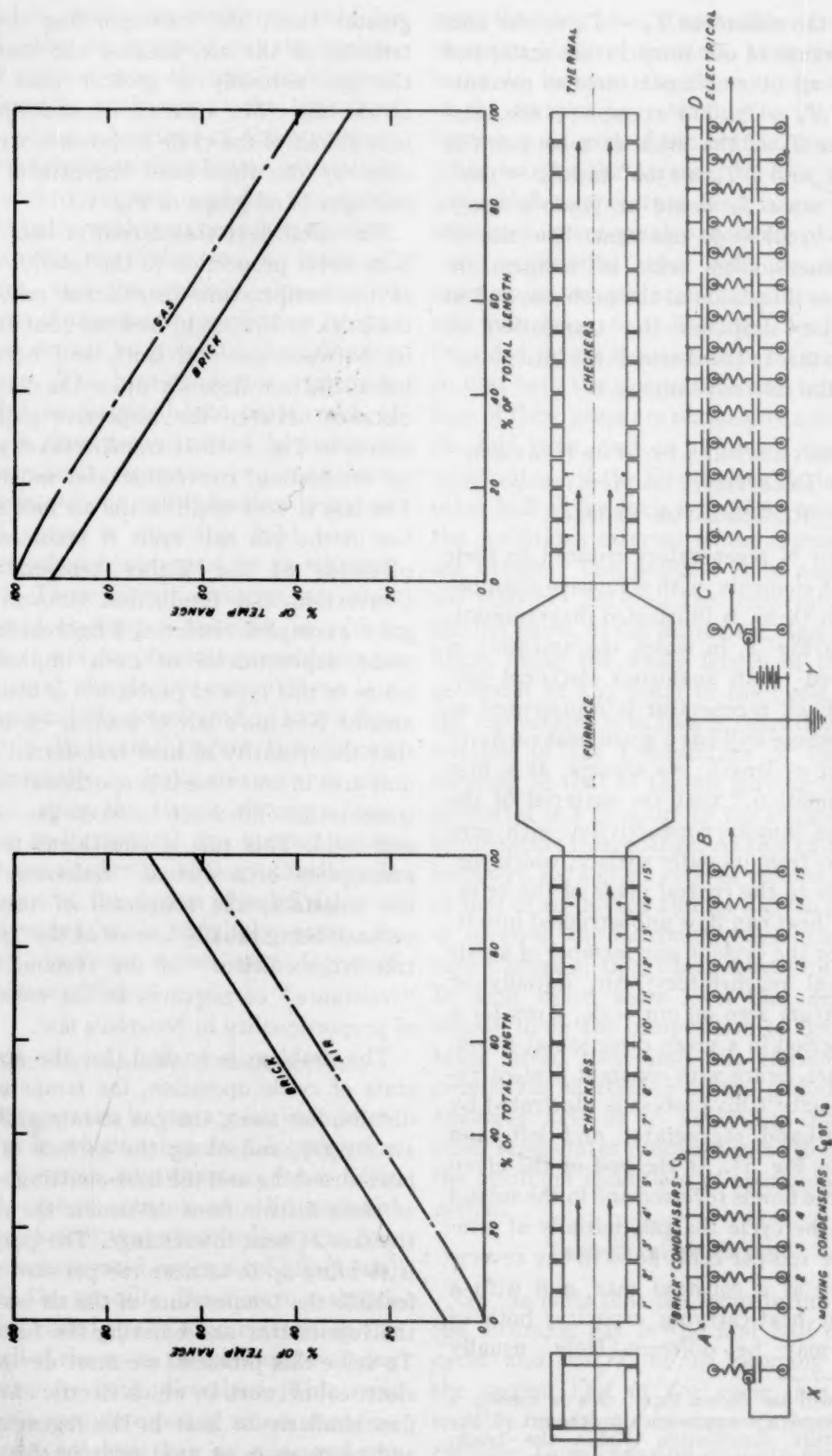


FIG. 1.—SCHEMATIC CROSS SECTION OF OPEN-HEARTH-FURNACE REGENERATOR SYSTEM AND ITS ELECTRICAL COUNTERPART.

work the voltage, which can be translated directly to temperature at the corresponding place in the regenerator. We may consider the flowing gas as a series of moving slices or cells, each carrying a certain quantity of heat, which is the product of the weight (or volume) of the gas, its mean specific heat and its temperature. The precise counterpart, from a mathematical standpoint, of this is a stream of moving electrostatic condensers, each of which has a capacity equivalent to the heat capacity of the gas cell, at a voltage equivalent to the temperature and moving at a speed corresponding to the rate of flow of the gas. The corresponding conditions are fulfilled, in that the heat content of the air or gas can safely be taken to be proportional to its temperature, and the electric charge of a condenser is measured by its potential. Moreover, as Newton's law of cooling corresponds to Ohm's law, an electrical resistance may be used to represent the surface "resistance" to heat transfer. The checker brick itself can be simulated by a set of larger stationary condensers to which the small condensers are intermittently connected through a resistor corresponding in amount to the surface "resistance."

Thus a proper analogue may be constructed from appropriate resistors and condensers, as indicated in the lower part of Fig. 1. Between *A* and *B*, for example, there are, in a horizontal row, 15 stationary condensers, which correspond to the 15 sections of brick of the regenerator tube above them. On a lower line another row of 15 condensers represents the heat capacity of the several moving gas or air cells opposite the respective brick sections at any moment. Since the gas or air drifts through the regenerator at a uniform rate, we must arrange that the corresponding condensers move at an analogous rate and must provide appropriate electrical moving contacts. The resistor between this contact and the condenser represents the resistance

to heat transfer at the brick surface; the other plate of the condenser is connected to a common grounded conductor. The number of separate condenser units should be great enough so that the voltage variation for a single contact time is quite small in relation to the total voltage drop through the whole series, thus giving a sufficiently close approximation to the continuous process of the actual regenerator.

The left-hand section of the diagram represents the air heating and the right the simultaneous gas cooling in one half of each cycle; in the alternate half periods, by a reversal of flow, the functions of left and right portions of the system are merely interchanged. In the electrical network the differences between heating and cooling phases of the period are: (1) in the direction of motion of the moving condenser-resistor units, and (2) in the state of charge of the moving condensers, which enter at battery potential during the gas half and at ground potential during the air half of the cycle. It is convenient to express the electric potential in terms of the battery voltage as 100 per cent and the ground as zero, so as to be in numerical correspondence with our temperature scale; this greatly simplifies translation of the electrical measurements into thermal terms, yet in no wise limits the generality of application.

Let us now follow the course of the cycle in the electrical network, to bring out how it corresponds to what happens in the regenerator, as described above. The moving "gas" condensers are charged, by the battery at *Y*, to 100 per cent potential (that of the battery), and gradually lose charge as they pass from *C* to *D*. The moving "air" condensers are brought to zero potential at *X*, and pick up charge from the stationary condensers as they move from *A* to *B*. Since we are mainly interested in the performance of the regenerator when it has reached a steady state, we must operate the analogue until two consecutive

cycles become identical; potential measurements then give directly the desired temperature distribution. Thus, if the analogy is perfect, the curves at the top of the figure represent the temperature distribution along the regenerator as well as the distribution of potential along the bank of

For the gas period, $m_g = l'/C'_g R'_g$

$$n_g = l'/C'_g R'_g$$

For the air period, $m_a = l'/C'_a R'_a$

$$n_a = l'/C'_a R'_a$$

The analogous quotients for the electrical system must also be dimensionless, and so

TABLE 1.—*Definition of Symbols Used*

QUANTITIES ON HEAT REGENERATOR		CORRESPONDING QUANTITIES ON ELECTRICAL ANALOGUE	
l'	Effective length in direction of flow, ft.		Series of 15 distributor contact segments
t'	Time between reversals, hr.	t	Time between reversals, sec.
C'_g	Heat capacity per sq. ft. surface of brick of half thickness	C_g	Capacity of "brick" condenser, microfarads
C'_a	Heat capacity of amount of gas or air flowing over 1 ft. circumference of brick per hour*	C_a	Corresponding "gas" and "air" capacities in electrical terms, microfarads
R'_g	Transfer resistance for air or gas per sq. ft. effective surface	R_g	Electrical ("gas" and "air") transfer resistance, ohms

* This is the heat capacity of the volume of gas or air that flows vertically per hour through the regenerator divided by the perimeter of all flues of any one horizontal cross section of the checker.

condensers. For convenience of reference we give in Table 1 and Table 2, the definitions of the corresponding symbols and the corresponding parts of the two systems.

the ratios of the corresponding m 's and n 's can be used directly as conversion factors to translate thermal into electrical quantities. Thus it is only necessary to choose the sizes of the electrical capacities and

TABLE 2.—*Correspondence between Regenerator and Electrical Network, as Shown Schematically for One Half of the Cycle in Figure 1*

HEAT REGENERATOR	ELECTRICAL NETWORK
Brick cells of capacity proportional to C'_g	"Brick" condensers of capacity C_g
Moving gas or air, of capacity per unit time, proportional to C'_g or C'_a	"Gas" or "air" (moving) condensers of capacity C_g or C_a
Heat flow from 1 to 2 limited by transfer resistance R'_g or R'_a , the reciprocal of the transfer coefficient	Flow from 1 to 2 limited by resistors R_g or R_a
Inflowing gas temperature (100 per cent)	Initial (battery) potential of "gas" condenser (100 per cent)
Inflowing air temperature (zero)	Initial (ground) potential of "air" condenser (zero)

QUANTITATIVE CORRESPONDENCE BETWEEN THERMAL AND ELECTRICAL UNITS

The question arises as to the proper selection of a relationship among the electrical capacities, resistances and time, so that this will correctly represent the given set of corresponding relationships between the thermal quantities. The mutual conversion of electrical and thermal constants is best accomplished if we can combine the respective constants in such a way as to obtain nondimensional quantities, which must then have the same values in both systems. We may define four nondimensional quantities, m_a , m_g , n_a and n_g , as:

resistances in such a way that the corresponding values of m and of n are identical with those derived from the constants of the regenerator system. Thermal data are based usually upon the hour, whereas electrical units are based upon the second as unit of time; hence steady-state operation of the analogue is attained in a few minutes instead of the days required in the actual regenerator system.

Earlier we postulated, for simplicity in the preliminary discussion, that the temperature of the brick is at all times uniform over its thickness; this is equivalent to the assumption that its heat conductivity is infinite in comparison with the heat-transfer coefficient. This approximation, which

simplifies the necessary electrical network, is legitimate if the period of reversal is long and the brick thin; but it may introduce considerable error when the period is short or the brick thick. These conditions are readily taken care of by applying the theory of electrical cables to the problem of temperature distribution in the brick in the following way.

The brickwork may be regarded as a large slab exposed on both faces to the same cyclic temperature variation; consequently the heat flow is symmetrical with respect to the center plane of the slab, and there is no heat flow through this plane. Hence the problem is the same as for a slab of half the thickness, thermally insulated on one face, and heated cyclically on the other. The variation of temperature at this face may be represented by a Fourier series, which comprises only the odd harmonics because of the symmetry of the time-temperature cycle; and as a first approximation the terms beyond the first may be neglected, which then represents a sinusoidal variation of temperature. This is precisely equivalent to electrical flow in a cable without inductance, to which case the Kelvin telegraph equation is applicable. This equation yields the distribution of voltage and current in such a cable, which in our case is fed with a sinusoidal voltage at one end and is an open circuit at the other. This case is exactly equivalent to a resistance in series with a condenser, the size of each being determined by the period of temperature fluctuation, the thermal resistance and heat capacity, respectively, of the slab that is to be imitated. This combination of resistance and capacity replaces the simple "brick condenser" considered hitherto, if we wish to include this refinement in the analogue. In terms of physical apparatus this means merely that a proper adjustment of the size of the heat-transfer resistance end of the brick condenser must be made.

The additional resistance and capacity required to take account of the true thermal conductivity of the brick are computed by analogy from the expression for the impedance of an unloaded cable fed by a sinusoidal potential, which is:

$$Z = \frac{\sqrt{\pi f c R_b}}{2\pi f c} (1 - j) \frac{\cosh Q \cos Q + j \sinh Q \sin Q}{\sinh Q \cos Q + j \cosh Q \sin Q}$$

where Z is the impedance, f the frequency of alternation, c the capacity and R_b the resistance of a length of cable L , j is $\sqrt{-1}$ and Q is $L \sqrt{\pi f c R_b}$. This relation may readily be translated into corresponding thermal quantities; thus f becomes the frequency of reversal, c the specific heat of the brick and R_b the specific resistance to the heat flow through a brick of half thickness L . Moreover, this relation comprises a real and an imaginary term, the former corresponding to the effective thermal resistance per unit of surface of a brick of half thickness; the latter being equal to $1/(2\pi f C_b)$, where C_b is the effective thermal capacity per unit of surface of a brick of half thickness.

This representation of the brick is accurate for a sinusoidal variation of temperature, which is very nearly the case when the brick does not exceed $2\frac{1}{2}$ in. in thickness and the complete cycle lasts 20 min. or more (that is, time of reversal is 10 min. or more). These conditions usually obtain in practice. For much thicker brick or shorter cycles, it would be necessary to include higher terms in the Fourier series, with a corresponding increase in the number of resistance-capacity units.

Another possible, but not absolutely necessary, refinement of the network would take into account the variability of the heat-transfer coefficient with temperature during the gas half cycle in which radiation plays an appreciable part in the transfer. Experiment has shown that the

transfer of heat by radiation between brick and air is very small, and that the total transfer coefficient is essentially constant during the air half cycle. In the gas half cycle the improved heat transfer—i.e., reduced resistance at the hot end—can be simulated with sufficient accuracy by reduction of the value of the resistors at this end. These adjusted resistors (not shown in Fig. 1 but appearing as a vertical ladder in Fig. 3) increase in the direction in which the temperature of the gas decreases. In most cases this added complication was found to be unnecessary, the mean value of the transfer coefficient over the total range of gas temperature being sufficient for the purpose.

Before describing the physical embodiment of the electrical analogue, we outline the several simplifying postulates introduced, most of which are necessary in any mathematical treatment to keep the problem from becoming too complex and undefined. These postulates follow:

1. That the temperature of the gas entering the regenerator is constant. In fact it varies somewhat, probably by not more than 5 per cent of its value on the absolute scale, but this introduces no error as far as a comparison of regenerators of different design is concerned.

2. That the heat capacity (specific heat) of the gas, of air, and of the brick is constant over the temperature range. This is a close approximation, the actual deviation being only 2 to 6 per cent. Any infiltration of outside air between checkers may be taken into account by increasing correspondingly the heat-carrying capacity value of the gas, C'_g , relative to that of air, C'_a .

3. That there is no flow of heat through the brick in the direction of the gas flow. Such a flow, which would mean lessened efficiency of the regenerator, is probably small by reason of the many joints between checker-brick layers and the small temperature gradient.

4. That the air to be heated follows a path through the checkers identical with that of the gas that supplies the heat. This condition seldom is fulfilled with short checkerwork of large cross section. Such erratic gas distribution can be treated by considering separately small sections of the whole regenerator chamber. If it occurs it should be eliminated as far as possible by proper design of the checkers.

5. That the rate of flow of gas (or air), and the temperature at any location, are constant over the cross section of the regenerator. This condition may not be attained perfectly, in which case it can be handled as above, by division into smaller elements of cross section, for each of which the postulate is closely approximated.

6. That the continuous change of temperature and effective heat capacity along the length of the regenerator is simulated in the model by a number of discrete steps, each such unit being at a certain potential (temperature) level. In our apparatus there are 15 condenser units; the accuracy of imitation will increase with the number used, but any large increase introduces difficulties of construction that may not be warranted in view of the satisfactory results we have obtained with 15 units.

7. That the rate of heat exchange between gas (air) and brick follows Newton's law of cooling. This is closely approximated except for the part of the gas-brick transfer that is due to radiation.

CONSTRUCTION OF ELECTRICAL ANALOGUE

The linear arrangement of the units of the network, as depicted schematically in Fig. 1, is obviously less convenient in practice than a rotation of the moving units whereby they can be charged, or discharged, before re-entering the cycle. Nor is it necessary to rotate the units themselves, but merely to provide good rotating contacts of the commutator type. The full number of "brick" condensers

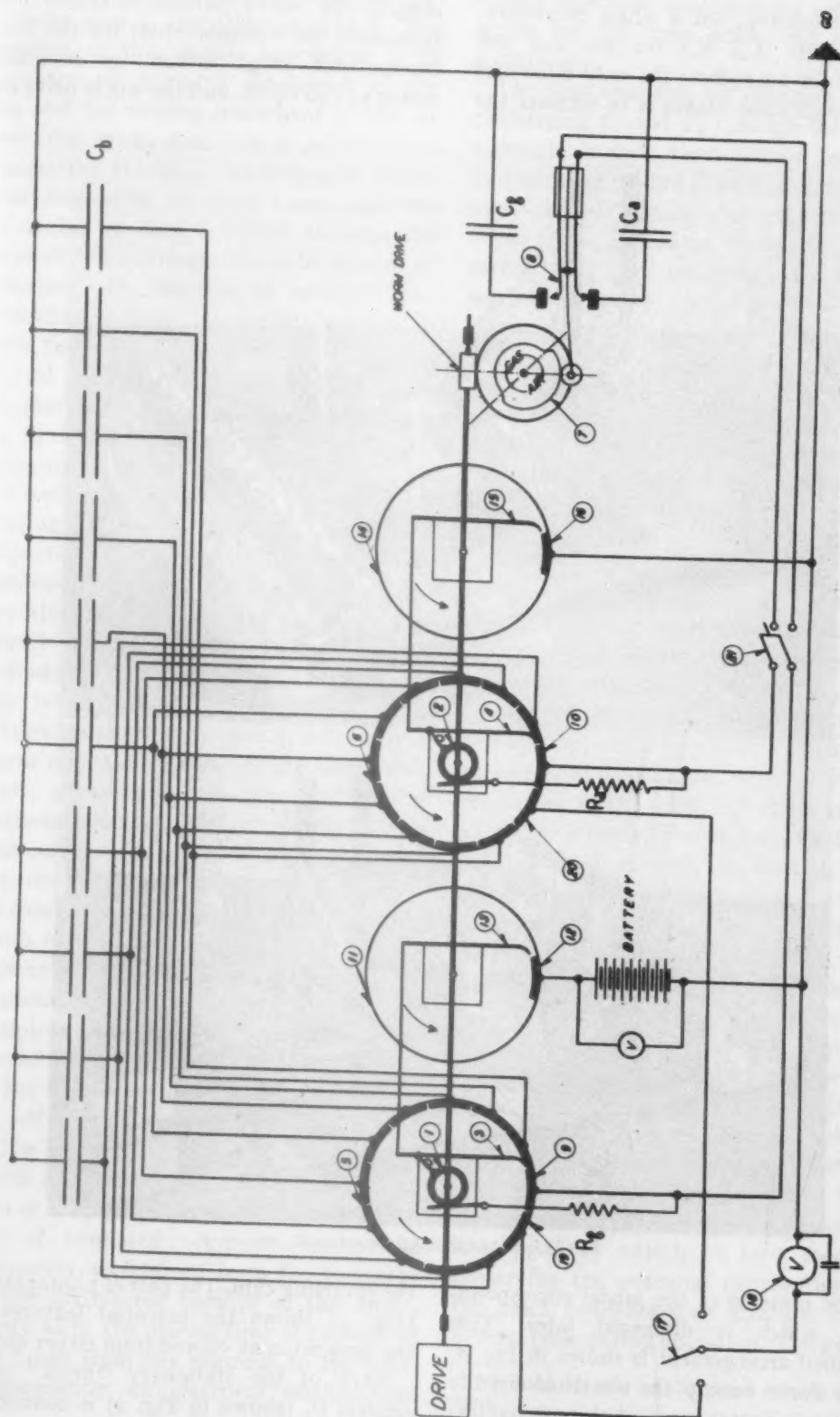


FIG. 2.—WIRING DIAGRAM OF ELECTRICAL ANALOGUE.

(C_b) is necessary, but a single condenser-resistor unit (C_g, R_g) for gas and one (C_a, R_a) for air suffice; the only difference this simplification makes is to increase the

details; the heavy horizontal center line represents the common shaft for the four commutator rings driven by a small motor at 940 r.p.m. and the worm drive on

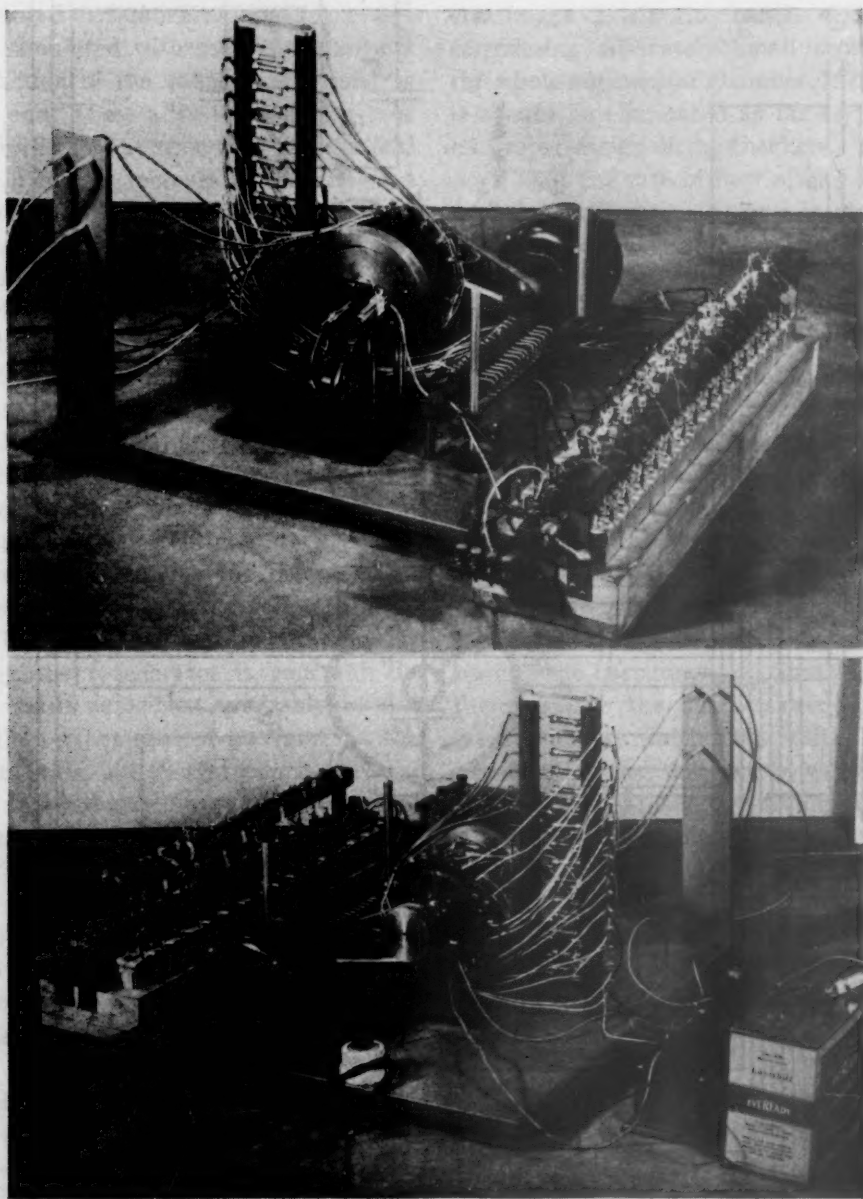


FIG. 3.—ELECTRICAL ANALOGUE.

time of rotation of the model correspondingly, which is discussed later. This simplified arrangement is shown in Fig. 2, which shows mainly the electrical circuits but also indicates some of the mechanical

the reversing cam. The pair of photographs (Fig. 3) shows the essential features of the apparatus as viewed from either end.

Each of the stationary "brick" condensers C_b (shown in Fig. 2) is connected

to two contact segments, one on distributor ring 5, the other on ring 6. The purpose of this double connection is to simulate the forward movement of the gas and the reverse movement of the air past the brick, and this is achieved by connecting the brick condensers in clockwise succession on ring 5 and counter-clockwise on ring 6, which obviates the necessity of shifting contact brushes or of reversing the direction of rotation. The commutator rings 5 and 6 are each made with three extra segments. On each ring one of these is extra and is left blank; another is the connection for charging C_g to the battery potential or for discharging C_a to ground (GD).

Condensers C_g and C_a represent the moving gas and air cells, R_g and R_a , the respective transfer resistances. Only one condenser-resistor unit is connected at any one time, the other being then on open circuit. The change from gas cycle to air is made by changing contact 8, which cuts one brush out and the other in. This reversal is effected by cam 7, driven by a worm reduction gear from the distributor shaft, ensuring a constant number of contacts per cycle; one revolution of this cam corresponds to a complete cycle of the regenerator. On contact at 8, C_g imparts its charge through R_g and the brush, ring-brush combination 1, 3 to the distributor segments on ring 5, thence to the brick condensers in proper order; the circuit is completed through the ground. Each revolution of the main shaft corresponds to the movement of the gas cell or of the air cell through the whole regenerator.

The length of time each contact lasts—which must be slightly less than the duration of one revolution divided by the number of insulated segments—cannot be accurately ascertained from the geometry of the distributor because of the uncertainty as to the precise time of passage of the brush from one segment to the next. Consequently an electrical method, de-

scribed later, was used, and the conversion factor for the time scale was adjusted accordingly.

The time available for charging and for discharging C_g and C_a through the special segments is very short, hence resistance during charging and discharging had to be avoided. This was done through two additional rings, 11 and 14, similar to 5 and 6 except that they comprise only a single segment. Brushes 3 and 13, 4 and 15, are interconnected so that segments 9 and 12, and 10 and 16, respectively, are brought directly into contact. In this way C_g is charged by the battery without significant resistance, and likewise C_a is discharged on each revolution, thus making the network in Fig. 2 equivalent to the linear arrangement in Fig. 1.

The several voltage levels are measured on electrostatic voltmeter 18, which has the advantage of responding accurately to the potential of the condenser without appreciably affecting its charge.* To obtain voltage values corresponding to exit gas and air temperatures, either segment 19 or 20 can establish contact with 18 on each revolution of the shaft; selection between 19 and 20 is made by switch 17, which may be connected or open as desired. These segments are in contact with C_g or C_a , respectively whose potentials are thus impressed on the voltmeter; these potentials are a measure of the temperature (on our scale) of the gas and air, respectively, as they leave the regenerator. The voltmeter is not restricted to these measurements; at the end of a gas or an air cycle it may be connected to each brick condenser to furnish the gradation of temperature of the brick along the length of the regenerator. Operation of the apparatus is stopped by switch 21 as a means of preserving the potential distribution over the brick condensers as attained at any desired time during operation. The appara-

* A cathode-ray oscillograph could also be used.

tus yielded the same result when started with all condensers discharged, or fully charged, or with any distribution of charges; that it should do so is requisite because the steady state, in which we are interested, requires the same distribution at a given point in the cycle, irrespective of the initial condition.

Constructional Elements Used in the Apparatus

The "brick" units C_b comprise two condensers, each of slightly over 2 mf. (type 228A, Western Electric paper condensers). These had very small leakage and were quite satisfactory. Fifteen such units, as used, had a total capacity of 62.5 mf. The "moving" units C_g , C_a , were assembled by grouping small mica condensers to make up a capacity ranging from 0.05 to 0.5 mf. The transfer resistances R_g , R_a ranged from 10,000 to 300,000 ohms to imitate a wide range of heat-transfer coefficients.

The commutator rings were made by setting copper segments firmly in a heavy, hard rubber ring, mounted on a rigid brass frame. To reduce error from leakage during operation and measurement, a gang switch (a series of mercury wells in a hard rubber block; not shown in Fig. 2 but recognizable in Fig. 3) was inserted in the leads to the brick condensers; it was opened simultaneously with switch 21, thus isolating the whole bank of condensers from the commutator.

The only serious experimental difficulty encountered was in the brushes 3 and 4 (Fig. 2), which must maintain good electrical contact over the whole of a commutator segment if the time scale is to have a well-defined value. Simple phosphor-bronze strips proved, on test with an oscillograph, to give irregular contact due to chattering, thus lessening the real contact time. After trial of several materials, the final choice was heavy strips of pure cold-rolled silver backed by phosphor-bronze strips and these in turn by $\frac{3}{8}$ -in. thick blocks of firm

live rubber. The contact ends of the silver strips were bent so that after a little wear they would, on leaving one segment, spring forward to the next with only a very small movement (0.003 to 0.005 in.), and the lost contact time was less than 1 per cent of the time of one revolution of the ring. All brush contacts were lubricated with a mixture of 20 per cent neatsfoot oil and 80 per cent tricresyl phosphate; this was very satisfactory and allowed us to run the apparatus many times before it was necessary to replace the rather soft silver strips.

OPERATION OF THE ANALOGUE

The first step is to calculate (by a method illustrated later) and adjust the values of the condenser-resistor units C_g - R_g , C_a - R_a , to correspond to a given design of the regenerator. With these in the network, the motor is started, switch 21 and the gang switch in the condenser bank are closed, and switch 17 is thrown to one side or the other. The approach to a steady state is now observed by watching the swings on the scale of the voltmeter 18, which is now reacting to the potential, either of C_g or of C_a as it leaves the system at the "cold end" or "hot end," respectively. Either potential varies in the course of the half cycle; the steady state is when the swings are alike for a number of successive cycles; that is, of revolutions of cam 7. Switch 17 may then be opened at a position of the cam that corresponds to the reversal point in the cycle, and the voltmeter then indicates the potential corresponding to gas or air temperature at the beginning or the end of each half cycle. If switch 21 is opened at the end of the "gas" or of the "air" period on the cam, the condenser bank is isolated, and its potential curve (the brick-temperature curve) at those points in the cycle is obtained by reading the potential on each condenser element C_b .

These measurements, which require about one quarter hour, furnish the essential data on the temperature distribution for a given design under given operating

brush and segment to the time of one revolution of the shaft may be determined experimentally by a series circuit containing a suitable battery, resistance, brush,

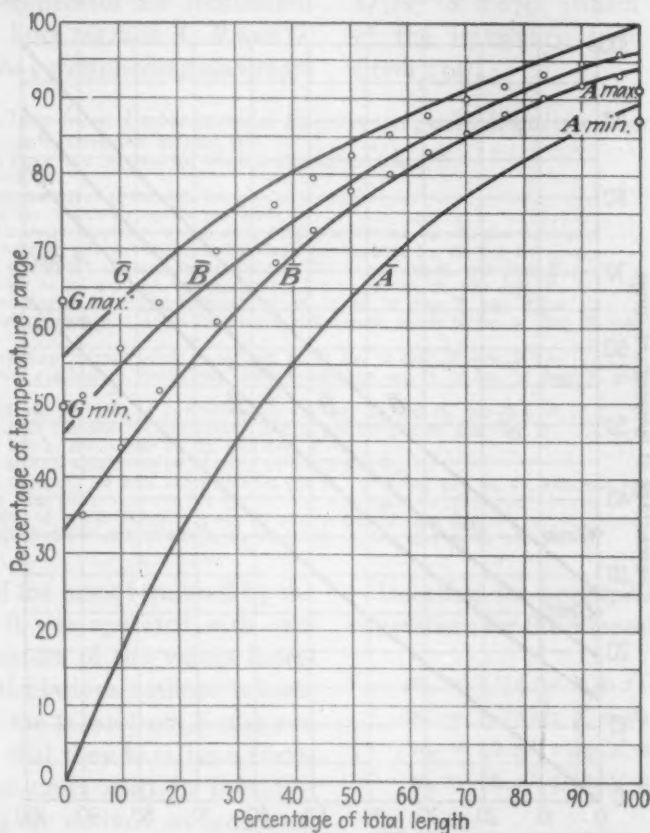


FIG. 4.—TEMPERATURE CONDITIONS IN EXPERIMENTAL REGENERATOR OPERATED AT 2.1:1 GAS TO AIR CAPACITY RATIO.

Curves and arrows show observed mean temperature; points indicated by small circles are corresponding extreme temperatures in a cycle, obtained by the analogue. B, G and A denote brick, gas and air, respectively.

conditions and on the corresponding efficiency. On repeated runs with an arbitrary initial voltage distribution on the "brick" condensers C_b , it proved feasible to reproduce the final observed potentials of these condensers to within ± 0.1 per cent, and those of C_g and C_a , as each leaves the system, to within ± 0.3 per cent, subject to the precautions: (1) that measurement was deferred until after a number of cycles of operation sufficient to realize the steady state; (2) that the brush contact on all segments is definite and uniform.

The ratio of actual time of contact of

segment and milliammeter. The shaft is then turned by hand until the circuit is closed by the brush and segment, when a milliammeter reading is made. The motor is now started and a second reading is made while the brush is uniformly rotated by the motor. The second reading divided by the first is the ratio of actual time to the time of one revolution of the shaft. In place of the milliammeter, a suitable resistance may be used and the voltage drop between its ends may be accurately determined by a potentiometer. Since a time ratio is measured, a knowledge of the

absolute value of the voltage, resistance, speed and the absolute calibration of the instrument is not necessary. The requirements are constancy of angular speed

accuracy and usefulness of the analogue by comparison of its indications with the temperatures measured in the regenerator systems studied. The first example is

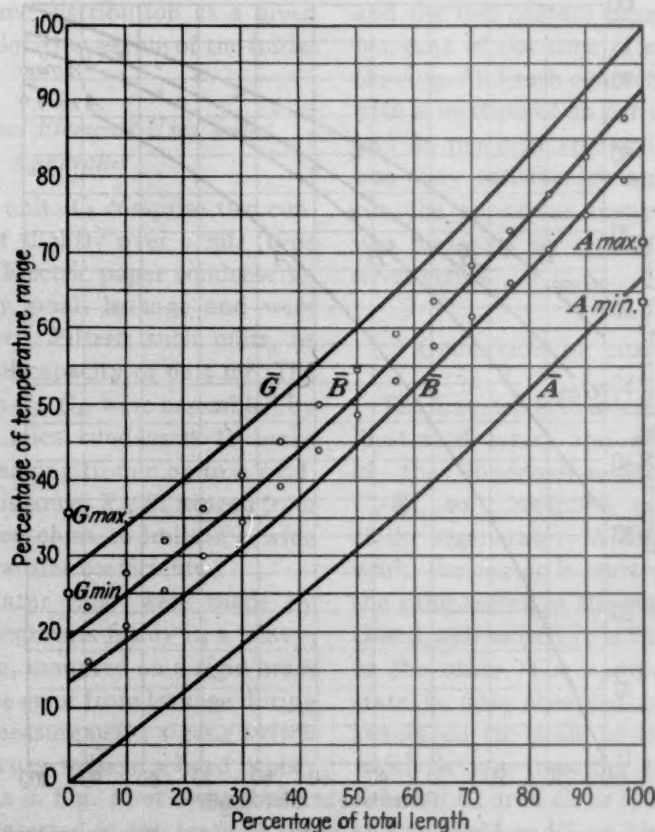


FIG. 5.—TEMPERATURE CONDITIONS IN EXPERIMENTAL REGENERATOR OPERATED AT 0.95:1 GAS TO AIR CAPACITY RATIO.

Curves and arrows show observed mean temperatures; points indicated by small circles are corresponding extreme temperatures in a cycle, obtained by the analogue. B , G and A denote brick, gas and air, respectively.

within any one revolution, constant battery voltage and proportionality between current and deflection of the instrument. The current-measuring instrument should be well damped to avoid oscillation of the needle.

METHODS OF CALCULATION AND RESULTS IN A FEW SPECIFIC CASES

The mode of calculation of the proper size of the condenser and resistor units is best illustrated by actual examples, which enable us, moreover, to show the degree of

experiment No. 17 from the work of Kofler and Kistner,³ on an experimental regenerator operated under as nearly ideal conditions as is feasible. This regenerator was a well-insulated airtight vertical shaft, of over-all dimensions $6\frac{1}{2}$ by $6\frac{1}{2}$ by 24 ft., with draft and gas temperature under accurate control. The various quantities pertaining to this experiment are listed in Table 3 together with the thermal constants of brick, gas, and air required to express Kofler and Kistner's data in terms of the quantities listed in Table 2. Their direct

measurements, when a steady state was reached, of the mean temperature of air, gas, and of the brick, during the gas and air half cycles, respectively, along the length of the regenerator are reproduced in Fig. 4 as the lines marked \bar{A} , \bar{B} and \bar{C} . The circles are the corresponding maximum

corr. = $0.454 + 0.050 = 0.504$ (items 10a, 11a). For the same reason a correction must be applied to the heat capacity, as given in Table 3; the corrected value is $1/(2\pi f' \times 0.079)$ (which is the coefficient of the imaginary term above) or 4.02 (item 15a).

TABLE 3.—Data from Experimental Regenerator, with Requisite Thermal Constants

1. Length of checkers in direction of flow, ft.	$P' = 16.4$
2. Perimeter of all flues in a horizontal section through checker, ft.	$= 194$
3. Thickness of brick, ft.	$= 0.262$
4. Time between consecutive reversals, hr.	$f' = 1$
5. Frequency; number of gas-air cycles per hour.	$f' = 0.5$
6. Volume of gas through checkers under standard conditions, cu. ft. per hr.	$V'_g = 99,000$
7. Volume of air through checkers under standard conditions, cu. ft. per hr.	$V'_a = 53,700$
8. Specific heat of gas at its average temperature, B.t.u. per cu. ft. per deg. F.	$S'_g = 0.0234$
9. Specific heat of air at its average temperature, B.t.u. per cu. ft. per deg. F.	$S'_a = 0.0205$
10. Heat-transfer resistance from gas to brick, sq. ft. \times hr. \times deg. F. per B.t.u.	$R'_g = 0.163$
10a. Total gas-transfer resistance, including brick resistance, sq. ft. \times hr. \times deg. F. per B.t.u.	$R'_g \text{ corr.} = 0.213$
11. Heat-transfer resistance from brick to air, sq. ft. \times hr. \times deg. F. per B.t.u.	$R'_a = 0.454$
11a. Total air-transfer resistance, including brick resistance, sq. ft. \times hr. \times deg. F. per B.t.u.	$R'_a \text{ corr.} = 0.504$
12. Heat capacity of gas per foot of perimeter, B.t.u. per hr. per ft. per deg. F.	$C'_g = V'_g S'_g / 194 = 11.9$
13. Heat capacity of air per foot of perimeter, B.t.u. per hr. per ft. per deg. F.	$C'_a = V'_a S'_a / 194 = 5.66$
14. Specific heat of brick, B.t.u. per cu. ft. per deg. F.	$C' = 34$
15. Static capacity of half thickness (0.131 ft.) of brick per sq. ft.	$= 4.45$
15a. Effective heat capacity of half thickness (0.131 ft.) of brick per sq. ft. exposed surface, B.t.u. per sq. ft. per deg. F.	$C'_b = 4.02$
16. Heat conductivity of brick, B.t.u. per sq. ft. per ft. per hr. per deg. F.	$1/R'_b = 0.83$
17. Heat flow (specific) resistance of brick, sq. ft. \times ft. \times hr. \times deg. F. per B.t.u.	$R'_b = 1.2$

and minimum of the brick furnished by the analogue when it was operated with condensers and resistors of the values determined by the calculations outlined below.

Items 1 to 11 are taken from Kofler and Kistner, except that they have been transformed into the units used in industry: items 12 and 13 are derived, as indicated, from items 8 and 10 or 9 and 11, respectively, along with item 2; item 14 is a recognized value of specific heat for this type of brick; item 16 is from direct measurement in this laboratory, and item 17 is the reciprocal of item 16.

When the appropriate values from Table 3 are inserted in the Kelvin equation (page 21) we obtain $Z = 0.050 - 0.079j$. The real term expresses the effective thermal resistance, which may be imagined as concentrated at the surface of the brick, to be added to the transfer resistance (items 10, 11) in order to take into account the temperature gradient in the brick caused by the cyclic variation of temperature. Thus the effective resistance $R'_g \text{ corr.} = 0.163 + 0.050 = 0.213$ and R'_a

Inserting the appropriate values in the expressions for the dimensionless constants:

$$m_g = 1/(4.02 \times 0.213) = 1.17$$

$$m_a = 1/(4.02 \times 0.504) = 0.493$$

$$n_g = 16.4/(11.9 \times 0.213) = 6.45$$

$$n_a = 16.4/(5.66 \times 0.504) = 5.73$$

These four quantities are those which the corresponding four quotients in the electrical system must likewise equal, so that:

$$1/C_b R_g = 1.17 \quad 1/C_g R_g = 6.45$$

$$1/C_b R_a = 0.493 \quad 1/C_a R_a = 5.73$$

The shaft of our analogue as built rotates at 940 r.p.m. The actual time of contact of each segment of the commutator per revolution, as measured electrically, was 0.0034 sec. The gear ratio of the reversing cam corresponds to 96 revolutions for a half cycle, and so the total contact time of brush and a segment is 96×0.0034 , or 0.326 sec. per half cycle. The brick mean capacity C_b for each of the 15 cells (or segments) is 4.16×10^{-6}

farads. Consequently

$$R_g = 0.326 / (4.16 \times 10^{-6} \times 1.17) = 67,000 \text{ ohms}$$

$$R_a = 0.326 / (4.16 \times 10^{-6} \times 0.493) = 158,300 \text{ ohms}$$

The electrical counterpart C_g (or C_a) of the rate of flow of heat capacity is a capacity divided by the time of contact (0.0034 sec.) of any one segment with the brush; and l is 15, as noted above. Hence

$$C_g = \frac{15 \times 0.0034}{67,000 \times 6.45} = 0.118 \times 10^{-6} \text{ farad}$$

$$C_a = \frac{15 \times 0.0034}{158,300 \times 5.73} = 0.056 \times 10^{-6} \text{ farad}$$

Resistances and condensers of these values were inserted in the network, the analogue operated and the several potentials observed as described previously.

These measurements on the analogue are plotted in Fig. 4 as small circles. The gas, at temperature 100 per cent, enters at the right and leaves at the left at a temperature, according to the analogue, ranging from 49.5 per cent (G min., Fig. 4) at the beginning, to 63.2 per cent (G max.) at the end, of the gas half cycle. Likewise the air, entering at temperature zero at the left, leaves at a temperature ranging from 87.2 per cent (A min) at the beginning to 91.2 per cent (A max.) at the end, of the air half cycle. It will be noted that curves G and A given by Kofler and Kistner end symmetrically within these limits. The upper set of small circles represents the analogue determinations of the maximum, the lower of the minimum, temperature attained by the brick along the path of flow of gas or air. For perfect correspondence these two sets of points should lie outside of the pair of curves BB , which represent mean values as observed by Kofler and Kistner; this is essentially so at the two ends but toward the center there is some deviation, which, however, is certainly no greater than is

to be expected from the degree of accuracy of Kofler and Kistner's observations.

By a modification of the procedure, the analogue can be made to yield the complete temperature curves of gas and air if there were any reason for knowing the whole course of these curves. In practice we are mainly interested in the final temperature of the air (and to some extent in that of the gas) leaving the regenerator, also in the two brick-temperature curves, since the area between this pair of curves is also a measure of the heat conveyed from gas to air, and therefore of the thermal efficiency of the regenerator system. The mean air temperature over the air cycle is proportional to the heat returned to the furnace; the difference between unity and the mean gas temperature over the gas cycle is proportional to the heat carried by the gas leaving the regenerator.

As a second illustration, take experiment No. 18 by Kofler and Kistner. In this the several items are as given in Table 3 except that the volumes of gas and of air (items 6, 7) are 75,500 and 89,000, respectively, and the transfer resistance $R'_g = 0.2325$, $R'_a = 0.345$ (items 10, 11); consequently C'_g is now 9.07, C'_a is 9.54 (items 12, 13). The correction for the impedance of the brick is the same as before. The values of the dimensionless constants for this case are

$$\begin{aligned} m_g &= 0.879 & n_g &= 6.39 \\ m_a &= 0.629 & n_a &= 4.345 \end{aligned}$$

whence, by calculation, as before,

$$\begin{aligned} R_g &= 89,000 \text{ ohms} \\ R_a &= 124,700 \text{ ohms} \\ C_g &= 0.090 \times 10^{-6} \text{ farad} \\ C_a &= 0.095 \times 10^{-6} \text{ farad} \end{aligned}$$

When these resistances and capacities were inserted in the network and the analogue operated, the results were as depicted in Fig. 5, the several lines and points on which correspond precisely with

those on Fig. 4. Again there is satisfactory agreement between the temperatures reported by Kofler and Kistner and the readings obtained from the electrical analogue.

It is to be noted that in the first case the volume of the gas passing, and consequently the amount of heat carried by it (C'_g), is greater than that carried by the air (C'_a); whereas in the second case C'_g is less than C'_a . Correspondingly the curves in the first case (Fig. 4) are concave to the abscissa; in the second case (Fig. 5), convex. When C'_g is equal to C'_a the curves are for practical purposes linear and symmetrical, as was actually demonstrated with the analogue. The second case, with C'_g less than C'_a , never occurs in an open-hearth system. The theoretical limiting values for C'_g/C'_a are in the range of about 1.05 to 1.30 for various fuels, but owing to air leakage the actual value may run much higher, from about 1.4 to 2.5. This was shown by an actual field test in which the C'_g/C'_a value was 2.33.

The two comparisons illustrated in Figs. 4 and 5 serve mainly as a confirmation of the essential validity of the postulates (listed on p. 22), which were deemed essential in order to idealize and simplify actual furnace conditions sufficiently to make the problem reasonably workable by either a mathematical or the electrical analogue treatment. The results indicate that these simplifying postulates do not appreciably distort the actual thermal conditions. The simpler problem of whether the construction and design of the analogue were such as to make it a reliable and accurate calculating device is really involved in these comparisons, but in order to obtain a more direct check with this aspect of the problem isolated from disturbing influences, it was thought desirable to match the analogue against a simple mathematically calculated set of conditions. In general, mathematical calculation is very difficult and time-consuming, but it can

be carried out for certain simple conditions—for instance, when the heat capacity of air and gas (C_a, C_g) per half cycle are equal, and the heat-transfer coefficient is the same in both halves of the regenerator cycle. These simple conditions never obtain in practice, but this in no wise prevents us from making the comparison to test the accuracy of the analogue data. The calculation for these conditions was made by Nusselt,¹ using the same assumptions as underlie the operation of the analogue and the following constants:

Total exposed area of checkers, sq. ft.	= 12,110
Period of reversal, hr.	= 4
Heat capacity of gas or air through regenerators, B.t.u. per hr. per deg. F.	$C'_g = C'_a = 11,025$
Heat capacity of half thickness of brick per sq. ft. of exposed surface, B.t.u. per sq. ft. per deg. F.	$C'_b = 4.1$
Heat-transfer resistance gas-brick or brick-air, sq. ft. \times hr. \times deg. F. per B.t.u.	$R'_g = R'_a = 0.24$
Heat conductivity of brick	$1/R'_b = \infty$
Heat-flow resistance of brick	$R'_b = 0$

On the basis of these data the dimensionless constants applicable to this case are $m_g = m_a = 2$, $n_g = n_a = 4.5$; hence the corresponding values to be inserted in the analogue network are $R_g = R_a = 39,200$ ohms, and $C_g = C_a = 0.289$ microfarad. Operation of the analogue yielded the several circles in Fig. 6, whereas the corresponding temperatures computed by means of the mathematical expressions given on pages 1053-4 of Nusselt's paper are shown as lines and arrows. The agreement is excellent, showing that the analogue as built and operated is in fact a satisfactory calculating device for this type of problem; and it gives us confidence in the results for the more complex practical cases when the mathematical calculation is impracticable.

CONCLUSION

The usefulness of the results obtainable by the use of an electrical analogue like that described in this paper, in the solution of the problems surrounding the proper design and operation of an efficient re-

generator system, depends upon the validity of the postulates adopted in treating the specific problem, and upon the accuracy of the analogue as a calculat-

Kistner, provided that the postulates adopted fit the conditions under which the regenerator is operated. Accordingly, we consider that this rapid method of using an

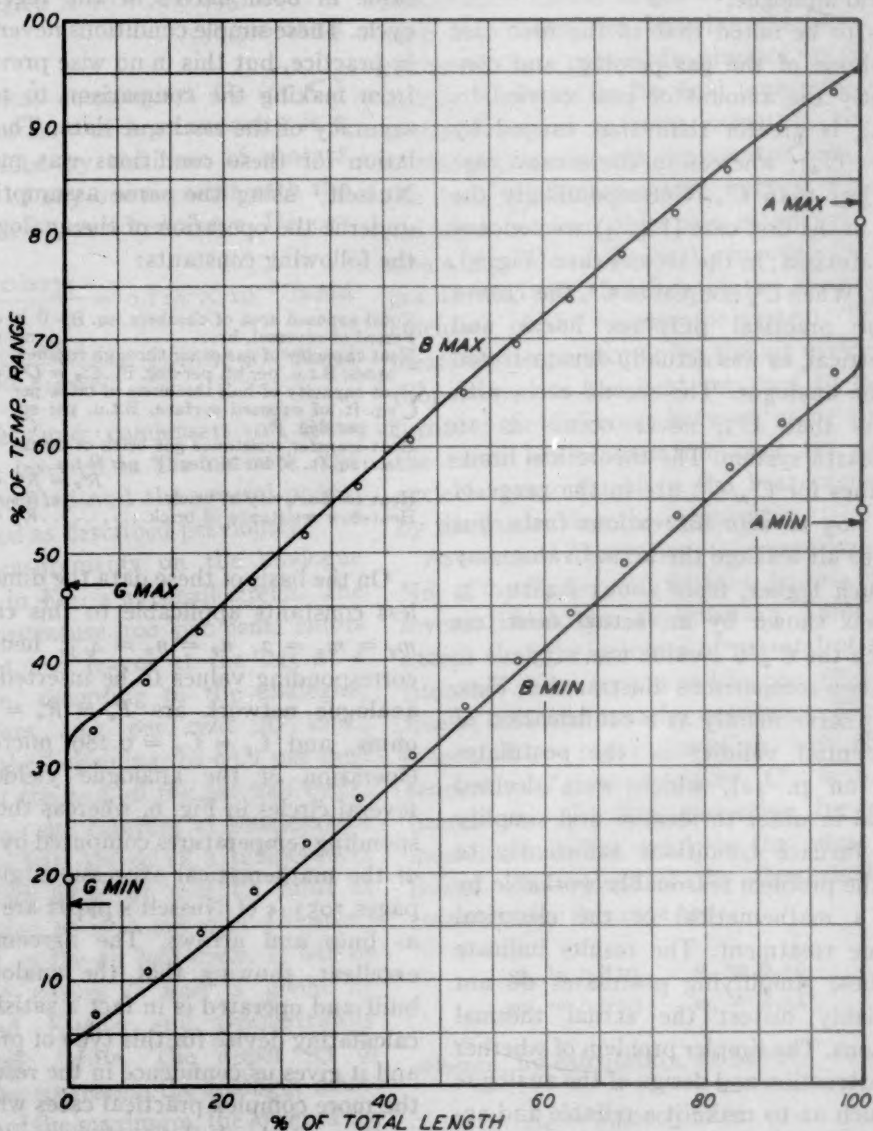


FIG. 6.—TEMPERATURE CONDITIONS IN A REGENERATOR AS DETERMINED MATHEMATICALLY (SOLID LINES AND ARROWS) AND BY THE ANALOGUE (SMALL CIRCLES).

ing device. The latter we have shown to be satisfactory by direct comparison with mathematical calculations, for a simplified set of conditions. The former we believe to be likewise satisfactory from comparisons with two runs recorded by Kofler and

electrical analogue on the analysis of the complex problems of the flow of heat in regenerator systems will aid in placing regenerator design on a rational basis and in indicating possible ways of improving the usefulness of existing installations.

ACKNOWLEDGMENT

The authors wish to acknowledge their indebtedness to Dr. John Johnston, for advice and criticism in the preparation of the paper, and to Mr. C. Siddall, for his collaboration.

REFERENCES

1. W. Nusselt: (a) The Theory of Air Preheaters. *Ztsch. ver. deut. Ing.* (1927) 71, 85-91; (b) The Steady State in the Air Preheater. *Ibid.* (1928) 72, 1052-1054.
2. G. Ackermann: The Theory of Heat Exchangers Having Heat Storage. *Ztsch. angew. Math. Mech.* (1931) 11, 192-205.
3. F. Kofler and H. Kistner: Experiments with a Full-scale Regenerator Chamber. *Archiv Eisenhüttenwesen* (1929-1930) 3, 25-42, 751-768.
4. F. Bruckmayer: An Electrical Analogue for the Solution of Heat-transfer Problems. *Archiv Warmewirtschaft Dampfkesselwesen* (1939) 20, 23-25.
5. V. Paschkis and H. D. Baker: A Method for Determining Unsteady-state Heat Transfer by Means of an Electrical Analogy. *Trans. Amer. Soc. Mech. Engrs.* (1942) 64, 105-112.

DISCUSSION

V. PASCHKIS.*—The authors are to be congratulated for an unusually interesting piece of work. It is remarkable that at approximately the same time, yet in two places and entirely independently, the idea of working with lumped resistance capacitance electrical networks has been evolved for the study of transient heat flow.

C. L. Beuken, in Maastricht, started his work by this method in 1935 also, and he published his results in 1937.⁶ Incidentally, almost at the same time, A. D. Moore published work on the hydraulic analogy method for study of transient heat flow.⁷

The writer has done some work on the heat and mass flow analyzer^{8,9} at Columbia University along lines similar to those published in the present paper. Since the equipment of the analyzer is rather extensive and flexible, it has been possible to choose an approach different from that selected by the authors. Instead of rotating one gas condenser and one

air condenser, a number of gas and air condensers were used. This made it possible to work with higher time ratios, which in turn facilitates measurements and improves their accuracy. The higher accuracy is achieved by reducing the time for leakage from the brick condensers. In this connection, it would be interesting to know what the authors call "very small leakage." In the equipment at Columbia, the condensers used have a leakage resistance in the order of magnitude of 50,000 to 100,000 megohms microfarad (these values are established by the voltage decay method).

The authors have assumed that the boundary conductance between gas and brick, and between air and brick, do not change with temperature. It is believed that this assumption does not hold and the proof of the authors, comparing their measurements with calculated values, is not conclusive; the calculated values have been based on the same assumption of constant properties, which in the opinion of the writer does not hold.

The heat transfer from the air to brick occurs by convection. The following formula was used to determine the boundary conductance:

$$h_c = T^{0.25} \left(0.9617 + \frac{0.243W_0}{d_h^{0.4}} \right)$$

The following notations are used:

h_c convective component of boundary conductance in k cal. per sq. m. per hr. per deg. C.

T absolute temperature, deg. Kelvin (deg. C. + 273).

W_0 air or gas velocity, m. per sec.

d_h hydraulic diameter, meters.

The formula was published by H. H. Boehm.⁹ The radiation component is approximately twice as great at 3000°F. as at 1500°F. for the gas period. The over-all boundary conductance calculated as indicated above varies within considerable limits; e.g., from 5.32 B.t.u. per sq. ft. per hr. per deg. F. at 2900°F. to 2.81 B.t.u. per sq. ft. per hr. per deg. F. at 800°F. for gas; or, in another experiment from 1.66 B.t.u. per sq. ft. per hr. per deg. F. at 2900°F.

* Columbia University, New York, N. Y.

⁶ Beuken, C. L.: *Economisch Technisch Tijdschrift*, Maastricht, Netherlands, 1937, No. 1.

⁷ A. D. Moore: *Ind. and Eng. Chem.* (1936) 704.

⁸ V. Paschkis: *Ind. Heating* (1942) 9, 1162.

⁹ H. H. Boehm: Versuche zur Ermittlung der konvektiven Waermuebergangszahlen und gemauerten engen Kanaelen. *Archiv Eisenhüttenwesen* (1933) 6, 423.

to 1.11 B.t.u. per sq. ft. per hr. per deg. F. at 200°F. for air.

The calculations of the brick values as shown by the authors appears unnecessary in view

comprises two scales, one starting with the beginning of the gas period and one with the beginning of the air period. The reversal period equals the sum of the maximum values of

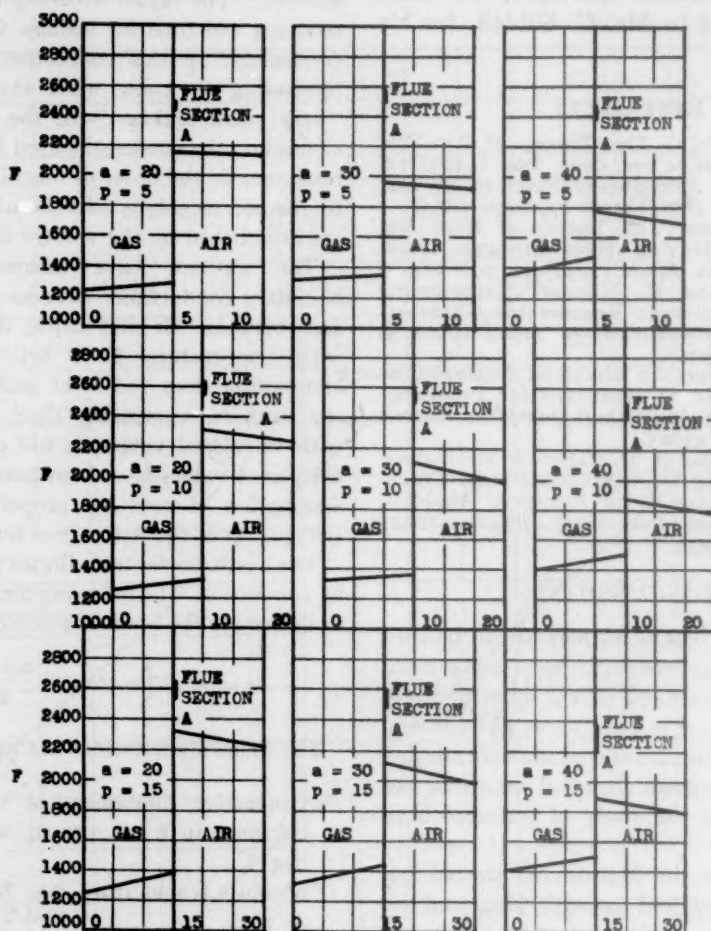


FIG. 7.

of the general correctness of the analogy between electric and heat flow.

The authors make mention of the efficiency of regenerators. The efficiency is of course a function of the gas and air quantity and can be made to approach unity with any design. The efficiency alone, however, is no suitable measure for the operation of a regenerator—rather, the product of the efficiency and a factor characteristic of the load. For example, such a factor may be the quantity of air per square foot of regenerator area.

To exemplify results, Fig. 7 is offered. In each graph, times are plotted as abscissas and temperatures as ordinates. The abscissa axis

both scales on the abscissa axis. The temperatures shown for gas are the temperatures at the exit of the gas and the temperatures shown for the air period are at the exit of the air.

On the ordinate separating the two halves of each graph a heavy line indicates the limit of temperature oscillations of the hottest part of the brick during any one reversal period. Each of the graphs on the chart holds for a different set of conditions, as indicated in the graph.

The results obtained indicate that it is desirable to work with thin bricks and with great lengths of the flue. There are, however, limits not only from the operational viewpoint

but also from the viewpoint of increased efficiency, which make it appear unnecessary to increase the lengths beyond certain values that depend upon the different variables.

The length of the reversal period does not appear to have major influence on the performance, at least not within the limits analyzed.

K. HEINDLHOFFER (author's reply).—One of the points raised by Dr. Paschkis pertains to the variability with temperature of the boundary conductance between gas and brick. The authors are aware of this fact and have taken this variation into account by using a set of graded resistors shown as a vertical ladder in Fig. 3. It is stated there that this extra complication could be avoided. The set of resistors could be replaced by a single resistance simulating the constant mean value of the heat-transfer coefficient without great loss of accuracy.

The calculation of the effective brick resistance, however, is important under conditions corresponding to practical reversal time and brick thickness. To neglect this calculation, as is proposed in the comments, would violate the analogy in an important way and would impair the accuracy of the results.

In answering the question of leakage resistance, the values were of the same order of magnitude as those quoted by Dr. Paschkis. Stated in equivalent terms, the leakage was about 1 per cent of the initial charge in 15 min. within a voltage range of 30 and 120.

Regarding the question of using many "gas" condensers instead of only one, reference is made to the paper. A great number of condensers require a great many brushes. Since the accuracy of the end result depends upon the proper adjustment of these brushes, it is desirable to have a minimum number of brushes. The leakage can be kept sufficiently low by proper design of the apparatus and by the use of good condensers.

B. M. LARSEN (author's reply).—With regard to the time ratio, it would perhaps be interesting if Dr. Paschkis would describe the details of his method for simulating the flow of gas and air capacity with multiple units. With condensers comparable to his, and the

best possible insulation in the circuit in general, we concluded that the time scale used permitted a negligible error over the range of heat-flow rates studied, especially in view of the presence of an appreciable leakage in the thermal system of any actual furnace. For very low time rates of heat flow, however, this source of error might become important, although it might then be so much of a factor in the thermal system as to require some provision for imitating it in the electrical analogy.

Our checks made to determine the accuracy of the analogue method included not only the comparison with a mathematical case of Fig. 6, but also the comparisons with an experimental regenerator shown in Figs. 4 and 5, and another comparison with a test on the regenerators in a commercial open-hearth furnace, which was not included here but which gave the same close agreement. As a result of these, we concluded that the refinement of a variable heat-transfer coefficient was unnecessary. Since all such refinements tend to diminish the flexibility of the analogue arrangement, a very essential part of the problem in any new type of application is to determine what simplifying assumptions are allowable.

In designing a regenerative furnace, the capacity desired plus the fuel to be used tend to fix the size and shape of the working chamber; this being determined, the optimum rate of fuel input is pretty much determined independently of the air preheat temperature; that is, although regenerator efficiency has a large effect on the rate of useful heat delivery, it does not much affect the maximum useful rate of fuel burning for a fixed size of working chamber, design of burners and ports, etc. With the maximum probable load thus pretty much fixed, the furnace designer wants to know the curve of regenerator efficiency vs. perimeter and depth of checkwork to decide the approximate point of diminishing returns in design, and the furnace operator wants to know the effect of reversal interval and of air leakage (that is, of degree of a symmetry between flow rates of air and gases of combustion) on regenerator efficiency. These are the reasons for introducing the efficiency term. It is true, of course, that many practical limitations enter into regenerator design, but a knowledge of the position and shape of the curves of effi-

ciency vs. depth or perimeter of exposed surface can nevertheless be a big help to the designer.

The average time loss on reversal is the biggest factor determining the optimum length of reversal period. However, the ideal efficiency curve does normally have an appreciable downward slope with increasing reversal

interval, and this curve is of some help in finding the best normal interval. Peak temperatures just before reversal are also of some importance to the refractory service in end walls and top checkerwork, and the analogue calculations can help here by showing the rate of increase in amplitude of brick-temperature oscillations with lengthening period.

A Completely Automatic Control of Open-hearth Reversal

By B. M. LARSEN,* MEMBER A.I.M.E. AND W. E. SHENK*

(New York Meeting, February 1945†)

THIS paper describes a method of reversal control of the open-hearth furnace that obtains in practice those effects considered below as essential to a completely automatic control, without appreciable interference with the natural rise and fall in temperature of the regenerative portions of the furnace system. Growing out of some studies of radiation pyrometry in open-hearth regenerators, it was developed during 1934-1938, and has been successfully applied to a number of commercial furnaces.

The goal of open-hearth furnace operation is the highest rate of production of steel of proper quality consistent with good refractory life and fuel economy. This requires rapid heat transfer from furnace to charge, which in turn is dependent upon heating the furnace refractories to the highest safe operating temperature. The greater the heat input to the melting chamber, the sooner this limiting temperature will be reached, so that control methods in general that are designed to protect against overheating of refractories should help to maintain maximum fuel input and production rate.

For the typical open-hearth system, with fixed regenerator capacity and with rate of fuel input usually restricted in its range of variation, our basic assumption is the

idea that the only other important variable—that is, the time interval between successive reversals—should also be held constant or within a small range. The present reversal control was designed therefore so that, under normal operating conditions, no arbitrary limitation is imposed other than to keep the reversal interval within the optimum time range. However, since a near approach to completely automatic operation involves protection of refractories through the balancing of furnace end temperatures as well as emergency protection against temperature peaks above some upper limit, it was also felt essential to employ, as an integral part of the control unit, a temperature-measuring instrument to register the true temperature of the refractory surfaces at some critical region in the hot ends of the regenerative zones.

As the basic elements of the control, we thus have one "maximum" and one "minimum" time relay and a potentiometer recorder-controller, combined with switches and relays to operate as follows:

1. Reversal *normally* occurs within an optimum range limited by the maximum and minimum settings to about 4 to 6 min. variation, but the actual interval usually is less variable and closer to the minimum setting.

2. The margin between minimum and maximum time is utilized, together with a "floating temperature limit" in the potentiometric control instrument, to correct any tendency toward temperature unbalance between ends of the furnace.

3. A second "maximum temperature

Manuscript received at the office of the Institute Dec. 1, 1944. Issued as T.P. 1830 in METALS TECHNOLOGY, June 1945. Reprinted in Open Hearth Proceedings, A.I.M.E., 1945.

* Research Laboratory, United States Steel Corporation, Kearny, New Jersey. W. E. Shenk now with American Transformer Co., Newark, N. J.

† Meeting canceled.

limit" in the potentiometer is utilized for reversal at less than the set minimum time as a means of emergency protection against overheating of the regenerator refractories.

OPTIMUM REVERSAL PERIOD

If the furnace were ideal it would be desirable to reverse it in rapid succession at short uniform intervals, thereby getting maximum efficiency of regeneration; that is, building up the temperature of the preheated air used in combustion at the maximum rate. In a practical furnace however, there is an unavoidable loss of heating time at each reversal because of the time taken to perform the mechanical operations of reversal and the time required to reestablish the flow of fuel and gases in the reverse direction and to establish proper fuel-air mixing and resultant combustion conditions. (The total interval is of the order of 30 to 60 sec. in a practical open hearth, depending upon its size.) This irreducible minimum of lost heating time in every reversal limits the period to one that is several times longer than this lost time, which suggests that the period should be long for maximum regenerator efficiency. In a long reversal period, however, this advantage is counterbalanced by the diminishing heat interchange in the regenerator as portions of its brickwork approach the temperature of the waste gases or the air; consequently the optimum period is neither short nor long but is determined by proper balancing of these two factors. This may be illustrated by the schematic curves of Fig. 1, where the "ideal" curve represents mean preheat temperature of the air vs. reversal interval, assuming no lost time on reversal. In the actual case, the time loss approaches 100 per cent at small intervals of the order of 60 to 100 sec., so that in terms of regenerated heat returned to the melting chamber (as sensible heat in air that was

rich enough in oxygen to give proper combustion), the actual regenerator efficiency (or mean air preheat temperature) would be low for such short reversal intervals. The percentage loss on reversal decreases rapidly with longer intervals, and when subtracted from the "ideal" curve gives an "actual" curve of the general form shown here. It changes slowly over several minutes near its optimum value, so that an appreciable range for the margin between "maximum" and "minimum" time settings is available without much lowering of regenerator efficiency.

PRINCIPLE OF CONTROL

If the furnace and charge were symmetrical, it would normally be necessary only to operate in accordance with the conditions of maximum rate of combustion, and to reverse at uniform time intervals equal to the optimum. However, no furnace is ever quite symmetrical in structure and combustion conditions; moreover, it is not generally possible to distribute the charge in a symmetrical manner. This often tends to cause different heating rates of the two regenerators, resulting in an asymmetry of temperature levels; this, if not counteracted, tends to increase the asymmetrical character of the furnace by burning the refractories away at a different rate at the two ends of the furnace. (Other causes of asymmetry, such as variable air leakage, may also be present.) The problem, therefore, is to extend heating time on the cooler and/or more slowly heating regenerator, so as to achieve temperature equality of the successive heating regenerators. The control method discussed here meets this requirement by imposing a maximum and a minimum reversal time upon the furnace, the optimum time being intermediate. The actual reversal time between these limits is automatically selected by a floating control switch in the checker

temperature recorder, in accordance with the temperature of the hotter regenerator, so as to give the minimum period to it and sufficient time within the maximum

time as the refractories in the melting chamber reach theirs. The approach to the danger temperature of the refractories in the melting chamber must therefore be

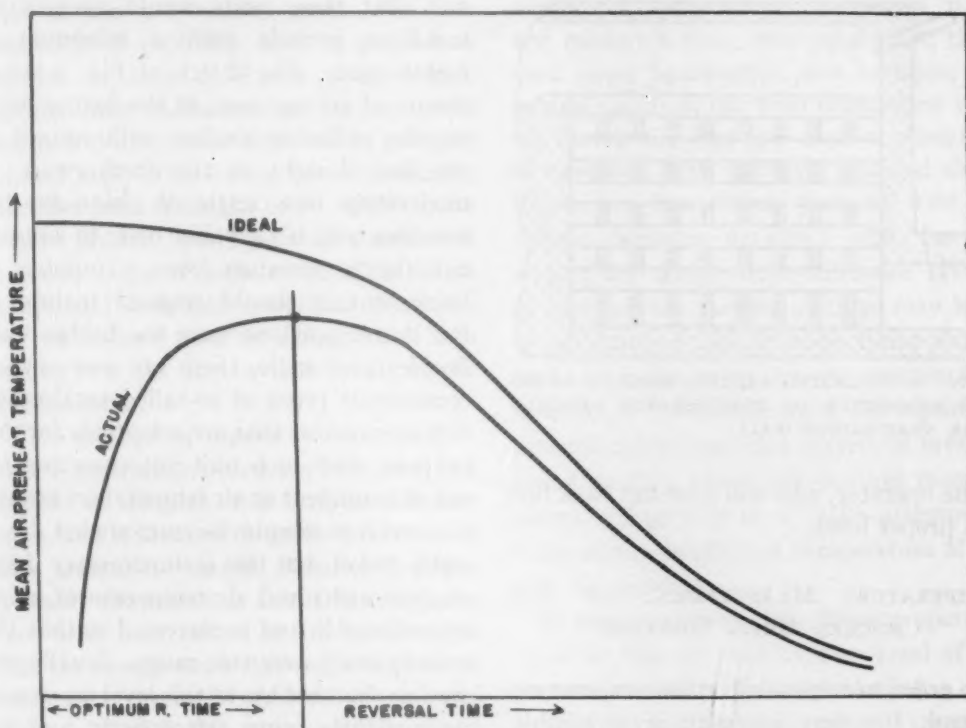


FIG. 1.—SCHEMATIC CURVES OF RELATIONSHIP BETWEEN REVERSAL INTERVAL AND EFFICIENCY OF HEAT INTERCHANGE BY REGENERATION.

period to the cooler one to allow it time to attain the same temperature. When the "danger point" (that is, some desired upper limit of top checker temperature) is approached in the regenerators, it is necessary to shorten the reversal time even below the requirements of optimum operation in order to achieve the then more immediate objective of protecting the refractories. This is accomplished by an independent fixed temperature-control point, which takes over from the floating control when this emergency arises.

In the operation of this control in a well-proportioned furnace the refractories in the regenerators will not necessarily approach the danger point at the same

guarded against either by an automatic cutback of the fuel—which is not a part of this reversal control but is often combined with it as an automatic roof-temperature control—or manually by the furnace operator, either by use of a roof-temperature pyrometer as an indication, or by visual observation, since the melting-chamber refractories are readily observable from the operating floor. Even in absence of either automatic or manual fuel control to prevent overheating, the emergency operation of the reversing control at the danger point gives partial protection from overheating in the melting chamber, because of the reduced efficiency brought about by the materially shortened reversal

periods below the optimum period. Furthermore, in the absence of automatic control of fuel input, this frequent reversing of the furnace cannot fail to attract the attention

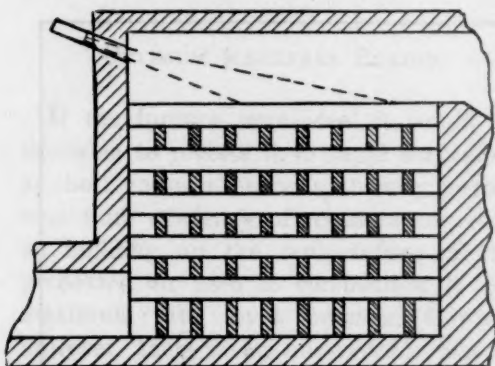


FIG. 2.—SIGHTING ARRANGEMENT OF RADIATION PYROMETER ON REGENERATOR CHECKERWORK NEAR BRIDGE WALL.

of the operator, who will then cut back fuel to a proper level.

TEMPERATURE MEASUREMENT OF TOP CHECKER BRICK SURFACE

In order to achieve effective temperature control, the first necessity is a reliable temperature indication from the hotter end of each regenerative zone. This presents a difficult problem because of: (1) the high temperature involved, (2) the presence of flame and corrosive dust in the combustion gases, and (3) the difficulty of maintenance of the sensitive element. Since, as has been pointed out, the factor that limits the maximum heating rate of the furnace is primarily the refractory temperature, it is necessary to measure the temperature of a specific refractory surface with as little disturbance from the flame and gases as possible. This is most conveniently done, especially where a large area of refractory is involved, by measurement of radiation from the heated surface.

In studies of checker-brick temperature measurement leading up to the development of this control system, we found that

the true average temperature of the top courses of checker brick near the bridge wall is closely approximated by the response of either a total-radiation pyrometer or photocell unit* sighted on these brick, and that these units would operate for indefinite periods with a minimum of maintenance. The sketch of Fig. 2 shows the usual arrangement of the fixture holding the radiation receiver with respect to the line of sight on the checkerwork. A moderately wide angle of vision for the sensitive unit is probably best, to average out the temperature over a number of brick, but it should respond mainly to the hotter portions near the bridge wall. Besides photocells, there are now several commercial types of so-called total-radiation pyrometers that are adaptable for this purpose. Any such unit not corrected for variable ambient or air temperature around the receiver should be surrounded by a water jacket, but this is unnecessary if the receiver will stand air temperatures up to around 200°F. and is corrected so that the error is small over this range. Usually the checker chamber has at this level a pressure range slightly below atmospheric, and the lens or window can be kept clean merely by allowing a small air leak through its sighting tube. If the pressure inside becomes positive at times, it is advisable to provide a small air flow through the sighting tube into the chamber. Under these conditions, maintenance normally is negligible, although an occasional inspection and checking with an optical pyrometer is advisable.

With a photocell unit, checked by optical pyrometer, there is only a small error from the true temperature of the brick surface (or of the iron oxide dust coating) under normal furnace conditions. With a radia-

* B. M. Larsen and W. E. Shenk: Temperature Measurement with Blocking-layer Photocells. In *Temperature, its Measurement and Control in Science and Industry*, 1150-1158. Amer. Inst. of Physics. New York, 1941. Reinhold Publishing Company.

tion unit sensitive to wave lengths longer than about 2.3μ , there is a high error of usually between 15° and 30°F. in the heating portion of the regenerator cycle, owing to the band radiation from the CO_2 and H_2O in the combustion gases. For this reason, it is probably best to provide a window or lens of Pyrex glass, which absorbs this radiation of longer wave length but transmits most of it between 0.4 and 2.5μ . With a long flame, or during excessive boils from the bath, actual flame may be present over the checkerwork, and this will cause a high error. This is an exceptional and bad condition, however, and we believe that an exaggerated high reading on the instrument is then not objectionable.

This method of measurement of regenerative-zone temperature has been used in a number of English and Continental furnaces, and it seems strange that it is not in more common use in American shops. Probably the reason is that thermocouples were used here, alone or in combination with the temperature-difference method of automatic reversal,* before commercial designs of radiation receivers had been well developed. The thermocouple, in the zone above the checkerwork, is subject to considerable maintenance because of the high temperature level, and in the flues or below the checkerwork has the disadvantage of being too far away from the more critical regions of the regenerative system. Besides, it tends to measure some indefinite temperature between that of the gases around it and the average of the hot wall surfaces visible to it. These disadvantages are all eliminated by the use of a radiation receiver.

CONTROL SETTINGS

The necessary control points for this reversal control are set by consideration

* M. J. Bradley and J. W. Kinnear, Jr.: The Automatic Reversing of Open Hearth Furnaces by the Temperature Difference Method. *Iron and Steel Eng.* (October 1930).

(1) of the safe upper limit of operating temperature of the regenerator refractories and (2) of the optimum reversal time from a study of the furnace design. There are just three settings to be made: namely, maximum temperature, maximum time, and minimum time; once established these need never be changed. For example, the control points of one trial installation were set during the first few days of operation in 1938 and have not been changed since. Experience has shown that, at least on certain furnaces provided with, for example, the temperature-difference system of reversal, the control settings may have to be changed one or more times during each heat in order to get satisfactory reversal at somewhere near the optimum interval. Moreover, in a system of reversal based on time alone, the settings must be altered frequently in a futile attempt to bring about equality of temperature of the two regenerators.

In actual operation the furnace operator must be able to take over reversal of the furnace at will without producing a prolonged disturbance of the general temperature balance in the furnace system. For example, during charging, making additions to the bath, taking samples, etc., it is often thought desirable to cut out the automatic control and to reverse the furnace manually without regard to temperature balance. This is accomplished simply by superimposing a push-button control on the automatic feature and whenever necessary, by completely opening the automatic circuits to prevent control except at the will of the operator. When the need for manual control is over, the operator restores automatic control by closing the switch actuating the automatic circuits, whereupon the system, even in the most severe unbalance resulting from this sort of operation, is able to restore balance within a few reversal cycles.

APPARATUS AND OPERATING RESULTS

Figs. 3 and 4 show the main units and the schematic circuit diagram, respectively. Details of the units and of operating se-

ture, although in any given installation the water-cooling and/or the air supply shown here might not be required.

There are actually four different modes

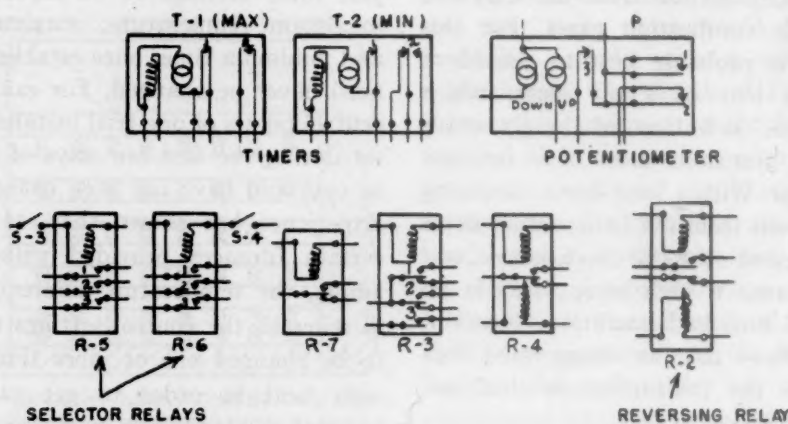


FIG. 3.—UNITS IN REVERSAL CONTROL CIRCUIT.

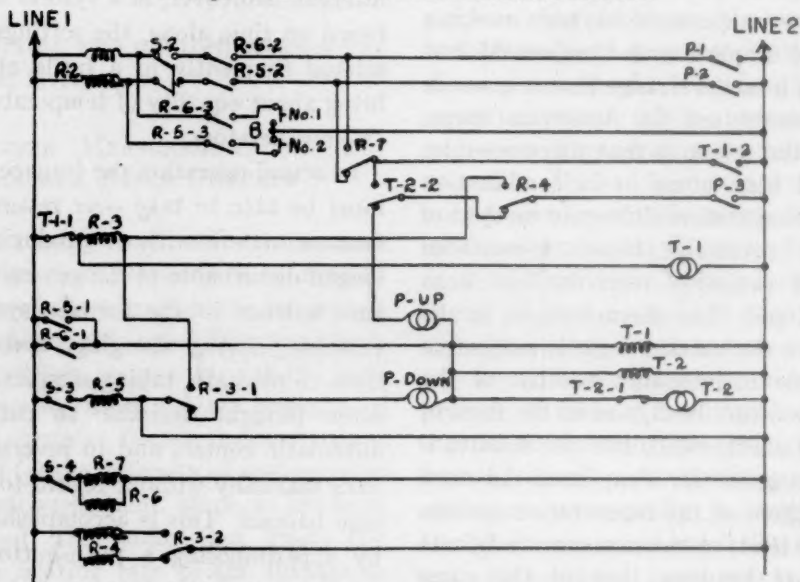


FIG. 4.—SCHEMATIC CIRCUIT DIAGRAM.

quences in this circuit are given in the Appendix. Fig. 5 is a front view of the control panel on an installation at a furnace fired with mixed liquid and gaseous fuel, and Fig. 6 shows the relay panel on this unit. Fig. 7 is a view of a pyrometer unit installed in an end-wall panel of a checker chamber; it illustrates a receiver properly set to record top checker-brick tempera-

of reversal by this circuit arrangement, the details of which are described in the Appendix:

1. Manual reversal by push button whenever desired by the furnace operator.
2. Automatic reversal by the floating temperature limit between minimum and maximum time intervals, this being the normal mode in operation.

3. Reversal at maximum time when checker temperature levels are falling.

4. Reversal at maximum temperature by the fixed limit in the controller.

The arrangements to effect 1 and 4 are conventional, as in all such automatic control equipment. Modes 2 and 3 are brought about by operation of the floating-temperature limit switch, the tripping point of which is moved up or down the temperature scale by a small reversible motor in the recorder-controller in such a manner that it always follows the peak temperature naturally attained in the hotter chamber by the surface of those hottest checker brick that are near the bridge wall, adjacent to the fantail and slag-pocket zones. Actually, only two or three extra relays and switches (in addition to the limit switches, reversing and selector switches, interlocks, etc., necessary for proper safeguarding on full automatic operation) are required to do this, and although the interactions of the various elements may appear complex, the operation is really quite simple and entirely automatic. Besides giving a continuous record of true refractory temperature in the most critical portion of the regenerative zones, this control equipment causes a minimum of interference with natural variations of temperature level, keeps the two ends of the furnace in balance and the reversal interval near its optimum value.

The various measuring and recording instruments, relays, timers, etc., employed in the installations have been mainly of common commercial types; it is important to use reliable, well-designed units, especially of the automatic reset time relays.

Experience on a typical installation of this reversal control on a commercial furnace showed a negligible amount of maintenance over a period of several years service. The equipment for measuring checker temperature, whether or not it is used in combination with automatic reversal, always requires some small

amount of regular inspection and maintenance, and this is likewise true of all automatic fuel valves, motors, etc. However, it was found that the extra timers



FIG. 5.—FRONT PANEL OF REVERSAL CONTROL UNIT FOR FURNACE WITH COMBINATION OF LIQUID AND GASEOUS FUELS.

and other relays, switches, etc., in this particular system added relatively little to the maintenance problem. The time period and maximum temperature settings, once properly adjusted, could be left alone indefinitely.

In general, the control was so nearly completely automatic that the furnace operator could perform his duties with no thought about furnace reversal (except as he might occasionally wish to employ

manual reversal for some special reason), with the consequent chief advantage that he could perform his other and more important tasks with greater efficiency.

CONCLUSION

The general desirability of automatic control of reversal of the open hearth is still a matter of dispute among steelmakers.

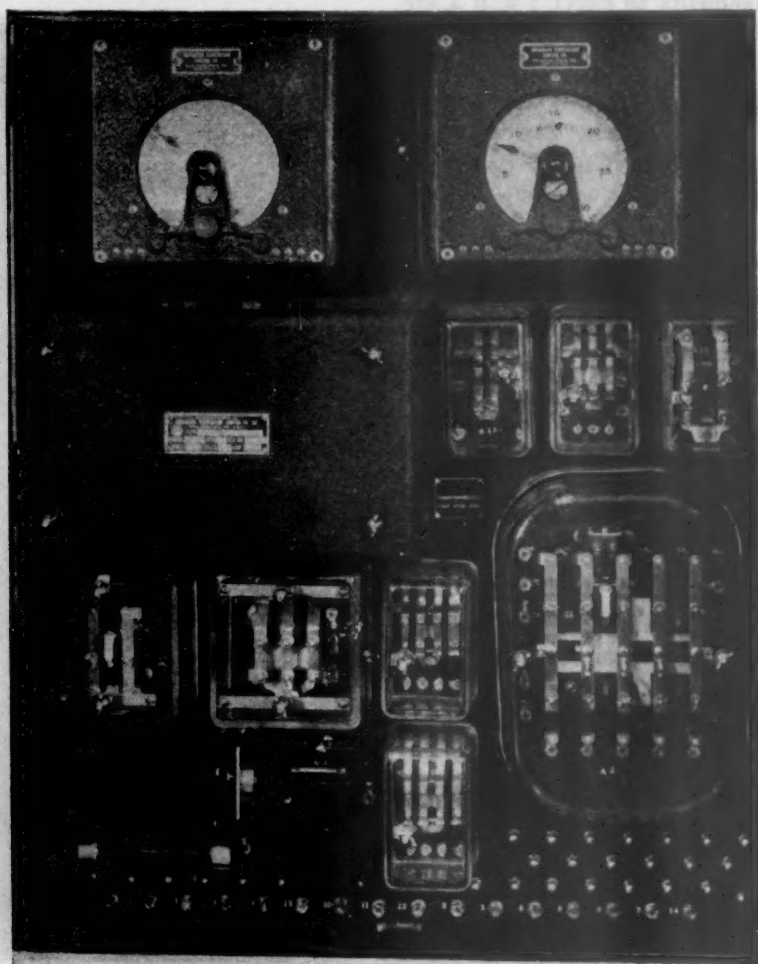


FIG. 6.—RELAY PANEL IN UNIT SHOWN IN FIG. 5.

Operating records indicate a small reduction in fuel consumption. The most important effect on operation, aside from the labor-sparing aspect, has been the evening up of the two ends of the furnace and the protection of end and checker zones from occasional excessive heating, so that a few extra heats usually were added to each furnace campaign. Savings from these sources alone indicate that the equipment cost was recovered in about a year.

This is partly because of the problems present in all automatic control methods in the open-hearth shop. Conditions of dirt, vibration and accidental shock are so severe that all controls must be rugged, reliable, and as free as possible from maintenance difficulties. The furnace process probably never can proceed with the clocklike precision and regularity of most industrial processes. All developments toward more instrumentation involve, moreover, the presence in the plant of a

few men skilled in repair and maintenance; against this, however, there is usually the compensating factor of a reduction in amount of routine labor and of attention

cated scheme. If the problem is conceived to be that of simply relieving the first helper of this mechanical operation, this method would seem the best solution, if

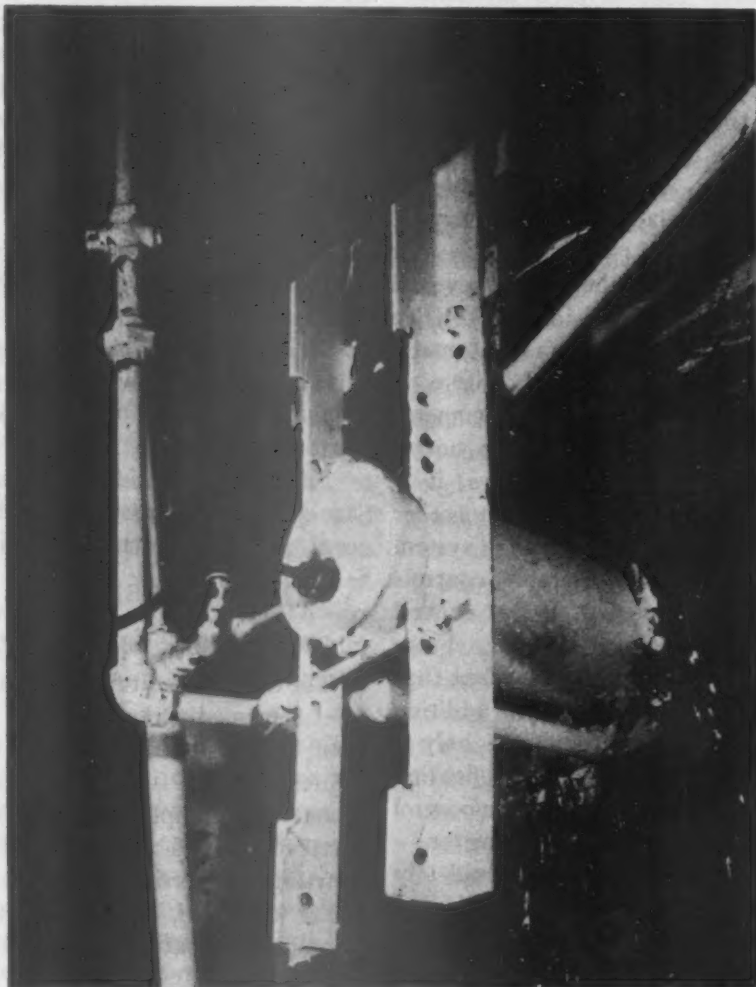


FIG. 7.—RADIATION-SENSITIVE MEASURING UNIT AS INSTALLED IN REGENERATOR END-WALL PANEL.

to details of operating control. This reduction is perhaps especially difficult in the open-hearth shop, but elimination of the simple but tiresome and repetitious job of reversing the furnace should help appreciably in this direction, for the first helper is then freer to give his attention to the control of actual steelmaking.

The simple mechanical operation of reversal is accomplished by a time relay unit about as well as by any more compli-

we take the view advanced earlier in this paper; i.e., that reversal should be based fundamentally on certain time intervals. However, the first helper also would like to know the temperature levels in the top-checker and end zones of his furnace, which are not accessible for routine direct observation, so that he can keep the two ends in balance, avoid excessive temporary peak temperatures, and recognize when conditions such as too fast driving, delayed

combustion or excessive air leakage, are producing too high an average level of checker temperature. The best solution to this problem appears to be to use radiation units sighted on the surfaces of the hottest checker brick and to record these temperatures on a two-point or four-point recording instrument. With such a record, the first helper can then adjust his reversal intervals to balance up the two ends and avoid excessive peaks, and is better able to recognize other maladjustments in furnace operation.

The development of the present reversal control was based on the idea that if we assume the desirability of (1) automatic reversal at intervals limited within a certain optimum range and (2) a temperature record of some region in the hotter portions of the regenerative zones, it is then only logical to try to bring together these basic elements to form a system accomplishing all the desirable controls related to furnace reversal, so that control would be completely automatic. From the foregoing description it is evident that the actual *extra* units needed in addition to these basic elements comprise only a few relays and switches and the floating limit and maximum temperature-control contacts in the recording potentiometer.

The desirable features of a completely automatic reversal control appear to us to be as follows:

1. Period between successive reversals should always be within a certain optimum range, except when a shorter period is needed for some secondary purpose or to avoid a peak of excessive temperature.

2. Measurement of brick temperature at some point in the hotter regenerative zones of fantails or top checker brick by radiation units, so that maintenance difficulties with thermocouples at such temperature levels are avoided and more specific temperature values on refractory surfaces may be obtained, with provision for shortening of reversal period when a

desired maximum of this temperature is approached.

3. Continuous balancing between ends at all times when on automatic control; provision for manual reversal at any time, with rapid readjustment to balance by automatic reversal after the unbalance produced by exceptional conditions or by manual reversals during temporary periods.

4. A continuous record of the measured temperatures in top-checker or fantail zones to give the operator a better basis for control of such factors as rate of driving and air leakage above floor level.

5. Absence of need for periodic or occasional change in any temperature or time setting in the control units, thus making the control more nearly completely automatic.

From our experience, these conditions are all met successfully by the reversal control system described in this paper.

APPENDIX

Reversal Control Circuit

The essential units in the control circuit* are shown diagrammatically in Fig. 3, and the schematic diagram of Fig. 4 represents the fundamental elements in about the simplest form on the basis that reversal is accomplished merely by starting a reversing motor, in one or the other direction, by closing one of two contacts alternately in the reversing relay *R-2*.

T-1 and *T-2* are automatic reset timers, each having a synchronous motor, a clutch coil for engaging the contact mechanism with the motor, a contact (*T-1-1*, *T-2-1*) for stopping the motor when the set interval has elapsed and main contacts (*T-1-2*, *T-2-2*), which operate when the time period has elapsed. When the relay has tripped at the end of its period it remains in that position until the clutch-coil circuit is broken, when a

*Larsen and Shenk: U. S. Patent No. 2139861 (July 14, 1938).

spring mechanism resets it immediately to its starting position.

P represents the potentiometer recorder-controller that records (in this case) the energy received from two radiation units sighted on the hottest checker brick near the bridge wall in a chamber at each end of the furnace. (The usual range of temperature is 1200° to 2600°F.) In the diagrams, *P-1* and *P-2* are maximum temperature contacts, which remain set to close at a manually adjusted position on the temperature scale; *P-3* is a "floating" contact, which is moved up or down along the temperature scale by the motors labeled "up" and "down" (these represent a small reversible synchronous motor) as described below.

Relays *R-2* and *R-4* are latched relays, which pick up on a momentary closing of the (upper) pickup coil and remain picked up by a latch unless dropped by the latch coil, being energized with the pickup coil circuit broken. *R-3*, *R-5* and *R-6* are ordinary magnetic relays, each of which is picked up only as long as its coil is energized. Switches *S-3* and *S-4* are limit switches on the furnace damper mechanism. They are adjusted so that, for example, *S-3* is closed only when the dampers are set for fuel burning at No. 1 end of the furnace, *S-4* closed only when on No. 2 end, both switches being open during reversal of the dampers. These switches actuate the coils of the selector relays *R-5* and *R-6*, which function as described below.

The various modes of reversal are all controlled by limit switches *S-3* and *S-4*, which determine whether selector relay coil *R-5* or *R-6* is energized. Thus, reversal can occur only in the proper direction at any time, and no reversal contact can be completed while the reversing dampers are in motion or when stalled in any intermediate position. In Fig. 4 it is shown that push buttons *B-1* and *B-2* will actuate *R-2* coils to up or down positions, to reverse the furnace in the proper direction, only as

determined by selector relay contacts *R-6-3* or *R-5-3*. If the operator pushes the wrong button, nothing happens. This manual reversal by push button can occur whenever desired, with hand switch *S-2* open or closed, but automatic reversal through selector contacts *R-6-2* and *R-5-2* will occur only with *S-2* closed.

P-1 or *P-2* contacts in the recorder will reverse the furnace independently of the time relays at any time, but this will occur only when excessively high checker temperatures are reached, the setting for *P-1* and *P-2* being usually around 2300° or higher on the recorder scale.

The most frequent condition is that of a gradually rising level of checker temperature. If the two ends are in balance, the heating checker usually will reach a higher level than that reached by the other checker on the previous half cycle. Suppose now that the minimum time interval on *T-2* is set at 12 min. and the maximum on *T-1* at 18 min. If (as usually happens under the condition described) the floating temperature-limit switch *P-3* closes before the 12-min. period has elapsed, *T-2-2* contact is down as shown and a circuit is made through *P-3*, *R-4*, *T-2-2* and the "up" motor, through *R-5-1* or *R-6-1*. The "up" motor runs and raises the operating position of *P-3* until it is just above the checker temperature; *P-3* then opens and the motor stops. Thus the *P-3* floating limit will normally be raised one or more steps as the temperature of the checker brick rises, until the minimum timer *T-2* trips at the end of 12 min. *T-2-2* is now picked up, so the next time *P-3* closes, the reversal contact is made through *R-5-2* or *R-6-2*. Reversal thus will occur usually shortly after the end of the minimum time period if the checker temperature levels are rising, or at some time between the 12 and 18-min. periods at the temperature-operating point of *P-3*, if these levels remain fairly constant; always tending to balance the two ends, however, since the *P-3* level will be reached

more slowly by the colder checker, which is then given more heating effect in one half cycle and less cooling effect in the other.

The only other condition of reversal is when the maximum time elapses before *P-3* closes, usually when one or both checker temperature levels has fallen off for some reason. In this case, contact *T-1-2* closes and reverses the furnace through *R-5-2* or *R-6-2*, etc. Another problem is present in this case, however. The reason for lapse of the maximum time period before reversal is that the "up" motor has pushed the *P-3* contact operating point up so high on the temperature scale that it is not operative, so we have the problem of getting it down again whenever *T-1* times out. *T-1* motor is directly across the line through its own hold-in contact *T-1-1*, so that it runs continuously except when *T-1* trips on an occasional maximum time reversal. Otherwise the only thing occurring to *T-1* on reversal is the breaking of its clutch-coil circuit by the limit switch and selector relays, allowing it to reset on any reversal, its motor running continuously. When the maximum time elapses without a reversal contact by *P-3* (or *P-1* or *P-2*) however, the motor hold-in contact *T-1-1* opens; besides stopping the motor, this also breaks the *R-3* pickup-coil circuit, which drops *R-3-1* and *R-3-2* into the positions shown in the diagram. The "down" motor is now in circuit through *R-5-1* or *R-6-1* (except during the period of a few seconds while the dampers are moving) and begins to move the operating point of *P-3* down the recorder scale. *R-3-2*, being dropped also, breaks *R-4* latch coil and makes *R-4* pickup coil, so that *R-4* contact picks up and when the *P-3* operating point has been moved down to one of the existing checker temperature levels and closes, *R-3* coil will be in circuit again (since *T-1* reset to close *T-1-1* as soon as reversal began) and with the picking up of *R-3-1* the "down" motor

will stop. At the same time, *R-3-2*, picking up, will restore *R-4* to the down position and the "up" motor will operate until *P-3* breaks again. The circuit is now restored to the same condition as before the tripping of maximum timer *T-1* except that *P-3* is now restored to its normal position just above the temperature level of the hotter checker chamber.

Auxiliary Control Elements

The circuit shown in Figs. 3 and 4 includes the essential elements required but in most actual cases certain extra operations during reversal may be needed, usually involving quite simple extensions of the circuit. Extra contacts may be included in the selector and reversing relays. In burning oil or tar fuel with steam atomization, an extra contact may be included in each limit switch. When reversal begins, this contact may close as one switch opens, turning steam on the opposite burner. With both switches open during damper movement, steam flows in both ends, ensuring steam flow on one before the fuel comes on, and purging of the other burner for a few seconds after its fuel is turned off. If more than one fuel is used, a cam timer may be employed to turn on the fuels in proper order and to delay the fuel on the oncoming end to allow complete reversal of gas flow and preheated air, so that proper combustion will be established at the burner as soon as the fuel comes on. If automatic draft and/or roof-temperature controls are employed, it may be desired to include an extra time-delay relay to cut these controls for a number of seconds during the reversal operation, while the normal furnace conditions are being disturbed. These auxiliary elements are used normally to ensure the completely automatic functioning of the system, so that a minimum of attention from the operator is required.

A Rapid Laboratory Method for Estimating the Basicity of Open-hearth Slags

BY W. O. PHILBROOK,* A. H. JOLLY, JR.,* MEMBERS A.I.M.E., AND T. R. HENRY*

(Cleveland Meeting, October 1944)

IN the course of a study of slag-control methods, the authors devised a laboratory technique by which the basicity of basic open-hearth furnace slags could be estimated with sufficient accuracy to make the method of possible interest for slag-control purposes. The process consisted of measuring the slight basicity of an extract of the powdered slag in water. The procedure was presented, for the benefit of those who might care to experiment with it, in a paper submitted in the 1944 McKune Award Contest and presented at the 1944 Open-hearth Conference in Pittsburgh.¹ Interest expressed at that meeting and favorable operating experience with the method at a neighboring plant, as described in a related paper by Michael Tenenbaum and C. C. Brown,² have encouraged us to present further details of the development, technique, and pitfalls of the method and some additional data not included in our first report.

At the outset it must be admitted that this method of estimation of slag basicity is not perfect; neither is any other that we know of. It is subject to somewhat greater errors than would be desirable, but compares favorably with other techniques in this respect. It has the disadvantage that it places the final determination of slag basicity in the hands of a laboratory technician rather than the furnace oper-

ator, although it can be operated in a control laboratory adjacent to the furnaces. It requires close attention to certain details, as do most laboratory procedures. On the favorable side, it eliminates the "human factor" of personal judgment inherent in estimation from pancakes or powdered samples. The procedure can be placed in practice much more rapidly and presents much less of a training problem than visual methods of estimation.

The principle and operation of the method are so simple that it would not be surprising if others have experimented with the same or similar procedures, but we are not aware of any prior publication of details. Our own shop has been operating fairly successfully for several years with the aid of slag pancakes. Since the past year or two have not been favorable for the expenditure of time and energy where the need was not urgent, we have not introduced the new practice for actual slag control and hence do not have extensive operating data. In presenting this method, therefore, we make no claims as to theoretical justification nor guarantees as to practical applicability, but offer it as an empirical observation. We believe it has sufficient merit to warrant its investigation by those just instituting a slag-control program or in search of supplementary methods for judging slag basicity

Manuscript received at the office of the Institute Oct. 20, 1944. Issued as T.P. 1862 in METALS TECHNOLOGY, August 1945.

* Wisconsin Steel Works, International Harvester Co., Chicago, Illinois.

¹ References are at the end of the paper.

PRINCIPLE OF THE METHOD

It is well known that when burnt lime or slaked lime is shaken up with water it

dissolves to some extent and produces an alkaline reaction. Even substances that ordinarily are considered insoluble dissolve to some slight degree in water and may

which applies within limitations over an important range of basic open-hearth slags and which may be exact enough to be useful for control purposes.

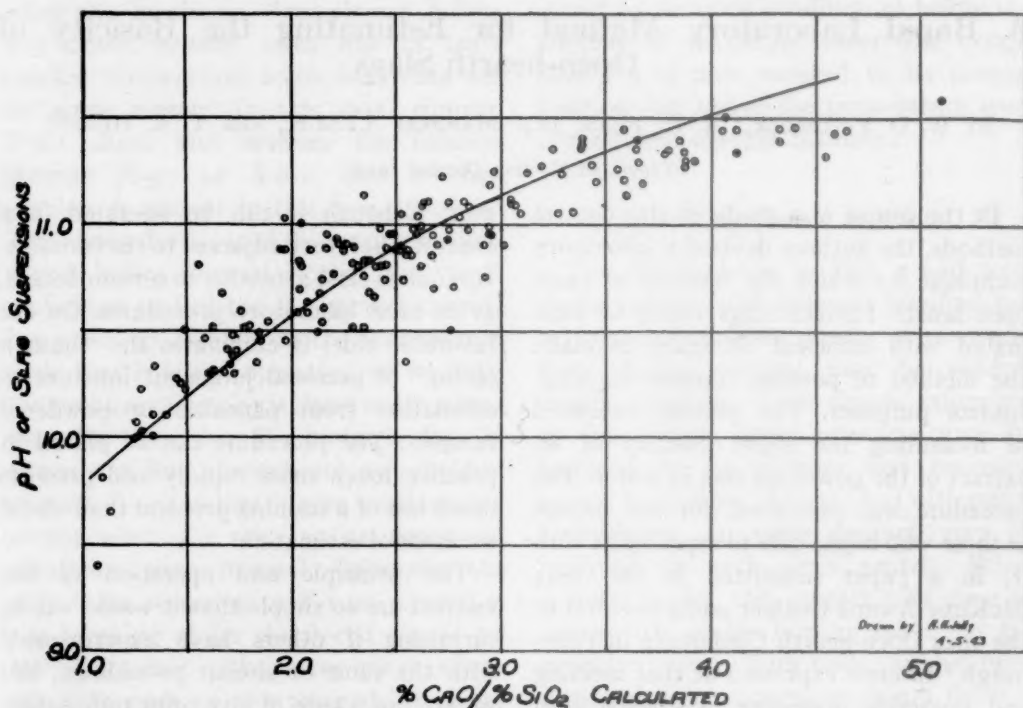


FIG. 1.—pH MEASUREMENTS COMPARED WITH LIME-SILICA RATIO OF 172 SLAGS.

produce either mild acidity or mild alkalinity. If the reaction is fairly strong, as with lime water, the alkalinity may be measured by titrating with a standard acid. In other cases more delicate means of measurement are necessary. It was found by experiment that when powdered slags were shaken up with water, they produced different degrees of alkalinity, depending upon the slag basicity, which could be measured by a glass-electrode pH meter.

After a number of experimental details had been worked out and a standard procedure had been decided upon, it was found that the pH value of the slag suspensions increased quite definitely as the lime-silica ratio of the slag increased. There is some chemical "sense" to this, but it would be hard to give an ironclad theoretical justification for it. We prefer to present it merely as an experimentally observed relationship,

Using the standard technique, which will be given later, pH measurements were made of suspensions of 172 slags. These are compared in Fig. 1 with the ratio of $\frac{\% \text{CaO}}{\% \text{SiO}_2}$ calculated from the chemical analysis of the slags. The line shown is a line of regression calculated as explained later in connection with Fig. 3. A very definite relationship is indicated, but there is a fairly broad scatter band. Attempts were made to reduce or explain this scatter. Taking MgO into consideration as a base by plotting pH against $\frac{\% \text{CaO} + \% \text{MgO}}{\% \text{SiO}_2}$ did not improve the relationship. The inclusion of P_2O_5 in the ratio by comparing pH with

$$\frac{\% \text{CaO}}{\% \text{SiO}_2 + \% \text{P}_2\text{O}_5}$$

seemed to result in a slight improvement, but the ratio $\frac{\% \text{CaO} + \% \text{MgO}}{\% \text{SiO}_2 + \% \text{P}_2\text{O}_5}$ gave as much or more scatter than the simple $\frac{\text{CaO}}{\text{SiO}_2}$ ratio. The slags were grouped into various ranges of iron oxide content, and pH plotted against $\frac{\text{CaO}}{\text{SiO}_2}$ for each range of iron oxide content. The average lines crossed at random and did not show any indication that iron oxide content influenced the relationship between pH and lime-silica ratio to any significant extent. It has not been possible to apply statistical or mathematical methods of analysis to these data to explain the scatter because of the pressure of other duties, but the purely qualitative indications obtained by graphing discourage any great hope for marked success along such lines. Later work has indicated that certain refinements of technique are advisable, such as close control of suspension temperature. More rigid standardization of technique might reduce the scatter to a small degree.

It was realized that many slags with some undissolved constituents were included among the samples, and that the chemical analyses were therefore not truly representative of the slags in some cases. A selection was accordingly made of about 90 slags, which were taken about an hour or more after melt, and at least an hour after additions of burnt lime or ore. A reasonable approach to a homogeneous slag should be expected for these selected samples. The pH of the slag suspensions is plotted against the calculated lime-silica ratio of these slags in Fig. 2. In this chart, the line has been fitted by eye. Although the scatter is still considerable, it may be seen from comparison with Fig. 1 that some of the worst points have been eliminated. The same 90 slags were plotted in Fig. 4; this time the V value assigned the pancake on the floor was

plotted against the V_c , or V value obtained from the analyzed samples. This plot was included for comparison purposes and will be discussed later.

It was noted that the relationship between pH and calculated V ratios followed a curved line. It looked as though a plot of pH against the logarithm of the V ratio might give a straighter line. This proved to be true, as is shown in Fig. 3, which includes all the data. In this case, too, there is a little chemical reason, involved in the definition of pH, why the semilog plot might be a straight line, but it is not very rigorous and it is best to remain within the limits of experimental observation. The line seems to be fairly straight on the semilog plot between 10.2 and 11.3 pH (basicity from 1.5 to 3.5) but curves away both above and below this range. The straight line shown in Fig. 3 is the line of regression of $\log \frac{\% \text{CaO}}{\% \text{SiO}_2}$ on pH (since it is desired to predict basicity from pH) calculated by statistical methods from the data. It is obvious, however, that there is some curvature in the points at either end, and closer inspection leads to the suspicion that the data do not conform to "chance distribution," so the line of regression thus calculated may not be the best one for prediction within a more limited range.

From an inspection of the charts, particularly Fig. 2, it appears that the pH of suspensions of powdered slags might be useful for estimating slag basicity over the V range from 1.5 to 3.5 or 4.0. Above 4.0 basicity, the change of pH with increasing basicity is too small to be useful. Most of the time, the estimate should be accurate within 0.3 V ratio, with occasional errors as great as 0.5 V units.

Since it has been shown that the pH of a slag suspension might be useful to give a rough estimation of the basicity of the slag, the question naturally arises as to whether this technique is more or less

accurate than the slag-pancake method. As one method of comparison, the basicities estimated from slag pancakes are plotted against the lime-silica ratios calcu-

in which sampling was started too late in the heat, the full background was not available, and the observer was thrown "off stride." This is not representative of

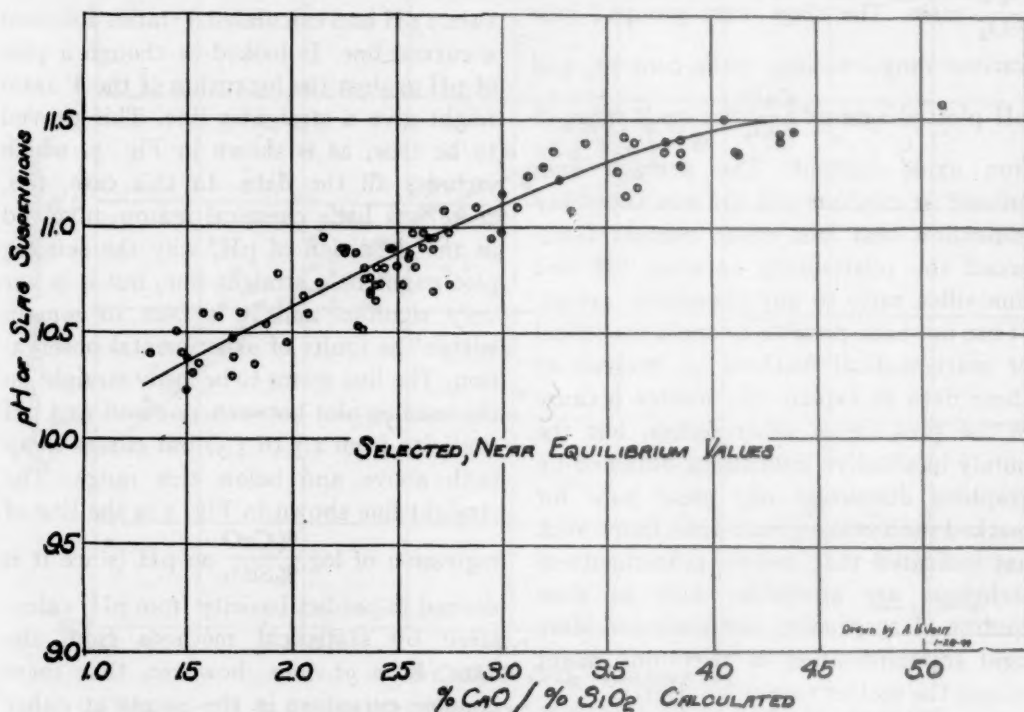


FIG. 2.—pH OF SLAG SUSPENSIONS PLOTTED AGAINST CALCULATED LIME-SILICA RATIO OF 90 SLAGS.

lated from the analyses in Fig. 4 for the same 90 slags used in Fig. 2, which were assumed to be fairly well digested. When Fig. 4 is compared with Fig. 2, it may be seen that the scatter is much worse in Fig. 4, particularly at the higher basicities above 3.0. From this it would appear that the pH method is more reliable than the slag-pancake estimation. Certain qualifications should be pointed out, however. The slag-pancake estimations were made during a transition period shortly after flush practice had been introduced into the shop. Some of the heats were made with flush practice and some were scrap-hot metal practice with no ore charged. Such conditions are not the most favorable for pancake estimation. In addition, several of the high-basicity points are from a heat

usual performance in the "reading" of slag pancakes, but the points are included to illustrate that the pancake method may be subject to serious errors occasionally in the high-basicity range. The estimations were made by one metallurgist; other observers might be either more or less skilled in pancake reading.

We feel that a check-up of the pancake readings is beneficial from time to time in order to permit the persons making the floor observations to check their efforts. To the man who is able to hit his slags most of the time within 0.2 to 0.4 V, a pat on the back or a "well done" is in order. Further, a periodic check will permit the melters to gain confidence in the information given them and give the new personnel a chance to see that the pancakes are not

something that was pulled out of thin air, but rather that they are a fairly accurate method of estimating slag conditions.

Our general impression is that the pan-

experimental technique that influenced the results and also showed that a standardized procedure must be followed to obtain reproducible pH readings from the

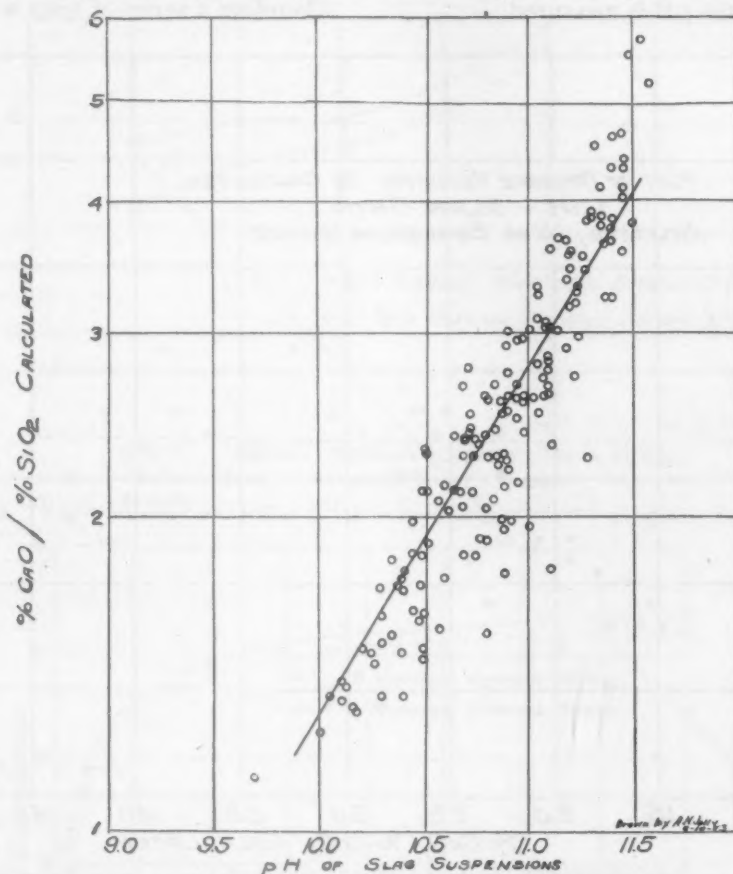


FIG. 3.—RELATIONSHIP BETWEEN pH OF SLAG SUSPENSIONS AND LOGARITHM OF CALCULATED LIME-SILICA RATIO.

cake practice is equal or superior to the pH technique at V ratios below 1.5; the two are of approximately equal accuracy at basicities between 1.5 and 2.5; and the pH method is definitely superior for slags of lime-silica ratios from 2.5 to 4.0. Neither method is of much utility above V ratios of 4.0, but there is seldom any need for carrying greater basicity than this in conventional basic open-hearth practice.

TECHNIQUE AND PROCEDURE FOR THE pH METHOD

Rather extensive investigation showed that there were a number of variables of

same slag. In developing a method of chemical analysis, it is possible to make up known samples and to settle upon a procedure that gives the right results. In a purely arbitrary and empirical method such as this one, there is no "right" result. It is, however, essential to establish a routine that is best suited to give consistent repetitive results, and then to ascertain whether the values so obtained will furnish a useful correlation with the property it is intended to estimate, in this case slag basicity. The following are the most important factors that were found to influence the pH measurements:

1. Particle size of the slag powder used.
2. Weight of sample used per given volume of water.
3. Time of shaking and standing allowed before the pH is measured.

not available, nor would the persons charged with the preparation of such samples devote the care needed for proper quartering and sizing.

Therefore a series of tests was made, in

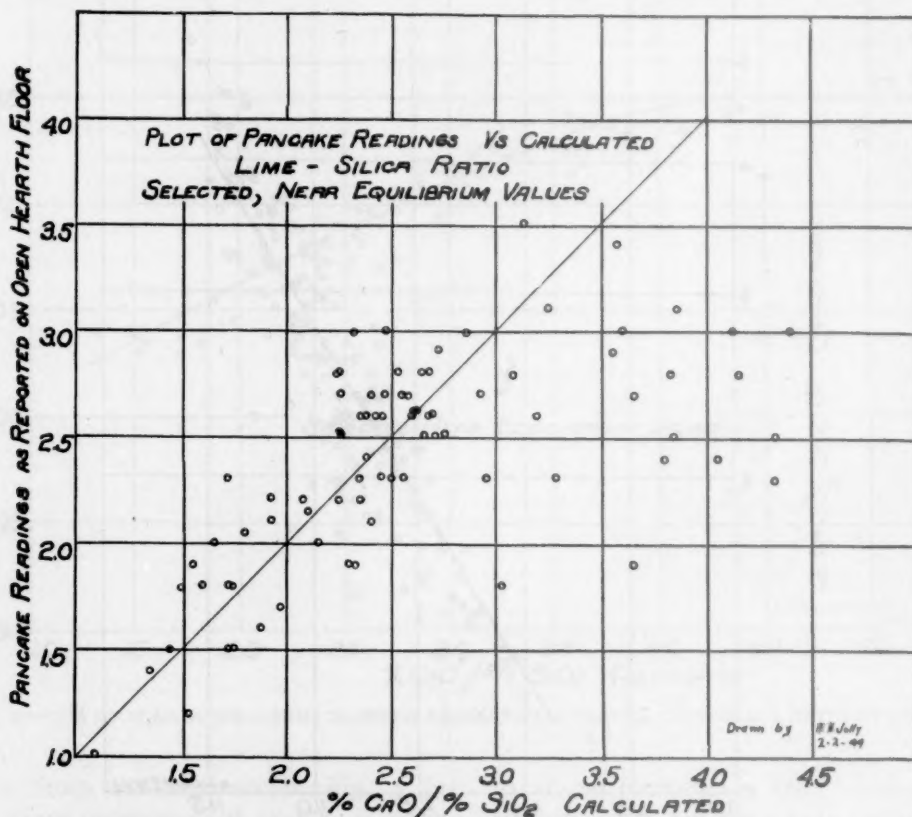


FIG. 4.—PLOT OF PANCAKE READINGS VERSUS CALCULATED SELECTED LIME-SILICA RATIOS (NEAR EQUILIBRIUM VALUES).

4. Exclusion of free access of atmospheric carbon dioxide to the suspension.
5. Temperature of the extract at the time the pH is measured.

Particle Size of Slag Powder

One of the first variables investigated was the screen size of the slag powder, because it was obvious that differences in particle size might influence the rate of solution or hydrolysis of the slag constituents. It was recognized that in any routine procedure the time required to crush an entire slag pancake so that all of it would pass a certain size screen was

which one half of a pancake was carefully prepared by crushing until all passed 40 mesh, quartering, removing metallic iron magnetically, and progressively screening. The weight of sample retained on each sieve was noted, and a pH measurement was made on an extract from each screen portion. The results of one such test are shown in Fig. 5. By taking the weighted average of all screen fractions, an average pH, of somewhat dubious significance perhaps, was calculated for the entire pancake. In order to determine what discrepancy would arise from somewhat more slipshod handling, a small chunk of slag taken

from the other half of the pancake at random, was pounded up and screened without quartering, pieces over 40 mesh being discarded, and pH measurements

what of a plateau at about 100 mesh (Fig. 5). It is concluded that in an unscreened sample the pH reading would be predominantly influenced by the relative

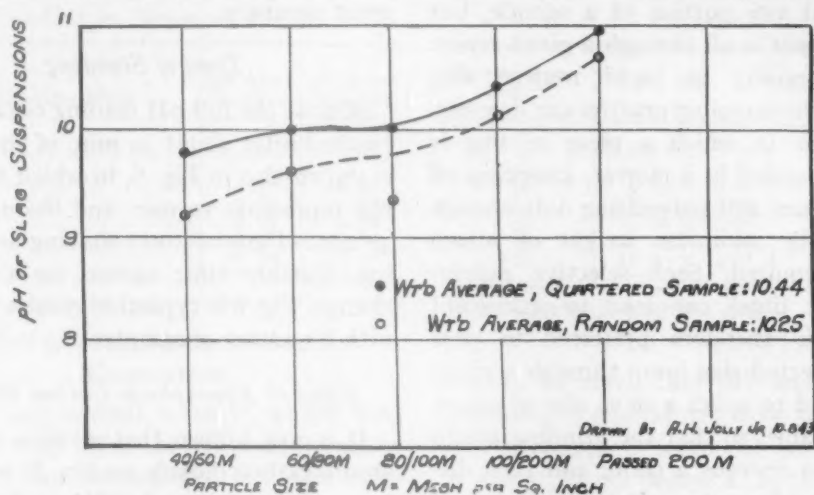


FIG. 5.—RELATIONSHIP BETWEEN pH AND PARTICLE SIZE OF POWDERED SLAGS.

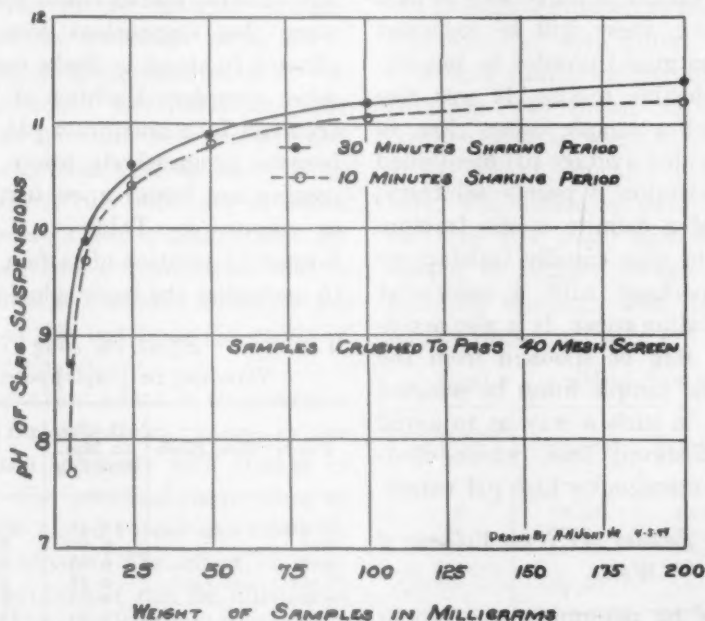


FIG. 6.—WEIGHT OF SLAG POWDER PER UNIT VOLUME OF WATER.

were taken on the various screen fractions. As indicated in Fig. 5, a difference from the more carefully prepared sample was found of about 0.3 pH unit, roughly equivalent to 0.35 V.

The pH of the extract increases as the powder particle size decreases, with some-

abundance of very fine powder, and that the greatest contribution to the pH value is from the minus 200-mesh fraction. It is indicated from this chart that most consistent results might be obtained by sieving on 100 and 200-mesh screens, discarding both the plus 100 and the minus 200-mesh

sizes and using only the intermediate fraction.

As a general rule, however, it is poor practice and constitutes a bad precedent to discard any portion of a sample, but rather to put it all through a given screen size. Especially in rapid routine slag analysis, the sampling practice can degenerate to one in which a piece of slag is hastily pounded in a mortar, knocking off a few corners and pulverizing only enough to give the minimum weight of screen sample required. Such selective pulverization at times can lead to significant errors. We therefore preferred to pass all the selected slag lump through a given screen, and to select a sieve size as coarse as practicable, so that the grinding would not be too onerous a chore and thus discourage good practice. It was determined that if all the sample is pulverized to pass a 40-mesh sieve, there will be sufficient fine (minus 200 mesh) powder in 200 mg. to give reproducible results. It was also found that such a sample comes close to giving the weighted average pH mentioned above. This selection is purely arbitrary, and the use of a definite screen fraction would no doubt give equally satisfactory results, but perhaps with a somewhat different correlation curve. It is also necessary that the slag be spooned from the furnace and the sample lump be selected from the cake in such a way as to avoid lumps of undissolved lime, which obviously will give erroneously high pH values.

Weight of Slag Powder per Unit Volume of Water

Experiments to determine the proper proportions of powder and water showed that the pH values increased as the weight of minus 40-mesh powder suspended in 100 ml. of water increased from 5 mg. up to 200 mg. Beyond 200 mg. per 100 ml. there was no further appreciable increase in pH, as shown in Fig. 6. This is very convenient, as it is necessary only to have

a minimum of 200 mg. of slag per 100 ml. of water; a moderate excess of slag does no harm. It is therefore not necessary to weigh or measure the slag and water with great accuracy.

Time of Standing

Almost the full pH reading obtainable is reached after about 10 min. of shaking, as is shown also in Fig. 6, in which the lower line represents 10 min. and the upper line 30 min. of intermittent shaking and standing. Further time caused no significant change. Fig. 6 is typical of results obtained with a number of samples.

Effect of Atmospheric Carbon Dioxide

It is well known that alkaline solutions absorb carbon dioxide readily. It was therefore not surprising when it was found that reproducible results could not be obtained when slag suspensions were shaken and allowed to stand in flasks open to the air. After complete leaching of the slag had occurred to a maximum pH, the readings became progressively lower (solution becoming less basic) upon further standing, as shown in Table I. Carbonic acid formed by solution of carbon dioxide tends to neutralize the basic solution.

TABLE I.—*Effect on Slag Suspensions of Standing in Unstoppered Flasks*

Powder Size, Mesh	pH After 10 Min. Standing	pH After 2 Hr. Standing	pH After 3 Hr. Standing
Unsize.....	10.48	10.31	10.08
+60.....	9.20	8.70	9.04
+80.....	9.66	9.35	9.18
+100.....	9.38	9.28	9.20
+200.....	10.26	9.99	9.88
-200.....	10.70	10.32	10.30

Fortunately, it was found that the simple expedient of keeping the flasks tightly stoppered during the 10-min. extraction period was sufficient to give reproducible results. Ordinary distilled water is satisfactory, it need not be freshly boiled nor specially purified; neither is it

necessary to purge the flasks initially nor to take special precautions during the brief period of making the pH measurement.

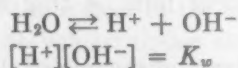
TABLE 2.—*Effect on Slag Suspensions of Standing in Stopped Flasks*

Powder Size, Mesh	pH After Standing 10 Min.	pH After Standing 25 Min.
Unsize.....	10.50	10.52
+60.....	9.60	9.58
+80.....	9.91	9.90
+100.....	9.78	9.80
+200.....	10.30	10.31
-200.....	10.74	10.72

Effect of Temperature on the pH Measurement

There are several ways in which temperature may influence pH measurements, and they can be classified into two categories. The first of these has to do with factors involved in the laws of electrochemistry and the technique of measurement. The electrical characteristics of the glass and reference electrodes and the proportionality constant between pH and e.m.f. of the electrode system both change with temperature. It is necessary to follow the instructions of the manufacturer for making temperature compensation and to calibrate against a standard buffer at the temperature of the test to avoid errors in the pH measurement.

A more important effect of temperature variations arises from the change in the true pH of the solutions with change in temperature. The practical importance of this factor was called to our attention by Mr. M. Tenenbaum. The effect of temperature on actual pH can be illustrated strikingly by the data for the dissociation of pure water:



Selected values for the dissociation constant for water at various temperatures, taken from a tabulation by Millard³ of results obtained by several investigators, are

shown in Table 3, together with the calculated pH values.

TABLE 3.—*Selected Values for Dissociation Constant for Water and Calculated pH Values*

Temperature, Deg. C.	K_w	Calculated ^a pH
0	0.12×10^{-14}	7.46
10	0.31×10^{-14}	7.26
18	0.59×10^{-14}	7.11
25	1.04×10^{-14}	6.99
50	5.66×10^{-14}	6.62
75	(23×10^{-14})	(6.32)
100	58.2×10^{-14}	6.12

$$^a K_w = [\text{H}^+][\text{OH}^-]; [\text{H}^+] = \sqrt{K_w};$$

$$\text{pH} = \log 1/[\text{H}^+] = \log 1/\sqrt{K_w}.$$

It may be noted that pH decreases with increasing temperature; close to 25°C. the rate of change is 0.016 pH per degree C. or 0.009 pH per degree F. In the solutions of acids, bases, or salts, the rate of change of pH with temperature may be greater or less than that with water.

A very similar change in pH with temperature was found with several slag-powder extracts. Measurements were taken of the pH of solutions at room temperature. The solutions were then cooled to 70°, the pH read, and then they were heated to slightly elevated temperatures and pH readings were taken, with the results shown in Table 4.

TABLE 4.—*pH of Sample Solutions*

Temperature, Deg. F.	Sample A	Sample B	Sample C
70	10.81	10.60	11.00
81	10.61	10.41	10.80
86	10.61	10.41	10.79
100		10.31	10.60
102	10.40		

This change appears to be reversible in that the suspensions will return to the initial pH upon return to room temperature after heating or cooling.

It may thus be seen that an increase in temperature causes a decrease in the pH of the slag solutions of a magnitude similar to the pH change for water. Seasonal

swings in laboratory temperature would therefore shift the pH readings obtained for the same slag basicity and cause an apparent error, or else a shift of the corre-

probably be accounted for by variations in temperature and other experimental error. This makes it possible to check the pH of a slag for "post-mortem" purposes

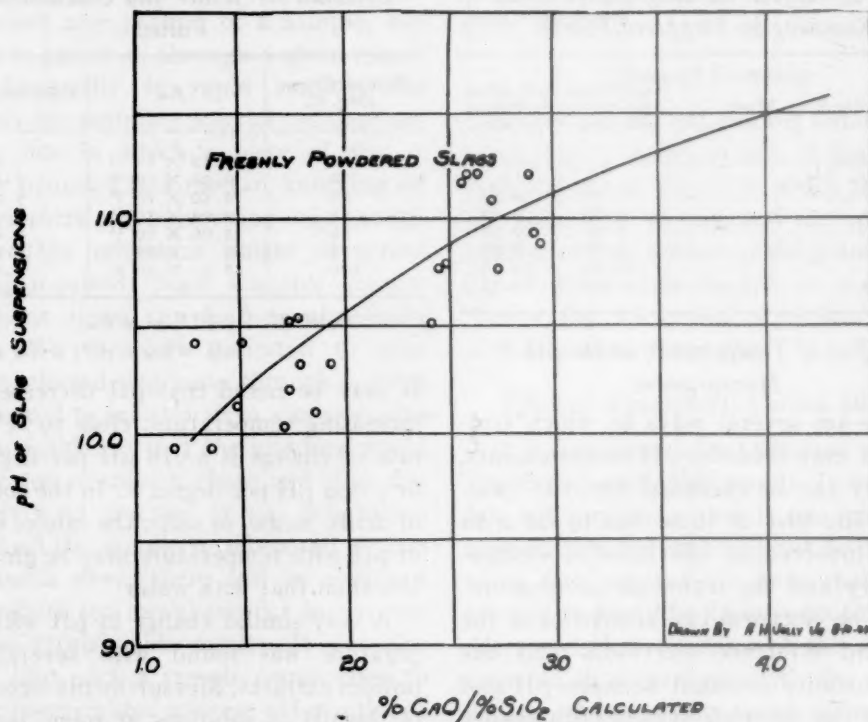


FIG. 7.—pH MEASUREMENTS COMPARED WITH LIME-SILICA RATIO OF SLAGS.

lation curve, of as much as 0.5 lime-silica ratio or more. It is therefore recommended that all pH measurements be made at temperatures held within a fairly close range, such as 75° to 80°F.*

Change of pH with Time

Investigation has failed to prove any consistent drift in the pH of slags pulverized at various intervals after pouring up to 10 days. The small deviations noted can

several days after the production of a heat. It is recommended, however, that correlation curves be based upon freshly crushed powder from recent slags to be consistent with operating practice and to avoid possible errors from air slaking of the slags.

Procedure for pH Measurement

The slag sample should be spooned from the furnace with the usual precautions to obtain a representative sample and to avoid lumps of undissolved constituents. It may be poured into a pancake mold or any convenient form; a thin section will cool faster.

Crush a lump of the cooled slag until all the sample passes a 40-mesh screen (60, 80, or 100 mesh may be used if preferred). Remove metallic iron and mix the powder well. Place about 100 ml. of water in a 250-ml. Erlenmeyer flask. Add about 200

* It appears to be a coincidence of nature that the error caused by failure to use the temperature compensator is in the opposite direction and of approximately the same magnitude as the true change in pH of the slag extracts with temperature, when the customary buffers of about pH 4 are used for calibration. Thus, if the pH meter is standardized against a pH 4 buffer at 25°C. and the temperature compensator is left at this temperature, approximately constant pH readings will be obtained for slags regardless of temperature because of compensatory errors. It is not recommended that this coincidence be depended upon for accurate results.

mg. of slag powder. Since the weight need not be highly precise, a small scoop of appropriate volume may be used to measure the powder. Stopper the flask well. Shake the flask intermittently and let stand for a period of 10 min. In the meantime, check the pH meter for the usual adjustments and temperature compensation. Adjust the temperature of the slag suspension to 75° to 80°F. Rinse the glass electrode and sample cup twice with the extract and then read the pH. It is immaterial whether or not slag particles are in suspension in the sample cup at the time of pH reading. Obtain the lime-silica ratio of the slag by reference to a correlation curve or table obtained from numerous pH measurements of analyzed samples, taken under standard conditions on slags under one day old.

It is recommended that the operator familiarize himself with the details of design, adjustments, and possible errors of the particular pH meter used. It is also suggested that a buffer solution of about pH 10 be used for standardization and that all temperatures be held close to 25°C. (77°F.). Inexpensive and convenient buffer tablets are now available for any pH range. It is also necessary to rinse the sample cup and glass electrode with the solution to be measured before making a reading, or the result will be influenced by water or solution remaining from a previous determination.

DISCUSSION AND CONCLUSIONS

Our first results, given in Figs. 1 to 3, were obtained before the effect of temperature variation was fully recognized. This factor may account for a small amount of the scatter in the original data. More recent values, under closer control, have been plotted in Fig. 7, superimposed upon the correlation curve of Fig. 1. The scatter is still considerable, but there is no significant indication of a general shift in the correlation curve over a period of about 18 months.

As previously indicated, we believe this method offers a possible means of estimating slag basicity with sufficient rapidity to be useful for open-hearth slag control. The estimations admittedly are not precise, and may be in error by as much as 0.5 V ratio at times. For shops having no technique for basicity control, this method may be instituted fairly rapidly and does not present any great training problem. The procedure can be handled by men or women of average intelligence without a high degree of technical training. For shops that now use slag pancakes, the method may be useful as an independent check on the pancake. The accuracy would appear to be roughly equivalent to that of slag pancakes for slags of lime-silica ratio less than 2.5, and should result in an improvement in accuracy for more basic slags up to 4.0 V, beyond which the technique is of little value. The entire procedure is purely empirical, and correlation curves must be prepared for the individual shop and practice in question.

ACKNOWLEDGMENT

We wish to express our indebtedness to Mr. A. A. Bartz, research chemist, for his assistance and suggestions in the slag analyses and pH determinations. The interest of Inland Steel Co. in our method and Mr. Tenenbaum's collaboration in keeping us informed of their results are greatly appreciated. Acknowledgment is made to the International Harvester Co. and the management of Wisconsin Steel Works for their interest in our work and permission to publish the results.

REFERENCES

1. W. O. Philbrook and A. H. Jolly, Jr.: A Survey of Slag-control Methods. *Open Hearth Proc.*, A.I.M.E. (1944) **27**, 233; *Blast Furnace and Steel Plant* (July and Aug. 1944) **32**, 793-797, 938-942.
2. M. Tenenbaum and C. C. Brown: Application of pH Slag-basicity Measurements to Basic Open-hearth Phosphorus Control. This volume, page 60.
3. E. B. Millard: *Physical Chemistry for Colleges*. Ed. 3, 279. New York, 1931. McGraw-Hill Book Co.
(See discussion on page 69.)

Application of pH Slag-basicity Measurements to Basic Open-hearth Phosphorus Control

BY MICHAEL TENENBAUM* AND C. C. BROWN,† JUNIOR MEMBERS A.I.M.E.

(Cleveland Meeting, October 1944)

IN recent years, the importance of slag control in basic open-hearth operations has been universally recognized. To effect such control during the working period of the heat, methods have been developed to measure or estimate slag oxidation and slag basicity. While satisfactory rapid chemical methods have been developed to determine slag oxidation, no completely adequate method of evaluating basicity has yet been provided. The most generally accepted control methods of measuring slag basicity are based on visual estimates. While considerable benefit may be derived from such estimates, the need for some measurable indication of slag basicity has become increasingly apparent.

In a recent paper, Philbrook and Jolly† suggested a promising technique for making the basicity determination. Their method consists of measuring the pH of a mixture of powdered open-hearth slag and distilled water. It was found that a relation could be established between the slag basicity and the alkalinity of the water mixture as measured by the hydrogen-ion concentration. The general procedure followed in making the measurements and the considerations involved in constructing the original curves are given in the paper of

Philbrook and Jolly and need not be repeated. It is the purpose of this paper to discuss some of the factors considered in applying the pH measurements to actual slag control and to present some of the results of its application.

FACTORS INVOLVED IN MEASURING pH OF WATER-SLAG MIXTURES

To facilitate the application of the pH control system, it was desirable that no alteration be made in the routine methods of sampling and crushing the furnace slag. Some of the factors considered before establishing a curve to relate slag basicity with the pH reading are reviewed individually in the following paragraphs.

EFFECT OF COOLING RATE

Under actual operating conditions there can be considerable variation in the temperature of the piece of slag crushed for the pH determination. To determine whether variations in crushing temperature or in cooling rate would affect the pH reading, a series of four samples was prepared from each of two separate slags. These samples represented conditions far more extreme than would actually be encountered. To obtain these samples, a thick pancake of slag was poured. One piece of this pancake was crushed immediately after it had solidified. Another piece was water-quenched and then crushed. A third piece was allowed to air-cool to room temperature before crushing. The fourth sample was prepared from a chilled slag. This sample was poured onto a heavy inclined steel plate at the

Manuscript received at the office of the Institute Nov. 2, 1944. Issued as T.P. 1863 in METALS TECHNOLOGY, August 1945.

* Metallurgist, Inland Steel Co., East Chicago, Indiana.

† Metallurgist, Inland Steel Co., East Chicago.

‡ W. O. Philbrook and A. H. Jolly, Jr.: A Survey of Slag-control Methods. *Open Hearth Proc.*, A.I.M.E. (1944) 27, 233; *Blast Furnace and Steel Plant* (July and Aug. 1944) 793-797, 938-942. See also this volume, page 49.

same time as the pancake. The pH readings obtained are shown in Table 1.

Despite the extreme variation of conditions in preparing the samples, no difference in pH reading was noted in the less basic sample. In slag No. 2, which was highly basic, there was some difference in the reading, indicating that some air slaking of the lime took place. In addition to the data given in Table 1, pH readings

TABLE 1.—*Effect of Crushing Temperature and Cooling Rate on pH Reading*

Slag	pH Reading			
	Crushed Red Hot	Water Quenched	Air Cooled	Chilled
No. 1.....	10.80	10.80	10.80	10.80
No. 2.....	11.10	11.20	11.25	11.25

were made on samples taken from various regions in a uniform slag pancake. No significant difference was noted. Since the variations encountered in actual practice are far less than the extremes represented by these conditions, it was concluded that no special precautions would be needed in selecting and cooling the samples for pH determination.

Effect of Screen Size

Early studies showed that probably the most important variable to be considered in making the pH measurements was the screen size of the sample. To evaluate this factor, a series of samples was prepared from each of three slags. These samples were prepared by crushing the *entire* slag, so that it would pass in turn through 20, 40, 80 and 200-mesh screens. At each stage in this crushing operation, a sample was removed for pH measurement. In addition, for each screen size, a determination was made of the percentage of the sample that would pass through a 200-mesh screen. The pH readings are given in Table 2.

The increase in pH reading with finer sizing, as shown in Table 2, is attributed to the added lime made available as greater

TABLE 2.—*Effect of Screen Size on pH Reading*

Screen Size through Which Sample Was Passed	pH Reading		
	Slag A	Slag B	Slag C
- 20 mesh.....	9.50	10.30	10.40
- 40 mesh.....	10.10	10.50	10.65
- 80 mesh.....	10.10	10.60	10.70
- 200 mesh.....	10.35	10.75	10.80
Analyzed CaO:SiO ₂ ratio..	1.61	2.31	2.37

surface areas become exposed. These data are shown graphically in Fig. 1, in which the pH is plotted as a function of that fraction of the sample that is minus 200-mesh. The coarser end of the curve represents the minus 20-mesh sample. In this range, screen size exerts a very marked effect on the pH reading. Between 50 and 80 per cent minus 200-mesh, the slope of each curve is small. As more than 80 per cent of the slag sample was crushed finer than 200-mesh, the slope of the curve increased. For routine basicity determinations, it was considered desirable to use slag samples that included between 55 and 60 per cent minus 200-mesh material. In this range minor variations in screen-size distribution would have the least effect on the pH reading. It was found that this screen size could be attained with reasonable regularity by merely using the part of a rapidly crushed slag sample that passed through an 80-mesh screen.

TABLE 3.—*pH Readings of Four Screen-size Fractions of Three Different Slags*

Screen-size Fraction, Mesh	pH Reading			Analyzed CaO:SiO ₂ Ratio		
	Slag A	Slag B	Slag C	Slag A	Slag B	Slag C
- 20 + 40	8.90	9.40	9.40	1.59	2.32	2.40
- 40 + 80	9.00	9.50	9.70	1.60	2.33	2.40
- 80 + 200	9.60	9.85	10.10	1.63	2.27	2.34
- 200	10.30	10.50	10.60	1.60	2.27	2.31

In order to determine the contribution to the pH reading made by material in the

various size ranges, a piece of each of the three slags considered in Table 2 was crushed. The crushed sample was then separated into four fractions according to

determinations were made of the percentage of lime and silica in each screen-size range. It was found that in the finer screen sizes there was actually a slight

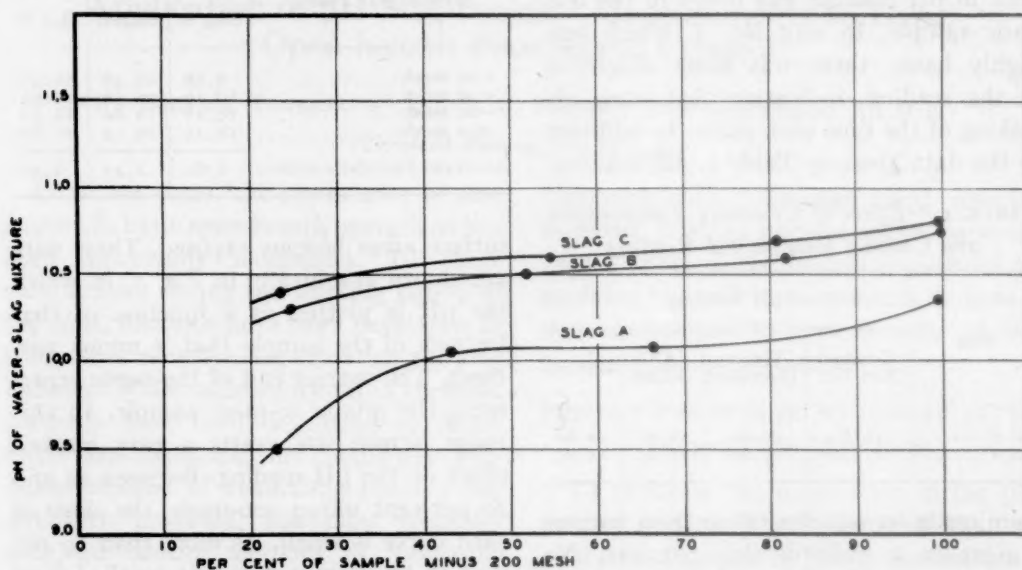


FIG. 1.—EFFECT OF SCREEN SIZE ON pH OF WATER-SLAG MIXTURE.

screen size. pH determinations made on these samples are given in Table 3 together with the actual analyzed basicity of each fraction.

As would be expected, the finer sized samples gave the highest pH reading. In making this type of separation, it seemed possible that some segregation of the lime-bearing minerals in the finest size groups might occur. If this were the case, the readings on the minus 200-mesh fraction would be expected to be higher than those obtained when the entire sample was crushed to pass through this size screen. A comparison of Tables 2 and 3 shows that the readings were actually lower in the minus 200-mesh fraction. This slight difference was probably the result of the finer grinding required to pass the entire sample through the 200-mesh screens.

A study made of these samples in the petrographic microscope indicated that the phase distribution was very similar in the various fractions. In addition, chemical

increase in both the lime and silica content. As shown in Table 3, however, the changes in the calculated lime-silica ratio were not large enough to be significant in this type of measurement. Accordingly, it was concluded that the variations in pH between the different screen-size fractions were caused by differences in particle size rather than differences in composition. For this reason it was decided that little error would be introduced in the basicity determination if only that fraction of the slag passing through an 80-mesh screen after a single crushing were used as the sample.

Effect of Aging

It is often desirable to measure the slag basicity several days after a heat is tapped. To investigate the effect of aging on the slags, pH readings were made on 20 random samples each day for two weeks. The changes taking place during this period were too small to be considered significant.

Effect of Contact Time of Water and Slag on pH Reading

Since the slag samples used for this work were crushed to pass through a finer screen

Relation between pH Reading and Slag Basicity

The routine procedure used in sampling the slag and determining the pH of the

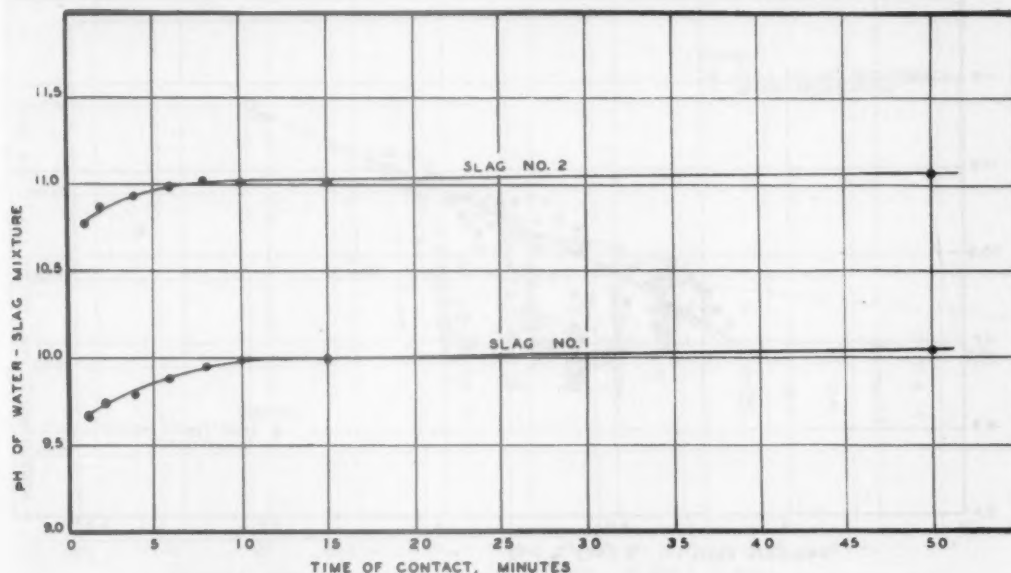


FIG. 2.—EFFECT OF WATER-SLAG CONTACT TIME ON pH READING.

size than that suggested by Philbrook and Jolly, a study was made to determine whether the time required for the slag and water to be in contact could be shortened. The rate at which the pH increased after the initial mixing for two different slags is shown in Fig. 2. The pH rose rapidly for 9 min. in the acid slag and 7 min. in the basic slag. In both samples, there was little further significant increase in pH after 10 min. For routine measurements, a standard time of 10 min. between mixing and reading the pH was adopted. It was felt that this timing would ensure an adequate approach to the maximum reading and still allow the results to become available to the operators within a reasonable length of time.

While numerous other variables were considered in applying pH measurements to plant operations, the results of the studies made merely reaffirmed the work of Philbrook and Jolly.

water mixture was similar to that used for other analyses. A slag sample was taken from the furnace by means of a test spoon and poured into the usual slag pan. The cake was allowed to cool below a red heat. A piece of the cake was broken off and crushed in a hardened steel mortar. The minus-80 fraction was removed from the crushed sample. Two tenths of a gram of the minus 80-mesh material was weighed and mixed with 100 c.c. of distilled water. After 10 min., during which time the mixture was shaken once, the pH of the liquid was determined.

It is to be expected that the actual relation between slag basicity and the pH reading would differ somewhat for each specific set of operating conditions. To establish this relation, chemical analyses were made of a series of slag samples after the pH measurement had been completed. In all work, the ratio of percentage of lime to percentage of silica was used as a meas-

ure of slag basicity. The curve relating slag basicity and the pH reading differed only slightly from that given originally by Philbrook and Jolly. The relation is

unreacted ore, on the other hand, caused the readings to be low. It was often possible to detect such errors in the basicity reading by comparing the color of the sample with

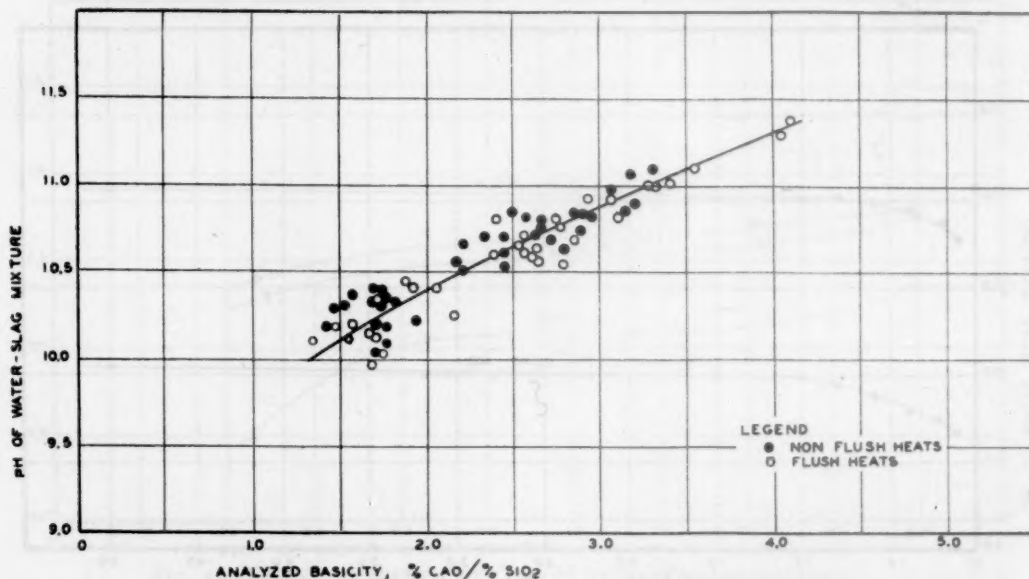


FIG. 3.—RELATION BETWEEN SLAG BASICITY AND pH READING OF WATER-SLAG SOLUTION (0.200 GRAM SLAG IN 100 MILLILITERS WATER FOR TEN MINUTES).

plotted in Fig. 3. The points on which this curve is based are divided into two groups, depending on whether the samples were taken from heats made by flush or nonflush practice. There was a slight difference between the best curves for the two practices. It was felt, however, that for routine control the slight added accuracy arising from using two curves would be more than offset by the inconvenience of the double calibration. Accordingly, a single curve is shown.

APPLICATION OF pH READINGS TO PHOSPHORUS CONTROL

In applying the pH method, it was necessary to recognize several factors that complicated the interpretation of the reading. It was absolutely necessary that the sample be free from any undissolved lime. The presence of such material resulted in high pH readings that did not represent the actual liquid slag. The presence of

standard powdered slags or by recognizing a discrepancy between the reading and the appearance of the slag pancake. By using a series of tests on each heat, the trend of basicity changes could be established, thus making it possible to recognize erroneous readings.

It seemed that by using a dip test rather than the conventional spoon for removing slag from the furnace, the errors caused by sample contamination might be reduced. While slightly more accurate results were obtained when this modified testing method was used, the benefit was not sufficient to warrant introducing a new sampling procedure.

Some results obtained by using the pH slag-basicity measurement for routine control are given in Figs. 4 to 8. The data represented on each of these figures demonstrate that the pH measurement provides an effective indication of the ability of the slag to retain phosphorus. Each graph

represents the relation between slag basicity just before deoxidation and the last analysis of ladle phosphorus. All basicity measurements were made by the pH method.

in plotting basicity against ladle phosphorus considerable spread would exist between individual points.

Fig. 4 shows the effect of finishing slag basicity on ladle phosphorus for 200 basic

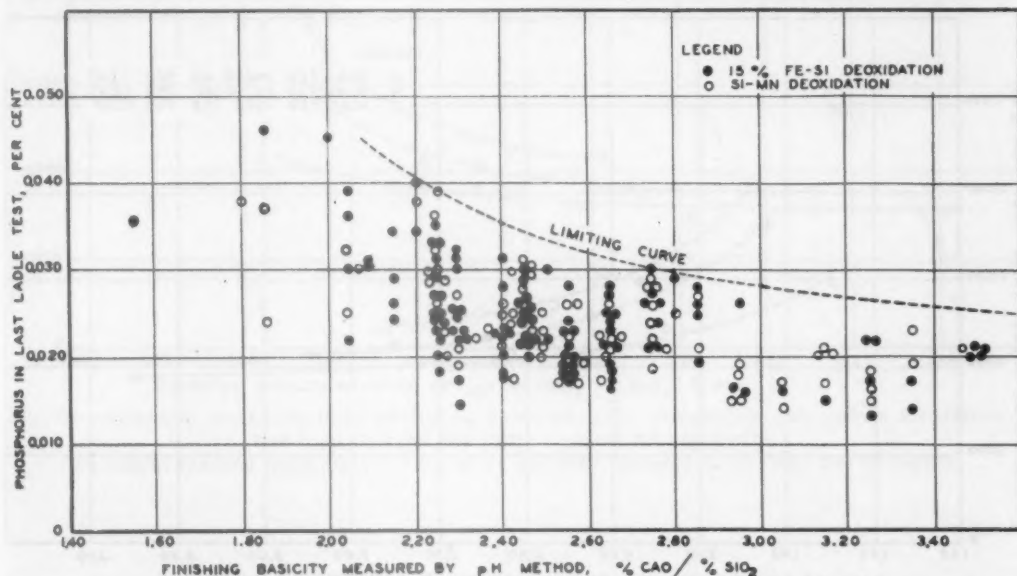


FIG. 4.—RELATION BETWEEN SLAG BASICITY AND LADLE PHOSPHORUS FOR 0.30 TO 0.50 PER CENT CARBON KILLED STEEL.

Principal furnace deoxidizer: 22 lb. of 15 per cent ferrosilicon per net ton of ingots or 21 lb. of silicomanganese per net ton of ingots.

Since killed grades of open-hearth steel are the most susceptible to phosphorus reversion, the slag-basicity control was initially limited to heats of this type. On these grades, it has been found that the magnitude of the reversion depends largely on the amount and type of furnace deoxidizing additions. The curves of Figs. 4 to 8 represent four different furnace deoxidations, ranging from the use of 22 lb. per net ton of silicomanganese or 15 per cent ferrosilicon to practices including no furnace deoxidizer.

In considering the elimination of phosphorus from the basic open hearth, it must be remembered that numerous variables, other than basicity, affect the reaction. Most prominent among these variables are slag and bath oxidation, temperature, phosphorus content of the system, and slag weight. It is to be expected, therefore, that

open-hearth heats. The principal furnace deoxidizer used in these heats was either 15 per cent ferrosilicon or silicomanganese. About 22 lb. of these ferroalloys was used per net ton of ingots. All heats were made to approximately the same chemical analysis. As was expected, there was considerable scattering of the resultant points.

The same general spread of points was obtained with either the ferrosilicon or the silicomanganese deoxidation. Despite this wide spread, a limiting curve could be drawn showing the maximum percentage of phosphorus obtained throughout the basicity range studied. This limiting curve shows that in order to maintain the ladle-phosphorus content below 0.035 per cent with normal variations in operating conditions, it is necessary to maintain the slag basicity above 2.40. If a limit of 0.040 per cent phosphorus is placed on the

open-hearth analysis, the minimum allowable basicity can be lowered to 2.20. Further reductions in basicity may be made as the maximum allowable phosphorus is increased.

furnace deoxidizer was 17 lb. of 15 per cent ferrosilicon per net ton of ingots. The pattern of the curves is similar to that of the preceding figure. Because of the lower carbon and the reduction in the weight of

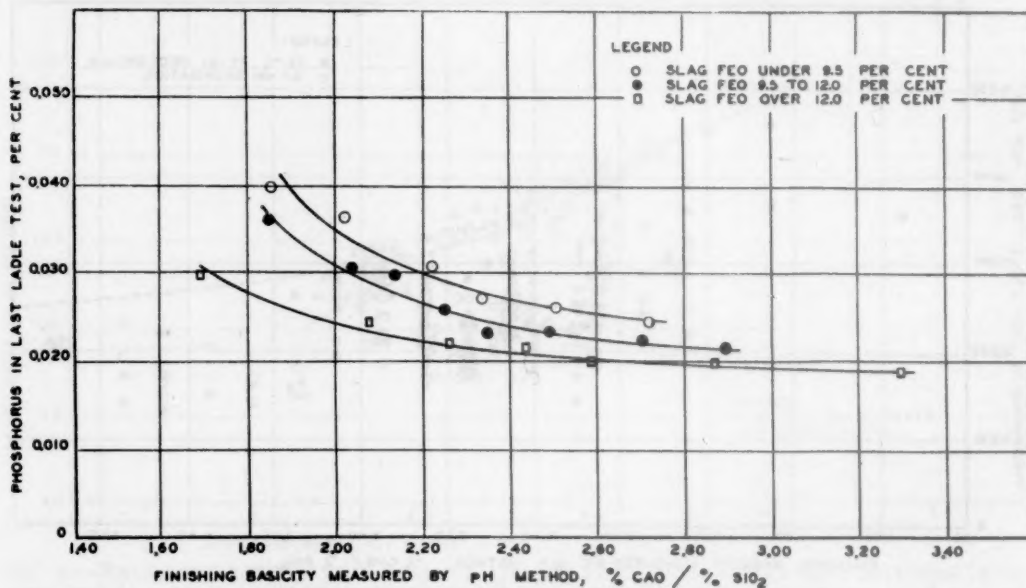


FIG. 5.—AVERAGE RELATION BETWEEN SLAG BASICITY, SLAG OXIDATION AND LADLE PHOSPHORUS FOR 0.30 TO 0.50 PER CENT CARBON KILLED STEEL.

Principal furnace deoxidizer: 22 lb. of 15 per cent ferrosilicon per net ton of ingots or 21 lb. of silicomanganese per net ton of ingots.

In an attempt to eliminate the effect of the numerous other active variables, the data of Fig. 4 were averaged and then replotted in three separate curves according to FeO content of the finishing slag. A definite relation became apparent, which is shown in Fig. 5. The curves emphasize the importance of slag oxidation as well as slag basicity in controlling phosphorus in the basic open hearth. Where slag oxidation is sufficiently high, it is possible to prevent phosphorus reversion despite low slag basicity. From Figs. 4 and 5, aim basicity ranges were established for routine practice on this grade of steel.

The averaged curves for three other deoxidation practices and steel analyses were also determined. Fig. 6 illustrates the relation between slag basicity, slag oxidation and ladle phosphorus for 0.20 to 0.30 per cent carbon steel. The principal

deoxidizer, the general ladle phosphorus level is lower than in Fig. 5.

The average curves for a 0.65 to 0.75 per cent carbon grade deoxidized in the furnace with ferromanganese is given in Fig. 7. Fifteen pounds of the ferroalloy per net ton of ingots was used. The general phosphorus level was about the same as was obtained on the 0.20 to 0.30 per cent carbon steel in Fig. 6. Again, the data were divided into three groups to emphasize the importance of slag oxidation on ladle phosphorus.

The averaged relation between ladle phosphorus and slag basicity for the extreme practice where no furnace deoxidizer was used is given in Fig. 8. This practice was used on 0.75 to 1.00 per cent carbon killed steel. The available data in the higher basicity ranges were limited. In the lower basicity ranges, this grade was less susceptible to phosphorus

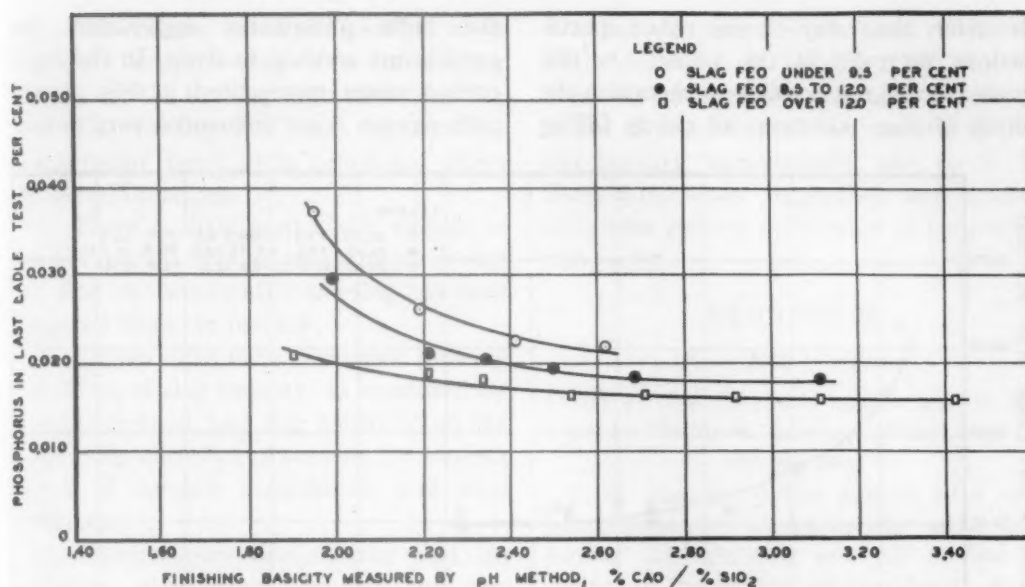


FIG. 6.—AVERAGE RELATION BETWEEN SLAG BASICITY, SLAG OXIDATION AND LADLE PHOSPHORUS FOR 0.20 TO 0.30 PER CENT CARBON KILLED STEEL.

Principal furnace deoxidizer: 17 lb. of 15 per cent ferrosilicon per net ton of ingots.

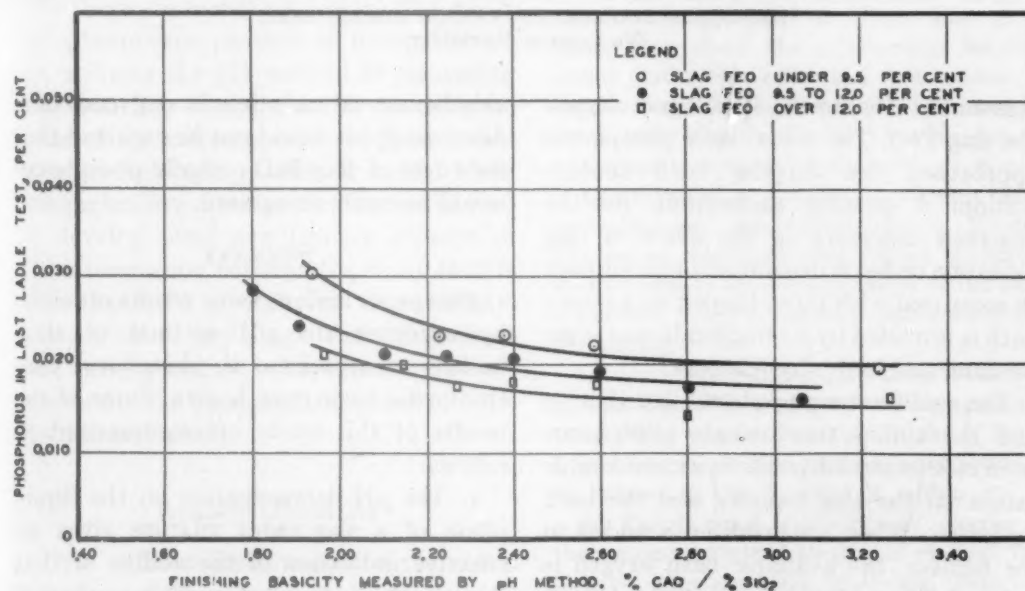


FIG. 7.—AVERAGE RELATION BETWEEN SLAG BASICITY, SLAG OXIDATION AND LADLE PHOSPHORUS FOR 0.65 TO 0.75 PER CENT CARBON KILLED STEEL.

Principal furnace deoxidizer: 15 lb. of 80 per cent ferromanganese per net ton of ingots.

reversion than any of the other specifications surveyed in this paper. On this grade, it was not possible to recognize the effect of slag oxidation, all points falling

the ladle phosphorus approaches the equilibrium residual analysis. In the high-carbon range represented in Fig. 8, the bath oxygen is not influenced very notice-

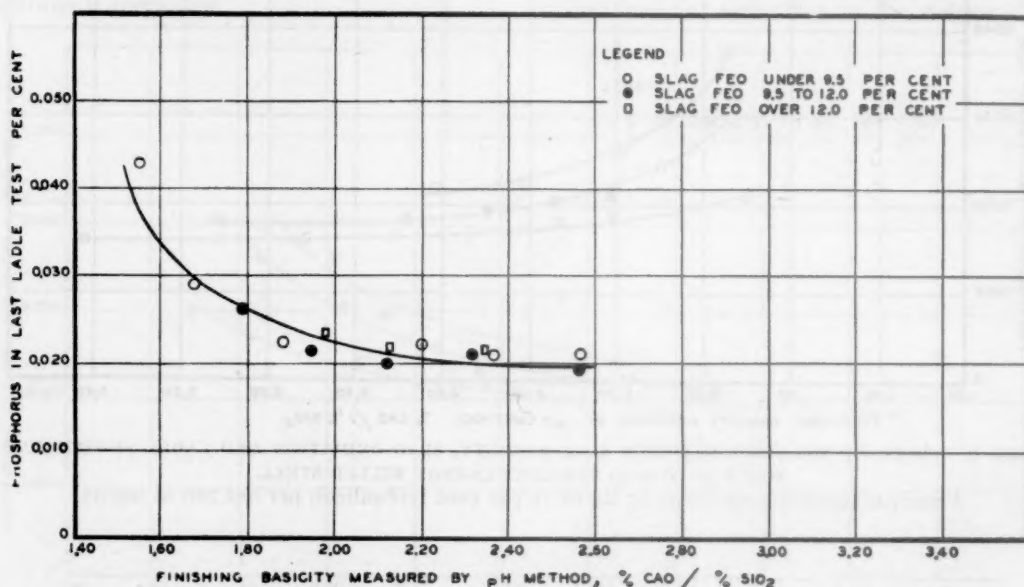


FIG. 8.—AVERAGE RELATION BETWEEN SLAG BASICITY, SLAG OXIDATION AND LADLE PHOSPHORUS FOR 0.75 TO 1.00 PER CENT CARBON KILLED STEEL. No furnace deoxidizer.

reasonably close to the same curve despite the slag FeO. The actual ladle phosphorus approached the tapping bath concentration. A possible explanation for the observed difference in the effect of slag oxidation on heats deoxidized in the furnace as compared with those tapped on an open bath is provided by a consideration of some fundamental bath-slag relations.

The equilibrium phosphorus distribution and the ability to eliminate phosphorus from molten steel depends to a considerable extent on the slag basicity and the bath oxidation. When a deoxidizer is added to the furnace, the available bath oxygen is reduced. The ability of the slag to retain phosphorus after the addition is then dependent on the oxygen in the slag. Consequently, the extent of any phosphorus reversion during furnace deoxidation would be influenced considerably by the slag FeO

When no furnace deoxidizer is added,

ably by normal variations in slag oxidation. Accordingly, it would not be expected that the effect of slag FeO on ladle phosphorus would be easily recognized.

SUMMARY

This paper reviews some results obtained by applying the pH method of slag-basidity measurement to phosphorus control in the basic open hearth. Some of the results of this study are summarized as follows:

1. The pH determination on the liquid phase of a slag-water mixture gives an effective indication of the ability of that slag to retain phosphorus. This method of slag-basidity measurement was used successfully to control ladle phosphorus in actual open-hearth operations.

2. The screen size of the sample is probably the most important physical variable influencing the pH reading.

3. The minus 80-mesh fraction of a hurriedly crushed slag is a satisfactory sample for the basicity determination.

4. The cooling rate and the crushing temperature exert little significant effect on the pH reading.

5. There is little appreciable change in the pH reading of powdered samples during the first two weeks after the slag has been removed from the furnace.

6. Curves have been developed showing the effect of slag basicity, as measured by the pH method, and slag oxidation on the final ladle-phosphorus content for various types of furnace deoxidation and steel analyses.

7. These curves demonstrate that for effective phosphorus control, the slag composition should be adjusted according to the weight and type of furnace deoxidizers that are to be used in finishing the heat.

It has been pointed out in this paper that there are numerous factors that affect the phosphorus content of finished steel. By utilizing the pH method of measuring slag basicity, it was possible to evaluate some of the more apparent of these variables on selected grades of steel. More comprehensive studies would be needed to develop some quantitative concept of the interrelation between the many factors affecting ladle phosphorus. Accordingly, the control of any single variable such as slag basicity cannot be expected to regulate absolutely the phosphorus content of basic open-hearth steel.

ACKNOWLEDGMENT

The authors are grateful to the many members of the metallurgical and chemical departments of Inland Steel Co. who advised and assisted the preparation of this paper. They are indebted to the management of that organization for permission to publish the data presented in the paper.

Acknowledgment is also due to W. O. Philbrook and A. H. Jolly, Jr., of Wisconsin Steel Works, for their help and assistance in the development of the method of pH slag-basicity measurement, and to T. S. Washburn, whose suggestions and helpful criticisms proved invaluable in preparing this paper.

DISCUSSION

(E. G. Hill presiding)

(Most of this discussion applies also to the paper by Philbrook, Jolly and Henry, page 49. this volume.)

J. G. MRAVEC.*—The authors have presented some very interesting information concerning this relatively new pH method of measuring the basicity of open-hearth slags. I was rather surprised to learn that the screen size of the powdered slag exerted such a considerable effect on the pH of the slag and water mixture. In Fig. 1, the authors show for slag test A a variation of 0.8 pH units between samples consisting of from 23 to 100 per cent minus 200-mesh particles. From Fig. 3, in which they show the relationship between actual CaO-SiO_2 ratios and pH values of various slags of similar screen size, it may be noted that a variation of 0.8 pH units is equivalent to a spread in CaO.SiO_2 , or V-ratio of approximately 1.7; each 0.1 pH unit being equivalent to approximately 0.2 V-ratio. The screen size of the slag sample is indeed, as concluded by the authors, probably the most important physical variable influencing the pH reading.

In our plant, we are estimating both the V-ratio and FeO content from slag-pancake tests. Most of our slags fall in the V-range from 1.0 to 2.8. Within this range our accuracy of estimating the V-ratios is within 0.2 to 0.3V. This is equal apparently or superior to the accuracy obtained by the pH method. Our furnace operators and observers, however, have had several years of experience in reading slag pancakes.

In regard to the curves showing the relationships between slag basicity, slag oxidation, and ladle phosphorus for steels deoxidized by

* Research Metallurgist, The Timken Roller Bearing Co., Canton, Ohio.

various furnace deoxidizers, I should like to point out that for a given V-ratio before deoxidation, the ladle phosphorus decreased as the amount of silicon deoxidizer used decreased. This is as one might expect, since the less SiO_2 is formed during deoxidation, the less will be the decrease in the basicity of the tapping and ladle slags. I might add, also, that the relationship between slag FeO and ladle phosphorus as shown by the authors is in agreement with our experience.

There is one question I should like to ask. In looking closely at the spreading of the points in Fig. 4, it seems to me that their vertical limits could be more accurately outlined by four separate curves of similar shape, two above and two below. The bottom two curves could be drawn approximately parallel to the upper curves.

My question is: Is the point where the curves come up to a peak, a critical point of some sort, or does it happen to occur simply by chance?

K. L. FETTERS.*—As a matter of record, two unpublished theses written at the Massachusetts Institute of Technology should be cited among the references.

In 1944, D. J. Sullivan and H. J. Stievater wrote on the subject of the Basicity of Open-hearth Slags. They made a series of experiments to determine a measure of the free lime, or basicity of open-hearth slags by the amount of ammonia released from a solution of ammonium sulphate $(\text{NH}_4)_2\text{SO}_4$ under standardized conditions of concentration and time. The results gave a basicity value that correlated well with theoretically calculated basicity values and with lime-silica ratios of the slag.

The Study of Basic Open-hearth Slag in Relation to Basic Open-hearth Steel Products, by D. C. Nickle, of M.I.T., in 1927, attempted to develop a method for determining directly the free lime of slags, but met with little success.

The authors of the present paper show correlations between lime-silica ratio and pH value. I believe that correlations between pH and "free lime" calculated on some arbitrary base would show a better relationship.

Any slag test is made primarily to give an indication of the effectiveness of the slag as

far as basicity and oxidizing power are concerned. Inasmuch as these properties are not linear functions of basicity, it might be preferable to consider them in relation to free lime, or possibly directly in terms of pH. The point I wish to make is that the authors are trying to show how good an approximation they can make to the lime-silica ratio by means of their pH tests, and I think that perhaps they already have a better measure of what they want to know about a slag in their pH test than they have in the ordinary lime-silica ratio.

In connection with their remarks on the slag pats, there is an observation we might make; that is, that in numerous cases when we take slag pats, we find that the estimated basicity will tell us more than the chemically determined and calculated lime-silica ratio. For that reason, I think the slag pats frequently offer advantage in the practical control of a heat, because they take into account, even better than the pH measurements, the amount of free lime or the amount of undissolved lime, which does not have any effect on the actual basicity of the slag. In the slag pats, the constituents that have been liquid solidify to form a particular pattern and a particular luster of surface, and this appearance is affected only very slightly by the amount of undissolved constituents, and thus the measure gives us, I believe, a more effective measure of the functioning basicity value of the slag.

N. J. GRANT.*—The curve in Fig. 4 contains values from 0.050 down to 0.010 per cent P. It seems to me that with such slags, which take four mols of lime to neutralize each mol of P_2O_5 , with the P_2O_5 varying in such wide limits, correction for it should have been made in the lime-silica ratios. Going further than that, as Dr. Fettes has suggested, the more practical value would have been free lime, which is the value sought.

Another question—I would like to ask the authors what the basis was of their ladle sample; that is, whether all their samples were taken from the middle ingot, or from the first ingot? I would like to know whether any of the analyses from the last three or four ingots were

* Youngstown Sheet and Tube Co., Youngstown, Ohio.

* Massachusetts Institute of Technology, Cambridge, Massachusetts.

included in getting the ladle phosphorus, which would give a very misleading picture.

One final item is this: Was there a ladle deoxidation, and if so, how was that taken into consideration in all these things? After all, during ladle deoxidation, oxygen is removed from the metal, which means that equilibrium between the slag and the metal is further and further away. Later oxygen is again going into the metal and decreasing in the slag as closer equilibrium is striven for, which means in either case better conditions for phosphorus reversion.

N. METCALF.*—It is noted that the difference in pH produced by variations of crushing temperatures and cooling rates have little practical significance. However, in regard to such variations it is felt that the authors could have gone a step further and checked what effect the temperature of the slag at the time of sampling might have on the pH value. Since temperature is a controlling factor as regards slag constitution, it is probable that this or the maximum temperature the slag had attained prior to sampling would have a greater bearing on the question than any treatment after solidification.

Figs. 4 to 8 show very clearly how slag oxidation affects the slag's ability to hold phosphorus in face of additions of deoxidizers to the bath. However, more direct reasoning concerning the mechanics of the reversion is preferred from that presented by the authors, and is as follows: the ferrosilicon acts directly on the slag, reducing the tricalcium or tetracalcium phosphate. Buckwheat coal, or other form of carbon added to the slag, which did not contact the metal at all, would act in the same way. Naturally a slag carrying a higher FeO content would counteract such reducing action more than a slag not so highly oxidized. This is borne out by Fig. 8, which shows that in the absence of reducing material (ferrosilicon) the phosphorus content is the same for the full range of slag oxidation considered, which of course controls the bath oxygen. If reversion of phosphorus was due directly to lowered bath oxygen, the phosphorus should be higher in such cases, regardless of how such a lowering

of oxygen content was arrived at, but this does not happen, as is shown in Fig. 8.

W. J. REAGAN.*—This paper, with its great amount of detailed data, is a very interesting piece of work. However, from the angle of both the basic electric furnace and the basic open hearth, I do not believe it has any practical value.

In the curve in Fig. 3 showing the relationship of slag basicity with the pH reading of water-slag solution, the pH values in the range of 2.0 to 3.0 slag basicity are so close to one another that it would be very difficult to use them for correcting slag basicity.

Furthermore, in my experience phosphorus control is not a problem. By the use of the usual slag cakes and one or two chemical phosphorus determinations, the phosphorus control problem becomes very simple.

M. TENENBAUM (author's reply).—In answer to Mr. Mravec's remarks, I just suspect that the program of slag pancakes that has been established and is functioning satisfactorily is probably as good or better than the pH method, but, as he pointed out, it had been used at his plant for two years and probably a considerable period before that was required before the shop was educated to a point where it could make satisfactory use of the slag-pancake technique.

In contrast to that, the technique of slag basicity measurements by the pH method was established after about a one-week period to establish a satisfactory calibration. It is merely a question of time, and sometimes the problems associated with educating a large open-hearth furnace shop on the techniques of reading slag basicity by reading the pancakes is almost too difficult to overcome. This is especially true at the present time, with the rapid turnover of operating personnel.

As for the question that he asked about the slight peak in the curve at the basicity of 2.65. I am not in position to give any satisfactory explanation for its appearance. It did occur there. It still seems to occur with our more recent data.

Mr. Grant asked where the ladle tests were taken. All ladle tests were taken near the

* Chief Metallurgist, Burlington Steel Co., Hamilton, Ont., Canada.

* Research Metallurgist, Alloy Steel Unit, Copperweld Steel Co., Warren, Ohio.

end of the heat. They were always in the last three ingots poured.

All grades of steel shown in these four curves did receive some ladle deoxidation. Aluminum, manganese and silicon were added to bring them up to specification. The paper was presented merely to show the application of the pH system, and not to evaluate the various factors so much affecting the reversion of the phosphorus.

Mr. Metcalf has suggested the possible effect of slag temperature on pH values. Since slag temperature is not a factor that can be controlled by personnel making the pH determination, and since such temperature effects on slag constitution are more or less intangible, we do not feel that a study of this variable would have any easily recognizable practical significance.

Mr. Metcalf's reasoning concerning phosphorus reversion does not appear entirely adequate. In many practices the deoxidizers are not in any prolonged contact with the slag; yet there often is a considerable reversion. In addition, such reasoning does not explain why considerable phosphorus reversion can

occur despite the fact that there is no perceptible change in slag analysis.

With regard to the relation between slag and bath oxidation, it has been established fairly definitely that, in higher carbon ranges, the effect of slag oxygen on bath oxygen is minor compared with the effects of carbon and transient bath conditions.

Several discussers have suggested the possibility that free lime governs the pH reading. This is undoubtedly true. However, our current knowledge of slag constitution is not adequate to define or evaluate exactly the free lime content. For this reason, attempts to plot the pH reading against arbitrary measures of free lime content resulted in no better relationship than was obtained using the simple and familiar lime-silica ratio.

Dr. Fetter's suggestion that the actual pH reading may prove to be a better index of slag basicity than the lime-silica ratio appears reasonable. However, since pH units are entirely foreign to most open-hearth personnel, it seems more desirable in establishing a slag-control program to use the basicity index that is familiar to the operators.

Effect of Ingot Delivery Time as a Factor in Quality of Bessemer Steel

BY HOWARD C. DUNKLE,* MEMBER A.I.M.E.

(Cleveland Meeting, October 1944)

Various factors can affect the quality of B1112 and B1113 steel as produced in a bessemer plant; among them: vessel-charging practice, blowing practice, ingot-pouring practice, ingot delivery-time practice, pit-heating practices, and ingot-rolling practice. Evaluation of the influence of ingot delivery time on quality has been chosen as the subject for this paper because this time is completely within the control of the operator, and on this particular factor there is a tremendous amount of information in the dusty archives of the average steel plant.

In order to know how much improvement can be made and when attention should be directed to other factors that influence quality, in the continual struggle for improvement, the effect of ingot delivery time must be accurately evaluated. Once this is done, the importance of other variables can be accurately obtained, thus eliminating the necessity of resorting to opinions that are of doubtful value at best.

In the study described herein, extensive use was made of the statistical card system as a method of determining the effect of ingot delivery time as a quality factor in bessemer screw-stock grades by simple direct correlation. The value of this

statistical method as a means of accurately determining the influence of various factors has been amply demonstrated by Work¹ for the bessemer process and by Hand and Gould² and Fetters and Chipman³ for the open-hearth process. The quality records of 300,000 tons of bessemer screw-stock billets were used in this study of the effect of ingot delivery time on the rejections for breaks, pipe, check and seams.

The reduction in the number of rejections for poor quality reduces the costs and increases the productivity per man-hour. The operator today, more than ever before, must know how to keep costs down, how to do it most quickly and in the best way, and how to obtain the highest quality in line with the ever increasing demands of the customer. It is necessary for him to know the individual relations and inter-relations between various factors affecting the quality of the manufactured product if he is to produce material that will meet competitively the cost, performance, and quality demands of the trade.

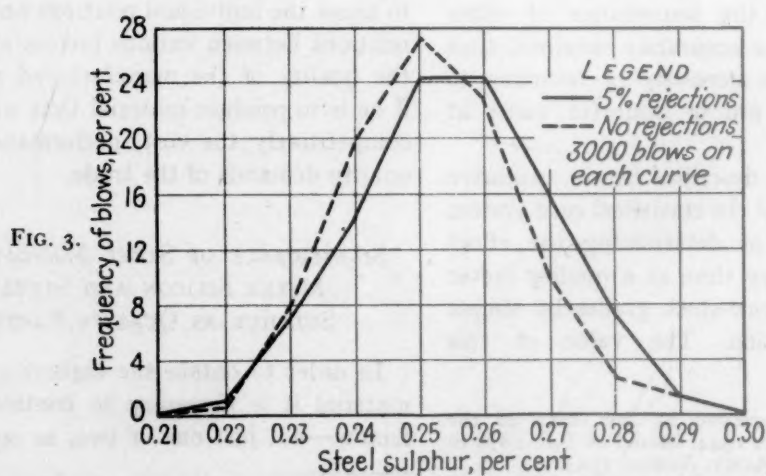
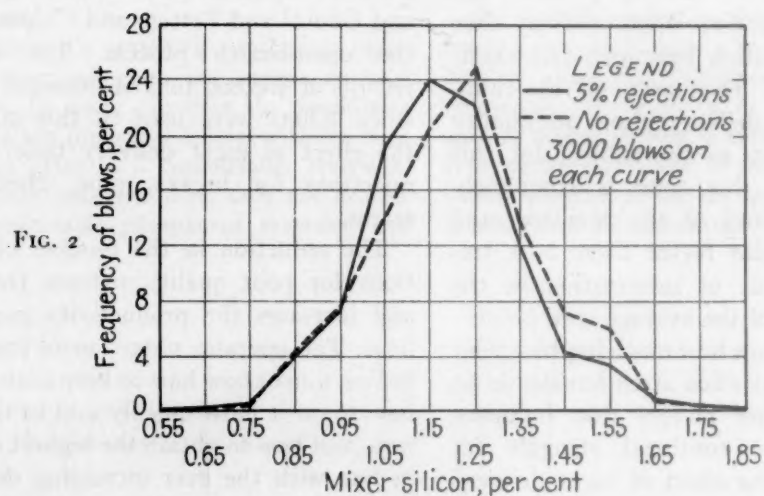
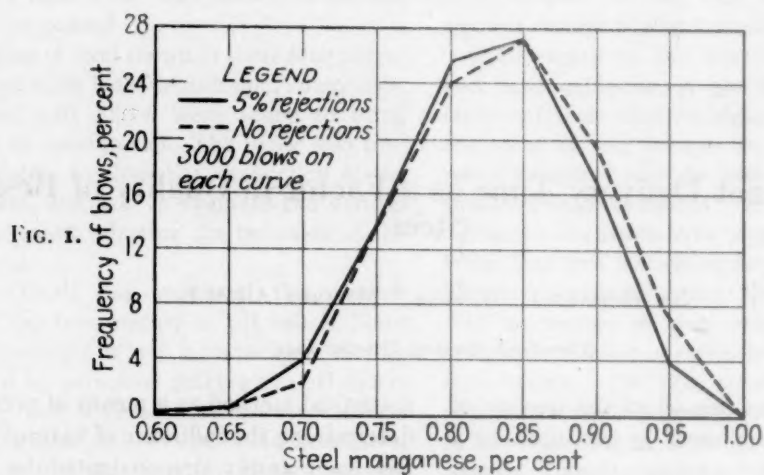
SIGNIFICANCE OF STEEL MANGANESE, MIXER SILICON AND STEEL SULPHUR AS QUALITY FACTORS

In order to obtain the highest grade of material it is necessary to control many factors—not just one or two, as operators

Manuscript received at the office of the Institute Nov. 28, 1944. Issued as T.P. 1878 in METALS TECHNOLOGY, August 1945.

* Mill Metallurgist, Republic Steel Corporation, Youngstown, Ohio.

¹ References are at the end of the paper.



FIGS. 1-3.—FREQUENCY DISTRIBUTION ON BLOWS WITH AND WITHOUT SCRAP REJECTIONS; GRADE OF STEEL, AISI-B1113.

sometimes do. This point is well illustrated in Figs. 1, 2, and 3, which show the frequency distribution of three quality factors that have to do with the chemistry of the steel. On each of these three figures are shown two frequency-distribution curves, each composed of 3000 blows. The solid line represents blows with 5 per cent or more rejections for breaks, pipe, check, and seams while the dotted line shows that no rejections for these defects were made. Data on these curves were taken from the bessemer chipping records of high-sulphur small billets (3 by 3 in. and under).

The similarity between the two curves on each of these three figures shows how little one factor can account for quality of steel. Fig. 1 shows very little difference in the manganese distribution between the blows with and without rejections. In Fig. 2 the blows with no rejections, indicated by the dotted line, show that better quality is obtainable if the average silicon in the iron is held at 1.25 per cent rather than under this value. The influence of sulphur on quality is well known and, as shown in Fig. 3, the blows without rejections have a lower average sulphur content. Summarizing the total effect of these three quality factors indicates that they account for only a part of the total quality.

TIME AS A FACTOR IN STEELMAKING

The time element is considered one of the most important factors in the making and treating of steel.⁴ Time plays a vital role in the blowing, pouring, cooling, heating, and rolling of bessemer steel. It is so deeply tied up with steel quality and production that most studies involving any part of the manufacturing process must necessarily include the time element, either directly or indirectly. One time interval that was considered herein to have an effect on quality of bessemer steel

was the period of time that elapses after the ingots are poured until they are charged into the soaking pits, which hereafter will be designated as the "ingot delivery time." One phase of this cooling period that was investigated was the length of time after each blow was stripped until it was charged into the soaking pits, and this will be referred to as the "finish strip to finish charge time."

Delivery of Ingots to Soaking Pits

Because of the short distance between the bessemer pouring platform and the mold-stripping crane, which is on the converter side of the soaking-pit building, most of the ingots were charged into the pits within 30 to 60 min. after pouring. Ingots not charged within 90 min. after pouring were either side-tracked or sent to the yard to be charged several hours or days later as cold steel. All ingots were poured into 18 by 25 by 69-in. molds. Observers were stationed at the soaking pits to record the ingot delivery time on each blow by 10-min. intervals. These data were later transferred to the statistical punched card to be used in correlations of quality.

Finish Strip to Finish Charge Time

Because of the rapid cooling of the ingots during the finish strip to finish charge time, a study was first undertaken to determine the influence of this cooling period on quality. Data were obtained on 12,000 tons of high-sulphur ingots, which were equally distributed between the B1112 and B1113 steels. The graphs in Figs. 4 and 5 show the total rejections on small billets for these two grades of steel. The total rejections on B1112 increase 1.3 per cent in 8 min. (Fig. 4) and on B1113 the total rejections (Fig. 5) increase 4.8 per cent

for the same period of time, indicating that the ingots of higher sulphur content are much more sensitive to the cooling

Ingot Delivery Time

Both chipping and scarfing quality records were used to evaluate the influence

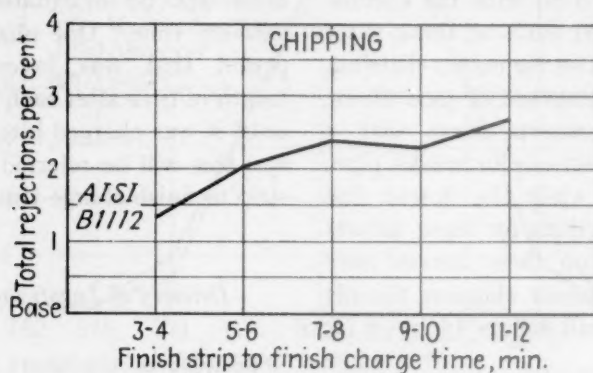


FIG. 4.—EFFECT OF FINISH STRIP TO FINISH CHARGE TIME ON TOTAL REJECTIONS (BREAKS, PIPE, CHECK AND SEAMS).

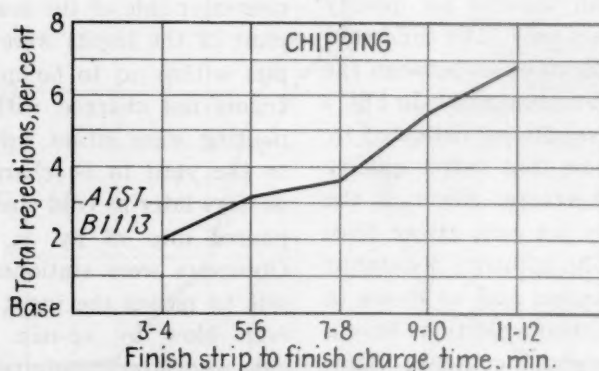


FIG. 5.—EFFECT OF FINISH STRIP TO FINISH CHARGE TIME ON TOTAL REJECTIONS (BREAKS, PIPE, CHECK AND SEAMS).

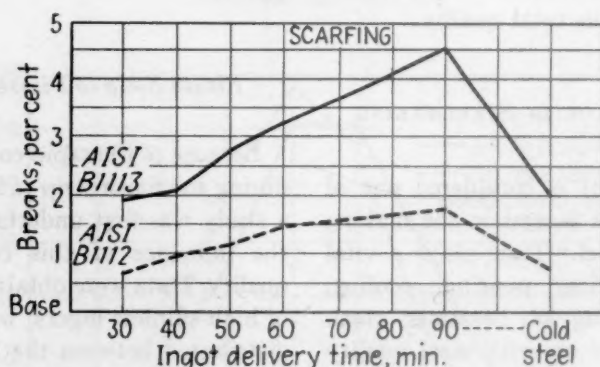


FIG. 6.—EFFECT OF INGOT DELIVERY TIME ON PERCENTAGE OF STEEL REJECTED FOR BREAKS.

effect during this period. The greatest improvement in quality is to be obtained by concentrating on this phase of the cooling cycle.

of ingot delivery time on the quality of B1112 and B1113 steels for various kinds of defects. Data from 140,000 tons of chipped small billets and 130,000 tons

of scarfed large billets were used in this study. The chipped small billets ranged from $1\frac{1}{2}$ to 3 in. square and the scarfed large billets ranged from 4 to 6 in. square,

charged into the soaking pits at atmospheric temperature.

Figs. 6 to 15 show the effect of ingot delivery time on individual and total

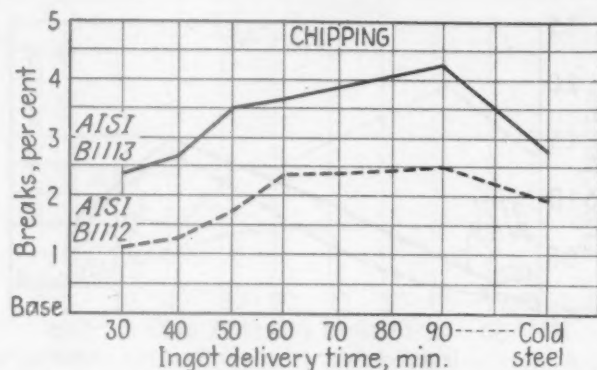


FIG. 7.—EFFECT OF INGOT DELIVERY TIME ON PERCENTAGE OF STEEL REJECTED FOR BREAKS

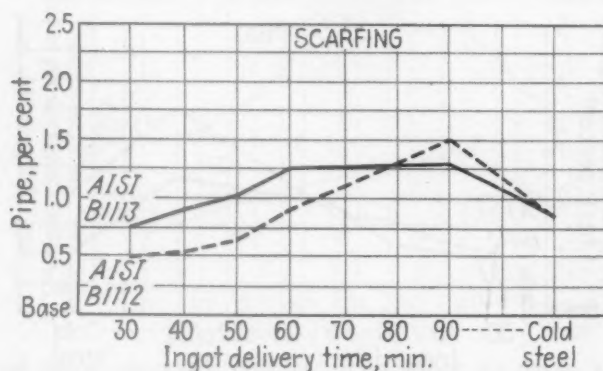


FIG. 8.—EFFECT OF INGOT DELIVERY TIME ON PERCENTAGE OF STEEL REJECTED FOR PIPE.

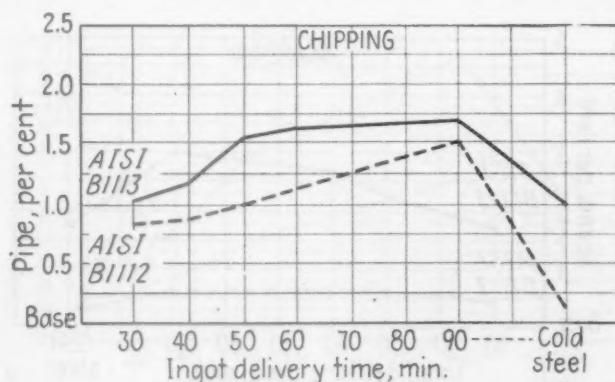


FIG. 9.—EFFECT OF INGOT DELIVERY TIME ON PERCENTAGE OF STEEL REJECTED FOR PIPE.

inclusive. Rejections were plotted for 10-min. intervals from 30 up to and including 90 min. ingot delivery time. The cold steel represents ingots that had been

steel rejections as found by simple correlations. All types of rejections increased with the ingot delivery time up to and including 90 min. On cold steel the per-

centage of rejections drops to approximately the same level as the 40 to 50-min. ingot delivery time. This would mean that rejections increase to a maximum peak

duced in the ingot when charged into the soaking pits, and in combination with the effects of rolling the ingots in the blooming mill.

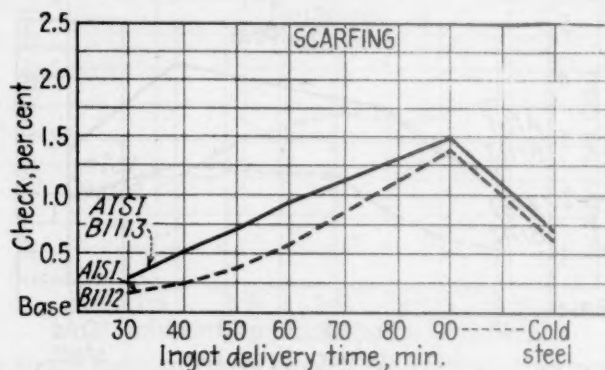


FIG. 10.—EFFECT OF INGOT DELIVERY TIME ON PERCENTAGE OF STEEL REJECTED FOR CHECK.

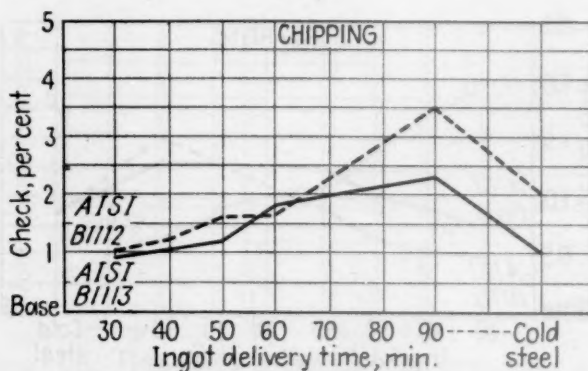


FIG. 11.—EFFECT OF INGOT DELIVERY TIME ON PERCENTAGE OF STEEL REJECTED FOR CHECK.

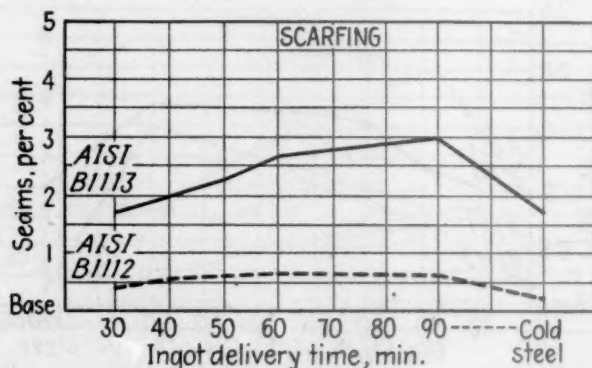


FIG. 12.—EFFECT OF INGOT DELIVERY TIME ON PERCENTAGE OF STEEL REJECTED FOR SEAMS.

and then decrease to the point indicated by results on cold steel. One explanation for this may be the thermal shock and temperature-gradient stress variations pro-

Rejections

For Breaks.—Breaks are affected to a great extent by the ingot delivery time, as shown in Figs. 6 and 7. From 30 to 90 min.

inclusive, the percentage of breaks on B1112 and B1113 steels increase 1 to 1.25 and 2 to 2.5 per cent, respectively.

tions on B1112 steel increase 0.5 to 0.75 per cent and on B1113 they increase 0.75 to 1 per cent.

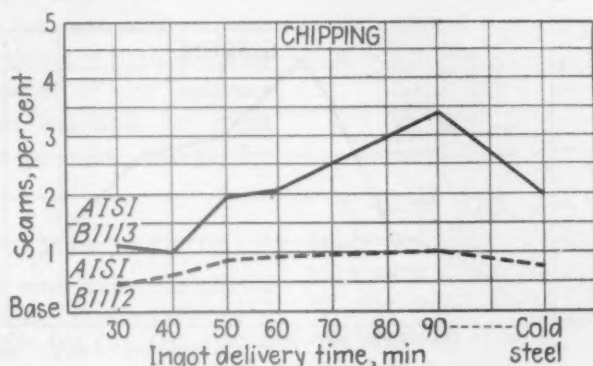


FIG. 13.—EFFECT OF INGOT DELIVERY TIME ON PERCENTAGE OF STEEL REJECTED FOR SEAMS.

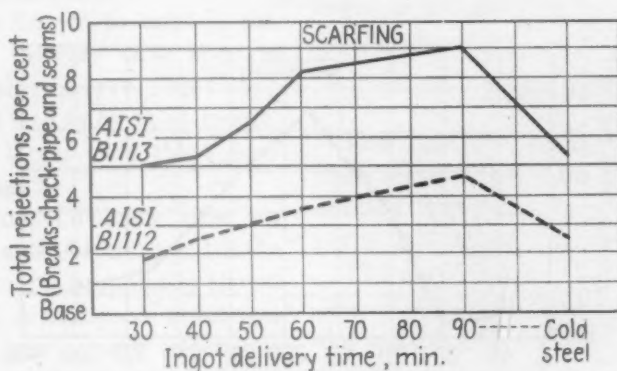


FIG. 14.—EFFECT OF INGOT DELIVERY TIME ON PERCENTAGE OF STEEL REJECTED FOR TOTAL REJECTIONS (BREAKS, PIPE, CHECK AND SEAMS).

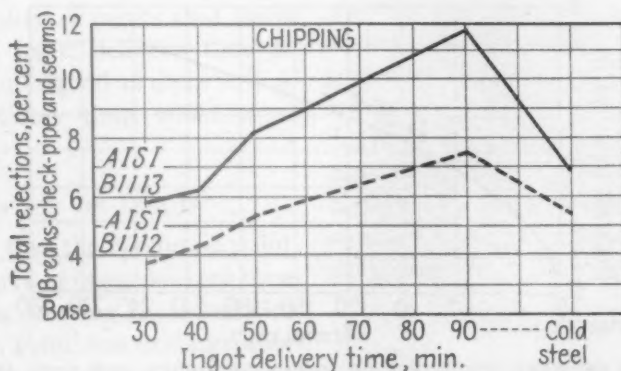


FIG. 15.—EFFECT OF INGOT DELIVERY TIME ON PERCENTAGE OF STEEL REJECTED FOR TOTAL REJECTIONS (BREAKS, PIPE, CHECK AND SEAMS).

For Pipe.—Figs. 8 and 9 show that pipe is affected the least by ingot delivery time. Up to 90 min., inclusive, pipe rejection

For Checked Steel.—Rejections for checked steel (Figs. 10 and 11) increase 1.25 to 2.5 per cent on B1112 and 1.25 to

1.5 per cent on B1113 steel for the 30 to 90-min. ingot delivery time. The term "checked steel" as referred to in this

for seams on the B1112 steel (Figs. 12 and 13). However, the increase in percentage of rejections on the higher sulphur grade

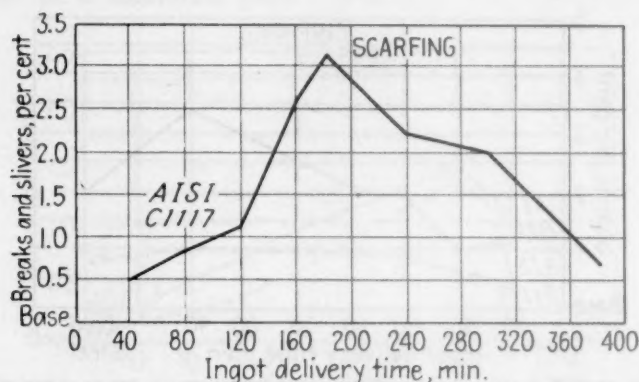


FIG. 16.—EFFECT OF INGOT DELIVERY TIME ON PERCENTAGE OF REJECTIONS FOR BREAKS AND SLIVERS.

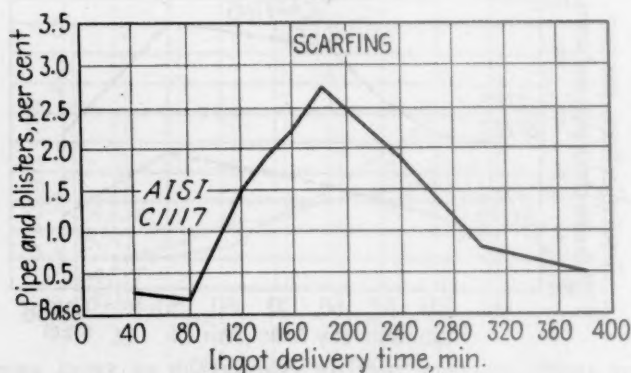


FIG. 17.—EFFECT OF INGOT DELIVERY TIME ON PERCENTAGE OF REJECTIONS FOR PIPE AND BLISTERS.

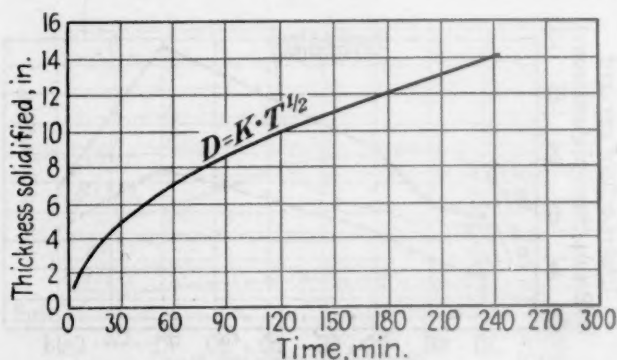


FIG. 18.—RELATION BETWEEN THICKNESS OF METAL SOLIDIFIED AND TIME AFTER METAL IS IN CONTACT WITH MOLD WALL.

paper is a slivered condition found on one or more corners of the billet.

For Seams.—The ingot delivery time does not have much effect on rejections

is very noticeable and seams increase 1.25 to 2.5 per cent from 30 to 90 minutes.

Total Number.—The relationship between total number of rejections and ingot

delivery time is given in Figs. 14 and 15, which summarizes the four types of defects shown in Figs. 6 to 13 inclusive. Total rejections increase 2.9 to 3.6 per cent on B1112 and 4 to 5.9 per cent on B1113 for 30 to 90-min. ingot delivery time. Because of the physical aspects of our bessemer plant, no data are available on ingot delivery time after 90 min., except for cold steel.

INGOT DELIVERY TIME ON C1117

In order to show more fully the effects of ingot delivery time, the results for a statistical study on about 150,000 tons of C1117 small billets have been included herein. This steel was selected because of the large variation known to exist in the open-hearth ingot delivery time and its similarity in analysis to B1112. This C1117 steel was all poured into 23 by 25-in. molds, which are a little larger than those used for the bessemer ingots.

The effect of ingot delivery time on rejections for pipe and blisters, and breaks and slivers for C1117, is graphically shown in Figs. 16 and 17. A maximum point was reached at 180 min., with rejections increasing more rapidly as the delivery time increased to 180 min. than they declined as delivery time increased beyond 180 min. The quality of ingots that have more than 6 hr. ingot delivery time is shown to be almost as good as those with a 40 to 80-min. delivery time, which were the best in quality.

SOLIDIFICATION OF INGOTS

It was thought that the maximum point reached on the curve of ingot delivery time was related to the freezing characteristics of the ingot. A. L. Feild⁵ has demonstrated mathematically that the depth of thickness solidified in from the mold wall is directly proportional to the square root of the time elapsing after pouring. The relation between depth solidified and time may be expressed by the following equation:

$$D = K \times T^{1/2}$$

D = depth of solidification in from the mold wall.

T = time elapsing after pouring (minutes).

K = a constant that depends on the type and size of mold, temperature of steel above its melting point, analysis of steel, etc.

A curve (Fig. 18) was obtained by applying this formula to various mold sizes using the constant K as 0.90, required by the mold size employed. The total solidification of a 23 by 25-in. ingot was found to be about 165 min. after pouring, which corresponds fairly well to the peak found in the curve of ingot delivery time for C1117.

CONCLUSIONS

The apparent similarity of the frequency-distribution curves for blows with and without rejections shows how little one factor can account for steel quality.

The effect of finish strip to finish charge time is considerably more important than the ingot delivery time for the same length of time.

The best quality for high-sulphur steels (B1112, B1113, and C1117) is obtained when the ingot delivery time is the shortest, or from ingots charged into the pits as cold steel. Rejections of these increase to a maximum and then decline as the ingot delivery time increases. It is tentatively concluded that this maximum point corresponds approximately to the time necessary to complete the solidification of the ingot.

ACKNOWLEDGMENT

The author wishes to express his appreciation to Mr. E. C. Smith, Chief Metallurgist of the Republic Steel Corporation, and to Dr. D. E. Babcock, Assistant Chief Metallurgist of the Youngstown district, for their helpful comments and suggestions

on this paper, and to the executives of the Youngstown district of the Republic Steel Corporation for permission to present these data. In addition, he would like to acknowledge his debt to Mr. P. J. Kloss, whose work with the statistical card system contributed much to this paper.

REFERENCES

1. H. K. Work: *Trans. A.I.M.E.* (1941) **145**, 132.
2. H. K. Hand and Gould: *Trans. A.I.M.E.* (1942) **150**, 76-84.
3. K. L. Fetters and J. Chipman: *Trans. A.I.M.E.* (1940) **140**, 170-203.
4. J. Johnson: *Trans. A.I.M.E.* (1942) **150**, 13-29.
5. A. L. Feild: *Trans. Amer. Soc. Steel Treat.* (1927) **11**, 264-276.

[DISCUSSION

(H. K. Work presiding)

MEMBER.—Has any attempt been made, in analyzing these data on delivery time, on the part of freezing the ingot and total transit time, to get the correlation with rejection in that manner? What I want is to try to separate the effects of the superfreeze or any other factor in the freezing of the ingot from the actual time the ingot stood after frozen. Did the various thermal gradients after going to the soaking pit have any effect, or is it merely the time in the solidification of the ingot?

C. E. SIMS.*—This paper is very interesting, in view of some experiments done at Battelle several years ago. The particular reason for the experiments was some tests to determine whether suitable substitutes for manganese could be found that would aid in reducing the hot shortness of steels. We were testing these steels for forgeability, which of course would relate to their rollability as well.

We found a very important effect in regard to cooling. This work was done on small ingots, not much over 3 or 4 in. in diameter, which would freeze in about 6 min. If these ingots were allowed to cool to room temperature and then were reheated for forging or rolling, we got results that were very much better than if the ingots were taken out of the mold immediately after freezing and put into a

reheating furnace and maintained at a forging temperature.

In short, the results were markedly different. If we wanted results that bore any relation to practice, it was necessary to strip the ingots while they were still hot and put them in a hot furnace.

That coincides very closely with the data that were shown here. The coincidence between the apparent solidification time of the ingot and the peak of rejections looks very good, but I am wondering if it might be only a coincidence, in view of the results I have just described.

In examining the steels as to reasons for this, we found quite a marked difference in the conformation of the sulphides. There was a difference in the character of the sulphides, which might readily account for the difference in the forgeability of these steels.

G. SOLER.*—We are led to wonder if the trouble is not at the soaking pits. The delivery time seems to follow a frequency curve. Apparently delivery is not under control.

In the heating of cold steel, most mills take a little more care in heating and will chill the pits. This should be done with long delivery times.

H. B. EMERICK.†—I think, with Mr. Soler, that the ratio of ingot heating time to ingot delivery time is probably one explanation for this curve of ingot delivery time versus rejections reaching a peak. It has been our experience that if the track time, or ingot delivery time as Mr. Dunkle calls it, becomes excessively long, the natural tendency is to rush the heating on those blows in the soaking pits so that they can follow through in sequence on the mill, and they are frequently rolled at low temperature. That circumstance does not obtain, of course, on ingots that are charged fairly rapidly after finish pour.

I would like to ask Mr. Dunkle a question. When working with high-sulphur steels, is it not possible to get them into the pits too fast? It has been our experience that ingot delivery time under 35 min. on B-1112 grade, or under 45 min. on B-1113 grade, will cause a condition that we call "bellying" in the rolling mill,

* Timken Roller Bearing Co., Canton, Ohio.

† Steel Works Metallurgist, Jones and Laughlin Steel Corporation, Aliquippa, Pennsylvania.

* Battelle Memorial Institute, Columbus, Ohio.

which results in unsound interior structures in the finished billet. We have found it necessary to cut back on these delivery times, particularly on B-1113, because of that difficulty. Our mold size is 25 by 25 in. square, 80 in. tall.

H. C. DUNKLE (author's reply).—No attempt has been made to correlate rejections with the ingot delivery time after solidification of the ingot.

Mr. Sims' comments on the experiments conducted at Battelle are interesting and bring up a point regarding the characteristics of the sulphides of which we have made no investigation.

We are certainly willing to agree with Mr. Soler that there are many variables in the heating of ingots in the soaking pits, which materially affect the surface quality of steel. The kind of fuel, the characteristics of the heaters, the number of ingots per pit, and the working condition of the pit equipment are but a few

of the factors that can and will have a bearing on quality. These influencing conditions were recognized and it was felt that their effect would be distributed throughout the ingot delivery time when a large mass of data was used as in this investigation.

It is doubtful whether any economic advantage is to be gained by charging low-carbon bessemer-screw-stock cold steel into chilled pits. The cost of increased fuel consumption would be greater than the savings made in reduced rejections, if any.

In reply to Mr. Emerick's question about the bellying of ingots in the rolling mill because of short ingot delivery time, I would say this could easily happen when using a 25 by 25-in. mold. With 18 by 25-in. molds and 30-min. ingot delivery time, we find practically no bellying of ingots. Hot ingots that are stripped without the plunger breaking through the ingot top and are not properly "set" in the soaking pits will often belly when rolled.

Creep Properties of Some Binary Solid Solutions of Ferrite

BY CHARLES R. AUSTIN,* MEMBER A.I.M.E., C. R. ST. JOHN,† AND R. W. LINDSAY‡

(New York Meeting, February 1945§)

MANY of the factors influencing the creep behavior of ferrous alloys have been investigated and reported upon in the literature, including such variables as grain size, steelmaking practice, nature and stability of the microstructure, and the effect of alloying elements in steels. However, with respect to the latter, the microstructures involved are usually heterogeneous and as a result the effect of the addition is related to its effects on the various phases present in the microstructure. In the instances where this structure consists of ferrite and carbide, the behavior of the alloy addition will be related to its action in strengthening ferrite and in opposing temperature softening of ferrite as well as coalescence of carbide.

The present paper is the third in a series comprising a comprehensive review of investigations on the properties of iron binary alloys.^{1,2} Its purpose is to describe the results of isolating one microstructural phase, namely ferrite, and studying its creep characteristics in both the unalloyed and alloyed conditions. This should aid in establishing to a large degree the importance of ferrite in the creep behavior of steels consisting of the previously mentioned ferrite-carbide aggregate.

Manuscript received at the office of the Institute Dec. 15, 1944. Issued as T.P. 1837 in METALS TECHNOLOGY, August 1945.

* Professor of Metallurgy, The Pennsylvania State College, State College, Pennsylvania.

† Metallurgical Engineer, Aluminum Company of America, and graduate of the department of Metallurgy, The Pennsylvania State College.

‡ Assistant Professor of Metallurgy, The Pennsylvania State College.

§ Meeting canceled.

¹ References are at the end of the paper.

REVIEW OF PREVIOUS WORK

In view of the fact that the present investigation deals only with the effects of silicon, manganese, chromium, molybdenum, nickel, and cobalt, and to a certain extent with the effects of carbon, the review of previous literature will be confined to these elements. Practically no references were encountered dealing with the influence of these elements on the creep characteristics of the isolated phase. However, various contributions have dealt with the creep behavior of low-carbon steels alloyed with the elements under consideration. A particularly concise review in this respect is given by Bullens (Battelle)³ and much of this material has been drawn upon.

The definite improvement in creep resistance and high-temperature strength conferred by molybdenum is well known. Published suggestions by the A.S.M.E.⁴ permit of an increase of some 2000 to 5000 lb. per sq. in. in permissible design loads over a temperature range from 650° to 1000°F. as a consequence of additions of 0.40 to 0.60 per cent of this element in carbon steels of the order of 0.25 to 0.35 per cent carbon content.

Babcock and Wilcox Tube Co.⁵ has published data showing the pronounced increase in stress necessary to cause one per cent creep per 10,000 hr. when additions of 0.5 or 1 per cent molybdenum are made to a plain carbon steel. These data apply to temperatures over a range from 800° to 1000°F.

Members of the U.S. Steel Corporation research staff⁶ investigated the creep resistance of a steel with 0.11 per cent C and 0.54 per cent Mo in the normalized and tempered condition. The best results were coincident with a fine precipitation of what apparently was molybdenum-rich carbide throughout the ferrite matrix. This structure exhibited definite stability. The testing temperature was 1100°F. in this investigation.

creep resistance, but further additions of chromium of the order of 2.5 and 5 per cent (with the same amount of molybdenum) decreased it. The temperatures employed were 800°, 1000°, and 1200°F. The effects of chromium on oxidation and corrosion resistance are probably quite definitely related to the increased load-carrying ability in some instances of steels containing this element, particularly at the higher test temperatures.

TABLE I.—*Chemical Analyses of Alloys Investigated*
Weight Per Cent Alloying Element

Alloy	C	Cr	Co	Ni	Mn	Mo	Si	P	S
Pure iron.....	0.02	0.003	0.005	0.032	0.03	0.004	0.003	0.010	0.013
Carbon.....	0.23	0.003	0.005	0.040	0.03	0.004	0.005	0.011	0.014
Carbon.....	0.53	0.003	0.005	0.030	0.03	0.004	0.010	0.010	0.016
Carbon.....	0.91	0.003	0.005	0.034	0.03	0.004	0.006	0.010	0.011
Chromium.....	0.03	0.45	0.005	0.032	0.05	0.004	0.012	0.011	0.011
Chromium.....	0.02	0.99	0.005	0.034	0.03	0.004	0.004	0.010	0.013
Chromium.....	0.03	4.83	0.005	0.023	0.03	0.004	0.008	0.012	0.015
Cobalt.....	0.03	0.003	0.52	0.037	0.03	0.004	0.004	0.012	0.014
Cobalt.....	0.05	0.003	1.00	0.043	0.05	0.004	0.004	0.010	0.019
Cobalt.....	0.03	0.003	5.08	0.08	0.03	0.004	0.004	0.012	0.015
Nickel.....	0.03	0.003	0.005	0.57	0.03	0.004	0.004	0.010	0.011
Nickel.....	0.02	0.003	0.005	1.15	0.03	0.004	0.004	0.010	0.015
Nickel.....	0.02	0.003	0.005	4.83	0.03	0.004	0.004	0.010	0.016
Manganese.....	0.02	0.003	0.005	0.032	0.69	0.004	0.004	0.010	0.014
Manganese.....	0.06	0.003	0.005	0.030	1.33	0.004	0.004	0.011	0.020
Manganese.....	0.03	0.003	0.005	0.035	7.25	0.004	0.13	0.012	0.022
Molybdenum.....	0.03	0.003	0.005	0.054	0.03	0.11	0.004	0.010	0.014
Molybdenum.....	0.03	0.003	0.005	0.023	0.03	0.54	0.004	0.010	0.014
Molybdenum.....	0.04	0.003	0.005	0.016	0.03	1.50	0.004	0.011	0.014
Silicon.....	0.03	0.003	0.006	0.033	0.03	0.004	0.22	0.012	0.015
Silicon.....	0.02	0.0045	0.005	0.032	0.03	0.004	0.59	0.011	0.018
Silicon.....	0.02	0.003	0.005	0.055	0.03	0.004	1.21	0.010	0.012

The limited amount of data relating to manganese would indicate that increase of this element may be helpful. However, the data available on this point do not permit any definite conclusions.⁷ The steels used contained 0.15 per cent C and testing was carried out at 800°, 1000°, and 1200°F.

Chromium may increase slightly the creep resistance, but again the results are not too clearly defined. Some data⁸ would seem to indicate that the addition of 1 to 1.5 per cent Cr (in conjunction with 0.40 to 0.60 per cent Mo) increased the

Bullens points out that nickel or silicon, which are ferrite strengtheners at ordinary temperature, are almost without effect on creep at high temperature. Cross and Lowther⁹ have shown that the addition of silicon to pure iron does increase the creep resistance at 850°F. Of course, silicon will confer increased oxidation and corrosion resistance.¹⁰

The work of Jenkins, Mellor, and Jenkinson¹¹ may be taken as representative of the effect of carbon on the creep properties of steels. Their research indicates that an increase in carbon results in a

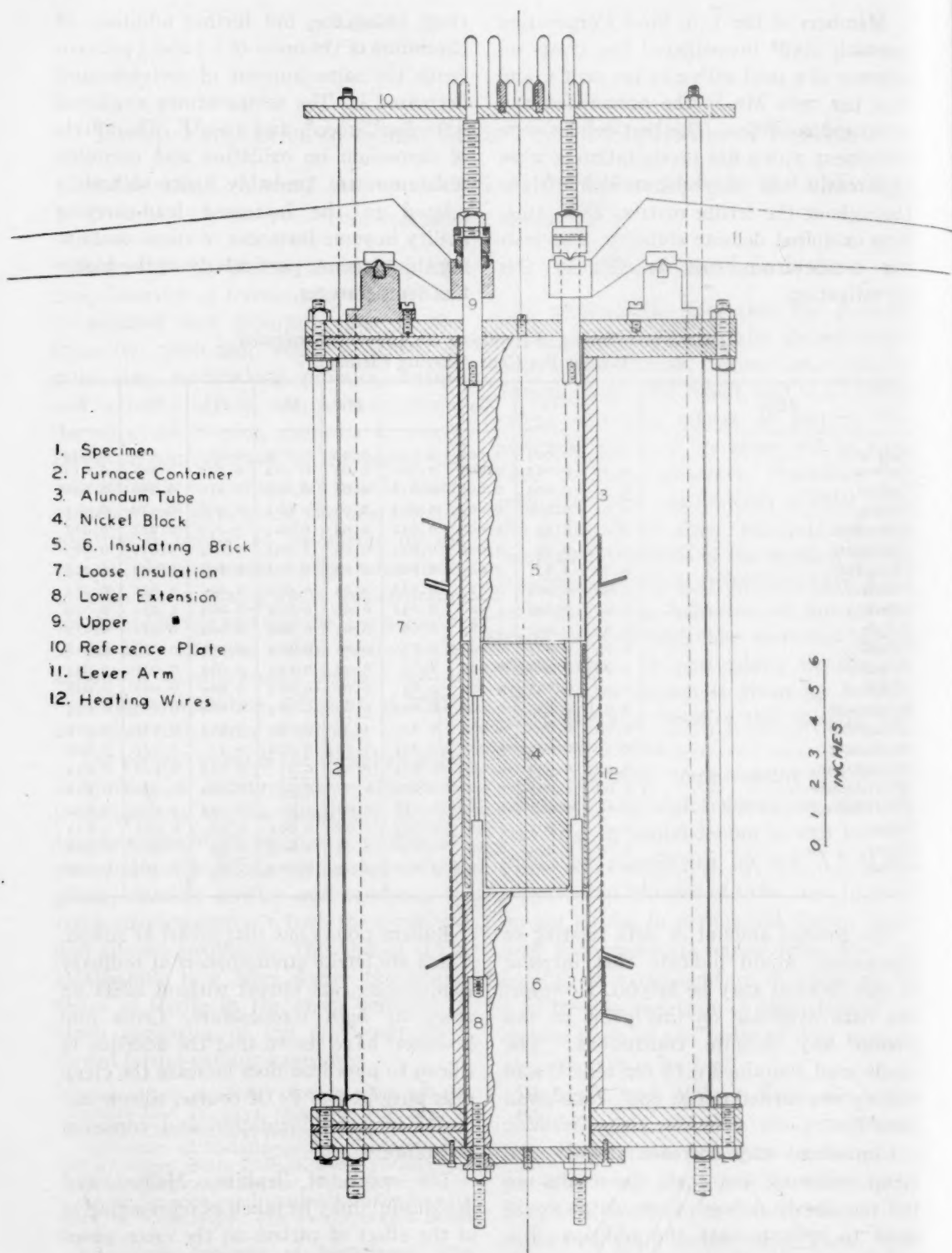


FIG. 1.—SECTIONAL VIEW OF CREEP-TESTING ARRANGEMENT

The standard bar, which furnishes a means for correction for dimensional changes other than those due to creep, is centrally located within the furnace core and positioned lengthwise in the same manner as the bars shown.

general increase in creep strength up to temperatures of the order of 630° to 750°F . Above this temperature on up to the lower critical an increase in carbon content up to

mium, molybdenum, silicon, manganese, nickel, and cobalt. These alloys were prepared from hydrogen-annealed electrolytic iron by induction melting in about 150-lb.

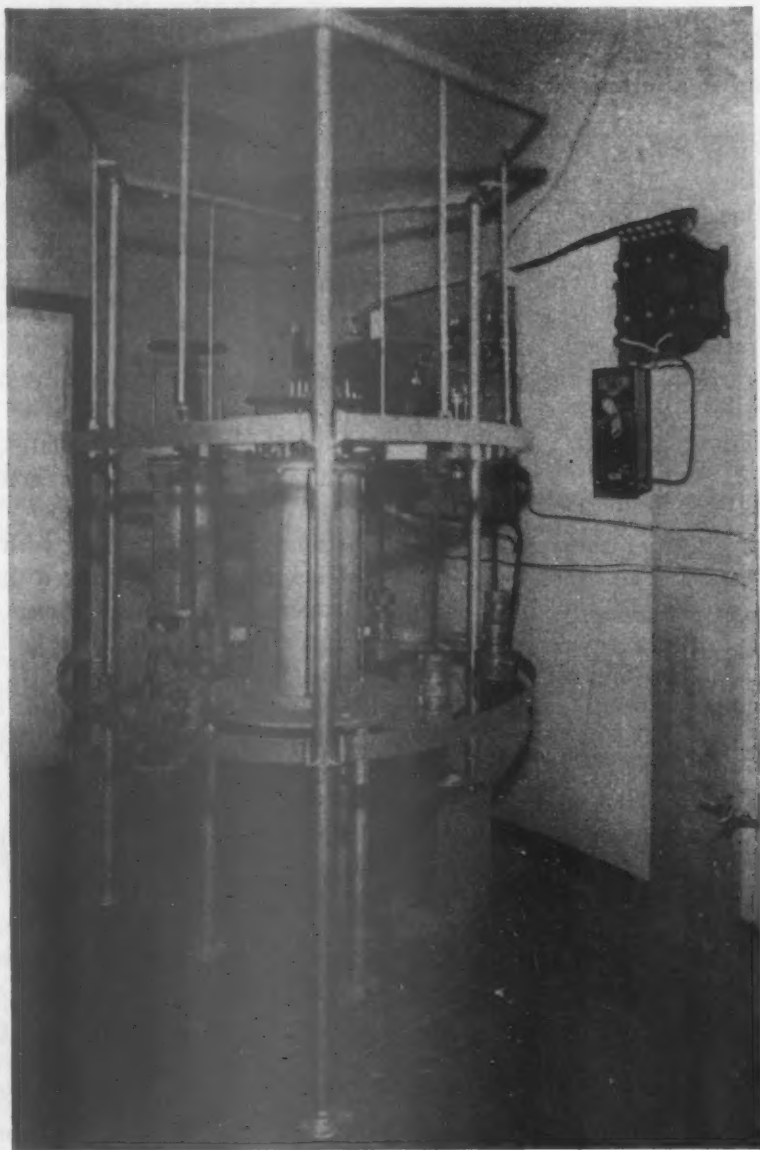


FIG. 2.—FURNACE ASSEMBLY.

1.25 per cent shows no pronounced strengthening action.

IRON BINARY ALLOYS INVESTIGATED

The iron binary alloys investigated were ferritic solid solutions of six of the more important alloying elements; namely, chro-

lots in magnesia crucibles. Melting was carried out under an atmosphere of hydrogen, the melt in each case being permitted to solidify in the crucible. The alloy was just remelted under hydrogen and again allowed to solidify in the crucible, the purpose being to minimize porosity.

The ingots were forged to about 2-in. square sections and rolled to $\frac{3}{8}$ -in. diameter bar stock. Half of this bar stock (from the bottom end of the ingot) was rolled down to $\frac{5}{16}$ -in. diameter. The tensile creep test bars were prepared from this bar stock by centerless grinding of the gauge section to a form indicated later in the paper.

The chemical analyses of the alloys are given in Table 1. All of the alloys were given an annealing treatment in vacuum at 1790°F. One of the purposes of this annealing treatment was to relieve as completely as possible any stresses present in the alloys prior to creep testing. The anneal was carried out on the creep specimens in the final machined and centerless ground condition.

TESTING ARRANGEMENT

Some description of the testing equipment is necessary. The general principles are similar to those described by one of the present authors some years ago¹² except that dead loading was substituted for spring loading.

Furnace Construction

A sectional view of the furnace is shown in Fig. 1 and a photograph of the general assembly is included as Fig. 2. Attention may be called to a few salient details. The samples (1) are enclosed in a nickel block (4) which rests upon the lower insulating brick (6) and supports the upper insulating brick (5). The purpose of this nickel block is to promote uniformity of heat distribution over the gauge length of the specimen.

The furnace holds six specimens and a standard. The standard is at the center of the furnace and the six specimens are arranged symmetrically around it. This standard is an unreduced length of the alloy with 4.83 per cent Cr and is only slightly stressed by spring loading. The aim is to provide a correction by means of this standard for any minute dimensional

changes not attributable to creep. Gauge readings on this standard are referred to an arbitrary value measured on the same gauge at the beginning of the test period and deviations from this arbitrary value are added to or subtracted from the readings on the specimens under test. The actual creep-test sample consists of a $\frac{5}{16}$ -in. diameter bar, 10 in. long and threaded both ends. The gauge section, 4 in. long, is reduced accurately to 0.125-in. diameter by centerless grinding.

All specimens are held by extension members (8 and 9), which screw on to each end of the specimen. The lower extension member is anchored to the base plate of the furnace and the upper extension member protrudes through the top of the furnace and above the reference plate (10).

The furnace windings consist of the conventional main, upper, and lower auxiliary coils. Together with the use of nickel block, this permitted the maximum temperature variation over the gauge length of the specimen to be held to 2°F. Constancy of temperature is maintained by control of the main heating circuit using a sensitive photoelectric potentiometric control unit.

The furnace assembly is in a constant-temperature room, where the temperature is maintained constant to $\pm 1.5^\circ\text{F}$. by an air-conditioning unit.

Measurement of Deformation

Three seatings are inserted in the reference plate in symmetrical fashion about each top extension member, for the purpose of seating the measuring device. Each set of seatings consists of two conical points and a flat contact area. These match a hollow cone, a V-cut, and a conical point, respectively, on the feet of the measuring device. This provides a means of setting the measuring gauge on the reference plate in the same fixed position for each reading. The reference plate is fixed with respect to the lower stationary ends of the specimens

by three Invar rods outside of the furnace, which are attached to the base plate.

A Starrett gauge is used for measuring changes in length. Readings can be estimated to the nearest 0.00001 in. and reproducibility is of the order of 0.00005.

Application of Loads

The load is applied to the specimen by a lever system (II, Fig. 1). The lever ratio is such as to give an advantage of 6 to 1 for added loads. The lever is attached to the upper extension member between the top of the furnace and the reference plate. When weights are being added to the hanger at the end of the lever arm, the latter is brought to a stop by a screw, so that the weights can be added without exerting shock on the specimen. The load may be applied upon releasing the lever arm by simply turning down the screw so that it makes contact no longer with the arm.

METHOD OF TESTING

The method employed is a step-up loading test, which has the advantage of conserving time and material. The initial load applied to the samples is 5000 lb. per sq. in., and after this load has been held for 600 to 700 hr. while the time vs. extension relationships are established, the load is stepped up to 7500 lb. per sq. in. and again held for 600 to 700 hr.

This is the general procedure, then, to step up the load by increments of 2500 lb. per sq. in. and hold under the load in question for the stated time, which seemed to be ample to establish the creep rate in the so-called second stage of creep where the time-extension plot is approximating a straight line. Such loading was continued until either the sample failed or had deformed to such a degree that further loading would be useless.

The value of this method of loading has been established and discussed in a previous investigation.¹²

The creep behavior of these alloys was investigated most completely at 800°F., but sufficient work was conducted at 1000°F. to establish the significance of temperature.

PRESENTATION OF DATA

Tests at 800°F.

The total deformation readings under a given loading were taken twice daily and plotted against time of test. In most instances a steady rate of deformation was entered into after some 100 to 200 hr. of test and continuing the test period to 600 to 700 hr. allowed time to establish this rate of deformation. Then the load was increased and the procedure repeated for the new loading, in order to again determine deformation rate. In this manner the rate was established for each load increment to which the test bar was subjected. These relationships between deformation expressed as inches per inch, loads in pounds per square inch, and time in hours, were assembled into composite diagrams for the entire testing life of any given sample. The diagrams for the tests at 800°F. are presented as Figs. 3 and 4, the purpose of Fig. 4 being to show the results for the three stronger alloys on extended scale. In each case the dotted line represents the behavior of commercially pure ferrite.

On each of these plots there has been included a schematic representation of the slopes (elongation vs. time) associated with various creep rates per 1000 hr. This permits ready evaluation of the order of magnitude of the various sections of the elongation-time curves in terms of creep rate.

The actual creep rates at the various stresses investigated for the several binary alloys at this temperature are presented in Table 2.

The considerable amount of data accumulated at 800°F. over a period of several

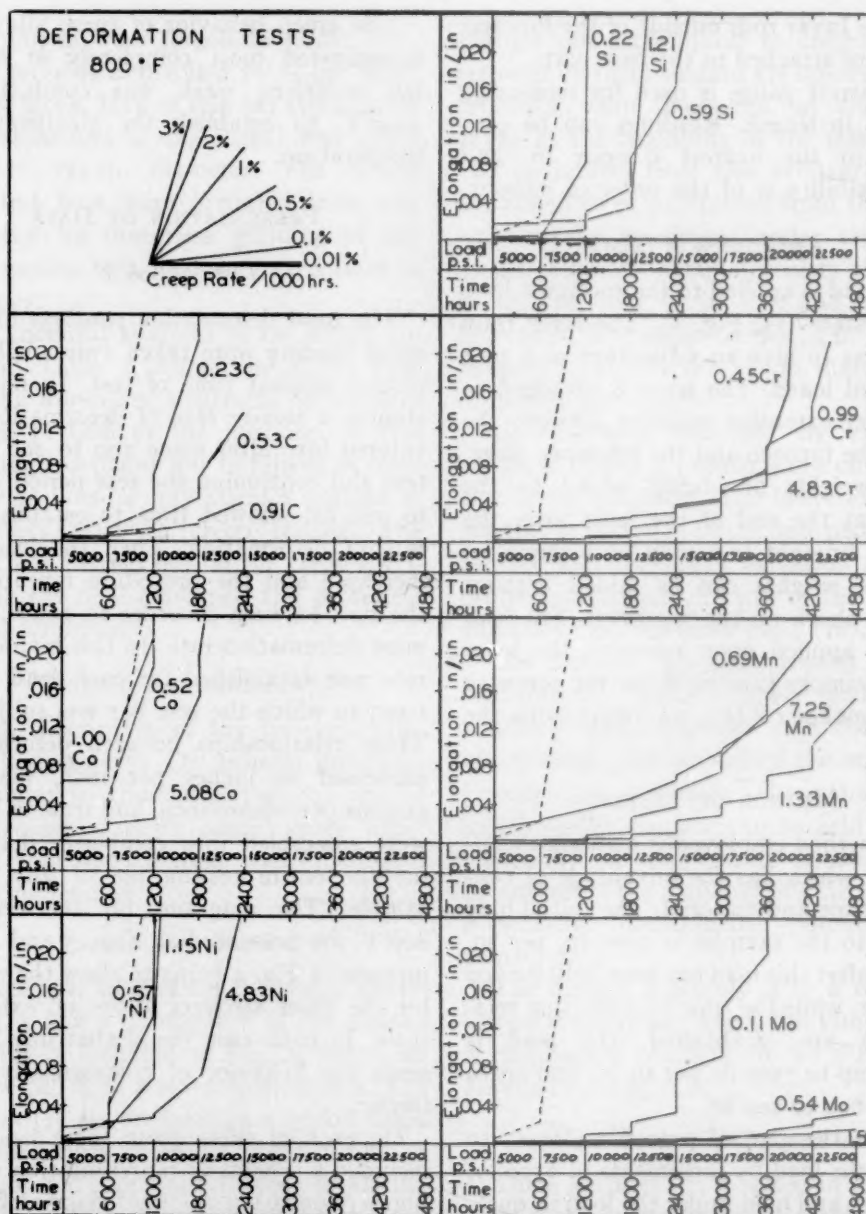


FIG. 3.—EFFECT OF VARIOUS ELEMENTS ON DEFORMATION CHARACTERISTICS OF IRON AT 800°F.

It should be pointed out that the strain increments accompanying periodic stress increments are not indicative of initial elongation in the test sample. These strain increments represent a summation of plastic and elastic strain in the gauge plus elastic strain in the upper and lower extension members and in the shank sections of the test bars. The slope of the creep curves alone is characteristic of the alloy under test.

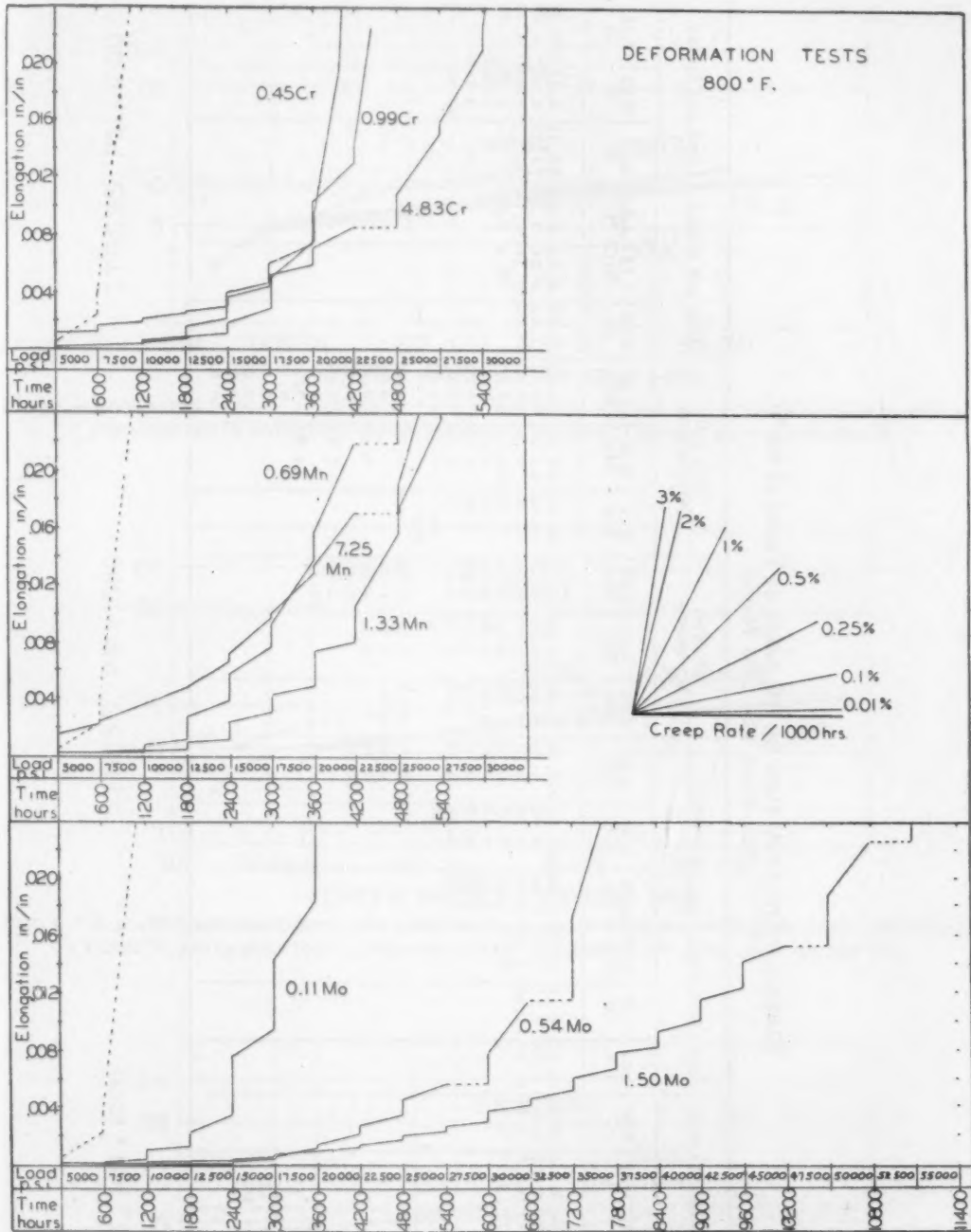


FIG. 4.—EFFECT OF CHROMIUM, MANGANESE AND MOLYBDENUM ON DEFORMATION CHARACTERISTICS OF IRON AT 800°F.
See note under Fig. 3.

TABLE 2.—Creep-rate Data for All Alloys as Tested at 800°F.
PER CENT PER 1000 HOURS

Load, Lb. per Sq. In.	Iron and Carbon			Iron and Cobalt			Iron and Chromium			Iron and Manganese			Iron and Molybdenum			Iron and Nickel			Iron and Silicon		
	0.23 C	0.53 C	0.91 C	0.52 Co	1.00 Co	5.08 Co	0.45 Cr	0.99 Cr	4.83 Cr	0.69 Mn	1.33 Mn	7.25 Mn	0.11 Mo	0.54 Mo	1.50 Mo	0.57 Ni	1.15 Ni	4.83 Ni	0.22 Si	0.59 Si	1.21 Si
5,000	0.08	<0.01	0.03	0.03	0.11	0.12	0.02	<0.01	<0.01	0.01	<0.01	0.17	<0.01	<0.01	<0.01	0.05	0.05	<0.01	<0.01	0.04	<0.01
7,500	4.54	0.34	0.08	0.07	2.32	2.16	0.10	0.01	0.02	0.03	<0.01	0.18	0.04	<0.01	<0.01	1.64	0.91	0.20	1.35	0.08	0.01
10,000	62.0	2.16	0.36	0.16	31.16	11.00	1.42	0.01	0.02	0.07	0.08	0.20	0.06	0.01	0.01	20.00	11.31	0.74	12.73	0.41	0.20
12,500	12,500	46.77	5.00	1.13			10.72	0.05	0.08	0.05	0.20	0.29	0.16	<0.01	<0.01		86.4	5.02		1.50	11.25
15,000							0.13	0.08	0.07	0.32	0.09	0.35	0.23	0.01	0.02					3.55	
17,500							0.20	0.18	0.07	0.54	0.14	0.45	0.80	0.06	0.01					9.10	
20,000							2.24	0.44	0.21	1.06	0.30	0.57	2.10	0.09	0.03					93.00	
22,500							2.50				0.78		400	0.13	0.03						
25,000									0.27	2.68	1.66	0.89	app.	0.18	0.04						
27,500									0.53	15.40	5.57	1.21			0.05						
30,000									1.00		14.55	1.90		0.57	0.06						
32,500									10.34			2.40			0.08						
35,000												3.88		1.52	0.09						
37,500												10.35			0.06						
40,000														14.63	0.10						
42,500															0.11						
45,000															0.15						
50,000															0.49						
55,000															0.61						
60,000															0.81						

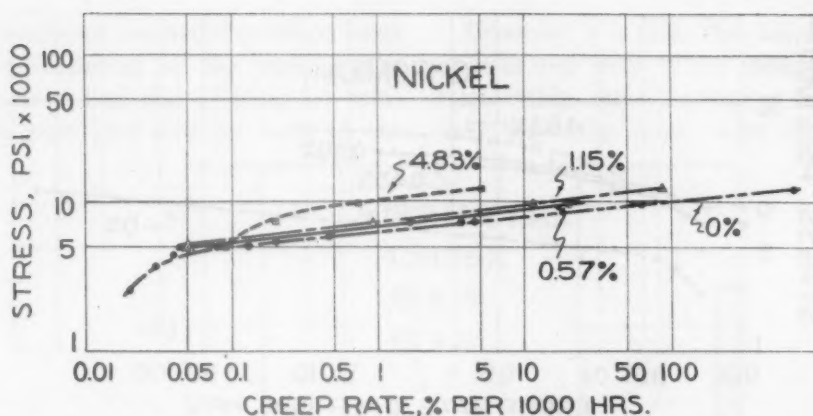


FIG. 5.—LOGARITHMIC PLOT SHOWING RELATION BETWEEN STRESS AND STRAIN RATE FOR NICKEL FERRITIC SOLID SOLUTIONS COMPARED WITH COMMERCIAL PURE IRON AT 800°F.

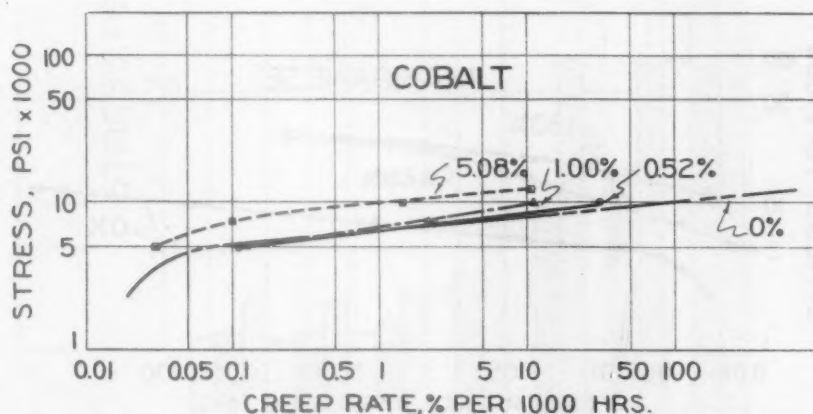


FIG. 6.—LOGARITHMIC PLOT SHOWING RELATION BETWEEN STRESS AND STRAIN RATE FOR COBALT FERRITIC SOLID SOLUTIONS COMPARED WITH COMMERCIAL PURE IRON AT 800°F.

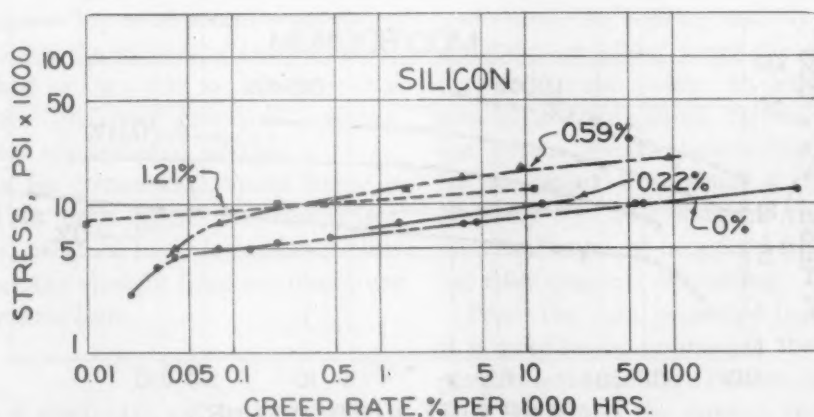


FIG. 7.—LOGARITHMIC PLOT SHOWING RELATION BETWEEN STRESS AND STRAIN RATE FOR SILICON-FERRITE SOLID SOLUTIONS COMPARED WITH COMMERCIAL PURE IRON AT 800°F.

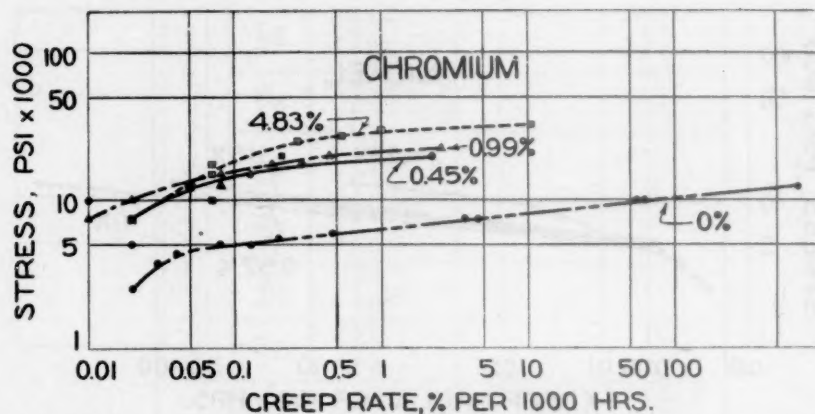


FIG. 8.—LOGARITHMIC PLOT SHOWING RELATION BETWEEN STRESS AND STRAIN RATE FOR CHROMIUM-FERRITE SOLID SOLUTIONS COMPARED WITH COMMERCIAL PURE IRON AT 800°F.

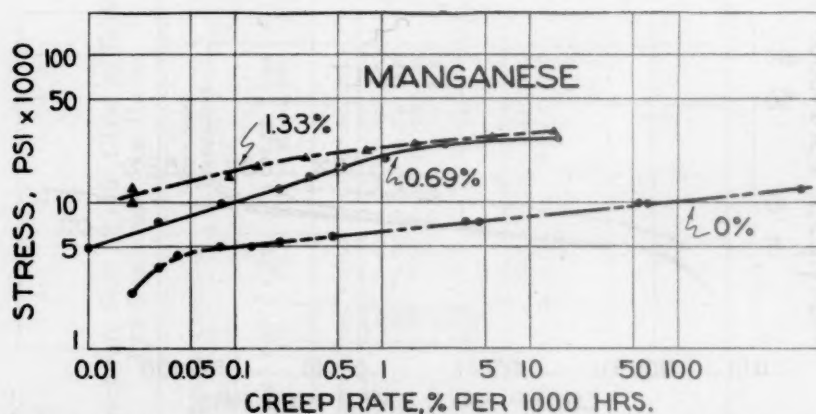


FIG. 9.—LOGARITHMIC PLOT SHOWING RELATION BETWEEN STRESS AND STRAIN RATE FOR MANGANESE FERRITIC SOLID SOLUTIONS COMPARED WITH COMMERCIAL PURE IRON AT 800°F.

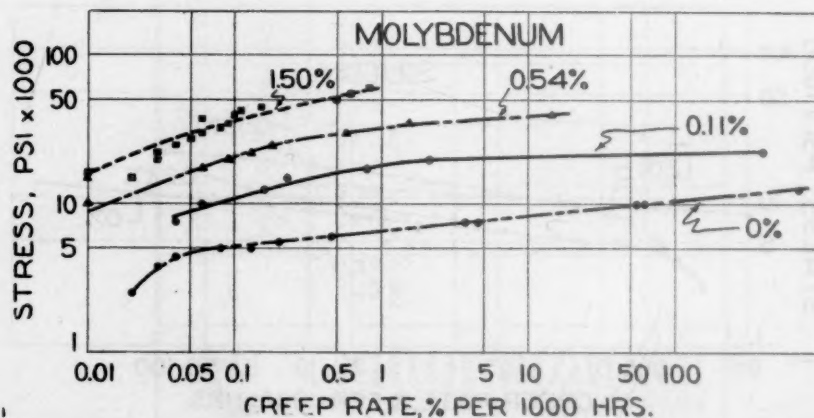


FIG. 10.—LOGARITHMIC PLOT SHOWING THE RELATION BETWEEN STRESS AND STRAIN RATE FOR MOLYBDENUM-FERRITE SOLID SOLUTIONS COMPARED WITH COMMERCIAL PURE IRON AT 800°F.

years provides an unusually excellent basis for an examination of the relationships between stress and rate of creep for commercially pure iron and for each of the

However, it is clear that where linearity persists over most of the stress-strain rate relationship some curvature is noted at very low creep rates under conditions of

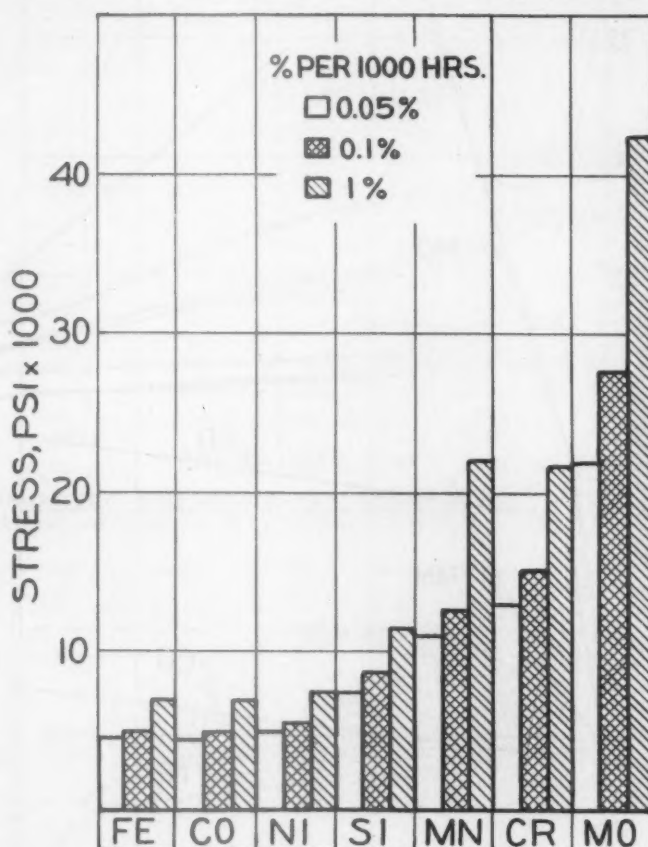


FIG. 11.—STRESSES CAUSING INDICATED CREEP RATES AT 800°F. IN FERRITIC SOLID SOLUTIONS CONTAINING ONE PER CENT BY WEIGHT OF EACH ELEMENT.

binary alloys. The more recently published researches on the subject of creep indicate the method of log stress vs. log creep rate to be the preferred graphical analysis. Such plots are included as Figs. 5 to 10. The data for commercially pure ferrite is included in each figure for comparison purposes. Most of these logarithmic plots are essentially straight lines and hence are of the general form:

$$y = mx^n \quad [13]$$

where y = creep rate, per cent per hour

x = stress in lb. per sq. in.

m and n are constants.

low stress. In others, notably with the molybdenum alloys when the creep rates obtained even with moderately high stresses are quite small, the relationship is not linear. These observations are similar to recent deductions of Nadai and McVetty¹⁴⁻¹⁶ and indicate that further information might be gained from employing their concepts of plotting.

From the data presented in this paper, it is possible to summarize the results in graphic fashion. Fig. 11 shows in the form of a bar graph the stresses causing 0.05, 0.1 and 1 per cent creep per 1000 hr. at 800°F. for an addition of one per cent by

weight of each of the elements in question. Such information was obtained by interpolating the stresses causing these three

6 that the presence of even 5 weight per cent (approximately) of either of these two elements in solid solution has but little

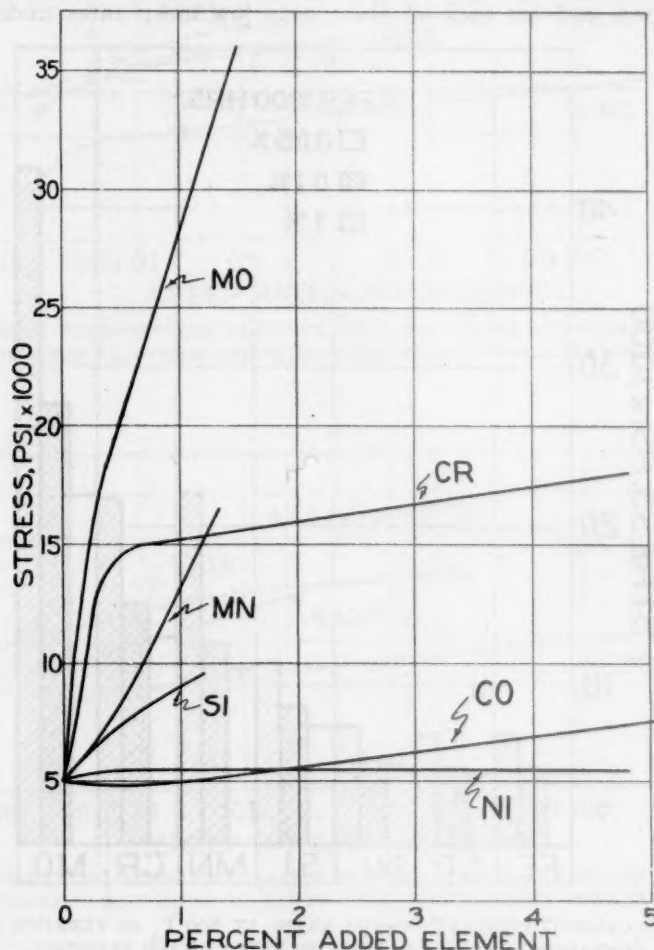


FIG. 12.—STRESSES NECESSARY TO CAUSE 0.1 PER CENT CREEP PER 1000 HOURS FOR EACH ELEMENT INVESTIGATED.

Interpolation at one weight per cent added element furnishes part of data plotted in Fig. 11.

rates of creep from each individual log-log plot (Figs. 5 to 10) and then replotting these stresses against the weight percentages of added alloying elements. From such working plots (Fig. 12 for the stresses necessary to cause 0.1 per cent creep per 1000 hr.) it was possible to interpolate the stresses indicated in Fig. 11.

Thus it is at once evident that the addition of either nickel or cobalt up to one per cent by weight is ineffective in strengthening commercially pure ferrite against creep at 800°F. It will be noted from Figs. 5 and

effect in raising the creep strength of unalloyed ferrite.

The addition of one per cent silicon has a moderate strengthening action, since it raises the creep strength of the iron by approximately 2500 to 4500 lb. per sq. in. The effect of this amount of silicon appears comparable to that of 5 per cent nickel or cobalt (Figs. 5, 6 and 11).

Chromium and manganese are quite comparable in their action (Fig. 11) and are definitely more effective than silicon. The alloy containing approximately 5 per

cent chromium showed a further definite improvement above that effected by an addition of 1 per cent of the element. This is apparent from Fig. 8.

To further emphasize the contrast between these six elements, a semilogarithmic plot has been included as Fig. 13, in which stress is represented on a regular coordinate

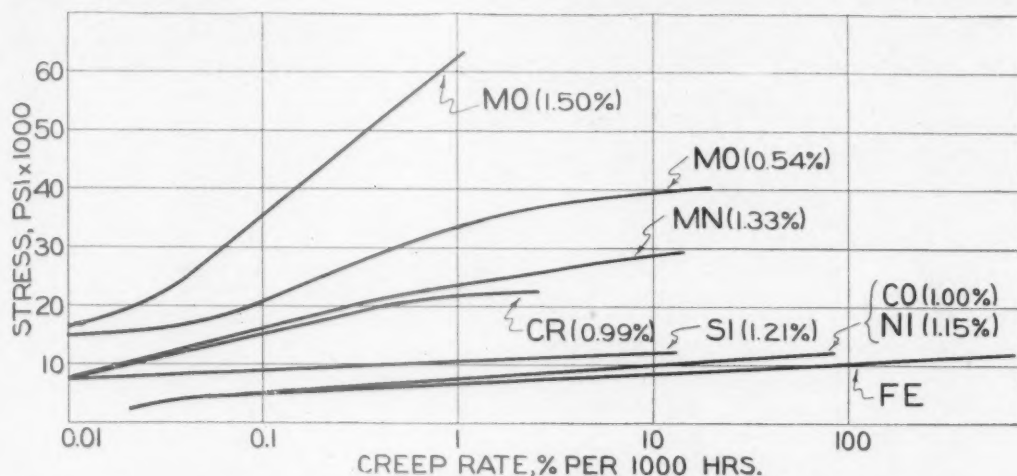


FIG. 13.—SEMILOGARITHMIC PLOT SHOWING COMPARISON BETWEEN BEHAVIORS OF ELEMENTS IN FERRITIC SOLID SOLUTION AT APPROXIMATELY ONE WEIGHT PER CENT.

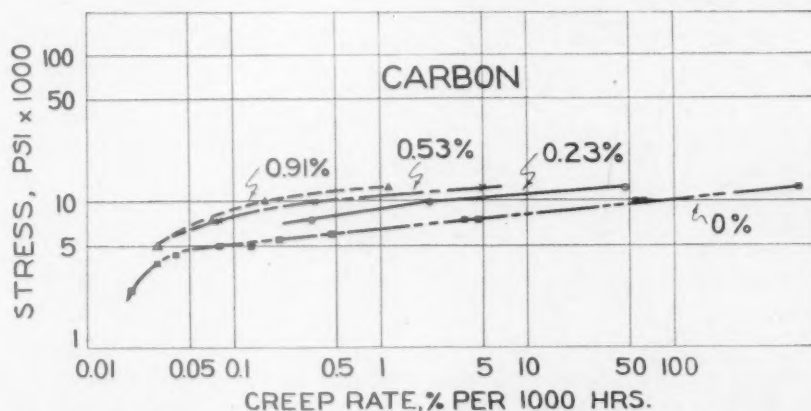


FIG. 14.—LOGARITHMIC PLOT SHOWING RELATION BETWEEN STRESS AND STRAIN RATE FOR IRON-CARBON ALLOYS COMPARED WITH COMMERCIAL PURE IRON AT 800°F.

Molybdenum additions exhibit a profound effect on raising the creep strength of ferrite at 800°F., since as little as 0.11 per cent of this element accomplished almost the same result as one per cent of either chromium or manganese (Figs. 10 and 11). Further additions of molybdenum to the total amount of 0.54 and 1.50 per cent have a still more striking effect being far superior to any of the other alloys tested.

scale against creep rate on a logarithmic scale. These curves illustrate the behavior of alloys with approximately one weight per cent of added element (actually 0.99 per cent Cr, 1.5 per cent Mo, 1.33 per cent Mn, 1.21 per cent Si, 1.15 per cent Ni, and 1.00 per cent Co). The relative effects of these elements are again clearly evident.

These results at 800°F. seem to confirm previous published results in some cases and to contradict them in others. It is

evident that nickel, which associates itself with the ferritic phase, does not strengthen this phase in creep to any extent. Cobalt acts quite similarly to nickel. Silicon ap-

improvement in creep strength resulting from additions of molybdenum is well known, but in commercial steels there is a tendency to attribute the major propor-

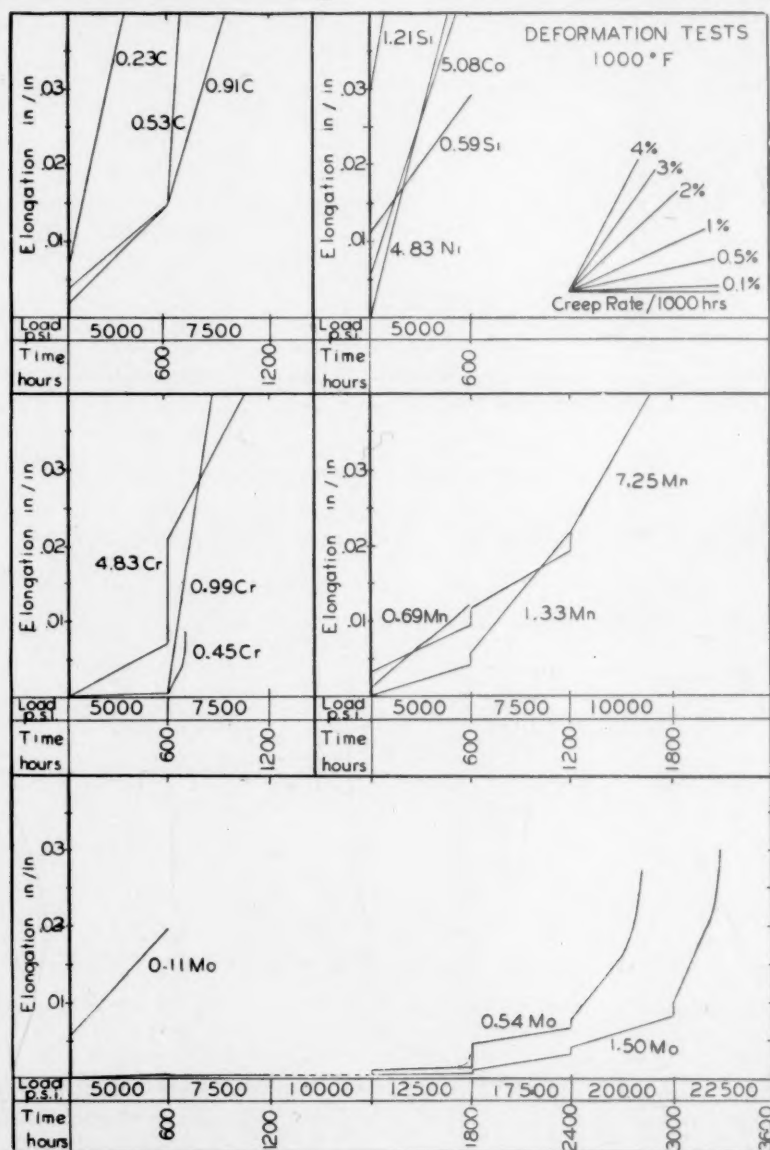


FIG. 15.—EFFECT OF VARIOUS ELEMENTS ON DEFORMATION CHARACTERISTICS OF IRON AT 1000°F.

pears to have a definite, although moderate strengthening action in contrast with some published remarks.³ On the other hand, the present results confirm the work of Cross and Lowther.⁹ The definite strengthening action of chromium and manganese appears also to contradict previous results.³ The

tion of its effect to its relation to the behavior of the carbide phase. While molybdenum is a carbide-forming element, the present investigation shows that even as small an amount as 0.1 per cent has a pronounced strengthening action on the ferritic phase.

Iron-carbon Alloys.—While iron-carbon alloys cannot be included in a general analysis of ferrite strengthening at elevated temperatures by elements in solid solution, the behavior of such alloys is of paramount importance. Accordingly the results of some studies at 800°F. on unalloyed steels containing 0.23, 0.53, and 0.91 per cent carbon (see Table 1) are included here. The behavior of these alloys is indicated in Fig. 14.

Jenkins and co-workers¹¹ regarding the effect of carbon in this temperature range.

Tests at 1000°F.

The results at 1000°F. are presented in Fig. 15 and Table 3. These results are not so comprehensive as those at 800°, but they do provide some further interesting points regarding the behavior of the alloys. It was found that the resistance of com-

TABLE 3.—*Creep-rate Data for All Alloys as Tested at 1000°F.*
PER CENT PER 1000 HOURS

Load, Lb. per Sq. In.	Iron	Iron and Carbon			Iron and Cobalt			Iron and Chromium		
		0.23 C	0.53 C	0.91 C	0.52 Co	1.00 Co	5.08 Co	0.45 Cr	0.99 Cr	4.83 Cr
5,000	430	9.85	2.14	1.83			6.75	0.04	0.09	1.16
7,500			36.4	8.32				4.43	16.5	4.42

Load, Lb. per Sq. In.	Iron and Manganese			Iron and Molybdenum			Iron and Nickel			Iron and Silicon		
	0.69 Mn	1.33 Mn	7.25 Mn	0.11 Mo	0.54 Mo	1.50 Mo	0.57 Ni	1.15 Ni	4.83 Ni	0.22 Si	0.59 Si	1.21 Si
5,000	1.81	0.61	1.03	2.43	0.05	0.05			8.76		3.00	12.16
7,500					<0.01	0.01						
10,000												
12,500					0.05	0.01						
17,500					0.34	0.14						
20,000					2.88	0.69						
22,500						5.14						

At this temperature, at least, progressive increase of carbon content up to 0.91 per cent has a continuous strengthening action on the commercially pure iron. It is interesting to note further that the strengthening action of carbon approximates that of silicon, but is inferior to chromium, manganese, and molybdenum (compare Fig. 14 with Figs. 5 to 10). Thus the action of the carbide phase, which was initially in the lamellar form resulting from a prior annealing treatment, is not so favorable as that of any of the latter three elements in solid solution in ferrite. The results for the iron-carbon alloys are in good agreement with the conclusions of

commercially pure ferrite to creep at 1000° is extremely small at the stresses investigated, hence no indication of its behavior is given in Fig. 15. However, Table 3 shows its high rate of deformation at a stress of 5000 lb. per sq. in. Generally the molybdenum alloys were the only binary solid solutions of this group to exhibit noteworthy resistance to plastic flow at this temperature. The manganese and chromium alloys showed fair creep resistance at 5000 lb. per sq. in. but when loaded to 7500 lb. per sq. in. or higher they deformed at a rapid rate. As may be anticipated from the data for 800°F., all of the alloys in the nickel, cobalt, or silicon group exhibited

very low creep resistance, comparable to unalloyed ferrite at this higher temperature.

In view of the high creep rates of the alloys at 1000°F., it is not possible to show

stant stress levels at 800°F. and 1000°F., while Fig. 16 shows the trend of change in stress as a function of temperature for 0.1 per cent and 1.0 per cent creep rate.

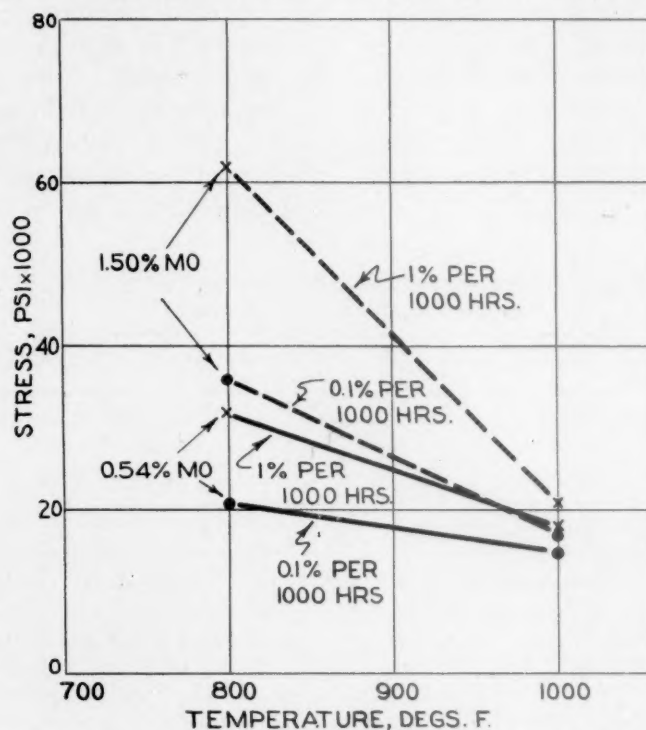


FIG. 16.—TREND OF EFFECT OF TEMPERATURE ON CREEP RATE FOR TWO MOLYBDENUM ALLOYS.

any comprehensive comparison of the significance of temperature. However, an attempt has been made to indicate this

TABLE 4.—Comparison of Creep Rates at 800° and 1000°F. for Three of the Alloys PER CENT PER 1000 HOURS

Stress, Lb. per Sq. In.	0.99 Cr.		1.33 Mn		1.50 Mo	
	800°F.	1000°F.	800°F.	1000°F.	800°F.	1000°F.
5,000	<0.01	0.09	<0.01	0.61	<0.01	0.05
7,500	0.01	16.5	<0.01	3.45	<0.01	0.01
10,000	0.02		0.02		<0.01	
12,500	0.08		0.02		<0.01	0.01
17,500	0.18		0.14		0.01	0.14
20,000	0.44		0.30		0.03	0.69
22,500	2.56		0.78		0.03	5.14

significance in Table 4 and in Fig. 16. Table 4 embraces a comparison of the creep rates obtained in some of the alloys at con-

Iron-carbon Alloys.—None of the iron-carbon alloys showed any marked resistance to creep at this temperature. The alloys with 0.53 and 0.91 per cent carbon behaved rather similarly and responded somewhat better than the alloy with 0.23 per cent carbon. Again the results seem to be in definite agreement with those of Jenkins and his co-workers as stated in the literature review.

DISCUSSION OF DATA

Binary Solid Solutions

The actual and relative behaviors of the six elements under investigation have been portrayed in Figs. 5 through 10. Comments regarding their strengthening actions were offered in the preceding section and a

graphical comparison has been made in Figs. 11 and 13.

Work-hardening and temperature-softening opposing work-hardening are recognized generally to be two of the most important properties in determining the creep behavior of metals and alloys. Gillett¹⁷ has stated: "The most important phenomenon in the creep of a stable material is the development or lack of development of strain-hardening under the tiny deformation rate and the temperature obtaining. Creep curves are most sensitive indicators of strain hardening, and probably the only sufficiently sensitive indicators." The profound effects of minute amounts of deformation on increasing resistance to plastic flow have also received experimental analysis by one of the present authors.¹⁸ It is of interest to note Gillett's reference to minute deformation rate and his further reference to temperature-softening as crystal relief annealing. There is too often an inclination to use loosely the term "recrystallization" with respect to temperature-softening in the process of creep. Gillett has indicated that frequently there is no evidence of recrystallization even where the creep curves indicate progressive removal of strain-hardening by annealing concomitant with an amount of deformation far beyond that allowable in service.

The lack of apparent change in structure has been noted frequently as recorded in some of the investigations of one of the present authors^{12,19} Furthermore, the fact that certain property changes can occur in the annealing of strain-hardened metals and alloys without accompanying change in microstructure is well known under the nomenclature of recovery.²⁰ In view of these remarks, it is not surprising that no definite microstructural evidence was found regarding the work-hardening and temperature-softening occurring during creep of these alloys. Definite evidence of such structural changes has been recorded, how-

ever, where creep tests have been carried out in vacuum on polished specimens.^{11,21} The effect of the various elements with regard to their strengthening action on the creep behavior of commercially pure ferrite seems to be rather well related to their respective effects in the annealing response of cold-rolled iron binary alloys.

In a separate study² it was shown, for materials work-hardened by cold-rolling, that certain of these elements definitely raised the temperature of softening as compared with the base line ferrite. It is these same elements that strengthen ferrite in creep. Thus, it appears that although the type and degree of deformation is different in these cold-rolling studies as contrasted with creep, the softening temperatures of the cold-rolled alloys in relation to the unalloyed ferrite may be approximate indicators of creep behavior. The same has held true for tests on additional ferrite solid solutions as yet unpublished.²² Generally it may be said that for 5 per cent reduction in thickness of unalloyed ferrite by cold-rolling, the softening temperature (based on 1 hr. annealing periods) was found to be 870°F. This temperature was relatively unaffected by the presence of nickel or cobalt in solid solution, slightly raised by silicon and definitely increased by chromium, manganese, and molybdenum additions. The latter three elements were also most effective in their strengthening action with regard to creep.

In view of the recognized significance of grain size in some materials in creep testing, an effort was made to establish a uniform A.S.T.M. grain size of 4 to 5 in all of the creep bars. However, because of prior processing, the grain sizes obtained ranged from 1 to 7 (Table 5) and in each instance the grain size was finest with the highest alloy content. The only exception was noted in the silicon alloys. The effect of grain size has been recognized and related particularly to an ill-defined term called equicohesive temperature. Thus, in refer-

ring to the effect of prior austenitic grain size in steels tested at 800°F. and above, data have been presented^{3,17} which indicate that grain-size effect may be large or negligible. Furthermore it appears that other factors such as melting practice may exert so much influence as to render impossible any clear statement on the role of grain size.

TABLE 5.—A.S.T.M. Grain Sizes of Ferritic Solid Solutions Prior to Testing

Alloy	Grain Size	Alloy	Grain Size
Iron.....	1		
0.52 Co.....	1	0.11 Mo....	3
1.00 Co.....	2½	0.54 Mo....	4½
5.08 Co.....	3	1.50 Mo....	6
0.45 Cr.....	1	0.57 Ni.....	1
0.99 Cr.....	2½	1.15 Ni.....	3
4.83 Cr.....	4½	4.83 Ni.....	7
0.69 Mn.....	2½	0.22 Si.....	1
1.33 Mn.....	6	0.59 Si.....	5
7.25 Mn.....		1.21 Si.....	1

Perhaps a recent study of the creep characteristics of copper²³ is more relevant to the present investigation. In this cited research Parker and Riisness found that variation in grain size had little influence under the particular testing conditions employed. Accordingly the authors feel that differences in behavior within a given alloy group are likely to be small with respect to any grain-size variation and that observed differences are related essentially to the strengthening action of the alloy. This conclusion can be confirmed directly if consideration is directed toward the behavior of molybdenum, chromium, and manganese alloys, compared with iron binaries containing nickel or cobalt. Thus with alloys having an approximately constant A.S.T.M. grain size No. 3, it may be noted that for a creep rate of 0.1 per cent per 1000 hr. at 800°F. an alloy with 0.11 per cent molybdenum approaches closely in its creep behavior to alloys with 0.99 per cent chromium or 0.69 per cent manganese, and all showed marked superiority

to alloys with 1.15 per cent nickel, or 1 or 5 per cent cobalt.

Reference must be made to the alloy with 7.25 per cent manganese. The extension-time behavior of this alloy was included in Figs. 3 and 4 but data were omitted from Fig. 9, since the structure was duplex or Widmanstätten in nature. It was considered that this structure was responsible for the relatively high creep resistance exhibited by the alloy. It is interesting to note, however, that the solid solutions containing 0.54 and 1.5 per cent molybdenum have superior creep properties.

The effect of a marked rise in test temperature, from 800° to 1000°F., on the resistance to deformation of all the binary alloys was to be anticipated. The profound decrease in strength of even the molybdenum alloys is well shown in Fig. 16, where the trend of stress-temperature relationship for 0.1 and 1 per cent creep rate per 1000 hr. is portrayed. However, this behavior correlates satisfactorily with the data presented in an earlier paper² on the effect of annealing the cold-rolled alloys on temperature-softening as revealed by the studies on change in hardness. Indeed, it would appear that the effect of temperature increments on decrease in creep resistance could be roughly predicted from the cited cold-working and temperature-softening studies. Thus molybdenum was shown to be quite effective in retarding softening at temperatures in the vicinity of 1000°F. and the same is true to lesser extent of chromium and manganese. This reaction to temperature is reflected in the fact that the molybdenum alloys retain a fair measure of creep resistance at 1000°F. even under fairly high loads (17,500 lb. per sq. in.), while the chromium and manganese alloys show a marked superiority in creep resistance at 5000 lb. per sq. in. load over those containing nickel, cobalt, or silicon.

Iron-Carbon Alloys.—The structures of the three iron-carbon alloys prior to testing

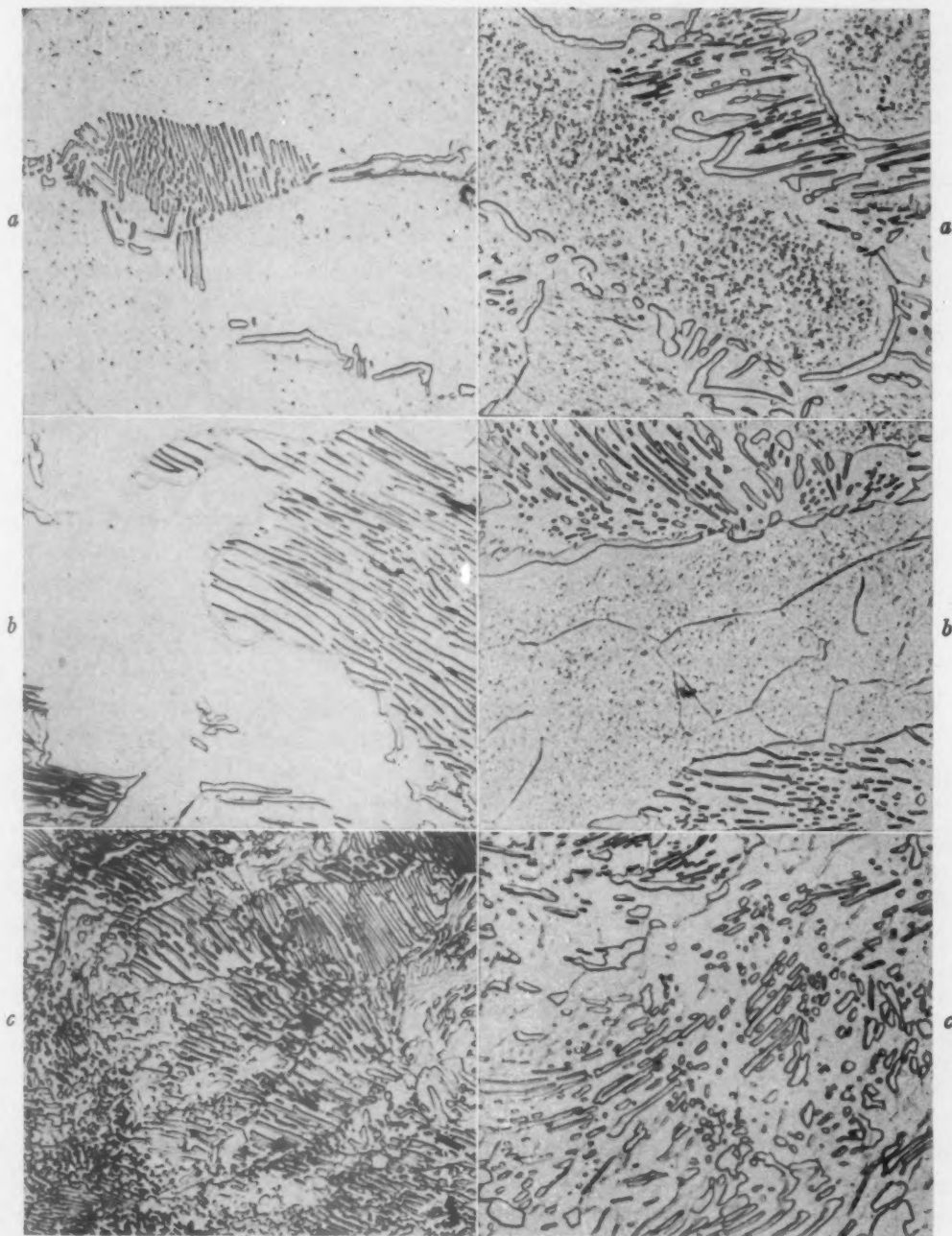


FIG. 17.

FIG. 18.

FIG. 17.—MICROSTRUCTURES OF IRON-CARBON ALLOYS AS ANNEALED AT 975°C. AND FURNACE-COOLED. $\times 750$.

a. 0.23 per cent C. *b.* 0.53 per cent C. *c.* 0.91 per cent C.

FIG. 18.—MICROSTRUCTURES OF IRON-CARBON ALLOYS AFTER CREEP TESTS AT 1000°F. $\times 750$.

a. 0.23 per cent C. 600 hours at 1000°F.

b. 0.53 per cent C. 920 hours at 1000°F.

c. 0.91 per cent C. 1200 hours at 1000°F.

are shown in Fig. 17. The lamellar structure in the pearlite areas was maintained throughout the testing period at 800°F. Comment has been made previously on the strengthening action at this temperature of increasing amounts of carbon.

When these alloys were tested at 1000°F., the structures showed a pronounced tendency to spheroidize, as is evident in Fig. 18. This reflects naturally in the decreased creep resistance of these alloys at this temperature. The alloy containing 0.53 per cent carbon showed some improvement as compared with the alloy with 0.23 per cent, but further increase of carbon to 0.91 per cent resulted in no further strengthening. The lack of structural stability leading to spheroidization is recognized as resulting in increased rates of creep.^{3,17}

SUMMARY

The results of this investigation permit several conclusions regarding the creep characteristics at 800° and 1000°F. of the ferritic phase in both the unalloyed and alloyed conditions.

It is evident that commercially pure ferrite possesses a relatively low creep resistance at 800°F. While nickel or silicon in solid solution raise the tensile strength and hardness of ferrite at room temperature, these elements have only minor effects on raising the resistance to deformation at elevated temperatures. Cobalt is similarly ineffective in raising the creep strength of ferrite but normal-temperature tensile strength and hardness of cobalt solid solutions are not markedly different from the values for the unalloyed iron. On the other hand, while chromium does not markedly influence the strength of ferrite at ordinary temperatures, this element definitely increases the creep strength of ferrite by its presence in solid solution. Manganese and molybdenum in solid solution are ferrite strengtheners, and also increase the creep resistance of ferrite.

Molybdenum has an especially pronounced action in the latter respect.

It would seem that any marked increase in tensile strength or hardness of ferrite as a consequence of the formation of solid solution is no definite criterion that creep strength will be improved similarly. However, experimental evidence has been presented to show that creep characteristics of various ferrite solid solutions are closely related to temperature-softening behavior of the cold-worked alloys. Thus, it was found in previously published work on annealing characteristics of cold-rolled binary ferrite solid solutions that molybdenum additions were markedly effective in opposing temperature-softening in the work-hardened alloys. Chromium and manganese were somewhat less effective in this respect, but were definitely more potent than silicon. Nickel and cobalt in solid solution had relatively little effect in modifying the temperature-softening characteristics of ferrite. This order of decreasing potency with respect to opposing temperature-softening in work-hardened alloys is the same as that obtaining in listing the elements with respect to their behavior on the creep strength of ferrite at 800°F. Molybdenum was the most potent element in raising creep strength, while nickel and cobalt at the other end of the list were relatively ineffective.

When the testing temperature was increased to 1000°F., the results were as might be anticipated from the results on temperature-softening. Thus it had been shown that molybdenum raised the softening temperature of the cold-worked ferrite solid solution well above 1000°F. The molybdenum alloys with 0.54 and 1.5 per cent molybdenum in solid solution were the only ones to retain any measure of creep resistance at this higher temperature. Although chromium and manganese were also effective in raising softening temperature, they were not nearly so effective as molybdenum in strengthening ferrite at

this temperature level. It may be noted, however, that molybdenum promotes solid solution hardening to a greater degree than either chromium, or manganese.

Some study was also devoted to investigating the effects of the addition of 0.23, 0.53 and 0.91 per cent carbon on the creep characteristics of ferrite. It was found that increasing the amount of carbon progressively increased the creep strength at 800°F. However, the increase in creep resistance produced by the presence of the carbide phase in lamellar distribution did not equal that produced by chromium, manganese or molybdenum in solid solution. When these iron-carbon alloys were tested at 1000°F. their creep resistance was little greater than that of single-phase ferrite and they were structurally unstable, showing definite tendency to spheroidize.

ACKNOWLEDGMENT

It is a pleasure to record the valuable assistance received in the development of this program of research. In particular should be mentioned Mr. P. H. Brace, Westinghouse Electric and Manufacturing Co., who prepared the binary alloy ingots and Dr. Miles K. Smith, Latrobe Electric Steel Co., who supervised fabrication of the alloys. Dr. C. H. Samans, formerly associated with the department of metallurgy at The Pennsylvania State College, was instrumental in collecting much of the experimental data reported in the paper.

REFERENCES

1. C. R. Austin: Effect of Elements in Solid Solution on Hardness and Response to Heat Treatment of Iron Binary Alloys. *Trans. Amer. Soc. Metals* (1943) **31**, 321-339.
2. C. R. Austin, L. A. Luini and R. W. Lindsay: Annealing Studies on Cold-rolled Iron and Iron Binary Alloys. *Amer. Soc. Metals Preprint* 40 (Oct. 1944). 35 pages.
3. D. K. Bullens: Steel and Its Heat Treatment, II, 336-370. New York, 1939. John Wiley and Sons.
4. Allowable Working Stresses for Ferrous Materials. *Mech. Eng.* (1938) **60**, 170-171.
5. Babcock and Wilcox Tube Co.: Properties of Carbon and Alloy Steel Tubing for High Temperature-High Pressure Service. *Tech. Bull.* No. 6-D. 1941.
6. R. F. Miller, R. F. Campbell, R. H. Aborn, and E. C. Wright: Influence of Heat Treatment on Creep of Carbon-Molybdenum and Chromium-Molybdenum-Silicon Steel. *Trans. Amer. Soc. Metals* (1938) **26**, 81-105.
7. A. E. White and C. L. Clark: Influence of Grain Size on the High Temperature Characteristics of Ferrous and Non-ferrous Alloys. *Trans. Amer. Soc. Steel Treat.* (1934) **22**, 1069-1098.
8. Timken Steel and Tube Co.: Digest of Steels for High Temperature Service, Nov. 1934.
9. H. C. Cross and J. G. Lowther: Study of Effect of Variables on the Creep Resistance of Steels. *Proc. Amer. Soc. Test. Mat.* (1940) **40**, 125-158.
10. M. J. Day and G. V. Smith: Iron Alloy Sealing. *Iron and Steel* (London) (Feb. 1944) 255-259.
11. C. H. M. Jenkins, G. A. Mellor, and E. A. Jenkinson: Investigation of the Behavior of Metals under Deformation at High Temperatures, II—Structural Changes in Carbon Steels Caused by Creep and Graphitization. *Jnl. Iron and Steel Inst.* (1942) **145**, 51, 86.
12. C. R. Austin and H. D. Nickol: Comparison of the Tensile Deformation Characteristics of Alloys at Elevated Temperatures. *Jnl. Iron and Steel Inst.* (1938) **137**, 177-221.
13. F. H. Norton: Creep of Steel at High Temperatures. New York, 1929. McGraw-Hill Book Co.
14. P. G. McVetty: Creep of Metals at Elevated Temperatures—The Hyperbolic Sine Relation between Stress and Creep Rate. *Trans. Amer. Soc. Mech. Engrs.* (1943) **65**.
15. A. Nadai and P. G. McVetty: Hyperbolic Sine Chart for Estimating Working Stresses of Alloys at Elevated Temperatures. *Proc. Amer. Soc. Test. Mat.* **43**, 735-748.
16. P. G. McVetty: Interpretation of Creep Test Data. *Proc. Amer. Soc. Test. Mat.* (1943) **43**, 707-734.
17. H. W. Gillett: Some Things We Don't Know About the Creep of Metals. *Trans. A.I.M.E.* (1939) **135**, 15-58.
18. C. R. Austin and J. R. Gier: Comparative Studies on Creep of Metals Using a Modified Rohn Test. *Trans. A.I.M.E.* (1934) **111**, 53-74.
19. C. R. Austin and C. H. Samans: Effects of Temperature of Pretreatment on Creep Characteristics of 18-8 Stainless Steel at 600° to 800°C. *Trans. A.I.M.E.* (1940) **140**, 459-474.
20. R. F. Mehl: Recrystallization. *Metals Handbook*, 1939 Ed., 207-213. Amer. Soc. Metals.
21. D. Hanson: The Creep of Metals. *Trans. A.I.M.E.* (1939) **133**, 15-57.
22. Unpublished research on iron binary alloys. The Pennsylvania State College.
23. E. R. Parker and C. F. Riisness: Effect of Grain Size and Bar Diameter on Creep Rate of Copper at 200°C. *Trans. A.I.M.E.* (1944) **156**, 117.

Recovery of Cold-worked Aluminum Iron as Detected by Changes in Magnetic Properties

BY J. K. STANLEY,* JUNIOR MEMBER A.I.M.E.

(Cleveland Meeting, October 1944)

It has been known for many years that the magnetic properties of a ferromagnetic material are very sensitive to internal strain. Any structure-sensitive property such as ferromagnetism, which is a function of the regularity of the atomic arrangement, and discontinuities such as grain boundaries must show deviations from an equilibrium state when the regularity of the lattice is disturbed. Experience has shown that such distortions have a marked effect on the magnetic properties of a ferromagnetic material. The purpose of this paper is to show the feasibility of using magnetic methods in detecting internal strains. More specifically, it will be shown how such properties as permeability, remanence, and coercive force change on cold-working of aluminum iron and how these magnetic properties change during the annealing below the recrystallization temperatures. This work was conducted for two reasons. One was the desire to see in what manner strains are relieved in aluminum iron at low temperatures—a subject of practical importance in soft magnetic materials—and the other was the feeling that a study of cold-working and strain relief might shed some light on our understanding of what takes place in the deformation of metals.

DEFINITION OF TERMS

It is necessary to define the terminology used in this paper because magnetic

nomenclature is usually unfamiliar to the metallurgist, and certain other terms, such as recovery, have been used ambiguously by metallurgists and others.

Magnetic terms are best explained by reference to the common hysteresis loop of ferromagnetic materials (Fig. 1). In Fig. 1 the coordinates are magnetic induction, B , (ordinate) and magnetizing force, H , (abscissa). The c.g.s. unit for the magnetic induction is the gauss, the number of flux lines per square centimeter, and the unit for the magnetizing force is the oersted, the number of lines of force per centimeter in air or vacuum.

If one starts with a completely demagnetized specimen and magnetizes it, a typical virgin magnetization curve beginning at the origin is obtained. This curve is also the locus of tips of a family of smaller hysteresis loops. From this curve it is to be noted that the induction is not proportional to the magnetizing force, and that it appears to approach a limiting induction called the saturation value, and does so for values of H of 1000 oersteds.

The ratio of the magnetic induction (gauss) to the magnetizing force (oersteds) is called permeability, μ . Thus

$$\mu = B/H$$

and if the magnetizing force H (oersteds) is specified as 10 or 100 oersteds, the permeability is written as μ_{10} or μ_{100} . This is the accepted notation, and will be used in this paper. The values of permeability for $H = 10$ or 100 are chosen as indices for

Manuscript received at the office of the Institute June 27, 1944. Issued as T.P. 1767 in METALS TECHNOLOGY, January 1945.

* Research Engineer, Research Laboratories, Westinghouse Electric and Manufacturing Co., East Pittsburgh, Pa.

comparison, as experience with soft magnetic materials has shown that these values yield useful information. The μ_{10} value has been useful because small com-

If the magnetizing force H of Fig. 1 is reduced from the maximum value, the new $B-H$ curve does not coincide with the virgin curve; instead, it traces out a

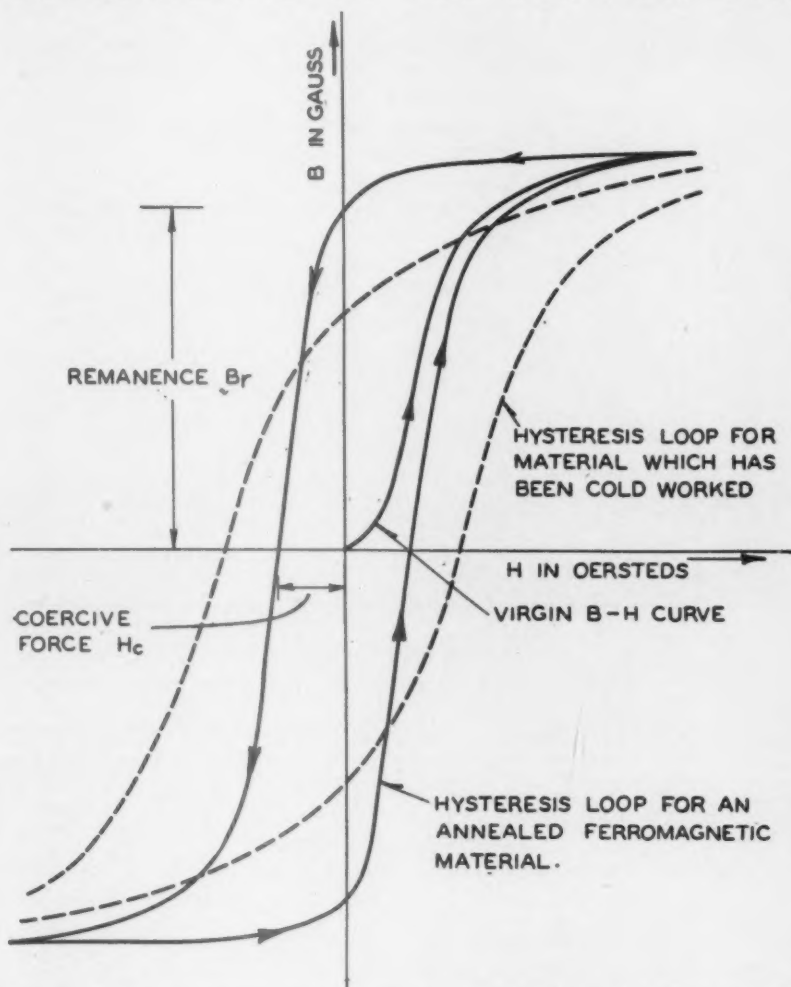


FIG. 1.—SCHEMATIC REPRESENTATION OF CHANGE IN HYSTERESIS LOOP ON COLD-WORKING.

mercial transformers operate at approximately this value and the μ_{100} value, along with the μ_{10} , serves as a measure of the degree of orientation.*

* It should be borne in mind that ferromagnetic materials are inherently anisotropic, both after cold-rolling and after recrystallization. In recent years considerable work has been done in the transformer industry to obtain a material with good preferred orientation. The changes in the permeabilities have been used as an index of the degree of orientation. The closer the value of μ_{100} approaches the saturation value for the given ferromagnetic material, the better is the degree of orientation. The goal is to attain single-crystal properties.

hysteresis loop. Even when the magnetizing force is zero, a certain residual induction B_r remains. Then, in order to reduce this residual induction, B_r , to zero, the magnetizing force must be reversed. The value of the reversed magnetizing force required to bring the induction to zero is called the coercive force, H_c . If the magnetization is carried from a maximum value in one direction to the maximum value in the opposite direction, and back again, the complete hysteresis loop is obtained.

The area of this loop is proportional to the amount of energy expended in carrying the magnetization through one cycle, and

row hysteresis loops. The presence of strains causes a distortion of the crystal lattice and enlargement of the loop and

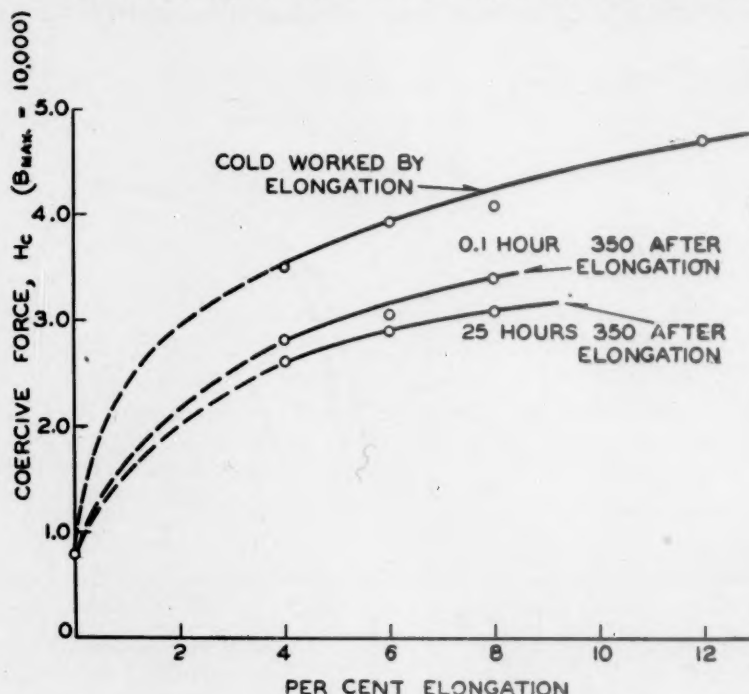


FIG. 2.—CHANGE IN COERCIVE FORCE ON COLD-WORK (ELONGATION).

TABLE 1.—Relief of Strain at Various Deformations at Constant Temperature

Sample	Elongation, Per Cent	Treatment	Permeability ^a		Coercive Force ^b H_c	Remanence ^b B_r	H for $B = 10,000$
			μ_{10}	μ_{100}			
11B	4	10 hr. 800°C.	1,530.0	178.5	0.82	8,500	1.84
		After elongation	575.0	179.0	3.5	3,150	20.0
		0.1 hr. (total) at 350°C.	765.0	178.5	2.83	4,200	15.5
		1.0 hr. (total) at 350°C.	780.0	177.0	2.78	4,200	15.0
		10.0 hr. (total) at 350°C.	830.0	175.0	2.68	4,600	14.0
11C	6	25.0 hr. (total) at 350°C.	840.0	174.5	2.62	4,600	13.9
		10 hr. 800°C.	1,540.0	179.5	0.8	8,500	1.76
		After elongation	469.0	177.5	3.9	2,800	24.7
		0.1 hr. (total) 350°C.	695.0	176.5	3.05	4,100	17.7
		1.0 hr. (total) at 350°C.	715.0	176.5	3.00	4,100	17.1
11D	8	10.0 hr. (total) at 350°C.	775.0	174.5	2.85	4,600	15.7
		25.0 hr. (total) at 350°C.	775.0	174.0	2.88	4,600	15.8
		10 hr. 800°C.	1,540.0	179.0	0.8	8,400	1.82
		After elongation	395.0	175.0	4.09	2,650	28.8
		0.1 hr. (total) at 350°C.	652.0	177.0	3.42	4,100	19.0
14A	12	1.0 hr. (total) at 350°C.	665.0	175.0	3.28	4,100	18.9
		10.0 hr. (total) at 350°C.	750.0	174.0	3.10	4,700	16.7
		25.0 hr. (total) at 350°C.	750.0	173.0	3.10	4,600	16.7
		10 hr. 800°C.	1,560.0	180.0	0.80	8,500	1.65
		After elongation	300.0	171.0	4.7	2,200	36.0

^a Permeability for $H = 10$ and $H = 100$ oersteds, respectively.

^b Coercive force in oersteds (H) and remanence in gauss (B_r) determined for $B_{max} = 10,000$.

might be looked upon as a measure of magnetic "friction."

A strain-free material has small or nar-

consequently a change in permeability, coercive force, and residual induction. This is schematically shown in Fig. 1. In other

words, a measure of good magnetic quality is low coercive force, and high permeabilities (μ_{10}) and remanence.

The word "recovery" as used in this

by a release of the load, and then immediately reapplied, the stress continues from the point of interruption. If, on the other hand, some time elapses, or if the specimen

TABLE 2.—*Recovery at Various Temperatures at Constant Strain*

Sample	Elongation, Per Cent	Treatment	Permeability ^a		Coercive Force ^b H_c	Remanence ^b B_r	H for $B = 10,000$
			μ_{10}	μ_{100}			
12B	6	10 hr. 800°C.	1,550	180.0	0.76	8,500	1.55
		After elongation	445	172.0	3.68	2,700	26.0
		0.1 hr. at 150°C.	450	176.0	3.71	2,700	25.8
		1 hr. (total) at 150°C.	455	173.0	3.70	2,700	25.6
		10 hr. (total) at 150°C.	460	176.0	3.66	2,800	25.2
14B	6	25 hr. (total) at 150°C.	485	182.0	3.65	2,900	24.0
		10 hr. 800°C.	1,560	181.0	0.79	8,500	1.63
		After elongation	435	172.0	3.85	2,700	26.8
		0.1 hr. at 250°C.	585	176.0	3.50	3,600	21.2
		1 hr. (total) at 250°C.	625	174.0	3.30	3,800	20.0
11C	6	10 hr. (total) at 250°C.	660	178.5	3.25	4,200	19.0
		25 hr. (total) at 250°C.	670	180.0	3.28	4,000	18.5
		10 hr. 800°C.	1,540	179.5	0.80	8,500	1.76
		After elongation	469	177.5	3.90	2,800	24.7
		0.1 hr. at 350°C.	695	176.5	3.05	4,100	17.7
15A	6	1 hr. (total) at 350°C.	715	176.5	3.00	4,100	17.1
		10 hr. (total) at 350°C.	775	174.5	2.85	4,600	15.7
		25 hr. (total) at 350°C.	775	174.0	2.88	4,600	15.8
		10 hr. 800°C.	1,560	181.0	0.75	8,600	1.53
		After elongation	455	175.0	3.68	2,700	26.1
15B	6	0.1 hr. at 450°C.	830	174.0	2.69	4,800	14.1
		1 hr. (total) at 450°C.	865	172.5	2.60	4,800	13.1
		10 hr. (total) at 450°C. (No 25-hr. anneal)	996	173.0	2.40	5,200	9.4
		10 hr. 800°C.	1,560	181.0	0.75	8,600	1.55
		After elongation	455	175.0	3.66	2,700	26.1
		0.1 hr. at 550°C.	1,090	179.5	2.20	5,300	8.56
		1 hr. (total) at 550°C.	1,185	177.5	2.00	5,500	6.88
		10 hr. (total) at 550°C.	1,382	177.0	1.80	6,100	4.88

^a Permeability for $H = 10$ and $H = 100$ oersteds, respectively.

^b Coercive force in oersteds (H_c) and remanence in gauss (B_r) determined for $B_{max} = 10,000$.

text is not to be confused with recrystallization, although Fetz¹ has used it in connection with changes in properties occurring on recrystallization of cold-worked metals. "Recovery" as used here is concerned only with changes in internal strain or structure as manifested by corresponding changes in magnetic properties. These internal changes cannot be observed microscopically. Recrystallization, on the other hand, is a process of formation of new grains in a deformed matrix by nucleation and growth² and is visible microscopically.

Recovery, sometimes called crystal recovery, often is referred to in connection with physical testing. The application of a load to metal specimens results in a characteristic stress-strain curve. If this curve is interrupted at some stress before failure,

is heated before the load is reapplied, the stress starts at a very low point. In such procedure the strain-hardening has been lost even though no recrystallization occurred. The specimen has undergone recovery.

Other properties, such as electrical resistivity, thermoelectric force and "spring-back,"* show variations during the recovery period. Mehl³ gives a good discussion of the phenomenon of recovery.

Recovery, in general, is considered a low-temperature phenomenon while recrystallization can be considered a high (relatively speaking) temperature phenomenon.

* Springback is the measure of the change of diameter of a cold-worked strip after it is removed from a mandrel.

Not all effects of cold-work are removed by recovery, as will be seen from the results of this investigation. (See Figs. 4, 5, and 6.)

by Smith and Wood,¹⁶ for example, it appears that diffraction patterns of pure iron can be used to detect recovery of a deformed lattice. In their work the fol-

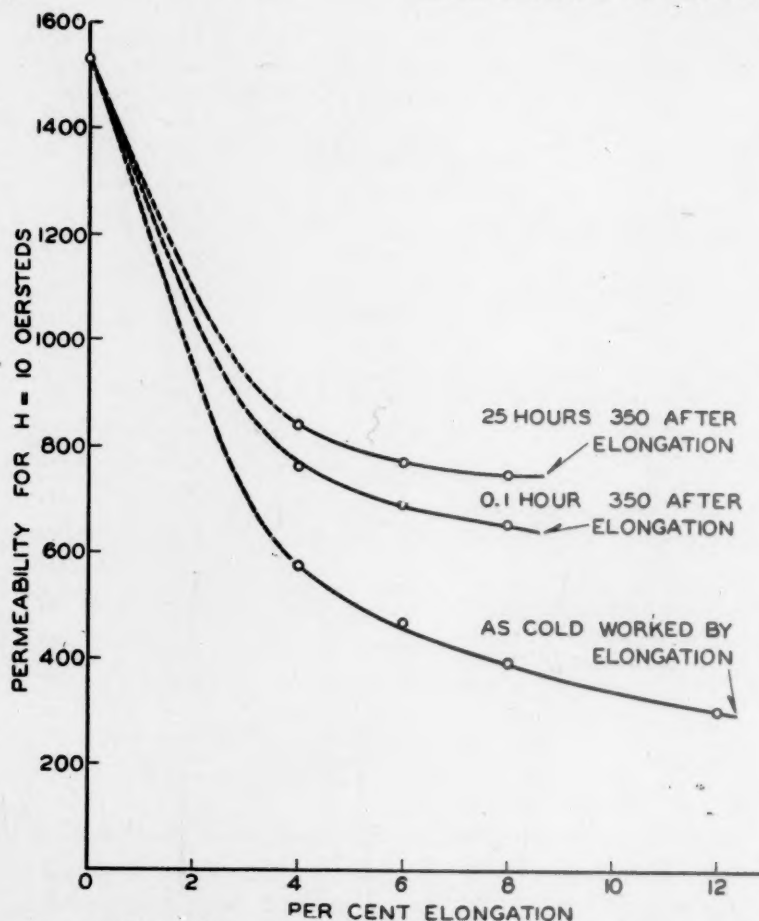


FIG. 3.—CHANGE IN MAGNETIC PERMEABILITY AT $H = 10$ ON COLD-WORK (ELONGATION) AND RECOVERY.

LITERATURE

Numerous methods have been used for the determination of internal strains and stresses but many of them are mechanical in nature⁴ and often suffer from limitations of one kind or another. Accurate data, however, are possible.^{5,6}

The internal-friction method has yielded useful information about cold-work and recovery because of the sensitivity of the method.⁷⁻¹³

X-ray methods,¹⁴ particularly with the back-reflection cameras, can be used to detect elastic strains. In the light of work

lowing back-reflection spectrometer data are of special interest:

Diameter of diffraction ring (310) under different conditions:

Initial state.....	6.68 cm.
Loaded 28,000 lb. per sq. in.....	6.61
After removal of load.....	6.73
Annealed 1 hr. 100°C.....	6.73
Annealed 1 hr. 200°C.....	6.73
Annealed 1 hr. 300°C.....	6.69

The work of Smith and Wood would mean then that lattice recovery in pure

iron occurs at relatively low temperatures and apparently is quite rapid.

Laue photograms of an aluminum crystal that had been elongated 15 per cent and annealed $\frac{1}{2}$ hr. at 400°C . did not show

study of strains. The work reported here will illustrate the use of such measurements.

EXPERIMENTAL PROCEDURE

Material chosen for these tests was an aluminum iron of the following composi-

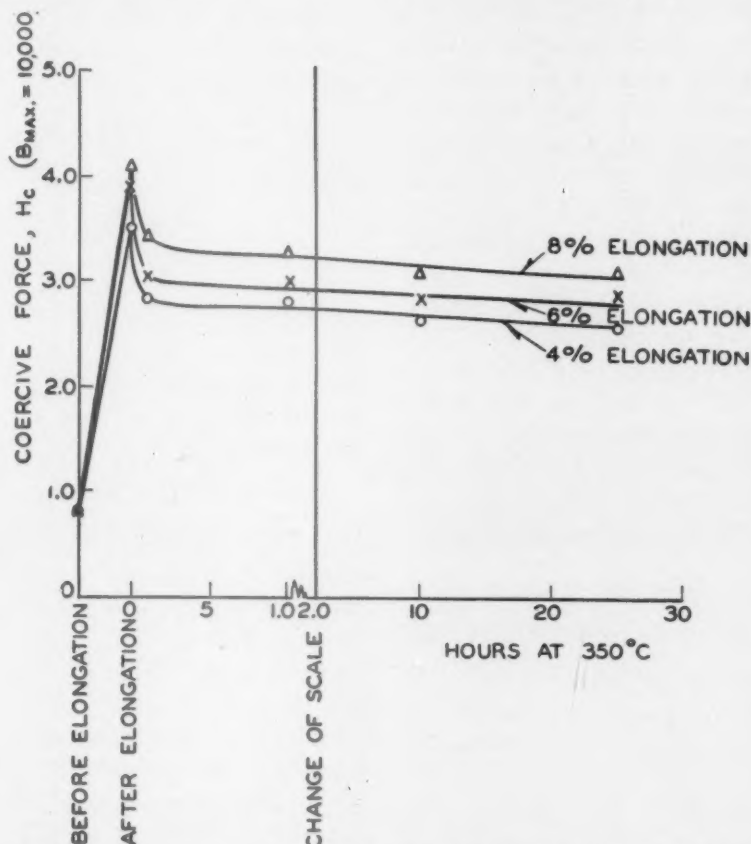


FIG. 4.—DECREASE OF COERCIVE FORCE WITH ANNEALING TIME AT CONSTANT TEMPERATURE FOR VARIOUS ELONGATIONS.

any change in asterism but apparently shows a change in lattice dimensions¹⁶ if the photograms were taken under identical conditions.

The measurement of strain by magnetic methods is not new and has been reviewed by Barrett.¹⁷ Little, however, has been done to use magnetic measurements to follow changes due to cold-work¹⁸ and recovery. The method, naturally, is applicable only to ferromagnetic materials but offers for them an excellent tool—extreme sensitivity and ease of measurement—for

tion: aluminum, 3.16 per cent; silicon, 0.03; manganese, 0.007; carbon, 0.007.

The strips were prepared by cold-rolling the 0.50-in. hot-rolled strip to 0.010 in. Strips about 15 in. long were cut in the rolling direction and were milled to 1-in. widths to have parallel edges. After milling, all the strips were sorted into groups of five strips, and all samples were annealed for 10 hr. at 800°C . in a hydrogen atmosphere (-60°C . dewpoint).

Magnetic tests for permeability, remanence, and coercive force were made after

the anneal by the Epstein test, which has been described by Burgwin.¹⁹

After magnetic testing, the strips were pulled in a Tinius-Olsen tensile machine of 5000 lb. capacity. Usual grips were used but care was exercised to obtain axial loading. Strips were slowly loaded by hand and extensions were measured by dividers over a 7-in. gauge length. The elongations were measured to 0.01 in. After elongation, ends of the strips with grip marks were cut off with a jeweler's saw to make a strip 11 in. long. The samples were magnetically tested, and after the test were annealed at various times and temperatures as shown in the tables. The samples were annealed under identical conditions. They were heated at a uniform rate of 4° per minute; they were held at $\pm 5^\circ$ of the desired temperature; and at the end of the anneal they were furnace-cooled to room temperature. After each heat-treatment the samples were tested and then reannealed.

RESULTS*

Effect of Cold-work on Magnetic Properties

Information on the effect of cold-work on aluminum iron is contained in Table 1, and some of this information is plotted in Figs. 2 and 3. In Fig. 2, where the coercive force is plotted against the cold-work,† the following expression can be written for the parabolic curve:

$$H_c = aE^b + C$$

or for the data

$$H_c = 1.78E^{0.308} + 0.8$$

where E is the elongation in per cent.

The permeability for $H = 10$ is markedly affected by the cold-work, indicating that permeabilities at low magnetizing forces

are structure sensitive. The permeability for $H = 100$ is virtually unaffected by the cold-work (see Table 1) because for this magnetizing force the curve is approaching the saturation value, which is a function of the material composition only.

The effect of cold-work on the permeability, μ_{10} , can be expressed by the following equation:

$$\mu_{10} = C - aE^b$$

or for the data obtained here

$$\mu_{10} = 1540 - 716(E)^{0.226}$$

The remanence and the magnetizing force for a flux density of $B = 10,000$ are also markedly affected by cold-work, as can be seen from Table 1; the remanence is decreased and H for $B = 10,000$ is increased.

Recovery of the Cold-worked Aluminum Iron at Constant Temperature

Strips of aluminum iron that had been elongated 4, 6, and 8 per cent and magnetically tested were annealed for 0.1 hr., 1 hr., 10 hr. and 25 hr. at 350°C. The data for these heat-treatments are found in Table 1, and indicate that the coercive force and the magnetizing force H for $B = 10,000$ decrease, and that the permeability for $H = 10$ and remanence increase with annealing time. The greatest changes of these properties occur in the first few minutes of the anneal and then each property seems to reach a limiting value. The coercive force has been plotted as a function of time in Fig. 4. A residual effect remains apparently after lattice recovery has occurred.

Recovery of Cold-worked Aluminum Iron at Various Temperatures

Strips of aluminum iron that had been elongated 6 per cent were annealed at various temperatures (150°, 250°, 350°, 450°, and 550°C.) for 0.1 hr., 1 hr., 10 hr. and 25 hr. The information obtained

* The same characteristic results obtained on aluminum iron were found for pure (electrolytic) iron. Insufficient data, however, precluded its reporting at this time.

† The yield-point elongation of the material is close to 4 per cent and for this reason lower degrees of cold-work could not be studied; i.e., the deformation would not be uniform throughout the strip.

from this study is tabulated in Table 2. There is virtually no change in the magnetic properties of material annealed at 150°C. At all other temperatures there is improve-

different temperatures. Grain sizes were identical; there was no evidence of recrystallization. The grain size of all materials was A.S.T.M. 5.

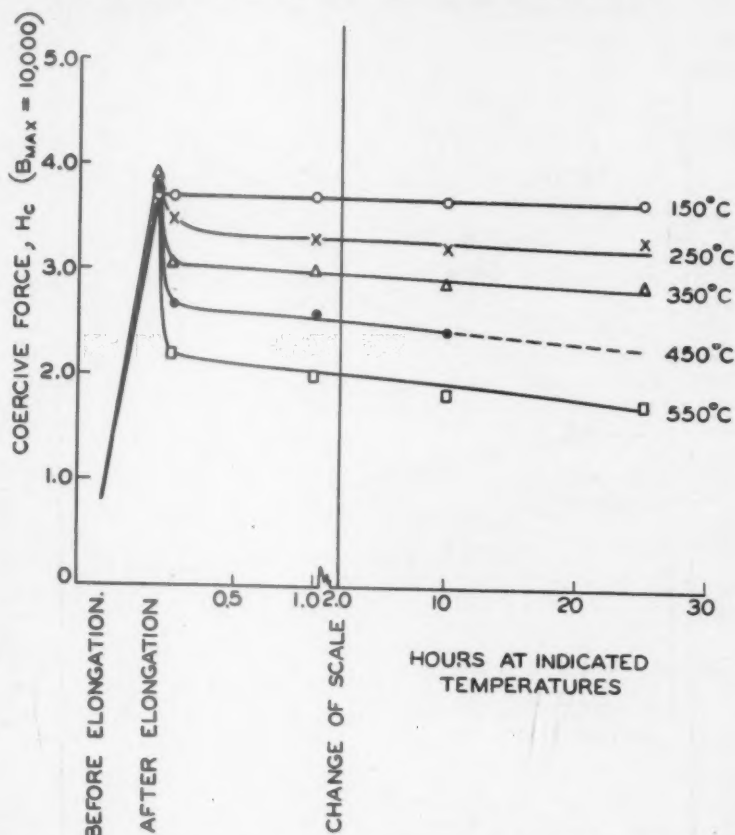


FIG. 5.—DECREASE IN COERCIVE FORCE WITH TIME AT VARIOUS TEMPERATURES FOR AN ELONGATION OF 6 PER CENT.

ment in magnetic quality of the aluminum iron; i.e., the coercive force, and the magnetizing force H for $B = 10,000$ decrease and the permeability μ_{10} and remanence increase. The higher this annealing temperature, the greater is the improvement in properties mentioned.

The change of coercive force with time at these temperatures is plotted in Fig. 5, and the change of permeability and coercive force as a function of temperature is plotted in Fig. 6. In no case under experimental conditions considered here were the initial magnetic properties obtained.

Metallographic examination was carried out on all samples annealed 25 hr. at the

Apparently the phenomenon discussed here is similar to that mentioned by Smith and Wood,¹⁵ inasmuch as the strained lattice tends to recover very quickly at low temperatures. A certain amount of internal damage remains because of the cold-work even after the lattice has recovered, as can be seen from the fact that the initial magnetic properties are not obtained by this low-temperature annealing.

SUMMARY

The changes in magnetic properties such as coercive force, remanence, and permeability (at $H = 10$ oersteds) can be used

to study the effect of cold-work and recovery in aluminum iron.

The coercive force and the value H for $B = 10,000$ are increased and the permeability (μ_{10}) and remanence are decreased

The annealing of cold-worked (4, 6, and 8 per cent elongation) aluminum iron at 350° results in a rapid relief of strain and then appears to reach limiting values for the respective elongations.

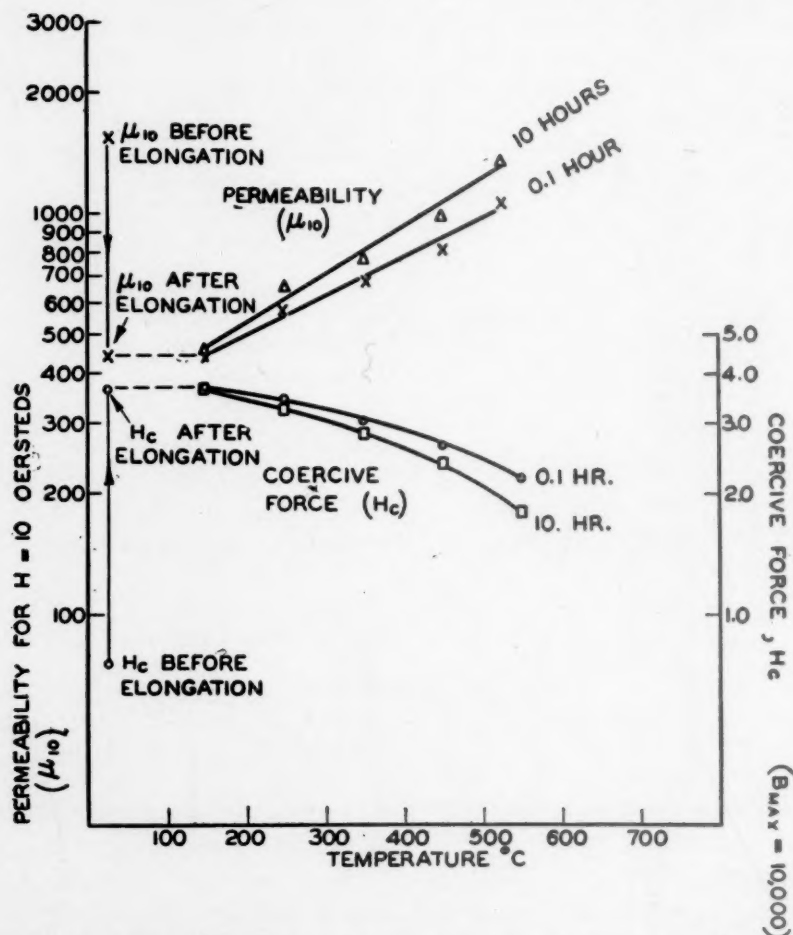


FIG. 6.—CHANGE IN PERMEABILITY AND COERCIVE FORCE AS A FUNCTION OF TEMPERATURE. 6 per cent elongation.

with increasing cold-work. The change in coercive force can be expressed by an equation of form

$$H_c = aE^b + C$$

and the permeability by an equation of form

$$\mu_{10} = C - aE^b$$

where a , b , and C are constants and E is the elongation.

The annealing of cold-worked (6 per cent elongation) aluminum iron at 150° , 250° , 350° , 450° , and 550°C. results in a very rapid relief of strain at all temperatures except 150°C. , at which nothing occurs. The higher the temperature, the greater is the recovery and the closer is the approach of magnetic properties to the original annealed material. No recrystallization was found in any of the samples.

ACKNOWLEDGMENT

The writer acknowledges the assistance of E. U. Powell, Eldon Bissett, L. C. Ammodt, and W. J. Carr, all of the Westinghouse Laboratories, for carrying out the magnetic testing.

REFERENCES

1. E. Fetz: *Trans. Amer. Soc. Metals* (1941) 29, 210.
2. J. K. Stanley and R. F. Mehl: *Trans. A.I.M.E.* (1942) 150, 260.
3. R. F. Mehl: Recrystallization. *Metals Handbook* (1939) 210. Amer. Soc. Metals.
4. G. Sachs and K. R. Van Horn: Practical Metallurgy, Chap. VI. Amer. Soc. Metals.
5. G. Sachs and G. Espey: *Trans. A.I.M.E.* (1942) 147, 74.
6. L. W. Kempf and K. R. Van Horn: *Trans. A.I.M.E.* (1942) 147, 250.
7. R. H. Canfield: *Trans. Amer. Soc. Steel Treat.* (1932) 20, 549.
8. R. L. Wegel and H. Walther: *Physics* (1935) 6, 141.
9. F. Forster and W. Koster: *Ztsch. Metallkunde* (1937) 29, 116.
10. F. Forster and H. Breitfield: *Ztsch. Metallkunde* (1938) 30, 343.
11. W. Koster and K. Rosenthal: *Ztsch. Metallkunde* (1938) 30, 345.
12. T. A. Read: *Trans. A.I.M.E.* (1941) 143, 30.
13. C. Zener, H. Clarke and C. S. Smith: *Trans. A.I.M.E.* (1942) 147, 90.
14. C. S. Barrett: Structure of Metals, Chap. XIV, New York. McGraw-Hill Book Co.
15. S. L. Smith and W. A. Wood: *Proc. Roy. Soc. London* (1941) 178-A, 93.
16. R. Karnop and G. Sachs: *Ztsch. Phys.* (1927) 42, 283.
17. C. S. Barrett: *Metals and Alloys* (1934) 5, 134.
18. E. V. Potter: U.S. Bur. Mines R.I. 3400 (1938) 41. Potter has measured the coercive force of iron, iron-nickel, and nickel rods on torsion.
19. S. L. Burgwin: *Proc. Amer. Soc. Test. Mat.* (1941) 41, 779.

Effect of Variables on the Recrystallization of Silicon Ferrite in Terms of Rates of Nucleation and Growth

BY JAMES K. STANLEY,* JUNIOR MEMBER A.I.M.E.

(New York Meeting, February 1945†)

WHEN a plastically deformed metal is heated to a certain temperature, it undergoes a complete change in microstructure, the consequence of which is a marked alteration of mechanical properties such as hardness, strength and ductility. This change in microstructure occurs by recrystallization and is a process involving the formation and growth of strain-free nuclei in the deformed matrix. These nuclei continue to form with time and grow until a new grain structure replaces the cold-worked structure. The formation of the nuclei in the deformed sheet of 1 per cent silicon ferrite is illustrated in Fig. 1.

If a recrystallization is conducted isothermally, a measurement of the fraction of the matrix recrystallized plotted against time leads to an isothermal recrystallization curve, first established in 1942.¹ Such recrystallization curves are shown in Fig. 4. These curves show that the recrystallization of a cold-worked metal is best considered as a rate process rather than a time independent process such as is suggested by the improperly named and misleading recrystallization diagrams involving deformation, temperature, and grain size.²⁻⁵

Any study of the rate of recrystallization resolves itself into a study of the component rates of nucleation and growth. The previous paper¹ provided an account of the determination of the rates of

nucleation; N , the number of nuclei formed per unit time per unit of unrecrystallized area, and growth, G , the radial growth in unit time, in the recrystallization of silicon ferrite (1 per cent Si). A method was developed to furnish experimental data for evaluating the effect of the recrystallization variables on N and G . The mathematical analysis for the derivation of the isothermal recrystallization curve was developed for a two-dimensional case (in thin sheets where the diameter of the recrystallized grain is greater than the sheet thickness).

The present paper is a continuation of the study of recrystallization of 1 per cent silicon ferrite begun in 1942.¹ In this work the effect of the factors deformation, temperature, grain size, composition, and recovery is studied with respect to the rates of nucleation and growth. At the same time it is shown how the cooperation of N and G affects the isothermal recrystallization curve. The study of these variables on N and G has a definite bearing on the mechanism of recrystallization and should lay a foundation for a rational theory on the subject.

PROCEDURE

The procedure used in these experiments was essentially the same as that described previously but in certain details some changes were made in the interests of speed. With few exceptions, the procedure is the same for the study of all the variables. Where the procedure is different from standard manipulations attention is called to this fact.

Manuscript received at the office of the Institute, Dec. 11, 1941. Issued as T.P. 1840 in METALS TECHNOLOGY, August 1945.

* Research Engineer, Research Laboratories, Westinghouse Electric and Manufacturing Co., East Pittsburgh, Pennsylvania.

† Meeting canceled.

¹ References are at the end of the paper.

The material used in this investigation is the same as that used in the previous work. This 1 per cent silicon ferrite had the composition given in Table 3 of this

unrecrystallized material was obtained with 15 per cent nital.

The material was photographed on photographic paper (P.M.C. bromide

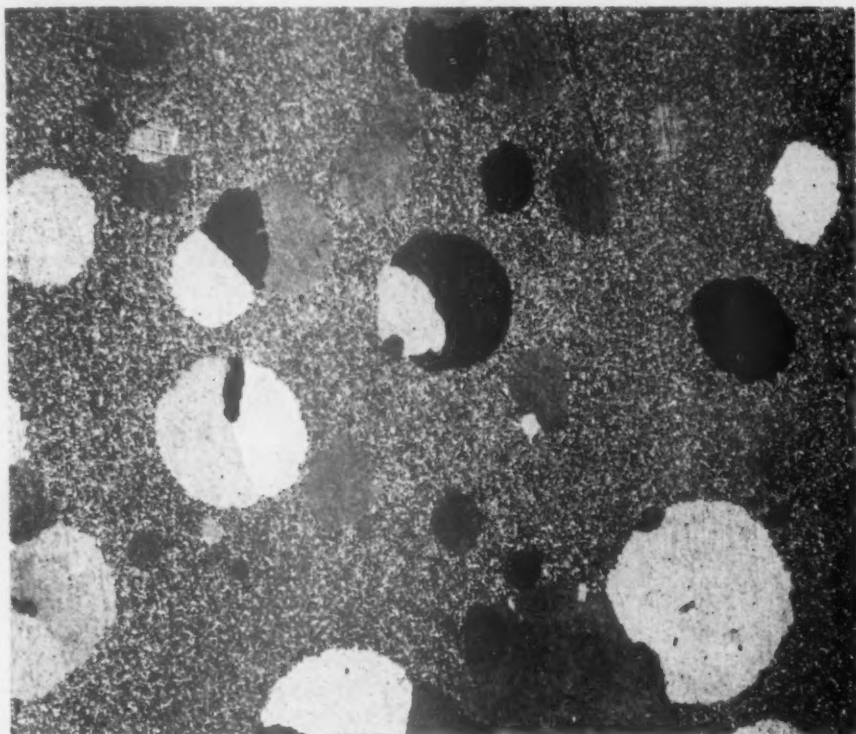


FIG. 1.—NUCLEI GROWING IN A DEFORMED MATRIX. $\times 7$. ETCHED IN 15 PER CENT NITAL.

paper. The hot-rolled material was first ground on both sides from 0.10 to 0.09 in. on a precision grinder to remove the surface and eliminate variations in gauge. This material was then cold-rolled on a four-high mill to 0.012 in. The strip was cut to 12-in. lengths and was annealed by suspending it in a vertical furnace for 25 hr. at $825^{\circ}\text{C.} \pm 5^{\circ}$ in dry hydrogen (minus 60°C. dew point). The grain size in the plane of the sheet is seen in Fig. 2; this grain size corresponds to an A.S.T.M. grain size of 6.

The cold-work was done by elongation in a tensile machine, as this represents a simple deformation and one that is readily controlled. All annealing was carried out in a salt pot in which the temperatures were held to $\pm 2^{\circ}\text{C.}$ Cleaning of the samples was carried out in hot 50-50 HCl and the contrast between the recrystallized and

paper) using it as paper negatives, which, when dry, could be used for planimeter measurements and counting, avoiding the tediousness of making tracings from negatives. The new method was not only rapid and time saving, but very inexpensive.

All data presented here are for isothermal recrystallization. Specimens approximately one square inch in area were introduced into the salt pot in numbers from 1 to 15 and reached the temperature of the molten salt in 2 to 30 sec., respectively. This time error is very small compared with the recrystallization times and was disregarded.

While precautions were taken to control the grain size, temperature, and deformation in order to minimize fluctuations in the nuclei formed, occasional variations were noted. This probably means that

while it is possible, by careful manipulation, to obtain uniform macroscopic deformations, this will not assure uniform microscopic deformations. These fluctua-

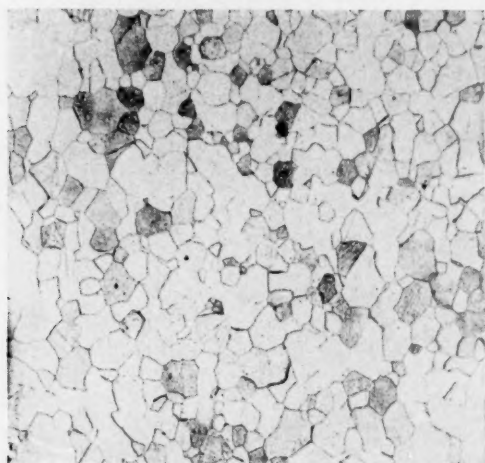


FIG. 2.—ONE PER CENT SILICON IRON ANNEALED 25 HOURS AT 825°C. $\times 100$, A.S.T.M. GRAIN SIZE NO. 6.

tions in recrystallization can be reduced by the use of statistical methods; i.e., by the employment of a number of samples.¹

From each group of such samples at each time interval, the following information was obtained: the average percentage of the area recrystallized, the average number of nuclei formed per area, and the average diameter of the largest nucleus in each sample. New samples were taken for the other time intervals.

The isothermal recrystallization curve (fraction recrystallized vs. time) can be plotted directly from the data if sufficient points are obtained, but this is laborious and time-consuming. In order to speed up the accumulation of data, a short cut based on theoretical calculations was resorted to; the number of points necessary to establish the curve was thereby reduced, but the number of samples required to establish a point was the same as before; namely, five to eight samples.

By the use of the reaction-rate paper originated by Johnson,⁶ on which he plots the logarithm of the natural logarithm of

the reciprocal of the fraction of material unrecrystallized against the logarithm of time, the recrystallization data form a straight line.* This type of paper is shown

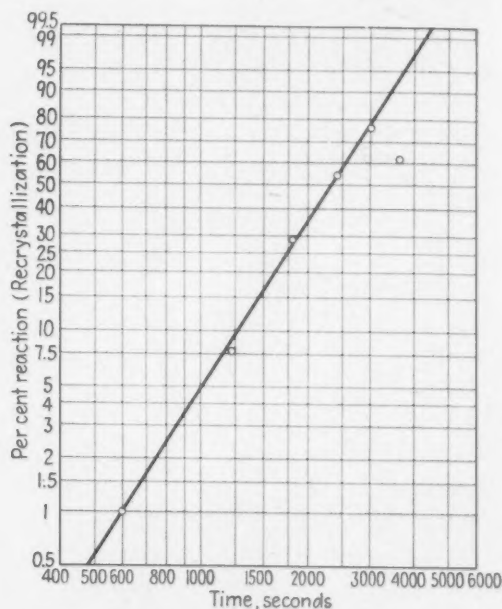


FIG. 3.—REACTION-RATE PLOT DUE TO JOHNSON⁶ FOR ISOTHERMAL RECRYSTALLIZATION AT 800°C.; 5 PER CENT ELONGATION.

in Fig. 3 with data plotted for recrystallization at 800°C. Such curves for various temperatures and conditions can then be replotted on rectangular coordinates as shown in Fig. 4 for 770°C. This is desirable because the progress of recrystallization is easier to visualize on undistorted coordinates.

* Using the notation first given by Johnson and Mehl⁷ and later adopted in the study of "two-dimensional" recrystallization,¹ the fraction of the sample recrystallized at time t is given as $f(t)$. The reaction equation for constant N (actually N varies with time) and G is

$$f(t) = 1 - e^{-\frac{\pi G^2 N t^3}{3}}$$

By definition $u(t)$ is the fraction unrecrystallized at time (t) , so that

$$f(t) = 1 - u(t)$$

$$\text{or } 1 - u(t) = 1 - e^{-\frac{\pi G^2 N t^3}{3}}$$

Taking the natural logarithm of the above

The evaluation of the rate of nucleation was carried out by plotting the number of nuclei formed per unit of unrecrystallized area n against time on semilogarithmic paper and drawing the best straight line through the data. This is permissible because it was previously shown¹ that the nuclei that form per unit time at the beginning of the recrystallization can be represented by the equation of the type*

$$n = ae^{bt} \quad [1]$$

where a and b are constants.

From this best straight line, the number of nuclei per unrecrystallized area are plotted against time on rectangular coordinates. From this exponential curve the uncorrected rate of nucleation N is determined by graphical methods. This rate of nucleation is then corrected for the fraction of the area recrystallized at that time. The rate of nucleation is given as the number of nuclei formed per second per square centimeter.

Since the rate of growth G is known to be constant,¹ the rate can be determined from the slope of the plot of the radius of the largest grain against time. The rate of growth is expressed in centimeters of radial growth per second, obtained from the measurement of the diameter of the largest grain at various time intervals on the assump-

expression,

$$\ln \frac{1}{u(t)} = + \frac{\pi G^2 N t^3}{3}$$

If the \log_{10} is taken of the above equation

$$\log \left[\ln \frac{1}{u(t)} \right] = \log \left(\frac{\pi G^2 N}{3} \right) + 3 \log t \\ = \text{constant} + 3 \log t$$

Hence, when $\log \left[\ln \frac{1}{u(t)} \right]$ is plotted against $\log t$ a straight line results. The advantage of this type of plot is in determining the isothermal recrystallization curves of Fig. 4 and others because it is easier to draw a straight line, rather than a curved one, through scattered points. Such a plot is useful for extrapolation if data are scarce.

* This relation is valid for early stages of recrystallization [$f(t) = 0.3$ or 0.4] but does not hold for higher fractions recrystallized.¹ The first-formed nuclei play a dominant role in the rate of recrystallization and those formed at longer times only a minor one.

tion that the largest grain in any sample had formed at the first instant of reaction. Growth curves can be represented by a straight-line equation of the form

$$r = G(t - C) \quad [2]$$

where C is a time constant or the so-called incubation or induction period.

EFFECT OF DEFORMATION

Increasing the deformation is known to affect greatly the recrystallization of metals. In general it can be said that the greater the deformation, the more rapid is the recrystallization, the lower is the temperature at which the material recrystallizes in a given time, and the finer is the resultant grain size.

Little is known of the effect of deformation on the rates of nucleation and growth and consequently on the isothermal recrystallization curve. The literature in regard to N and G has been reviewed,¹ and while there exists some information on the effect of deformation on N and G , it is of doubtful value because of the experimental methods employed and the method of evaluating the two factors. All investigators however are in common agreement that cold-work increases both N and G .

The isothermal recrystallization curves for silicon ferrite of A.S.T.M. grain size 6.0 (Fig. 2) deformed 5, 6, 7, and 8 per cent, and annealed at 770°C. are shown in Fig. 4. These curves show the increase in the rate of recrystallization with increasing cold-work.

The rates of nucleation (Figs. 5 and 6) and growth (Fig. 7)* show that this change in recrystallization is due both to the increase in the rates of nucleation and growth with deformation.

The effect of deformation on the change in the rate of nucleation N is seen in Fig. 5. Deformation has a strong effect in increasing the rate of nucleation. For sake of comparison, the rate of nucleation has been determined for fractions recrystal-

* The slope of the curves is the rate of growth.

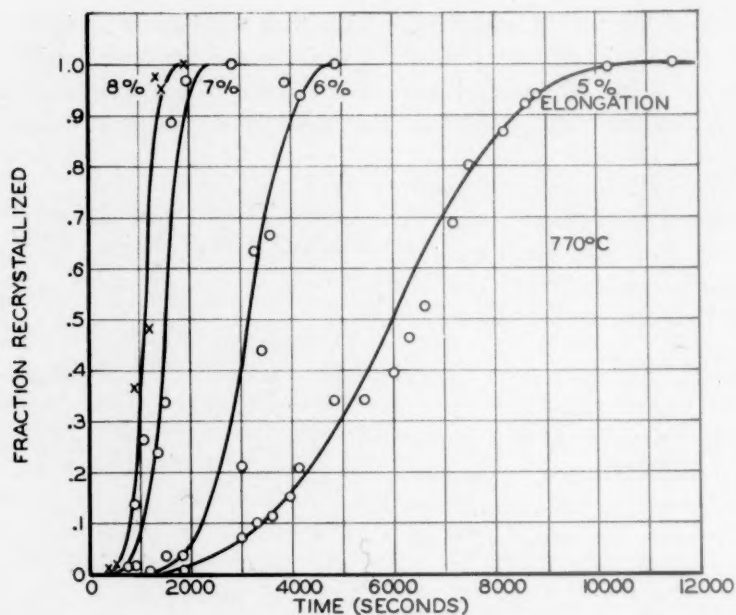


FIG. 4.—EFFECT OF DEFORMATION ON RECRYSTALLIZATION.

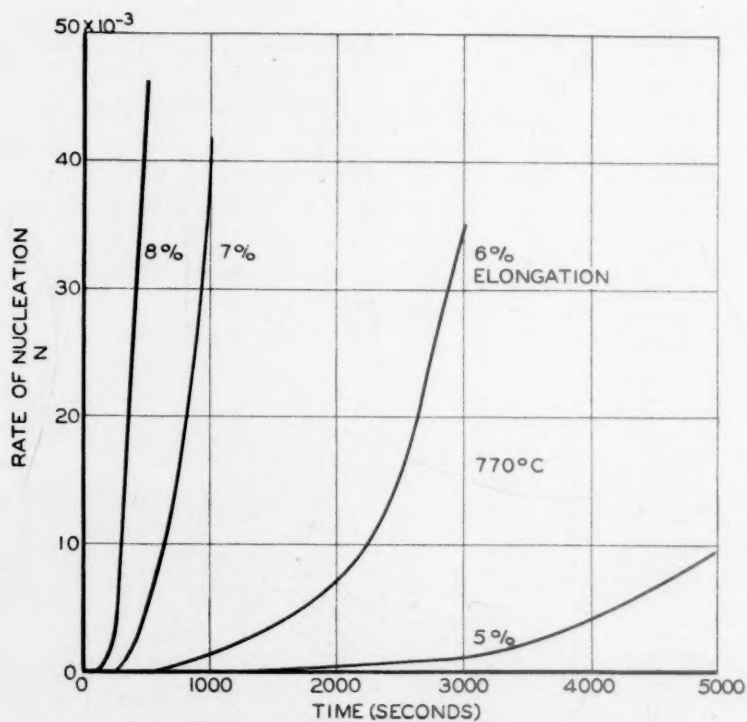


FIG. 5.—CHANGE IN RATE OF NUCLEATION WITH TIME.

lized 0.1 and 0.2 (Table 1).^{*} This change in the rate of nucleation is plotted on a

The coefficients c and d were determined by the method of averages for $f(t) = 0.2$.

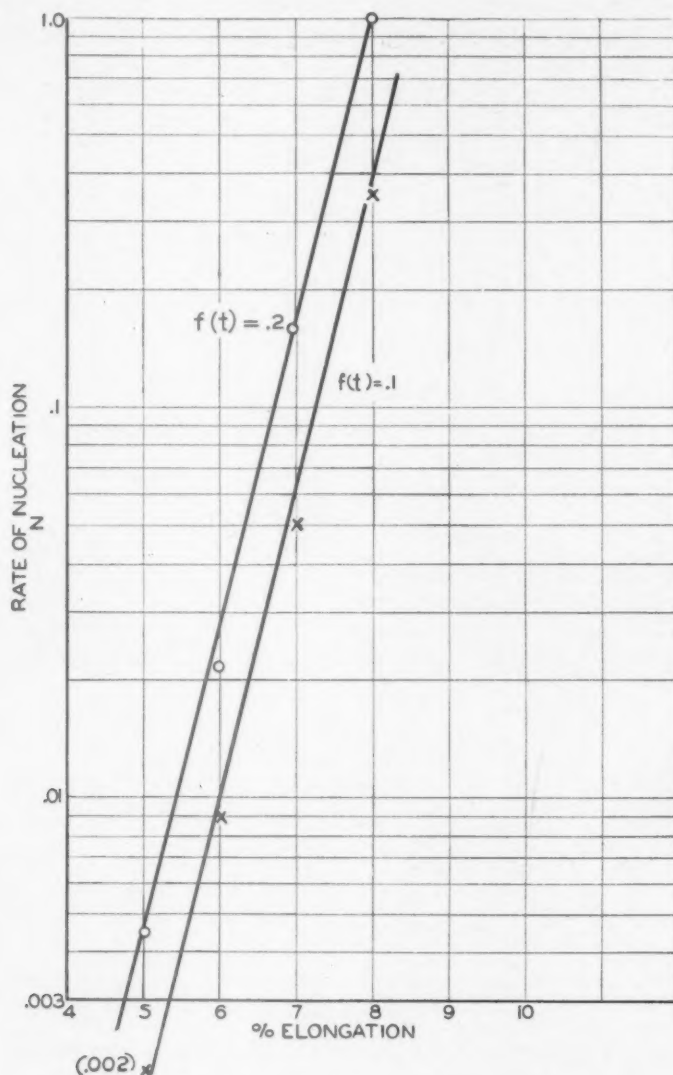


FIG. 6.—EFFECT OF DEFORMATION ON NUCLEATION.

semilog scale in Fig. 6. The equation for the lines is

$$N = ce^{dE} \quad [3]$$

where N is the rate of nucleation,

c and d are constants,

E is the percentage of elongation.

^{*} Comparisons above 0.2 fraction recrystallized are difficult to make because of the high rate of nucleation and the impingement errors; below 0.2, comparisons can be made at any arbitrarily chosen fractions and will yield equivalent data.

The equation then becomes

$$N = 2.56 \times 10^{-7} e^{1.9E} \quad [4]$$

The rate of growth, like nucleation, is also increased with increasing deformation. This is shown in Fig. 7. In this figure the radius of the largest grain is plotted against time for each deformation and the slope of these lines is the rate of growth G in centimeters per second.

The rate of growth G and the time intercept C , or the so-called period of incuba-

tion, are given in Table 1 and are plotted as a function of the elongation in Fig. 8.

An attempt was made to calculate the isothermal recrystallization curves of Fig.

and actual isothermal recrystallization curves was fair for the 5 per cent elongation, but agreement was closer at higher elongations. For a comparison of the cal-

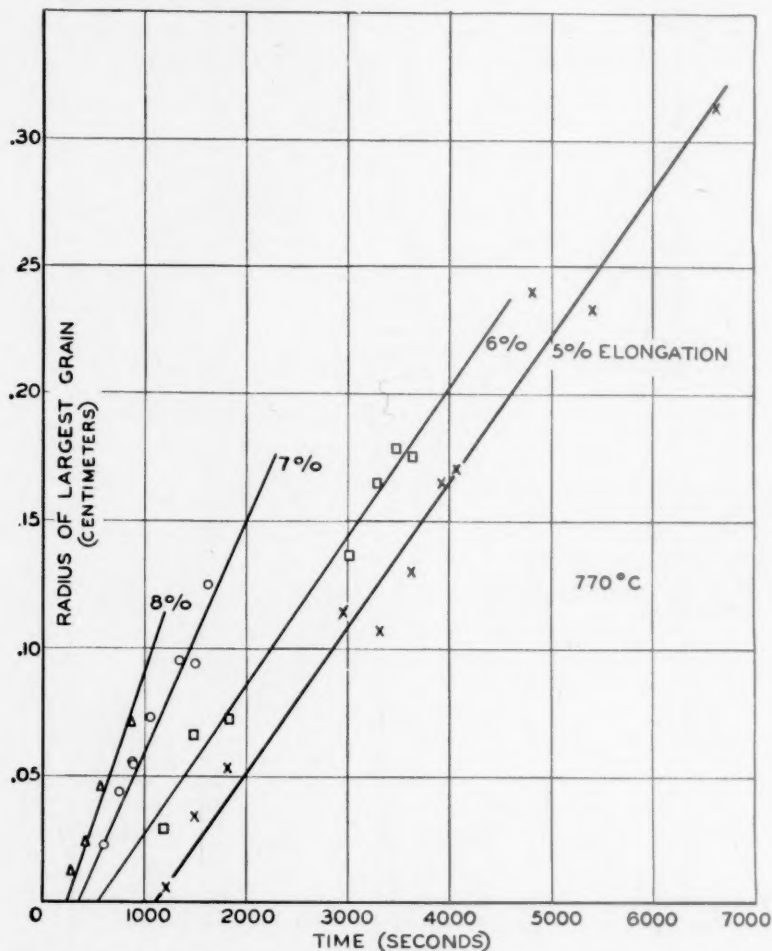


FIG. 7.—RADIAL GROWTH OF THE LARGEST GRAIN FOR VARIOUS DEFORMATIONS.

4, since the analytical expression for this isothermal recrystallization was obtained previously.¹ The expression for two-dimensional recrystallization is:

$$f(t) = 1 - e^{-\frac{2\pi G^2 a}{b^2} \left(\frac{e^{bt}}{b} - \frac{bt^2}{2} - \frac{1}{b} - t \right)} \quad [5]$$

where G is the rate of growth.

a and b are coefficients of the rate of nucleation curve for each deformation.

t is time.

The agreement between the calculated

and actual recrystallization curves see reference 1.

EFFECT OF TEMPERATURE

Temperature is known to affect the recrystallization of a cold-worked metal and the cited literature gives its general effects. Literature on the effect of temperature on nucleation and growth is very fragmentary and no reliable data exist on these processes.¹

The isothermal recrystallization curves for silicon ferrite are plotted in Fig. 9 for

temperatures of 740°, 770°, and 800°C. This composite plot shows the large effect of temperature in increasing the rate of recrystallization. This effect is better seen by comparing the times required for a 0.2 fraction recrystallized for the various deformations at the different temperatures (Table 2).

The nucleation and the growth of the

TABLE 1.—Change of N and G with Temperature

Temperature, Deg. C.	Elongation, Per Cent	N^a for		G^b	C , Sec.
		$f(t) = 0.1$	$f(t) = 0.2$		
740	6	0.005	0.010	2.4×10^{-5}	1,210
	7	0.028	0.055	3.5×10^{-5}	340
770	5	0.002	0.0045	5.4×10^{-5}	1,030
	6	0.009	0.0218	6.2×10^{-5}	530
	7	0.052	0.162	8.6×10^{-5}	270
800	8	0.355	1.04	11.5×10^{-5}	210
	4	0.002	0.006	9.5×10^{-5}	320
	5	0.007	0.013	10.5×10^{-5}	70

^a Rate of nucleation expressed as number of nuclei per sec. per sq. cm. unrecrystallized area.

^b Rate of growth in centimeters radial growth per second.

nuclei were found to increase with temperature. Since the rates of nucleation are known to increase with time (Fig. 10), the expedient of comparing the rates of nucleation at 0.2 fraction recrystallized was resorted to. Such comparison is given in Table 1. The rate of growth is easy to compare because G is constant with time. The rate of growth, along with the time intercept C , is also given in Table 1. The change in the rate of growth at the various temperatures is shown in Fig. 11.

The temperature dependence of N and G has been found by Anderson and Mehl⁸ to be of the exponential equation so familiar in reaction-rate studies.^{9,10} Thus the rates of nucleation and growth can be written

$$N = Ae^{-\frac{Q_N}{RT}} \quad [6]$$

or

$$\ln N = \ln A - \frac{Q_N}{RT} \quad [7]$$

and

$$G = Be^{-\frac{Q_G}{RT}} \quad [8]$$

or

$$\ln G = \ln B - \frac{Q_G}{RT} \quad [9]$$

where Q_N and Q_G are the activation energies for nucleation and growth, respectively,

T is absolute temperature,

R is the gas constant in calories per degree, and A and B are constants.

The activation energies Q_N and Q_G represent the slopes of plots of $\ln N$ or $\ln G$ against $\frac{1}{T}$, respectively, and are independent of the amount of recrystallization. N and A will vary with the percentage of recrystallization, since N varies with time, but G and B do not vary because G is invariant with time.

TABLE 2.—Time Required for Recrystallization at Various Temperatures

Temperature, Deg. C.	Elongation, Per Cent	Time, Sec., for $f(t) = 0.2$
740	6	6,700
	7	2,800
770	5	4,200
	6	2,550
	7	1,220
800	8	900
	4	3,200
	5	1,600

An attempt was made to estimate the order of magnitude of the activation energies. The activation energy for nucleation Q_N was determined first in the following way. The data for N at 770°C. were plotted against deformation on semilog paper (as was done in Fig. 6) and then the points for the other temperatures were plotted. Through these points lines were drawn parallel to the 770°C. data, assuming that the effect of deformation on nucleation is the same at the various temperatures as it is for 770°C. From such plots the relation between N and temperature was established. In Fig. 12, the logarithm of the rate of nucleation is plotted against $\frac{1}{T}$ where T = absolute

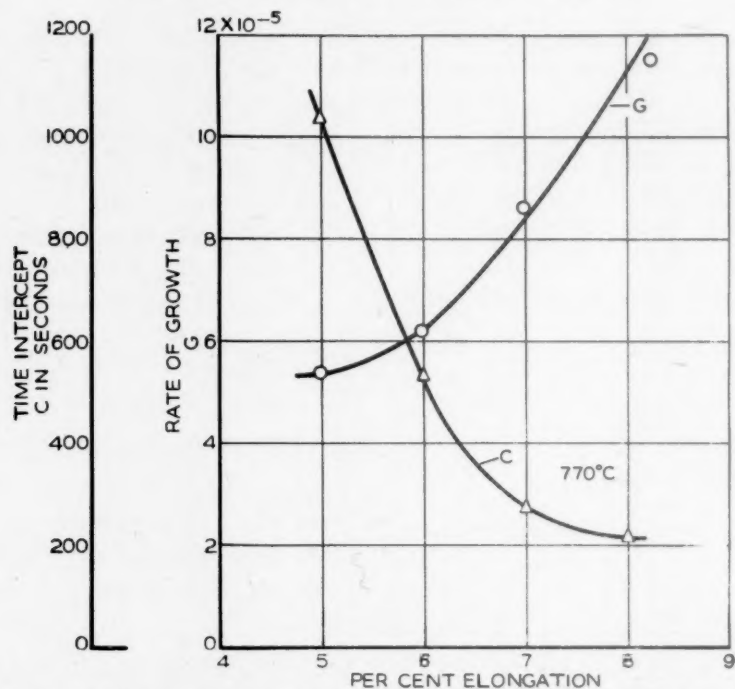


FIG. 8.—CHANGE OF GROWTH AND INDUCTION PERIOD WITH DEFORMATION

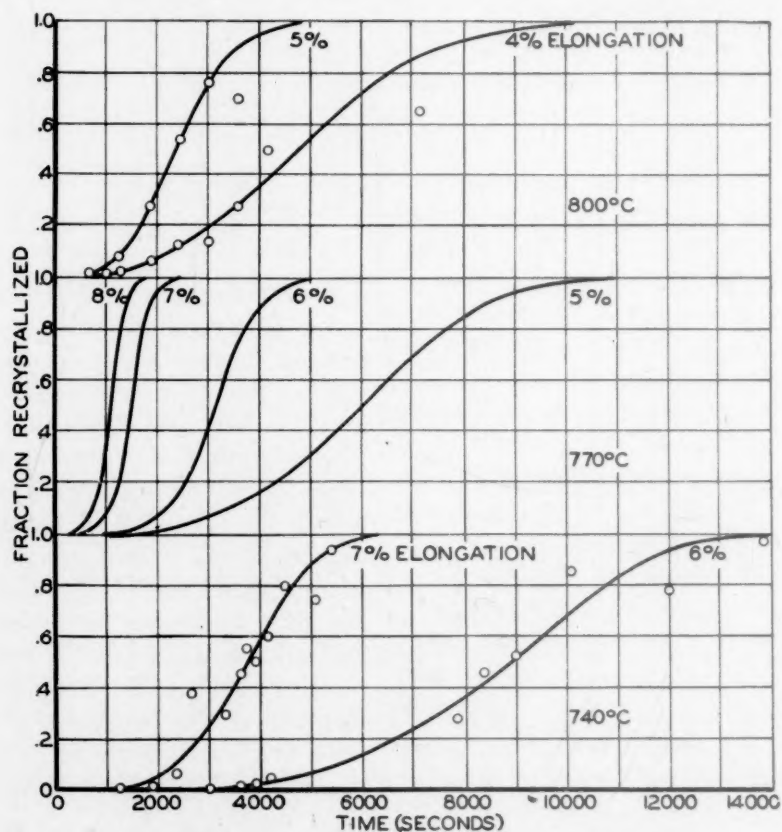


FIG. 9.—EFFECT OF TEMPERATURE ON RECRYSTALLIZATION.

temperature. From the straight lines that result, the activation energy can be derived.

lines then yields the activation energy. The calculation of the unknowns in Eq. 8 leads to the following equation for the

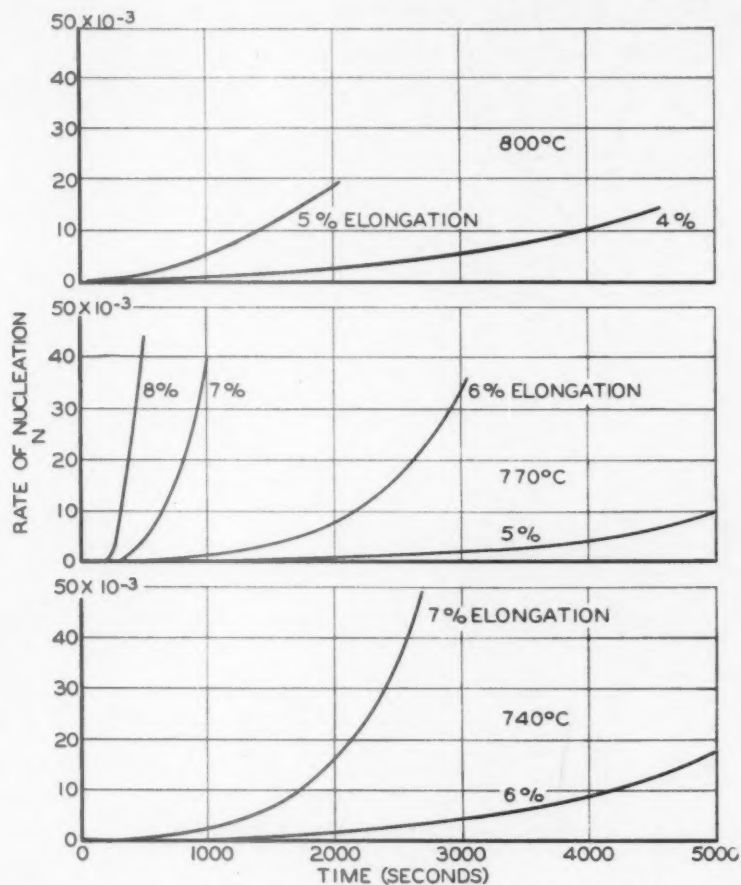


FIG. 10.—EFFECT OF TEMPERATURE ON NUCLEATION.

The calculation of the unknowns in Eq. 6 for 7 per cent elongation gives the following result

$$N = 3.72 \times 10^{13} e^{-\frac{69,000}{RT}} \quad [10]$$

The activation energy of 69,000 cal. represents the activation energy that must be supplied to the cold-worked material to cause the nuclei to form.

A similar procedure was carried out to estimate the activation energy Q_N , required for the growth of the nuclei. To estimate this energy, the logarithm of G is plotted against $\frac{1}{T}$ in Fig. 13; the slope of these

rate of growth

$$G = 1.7 \times 10^{11} e^{-\frac{73,000}{RT}} \quad [11]$$

The activation energy for growth, Q_G , is 73,000 cal., and represents the energy required for the nuclei to grow in the deformed matrix.

The data obtained here are insufficient to determine the variation, if any, of Q_N or Q_G with deformation.

By way of recapitulation, it can be said that a rise in temperature causes a cold-worked metal to recrystallize more rapidly because both the rates of nucleation and of growth are increased by a rise in temperature.

EFFECT OF GRAIN SIZE

The initial grain size of a metal upon which is imposed a cold deformation is known to affect the response of this material to recrystallization. Little is known,

fine-grained material was then elongated 5 per cent, as was a similar piece of coarse-grained material (A.S.T.M. 6.0, Fig. 2). These materials were then recrystallized at 770°C.

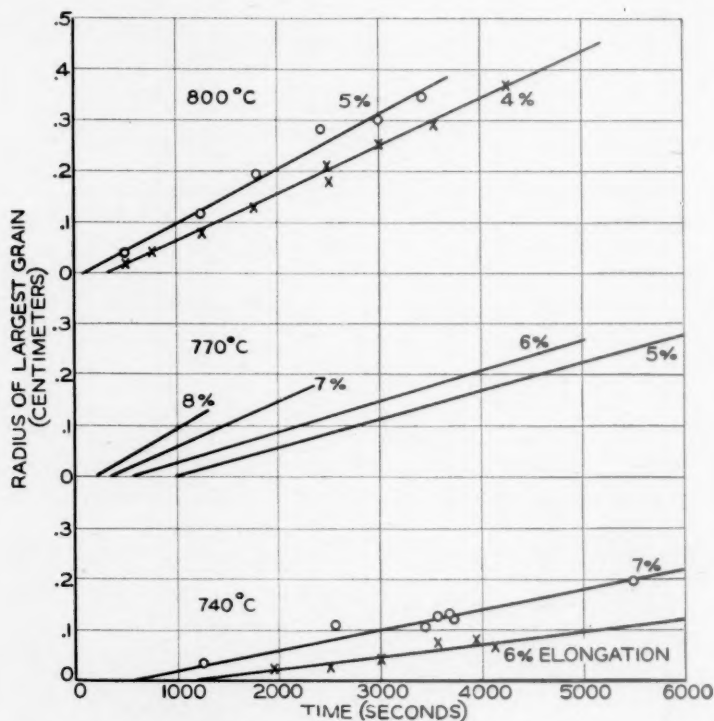


FIG. 11.—EFFECT OF TEMPERATURE ON RATE OF GROWTH.

however, as to the effect of grain size on the rates of nucleation and growth. There appears to be no literature on the effect of this variable in connection with rates of nucleation and growth, though one might surmise that both rates are increased by decreasing the grain size since fine-grained materials recrystallize more rapidly than coarse-grained materials.

Effect of a Uniform Equiaxed Grain Structure

Material of a smaller grain size than was used for deformation and temperature studies was prepared by annealing the cold-rolled silicon ferrite for 1 hr. at 700°C. The resultant grain size, corresponding to an A.S.T.M. 9.0, is shown in Fig. 14. This

By the usual analysis, the isothermal recrystallization curves (Fig. 15), the rate of nucleation curve (Fig. 16), and the growth curves (Fig. 17), were obtained.

The striking difference in the isothermal recrystallization curves (Fig. 15) is the rapidity of the recrystallization of the fine-grained material. The fine-grained material had completed half of the recrystallization, $f(t) = 0.5$, in 21 min. (1250 sec.) whereas the coarse-grained material required 100 min. (6000 sec.).

A study of the rate of nucleation (Fig. 16) shows that the nucleation is extremely rapid in the fine-grained material. For instance, the rate of nucleation N at 0.2 fraction recrystallized is 0.718 for the fine-grained silicon ferrite, whereas for coarse-

grained ferrite under otherwise identical conditions N is 0.0045. and in the coarser grained material

$$G = 5.4 \times 10^{-5}$$

The curve of the rate of growth (Fig. 17) shows that the rate of growth G is appar-

However, the period of incubation is very

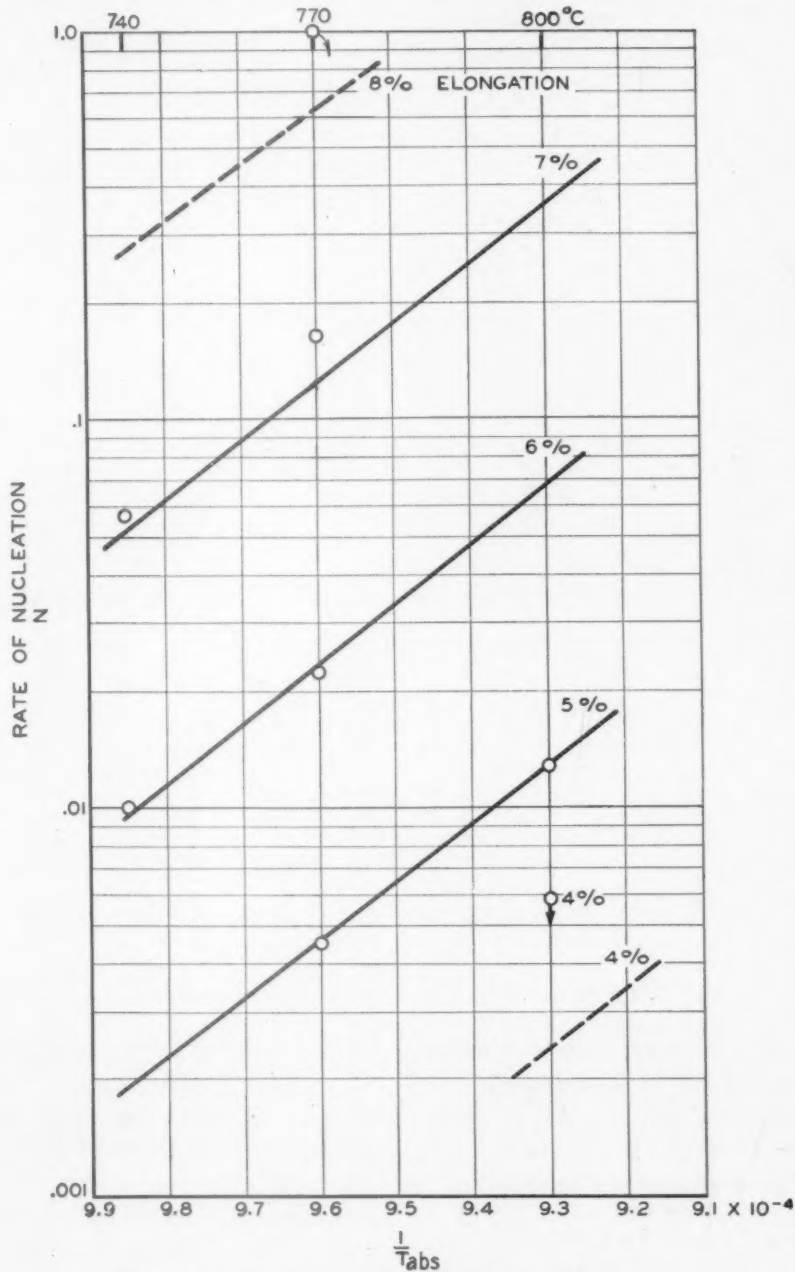


FIG. 12.—EFFECT OF TEMPERATURE ON NUCLEATION.

ently constant for these two grain sizes. In the fine-grained material

$$G = 5.7 \times 10^{-5}$$

small for the fine-grained, if it actually exists at all; here $C = -6.0$ sec., or zero. The period of incubation C for the coarse-grained iron is 1030 seconds.

From this study, it can be said that fine grain size causes the cold-worked silicon ferrite to recrystallize more rapidly, because of the large differences in the rates

grain size on which had been imposed an elongation of 5 per cent gave a rather non-uniform structure on recrystallization. This is seen in Fig. 19 at 50 diameters At

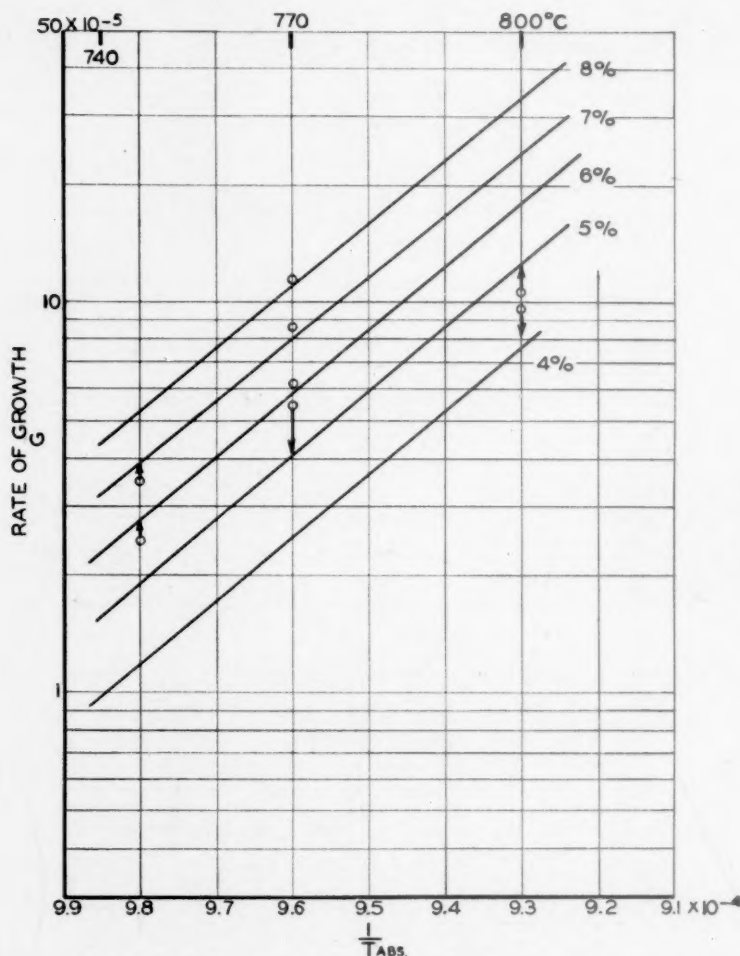


FIG. 13.—EFFECT OF TEMPERATURE ON RATE OF GROWTH.

of nucleation—the rate of nucleation being greater for the fine-grained material than for the coarse-grained. The rate of growth appears not to be affected by the grain size in the range of grain sizes examined.

Effect of a Nonuniform Grain Structure

Material of a nonuniform grain structure, as in Fig. 18, could not be studied in the usual fashion, because it did not give the customary nuclei that could be distinguished as such by the present technique. This material with a nonuniform

7 diameters, at which most recrystallization pictures were taken, no useful information could be obtained, although it did appear that the material had all recrystallized.

Apparently the grain size must be uniformly fine, and equiaxed within certain limits, to get circular nuclei that can be distinguished in a cold-worked matrix.

EFFECT OF COMPOSITION

It is common knowledge that the recrystallization of metals is markedly affected

by elements entering into solid solution. In general, such materials tend to recrystallize at higher temperatures than do pure or less alloyed metals.

There appears to be no information on the effect of composition on the rates of nucleation and of growth, but judging from the literature it appears that either the rate of nucleation or the rate of growth, or possibly both, are affected by the presence of additions forming solid solutions.

TABLE 3.—Composition of the Silicon Alloys
PER CENT

Constituent	Low-silicon Alloy	High-silicon Alloy
Silicon.....	1.04	3.12
Sulphur.....	0.009	0.013
Phosphorus.....	0.010	0.005
Manganese.....	0.035	0.11
Carbon.....	0.006	0.007

In an attempt to establish the effect of change in composition, a comparison was

believed that the effect of composition is none the less indicated; the rates of

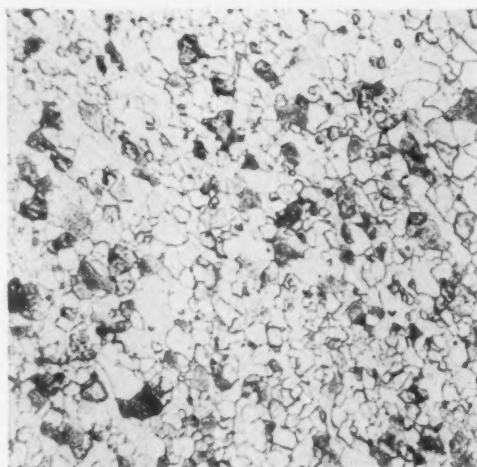


FIG. 14.—ONE PER CENT SILICON IRON ANNEALED ONE HOUR AT 700°C. $\times 100$. A.S.T.M. GRAIN SIZE NO. 90.

nucleation would suffer most from an incompleteness of the data.

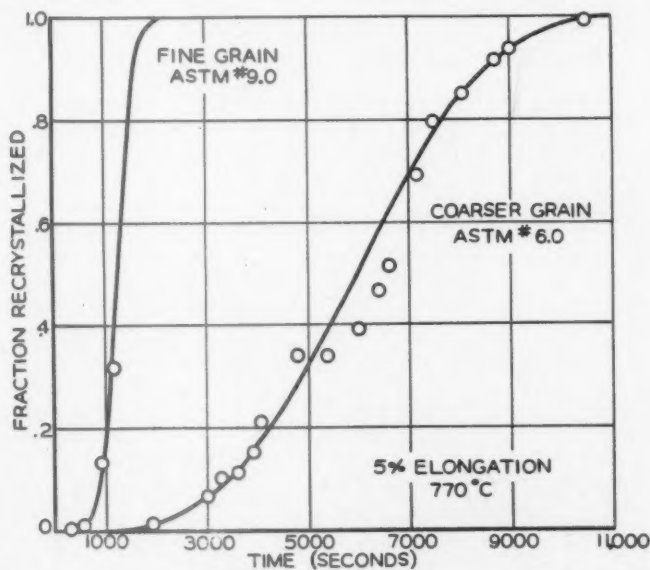


FIG. 15.—EFFECT OF GRAIN SIZE ON ISOTHERMAL CURVE.

made between alloys containing 1 and 3.1 per cent silicon, respectively (Table 3). While the data on the effect of composition is not as extensive as that on the other factors affecting the recrystallization, it is

The impurities of the high-silicon alloy compare fairly well with those of the low-silicon alloy except that the manganese is somewhat higher (0.11 versus 0.035). This may lead to no great error, owing to the

presence of such large amounts of silicon. Another difference between the two materials is that the 3.12 per cent silicon iron is

recrystallization of this oriented 3.12 per cent silicon iron, no anisotropy of growth (elliptical nuclei) was noted.

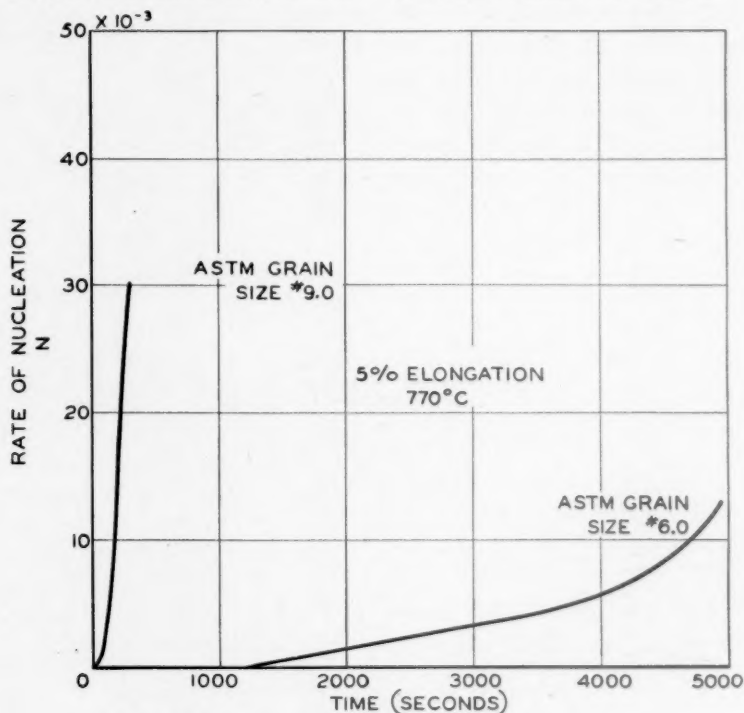


FIG. 16.—EFFECT OF GRAIN SIZE ON NUCLEATION.

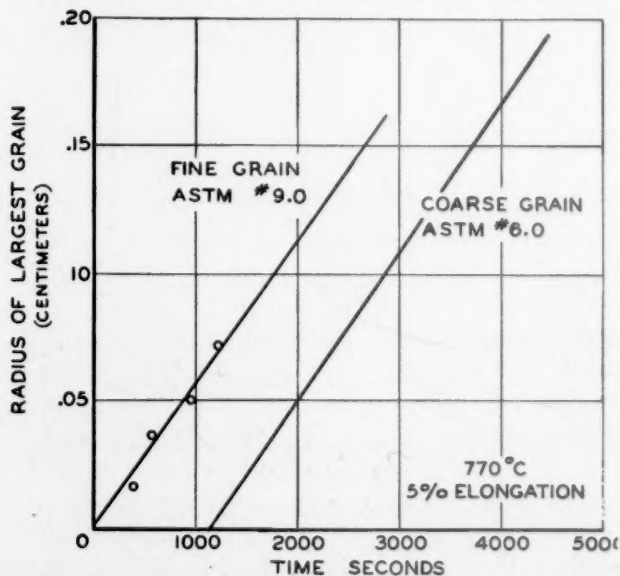


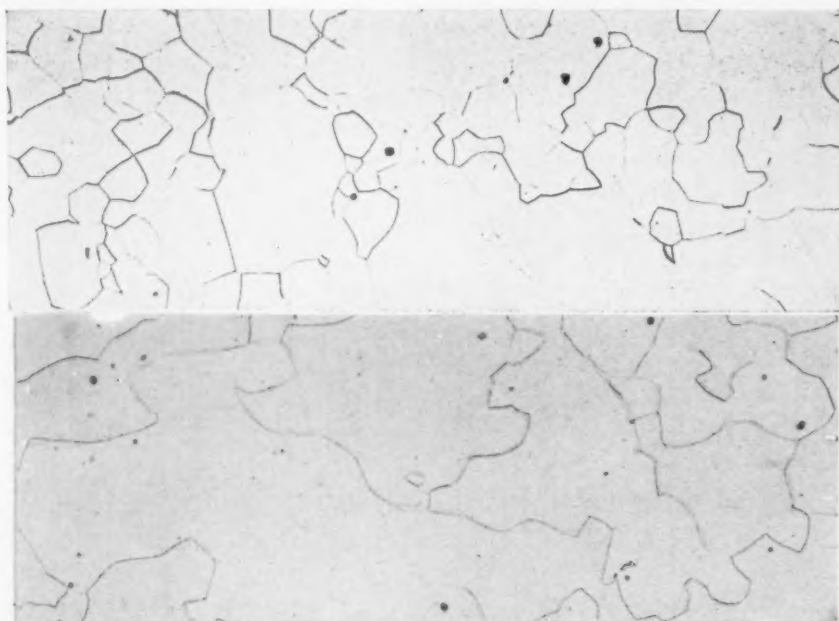
FIG. 17.—EFFECT OF GRAIN SIZE ON RADIAL GROWTH OF LARGEST GRAIN.

better oriented than the 1 per cent silicon iron, since it is magnetic strip specially processed for preferred orientation. During

An attempt was made to obtain material of essentially the same grain size, as this factor has been shown to have a great effect

on the isothermal recrystallization curve. The grain size of both silicon alloys was A.S.T.M. 6.0, Fig. 2.

with the 1 per cent silicon alloy. The isothermal recrystallization curves are shown in Fig. 20, which indicate that the recrystallization is considerably retarded by the presence of silicon. For the 6 per cent elongation at $f(t) = 0.5$, half the low-alloy



18

19

FIG. 18.—ONE PER CENT SILICON IRON ANNEALED 25 HOURS AT 875°C. $\times 100$.
FIG. 19.—ONE PER CENT SILICON IRON, 5 PER CENT ELONGATION, 40 MINUTES AT 770°C. INITIAL GRAIN SIZE AS IN FIG. 18. $\times 100$.

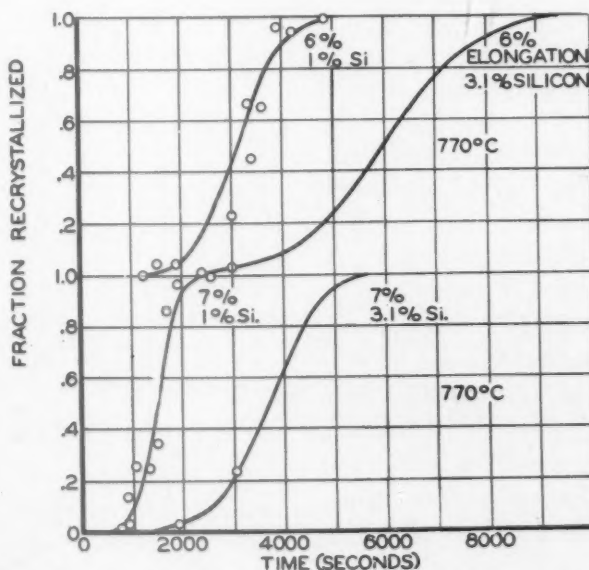


FIG. 20.—EFFECT OF COMPOSITION ON RECRYSTALLIZATION OF SILICON FERRITE.

The 3.1 per cent silicon alloy was elongated 6 and 7 per cent and was annealed at 770°C.; it was then compared

tallization is considerably retarded by the presence of silicon. For the 6 per cent elongation at $f(t) = 0.5$, half the low-alloy

material is recrystallized in 53 min., but the high-alloy material takes 1 hr. 40 min., or approximately twice as long. For the 7 per cent elongation, half the low-alloy

to be initially restrained by the presence of silicon. The rate of growth is definitely reduced. A combination of these effects results in a slower rate of recrystallization.

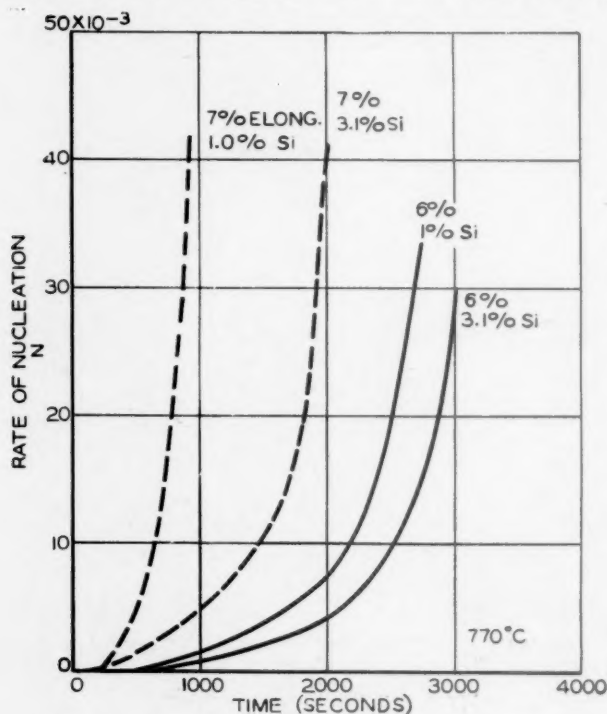


FIG. 21.—EFFECT OF COMPOSITION ON NUCLEATION.

material is recrystallized in 25 min. but the other requires about an hour—also twice as long.

The curve of the rate of nucleation for the 3.1 per cent alloy (Fig. 21) shows that the rate of nucleation with time is initially decreased in comparison with that of the 1 per cent alloy but eventually the rate becomes quite rapid. In Table 4, a comparison is made of the rates for the fraction recrystallized equal to 0.05, because comparisons at greater fractions are misleading since the rates are so very high. The rate of growth G and the incubation period C are also decreased by the addition of silicon, as shown in Table 4.

From this information, it can be said that the effect of more silicon in solid solution causes the material to recrystallize more slowly. The process of nucleation appears

TABLE 4.—Effect of Composition on N , G , and C

Elongation, Per Cent	N^a for $f(t) = 0.05$		G , Cm. per Sec.		C , Sec.	
	Low Silicon	High Silicon	Low Silicon	High Silicon	Low Silicon	High Silicon
6	0.005	0.045	6.2×10^{-5}	1.4×10^{-5}	530	465
7	0.032	0.071	8.6×10^{-5}	1.8×10^{-5}	270	42

^a Rate of nucleation expressed as number of nuclei per sec. per unit unrecrystallized area.

RECOVERY

Recovery of a cold-worked material usually refers to changes in certain properties occurring in the material at room temperature or somewhat above room temperature but below the temperature at which first signs of recrystallization occur. Such low-temperature heat-treatments are known to relieve stresses, and atomic

properties such as electrical resistivity, thermoelectric force, and magnetic characteristics are improved; i.e., they tend

Workers on recrystallization are not at all in agreement on the effect of recovery on nucleation.¹

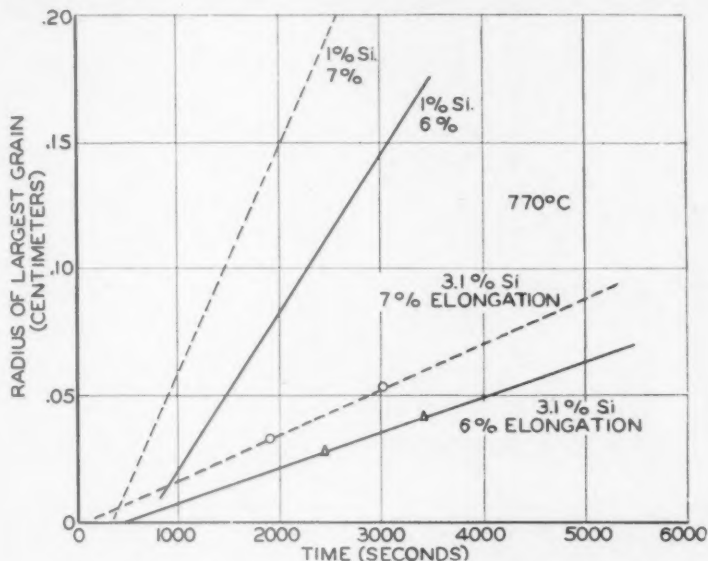


FIG. 22.—EFFECT OF COMPOSITION ON RADIAL GROWTH.

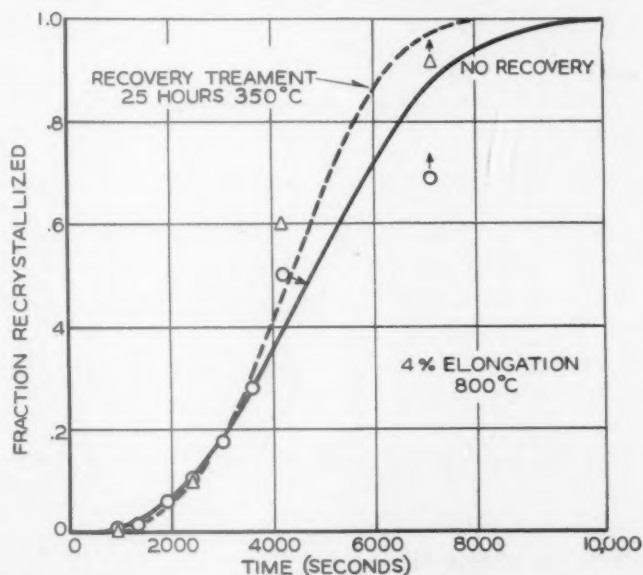


FIG. 23.—ISOTHERMAL RECRYSTALLIZATION FOR RECOVERED AND UNRECOVERED SAMPLES.

to approach values for annealed materials. Magnetic properties of ferromagnetic materials offer simple means of studying the changes due to recovery,¹¹ and this method has been used here to indicate changes in the cold-worked silicon ferrite before recrystallization.

An observation had already been made¹ that N appeared to decrease with recovery but no detailed or systematic investigation had been attempted at that time.

To establish the effect of recovery on silicon ferrite, the material was elongated 4 per cent and was annealed at 350°C. for

25 hr. The changes in magnetic properties after various intervals, 0.1, 1, 10, and 25 hr., were determined to show the progress of the recovery (Table 5). The coercive force*

materials are shown in Fig. 23. There is a slight difference in these curves. While at the start of recrystallization the curves are almost identical, they show a little de-

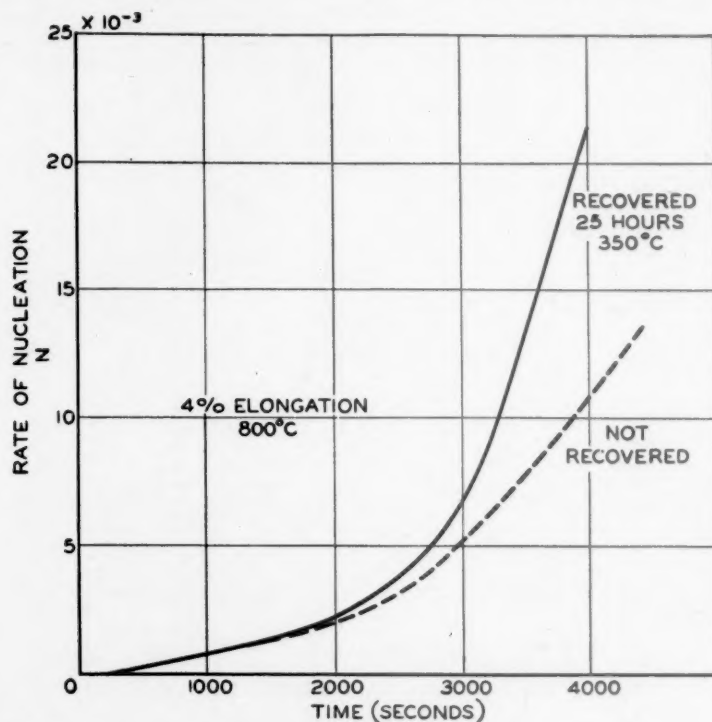


FIG. 24.—CHANGE IN NUCLEATION WITH TIME IN RECOVERED AND UNRECOVERED SAMPLES.

is of particular significance because it is a measure of the internal strain of the material. Note how elongation changes the coercive force from 0.81 oersteds for the annealed material to 2.90 for the cold-worked. Note also the rapid decrease in the coercive force at the start of the recovery treatment and the gradual change for succeeding periods.

After the elongated material had received the recovery treatment, it was recrystallized at 800°C. with material similarly elongated but not recovered. The grain size of this material was A.S.T.M. 6.0, Fig. 2.

The isothermal recrystallization curves for the recovered and unrecovered mate-

rials are shown in Fig. 23. There is a slight difference in these curves. While at the start of recrystallization the curves are almost identical, they show a little de-

TABLE 5.—Changes in Magnetic Properties on Recovery of One Per Cent Silicon Iron at 350°C.

Treatment	Permeability ^a		Coercive Force H_c	Remanence ^b B_r
	μ_{10}	μ_{100}		
25 hr. at 825°C.....	1,540	178	0.81	9,000
After 4 per cent elongation.....	805	176	2.90	4,000
0.1 hr. at 350°C.....	850	177	2.59	4,100
1.0 hr. (total) 350°C.....	885	178	2.50	4,200
10.0 hr. (total) 350°C.....	990	178	2.40	4,400
25.0 hr. (total) 350°C.....	1,015	178	2.35	4,400

^a Permeability for $H = 10$ and $H = 100$ oersteds, respectively, where permeability is B/H and B is given in gauss.

^b Coercive force in oersteds (H_c) and remanence in gauss (B_r) determined for $B_{max} = 10,000$.

* See ref. 11 for a discussion of these properties.

An analysis of the recrystallization curve discloses the behavior of the nucleation and growth of the nuclei that can account for the difference in the recrystallized

curve by decreasing the time for recrystallization. Recovery appears to increase the rate of nucleation but decreases the rate of growth. The rate of nucleation,

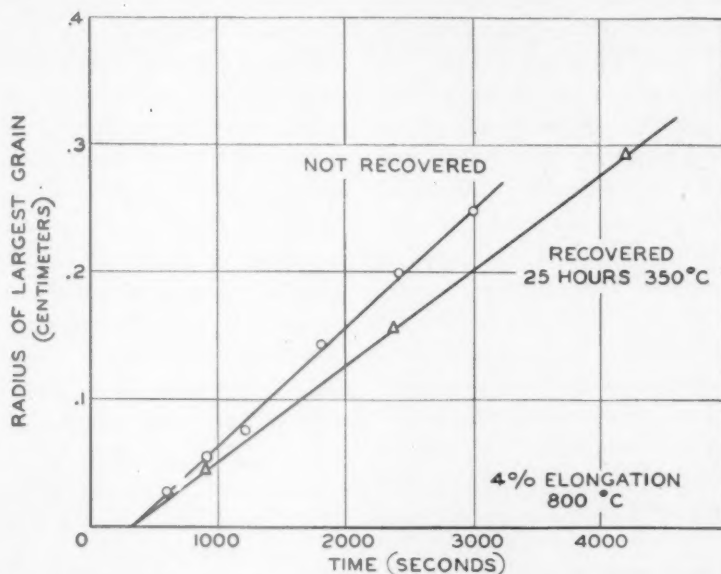


FIG. 25.—RADIAL GROWTH OF LARGEST GRAIN FOR RECOVERED AND UNRECOVERED SAMPLES.

curves. The rate of nucleation as a function of time for the recovered and unrecovered samples is shown in Fig. 24. Here the rates are about the same when recrystallization first starts, but after about 2000 sec. the recovered material has a higher rate of nucleation than the unrecovered material. More specifically, and by way of comparison, the rate of nucleation N at $f(t) = 0.2$ is 5.95×10^{-3} for the unrecovered material and 7.7×10^{-3} for the material recovered at 350°C .

There is also a difference in the rate of growth in the recovered and unrecovered silicon alloy (Fig. 25). The material that had been given a recovery treatment had a lower rate of growth G than the material that had no such treatment. The rate of growth G for the recovered material was 7.6×10^{-5} , and for the unrecovered material it was 9.56×10^{-5} . The period of incubation C is the same for both materials.

By way of summary, recovery slightly affects the isothermal recrystallization

however, is of such magnitude that it offsets the decreased rate of growth, resulting in a more rapid recrystallization. The increase in the rate of nucleation is surprising, because a decrease with recovery would be expected, since it is assumed that points of high stress are relieved by recovery.

DISCUSSION OF RESULTS

The rate of recrystallization of silicon ferrite has been shown to increase with increasing deformation, increasing temperature, and decreasing grain size; the rate is decreased by solid solution elements such as silicon; the rate is little affected by recovery, but little as the effect is, it increases the rate of recrystallization slightly.

Since the isothermal recrystallization curve is the result of the nucleation and growth processes, a consideration of these

processes is highly informative. Increasing the deformation increases both the rates of nucleation N and growth G . The rate of nucleation is principally effective in causing the increased rate of recrystallization. Increasing temperature, of course, increases both the rates of nucleation and growth—as might be expected, since both N and G are known to be activation types of reactions. Material of fine grain size has a high rate of nucleation compared with a coarser grained material, but the rate of growth for the grain sizes used is apparently constant. The addition of more silicon to the alloy initially decreases the rate of nucleation but subsequently the rate of nucleation becomes quite rapid; the rate of growth is reduced considerably. Recovery appears somewhat to increase the rate of nucleation and decreases the rate of growth, which is an unexpected result.

Some thoughts on nucleation itself are not out of order, but it should be borne in mind that most of these ideas are conjectures and an insight into the actual mechanism must await further work.

Recrystallization nuclei originate in the grain (or twin) boundaries, apparently from debris formed when a metal is cold-worked; this was observed as early as 1914.¹² With this idea in mind, one may visualize how the various factors influencing recrystallization may effect nucleation. As the strained metal is heated, the formation of nuclei from the grain-boundary debris might be considered as taking place in one of two ways. Fragments from parent grains might merely spheroidize or several fragments might coalesce into a more or less spherical particle. In either way, the particle or nucleus would grow into the strained matrix. Increasing the deformation would increase the amount of grain-boundary debris and thereby give rise to increased nucleation. Temperature would increase nucleation by hastening the diffu-

sion processes that affect the agglomeration and growth, so that nuclei would become visible in a shorter time. Grain size should markedly increase the nucleation because additional grain boundaries are provided in which more grain debris can form. Recovery would be expected to increase the rate of nucleation because the grain-boundary material would have additional time at a low temperature to coalesce and grow, and would have an advantage over material not recovered. The effect would be small as found, because the relatively low temperature of the recovery treatment would retard the formation of the nucleus. The manner in which composition would affect nucleation is difficult to postulate, unless the silicon would delay the coalescence of the grain debris.

The increase in the rate of nucleation with time might be explained in the following manner: During cold-work the regions of highest stress are those in the grain boundaries, and it is in these sites that fragmentation of the grains first begins. The formation of grain-boundary material or debris would probably follow a Maxwellian distribution as to size. Thus the potential nucleus is formed as the metal is cold-worked. On heating, the grain-boundary debris undergoes a coalescence or spheroidization and immediately begins to grow in the deformed matrix. The larger the coalesced particle, the sooner it becomes visible. Since there are few large particles according to the Maxwellian distribution, only a few nuclei will be visible in the early stages of the recrystallization. The next smaller coalesced particles require longer time for growth to be visible, but there are many more of them. This situation leads to an increased rate of nucleation, which is observed. Finally, the smallest coalesced particles would require the longest time to grow to be visible and would be fewer in number. The rate of nucleation would then

decrease. That such a state of things probably exists is verified by a crude grain-size distribution curve shown in an earlier paper,¹ of a study in which few large and small grains were found and many of intermediate size.

The occurrence of nuclei with multiple orientations (Fig. 1) might be explained by the idea that grain-boundary material becomes detached from the parent grain, serving either as a fragment, which would spheroidize, or as several fragments, which would coalesce into one orientation. Sometimes the debris would come from a single grain giving a nucleus of a single orientation. At other times the grain-boundary material would be a composite particle formed from two grains, the original grain boundary being a plane of symmetry in the nucleus, which might give a nucleus with two orientations. At still other times the greatest stress of the grain boundary would be at the intersection of three or more grains and a potential nucleus might form from debris from all these grains, which might give rise to nuclei of multiple orientations. It should not be forgotten that some nuclei with different orientations can form by impingement; if nuclei form too close together, such grains appear like buds along the periphery of a large grain.

Since the growth of nuclei is a process akin to self-diffusion, growth can be considered in terms of diffusion mechanisms. While the picture is entirely qualitative, it does offer an explanation of some observed facts. It is conceivable that one of the consequences of cold-work is the introduction of vacancies or voids in a crystal lattice, as postulated by Huntington and Seitz¹³ and by Huntington.¹⁴ If so, it follows that the greater the cold-work the greater the number of vacancies and the more rapid the growth, when the material is recrystallized. Temperature would affect the growth by increasing the rate of interchange between the strained and

unstrained material. The grain size might be expected to be ineffective in affecting the number of vacancies formed, but composition (increase in solid solution elements) would be expected to retard the formation of vacancies by the strengthening effect of the addition. Recovery also might be expected to decrease the number of vacancies because of a "healing" action of recovery, which would cause some of the vacancies to diffuse out.

SUMMARY

1. Data are presented on the effect of deformation on the recrystallization of 1 per cent silicon ferrite. It is shown that increasing deformation increases the rate of recrystallization because both the rates of nucleation and growth are increased.

2. The effect of temperature was studied at 740°, 770°, and 800°C. on the isothermal recrystallization curves. Temperature increases the rates of nucleation and growth and thereby increases the rate of recrystallization. An estimate is made of the activation energies for nucleation and growth, since both are reaction-rate processes.

3. A fine-grained material recrystallizes more rapidly than a coarse-grained material because of the great effect of the grain size on the rate of nucleation. The rate of growth is practically constant.

4. The addition of a solid solution element like silicon to iron decreases the rate of recrystallization because the alloy addition initially delays the rate of nucleation, though eventually it becomes quite rapid. The silicon addition decreases the rate of growth.

5. Recovery of cold-worked 1 per cent silicon ferrite for 25 hr. at 350°C. results in a very slight increase in the rate of recrystallization. Recovery appears to increase the rate of nucleation and decrease the rate of growth.

REFERENCES

1. J. K. Stanley and R. F. Mehl: *Trans. A.I.M.E.* (1942) **150**, 260.
2. J. Czochralski: *Moderne Metallkunde*. Berlin, 1924. Julius Springer.
3. R. F. Mehl: *Metals Handbook* (1939) 207. Amer. Soc. for Metals.
4. G. Tammann: *Lehrbuch der Metallkunde*, 183. 1932, Leopold Voss.
5. E. Schmid und W. Boas: *Kristall Plastizität*, 24. Berlin, 1935. Julius Springer.
6. Discussion by W. R. Johnson of paper by F. C. Hull, R. A. Colton, and R. F. Mehl: *Trans. A.I.M.E.* (1942) **150**, 208.
7. W. A. Johnson and R. F. Mehl: *Trans. A.I.M.E.* (1939) **135**, 416.
8. W. A. Anderson and R. F. Mehl: *Recrystallization of Aluminum in Terms of Rate of Nucleation and Rate of Growth*. *Trans. A.I.M.E.* (1945) **161**, 140.
9. J. A. M. van Liempt: *Ztsch. anorg. allg. Chem.* (1931) **195**, 366.
10. R. Becker: *Ztsch. techn. Physik* (1926) **7**, 547.
11. J. K. Stanley: This volume, page 106.
12. C. Chappell: *Jnl. Iron and Steel Inst.* (1914) **89**, 460.
See also H. C. H. Carpenter and F. Elam: *Jnl. Inst. for Metals* (1921) **25**, 303.
13. H. B. Huntington and F. Seitz: *Phys. Rev.* (1942) **61**, 315.
14. H. B. Huntington: *Phys. Rev.* (1942) **61**, 325.

DISCUSSION

R. WARD* and C. G. DUNN.†—Changes occurring on heat-treating a polycrystalline material previously deformed a small amount may be one of recrystallization, grain growth or recovery, or a combination of these phenomena. In general, grain refinement is often considered¹⁵ sufficient proof of recrystallization, but a refinement of grain size is not necessarily a criterion of this phenomenon. The main distinction between recrystallization and grain growth is that in recrystallization new grains, essentially strain free, appear and grow, whereas for grain growth some grains may recover, at least partially, and grow at the expense of their neighbors. This latter phenomenon, like the former, may be described in terms of rates. It is not evident that grain growth alone is excluded as a possibility in the present work and it appears to us that the author has not offered sufficient proof¹⁶ of nucleation. Actual proof of nucleation is

* Research Metallurgist, General Electric Co., Pittsfield, Mass.

† Research Physicist, General Electric Co., Pittsfield, Mass.

¹⁵ H. C. H. Carpenter and F. Elam: *Crystal Growth and Recrystallization in Metals*. *Jnl. Inst. of Metals* (1920) **24**, 83-154.

absent also in other papers^{1,8} dealing with recrystallization.

Not only does grain growth in deformed material show certain time effects as does recrystallization, but grain growth following recrystallization may do the same. For example, it has been observed in this laboratory, for copper and for silicon ferrite, that abnormal grain growth from a fine-grained recrystallized matrix shows a time dependence similar to that shown by the author, by Stanley and Mehl¹ and by Anderson and Mehl⁸ for their work on deformed fine-grained samples of silicon ferrite and of aluminum. In copper that has been cold-rolled above 90 per cent and annealed at a high temperature to produce a fine-grained recrystallized matrix, it is found that large modular grains grow after a period of time in excess of the time required for complete recrystallization. Little is known about the process that requires time before abnormal growth begins (an incubation period for such growth). However, in the case of recovery and growth in deformed grains of silicon ferrite (also observed in this laboratory) it is known that deformed grains do recover at least partially before growth begins and time is required for this process.

A number N might be convenient to use in computing rates of transformation in recrystallization and in abnormal grain-growth processes, but numerical values do not prove that a nucleation process such as the formation of new grains at grain boundaries, at twin boundaries, or along slip planes really takes place. We agree with Maddigan¹⁶ that large-grained samples would be preferable to small-grained samples in order to observe the early stages of recrystallization. However, even here difficulty may arise because it has been observed¹⁷ that early nuclei do not always survive during recrystallization. In fact, most of them did not in the case cited.

Granting that the author does have true recrystallization, two other points should be discussed.

First, there is the effect of recovery on recrystallization. It is known, for instance, that certain physical properties can be entirely

¹⁶ *Trans. A.I.M.E.* (1942) **150**, 271.

¹⁷ C. G. Dunn: *Orientation Changes during Recrystallization in Silicon Ferrite*. *Trans. A.I.M.E.* (1945) **161**, 98.

recovered in some metals below the recrystallization temperature. It is also known that recovery may continue concomitantly with recrystallization. In one case of this type it was observed¹⁸ that lattice perfection in silicon ferrite crystals was restored to a remarkable degree. Now, if lattice perfection mainly could be restored by a recovery process, it is reasonable to suppose that nearly all physical properties then would recover nearly 100 per cent. It may be noted from the data of Table 5 that the coercive force is still 190 per cent over the original value, even after the recovery treatment. We may conclude from this that recovery is far from complete and that the sample is in a state of partial recovery.

Treatments that put a sample into a state of partial recovery could, we think, leave the sample in an uncertain position relative to an untreated one. For instance, the partially recovered sample might recrystallize more rapidly because some recovery apparently always precedes recrystallization, or it might recrystallize more slowly or not at all because fairly complete recovery interferes with both nucleation¹⁹ and growth.¹⁸

Secondly, in regard to grain-size uniformity, isothermal curves for initially different grain-size materials show that recrystallization of material having a fine grain size is more rapid than for the material having the larger grains. These conclusions are drawn from materials that previously have been annealed at 700° and 825°C. to produce grain sizes of A.S.T.M. 9.0 and 6.0, respectively. However, when the author anneals material at 875°C. he fails to obtain the circular nuclei obtained with the aforementioned anneals. This failure he attributes to the nonuniformity of grain size obtained. It appears to us that in view of the previous results it would be more logical to attribute the lack of growth of circular nuclei to the average grain size than to nonuniformity. In fact, one would expect that in material having a nonuniform grain size the value of N might assume some intermediate value between the value of N for the smaller and the larger size, provided, of course, that circular

growth takes place for both these sizes. It has been observed in this laboratory that growth similar to that described in the present paper is found in copper when the initial grain size is uniformly fine, and even when the grain size varies from 494 to 23 gr. per sq. mm. within the same material. However, when the initial uniform grain size is 23 gr. per sq. mm., no circular nuclei appear. Anderson and Mehl⁸ further show that no data could be obtained with material having an initial large grain size. Further studies should be made to establish the effect of grain-size uniformity on the process being studied.

W. A. ANDERSON.*—Mr. Stanley's paper is of considerable interest. Dr. R. F. Mehl and I recently completed a similar investigation on aluminum⁸ and found that the rates of nucleation and growth increase with increasing temperatures and increasing degrees of deformation and decrease with increasing grain sizes. These results are substantially the same as those of Mr. Stanley. The agreement suggests that these behaviors may be expected in other metals and solid solution alloys.

I am inclined to disagree with Mr. Stanley, however, on the interpretation of the structures shown in Figs. 18 and 19. I believe that the structure represented in Fig. 19 is unrecrystallized, for two reasons: (1) the grain size of this sample is essentially the same as that of the unstrained sample shown in Fig. 18, and in all of Mr. Stanley's previous work it has been shown that the recrystallized grains are many times larger than the grains in the matrix of the unrecrystallized metal (Fig. 1); (2) since the material in question has the coarsest grain size of any used in this investigation, it should be the slowest to recrystallize. The sample in Fig. 19, however, has been heated for only 40 min. at 770°C. As shown on the recrystallization curves in Fig. 15, this is sufficient time for only a small percentage of recrystallization in a series of samples with a much finer grain size. It appears doubtful, therefore, that any recrystallization would occur under similar experimental conditions in a material with a much larger grain size.

J. K. STANLEY (author's reply).—Ward and Dunn raise the question whether or not one is

¹⁸ C. G. Dunn: Recrystallization and Twin Relationships in Silicon Ferrite. *Trans. A.I.M.E.* (1944) **158**, 372-386.

¹⁹ J. A. Collins and C. H. Mathewson: Recrystallization of Aluminum Single Crystals. *Trans. A.I.M.E.* (1940) **137**, 150-169.

* Aluminum Research Laboratories, New Kensington, Pennsylvania.

actually observing recrystallization. They seem to feel that one may be observing grain growth. To the writer there appears little doubt that the process discussed in the present paper is one of recrystallization—namely, that strain-free grains form and grow in the cold-worked strained matrix. That the phenomenon is not grain growth is shown by the fact that the process does not have the characteristics of grain growth—namely, the general slow rate of grain growth even at elevated temperatures, the difficulty of calling any particular grain a nucleus different in some manner from its neighbors, and the fact that usually the grains during grain growth are more or less of the same size.

In the present study, the origin of the nuclei in the deformed matrix was not established. Two possibilities exist for their origin. In the first case the nuclei may occur in the points of highest strain at grain boundaries and twin planes; this is old knowledge.¹² See also the fine photograph of partly recrystallized admiralty metal,²⁰ which shows nuclei in old grain boundaries and on twin planes. In the second case the nucleus might originate as a favored grain in the deformed matrix, for some reason or other, and begin to grow rapidly into its neighbors. This type of nucleus has not been observed and, furthermore, if such mechanism were operative for recrystallization, there could never be refinement in the grain size, which, as everyone knows, is a characteristic of deformed (not necessarily completely fragmented) and recrystallized metals.

It has been shown recently, by Barrett,²¹ that deformed grains are not strain free until they are recrystallized. Yet it is well known that recrystallized metals show grain growth. Ward and Dunn, however, suggest that during grain growth some grains may recover (become partially strain-relieved) and grow at the expense of their neighbors. That strained grains do recover is not questioned, but the implication is that grain growth is determined by variations in strain energy in the various grains. Experimental evidence of this point would be welcome, as would data on rates (assuming that Ward and Dunn are talking about rates of nucleation and growth).

²⁰ W. Campbell: *Trans. A.I.M.E.* (1926) **73**, 1135, Fig. 1.

²¹ C. S. Barrett: *Trans. A.I.M.E.* (1945) **161**, 15.

In regard to time and temperature for recrystallization and grain growth, it can be said, in general, that recrystallization will occur in relatively short times and at low temperatures as compared with grain growth, which takes place at higher temperatures and requires considerably longer annealing times.

Hardness measurements of partially recrystallized silicon ferrite show that the recrystallized material (nuclei) are softer (strain-free) than the matrix from which they grow. Hardness measurements were carried out on the Tukon tester, on which Knoop hardness numbers were obtained. Polished specimens that had been elongated 6 per cent and were recrystallized at 740°C. were used for the tests. Four readings were taken for each of the following averages:

Specimen	Recrystallized (Nuclei), K.H.N.	Unrecrystallized Matrix
1.....	118	127
2.....	137	147

Ward and Dunn make some unusual observations on the grain growth of copper and claim a time dependence for this mechanism similar to that reported for silicon ferrite. Detailed information on this study would be appreciated.

Discussion as to the effect of recovery on recrystallization is appreciated, but it must be borne in mind that this phase of the study is far from complete. It appears doubtful that lattice perfection can be restored completely in a cold-worked metal unless it is recrystallized.²¹

The remarks of Ward and Dunn and of W. A. Anderson on the effect of grain structure are well taken. Certainly there remains much work to be done to settle this question. Dr. Anderson believes that the structure in Fig. 19 is not recrystallized. About this point the writer is not certain, although microscopic examination seemed to show some difference between the unannealed and annealed samples. This point was not pursued further, because all that the writer wished to indicate was that a fine, uniform grain size is a prerequisite to circular growth of the nuclei under the annealing conditions of the experiment.

Oxide-metal Layers Formed on Commercial Iron-silicon Alloys Exposed to High Temperatures

BY RAYMOND WARD,* JUNIOR MEMBER A.I.M.E.

(New York Meeting, February 1945†)

IN the past few years several papers have appeared dealing with different aspects of the oxidation of dilute alloys, especially with respect to the formation of internal oxides or subscales. Subscale has been defined¹ as that layer or zone of oxide particles precipitated in a matrix of metallic metal in which the oxide particles are dispersed uniformly and occur by diffusion of the oxygen inward from the metal surface. Alloys composed of a solvent metal more noble than the alloying elements are subject to subscale or internal oxidation. In these alloys the solute must be present in such quantities that if the alloy is exposed to an oxidizing atmosphere at elevated temperatures, the rate of diffusion of the oxygen into the metal will be greater than the rate of diffusion of the solute outward. There is a composition range of the iron-silicon system that falls into this classification.

Knowledge of the nature and rates of oxidation of iron-silicon alloys is of great commercial importance, but very little information of this nature is available. Darken² recently has made calculations to show the limits of concentration of silicon for which subscales are produced in iron-silicon alloys; however, the main thesis of his paper was to analyze and to explain the already existing data. The purpose of this paper is to present the effect of com-

position, temperature, time, and atmosphere on the type of scale-metal layer obtained and to give some qualitative indication of the effect of these variables on the rates of oxidation. Since this paper is a study of silicon steels that are available commercially, extremely low-silicon and high-silicon alloys are not included.

EXPERIMENTAL PROCEDURE

The alloys used in the experiment were taken from heats of silicon steel that ranged in analysis from 0.70 to 5.8 per cent silicon. This composition range takes in most of the commercial silicon steels. In Table I are listed the compositions of alloys used. Other than iron and silicon, the alloys normally contained approximately the following impurities: carbon, 0.03 per cent; manganese, 0.07; phosphorus, 0.008; sulphur, 0.02; copper, 0.07; tin, 0.01, and from nil to a trace of chromium, nickel and copper. All of the alloys used were melted in open-hearth furnaces, except where otherwise noted, and were hot-rolled to 0.100-in. plate. Samples approximately 1/2 in. square were then cut from these materials. So that the surface conditions of the samples used for oxidation would be standardized, each sample was ground through 000 emery paper immediately before oxidation.

Two different techniques were employed in carrying out the oxidizing treatments. One consisted simply of heating the samples with free access to air. In this treatment the samples were set on edge on a refrac-

Manuscript received at the office of the Institute Nov. 29, 1944. Issued as T.P. 1832 in METALS TECHNOLOGY, August 1945.

* Research Metallurgist, General Electric Co., Pittsfield, Massachusetts.

† Meeting canceled.

¹ References are at the end of the paper.

TABLE I.—*Conditions of Oxidation*
TIME OF OXIDATION IN MINUTES

Oxidation Media.....		Air/			Fe ₂ O ₃							Fe ₃ O ₄ + H ₂ O				Fe ₂ O ₃ + Fe				Fe ₃ O ₄ + Fe + H ₂ O				
Temperature, deg. C.....		800	900	1000	600	700	800	900	1000	1100	1200	800	900	1000	1100	1200	800	900	1000	1100	1200	800	900	1000
Steel No.	Si, Per Cent	none	none	120	120	120	120	120 ^a	120 ^a	120	120	none	none	none	none	none	none	none	none	none	none	none	none	none
1	0.70	none	none	120	120	120	120	120	120 ^a	120	120	120	120	120 ^a	120 ^a	120 ^a	120 ^a	120	120	120	120	120	120	120
2	1.28	30 ^b	120	5	none	none	2700	120	120 ^a	120	120	120	120	120 ^a	120 ^a	120 ^a	120	120	120	120	120	120	120	120
3	1.30	none	none	120	120	120	120	120	120 ^a	120	120	120	120	120 ^a	120 ^a	120 ^a	120	120	120	120	120	120	120	120
4	1.56	none	none	120	120	120	120	120	120 ^a	120	120	120	120	120 ^a	120 ^a	120 ^a	120	120	120	120	120	120	120	120
5	2.55	10 ^c	120	20	120	120	120	120	120	120	120	120	120	120 ^a	120 ^a	120 ^a	120	120	120	120	120	120	120	120
6	2.78	30 ^c	120	none	none	none	120 ^d	120	120 ^a	120	120	120	120	120 ^a	120 ^a	120 ^a	120	120	120	120	120	120	120	120
7	3.11	30 ^b	120	5	120	120	120 ^d	120 ^d	120 ^a	120	120	120	120	120 ^a	120 ^a	120 ^a	120	120	120	120	120	120	120	120
8	3.17 ^a	10 ^c	120	20	none	none	2700	120	120 ^a	120	120	120	120	120 ^a	120 ^a	120 ^a	120	120	120	120	120	120	120	120
9	4.24	10	120	20	none	none	120	120	120 ^a	120	120	120	120	120 ^a	120 ^a	120 ^a	120	120	120	120	120	120	120	120
10	4.28	30 ^c	120	120	120	120	120 ^d	120 ^d	120 ^a	120	120	120	120	120 ^a	120 ^a	120 ^a	120	120	120	120	120	120	120	120
11	4.69	10	120	20	none	120	2700	120	120 ^a	120	120	120	120	120 ^a	120 ^a	120 ^a	120	120	120	120	120	120	120	120
12	5.81	7200	none	120	120	120	120	120	120 ^a	120	120	120	120	120 ^a	120 ^a	120 ^a	120	120	120	120	120	120	120	120

^a Arc-furnace heat.^b Also treated at 5, 240, 1200, 2700, 6000, 7200, 14400 minutes at temperature.^c Also treated at 2700, 6000, 7200, 14400 minutes at temperature.^d Duplicate samples run for these conditions.^e Also treated at 0, 10, 30, 60, 600 minutes at temperature.^f Many other samples not listed were given air oxidizing treatments at 800°C. with negative results.

tory in an electrically operated and controlled muffle furnace. The second method used was one that maintained a definite atmosphere during heat-treatment. Samples were packed in iron tubes with ferric oxide (Fe_2O_3) and with a mixture of ferric oxide and iron powder to form effectively the magnetic oxide Fe_3O_4 . In a few special cases a small amount of water was added to the tube to determine the effect of water vapor on the oxidation process.

Samples were heated in air at 800°, 900° and 1000°C. and in closed containers containing oxidizing agents at 600°, 700°, 800°, 900°, 1000°, 1100° and 1200°C. The time factor varied from 5 min. to 240 hr. for air oxidation and from time to reach temperature to 10 hr. for the samples heated in the tube container. Heat-treatments were given according to the schedule shown in Table 1.

After heat-treatment, each sample was sectioned across the center and perpendicular to the broad face, mounted and polished by the usual methods with special effort to maintain the outer oxide layer. No etchants were used, as the scale layers were revealed after the polishing operation.

OBSERVATIONS

For any oxidation condition that allows subscale formation there usually is a composition limit above which subscale is no longer observed. This limit depends on the oxidizing conditions imposed. Variations of temperature, oxidizing media, and to some extent time, all have an effect upon the oxidation characteristics. Micrographs illustrating the effect of these variables are shown in Figs. 1 to 5 and are discussed below.

Effect of Composition and Temperature

Alloys below 2.55 Per Cent Silicon.—Limiting the atmospheres to an oxygen content of the decomposition pressure of Fe_2O_3 and the time at 2 hr., it is noted that in the main the precipitation of oxides

follows the same general pattern noted previously.^{1,3} For a 0.7 per cent silicon alloy oxidized at 800°C., precipitation takes place mainly along grain boundaries (Fig. 6). Close observation shows that although the front of advance is mainly by grain-boundary oxidation, precipitation in arrears is taking place within the grain. This intragrain pattern is somewhat similar in appearance to alpha veining.

An increase in the temperature gives rise to more general precipitation throughout the grain (Fig. 1a) and, in addition, an increase in temperature straightens the subscale-metal boundary. To obtain general precipitation and straight subscale-metal boundaries on samples with increased silicon content, higher temperatures of oxidation are necessary. For example, the subscale-metal boundary in the 0.7 per cent silicon alloy at 1000°C. is much straighter than the boundary in an alloy containing 1.3 per cent silicon; likewise, precipitation in the 1.56 per cent silicon alloy at 1000°C. appears to take place first by diffusion of the oxygen at the grain boundaries and then diffusion from this locality to the center of the grain. The oxidation process produces a fine precipitate, which outlines the grain boundary. This is in distinct contrast to the 0.7 per cent silicon steel treated at the same temperature, which gives an evenly distributed precipitate although the boundary is somewhat irregular. At temperatures in the neighborhood of 1200°C. all alloys up to and including 1.56 per cent silicon have regular bands of evenly dispersed oxides similar to Fig. 7. It thus appears that even at high temperatures preferential grain-boundary precipitation takes place, as is evidenced in the 1.56 per cent silicon alloy cited above and is further illustrated in the 1.3 per cent silicon alloy oxidized at 1100°C. (Fig. 3d) and at 1000°C. for a longer period of time (Fig. 4e).

Alloys of 2.55 Per Cent Silicon and Above.—Alloys ranging from 2.55 per cent

Steel No.

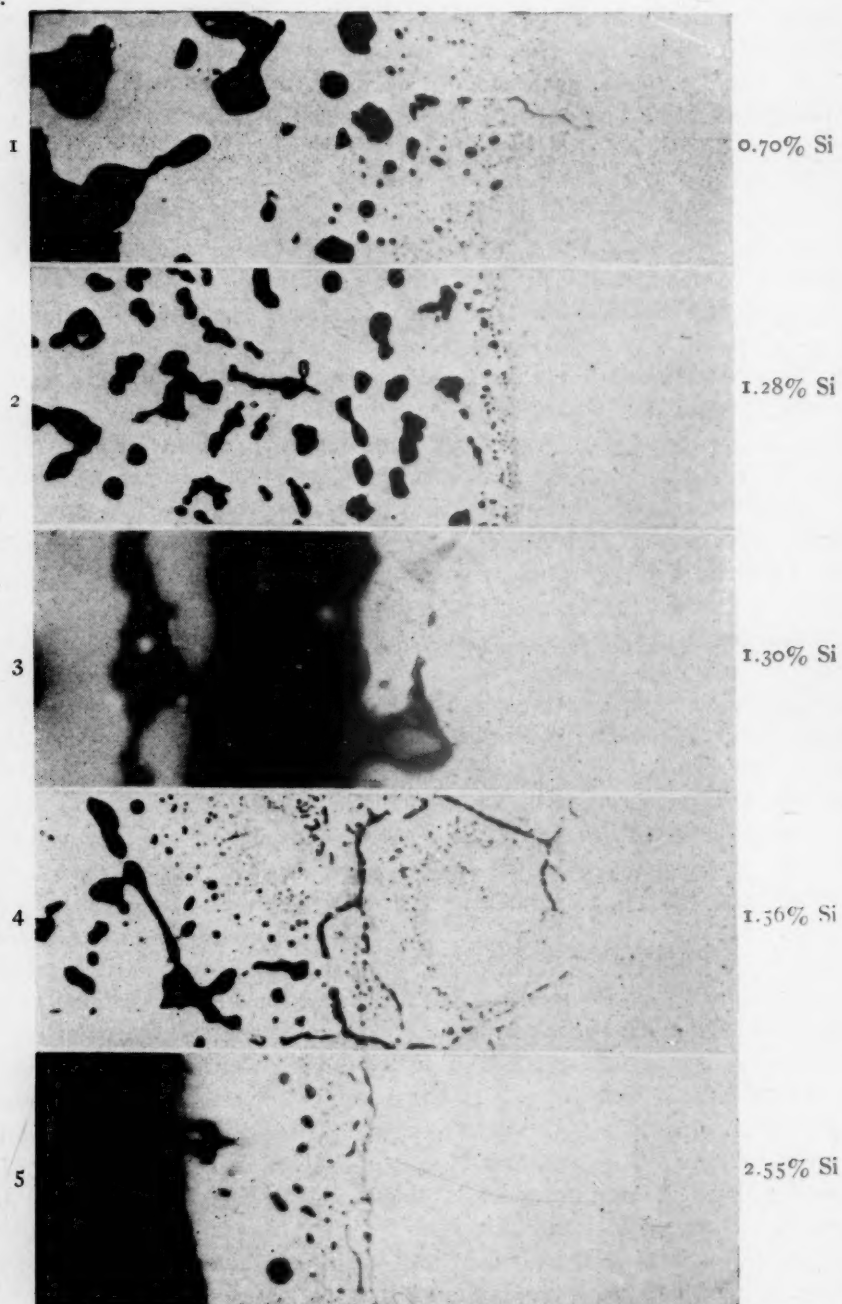


FIG. 1.—IRON-SILICON STEELS OXIDIZED IN Fe_2O_3 2 HOURS AT 1000°C . $\times 600$ UNETCHED. External surface at left side.

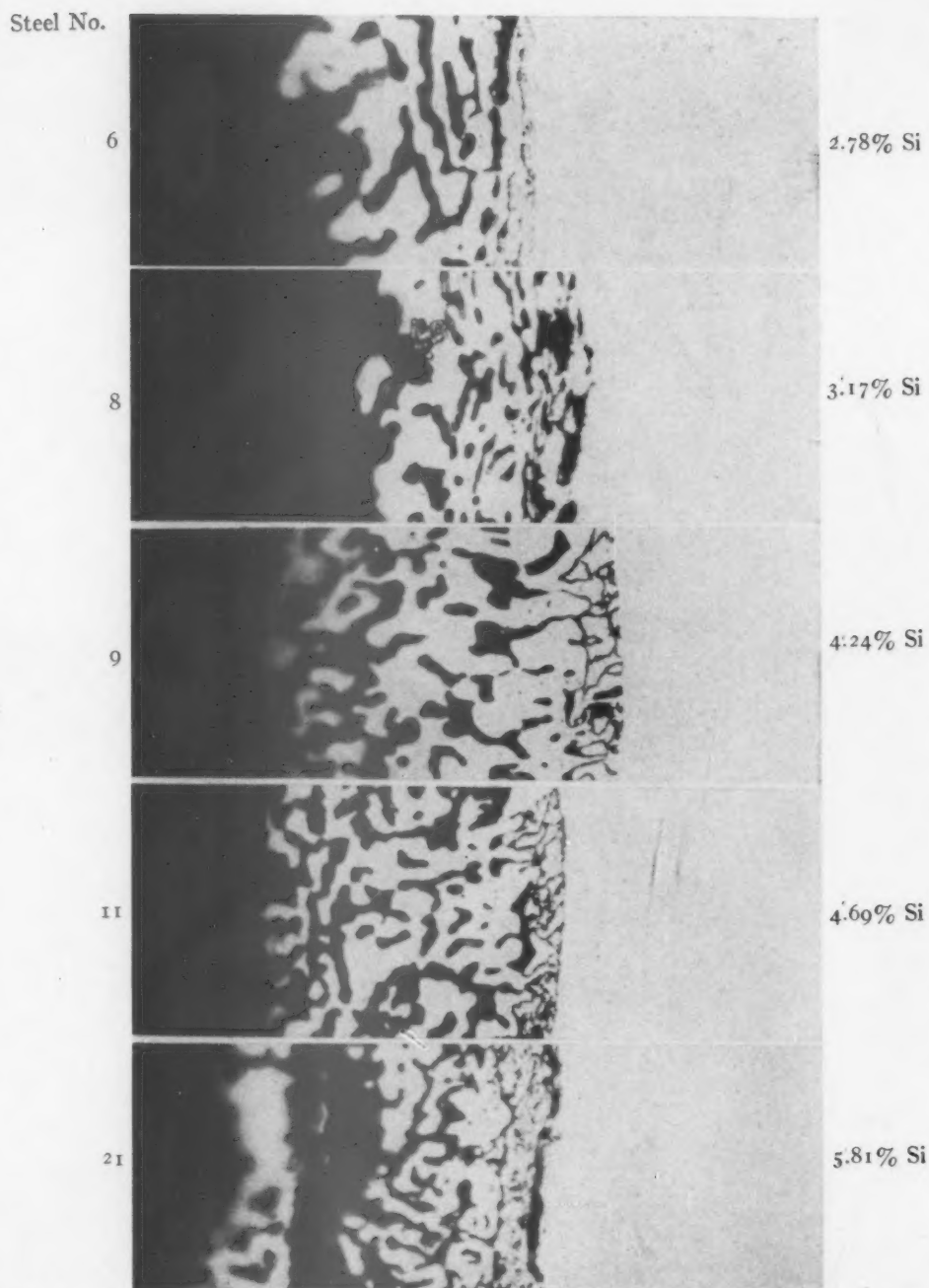


FIG. 2.—IRON-SILICON STEELS OXIDIZED IN Fe_2O_3 2 HOURS AT 1000°C . $\times 600$. UNETCHED.
External surface at left side.

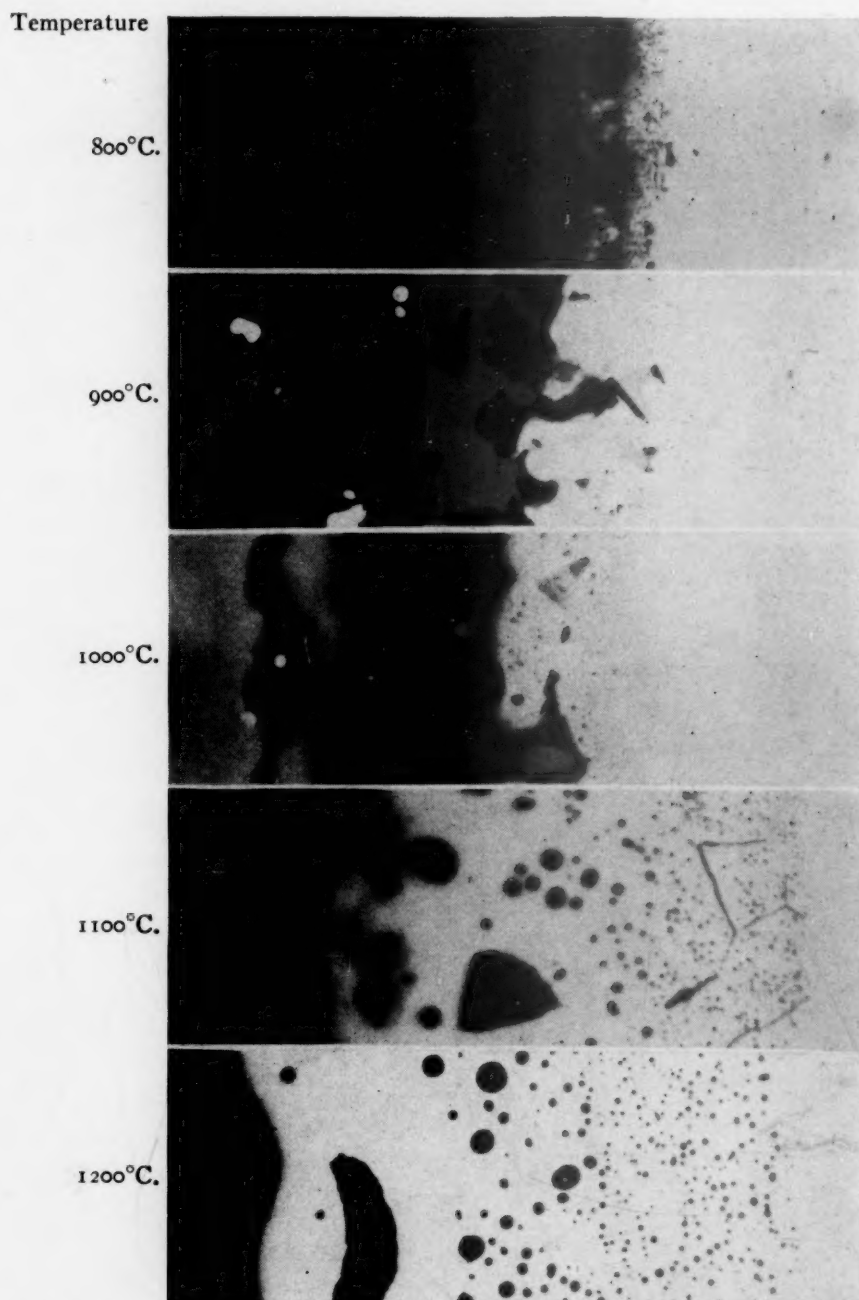


FIG. 3.—STEEL NO. 3 (1.30 PFR CENT Si) OXIDIZED IN Fe_2O_3 2 HOURS. $\times 600$. UNETCHED.
External surface at left side.

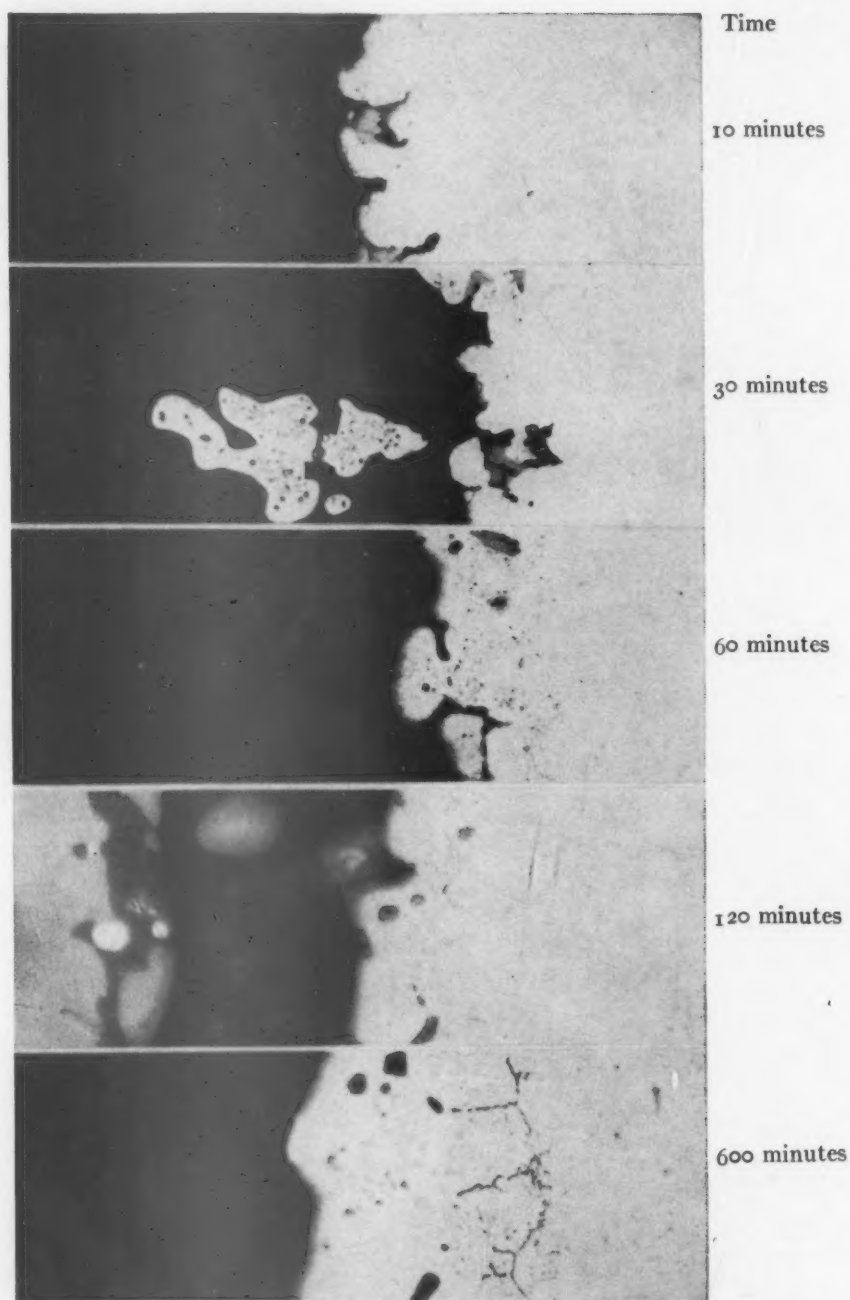


FIG. 4.—STEEL NO. 3 (1.30 PER CENT Si) OXIDIZED IN Fe_2O_3 AT 1000°C . $\times 600$. UNETCHED.
External surface at left side.

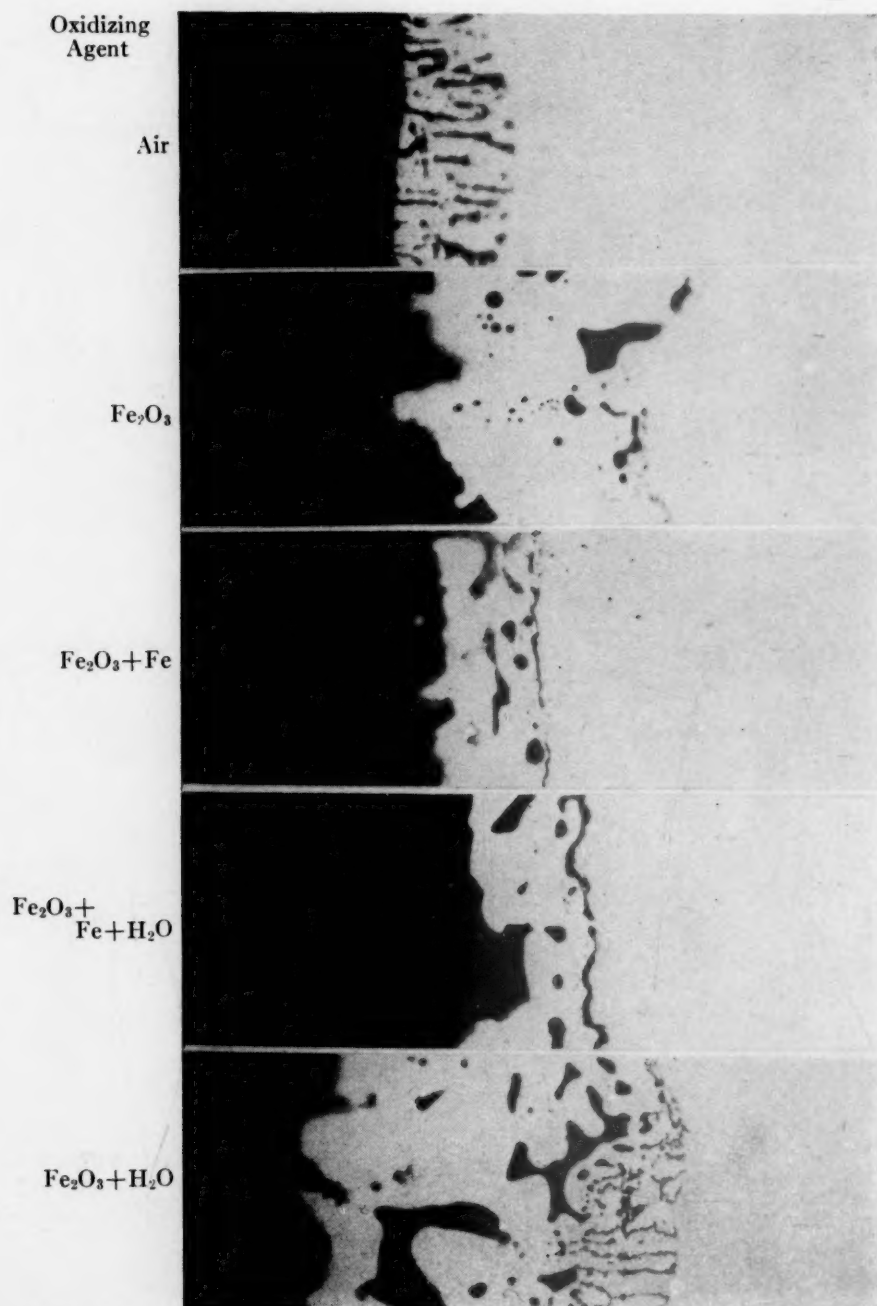


FIG. 5.—STEEL NO. 7 (3.11 PER CENT Si) OXIDIZED 2 HOURS AT 1000°C. $\times 600$. UNETCHED. External surface on left.

silicon and up oxidize in a manner different from those in the lower silicon brackets. Irregular shaped complex oxide particles are formed, which increase in number as the silicon content is increased. There is for these higher silicon alloys a temperature-composition interdependence which results in scale-metal layers that are different in appearance from those alloys discussed above.* In the region of 700°C., some samples develop scale-metal layers in which the precipitate occurs as lamellae in a direction perpendicular to the surface of the specimen and at distances from each other that apparently depend on the orientation of the grain with respect to the sectioned surface (Fig. 8). To distinguish this type of layer from other scale-metal structures, the layer will be referred to as a "pearlitic" type because of the similarity in appearance to the pearlite of iron-carbon alloys. This type of scale-metal layer occurs in steels having 2.55 per cent to 5.8 per cent silicon when oxidized at 700°C., and to a limited extent in the same composition range at 800°C., but occurs more predominantly in alloys above 4 per cent silicon at this higher temperature. Grains appear well differentiated by virtue of the difference in spacing of the lamellae. Evidence of the fact that the structure observed in the scale-metal layer existed from the beginning of the oxidation process is gained from observation of the scale layer. In the scale layer the same "pearlitic" structure is seen, except that the metal of the scale-metal layer is now replaced by oxides and the structure is much less clear. Close observation shows evidences of previous grains and grain boundaries in the scale layers. No struc-

tures of the "pearlitic" type are seen above temperatures of 800°C. for the range of alloys studied.

At 800°C. layers of oxide alternated with

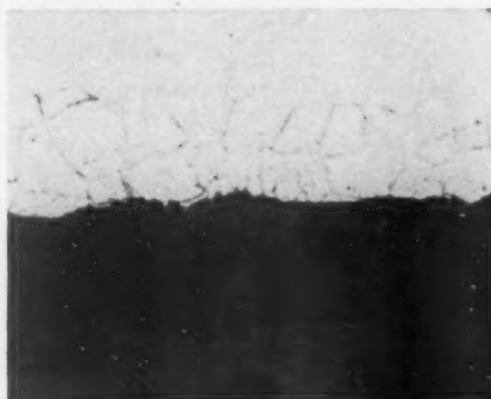


FIG. 6.—STEEL NO. 1 (0.7 PER CENT Si) OXIDIZED IN Fe_2O_3 2 HOURS AT 800°C.

Shows oxidation taking place along grain boundaries. Note faint lines of precipitate in grains behind most advanced grain-boundary oxides. External surface at bottom.

layers of metal parallel to the metal surface appear to be the stable type of oxide structure (Figs. 9a, 10a and 11a). The layers appear very much akin to Liesegang⁶ structures and the oxides become increasingly more plentiful as the concentration of silicon in the alloy is increased. A difference between the structures heretofore seen in other alloy systems and the present structure is that we believe the present oxide layers are composed of solute oxide plus solvent oxide. The explanation for layers of this type probably falls along similar lines of reasoning that is used to explain the formation of Liesegang rings, but is somewhat more complex, since here the formation of an iron oxide as well as silicon dioxide must be accounted for. This type of structure obtains up to temperatures of about 1000°C. At these temperatures the oxide particles become more spheroidal (Figs. 9b, 10b, 11b).

The particles in the scale-metal layers obtained at temperatures from 1000° to 1200°C. are much more easily identified because of their coarseness of structure.

* The layers on these higher silicon alloys are similar to the layers on the alloys containing lesser amounts of silicon, in that there are oxides present in a matrix of pure metal, but differ in that in a number of cases the oxides found are connected to the outer scale. For this reason the layers on these higher silicon compositions will hereafter be termed scale-metal layers.

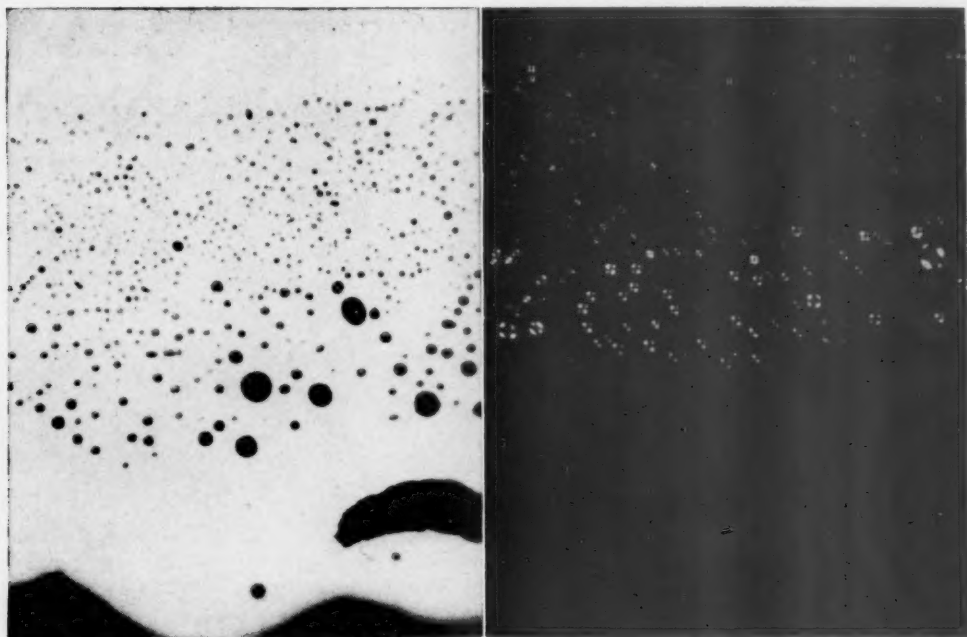


FIG. 7.—STEEL NO. 3 (1.30 PER CENT Si) OXIDIZED IN Fe_2O_3 2 HOURS AT 1200°C . $\times 600$.
UNETCHED.

Shows appearance of oxide particles (a) with bright-field illumination and (b) with polarized light. External surface at bottom.

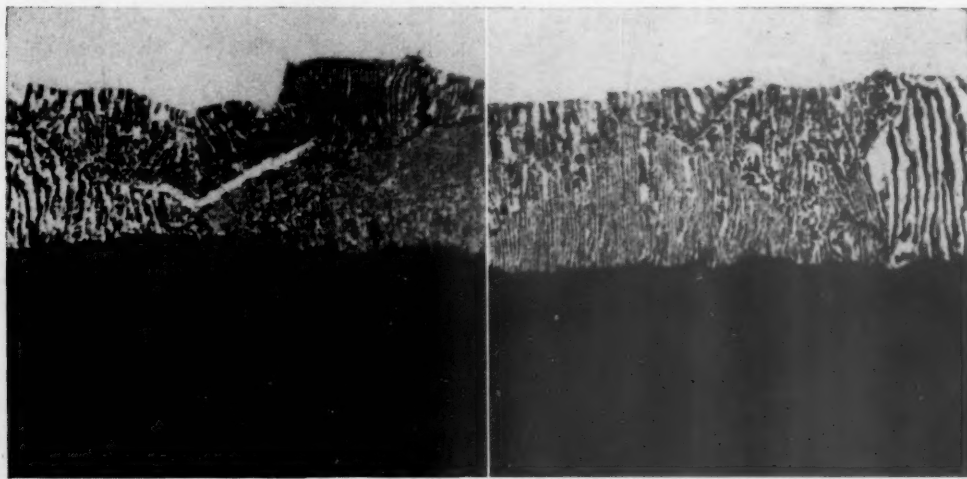
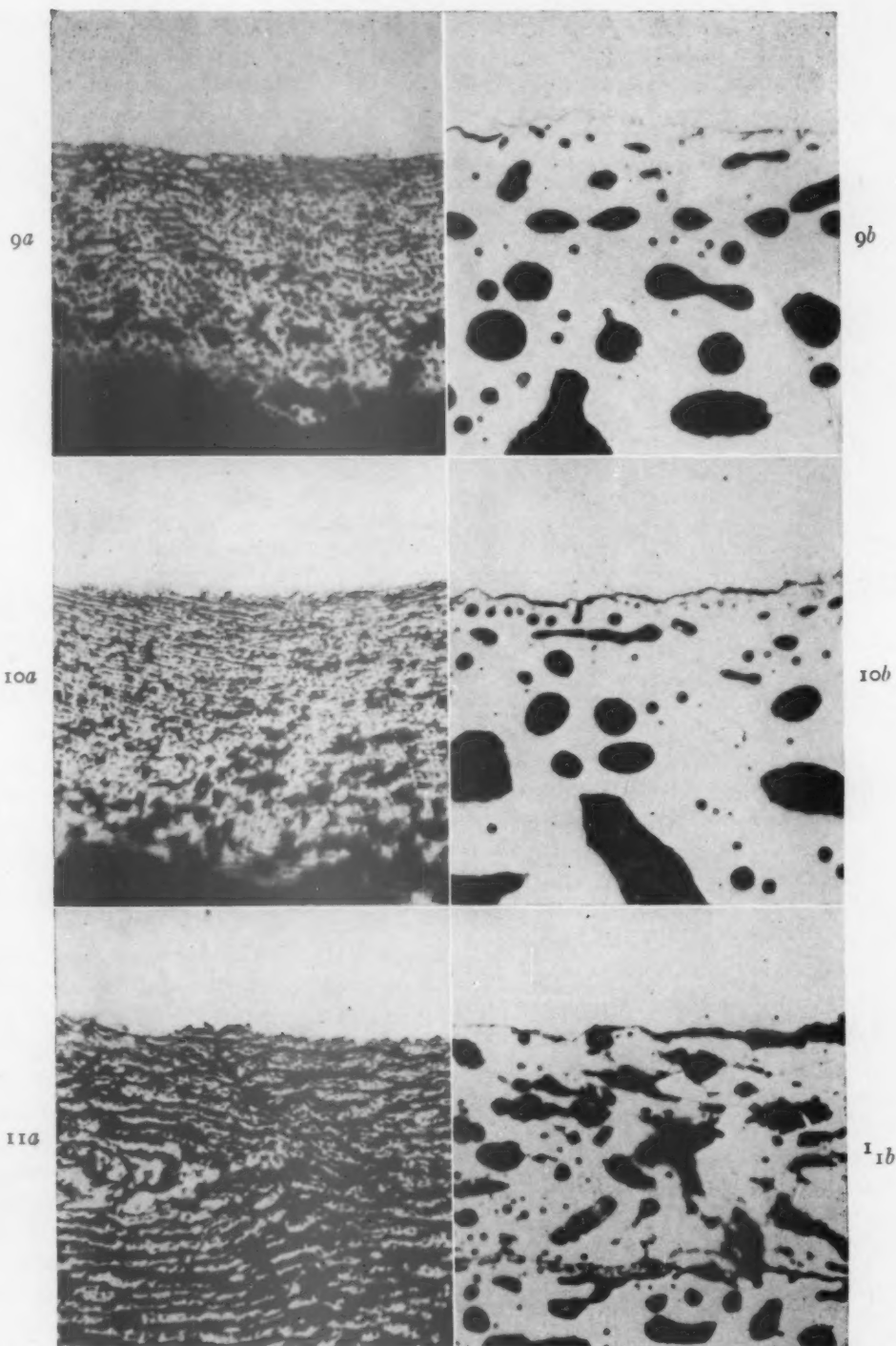


FIG. 8.—STEEL NO. 12 (5.81 PER CENT Si) OXIDIZED 2 HOURS AT 800°C . IN FERRIC OXIDE. $\times 600$.
UNETCHED.

Two areas of same specimen showing development of oxide structures perpendicular to outside surface. Outer scale shown at bottom. Both "pearlitic" and "Liesegang" scale-metal structures have been seen on samples containing 5.81 per cent Si. Pearlitic structures appear to be prevalent below 800°C ., whereas Liesegang structures are prevalent above 800°C .



FIGS. 9-11.—COMPARISON OF SCALE-METAL LAYERS WITH VARIATIONS OF COMPOSITION AND TEMPERATURE. $\times 600$. UNETCHED.

Oxidized 2 hours in ferric oxide (a) at 800°C .; (b) at 1200°C .

Fig. 9. Steel No. 5; 2.55% Si.

Fig. 10. Steel No. 8; 3.17% Si.

Fig. 11. Steel No. 12; 5.81% Si.

External surface at bottom.

Identification by microexamination revealed a number of pure or nearly pure silica particles near the metal to scale-metal boundary, the number of which decreases

was possible during oxidation at temperatures of 1200°C., but none was observed, probably because the amount of eutectic available for melting was very small.

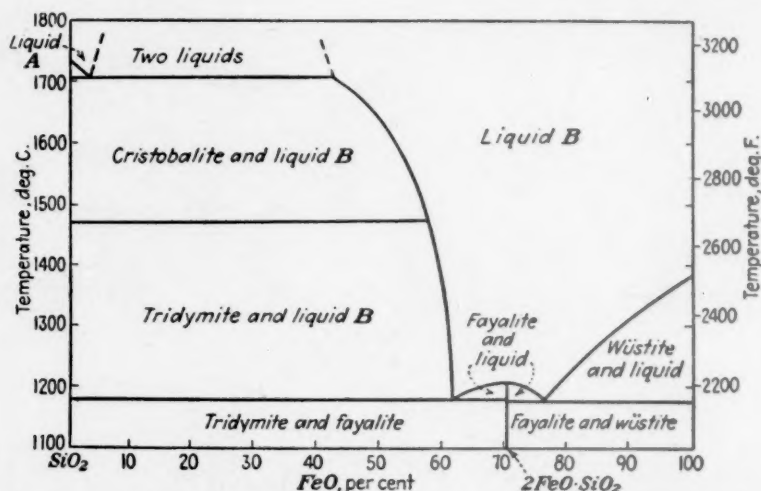


FIG. 12.—SYSTEM FeO-SiO_2 ACCORDING TO BOWEN AND SCHAIRER.⁶

with an increase in silicon content until at 5.8 per cent silicon no pure silica particles are found at any temperature up to and including 1200°C. Intermixed with these, and increasing in number and size toward the outer scale, are globules of oxides that are rich in iron oxide content. These globules become more irregular in shape as the surface of the metal is approached and, in addition, decomposition of the iron oxide (wüstite) due to cooling at room temperature becomes more prevalent. (Iron oxide in combination with silica as an iron silicate is found at the front of furthest oxygen advance.) A line of oxide, presumably largely SiO_2 , extending along the metal to scale-metal interface, and presenting a solid front as a barrier to further oxidation, is found in nearly all these alloys and must coalesce with increasing time, since only in very few cases are these fronts to be seen in the band itself. This must be true unless the solid front is formed during cooling to room temperature.

Liquation of eutectics of iron silicates

Effect of Time and Oxidizing Media

Except for the lower silicon steels, the effect of time on the character of the scale-metal layers produced is negligible. In the composition range where fine precipitates are seen, the beginning of oxidation at 1000°C. in Fe_2O_3 takes place at grain boundaries. With the elapse of a small increment of time, coarse iron oxides form near the surface and are surrounded by a fine precipitate. An hour at temperature shows a band formation irregular in outline. The depth to which the band occurs and the evenness of the boundary increases with time (Fig. 4). After 10 hr. at temperature a definite band parallel to the edge of the sample is formed. Heavy grain-boundary precipitation is visible, although little grain-boundary precipitate is seen in the bands after periods of 1 to 2 hr. at temperature. No variation of this nature is seen in alloys above 2.55 per cent silicon where the nature of the scale-metal layer remains the same and only the thickness of the scale-metal layer increases. Compare Figs. 2d and 13.

Measurements were made of the thickness of the original sample and the thickness of the unoxidized metal after oxidation treatments at 1000°C. in Fe_2O_3 for 0, 10, 30, 60, 120 and 600 min. at temperature. Because the amount of scaling is small, errors introduced by variations in cutting and polishing that produced surfaces not truly perpendicular to the edge of the sample were sufficient to cause large percentage variations in the final values. These values were erratic and therefore are not included.

Change in oxidizing media has a profound effect upon the amount of scale-metal layer formed. For the same conditions of temperature and time a decrease in the oxygen partial pressure decreases the thickness of the layer formed and an increase in oxygen increases the depth of the layer produced. This seems to be in conflict with previous experiments,⁴ where the depth to which subscale occurred increased with decreased oxygen partial pressure. It should be noted, however, that in previous experiments the decreased oxygen pressure was low enough to exclude the formation of a scale layer, whereas in the present experiment scale layers formed in all cases.

Scale-metal layers produced in alloys heated in air for various lengths of time are small in comparison with those produced in samples embedded in Fe_2O_3 . The low-silicon alloys have only faint traces of precipitated oxides and in the high-silicon alloys (5.81 per cent) spalling of the scale was prevalent. The intermediate range of 3 per cent silicon produced the greatest depth of scale-metal layer. The effect of atmosphere on the characteristics of scale-metal layer formation are shown in Fig. 5.

DISCUSSION OF RESULTS

From the foregoing observations it is evident that there is a definite break in the nature of the oxidation process of

silicon alloys between 1.5 and 2.5 per cent silicon. Layers of fine precipitate uniformly distributed, in which the size of the particle increases toward the outer surface

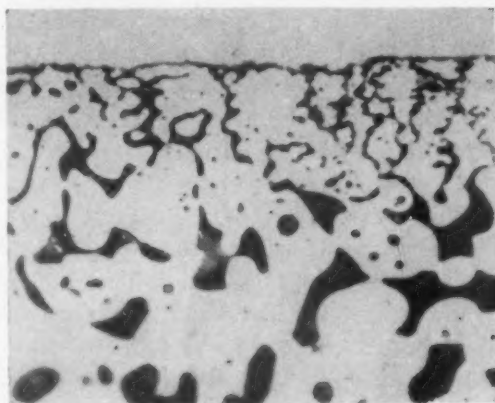


FIG. 13.—STEEL NO. 11 (4.69 PER CENT Si) OXIDIZED 10 HOURS AT 1000°C. IN FERRIC OXIDE. External surface at bottom.

of the metal, are found in all alloys, especially at high temperatures. Although individual oxide particles appear in a band of steels of 2.55 per cent silicon and greater, the particles themselves are no longer consistent in size or shape. As the silicon content is increased, the irregular shaped particles tend to become more elongated and often they are found to connect the inner layer to the surface scale.

The composition limit for the formation of subscales is not clearly defined. If oxide particles of any composition, size, shape or distribution that are grouped in band formation are taken as subscales, then subscales can be said to exist even in 5.8 per cent silicon steels when treated at 1200°C. If subscales are limited to the conditions that there is a band of uniformly dispersed oxide particles precipitated in a metallic matrix and that a layer of metal relatively free from oxides and adjacent to the outer scale is retained, then there is composition limit for the formation of subscale and this limit is somewhere between 1.5 and 2.5 per cent silicon. Darken² has stated that subscale formation

for iron-silicon alloys is limited to steels having a maximum of 3.25 per cent silicon when they are oxidized, so that scaling takes place on the outer surface. This conclusion was based on mathematical calculations and an experiment wherein a silicon steel having 3.25 per cent silicon oxidized in atmosphere of CO_2 at 1000°C . developed subscale only in patches. Since no samples in this experiment were oxidized in a CO_2 atmosphere, no direct comparisons can be made. However, no definite break in the nature of oxidation of silicon steels was observed in this composition range. While it is true that small additions of alloying elements may affect the subscale formation, only in a few isolated cases were any subscales seen that could be attributed to alloying elements other than silicon. Minor variations in scale-metal layers were noted in samples run for checks, but in no case were such variations sufficient to change the general characteristics of the scale-metal layer formations.

The formation of the complex oxide particles in alloys of 2.55 per cent silicon apparently are obtained first by precipitation of a silica particle and then changed either through the solution of iron or the formation of iron oxides in the immediate vicinity of the particle and the solution of these oxides. Particles of different composition and different phases are easily formed merely by the solution of more iron oxide to form a compound $2\text{FeO} \cdot \text{SiO}_2$ (Fig. 12).

It is interesting to note that the method for oxygen diffusion from the metal surface inward changes not only with temperature but with concentration. Oxygen diffuses in low-silicon alloys at low temperatures by diffusion along grain boundaries, whereas diffusion appears to take place through the crystal lattice with greater silicon concentrations. At the present no explanation can be offered for the changes in the nature of scale-metal layer from one type to a layer of an entirely different character

above 800°C . The fact that the type of layer seen on a 3.11 per cent alloy oxidized in air at 1000°C . is similar to those scale-metal layers seen at 700°C . indicates that oxidizing media, as well as temperature and composition, may play a very important role in determining the character of the scale formed.

CONCLUSIONS

1. At temperatures below 800°C . and compositions below 1.56 per cent silicon diffusion of oxygen takes place preferentially along grain boundaries.
2. At temperatures below 800°C . and concentrations above 2.55 per cent silicon diffusion of oxygen appears to proceed by lattice diffusion.
3. For alloys lean in silicon that are oxidized above 800°C . a layer of oxide particles is precipitated; the layer increases in depth with an increase in temperature and time.
4. For alloys above 2.55 per cent silicon, the character of oxidation changes from a "pearlite" type to a structure similar to "Liesegang" bands at 800°C . and to a globular type of structure above 1000°C .
5. The globules of iron silicates formed at high temperatures in a number of cases are obtained first by precipitation of the silica particles and then by gradual solution of either iron or iron oxides that have been formed adjacent to the particle. A number of the silica particles can possibly be precipitated in a concentration gradient where the silicon content has been reduced sufficiently to allow precipitation of the particle.
6. Spalling of the metal-oxide layers is frequent where the Liesegang structure is obtained, whereas scales of the pearlite type are most often adherent.
7. The character of the metal-oxide layers on the surface is dependent on the composition, temperature, rate of oxygen delivery to the surface, and to a limited

extent, time. None of these factors can be overlooked in predictions of the type of scale to be formed.

SUMMARY

Structures of iron-silicon alloys containing from 0.70 to 5.8 per cent silicon have been oxidized in air and also in closed containers containing ferric oxide and mixtures of ferric oxide, iron powder and water at temperatures from 600° to 1200°C. Characteristics of the metal-oxide layers that were produced by these various treatments have been described and discussed.

REFERENCES

1. F. N. Rhines: A Metallographic Study of Internal Oxidation in the Alpha Solid Solutions of Copper. *Trans. A.I.M.E.* (1940) **137**, 246.
2. L. S. Darken: Diffusion in Metal Accompanied by Phase Change. *Trans. A.I.M.E.* (1942) **150**, 152.
3. F. N. Rhines and A. H. Grobe: Internal Oxidation of Dilute Alloys of Silver and Some White Metals. *Trans. A.I.M.E.* (1942) **147**, 318.
4. F. N. Rhines and B. J. Nelson: Structure of Copper-zinc Alloys Oxidized at Elevated Temperatures. *Trans. A.I.M.E.* (1944) **156**, 171.
5. C. S. Smith: *Min. and Met.* (1930) **11**, 213; (1932) **13**, 481.
6. N. L. Bowen and J. F. Schairer: The System FeO-SiO₂. *Amer. Jnl. Sci.* (1932) [7] **24**, 177.

The Liquidus-solidus Temperatures and Emissivities of Some Commercial Heat-resistant Alloys

BY JAMES T. GOW,* ANTON DE S. BRASUNAS,* JUNIOR MEMBER, AND OSCAR E. HARDER,*
MEMBER A.I.M.E.

(New York Meeting, February 1945†)

THIS paper deals with the results obtained and the techniques employed in determining:

1. Liquidus and solidus temperatures of the HH and HT type heat-resistant alloys.‡

2. The relation of true temperatures (thermocouple) to apparent temperatures (optical pyrometer) for the molten HH and HT type alloys.

This work was the outgrowth of needing to know something definite about these temperatures in order to study the effect of pouring temperatures, shake-out times, and heat-treatments on the properties of some heat-resistant alloys. The information developed is thought to be of interest to industry for guidance in foundry practices and the industrial heat applications of the alloys. This paper is based upon work that has been done for the Alloy Casting Institute at Battelle Memorial Institute.

LIQUIDUS AND SOLIDUS TEMPERATURES OF HH AND HT TYPE ALLOYS

Experimental Procedures

Temperature-time curves were obtained during the cooling and solidification of several HH and HT type alloys. The metal

Manuscript received at the office of the Institute Dec. 1, 1944. Issued as T.P. 1838 in METALS TECHNOLOGY, August 1945.

* Assistant Supervisor, Research Engineer, and Assistant Director, respectively, Battelle Memorial Institute, Columbus, Ohio.

† Meeting canceled.

‡ Alloy designations of the Alloy Casting Institute applying to the following type compositions: HH, 26 per cent Cr, 12 per cent Ni; HT, 16 per cent Cr, 36 per cent Ni.

was melted in an Ajax high-frequency induction furnace and poured into a core-sand mold for cooling.

The temperature measurements were obtained by means of a platinum, platinum-rhodium thermocouple contained within a fused silica sheath, which was extended through the side wall of the dry core-sand mold to a point at about the center of the mold cavity, which was 3 in. in diameter by 5 in. deep. The cold junction of the thermocouple was kept in an ice bottle, and the temperature was recorded automatically on a direct-reading potentiometer recorder. Through a switching arrangement, the temperature recorded was checked occasionally with a portable Leeds and Northrup potentiometer indicator. Less than a 5°F. variation in the two instruments was always found. This is within the limit of accuracy of readings. The thermocouple used was checked for accuracy against a standard couple, both before use on this work and after completion of the work, by the instrument laboratory.

Temperature-time Cooling Curves

Fig. 1 is an enlarged reproduction of a part of one of the cooling curves over the temperature range of 2600° to 2200°F. for an alloy of the HT type with 0.45 per cent carbon, 16 per cent chromium, and 36 per cent nickel. This is a typically shaped cooling curve as obtained for the alloys.

It will be noted that two temperatures are shown on Fig. 1 for the liquidus temperature. It is thought likely that the higher temperature, *A*, at the point at

which the slope of the curve begins to change, represents the true start of nucleation or solidification, but for practical

The solidus temperature was rather clearly marked for most of the alloys in the manner shown in Fig. 1. However, in

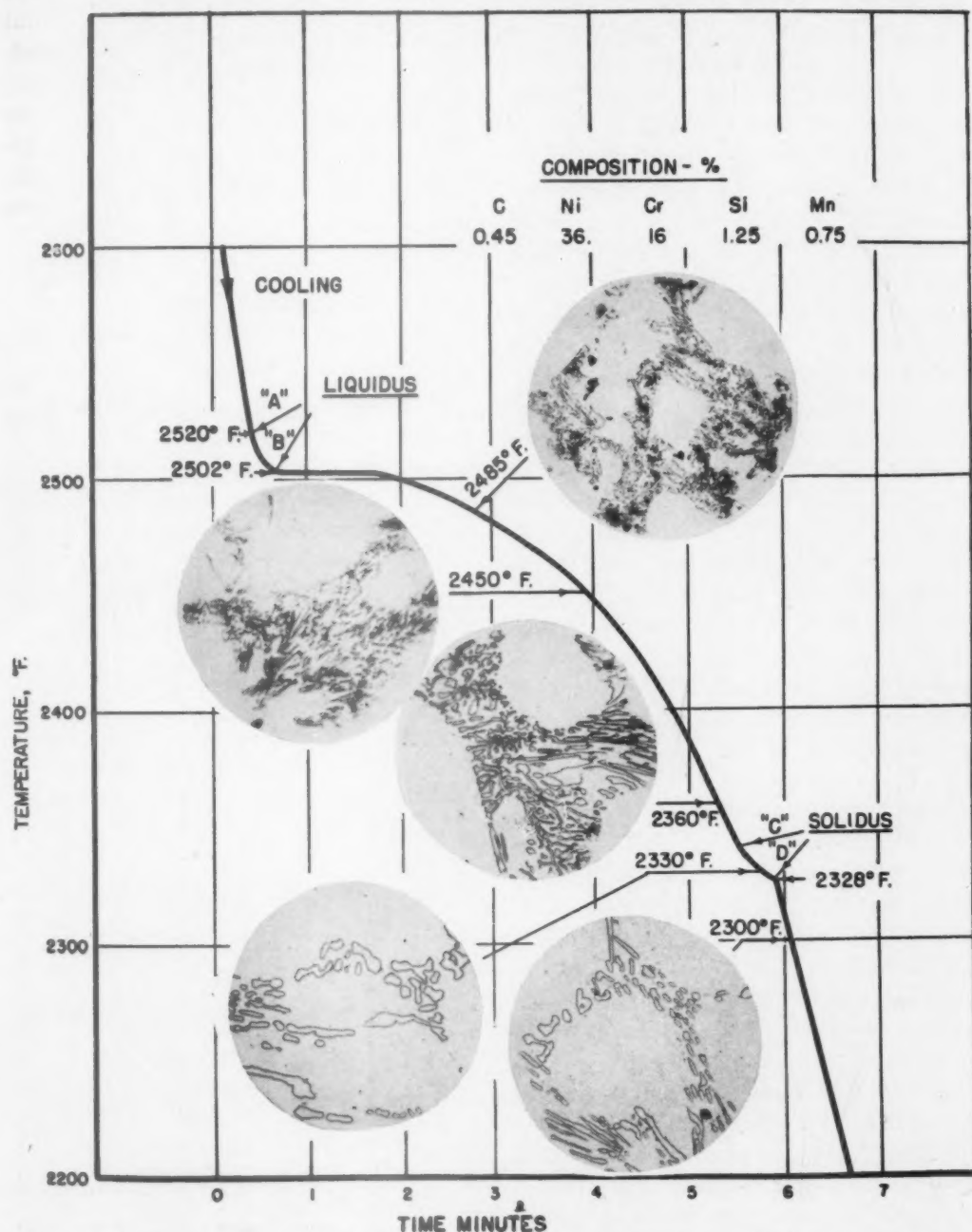


FIG. 1.—TEMPERATURE-TIME COOLING CURVE FOR HT TYPE ALLOY, AND MICROSTRUCTURES FOR SPECIMENS QUENCHED FROM TEMPERATURES SHOWN ON CURVE.

consideration, the lower temperature, B, at which solidification is definitely underway, is the one of importance.

some instances it was less evident, so that the temperatures selected may differ from $\pm 15^\circ\text{F}$. the actual temperature. The

change in slope of this curve, starting at about C, 2340°F., and ending at about D, 2330°F., is thought to represent the final solidification and rejection of the carbide-austenite eutectic, which is present in alloys of this carbon content.

In order to have more definite evidence as to the significance of the changes in slope for the cooling curves of Fig. 1, specimens of the as-cast alloy were heated to temperatures in the range of 2300° to 2500°F., held $\frac{1}{2}$ hr. at temperature, and then quenched directly into water at room temperature. The actual temperatures employed and details of the resulting structures are given on Fig. 1. The appearance of the eutectic carbide areas is observed to differ as the quenching temperature varied. The appearance of the eutectic carbide network for the specimen quenched at 2300°F. is very similar to what would be found for the as-cast alloy. The specimen quenched at 2330°F. shows but little change, except possibly some tendency for spheroidization or agglomeration of the eutectic carbide particles, indicating that no melting occurred at this temperature in $\frac{1}{2}$ hr. The specimen at 2360°F. shows a greater divorcement of the eutectic carbides than either the 2300°F. or the 2330°F. specimens. This, it would seem, definitely indicates that at 2360°F. what had been the eutectic carbide areas were molten metal, so that, on quenching, a new eutectic pattern of carbide and austenite was formed. The relatively fast cooling obtained by the quench would result in a refinement of carbide-particle size. The 2450°F. and 2485°F. specimens show still further refinement in the eutectic carbide-particle size, and it is definite that the eutectic-appearing areas of the photomicrographs were liquid at those heating temperatures. From the appearance of the structure of the specimen heated to 2485°F., it is thought likely that some proeutectic austenite, which had been liquid at 2485°F., separated out while the

temperature dropped to that at which the eutectic developed, from the last liquid to solidify.

These microstructures are suggestive of what might be obtained by knocking out castings before solidification is completed, thereby producing finely divided eutectic, and the effects of reheating below the solidus temperature, which tends to agglomerate the carbides of the eutectic but may also dissolve some of the carbides into the matrix.

LIQUIDUS-SOLIDUS TEMPERATURES OF TERNARY IRON-NICKEL-CHROMIUM ALLOYS

Published data by C. Jenkins and co-authors¹ give the liquidus and solidus temperatures for essentially pure Fe-Cr-Ni alloys. Data from that paper, for the alloy ranges of present interest, are given in Table 1. These relatively pure ternary

TABLE 1.—*Liquidus-solidus Temperatures of Relatively Pure Ternary Iron-nickel-chromium Alloys^a*

A. The 26 Per Cent Cr—12 Per Cent Ni Range			
Nickel, Per Cent	Chromium, Per Cent		
	24	26	28
10	L = 2655°F. S = 2595°F.	L = 2660°F. S = 2595°F.	L = 2660°F. S = 2600°F.
12	L = 2625°F. S = 2580°F.	L = 2625°F. S = 2575°F.	L = 2635°F. S = 2575°F.
14	L = 2615°F. S = 2575°F.	L = 2615°F. S = 2570°F.	L = 2615°F. S = 2565°F.
B. The 35 Per Cent Ni—15 Per Cent Cr Range			
Nickel, Per Cent	Chromium, Per Cent		
	10	15	20
30	L = 2655°F. S = 2575°F.	L = 2620°F. S = 2550°F.	L = 2595°F. S = 2510°F.
35	L = 2645°F. S = 2565°F.	L = 2610°F. S = 2530°F.	L = 2585°F. S = 2505°F.
40	L = 2630°F. S = 2555°F.	L = 2600°F. S = 2515°F.	L = 2575°F. S = 2495°F.

^a Data interpolated from the isothermal contours of Figs. 10 and 11 of the paper by Jenkins and others.¹

¹ References are given at the end of this paper.

Fe-Cr-Ni alloys are stated to have, as their main impurity, Cr_2O_3 in varying amounts, but not exceeding 0.75 per cent, and silicon which never exceeded 0.16 per cent.

The liquidus and solidus temperatures are very similar for (1) the alloy containing 26 per cent Cr, 12 per cent Ni, bal. Fe, and (2) for that containing 35 per cent Ni, 15 per cent Cr, bal. Fe. The former alloy, as contrasted with the latter, is shown to have liquidus and solidus temperatures 15° and 45°F. higher, respectively. Thus the temperature range over which solidification occurs is shown to be about 50°F. for the first alloy and some 80°F. for the second.

The trend of influence of increasing the

nickel content from 10 to 14 per cent at constant chromium levels of from 24 to 28 per cent is to lower the liquidus about 10°F. and to lower the solidus about 7°F. for each 1 per cent increase in nickel content. Increasing chromium contents from 24 to 28 per cent at constant nickel levels of 10, 12, and 14 per cent is indicated to have no definite effect on these temperatures.

In the alloys of higher nickel and lower chromium content, both the liquidus and the solidus temperatures are lowered about 2°F. for each 1 per cent nickel increase in the range of 30 to 40 per cent nickel at chromium levels of 10 to 20 per cent. Each 1 per cent chromium increase is

TABLE 2.—Compositions and Liquidus-solidus Temperatures of Some HH and HT Alloys

Alloy No.	Chemical Composition, Per Cent					Temperature, Deg. F.			
						Liquidus ^b		Solidus ^b	
	C	Ni	Cr	Si	Mn	A	B	C	D
HH Type Alloys									
AX-4R.....	0.34	10.60	27.4	1.58	0.92	2595	2578	2480	2465
No. 1.....	0.38	10.30	26.4	1.51	0.95	2570	2558	2490	2475
AS-1R.....	0.35	12.36	22.7	1.84	0.96	2575	2553	2500	2485
AG-R.....	0.53	12.50	24.7	1.77	0.78	2540	2522	2320	2300
No. 9.....	0.54	13.00	24.8	1.40	0.90	2535	2522	2335	2310
HT Type Alloys									
D-1.....	0.06	35.69	16.11	1.25	0.75		2560	2470	2450
D-3.....	0.12	35.33	16.42	1.27	0.84		2525	2480	2460
D-2.....	0.15	35.84	16.05	1.12	0.90		2540	2490	2460
D-20.....	0.46	36 ^a	16 ^a	0.44	0.80		2505	2340	2330
D-21.....	0.43	36 ^a	16 ^a	1.64	0.80		2475	2340	2320
D-22.....	0.45	36 ^a	16 ^a	2.61	0.80	2445	2440		2240
D-4.....	0.41	33.97	14.21	1.38	0.90		2520	2355	2335
D-11.....	0.41	37.11	13.82	1.29	0.84		2495	2330	2315
D-15.....	0.40	38.52	14.10	1.27	0.85		2495	2330	2305
D-5.....	0.40	32.98	15.73	1.31	0.80		2495	2335	2325
No. 1.....	0.46	36 ^a	10.18	1.31	0.75	2520	2502	2340	2330
D-12.....	0.42	37.62	15.85	1.35	0.90		2480	2330	2310
D-16.....	0.40	39.95	16.65	1.24	0.85		2480	2340	2320
D-6.....	0.40	32.64	18.22	1.23	0.81		2490	2345	2310
D-9.....	0.44	34.53	18.26	1.22	0.83		2495	2350	2335
D-13.....	0.40	37.75	17.85	1.38	0.83		2480	2350	2315
D-17.....	0.42	40.04	18.17	1.35	0.83		2480	2355	2330
D-7.....	0.44	33.83	20.11	1.31	0.86		2485	2355	2335
D-10.....	0.43	36.77	19.81	1.36	0.84		2490	2360	2345
D-14.....	0.40	37.53	19.90	1.29	0.89		2475	2340	2320
D-18.....	0.44	39.38	19.95	1.29	0.77		2475	2345	2320
M8R.....	0.65	35.6	15.9	2.19	0.84	2470	2455	2350	2330
77R.....	0.17	35.58	15.3	3.06	0.72		2500	2400	2390
80R.....	0.36	35.91	15.3	2.99	0.65	2490	2475	2270	2250
57R.....	0.56	35.99	14.9	3.64	0.70	2440	2420	2285	2250

^a Intended composition but not determined by analysis.

^b See Fig. 1 for meaning of points A, B, C, and D.

shown to lower the liquidus and solidus temperatures about 6°F. at nickel content levels of 30 to 40 per cent.

LIQUIDUS-SOLIDUS TEMPERATURES OF COMMERCIAL HEAT-RESISTANT ALLOYS

Table 2 gives the values for the liquidus and solidus temperatures as obtained from the temperature-time cooling curves for a total of 28 heats, of which 5 are of the general HH type of composition and 23 of the HT type.

A comparison of the temperature levels for the liquidus-solidus temperatures of the ternary alloys (Table 1) with the similar temperature levels for the commercial compositions (Table 2) shows that a definite lowering occurs when the additional elements, carbon, silicon, and manganese, are present. The data of Table 3 show the extent of difference in these temperatures between the ternary Fe-Cr-Ni alloys of 26 per cent Cr, 12 per cent Ni and 36 per cent Ni, 16 per cent Cr and commercial compositions with these same nickel and chromium contents. Only the *B* and *D* values of Table 2 are used in Table 3. Under each temperature for the commercial alloys, the lowering in temperature as compared with the pure ternary alloys is shown in parentheses. The data given in Table 2 may be used also to give a more extensive picture of the effect of carbon on the liquidus and solidus temperatures.

The effect of the additional elements present in both types of commercial alloys in lowering the liquidus temperature is less pronounced than in lowering the solidus temperature, being about 100°F. for 0.50 per cent carbon and the other alloying elements present (Table 3). On the other hand, the solidus temperatures for commercial alloys of this carbon content are lowered about 275°F. and 190°F., respectively, for the HH and HT alloys. For the lower carbon alloys studied, the effect of carbon on the solidus temperature is mild

(C up to 0.35 per cent in the HH alloys and to 0.15 per cent in the HT alloys); but with further increases in carbon, the effect is more pronounced until there is some eutectic formed at about 0.40 to 0.50 per cent carbon in the HH alloys and about 0.30 to 0.40 per cent carbon in the HT alloys, both of which result in a minimum solidus temperature of around 2300° to 2320°F., which appears to be the eutectic temperature for these alloys. The data now available do not make it possible to establish completely the contours of the solidus lines for these two types of commercial heat-resistant alloys.

TABLE 3.—*Liquidus and Solidus Temperatures of Essentially Pure Iron-nickel-chromium Alloys as Contrasted with Commercial Alloys of the Same Nickel and Chromium Contents*

A. The 26 Per Cent Cr, 12 Per Cent Ni Type Alloy

	Alloy Identification		
	Jenkins and Others ¹	Alloy AS-1R	Alloy AG-R
Main elements other than 26 per cent Cr, 12 per cent Ni, bal. Fe.	Essentially pure	C-0.35 Si-1.84 Mn-0.96	C-0.53 Si-1.77 Mn-0.78
Liquidus temperature. ^a	2625°F.	2555°F. (-70°F.)	2520°F. (-105°F.)
Solidus temperature. ^a	2575°F.	2485°F. (-90°F.)	2300°F. (-275°F.)

B. The 36 Per Cent Ni, 16 Per Cent Cr Type Alloy

	Alloy Identification		
	Jenkins and Others	Alloy D-2	Alloy No. 1
Main elements other than 36 per cent Ni, 16 per cent Cr, bal. Fe.	Essentially pure	C-0.15 Si-1.12 Mn-0.90	C-0.46 Si-1.31 Mn-0.75
Liquidus temperature. ^a	2605°F.	2340°F. (-65°F.)	2500°F. (-105°F.)
Solidus temperature. ^a	2520°F.	2460°F. (-60°F.)	2330°F. (-190°F.)

^a The values given are the *B* and *D* values from Table 2.

These relations are considered to be in general agreement with microstructures

found in these commercial heat-resistant alloys. These deductions, however, are restricted to alloys having silicon and manganese contents in a relatively narrow range, and separate considerations must be given to their effects.

TABLE 4.—*Liquidus and Solidus Temperatures of Alloys of 36 Per Cent Nickel, 16 Per Cent Chromium and Silicon and Carbon as Shown*

Alloy No.	Carbon, Per Cent	Silicon, Per Cent	Liquidus, Deg. F. ^a	Solidus, Deg. F. ^a
D-20	0.46	0.44	2505	2330
No. 1	0.46	1.38	2500	2330
D-21	0.43	1.04	2475	2320
D-22	0.45	2.61	2440	2240
77R	0.17	3.06	2500	2392
80R	0.36	2.99	2475	2250
57R	0.56	3.64	2420	2250

^a The values given are the B and D values in Table 2.

Silicon is also indicated to have some influence on the liquidus and solidus temperatures. The data of Table 4 show the trend of change for these temperatures as a function of silicon content. The first four alloys are closely similar in composition except for silicon content. The most marked change in these temperatures occurs in going from 1.75 to 2.50 per cent silicon. Two alloys of somewhat higher silicon content, 80R and 57R, are shown to have liquidus and solidus temperatures in line

with the 2.50 per cent silicon alloy D-22. Alloy 77R of 3.06 per cent silicon and but 0.17 per cent carbon is also included in this table, so that the trend of influence of carbon content at this high silicon content is brought out. It is again of interest to note that a rather abrupt drop in the solidus temperature is indicated to occur at some carbon content above 0.17 per cent carbon and below 0.36 per cent.

Table 5 presents the liquidus-solidus data for a group of alloys with nickel and chromium contents varying in the commercial range of the HT alloys. They are closely similar in carbon, silicon and manganese contents. The following trends of influence of chromium and nickel content variations are apparent.

Increased amounts of chromium, from 14 to 20 per cent, at constant nickel levels in the range of 34 to 40 per cent, are shown by the data of Table 5 to result in a moderate lowering of the liquidus temperature. The average decrease in liquidus temperature per 1 per cent chromium increase for this range of compositions is indicated to be about 4.5°F. Increasing nickel contents from 34 to 40 per cent at constant chromium levels in the range of from 14 to 20 per cent also results in a moderate lowering in the liquidus temperature. The lowering in the liquidus

TABLE 5.—*Liquidus and Solidus Temperatures of Alloys of Nickel and Chromium Contents as Shown and with About 0.45 Per Cent Carbon, 1.20 Per Cent Silicon, and 0.80 Per Cent Manganese*

Approximate Nickel, Per Cent	Approximate Chromium, Per Cent			
	14	16	18	20
33-34	D-4 ^a L = 2520°F. S = 2335°F.	D-5 ^a L = 2495°F. S = 2325°F.	D-6 ^a L = 2490°F. S = 2310°F.	D-7 ^a L = 2485°F. S = 2335°F.
35-36		No. 1 ^a L = 2500°F. S = 2330°F.	D-9 ^a L = 2495°F. S = 2335°F.	D-10 ^a L = 2490°F. S = 2345°F.
37-38	D-11 ^a L = 2495°F. S = 2315°F.	D-12 ^a L = 2480°F. S = 2310°F.	D-13 ^a L = 2480°F. S = 2315°F.	D-14 ^a L = 2475°F. S = 2320°F.
39-40	D-15 ^a L = 2495°F. S = 2315°F.	D-16 ^a L = 2480°F. S = 2320°F.	D-17 ^a L = 2480°F. S = 2330°F.	D-18 ^a L = 2475°F. S = 2320°F.

^a These are the alloy identification numbers. Chemical analyses of alloys are given in Table 2.

temperature per 1 per cent nickel increase is indicated from these data to be about 3°F. The maximum variation in the liquidus temperatures of these HT alloys was found to be only 45°F. The trend of change in the solidus temperature with alteration in the nickel and chromium contents is less clearly indicated. The maximum difference between the solidus temperatures obtained for this group is only about 25°F.

RELATION OF TRUE TEMPERATURES (THERMOCOUPLE) TO APPARENT (OPTICAL) TEMPERATURES FOR MOLTEN HH AND HT TYPE ALLOYS

Both the Leeds and Northrup and the Pyro optical pyrometers are capable of determining temperatures under black-body conditions quite accurately.

Since the radiant energy emitted from the surface of molten metals varies, both with the chemical composition and the temperature of the metal, and is less than that radiated by a perfect black body at the same temperature, the currently used optical pyrometers are not capable of giving true molten-metal temperatures, and the temperatures indicated, therefore, are to be considered only as apparent temperatures.

For molten steel and iron, an attempt has been made by the instrument manufacturers to correct the optical readings so as to be closer to the true temperatures, by assuming an emissivity value of 0.40. In the Leeds and Northrup instrument, a second filter is introduced to compensate for an emissivity of 0.40 for molten steel, and the readings are taken from the same calibrated scale as for observations with black-body conditions. The Pyro optical pyrometer does not introduce a second filter but has two calibrated scales; the one (black) being read for temperatures under black-body conditions, and the other (red) being read for molten-steel temperatures.*

* Both these instruments are manufactured

There is some interest, therefore, in obtaining the relation of true temperature (thermocouple) to apparent temperatures (optical) for the HH and HT types of heat-resistant alloys. This has entailed working out a method for obtaining true temperatures by means of an immersion thermocouple and a technique of obtaining simultaneous readings with this thermocouple and an optical pyrometer, for both the furnace bath and the metal stream upon pouring.

Calibration charts for the L. and N. and the Pyro optical pyrometers have been worked out for the HT and HH types of alloys. These charts (Figs. 4, 5 and 6) may serve for correcting the optical readings to true or actual temperatures.

Of at least academic interest are the calculated values of emissivity, which range from about 0.34 to 0.49 for the HT alloys and from 0.49 to 0.63 for the HH alloys for the clear stream of molten metal upon pouring. These values are raised about 0.10 when readings are made on the open bath; this may be caused by the formation of a film on the metal surface, even though an attempt was made to obtain open bath readings on clear metal. This means that when sighting on the HT (36 per cent Ni, 16 per cent Cr) alloy, using the 0.4 emissivity correction assumed by instrument makers as standard for molten steel and iron, the temperature indicated will be close to the true temperature of the metal. However, when sighting on the HH type (26 per cent Cr, 12 per cent Ni), using this same emissivity correction, the apparent temperatures will be some 50° to 100°F. higher than the true temperatures.

METHOD OF DETERMINING ACTUAL BATH TEMPERATURE

An apparatus was constructed to take immersion temperature readings with a

with only one scale (black-body), and some users determine only apparent temperature and make their own corrections for emissivity.

platinum-platinum-10 per cent rhodium thermocouple. The protection tube was designed after the methods used by Schofield and Grace^{2,3} so successfully. All

mersion at 3150°F. is shown to the right-hand side of the photograph, and excessive slagging of the block and complete softening of the tube are evident. The wires

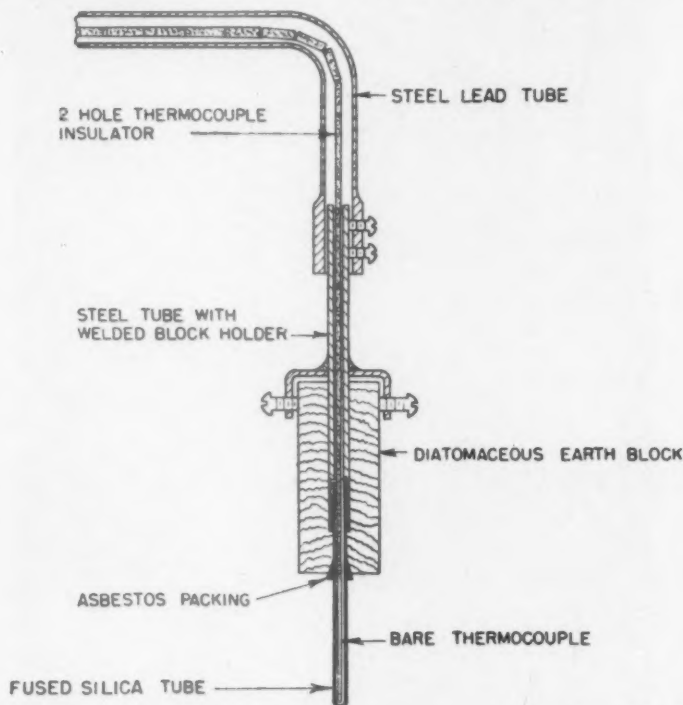


FIG. 2.—SECTION THROUGH IMMERSION THERMOCOUPLE APPARATUS. ONE FOURTH ACTUAL SIZE.

the materials needed are easily obtainable and are as shown in Fig. 2. The apparatus is readily assembled, and parts can be replaced very easily. The diatomaceous earth block, which gives slag-line protection to the silica tube containing the thermocouple, is the commercial Sil-O-Cel. Such a block is readily cut to size with woodworking tools, and although care is necessary in handling the material before use, because it is very friable, it becomes a hard and rather tough material after the first immersion.

Fig. 3 shows the assembled immersion apparatus ready for its first immersion. A block and silica tube after 12 immersions at temperatures of from 2665° to 2880°F., which is the probable limit of its life, is shown at the center of the photograph. Also, a block and silica tube after one im-

shown around the block are placed there as a protection against the falling away of any part of the block that may crack. These wires are not thought essential. At the range of temperatures used for the heat-resistant alloys, the block and tube should last for at least six immersions. Failure of the block occurs by a slagging action. The silica tube generally fails from solidification of metal or slag on the tube, causing it to crack through differences in contraction characteristics. However, at temperatures sufficiently high, the metal or slag will not adhere to the tube, and a slagging action eventually will cause it to fail.

A thin-walled iron tube was used in the early work as a protection tube over the silica tube. The main thought was that it might lessen heat shock on the silica tube. Such an iron tube will not melt off at the

lower temperatures, but it requires a longer immersion time to obtain a temperature reading and appeared to be quite unneces-

able for larger furnaces. A 22-gauge platinum thermocouple, 3 ft. long, was used. The handle end of the lead tube

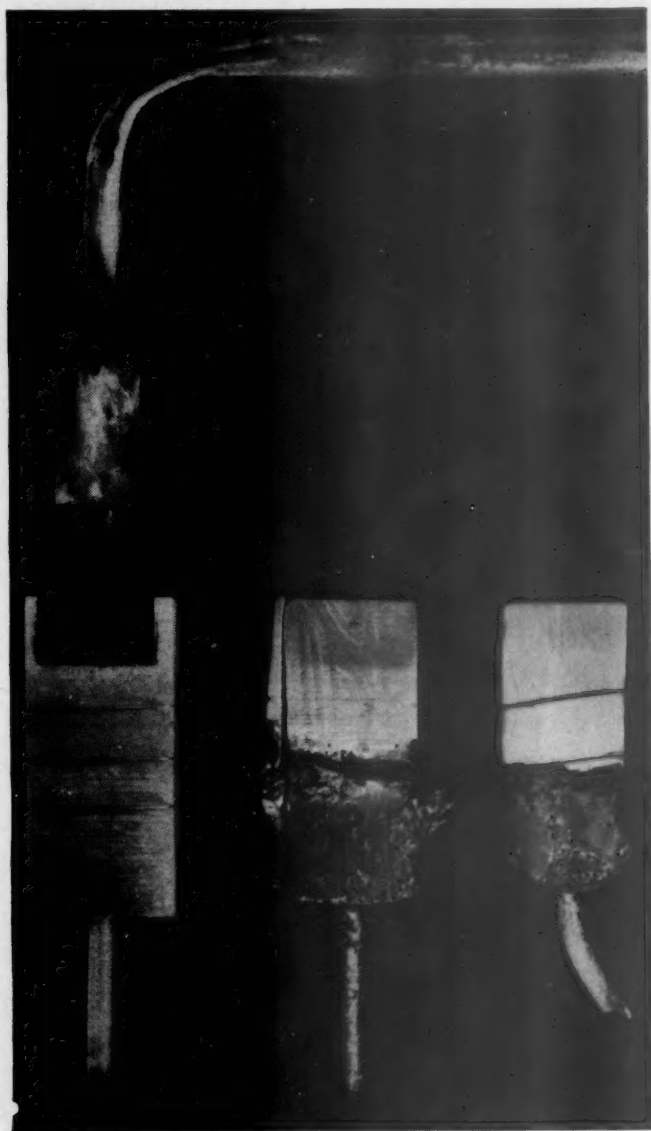


FIG. 3.—IMMERSION APPARATUS.

Left. Assembled immersion thermocouple ready for use.

Center. Replaceable block and silica tube after 12 immersions at temperatures from 2665° to 2880°F.

Right. The same after one immersion at 3150°F.

sary when a bare silica tube could withstand as many as 12 immersions.

A steel lead tube about 3 ft. long, as used in this work, is convenient for taking temperatures in furnaces up to 1000 lb. capacity, but a longer tube may be desir-

able for larger furnaces. A 22-gauge platinum thermocouple, 3 ft. long, was used. The handle end of the lead tube should be insulated, so that temperatures, in an induction-furnace bath, can be taken with the power on.

A portable L. and N. potentiometer indicator was used in conjunction with the thermocouple to determine the tempera-

tures. An ordinary thermometer inserted in the handle of the lead tube, where the cold junction of the thermocouple and copper lead wires occurs, was used to determine the cold junction correction to be applied. With this setup, the temperature of the bath can be obtained with immersion times of from 5 to 10 seconds.

The thermocouple was checked against a standard several times during this study and reached a maximum error of plus 6°F. at 2600°F., from which it did not deviate with further use.

Immersion temperatures thus obtained were considered true temperatures.

MEASURING APPARENT METAL TEMPERATURES (OPTICAL)

Both the Pyro optical pyrometer and the potentiometer direct-reading model Leeds and Northrup optical pyrometer were used to determine apparent temperatures. These instruments were checked frequently against a standard light source.⁴

To determine apparent temperatures for emissivity calculations, it is necessary to use the black scale on the Pyro and the high scale on the L. and N., which assume black-body conditions; but the other scale readings applicable to molten steel, with the emissivity assumed as 0.40, were recorded wherever possible so that true vs. apparent temperature curves could be obtained for these readings also.

METHOD OF OBTAINING TRUE TEMPERATURES (THERMOCOUPLE) AND CORRESPONDING APPARENT TEMPERATURES (OPTICAL PYROMETER)

The sequence in which temperatures were determined for some heats was as follows: (1) Open-bath optical temperatures, (2) immersion or true temperatures, and (3) pouring temperature—optical.

Except when noted differently in the tables, the power to the furnace was

turned off just prior to determination of the immersion temperatures. In any case, these operations were carried out rapidly. Approximately 50°F. higher temperatures, as determined by the optical pyrometer, were found on the open bath than on the pour. It is thought that this does not represent actual temperature loss from the time the first optical reading was taken until the time that the last one was taken. Certainly some temperature loss occurs; however, it is likely that a thin film, on what appeared to the eye to be a clear metal surface on the open bath, causes a higher temperature reading than if such a film were not present. Actual temperature loss is possibly of a magnitude of about 10°.

For some of the heats of the HT alloys, temperatures were obtained with the optical pyrometer sighted upon a filmed surface. The surface of this metal remains clear when the metal temperature is above about 2800°F. (true temperature), and it became increasingly difficult to obtain a clear metal surface for sighting upon, with the optical pyrometer, as the temperature drops below 2800°F. toward the liquidus temperature. It was deemed advisable, therefore, to learn the relationship between the apparent temperature obtained when sighting on this filmed-over surface and the true temperature of the bath. The results obtained show the importance of knowing the condition of the surface sighted upon. It also is intended to extend the calibration of the optical pyrometers to molten-metal surface conditions, which could be more readily controlled under commercial foundry conditions, when handling the metal at temperatures at which it is difficult to obtain a clear metal surface for sighting upon.

Calibration Curves for the Optical Pyrometer

For the two types of alloys, the following curves were obtained for clear metal-surface conditions:

TABLE 6.—*Temperature Measurements Obtained on Commercial Alloy Heats for Purposes of Calibration of Optical Pyrometers and Emissivity Determinations*

A. Optical Pyrometers Sighted on Open Bath					
Alloy No.	True Temperature, Deg. F., Thermocouple	Open Bath Temperature, Deg. F.			
		Pyro-Red	Pyro-Black	L. and N. High	L. and N. $0.4E_{\lambda}$
HH Type Alloys					
AS-1R....	2613	2740	2520		
	2790	2930	2680		2880
	2715	2840	2600		2790
	2796	2940	2690		
AX-4....	2820	2965	2715		
No. 9....	2859	3000	2750		
No. 10....	2882	3050	2790		
HT Type Alloys					
57R.....	2850	2940	2690		
M8.....	2917	3010	2755		
77R.....	2765	2830	2595		
80R.....	2930	3050	2790		3000
No. 1 (re-melt)...	2765	2830	2595	2580	2830
No. 1 (re-melt)...	2780	2850	2610	2600	2835
D-21.....	2955			2810	3090
D-20.....	2950	3015	2760		
No. 1.....	2765	2850	2610		
B. Optical Pyrometers Sighted on Stream during Pour					
Alloy No.	True Temperature, Deg. F., Thermocouple	Pouring Temperature, Deg. F.			
		Pyro-Red	Pyro-Black	L. and N. High	L. and N. $0.4E_{\lambda}$
HH Type Alloys					
AG-R....	2796	2900	2660		
AX-4....	2820	2910	2665		
No. 9....	2859	2945	2695		
No. 10....	2882	3000	2750		
HT Type Alloys					
No. 1....	2869	2900	2660		
	2877	2880	2640		
	2876	2920	2675		
	2840			2620	
	2672			2440	
	2695			2465	
	2873	2930	2680		
	2896	2980	2735		

TABLE 6.—(Continued)

C. Optical Pyrometers Sighted on Film Over Surface of Bath

Alloy No.	True Temperature, Deg. F., Thermocouple	On Film			
		Pyro-Red ^a	Pyro-Black ^a	L. and N. High	L. and N. 0.4E _λ
HT Type Alloys					
No. 1 (re-melt)...	2560	2770-2770	2545-2545	2530	2755
	2592	2830-2820	2595-2585	2575	2815
	2605	2815-2820	2580-2585	2575	2810
	2650	2910-2900	2665-2660	2645	2890
	2723	3015-2980	2760-2735	2710	2950
	2735	2995-3010	2745-2755	2725	2970
	2765	3010	2755		2980
	2711	2960-2960	2710-2710	2690	2930
	2777	3030	2770	2750	2995

^a Simultaneous readings taken by two operators.

1. Black-scale Pyro and high-scale L. and N. temperatures *taken on the open bath* against true temperature;

2. Red-scale Pyro and $0.4E_\lambda$ scale L. and N. temperatures *taken on the open bath* against true temperature;

3. Black-scale Pyro and high-scale L. and N. temperatures *taken on the pour* against true temperature; and

4. Red-scale Pyro temperatures *taken on the pour* against true temperature.

For the HT type alloy, two additional curves were obtained for a filmed-over surface condition. They are:

1. Black-scale Pyro and high-scale L. and N. temperatures *taken on a filmed-over bath surface* against true temperature; and

2. Red-scale Pyro and $0.4E_\lambda$ scale L. and N. temperatures *taken on a filmed over bath surface* against true temperature.

These curves of Figs. 4, 5, and 6 are actually calibration charts for these two types of optical pyrometers when used with HT and HH alloys, respectively.

The data used to construct the curves are given in Table 6. The chemical compositions of these alloys are given in Table 2.

True vs. Apparent Temperatures for HH Alloys

Fig. 4 shows the relation between true temperature and apparent temperature

2650°F. on the stream of pouring metal; nearly 2700°F. on the open bath. Thus, these readings would be from 100° to 150°F. lower than the true temperature. Using the

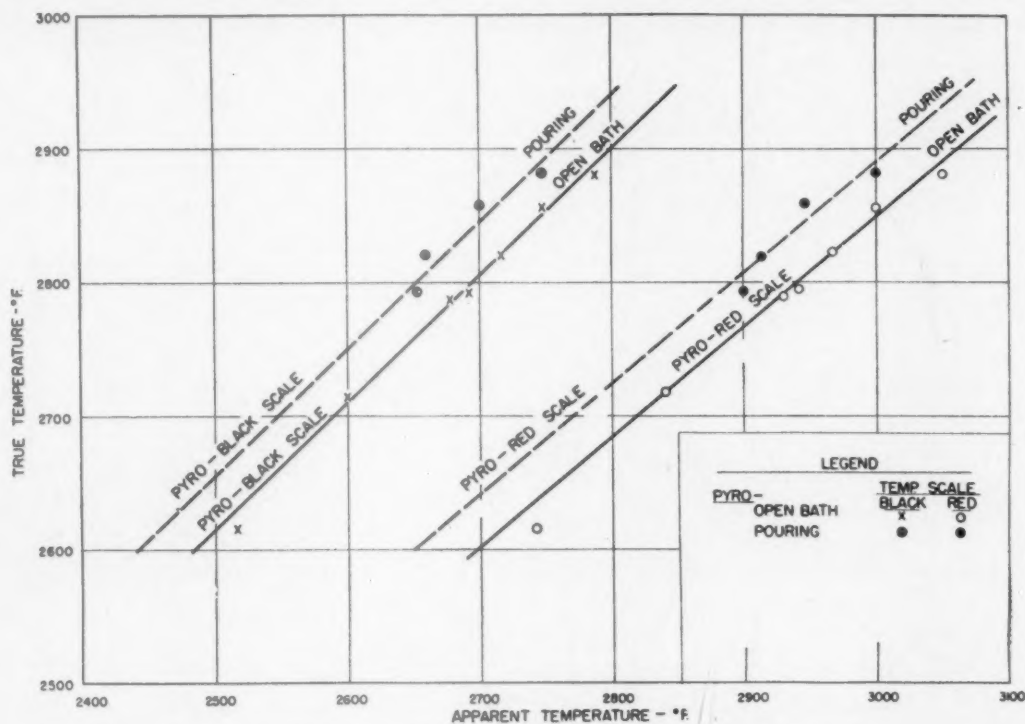


FIG. 4.—TRUE VS. APPARENT TEMPERATURES OF HH TYPE ALLOYS.
26 per cent Cr, 12 per cent Ni.

as read on the Pyro instrument, using the black scale sighted against the open bath and the stream of molten metal in pouring, and also as read from the red scale of the Pyro instrument. Curves have not been taken for the L. and N. instrument for this type of alloy, but it is thought that such readings would coincide closely with those of the Pyro instrument.

It is observed, first, that there is a substantial difference in the readings for the open bath as compared with the stream of molten metal during pouring and that the open bath gives a somewhat higher temperature. The significance of this chart can be illustrated by comparing the apparent temperatures with the true temperatures; for example, at 2800°F. Using the Pyro black scale, the temperature is about

corrected scales, Pyro red. (0.4 E_{λ}), the temperature on the metal stream is nearly 2900°F., and in the open bath is about 2940°F. Thus, for this type of alloy at a true temperature of 2800°F., a temperature is obtained that is 100°F. or more too low if the black-body scale is used, and nearly an equally too high a temperature if the scale as corrected by the instrument company for molten steel is used. It is to be noted, however, that all these data are for the HH alloys, essentially free from a film, and it will be brought out in the discussion of the HT alloys that, under a film condition, which exists at temperatures below about 2800°F., the alloys gave optical readings on the black-body scale that are close to the true temperatures.

True vs. Apparent Temperatures for HT Alloys

The true and apparent temperatures for HT alloys are shown in Figs. 5 and 6.

scale, the readings obtained by sighting on the stream of metal during pouring would be of the order of 200°F. below the true temperature. Again, there is a differ-

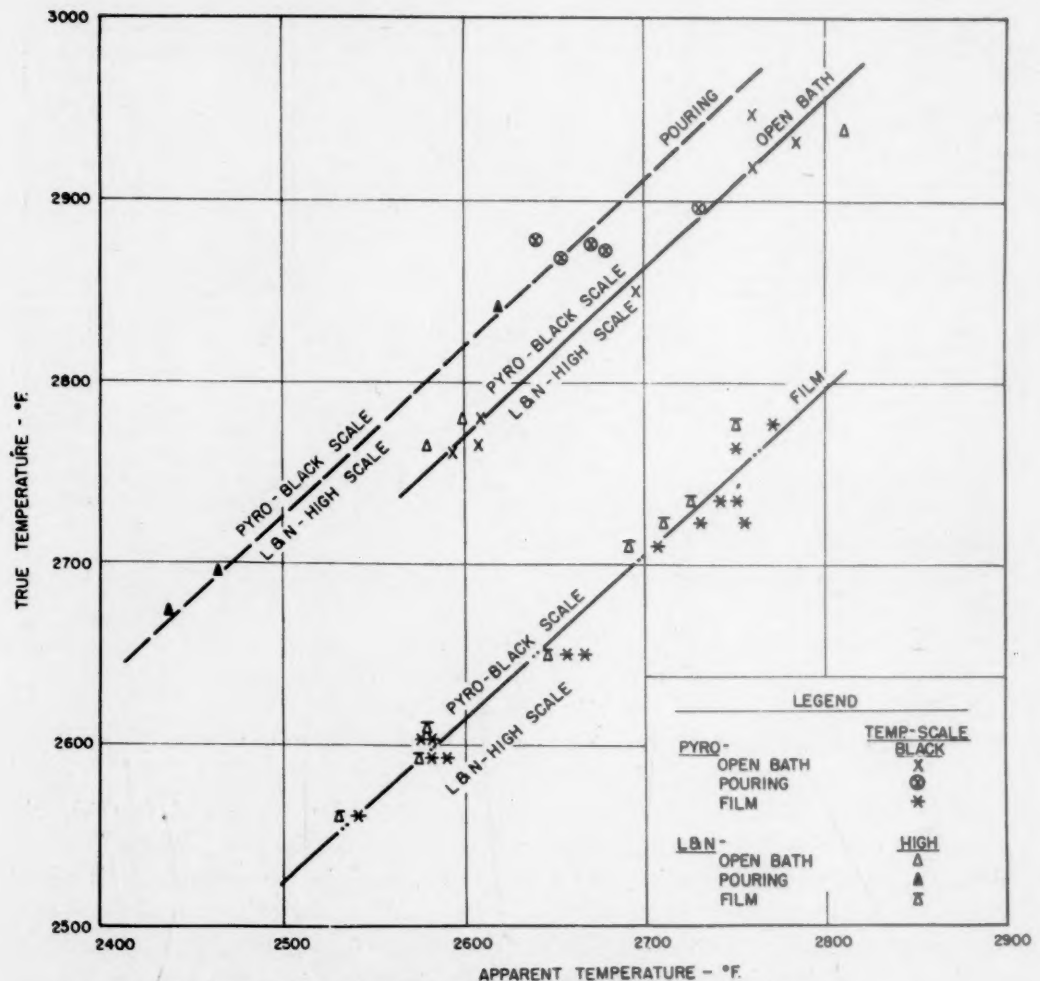


FIG. 5.—TRUE VS. APPARENT TEMPERATURES OF HT TYPE ALLOYS.
36 per cent Ni, 16 per cent Cr.
Black-body scales with clear and filmed surfaces.

Fig. 5 shows the relations between the true temperature and the apparent temperature, using the black-body scales of the two instruments when sighted on the stream of molten metal and on the open metal bath, and also the relation for the metal covered with a film, the latter condition being for temperatures below 2800°F. Again, using a true temperature of 2800°F. and with the pyrometer on the black-body

ence of about 50°F. between the temperature reading on the metal during the pour and on the open bath. For lower temperatures, below about 2800°F., if the metal is permitted to form a film on the open surface, and this is almost unavoidable, it will be noted that there is fairly close agreement between the true temperature and the temperature read with the optical pyrometer, using the black-body scale. It is to be

emphasized that the relations pointed out in Fig. 5 for the corrections for the black-body scale in sighting on clear metal will not apply at the lower temperatures where

the true temperature. However, if the reading is made on the open metal bath, the apparent temperature is some 75°F. above the true temperature. As mentioned

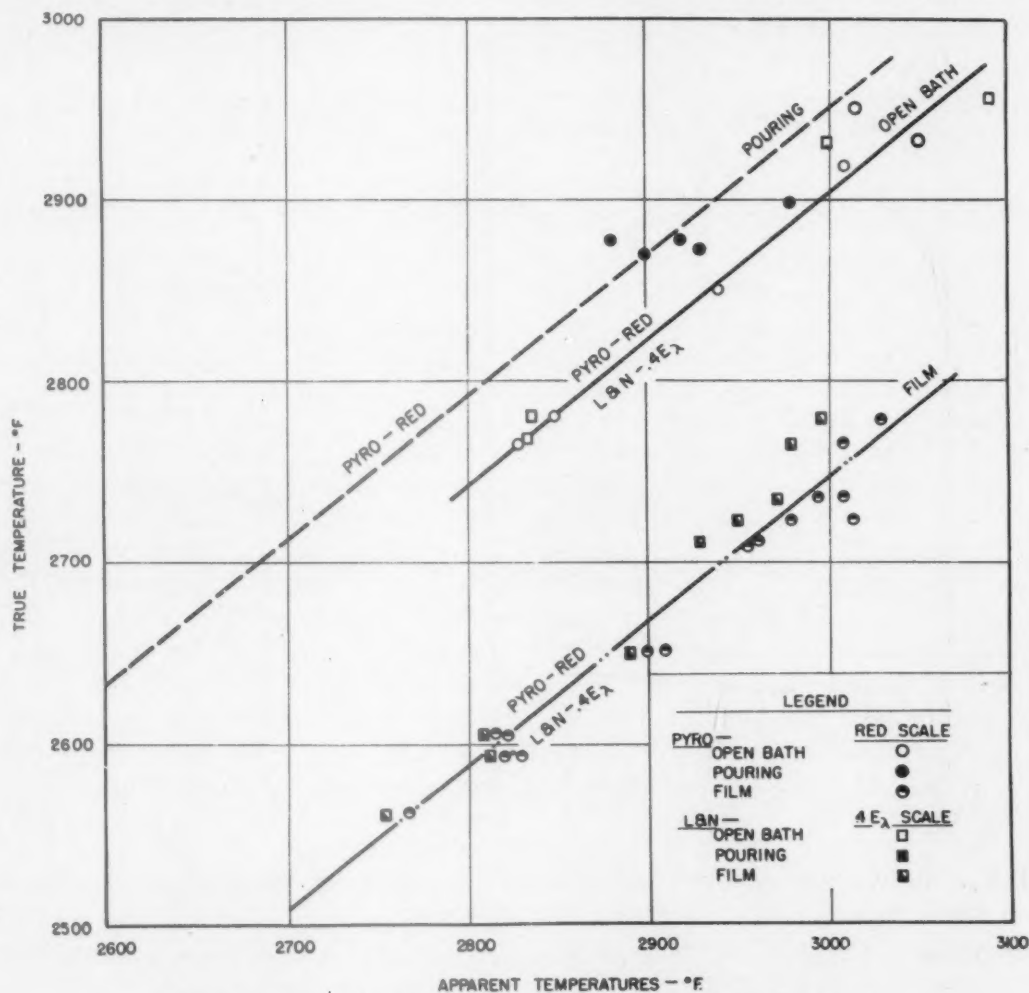


FIG. 6.—TRUE VS. APPARENT TEMPERATURES OF HT TYPE ALLOYS.
36 per cent Ni, 16 per cent Cr.
Corrected scales ($0.4E_\lambda$) with clear and filmed surfaces.

this type of metal forms a film that appears to approach black-body conditions in emissivity.

Fig. 6 shows the relation between the true temperature and the apparent temperature when using the two instruments and using the scales corrected to read steel temperatures. Using the temperature of 2800°F., the reading on the stream of molten metal is only very slightly above

previously, probably this is the result of an unavoidable slight film on the metal bath.

Fig. 6 also shows the relation of true temperature to apparent temperature when the readings are made on a bath covered with the film and using the scales for reading on molten steel. At a true temperature of 2700°F., the reading on this scale would be over 2900°F., or would introduce an error of over 200°F. These experiments

with the HT type of alloy suggest that the optical readings will be relatively close to the true temperature if, at the high tem-

somewhat above 2800°F. and film formation taking place, the apparent temperature might indicate that the temperature

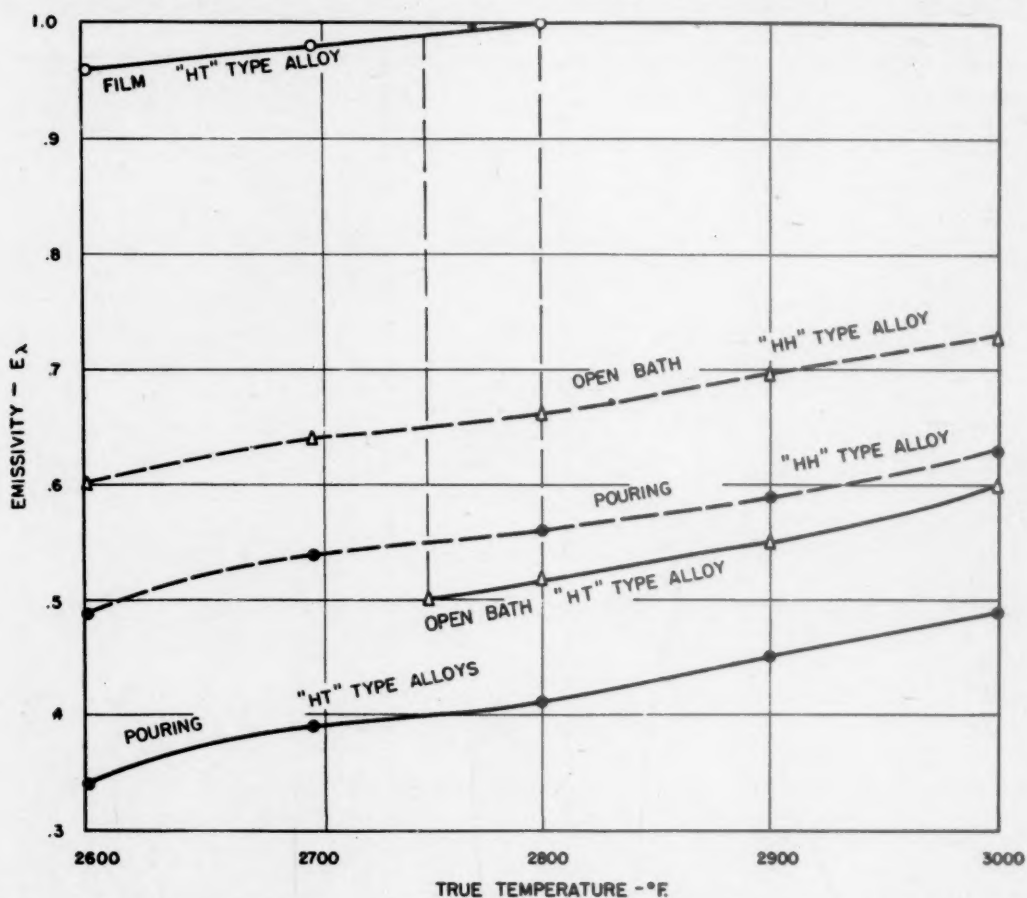


FIG. 7.—VARIATION OF EMISSIVITY OF HH AND HT TYPE ALLOYS WITH TEMPERATURE AND SURFACE CONDITION.

peratures and under conditions of open bath or stream of molten metal, the readings are made on the scales designed for use on molten steel; and, if the readings are below about 2800°F. and the metal has become covered with a film, the readings should be made on the black-body scale. The conditions observed would suggest that, if the temperature of molten HT alloys is being followed with an optical pyrometer, and if it is heated to slightly above 2800°F. and the film disappears, the apparent temperature might show a decrease, whereas the true temperature had been increased. Likewise, on cooling from

of the bath is increasing, whereas in fact it had decreased substantially.

While detailed measurements have not been made on the HH type of alloy, it is known that the alloy forms a film similar to the HT type, at about the same temperature on cooling, and it is considered likely that the effect on the apparent temperature is of about the same order and in the same direction as with the HT type of alloy.

EMISSIVITY CALCULATIONS AND CURVES

Two emissivity curves were calculated for the HH type alloy and three for the HT type alloy from the true temperature vs.

apparent temperature curves. At least five points along each straight line of the relation of true to apparent temperature were taken arbitrarily, and from the data of each point, an emissivity value was calculated using the formula:⁵

$$\ln E_{\lambda} = \frac{C_2}{\lambda} (T_t^{-1} - T_a^{-1})$$

in which

T_t = true (immersion) temperature in deg. Kelvin,

T_a = apparent (black scale optical) temperature in deg. Kelvin,

λ = wave length of filter employed in optical pyrometer, 0.65μ ,^{*5}

C_2 = second radiation constant, $14,360\mu$ deg.,⁶ and

E_{λ} = emissivity.

The emissivity for each true temperature used was then plotted, and the slightly S-shaped curves were drawn through the points to construct Fig. 7. The solid lines are for type HT alloys, while the broken lines are for type HH.

The significance of these curves is purely academic at the present time. Optical-pyrometer temperatures are relative, and it would be of no value to put in a special filter to compensate for the emissivity of each alloy. With the use of the true vs. apparent temperature curves, just as reliable a relative value can be obtained to correspond to a given true temperature. Furthermore, the variation of emissivity with temperature makes emissivity a value worth very little in actual practice.

The emissivity values calculated from the pouring temperatures probably are the most reliable for a film-free metal surface. Taking this value for the HT alloy, it can be said that the emissivity of such an alloy varies from 0.34 to 0.49 for temperatures of 2600° to 3000°F ., respectively.

* This conventional value has been used in the calculations of emissivities, but it is obvious that variations in the wave lengths of filters will make a difference in the calculated values.

Under similar conditions, the emissivity of the HH alloys ranges from 0.49 at 2600°F . to 0.63 at 3000°F . If the HT alloy is covered with a film, the emissivity is approximately 1.0 in the range of 2600° to 2800°F ., as shown in the upper curve of Fig. 7.

From the wide range of analyses of the alloys upon which emissivity measurements were made, it is evident that minor alloying elements, such as carbon, silicon, and manganese, in the normal range, have little effect upon emissivity. Probably there is a minute effect, but it was not detected. Even a variation of 4 per cent of chromium or nickel for the HT type of alloy and 6 per cent of these elements for the HH type was indicated not to cause a measurable variation in emissivity.

Thus, the two types of alloys can be given a definite emissivity range. The true vs. apparent temperature curves will probably be more useful than the emissivity curves in actual foundry operations.

Should temperature control become a critical factor in the pouring of heat-resistant alloys, foundries may find it useful economy to employ an immersion thermocouple apparatus. With the immersion couple, absolute temperature control could be maintained. The initial cost of an immersion couple apparatus is no greater than that of an optical pyrometer, and the cost of the silica protection tube and slag-line block replacements would not amount to more than a few cents per temperature determination.

SUMMARY AND CONCLUSIONS

The liquidus and solidus temperatures of two types of commercial heat-resistant alloys have been determined. These alloys were of the HH type (26 Cr, 12 Ni) and of the HT type (36 Ni, 16 Cr).

Temperature-time cooling curves were taken, using a platinum, platinum-rhodium thermocouple, and comparisons have been

made between the data obtained for these commercial alloys and essentially pure alloys of iron, nickel, and chromium at the same nickel and chromium levels.

The carbon and silicon additions for the commercial alloys are shown to lower the liquidus and solidus temperatures. The liquidus temperature of the commercial HH alloys is reduced about 70°F. by 0.35 per cent carbon and about 105°F. by 0.53 per cent carbon when the silicon contents were about 1.75 per cent and the manganese contents about 1.0 per cent. Essentially the same reductions were found in the liquidus temperature of the HT alloys for carbon contents of 0.15 and 0.46 per cent. The solidus temperatures were lowered more than the liquidus temperatures, being reduced about 275° and 190°F. for around 0.50 per cent carbon in the HH and HT alloys, respectively.

Some eutectic was encountered in alloys of the HH type composition with about 0.40 to 0.50 per cent carbon present, and it was apparent with 0.30 to 0.40 per cent carbon for the alloys of the HT type. With normal silicon and manganese contents, the indicated minimum solidus temperature, or eutectic temperature, was found to be about 2300° to 2320°F. for both the HH and HT type alloys.

For alloys coming within the range of commercial HT type with chromium in the range of 14 to 20 per cent, nickel in the range of 34 to 40 per cent, and with carbon, silicon, and manganese constant at about 0.42, 1.25, and 0.85 per cent, respectively, the liquidus and solidus temperatures are moderately lowered as alloy content is increased. The maximum lowering found in the liquidus temperatures was about 45°F. and in the solidus temperatures only about 25°F.

Correlations have been determined between the true or thermocouple temperatures and the apparent or optical-pyrometer temperatures of the HH and HT types of alloys. Metal in the open bath that

appeared to have a clear surface gave a higher temperature reading than the molten stream of metal poured immediately after taking the reading on the clear bath. It appears that the bath, although appearing to be clear, has some film which increases its emissivity. It is shown that the corrections that have been applied to optical pyrometers for reading molten-steel temperatures give readings that are somewhat too high for clear surfaces or for the stream of molten metal of the HH alloys, and that the disparity is less for the HT alloys. The black-body temperature scales give readings that are too low when sighting on the clear metal surface, but when the true temperature of the metal is 2800°F. or less, a surface film tends to form, which gives readings on the black-body scales that are quite close to true temperature.

The emissivities of these heat-resistant alloys vary with the temperature of the bath and also the surface condition of the bath. Curves have been drawn to show the emissivities of these two types of alloys as a function of these variables. Calibration charts have been drawn, which may be used in converting apparent temperatures made with two types of optical pyrometers under various conditions to true temperatures. The importance of knowing the condition of the surface sighted upon is shown. The difficulties arising from the variable surface conditions of the bath have been pointed out, and the feasibility of using an immersion thermocouple suggested.

ACKNOWLEDGMENTS

The authors wish to express appreciation to the Alloy Casting Institute and Battelle Memorial Institute for permission to publish the information contained in this paper. The assistance of Herbert S. Kalish, formerly of the Battelle staff and now in the Armed Services, in the early phases of this study is gratefully acknowledged.

REFERENCES

The following publications are valuable sources of information on closely related studies reported in the technical literature:

1. C. H. M. Jenkins, E. H. Bucknall, C. R. Austin and G. A. Mellor: Some Alloys for Use at High Temperatures: Part IV. The Constitution of the Alloys of Nickel, Chromium, and Iron. *Jnl. Iron and Steel Inst.* (1937) 136.
2. F. H. Schofield and A. Grace: Second Report of the Liquid Steel Temperature Subcommittee (Eighth Report on the Heterogeneity of Steel Ingots). Iron and Steel Inst. Special Rept. No. 25 (1939) 235-264.
3. Third Report of Liquid Steel Temperature Subcommittee. *Jnl. Iron and Steel Inst.* (1942) 213-243.
4. C. F. Lucks and H. W. Russell: The Fluorescent Mercury-Vapor Lamp as a Light Source for a Single-Point Check on Optical Pyrometers. *Jnl. Optical Soc. Amer.* (Apr. 1940) 30 (4), 163-167.
5. G. N. Goller: The Emissivity of Molten Stainless Steels. *Trans. Amer. Soc. Metals* (1944) 32, 239-254.
6. H. T. Wensel: International Temperature Scale and Some Related Physical Constants. Nat. Bur. Stds. *Jnl. of Research* (Apr. 1939) 22, 375.

DISCUSSION

G. N. GOLLER.*—I read this paper with considerable interest and feel that from a practical standpoint the data presented by the authors should be of value to foundries and other shops melting the HH and HT heat-resisting alloys.

In studying the data in this paper, I noted that wherever a comparison can be made between readings obtained with the Pyro and the Leeds and Northrup optical pyrometers, the Pyro instrument consistently read 15° to 20°F. higher than the Leeds and Northrup instrument. This should not be, since both instruments were checked frequently against a standard light source. It is my experience that great care must be taken when setting the lamp current on the Pyro and that it may have to be reset often. A change of one division on the milliammeter scale will affect the temperature reading by approximately 35°F. Improper setting of the lamp current may account for the wide deviation of points obtained with the Pyro as compared with the Leeds and Northrup optical pyrometer readings.

The calibration line in Fig. 5, obtained by

plotting readings taken on the oxide film covering the metal surface, should be adjusted slightly, since the Leeds and Northrup readings appear to be the most reliable. This is substantiated by the fact that some of the Pyro readings indicate emissivities of more than one.

The statement made by the authors that "even a variation of 4 per cent of chromium or nickel for the HT type of alloy was indicated not to cause a measurable variation in emissivity" is not borne out by the data, since the heats on which emissivity data are available have chromium and nickel contents within a very narrow range.

At our plant, an immersion thermocouple similar to one described by the authors, but designed for the measurement of the bath temperature in large electric-arc furnaces, has been in constant use for more than a year on commercial heats of stainless steel. Each furnace in our melt shop is equipped with a number of immersion couples and an electronic recording instrument, which are maintained daily. This installation has been described by L. F. Weitzenkorn.⁷

When the immersion couple is used in large furnaces it has been found necessary to replace the fused silica protection tube after each reading. The cost per reading in our shop amounts to \$0.98, of which \$0.67 is the cost of the silica tube. The seemingly expensive platinum costs less than \$0.30 per reading.

In the foundry, even on small furnaces, it may also be necessary to replace the silica tube after each reading, since most immersions will be made in molten metal having a temperature of 3000°F. or more, especially when small castings are to be poured.

By the measurement of bath temperatures with the immersion couple before the steel is tapped from the furnace and the use of optical pyrometer readings taken during the pouring of the ingots and corrected according to the grade, we have one temperature scale in our shop, which is the true temperature. It is important that an observer making optical pyrometer measurements of molten-steel temperatures take care when an oxide film is forming on the surface of the metal. Readings must be made on either the clear metal or the oxide

* Supervising Metallurgist, Rustless Iron and Steel Corporation, Baltimore, Maryland.

⁷ *Proc. Electric Furnace Steel Conference*, 1944, A.I.M.E., 143.

film and corrections made accordingly. This point was stressed by the authors.

By the use of the data presented by the authors and similar data on other grades, the foundry will become more familiar with the influence of the temperature of the metal during melting and pouring upon the properties and quality of their castings. If temperature control is needed the quick immersion platinum thermocouple is recommended as a very practical tool for the foundry.

J. T. Gow (authors' reply).—We were fully aware that the Pyro optical pyrometer used read consistently higher than the Leeds and Northrup instrument. This had been noted by numerous operators. The statement made by Mr. Goller, "this should not be, since both instruments were checked frequently against a standard light source," is not wholly agreed with. For the reported studies, the lamp-current setting of the Pyro optical pyrometer was properly adjusted at each use of the instrument. Our instrument laboratory periodically calibrates all of our optical pyrometers, using a wide-ribbon, tungsten-filament standard lamp. We also have the fluorescent mercury-vapor lamp setup in our foundry for a convenient single-point check on the optical pyrometers

by the operators. The instrument laboratory has record of optical pyrometers agreeing on the tungsten standard lamp and not agreeing on the fluorescent mercury-vapor lamp. The latter is pink in color, and the differences mentioned are believed to result from a difference in filter characteristics of the optical pyrometers. Without knowing definitely the wave length of the filter employed in the commercial instruments, but accepting the conventional value of 0.65μ , emissivity values calculated from the average straight-line curves of the relation of true to apparent temperature are necessarily in error a small amount.

It was one of our main objectives to stress the importance of knowing the condition of the molten-metal surface sighted upon, by developing the relationship between the apparent and true temperature of the molten heat-resistant alloys when sighting on an open bath, on a more film-free surface such as obtained for the stream of metal on pouring, or when sighting on a filmed-over surface, as would occur as the ladle temperature drops below 2800°F .

The reference to Mr. Weitzenkorn's recently published paper is appreciated, as it shows definitely that the immersion platinum thermocouple has found practical application in the foundry.

Ar'' in Chromium Steels

By EUGENE P. KLIER,* JUNIOR MEMBER, AND ALEXANDER R. TROIANO,† MEMBER A.I.M.E.

(New York Meeting, February 1945†)

SINCE the very early work on quenched structures, where the products of the martensite transformation had been recognized, this transformation has provoked much interest and study. Theoretically it was desirable to account for the extreme changes in physical properties resulting from the formation of martensite, as that information might lead to results of practical importance. Desirable information, therefore, was on the kinetics of transformation from austenite to martensite as well as on the physical constitution of the martensite.

It has been known for years that certain steels quenched to room temperature will contain persistent austenite as well as martensite. Other important and now well-established features of the martensite reaction are the progress of the reaction on cooling only and the independence of Ar'' with cooling velocities exceeding the critical velocity. These facts have been experimentally determined by various methods and investigators. Notable among the early investigators were Tammann and Scheil¹ and Wever and Engel.² Unfor-

tunately, all investigators did not fully interpret their results, which, coupled with several investigations that yielded conflicting results, caused a state of confusion that was not clarified until quite recently.

X-ray investigations of martensite in steels³⁻⁶ indicate it to be a supersaturated solid solution of carbon in alpha iron. This supersaturation is evident from the appearance of a body-centered tetragonal structure with the addition of sufficient carbon. The dimensions of this tetragonal structure are a linear function of the carbon content within the limits of accuracy of the determinations. Slight tempering of tetragonal martensite leads to the destruction of the tetragonal structure, which is converted to a body-centered cubic structure. This phenomenon has precipitated a controversy concerning the nature and mechanism of the tempering of martensite. The facts in the case have been outlined by Epstein⁷ and more recently by Antia, Fletcher, and Cohen.⁸

The significance of Ar'' on theoretical grounds is not clear, however, although considerable study has been devoted to its determination. The precise position of Ar'' as a function of carbon content was first stated by Greninger and Troiano⁹ for steels covering a range of approximately 0.7 to 1.8 per cent carbon. The effect of alloying elements on Ar'' has recently been the subject matter of investigation by various methods.

Most of the material presented in this paper has been abstracted from a thesis submitted by E. P. Klier in partial fulfillment of the requirements for the degree of Master of Science, University of Notre Dame, May 1942. Manuscript received at the office of the Institute Nov. 29, 1944. Issued as T.P. 1799 in METALS TECHNOLOGY, February 1945.

* Instructor in Metallurgy, Pennsylvania State College, State College, Pennsylvania.

† Associate Professor of Metallurgy, University of Notre Dame, Notre Dame, Indiana.

‡ Meeting canceled.

§ References are at the end of the paper.

All the common alloying elements have been studied to some degree.^{10-16*} However, with the possible exception of those for the work on manganese,^{10,15} no systematic data exist over a wide range of carbon and alloying element for any of the alloying elements. Such a study for chromium steels is presented here. It is interesting to note that most of the alloying additions studied either have no effect or lower Ar''. Two notable exceptions, aluminum and cobalt, raise Ar''.

EXPERIMENTAL WORK

Materials.—The Ar'' determinations were made on 17 chromium steels of rather

TABLE 1.—Data on Steels Investigated

Steel	Analyses, Per Cent						Austenitizing	
	C	Mn	Si	P	S	Cr	Temperature, Deg. C.	Time, Hr.
3-Cr-40	0.38	0.20	0.18	0.018	0.013	2.98	1200	2
6-Cr-40	0.43	0.23	0.20	0.015	0.013	5.53	1200	2
9-Cr-40	0.41	0.23	0.17	0.017	0.012	8.77	1200	2
12-Cr-40	0.46	0.25	0.19	0.009	0.012	11.75	1200	3
15-Cr-40	0.42	0.25	0.18	0.016	0.011	14.61	1150	20-28
3-Cr-70	0.69	0.22	0.12	0.022	0.011	3.00	1200	2
6-Cr-70	0.69	0.27	0.18	0.020	0.014	5.75	1200	2
9-Cr-70	0.71	0.22	0.20	0.010	0.012	8.73	1200	3
12-Cr-70	0.76	0.26	0.21	0.018	0.014	11.55	1200	4
15-Cr-70	0.73	0.28	0.20	0.014	0.014	14.82	1200	5
1-Cr-100	1.04	0.34	0.28	0.010	0.012	0.95	1200	1/2
3-Cr-100	1.02	0.33	0.35	0.020	0.012	2.89	1200	2
4-Cr-100	1.04	0.18	0.35	0.00	0.00	3.97	1200	2
6-Cr-100	1.05	0.31	0.35	0.017	0.012	5.69	1200	2
9-Cr-100	1.02	0.33	0.35	0.016	0.011	8.81	1200	10-12
3-Cr-130	1.28	0.29	0.37	0.019	0.017	2.69	1200	2
6-Cr-130	1.28	0.30	0.37	0.017	0.016	5.75	1175	20-24

low manganese content of which the compositions are given in Table 1. The selection of these steels was made after a consideration of the equilibrium diagram for the

* Not listed here are many papers from the Kaiser-Wilhelm-Institut für Eisenforschung, which have appeared in the last 15 years and which contain considerable information dealing with the effect of alloying additions on Ar''. For the most part, those papers are not devoted to a systematic study of composition versus Ar'', hence much of the information is fragmentary.

iron-carbon-chromium system by Tofaute, Sponheuer, and Bennek¹⁷ and by Tofaute, Küttner, and Büttinghaus.¹⁸

Austenitizing Furnace.—A vertical sillimanite tube furnace wound with platinum, 20 per cent rhodium alloy wire was employed for austenitizing. The atmosphere was dried nitrogen, purified by passing over heated copper gauze. To minimize decarburization effects, it was necessary to insert a graphite plug in the furnace at a distance of approximately 1/4 in. below the specimen. The atmosphere thus obtained was sufficient to prevent any observable decarburization in a specimen of high carbon content after more than 24 hr. at 1200°C. The austenitizing times and temperatures for the various steels are listed in Table 1.

Determination of Ar''.—The quench-temper method developed by Greninger and Troiano⁹ was employed. Various quenching media were used, as follows:

400° to 75°C..... Wood's metal
 65° to 5°C..... water
 30° to -38°C..... mercury
 20° to -15°C..... 10 per cent solution of sodium hydroxide in water
 -38° to -77°C..... dry ice and acetone
 -77° to -192°C..... liquid air

The water was employed after a rapid quench in Wood's metal to near 100°C., followed by cooling in the water in the temperature range 65° to 25°C. The dry ice and acetone and the liquid air were employed after the specimens had been quenched to room temperature in water. It is significant to note that the quenches into warm water, dry ice and acetone, and liquid air were interrupted at some higher temperature. Direct transfers to warm water, dry ice and acetone, and liquid air yield a slow and unsatisfactory quench.

Ar'' was determined as that temperature at which there was unmistakable evidence of martensite with none evident at 10°C. higher. The accuracy of the method for

any given specimen is considered good to $\pm 5^\circ\text{C}$. However, such variables as inhomogeneity probably restrict the over-all accuracy for the system to not better

0.40 Per Cent Carbon Series

Certain data for the steels of the 0.40 per cent C series have been presented by

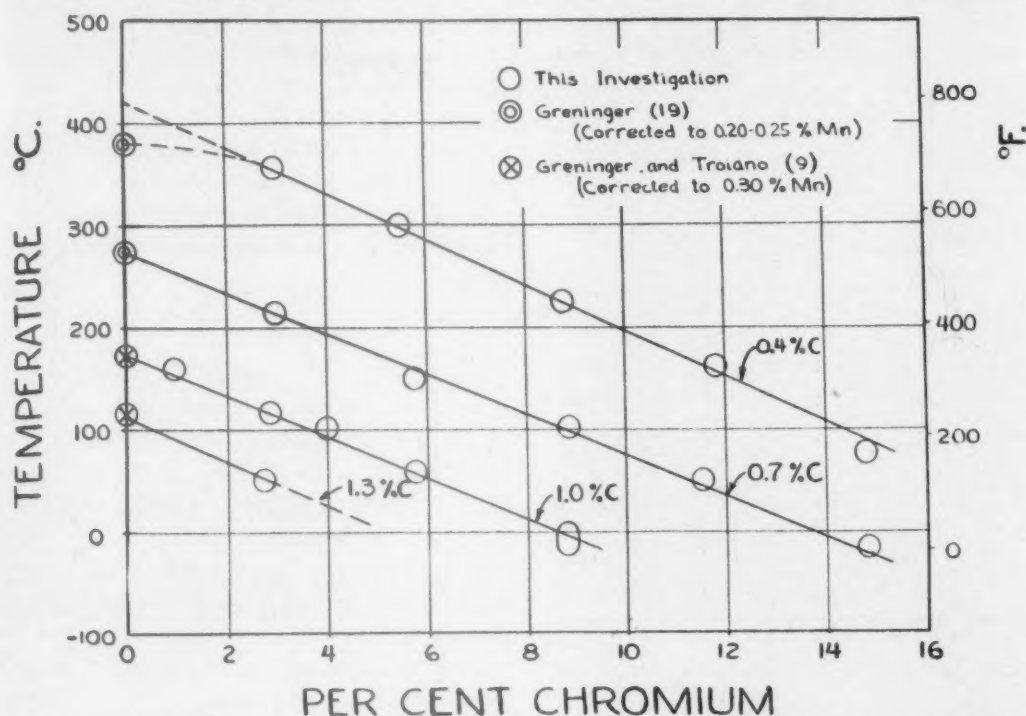


FIG. 1.—INFLUENCE OF CHROMIUM ON Ar'' IN 0.40, 0.70, 1.0, AND 1.3 PER CENT CARBON STEELS.

than $\pm 10^\circ\text{C}$. The several exceptions to this degree of accuracy are clearly stated in the text.

Specimen Size.—Initial Ar'' determinations were made with specimens $\frac{1}{4}$ in. in diameter and $\frac{1}{4}$ in. high. Almost all the Ar'' points were checked using specimens $\frac{1}{16}$ by $\frac{1}{8}$ by $\frac{1}{2}$ in. In a few cases final checks were made with specimens $\frac{1}{32}$ by $\frac{1}{32}$ by $\frac{1}{2}$ in. In one or two cases to be described later, other sizes of specimens were employed.

EXPERIMENTAL RESULTS

The determined Ar'' temperatures are given in Table 2, together with corresponding values after correction for slight carbon variations. These data are plotted in Fig. 1. The following remarks are pertinent.

the authors.¹² The salient features can be summarized briefly. Ar'' for a 0.40 per cent C, 0.20 per cent Mn steel as taken from Greninger's data¹⁹ is approximately 380°C . If this series is extrapolated to 0 per cent Cr, a value of approximately 425°C . is obtained. This discrepancy is well outside the accepted limits of over-all accuracy of the results. Thus it appears that the initial additions of chromium are not very effective in lowering Ar'' , and might in fact actually raise Ar'' . The data of Rose and Fischer¹⁶ indicate that this actually occurs with chromium steels containing 0.20 per cent C.

Additions above 3 per cent cause a lowering of Ar'' , in a linear relationship. The rate of lowering is approximately 23°C . per 1 per cent Cr. The value for 15-Cr-40 appears to be slightly low.

However, this is probably an effect of stabilization, to be discussed later, and it is believed that a more fundamental value is obtained by a straight line.

TABLE 2.—Ar'' Temperatures

Steel	Ar'' Observed		Ar'' Corrected for Carbon	
	Deg. C.	Deg. F.	Deg. C.	Deg. F.
3-Cr-40	365	689	358	676
6-Cr-40	290	554	301	574
9-Cr-40	223	433	226	439
12-Cr-40	138	280	160	320
15-Cr-40	65	149	72	162
3-Cr-70	220	428	217	423
6-Cr-70	153	307	150	302
9-Cr-70	100	212	103	217
12-Cr-70	30	86	50	122
15-Cr-70	-25	-13	-15	5
1-Cr-100	155	311	163	325
3-Cr-100	115	239	119	246
4-Cr-100	94	201	102	216
6-Cr-100	50	122	60	140
9-Cr-100	-5 to -15	23 to 5	-1 to -11	30 to 12
3-Cr-130	55	131	51	124
6-Cr-130	lower than -38	lower than -36		

0.01 per cent C = 2°C (correction factor 1.0 and 1.3 per cent C)

0.01 per cent C = 3.5°C (correction factor .40 and .70 per cent C)

0.70 Per Cent Carbon Series

The Ar'' curve for the 0.70 per cent C series is a straight line of very nearly the same slope as the 0.40 per cent C series. The extrapolated value to 0 per cent Cr agrees reasonably well with the value expected for a 0.70 per cent plain carbon steel with 0.25 per cent manganese.

Considerable difficulty was experienced in the determination of Ar'' for steel 15-Cr-70. In this connection the following observations are to be considered:

1. Ar'' as determined for the larger specimens was between -38°C. and -77°C. The quenching media were refrigerated mercury, dry ice and acetone.

2. Ar'' as determined for the small specimens was -25°C. (corrected for carbon to -15°C.). The quenching medium was refrigerated mercury.

3. The extrapolated value for this steel from the carbon corrected curve is about

-15°C. This is in agreement with the determination as listed above.

1.00 and 1.30 Per Cent Carbon Series

Both the 1.00 and the 1.30 per cent C series exhibit the same type of straight-line relationship as is shown in the 0.40 and 0.70 per cent C series, although the 1.3 per cent C series is based on only one determination in a chromium steel. The values for 9-Cr-100 and 6-Cr-130 will be considered in the discussion on stabilization.

Microstructure of Martensite

One of the distinctive features of a martensite structure is its shape. That this shape varies under different conditions has long been recognized. However, the factors involved in these variations have not been understood.

In the results considered here three factors may be considered as effective in altering the shape of the martensite volumes. These are carbon content, chromium content, and temperature of formation. Grain size may be considered a fourth variable, but its influence on the relatively large-grained specimens employed in this study was negligible.

In work on plain carbon steels, Whitely²⁰ was led to distinguish four types of martensite depending on the carbon content. He neglected the factor of temperature in this series. In fact, a series of this type does not allow the temperature factor to be isolated. Fortunately a series of the type presented here will have steels of widely different compositions with very nearly the same Ar''. Obviously, this will allow a comparison of the relative effects of composition versus temperature.

For example, steels 3-Cr-70 (Fig. 2) and 9-Cr-40 (Fig. 3) have Ar'' temperatures near 220°C. The martensite structures are very similar. A similarity also exists between the structures in steels 9-Cr-70 (Fig. 4), 3-Cr-100 (Fig. 5), and 3-Cr-130

(Fig. 6), all of which have $A_{r''}$ within a temperature range of approximately 60°C . The steels for these examples were selected with reasonably the same $A_{r''}$ temperatures without regard for composition. The results indicate that the temperature of formation of the martensite is a more important factor governing the microstructure than is the composition.

The general variation in the microstructure of martensite obtained in plain carbon steels with increasing carbon content is quite like that observed for steel 3-Cr-40 (Fig. 7) compared with steel 12-Cr-40 (Fig. 8). In these two steels, the microstructural differences must be caused by either the difference in chromium or in $A_{r''}$. Carbon content obviously is not a variable. However, as stated above, the same type of microstructural variations are found in plain carbon steels. This lends increased weight to the concept that the shape of a martensite volume is primarily dependent upon its temperature of formation.

The martensite volumes in steel 3-Cr-40 are lathlike in shape, of uniform size, and do not possess a midrib. The martensite volumes in steel 12-Cr-40 are of two distinctive types; that noted for steel 3-Cr-40, and a more massive type, relatively larger in all dimensions, platelike, and possessing a distinct midrib. From geometrical considerations it is evident that the midribbed structure formed prior to the finer structure.

A consideration of the structures shown in Figs. 8, 4, 5, and 6 indicates an alteration in the amount of the massive midrib type of martensite relative to the total amount of martensite. There appears to be an increase in the amount of the midribbed martensite as $A_{r''}$ decreases. This comparison extends to steels 6-Cr-130 (Fig. 9) and 9-Cr-100 (Fig. 10). Both these steels have $A_{r''}$ below room temperature, and exhibit martensite volumes characterized by midribs although the size of these volumes vary considerably.



FIG. 2.—STEEL 3-Cr-70. QUENCHED TO 152°C ., HELD TWO MINUTES, TRANSFERRED TO 302°C ., HELD 1 MINUTE AND QUENCHED INTO WATER.

FIG. 3.—STEEL 9-Cr-40. QUENCHED TO 192°C ., HELD TWO MINUTES, TRANSFERRED TO 338°C ., HELD 3 MINUTES AND QUENCHED INTO WATER.

Both $\times 500$ and etched with Vilella's reagent.



Fig. 11 shows the character of another type of martensite obtained in steel 6-Cr-130 and 9-Cr-130 after compressing a $\frac{3}{8}$ -in. round by $\frac{3}{8}$ -in. high specimen approximately 25 per cent, and then tempering slightly to accentuate the structure. Tempering did not produce this structure because the specimen became slightly ferromagnetic after deformation but prior to tempering. The characteristic "deformation markings" were also obtained by drastic quenching in steels 15-Cr-70, 9-Cr-100, and 6-Cr-130. These markings apparently delineate the $\{111\}$ (slip) planes of the austenite. X-ray diffraction patterns show them to have a crystal structure based on the body-centered cubic structure (very probably distorted body-centered tetragonal).

Discussion of Microstructures

From the statements above, certain generalizations are possible.

1. Alterations in carbon and chromium content in steel result in microstructural changes. These changes are not directly dependent on the alloying additions but rather result from the alteration in Ar'' caused by the alloying addition.

2. Two types of regular martensite structures are recognized: (a) a fine, poorly defined, lathlike structure, which is characteristic of martensite formed at high temperatures; (b) a well-defined platelike structure usually characterized by a mid-rib, and formed at intermediate and low temperatures. The transition between the structures of a and b is continuous with decreasing temperature.

FIG. 4.—STEEL 9-Cr-70. QUENCHED TO 25°C., TEMPERED 296°C. FOR ONE MINUTE AND QUENCHED INTO WATER.

FIG. 5.—STEEL 3-Cr-100. QUENCHED TO 25°C., TEMPERED 370°C. FOR ONE MINUTE AND QUENCHED INTO WATER.

FIG. 6.—STEEL 3-Cr-130. SAME TREATMENT AS FOR FIG. 5.

All $\times 500$ and etched with Vilella's reagent.

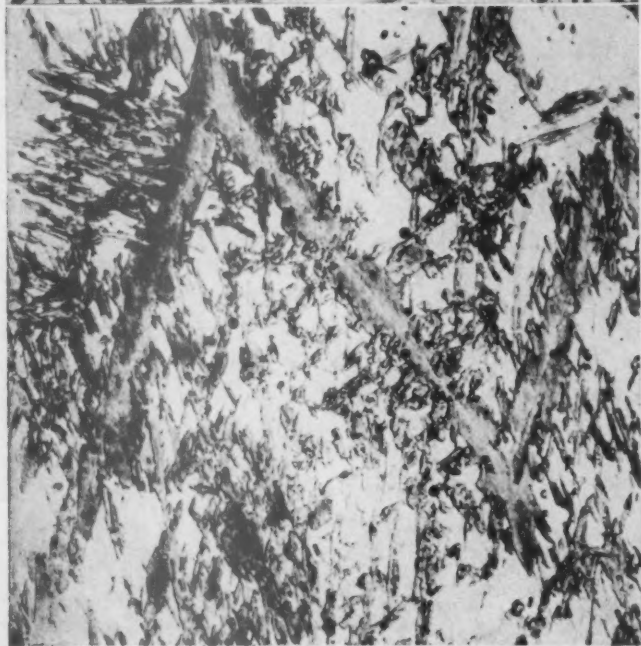
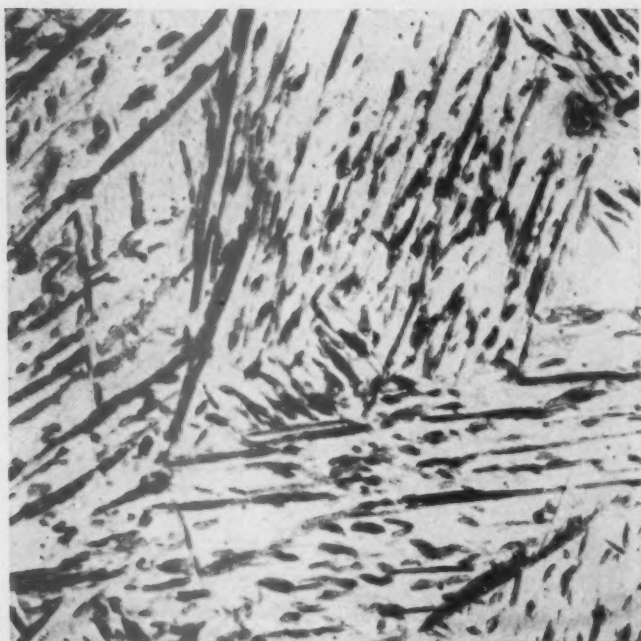


FIG. 7.—STEEL 3-Cr-40. QUENCHED TO 308°C ., HELD 30 SECONDS AND QUENCHED INTO WATER.

FIG. 8.—STEEL 12-Cr-40. QUENCHED TO 92°C ., HELD TWO MINUTES, TRANSFERRED TO 302°C ., HELD ONE MINUTE AND QUENCHED INTO WATER.

Both $\times 500$ and etched with Vilella's reagent.



3. The temperature range through which martensite forms is not a constant temperature interval.

"Deformation markings" were also observed in certain steels. Because of the nature of the formation of these markings, they must be classified as a type of martensite. The same type of markings as those revealed in this study have been obtained in other systems, both ferrous and nonferrous, under similar conditions. One of the best known examples is Hadfield manganese steel.

STABILIZATION

It is well known that the martensite reaction progresses on continuous cooling. It might be anticipated, therefore, that the rate of cooling through the martensite range would affect in some way the course of the transformation. If a specimen of the steel in the austenitic condition is cooled, say halfway through the martensite range, approximately 50 per cent of the austenite will transform to martensite. If the specimen is held at this temperature for an appreciable time before being cooled further, the martensite reaction does not set in immediately on continued cooling, and no austenite transforms until a temperature interval, dependent on the time of holding at temperature, has been passed through. This phenomenon has come to be known as "stabilization of the austenite" or simply as "stabilization." As will be shown, analogous treatment of certain chromium steels in the austenitic state results in a lowering of Ar'' for the steel. Stabilization as considered here has reference to this latter phenomenon.

FIG. 9.—STEEL 6-Cr-130. QUENCHED INTO WATER, TRANSFERRED TO LIQUID AIR, TEMPERED 15 SECONDS 450°C. $\times 500$.

FIG. 10.—STEEL 9-Cr-100. SAME TREATMENT AS FOR FIG. 9. $\times 500$.

FIG. 11.—STEEL 9-Cr-100. QUENCHED INTO WATER. SEVERELY DEFORMED AND TEMPERED TWO MINUTES 280°C. $\times 400$.

All etched with Vilella's reagent.

A brief initial report of some of this work has already been presented.²¹ No systematic study of stabilization in this system was attempted. The study of stabilization was made only as far as it was necessary to evaluate its effect on the determination of Ar'' in certain specific steels.

The work of Gordon and Cohen,²² in which this phenomenon was first quantitatively studied, was carried out under unique conditions. The steel studied (18-4-1 high-speed tool steel) was quenched partially through the martensite range and the stabilization study was carried out on specimens containing considerable amounts of martensite. It was suggested that stabilization could possibly result from the effect of stress relief caused by the prior formation of martensite. A later paper by Fletcher and Cohen²³ dealt with the same type of stabilization study as that reported in the high-speed steel investigation. The results considered here pertain to a lowering of the Ar'' point, a quite different situation from that previously investigated. It is believed that most of the steels in this set will exhibit stabilization under proper conditions. However, steels 15-Cr-40, 15-Cr-70, 9-Cr-100, and 6-Cr-130 were so sensitive to stabilization that special precautions were necessary to be certain that stabilization did not influence the results. In fact, for the case of 6-Cr-130 it is felt that the experimental methods at hand were not capable of eliminating the effects of stabilization.

The following observations relevant to the determination of Ar'' are significant.

15-Cr-40

An interruption of only several seconds at 395°C. in the cooling lowered Ar'' for the 15-Cr-40 steel to slightly below room temperature. In addition, the larger specimens gave lower Ar'' values than the slivers. Obviously this steel was so sensitive to stabilization that the most rapid cooling velocities were necessary. It is possible that

the slightly low value obtained (as compared with the extrapolated value) could be explained on the basis that a sufficiently rapid cooling velocity was not obtained.

15-Cr-70

1. Ar'' using slivers $\frac{1}{32}$ by $\frac{1}{32}$ by $\frac{1}{2}$ in. of steel 15-Cr-70 quenched into refrigerated mercury was -25°C .

2. By increasing the specimen size to $\frac{1}{4}$ by $\frac{1}{4}$ by $\frac{1}{4}$ in. and quenching into water, then immediately transferring to dry ice and acetone, Ar'' was lowered to somewhere between -38° and -77°C .

3. Quenching a specimen to room temperature and holding for one hour, Ar'' was lowered to some value below -77°C .

4. By holding the specimen of part 2 for one year at room temperature, no added martensite was formed on cooling to liquid-air temperatures.

This steel obviously was extremely sensitive to stabilization. An interruption in cooling of several seconds at room temperature was sufficient to lower Ar'' more than 55°C ., and one hour at room temperature lowered Ar'' more than 100°C .

9-Cr-100

1. Quenching specimens $\frac{1}{4}$ by $\frac{1}{4}$ by $\frac{1}{4}$ in. of steel 9-Cr-100, and also slivers $\frac{1}{32}$ by $\frac{1}{32}$ by $\frac{1}{2}$ in., into refrigerated mercury yielded an Ar'' value below -38°C .

2. A series of six specimens was quenched directly into a refrigerated 10 per cent solution of sodium hydroxide in water. These specimens were sized from $\frac{1}{32}$ by $\frac{1}{32}$ by $\frac{1}{2}$ in. up to $\frac{1}{4}$ by $\frac{3}{8}$ by $\frac{5}{8}$ in. Neither the smallest nor the largest of these specimens showed any martensite on quenching to -15°C . However, the specimens of intermediate size yielded Ar'' values in the range of -5 to -15°C (uncorrected). A more precise determination was not possible; but the results described above were generally reproducible.

The sodium hydroxide solution was the most efficient quenching medium employed

in this investigation. Thus we see that this steel was extremely sensitive to stabilization. The largest specimen was unable to attain as rapid a cooling velocity as were the smaller specimens. However, this leaves unexplained the failure of the sliver to exhibit any martensite when quenched into the sodium hydroxide solution at -15°C . This is considered to be a real specimen-size effect and not the indirect effect obtained with large specimens, which is actually a cooling-velocity effect. One of the authors has had an experience similar to this with a nickel steel in which Ar'' was slightly above room temperature. When filings were quenched to room temperature, no martensite was observed, but slivers quenched under identical conditions did yield martensite.

6-Cr-130

Attempts to obtain an accurate value for steel 6-Cr-130 were unsuccessful. Direct quenches into refrigerated mercury down to -38°C . did not yield martensite. Sufficient data are not available at this time to state definitely whether the abnormally low Ar'' value obtained is real or similar to the previously discussed cases, where it was observed that stabilization could influence the determination of Ar''.

DISCUSSION OF RESULTS

The effect of chromium on Ar'' has been determined for 17 steels covering a wide range of compositions. The Ar'' surface for this system appears to be plane over most of the composition range investigated, but in the dilute alloys the surface may be warped, as indicated by the 0.40 per cent C series and the data of Rose and Fischer.¹⁶ More study is desirable in this range in both this and other systems. However, in relatively low-alloy steels containing less than 0.40 per cent carbon, the microscopic method employed here is unsatisfactory; other methods should be employed. The action of steel 6-Cr-130 suggests a deviation

from a plane surface in this region also; but at present it is considered that this is a secondary effect of stabilization rather than a fundamental deviation in the action of the alloying element as it affects Ar''.

The curves in Fig. 1 show, if Ar'' is plotted versus carbon content for the various chromium series, that the rate of lowering Ar'' in chromium steels is much the same as in plain carbon steels; that is, small additions of carbon have a relatively greater effect than large additions.

A study of the microstructures obtained in this system demonstrate quite conclusively that the shape of a given martensite volume is dependent to a far greater extent upon the temperature of formation than upon the composition.

Several of the steels studied were shown to be extremely sensitive to stabilization. In several of the alloys only a momentary interruption in cooling was sufficient to lower Ar'' from 50° to 100°C . In fact, a slow cooling velocity (well above the critical velocity) was sufficient to initiate stabilization and yield abnormally low Ar'' values. Thus it becomes obvious that a systematic study of Ar'' in most of the alloy-steel systems must carefully evaluate the possible effect of stabilization.

It has been shown that stabilization can occur without previous decomposition of austenite to martensite or any of the other recognized decomposition products. Obviously, the stress-relief hypothesis of Gordon and Cohen²² will not apply to the phenomena observed here, and thus cannot afford an explanation for the general case of stabilization. It is quite probable that the relief of stress plays some role where there has been some decomposition of austenite.

ACKNOWLEDGMENTS

The authors wish to acknowledge the interest and cooperation of Dr. E. G. Mahin, head of the Department of Metallurgy, University of Notre Dame, and to

thank Mr. G. V. Luersson, of the Carpenter Steel Co., and Mr. W. G. Hildorf, of the Timken Roller Bearing Co. for their help in obtaining most of the steels investigated.

REFERENCES

1. G. Tammann and E. Scheil: Die Umwandlungen des Austenits und Martensits in gehärteten Stählen. *Ztsch. anorg. allg. Chem.* (1926) **157**, 1-21.
2. F. Wever and N. Engel: Ueber den Einfluss der Abkühlungsgeschwindigkeit auf die Umwandlungen der Stähle. *Mitt. K-W-I. Eisenforschung* (1930) **12**, 93-114.
3. W. Fink and E. Campbell: Influence of Heat Treatment and Carbon Content on the Structure of Pure Iron-Carbon Alloys. *Trans. Amer. Soc. Steel Treat.* (1926) **9**, 717-754.
4. G. Hägg: X-ray Investigations on the Structure and Decomposition of Martensite. *Jnl. Iron and Steel Inst.* (1934) **130**, 439-451.
5. E. Öhman: X-ray Investigations on the Crystal Structure of Hardened Steel. *Jnl. Iron and Steel Inst.* (1931) **123**, 445-463.
6. K. Honda and Z. Nishiyama: On the Nature of the Tetragonal and Cubic Martensite. *Sci. Repts., Tohoku Imp. Univ.* (1932) **21**, 299-331.
7. S. Epstein: The Alloys of Iron and Carbon, **1**, 210-220. New York, 1936. McGraw-Hill Book Co.
8. D. Antia, S. Fletcher, and M. Cohen: Structural Changes during the Tempering of High Carbon Steel. *Trans. Amer. Soc. Metals* (1944) **32**, 290-332.
9. A. B. Greninger and A. R. Troiano: Kinetics of the Austenite-Martensite Transformation in Steel. *Trans. Amer. Soc. Metals* (1940) **28**, 537-574.
10. J. V. Russell and F. T. McGuire: A Metallographic Study of the Decomposition of Austenite in Manganese Steels. *Trans. Amer. Soc. Metals* (1944) **33**, 103-125.
11. H. Chiswick and A. B. Greninger: Influence of Nickel, Molybdenum, Cobalt and Silicon on the Kinetics and Ar'' Temperatures of the Austenite to Martensite Transformation in Steels. *Trans. Amer. Soc. Metals* (1944) **32**, 483-520.
12. E. P. Klier and A. R. Troiano: Discussion to reference 11.
13. P. Payson and C. H. Savage: Martensite Reactions in Alloy Steels. *Trans. Amer. Soc. Metals* (1944) **33**, 261-280.
14. V. Zyuzin, V. Sadovski and S. Baranchuk: Influence of Alloy Elements on Position of Martensite Point, Quantity of Retained Austenite, and Stability of Retained Austenite during Tempering. *Metallurg* (1939) **14**, 75-80.
15. F. Wever and K. Mathieu: Ueber die Umwandlungen der Manganstähle. *Mitt. K-W-I. Eisenforschung* (1940) **22**, 9-20.
16. A. Rose and W. Fischer: Einfluss der Abkühlungsgeschwindigkeit auf die Umwandlungen und die Eigenschaften der Chromstähle. *Mitt. K-W-I. Eisenforschung* (1939) **21**, 133-149.
17. W. Tofaute, A. Sponheuer, and H. Bennek: Unwandlungs-, Hartungs- und Anlassvorgänge in Stählen mit Gehalten bis 1% C und bis 12% Cr. *Archiv Eisenhüttenwesen* (1934-1935) **8**, 499-506.
18. W. Tofaute, C. Küttner, and A. Büttinghaus: Das System Eisen-Chrom-Chromkarbid Cr₇C₃-Zementit. *Archiv Eisenhüttenwesen* (1936) **9**, 606-616.
19. A. B. Greninger: The Martensite Thermal Arrest in Iron-Carbon Alloys and Plain Carbon Steels. *Trans. Amer. Soc. Metals* (1942) **30**, 1-26.
20. J. Whitely: Observations on Martensite and Troostite. *Jnl. Iron and Steel Inst.* (1925) **3**, 315-349.
21. A. R. Troiano: Discussion to reference 22.
22. P. Gordon and M. Cohen: The Transformation of Retained Austenite in High Speed Steel at Subatmospheric Temperatures. *Trans. Amer. Soc. Metals* (1942) **30**, 569-591.
23. S. G. Fletcher and M. Cohen: The Dimensional Stability of Steel. Part I—Subatmospheric Transformation of Retained Austenite. *Amer. Soc. Metals Preprint* 27 (1944).

DISCUSSION

C. ZENER.*—The linear variation of Ar'' with chromium content found by Klier and Troiano has a very interesting theoretical significance. The anomalous shape of the gamma loop in the iron-chromium system implies that the activity of chromium is not a linear function of its concentration for temperatures above 800°C. Upon combining the results in this paper with the thermodynamical interpretation of the Ar'' temperature recently presented by the author, one concludes that the activity of chromium in the alpha and gamma phases of iron is a linear function of its concentration at least below 400°C. The observed slope of Ar'' vs. concentration curves gives 1500 cal. as the heat that would be absorbed in the transfer of one mol of chromium from the gamma to the alpha phase.

* Principal Physicist, Watertown Arsenal, Watertown, Mass. (On leave, Professor of Physics, Washington State College.)

Transformation of Austenite in a Steel Containing 3 Per Cent Chromium and 1 Per Cent Carbon

By E. P. Klier,* JUNIOR MEMBER A.I.M.E.

(Cleveland Meeting, October 1944)

THE work of Klier and Lyman¹ on the bainite reaction has led to the full description of this reaction for medium-carbon low-alloy steels. Certain experimental data reported by Klier and Lyman appear, however, to be improbable of obtaining in very high-carbon steels.

The study herein reported consists of an analysis of the transformation characteristics of a 3 per cent chromium, 1 per cent carbon steel by means of X-ray and metallographic methods. From the results obtained it is concluded that the bainite reaction in this steel is more complicated than that reported by Klier and Lyman for the low-carbon low-alloy steels. However, the mechanism of bainite formation in this steel appears to be essentially the same as proposed for the low-carbon low-alloy steels with the modification that the first volumes to transform are carbon-rich rather than carbon-poor.

EXPERIMENTAL PROCEDURE

The analysis of the steel studied was: Cr, 2.89; C, 1.02; Mn, 0.33; Si, 0.35; S, 0.012; P, 0.020. The stock was received from the Carpenter Steel Co. in rolled bars.

Specimen Preparation

Specimens were austenitized at 1200°C. (2192°F.) for 25 min. in purified nitrogen.

Manuscript received at the office of the Institute Aug. 8, 1944. Issued as T. P. 1855 in METALS TECHNOLOGY, September 1945.

* Instructor in Metallurgy, The Pennsylvania State College, State College, Pennsylvania.

¹References are at the end of the paper.

The resultant A.S.T.M. austenite grain size was 0-1. Isothermal transformation was allowed by quenching the specimens into liquid metal baths controlled to $\pm 5^\circ\text{C.}$ at 540°C. (1004°F.) and above, and to $\pm 2^\circ\text{C.}$ at 490°C. (914°F.) and below. Following the desired degree of transformation all specimens were water quenched.

Metallographic Examination

Specimens $\frac{1}{4}$ in. round by $\frac{1}{4}$ in. were used for metallographic examination. Etchants used were Vilella's reagent (1 gram picric acid, 10 ml. hydrochloric acid to make 100 ml. ethyl alcohol solution) and alkaline sodium picrate (electrolytic).

Vilella's reagent was effective in revealing all microconstituents, while the alkaline sodium picrate developed the carbon-rich structures or carbides only.

X-ray Examination

Two X-ray techniques were used—the Debye-Scherrer method and a back-reflection method. The small specimens necessary for the Debye-Scherrer method were austenitized and then allowed to transform, or were cut from the larger metallographic specimens. The metallographic specimens were used for the back-reflection X-ray analysis.

When it was desirable to determine the structure of the carbide present, sliver specimens were electrolytically etched to develop a carbide coating, then were exposed in the cameras. This technique was frequently necessary to allow positive identification of the carbide.

Chromium-K filtered radiation was used for exposures by the Debye method; iron-K unfiltered radiation was used for the back-reflection exposures.

EXPERIMENTAL RESULTS*

Metallographic

The results of the metallographic study are in part summarized in the conventional isothermal transformation diagram presented in Fig. 1. At temperatures above 490°C. (914°F.) the lines may be considered as representing within very close limits the exact beginning or end, as the case may be, of transformation. Below this temperature the curve for start of transformation is reasonably well determined, but the curve for end of transformation may be subject to relatively large error, as the decomposition of austenite in this range was not carried to more than 95 per cent completion.

Ar'' for this steel as determined by the quench-temper procedure² was 110°C.

At all temperatures above 690°C. (1274°F.) proeutectoid carbide was precipitated, while at 640°C. (1184°F.) conclusive

evidence for such carbide precipitation was not obtained.

At 690°C. and higher, lamellar structures were formed subsequent to formation

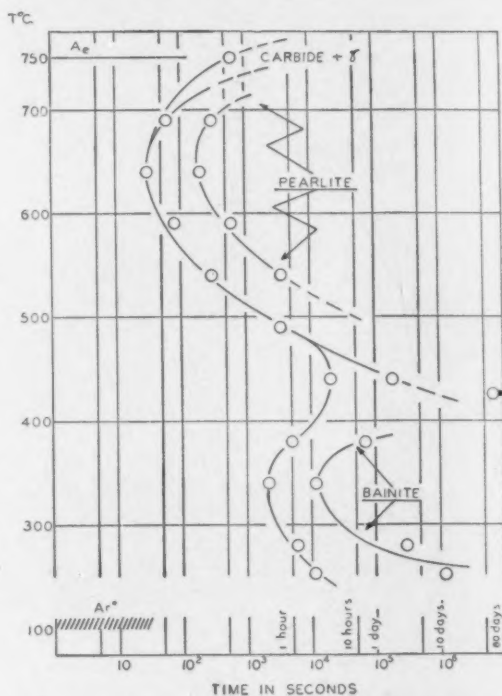


FIG. 1.—ISOTHERMAL TRANSFORMATION DIAGRAM FOR A 3 PER CENT CHROMIUM, 1 PER CENT CARBON STEEL.

* To facilitate discussion of the material to be presented, it has been convenient to use certain nomenclature in somewhat different sense than is commonly accepted. This has largely been necessitated by the results of Klier and Lyman¹ which have shown that the reaction that yields the lamellar pearlite above the "nose" of the S-curve does not produce the bainite structures below this point, but rather yields a massive dark-etching structure, which forms concurrently with or subsequent to bainite formation in an S.A.E. 1037 steel.

Alloy additions normally tend to separate the temperature ranges in which pearlite and bainite form (true also for nickel and manganese additions,³⁻⁵) primarily by lowering the range in which bainite forms. The obvious consequence of this is that the transformation diagrams for such steels exhibit an upper and lower nose, or two temperatures of high reaction rate excluding consideration of the martensite reaction.

Under the conditions outlined above it is no longer proper to call bainite those structures developed on the lower part of the upper nose of the S-curve. In this discussion these structures will be called pearlite, because of their possible generic relatedness to the lamellar structures formed at higher temperatures.

of carbide. At 725°C. (1337°F.) the structure developed was fine pearlite. At 690°C. the structure developed was nodular, but was resolved by an objective of N.A. 1.30 and found definitely to be constituted of lamellar components.

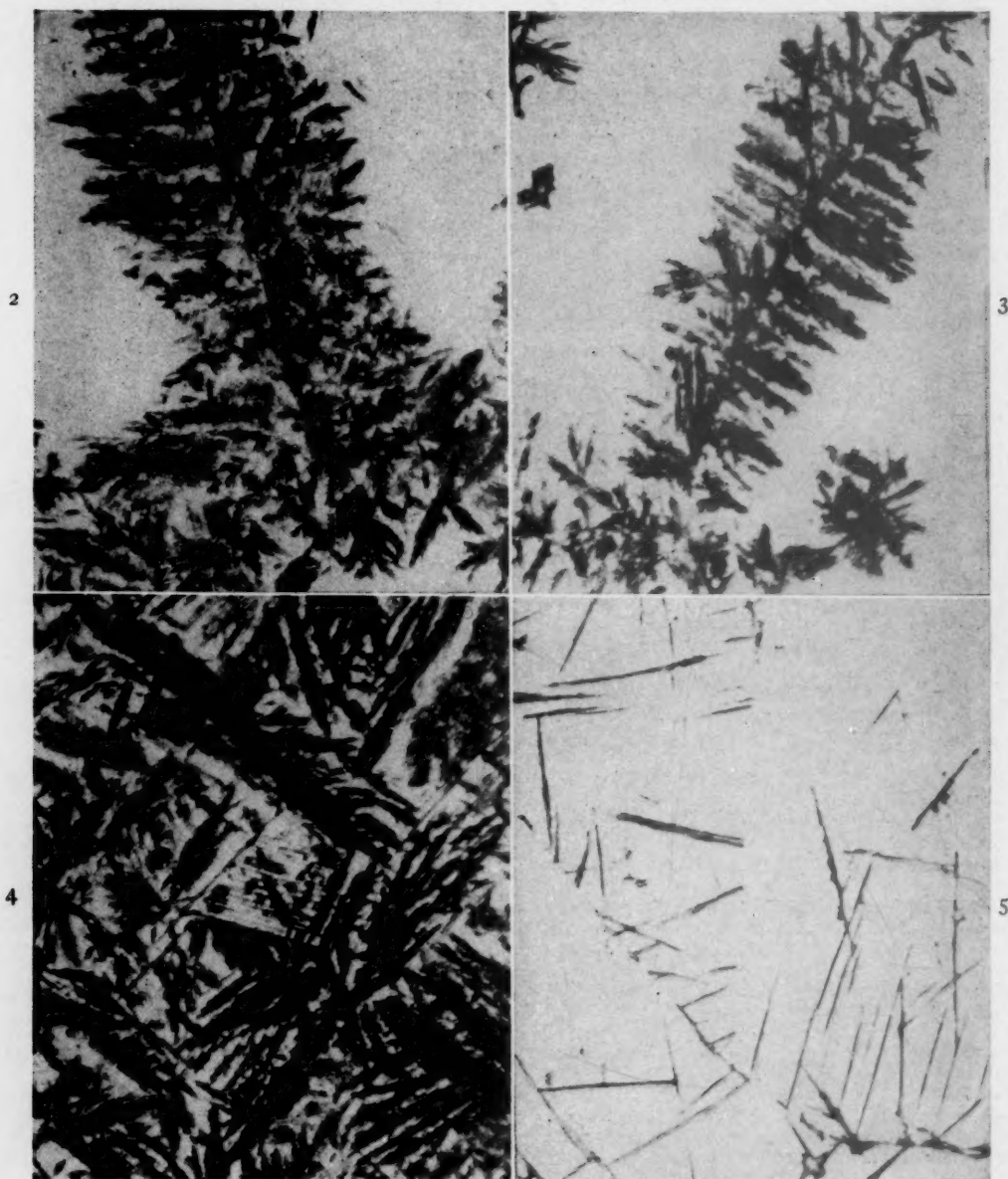
Nodular structures were developed by transformation at all temperatures from 690°C. (1274°F.) to 490°C. (914°F.). Further, as might be expected, austenite grain boundaries played an important role in the initiation of this transformation (Figs. 2 and 3).

The structures under discussion were not resolved; i.e., they appeared black even when examined under an objective of N.A. 1.30. It is necessary to conclude, therefore, that these structures are finely divided, which necessitates that they be

formed either of minute particles of a carbon supersaturated product—analogueous to the precipitates in age-hardening sys-

decomposes. However, there appears to be no evidence to support this latter view.

At temperatures 640°C. (1184°F.)



FIGS. 2-4.—STEEL CONTAINING 3 PER CENT CHROMIUM AND 1 PER CENT CARBON.

Fig. 2. Transformed at 540°C. for 16 minutes.

Fig. 3. Transformed at 490°C. for 65 minutes.

Fig. 4. Transformed at 490°C. for 4 hours.

Fig. 5. Transformed at 440°C. for 9½ hours.

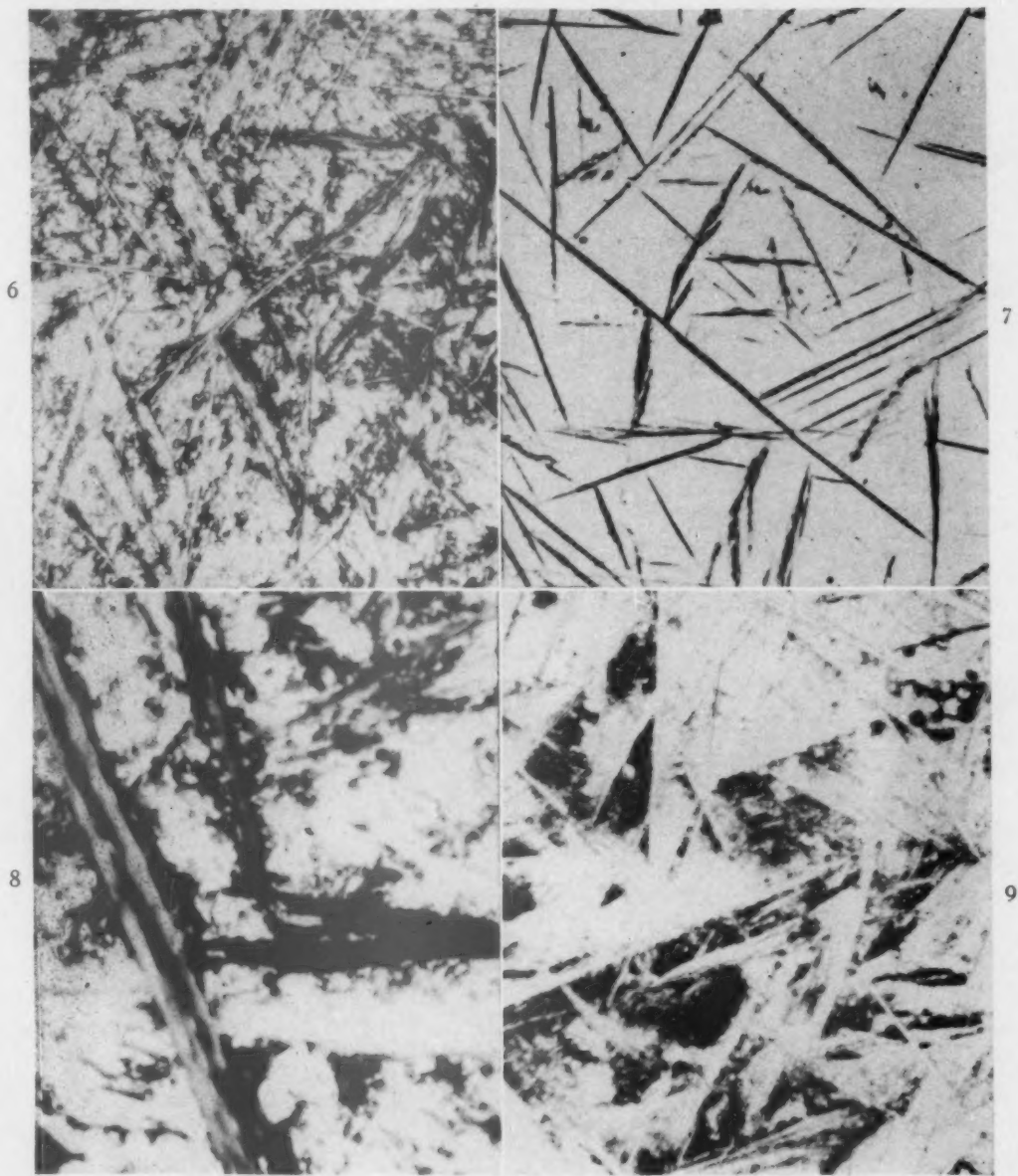
All × 500. Etch, Vilella's reagent.

tems—or of small particles of ferrite and carbide. It may be argued that precipitation takes place by the formation of a supersaturated structure, which in turn

through 540°C. (1004°F.) the pearlite reaction accounted for complete decomposition of the austenite. At 490°C. (914°F.) however, a new reaction product was

observed, forming during the course of the pearlite reaction. This is clearly brought out from a consideration of Figs. 3 and 4.

At 440°C. (824°F.) the first precipitate structure to appear is acicular and obviously is related to the acicular structure



FIGS. 6-9.—STEEL CONTAINING 3 PER CENT CHROMIUM AND 1 PER CENT CARBON, TRANSFORMED AT 440°C. FOR 16 $\frac{2}{3}$ HOURS.

Fig. 6. $\times 500$. Etch, Vilella's reagent.

Fig. 7. $\times 500$. Etch, sodium picrate.

Fig. 8. $\times 2500$. Etch, Vilella's reagent.

Fig. 9. $\times 500$. Etch, Vilella's reagent.

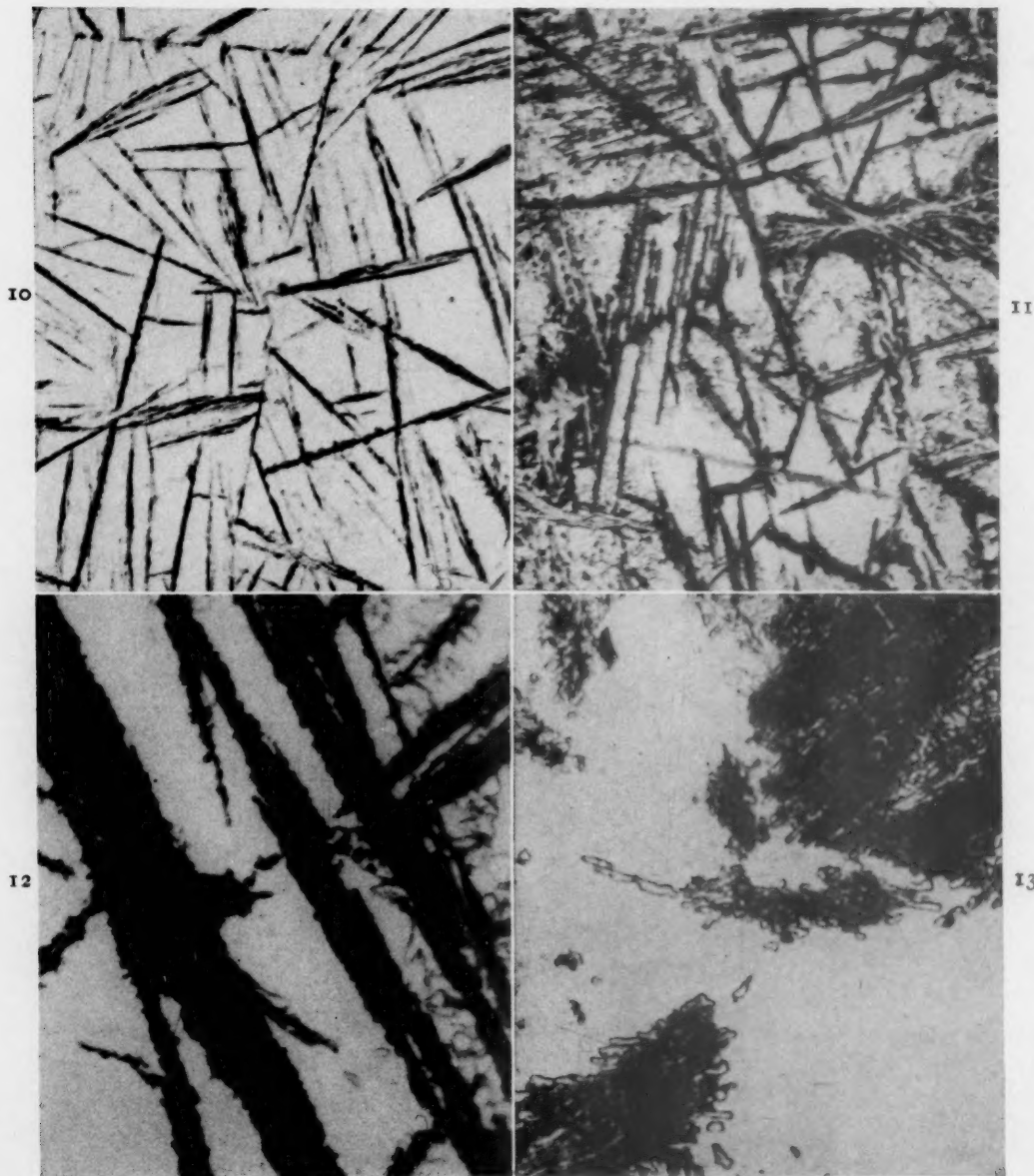
The acicular product is considered as the new reaction product. It is of interest that the total volume of this acicular product is quite small.

observed at 490°C. (914°F.). After 9 hr. at temperature, transformation has progressed to the extent indicated in Fig. 5. On transforming for 16 hr. and 20 min. the

acicular product has increased in quantity while a second massive structure is now present (Fig. 6). Etching in alkaline

carbon-rich and the massive structure carbon-poor.

An examination under an objective of



FIGS. 10-13.—STEEL CONTAINING 3 PER CENT CHROMIUM AND 1 PER CENT CARBON.

Fig. 10. Transformed at 440°C. for 120 hours. $\times 500$. Etch, sodium picrate.

Fig. 11. Transformed at 425°C. for 82 days. $\times 500$. Etch, Vilella's reagent.

Fig. 12. Transformed at 425°C. for 82 days. $\times 2500$. Etch, Vilella's reagent.

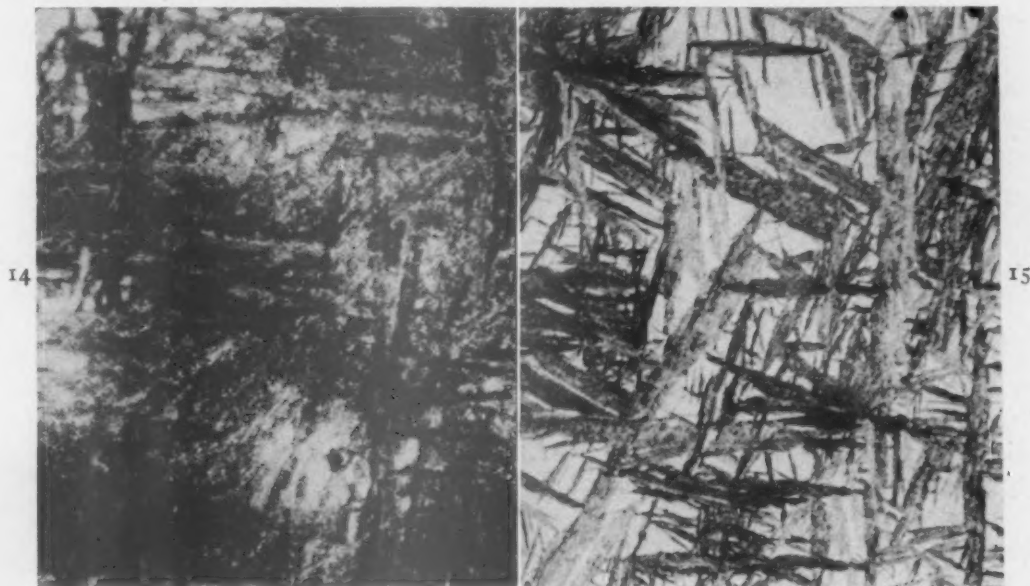
Fig. 13. Transformed at 390°C. for 4 hours. $\times 2000$. Etch, Vilella's reagent.

sodium picrate stains the acicular structure but does not affect the massive structure (Fig. 7). Tentatively, then, it may be stated that the acicular structure is

N.A. 1.30 of the structures developed in the 16-hr. 20-min. specimen by etching in Vilella's reagent and in alkaline sodium picrate revealed certain discrepancies in

the width of the precipitate carbide structure. The specimen, therefore, was heavily etched in Vilella's reagent and photographed, with the results indicated in Fig.

the amount of pearlite is very small even after 82 days at temperature. Fig. 11 shows the relative amounts of the transformation products after 82 days at 425°C. More



FIGS. 14 AND 15.—STEEL CONTAINING 3 PER CENT CHROMIUM AND 1 PER CENT CARBON.

Fig. 14. Transformed at 340°C. for 3 hours. $\times 500$. Etch, Vilella's reagent.

Fig. 15. Transformed at 275°C. for 4 hours. $\times 500$. Etch, Vilella's reagent.

8. It is quite evident that the indicated precipitate structure consists of a core, which is not attacked by the etchant to the same degree as is the area immediately surrounding it. This is fair evidence that the zone immediately surrounding the carbide is depleted in carbon.

Transformation at 440°C. (824°F.) for 120 hr. causes further precipitation of the carbon-rich and carbon-poor structures, while it is revealed that the pearlite reaction has progressed to a considerable extent (Fig. 9). The increase with time at temperature in amount of the acicular product is evident from a comparison of Figs. 5, 7, and 10. Further, the increase in amount of the acicular product on lowering transformation temperature is shown by comparing Figs. 4 and 10.

Transformation at 425°C. (797°F.) takes place in a manner similar to that at 440°C. (824°F.). At this temperature, however,

detailed examination of the microconstituents is allowed in Fig. 12. At least four microconstituents are clearly distinguishable. The acicular structure appears to be fibrated, but it must be remembered that this structure has been subjected to an extreme tempering process, which also can account for this feature. The pearlite structure is not resolved and again presents the aspect of being finely divided. The massive white structure appears to be ferrite. Of considerable interest is the matrix structure. The etchant, while evidently corroding away an appreciable amount of this structure, has not revealed any evidence of martensite. Further, from a consideration of the obvious growth of the other constituents in this matrix, it is considered as possibly austenite. On tempering this specimen at 700°C. (1292°F.) for three min. the matrix was completely decomposed. The resultant microstructure

did not appear to contain tempered martensite.

The changes in microstructure produced by lowering the temperature of transformation is revealed in an examination of Figs. 13, 14 and 15.

The reaction products, while remaining massive, pass through a pseudonodular form at about 340°C. (644°F.). At lower temperatures the structure is definitely acicular, in large measure resembling the martensite structure developed in this steel by quenching to room temperature.

X-ray Analysis

Isothermal transformation of this steel at 440°C. (824°F.) resulted in the formation of a carbide-like precipitate. Assuming this precipitate to consist of a uniform crystal structure, it should be amenable to analysis by X-ray diffraction methods. Thus it should be possible to identify the precipitate as Fe_3C , or possibly some different carbide that could develop in this steel.

TABLE 1.—Carbide Structures Developed on Isothermal Transformation of Steel 3 Per Cent Chromium, 1 Per Cent Carbon at 440°C.

Transformation Time, Hr.	Specimen Preparation	Structure
5.0	Etched in HCl	No carbide
7.25	Electrolytic etch	No carbide
9.75	Electrolytic etch	Fe_3C (?)
17.75	Etched in HCl	Fe_3C (?)
27.5	Etched in HCl	Fe_3C
32.	Etched in HCl	Fe_3C

In Table 1 are presented the results of X-ray analysis employing in indicated instances the special electrolytic etching process to develop the carbide structure.

It is to be noted that even after 17.75 hr. at 440°C. (824°F.) the X-ray pattern does not show positively the Fe_3C crystal structure. The identifications marked as questionable are based on the observation of several faint lines at angles of reflection

at which are found strong Fe_3C lines when this structure is present.

When an electrolytic etch was used, conditions were optimum for the development of the carbide pattern. The etching treatment virtually eliminated the ferrite lines normally obtained and only faint traces of the $(110)_\alpha$ were observed.

The residue left on the specimen after etching was not graphite, as was plainly evident in handling it. It is concluded, therefore, that this constituent is a poorly formed carbide, which, being unstable, decomposes to form Fe_3C on continued holding at 440°C.

The results of a cursory examination of carbide structures formed at various temperatures are presented in Table 2.

TABLE 2.—Carbide Structures Developed on Isothermal Transformation of Steel 3 Per Cent Chromium, 1 Per Cent Carbon at Various Temperatures

Transformation		Structure
Temperature, Deg. C.	Time	
750	22.5 hr.	$\text{Fe}_3\text{C} + \text{Cr}_7\text{C}_3$
715	.5 hr.	Fe_3C
490	4.25 hr.	Fe_3C
270	25 days	Fe_3C

The carbide normally observed as a consequence of isothermal transformation has the crystal structure of cementite. The specimen transformed at 270°C. (518°F.) yielded a pattern that, while quite complete, consisted of diffuse broad lines. This is considered as indicating a very fine particle size existing for the precipitated Fe_3C .

The tetragonal martensite formed from the decomposing austenite on cooling to room temperature varied in carbon content with the time at 440°C. (824°F.). The results for measurements of the tetragonality of these martensites are presented in Table 3 and are plotted in Fig. 16.

The tetragonality of the martensite formed remained virtually constant until after holding at 440°C. (824°F.) for nearly 10 hr. After 10 hr. at 440°C. the tetrag-

onality of the martensite was definitely reduced. This reduction of carbon in the transforming austenite continued for 30 hr., after which time an axial ratio of 1.025 was obtained, corresponding to a carbon content of about 0.55 to 0.65 per cent. After 42.5 hr. at temperature, the axial ratio obtained was still 1.025, while holding for 53.25 hr. resulted in such weak lines that accurate measurements were not possible.

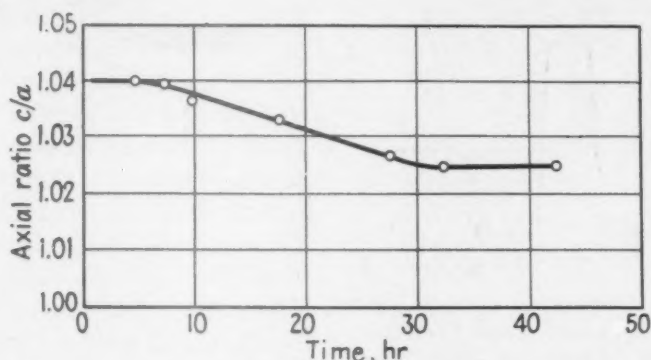


FIG. 16.—AXIAL RATIO OF MARTENSITE FORMED IN A 3 PER CENT CHROMIUM, 1 PER CENT CARBON STEEL SUBSEQUENT TO TRANSFORMATION AT 440°C. FOR VARIOUS TIMES.

onality of the martensite was definitely reduced. This reduction of carbon in the transforming austenite continued for 30 hr., after which time an axial ratio of 1.025 was obtained, corresponding to a carbon content of about 0.55 to 0.65 per cent. After 42.5 hr. at temperature, the axial ratio obtained was still 1.025, while holding for 53.25 hr. resulted in such weak lines that accurate measurements were not possible.

TABLE 3.—Axial Ratio (c/a) of Martensite Formed on Cooling to Room Temperature after Partial Transformation of Steel 3 Per Cent Chromium, 1 Per Cent Carbon at 440°C.

MEASUREMENT ON (200) DOUBLET			
TIME, HR.	c/a	TIME, HR.	c/a
0	1.040	17.75	1.035
5	1.038	27.5	1.027
7.25	1.038	32	1.025
9.75	1.038	42.5	1.025

An attempt was made to follow the lattice-parameter changes taking place in the transforming austenite. Back-reflection patterns using a Sachs-type camera with rotating specimen were obtained. This approach was of little value, as good austenite lines could not be obtained con-

sistently. Thus a specimen transformed at 440°C. (824°F.) for 16 hr. and 20 min. did not yield a good pattern. The lines were inconsistently broad and diffuse.

Better lines for measurement could be obtained from the specimen transformed for 42.5 hours. In an attempt to solve this ambiguity, a back-reflection Laue pattern of this specimen was obtained. For the camera setup used, and with iron radiation, the reflection circle for the $(311)_\gamma$ had a diameter of about 13 cm. This reflection circle, however, consisted of two circles for the case under consideration. One circle was roughly 0.5 cm. less in diameter. (This is not to be confused with a resolution of the K_α doublet, which for the conditions here did not occur.) This indicates that an austenite of somewhat less carbon content than the matrix austenite was present.

Considering the difficulties to be surmounted, precision lattice measurements could not be carried out. Qualitatively, though, it may be stated that austenite lattice adjustments took place in keeping with the results reported for the martensite axial ratio.

Concerning back-reflection studies carried out for transformation at 340°C. (644°F.) and 270°C. (518°F.) the following may be said:

1. Measurable displacement of the austenite lines did not occur at either

temperature throughout the course of transformation.

2. The intensity of the austenite lines reached a maximum for both tempera-

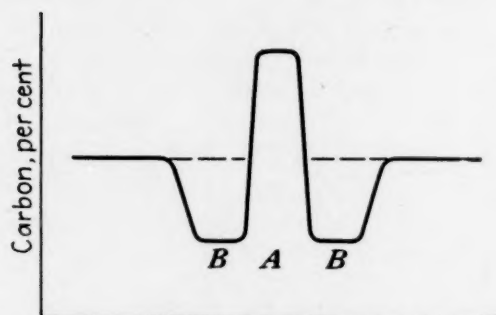


FIG. 17.—CARBON CONCENTRATION GRADIENT THROUGH CARBIDE STRUCTURE FORMED ISOTHERMALLY AT 440°C.

tures after partial decomposition at constant temperature. The austenite lines were sharper in the latter instances.

DISCUSSION OF RESULTS

The description of the bainite reaction in low-alloy hypoeutectoid steels as presented by Klier and Lyman¹ does not fully account for the data presented in the foregoing pages. It must be assumed then that this is a more general type of bainite reaction than that reported earlier.

Klier and Lyman report that for the type of steels they studied bainite formation takes place by the initial setting up of austenites of high and low carbon concentrations. Following this the austenite of low carbon concentration transforms to bainite (Klier⁶). This is exactly contrary to the observations obtained on this steel.

For this 3 per cent Cr, 1 per cent C steel, the carbon content of the austenite is altered so that a carbide may be precipitated. The manner in which this takes place leaves the carbide enclosed in a carbon-depleted shell; thus the carbon contained in the carbide is obtained from the austenite immediately surrounding. In terms of carbon-concentration gradients, a section through this precipitate structure

would conform to the idealized case in Fig. 17. *A* is the center of the precipitate particle while *B-B* is the carbon-depleted zone immediately surrounding it. A very similar instance has been reported by Greninger and Troiano⁷ for work carried out on a plain high-carbon steel.

The failure to determine the crystal structure of this carbide must be owing to its nonuniform structure. Thus the lattice parameter from the center of the structure to its boundaries varies continuously and as a consequence does not meet the optimum requirements for a diffraction grating for X-rays. However, by the use of special X-ray techniques, it may be possible to obtain more information concerning this structure.

In addition to the carbon-rich structure considered above, transformation may take place with the formation of a carbon-poor structure, apparently as in the hypoeutectoid low-alloy steels.

When the temperature of transformation is lowered, the microstructural changes indicate a gradual merging of the two precipitate structures. This merging of the two reaction products would consist in their continuous approach to the composition of the matrix. Thus at some temperature transformation evidently takes place without macroscopic carbon diffusion. This seems to be borne out metallographically but the X-ray analysis yielded no positive data on this point.

For this steel, then, bainite formation is considered as taking place as follows:

1. Owing to carbon adjustments in the transforming austenite, regions of carbon enrichment and depletion are set up.
2. Both the carbon-rich and carbon-poor zones may then transform to bainite, which thus may be either an unstable carbide-carbon dilute Fe_3C (?) or a supersaturated ferrite.
3. The completion of the reaction is temperature dependent—as the temperature is lowered, more bainite is formed,

until a temperature is reached at which all austenite transforms to bainite.

4. At the temperature indicated in conclusion 3, there may be no macroscopic diffusion effect such as is observed on transforming at higher temperatures. It appears, however, that the two phenomena need not be associated except by chance.

REFERENCES

1. E. P. Klier and T. Lyman: The Bainite Reaction in Hypoeutectoid Steels. *Trans. A.I.M.E.* (1944) **158**, 394.
2. A. B. Greninger and A. R. Troiano: Kinetics of the Austenite to Martensite Transformation in Steel. *Trans. Amer. Soc. Metals* (1940) **28**, 537.
3. J. V. Russell and F. T. McGuire: A Metallographic Study of the Decomposition of Austenite in Manganese Steels. *Trans. Amer. Soc. Metals* (1944) **33**, 103.
4. F. Wever and K. Mathieu: Ueber die Umwandlungen der Manganstähle. *Mill. K.W.I. Eisenforsch.* (1940) **22**, 9.
5. H. Lange and K. Mathieu: Ueber den Ablauf der Austenitumwandlung im unterkühlten Zustand bei Eisen-Nickel-Kohlenstoff-Legierungen. *Mill. K.W.I. Eisenforsch.* (1938) **20**, 125.
6. E. P. Klier: Discussion of Amer. Soc. Metals Preprint No. 19, by J. R. Ham, Oct. 1944.
7. A. B. Greninger and A. R. Troiano: Crystallography of Austenite Decomposition. *Trans. A.I.M.E.* (1940) **140**, 307.

Isothermal Transformation of Austenite in One Per Cent Carbon, High-chromium Steels

By TAYLOR LYMAN,* JUNIOR MEMBER, AND ALEXANDER R. TROIANO,† MEMBER A.I.M.E.

(New York Meeting, February 1945‡)

STUDIES of the transformation of austenite at constant subcritical temperatures have been numerous since the work of Davenport and Bain.¹ Considerable information has been obtained on low-alloy steels and on high-carbon alloys containing undissolved carbide or graphite at the austenitizing temperature. Little is known of the isothermal transformation of austenite containing in solution large amounts of both carbon and a single alloying element.

In this investigation four steels containing one per cent carbon and with chromium in the range 3 to 9 per cent have been examined with the view to establishing the fundamental character of the isothermal reactions when all carbon and chromium are initially in solution in austenite.

EXPERIMENTAL PROCEDURE

Alloys

The chemical compositions of the steels investigated are given in Table 1. The 4 per cent Cr alloy is a commercial steel. The other steels were made by the Carpenter Steel Co. as 50-lb., induction-furnace heats and rolled to 5/8-in. round bars. Bars were softened at 650° to 700°C. before the specimens were cut.

Manuscript received at the office of the Institute Dec. 1, 1944. Issued as T.P. 1801 in METALS TECHNOLOGY, September 1945.

* Instructor in Metallurgy, University of Notre Dame, Notre Dame, Indiana.

† Associate Professor of Metallurgy, University of Notre Dame.

‡ Meeting canceled.

¹ References are at the end of the paper.

TABLE 1.—*Compositions of Steels Investigated*

Steel	Composition, Per Cent					
	C	Cr	Mn	Si	P	S
3 % Cr	1.02	2.9	0.33	0.35	0.020	0.012
4 % Cr	1.04	4.0	0.18	0.35	<0.01	<0.01
6 % Cr	1.05	5.7	0.31	0.35	0.017	0.012
9 % Cr	1.02	8.8	0.33	0.35	0.016	0.011

Metallographic Method

Most of the lines on the transformation diagrams presented here have been placed on the basis of the microscopic examination of partially reacted specimens. The specimens were approximately 1/2 by 1/4 by 1/8 in. in size. Specimens of the 9 per cent Cr steel were held 10 to 12 hr. at 1200° to 1225°C. before quenching to the various subcritical temperatures. The other steels were held for 2 to 2 1/2 hr. at 1200°C. before quenching. These treatments, carried out in an atmosphere of purified nitrogen, produced an austenite grain size larger than A.S.T.M. No. 1, some grains being 1 to 2 mm. in diameter. There were a few undissolved carbide particles in some specimens of the 9 per cent Cr steel. It is believed, however, that any errors in the results due to incomplete solution of carbon and chromium in austenite are negligible; that is, austenite compositions may be considered as being those listed in Table 1.

X-ray Methods

Constituents were identified and martensite axial ratios determined from Debye

patterns obtained using the K-alpha radiations from chromium or cobalt. X-ray specimens were about $\frac{1}{16}$ by $\frac{1}{16}$ by $\frac{1}{2}$ in. in size. These specimens were first sealed in evacuated quartz tubes, given the same austenitizing treatments as the metallographic specimens and water-quenched. The large grain size produced by these austenitizing treatments, while facilitating microscopic examination, was undesirable in the X-ray specimens. In order that a large number of austenite grains should contribute to the diffraction effects, X-ray specimens were tempered for 1 to 2 min. at 300°C. (specimens of the 9 per cent Cr steel were first cooled in liquid air to form martensite) after the regular solution treatment. Individual specimens were then attached to iron wires, reaustenitized for 2 to 3 min. at 1200°C. and quenched to the various subcritical temperatures for isothermal transformation. All X-ray specimens were examined microscopically before being carefully ground on emery paper, etched and placed in the cameras.* When it was desired to check the presence or absence of carbides, X-ray specimens were etched electrolytically in a 5 per cent aqueous solution of hydrochloric acid.

Dilatometric Method

The progress of isothermal transformation was followed dilatometrically in three of the steels in the temperature region 270° to 380°C. The dilatometer employed was a modification of the type used by Davenport and Bain. Dilatometer specimens were $\frac{1}{16}$ in. thick and 1 in. long. These specimens were bound together in batches of 10, placed in a small crucible of the 4 per cent Cr steel, austenitized for

2 hr. at 1200°C. in purified nitrogen and oil-quenched. Individual specimens that had been given this treatment were then reaustenitized for 3 to 5 min. at 1200°C. and transferred from austenitizing furnace to dilatometer by means of attached wires.

GRAPHICAL PRESENTATION OF RESULTS

In most cases the beginning of a transformation, at a given temperature, has been placed between a specimen observed microscopically to contain no decomposition product (or only a few scattered traces) and one containing the first uniformly distributed amounts. Two points—corresponding to such pairs—have been plotted on the diagrams. The end of transformation (complete disappearance of austenite) has likewise been bracketed between two specimens.

At temperatures below 380°C. where the "intermediate reaction" products appear, dilatometric data have been represented by drawing a horizontal line at the temperature of the run, the end points of the line corresponding to the times for 2 and 98 per cent of the expansion during the initial, rapid part of the reaction.

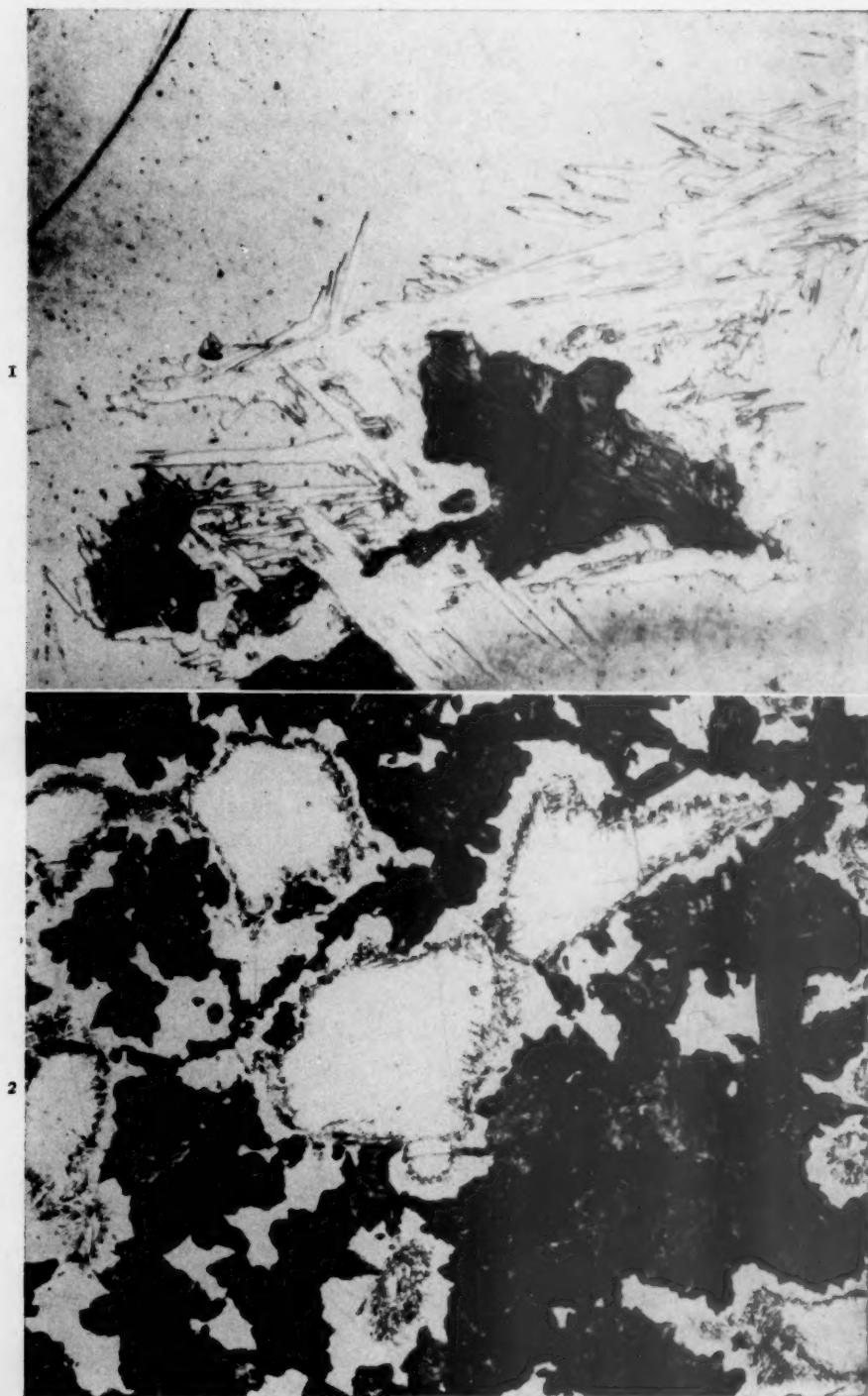
The lines marked A_{E_1} are the approximate lowest temperatures for the existence of austenite as a stable phase in the various steels. These temperatures were taken from the data of Tofaute, Sponheuer and Bennek.^{2,3} The $A_{r''}$ temperatures are from the data of Klier and Troiano.⁴

RESULTS

Steel with 9 Per Cent Chromium

A specimen of the steel with 9 per cent Cr water-quenched from 1200° to 25°C. contains no martensite needles. Subsequent cooling in liquid air leads to the formation of tetragonal martensite of axial ratio 1.043 (very closely the same as the martensite axial ratio of a 1.0 per cent carbon, plain carbon steel). This result may be accepted as proof that chromium has only

* As would be expected, the decomposition of austenite proceeded at a greater rate in these fine-grained X-ray specimens (when transformations started at grain boundaries) than in the coarse-grained metallographic specimens that were used as the basis for constructing the transformation diagrams. Qualitatively, the course of transformation was always the same, at a given temperature, in the two sets of specimens.



FIGS. 1 AND 2.—9 PER CENT CHROMIUM STEEL QUENCHED FROM 1200°C. TO 750°C. AND HELD FOR TIMES INDICATED.

Fig. 1. 2200 seconds. $\times 750$.

Fig. 2. 5000 seconds. $\times 75$.

Etched in Vilella's reagent.

a small or negligible effect upon the axial ratio of a 1 per cent carbon martensite, a conclusion in agreement with the results of Nishiyama.⁵

After about $\frac{1}{2}$ hr. at 750°C., lamellar pearlite begins to form in this steel. About one half of this first pearlite to appear can be resolved microscopically with an objective of numerical aperture 1.3. In addition to pearlite, martensite is present in the microstructures of specimens partially reacted at 750°C. and quenched to room temperature. It may be judged from Figs. 1 and 2 that as transformation proceeds the martensitic regions (in quenched specimens) extend to greater distances from the reaction interface. An X-ray specimen held for 1 hr. at 750°C. contained martensite of axial ratio 1.027 after quenching.

Specimens partially reacted at the knee of the S-curve and quenched to room temperature contain nodular pearlite surrounded by martensite (Fig. 3). This martensitic border is very narrow, regardless of the degree of advancement of the reaction at this temperature.

At 630°C. the reaction product is nodular and martensite is present as after transformation at the higher temperatures. With decreasing reaction temperature there is an increasing tendency for the matrix to be entirely martensitic (after quenching to room temperature) before the isothermal transformation has proceeded to completion.

Fig. 4 is illustrative of the decomposition progress after 10,000 sec. at 565°C. A specimen held for 15,000 sec. at this temperature shows a much smaller amount of austenite in the martensite-austenite residuum, although the degree of advancement of the reaction is not much greater than that shown in Fig. 4.

The axial ratios of martensite in partially reacted specimens are given in Table 2.

Since the axial ratio of martensite is a

function of the carbon content only, it is evident that the unreacted matrix becomes greatly impoverished in carbon during the course of transformation. The time interval

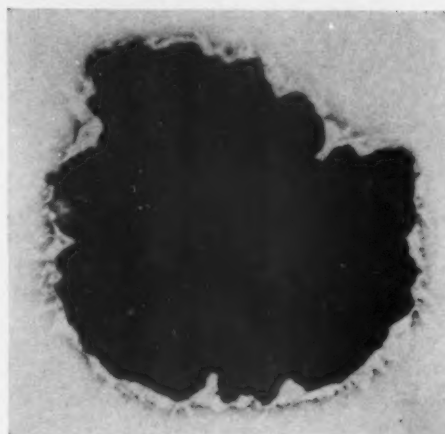


FIG. 3.—9 PER CENT CHROMIUM STEEL QUENCHED FROM 1200°C. TO 685°C. AND HELD FOR 350 SECONDS. $\times 1000$. ETCHED IN VILELLA'S REAGENT.

during which this carbon diffusion occurs is a relatively small part of the total time required for transformation. The micrograph of Fig. 5 shows that there is a large amount of austenite in a specimen

TABLE 2.—Axial Ratios of Martensite in 9 Per Cent Chromium Steel after Partial Transformation of Austenite^a

Temperature, Deg. C.	Time, Sec.	c/a
Quenched from 1200° to -192°C.....		1.043
750.....	3,600	1.027
515.....	50,000	1.032
515.....	70,000	1.027
515.....	100,000	1.019
475.....	700,000	1.027
475.....	1,000,000	1.025

^a See footnote on page 197.

quenched to room temperature after 10^6 sec. at 475°C. A specimen held for 1.5×10^6 sec. showed only slightly more isothermal decomposition product but the matrix was almost entirely martensitic. Decomposition was 80 to 90 per cent complete after 200 days at 475°C.

It is to be noted in Fig. 5 that well-formed martensite needles are present in the matrix, not only in immediate contact with the transformation product but also

about one month and a specimen held for 141 days showed less than 5 per cent of the dark-etching product. Specimens held for 200 days at 300°, 225°, and 165°C. con-

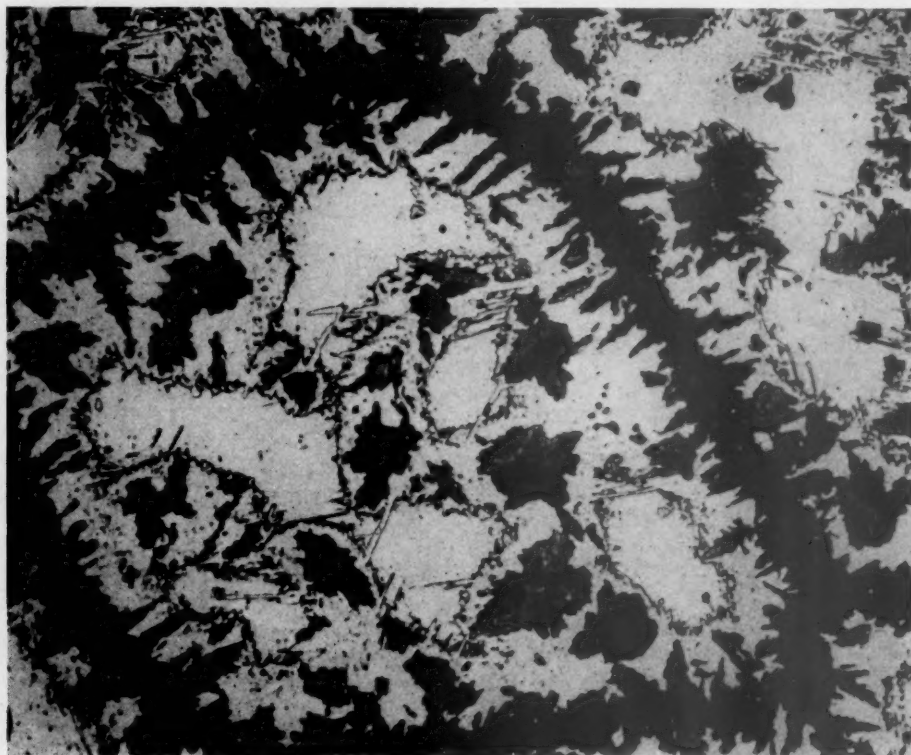


FIG. 4.—9 PER CENT CHROMIUM STEEL QUENCHED FROM 1200°C. TO 565°C. AND HELD FOR 10,000 SECONDS. $\times 300$. ETCHED IN VILELLA'S REAGENT.

in areas farthest from the product. This is in contrast with the appearance of the specimen treated at 565°C. (Fig. 4), which shows about the same degree of advancement of transformation but no martensite needles at maximum distance from the product. This difference suggests that there may be an "inverse-stabilization" process accompanying the concentration change at the lower temperature; that is, martensite may have formed "prematurely" on cooling from the reaction temperature, under the influence of some variable other than concentration change. In the absence of accurate knowledge of the concentration gradients in the matrix, this idea has only speculative interest.

At 415°C., transformation began after

tained no isothermal product and no martensite.

The transformation diagram for this steel has been drawn from the microscopic evidence and is shown in Fig. 6. After about half reaction at temperatures below the knee of the S-curve, the rate of transformation is considerably decreased. Some microstructural differences have been noted between the dark-etching transformation product formed during this later period and that formed earlier at the same temperature. These differences are probably imposed by the concentration change in the matrix austenite. The matrix has been shown to be low in carbon during the later part of the reaction; it may also be low in chromium.



FIG. 5.—9 PER CENT CHROMIUM STEEL QUENCHED FROM 1200°C. TO 475°C. AND HELD FOR 1,000,000 SECONDS. $\times 300$. ETCHED IN VILELLA'S REAGENT.

By way of summary of the structures produced by isothermal decomposition of austenite in this steel: The product of transformation changes in a gradual man-

formed at the higher temperatures is that of pearlite, the reaction might be designated as the pearlite reaction over the entire range. Such a designation is lacking

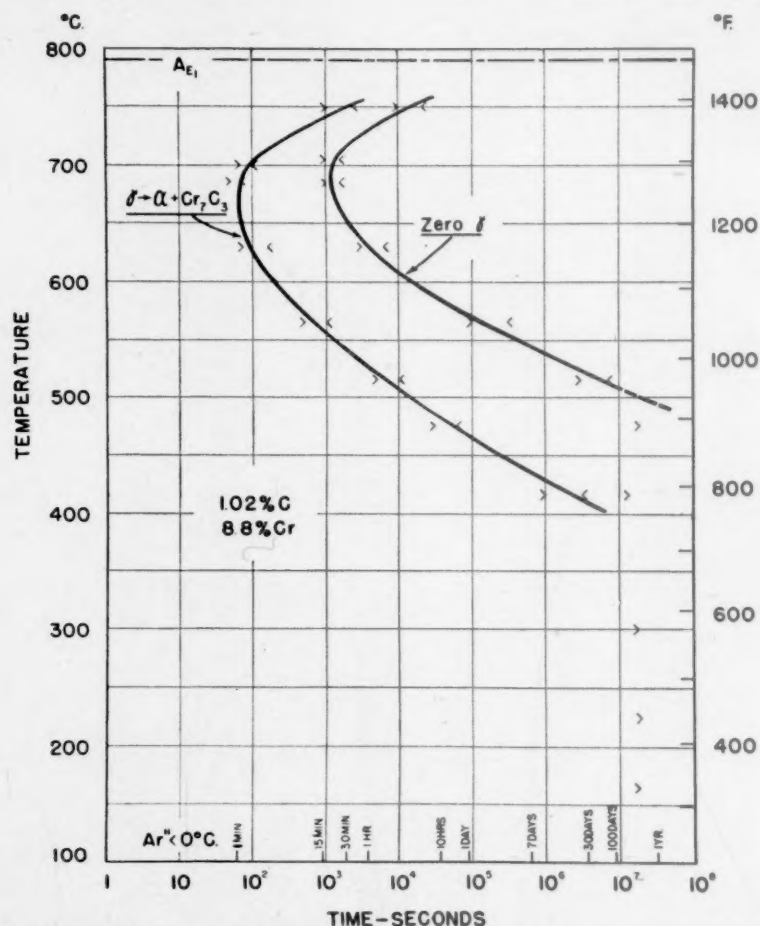


FIG. 6.—ISOTHERMAL TRANSFORMATION DIAGRAM FOR 9 PER CENT CHROMIUM STEEL.

ner with the temperature of formation, being always dark-etching and rather massive. There is qualitative similarity in the austenite-martensite relationships in the unreacted portions of partially transformed specimens quenched from all temperatures where decomposition was observed. The reaction, both above and below the temperature of maximum rate, decreases the carbon content of the matrix austenite. It is concluded, therefore, that the transformation of austenite at all of these temperatures is fundamentally the same. Since the appearance of the product

in specificity since it conveys nothing at all regarding the nature of the carbide phase or phases that form from austenite during the reaction.

In an effort to identify the crystal structure of the carbide formed during isothermal reaction in this steel, X-ray diffraction patterns were obtained from specimens reacted at various temperatures. In no case was there positive evidence of the presence of the orthorhombic carbide Fe_3C .^{*} Transformation times and tem-

* The orthorhombic and trigonal carbides will be designated Fe_3C and Cr_7C_3 , respec-

peratures where a carbide having the crystal structure of Cr_7C_3 could be identified are given in Table 3. Certain patterns obtained from specimens held for shorter

TABLE 3.—Transformation Times and Temperatures at Which Diffraction Patterns of Cr_7C_3 Were Obtained with the 9 Per Cent Chromium Steel

TEMPERATURE, DEG. C.	TIME, SEC.
750	2,200
750	35,000
685	3,000
650	85,000
515	700,000
515	18,000,000
475	3,000,000

times than those listed in Table 3 were not conclusive; carbide lines were too indistinct for identification of the crystal structure. The reaction has been designated as gamma-to-alpha-plus- Cr_7C_3 on the transformation diagram of Fig. 6.

Steel with 3 Per Cent Chromium

The data on the steel with 3 per cent Cr are an extension and, in some respects, a confirmation of previous work by E. P. Klier⁶ on the same alloy.

The proeutectoid carbide formed above 700°C. has the crystal structure of Fe_3C . This carbide reaction merges with the pearlite reaction at the knee of the S-curve. Nodular pearlite is formed at 630°C. At 565°C. the product has some resemblance to nodular pearlite but growth is not truly radial (Fig. 7). There is considerable similarity between this structure and the "arborescent, granular structure" observed by Jolivet⁷ at 550°C. in a steel containing 0.75 per cent C, 1 per cent Cr and 0.6 per cent Mo. There is no microscopic evidence of carbon diffusion accompanying this reaction in the manner observed in the 9 per cent Cr Steel. A series of X-ray specimens partially reacted at 565°C. showed that the axial ratio of the matrix martensite was constant at 1.044 (the same as the as-quenched value) as long as there

was enough of the tetragonal structure present for measurement.

At 515°C. carbide of platelike habit forms from austenite as well as the dark-etching structure (Fig. 8). The two reactions begin together and proceed simultaneously until all of the austenite has transformed.

At 450°C. carbide, identified as Fe_3C , appears before the dark-etching structure (Fig. 9). Considerably more of this plate carbide forms at 450°C. than at 515°C. As would be expected, the carbon content of austenite decreases as the amount of Fe_3C increases at 450°C. This relationship is derived from the data of Fig. 10, in which the martensite axial ratio is plotted as a function of time at 450°C. By the time the carbon content of the matrix has been reduced to about 0.6 per cent (as judged by the axial ratios) recognizable ferrite particles begin to appear in the microstructure, and the ferrite and carbide reactions proceed together. Correlating the X-ray data with the microstructures, it is seen that during this period of simultaneous formation of ferrite and carbide the axial ratio of martensite decreases at a much lower rate. This indicates that carbon impoverishment of the austenite due to the formation of Fe_3C is almost counterbalanced by carbon enrichment due to the ferrite precipitation. Martensite axial ratios were less accurately measurable after about 100,000 sec. at this temperature, the Debye lines being more diffuse than after shorter holding times. The microstructure obtained on holding for 1,000,000 sec. at 450°C. is shown in Fig. 11.

At 415°C. Fe_3C is again the first decomposition product to appear, followed by ferrite. The dark-etching product is considerably less prominent in microstructures obtained at this temperature than in those obtained at all higher temperatures. (Cf. Figs. 11 and 12, for example). Comparing Figs. 12 and 13, it can be seen that the three reactions proceed simultaneously,

tively, but it is understood that these formulas do not express the chemical compositions of the phases in ternary Fe-C-Cr alloys.



FIG. 7.—3 PER CENT CHROMIUM STEEL QUENCHED FROM 1200°C. TO 565°C. AND HELD FOR 500 SECONDS. $\times 500$. ETCHED IN VILELLA'S REAGENT.

FIG. 8.—3 PER CENT CHROMIUM STEEL QUENCHED FROM 1200°C. TO 515°C. AND HELD FOR 5000 SECONDS. $\times 1000$. ETCHED IN PICRAL PLUS NITAL.

most of the austenite transformation during 174 days at temperature being by separate carbide and ferrite reactions, rather than

ture outlining twin bands in the austenite grains (Fig. 14). After careful etching in dilute reagents, this twin-band

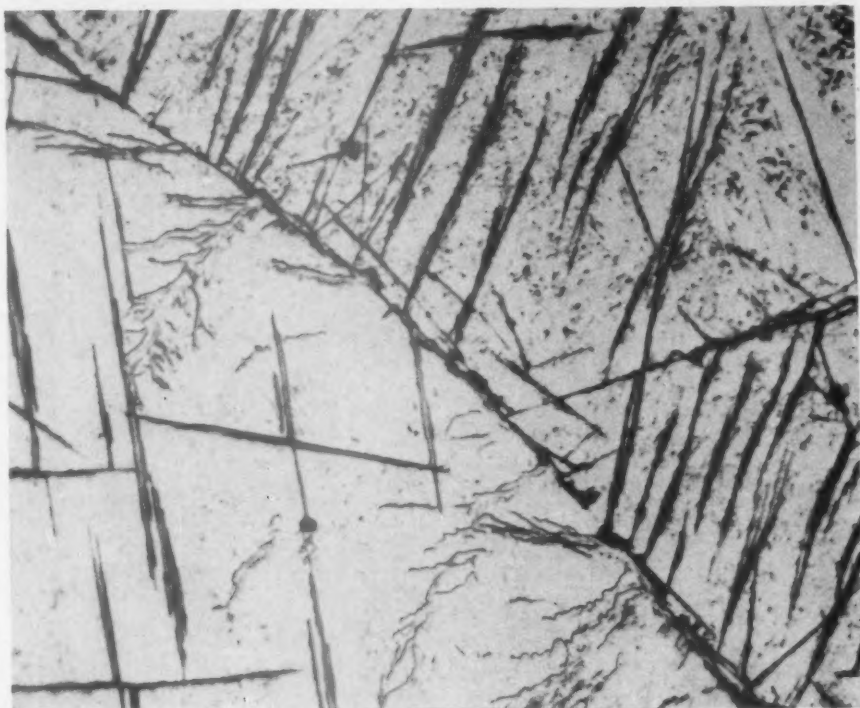


FIG. 9.—3 PER CENT CHROMIUM STEEL QUENCHED FROM 1200°C. TO 450°C. AND HELD FOR 20,000 SECONDS. $\times 1000$. ETCHED IN VILELLA'S REAGENT.

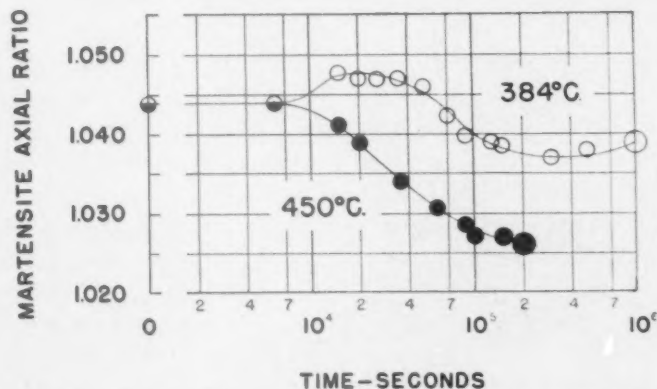


FIG. 10.—DEPENDENCE OF MARTENSITE AXIAL RATIO UPON TIME AT 450°C. AND AT 384°C. DURING ISOTHERMAL TRANSFORMATION IN THE 3 PER CENT CHROMIUM STEEL.

by formation of the dark-etching aggregate structure.

Transformation proceeds slowly at 395°C. and a specimen held for 100,000 sec. contains rather uniformly distributed Fe₃C plates and a darker-etching struc-

ture boundary structure appears as resolvable particles (Fig. 15), much like the ferrite formed at 450°C. and 415°C. An important difference in the kinetic phenomena is to be noted, however: At 395°C. the ferrite reaction is not dependent upon prior for-

mation of carbide (and resultant carbon depletion of the austenite); it is only after considerably longer holding times at 395°C. that ferrite forms in the near vicinity of

axial ratio that follows has been correlated with the formation of carbide plates of the same microappearance as those observed at temperatures above 384°C. Ferrite and



FIG. 11.—3 PER CENT CHROMIUM STEEL QUENCHED FROM 1200°C. TO 450°C. AND HELD FOR 1,000,000 SECONDS. $\times 1000$. ETCHED IN VILELLA'S REAGENT.

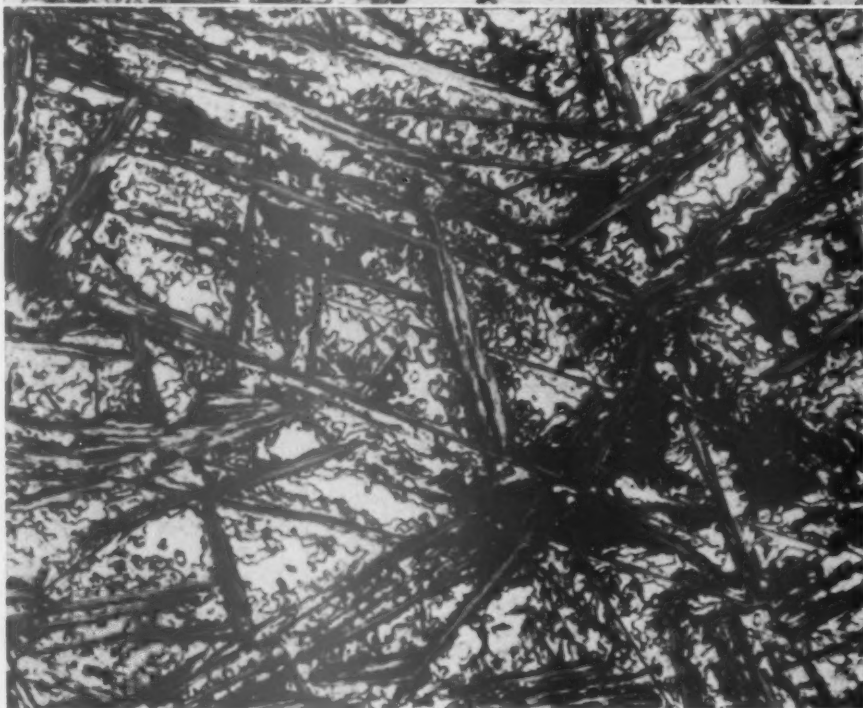
carbide plates in the manner observed at 415° and 450°C.

At 384°C. initial transformation is more rapid than at 395°C. and the structure is that shown in Figs. 16 and 17. At highest magnification many ferrite particles can be seen. These particles are closely associated with the unresolved part of the structure. It has been assumed that there is only one decomposition product present; the microstructure is considered as being made up of ferrite of varying particle size. Fig. 10 shows the variation in the axial ratio of martensite as a function of transformation time at 384°C. The initial increase in axial ratio accompanies formation of the product of Fig. 17; that is, ferrite formation results in carbon enrichment of the matrix austenite. The decrease in

carbide continue to form slowly by separate reactions on further holding and after 10^6 sec. the microstructure is that shown in Fig. 18. At this temperature, as at 450°C., correlation of microscopic and X-ray data indicates that during the period when the two reactions are running simultaneously they almost counterbalance each other in their effect upon the carbon content of the matrix. The axial ratio-time curve shows that the carbon content of the matrix is not much less than the original 1 per cent after 10^6 sec. at 384°C. The simplest interpretation that can be placed upon the X-ray and microscopic data is that given; namely, that austenite decomposition takes place by two reactions (gamma-to-alpha and gamma-to-carbide) which start at different times but



12



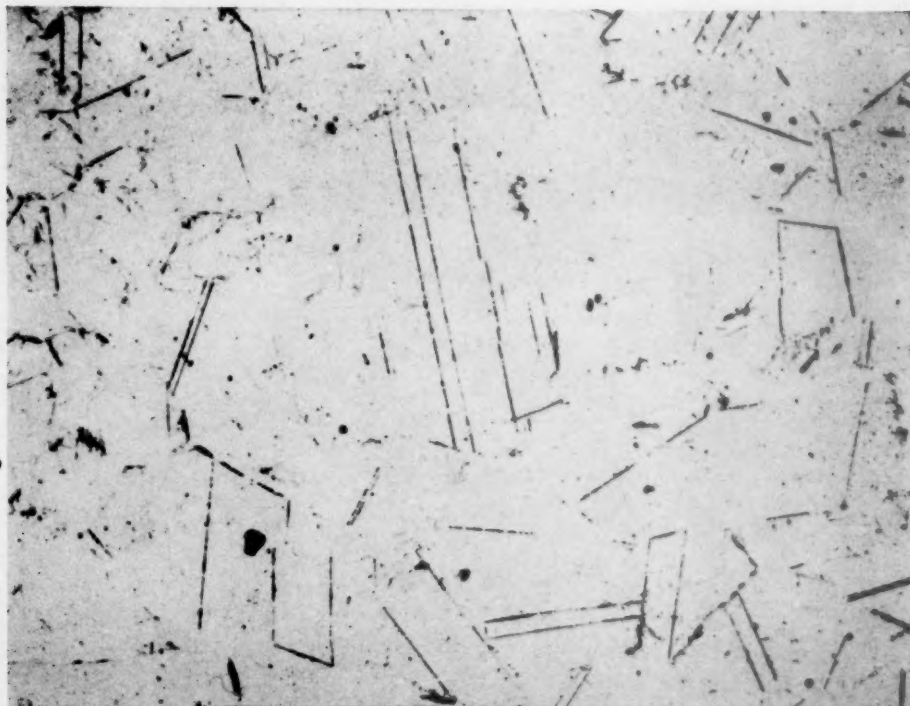
13

FIGS. 12 AND 13.—3 PER CENT CHROMIUM STEEL QUENCHED FROM 1200°C. TO 415°C. AND HELD FOR TIMES INDICATED. $\times 1000$. ETCHED IN VILELLA'S REAGENT.

Fig. 12. 1,000,000 seconds (11 days, 14 hours).

Fig. 13. 15,000,000 seconds (174 days).

14



15

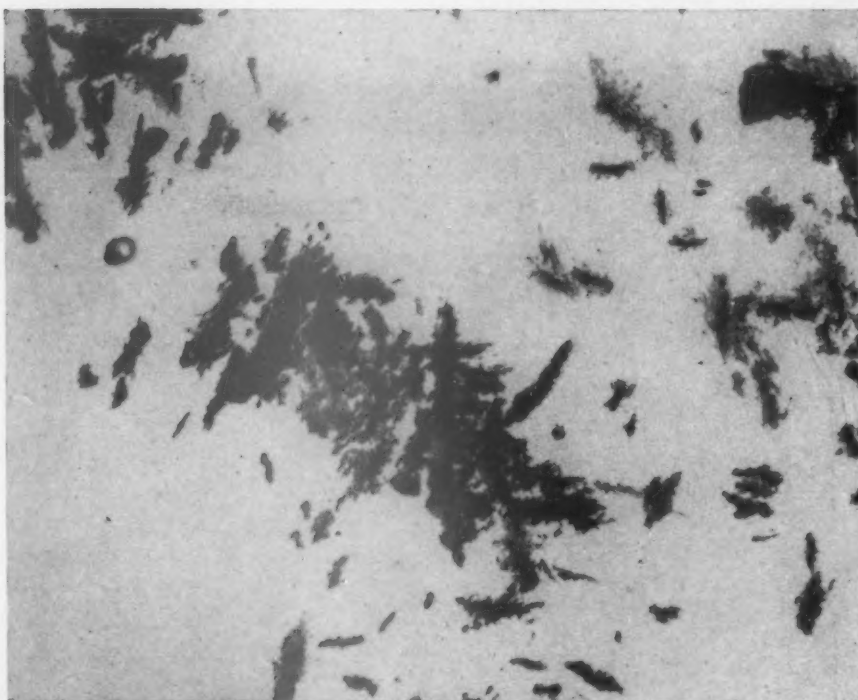


FIGS. 14 AND 15.—3 PER CENT CHROMIUM STEEL QUENCHED FROM 1200°C. TO 395°C. AND HELD FOR 100,000 SECONDS.

Fig. 14. $\times 75$.

Fig. 15. $\times 2500$.

Etched in nital.



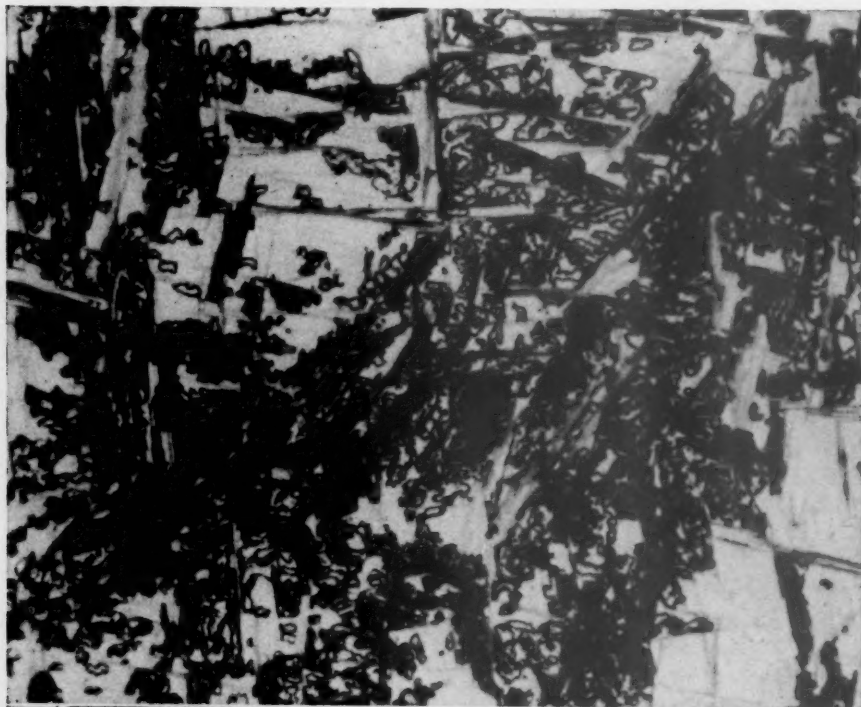
16



17

FIGS. 16 AND 17.—3 PER CENT CHROMIUM STEEL QUENCHED FROM 1200°C. TO 384°C. AND HELD FOR 10,000 SECONDS.
Fig. 16. $\times 500$.
Fig. 17. $\times 2500$.
Etched in nital.

18



19

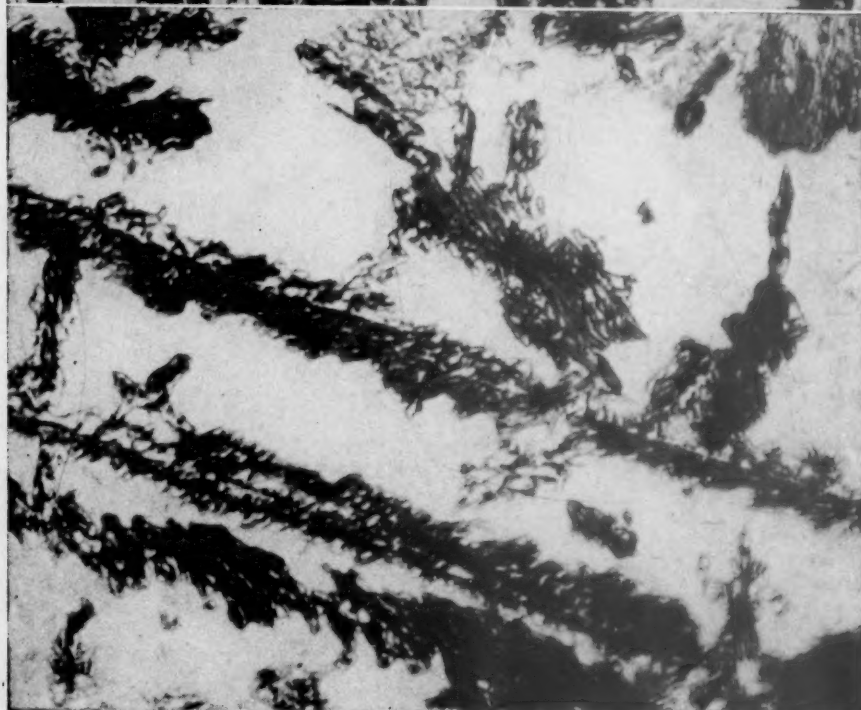


FIG. 18.—3 PER CENT CHROMIUM STEEL QUENCHED FROM 1200°C. TO 384°C. AND HELD FOR 1,000,000 SECONDS. $\times 1000$. ETCHED IN VILELLA'S REAGENT.

FIG. 19.—3 PER CENT CHROMIUM STEEL QUENCHED FROM 1200°C. TO 370°C. AND HELD FOR 10,000 SECONDS. $\times 2000$. ETCHED IN NITAL.

proceed simultaneously after carbide begins to form.

The microstructure changes markedly with the reaction temperature in the range 384° to 325°C . (Figs. 17, 19, 20, 21). There seems to be a continuous variation from the particle ferrite of Fig. 17 to the typical bainite of Fig. 21.

Dilatometric measurements during reaction in this temperature range show that, at a given temperature, there is an initial period of expansion, after which the specimen length is essentially constant or decreases slightly with time. Microstructures show that the reaction stops or proceeds at a very low rate after this initial expansion. This feature is so well marked that it has been thought worth while to indicate on the transformation diagram (Fig. 22) the times at which the initial, relatively rapid transformation (representing only partial decomposition of austenite) is complete. The magnitude of the initial expansion increases very rapidly with decreasing temperature (Fig. 23). In terms of the transformation, this indicates that the degree of advancement which the reac-

hypoeutectoid chromium steels. It is also worthy of note that in the hypereutectoid alloy reported here, as well as in the hypoeutectoid 3 per cent Cr steel previ-

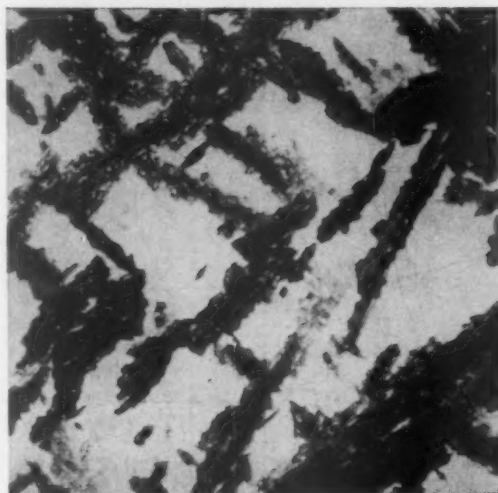


FIG. 20.—3 PER CENT CHROMIUM STEEL QUENCHED FROM 1200°C . TO 355°C . AND HELD FOR 7000 SECONDS. $\times 1000$. ETCHED IN NITAL.

ously reported, the structure forming initially from austenite at highest temperatures in the intermediate range is ferrite



FIG. 21.—3 PER CENT CHROMIUM STEEL QUENCHED FROM 1200°C . TO 325°C . AND HELD FOR 6000 SECONDS. $\times 750$. ETCHED IN VILELLA'S REAGENT.

tion can attain increases with decreasing reaction temperature. These characteristics of the intermediate reaction were previously noted by Klier and Lyman⁸ in

and the matrix austenite becomes enriched in carbon. In both cases, enriched austenite transforms on continued holding by a distinctly different reaction.

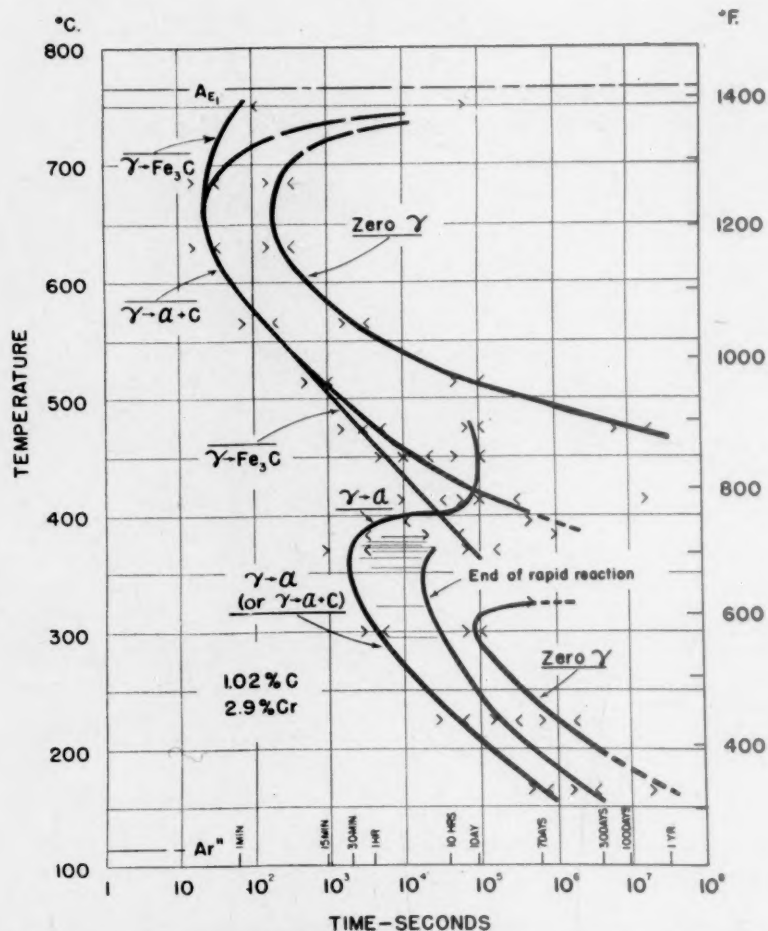


FIG. 22.—ISOTHERMAL TRANSFORMATION DIAGRAM FOR 3 PER CENT CHROMIUM STEEL. Horizontal lines at temperatures between 290° and 390°C. represent time periods of initial, relatively rapid dilatometric expansion during isothermal transformation.

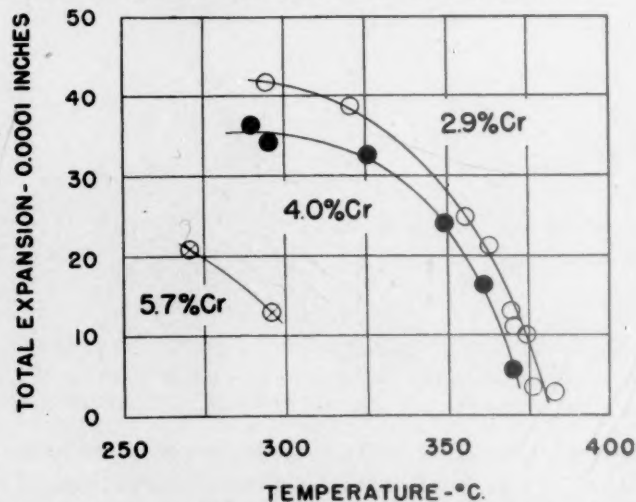


FIG. 23.—DEPENDENCE OF TOTAL DILATOMETRIC EXPANSION DURING INITIAL, RAPID TRANSFORMATION UPON REACTION TEMPERATURE. All dilatometer specimens 1 inch long

All of the austenite transformed to bainite at 300°C. and at 225°C. At 165°C. the bainite transformation proceeded to a high degree of completion during the

to those of the orthorhombic structure. Transformation times and temperatures at which only Fe_3C was found are given in Table 4.

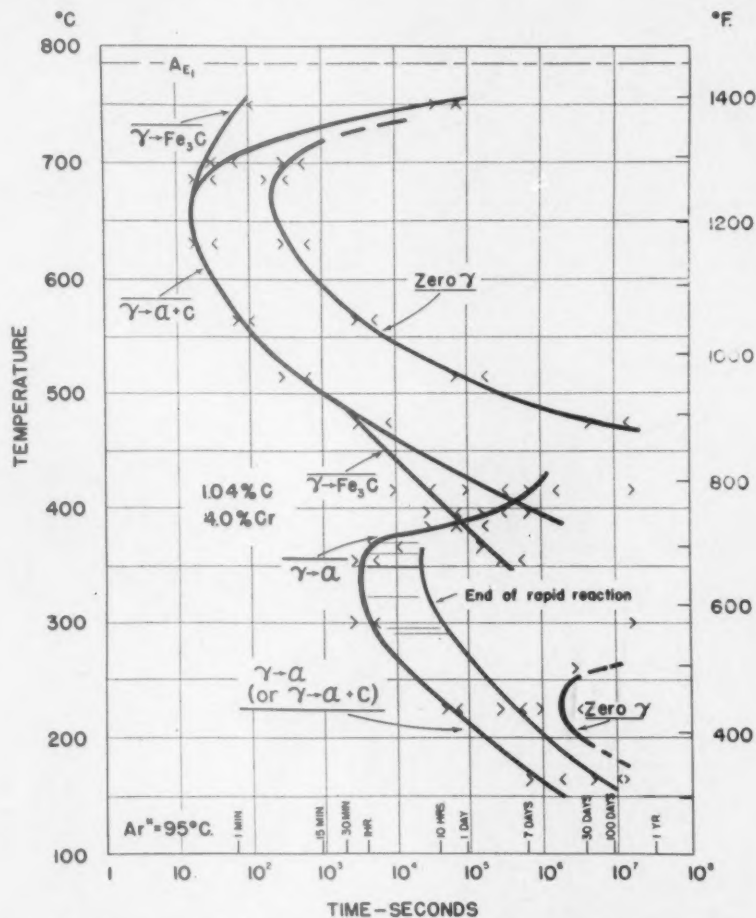


FIG. 24.—ISOTHERMAL TRANSFORMATION DIAGRAM FOR 4 PER CENT CHROMIUM STEEL.

Horizontal lines at temperatures between 290° and 370°C. represent time periods of initial, relatively rapid dilatometric expansion during isothermal transformation.

second, third and fourth weeks at temperature. Further transformation was much slower, austenite decomposition being 99 per cent complete in a specimen held for 232 days.

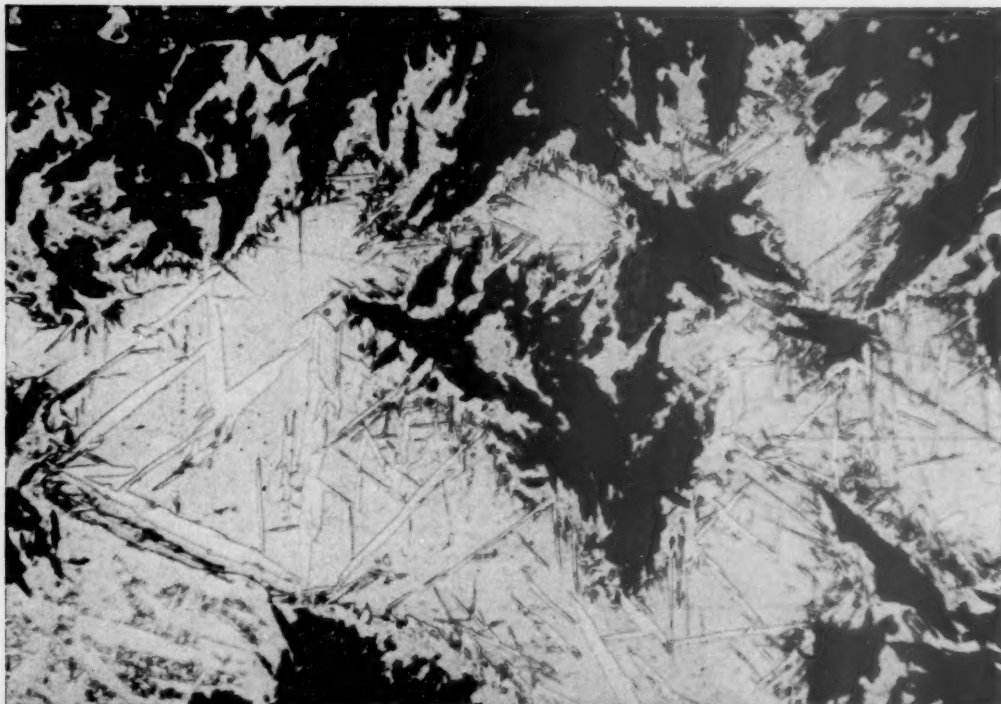
A number of specimens have been re-acted isothermally and diffraction patterns obtained to determine the identity of carbides. Whenever an identification was possible, Fe_3C was present. In one specimen, held for 1.5×10^6 sec. at 515°C., weak Cr_7C_3 lines were present in addition

TABLE 4.—Transformation Times and Temperatures at which Fe_3C Was the Only Carbide Obtained with the 3 Per Cent Chromium Steel

TEMPERATURE, DEG. C.	TIME, SEC.
775	35,000
650	300
650	85,000
565	900
450	500,000
415	7,000,000
384	1,000,000

The pearlite reaction is labeled gamma-to-alpha-plus-carbide on the transformation diagram. The intermediate reaction

25



26



FIG. 25.—6 PER CENT CHROMIUM STEEL QUENCHED FROM 1200°C. TO 565°C. AND HELD FOR 3000 SECONDS. $\times 500$. ETCHED IN VILELLA'S REAGENT.

FIG. 26.—6 PER CENT CHROMIUM STEEL QUENCHED FROM 1200°C. TO 415°C. AND HELD FOR 200 DAYS. $\times 750$. ETCHED IN VILELLA'S REAGENT.

is designated gamma-to-alpha and, parenthetically, gamma-to-alpha-plus-carbide. Further consideration of this matter will be given in a later section.

Steel with 4 Per Cent Chromium

The transformation diagram for the 4 per cent Cr steel (Fig. 24) is qualitatively the same as that for the 3 per cent Cr steel. Dilatometric measurements in the upper intermediate range reveal a similar temperature dependence of the degree of advancement that can be attained by the initial reaction (Fig. 23). The separation in time of the incomplete intermediate reaction and the carbide reaction that follows is somewhat greater than in the steel of lower chromium content. At 355°C. relatively rapid reaction takes place during the first 6 hr. at temperature; after about five days the remaining austenite begins to precipitate carbide.

The intermediate reaction goes nearly to completion in less than one day at 300°C. However, the austenite that remains does not completely decompose on continued holding for 200 days. Only at 225°C. was complete transformation of austenite to bainite observed.

The results of X-ray identifications of carbide structures are given in Table 5.

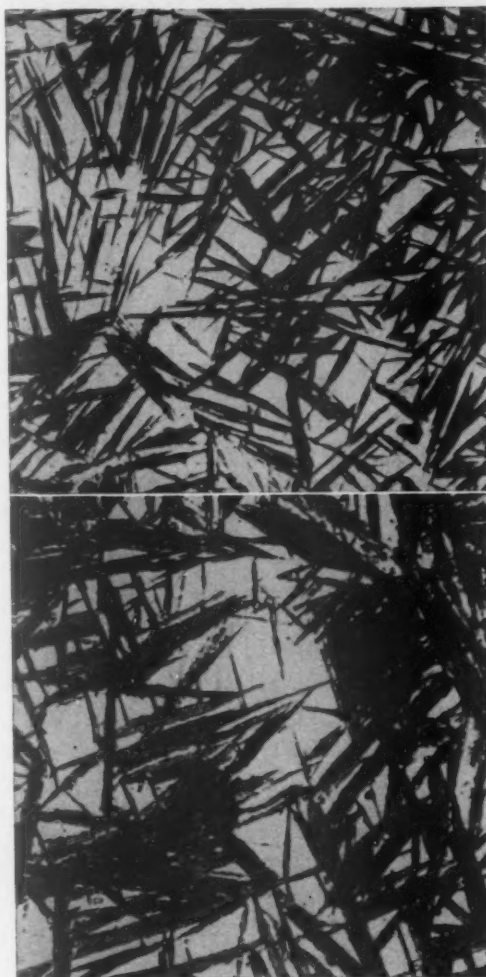
TABLE 5.—Carbide Identifications Obtained with the 4 Per Cent Chromium Steel

Temperature, Deg. C.	Time, Sec.	Carbide
725	7,000	$\text{Fe}_3\text{C} + \text{Cr}_7\text{C}_3$ (?)
650	85,000	$\text{Fe}_3\text{C} + \text{Cr}_7\text{C}_3$
630	700	$\text{Fe}_3\text{C} + \text{Cr}_7\text{C}_3$
515	5,000	Fe_3C
515	10,000	Fe_3C
515	50,000	$\text{Fe}_3\text{C} + \text{Cr}_7\text{C}_3$
515	3,000,000	$\text{Fe}_3\text{C} + \text{Cr}_7\text{C}_3$
475	700,000	$\text{Fe}_3\text{C} + \text{Cr}_7\text{C}_3$
415	75,000	Fe_3C
415	150,000	Fe_3C
415	700,000	Fe_3C

Steel with 6 Per Cent Chromium

Transformation of austenite in the 6 per cent Cr steel has features in common with the transformations in steels of both higher and lower chromium contents.

At 565°C. decomposition takes place with accompanying carbon diffusion in the manner observed in the 9 per cent Cr steel (Fig. 25). The same phenomenon was



FIGS. 27 AND 28.—6 PER CENT CHROMIUM STEEL QUENCHED FROM 1200°C. TO 300°C. AND HELD FOR TIMES INDICATED. $\times 300$.

Fig. 27. 500,000 seconds (5 days, 19 hours).

Fig. 28. 17,500,000 seconds (200 days).

Etched in Vilella's reagent.

observed at other temperatures. After 3000 sec. at 565°C., martensite in the quenched specimen has an axial ratio of 1.030. (Martensite formed on a direct quench from 1200°C. in this steel has an axial ratio of 1.046.)

At 415°C. both carbide and the dark-etching aggregate structure form slowly

(Fig. 26). A specimen held for 35 days at 384°C. contained carbide but none of the dark-etching product.

The structure formed during the first six days at 300°C. is shown in Fig. 27. As is evident from comparison of Figs. 27 and 28, continued holding for 200 days at this temperature results in no appreciable reduction in the amount of austenite present. Specimens held for more than one day at 300°C. contain no martensite. Greninger and Troiano,⁹ in studying a 1.78 per cent carbon steel, were the first to observe metallographically a lowering of the martensite range during isothermal transformation at low temperatures. Although about 90 per cent of the austenite transformed to bainite at 225°C. during the first 80 days at temperature, no decomposition was observed 60°C. lower, at 165°C., even after 200 days.

The X-ray results for this steel are summarized in Table 6 and the transformation diagram is given in Fig. 29. The X-ray results indicate that at 650°C. Fe_3C forms from austenite as a part of the pearlite aggregate but on continued holding transforms to Cr_7C_3 .

TABLE 6.—Carbide Identifications Obtained with the 6 Per Cent Chromium Steel

Temperature, Deg. C.	Time, Sec.	Carbide
785	110,000	Fe_3C
650	600	$\text{Fe}_3\text{C} + \text{Cr}_7\text{C}_3$ (?)
650	1,000	$\text{Fe}_3\text{C} + \text{Cr}_7\text{C}_3$ (?)
650	85,000	Cr_7C_3
565	3,000	Fe_3C (?)
515	3,000,000	Cr_7C_3
260*	1,000,000	Fe_3C

* A specimen quenched from 1200°C. to room temperature, cooled in liquid air and tempered 500,000 seconds at 260° contained Fe_3C .

DISCUSSION OF RESULTS

The Isothermal Reactions

The isothermal reactions of austenite in the steels studied are of three types: gamma-to-carbide, gamma-to-alpha, and gamma-to-alpha-plus-carbide.

The gamma-to-carbide reaction is the most easily distinguished because the precipitate is the most nearly constant microscopically. The other reactions lead to a greater variety of structures, some of which cannot be resolved with the optical microscope. Furthermore, the X-ray diffraction patterns produced by these unresolvable structures do not lend themselves to precise interpretation. It is apparent that if distinctions are to be made in these doubtful cases, they must be based upon indirect evidence.

In the 9 per cent Cr steel, carbon flow from matrix to product was observed at temperatures both above and below the knee of the S-curve. This characteristic, common to both high- and low-temperature transformation, and the identification of the carbide allowed the reaction in this steel to be designated gamma-to-alpha-plus- Cr_7C_3 . This reaction in its more general form (gamma-to-alpha-plus-carbide) can be traced through the series of steels. The large-scale diffusion of carbon was observed in the 6 per cent Cr steel although the pearlite reaction is gamma-to-alpha-plus- Fe_3C at some or all temperatures. The microstructural similarities permit extension to the 3 and 4 per cent chromium steels.

It has been shown that a gamma-to-alpha reaction occurs in the 3 per cent Cr steel between 475° and 370°C. The curve for beginning of transformation is continuous from 370°C. to the lowest temperature investigated. Continuity of structure is evident, particularly below 325°C., where acicular structures are formed. Between 325° and 380°C., where the microstructure of the reaction product changes rapidly with temperature of formation, the degree of advancement attainable by the reaction also varies with temperature. This temperature dependence of the degree of advancement of the intermediate reaction is found in steels of widely varying carbon and alloy content; it is not associated with a

particular microstructure. This feature of transformation seems to be a more general and definitive characteristic of the intermediate reaction than does microstructure.

upon the microscopic recognition of ferrite between 400° and 370°C . Since direct structural evidence is lacking at the lower temperatures, the designation gamma-

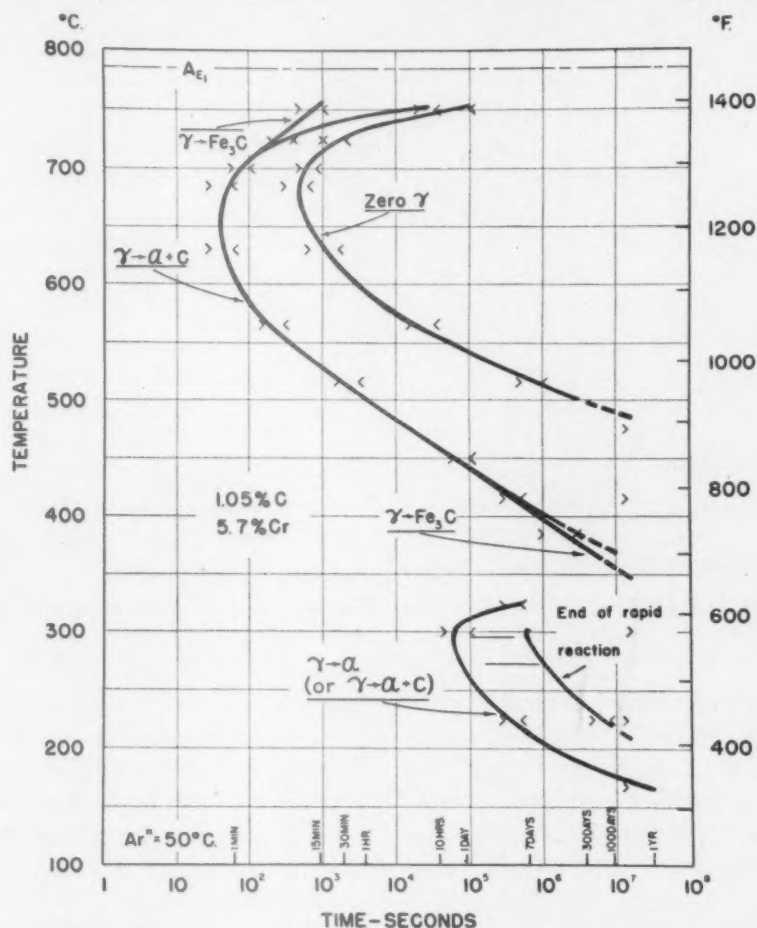


FIG. 29.—ISOTHERMAL TRANSFORMATION DIAGRAM FOR 6 PER CENT CHROMIUM STEEL.

Specification of the intermediate reaction as gamma-to-alpha implies that carbide forms only from a supersaturated ferrite (never from austenite) at temperatures where this reaction goes to completion. This is essentially the original point of view of Davenport and Bain¹ with respect to the acicular structures now called bainite. The alternative concept is that both carbide and ferrite form from austenite to produce bainite.

The postulation, made herein, that the intermediate reaction is a gamma-to-alpha reaction over the whole range relies heavily

to-alpha-plus-carbide has been inserted parenthetically.

With decreasing temperature below 650°C , there is an increasing tendency for austenite to transform by separate ferrite and carbide reactions that proceed simultaneously. For instance, with the 3 per cent Cr steel at temperatures between 450° and 384°C , the reactions gamma-to-alpha and gamma-to-carbide proceed together with simultaneous carbon enrichment and carbon impoverishment of the matrix. The concurrent existence of two such different processes in a single austenite crystal

has not been observed in hypoeutectoid steels.

The carbide phases formed during isothermal transformation of austenite may

elimination of the gamma-to-Fe₃C reaction, both above and below the temperature of maximum rate of pearlite formation. No gamma-to-carbide reaction

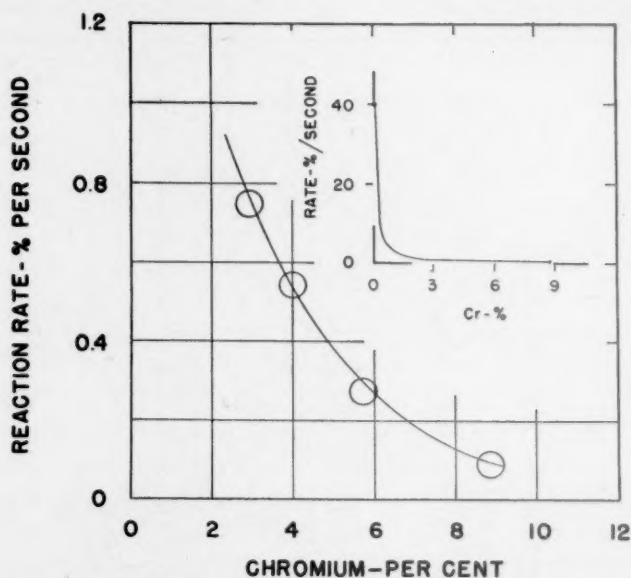


FIG. 30.—DEPENDENCE OF REACTION RATE TO PEARLITE (AT THE KNEE OF THE S-CURVE) UPON CHROMIUM CONTENT OF 1 PER CENT CARBON STEELS.

Insert shows, approximately, the relationship over the range 0 to 9 per cent Cr.

change their compositions and their crystal structures during and after decomposition of austenite. These carbide reactions may be rapid or slow. There is evidence that Fe₃C, formed during the pearlite reaction in the 6 per cent Cr steel, transforms to Cr₇C₃ after austenite decomposition is complete. This reaction has also been observed by Crafts and Offenbauer¹⁰ during tempering at 600°C. of a 0.40 per cent C, 2.56 per cent Cr steel. Additional information on the kinetics of such changes in carbides, both on tempering and after isothermal transformation of austenite, is needed.

Effect of Chromium upon the Reactions

The effect of chromium dissolved in austenite upon the reactions in these steels of constant carbon content can now be evaluated.

Increasing chromium causes the gradual

was observed in the 9 per cent Cr steel. As the carbide reaction is eliminated, the character of the pearlite transformation changes; carbon movement, especially during the first half of the reaction, leaves the unreacted austenite considerably impoverished in carbon.

Increasing chromium has three main effects upon the intermediate reaction: The reaction is shifted to longer times and to lower temperatures (with an accompanying decrease in the rate of transformation), and the temperature region of incomplete transformation becomes wider. The intermediate reaction was not observed in the steel with 9 per cent Cr. Increasing chromium from 2.9 to 5.7 per cent lowers the temperature of minimum induction time by 60° to 70°C. In the same steels, Ar'' is lowered the same amount by increased chromium. It is of interest that in molybdenum steels, both the martensite and intermediate temperature ranges

are relatively insensitive to molybdenum content.^{11,12}

The rate of pearlite formation at the knee of the S-curve has been plotted as a function of chromium content in Fig. 30. These rates have been obtained by dividing into 100 the number of seconds between beginning and end of reaction as taken from the transformation diagrams. When plotted on an expanded scale, there appears to be a rather marked variation. However, this variation is small in comparison with that encountered in the range 0 to 3 per cent Cr, as is evident from the insert of Fig. 30. The rate is decreased by a factor of about 400 in the range 0 to 9 per cent; this factor is about 7 in the range 3 to 9 per cent.

It has been shown here that little, if any, Cr_7C_3 forms from austenite in the 3 per cent Cr steel while little, if any, Fe_3C forms in the 9 per cent Cr steel. This change in the structure of pearlite with increasing chromium implies a change in the composition of the carbide phase. If pearlite is nucleated by carbide, a change in the "active nucleus" is also implied. In spite of these changes the rate of reaction near 650°C . is affected by a factor of less than 10 over the composition range 3 to 9 per cent Cr. On the other hand, in the dilute alloy range below 3 per cent Cr, where Fe_3C is always the carbide phase in pearlite, the rate of reaction changes very rapidly with increasing chromium content (Fig. 30, insert). It seems unlikely that the diffusion of chromium into the carbide phase during the pearlite transformation is the rate-controlling factor in this reaction in both the dilute and the high-chromium alloys. It remains to be shown what role the diffusion of chromium may play in either case.

SUMMARY

1. Microscopic, X-ray and dilatometric methods have been employed in determining the isothermal transformation diagrams

for four steels containing 1 per cent carbon with chromium contents of 3, 4, 6, and 9 per cent.

2. The following isothermal reactions were observed: gamma-to- $(\text{Fe,Cr})_3\text{C}$, gamma-to-alpha, gamma-to-alpha-plus- $(\text{Cr,Fe})_7\text{C}_3$, gamma-to-alpha-plus- $(\text{Fe,Cr})_3\text{C}$, $(\text{Fe,Cr})_3\text{C}$ -to- $(\text{Cr,Fe})_7\text{C}_3$.

3. Near 400°C ., in the 3 and 4 per cent Cr steels, austenite decomposition occurs mainly by separate carbide and ferrite reactions, which proceed simultaneously.

4. The reaction gamma to alpha occurs at highest temperatures in the intermediate range in the 3 and 4 per cent Cr steels. The degree of advancement the intermediate reaction can attain increases rapidly with decreasing temperature. This reaction can go to completion in the lower part of the intermediate range in the 3 and 4 per cent Cr steels.

5. Increasing chromium causes the gradual elimination of the gamma-to-carbide reaction. In the 6 and 9 per cent Cr steels, where the gamma-to-carbide reaction is weak or absent, carbon impoverishment of matrix austenite takes place during the formation of pearlite.

6. Increasing chromium lowers the intermediate range about the same amount as it lowers the martensite range.

7. The rate of the pearlite reaction at the knee of the S-curve is decreased by chromium in the composition interval 3 to 9 per cent to a much less extent than in the 0 to 3 per cent chromium alloys. It is considered unlikely that the diffusion of chromium into the carbide phase is the rate-controlling factor in pearlite formation in both dilute and high-chromium alloys.

ACKNOWLEDGMENTS

The authors wish to acknowledge the contributions of Mr. John F. Collins and Mr. Stuart Lyman, who assisted in the metallographic work. The advice and cooperation of Dr. E. G. Mahin, Head of the

Department of Metallurgy, University of Notre Dame, is appreciated.

REFERENCES

1. E. S. Davenport and E. C. Bain: Transformation of Austenite at Constant Subcritical Temperatures. *Trans. A.I.M.E.* (1930) **90**, 117.
2. W. Tofaute, A. Sponheuer and H. Bennek: Umwandlungs-, Härtings- und Anlassvorgänge in Stählen mit Gehalten bis 1% C und bis 12% Cr. *Archiv Eisenhüttenwesen* (1935) **8**, 499.
3. A. B. Kinzel and W. Crafts: Alloys of Iron and Chromium, I—Low-Chromium Alloys. New York, 1937. McGraw-Hill Book Co.
4. E. P. Klier and A. R. Troiano: Ar'' in Chromium Steels. This volume, page 175.
5. Z. Nishiyama: X-ray Investigation of Austenite and Martensite in some Special Steels. *Sci. Repts. Sendai* (1935) **24** (1), 128.
6. E. P. Klier: Subcritical Decomposition of Austenite in Chromium Steels. Ph. D. Dissertation, University of Notre Dame, 1944.
7. H. Jolivet: Transformation of Austenite on Cooling; Morphology and Genesis of the Aggregates Formed. *Jnl. Iron and Steel Inst.* (1939) **140**, 95.
8. E. P. Klier and T. Lyman: Bainite Reaction in Hypoeutectoid Steels. *Trans. A.I.M.E.* (1944) **158**, 394.
9. A. B. Greninger and A. R. Troiano: Crystallography of Austenite Decomposition. *Trans. A.I.M.E.* (1940) **140**, 307.
10. W. Crafts and C. M. Offenbauer: Carbides in Low-chromium Steel. *Trans. A.I.M.E.* (1942) **150**, 275.
11. J. R. Blanchard, R. M. Parke, and A. J. Herzig: The Effect of Molybdenum on the Isothermal, Subcritical Transformation of Austenite in Eutectoid and Hypereutectoid Steels. *Trans. Amer. Soc. Metals* (1943) **31**, 849.
12. H. H. Chiswick and A. B. Greninger: Influence of Nickel, Molybdenum, Cobalt and Silicon on the Kinetics and Ar'' Temperatures of the Austenite to Martensite Transformation in Steels. *Trans. Amer. Soc. Metals* (1944) **32**, 483.

DISCUSSION

J. H. HOLLOMON,* L. D. JAFFE,† and C. ZENER.‡—The authors are to be congratulated on the systematic and complete study of the effects of chromium on the isothermal decomposition of austenite. This study will certainly aid in an understanding of these transformations.

* Captain, Ordnance Department, Watertown Arsenal, Watertown, Massachusetts.

† Metallurgist, Watertown Arsenal, Watertown, Mass.

‡ Principal Physicist, Watertown Arsenal, Watertown, Mass. (On leave, Professor of Physics, Washington State College.)

It is of interest to note that the present paper confirms several results of the Russian investigators, Steinberg and Susin, which have attracted little attention in the United States. These authors found that the bainite reaction does not go to completion^{13,14} (at certain temperatures), that partial transformation to bainite lowers the M_s temperature of the remaining austenite^{13,14} that holding (presumably hypereutectoid) steel in the pearlite temperature range raises the M_s temperature because the carbon content of the remaining austenite is lowered^{13,14,15} (earlier noted but not explained in this way by Wever and Engel¹⁶), and that the bainite reaction in 9 per cent chromium steel (even with only 0.35 per cent carbon) commences only after extremely long times.¹⁵

The authors' work also clarifies the previously puzzling observation of Jolivet⁷ that cementite needles may form in hypereutectoid steel at temperatures below the pearlite nose. The present paper indicates that the time for the apparent commencement of primary cementite formation is less dependent upon temperature than the time for apparent commencement of pearlite formation.

The observations of Messrs. Lyman and Troiano and Steinberg and Susin concerning the bainite transformation may be readily explained in terms of the interpretation of austenite decomposition recently presented.¹⁷

According to this interpretation, the initial stage in the formation of bainite is the transition of the face-centered structure of austenite into the body-centered structure of ferrite without a change in carbon concentration. This transition is associated with a critical temperature just like any other polymorphic transition.

¹³ S. Steinberg and V. Susin: Etude sur les transformations de l'austenite dans un acier au chrome. *Rev. Métal.* (1934) **31**, 554-559.

¹⁴ S. Steinberg and V. Susin: Die Umwandlung des Austenits im Schnellarbeitsstahl. *Archiv Eisenhüttenwesen* (1934) **7**, 537-538.

¹⁵ S. Steinberg, V. Susin, and I. Goldin: Etude sur les transformations de l'austenite dans un acier au chrom-silicium. *Rev. Métal.* (1937) **34**, 190-194.

¹⁶ F. Wever and N. Engel: Ueber den Einfluss der Abkühlungsgeschwindigkeit auf die Temperatur der Umwandlungen, das Gefüge und den Feinbau der Eisen-Kohlenstoff-Legierungen. *Mitt. K-W-I. Eisenforschung* (1930) **12**, 93-114.

¹⁷ C. Zener: Kinetics of the Decomposition of Austenite. *A.I.M.E. Tech. Pub.* 1856 (1945).

Martensite is also regarded essentially as a supersaturated ferrite, but in which the carbon atoms occupy certain preferred interstitial sites, this preferred distribution giving rise to the slight tetragonality. The residual stresses introduced by the formation of martensite lower its transformation temperature below that of bainite by an amount that is independent of composition. Any alloy therefore lowers, or raises, the critical temperature for bainite and for martensite formation by the same amount, as has been found by the authors to be the case for chromium.

The authors state, and vividly demonstrate in their Fig. 23, that the bainite reaction may be regarded as virtually ceasing after a certain fraction of the austenite has transformed, this fraction increasing with decreasing temperature. This phenomenon has been explained¹⁷ as the direct consequence of the diffusion of carbon out of the growing bainite grain into the surrounding austenite matrix. The increase in carbon concentration in the surrounding austenite lowers the critical transformation temperature, thereby retarding growth. The growth of a bainite grain may be permanently stopped by the precipitation of a cementite film along its boundary. As the temperature is lowered, and the diffusion of carbon consequently reduced, the retardation of bainite growth by carbon diffusion becomes less effective.

The converse phenomenon of a raising of the bainite transformation temperature by a lowering of the carbon concentration in the austenite through precipitation of free cementite is demonstrated in Fig. 22.

T. LYMAN and A. R. TROIANO (authors' reply).—The discussers, in accepting the results of Steinberg and Susin, appear to have accepted also a doubtful interpretation of some of these results. For instance, Steinberg and Susin¹⁴ report that in 18-4-1 high-speed steel held for 70 hr. at 600°C., or for 150 min. at 700°C., transformation of unreacted austenite during subsequent cooling begins at about 500°C instead of at the normal M_s temperature of 180°C. It was assumed by these investigators that this represented an elevation of the austenite-to-martensite transformation range. More recent and more comprehensive work by

Gordon, Cohen and Rose¹⁸ has shown clearly, however, that transformation to bainite will occur at temperatures below 500°C. during cooling of high-speed steel at comparable rates after holding in the temperature range 500° to 650°C.

It is obvious that the magnetometric data of Steinberg and collaborators^{13,14,15} do not constitute proof of changes of carbon content in the matrix austenite. In the absence of direct evidence, these authors assumed that the elevation of the low-temperature transformation range was due to carbon impoverishment of austenite accompanying carbide precipitation. The plausibility of this assumption is scarcely to be denied, since undissolved carbide was present after austenitizing of the steels used in all of these investigations; growth of these carbide particles prior to and during pearlite formation would lower the carbon content of austenite and raise the low-temperature transformation range. This explanation becomes even more probable in the light of the results given in the present paper, where it is shown that free carbide may form at temperatures as low as 400°C., even in the absence of pre-existing nuclei.

While carbon impoverishment of austenite is a necessity with simple carbide precipitation, this is not true with the austenite-to-pearlite transformation. Therefore, the observation of the present paper that pearlite formation can cause a carbon depletion of matrix austenite is most striking. Such a result cannot be predicted from any previous experimental or theoretical studies of the pearlite reaction.

It is not made clear by Messrs. Hollomon, Jaffe and Zener in what way the data of Wever and Engel,¹⁶ obtained on continuous cooling of plain carbon steels, are pertinent to the present paper. We suppose, however, that their reference is to the variation of martensite axial ratio with cooling velocity observed by these investigators in a 1.28 per cent carbon steel. This result was discussed several years ago by Greninger and Troiano⁹ in connection with more complete data. It was shown that the observed effect is due to the formation of free cementite during cooling, thus providing

¹⁸ P. Gordon, M. Cohen and R. S. Rose: The Kinetics of Austenite Decomposition in High Speed Steel. *Trans. Amer. Soc. for Metals* (1943) 31, 161.

another example of the ease of carbide formation in hypereutectoid steels.

We have noted on page 216 that specimens of the 6 per cent Cr steel held for more than one day at 300°C. contained no martensite after quenching to room temperature; that is, M_s was lowered by partial transformation to bainite. It is of interest, in this connection, to note that although Steinberg and Susin attributed the

elevation of M_s to carbon depletion of austenite, they did not assume that the lowering of M_s after partial transformation to bainite was due to carbon enrichment of austenite.

Since our paper was written, additional X-ray evidence on the bainite transformation at 300°C. in the 6 per cent Cr steel has been obtained. This evidence, given in Table 7, shows that neither the lowering of M_s nor the stopping of the bainite reaction is caused by an increase in the carbon content of austenite. It is still pertinent to ask:

1. Why does bainite formation stop, leaving large volumes of austenite of the original composition free from transformation?

2. What change in this unreacted austenite is responsible for the lowering of its M_s temperature?

We do not find any answer to these fundamental questions in Dr. Zener's theory, as outlined by the discussers.

TABLE 7.—*Axial Ratio of Martensite in the 6 Per Cent Cr Steel after Partial Transformation at 300°C. and Subsequent Cooling in Liquid Air*

Time	Approximate Per Cent Bainite	Axial Ratio
0	0	1.046
36 hours	10	1.046
9 days	30 ^a	1.046
14½ days	30 ^a	1.046

^a Cf. Figs. 27 and 28.

Time-temperature Relations in Tempering Steel

By J. H. HOLLOMON* AND L. D. JAFFE,† JUNIOR MEMBERS A.I.M.E.

(New York Meeting, February 1945†)

THE effect of tempering temperature and time upon the properties of quenched steel is clearly a subject of great practical importance, as well as of considerable theoretical interest. It would be very desirable to be able to predict the properties of a quenched steel when given any selected tempering cycle, with a minimum of experimental work upon that heat or even type of steel.

Two problems are involved: one consists of relating the structure obtained to the physical properties, and will not be discussed here; the other, with which this paper deals, involves the relations of time, temperature and composition with the structure obtained on tempering.

Indentation hardness is perhaps the most convenient quantitative measure of the tempered structure, or of what might be called the "degree of tempering." Undoubtedly, it is not an exact measure, and in some cases (as when temper-brittleness occurs) pieces of the same quenched and tempered steel may have widely differing properties at the same hardness. However, hardness has the advantage of being simple to determine and is certainly the most widely used indication of the degree of tempering. Moreover, for fully quenched steels that are not temper-brittle and do not contain retained

austenite when quenched, it appears that, in general, if the hardness of the steel is the same, the tensile and impact properties will also be identical, whether a high or a low tempering temperature is used.

The tempering charts available in the metallurgical literature usually give the hardness as a function of tempering temperature for only one tempering time. However, in practice, tempering times frequently vary, and a method of converting tempering curves for one time to tempering curves for some other time would be very valuable. It is also advantageous, in determining the tempering treatment necessary for a given part, not to have to temper samples at several temperatures for the time used for the commercial tempering operation. A more satisfactory procedure would be to employ times of the order of 10 to 30 min., rather than 5 or 10 hr., and if possible to use only one temperature. Furthermore, it is frequently desirable, for reasons such as temper-brittleness,* to obtain a given hardness with short times at relatively high temperatures, and it would be convenient to be able to compute without tests the time required to produce this hardness.

Remarkably few quantitative studies of the hardness of quenched steel tempered over wide ranges of temperature and time

The statements or opinions in this article are those of the authors and do not necessarily express the views of the Ordnance Department. Manuscript received at the office of the Institute Nov. 17, 1944. Issued as T.P. 1831 in METALS TECHNOLOGY, September 1945.

* Captain, Ordnance Department, Watertown Arsenal Laboratory, Watertown, Mass.

† Metallurgist, Watertown Arsenal Laboratory.

‡ Meeting canceled.

* For steels susceptible to temper-brittleness, tempering between about 600° and 1050°F. is undesirable, since such tempering may result in inferior impact properties. One way to eliminate possible temper-brittleness is to produce the desired hardness at a tempering temperature sufficiently high to avoid the precipitation that causes temper-brittleness, and then quench from this temperature.¹

¹ References are at the end of the paper.

have been published,^{2-4,6} and apparently none of these investigations systematically included the effect of carbon content. It was decided, therefore, to study the tempering of a series of fully quenched steels differing only in carbon content, tempered over a wide range of time at temperatures from room to just below the critical, in order to obtain more systematic knowledge of the effects of carbon content, temperature, and time, and if possible to establish a method of finding the various combinations of temperature and tempering time that produce the same hardness. The experimental details and results will be discussed in part I of this paper, and the method obtained will be presented in part II.

diameter and approximately $\frac{1}{4}$ in. thick, by cutting these rounds transversely.

TABLE 2.—*Normalizing and Quenching Temperatures*

Heat	Carbon, Per Cent	Normalizing Temperature, Deg. C.	Quenching Temperature, Deg. C.
V	1.15	960	925
W	0.89	880	840
T	0.74	870	760
S	0.56	890	820
U	0.31	925	840
R	0.98	875	870

Heat-treatment

The samples were given a normalizing treatment of one hour at the temperatures indicated in Table 2, which had been chosen

TABLE 1.—*Analyses*
PER CENT

Steel	C	Mn	Si	S	P	Ni	Cr	Cu	Mo	V	Al Added
V	1.15	0.58	0.09	0.021	0.012	Tr.	0.01		Tr.	Nil	None
W	0.89	0.55	0.06	0.020	0.012	Tr.	0.01	0.08	Tr.	Nil	None
T	0.74	0.66	0.18	0.021	0.009	Nil	0.01		Nil	Nil	None
S	0.56	0.54	0.18	0.015	0.012	Nil	0.02		Nil	Nil	None
U	0.31	0.52	0.10	0.026	0.007	Nil	0.015	0.06	Nil		None
R	0.98	0.30	0.30	0.021	0.007	Tr.	0.03	0.055	Nil	Nil	None

I. EXPERIMENTAL WORK AND DISCUSSION

Materials

Six heats of plain carbon steel were used in the experimental work. Five of these (S, T, U, V, W) constituted a series of 200-lb. heats nominally differing only in carbon content and melted with the same practice in an acid-lined, high-frequency induction furnace. The check analyses are given in Table 1. Each of these heats was poured into a single ingot, which was forged down to $\frac{5}{8}$ in. square. The sixth heat, designated R, whose analysis is also given in Table 1, was obtained in the form of $\frac{3}{4}$ -in. hot-rolled rounds of a commercial plain carbon tool steel. Some of the bars from each heat were ground to $\frac{1}{2}$ -in. rounds. About 50 samples per heat were obtained in the form of disks $\frac{1}{2}$ in. in

on the basis of the equilibrium iron-carbon diagram. Preliminary tests were then run to determine a suitable quenching temperature for each heat. Temperatures selected to give austenite with no undissolved ferrite or carbide and a Shepherd fracture grain size of 5 to $5\frac{1}{2}$ are also listed in Table 2. The samples were austenitized in air for one hour at these temperatures and then quenched in brine. Since it was desired to start the tempering from a fully martensitic structure, the 1.15 per cent carbon steel (V) was cooled in liquid nitrogen to -190°C . immediately after the quench, in order to minimize retention of austenite, while the other steels were cooled to minus 70°C . in a mixture of dry ice and alcohol.*

* The as-quenched hardness indicates that the specimens of the low-carbon steel U were probably not completely martensitic.

A specimen from each heat was then tempered for each of the selected times, at each of the selected temperatures. These temperatures were: 100°, 150°, 200°, 250°, 300°, 400°, 500°, 600°, and 700°C. Tempering media were water (at 100°C.), oil (for steels R, S, and T at 150°C.) molten salt (for steels U, V, W, at 150°C. and all steels at 200° to 500°C.), and molten lead (at 600° to 700°C.). The times in the tempering baths were 10 sec., 90 sec., 15 min., 2½ hr., 24 hr. Times were controlled manually and varied perhaps ±10 per cent from the nominal for shorter times and somewhat less for the longer, as is usual in heat-treatment. The 100°C. temperature was obtained simply by tempering in boiling water, but for all higher temperatures thermostatic control that maintained the temperature constant within ±2°C. was used. In the few cases in which the measured temperature was found to differ slightly from the nominal, the measured temperature was recorded and was used in all calculations. The accuracies of the

temperature measurements were limited by uncertainties in thermocouple calibration, which did not exceed ±4°C. During the tempering operation, the heat R samples were suspended from wires for ease in handling, but the disks from the other heats were tempered in small perforated sheet-metal containers.

All specimens were quenched in water following the temper. They were then ground to a depth of 0.050 in. on a wet surface grinder, and four Rockwell C hardness measurements were made on each. The average of these hardness measurements for each specimen is given in Tables 3 to 8.

Functional Relationship for Experimental Steels

Probably the most obvious assumption as to the relation between time and temperature of tempering is that it takes the usual form of diffusion equations, the hardness being some function of the parameter:

$$te^{-Q/RT}$$

TABLE 3.—Steel R (0.96 Per Cent C)

Brine quenched after 1 hour at 870°C.; cooled to -70°C. before tempering. As-quenched hardness, 66.5 Rc

Rockwell C Hardness Obtained by Tempering at Indicated Time and Temperature									
Nominal Time of Tempering	100°C.	150°C.	200°C.	250°C.	300°C.	406°C.	500°C.	602°C.	700°C.
10 sec.....	66.5	67.0	68.0	66.5	65.0	60.5	52.5	43.5	35.5
90 sec.....	65.5	66.5	66.5	62.5	61.0	52.5	44.5	35.5	27.5
900 sec. (15 min.).....	67.0	65.5	63.5	60.0	56.5	49.5	41.5	28.5	22.5
9,000 sec. (2½ hr.).....	67.5	64.5	62.5	57.5	55.5	45.5	35.5	23.5	14.5
86,400 sec. (24 hr.).....	66.5	63.5	60.5	56.0	52.5	43.5	30.5	4.5	4.5

TABLE 4.—Steel V (1.15 Per Cent C)

Brine quenched after 1 hour at 925°C.; cooled to -190°C. before tempering. As-quenched hardness, 64.5 Rc

Rockwell C Hardness Obtained by Tempering at Indicated Time and Temperature									
Nominal Time of Tempering	100°C.	150°C.	200°C.	250°C.	300°C.	400°C.	500°C.	600°C.	700°C.
10 sec.....	65.0	63.5	65.0	66.5	64.0	57.5	49.0	42.5	37.5
90 sec.....	64.5	65.0	64.5	61.5	60.0	52.0	44.0*	38.5	32.0*
900 sec. (15 min.).....	65.5	66.0	62.5	59.5	55.5	49.5	41.0	32.5	24.5
9,000 sec. (2½ hr.).....	66.5	64.0	60.0*	57.5	53.0*	46.5	37.5*	30.5*	18.0
86,400 sec. (24 hr.).....	65.0	61.0	60.5	55.5	50.5	42.0*	32.0*	23.0	4.5

* Average of two specimens.

TABLE 5.—*Steel W (0.89 Per Cent C)*

Brine quenched after 1 hour at 840°C.; cooled to -70°C. before tempering. As-quenched hardness, 67.0 Rc

Rockwell C Hardness Obtained by Tempering at Indicated Time and Temperature									
Nominal Time of Tempering	100°C.	150°C.	200°C.	250°C.	300°C.	400°C.	500°C.	600°C.	700°C.
10 sec.	67.0	67.5	67.5	67.5	64.5	58.5	48.5	43.0	37.5
90 sec.	67.5	67.5	65.5	62.5	59.5	52.5	45.5	38.0	31.5
900 sec. (15 min.)	68.0	66.5	64.5	60.5	57.5	50.5	42.5	34.0	25.5
9,000 sec. (2½ hr.)	68.5	63.5	61.5	58.5	54.0	46.5	38.0	28.5	18.0
86,400 sec. (24 hr.)	67.5	62.5	59.5	55.5	52.5	44.5	33.0	22.5	12.0

TABLE 6.—*Steel T (0.75 Per Cent C)*

Brine quenched after 1 hour at 760°C.; cooled to -70°C. before tempering. As-quenched hardness, 66.5 Rc

Rockwell C Hardness Obtained by Tempering at Indicated Time and Temperature									
Nominal Time of Tempering	100°C.	150°C.	200°C.	250°C.	300°C.	400°C.	500°C.	600°C.	700°C.
10 sec.	67.0	67.5	67.5	67.0	65.5	61.5	51.5	42.5	36.5
90 sec.	66.5	67.5	65.0	61.5	58.5	51.5	44.5	38.5	29.0
900 sec. (15 min.)	67.5	66.5	62.5	59.5	56.5	49.5	42.5	34.5	22.5
9,000 sec. (2½ hr.)	66.5	64.5	59.5	58.0	53.5	47.5	38.5	28.5	16.5
86,400 sec. (24 hr.)	65.5	61.5	58.5	55.0	51.5	44.5	34.5	21.5	7.5

TABLE 7.—*Steel S (0.56 Per Cent C)*

Brine quenched after 1 hour at 820°C.; cooled to -70°C. before tempering. As-quenched hardness, 63.0 Rc

Rockwell C Hardness Obtained by Tempering at Indicated Time and Temperature									
Nominal Time of Tempering	100°C.	150°C.	200°C.	250°C.	300°C.	400°C.	500°C.	600°C.	700°C.
10 sec.	62.5	62.5	63.5	62.5	61.5	56.0	48.5	38.5	31.5
90 sec.	63.5	62.5	60.5	57.5	54.5	48.5	40.5	32.5	25.5
900 sec. (15 min.)	63.5	61.5	58.5	54.5	52.0	45.0	36.5	28.5	19.0
9,000 sec. (2½ hr.)	61.0	61.0	56.5	53.5	50.5	42.0	34.5	25.0	12.5
86,400 sec. (24 hr.)	60.5	58.5	54.5	50.5	47.5	40.5	31.5	18.5	1.5

TABLE 8.—*Steel U (0.31 Per Cent C)*

Brine quenched after 1 hour at 840°C.; cooled to -70°C. before tempering. As-quenched hardness, 46.5 Rc

Rockwell C Hardness Obtained by Tempering at Indicated Time and Temperature									
Nominal Time of Tempering	100°C.	150°C.	200°C.	250°C.	300°C.	400°C.	500°C.	600°C.	700°C.
10 sec.	47.5	48.0	49.0	49.0	46.5	45.5	35.5	26.5	21.5
90 sec.	49.0	46.0	49.5	47.5	43.5	39.5	30.5	22.5	16.0
900 sec. (15 min.)	49.0	47.5	48.0	46.0	42.5	35.5	25.5	18.5	13.5
9,000 sec. (2½ hr.)	47.5	47.0	46.5	44.0	39.5	30.5	19.5	16.0	7.0
86,400 sec. (24 hr.)	48.5	47.5	44.0	42.5	37.5	28.5	21.0	12.5	3.5

where t is the time, T the absolute temperature, Q a constant characteristic of the steel, and R the universal gas constant. This type of relationship was tried first, there-

to the hardness found), it was discovered that the parameter did not vary smoothly with the hardness, but was constant within the scatter found. From these facts, a new

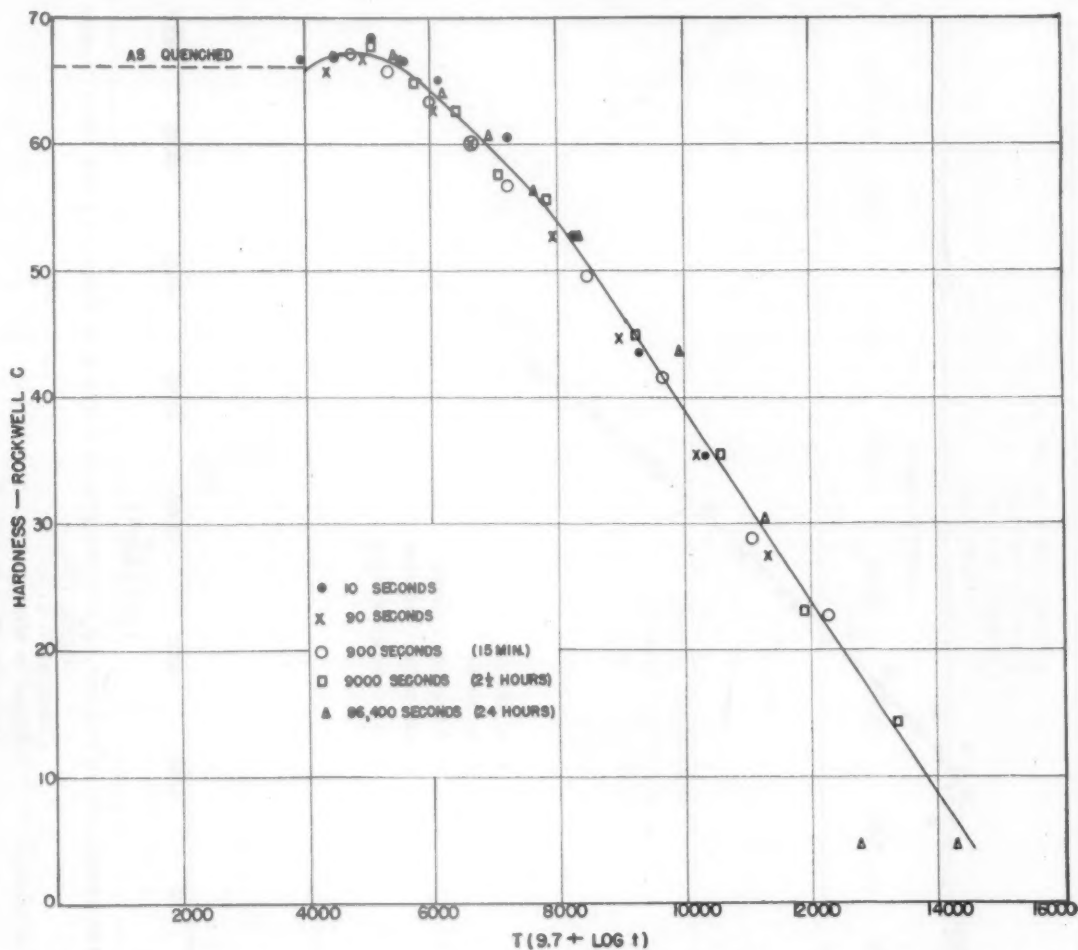


FIG. 1.—HARDNESS VS. TIME-TEMPERATURE PARAMETER FOR TEMPERING FULLY QUENCHED 0.96 PER CENT CARBON STEEL (R).

Constant = 9.7

Time t in seconds.

Temperature T in deg. K.

fore, using data on steel R. Q was calculated from the time-temperature combinations giving the same hardness, and was found not to be a constant but to vary with the hardness from 50,000 cal. per mol at Rockwell C-20 to about 12,000 cal. per mol at Rockwell C-65. Moreover, when the times and temperatures used for steel R were substituted in the parameter $te^{-Q/RT}$ (together with the value of Q appropriate

functional relationship was deduced as explained in appendix A. This may be put in the form:

$$\text{Hardness} = f(T \log t/t_0) \quad [1]$$

where t_0 is a constant, characteristic of the steel. An equivalent form, useful for numerical calculation, is:

$$\text{Hardness} = f[T(c + \log t)] \quad [2]$$

where c is a constant, characteristic of the steel. These equations imply nothing as to the way in which hardness varies with the parameter $T \log t/t_0$ or $T(c + \log t)$,

long tempering time and a low temperature, but nothing is said as to what that hardness is.

To obtain a numerical value of c ,

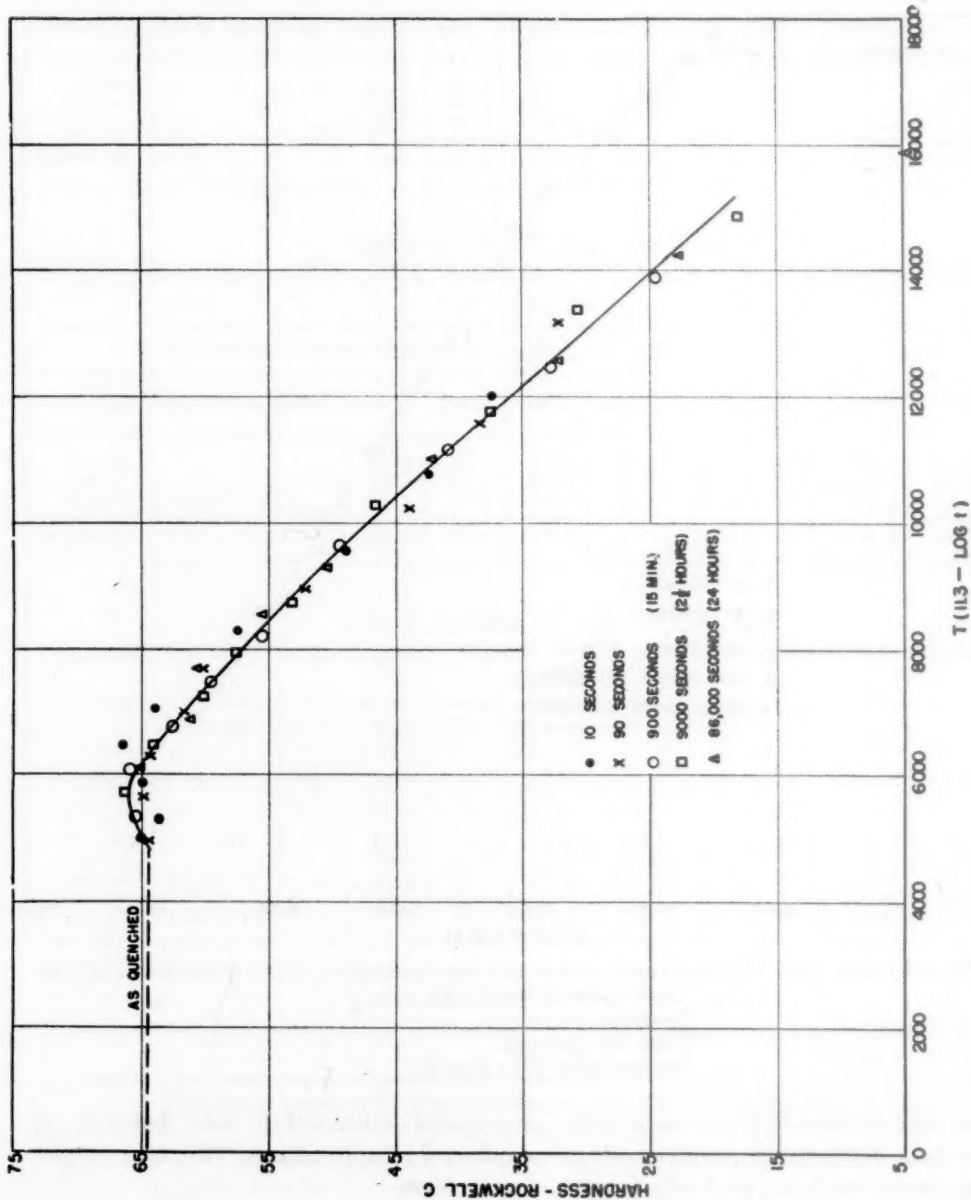


FIG. 2.—HARDNESS VS. TIME-TEMPERATURE PARAMETER FOR TEMPERING FULLY QUENCHED 1.15 PER CENT CARBON STEEL (V).

Constant = 11.3.

Time t in seconds.

Temperature T in deg. K.

but merely state that a functional relationship between hardness and parameter exists. In other words, as long as the parameter has a constant value, the same hardness is produced with a short tempering time and a high temperature as with a

combinations giving the same hardness were found for steel R by plotting the hardness data of Table 3 against time (on a logarithmic scale) for each temperature and interpolating to obtain the time necessary to give about 15 different hard-

nesses. Pairs of time and temperature combinations that gave equal hardnesses 3 were then substituted in Eq. 2, and the results were plotted in Fig. 1. All points

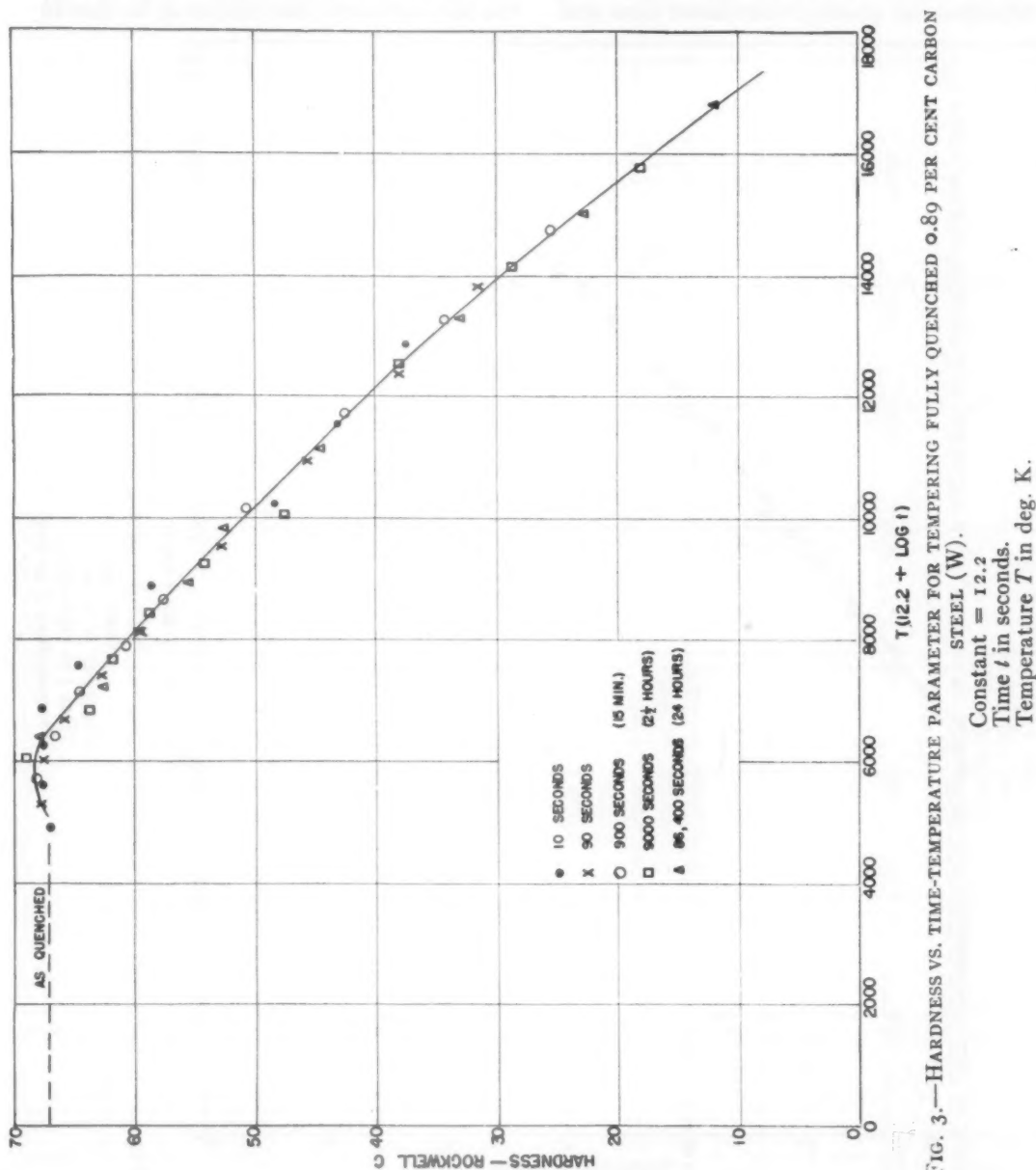


FIG. 3.—HARDNESS VS. TIME-TEMPERATURE PARAMETER FOR TEMPERING FULLY QUENCHED 0.89 PER CENT CARBON

were substituted in the derived equation:

$$-c = \frac{T_1 \log t_1 - T_2 \log t_2}{T_1 - T_2} \quad [3]$$

The values obtained with the various pairs of combinations used were simply averaged, with the result $c = 9.7$ (for times in seconds). The experimental data of Table

but one fall on a single line, with a scatter of less than $\pm 1\frac{1}{2}$ points Rockwell C, which is little more than the scatter expected in the hardness measurements. Since Eq. 2 worked so well for steel R, it was next tried on the other experimental heats, a value of c being computed separately for each one. Figs. 2 to 6 show the

results. Again, the scatter is in general no more than would be expected from the experimental errors in hardness, time and

specimens delayed the heating. A few other points also deviate somewhat from the plotted curve, but this may be due to

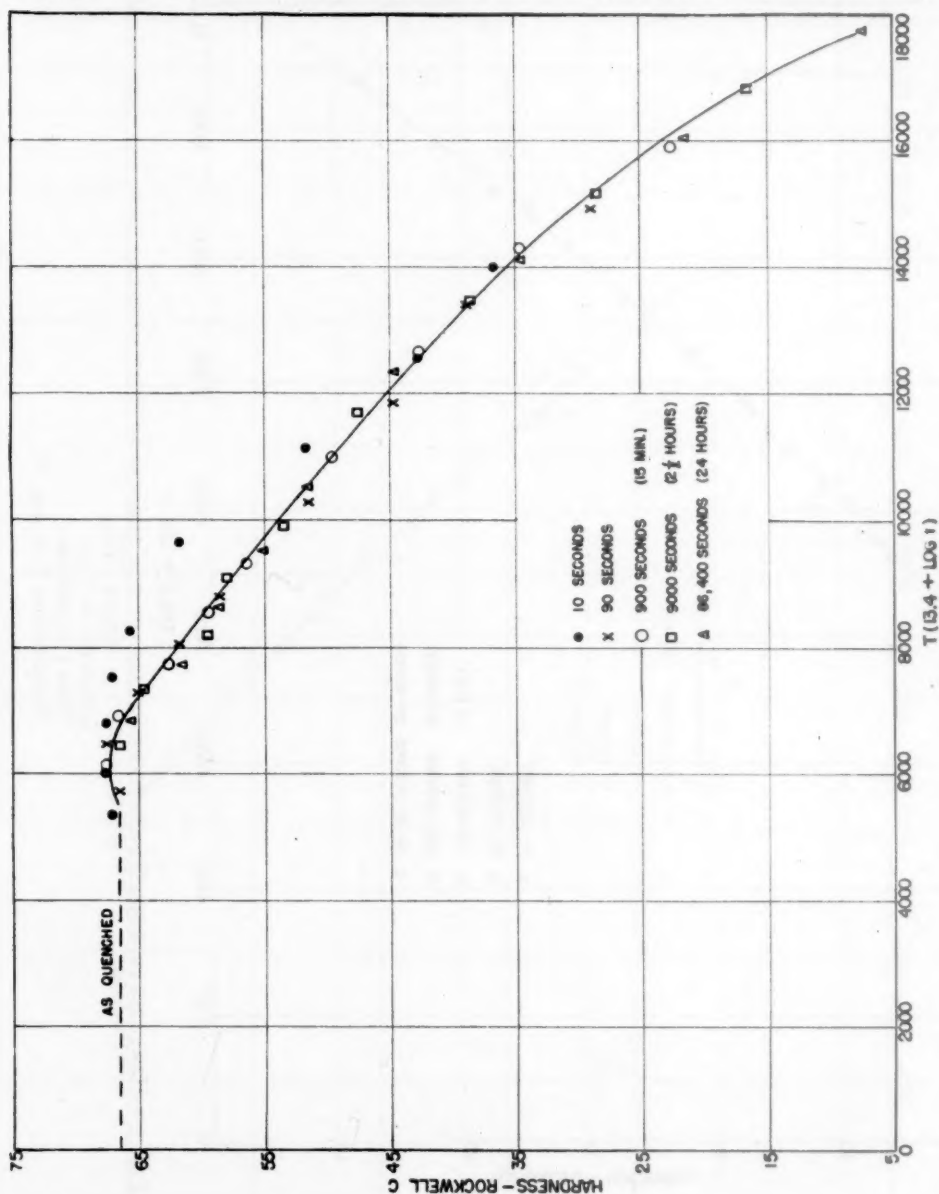


FIG. 4.—HARDNESS VS. TIME-TEMPERATURE PARAMETER FOR TEMPERING FULLY QUENCHED 0.74 PER CENT CARBON STEEL (T).

Constant = 13.4.

Time t in seconds.

Temperature T in deg. K.

temperature measurements. The hardnesses for the disks tempered 10 sec. form an exception, falling on the high side of the curves. This deviation merely indicates that the time at temperature was significantly less than the nominal 10 sec., presumably because the perforated sheet-metal containers used in treating these

minor errors in the heat-treatment, grinding, or hardness measurement.

Application of Functional Relationship to Data in the Metallurgical Literature

In order to determine whether the relation was valid for the tempering of alloy steels, it was applied to the data for

seven steels given by Bain.⁴ These steels were stated to be quenched and presumably had a martensitic structure before

for each steel, Eq. 2 fits the data very well, even though several of the steels displayed marked secondary hardening. (Fig. 7 is an

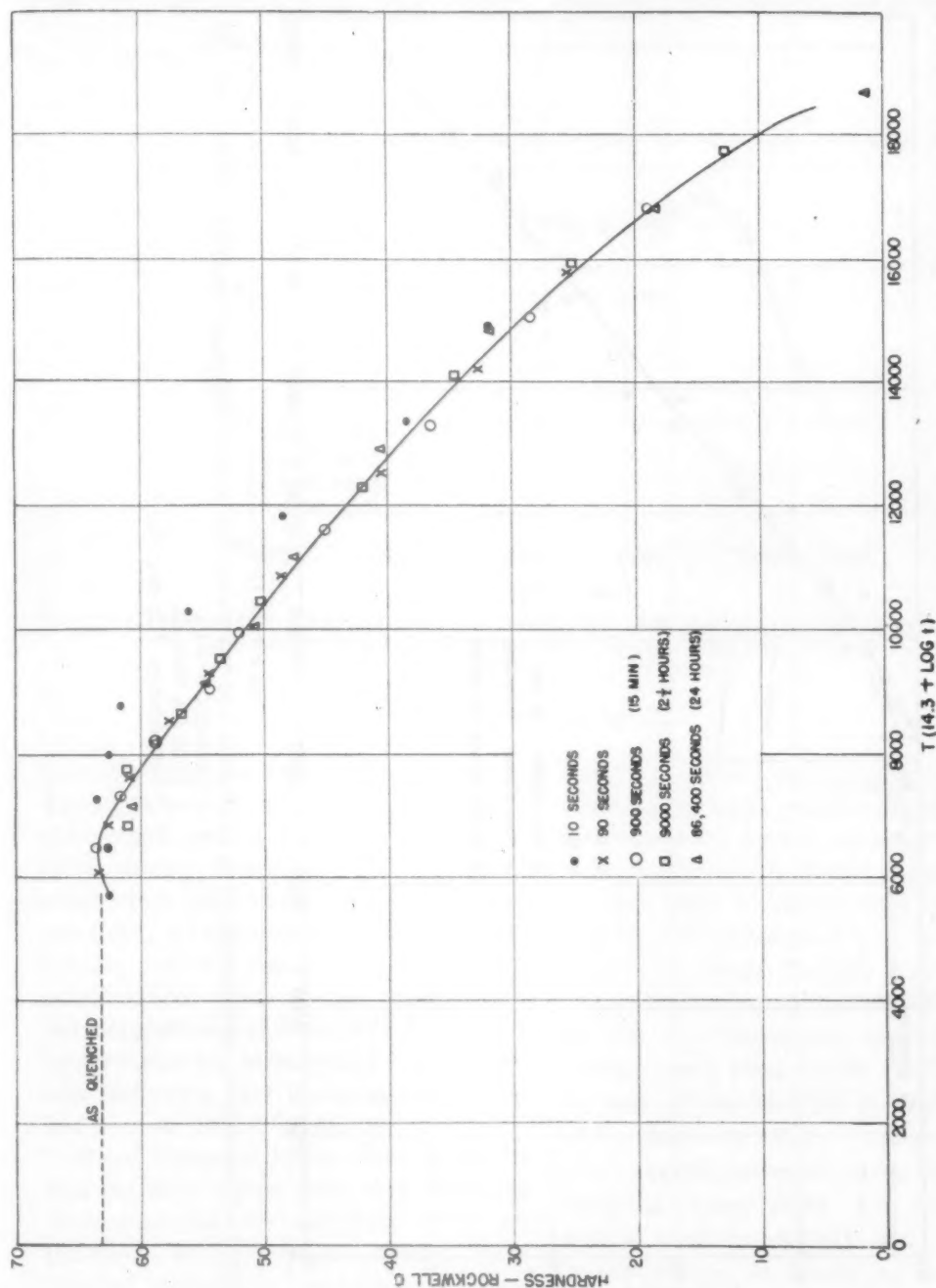


FIG. 5.—HARDNESS VS. TIME-TEMPERATURE PARAMETER FOR TEMPERING FULLY QUENCHED 0.56 PER CENT CARBON STEEL (S).
Constant = 14.3.
Time t in seconds.
Temperature T in deg. K.

tempering, but apparently no precautions were taken to eliminate retained austenite. It was found that, with the c computed

example.) Occasional deviations can be accounted for readily, if it is considered that Bain did not give any experimental

points (except for one plain carbon steel) and the values had to be taken from his smoothed curves.

could be found in the literature.* These include the values obtained by Austin and Norris² on six plain carbon hypereutectoid

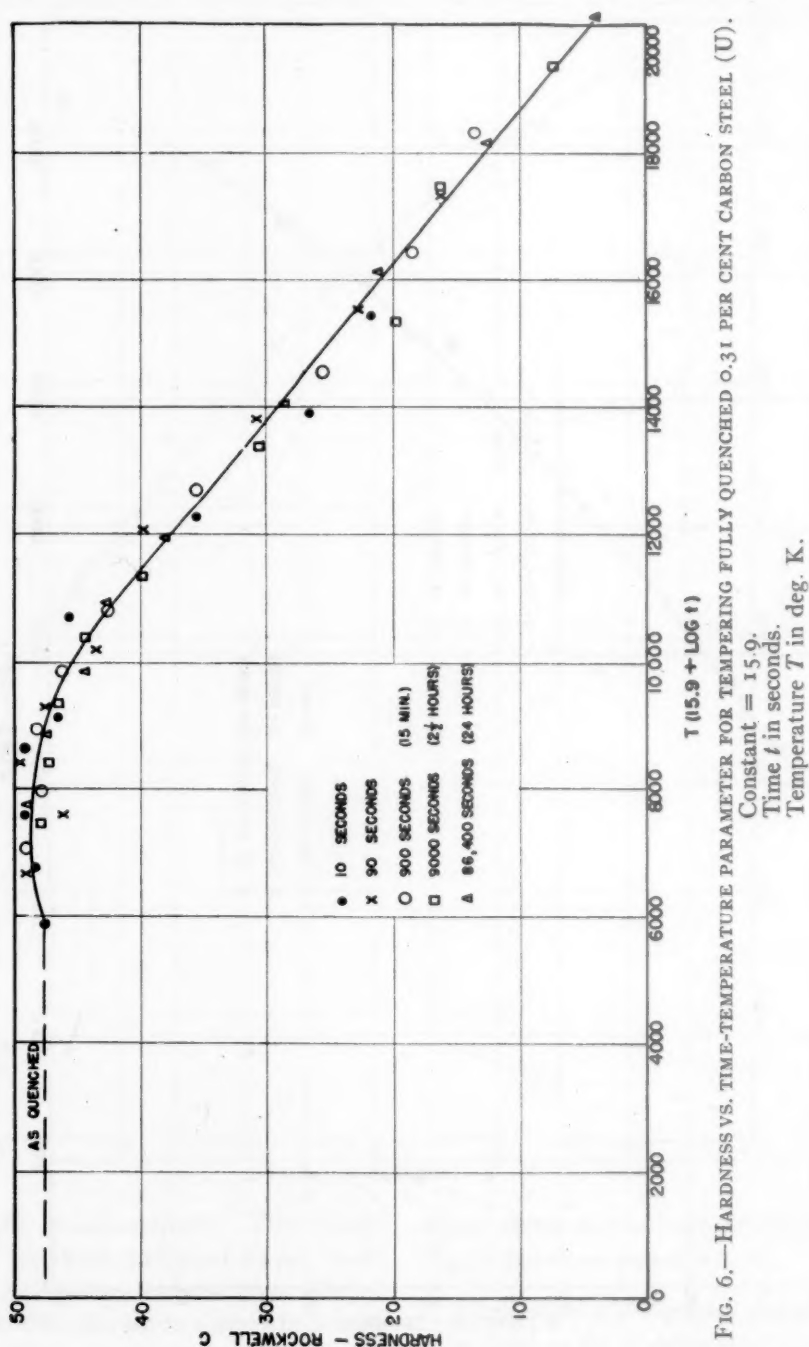


FIG. 6.—HARDNESS VS. TIME-TEMPERATURE PARAMETER FOR TEMPERING FULLY QUENCHED 0.31 PER CENT CARBON STEEL (U).

In order to test Eq. 2 further, it was applied to all the data covering a wide range of times and temperatures that

steels austenitized one hour at 1000°C.,

* Subsequent to the preparation of this manuscript, some additional data were found.

quenched in water in the form of pieces $\frac{1}{2}$ -in. long and $\frac{3}{8}$ in. in diameter, tempered at three temperatures for times varying from 30 min. to 125 hr., and water-

for each. Curves are plotted in Fig. 12 for all four initial structures, using the average value of c . Each initial structure gives a curve with little scatter when plotted in this

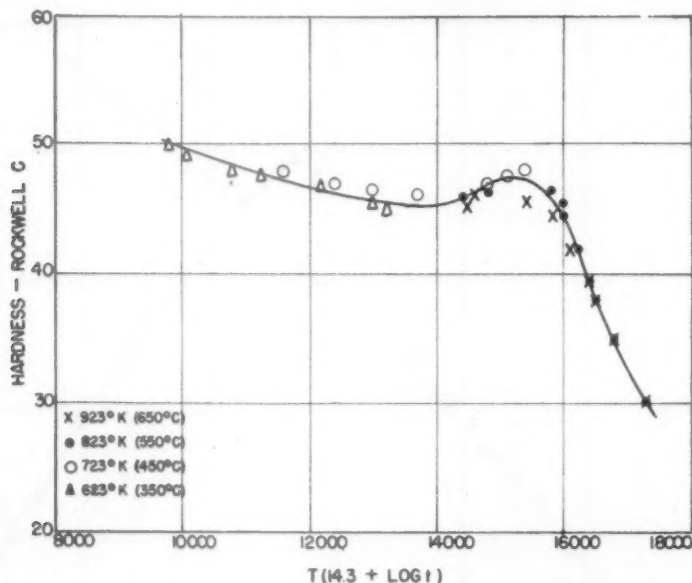


FIG. 7.—HARDNESS VS. TIME-TEMPERATURE PARAMETER FOR TEMPERING QUENCHED 2 PER CENT MOLYBDENUM, 0.35 PER CENT CARBON STEEL. (Data from Bain.⁴)

Constant = 14.3.

Time t in seconds.

Temperature T in deg. K.

quenched from the tempering temperature. The steels were of interest in that considerable graphitization occurred in some of them during tempering. For the three steels where there was little graphitization, practically all the points fall along smooth curves; for the steels that graphitized considerably, most of the points again fall along smooth curves, but a few for the longer times fall considerably lower, probably indicating that the combined carbon had been reduced (Fig. 8).

Engel³ tempered $\frac{1}{10}$ -in. thick disks of a 0.94 per cent carbon steel after obtaining microstructures of martensite (plus retained austenite), lower bainite (plus retained austenite), fine nodular pearlite, and moderately coarse pearlite. Figs. 9 to 11 show hardness versus the time-temperature parameter for the first three of these, the value of c being calculated separately

way, except for the samples nominally tempered for 2 sec., which clearly were not at temperature for this whole time.

In a recent paper, Loria⁶ has given data for five heats of cobalt steel, containing 0.70 per cent carbon and ranging from 0 to 11 per cent cobalt. Samples were quenched to martensite, then tempered for 1, 10 and 30 min. at temperatures ranging, for the various steels, from 100° to 710°C. As may be seen by the example in Fig. 13, most of the points fall within ± 1 point Rockwell C of a smooth parametric curve, the extreme deviation being about ± 2 points. The scatter increases slightly with increasing cobalt content. It should be noted, however, that the data of Loria are insufficient to permit determination of the best value for c ; the latter had to be approximated by a method that is described later.

Value of Constant c

To determine the effect of carbon content upon c , the values of c obtained for the series of five experimental induction-

pairs of time-temperature combinations giving the same hardness scatter very widely, and their average cannot be considered very accurate. Moreover, since the

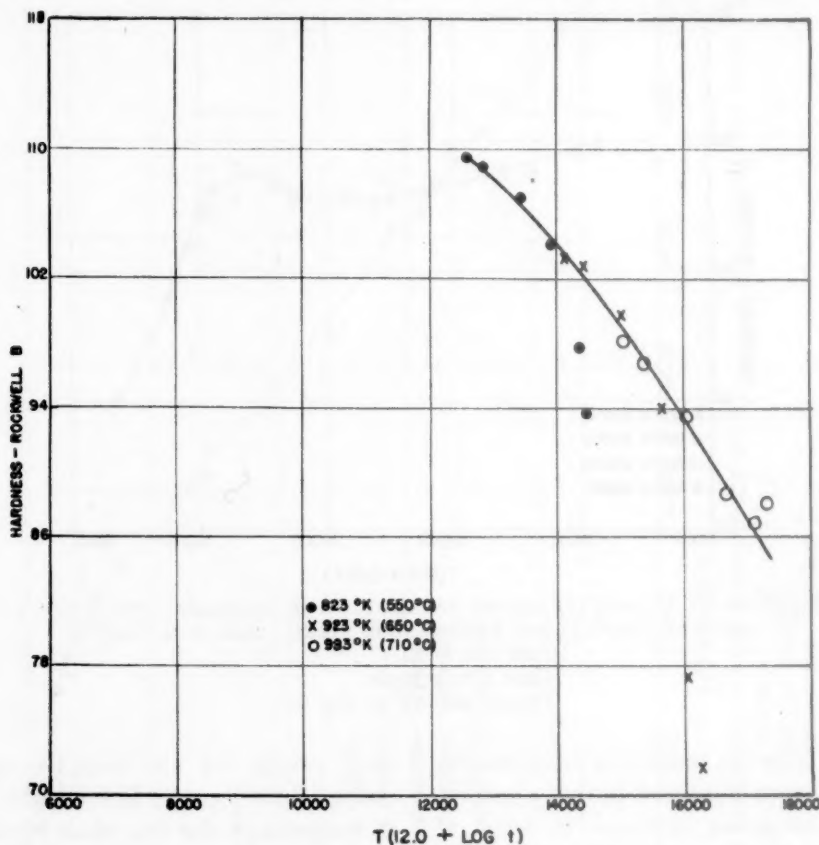


FIG. 8.—HARDNESS VS. TIME-TEMPERATURE PARAMETER FOR 0.97 PER CENT CARBON STEEL (F) WHICH GRAPHITIZED DURING TEMPERING. (Data from Austin and Norris.²)

Constant = 12.0.

Time t in seconds.

Temperature T in deg. K.

furnace heats (S, T, U, V, W) are plotted in Fig. 14. The points fall very close to a straight line, corresponding to the equation:

$$c = 17.7 - 5.8 \times (\text{per cent carbon}),$$

for time in seconds [4]

$$c = 21.3 - 5.8 \times (\text{per cent carbon}),$$

for time in hours

A survey of the values of c obtained for heat R and for the steels considered in the literature indicates that they do not fall close to this curve. However, the numerical values of c obtained from the different

scatter of the hardness data from the resulting functional curve is always small, it is clear that this scatter must be rather insensitive to the value of c used.

To check this insensitiveness to variation in the value of c , the data for steel R were plotted using the value of c indicated by Fig. 14, and the data for the other five experimental heats were plotted using the value $c = 13.0$ (for time in seconds), which is about the average for the five steels. The scatter was found to be but little greater than that found when a separate c

was used for each, as may be seen from the instance shown in Fig. 15.

As another check of the slight effect that the value of c has upon the results,

obtained with $c = 10.0$ and $c = 16.0$ are within $\pm 10^\circ\text{C.}$ of that with $c = 13.0$. To determine the effect of such variation upon the hardness, the derived tempera-

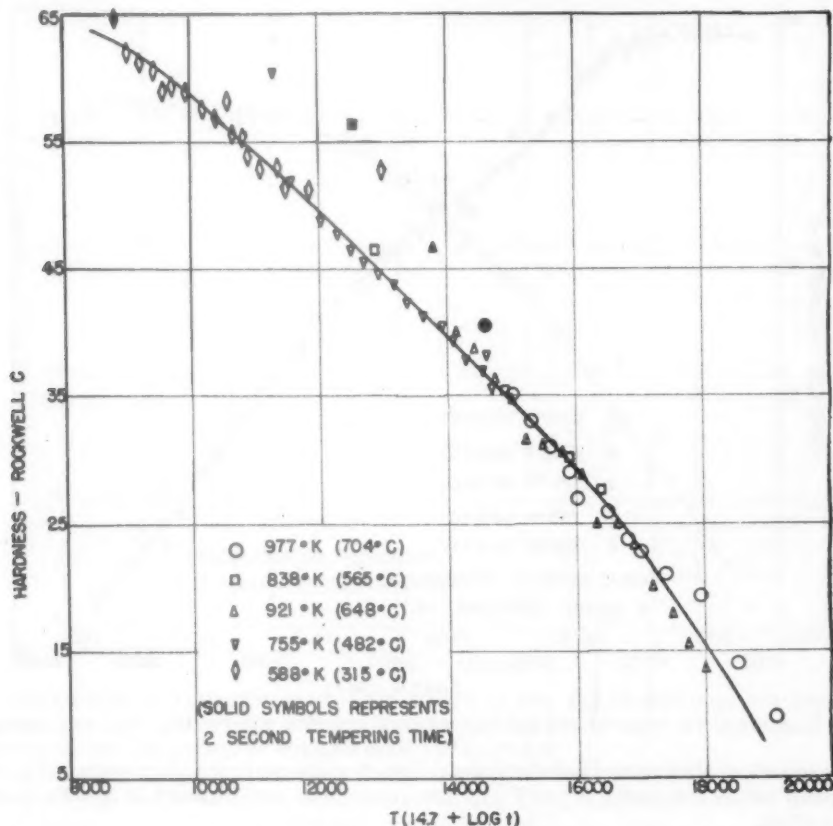


FIG. 9.—HARDNESS VS. TIME-TEMPERATURE PARAMETER FOR TEMPERING 0.94 PER CENT CARBON STEEL. (Data from Engel.³)

Structure before tempering: martensite (plus retained austenite)

Treatment before tempering: 1500°F., 10 min., brine quench.

Constant = 14.7.

Time t in seconds.

Temperature T in deg. K.

there was calculated the temperature necessary to obtain with a 10-hr. temper the hardness reached in 1 hr. at 550°C. The following relationship for constant degree of tempering, readily obtained from Eq. 2, was used:

$$T_1(c + \log t_1) = T_2(c + \log t_2) \quad [5]$$

If the value of c (for time in seconds) is assumed to be 10.0, 13.0, and 16.0, the temperature is found to be 493° , 503° , and 510°C. , respectively, so that the values

and their corresponding time of 10 hr. were substituted in the parameter for the experimental steel T , using $c = 13.0$, and the resultant hardnesses were found from the hardness vs. parameter plot for that steel. These hardnesses are 36.5, 35.4, and 34.9 Rockwell C, respectively. Thus, for this typical case, it appears that the use of an average c value of 13.0 in cases where the true value is 10.0 or 16.0 introduces a hardness error of the order of but one point Rockwell C.

Form of the Function

Nothing has been said yet concerning the particular function of the hardness parameter that represents the hardness

scale (though in opposite direction) and apparently is not affected by the use of $T(c + \log t)$ in place of $\log t$. In either case, marked deviations from linearity

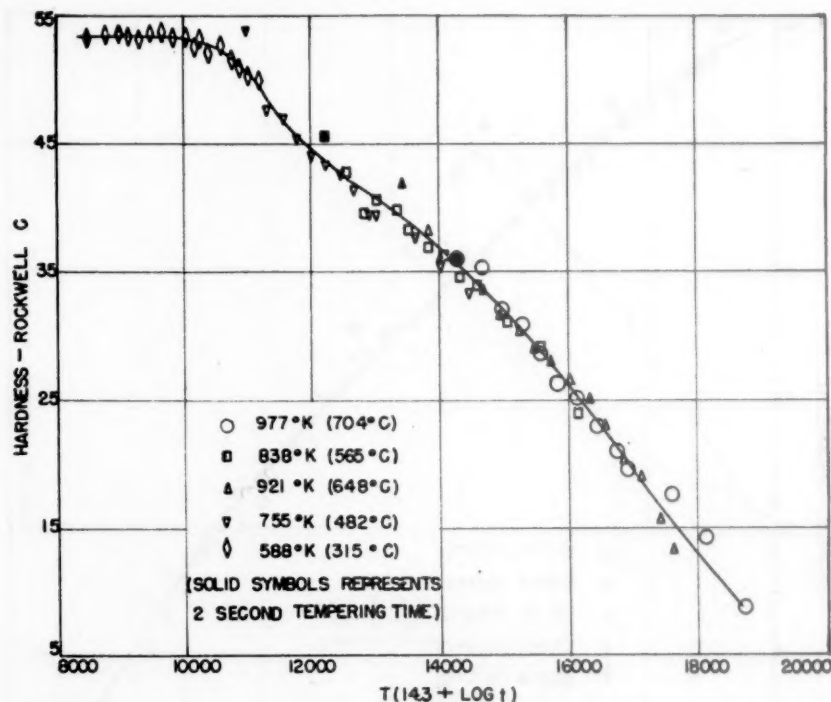


FIG. 10.—HARDNESS VS. TIME-TEMPERATURE PARAMETER FOR TEMPERING 0.94 PER CENT CARBON STEEL. (Data from Engel.³)

Structure before tempering: bainite (plus retained austenite).

Treatment before tempering: 1500°F., 10 min.; quench in lead-bismuth at 600°F., hold 30 min. Quench in water.

Constant = 14.3.

Time t in seconds.

Temperature T in deg. K.

(other than that it is univalued). Previous investigators²⁻⁴ have noted that, over a considerable range, the hardness for a particular tempering temperature varies almost linearly with the logarithm of the time, and they state that this linearity range is somewhat better when Brinell rather than Rockwell hardness is used. The figures indicate that the Rockwell hardness also varies almost linearly with the time-temperature parameter $T(c + \log t)$. The hardness data for steel S were replotted against $T(c + \log t)$ after conversion⁷ to the Brinell scale. The deviation from linearity was about the same with either

occur at hardnesses within 3 Rockwell C (about 30 Brinell or Vickers) of the hardness of the untempered steel, as well as over a wide range in steels (containing large percentages of carbide-forming elements) that display pronounced secondary hardening.

It was found that Rockwell C hardnesses of the five plain carbon steels S, T, U, V, W, when plotted (for times in seconds) against $T(13.0 + \log t)$, lie on curves having approximately the same slope. The average slope for the five steels was found to be -0.00457 Rockwell C per unit of $T(13.0 + \log t)$, where T is in degrees K.

and t is in seconds. The intercepts of the (extrapolated) linear hardness curves with $T(13.0 + \log t) = 0$ lie on a smooth curve when plotted as a function of carbon con-

use of the Rockwell C scale is generally not recommended. At the high hardness end, the equation does not hold when closer than 3 points Rockwell C to the

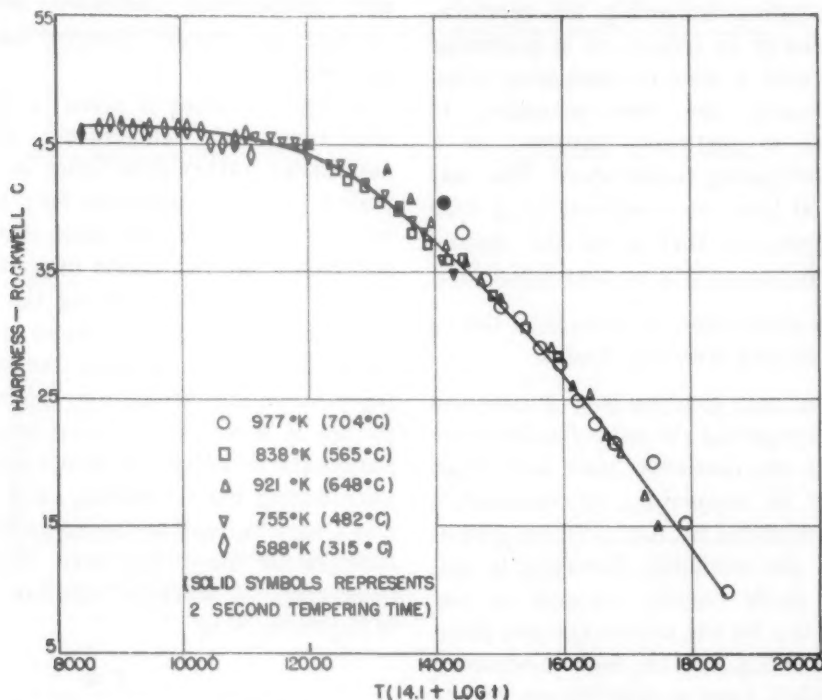


FIG. 11.—HARDNESS VS. TIME-TEMPERATURE PARAMETER FOR TEMPERING 0.94 PER CENT CARBON STEEL. (Data from Engel.³)

Structure before tempering: fine pearlite.

Treatment before tempering: 1500°F., 10 min. Quench in lead at 900°F., hold 30 sec. Quench in water.

Constant = 14.1.

Time t in seconds.

Temperature T in deg. K.

tent. Thus, the straight-line portion of the tempering curves for the five plain carbon steels is given simply by the equations:

$$R_c = H_c - 0.00457T(13.0 + \log t), \text{ for } T \text{ in deg. K., } t \text{ in sec. [6]}$$

$$R_c = H_c - 0.00254T(13.0 + \log t), \text{ for } T \text{ in deg. R., } t \text{ in sec.}$$

Here, R_c is the Rockwell C hardness of the steel and H_c is the "characteristic hardness" given for these steels in Fig. 16, being the hardness found by extrapolating the straight-line portion of the curves to $T(13.0 + \log t) = 0$. This relation begins to fail below 25 Rockwell C; where the

hardness before tempering (see Fig. 15).^{*} Since non-carbide-forming elements apparently shift the tempering curve with little change of slope,⁴ Eq. 6 should apply to alloy steels not containing large quantities of carbide-forming elements, provided the value of H_c appropriate to the steel and the structure prior to tempering is used. Within these limitations, the accuracy of the equation is perhaps ± 3 points Rockwell C.

* The hardness before tempering for fully hardened steel is available in the literature.⁴ For incompletely hardened steel, the hardness before tempering is a function of the cooling rate and composition, but the linear relationship and its slope should still apply (Fig. 12).

II. APPLICATIONS

The results described in the foregoing pages should find their greatest practical use in calculating, for any steel and any structure before tempering, the temperature necessary to temper to a particular hardness with a selected tempering time, or, conversely, the time necessary to temper to a particular hardness at a selected tempering temperature. The case in which at least one combination of time and temperature that gives the desired hardness is known will be considered first.

One Time-temperature Combination Giving Desired Hardness Known

If two or more combinations of time and temperature giving the same hardness are known for the particular steel and structure prior to tempering, the constant c may be calculated by Eq. 3. Unless extensive data are available, however, it will probably prove equally accurate to use the value of c for the carbon content given by Fig. 14 or Eq. 4. If the highest accuracy is not needed, some average figure, appropriate to the range of carbon contents under consideration, may be used. Thus, for the usual steels for heat-treated parts, containing 0.25–0.40 per cent carbon, a value of 16 for times in seconds or $19\frac{1}{2}$ for times in hours should be sufficiently close, while for tool steels of 0.90 to 1.20 per cent carbon the constant could be taken as $11\frac{1}{2}$ for times in seconds or 15 for times in hours.

Once the value of the constant and one combination of time and temperature giving the desired hardness are known, other combinations are readily found by Eq. 5. To reduce the amount of calculation still further, Figs. 17 and 18, in which this equation has been plotted for $c = 19\frac{1}{2}$ and $c = 15$, respectively (for times in hours), may be used.

To use these charts, locate on the pertinent graph the point corresponding to the time and temperature that are

known to produce the desired hardness. Draw a line (real or imaginary) through this point and parallel to the neighboring lines of the chart. All combinations of time and temperature indicated by values on this line should produce the desired hardness.

Tempering times as given in this paper are times at temperature (at least nominally), rather than times in the tempering furnace. Correction may be made, by integration of the time-temperature parameter, for the effects of slow heating or slow cooling in increasing the effective tempering time but in most cases the correction can be neglected (see example 2 below). For this integration, it is necessary to use a form of the time-temperature parameter in which the temperature may vary during the tempering. (Eqs. 1, 2, 3, and 5 were derived on the assumption that temperature does *not* vary during the tempering.) A suitable equation, derived in appendix B, is:

$$dM = \frac{T dt}{(2.303) 10^{\frac{M}{T} - c}} \quad [7]$$

where M is the parameter that reduces, when T does not vary during the cycle and for appropriate boundary conditions, to the $T \log t/t_0$ and $T(c + \log t)$ used in Eqs. 1 and 2. Eq. 7 is of use not only for cases of slow heating or cooling, but also when dealing with cases where a tempered part is subsequently reheated to a temperature at which further tempering may occur, as in stress-relieving treatments.

A few words may be desirable as to the matter of units. The hardness (structure, or degree of tempering) may be expressed in any system, since Eq. 5 applies only when the hardness (structure, or degree of tempering) is kept constant. Temperature appears as a ratio, so either Centigrade Absolute ($^{\circ}\text{K.} = ^{\circ}\text{C.} + 273$) or Fahrenheit Absolute ($^{\circ}\text{R.} = ^{\circ}\text{F.} + 460$) may be used. The constant c must be in units consistent

with t ; changing from seconds to hours, however, simply involves adding $\log 3600 = 3.57$ to c for seconds. Also, the values for c mentioned apply when using \log_{10} . If

1150°F., while obtaining the same hardness. What should the tempering time be at this temperature?

Solution.—Since this is a 0.30 per cent

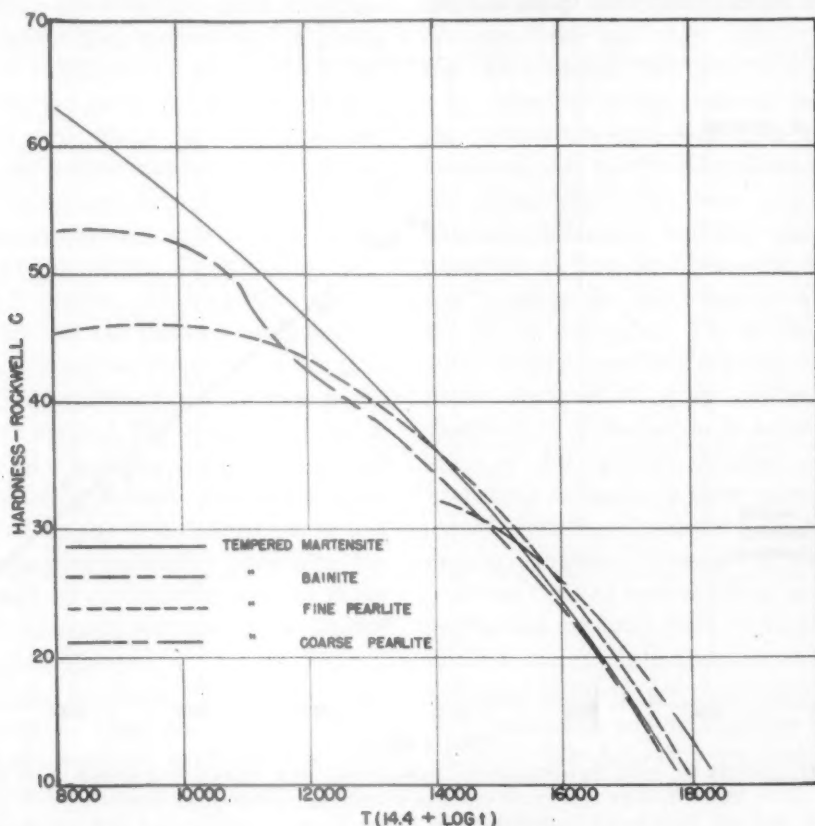


FIG. 12.—HARDNESS VS. TIME-TEMPERATURE PARAMETER FOR TEMPERING 0.94 PER CENT CARBON STEEL FROM VARIOUS INITIAL STRUCTURES. (Data from Engel.³)

Temperature of formation of isothermal structures: bainite, 600°F.; fine pearlite, 900°F.; coarse pearlite, 1200°F.

Constant = 14.4
Time t in seconds.
Temperature T in deg. K.

it is desired to use \ln , the values quoted for c (and for the parameter) must be multiplied by $\ln_{10} 10 = 2.30$.

Example No. 1.—A nickel-chromium-molybdenum steel containing 0.30 per cent carbon is found to have a hardness of Rockwell C-34½ when austenitized 1 hr. at 1600°F., oil-quenched as a ⅝-in. square, tempered 5½ hr. at 1020°F. and water-quenched from the temper. To avoid the possible effects of temper-brittleness, it is desired to change the temperature to

carbon steel, refer to Fig. 17. It is there found that the point for 5½ hr. at 1020°F. is slightly above the line marked "Hardness Difference = 64." An imaginary line through this point parallel to line 64 intersects the 1150° abscissa at 0.14 hr., or 8 minutes.

Alternative Solution.—The time can also be found without Fig. 17 by using the parameter $T(c + \log t)$. Since this is a 0.30 per cent carbon steel, take $c = 19.5$. Substituting in Eq. 5, $T_1 = 1480^\circ\text{R.}$,

$T_2 = 1610^\circ\text{R.}$, and $t_1 = 5.5$; and solving for t_2 , it is found that $t_2 = 0.128 \text{ hr.} = 7.7 \text{ minutes.}$

Experimental Result.—Samples of the steel were austenitized and quenched as

carbon steel, assume (Fig. 14) $c = 19$. At the end of 4 hr., the parameter

$$M = T(c + \log t) = 1600(19 + \log 4) = 31,363$$

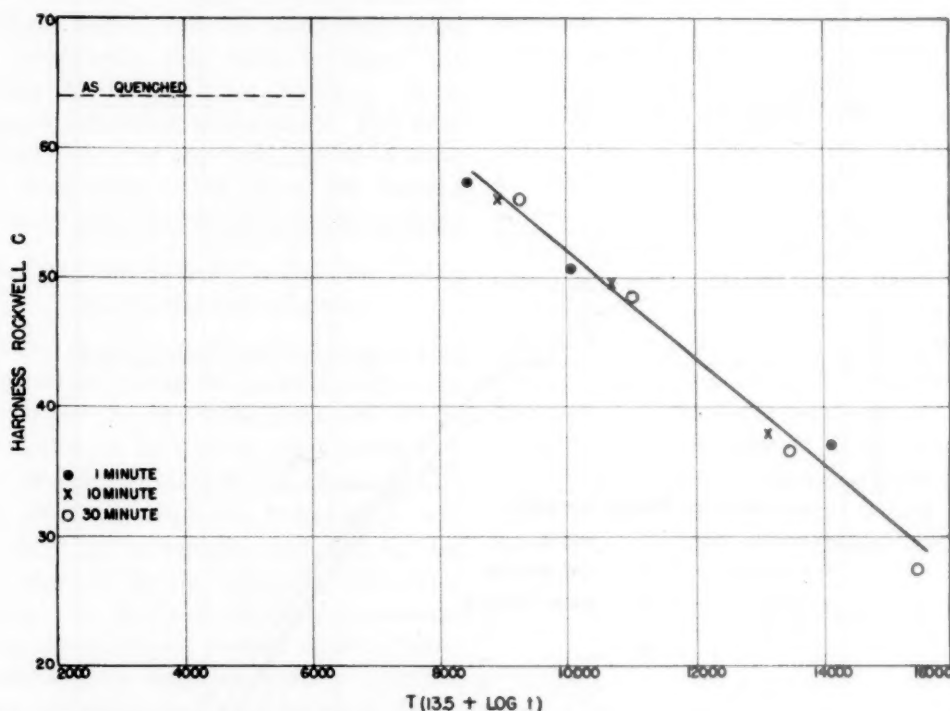


FIG. 13.—HARDNESS VS. TIME-TEMPERATURE PARAMETER FOR FULLY QUENCHED 4.20 PER CENT COBALT, 0.71 PER CENT CARBON STEEL (C). (Data from Loria.⁶)

Constant = 13.5.

Time t in seconds.

Temperature T in deg. K.

described, then tempered in salt for 8 min. at 1150°F. and water-quenched from the temper. The average hardness was found to be Rockwell C-34½.

Example No. 2.—A specimen of high-alloy steel containing 0.40 per cent carbon is tempered 4 hr. at 1140°F. (1600°R.) and then cooled at a constant rate of 500°F. per hour down to 140°F. (600°R.). It is desired to obtain the same hardness in another specimen of the steel (which received the same treatment prior to tempering) also tempered at 1140°F. but quenched from the temper. What should the tempering time be for this second specimen?

Solution.—Since this is a 0.40 per cent

For times between 4 and 6 hr., Eq. 7 must be used, substituting $T = 3600 - 500t$. Using the initial condition $M = 31,363$ at $t = 4$ and integrating step by step, it is found that $M = 31,378$ at $t = 6$. Substituting this value in $M = 1600(19 + \log t)$, t is found to be 4.085 hr., or 4 hr., 5 minutes.

No Time-temperature Combination Giving Desired Hardness Known

If it is desired to determine the time or the temperature to temper a steel to a desired hardness, using a selected temperature or time, and no combination of time and temperature that gives this hardness is known, the recommended procedure is

to find one such combination and then apply the methods of the preceding section.

If the hardnesses obtained with two or more combinations of time and temperature are known for the steel and initial structure under consideration, a combination giving the desired hardness can usually be found by interpolation methods. If all the known hardnesses were found for one tempering time, the hardnesses may be plotted against temperature on any convenient scale. If all the known hardnesses were found for one tempering temperature, the hardnesses may be plotted against the logarithm of the time (or against the time on semilogarithmic paper). If neither temperature nor time has been kept constant, the hardnesses can be plotted against $T(c + \log t)$, choosing the value of c and the units as explained in the preceding section. Except for hardnesses close to the untempered value and for steels showing secondary hardening, the plots should be sufficiently close to linear to permit interpolation and, to a limited extent, extrapolation.

If only the hardness obtained with one combination of time and temperature is known, and secondary hardness is believed absent, it is possible to obtain an approximate answer by the use of Eq. 6, or of the hardness difference values (derived from Eq. 6 as $H_c - R_c$) that are indicated on Figs. 17 or 18.* For this purpose, the hardness difference value indicated by the figure or equation is simply added to the measured hardness value to give a so-called "characteristic hardness" of the steel (which depends on the composition and the structure before tempering, but is not equal to and should not be confused with the hardness before tempering). To obtain

approximately the hardness that will result from any selected combination of time and temperature, the hardness difference corresponding to this combination is read from the figure (or computed by the equation) and then subtracted from the characteristic hardness just found. If it is desired to obtain, instead, the tempering treatment that will give a desired hardness, this hardness is subtracted from the characteristic hardness to give a new hardness difference, and the various combinations of time and temperature sought will be along the chart line (or will satisfy Eq. 6) for this value. The hardness difference values do not hold for steel hardnesses below Rockwell C-25 or within 3 points Rockwell C of the hardness before tempering, or for steels showing secondary hardening (containing large percentages of carbide-forming elements such as molybdenum, tungsten, chromium or vanadium).

If one type of steel is being used for the production of some part, it is possible to make a rather close approximation of the time and temperature combinations necessary to produce a given hardness in various heats by the following method: For one heat of steel, quench to the structure that is being produced by the heat-treatment employed. Temper pieces for a convenient time at various temperatures and plot the hardness obtained as a function of temperature. For subsequent heats, the hardness at only one temperature need be determined (using the tempering time for which the plot was drawn), and a line parallel to the originally constructed curve can be drawn through this one point. The temperature necessary to produce the desired hardness with the selected time can be then read from this new curve. If in production it is desired to use some other tempering time, the equivalent temperature can now be readily found by using the parametric form, or Fig. 17 or 18. (This method will not hold if the composition or quenching conditions

* Because the ϵ values employed in Figs. 17 and 18 are somewhat different from those of Eq. 6, a hardness difference value ($H_c - R_c$) calculated from the equation is not exactly constant over the entire length of the lines on the figures. Those values shown satisfy Eq. 6 at time = 3 hr. (selected as an average tempering time), and the deviations from Eq. 6 at the other times are negligible in view of the relatively low accuracy of that equation.

change so much from heat to heat that different metallurgical structures are obtained prior to tempering.)

It is not believed that, at present, accu-

1.50 per cent tungsten, 0.80 per cent chromium, and 0.20 per cent vanadium. The lower critical temperature (A_{c1}) is 1350°F. The hardness after normalizing in

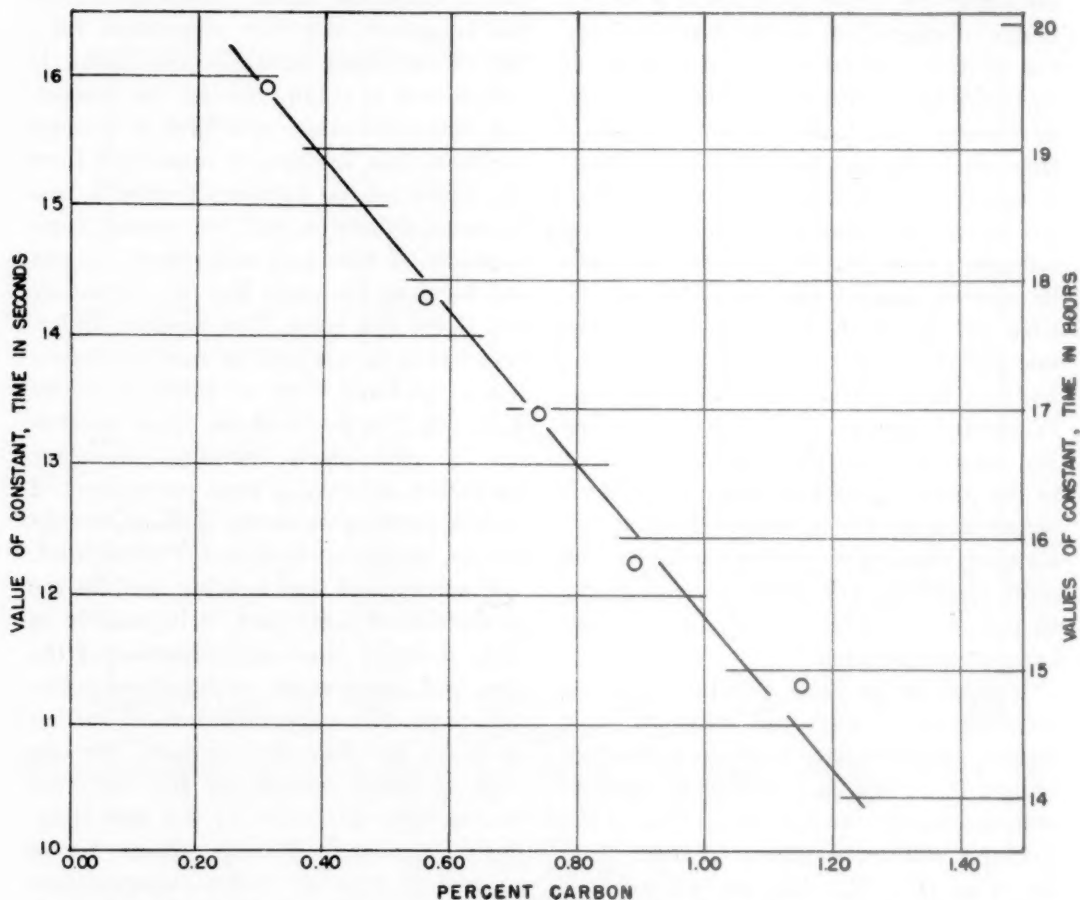


FIG. 14.—VARIATION OF CONSTANT IN TIME-TEMPERATURE PARAMETER WITH CARBON CONTENT FOR TEMPERING FULLY QUENCHED PLAIN-CARBON STEELS.

rate tempering predictions can be made on a steel for which there are no experimental tempering data. A rough approximation is possible, however, by comparison with tempering data for other steels of similar composition, together with the use of Eq. 6 or Fig. 17 or 18.

Example No. 3.—It is desired to determine (without experimental work) whether it is practical to soften a nondeforming tool steel to Rockwell B-96 (C-19) by subcritical annealing (tempering) after normalizing in 2-in. rounds. The composition of the steel is: 1.15 per cent carbon,

2-in. rounds and tempering 1 hr., is known to be:

TEMPERING TEMPERATURE, DEG. F.	HARDNESS ROCKWELL C
900.....	41
1000.....	40
1100.....	37
1200.....	31
1300.....	25

(These values are hypothetical, being assumed for purposes of illustration.)

Solution.—The hardness obtained with 1-hr. tempering are plotted (on linear coordinate paper) against the tempering

temperatures. Above 1100°F., the curve is almost linear, and when extrapolated to Rockwell C-19 indicates a tempering

1400°F. will be obtained at 1325° in 4½ hr. This is a practical time for tempering, therefore it appears that the desired

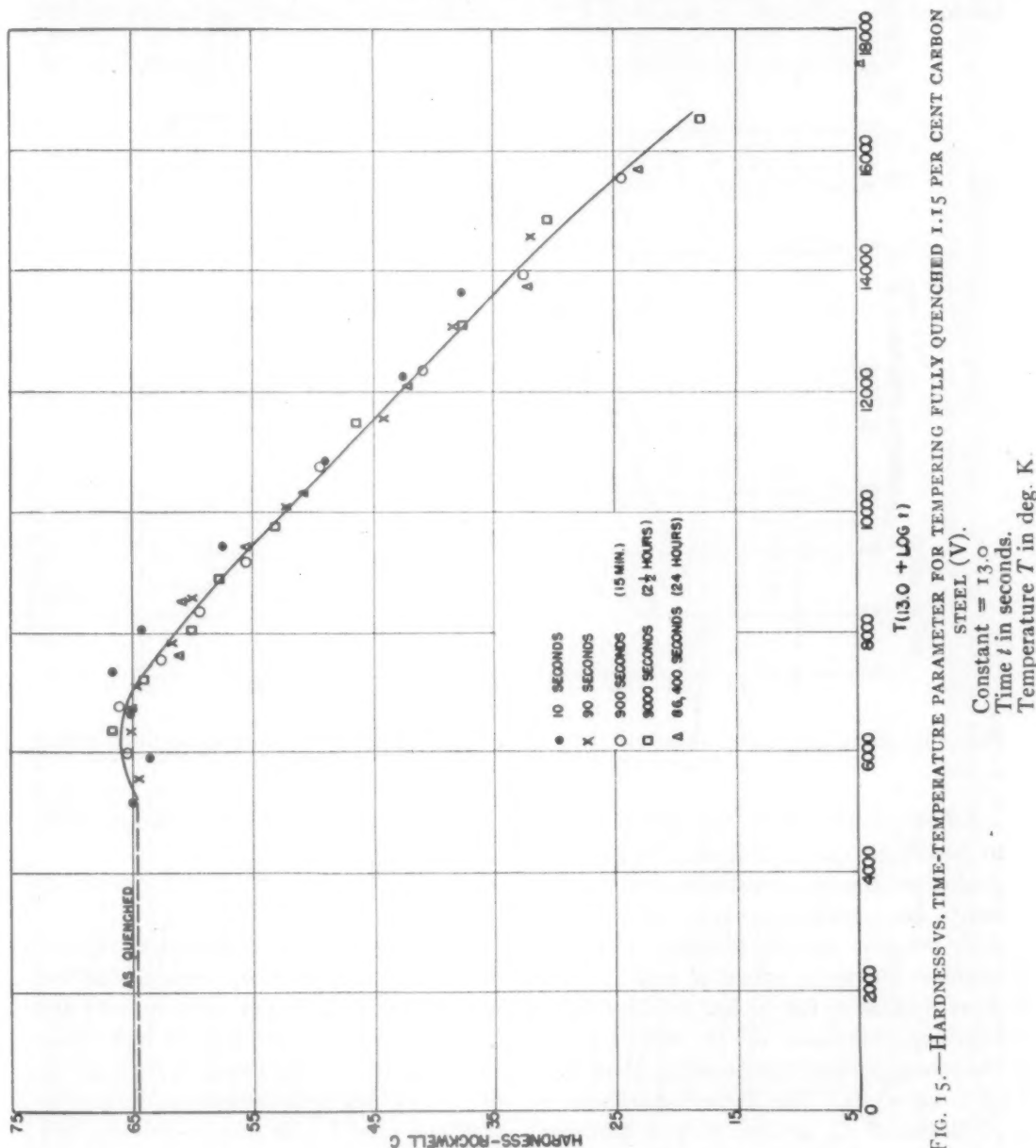


FIG. 15.—HARDNESS VS. TIME-TEMPERATURE PARAMETER FOR TEMPERING FULLY QUENCHED 1.15 PER CENT CARBON STEEL (V).

Constant = 13.0

Time t in seconds.

Temperature T in deg. K.

temperature of 1400°F. This is, however, above the critical temperature of 1350°F.; the highest practical tempering temperature would be about 1325°F. Since the steel contains 1.15 per cent carbon, reference is made to Fig. 18. This indicates that the hardness obtained in 1 hr. at

hardness can be attained by tempering the normalized steel at 1325°F.

Example No. 4.—It is desired to find the tempering temperature that will give 260 Brinell (26 Rockwell C) in a 0.20 per cent carbon, 5 per cent nickel, 0.25 per cent molybdenum steel, water-quenched

and tempered 2 hr. It is known that when water-quenched in the same section and tempered 1 hr. at 1100°F., the steel has a hardness of 330 Brinell (35 Rockwell C).

indicates that, for the desired hardness difference of 75, the tempering time should be 14 hr. This, it must be remembered, is a rough approximation only, though the best

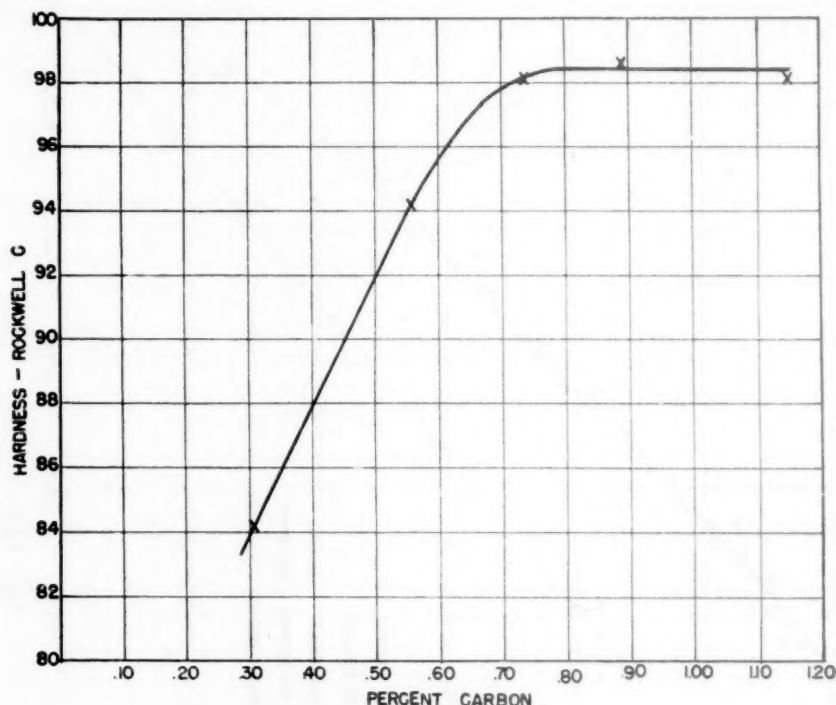


FIG. 16.—CHARACTERISTIC HARDNESS (H_c) VS. CARBON CONTENT FOR EXPERIMENTAL FULLY QUENCHED PLAIN-CARBON STEELS (S,T,U,V,W).

Solution.—The data are not sufficient to permit an exact solution. Since only a moderate amount of carbide-forming elements are present, however, an approximate solution can be obtained from the hardness difference values of Fig. 17. This chart indicates for 1 hr. at 1100°F. a hardness difference of 66 Rockwell C. The characteristic hardness is, therefore, $66 + 35 = 101$. The desired hardness is 26 Rockwell C, so the desired hardness difference is $101 - 26 = 75$. For a hardness difference of 75 and a time of 2 hr., Fig. 17 gives a temperature of 1290°F. This will almost certainly be above the lower critical temperature, which, for this steel, can be estimated as approximately 1240°F. If 1220°F. is considered the highest practical tempering temperature, Fig. 17

that can be obtained with the available data.

SUMMARY

Six heats of plain carbon steel, five of which differed only in carbon content (ranging from 0.31 per cent to 1.15 per cent), were fully quenched to martensite and tempered for times ranging from 10 sec. to 24 hr. at temperatures of 100° to 700°C. (212° to 1292°F.). It was found that the hardnesses obtained were functions of the parameter $T(\log t/t_0)$, equivalent to $T(c + \log t)$, where T is the absolute temperature, t the time, and t_0 and c constants of the steel.

This functional relationship was found to hold very closely (within about ± 1 point Rockwell C) for all appropriate

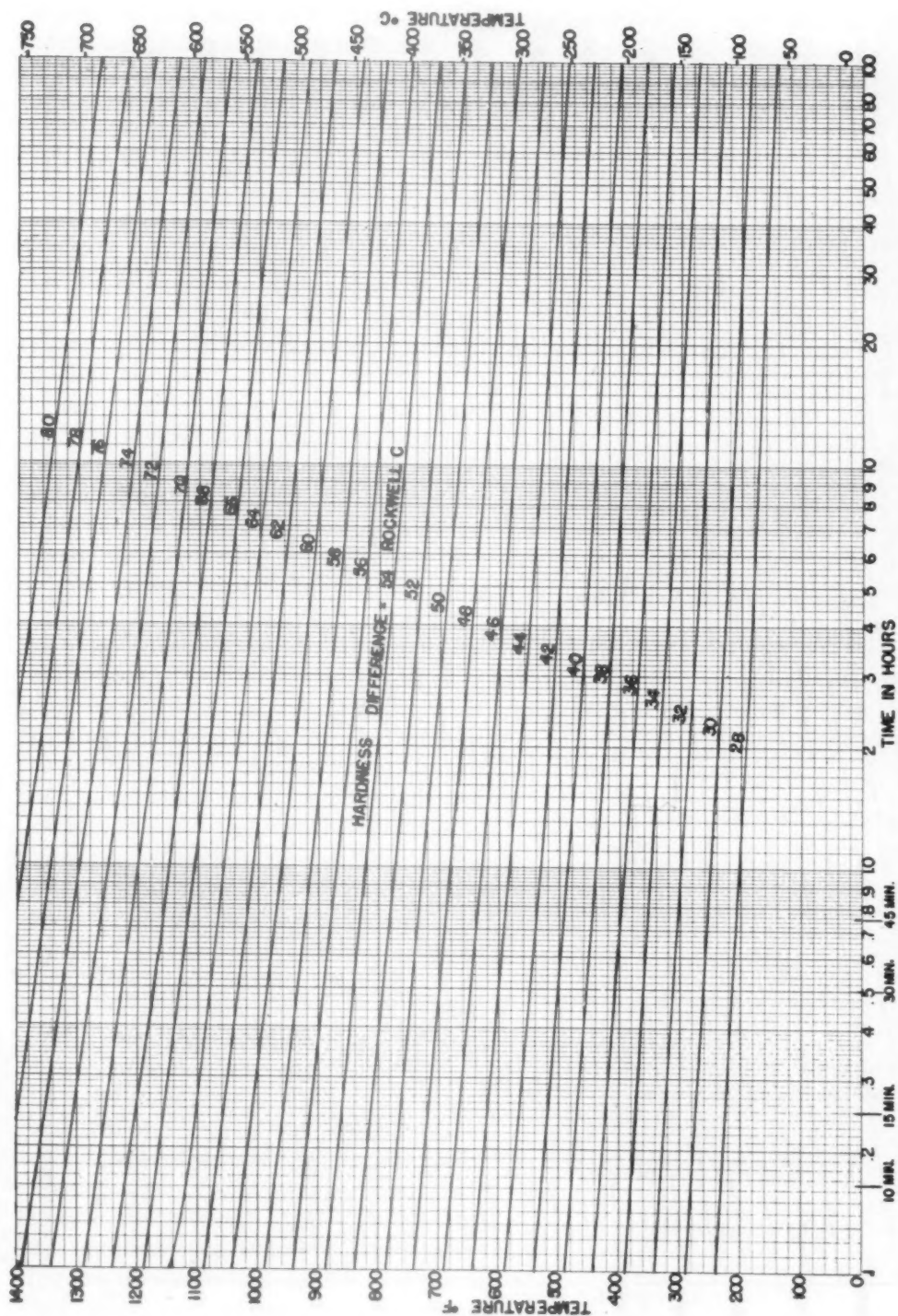


FIG. 17.—CHART FOR FINDING TIME-TEMPERATURE COMBINATIONS GIVING EQUIVALENT TEMPERING.
Approximate hardness-differences for steels not containing large percentages of carbide-forming elements are also shown.
Primarily for steels containing 0.20-0.40 per cent carbon.
 $c = 19.5$ (time in hours).

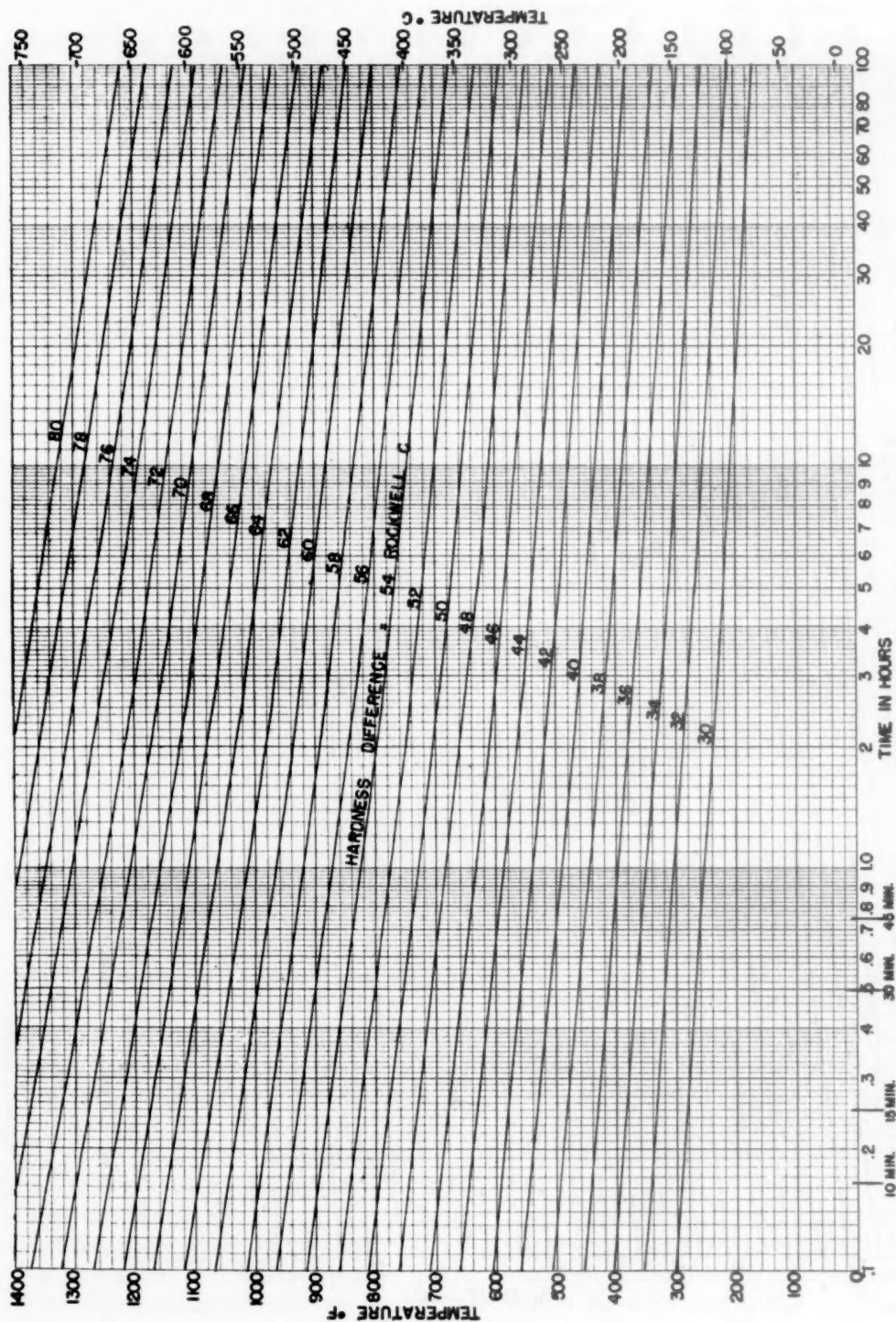


Fig. 18.—CHART FOR FINDING TIME-TEMPERATURE COMBINATIONS GIVING EQUIVALENT TEMPERING. Approximate hardness-differences for steels not containing large percentages of carbide-forming elements are also shown. Primarily for steels containing 0.90–1.20 per cent carbon.

tempering data noted in the metallurgical literature, except when graphitization took place. This was true whether the initial structure was martensite (with or without retained austenite), bainite, or pearlite, and whether or not secondary hardening occurred. The data covered temperatures ranging from 210°F. (100°C.) to 1310°F. (710°C.), times from 6 sec. to 1000 hr., carbon contents from 0.31 to 1.15 per cent, and alloy contents from none up to 5 per cent molybdenum with 5 per cent chromium.

The value of the constant c was found to vary somewhat for different steels, and appears to decrease linearly with increasing carbon content. However, the value is not critical. The important practical application of the relationship is the determination of the various combinations of tempering temperature and time that result in a given hardness, when one such combination is known for the steel. For this purpose, it appears sufficiently accurate (within $\pm 1\frac{1}{2}$ points Rockwell C over the usual range of times) to use $c = 19\frac{1}{2}$ for ordinary carbon and alloy steels (0.25 to 0.40 per cent carbon) and $c = 15$ for tool steels (0.90 to 1.20 per cent carbon), the times being expressed in hours. On the basis of these values, charts have been prepared by which the equivalent time-temperature combinations can be found readily.

For steels showing no secondary hardening, it was found that the Rockwell C or Brinell hardness varies almost linearly with the parameter over a considerable range, and that the slope of this linear relationship differs little among the various steels. This permitted inclusion in the charts of a feature that permits rapid calculation of the hardness obtainable with any tempering treatment (within certain limitations and within an accuracy of ± 3 points Rockwell C) when the hardness obtained with only one tempering treatment is known.

These results permit close estimation

of the hardness that will be obtained with any time and temperature of tempering, with much fewer experimental data than were formerly necessary.

REFERENCES

1. R. H. Greaves and J. A. Jones: Temper-Brittleness of Nickel-Chromium Steels. *Jnl. Iron and Steel Inst.* (1925) **III**, 231-255.
2. C. R. Austin and B. S. Norris: Effect of Tempering Quenched Hypereutectoid Steels on the Physical Properties and Microstructures. *Trans. Amer. Soc. Metals* (1938) **26**, 788-849.
3. E. H. Engel: The Softening Rate of Steel When Tempered from Different Initial Structures. *Trans. Amer. Soc. Metals* (1939) **27**, 1-17.
4. E. C. Bain: Functions of the Alloying Elements in Steel, 230-274. *Amer. Soc. Metals*, 1939.
5. *Ibid*, page 36.
6. E. A. Loria: Rates of Tempering in Cobalt Steels. *Amer. Soc. Metals Preprint* No. 4 (1944).
7. Hardness Conversion Table. *Amer. Soc. Metals Handbook* (1939) 127.

APPENDIX A.—Derivation of Time-temperature Parameter and Supplementary Equations for Cases When Temperature is Constant during Tempering

It was at first assumed that hardness

$$H = f_1(te^{-Q/RT}) \quad [A1]$$

It was found, however, that:

$$Q = f_2(H) \quad [A2]$$

and

$$te^{-Q/RT} = t_0 \quad [A3]$$

a constant. Taking the logarithmic form of A3, and equating the Q of A3 and A2, there is obtained:

$$Q = RT(\ln t - \ln t_0) = f_2(H) \quad [A4]$$

Then

$$H = f_3[e^{RT \ln t/t_0}] \quad [A5]$$

or

$$H = f(T \log t/t_0) \quad [A6]$$

$$= f[T(\log t - \log t_0)] = f[T(c + \log t)]$$

For constant hardness:

$$T_1(c + \log t_1) = T_2(c + \log t_2) \quad [A7]$$

or

$$-c = \frac{T_1 \log t_1 - T_2 \log t_2}{T_1 - T_2} \quad [\text{A8}]$$

and

$$\frac{T_2}{T_1} = \frac{c + \log t_1}{c + \log t_2} \quad [\text{A9}]$$

From Eq. A6:

$$c = -\log t_0 \quad [\text{A10}]$$

Since, as indicated in the text, c is of the order of 10 to 16 for times in seconds, t_0 is of the order of 10^{-10} to 10^{-16} seconds.

APPENDIX B.—*Derivation of Time-temperature Parameter for Cases when Temperature May Vary during Tempering*

Using the form of Eq. A6 (or Eq. 2):

$$H = f_1(M) \quad [\text{B1}]$$

where M is the unknown parameter.

For T constant during the tempering:

$$M = T \log (t/t_0) = \frac{T}{2.303} \ln (t/t_0) \quad [\text{B2}]$$

by Eq. A6, or:

$$t = t_0 10^{M/T} \quad [\text{B3}]$$

and

$$dM/dt = \frac{T}{2.303t} \quad [\text{B4}]$$

Substituting the value of t given by Eq. B3 in Eq. B4,

$$dM/dt = \frac{T}{2.303 t_0 10^{M/T}} = \frac{T}{(2.303) 10^{\frac{M}{T} - c}} \quad [\text{B5}]$$

It can be assumed that Eq. B5 holds even when T is not constant. It is then the desired differential equation for M . In general, the integration will have to be performed by step-by-step methods.

It may be of interest to solve Eq. B5 for the special case of constant T but with the general boundary condition $M = M_0$ at $t = t_0$. Here Eq. B5 gives:

$$e^{2.303M/T} d(2.303M/T) = dt/t_0 \quad [\text{B6}]$$

Integrating and substituting the boundary conditions:

$$e^{2.303M/T} - e^{2.303M_0/T} = 10^{M/T} - 10^{M_0/T} = (t - t_0)/t_0 \quad [\text{B7}]$$

$$M = T \log \left(\frac{t - t_0}{t_0} + 10^{M_0/T} \right) \quad [\text{B8}]$$

If Δt is the time spent at temperature T and M_0 the value of the parameter at the start of this time, Eq. B8 may be written:

$$M = T \log \left(\frac{\Delta t}{t_0} + 10^{M_0/T} \right) \quad [\text{B9}]$$

For the initial condition $M_0 = 0$, this reduces to:

$$M = T \log (\Delta t/t_0) \quad [\text{B10}]$$

which is necessarily equivalent to Eq. A6.

DISCUSSION

A. M. WHITE.*—The authors are to be congratulated on their interesting and extremely useful paper. The relations shown are particularly timely, inasmuch as they will effect considerable economies of time, which are so important in these days of accelerated production. This writer has attempted to use the described relations and has obtained results of accuracy at least equal to that claimed by the investigators.

A simplification in the presentation and use of Figs. 17 and 18 is suggested. In order to avoid the confusing concepts of "hardness difference" and "characteristic hardness" the charts could be drawn without actual notation of "hardness difference" values, merely stating that the spacings between the lines represent 2 points Rockwell C. Then, to obtain a different hardness for a steel that does not exhibit

* Associate Metallurgist, War Dept., Watertown Arsenal, Watertown, Mass. The opinions expressed are those of the writer only, and do not necessarily reflect those of the War Department.

secondary hardening, it is merely necessary to move from the known point vertically upward for a hardness decrease or vertically downward for a hardness increase, the distance moved being guided by the spacings between the lines of constant hardness.

Inasmuch as the factor in Eq. 6 apparently changes as the value of C changes, it would be advantageous to know the relationship between these two variables. This information would enable one to construct accurate charts for steels of carbon contents between 0.40 and 0.90 per cent.

The writer is attempting to apply the methods explained in this paper to yield strength instead of hardness. Present indications are that this can be done with considerable accuracy provided certain conditions such as the yield-tensile ratio are reasonably constant. It is hoped that the excellent work of the authors will stimulate other investigators to approach other metallurgical phenomena in a similar manner.

J. H. HOLLOMON and L. D. JAFFE (authors' reply).—Mr. White is correct in stating that, when considering a single steel, the concept of "characteristic hardness" and the numerical hardness difference values given in Figs. 17 and 18 are unnecessary. However, they should prove useful in comparing the response to tempering of different steels.

To obtain the factor in Eq. 6 suitable for other values of c , an equation such as

$$0.00457(13.0 + \log t) = Y(c + \log t)$$

may be used, where Y is the desired factor. It is evident that the calculated value of Y for any c will depend upon the time t . However, since Eq. 6 is not highly accurate, it appears satisfactory to use the value of Y computed for some average value of t . As explained in the last footnote (p. 241), this was done in preparing Figs. 17 and 18.

The authors await with interest the results of Mr. White's attempt to apply the methods explained in the paper to yield strength instead of hardness.

Time-temperature Transformation Curves for Use in the Heat-treatment of Cast Steel*

BY C. T. EDDY,† MEMBER A.I.M.E., R. J. MARCOTTE‡ AND R. J. SMITH‡

(New York Meeting, February 1945§)

THE objectives of the investigation herein reported were to determine: (1) the S-curves for certain selected cast steels, (2) whether or not the published S-curves for wrought steels are satisfactory for use on cast steels of similar composition, and (3) to prepare hardenability curves of the selected cast steels.

In order to make the final comparisons between cast and wrought steel more completely tangible, it was deemed advisable not only to determine S-curves for the steels submitted in the cast condition but also to roll some of the cast-steel test bars and determine comparison S-curves on such wrought material. This procedure eliminates the composition variable and makes it possible to reveal the differences resulting from plastic deformation of the cast structure in addition to providing the comparison with published data on wrought steels.

CAST STEELS

The cast steels selected for the preparation of S-curves, or time-temperature transformation curves, were similar to S.A.E. series 1030, 2330, 4130 and 4330.

* This article sets forth the results of research conducted by the Michigan College of Mining and Technology upon the initiative of the Steel Founders' Society of America and at the Society's expense. Copyright, 1945, by the Steel Founders' Society of America.

Manuscript received at the office of the Institute Dec. 1, 1945. Issued as T.P. 1846 in METALS TECHNOLOGY, September 1945. Reprinted by permission of the Steel Founders' Society of America.

† Professor of Metallurgical Engineering, Michigan College of Mining and Technology, Houghton, Michigan.

‡ Assistant Professor of Metallurgical Engineering, Michigan College of Mining and Technology.

§ Meeting canceled.

Of these the 1030 was supplied by The Crucible Steel Casting Co., Cleveland, Ohio, and the other three by The Sawbrook Steel Castings Co., Lockland, Ohio. The steels were furnished in the as-cast condition. The manufacturers supplied the chemical analyses and the properties that could be obtained in the heat-treated condition—all of which is summarized in Table I.

TABLE I.—Analyses, Treatment and Properties of Steels Tested

Steel No.....	1030	2330	4130	4330
Chemical Composition, Per Cent				
Carbon.....	0.30	0.28	0.32	0.33
Manganese.....	0.75	0.69	0.54	0.69
Silicon.....	0.46	0.41	0.36	0.41
Phosphorus.....	0.026	0.043	0.034	0.043
Sulphur.....	0.040	0.028	0.021	0.028
Nickel.....		3.30	0.07	1.41
Chromium.....		0.12	0.75	0.72
Molybdenum...		0.03	0.27	0.25
Treatment, Deg. F.				
Normalized.....	1650	1650	1650	1650
Quenched.....		Oil: 1575	Water: 1600	Oil: 1575
Tempered.....	1250	1200	1150	1200
Properties				
Tensile strength, lb. per sq. in.	74,500	109,400	137,000	129,325
Yield point, lb. per sq. in.	47,500	81,125	109,000	114,375
Elongation in 2 in., per cent.	31.0	20.0	13.5	21.0
Reduction of area, per cent.	50.6	34.4	31.2	44.6

PROCEDURE

The metallographic and dilatometric procedures and equipment were in general standard. The specific technique employed was described in a report of the Steel

Founders' Society of America.¹ However, the method of specimen preparation differed, of necessity, from that used for wrought materials. The cast coupons sup-

a ½-in. square. From this ½-in. square bar, specimens for the metallographic method, measuring 0.055 in. thick and ½ in. square, were cut on a radiac cutoff wheel. The stop

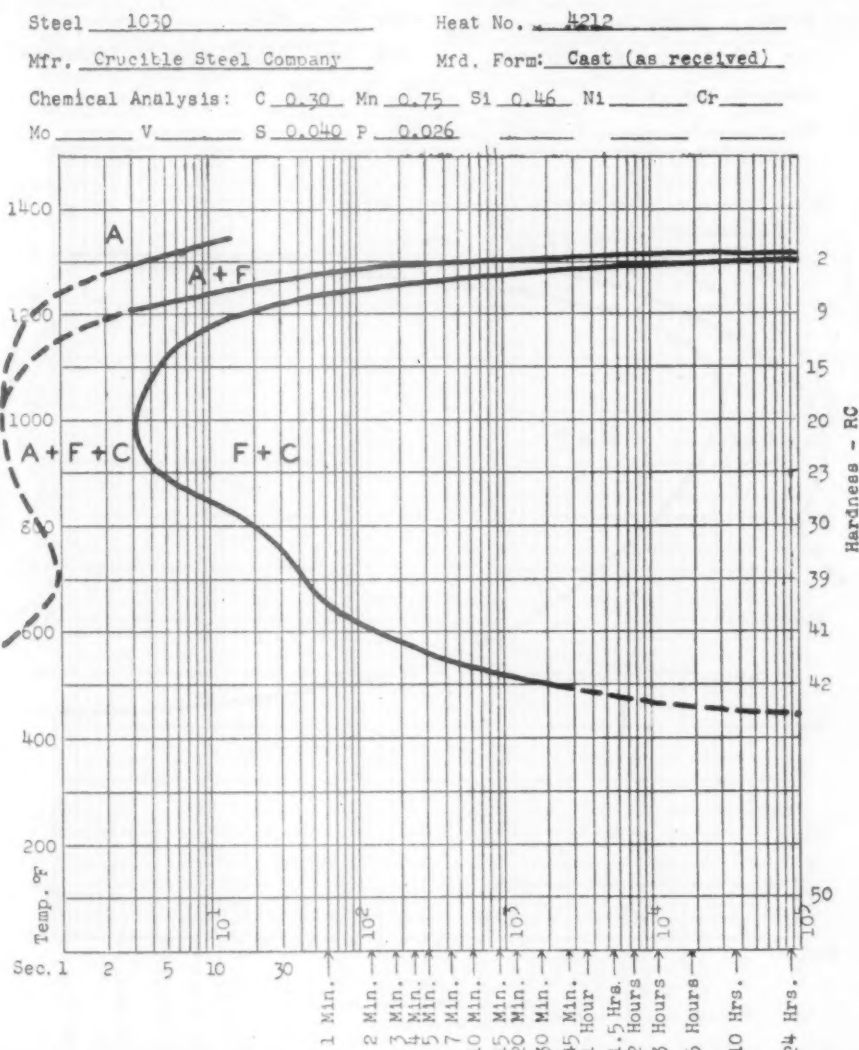


FIG. 1.—S-CURVE FOR CAST STEEL SIMILAR TO 1030.

plied measured approximately 1¼ by 1¼ by 7 in. After removal of the surface in a shaper, these coupons were milled longitudinally into two parts, each measuring about ½ by 1¼ by 7 in. From these bars, dilatometer specimens 0.035 in. thick, ½ in. wide and 4½ in. long were cut by milling until the bar was reduced to approximately

attached to the vise of the cutoff wheel permitted control of the specimen thickness to ± 0.002 in.

To facilitate the handling of the specimens in austenitizing, austempering and quenching, a No. 12 iron wire 6 in. long was spot-welded to a corner of the specimen. It is believed that this procedure for specimen preparation retains as nearly as is possible the average as cast characteristics.

¹ References are at the end of the paper.

The specimens for the wrought condition were prepared by hot-rolling the coupons down to strips of 0.055-in. and 0.035-in. thickness and cutting these strips into the

sent the data accumulated in making approximately 150 dilatometric analyses and in examining metallographically more than 1000 heat-treated specimens.

Steel 1030 Heat No. 4217
 Mfr. Crucible Steel Company Mfd. Form: Rolled from cast coupons
 Chemical Analysis: C 0.30 Mn 0.75 Si 0.46 Ni Cr
 Mo V S 0.040 P 0.026

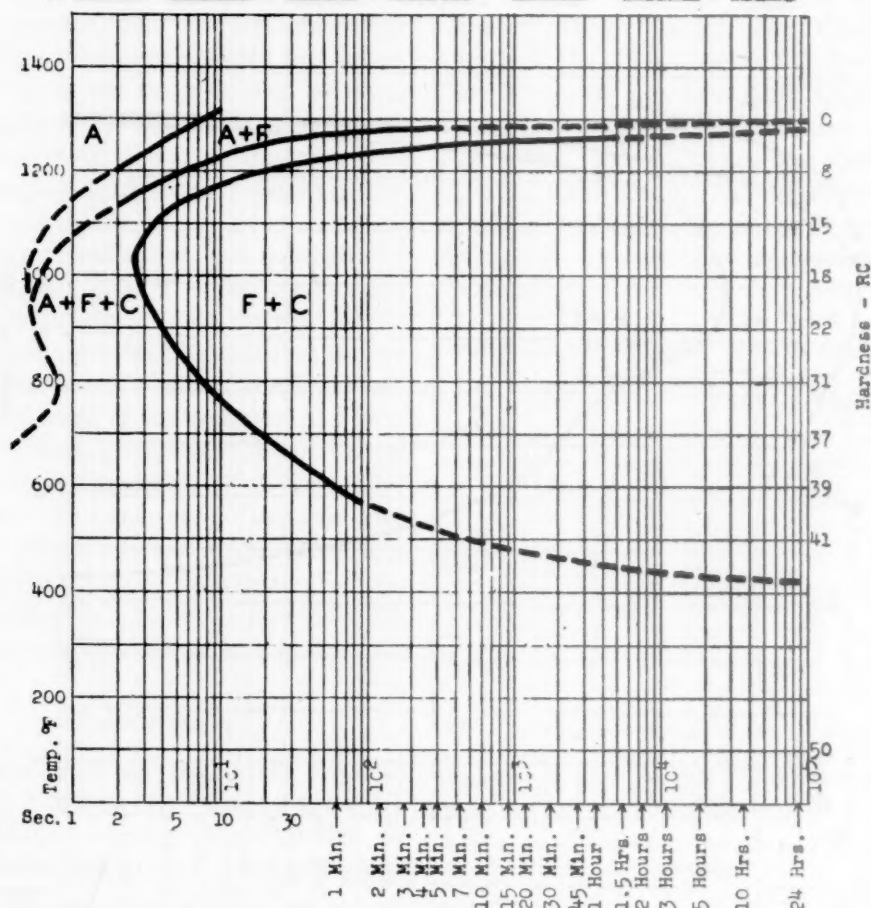


FIG. 2.—S-CURVE FOR CAST STEEL SIMILAR TO 1030. ROLLED FROM CAST COUPONS.

proper lengths for the metallographic and dilatometric specimens respectively.

S-CURVES

Figs. 1 to 14 represent the results of the determination of the S-curves, or time-temperature transformation curves, and the incident comparisons. None of the specific data collected for establishing the actual points that determine the curves are included. However, the curves repre-

The critical temperatures for the four steels investigated are listed in Table 2.

TABLE 2.—*Ac and Ae Temperatures*
DEGREES F.

Steel	Ac ₁	Ac ₂	Ae ₁ *
1030 (cast).....	1364	1517	1340
2330 (cast).....	1283	1382	1190
4130 (cast).....	1382	1517	1365
4330 (cast).....	1350	1445	1300

* No concerted effort was made to determine the Ae temperatures. Those listed above were estimated from observations.

The grain size for all steels was 7 to 8. In the experimental determination of the S-curve, all samples were given the same

Wherever Rockwell C hardness values appear on the figures, they represent the hardness at the completion of transforma-

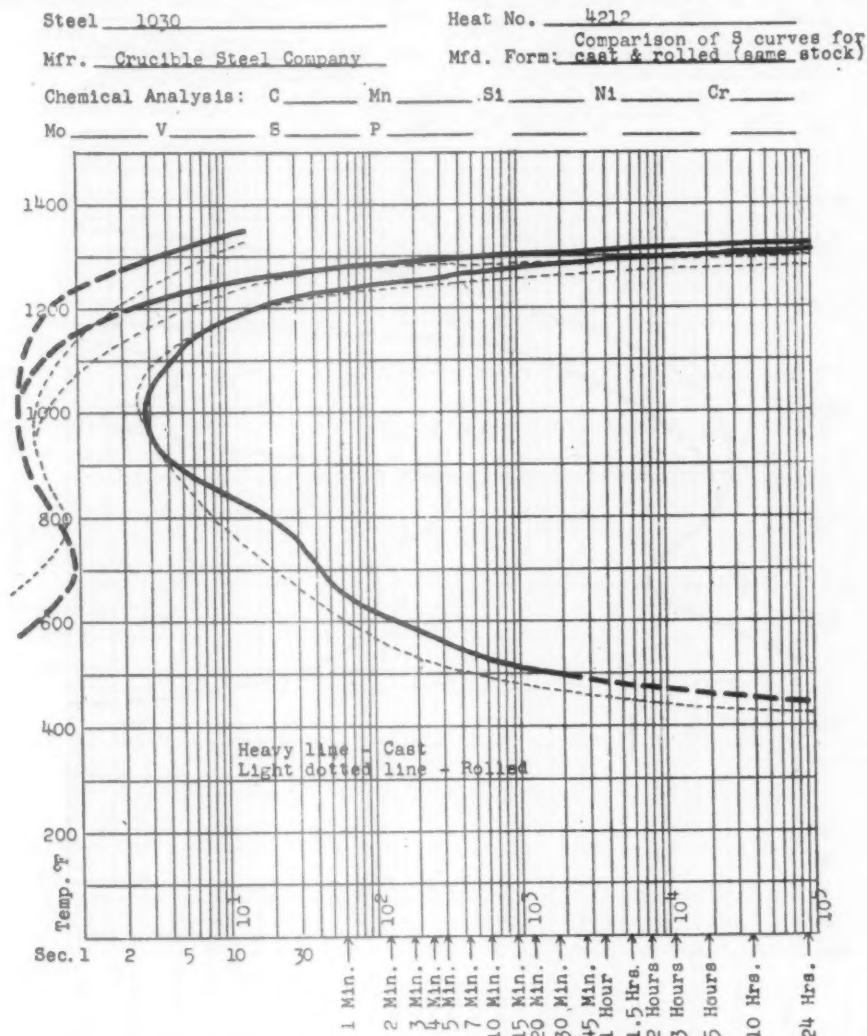


FIG. 3.—COMPARISON OF CAST AND ROLLED-CAST STEELS SHOWN IN FIGS. 1 AND 2.

austenitizing treatment; that is, 20 min. at 1660°F.

Figs. 1 to 14 represent the results. The rolled material upon which the curves in Figs. 2, 5, 8 and 12 are based was prepared by rolling cast coupons of the steels submitted.

tion for the temperatures indicated.

DISCUSSION OF RESULTS ON S-CURVES

An examination of Figs. 3, 6, 9 and 13, comparing the S-curves for the selected steels in the as-cast and rolled conditions leads to the following observations:

1. All of the comparisons indicate that there is general agreement between the cast and wrought conditions.

3. The A_{e1} temperature for the cast condition seems generally higher than it is for the wrought condition. However, this

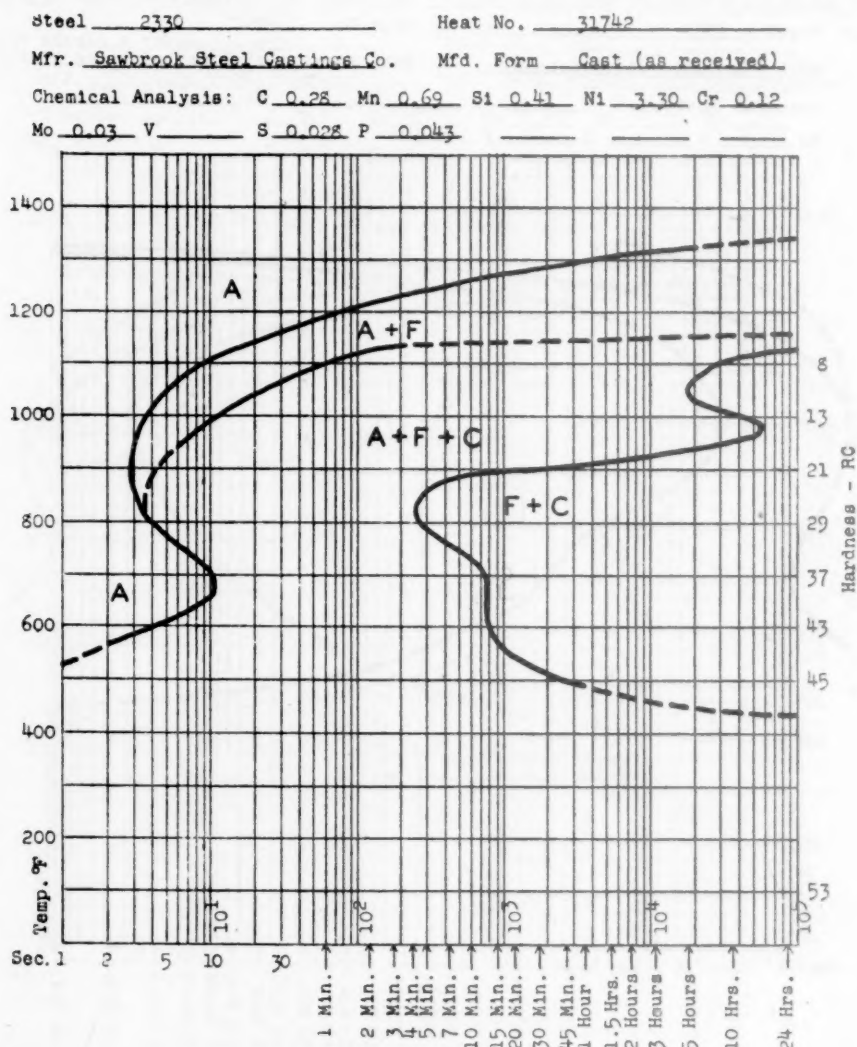


FIG. 4.—S-CURVE FOR CAST STEEL SIMILAR TO 2330.

2. There is a general tendency for a slight counterclockwise rotation of the S-curve for the cast condition. This implies that the rate of transformation of cast steel in the austenitic condition is accelerated at the higher subcritical temperatures and decelerated at the lower temperatures. This may be due to the inherent microscopic segregation in cast steel structures.

observation may be a direct result of the aforementioned apparent rotation of the curve.

4. Despite the general shifting of the upper part of the S-curve to the left, there seems to be little consistency as regards the tendency for beginning of ferrite precipitation. For example, in Fig. 3 the

ferrite line for the cast condition lies to the left of that for the wrought condition, while in Fig. 13 it lies to the right.

5. The so-called "martensite tempera-

ture" of the 4130 steel investigated by Parke and Herzig² (Fig. 10) is exceptional. However, the agreement of the curves for the 4330 steel shown in Fig. 14 is not as

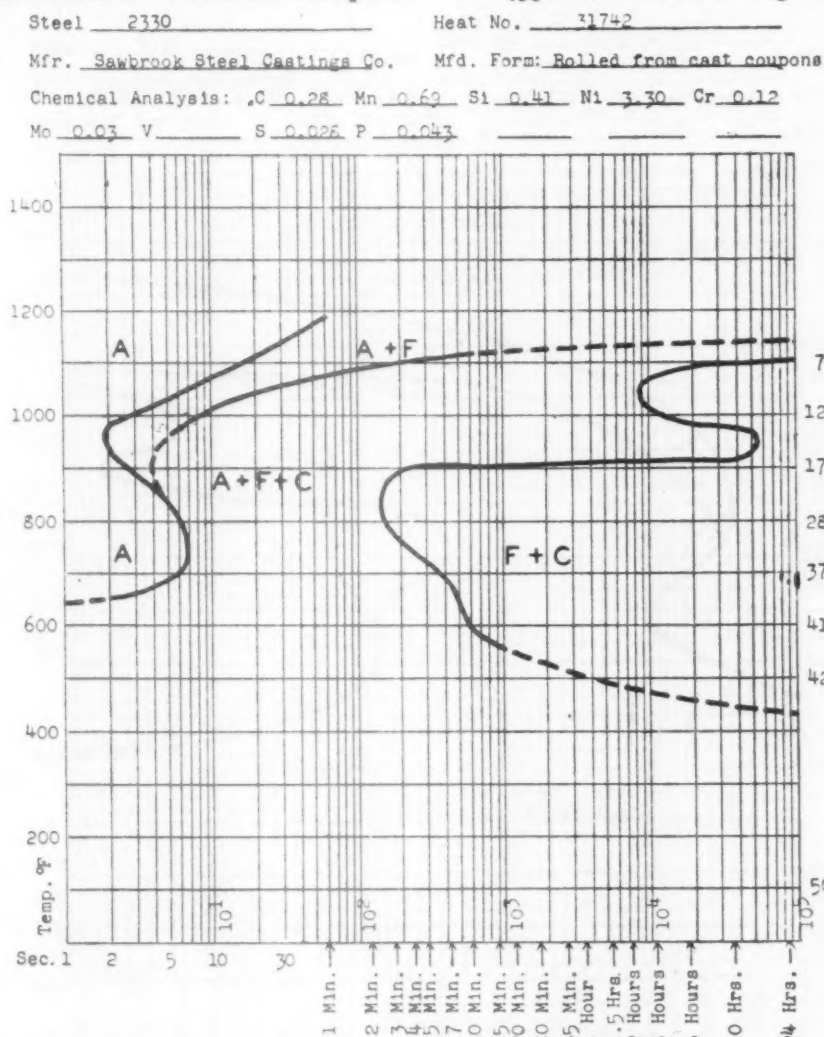


FIG. 5.—S-CURVE FOR CAST STEEL SIMILAR TO 2330. ROLLED FROM CAST COUPONS.

ture" for the cast condition is consistently lower (50° to 100°F.) than it is for the wrought condition. This also may be a direct result of the inherent microscopic segregation.

6. The time required for transformation (1 to 99 per cent) at temperatures just below the nose of the curve is greater for the cast than for the wrought condition.

The agreement between the S-curve of the 4130 steel in the as-cast condition with

close. Even though the temperature relations are in substantial agreement, it will be observed that the entire curve reported by Parke and Herzig² lies considerably to the right of that for the cast 4330 as determined in this investigation. This would indicate a greater hardenability for this particular wrought steel.

Admittedly there is no direct dependency of the entire S-curve upon hardenability. However, the general location of the nose

of the curve is an indication of relative hardenability. With this in mind, the hardenabilities of these two steels were calculated from their chemical compositions.³

mately the same, as would be expected from the close agreement of the S-curves.

Published data for 1030 and 2330 wrought steels were not available, there-

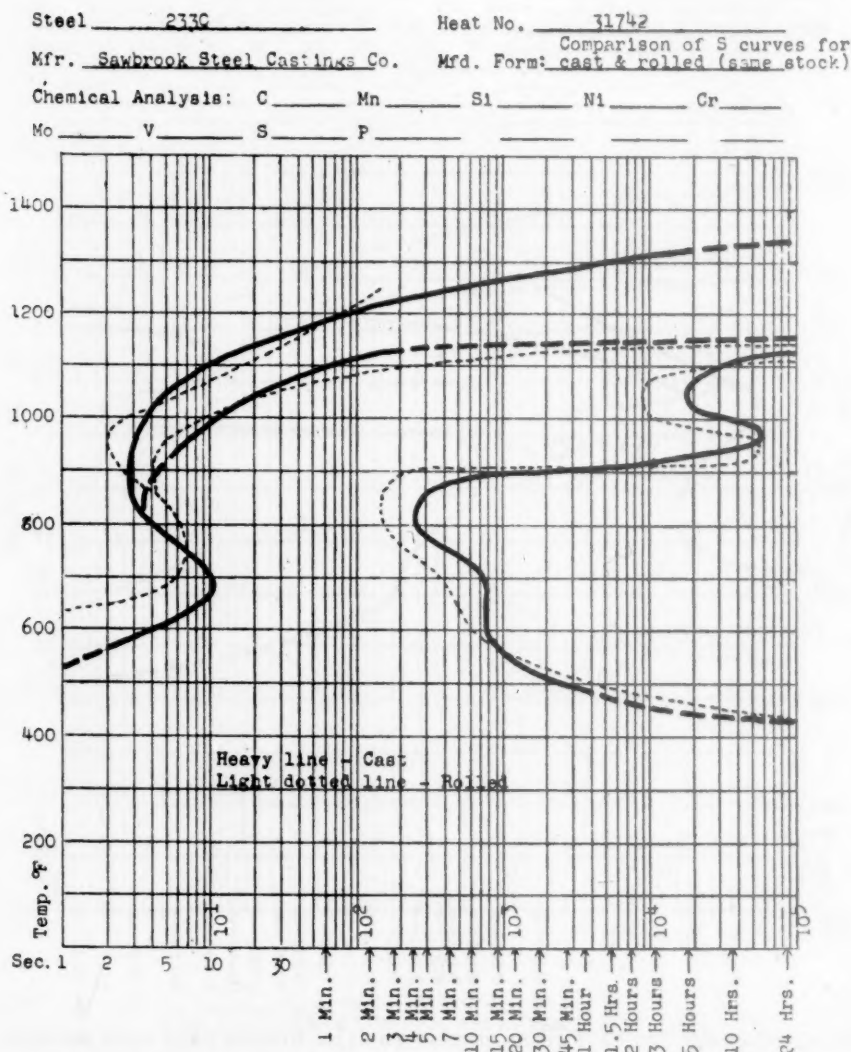


FIG. 6.—COMPARISON OF CAST AND ROLLED-CAST STEELS SIMILAR TO 2330.

It was found that because of differences in chemical composition, the steel investigated by Parke and Herzig had considerably greater hardenability. Had these steels been of the same chemical composition, their S-curves would most likely have been in closer agreement.

The calculated hardenabilities for the 4130 steels shown in Fig. 10 were approxi-

fore the direct comparisons could not be made. However, a comparison of the S-curve for the 2330 steel in the as-cast condition with that of a 2340 wrought steel investigated by Davenport⁴ reveals that his curve lies considerably to the left of that determined for the cast 2330. This would indicate that the hardenability of this particular cast 2330 was greater than

that of the wrought 2340, in spite of the higher carbon content of the latter. Oddly enough, the calculated hardenability of this particular cast 2330 is considerably

was obviously much less than the normal reduction in wrought steels rolled from the ingot.

However, the close agreement in Figs.

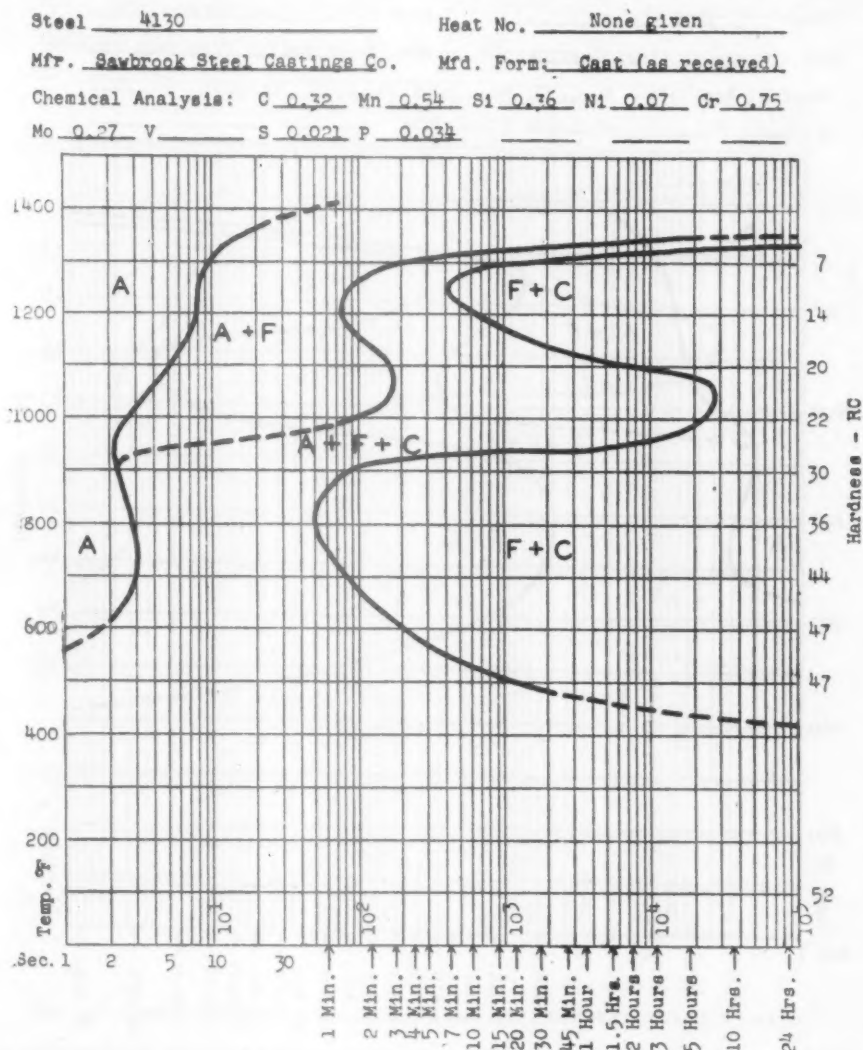


FIG. 7.—S-CURVE FOR CAST STEEL SIMILAR TO 4130.

greater than that of the S.A.E. 2340, and therefore justifies the relative location of the curves, especially in view of the fact that the chemical analysis of the cast 2330 steel shows chromium and molybdenum to be present.

Note should be taken of the fact that the rolled material used in the comparisons was rolled in the laboratory from relatively small cast coupons. The resultant reduction

9 and 10 between the 4130 rolled from cast coupons and the commercial wrought 4130 of practically the same calculated hardenability probably justifies the comparisons made of the cast and wrought conditions.

CONCLUSIONS RELATING TO THE S-CURVE FOR CAST STEELS

On the basis of the results of the investigation of the four selected cast steels, it

may be concluded that S-curves for wrought steels can be utilized in the heat-treatment of steel castings.

The investigation revealed that differ-

HARDENABILITY

The four cast steels of Table 1 were studied following the standard S.A.E. procedure for determining the harden-

Steel 4130 Heat No. None given
 Mfr. Sawbrook Steel Castings Co. Mfd. Form: Rolled from cast coupons
 Chemical Analysis: C 0.32 Mn 0.54 Si 0.36 Ni 0.07 Cr 0.75
 Mo 0.27 V — S 0.021 P 0.034

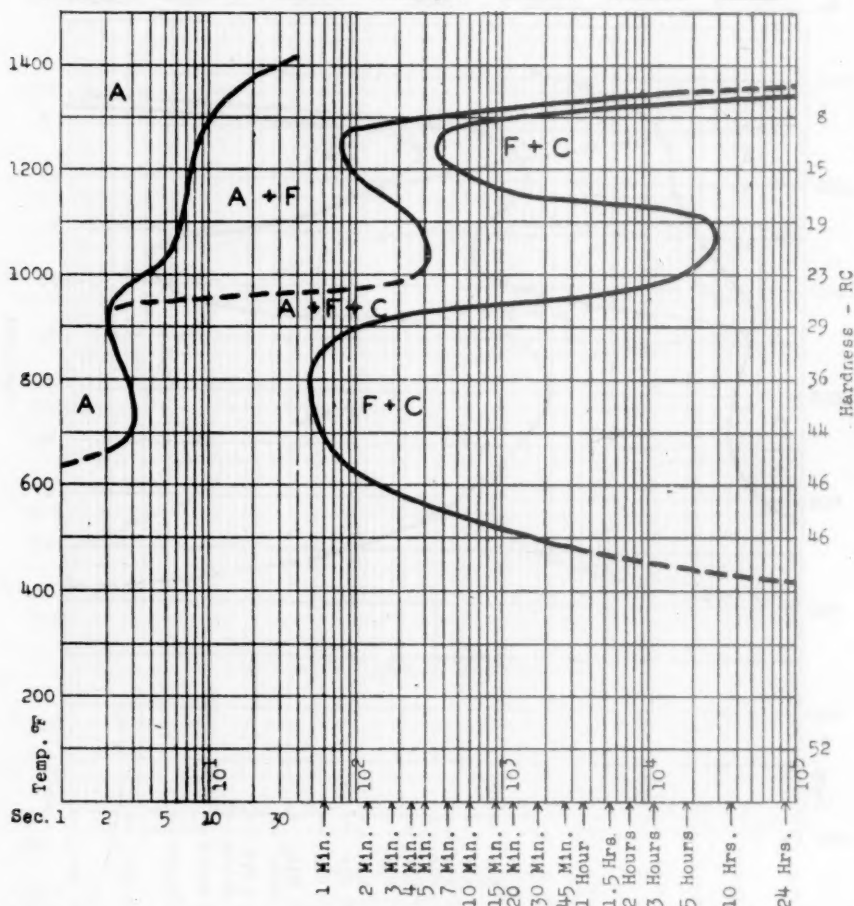


FIG. 8.—S-CURVE FOR CAST STEEL SIMILAR TO 4130. ROLLED FROM CAST COUPONS.

ences in the position of the S-curve due solely to the structural nature (cast or wrought) of the steels are minor in comparison with the differences resulting from normal variation in chemical composition of commercial heats. However, it must be remembered that this observation is based on the investigation of only four steels, even though these have been selected as representative of several classes.

ability of steel by the end-quench test,⁵ the type L-bar being employed throughout.

The first hardening temperatures used were in all cases 75°F. higher than the A_{c3} temperatures shown in Tables 2 and 3. The normalizing temperatures employed are also shown in Table 3.

Since the heating temperatures required for hardening cast steels are higher than those for wrought steels of similar analyses,

and, further, since the first hardening flats were ground to a depth of 0.025 in., temperature selected for this test was only slightly higher than that recommended for hardness readings again taken.

Steel 4130 Heat No. None given
 Mfr. Sawbrook Steel Castings Co. Mfd. Form: cast & rolled (same stock)
 Comparison of S curves for
 Chemical Analysis: C _____ Mn _____ Si _____ Ni _____ Cr _____
 Mo _____ V _____ S _____ P _____

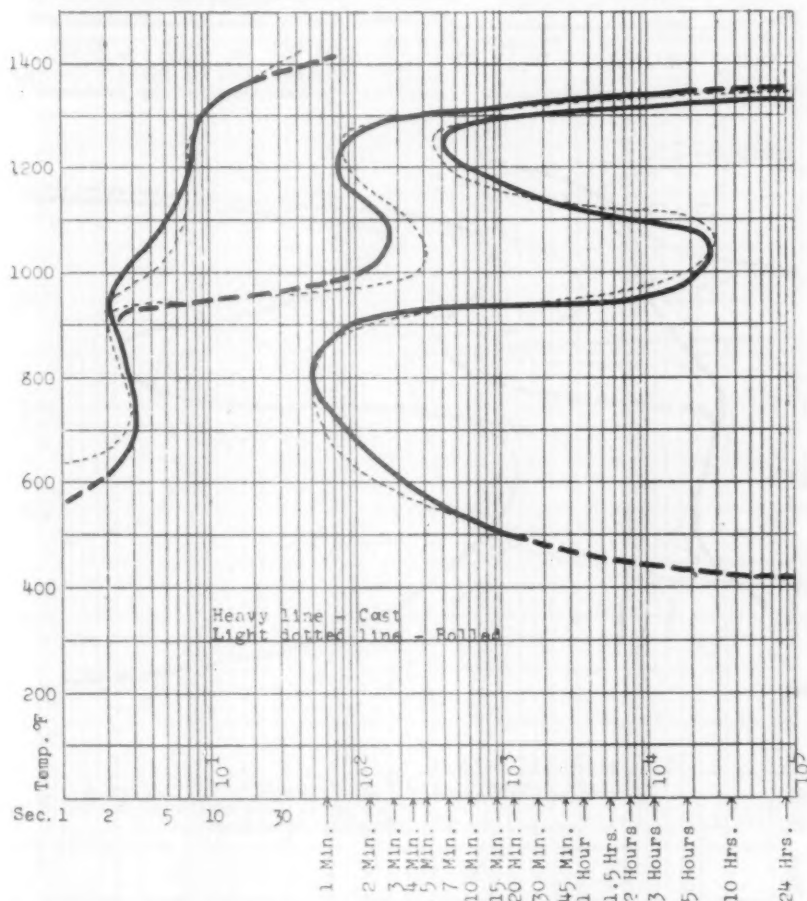


FIG. 9.—COMPARISON OF CAST AND ROLLED-CAST STEELS SIMILAR TO 4130.

wrought material, it was decided to repeat the hardenability test using higher hardening temperatures. These temperatures are listed in Table 3 as second hardening temperatures, and were in all cases 100°F. higher than the first temperatures. The original end-quench bars were ground free of any scale and without other treatment were again heated and quenched.* New

The hardenability curves obtained are shown in Figs. 15, 16, 17 and 18.

TABLE 3.—Normalizing and Hardening Temperatures

Steel No.	Degrees F.			
	Ac ₁	Normalizing	First Hardening	Second Hardening
1030	1517	1650	1529	1692
2330	1382	1650	1457	1560
4130	1517	1700	1592	1692
4330	1445	1650	1520	1620

* Although an admittedly inadvisable procedure, the second heating of the already tested bar was necessitated by lack of sufficient steel of the same analysis (same heat).

at the two temperatures for the cast steels and a comparison curve for a wrought steel of similar composition obtained from the literature⁶⁻¹⁰ are shown. The hardenabilities of all the cast steels compare favorably with those of the wrought.

the S-curves, is the subject of a current investigation and will be reported later.

ACKNOWLEDGMENTS

The authors wish to express appreciation to the Steel Founders' Society of America

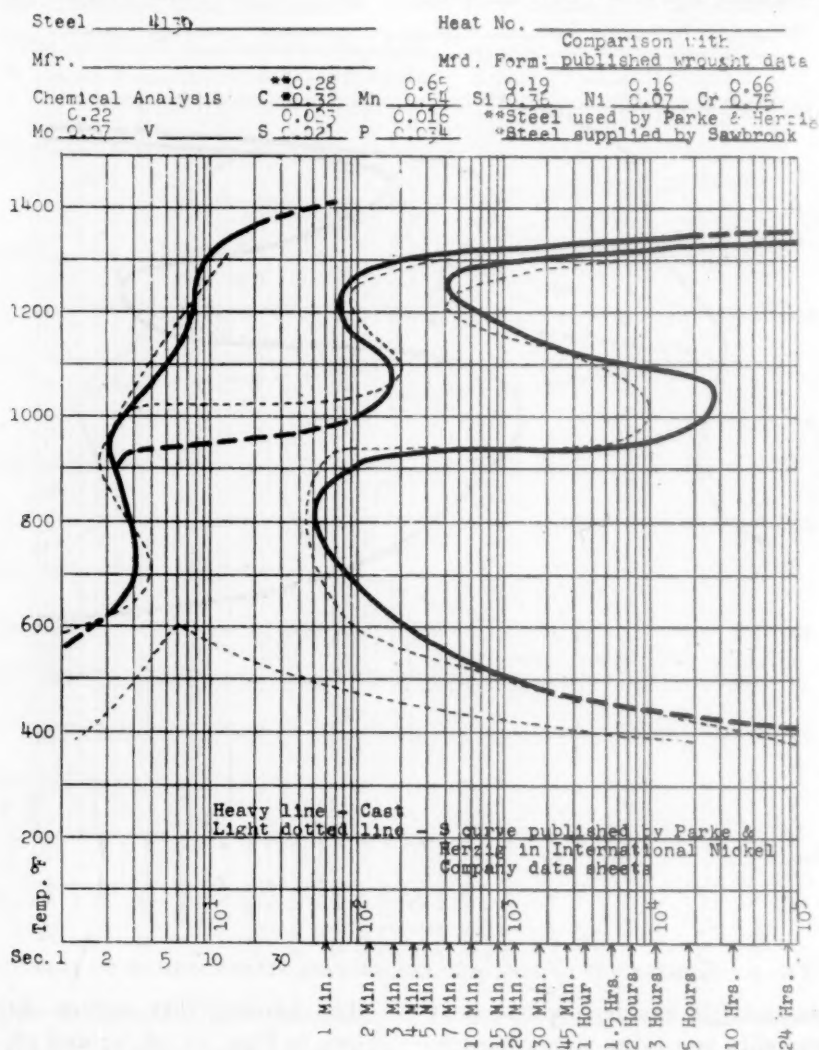


FIG. 10.—COMPARISON OF S-CURVES OF THE 4130 STEEL IN THE AS-CAST CONDITION SHOWN IN FIG. 7 WITH THAT FOR A 4130 WROUGHT STEEL DETERMINED BY PARKE AND HERZIG.²

The use of higher hardening temperatures resulted in higher hardenabilities in all cases, the increase probably resulting from improved homogenization and a possible slight increase in grain size. This effect, in addition to the general effects of austenitizing temperature in relation to

for the support given the investigation and for permission to publish the results. They wish particularly to thank Mr. Charles W. Briggs, Technical and Research Director of that Society, for his full cooperation in setting up and coordinating the project.

Acknowledgment is also made to the Sawbrook Steel Castings Co., of Lockland,

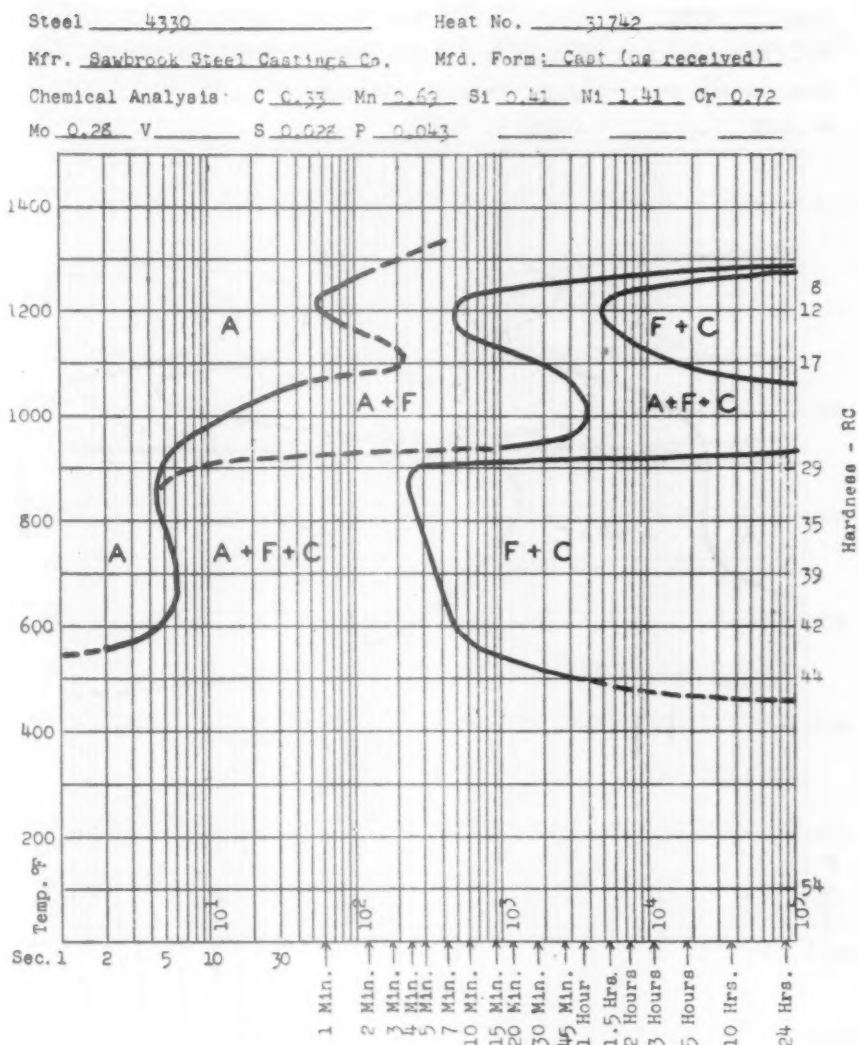


FIG. 11.—S-CURVE FOR CAST STEEL SIMILAR TO 4330.

Steel 4330 Heat No. 31742
 Mfr. Sawbrook Steel Castings Co. Mfd. Form: Rolled from cast coupons
 Chemical Analysis: C 0.33 Mn 0.69 Si 0.41 Ni 1.41 Cr 0.72
 Mo 0.28 V 0.028 P 0.043

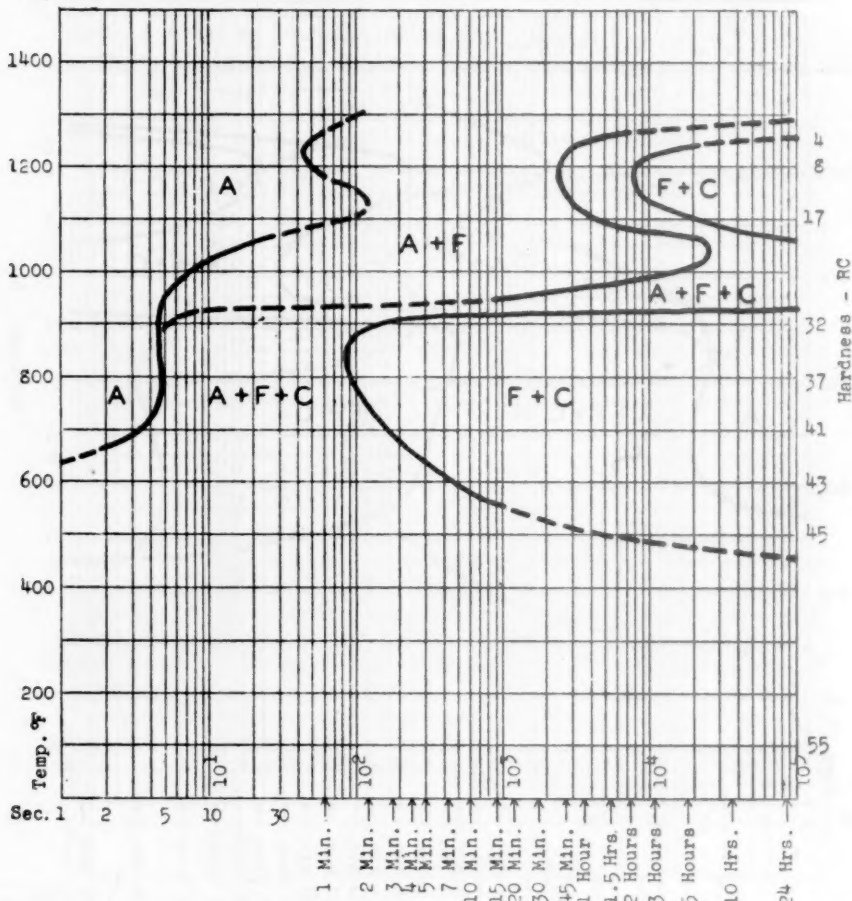


FIG. 12.—S-curve for cast steel similar to 4330. ROLLED FROM CAST COUPONS.

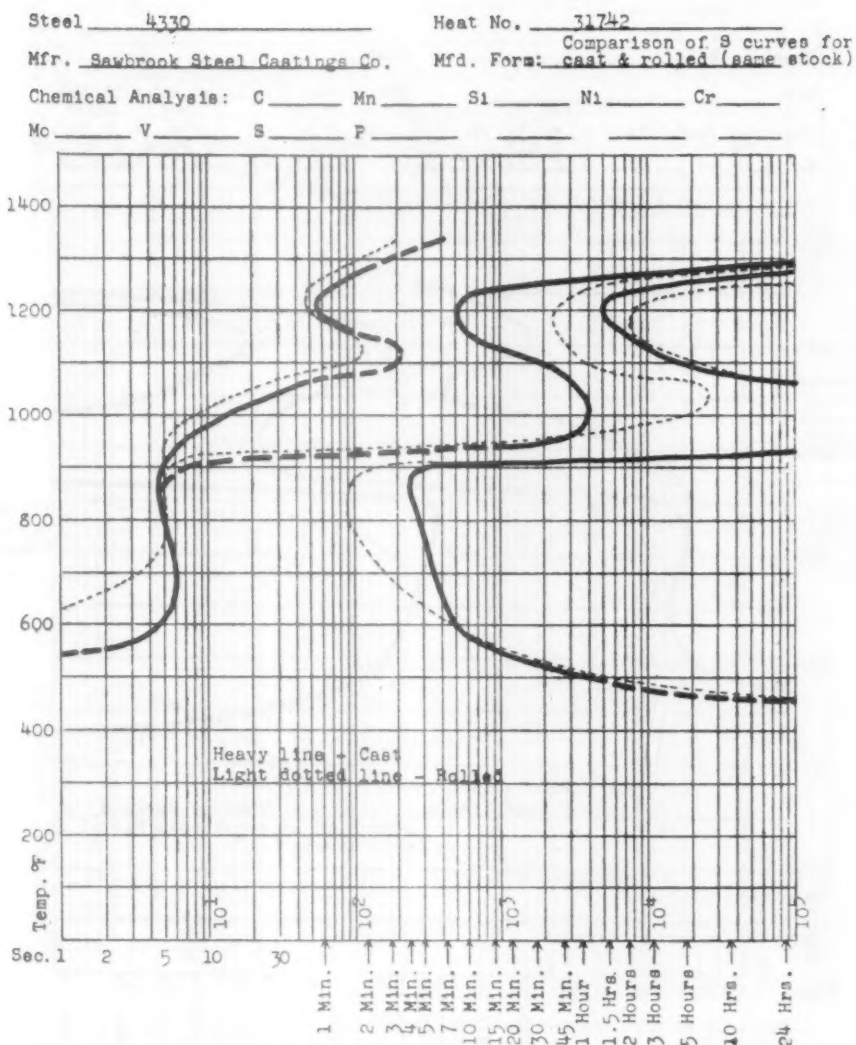


FIG. 13.—COMPARISON OF CAST AND ROLLED-CAST STEELS SIMILAR TO 4330.

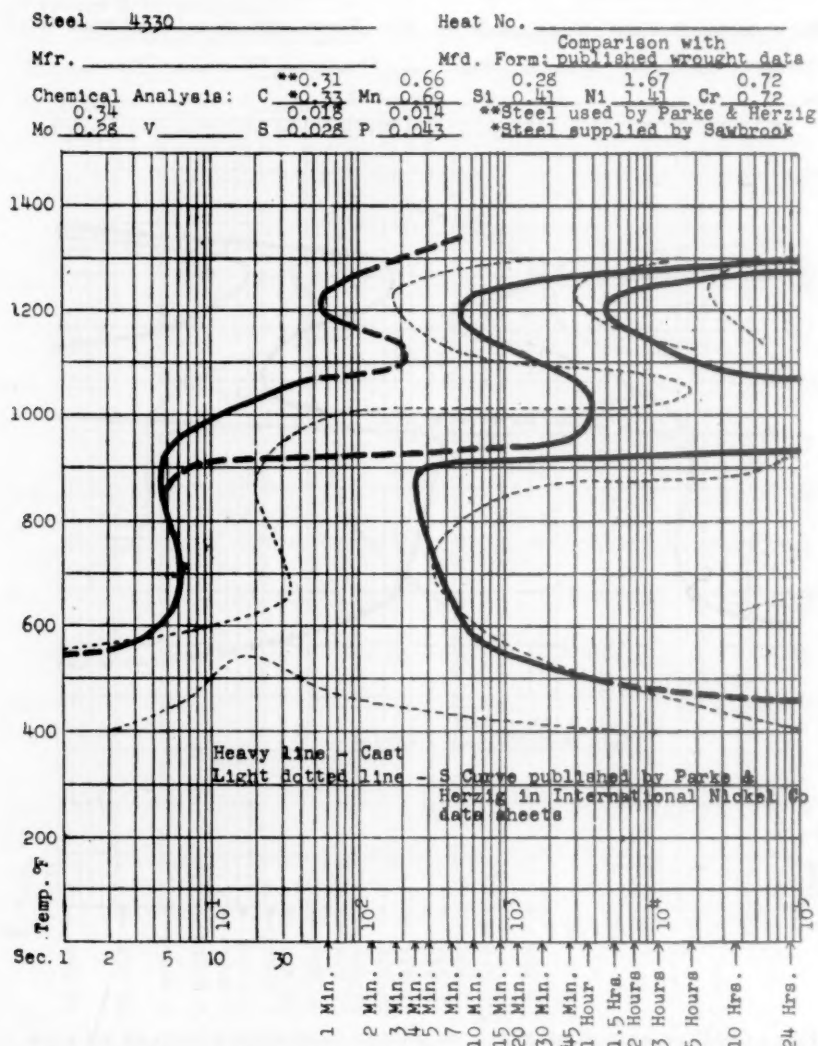


FIG. 14.—COMPARISON OF CAST AND WROUGHT STEELS SIMILAR TO 4130.

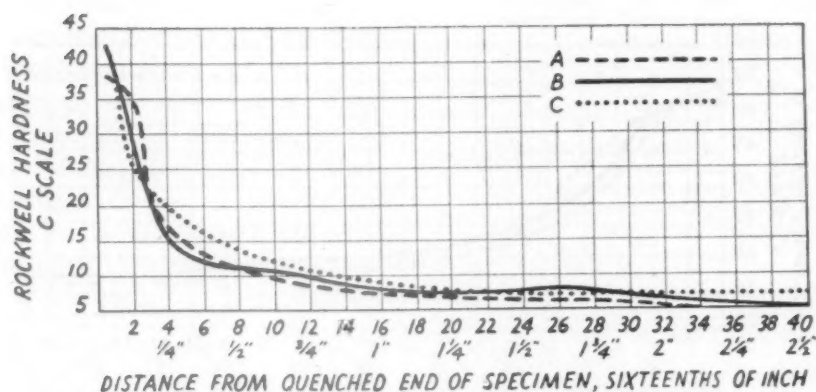


FIG. 15.—HARDENABILITY CURVE FOR CAST STEEL SIMILAR TO 1030.

Steel 1030	Composition, Per Cent					Quench, Temperature, Deg. F.	Grain Size
	C	Mn	P	S	Si		
A = Cast.....	0.30	0.75	0.026	0.040	0.46	1592	7-8
B = Cast.....	0.30	0.75	0.026	0.040	0.46	1692	7-8
C = Wrought.....	0.38	0.86				1525	Fine

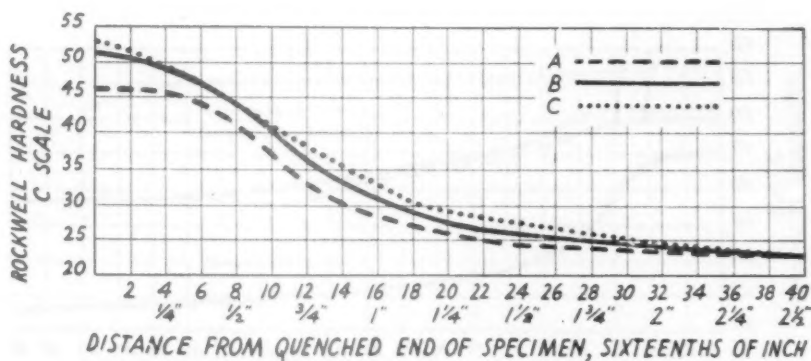


FIG. 16.—HARDENABILITY CURVE FOR CAST STEEL SIMILAR TO 2330.

Steel 2330	Composition, Per Cent								Quench, Temperature, Deg. F.	Grain Size
	C	Mn	P	S	Si	Cr	Ni	Mo		
A = Cast.....	0.28	0.69	0.043	0.028	0.41	0.12	3.30	0.03	1457	7-8
B = Cast.....	0.28	0.69	0.043	0.028	0.41	0.12	3.30	0.03	1560	7-8
C = Wrought.....	0.29	0.61					3.41		1505	7

Ohio, and the Crucible Steel Casting Co., of Cleveland, Ohio, for supplying the steels for the investigation.

The assistance of Prof. G. W. Boyd and Mr. R. B. Oliver, associates in the Department of Metallurgical Engineering at the Michigan College of Mining and Technology, in the microscopic work and in hardenability determinations is also gratefully appreciated.

REFERENCES

1. Technical Research Committee, S.F.S.A.: Final Report on Project No. 6, part I, Time-Temperature Transformation Curves (S-curves) for Use in the Heat Treatment of Cast Steels (Aug. 1944).
2. International Nickel Company data sheet: Isothermal Transformation Diagrams (S-curves) for Some Constructional Alloy and Carbon Steels.
3. M. A. Grossmann: Hardenability Calculated from Chemical Composition. *Trans. A.I.M.E.* (1942) **150**, 227.
4. *Trans. Amer. Soc. Metals* (Dec. 1939); also U.S.S. Atlas of Isothermal Transformation Diagrams.
5. Method of Determining Hardenability. S.A.E. Handbook, 1943 Ed., sec. 3, pt. 4.
6. M. Hill: Hardenability of Aircraft Steels. *Trans. Amer. Soc. Metals* (1943) **31**, 915, for S.A.E. 2330.
7. *Ibid.* for S.A.E. 4340.
8. T. A. Frischman: Carburizing the NE Steels, National Emergency Steels. *Amer. Soc. Metals* (Apr. 1943) **41**, for S.A.E. 4320.
9. W. E. Jominy: Hardenability Tests. Hardenability of Alloy Steels 85, for *Amer. Soc. Metals* for S.A.E. 1035.
10. R. M. Parke and A. J. Herzig: Hardenability of Molybdenum S.A.E. Steels. *Metals and Alloys* (1940) **11**, 12, for S.A.E. 4130.

Tensile Deformation

By JOHN H. HOLLLOMON,* JUNIOR MEMBER A.I.M.E.

(New York Meeting, February 1945†)

IN recent papers, O'Neill,¹ Vivian,² and Zener and Hollomon³ have reviewed some of the information concerning the relations between stress and strain during plastic deformation. Since further information has been obtained since these reviews were published, this paper attempts to further coordinate and amplify the knowledge concerning the plastic deformation of metals in simple tension.

Ordinarily the results of tensile tests of metals are presented as graphs in which the load divided by the original area is plotted as a function of the percentage of elongation measured over some specified gauge length. The interpretation of graphs of this sort is limited, since the stress required to deform the metal at any stage of the deformation is actually the load divided by the instantaneous rather than the original area. Furthermore, each increment of the deformation is performed on metal that has been previously deformed, and, as pointed out by Ludwik,⁴ the strain could be more effectively defined:

$$\epsilon = \ln \frac{A_0^\dagger}{A} \quad [1]$$

The statements or opinions in this article are those of the author and do not necessarily express the views of the Ordnance Department.

Manuscript received at the office of the Institute Dec. 19, 1944. Issued as T.P. 1879 in METALS TECHNOLOGY, June 1945.

* Captain, Ordnance Department, U. S. Army, Watertown Arsenal, Watertown, Mass.

† Meeting canceled.

‡ For large strains, the change in dimensions due to the change in volume accompanying elastic deformation will be small compared with the change in dimensions arising from plastic flow. If the actual area under load has been measured, the plastic strain is equal to $\ln \frac{A_0}{A} - 2\nu(S/E)$, where A is the area under load; ν , Poisson's ratio; S , the stress, and E , Young's modulus.

where ϵ is the strain and A_0 and A are, respectively, the original and instantaneous areas.

The results of the tensile tests can be more effectively presented and interpreted if the stress* (load divided by actual area) is plotted as a function of the strain as defined above. A schematic curve of this type is presented as Fig. 1.

In a previous paper,⁶ the concept of Ludwik⁷ concerning the flow and fracture of metals was successfully employed to explain some of the puzzling results of notched-bar impact tests of steel. It appears that the use of this concept is very fruitful and should be kept in mind in any study of the deformation characteristics of metals. Ludwik considered that a flow stress-strain curve of a metal was essentially a locus of points that described the stress required for plastic flow of an infinite number of specimens, each with a different strain history determined by the preceding part of the flow curve. Each of these specimens can also be considered to have a fracture strength. Unfortunately (or fortunately depending upon the point of view), all the specimens, except the one deformed to the fracture strain, flow and do not fracture. Even though the metals do not fracture, the concept of a fracture-strength curve seems

¹ References are at the end of the paper.

* After necking commences, the stress in the necked region is not strictly uniform nor uniaxial. The correction to the average tensile stress necessitated by the nonuniformity of the stress, has been recently developed by Bridgman.⁸ In moderately ductile metals, the correction to the average tensile stress as calculated above was found to be small.

to be effective in rationalizing many of the properties of metals, particularly of steels, to which the concept has been more frequently applied.

The entire problem of the mechanical behavior of metals resolves itself into the separate problems of determining and relating the effects of temperature, strain rate, stress combination, deformation, and metallurgical structure on the stress required for flow and the stress required for fracture. Since tensile deformation is the simplest type to which a metal may be subjected, the usual method of study is to consider the effects of the other variables on the tensile stress-strain curves. It appears, however, that such data can be more effectively interpreted by the concepts of Ludwik than by considering the stress-strain curve as an entity.* This paper will be concerned primarily with the effects of strain on the stress required for flow, as modified by changes in metallurgical structure. (It is hoped that the fracture problem may be developed in more detail in subsequent papers.) Unfortunately, most of the data on this subject have been obtained for steel, and, as a consequence, this discussion will have to be concerned primarily with that metal. The effects of temperature and rate of strain have been discussed to some extent elsewhere.^{3,8,9} For the most part, the data of this paper will refer to stress-strain curves obtained at or near 20°C. and at strain rates of the order of 10^{-4} sec.⁻¹ The effect of stress distribution will not be discussed in this paper.

INITIAL YIELDING

For the purpose of discussion, the tensile stress-strain curves can be divided into three distinct regions: the elastic, the initial yielding, and the plastic flow. The so-called elastic part of the deformation

will not be treated in this paper.* Suffice it to say that in polycrystalline metals during the elastic deformation the stress is essentially proportional to the strain,

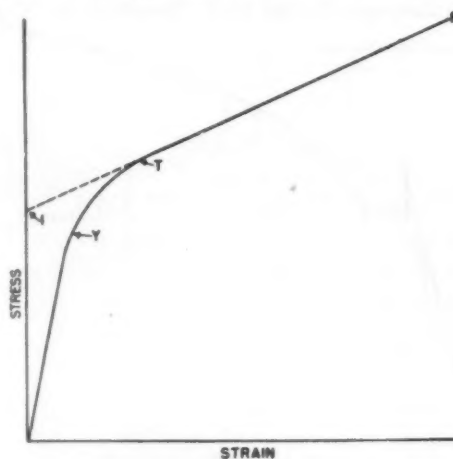


FIG. 1.—SCHEMATIC STRESS-STRAIN CURVE.

- I. Intercept.
- Y. Yield strength.
- T. Point at which necking begins.
- F. Fracture strength.

the constant of proportionality being referred to as the elastic modulus.

For some metals, the stress-strain curve deviates only gradually from this straight line; in others, the deviation is sharp. The discontinuous type of yielding is referred to variously as the Piobert effect, Lüders' deformation, etc.; it is the phenomenon that manifests itself in upper and lower yield points, and in discontinuous or heterogeneous deformation.† A schematic stress-strain curve of a metal that exhibits the heterogeneous yielding is presented as Fig. 2. This yielding phenomenon has been discussed in detail by Nadai¹⁰ and by Carpenter and Robertson.¹¹ Re-

* The little space assigned to elastic deformation should not be taken to imply that its study or a discussion of the properties of metals in this region is not important. The author understands that C. Zener will shortly publish a paper summarizing the inelastic effects in the elastic region.

† The entire specimen does not deform uniformly, but regions of the metal at angles of nearly 45° to the axis of the specimen deform. The deformation starts at stress concentrations and then transverse the specimen (see Nadai¹⁰).

* Difficulties attendant to interpreting the results of tensile tests on specimens previously deformed in torsion are cases in point.

cently, Edwards, Phillips and Liu¹² studied the effect in metals other than mild steel. In the United States, Winlock and Leiter¹³ have been perhaps the major contributors

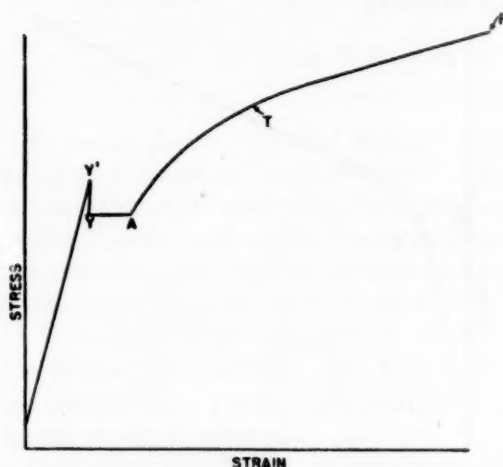


FIG. 2.—SCHEMATIC STRESS-STRAIN CURVE OF A METAL HAVING DROP IN LOAD AT YIELDING.

- Y'. Upper yield stress.
- YA. Lower yield strain.
- T. Point at which necking begins.
- F. Fracture strength.

to the knowledge of this phenomenon. It is generally conceded that in steels the presence of carbides or nitrides precipitated in the grain boundaries during cooling is responsible for this type of yielding. A possible mechanism has been suggested by several investigators, Nadai¹⁵ in particular, and has been discussed frequently.^{3,11,14}

Gensamer and Low¹⁶ have shown that if the carbon and nitrogen are removed from iron the metal does not yield initially in this manner. If, on the other hand, as little as 0.002 per cent of either of these elements is reintroduced into the metal, the Piobert effect is again manifest. It appears that in steels there are at least two conditions that must be fulfilled before this type of initial heterogeneous yielding occurs. Not only must there be a precipitate on the grain boundary, but also the carbide distribution within the grains must make possible a free path of ferrite from grain boundary to grain boundary. The more random the distribu-

tion of the carbides, and the more spheroidal the carbides, the more likely is the occurrence of the Piobert effect. This point of view is confirmed by the data of Gensamer and collaborators,¹⁷ who found that in eutectoid steels the heterogeneous yielding occurred at higher yield strengths when the carbides were spheroidal than when they were lamellar. In the latter case, it is difficult to imagine a continuous path in the ferrite from boundary to boundary (at the specified angle of nearly 45° to the axis of the specimen), except when the pearlite is very coarse. With spheroidal carbides (tempered martensitic steels), a continuous path in the ferrite is possible, even for relatively numerous, dispersed particles. It is not yet possible to apply this reasoning quantitatively to the yielding phenomenon, since the exact mechanism of the phenomenon is not known.

The height of the stress-strain curves for polycrystalline single-phase metals seems to be governed by the strength of the single crystals of the metal, as modified by the grain-boundary restraint. Sachs¹⁸ and G. I. Taylor¹⁹ have discussed in detail the stress-strain curves of such metals. Norbury²⁰ pointed out that the hardening effect of elements in solid solution was related to the difference in size between the solvent and solute atoms. For irons that showed little or no inhomogeneous initial yielding, Gensamer and Lacy²¹ found that increase in strength due to the introduction of solute elements was related to the atomic percentage of the alloying elements in the following manner:

$$\Delta S = kx^n$$

where ΔS is the increase in strength characteristic considered (tensile strength, etc.), x is the atomic percentage of solute, n a number of the order of magnitude of $\frac{3}{4}$ and k a constant that depends on the added element. The value of k is larger the greater the lattice distortion of the

solvent, engendered by the introduction of the solute. In general, the greater the amount of solute that can be accommodated (the greater the solubility), the smaller will be the value of k .

stress-strain curves of polycrystalline metals consisting of two phases seems to be controlled by the mean straight path through the continuous phase. Gensamer and co-workers¹⁷ first stated the principle

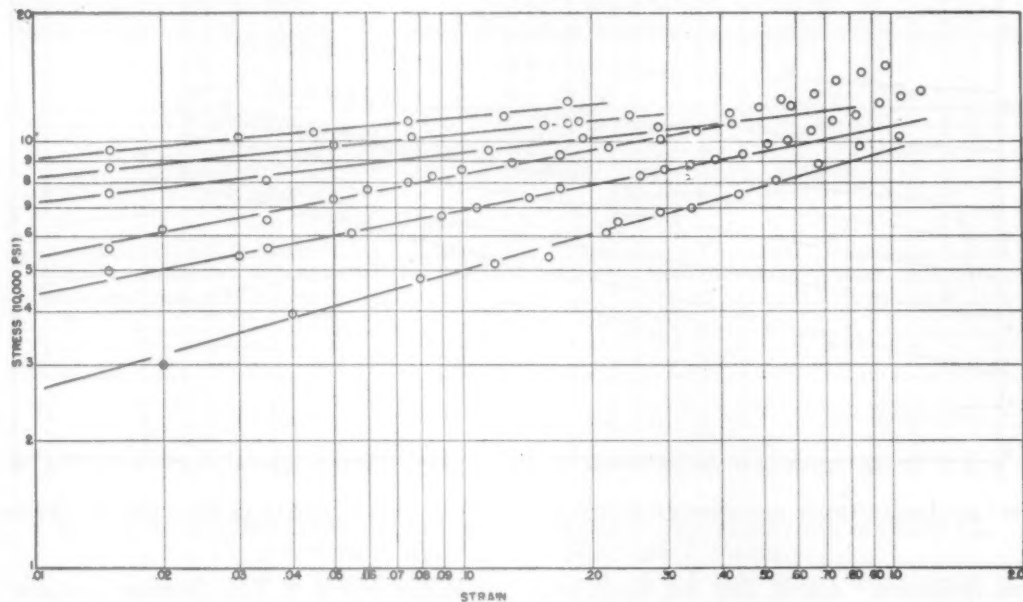


FIG. 3.—LOGARITHMIC STRESS-STRAIN CURVES OF S.A.E. 1020 STEEL (0.20 PER CENT C). (From Hollomon.²⁷)

Grain size also affects the yield strength (markedly, when the yielding is discontinuous) and the tensile strength. The smaller the grain size, the greater will be the strength at a given strain. Wood²² found that the hardness, which is a measure of both the yield strength and the slope of the initial plastic portion of the stress-strain curve, varied linearly as the reciprocal of the square of the average grain diameter. A relation of this type between the yield or tensile strengths and grain size was not found for the data for brass, which are discussed subsequently. Edwards and Pfeil²³ performed experiments to determine the effect of grain size on the tensile properties of iron. They found that the lower yield strength (Y of Fig. 2) increases more rapidly as the grain size decreases than does the rising part of the stress-strain curve (A to T of Fig. 2).

On the other hand, the height of the

in the following form: "The resistance to deformation of a metallic aggregate consisting of a hard phase dispersed in a softer one is proportional to the logarithm of the mean straight path through the continuous phase." As the average distance becomes smaller, the yield strength (stress at any given value of the strain) increases.

FLOW OF DEFORMED METALS

After the initial yielding, the shapes of the stress-strain curves of all metals are similar;* the stress increases with strain at a decreasing rate. Little attention has been given to the relation between stress and strain in this region, or to the effect of changes in metallurgical structure on the shape of this portion of the curve. It has been suggested, however, by Norris²⁴

* Except for steels in the blue-brittle range and a few other metals, in which case the stress-strain curves are serrated.

and by Nadai¹⁰ that the logarithm of the stress is very nearly a linear function of the "true tensile elongation,"* and MacGregor,²⁵ Gensamer and collaborators^{17,26}

dium steel containing 0.45 per cent carbon, which were quenched to martensite and tempered at five temperatures for one hour. The stress-strain curves for this steel are

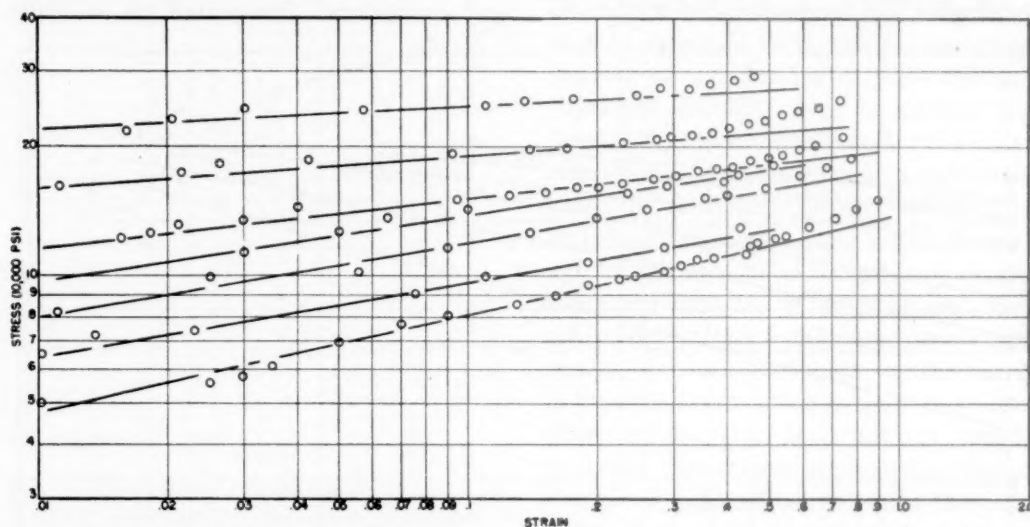


FIG. 4.—LOGARITHMIC STRESS-STRAIN CURVES OF S.A.E. 1045 STEEL (0.49 PER CENT C). (From Hollomon.²⁷)

and Hollomon²⁷ found that for steels the stress is a linear function of the strain from T (Figs. 1 and 2) to the fracture strain. Ludwik,⁴ in his early studies, found that during plastic flow, the following relation expressed approximately the relation between stress and strain:

$$S = S_0 - K(\epsilon)^m \quad [2]$$

where S_0 , and K and m are constants.

In Figs. 3, 4, 5, and 6, the data for variously heat-treated specimens of four plain carbon steels are plotted on logarithmic paper. The data of Figs. 3 and 4 are taken from a previous paper,²⁷ the data of Fig. 6 are taken from the results of Gensamer and co-workers.²⁶ The data of Fig. 5 are new, having been obtained with a series of plain carbon steel specimens quenched to martensite and tempered at each of four temperatures for one hour. In Fig. 7, the data are plotted for specimens of a chromium-molybdenum-vana-

presented in Fig. 8. The chemical composition of the steel was: C, 0.45 per cent; Mn, 0.75; Si, 0.34; S, 0.016; P, 0.022; Cr, 1.02; Mo, 0.38; V, 0.14. The specimens were $\frac{5}{8}$ in. round, taken transverse to forging direction, austenitized at 1650°F. for 1 hr. and quenched in oil and tempered 1 hr. at temperatures indicated in Fig. 8.

It is to be noted that for all the data the logarithm of the stress is essentially a linear function* of the logarithm of the strain, from strains of about 0.01 to about 0.4. For strains larger than about 0.4, the data in most cases diverge upward from the straight lines. The upward divergence from strains of about 0.4 to the fracture strain may possibly be associated with anisotropy, which, of course, will depend on the manner in which the strain occurs. In order to illustrate that the divergence of the stress-strain curves from linearity

* The ratio of the initial area to the actual area minus one.

* For steels that exhibit a drop in load at yielding and a lower yield-point elongation, this linearity of the logarithmic stress-strain curve commences when the stress begins to rise (after the lower yield elongation).

may be due to orientation effects, logarithmic shear stress-strain curves for a mild steel are plotted in Fig. 9. Curve *A* was derived³ from tensile stress-strain

large shear strains, while the torsion data diverge downward. A fundamental difference in the behavior in tension and torsion has been discussed in detail³ and has been

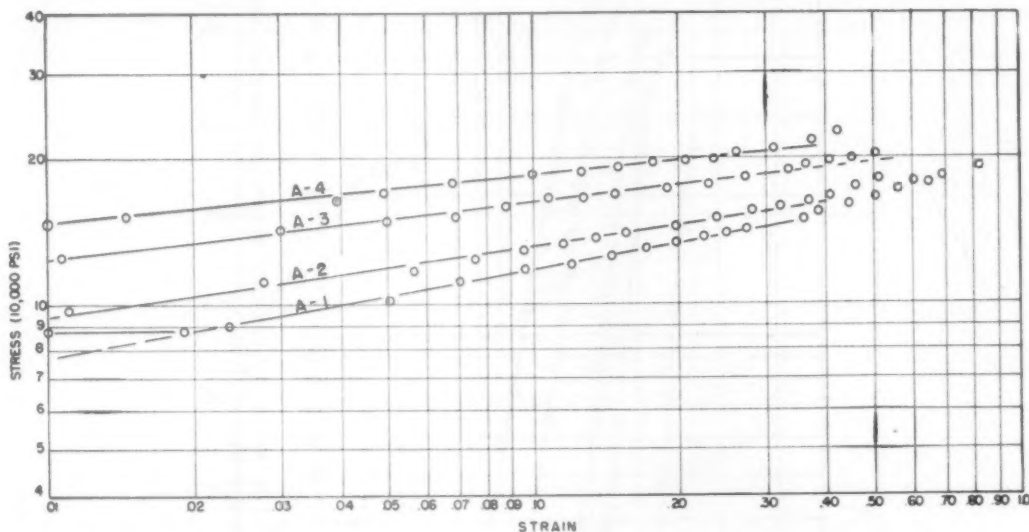


FIG. 5.—LOGARITHMIC STRESS-STRAIN CURVES OF S.A.E. 1055 STEEL (0.59 PER CENT C).

- A-1. 1600°F. water quench; draw 1300°F. 1 hour.
 A-2. 1600°F. water quench; draw 1200°F. 1 hour.
 A-3. 1600°F. water quench; draw 1100°F. 1 hour.
 A-4. 1600°F. water quench; draw 1000°F. 1 hour.

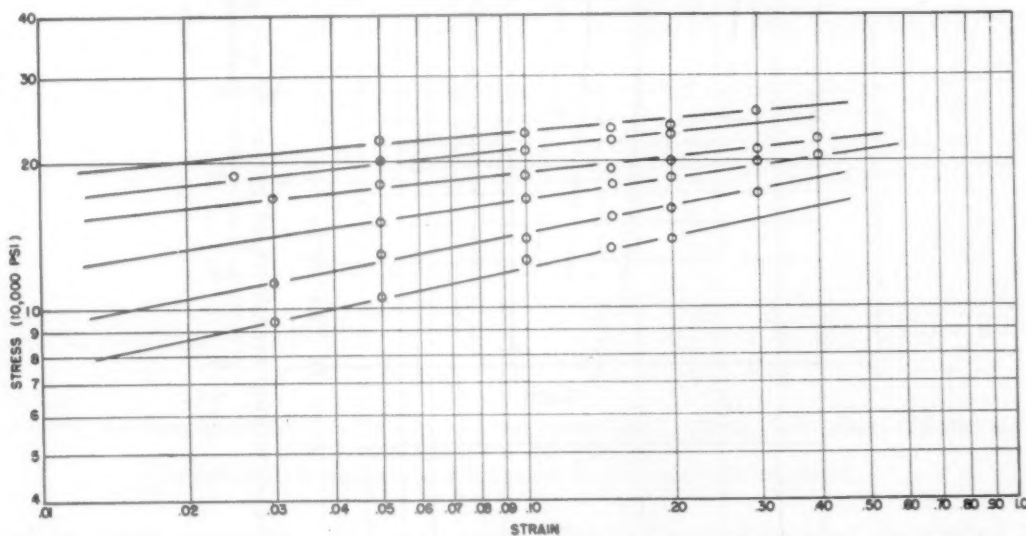


FIG. 6.—LOGARITHMIC STRESS-STRAIN CURVES (0.78 PER CENT C). (From Gensamer et al.²⁶)

data, utilizing Von Mises' viewpoint, and curve *B* was taken directly from a torsion test performed on the same material. The data derived from the tensile test diverge upward from the strain line for

ascribed to the difference in orientation effects (of carbides) associated with the two types of deformation.

For copper and brass, however, the linearity of the logarithmic stress-strain

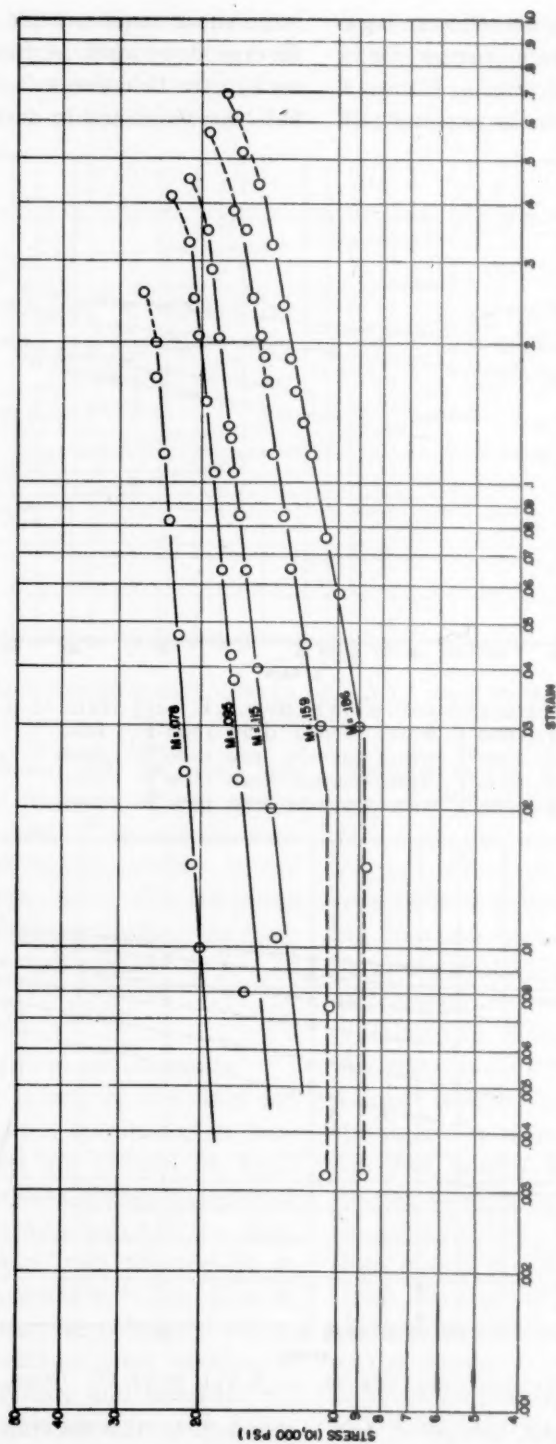


FIG. 7.—LOGARITHMIC STRESS-STRAIN CURVES OF 0.45 PER CENT C ALLOY STEEL AT VARIOUS STRENGTH LEVELS (ALL SPECIMENS TEMPERED MARTENSITE; SEE FIG. 8).

curves appears to continue to the fracture strain. When the stress-strain curves are plotted logarithmically, an anomalous behavior of these metals is revealed. An

annealing temperatures that would produce a range of grain sizes, and, on the basis of these experiments, the annealing temperatures listed in Table I were chosen.

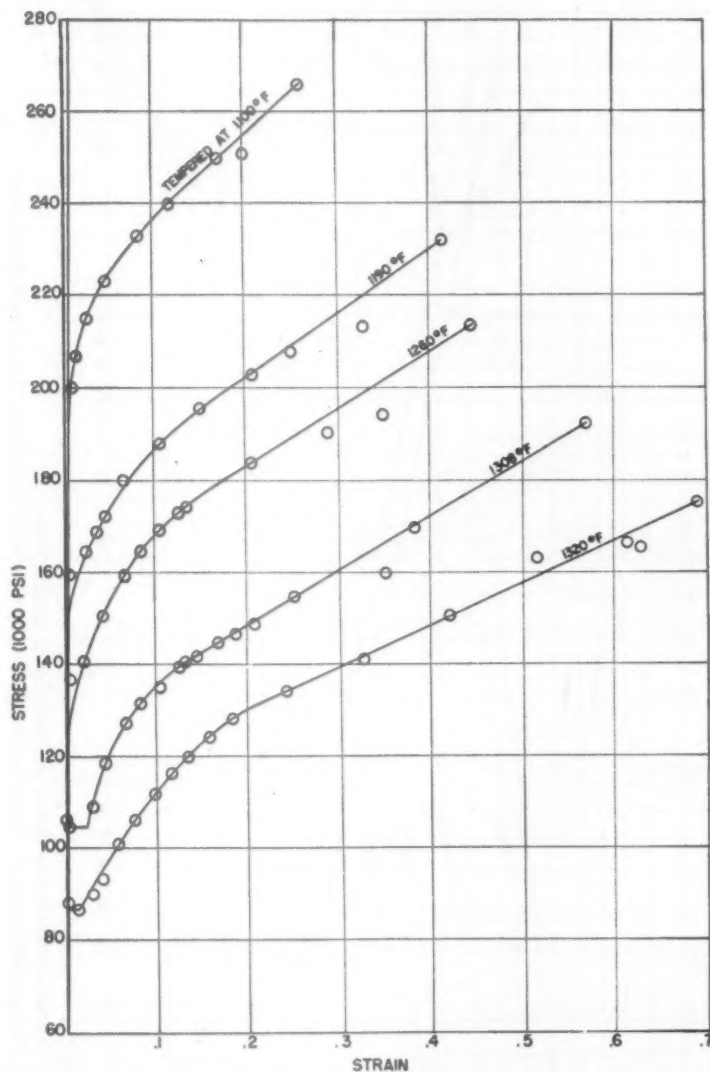


FIG. 8.—STRESS-STRAIN CURVES FOR 0.45 PER CENT CARBON STEEL CONTAINING CHROMIUM, MOLYBDENUM AND VANADIUM.
(Quenched to martensite and tempered to temperatures indicated.)

alpha brass containing 69.4 per cent OFHC copper, and the remainder zinc, was obtained in the annealed condition, in the form of $\frac{1}{2}$ -in.-diameter bar stock, with an average grain size of 0.015 mm. Certain preliminary annealing experiments were performed in order to determine the

The resultant grain sizes determined by metallographic examination and by comparison with the A.S.T.M. Standards, are also listed in this table.

After the annealing treatments, standard 0.357-in.-diameter tensile specimens having a 2-in. uniform gauge length were

machined from bar stock receiving all treatments. The specimens were then pulled in tension at a strain rate of approximately 10^{-4} sec. $^{-1}$ The load and elongation

replaced with a special diameter gauge. The diameter and load were then measured simultaneously to fracture. These measurements were made with the apparatus and

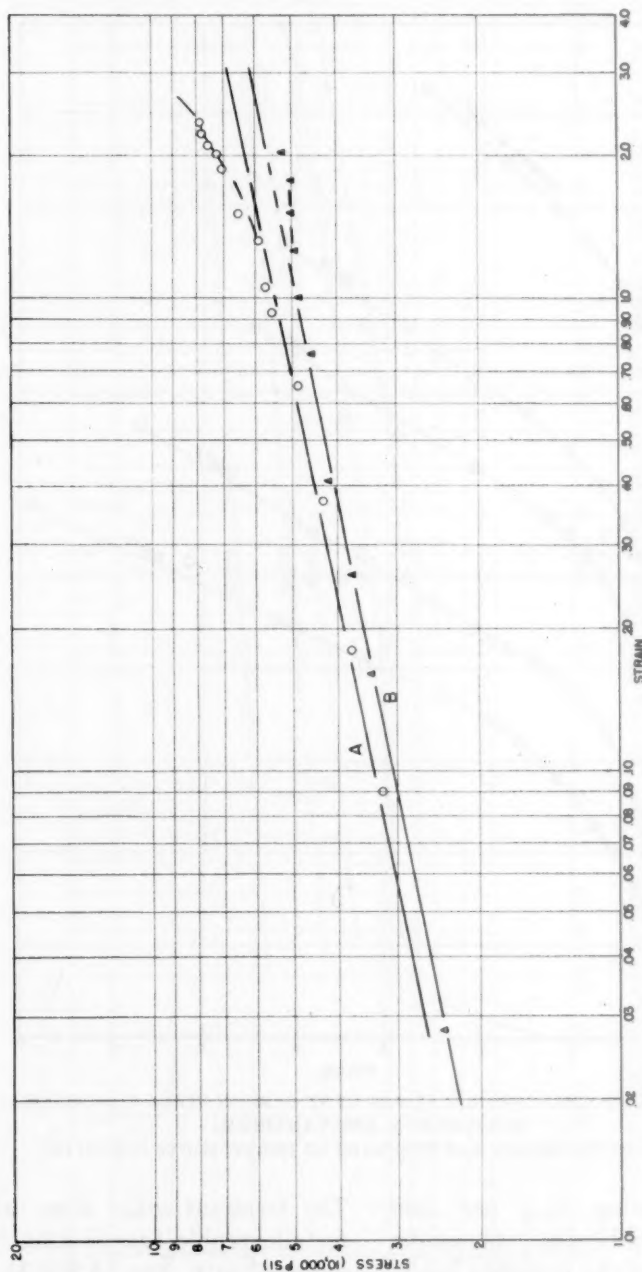
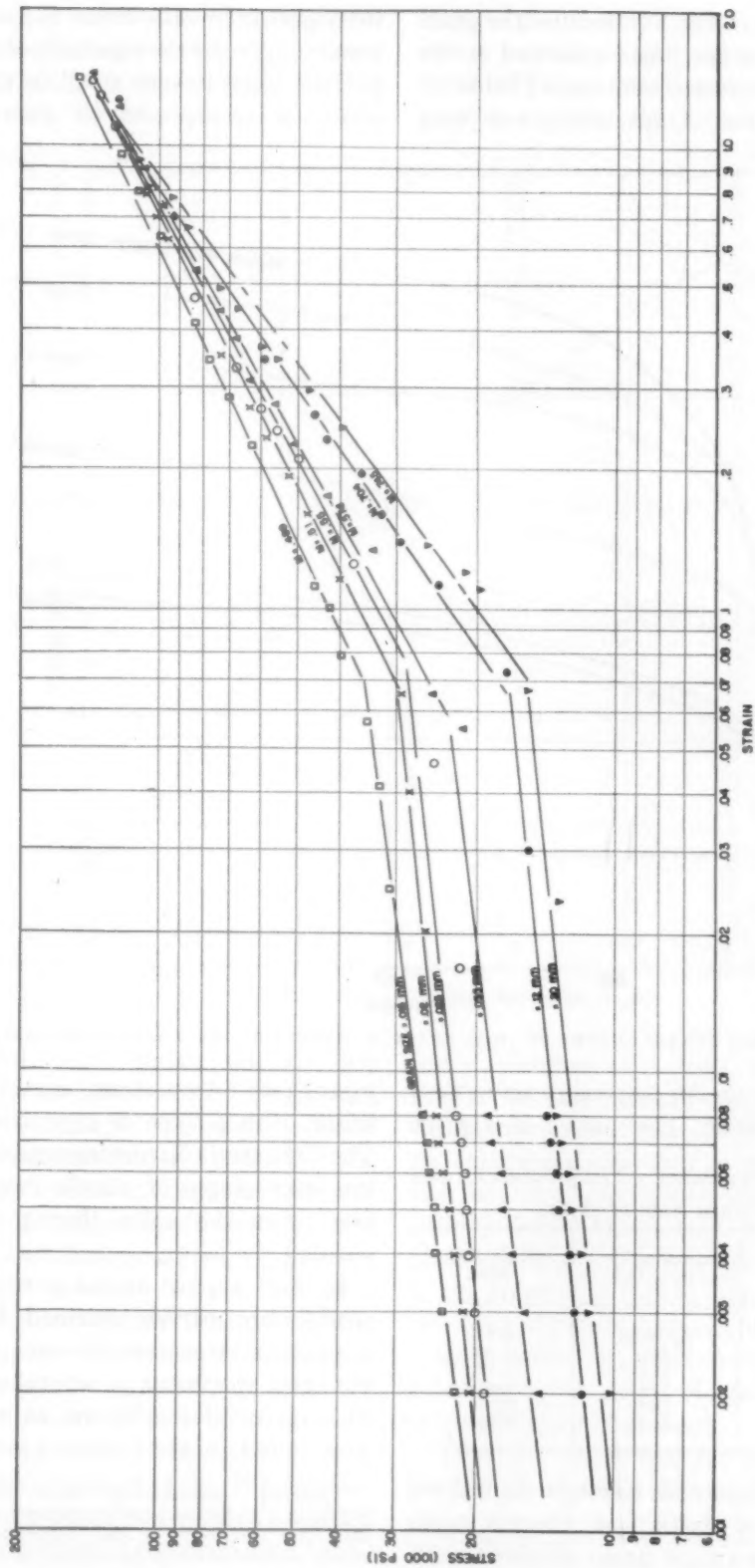


FIG. 9.—COMPARISON OF TENSION AND TORSION LOGARITHMIC STRESS-STRAIN CURVES.
A. Shear-stress strain curve derived from tensile test.
B. Shear-stress strain curve derived from torsion test data from Zener and Hollomon.³

were measured up to approximately a strain of 0.008, the elongation being measured with an Olsen extensometer. The extensometer was then removed and

by the technique described in a previous paper.⁸

The data for the brass specimens of various grain sizes are plotted on loga-



rithmic paper in Fig. 10. Because the grain size of the two specimens annealed at the highest temperatures were large (Table I), the deformation of specimens was very

the logarithm of the stress is essentially a linear function of the logarithm of the strain, but the slope is very small (0.1). From a strain of about 0.06 to fracture,* the

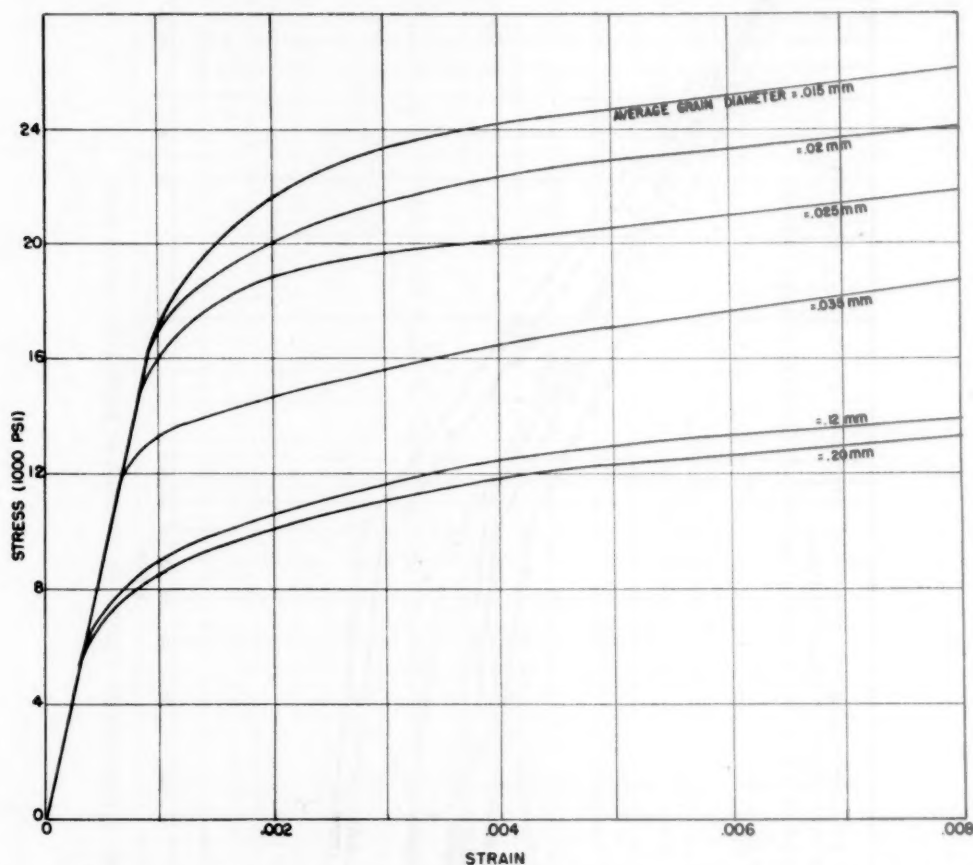


FIG. 11.—STRESS-STRAIN CURVES OF 70-30 BRASS OF DIFFERENT GRAIN SIZES (FOR SMALL STRAINS).

irregular and the stress-strain curves were somewhat erratic. The curves of Fig. 10

TABLE I.—Annealing Temperatures and Grain Size of Brass

Specimen No.	Annealing Temperature, Deg. C.	Grain Size, Mm.
1	As recd.	0.015
2	505	0.02
3	515	0.025
4	575	0.035
5	680	0.12
6	800	0.20

reveal a difference in behavior during the two regions of plastic flow. From a strain of about 0.002 to a strain of about 0.06,

logarithmic stress-strain curves are also linear, with a slope of approximately 0.5. Thus, the strain-hardening exponent during the later stages of plastic flow is about five times the value during the initial yielding.

In Fig. 11, the initial portions of the stress-strain curves obtained from load-elongation measurements are plotted for the brass specimens of several grain sizes. The curves of this figure, as well as the data found in the standard compilations

* Recent unpublished data obtained by Bridgman indicate that for copper in compression the linearity of the logarithmic stress-strain curves extends to strains of about 3.5.

of mechanical properties of commercial single-phase alloys, indicate that the stress-strain curves during the initial yielding rise only very slowly, even though it is

largest grain size.* The initial, slowly rising portion of the stress-strain curve followed by a second more sharply rising portion suggests that the nature of the

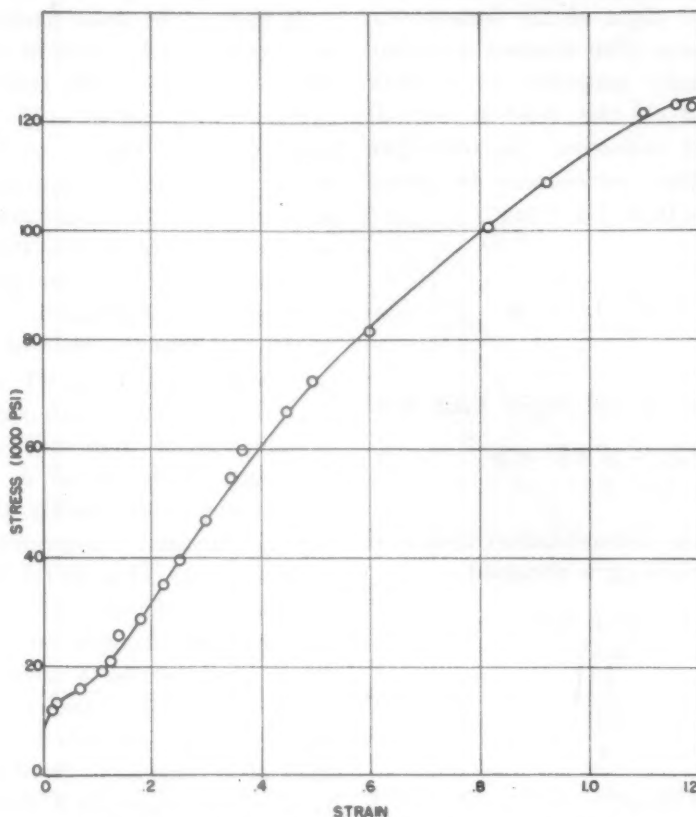


FIG. 12.—TYPICAL STRESS-STRAIN CURVE OF BRASS.

well known that these materials are extremely work-hardenable. Wilkins and Bunn,²⁸ for example, in their recently published compilation of data for the coppers and brasses, indicate that the yield strengths of copper and brass in the annealed condition measured at different small strains are very nearly the same. The significance of this behavior during the initial plastic flow has, however, not been discussed.

This anomalous behavior can also be illustrated by the stress-strain curves over the whole range of plastic deformation from yield to fracture. In Fig. 12, such a curve is presented for the brass having the

initial yielding of copper and brass is similar to that of mild steel. That the deformation does not occur completely by inhomogeneous flow is evidenced by the fact that the initial yielding is not sharply defined, as in steel. It is, however, most significant that there are two regions of the stress-strain curve that have fundamentally different characteristics. Recent English work¹² has demonstrated that this inhomogeneous type of yielding occurs in metals other than steel.

Thus, for steels and for at least some nonferrous metals, the relation between

* Similar curves were obtained for all of the brass specimens tested. Fig. 12 is typical.

stress (S) and strain (ϵ) in the plastic region after the initial yielding may be expressed by the following relation:

$$S = K(\epsilon)^m \quad [3]$$

where m is the slope of the logarithmic stress-strain curve. This relation is similar to that originally proposed by Ludwik (Eq. 2). Based on this relation, several interesting and important characteristics of the stress-strain curves may be developed. It follows from Eq. 3 that:

$$\frac{\frac{dS}{S}}{\frac{d\epsilon}{\epsilon}} = \left(\frac{dS}{d\epsilon}\right) \frac{\epsilon}{S} = m \quad [4]$$

Necking begins at maximum load and:

$$\begin{aligned} dL &= d(AS) = 0 \\ \text{since } L &= AS \end{aligned} \quad [5]$$

Carrying out the differentiation indicated in Eq. 5, the following is obtained:

$$\begin{aligned} AdS + SdA &= 0 \\ \text{or } \frac{\frac{dS}{S}}{\frac{dA}{A}} &= -1 \end{aligned} \quad [6]$$

But since from Eq. 1:

$$\frac{dA}{A} = -d\epsilon \quad [7]$$

Eq. 6 becomes:

$$\frac{dS}{d\epsilon} = S \quad [8]$$

This relation was developed by Gensamer²⁹ and indicates that necking (inhomogeneous or local deformation) will begin at the strain at which the slope of the stress-strain curve becomes equal to the stress. Substituting Eq. 8 in Eq. 4,

$$\epsilon_m = m \quad [9]$$

where ϵ_m is the strain at the maximum load.* Thus, the amount of uniform

* Conversations with M. Gensamer indicate that J. R. Low, formerly of Lehigh University, developed this relation independently.

deformation before necking begins is equal to the strain-hardening exponent. As indicated in the appendix, this relation permits a rapid approximate method of obtaining complete stress-strain curves.

In Fig. 13, the strain-hardening exponent is plotted as a function of the stress at a strain of 0.01 (yield strength) for the carbon steels whose stress-strain curves are plotted in Figs. 3 to 6. The strain-hardening exponent appears to depend only upon the yield strength, independent of the structure of the steel. The steels were of various structures: pearlite, bainite, and tempered martensite. The commonly held belief that the ratio of yield strength to tensile strength depends upon structure may be reconciled with these data, if it is remembered that fully quenched and tempered steels reveal a drop in load at yielding more readily than do steels having lamellar structures. The lower yield strength of a metal having a drop in load at yielding is greater than would be the yield strength (at a small strain) for a steel having a continuously rising stress-strain curve and the same tensile strength. Fully quenched steels, therefore, may often appear to have a larger yield-tensile ratio than steels having a lamellar structure. The specimen of 0.59 per cent carbon steel tempered at 1300°F. illustrates this phenomenon. This specimen reveals a drop in load at yielding and a pronounced lower yield-point elongation. As indicated in Fig. 5, the stress at a strain of 0.01 obtained by extrapolating the smooth stress-strain curve is about 14,000 lb. per sq. in. smaller than is the lower yield stress.

The equation of the straight lines of Fig. 13 may be written as:

$$\log m = K' - 0.94 \log S_{0.01} \quad [10]$$

where m is the slope of the logarithmic stress-strain curve, $S_{0.01}$ is the stress at a strain of 0.01, and K' is a constant that depends upon the carbon content

as indicated in Fig. 14. Thus, for the plain carbon steels investigated, the yield strength and carbon content together will determine, with the use of Fig. 14 and

at a strain of 0.01. These data have been collected over the last few years and seem to indicate that for alloy steels the strain-hardening exponent is slightly higher than

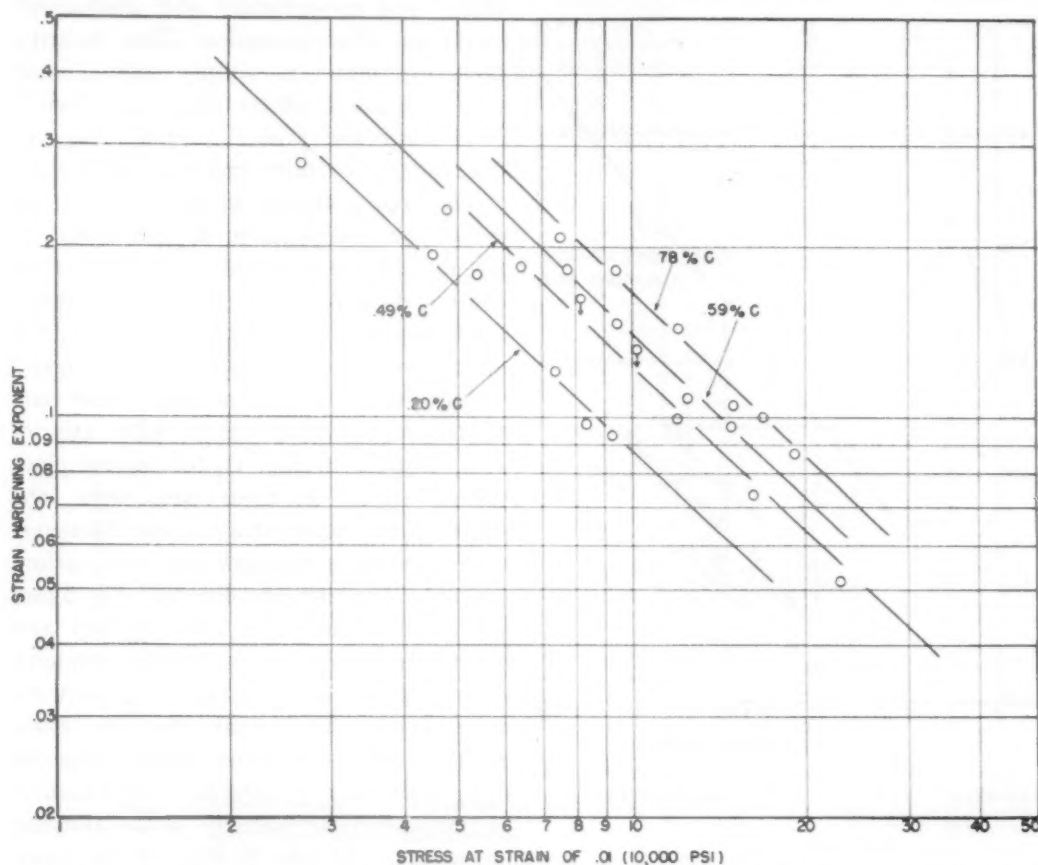


FIG. 13.—VARIATION OF SLOPES OF LOGARITHMIC STRESS-STRAIN CURVES WITH STRENGTH LEVEL, FOR SEVERAL CARBON CONTENTS.
(From Figs. 3, 4, 5 and 6.)

Eq. 10, the slope of the logarithmic stress-strain curve (in the range of strain from 0.01 to 0.4). For most practical purposes, the value of 0.94 may be made equal to one with the following result:

$$m = \frac{K}{S_{0.01}} \quad [11]$$

The strain-hardening exponents for a large number of forged medium alloy steels consisting of various metallurgical structures and of various compositions are plotted in Fig. 15, a function of the stress

for the corresponding plain carbon steels. No trend in the effects of individual alloying elements has been observed.

For the brass specimens, the dependence of the strain-hardening exponent on yield strength is of the same form as Eq. 10, except that for brass, the constant (0.94) is about 0.5. The relation between the strain-hardening exponent and the yield strength for the brass specimens whose stress-strain curves are plotted as Fig. 10 is plotted as Fig. 16. The slope of the straight line of this figure is approximately one half.

The strain to the maximum load may in many practical applications be a most important criterion of a metal's behavior. In deep-drawing operations, for example,

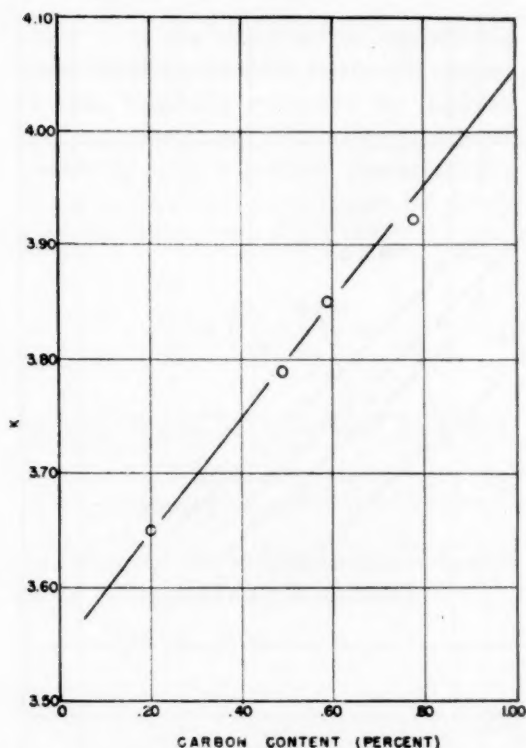


FIG. 14.—EFFECT OF CARBON CONTENT ON VARIATION OF SLOPE WITH YIELD STRENGTH (K OF EQUATION 3).

the extent to which the drawing may be carried out will be determined by the amount of strain (under the complex stress pattern) that occurs before "necking." As pointed out by Bartholomew³⁰ and MacGregor,³¹ the relative drawability of metals is related to the strain to maximum load. In this connection, the data of Fig. 13 lead to an interesting conclusion; for *equal yield strengths*, the strain to maximum load (strain-hardening exponent) is greater the higher the carbon content.

MacGregor²⁸ first pointed out that, at least for steels,* the stress-strain curves

* MacGregor's data also indicate that the stress-strain curves were linear in this region for cold-worked brass and copper. However, the data for brass just discussed are not in agreement with this conclusion.

are linear from about the strain to the maximum load (T of Figs. 1 and 2) to the fracture strain (F of Figs. 1 and 2). The data obtained subsequently by Gensamer and co-workers²⁶ and Hollomon²⁷ confirmed this conclusion. This linearity, however, may be simply coincidental; the orientation effects may be sufficient to modify the power relation (Eq. 3), that the stress-strain curve becomes linear.*

The slope of this linear part of the stress-strain curve appears to depend upon the strength of the steel and upon the carbon content. In Fig. 17, the slope of the strain-hardening curve is plotted as a function of the so-called "unstrained strength" (intercept of the extrapolated linear part of the stress-strain curve with axis of zero strain, I of Fig. 1), for several plain carbon steels. As these data show, the slope of the stress-strain curve increases with increasing strength for each carbon content. The straight line in this figure was obtained from the data of Lacy and Gensamer,²¹ who changed the strength of iron by the addition of alloying elements only. Their data indicate that the slope of the strain-hardening curve depends only upon the "intercept," independent of the amount or identity of the alloying elements in the iron. In Fig. 18, the maximum and minimum slopes of the stress curves are plotted as a function of carbon content. These curves are taken from the paper by Zener and Hollomon,³ except the point for zero carbon, which was taken from the data of Lacy and Gensamer.²¹ The effect of alloying elements on the latter portion of the stress-strain curve is not known; it appears, however, that metallurgical structure plays little role in determining the slope.

FRACTURE

The tensile stress-strain curve is terminated by fracture. As pointed out

* This relation between stress and strain after necking commences may not be of too great significance because of the nonuniformity of stress at the neck.⁵

previously, fracture occurs when the metal is so deformed that the tensile stress required for plastic flow becomes equal to the stress required for fracture. Ludwik,⁷

steels appears to be essentially independent of strain. Studies of such curves are complicated, because indirect means must be utilized for their determination,

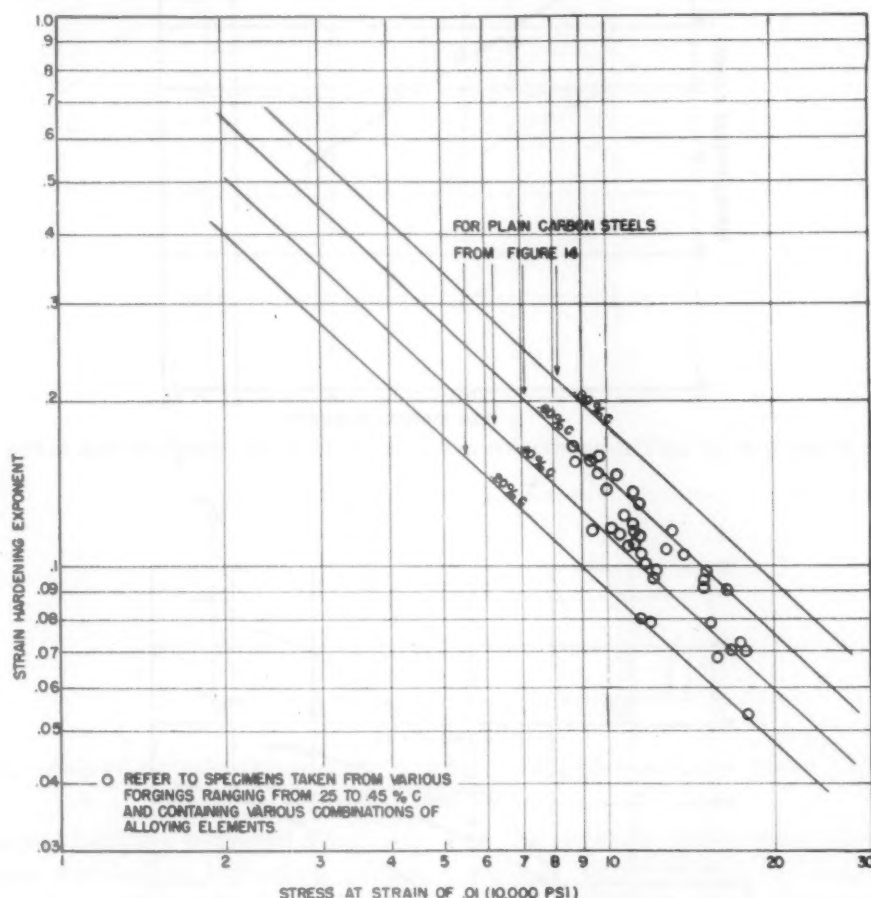


FIG. 15.—EFFECT OF STRENGTH LEVEL ON SLOPE OF LOGARITHMIC STRESS-STRAIN CURVE.

Kuntze,³² McAdam and co-workers,³³ Davidenkov and Wittmann,³⁴ Sachs and co-workers,³⁵ and Hollomon⁶ have used this concept effectively in interpreting the deformation and fracture characteristics of metals. The author in a previous paper⁶ suggested that the slope of the fracture-strength curve depends primarily upon the metallurgical structure. Schematic fracture and flow curves for steels of typical structures are presented as Fig. 19. The fracture curve of pearlitic steel increases rapidly with tensile deformation, while the curve for tempered martensitic

since plastic flow rather than fracture occurs under normal conditions. Furthermore, the change of the stress required for fracture with deformation is anisotropic, unlike the stress required for plastic flow. The entire problem of the behavior of metals under complex conditions of strain rate, stress distribution and temperature can be rationalized, however, by means of studies of these two curves. Using these concepts, an interpretation⁶ of the paradoxical notched-bar impact results of steels has been attempted recently. Future work will include primarily studies of

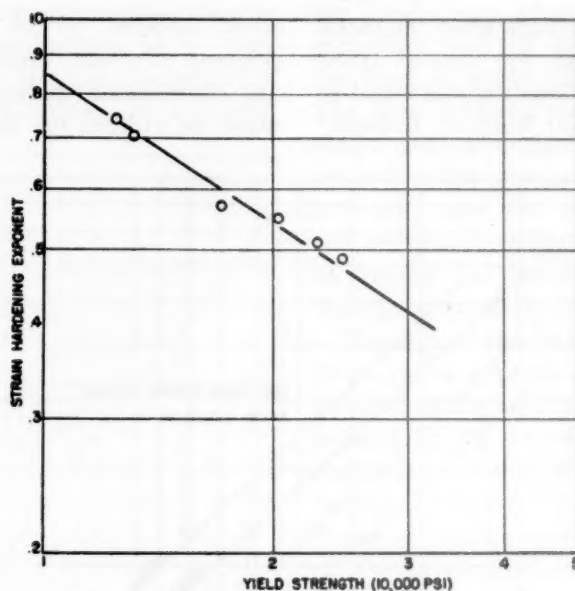


FIG. 16.—VARIATION OF STRAIN-HARDENING EXPONENT WITH YIELD STRENGTH FOR ALPHA BRASS.

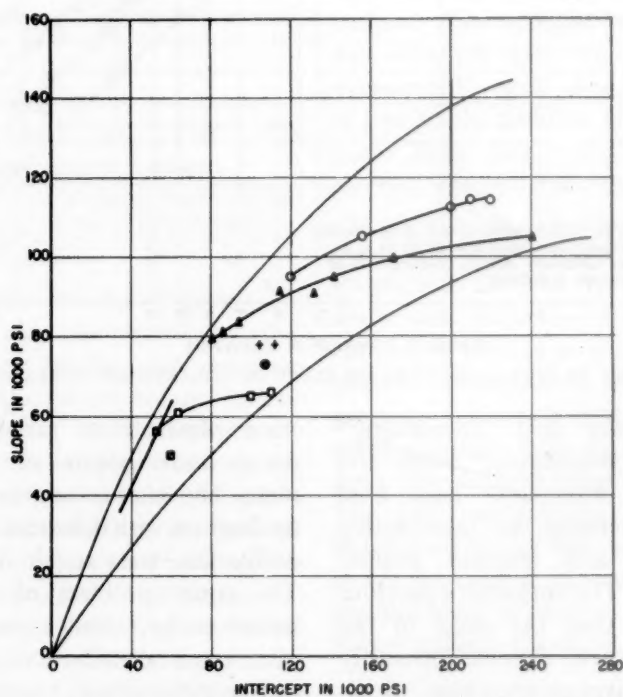


FIG. 17.—SLOPE VS. INTERCEPT FOR TENSILE STRESS-STRAIN CURVES.
After Zener and Hollomon³ except for the straight line, which is after Lacy and Gensamer.²¹

the relation between the conditions controlling fracture.

However, a study of the data (Fig. 8), for the alloy steel containing 0.45 per cent

of one half is the slope of the line of Fig. 20, and K is a constant.

Data for other steels are presently being obtained to test the general validity

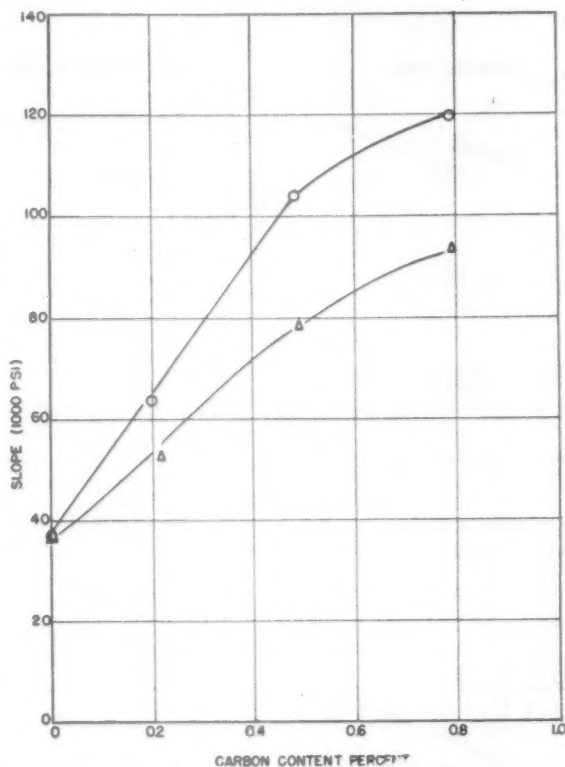


FIG. 18.—EFFECT OF CARBON CONTENT ON SLOPE OF STRAIN-HARDENING CURVE. (After Zener and Hollomon.³)

carbon and having a tempered martensitic structure revealed an interesting relation between the yield and fracture strengths. In Fig. 20, the logarithm of the stress required for fracture of this steel is plotted as a function of the logarithm of the yield strength. These data indicate that, at least for this steel and for this structure, the following relation between yield and fracture strengths is valid:

$$S_f = K(S_0)^{1/2} \quad [12]$$

where S_f is the tensile stress* required for fracture, S_0 is the yield strength, the value

* The correction suggested by Bridgman due to the nonuniform stress distribution across the neck has not been made.

of this relation. Such data for pearlitic steels is very difficult to interpret, for, as indicated in Fig. 19, the fracture strength of such steels depends markedly on strain, and, as the yield strength is changed, the strain before fracture also changes.

SUMMARY

The general problem associated with the study of mechanical properties of metals can be considered to the first approximation to consist of the separate problems of determining the effects of and the relations between the effects of strain rate, temperature, stress distribution, deformation and metallurgical structure on the tensile stress required for plastic flow and on the stress required for fracture.

In this paper, only the effects of tensile strain and changes of metallurgical structure on the stress required for plastic flow are discussed. Over a rather wide range of

tends to fracture. It is further shown that even the initial yielding of alpha brass is anomalous and may be similar to the inhomogeneous yielding of mild steels.

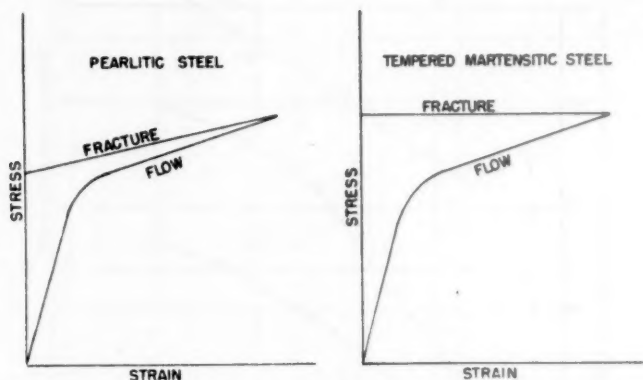


FIG. 19.—SCHEMATIC CURVES OF FRACTURE AND FLOW.

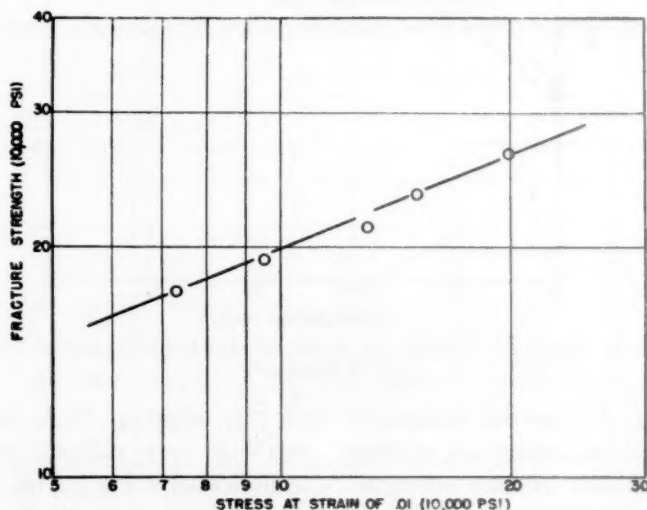


FIG. 20.—RELATION BETWEEN YIELD AND FRACTURE STRENGTHS OF A 0.45 PER CENT CARBON STEEL CONTAINING CHROMIUM, MOLYBDENUM AND VANADIUM.

strains, the stress required for plastic flow is found to vary with the strain to a small fractional power. For steels, this power relation extends from strains at least as small as 0.01 to strains of 0.4. Also for steels, the magnitude of the fractional power appears to be relatively insensitive to changes in structure or alloy composition, but appears to be primarily determined by the yield strength and the carbon content. For the brass and copper specimens studied, the power relation ex-

If the power relation between stress and strain is valid over the range of strain at which the maximum load occurs, the strain to the maximum load is exactly equal to the strain-hardening exponent (fractional power). Thus, the dependence of this power on the metallurgical structure is of prime importance for it is just this strain to maximum load that is so important in determining the drawability of the steels. The relations that have been developed permit the rapid determina-

tion of complete stress-strain curves (Appendix).

Although the fracture of metals is not discussed in detail in this paper, a new

(ϵ_n) may then be drawn through this point. This logarithmic stress-strain curve may then be replotted as a normal stress-strain curve up to a strain of 0.4, as

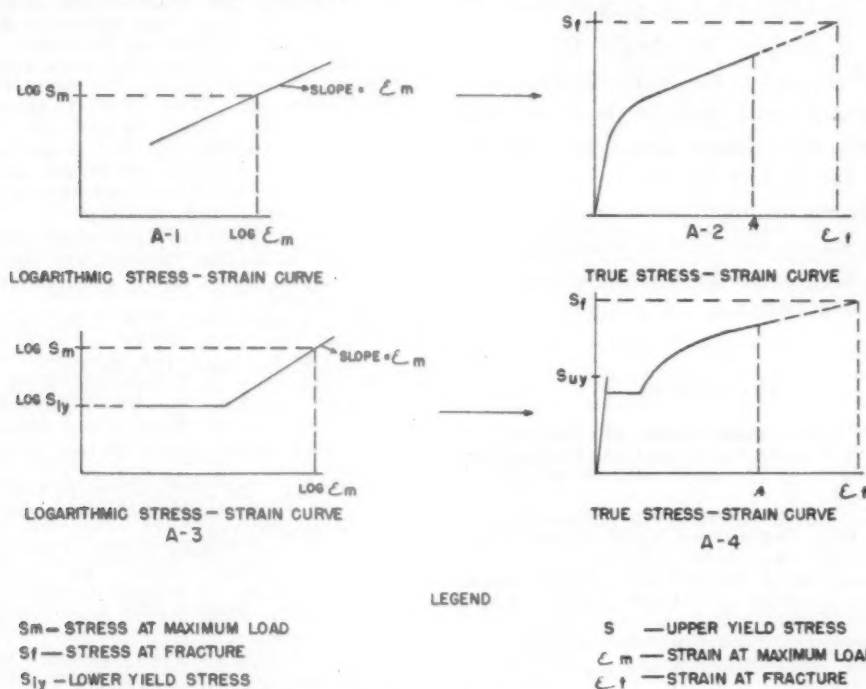


FIG. 21.—ILLUSTRATIONS OF THE METHOD OF OBTAINING THE TWO TYPES OF STRESS-STRAIN CURVES.

relation between the yield and fracture strengths of tempered martensitic steels is suggested. Later papers will be primarily concerned with the effects of metallurgical structure on the fracture of metals.

APPENDIX.—Simple Method of Determining Approximate Stress-strain Curves

The relations developed in this paper permit the approximate determination of stress-strain curves by a very simple procedure. It is only necessary to measure the initial diameter of the specimen, the maximum load and the elongation or the diameter at which the maximum load is reached. From these measurements, the stress and the strain at maximum load may be determined, and one point may be plotted on the logarithmic stress-strain curve. A straight line with a slope exactly equal to the strain at the maximum load

illustrated in Figs. A-1 and A-2 (Fig. 21). If the metal exhibits a drop in load at yielding, and a lower yield-point elongation, it is necessary to measure the upper and lower yield stresses as well as the maximum load and strain to maximum load. The lower yield stress is laid off on the logarithmic stress-strain curve as illustrated at A-3. The true stress-strain curve can be replotted then as illustrated at A-4, placing on this curve the upper yield stress.

The diameter at which necking begins may be determined very easily if the diameter over the gauge length of the tensile bar before testing is uniform. Before the maximum load is reached, the entire specimen deforms uniformly over the gauge length. When the maximum is reached, the specimen begins to neck and the metal at the necked region continues to deform and the material away

from the neck region ceases deforming. After the bar is broken, the diameter of the uniformly deformed* section of the specimen may be measured and the strain to the maximum load determined.

If it is desired to obtain the entire stress-strain curve, the final diameter and the breaking load† may be measured and a straight line drawn (on linear paper) between the part of the stress-strain curve that is linear on logarithmic paper (strain of about 0.4) to the point at which fracture occurs. This procedure is illustrated in Fig. 21, A-2 and A-4.

REFERENCES

1. H. O'Neill: Significance of Mechanical Test Properties of Metals. *Engineering* (July 2, 9, 16, 1943) **156**, 18-20, 38-40, 56-58.
2. A. C. Vivian: Mechanical Properties of Metals. *Engineering*, (July 23 and Aug. 6, 1943) **154**, 78-80, 118-120.
3. C. Zener and J. H. Hollomon: Plastic Flow and Rupture of Metals. *Trans. Amer. Soc. Metals* (1944) **33**, 163-235.
4. P. Ludwik: Elemente der technologischen Mechanik. Berlin, (1909). Julius Springer.
5. P. W. Bridgman: The Stress Distribution at the Neck of a Tension Specimen. *Trans. Amer. Soc. Metals* (1944) **32**, 553-574.
6. J. H. Hollomon: The Notched-bar Impact Test. *Trans. A.I.M.E.* (1944) **158**, 298.
7. P. Ludwik: Über die Bedeutung der Elastizitätsgrenze, Bruchdehnung und Kerbzähigkeit für den Konstrukteur. *Ztsch. Metallkunde* (1924) **16**, 207.
Streckgrenze, Kalt- und Warmspindigkeit. *Ztsch. ver. deut. Ing.* (1926) **70**, 379.
P. Ludwik and R. Scheu: Vergleichende Zug-, Druck, Dreh-, und Walzversuche. *Stahl und Eisen* (1925) **45**, 373.
8. C. Zener and J. H. Hollomon: Effect of Strain Rate upon the Plastic Flow of Steel. *Jnl. Applied Physics* (Jan. 1944) **15**, 22-32.
9. C. Zener and J. H. Hollomon: Conditions of Fracture of Steel. *Trans. A.I.M.E.* (1944) **158**, 283.
10. A. Nadai: Plasticity. New York, 1931. McGraw-Hill Book Co.
11. H. Carpenter and J. M. Robertson: Metals. New York, 1939. Oxford Univ. Press.
12. C. A. Edwards, D. L. Phillips and Y. H. Liu: The Yield Point in Steel. Iron and Steel Inst. Advance copy (Jan. 1943). Also, *Iron and Steel Eng.* (May 20, 1943) **16**, 370-374.
13. J. Winlock and R. Leiter: Some Factors Affecting the Plastic Deformation of Sheet and Strip Steel and Their Relation to the Deep Drawing Properties. *Trans. Amer. Soc. Metals* (1937) **25**, 163-205.
Some Observations on the Yield Point of Low-carbon Steel. *Trans. Amer. Soc. Mech. Eng.* (1939) **61**, 581-587.
14. C. A. Edwards, H. N. Jones and B. Walters: A Study of Strain-Age-Hardening of Mild Steel. *Jnl. Iron and Steel Inst.* (1939) **139**, 341-385.
15. A. Nadai: Über die unter einer Belastung sich bildenden Gleitflächen der festen Körper. *Ztsch. tech. Physik* (1924) **5**, 369-378.
16. M. Gensamer and J. R. Low, Jr.: Aging and the Yield Point in Steel. *Trans. A.I.M.E.* (1944) **158**, 207.
17. M. Gensamer, E. B. Pearsall, W. S. Pellini and J. R. Low, Jr.: The Tensile Properties of Pearlite, Bainite and Spheroidite. *Trans. Amer. Soc. Metals* (1942) **30**, 983-1020.
18. G. Sachs: The Derivations of the Conditions of Plasticity. *Ztsch. ver. deut. Ing.* (1928) **72**, 734.
19. G. I. Taylor: Plastic Strain in Metals. *Jnl. Inst. Metals* (1938) **62**, 307; The Mechanism of Plastic Deformation of Crystals. *Proc. Royal Soc.* (1934) **145**, 362, 388.
20. A. L. Norbury: The Volumes Occupied by the Solute Atoms in Certain Metallic Solid Solutions and Their Consequent Hardening Effects. *Trans. Faraday Soc.* (1924) **19**, 586-600.
21. C. E. Lacy and M. Gensamer: The Tensile Properties of Alloyed Ferrites. *Trans. Amer. Soc. Metals* (1944) **32**, 88-110.
22. W. A. Wood: X-Ray Study of Grain Size in Steels of Different Hardness Values. *Phil. Mag.* (1930) **10**, 1073-1081.
23. C. A. Edwards and L. B. Pfeil: The Tensile Properties of Single Iron Crystals and the Influence of Crystal Size upon the Tensile Properties of Iron. *Jnl. Iron and Steel Inst.* (1925) **112**, 79-110.
24. E. B. Norris: The Plastic Flow of Metals. *Bull. Virginia Polytechnic Inst. Engineering Expt. Station Series, Bull.* 27 (November 1936). **30**.
25. C. W. MacGregor: Relation between Stress and Reduction in Area for Tensile Tests of Metals. *Trans. A.I.M.E.* (1937) **124**, 208-228.
C. W. MacGregor and L. E. Welch: True Stress-strain Relations at High Temperatures by the Two-load Method. *Trans. A. I. M. E.* (1943) **154**, 423-437.
26. M. Gensamer, E. B. Pearsall, and G. V. Smith: The Mechanical Properties of the Isothermal Decomposition Products of Austenite. *Trans. Amer. Soc. Metals* (1940) **28**, 390-398.
27. J. H. Hollomon: Effect of Heat-treatment and Carbon Content on the Work-hardening Characteristics of Several Steels. *Trans. Amer. Soc. Metals* (1944) **32**, 123-133.

* Specimen having a long gauge length compared with the length over which necking occurs is necessary for this determination.

† In normal tensile tests, the breaking load is difficult to determine accurately, therefore special care must be taken to obtain accurate results.

28. R. A. Wilkins and E. S. Bunn: Copper and Copper-base Alloys. New York, 1943. McGraw-Hill Book Co.
29. M. Gensamer: The Yield Point in Metals. *Trans. A.I.M.E.* (1938) **128**, 104-117.
30. E. L. Bartholomew: Stress-Strain Measurements in the Drawing of Cylindrical Cups. *Trans. Amer. Soc. Metals* (1943) **31**, 582-598.
31. C. W. MacGregor: The Tension Test. *Trans. Amer. Soc. Test. Mat.* (1940) **40**, 508-534.
32. W. Kuntze: For survey and bibliography, see D. J. McAdams: *Trans. Amer. Soc. Mech. Engrs.* (1941) **63**, A-155 and *Trans. A. I. M. E.* (1942) **150**, 311.
33. D. J. McAdam, Jr.: The Technical Cohesive Strength of Metals. *Trans. Amer. Soc. Mech. Engrs.* (1941) **63**, A155-A165. Technical Cohesive Strength and Yield Strength of Metals. *Trans. A. I. M. E.* (1942) **150**, 311-357.
- D. J. McAdam, Jr., and R. W. Mebs: An Investigation of the Technical Cohesive Strength of Metals. This volume, page 474.
34. N. Davidenkov and F. Wittmann: Mechanical Analysis of Impact Brittleness. *Tech. Phys., U. S. S. R.* (1937) **4** (4), 3-17.
35. G. Sachs and J. Lubahn: Effects of Notching on Strained Metals. *Iron Age* (Oct. 8 and 15, 1942) **150**, 31-38, 48-52. Notched Bar Tensile Tests on Heat-Treated Low-Alloy Steels. *Trans. Amer. Soc. Metals* (1943) **31**, 125-160. Bursting Tests on Notched Alloy Steel Tubing. *Trans. Amer. Soc. Metals* (1943) **31**, 71-88.
- G. Sachs, J. D. Lubahn, and L. J. Ebert: Notched Bar Tensile Test Characteristics of Heat-Treated Low-Alloy Steels. *Trans. Amer. Soc. Metals* (1944) **33**, 340-395. The Effects of Notches of Varying Depth on the Strength of Heat-Treated Low-Alloy Steels. *Amer. Soc. Metals Preprint* **15** (1944).
- G. Sachs, J. D. Lubahn, L. J. Ebert, and E. L. Aul: The Effect of Fiber on Notched-Bar Tensile Strength Properties of a Heat-Treated Low-Alloy Steel. *Amer. Soc. Metals Preprint* **14** (1944).
36. M. Gensamer: Strength of Metals under Combined Stresses. *Amer. Soc. Metals*, Cleveland, Ohio, 1941.

DISCUSSION

C. ZENER.*—The author has stated that the shape of his stress-strain curves for brass indicates that the nature of the initial yielding in this metal is similar to that of mild steel. He may be interested to know that Sachs and Shoji³⁷ had previously reported that in single crystals of brass the initial portion of the stress-strain curve is flat up to a strain of 0.1, and

that some crystals even manifested a drop in load at yielding.

It appears that in brass the initial drop in load is more marked in single crystals than in polycrystals, just the reverse of iron. In this connection it may be pertinent to note that in brass eight slip planes are active, while in iron 84 slip planes are active. Propagation of a slip band from one crystallite to another should therefore be much more difficult in polycrystalline brass than in polycrystalline iron.

J. R. Low, JR.*—The author is to be congratulated on the analysis of the simple tension flow curve presented and the important generalizations stated. We have felt for some time that the so-called "mechanical properties" measured in the tensile test as it is usually performed (i.e., tensile strength, elongation in 2 in., etc.) are unsatisfactory measures of the plastic properties of a material, since they merely represent certain aspects of the mechanical behavior under a particular type of loading. The two material constants K and m in the expression $S = K(\epsilon)^m$ would appear to be much better measures of the plastic flow properties of a particular metal in a particular condition of heat-treatment. These two constants, together with the strain to fracture, completely define the plastic behavior in simple tension. Furthermore, it appears likely these two "properties" will also serve to define plastic flow under combined stresses, as the analysis of this latter, more complex, problem develops.

The relationship between the constant K of the author's Eq. 10 and the carbon content of steels, which is depicted in Fig. 14, appears to be valid even at very low carbon contents. The values of K in Table 2 were computed from true stress-strain data for low-carbon steel sheet and for steel sheets treated with wet hydrogen.³⁸

According to the author's Eq. 10 and Fig. 13, the strain-hardening exponent m for a fixed carbon content should increase continuously as the yield stress $S_{0.01}$ decreases. An exception to this relationship has been observed for S.A.E. 2340 specimens oil-quenched and tempered

* Development Engineer, Research and Development Division, Carnegie-Illinois Steel Corporation, Pittsburgh, Pa.

³⁸ Low and Gensamer: *Trans. A.I.M.E.* (1944) **158**, 207.

* Principal Physicist, Watertown Arsenal, Watertown, Mass.

³⁷ G. Sachs and H. Shoji: *Ztsch. Physik* (1927) **45**, 776.

for one hour at 400°F. and 500°F. In this particular case two specimens tempered at 400°F. had m values of 0.09 and 0.10 while a second pair tempered at 500°F. had m values of 0.045 and 0.05. The $S_{0.01}$ (yield strength at 1 per cent strain) values for the two tempering temperatures were approximately 270,000 and 260,000, respectively.

TABLE 2.—Values of K Computed from Stress-strain Data

Material	K	
	Observed	Predicted ^a
0.05 per cent C aluminum-killed temper rolled sheet...	3.56	3.57
Wet-hydrogen-treated aluminum-killed steel (C < 0.003 per cent).....	3.53	3.55
Wet-hydrogen-treated rimmed steel (C < 0.003 per cent)...	3.52	3.55

^a By extrapolation of straight line of Fig. 14.

In discussing the deviations from the straight-line relationship on logarithmic coordinates between true stress and true strain, particularly those at strains above 0.4, the author attributes the upward deviation for the tension case to orientation effects. Since these deviations are generally observed only after the specimen has necked down appreciably, it seems more probable that they result principally from the complex stress condition existing in the necked region. In general, one would expect the circumferential and radial stresses existing in the necked region to increase the longitudinal stress required for flow over the stress that would be required if simple tension conditions could be maintained.

J. H. HOLLOMON (author's reply).—The confirmation by Dr. Low of the effect of carbon content on strain-hardening is satisfying. Low's

data suggest that with the relations developed in the paper it will be possible to develop deep-drawing operations more scientifically. The author is in complete agreement with Dr. Low in his approach to the problem of mechanical properties. It should be possible to interpret all mechanical properties, qualitatively at least, in terms of the fundamental effects of strain, temperature, strain rate, metallurgical structure, and stress complex on the flow and fracture stresses.

Relations developed between the strain-hardening exponent and carbon content seem to apply only when the change in strength is brought about by a change in the shape, size, or number of carbide particles. Low's data for S.A.E. 2340 steel would seem to indicate that some new phase transformation has occurred. It is possible that the differences between the m values in Low's test are due to the differences in the amount of retained austenite.

It does not seem possible to account for the deviation of the logarithmic stress-strain curves in terms of the complex stress at the neck of the tension specimen. As Bridgman has indicated in his analysis, this stress distribution should be the same for all metals that have necked the same amount. Thus, copper and brass should show deviations from linear logarithmic stress-strain curves. Deviations in these metals do not appear to exist. Furthermore, the deviation does not exist for copper for strains much in excess of those suffered by steel before fracture in the ordinary tension test. Furthermore, the reorientation effect satisfactorily explains the downward deviation from linearity observed for torsion data.

The author would like to thank Dr. Zener for bringing to his attention a previous paper discussing peculiarities in initial yielding for brass. His comments concerning its source are most interesting.

Effects of Cold-rolling on the True Stress-strain Properties of a Low-carbon Steel

By F. J. MEHRINGER* AND C. W. MACGREGOR,† MEMBER A.I.M.E.

(New York Meeting, February 1945†)

VARIOUS investigations have been carried out to determine the effects of cold-rolling on the common physical properties as represented by the yield strength, tensile strength, percentage of elongation and ordinary reduction of area. Very little information is available in the literature with reference to the effects of cold-rolling on the true stress-strain properties.

Since the ordinary physical properties base both the stresses and the strains on the original dimensions of the test piece, which are greatly changed during the test, they are essentially empirical values and do not represent physically either true stresses or true strains. Consequently, they do not give an accurate picture of the effects of different conditions, both mechanical and metallurgical, on the strength and ductility of the material. It is not, however, the purpose of this paper to review the various advantages accruing from the use of true stress and true strain values, since these have been shown elsewhere,¹⁻¹² but to utilize them in representing the various effects considered.

The true stress S and true strain ($\epsilon = q'$) values mentioned above for the tension test are defined by¹

$$S = \frac{P}{A} \quad \text{and} \quad \epsilon = q' = \log_e \frac{A_0}{A} \quad [1]$$

where P , A , A_0 are the axial load, the

instantaneous area and the original area of cross section, respectively. From simultaneous readings of the axial load and the dimension or dimensions determining the instantaneous area of cross section, the true stress-strain curve is constructed by using the relations given in Eq. 1.

It is then the object of this paper to discuss the general effects of cold-rolling on the true stress and strain values for a low-carbon steel together with the effects of age-hardening and directionality on these properties.

PRELIMINARY INVESTIGATIONS

The material considered throughout the paper is a low-carbon steel of the following chemical analysis: C, 0.19 per cent; S, 0.118; P, 0.092; Mn, 0.85; Si, 0.01. The stock was received in bars, 7 by $\frac{3}{4}$ in., and was first annealed for one hour at 1650°F. followed by a furnace cool. Photomicrographs of this material showed considerable directionality even in the annealed condition.

In view of the possible effects of the nonhomogeneity and directionality in this material, it was considered important to investigate their influence on the true stress-strain diagrams. In addition, the effect of strain-aging in this steel was also made the subject of a preliminary study.

Effect of Aging on True Stress-strain Properties

Since a certain time element would elapse between the cold-rolling operation and the final tension tests, it was determined to investigate the aging character-

Manuscript received at the office of the Institute Nov. 29, 1944. Issued as T.P. 1849 in METALS TECHNOLOGY, September, 1945.

* Graduate Student, Massachusetts Institute of Technology, Cambridge, Massachusetts.

† Department of Mechanical Engineering, Massachusetts Institute of Technology.

‡ Meeting canceled.

¹ References are at the end of the paper.

istics. To study this, a number of bars of rectangular cross section were cold-rolled 5 per cent and tested after aging for different periods of time without any sub-

numerical values of the strength properties for each of the aging procedures. This shows that the ordinary tensile strength, in contrast with the above properties, increases

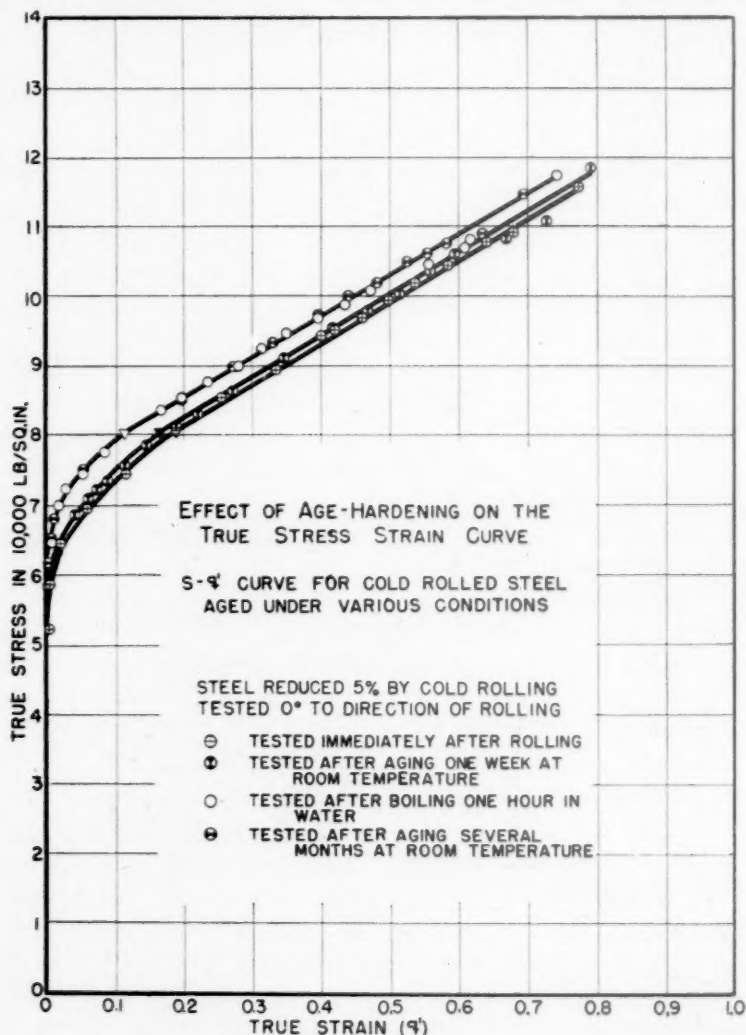


FIG. 1.

sequent machining. Fig. 1 shows the effects of the various aging treatments considered on the true stress-strain diagrams. As indicated, the true stress at the maximum load (indicated by inverted triangles) and the true stress at fracture remained practically unaffected. Similarly, the minimum modulus of strain-hardening $m = \partial S / \partial \epsilon$ was not changed to any appreciable extent of the aging treatments. Table 1 lists

continuously with the degree of aging. This is largely attributable to a decrease in the true uniform strain that occurs before the maximum load is reached. Table 1 also shows, in comparing the boiling-water treatment with the room-temperature aging of several months duration, that almost complete aging had taken place during the latter period. The tests to be described later depicting the influence of

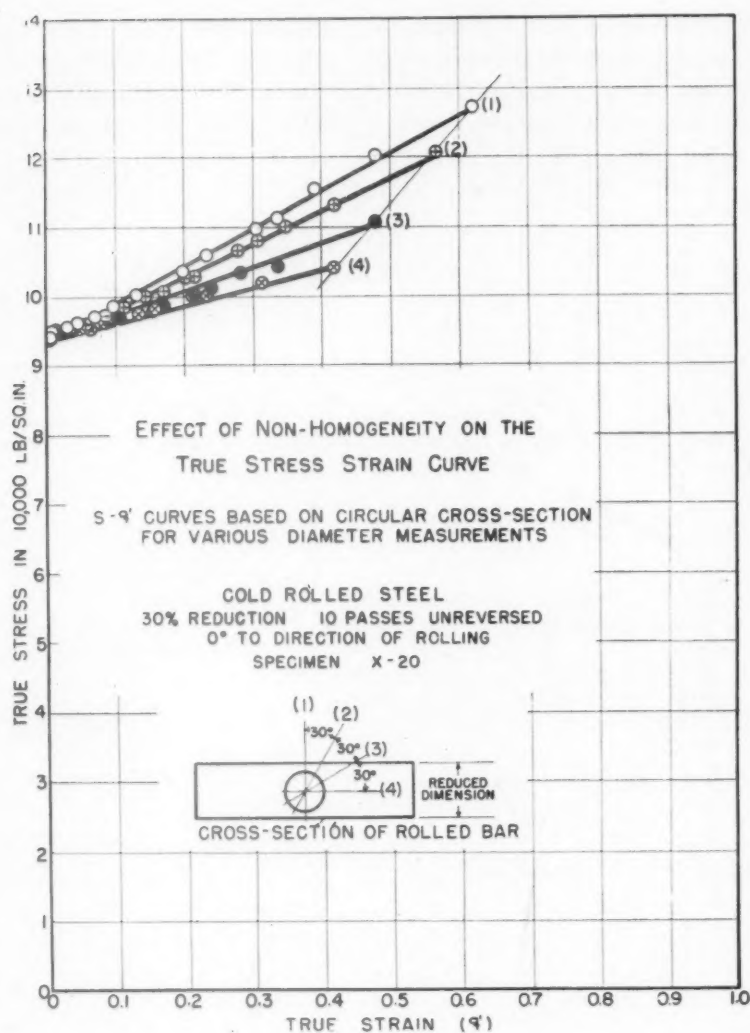


FIG. 2.

TABLE I.—Effect of Aging on Tensile-stress
Properties of a Low-carbon Steel Re-
duced 5 Per Cent by Cold-rolling

Property	Original	Aged Seven Days at Room Tem- pera- ture	Boiled in Water 1 Hr.	Aged Several Months at Room Tem- pera- ture
Tensile strength lb. per sq. in....	66,400	67,900	71,600	71,300
True stress, lb. per sq. in.:				
At maximum load.....	80,300	80,000	80,000	80,400
At fracture.....	115,800	117,800	114,300	118,000

cold-rolling on the true stress-strain prop-
erties were made on specimens that had
been cured for several months at room
temperature and thus were very nearly in
the fully aged condition.

Influences of Variations of Diameter in Same Cross Section

For most materials tested heretofore, it
had been found that they were sufficiently
homogeneous so that diameter measure-
ments taken at various positions around
the axis of the specimen did not differ
appreciably one from the other. The cross

sections then could be considered essentially circular in shape. The present steel is an exception in that, owing to the non-homogeneity, the cross sections become more and more elliptical as the test pro-

ceeds from the maximum load to fracture. These tension specimens were machined with their axes parallel to the rolling direction. The results of these tests are shown in Figs. 2 and 3.

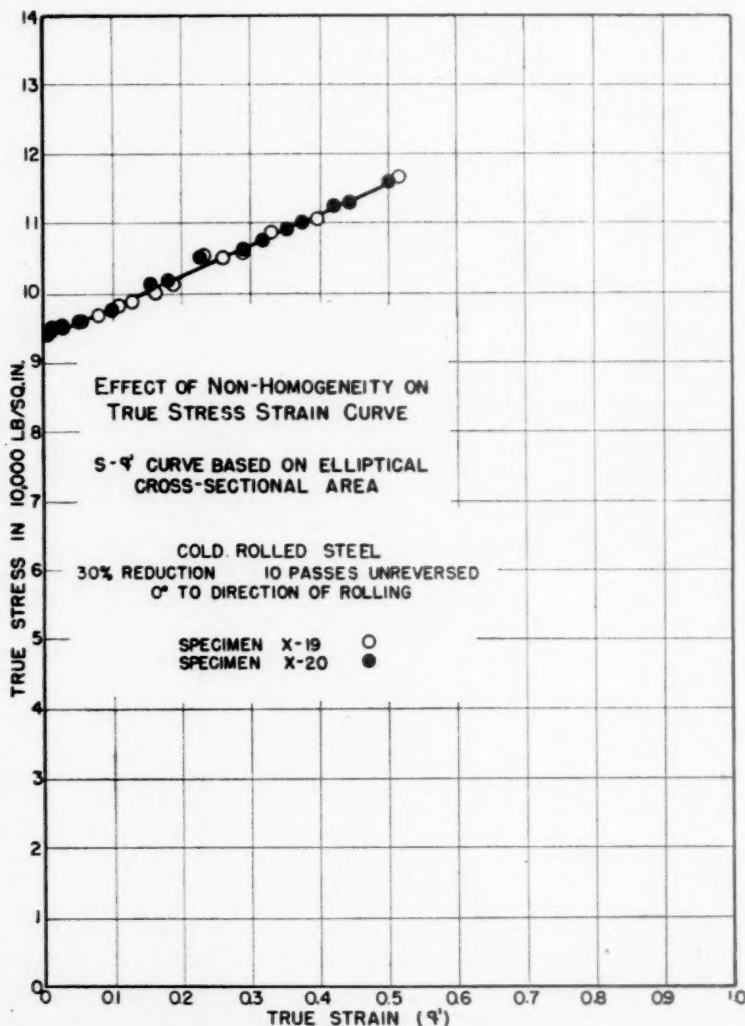


FIG. 3.

ceeds from the maximum load to fracture. No appreciable ellipticity is present at the maximum load point. Observations indicated that the major axis of the ellipse was parallel to the plane of the rolled bar.

A series of experiments was carried out in which the diameter measurements on the test bar were made at positions 0° , 30° ,

Each separate curve in Fig. 2 for 30 per cent reduction was constructed from diameter measurements taken only at one position relative to the normal of the surface of the original rolled bar. The areas were calculated assuming circular cross sections of that diameter. It can be seen that the lowest and shortest curve, No. 4,

was obtained from diameter measurements parallel to the plane of the rolled bar (horizontal). This diameter is the major axis of the ellipse. Each point on the upper

Thus when a true stress-strain curve appears to dip away from the straight line when testing a nonhomogeneous steel of this sort, it is probable that diameters may

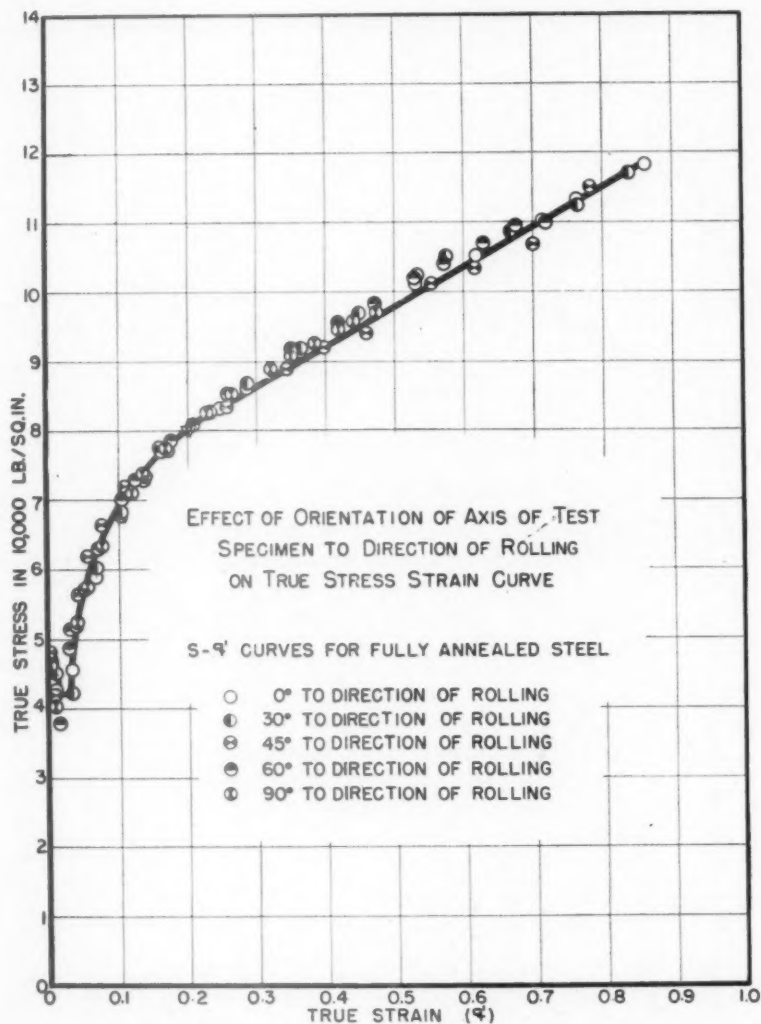


FIG. 4.

curve, No. 1, is based on a circular area of diameter equal to the minor axis of the ellipse, consequently this curve shows the greatest fracture stress and strain. An interesting feature of these curves is that if the cross section is considered to be a circle of diameter measured at a single position around the specimen axis, the stress based on this is linearly related to the strain in the region of local necking.

have been measured at somewhat different positions around the axis of the bar during the test. Similar results were obtained in tests on bars rolled to 15 per cent reductions.

Further, it may be shown, from a differentiation of the equations for true stress and true strain, that the slope of the true stress-strain curve at a given load is inversely proportional to the square of the

diameter. Hence, if there is a considerable variation in diameter around the axis of the test piece, a large difference in slope of the true stress-strain curve can be

areas computed from diameters taken at different positions around the axis from 104,000 lb. per sq. in. to 128,000 lb. per sq. in., while the 15 per cent reduction

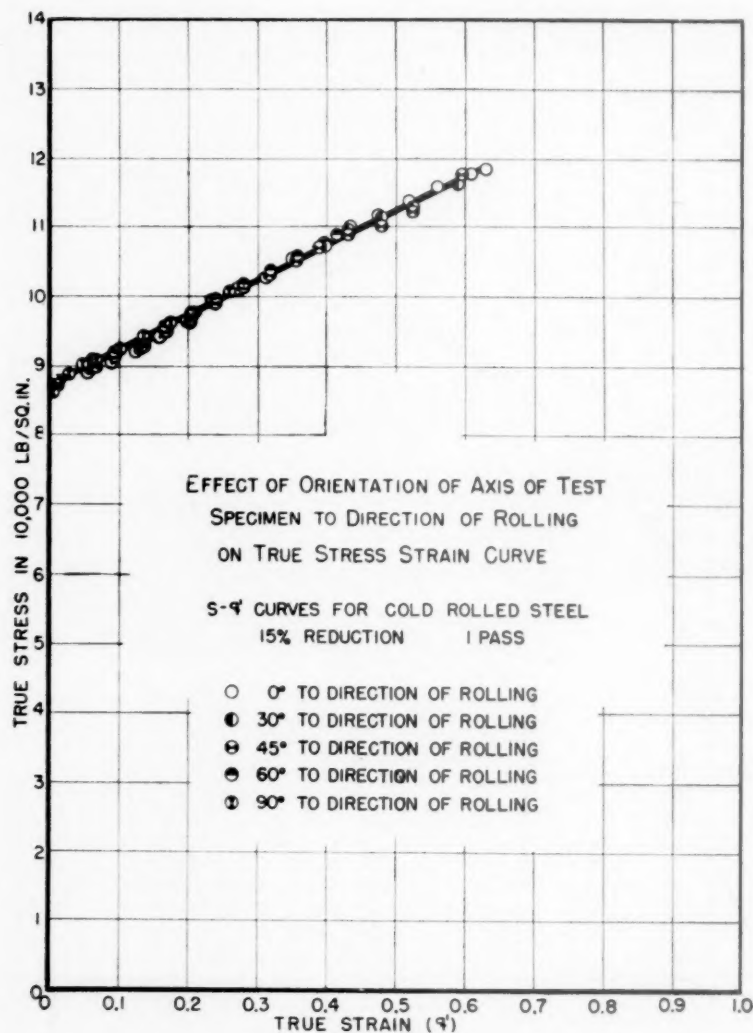


FIG. 5.

expected from diameter measurements taken at different positions around the axis. This is borne out by the experiments described.

The nonhomogeneity was greater for the 30 per cent reduction than for the 15 per cent reduction, as might be anticipated. The 30 per cent reduction showed a variation in fracture stress based on circular

indicated a variation from 108,000 to 122,000 lb. per sq. in. The variation in strains at fracture based on such considerations for the 30 per cent reduction was from 0.42 to 0.62, while for the 15 per cent reduction it was from 0.53 to 0.67. This wide range of values indicates the possible magnitude of scatter for a material of this type if the diameter measurements

are taken at random positions around the axis during the test without computing the actual elliptical areas.

The true stress-strain curve included in

complete such a test would be considerably greater than is generally spent. Fortunately, the true stress-strain curves for metals in this class may be determined

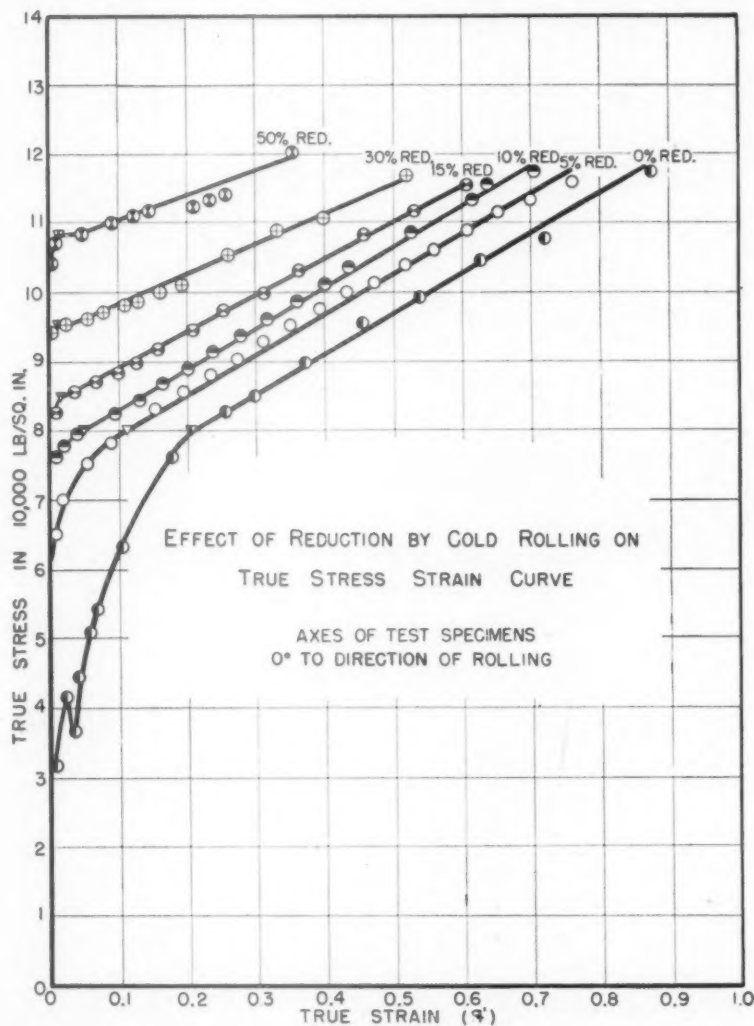


FIG. 6.

Fig. 3 is based on the actual elliptical areas of cross section. This curve coincides approximately with curve No. 2 in Fig. 2, which is based on diameters measured at a position 30° from the normal to the rolled surface. Very little scatter of the plotted points is evident. If the true elliptical areas of cross section are to be obtained for many points in the region of local necking for nonhomogeneous metals, the time to

with reasonably good accuracy without having to determine many points in the region of local necking, since use may be made of the experimental fact that despite the nonhomogeneity the curve is linear in this region. Tests have shown that the cross section does not become elliptical until the maximum load is passed, consequently the true stress-strain curve up to this point may be determined from diam-

eter measurements taken at any position around the axis of the test specimen. This establishes the curve up to the beginning of the straight-line portion. The elliptical area at fracture can be computed

geneous metals. This will explain also the reason why the fracture point is weighted more than some of the intermediate points in the region of local necking in some of the curves to be discussed later on.

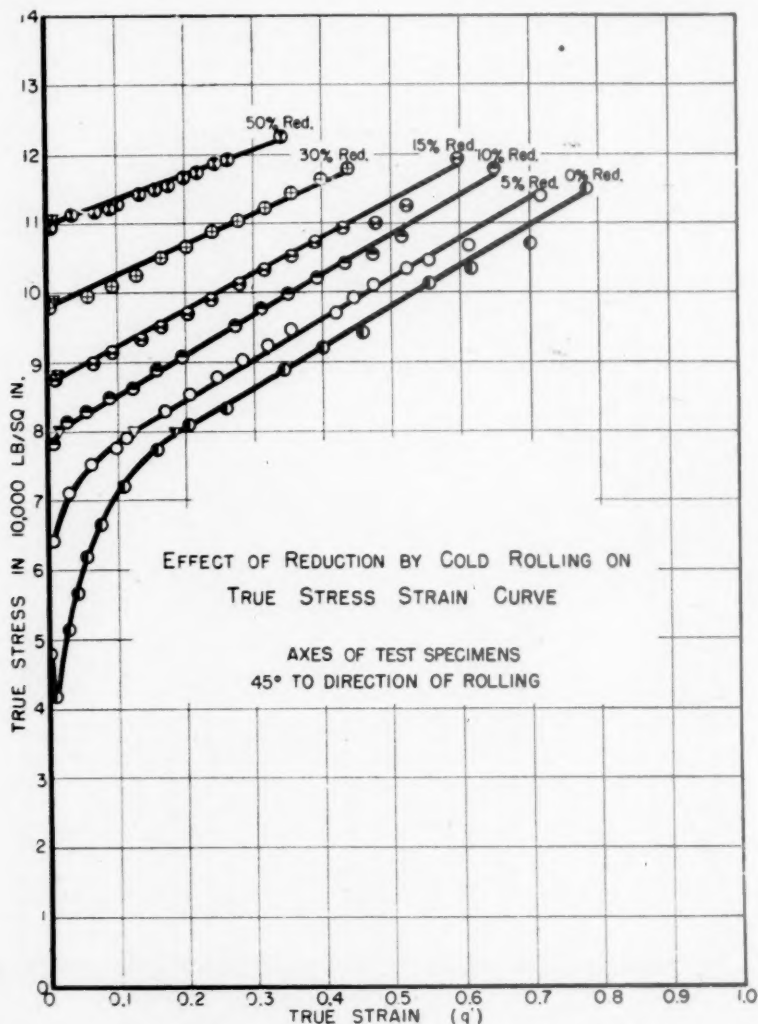


FIG. 7.

readily after the specimen is broken and the fracture stress and strain determined. A straight line between the fracture point and the maximum load point depicts the behavior in the necking region with reasonably good accuracy. This procedure determines the complete true stress-strain curve for such materials and takes very little longer to perform than for homo-

Influence of Orientation of Test Specimen to Direction of Rolling

The effect of the orientation of the test specimen is shown in Figs. 4 and 5. Specimens were cut from the plate with their axes at 0°, 30°, 45°, 60° and 90° to the direction of rolling and then tested in tension. These figures include the results on the annealed plate, and on plate cold-

rolled 15 per cent respectively. For this material, the main influence of changing the direction of the axis of the tension specimens from parallel to the rolling

15 per cent reduction in tension. As far as the true fracture strain is concerned, the cold-rolling tends to increase the initial directionality of the material.

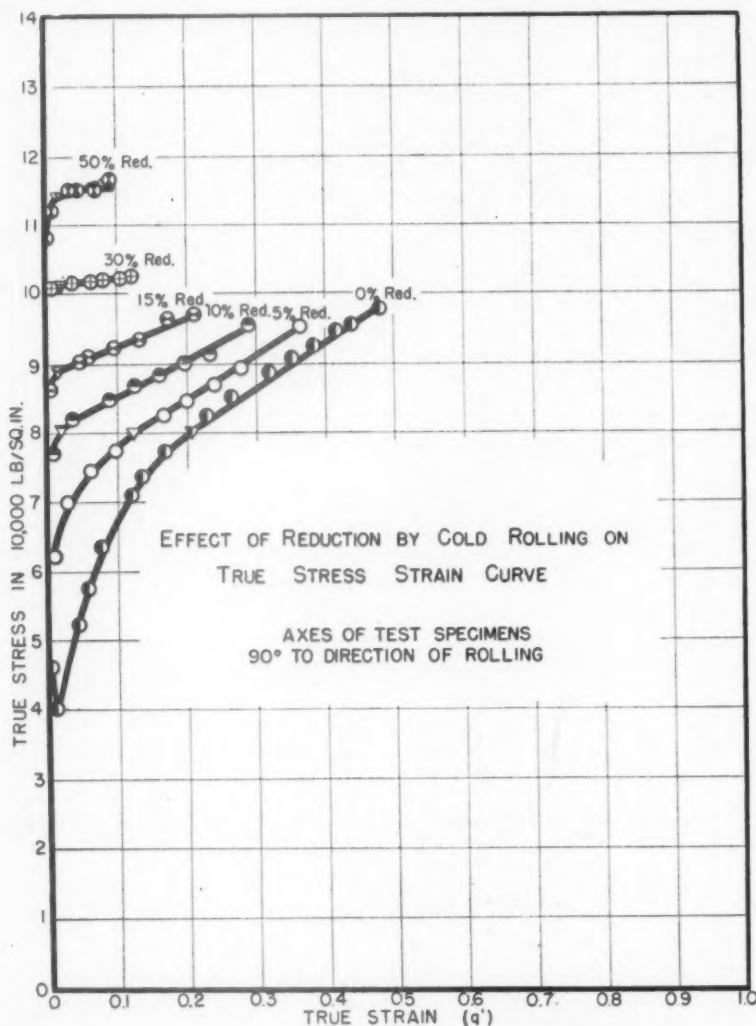


FIG. 8.

direction to transverse thereto is to continuously decrease the true fracture stress and the true fracture strain.

A numerical comparison of the effect of the orientation of the test specimen on the true fracture stress and strain is included in Table 2 for parallel and transverse specimens cold-rolled 5, 10 and 15 per cents and for a specimen pulled to

EFFECTS OF COLD-ROLLING ON TRUE STRESS-STRAIN PROPERTIES

In order to show the influence of cold-rolling on the true stress-strain properties for this steel, bars were rolled to various percentages of reduction and specimens were machined from them at different inclinations to the direction of rolling.

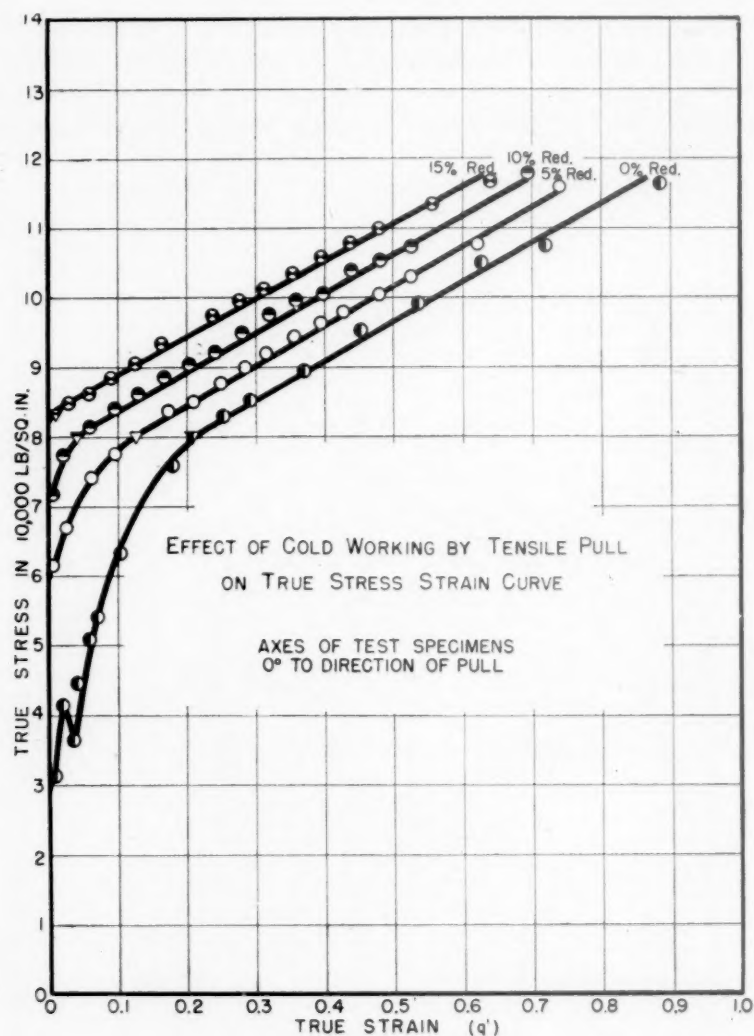


FIG. 9.

TABLE 2.—Effect of Orientation of Test Specimen on True Stress-strain Properties

Stress or Strain		Annealed	Cold-rolled			Cold-worked Pulled in Tension, 15 Per Cent Reduction
			5 Per Cent	10 Per Cent	15 Per Cent	
True fracture stress	Axis of specimen parallel to rolling...	118,000	116,000	118,000	116,000	116,000
	Axis of specimen perpendicular to rolling.....	97,000	95,000	95,000	97,000	95,000
	Ratio perpendicular to parallel.....	0.82	0.82	0.86	0.84	0.82
True fracture strain	Axis of specimen parallel to rolling..	0.86	0.76	0.71	0.61	0.63
	Axis of specimen perpendicular to rolling.....	0.48	0.37	0.29	0.21	0.28
	Ratio perpendicular to parallel.....	0.55	0.46	0.42	0.34	0.45

Tension tests of the true stress-strain type were made on test pieces prepared in this manner.

Figs. 6 to 8, inclusive, show both the

hardening $m = \partial S / \partial \epsilon$ is not greatly affected up to a reduction of 10 per cent. It decreases for higher reductions and the greatest decrease is for the 90° inclination

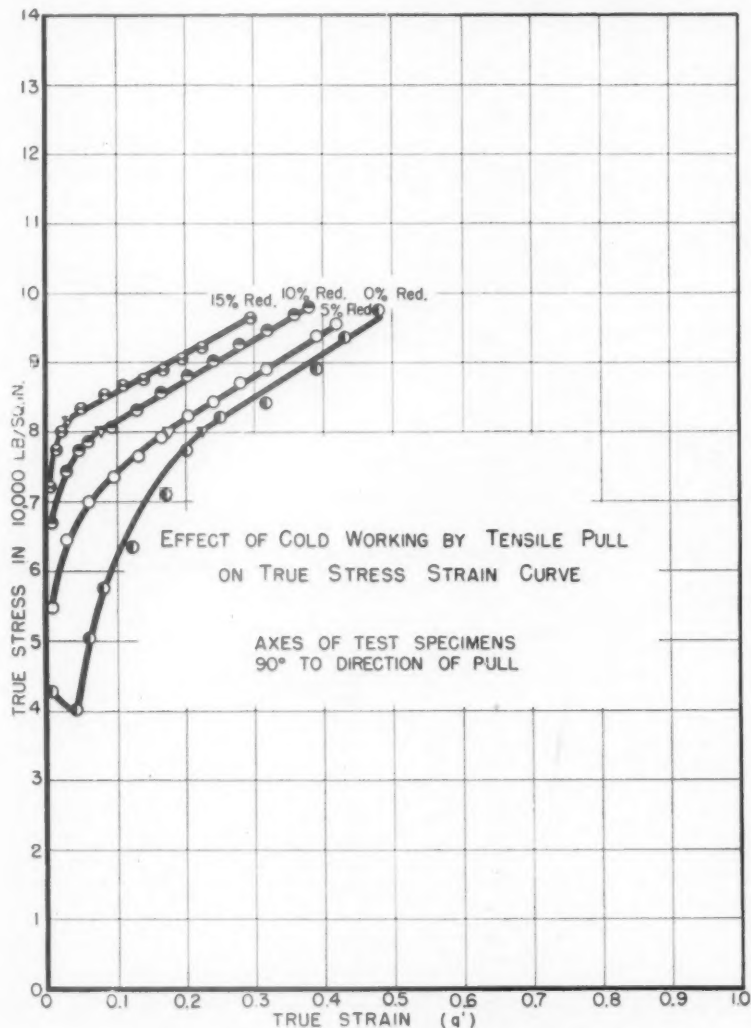


FIG. 10.

effects of the magnitudes of the reductions and the orientations of the test specimens to the direction of rolling on the true stress-strain diagrams for reductions up to 50 per cent. Although tests were made for inclinations of 0° , 30° , 45° , 60° and 90° to the rolling direction these figures include the 0° , 45° , and 90° degree inclinations only. From these curves it may be seen that the minimum modulus of strain

to the rolling direction. Increased reductions in rolling also reduce both the true uniform strains up to the maximum load points (indicated by inverted triangles), the local necking strains, and the true fracture strains. No appreciable increase in the true fracture stress takes place until about 30 per cent reduction is reached for all cases except the 90° specimens. The true stresses at the maximum loads, however,

are greatly increased by large reductions in rolling.

Figs. 9 and 10 are included to show the influence of cold-work by initial stretching

at 0° to the rolling direction. If Figs. 10 and 8 are compared, however, it is apparent that no such coincidence is present for specimens cut at 90° to the rolling direction.

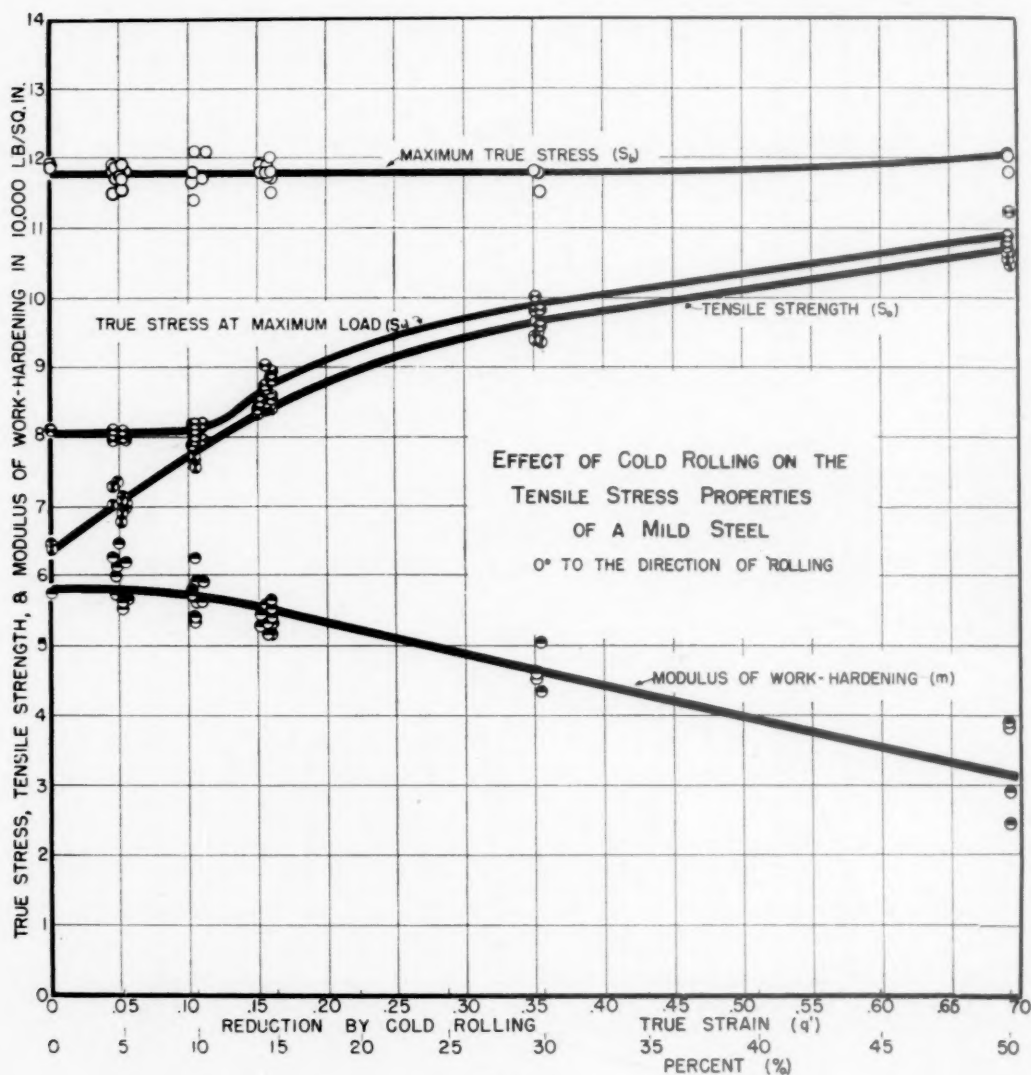


FIG. 11.

in tension on the true stress-strain properties rather than by cold-rolling as in the former experiments. A comparison of Fig. 9 with Fig. 6 indicates that the net effect on the true stress-strain properties for this steel of stretching up to 15 per cent is equivalent to cold-rolling to the same reductions on the specimens cut out

In this case the 10 per cent reduction by rolling has an effect that is about equivalent to a 15 per cent reduction by stretching.

A summary of the effects of cold-rolling on the various tensile properties, both ordinary and true stress-strain, is given in Figs. 11 to 18 inclusive.

Figs. 11 to 14 show the behavior of the maximum true stress (the true fracture stress), the true stress at the maximum load, the ordinary tensile strength and the

load remain essentially constant. Beyond these values, the true stress at the maximum load begins to increase rapidly, while the true stress at fracture either still

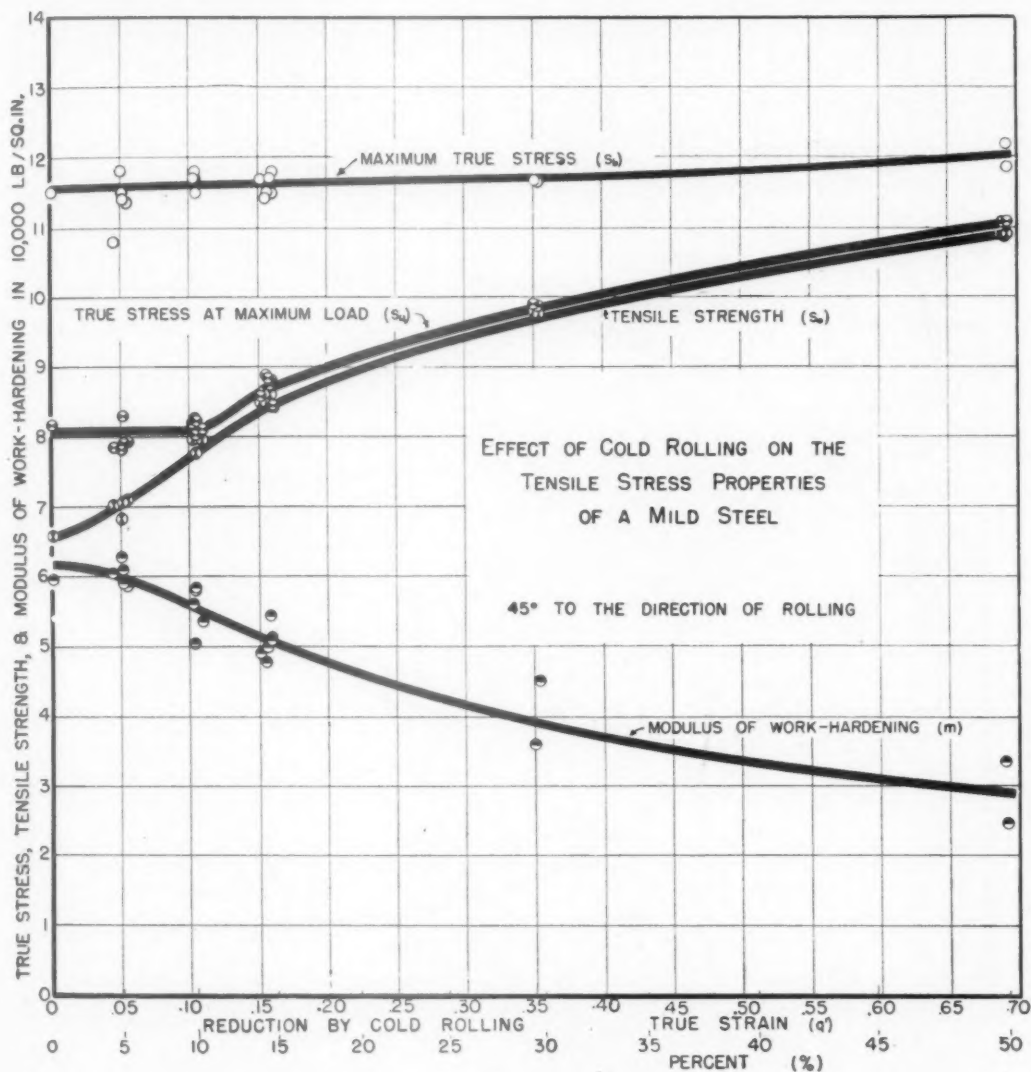


FIG. 12.

minimum modulus of work-hardening as a function of the reduction by cold-rolling. In most cases the influence of the cold-work on the tensile-stress properties is qualitatively the same for all inclinations of the test bars to the direction of rolling. The major variations lie only in the extent of the effect. For small reductions, both the true stress at fracture and at maximum

remains practically unaffected or increases slowly. For large reductions, both of these quantities increase in a parallel fashion. No appreciable increase in the true stress at fracture occurs for the 0° orientation until a 30 per cent reduction is reached. On the contrary, the 90° inclination exhibits an increase in the fracture stress at less than half of this amount of reduction.

The ordinary tensile strength increases just as soon as cold-working has begun. The remaining stress property—namely, the minimum modulus of work-hardening

instead of only to 50 per cent. The test specimens used for the higher reductions were rectangular in cross section. It had been found possible previously to compare

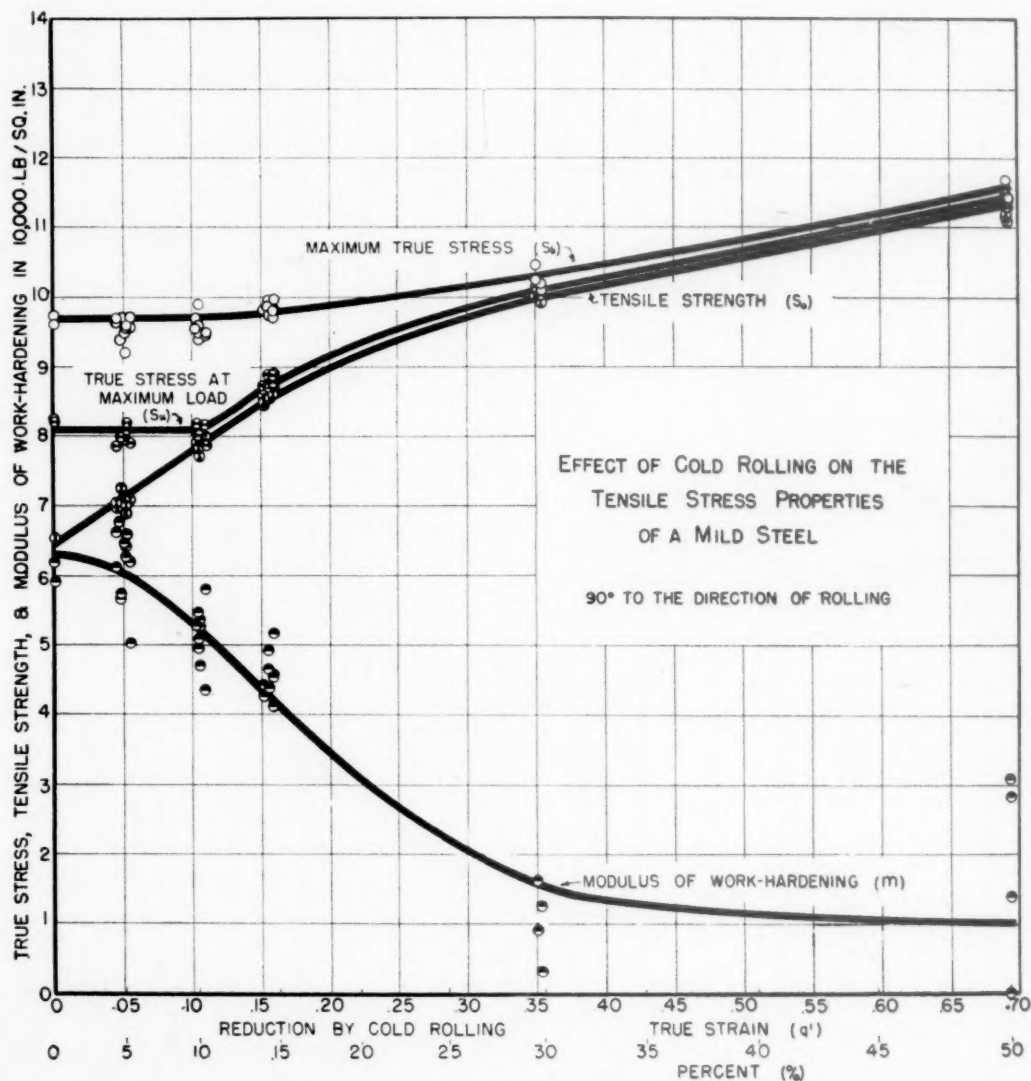


FIG. 13.

$m = \partial S / \partial \epsilon$ —decreases with increasing reductions. These figures disclose that the modulus of work-hardening decreases to a larger extent as the inclination of the test bar is greater with respect to the direction of rolling.

Fig. 14 is the same as Fig. 11 except that the reductions are carried to 95 per cent

directly the results of true stress-strain tests on rectangular and round specimens provided the ratio of width to thickness was not too great. For the large reductions, tests were made in a direction parallel to rolling only. The true stress at fracture increased from 118,000 lb. per sq. in. in the annealed condition to 120,000 lb. per

sq. in. at 50 per cent reduction and to 161,000 lb. per sq. in. at 95 per cent reduction. This final value represents an increase of about 33 per cent. The true

values indicated are the average of a number of readings taken over the cross section of the rolled bar, since no consistent variation of hardness across the section

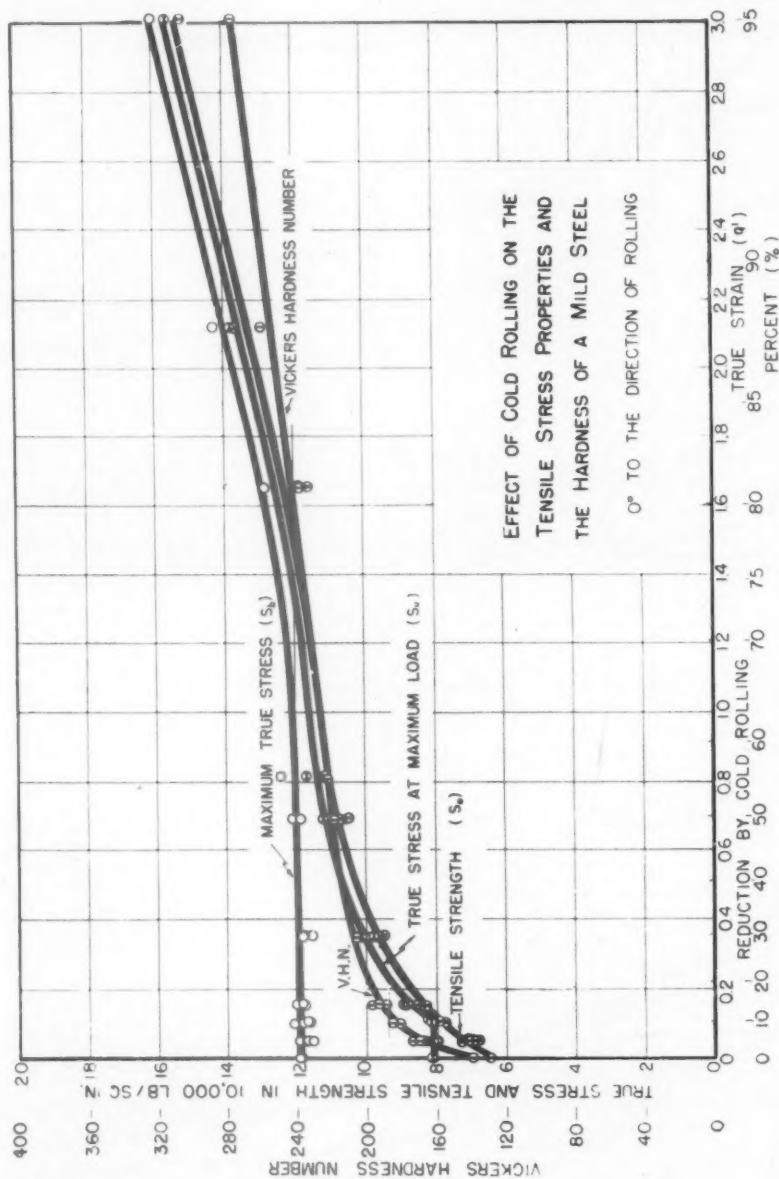


FIG. 14.

stress at the maximum load and the ordinary tensile strength have increased by even greater amounts.

The Vickers hardness is also plotted in Fig. 14. A 10-kg. load and a $\frac{3}{8}$ -in. objective were used in these determinations. The

was observable. The hardness increases rapidly with small reductions in rolling. The rate of increase of hardness decreases until a reduction of about 45 per cent is reached. Thereafter, the increase of hardness is at a uniform rate.

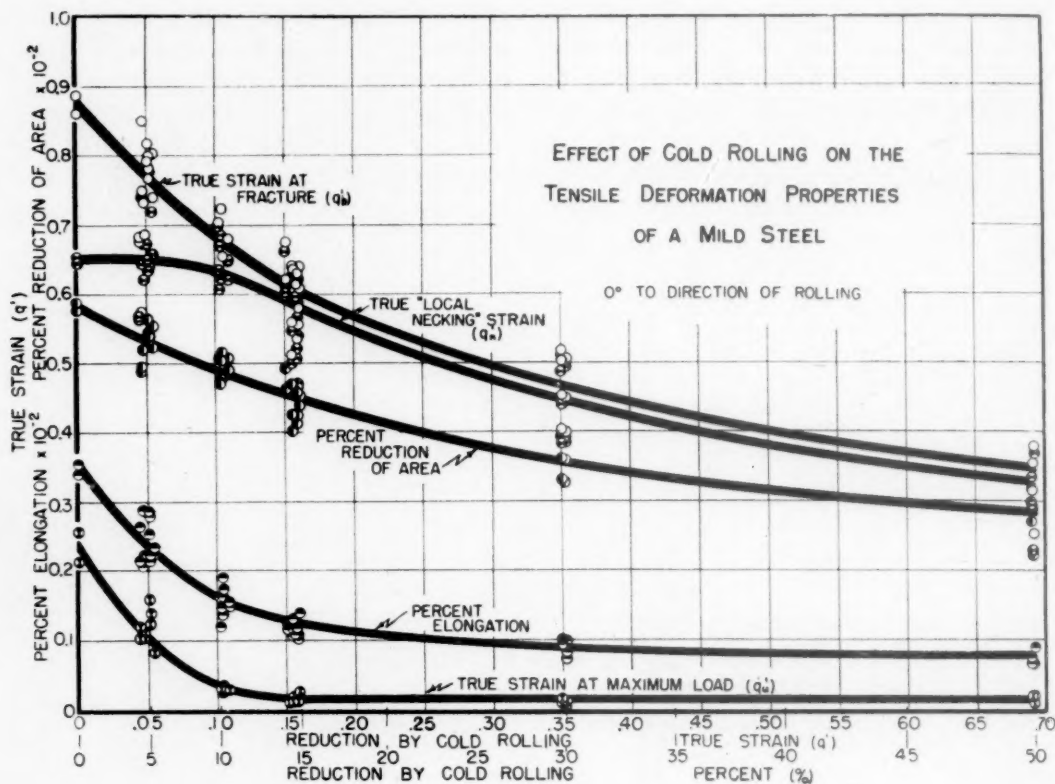


FIG. 15.

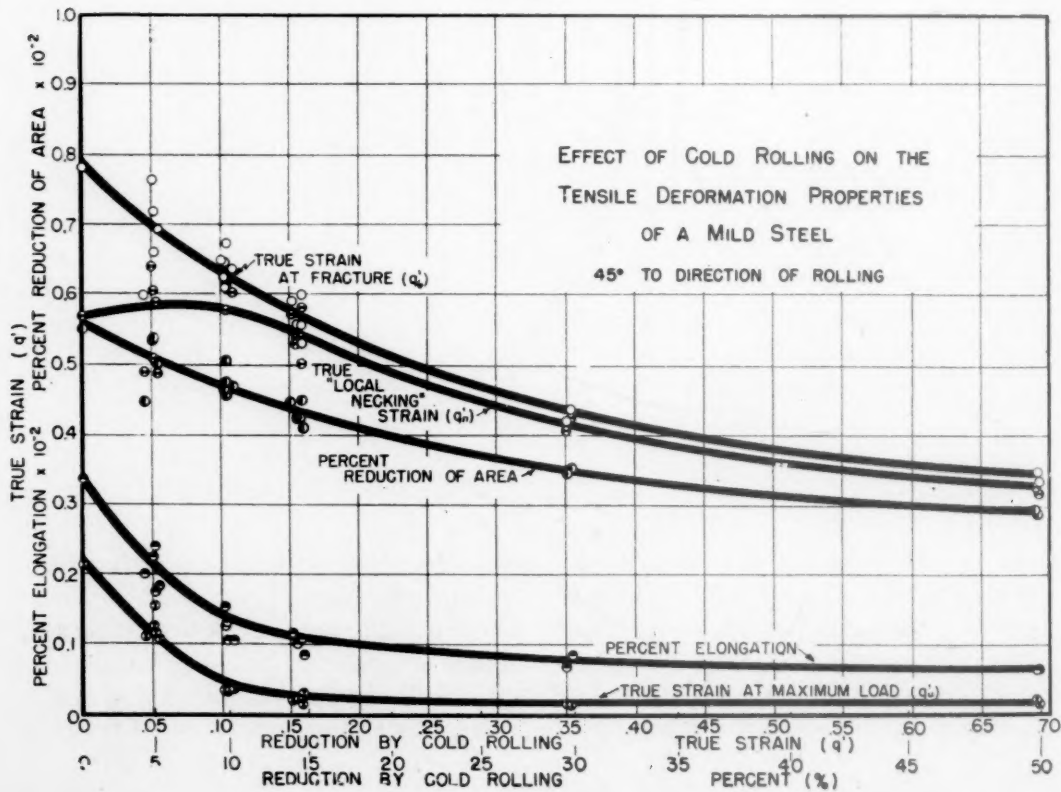


FIG. 16.

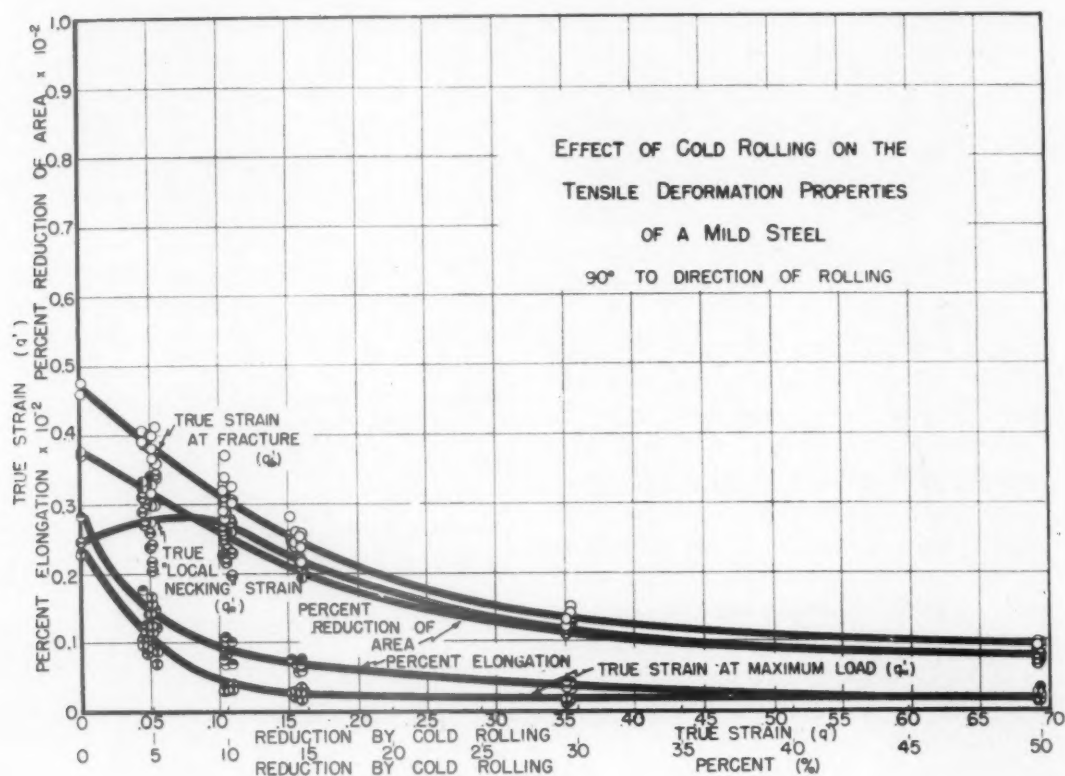


FIG. 17.

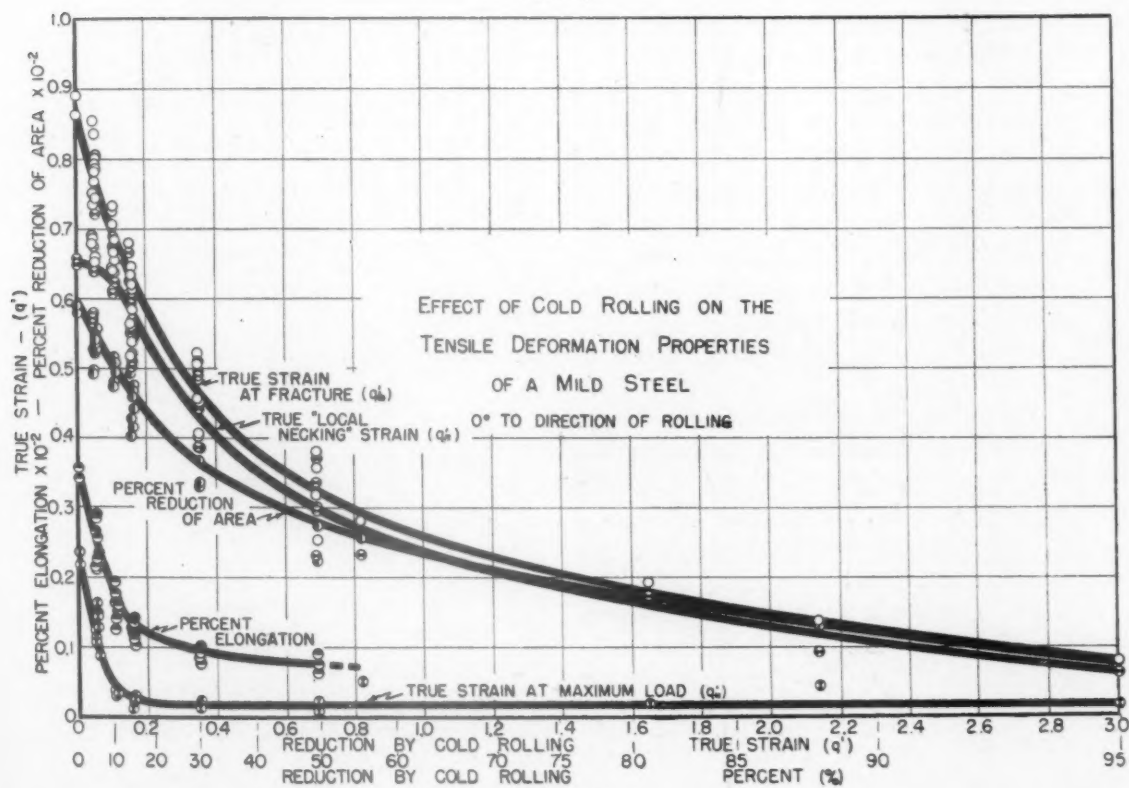


FIG. 18.

The effects of cold-rolling on the strain properties are shown in Figs. 15 to 18. The ordinary percentage of elongation and of reduction of area are plotted together with three true strain values.¹ The latter consist of the true fracture strain $q'_b = \epsilon_b$, the true uniform strain up to the maximum load $q'_\mu = \epsilon_\mu$, and the true local necking strain $q'_n = \epsilon_n$. The direct sum of ϵ_μ and ϵ_n is equal to ϵ_b .

The most significant curve of this series is that of the true strain at the maximum load $q'_\mu = \epsilon_\mu$, or the true uniform strain. The true uniform strain $q'_u = \epsilon_u$ is affected more by cold-rolling than the local necking strain until it reaches a value of 0.02 at 15 per cent reduction. This value then remains constant and all further cold-rolling merely decreases the local necking component of the total true strain. This behavior of the true uniform strain is the same independently of the orientation of the axis of the test specimen.

The true local necking strain $q'_n = \epsilon_n$ after about 10 per cent reduction tends to behave in a manner very similar to the true fracture strain $q'_b = \epsilon_b$.

The percentage of reduction of area behaves similarly to the true fracture strain. The magnitude of the effect of cold-rolling on the reduction of area is less than on the corresponding true fracture strain value. This indicates that the true strain is a more sensitive means of determining the effect of cold-rolling.

SUMMARY

The effects of cold-rolling on the true stress-strain properties of a low-carbon steel were investigated for total reductions up to 95 per cent. Tension tests of the true stress-strain type were made on the material after nearly complete aging had taken place. The influence of nonhomogeneity and of the orientation of the test bar relative to the rolling direction were studied in relation to their effects on these properties. The magnitude of strain-aging for

this material was also determined and pictured through the use of true stress-strain values. The general effects of cold-rolling on these physical properties were shown in a series of summary curves.

ACKNOWLEDGMENT

The authors would like to acknowledge the interest and support given to the work by Dr. Compton and Dr. Hunsaker. Assistance in the tests was received from Messrs. H. Majors, E. L. Bartholomew, Jr., and others. The photomicrographs (not reproduced here) were supplied by Mr. J. Connelly. For the careful machining of the test specimens the authors are indebted to Mr. H. Johnson.

REFERENCES

1. C. W. MacGregor: Relations between Stress and Reduction in Area for Tensile Tests of Metals. *Trans. A.I.M.E.* (1937) **124**, 208.
Differential Area Relations in the Plastic State for Uniaxial Stress. Stephen Timoshenko 60th Anniversary Volume. New York, 1939. The Macmillan Co.
The Tension Test. *Proc. Amer. Soc. Test. Mat.* (1940) **40**, 508-534.
A Two-load Method of Determining the Average True Stress-strain Curve in Tension. *Jnl. Applied Mechanics* (1939) **6**, A-156-158.
True Stress-strain Tension Test—Its Role in Modern Materials Testing. *Jnl. Franklin Inst.* (1944) **238**, 111-176.
2. M. Gensamer, E. B. Pearsall and G. V. Smith: The Mechanical Properties of the Isothermal Decomposition Products of Austenite. *Trans. Amer. Soc. Metals* (1940) **28**, 380-395.
3. B. Johnston and F. Opila: Compression and Tension Tests of Structural Alloys. *Proc. Amer. Soc. Test. Mat.* (1941) **41**, 552-570.
4. A. V. deForest, C. W. MacGregor and A. R. Anderson: Rapid Tension Tests Using the Two-load Method. *Trans. A.I.M.E.* (1942) **150**, 301.
5. F. J. Mehringer: True Stress-strain Plots of Flat Stock Steel. S.B. Thesis, Mass. Inst. of Tech., 1941.
6. D. J. McAdam, Jr.: The Technical Cohesive Strength of Metals. *Jnl. Applied Mechanics. Trans. Amer. Soc. Mech. Engrs.* (1941) **63**, A-155-165.
Technical Cohesive Strength and Yield Strength of Metals. *Trans. A.I.M.E.* (1942) **150**, 311.
7. D. J. McAdam, Jr., and R. W. Mebs: An Investigation of the Technical Cohesive Strength of Metals. This volume, page 474.

8. C. W. MacGregor and L. E. Welch: True Stress-strain Relations at High Temperatures by the Two-load Method. *Trans. A.I.M.E.* (1943) **154**, 423.
9. E. L. Bartholomew, Jr.: Stress-strain Measurements in the Drawing of Cylindrical Cups. *Trans. Amer. Soc. Metals* (1943) **31**, 582-593.
10. C. E. Lacy and M. Gensamer: The Tensile Properties of Alloyed Ferrites. *Trans. Amer. Soc. Metals* (1944) **32**, 88-105.
11. C. Zener and J. H. Hollomon: Plastic Flow and Rupture of Metals. *Trans. Amer. Soc. Metals* (1944) **33**, 163-215.
Effect of Strain Rate upon Plastic Flow of Steel. *Jnl. Applied Physics* (Jan. 1944) 22-32.
12. J. H. Hollomon: The Effect of Heat Treatment and Carbon Content on the Work Hardening Characteristics of Several Steels. *Trans. Amer. Soc. Metals* (1944) **32**, 123-131.

Distribution of Carbon between Titanium and Iron in Steels

BY W. P. FISHEL* AND BRISON ROBERTSON†

(Cleveland Meeting, October 1944)

THE carbide-forming tendencies of the various steel-alloying elements, or their affinities for carbon, is a subject that has received considerable attention, but little more than a probable arrangement of the elements as to their carbide-forming tendencies has been proposed.

The physical properties of alloy steels depend upon the relative proportions of the elements present and their combinations. One important phase of this subject is the distribution of carbon between the various elements present. The distribution of carbon between iron and other elements evidently will depend upon: (1) the affinity of each for carbon; (2) the relative atomic masses of the elements present; and (3) the possible formation of compounds between the alloying elements and iron and between the elements themselves. In ternary steels the case is simplified, especially in systems in which the element and iron form no compounds. In such systems iron and the alloying element are competing for the carbon present.

In this work the distribution of carbon between titanium and iron has been studied by measuring the relative amounts of iron carbide and titanium carbide present in a series of annealed steels in which the ratio of titanium to carbon extended from 0.527 to 4.61.

This paper is part of a thesis submitted by Brison Robertson in partial fulfillment of the requirements for a Master of Science degree at Vanderbilt University. Manuscript received at the office of the Institute March 16, 1944. Issued as T.P. 1763 in METALS TECHNOLOGY, October 1944.

* Professor of Metallurgy, Vanderbilt University, Nashville, Tennessee.

† Graduate Student, Vanderbilt University.

EXPERIMENTAL PROCEDURE

Ten Fe-Ti-C alloys, weighing about 250 grams each, were prepared by melting under a vacuum, in an induction furnace, Armco iron, carbon-free ferrotitanium (25 per cent Ti), and pure carbon. Vacuum melting prevented the formation of titanium oxides and nitrides, which would complicate the problem. The melts were made in graphite crucibles lined with sintered magnesium oxide. The ingots were cooled in the furnace under a vacuum and were then completely annealed at 950°C.

The determination of the amount of titanium carbide present was based upon the established insolubility of titanium carbide in boiling dilute (1:4) sulphuric acid, and the complete solubility of free titanium and titanium-iron compounds in this acid. High-carbon ferrotitanium, which had been treated to remove free Ti and Fe, was found to be completely insoluble in the acid; and the carbon-free ferrotitanium used in making the alloys was found to be completely soluble. Others^{1,2} have reported the insolubility of titanium carbide in sulphuric and hydrochloric acids.

Turnings from the ingots were digested with boiling sulphuric acid (1:4) until all action had ceased. The carbide residue was filtered off and analyzed for titanium, and in some cases for carbon. This represents the titanium that was united with carbon. The filtrate from the carbide residue contains the portion of the titanium that was in solid solution in the ferrite. Titanium

¹ References are at the end of the paper.

FIGS. 1-4.—CARBIDE IN ALLOYS 2, 5, AND 6. $\times 650$.

Fig. 1. Alloy 2, unetched.

Fig. 3. Alloy 6, unetched.

Fig. 2. Alloy 6, unetched.

Fig. 4. Alloy 5, etched with nital.

was determined in these filtrates. Titanium in both residues and filtrates was precipitated with Cupferron and determined gravimetrically according to the procedure suggested by the Chemists of the U. S. Steel Corporation.³ Total carbon was determined by standard combustion procedures. The carbon in the titanium carbide residue was filtered into combustion thimbles, which were dried and then burned

weight ratio of 4:1, as is shown by the last column.

2. In Fe-Ti-C steels practically 100 per cent of the titanium will be present as TiC so long as the weight ratio of Ti/C in the alloy is below a value somewhere between 3.57 and 4. This means that titanium is a very strong carbide former.

Further confirmation concerning the distribution of carbon was obtained by

TABLE 1.—*Compositions of Alloys and Distribution of Carbon*

Alloy No	Ti in Residue, Per Cent	Ti in Filtrate, Per Cent	Total Ti, Per Cent	Total C, Per Cent	Percentage of Total Ti in Carbide	Ratio Ti/C in Alloy	C in Residue, Per Cent	Ratio Ti/C in Residue
1	0.811	0.00	0.811	0.982	100	0.826		
2	0.483	0.00	0.483	0.915	100	0.527		
3	0.497	0.00	0.497	0.196	100	2.53		
4	0.476	0.00	0.476	0.416	100	1.15		
5	1.82	0.202	2.022	0.44	90	4.61	0.451	3.98
6	1.597	0.00	1.597	0.825	100	1.93	0.428	3.73
7	0.522	0.00	0.522	0.465	100	1.26		
8	0.649	0.00	0.649	0.29	100	2.24	0.156	4.16
9	1.536	0.240	1.776	0.388	86.5	4.57	0.39	3.94
10	1.24	0.00	1.24	0.353	100	3.57		

in a combustion furnace. Blanks were run during all combustions. The compositions of the alloys and the distribution of carbon are shown in Table 1. The results listed are the averages of not less than three separate determinations, which were in close agreement.

The titanium found in the filtrates of all alloys except 5 and 9 were recorded as zero. However, gravimetrically these values calculated from 0.01 to 0.03 per cent Ti. When fused and tested colorimetrically, none were above 0.01 per cent Ti. The amount of titanium found in these filtrates is independent of the ratio of titanium to carbon in the alloys. The small amounts of titanium found in these filtrates might have been the result of imperfect filtration of the carbide residues. It is believed that no titanium is present in solid solution in the ferrite, except in alloys 5 and 9.

Some conclusions can be drawn from the data of Table 1:

1. The formula of titanium carbide present in annealed steels is TiC, with a

microscopic examination and determinations of evolution of carbon on some of the alloys. The evolution method for carbon was developed in this laboratory several years ago. It closely resembles the method recently proposed by Donaldson.⁴

In this method the sample is treated with dilute hydrochloric acid. All evolved gases are swept out of the flask through a tube filled with hot CuO, which oxidizes all carbonaceous gases to CO₂. The CO₂ can be dried and absorbed in a Fleming bulb, or without purification may be absorbed in an ammoniacal barium chloride solution.

TABLE 2.—*Evolution of Carbon*

Alloy	Carbon by Evolution, Per Cent	Carbon in Carbide Residue, Per Cent	Sum	Total Carbon by Combustion, Per Cent
5	0.00	0.458	0.458	0.44
6	0.423	0.428	0.851	0.825
9	0.00	0.39	0.39	0.388
10	tr.			0.353

This method will detect and measure, fairly accurately, iron carbide and other carbides

decomposed by hydrochloric acid. TiC is not decomposed by this method. The results are presented in Table 2.

Alloys 5 and 9, which contained an excess of titanium above that required to form TiC with the carbon present, gave no carbon by evolution, showing that no iron carbide was present. Microscopic examination of these two steels showed that they contained no pearlite. For alloy 6, the sum of carbon by evolution, that present as Fe_3C plus that present as TiC is in fair agreement with the total carbon by combustion.

Microscopically TiC appears in the unetched sample as a yellow or light brown constituent, apparently forming a separate phase. Its appearance is little changed by treatment with nital. With low concentrations, the carbide appears as in Fig. 1. With higher concentrations, the TiC separates along the cleavage planes and as occasional cubes as in Figs. 2-4. Alloy 5 appears the same etched as unetched. No pearlite is present. Alloy 9, not shown here, was similar to alloy 5. Alloy 10 contained, in addition to the separated TiC, very small patches of pearlite. This confirmed the evolution results and showed that there was a slight excess of carbon beyond that required to form TiC with the Ti present.

The possible existence of a double titanium-iron carbide was investigated. About 50 grams of turnings from alloys 5 and 9 were completely digested with dilute sulphuric acid. The insoluble carbide residue was thoroughly washed until free from soluble iron salts. This residue was dissolved in nitric acid and was tested for iron. Only a very slight trace of iron was found. Therefore, a double or complex carbide does not exist as a true compound in annealed steels.

STANDARDS OF COMPARISON

The carbide-forming tendencies of the steel-alloying elements cannot be evaluated

without some standard of comparison. The equilibrium constants for the equations involved in the formation of iron carbide and the carbides of the various alloying elements may be compared.⁵ In the Fe-Ti-C system the equation is

$$\frac{(\text{Fe}_3\text{C})(\text{Ti})}{(\text{TiC})(\text{Fe})^3} = K$$

Minimum values may be substituted in this equation for Ti for steels similar to No. 1 and No. 2; and minimum values for Fe_3C in steels No. 5 and No. 6, from which values for K can be calculated. The data presented here show that the concentration of either Fe_3C or Ti is very small in all cases. Hence K must have a very small value. It is proposed to use as a basis of comparison the fraction or percentage of the equivalent proportion of the element to carbon in the carbide formed at which the alloying element begins to divide itself between the carbide and noncarbide phases. For example, the weight ratio of Ti to C in TiC is approximately 4 to 1 and the atomic ratio 1 to 1. This is the equivalent proportion. The data in Table 1 show that all the Ti is in the carbide phase up to and possibly beyond a weight ratio of 3.57, or an atomic ratio of 0.8925 to 1, which is 89.25 per cent of the equivalent proportion. The exact ratio at which Ti begins to divide between the two phases is being investigated further.

REFERENCES

1. Nat. Bur. Stds. *Circ.* 14 (1916) 9.
2. E. B. Shimer and P. W. Shimer: *Org. Com.* 8th Int. Congr. Appl. Chem. (1912) 1, 445.
3. Sampling and Analysis of Carbon and Alloy Steels. Reinhold Pub. Co., New York.
4. J. G. Donaldson: *Amer. Foundrymen's Assn. Reprint* 42-18.
5. K. K. Kelley: *U. S. Bur. Mines Bull.* 407 (1905).

DISCUSSION

L. D. JAFFE.*—Comparison with the extensive work of Tofaute and Buttinghaus⁶ indi-

* Metallurgist, Watertown Arsenal, Watertown, Mass.

⁶ W. Tofaute and A. Buttinghaus: *Die Eisenecke des Systems Eisen-Titan-Kohlenstoff. Archiv Eisenhüttenwesen* (1938) 12, 33-37.

cates that the present paper does not deal with equilibrium conditions at 950°C. but with phases formed at some lower temperature. Since the results are therefore dependent upon the cooling rate employed, would the authors give the manner, and if possible the rate, of cooling from 950°C.?

I. R. KRAMER.*—In their conclusions, the authors stated that when the ratio of titanium to carbon was below 3.57 or 4, the titanium was present as TiC. This statement implies that this would occur regardless of the austenitizing temperature. We feel that the authors meant their statement to apply for the annealing temperature used in their work; namely, 950°C. According to the iron-carbon-titanium equilibrium diagram proposed by Buttinghaus,⁷ for many of the steels reported here, the titanium could be dissolved at higher austenitizing temperatures. Further, Comstock⁸ has shown that the mechanical properties of steels containing titanium are dependent to a large extent upon the austenitizing temperature. The tensile strength of a steel containing 0.374 per cent C and 0.35 per cent Ti (Ti/C=0.95) was increased from 88,000 to 110,000 lb. per sq. in. by normalizing from 2150°F. instead of 1900°F.

* Division of Physical Metallurgy, Naval Research Laboratory, Anacostia, D. C.

⁷ A. Buttinghaus: The Iron End of the Fe-Ti-C System. *Tech. Mitt. Krupp A, Forschungsberichte* (1938).

⁸ G. F. Comstock: Some Effects of Heat Treatment on Low Alloy Titanium Steels. *Trans. Amer. Soc. for Metals* (1944) **33**, 324.

W. P. FISHEL (author's reply).—The questions raised by Mr. Jaffe and Mr. Kramer can be answered together. We had no intention to investigate the distribution of carbon between Ti and Fe at 950°C. We were concerned with the distribution in a completely annealed steel. The samples were held for 2 hr. at 950°C. and were allowed to cool in the furnace. I would judge that some 2 hr. was required for the ingots to cool to A₁.

We feel that as the melt cools TiC forms according to Buttinghaus, in the neighborhood of 1200°C. If undisturbed it segregates in the shapes shown in Figs. 1 to 4. This structure retains its form as the steel cools through the critical range. The TiC will certainly redissolve if heated sufficiently high and will separate again. After publication of the paper samples 5 and 9, which contained no Fe₃C, were heated to 1000°C. and held for 3 hr. They were then quenched in ice water and examined. The treatment had not changed the TiC structure. This proves that the carbide does not dissolve at that temperature.

I believe there is no disagreement between our findings and the hardening reported by Comstock. The hardening effect produced by Ti is present only if the steel has been worked from a fairly high rolling temperature down to near the critical temperature. The hardening could be explained by the breaking up of the segregated TiC particles. These particles segregate again when the steel is annealed.

Effect of Time of Storage on Ductility of Welded Test Specimens

BY CLARENCE E. JACKSON,* MEMBER A.I.M.E., AND GEORGE G. LUTHER*

(Cleveland Meeting, October 1944)

THE ever increasing array of information concerning the measurement of the effect of the welding process on the properties of a steel is an indication of the tremendous

specimen is prepared with a saw-notch placed so as to restrict deformation to the heat-affected zone under the bead weld when tested as a static bend. Failure is



FIG. 1.—NICK-BEND TEST FOR WELDABILITY.

effort that is being expended in this field. The methods that have been considered may be divided into two groups: first, those that measure directly the effect of welding on the ductility of a steel, and, second, those that observe the change in some property, such as the hardness of the heat-affected zone, and assume a direct correlation between this change and the resultant ductility.

The nick-bend test is a direct method designed for studying the effect of welding on the ductility of a steel. The test specimen (Fig. 1) consists of a bar cut from a plate with a bead weld on the surface. The

caused by rupture of the low-ductility metal in the heat-affected zone. The angle at maximum load is used as an index of the effect of the welding process on the material.

In the development of the nick-bend test considerable scatter was noted in some of the results, although the agreement of duplicate specimens welded at the same time and tested consecutively was excellent. Upon further investigation it was found that the change in ductility was dependent upon the interval of time between the welding operation and the testing of the specimen. For the six steels of Fig. 2, the angle at maximum load in four cases was doubled and in one case was tripled. All steels that have been studied show an improvement in the angle of bend for longer intervals between welding and testing.

This same behavior has been found in weldability tests using the Navy T-bend

This paper represents only the personal opinions of the authors and in no way reflects the official attitude of the U. S. Navy. Published by permission of the Navy Department. Manuscript received at the office of the Institute Aug. 11, 1944. Issued as T.P. 1772 in METALS TECHNOLOGY, January 1945.

* Division of Physical Metallurgy, Naval Research Laboratory, Anacostia Station, Washington, D. C.

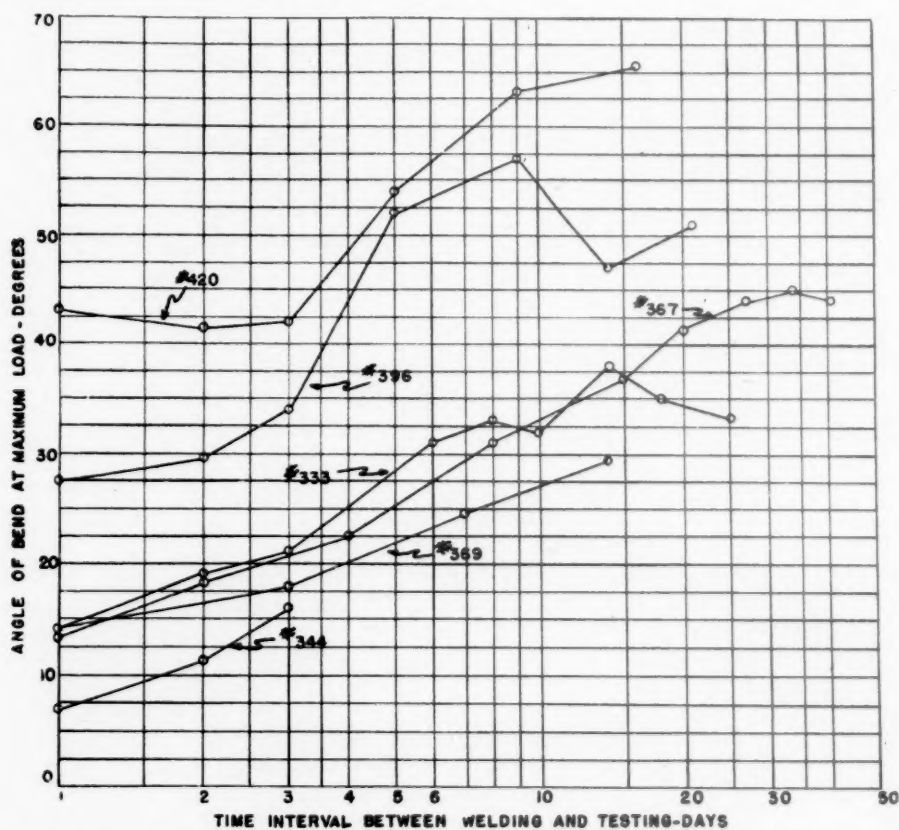


FIG. 2.—RELATION OF DUCTILITY TO TIME INTERVAL BETWEEN WELDING AND TESTING FOR NICK-BEND SPECIMENS.
See Table 1 for chemical composition.

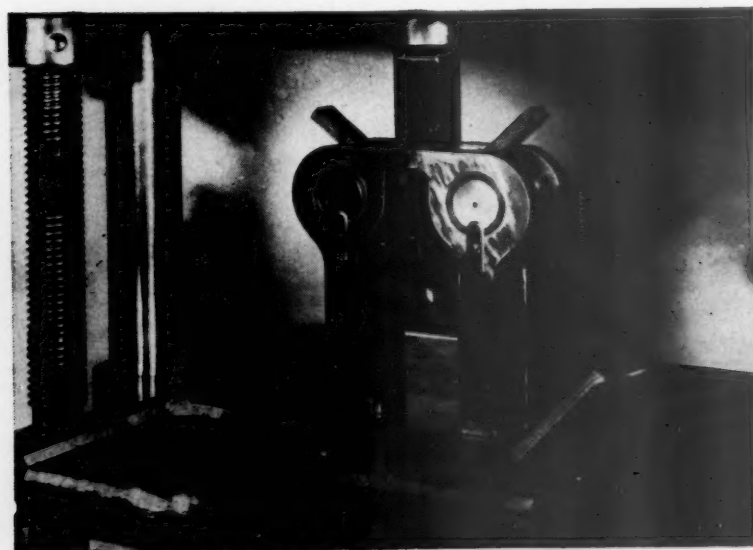


FIG. 3.—T-BEND TEST FOR WELDABILITY.

specimen in which a T-section is made by joining two plates by means of fillet welds. A special jig is used for bending the specimens (Fig. 3) and the angle to which the

a crack $\frac{1}{8}$ in. long was observed in the base metal, and the angle at failure was used as the index of ductility of the specimen.

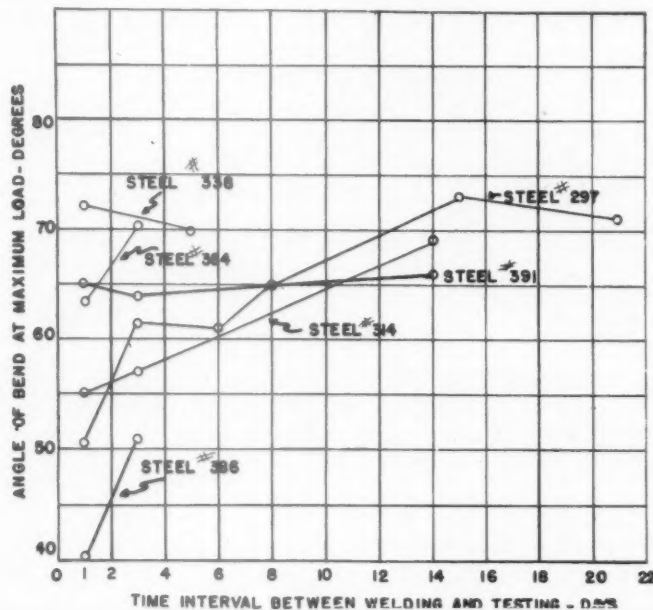


FIG. 4.—RELATION OF DUCTILITY TO TIME INTERVAL BETWEEN WELDING AND TESTING FOR T-BEND SPECIMENS.

base of the T is bent at maximum load is used as an index of the performance of the steel. Typical results are shown in Fig. 4.

Some of the more ductile steels having a high angle of bend at maximum load show no significant change in ductility with increasing time intervals between welding and testing, because the upper range of the T-bend test is limited to an angle at maximum load of approximately 70° . Hence an increase in angle can be expected only for steels that show low ductility one day after welding.

With these observations in mind, the results obtained with a longitudinal bead-weld bend specimen were scrutinized. This specimen was used in a study of the weldability of S.A.E. 4130 steel for aircraft service. The bead weld was deposited automatically and the specimen was bent to failure (Fig. 5) (or to the capacity of the test jig) with the bead weld in tension. The test specimen was considered to fail when

The ductility values observed in some of the test work showed excessive scatter, although, again, the agreement of duplicate specimens welded at the same time and tested consecutively was excellent. In order to check further the effect of the time interval between welding and testing, a series of 12 specimens of NE 9430 steel were tested one to seventeen days after welding, with results as shown in Fig. 6. There was a definite increase in the ductility of the test specimens with an increase in storage time.

All of these observations indicate that a gradual metallurgical change takes place in the welded test specimen. Four suggestions have been made, which offer some promise as a basis for a satisfactory explanation of this phenomenon: (1) hydrogen, (2) aging, (3) retained austenite, and, (4) the relief of residual stresses.

A search through the literature uncovered two investigations reporting be-

havior closely allied to that noted in tests reported here.

Reinhardt and Cutler,¹ reporting on the effect of time and temperature on the

They show that when all weld-metal specimens were held from 24 to 72 hr. at a temperature of 100°C., or for one hour at 300°C., and then tested in tension, the per-



FIG. 5.—LONGITUDINAL BEAD-WELD TEST SPECIMEN.

physical properties of medium carbon steel showed that the ductility of steel expressed by elongation is greatly improved by some equilibrium adjustment that takes place slowly at room temperature and much more rapidly at slightly increased temperature. In a discussion of these results, Langenberg favored the view that the changes in physical properties of the material were due to the relief of internal stress.

centage elongation and reduction of area were improved in the order of 30 to 50 per cent.

Dawson and Lytle offer no explanation of the improvement in ductility. They mention, however, that it has been stated in the literature that hydrogen when present in solid steel may have the effect of lowering these values, and also that heating at low temperatures is effective in removing

TABLE 1.—Chemical Composition of Specimens

Steel	C	Mn	Si	P	S	Ni	Cr	Mo	Cu	Al	Ti	V	Zr
297	0.14	0.59	0.82	0.026	0.033	0.075	0.48	0.08	0.20	0.034			0.05
314	0.18	1.10	0.16	0.018	0.020	0.11	0.03	0.02	0.23	0.01	0.01	0.003	
333	0.18	1.09	0.16	0.017	0.022	0.12	0.04	0.025	0.22	0.015			
338	0.20	0.54	0.04	0.012	0.024	0.06	0.01	0.02	0.10				
344	0.22	1.52	0.23	0.025	0.035	0.13	0.14	0.05	0.14	0.01	0.024	0.012	
367	0.16	1.16	0.26	0.019	0.027	0.08	0.05	0.02	0.19	0.02		0.09	
369	0.18	0.69	0.18	0.016	0.027	1.47	0.05	0.04	0.94	0.01			
384	0.18	1.28	0.24	0.021	0.032	0.10	0.05	0.03	0.20	0.02	0.007	0.002	
386	0.15	1.24	0.27	0.021	0.020	0.13	0.05	0.04	0.25	0.01	0.008	0.005	
391	0.16	1.26	0.24	0.020	0.020	0.06	0.04	0.038	0.15	0.012	0.01	0.01	
396	0.17	1.34	0.23	0.018	0.025	0.10	0.19	0.005	0.01	0.026	0.030		
420	0.23	0.50	0.003	0.010	0.053	0.10	0.05	0.02	0.15	0.01			

A more recent investigation, by Dawson and Lytle,² relates to the improvement in ductility of oxyacetylene welds by treatment at temperatures of 110° to 300°C.

¹ References are at the end of the paper.

hydrogen from steel. Whether the large increase in ductility can be attributed entirely to hydrogen is questionable.

A number of tests have been performed at the Naval Research Laboratory in an

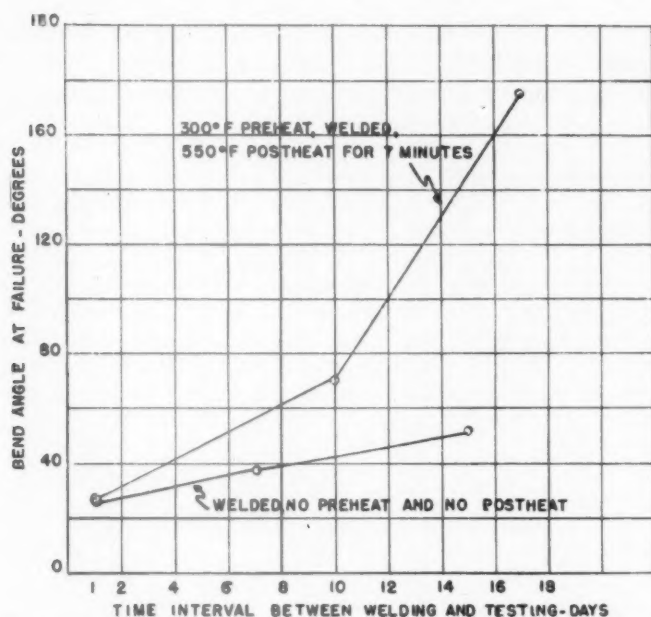


FIG. 6.—RELATION OF DUCTILITY TO TIME INTERVAL BETWEEN WELDING AND TESTING FOR LONGITUDINAL BEAD-WELD BEND SPECIMENS (NE 9430).

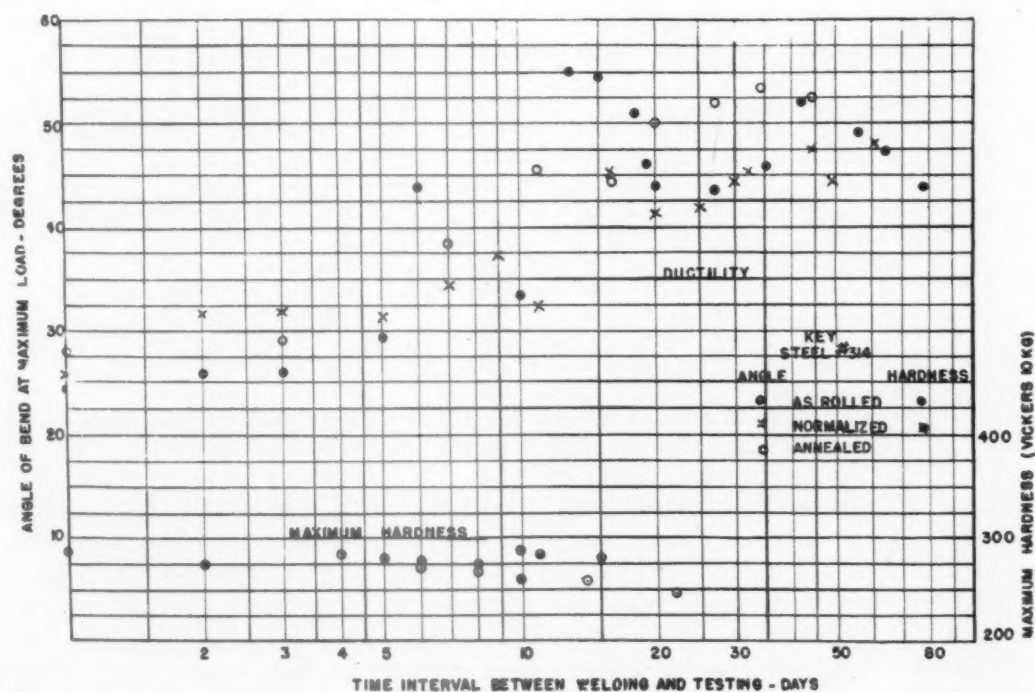


FIG. 7.—EFFECT OF CONDITION OF PLATE MATERIAL ON DUCTILITY FOR NICK-BEND TEST AND ON MAXIMUM HARDNESS IN HEAT-AFFECTED ZONE.

attempt to obtain some information regarding the mechanism controlling the change in ductility. A series of nick-bend tests was made on steel No. 314 (com-

served (Fig. 7). It may be possible that aging is responsible for the effects noted, although the exact mechanism is obscure.

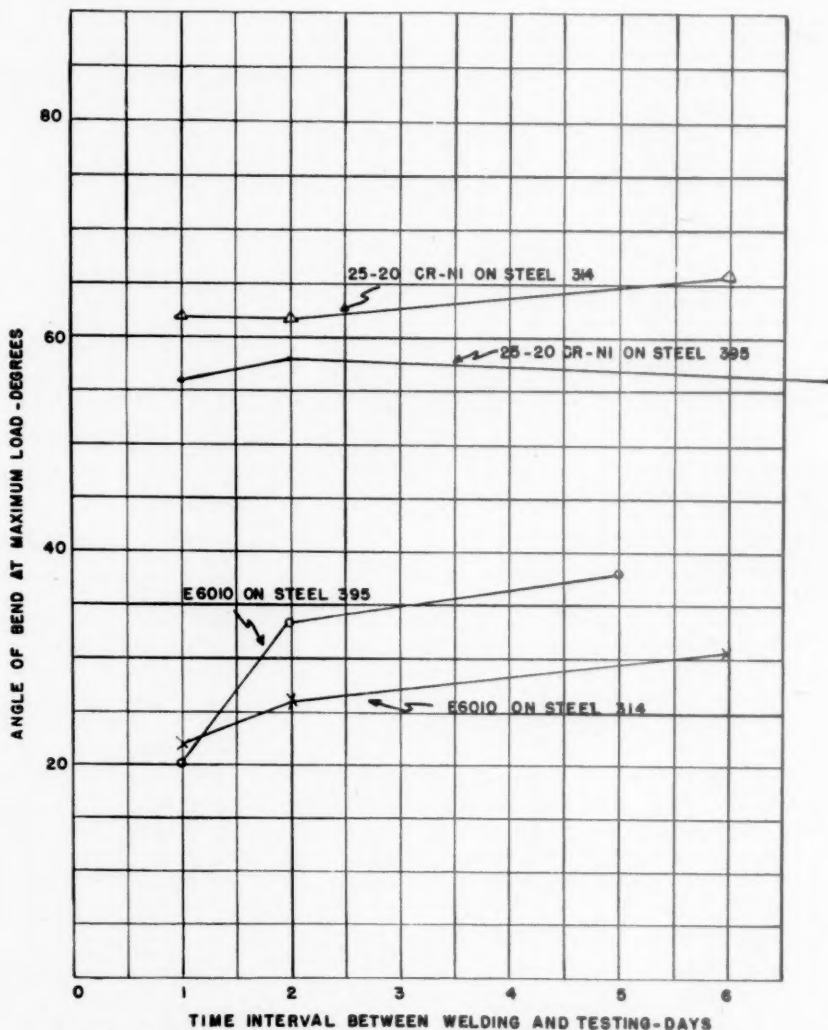


FIG. 8.—EFFECT OF TYPE OF ELECTRODE ON NICK-BEND TESTS.

position, Table 1) in the as-rolled, normalized (2 hr. at 900°C. [1650°F.]), and annealed conditions. In all tests an increase in ductility was observed; the initial condition of the steel having only a slight effect. Sections were obtained from these plates for measurement of the maximum hardness (Vickers 10 kg.) in the heat-affected zone under the bead weld. A slight decrease in maximum hardness was ob-

In line with work reported from this laboratory,³ the possibility was suggested that the gradual decomposition of retained austenite might cause the change in ductility. In order to check this hypothesis, a number of specimens were welded, treated in liquid air at -185°C. and then prepared for testing. The ductility obtained from specimens after treatment by liquid air was in line with that of specimens

not treated; hence, it appears that the change in ductility is not due to retained austenite.

To obtain information regarding the

mild-steel electrodes are shown in Fig. 8. This information adds to the argument that the change in ductility is probably the result of relief of stresses, since the low

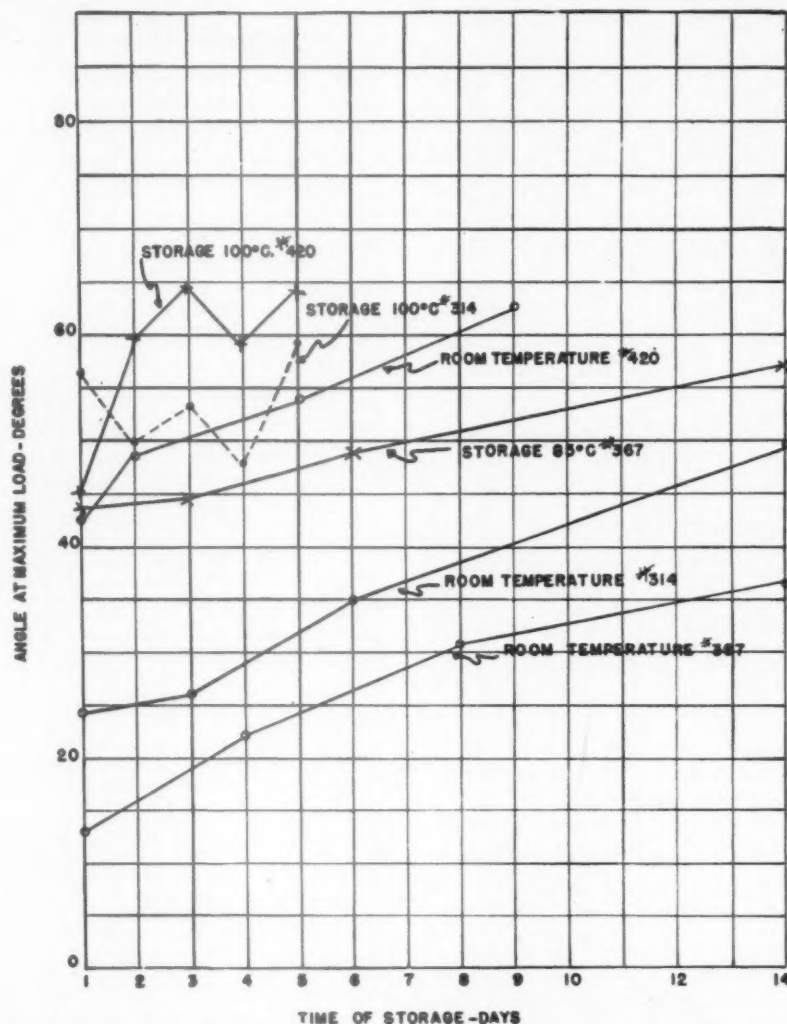


FIG. 9.—EFFECT OF TEMPERATURE OF STORAGE ON NICK-BEND TESTS.

effect of type of electrode, a number of nick-bend test plates were welded, using a 25-20 Cr-Ni type of electrode, for comparison with the data previously obtained for mild-steel electrodes of the A.W.S. E6010 type. Specimens welded with the 25-20 Cr-Ni electrodes showed no appreciable change in ductility with increasing time intervals between welding and testing. These results and those obtained using

yield strength of fully austenitic weld metal would tend to give lower stresses in the heat-affected zone.

If the increase in ductility is due to the relaxation of stresses, the effect should be augmented by an increase in the temperature. Specimens were placed in ovens maintained at 85°C. and 100°C. and were tested after various times of storage. The ductility was decidedly increased

by storing specimens at these elevated temperatures (Fig. 9).

From a practical standpoint, it is fortunate that the tests reported in this paper indicate that the ductility of a weldment improves rather than decreases. It confirms the statement often made by welding engineers that if a structure can be fabricated without cracking during the early periods of construction the chances for continued satisfactory performance are good.

Cognizance must be taken of the increase in ductility obtained after preparation of welded test specimens in order to obtain test results that are comparable and can be used for fundamental studies on the effect of welding on the properties of steel.

REFERENCES

1. G. A. Reinhardt and H. J. Cutler: Effect of Time and Low Temperature on Physical Properties of Medium-carbon Steel. *Trans. A.I.M.E.* (1920) **72**, 420-435.
2. J. R. Dawson and A. R. Lytle: Improving Ductility of Oxyacetylene Welds by Aging. *The Welding Jnl.* (1941) **20**, 109-s to 112-s.
3. C. E. Jackson, G. G. Luther and K. E. Fritz: Weldability Tests of Silicon-Manganese Steels. *The Welding Jnl.* (1944) **23**, 33-s to 43-s.

DISCUSSION

S. A. HERRES.*—The interesting effect of increasing ductility of welded test specimens with aging time, which was very well demonstrated by the authors' nick-bend tests, is also apparent in the testing of transverse tensile tests of welded joints. The tests reported by Zapffe and Sims⁴ in 1940 demonstrated that a similar recovery in ductility of weld metal is associated with escape of hydrogen, which is absorbed from the moisture and other hydrogen-bearing gases introduced into the welding atmosphere by electrode-coating ingredients.

* First Lieutenant, Ordnance Dept., Watertown Arsenal. The statements or opinions expressed in this discussion are to be considered those of the author and do not necessarily express the views of the Ordnance Department.

⁴ C. A. Zapffe and C. E. Sims: Defects in Weld Metal and Hydrogen in Steel. *Welding Jnl.*, Research Supplement (Oct. 1940) **19** (10).

Tests at Watertown Arsenal Laboratory⁵ demonstrated that hydrogen absorbed by the weld metal may also diffuse into the heat-affected zone to produce the flakelike underbead crack when hardenable steels are welded with electrodes having coatings high in moisture or hydrogen-bearing ingredients. It was further demonstrated that either ferritic or austenitic electrodes with a stainless type (lime-base) coating do not cause underbead cracking even though the maximum hardness or microstructure of the heat-affected base metal or the over-all stresses across the weld bead were not significantly different from specimens that developed underbead cracking. It was concluded that the lower hydrogen content and higher carbon dioxide content of welding atmospheres for stainless type coatings would reduce the hydrogen concentration in the weld metal and the consequent embrittlement of the heat-affected zone. Recent tests at Watertown Arsenal show that oil-quenched 0.25 per cent C alloy steel with the following properties, as quenched, 250,000 lb. per sq. in. tensile strength, 225,000 lb. per sq. in. yield strength, 40 per cent reduction⁷ of area, 30 ft.-lb. V-notch Charpy value, has less than 5 per cent reduction of area after cathodic hydrogen plating for 1 hr. in 10 per cent sulphuric acid (current density 4.4 amp. per sq. in.). Ductility of the hydrogen-charged samples recovers to about $\frac{3}{4}$ of the original reduction of area in 7 days at room temperature, 4 hr. at 212°F. or a very short time at higher temperatures.

In view of the extensive published evidence on the effects of hydrogen in welded joints, and particularly the decreased embrittlement of welds made with stainless electrodes, it is surprising that the authors did not devote more attention to consideration of hydrogen embrittlement.

C. A. ZAPFFE.*—Here is a paper based entirely upon the observation that weld metal gains in ductility over a period of standing at ordinary temperature, and in a shorter period at slightly elevated temperatures that are still too low to change the metal microstructurally.

⁵ S. A. Herres: Arc Welding of Alloy Steels. *Trans. Amer. Soc. for Metals* (1944) **33**, 531-565.

* Assistant Director, Research Division, Rustless Iron and Steel Corporation, Baltimore, Maryland.

In 1940, an extensive paper was presented before the American Welding Society which dealt with this matter, its cause, and its control in the greatest detail.⁶ The paper was

to be tested at other temperatures were stored on dry ice until needed.

Quoting from the section on Effect of Aging at Room Temperature: "The effusion of hydro-



FIG. 10.—ARC WELD ON MILD-STEEL PLATE IMMERSSED IN PAN OF GLYCERIN.

White cloud overlying weld is an island of foam caused by hydrogen escaping from the weld metal. $\frac{1}{3}$ natural size.

reprinted in full in a British Journal,⁷ in part in another American journal,⁸ and the essential information was included again in a second comprehensive paper presented before this society in 1941,⁹ and in a series of three papers later appearing in *Metal Progress*. In that work, not only tables and curves for physical properties were included, but photographs of fractures were presented illustrating the decrease in embrittlement occurring at room temperature over a period of two weeks. Because of this recovery at room temperature, all specimens

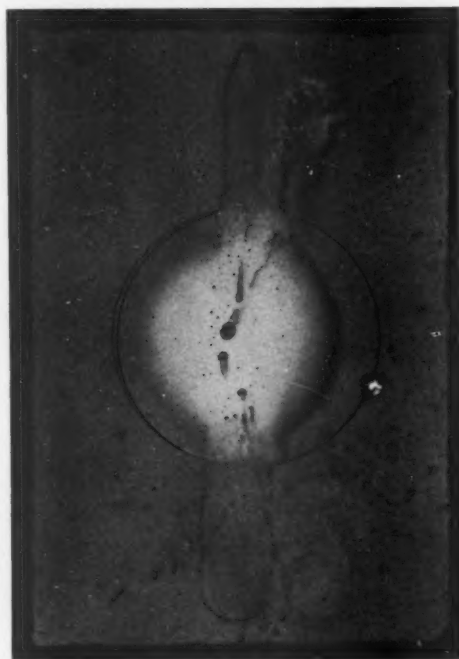


FIG. 11.—TEST SIMILAR TO THAT IN FIG. 10, WITH INVERTED COVER GLASS FOR GATHERING THE GAS.

Large visible bubbles are evident within a white, massive foam of tiny bubbles. Note foam island outside cover glass, which has floated to one side, exposing underlying weld bead. $\frac{1}{3}$ natural size.

gen from weld metal that occurs over a period of time at room temperature, though slow, is significant because welded structures can thereby attain some ductility without heat treatment." Why the "... search through the literature ..." professed by the authors of the present paper failed to uncover the work cited above is difficult to understand.

As for their four postulates, three can be collapsed into one; and the remaining one, retained austenite, should never have been included for the reason that the decomposition of austenite can only decrease ductility, not increase it. Thus, the behavior of hydrogen, which they list as postulate 1, is an aging function, which is their postulate 2; and escape of the gas from the metal relieves residual stresses, which is their postulate 4.

It seems difficult to believe that anyone

⁶ C. A. Zapffe and C. E. Sims: Defects in Weld Metal and Hydrogen in Steel. *Welding Jnl.* (1940) **19**, 337-S, 395-S.

⁷ *Sheet Metal Ind.* (1941) **15**, 791-796, 927-932, 1045-1051.

⁸ Hydrogen in Steel. *Blast Furnace and Steel Plant* (1940) **28**, 1163-1166.

⁹ Hydrogen Embrittlement, Internal Stress, and Defects in Steel. *Trans. A.I.M.E.* (1941) **145**, 225-271.

closely associated with welding has not yet ascertained for himself some of the more obvious relationships of this omnipresent and prime impurity when its presence is so easily

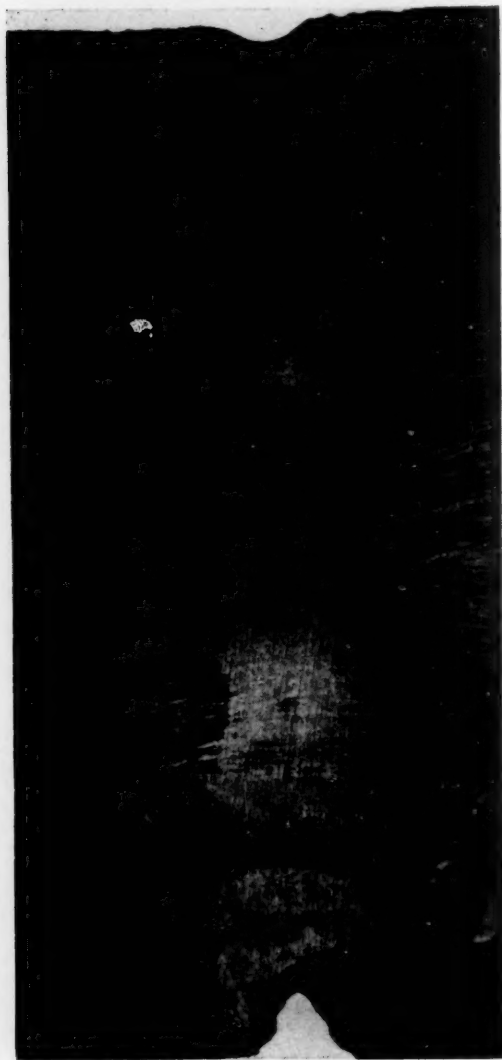


FIG. 12.—SURFACE OF HEAVY MILD-STEEL PLATE FIRED WITH A BLUE GLASS COATING AND SUBSEQUENTLY CHIPPED.

Obvious lack of adhesion over the weld metal is the result of hydrogen effusing there during firing to prevent the oxidation necessary for good adherence. $\frac{2}{3}$ natural size.

detected. For example, the escape of hydrogen even from welds made under the best conditions is easily detected by placing the weld under a liquid. The accompanying photographs,¹⁰ for

¹⁰ The writer wishes to express his appreciation to Mr. J. M. Cayford and Mr. Lewis

example, show the weld section of an arc-welded mild-steel plate immersed in a pan of glycerin. The whitish patch in Fig. 10 is a veritable island of foam directly overlying the weld, caused by hydrogen leaving the metal at room temperature. Fig. 11 shows another specimen, this time with an inverted cover glass collecting the copious foam. In Fig. 12, the nonadherence of vitreous enamel over the weld is another proof for a high hydrogen content of the weld metal.¹¹ These specimens were all arc-welded under normal conditions, and they display phenomena that any welder can observe without difficulty.

C. E. JACKSON (author's reply).—We appreciate the comments of Lieutenant Herres and Dr. Zapffe. We expected a rather vigorous reaction from those that insist that hydrogen is the "bad actor" in welding. We agree that in the tests reported in this paper hydrogen may be a contributing factor influencing the rate of increase in ductility. We have no quarrel with the statement that hydrogen is present in arc welds; its presence has been amply proved.

However, there are a number of other experimental results which we cannot explain simply on the basis of hydrogen. First, nick-bend tests on $\frac{1}{2}$ -in. plate thickness have much less change in ductility with time than those on $\frac{3}{4}$ or 1-in. thickness. Second, if the weld is deposited using a bare wire without the hydrogen-forming coating, the increase in angle at maximum load for the nick-bend specimen is still almost 30 per cent in tests at 14 days compared with 1-day tests. Third, the use of stainless-type coating on ferritic electrodes (Lieutenant Herres emphasizes that these electrodes produce no underbead cracking because of low hydrogen content) show an increase in angle at maximum load for nick-bend tests of more than 30 per cent for a 5-day interval compared with 1-day tests.

We fail to follow the application of Dr. Zapffe's comment that decomposition of austenite can only decrease ductility. In the steels in which

Breeze, Ceramic Engineers, Glascote Products, Inc., Cleveland, Ohio, who performed these experiments in the Glascote Laboratory and provided the photographs accompanying this discussion.

¹¹ W. W. Higgins and W. A. Derringer: Investigation of Fish-Scale Phenomena. *Jnl. Amer. Cer. Soc.* (1941) 24, 383-392.

the retained austenite transforms at a temperature only slightly below room temperature, the transformation during test by stress will produce a product with low ductility.¹² On the other hand, this transformation at room tem-

perature under the influence of welding stresses may relieve some of the nonhomogeneities in the heat-affected zone, so that improved ductility can be expected.

There evidence still points to the fact that there are other factors, in addition to hydrogen, that control the effect of time of storage on ductility of welded test specimens.

¹² C. E. Jackson, G. G. Luther, and K. E. Fritz: Weldability Tests of Silicon-Manganese Steels. *Welding Jnl.* (1944) **23**, 33-S.

Metallurgical Factors of Underbead Cracking

By S. L. HOYT,* C. E. SIMS,* AND H. M. BANTA, MEMBERS A.I.M.E.*

(New York Meeting, February 1945†)

OVER the past few years, metallic arc welding has been extended to steels of the hardenable type. As compared with other methods of fabrication, production has been facilitated, service performance frequently has been improved, and the overall results have been so favorable that engineers and production men have placed great emphasis on this application of welding. The metallurgist and welding engineer, however, have been confronted with new problems, since, for one reason, the harder steels are more apt to crack and special precautions must be taken if sound joints are to be procured. Some of the factors that are pertinent to this problem are metallurgical, and it is an object of this contribution to discuss steel manufacture and processing methods and to show how their control assists in reducing the hazard of cracking.

By this time, the problem of cracking—specifically underbead cracking, or “hard cracks,” or parent-metal cracks—is well known, and a large amount of work has been published, both here and abroad, dealing with this subject.¹ The tests described are made under restraint to facilitate cracking and are so designed that a semiquantitative, or at least a relative, value of the cracking tendency is obtained. As one would expect, it has been reported that the incidence of cracking increases with the carbon and alloy content of the steel. More specifically, the cracking

tendency is said to increase with the hardenability of the steel, though it is now recognized that the situation is not so simple. The phenomenon itself, on the other hand, has been but loosely described, and it is in only broad generalizations that this cracking has been related to steel metallurgy. Thus, while it has been abundantly demonstrated that the hardenable aircraft steel, S.A.E. 4130, must tend to crack when arc-welded, the problem still remains of why two lots of the same composition and the same hardenability can vary so greatly in cracking tendency, or what it is about the prior metallurgical history that so strongly affects the results. Further, while the efficacy of preheating and postheating in preventing cracking is recognized and utilized in production, the mechanism by which they function seems not to have been described.

These points are thought to be significant in the production of steel for fabrication by metallic arc welding and, hence, of interest to mill and process metallurgists and welding engineers. Consequently, it is another object of this paper to discuss the mechanism of parent-metal cracking, including the influence of the condition of the steel and the control of cracking by manipulation of the time-temperature conditions during and after welding.

A new method of rating the cracking tendency is also discussed, and the results of the test are related to steel composition and structure or prior history.

The work to be described was the outgrowth of work in 1940-41 at Battelle Memorial Institute on two projects, one

Manuscript received at the office of the Institute Nov. 29, 1944. Issued as T.P. 1847 in METALS TECHNOLOGY, June 1945.

* Battelle Memorial Institute, Columbus, Ohio.

† Meeting canceled.

¹ References are at the end of the paper.

of which involved the making and testing of simulated aircraft joints,² and the other a study of the utility characteristics of various welding electrodes in aircraft welding.² Both investigations involved welding the aircraft steel S.A.E. 4130, and it was soon discovered that while steel procured for one project welded satisfactorily, that secured for the other developed annoying cracks. A preliminary check on composition and other characteristics gave no clue as to why this should be. The same was true of a check of the literature and discussions with various metallurgists and welding engineers. It did develop, however, that the same thing had been observed by others, who were likewise unable to explain it, and mill metallurgists ran into the same peculiar behavior in their contacts in the field. It also developed that aircraft companies adopted the practice of preheating to avoid cracks developing in arc-welded structures, though it is probable that much of the steel could be welded without preheat.

Ultimately, it became obvious that there were some unknown factors, aside from chemical composition, that have an important bearing on parent-metal cracking in production welding. The logical answer to such a situation was a research aimed at uncovering the pertinent points and setting up a prescription for the production of steel that would give as great freedom from cracking as the analysis would permit.

A "restricted" research project, NRC-514, was set up in 1942 by the Office of Production Research and Development of the War Production Board under the supervision of the War Metallurgy Committee of the National Academy of Sciences—National Research Council. This project was to investigate the factors affecting the cracking tendency of hardenable steels, aside from composition, in an attempt to improve the welding quality. This work forms the basis of the present

paper, which has been released for publication by the Office of Production Research and Development.

To supervise the project, the War Metallurgy Committee appointed the following Project Committee:

A. J. Williamson, *Chairman*, Summerill Tubing Co.

R. S. Archer, Republic Steel Corporation.

J. J. Chyle, A. O. Smith Corporation.

G. Soler, Steel and Tube Div., Timken Roller Bearing Co.

C. L. Hibert, Consolidated-Vultee Aircraft Corporation.

M. Nelles, Office of Production Research and Development, W.P.B.

N. W. Fay, Iron and Steel Division, W.P.B.

This Project Committee maintained close contact with the work in progress, and we are deeply indebted to their constructive criticism and advice. Though small, the Committee was wisely selected to cover steel manufacture, steel processing, and production welding.

To describe the scope of the investigation, it was the variable behavior of presumably similar steels when welded in the same way under standard shop conditions that drew attention to the problem. For example, while cracking can be eliminated by using a different weld rod or by changing the welding practice, the problem was to find out what factors other than composition caused the variable behavior when steels were welded under standard conditions. This eliminates or holds constant certain factors or variables that now are recognized as affecting the incidence of cracks. Thus, while cracking is found, under some circumstances, in a steel with only 0.15 per cent C and 1.2 per cent Mn, of relatively low hardenability, even such a steel as S.A.E. 4340 is welded (under other conditions) without cracking. This comes about by the play of a number of factors, only a few of which are considered here. In particular, we are not dealing with the electrode, its size and

type, the speed of welding or rate of heat input, the joint design, the technique used, plate thickness or temperature as factors that affect cracking. Instead, we are

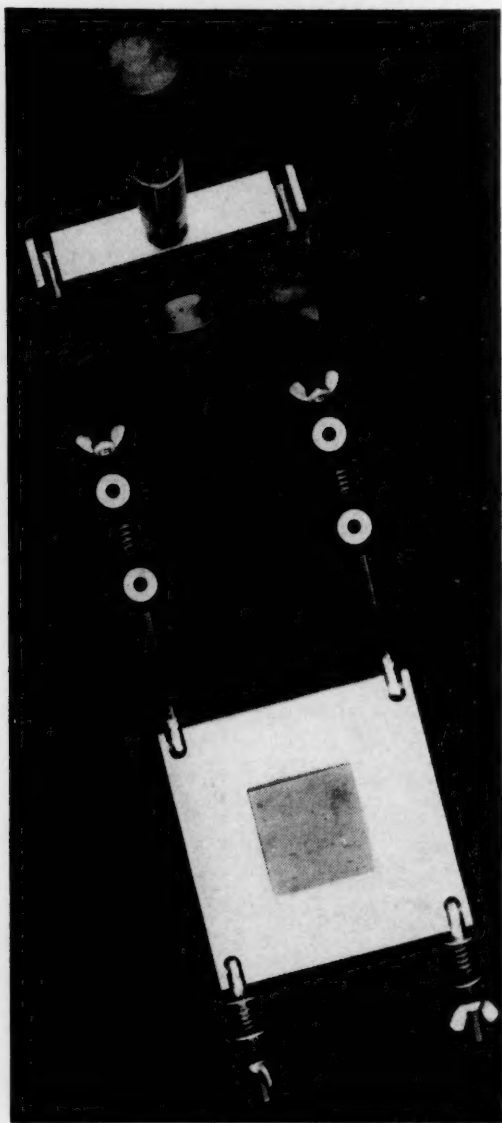


FIG. 1.—HINGED COPPER WELDING JIG FOR MAKING CRACK-SENSITIVITY TEST.

concerned with steel in the lighter gauges and methods of making and processing it to maintain a high level of welding quality. The welding conditions are held constant and are drastic enough at least to produce cracking in steels of lower "weldability."

ACKNOWLEDGMENTS

The appraisal of a proposed investigation is a highly critical procedure. At that stage we were fortunate in securing the advice of Mr. Earle Smith, Chief Metallurgist of the Republic Steel Corporation, and we gratefully acknowledge his timely and sage counsel.

To the War Production Board and the War Metallurgy Committee, we are grateful for the opportunity to work on this fascinating problem of welding metallurgy and appreciate their permission and that of Battelle Memorial Institute to publish an account of the results.

Various members of the Battelle staff have assisted in this work, and we are particularly indebted to C. B. Voldrich, Chief Welding Engineer, and G. A. Moore, Research Engineer.

CRACK-SENSITIVITY TEST

In order to establish the effect of the various metallurgical factors upon weld-crack sensitivity, it was first necessary to develop a usable crack-sensitivity test.³

The test finally devised is based upon the actual extent of cracking developed in welded specimens that are made under severe but closely controlled conditions. This procedure makes it possible to evaluate the crack sensitivity to a much finer degree than is possible by tests based on hardness and, in fact, corrects certain false generalizations based on hardness. The test is made by manually depositing a circular weld bead of approximately $1\frac{1}{4}$ in. outside diameter on a 2 by 2 by $\frac{1}{8}$ -in. steel specimen held in an appropriate jig as shown in Fig. 1. Both jig and specimen are preheated to 100°F. The bead is manually deposited in approximately 20 sec., allowing ± 0.5 second deviation. A $\frac{5}{16}$ -in. Wilson No. 520 electrode (type A.W.S., class E6013) is used with negative polarity at 50 to 55 amp. and 24 to 26 arc volts. The specimen is quenched in ice water immediately after welding and held at

60°F. for 24 hr., to permit cracking to develop. It is then drawn at 1050°F. for one hour to prepare it for the next step. The weld bead is then removed by grinding

crack sensitivity. Steels having an index of 100 or above are classified as insensitive, while those in the range of 90 to 100 are regarded as borderline cases and those

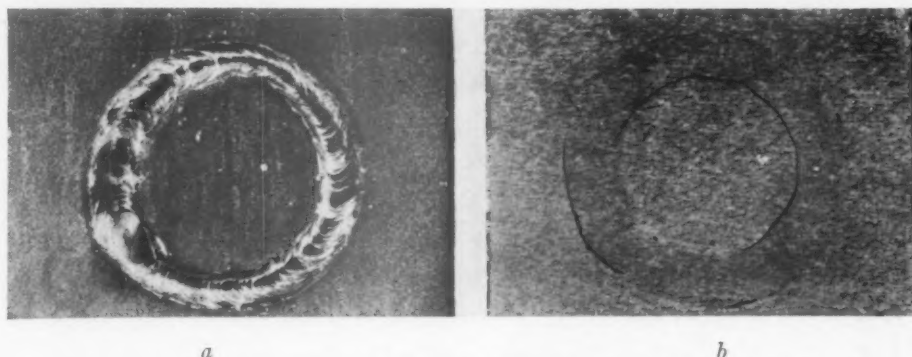


FIG. 2.—TYPICAL CIRCULAR BEAD-CRACK SENSITIVITY, WELD TEST SPECIMEN.

a. Circular bead weld test.

b. Bead side surface ground and Magnafluxed.

flush. After grinding, the specimens are Magnafluxed, and the total length of the cracks on the bead side is measured in degrees and related to the maximum crack length possible, or 720°. The test is illustrated in Fig. 2. The test is also adaptable to $\frac{3}{16}$ and $\frac{1}{4}$ -in. plate.

Extensive use of this test has revealed that at least six specimens are required for each steel tested. A control steel of known cracking tendency is also run with each group being tested, making it possible to assign to the unknown steel an index of crack sensitivity in terms of the control. This approach was found necessary because conditions could not be sufficiently duplicated from time to time to give a constant degree of cracking in a given steel. This seems now to be important in this field of testing, but since the difference in the degree of cracking between two steels was found to remain constant, even though the general level was shifted, the use of a control steel provided a means of overcoming the inherent variables associated with welding. The control used in this work was arbitrarily assigned an index value of 100, larger values indicating a less sensitive steel and lower values a greater degree of

below 90 as crack sensitive. A mathematical appraisal, based on an extensive number of tests, revealed the accuracy of the index as practically always within the limits of ± 3 and usually ± 2 .

COMPARISON OF SENSITIVE AND INSENSITIVE COMMERCIAL S.A.E. 4130 STEEL

Fortunately, there were available two lots of S.A.E. 4130 steel that were practically identical in chemical analysis but differed widely in weld-crack sensitivity, steel 581 being extremely crack sensitive as compared with steel 557. These steels were in the form of $\frac{1}{8}$ -in. plates processed to meet the "N condition" as required by the Army-Navy Specification AN-QQ-S-685.

In order to determine what metallurgical factors might account for this difference in crack sensitivity, the chemical analysis, tensile properties, hardenability, and grain-growth characteristics were investigated.

The check analyses of the two steels are practically identical (Table 1) except for the higher aluminum content found in steel 557. Although hardenability characteristics usually are assumed to be

TABLE 1.—*Check Analysis of Commercial S.A.E. 4130 Steels*
PER CENT

Steel No. ^a	C	Mn	P	S	Si	Cr	Mo	Ni	Al ^b
557	0.33	0.54	0.020	0.026	0.17	0.95	0.19	0.25	0.027
581	0.34	0.47	0.019	0.021	0.25	0.95	0.19	0.24	0.017

^a Steel 557 is insensitive and steel 581 sensitive.^b Aluminum values are the acid-soluble contents.

associated with cracking tendencies, end-quench tests revealed little difference between these steels (Fig. 3). The tensile

compared with 18.9 per cent for steel 557, the relative ratings being 83 and 100, respectively. These results are in good

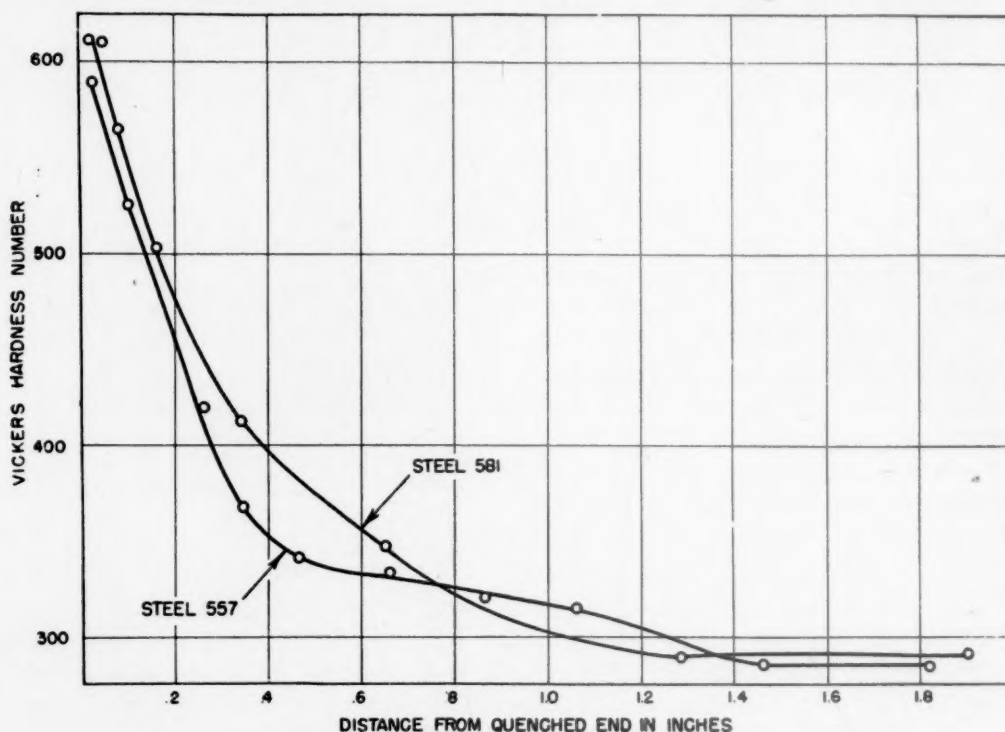


FIG. 3.—END-QUENCH HARDENABILITY CURVES FOR STEELS 557 AND 581.

A split-type hardenability specimen of standard Jominy dimensions was used, the $\frac{1}{8}$ -in. plate making up the middle section. After quenching, the middle section was removed and hardness determinations made along the longitudinal center line. Specimens heated 1 hr. at 1580°F.

properties of steel 581 are the higher (Table 2), especially the yield strength. A study of the grain-coarsening characteristics showed that steel 581 was more susceptible than 557 to grain growth at elevated temperatures. This would be expected from the difference in aluminum contents of these steels.

The results of crack-sensitivity tests are shown in Table 3. These data show that steel 581 cracked 54.6 per cent as

TABLE 2.—*Tensile Properties of the Commercial S.A.E. 4130 Steels*

Steel No.	Yield Strength, ^a Lb. per Sq. In.	Tensile Strength, Lb. per Sq. In.	Per Cent Elongation, 2 In.
557 (insensitive).....	65,800	94,100	21.0
557 (insensitive).....	64,800	93,700	22.0
581 (sensitive).....	79,300	99,450	18.5
581 (sensitive).....	79,700	101,060	18.0

^a Yield strength determined from stress-strain curve using load at 0.2 per cent offset.

agreement with previous observations in welding these two steels. However, the reason for this marked difference in crack sensitivity is not obvious, in view of the

data, are shown in Table 4; the cooling curves for both cycles, in Fig. 5.

From Fig. 5 it will be observed that when a slow heating and cooling cycle is

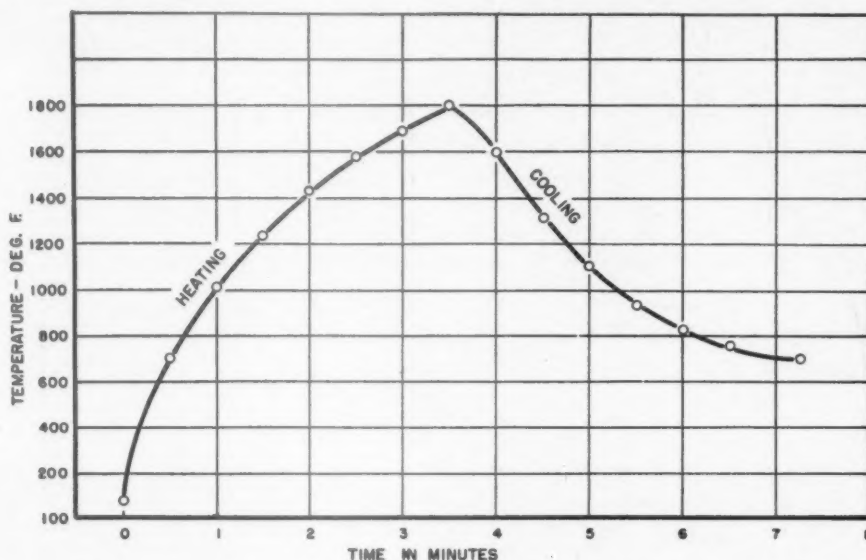


FIG. 4.—TYPICAL TIME-TEMPERATURE HEATING AND COOLING CYCLE FOR RAPID DILATOMETER TEST

similarity in chemical analysis and hardenability; and there is no reason to believe that the differences in physical properties or aluminum contents should directly affect the sensitivity to any appreciable extent.

TEMPERATURE-DILATION CHARACTERISTICS USING RAPID THERMAL CYCLE

Since metallic arc welding develops extremely rapid heating rates in the metal adjacent to the bead immediately followed by accelerated cooling, it appeared desirable to investigate the relative response of the sensitive and insensitive steel to rapid thermal cycles. This phase of the work was carried out by means of temperature-dilation studies using a rapid heating and cooling cycle. A typical time-temperature cycle is shown in Fig. 4. Slow heating and cooling rates were also used for comparison purposes.

The transformation temperatures observed when using the two heating and cooling cycles, together with other perti-

used, the crack-sensitive steel 581 has the higher Ar_3 temperature. When the rapid cycle is employed, this situation is reversed,

TABLE 3.—Results of Crack-sensitivity Test on Steels 557 and 581*

Steel No.	Specimen No.	Total Length of Cracks, Deg.	Average Total Length of Cracks, Per Cent	Crack-sensitivity Index
557	1	120	18.9	100
557	2	120		
557	3	70		
557	4	270		
557	5	120		
557	6	120		
581	1	470	54.6	83
581	2	360		
581	3	360		
581	4	380		
581	5	495		
581	6	295		

* In this work, Steel 557 was used as the control and was assigned the index value of 100.

the sensitive steel 581 having the lower apparent Ar_3 temperature. The reason for this is suggested by the microstructures of these two steels as shown in Fig. 6. The fine carbides in the sensitive steel go into

solution more rapidly, yielding a more highly alloyed austenite with a lower transformation temperature.

similar manner. During the short interval that the metal in the heat-affected zone is at an elevated temperature, the fine

TABLE 4.—Results of Dilatometer Test Data

Steel No.	Thermal Cycle	Average Heating Rate between 80° and 1800°F., Deg. per Min.	Time at Maximum Temperature, Min.	Average Cooling Rate between 1800° and 700°F., Deg. per Min.	Transformation Temperature, Deg. F.			
					Ac ₁	Ac ₃	Ar ₃	Ar ₁
557	Slow	41	18	18.3	1360	1460	1310	1210
581	Slow	42	19	18.3	1370	1470	1345	1240
557	Rapid	450-500	0	275-300	1400	1490	1020	940-830
581	Rapid	450-500	0	275-300	1390	1470	980	900-800

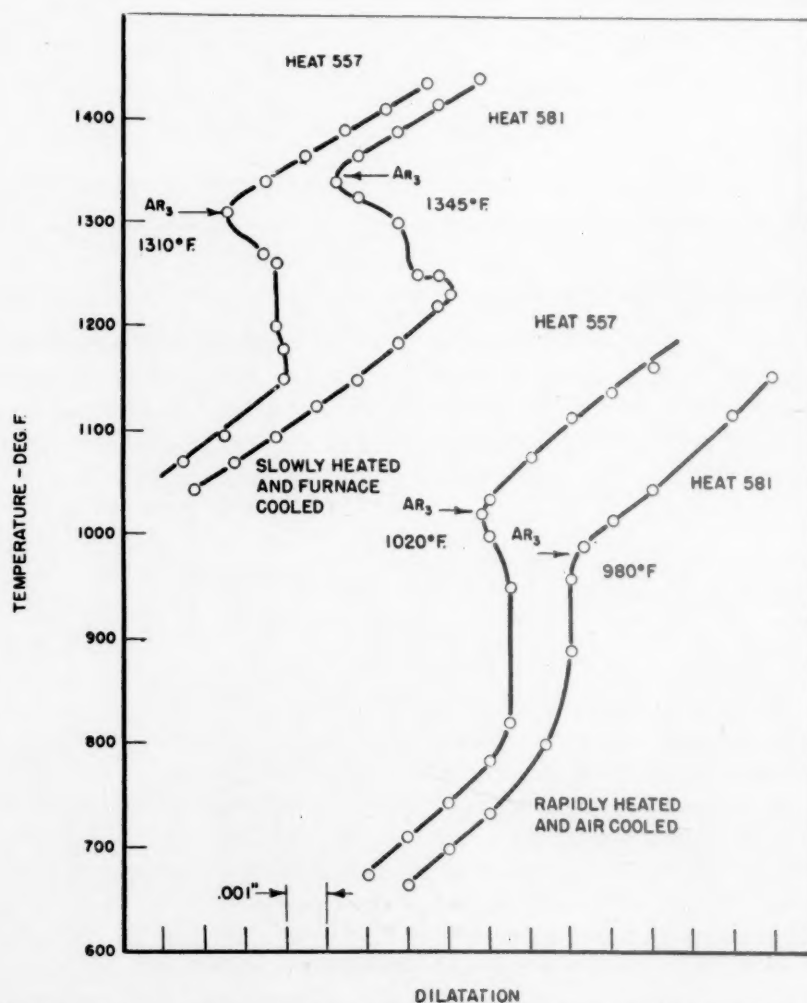


FIG. 5.—DILATOMETER COOLING CURVES, FOR BOTH SLOW AND RAPID THERMAL CYCLES, OF STEELS 557 AND 581.

The difference in crack sensitivity of these two steels may be explained in a carbides in the sensitive steel go into solution more completely. Upon cooling,

this high-carbon austenite establishes conditions favoring the mechanism by which cracks are formed. Coarser and less rapidly soluble carbides produce austenite of lower carbon and alloy content. The longer holding times of ordinary heat-treatment eliminate this difference in behavior, as is shown by the hardenability tests.

EFFECT OF STRUCTURE AND THERMAL HISTORY UPON CRACK SENSITIVITY

Since the data up to this point indicate that the structure may be an influential factor in crack sensitivity, the subject was further investigated by determining the crack sensitivity of various structures developed in steels 557 and 581. The following heat-treatments were used for this purpose:

1. Annealing to coarsen the carbide particle size.
2. Annealing followed by normalizing at 1900°F. for one hour.
3. Homogenizing for 100 hr. at 1900°F. followed by normalizing from 1900°F.

TABLE 5.—*Effect of Thermal Treatment upon Crack Sensitivity*

Steel No.	Thermal Treatment	Crack-sensitivity Index
557	As received. "Condition N"	100
581	As received. "Condition N"	83
557	Annealed	115
581	Annealed	117
557	Annealed and normalized	114
581	Annealed and normalized	125
557	Homogenized and normalized	82
581	Homogenized and normalized	89

These thermal treatments had a marked influence upon the sensitivity of the two steels (Table 5). Annealing greatly reduced the crack sensitivity of each steel; both steels having practically the same index number. Even more significant, normalizing at 1900°F. for one hour did not begin to obliterate the influence of the prior annealing treatment. This indicates that the effect of the final thermal treatment

may be practically nullified by the influence of the prior thermal history. The homogenizing treatment, followed by normalizing, developed the maximum crack sensitivity, the structure in both steels being very fine and both having essentially the same cracking index.

In these two steels, the difference in the carbide size in the as-received condition is fairly obvious from the microstructure. In some steels tested during the investigation, however, differences in carbide size could not be detected visually, after treatments designed to promote differences and when the rapid dilatometer and crack-sensitivity tests indicated that such differences did exist.

EFFECT OF ALUMINUM AND TITANIUM UPON CRACK SENSITIVITY OF S.A.E. 4130 STEEL

Since the examination of the two commercial steels revealed that coarse carbide steels were insensitive because the carbides are less readily soluble, and that aluminum content might be a factor in weld-crack sensitivity, these two factors were further investigated by means of induction-furnace heats.

A 300-lb. induction-furnace heat of S.A.E. 4130 was split into three parts, the first ingot being poured without an aluminum addition. The remainder of the steel in the furnace was deoxidized by an addition of 1½ lb. of aluminum per ton, after which the second ingot was poured. Sufficient ferrotitanium was then added to the furnace to yield a titanium content of 0.25 per cent in the third ingot. The purpose of this large addition of titanium was to form titanium carbides, which are extremely stable at high temperatures and therefore should decrease the crack sensitivity provided that carbide solubility is a factor. The chemical analyses of these three steels, which are identified as heats 9626-1, 2, and 3, are shown in Table 6.

All tests discussed in the following text were conducted on stock processed as follows:

1. Ingots forged and hot-rolled to $\frac{1}{4}$ -in. strips.
2. Annealed at 1300°F. for 12 hours.

In the third steel, the addition of titanium decreased the ultimate and the yield strength, the effect being much more pronounced on the latter. Accompanying the decrease in tensile strength, there was the usual increase in elongation.

TABLE 6.—*Chemical Analyses of Experimental Steels S.A.E. 4130*
PER CENT

Heat No.	C	Mn	P	S	Si	Ni	Cr	Mo	Ti	Al ^a
9626-1	0.36	0.52	0.011	0.029	0.40	0.03	1.00	0.18		0.00
9626-2	0.36	0.53	0.012	0.029	0.40		0.99	0.19		0.06
9626-3	0.37	0.55	0.010	0.029	0.44		1.00	0.18	0.25	0.09

^a Aluminum values are the acid-soluble contents. Ferrotitanium accounted for 0.03 per cent Al.

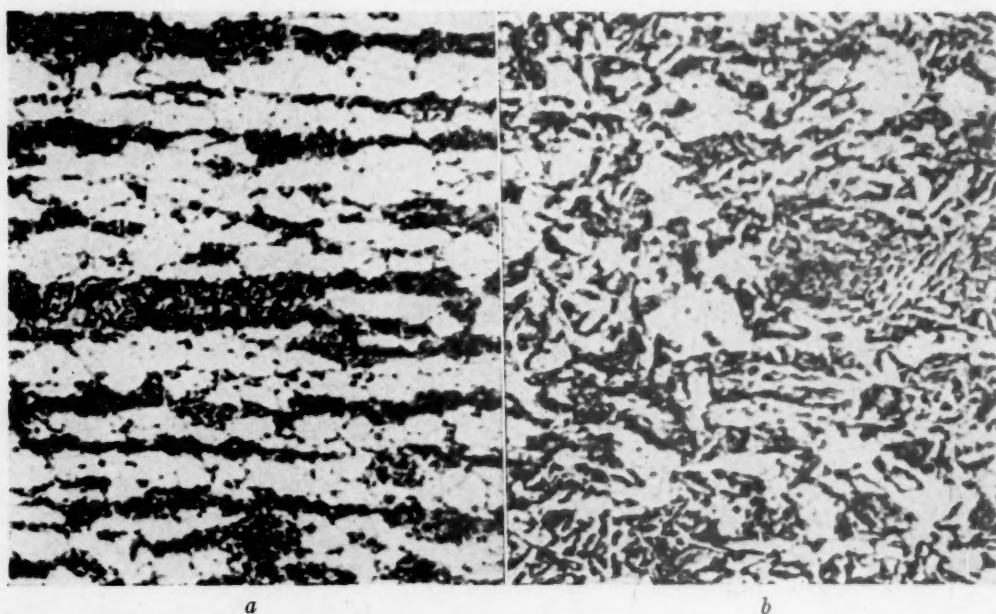


FIG. 6.—TWO COMMERCIAL S.A.E. 4130 STEELS THAT DIFFERED WIDELY IN CRACK SENSITIVITY.
× 1000. NITAL ETCH.

- a. Steel 557, insensitive.
- b. Steel 581, crack-sensitive.

3. Cold-rolled to 0.125-in. gauge.
4. Annealed at 1300°F. for 12 hours.
5. Normalized in a salt bath at 1640°F for one hour.
6. Drawn for one hour at 900°F.

Mechanical Properties

Table 7 indicates that the properties of the aluminum-free and the aluminum-treated steels are essentially identical.

TABLE 7.—*Tensile Properties of Heat 9626*

Heat No.	Deoxidation	Yield Strength, Lb. per Sq. In.	Tensile Strength, Lb. per Sq. In.	Elongation, Per Cent in 2 In.
9626-1	No aluminum	98,330	128,000	13.5
9626-1	No aluminum	98,330	128,760	12.5
9626-2	Aluminum	97,860	129,930	13.5
9626-2	Aluminum	97,040	128,620	13.5
9626-3	Al and Ti	84,930	124,130	17.5
9626-3	Al and Ti			



FIG. 7.—ANNEALED STRUCTURES. $\times 1000$. NITAL ETCH.

- a. Steel 9626-1, no aluminum.
- b. Steel 9626-2, $1\frac{1}{2}$ lb. Al per ton.
- c. Steel 9626-3, treated with Al and Ti.

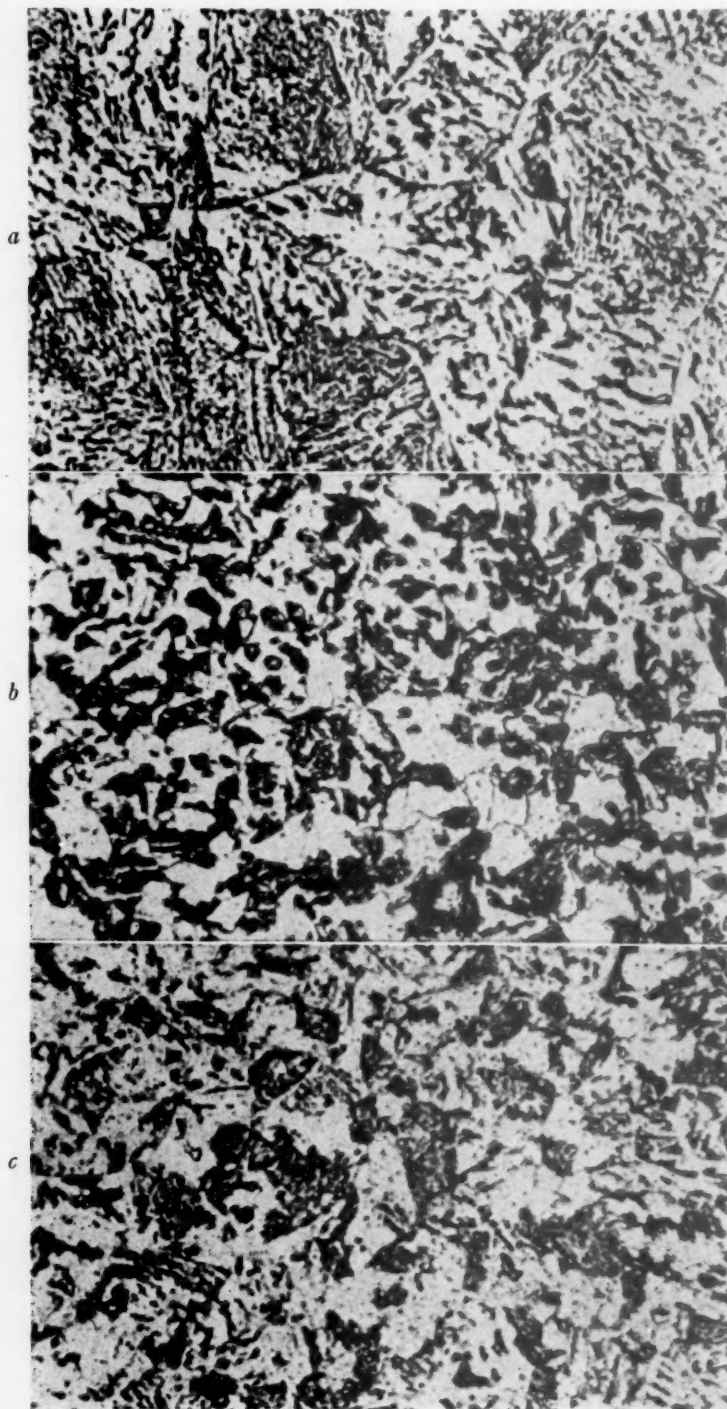


FIG. 8.—NORMALIZED STRUCTURES. $\times 1000$. NITAL ETCH.

a. Steel 9626-1, no aluminum.

b. Steel 9626-2, $1\frac{1}{2}$ lb. Al per ton

c. Steel 9626-3, treated with Al and Ti.

Microstructure

The structures prior to normalizing are shown in Fig. 7. At this stage of processing,

aluminum promotes carbide coalescence and that the addition of titanium apparently promotes nucleation of the carbide and produces a finer dispersion.

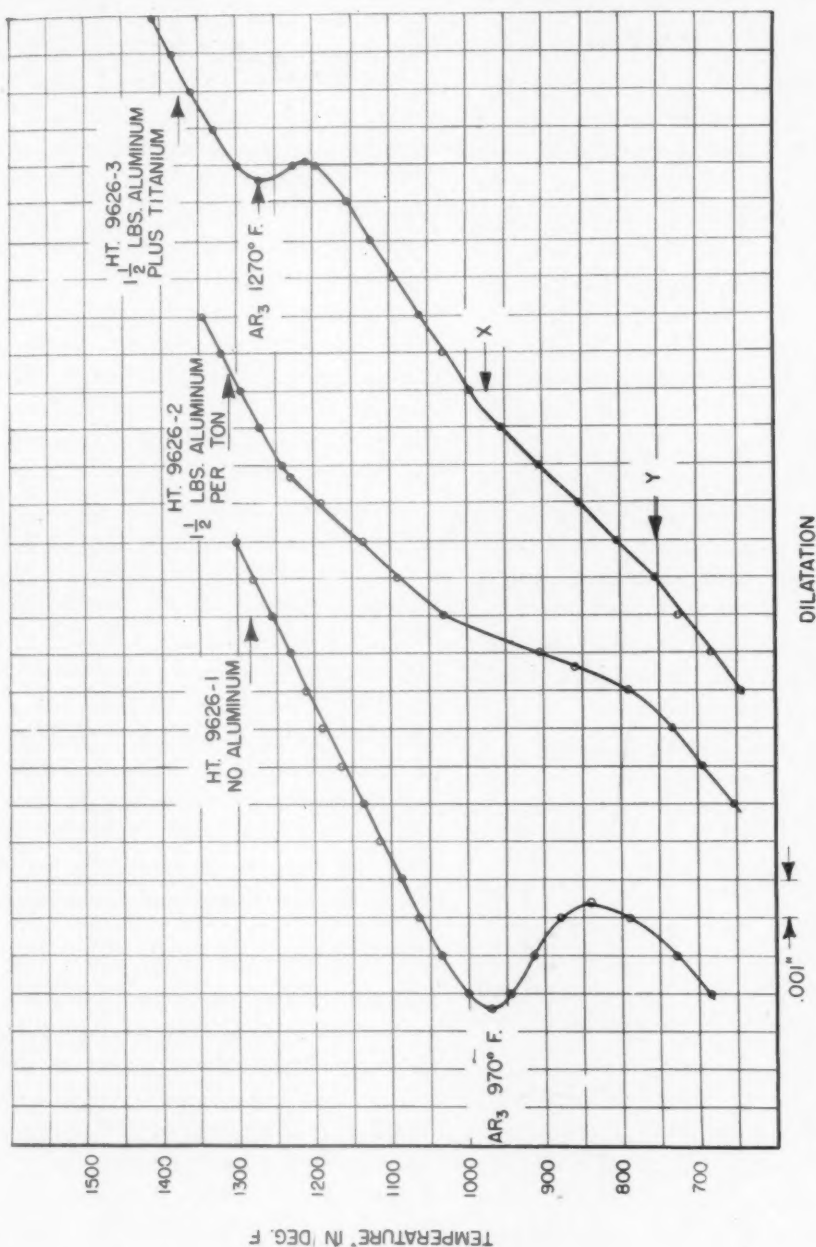


FIG. 9.—DILATOMETER COOLING CURVES SHOWING EFFECT OF ALUMINUM AND TITANIUM ADDITIONS.

the steels are in a spheroidized condition. The carbides in the aluminum-killed steel are appreciably larger than those in the aluminum-free steel, the smallest carbides being found in the aluminum-titanium steel. These results demonstrate that

The normalized and drawn structures, the condition in which the steels were tested, are shown in Fig. 8. The aluminum-free steel has an extremely large grain size with a more uniform distribution of carbide and smaller ferritic areas as compared

with the other two steels. There is some difference in the aluminum and aluminum-titanium steels, the latter having coarser carbide particles in the pearlite.

Rapid Dilatometer Tests

The dilatometer characteristics of the three steels were determined using the rapid heating and cooling cycle previously discussed. The data pertaining to these tests are shown in Table 8 and the cooling curves in Fig. 9. It is obvious from the cooling curves that temperature-dilatation characteristics of these steels vary widely.

The steel made without aluminum, No. 9626-1, has a much lower apparent A_{r3} temperature than the steel treated with aluminum and aluminum titanium. These results indicate that a higher alloyed austenite was developed during the rapid heating of the aluminum-free steel than in the two treated steels. Since the chemical analyses of these steels are almost identical, the low A_{r3} temperature of the aluminum-free steel signifies that the carbides of this steel are more readily soluble.

TABLE 8.—Dilatometer Data from Heat 9626

Heat No.	Average Heating Rate between 80° and 1800°F., Deg. per Min.	Average Cooling Rate between 1800° and 700°F., Deg. per Min.	Transformation Temperatures, Deg. F.			
			Ac_1	Ac_2	A_{r3}	A_{r1}
9626-1	570	300	1360	1440	970	840
9626-2	546	306	1370	1490	^a	^a
9626-3	573	347	1370	1490	^b	^b

^a Cooling curve not sufficiently sharp to locate A_{r3} and A_{r1} points; see Fig. 9.

^b Split transformation; see Fig. 9.

The cooling curve of the aluminum-killed steel shows that transformation starts at a relatively high temperature, 1240°F., which is approximately 140°F. higher than the similar point in the aluminum-free steel. Obviously, this reveals that the carbides in the aluminum-killed steel are less soluble than in the aluminum-free material. The cooling curve of the

aluminum-treated steel (Fig. 9) is relatively straight as compared with the S-shaped curve produced by the first steel.

The titanium-treated steel showed a typical split transformation during cooling, the first and principal transformation occurring between 1300° and 1200°F. The second transformation, which was of small magnitude, took place between 975° to 750°F. This curve indicates that most of the austenite formed during the short heating cycle was of relatively low carbon or alloy content, as revealed by the high temperature at which the first transformation occurred, small areas of a higher carbon concentration producing the lower transformation. These results indicate that the carbides in the titanium-treated steel are the least soluble.

Considering the first two steels, 9626-1 and 2, it is obvious from the dilatometer data that the normalizing treatment, although carried out at 1640°F. for one hour, did not obliterate the effect of the carbide size that was established during annealing. While the carbide size in the annealed titanium steel was smaller than in either of the other steels, the difference in size was more than compensated for by the occurrence of titanium carbide, which is more stable than iron and chromium carbides at elevated temperatures.

Crack-sensitivity Tests

The results of crack-sensitivity tests on steels 9626-1, 2, and 3 are summarized in Table 9. These data reveal a marked difference in the sensitivity of the aluminum-free steel as compared with the other two, the former having a sensitivity index of 94 as compared with 115 and 118 for the aluminum and the aluminum titanium-treated steels.

End-quench Hardenability

Rounds for Jominy end-quench hardenability tests were forged from each of the three ingots, followed by normalizing at

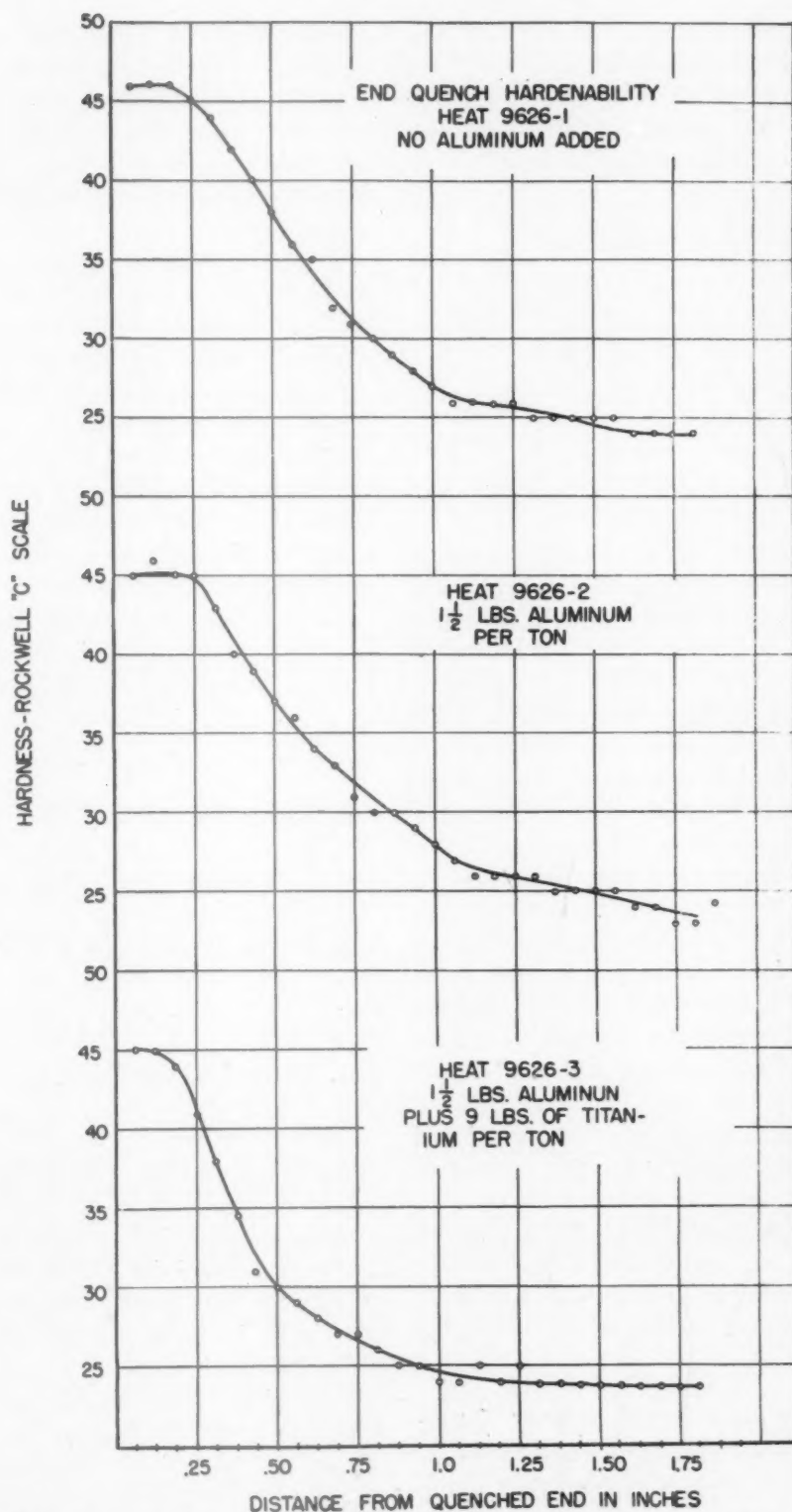


FIG. 10.—JOMINY END-QUENCH HARDENABILITY CURVES FOR STEELS 9226-1, 9226-2, AND 9226-3.

1650°F. for one hour. The standard test specimens were then heated to 1650°F. for one hour and quenched in the conventional manner. The results of these tests are illustrated graphically in Fig. 10.

TABLE 9.—*Summary of Crack-sensitivity Data from Heat 9626*

Heat No.	Deoxidation	Average Total Length of Cracks, Per Cent	Crack Sensitivity Index
9626-1	No aluminum	57.2	94
9626-2	Aluminum	14.8	115
9626-3	Al and Ti	11.0	118
557 ^a		43.9	100

^a Steel 557 used as control.

The hardenability curves for the aluminum-free and the aluminum-treated steels are practically identical, the titanium addition decreasing the hardenability, (when the usual quenching temperature is used) to an appreciable extent. These data again illustrate that hardenability, as determined by the Jominy end-quench procedure, is not necessarily a measure of the crack sensitivity. It has been suggested that if end-quenched test bars could be heated to the quenching temperature in a period of 2 or 3 min. a direct correlation might be found between the crack sensitivity and the hardenability, provided the microstructures of the two specimens were similar and had been arrived at by similar processing. However, this may not be strictly true because, as will be mentioned later, hardening and cracking appear to relate to somewhat different phenomena. For determining the effect of structures on cracking, the rapid dilatometer test is simple and accurate and has been valuable as an indirect check of the cracking tendency.

EFFECT OF ALUMINUM ADDITIONS, RANGING FROM 1 TO 4 POUNDS PER TON, UPON CRACK SENSITIVITY

Since it was demonstrated that the crack sensitivity of S.A.E. 4130 can be

decreased to an appreciable extent by deoxidation with 1½ lb. of aluminum per ton, it appeared advisable to investigate the effect of aluminum in greater detail and over a much wider range than would normally be used in this or similar grades of steel.

A 300-lb. induction-furnace heat, No. 10093, was made and poured into a number of ingots, which were deoxidized with aluminum additions ranging from 1 to 4 lb. per ton. All aluminum additions were made to the metal while in the furnace. The chemical analyses, including the acid-soluble aluminum content of these four steels, are shown in Table 10. With the exception of aluminum content, these four steels may be considered identical.

After forging and hot-rolling to 0.250 in., the stock from each ingot was divided into two lots and processed as follows:

Lot No. 1

1. Hot-rolled to 0.170 inch.
2. Annealed for 8 hr. at 1250°F.
3. Cold-reduced to 0.125 inch.
4. Normalized at 1650°F. for ½ hour.
5. Drawn at 900°F. for 1 hour.

Lot No. 2

1. Normalized at 1650°F. for 1 hour.
2. Drawn at 900°F. for 1 hour.

Properties Developed in Lot No. 1

From the chemical analyses and tensile properties, listed in Tables 10 and 11, it appears that steels 10093-1 to 4 are practically identical with the exception of the aluminum content.

The effect of aluminum content upon the crack sensitivity is shown in Table 12. There is a marked decrease in sensitivity as the aluminum content (acid-soluble) is increased from 0.02 to 0.09 per cent. Above the latter value, the effectiveness

decreases to the point where there is little to be gained from additional aluminum.

These data clearly illustrate the marked decrease in sensitivity that may be ob-

somewhat out of line with the results obtained from the first three ingots, and this value is questioned. There was not sufficient stock to repeat the test.

TABLE 10.—*Chemical Analyses of Heat 10093*
PER CENT

Heat No.	C	Mn	P	S	Si	Cr	Mo	Ni	Al ^a
10093-1	0.35	0.56	0.010	0.027	0.24	0.87	0.26	0.03	0.02
10093-2	0.34	0.56	0.011	0.027	0.25	0.89	0.27		0.05
10093-3	0.34	0.56	0.011	0.026	0.25	0.89	0.25		0.09
10093-4	0.34	0.57	0.011	0.026	0.25	0.89	0.22		0.12

^a The aluminum values are the acid-soluble contents.

tained, with no sacrifice in tensile properties, by increasing the aluminum content from the conventional value of 0.02 or 0.03

TABLE 11.—*Tensile Properties of Heat 10093, Lot No. 1*

Heat No.	Yield Strength, Lb. per Sq. In.	Tensile Strength, Lb. per Sq. In.	Elongation, Per Cent in 2 In.
10093-1	92,190	119,380	15.0
10093-1	92,940	120,550	15.5
10093-2	94,300	120,180	15.0
10093-2	90,920	118,620	13.0 ^a
10093-3	91,670	119,430	15.0
10093-3	93,590	120,620	15.0
10093-4	92,560	120,000	15.0
10093-4	91,860	119,510	15.5

^a Specimen broke short.

per cent to 0.09 per cent when using this type of processing practice.

Properties Developed in Lot No. 2

The steels in lot No. 2 were processed, as previously outlined, by hot-rolling to 1/4-in. gauge, followed by normalizing at 1650°F. and a 900°F. draw.

The tensile properties and crack-sensitivity values of these steels are shown in Tables 13 and 14. The tensile properties of all four steels are in very good agreement. From the crack-sensitivity data, it is obvious that the sensitivity of these steels was not affected by aluminum content as steels 10093-1 to 3, inclusive, have essentially the same index values.

The sensitivity of steel 10093-4 is

TABLE 12.—*Summary of Crack-sensitivity Data Heat 10093, Lot No. 1^a*

Heat No.	Aluminum Addition, Lb. per Ton	Average Total Length of Cracks, Per Cent	Crack-sensitivity Index
10093-1	1	73.9	84
10093-2	2	62.8	89
10093-3	3	54.0	93
10093-4	4	52.4	94

^a These steels were hot-rolled, annealed, cold-rolled, normalized, and drawn.

TABLE 13.—*Tensile Properties of Heat 10093, Lot No. 2^a*

Heat No.	Yield Strength, Lb. per Sq. In.	Tensile Strength, Lb. per Sq. In.	Elongation, Per Cent in 2 In.
10093-1	90,410	119,680	17.0
10093-1	91,510	120,480	16.5
10093-2	92,540	119,000	16.5
10093-2	93,040	120,000	17.5
10093-3	90,730	119,040	15.5
10093-3	92,220	119,840	16.0
10093-4	91,340	119,600	16.5
10093-4	92,220	120,040	15.5

TABLE 14.—*Summary of Crack-sensitivity Data Heat 10093, Lot No. 2^a*

Heat No.	Aluminum Addition, Lb. per Ton	Average Total Length of Cracks, Per Cent	Crack-sensitivity Index
10093-1	1	55.5	78
10093-2	2	57.9	77
10093-3	3	55.3	78
10093-4 ^b	4	39.2	85

^a These steels were hot-rolled, normalized, and drawn.

^b See text regarding crack-sensitivity values for steel 10093-4.

These data indicate that in these hot-rolled and normalized steels (i.e., which had not been given a spheroidizing anneal), the crack sensitivity was not influenced by

work in this investigation had demonstrated that the sensitivity is reduced by increasing the carbide size prior to normalizing. Therefore, the explanation con-

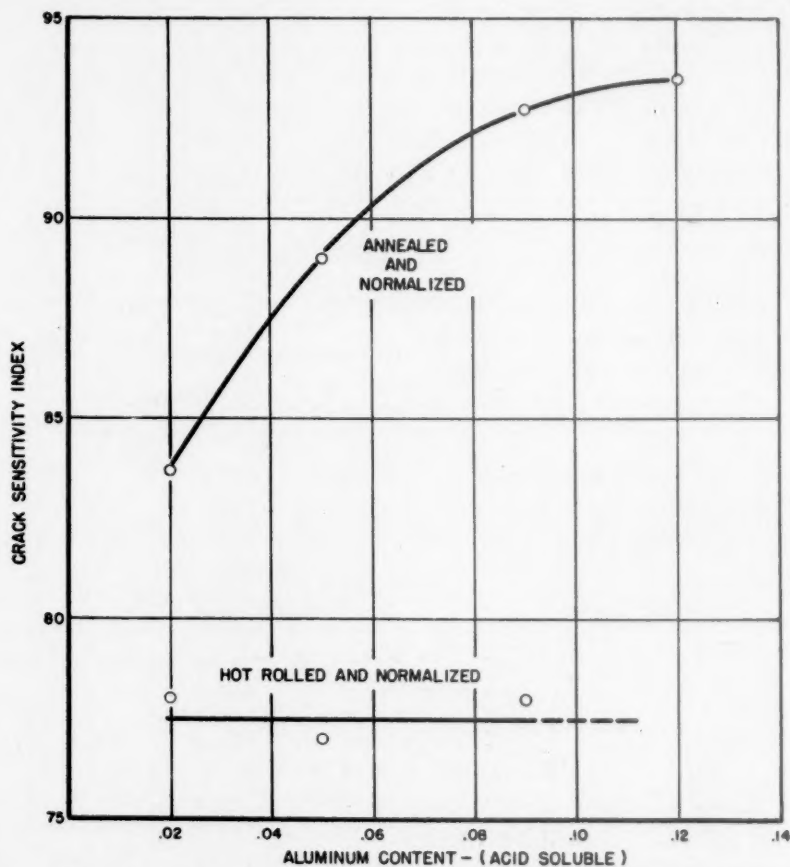


FIG. 11.—EFFECT OF PROCESSING AND ALUMINUM CONTENT UPON CRACK SENSITIVITY.

This graph shows that the crack sensitivity decreases with increased aluminum content only when the steel is annealed prior to normalizing.

aluminum content and was rather pronounced in all.

Comparison of Lots Nos. 1 and 2

The principal difference in the processing of these two lots was that lot No. 1 received cold-rolling and annealing treatment and lot No. 2 did not. Both steels were normalized and drawn as the final treatment. This indicates that the effect of aluminum is indirect and that it decreases the sensitivity by accelerating the rate of carbide coalescence during annealing. Previous

cerning aluminum appears satisfactory, since it accounts for the beneficial results obtained by the processing prior to normalizing. It is also in agreement with the fact that no improvement was obtained from increased aluminum content in the hot-rolled and normalized steels. In the latter, there was no opportunity for carbide growth, so the aluminum had no effect upon crack sensitivity.

Fig. 11 shows a comparison of the sensitivity of lot No. 1 with that of lot No. 2. This figure reveals the advantage of a combination of high-aluminum contents

aluminum deoxidation and the spheroidization of the carbides. With 2 lb. of aluminum per ton, a moderate to medium amount of cold-work and the usual subcritical anneal produce a good structure. The subsequent normalizing is then controlled to give the required properties. Tests of this point show that standard normalizing does not alter the structure sufficiently to vitiate the weldability; in fact, to do that, temperatures in excess of 1900°F. are required.

AN INVESTIGATION OF POSTHEATING

The effect of postheating conditions upon the extent of underbead cracking was investigated by making circular bead-crack tests on the sensitive steel 581. For these tests, the welding jig was modified by the addition of electric heating elements and a control system for maintaining the desired temperature. The jig and specimen were preheated to the test temperature and the circular bead was deposited as usual. The preheating was regarded only as a means of starting the postheat at the desired temperature and, as far as could be determined, does not have any other influence on the welding results.

Postheating conditions, ranging from room temperature to 1000°F. in steps of approximately 100°F., and time intervals of holding the test samples varying from one second to 24 hr. at each temperature, were investigated. The time range was covered in 17 steps, selected to give the maximum accuracy over the range of rapidly changing properties.

A summary of the data is shown in Fig. 12. These data need some explanation. While the tests were run as stated, the temperatures—"average effective temperature"—are those of the heat-affected zone adjacent to the weld bead as determined pyrometrically. This procedure was adopted to give a better understanding of the metallurgical conditions to which the test

samples were subjected. This appears to distort the curves in the high-temperature region—i.e., for the short-time intervals when the welding heat overbalances the direct heat from the jig—but the effect is relatively small in the low-temperature region with longer holding times. For postheating below about 500°F. the curves give an approximate idea of the times required to complete the austenite transformation and prevent cracking. The upper right region, which was only partly explored, shows that relatively long times would be required to prevent cracking if too high postheating temperatures were used. Furthermore, these results apply directly only to the welding conditions actually used, though in principle they are thought to hold for other conditions as well.

This chart consists of contour lines, each line representing a definite level of improvement obtained in the crack-sensitivity index rating by using the indicated postheating temperature and time of holding at temperatures. Thus by postheating at 600°F. for 1 min. the index was raised by 40 points. It will be noted that a marked improvement can be obtained by the proper selection of postheating conditions and that less time is required, in general, at the higher temperatures, up to about 1000°F.

While the cracking data were being collected, hardness surveys were made of the heat-affected zones in the crack-sensitivity specimens used in the postheating study. The maximum hardness developed in the heat-affected zone related to the incidence of cracking is shown in Fig. 13. These data reveal a good correlation between hardness and degree of cracking in the extremely hard and the soft specimens. However, with hardnesses of about 500 to 575 V.H.N. in the heat-affected zones, it was found that the crack sensitivity varied with the postheating history over a wide range. The reason for this apparent inconsistency was found in

the microstructure, the type of martensite shown in Fig. 14 being associated with cracking while the martensitic structure in Fig. 15 was not, or at least not to the

required may be short or long, depending on the temperature and the S-curve data, but the heat-affected zone is soft and weak. Intermediate temperatures are best suited

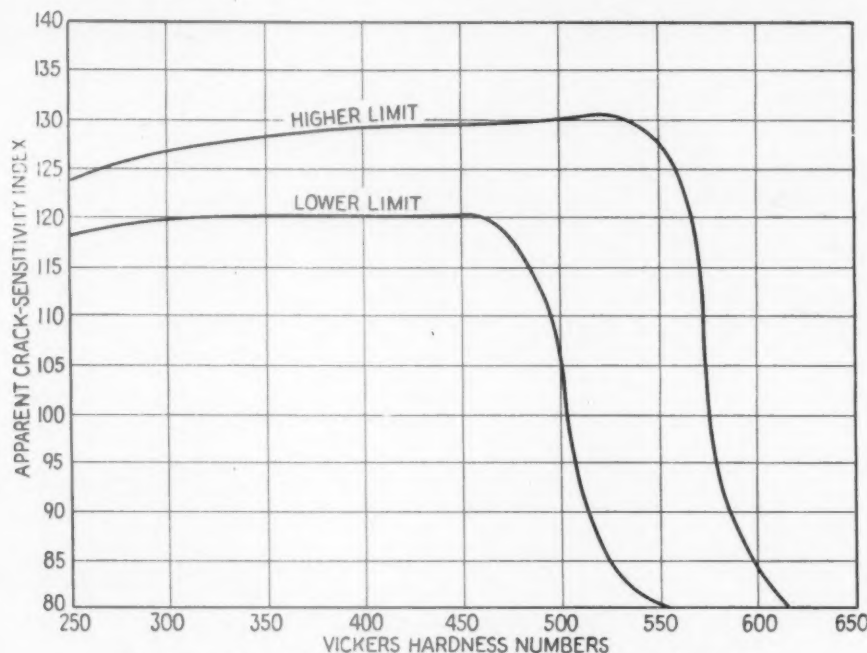


FIG. 13.—RELATIONSHIP OF CRACK SENSITIVITY TO HARDNESS.

same degree, although both structures were in the same hardness range.

The information obtained from this study indicated that the changes in properties of the heat-affected zone resulting from postheating may be predicted from an S-curve, taking into account that such curves are constructed from data obtained under ideal conditions, which permit transformation at constant temperatures. For most practical purposes, it appears that the postheating conditions that yield the most satisfactory results for freedom from cracking and high strength correspond to the conditions in the S-curve that are most favorable to the formation of bainite. To avoid cracking, the sole requirement for the test conditions employed was observed to be the practically complete transformation of the austenite that the welding heat produces alongside the weld. At high postheats the time

to give short times of postheat and maintain high strength in the heat-affected zone. Lower temperatures will eliminate cracking but the time is unduly lengthened and the heat-affected zone may be too hard and brittle.

It is obvious that the control of postheating to eliminate cracking follows S-curve data, but it is also clear that the variable temperature in the heat-affected zone superimposes another effect, which modifies the time-temperature relations.

THE CRACKING PHENOMENON

Inasmuch as the objective of this investigation was that of avoiding cracking when the hardenable steels were arc-welded, an understanding of the cracking phenomenon was highly desirable. As pointed out in the introduction, no authoritative statement on this point was available, but certain ideas were developed



FIG. 14.

FIGS. 14 AND 15.—STRUCTURES IN AREAS OF MAXIMUM HARDNESS FOLLOWING POSTHEATING. $\times 1000$. NITAL ETCH.
Fig. 14. Postheating 3 minutes at 197°F . to 137°F . V.H.N. 519-536. Sensitivity index 86.
Fig. 15. Postheating 3 minutes at 387°F . to 321°F . V.H.N. 514-548. Sensitivity index 113.

that led to the following conception of the broader aspects of underbead cracking. This picture includes the effects of the delayed transformation of retained austenite, hydrogen absorption, and stresses.

The presence of retained austenite was suspected from the finding that cracking occurred at about room temperature and that it progressed thereafter for a period of hours. A check by an X-ray method confirmed its presence, and this was held to be consistent with the results of the dilatometer tests and the effect of structure. The work on postheat treatment supported this idea, since, regardless of the hardness of the heat-affected zone, cracking was eliminated by causing the austenite to transform completely at some higher temperature. On this basis cracks are associated with the white martensite of Fig. 14, not because that structure is hard or brittle or weak but because that structure comes from the low-temperature transformation of austenite.

The effect of hydrogen absorption on underbead cracking has been discussed by Herres,⁴ who shows the vital role played by this gas. He suggests that the pressures produced when this gas precipitates at discontinuities may exceed the strength of the metal. Tests made in the present investigation completely substantiate his findings that hydrogen is necessary, and it was shown, for example, that the crack-sensitive steel 581 was crack-free when welded in the crack-sensitivity test with a nongassing weld rod.

It has been observed that underbead cracking always occurs in the most purely martensitic areas. This material has a strength in the neighborhood of 300,000 lb. per sq. in. and the stress that cracks it must exceed that figure. It is obvious, then, that shrinkage stresses alone are quite inadequate to initiate such cracks when it is realized that the unaffected parent metal has a yield strength under 100,000 lb. per sq. inch.

It has been demonstrated that retained austenite and the delayed decomposition to martensite play a vital part in the cracking. At the same time, decomposition of the retained austenite at room temperature in the absence of hydrogen does not cause cracking, and the fairly rapid decomposition of austenite at temperatures above 500°F. also does not lead to cracks.

Fitting these observations together, the mechanism seems to be as follows: During the welding operation with the usual weld rod, quantities of hydrogen are dissolved in the weld bead. This diffuses rapidly into the parent metal, which is heated above the transformation temperature. Hydrogen is soluble in austenite at all temperatures but is practically insoluble in cold ferrite or martensite. When the heat-affected zone transforms, therefore, hydrogen is rejected from all areas except those that remain austenitic. In these areas of austenite the hydrogen concentrates to relatively high values. When they later transform at room temperature and hydrogen is rejected, with no place to go, enormous aerostatic pressures are set up, which disrupt the adjacent structure even though it be hardest martensite. The cracks thus formed are undoubtedly quite small, and the principal function of thermal stresses probably is to cause the cracks to grow to visible size. This growth has been observed frequently and was demonstrated in the course of the present investigation. If this austenite is transformed at elevated temperatures, the hydrogen can diffuse sufficiently to prevent the maximum stress. This is a common experience with shatter cracks, which are never produced at temperatures above 400°F.

It follows, therefore, that the more hardenable steels are in general more crack sensitive because they tend more to retain austenite. Likewise, with greater solution of the carbides, the likelihood of retaining austenite is greater.

The very nature of the arc-welding process, with its steep temperature gradients, is ideal to set up local stresses of high magnitude, though the magnitude will depend on the degree of restraint imposed. While these stresses in themselves seem inadequate to cause cracking in the martensite, they are additive to the aerostatic stresses of the rejected hydrogen and might logically be the straw that breaks the camel's back. This is in line with the experience that sometimes cracks may form when welding is done under conditions of restraint but not when there is no restraint.

TECHNICAL CONTROL

The work described herein relates to light-gauge material and particularly to processing, which includes cold-rolling and subcritical annealing. Without aluminum deoxidation (2 lb. per ton) this processing is not as effective in coarsening the carbides; hence it is desirable to make steels of the S.A.E. 4130 class to fine grained practice. Fortunately the spheroidizing effect is not eliminated by production normalizing, and that step can be set up to meet the requirements for mechanical properties. Additional experience, not reported here, does suggest, however, that overspheroidization decreases the crack sensitivity more than is needed and increases the difficulty in meeting the strength required, particularly the yield strength.

The present contribution is advanced as a discussion of the fundamental principles involved in this field of metallurgy, or as a guide to the establishment of suitable practice. When the hardening elements are on the low side, the need of this control is less, but as the hardening elements increase, the effect of structure becomes more pronounced and the maintenance of good weldability requires a control of structure.

CONCLUSIONS

While this paper is essentially the conclusions of several years' work, together with a limited amount of supporting data, the results may be briefly summarized as follows:

1. The relative underbead cracking tendencies of hardenable steels, such as S.A.E. 4130, may be determined by a simple weld test made under carefully controlled conditions.

2. The extent of underbead cracking, crack sensitivity, can be correlated with the dilatometric characteristics obtained in a rapid thermal cycle.

3. The structure, as determined by the manufacturing and thermal history of the steel, has a marked effect upon the weld-crack sensitivity, a coarse carbide structure being less crack sensitive.

4. Increased aluminum content decreases the crack sensitivity of steels that have been annealed during processing prior to the final normalizing, the reason being that aluminum increases the rate of carbide coalescence during annealing.

5. The addition of sufficient titanium decreases the crack sensitivity because of the formation of extremely stable carbides.

6. The effect of postheating may be predicted from the S-curve, the most favorable strength to cracking ratio being obtained from the conditions most favorable to the formation of bainite.

7. With the exception of conditions of extremely high and low hardness in the heat-affected zone, no correlation was found between the hardness and the extent of cracking.

8. The origin of underbead cracks is thought to be in very high local aerostatic stresses developed by the sudden release of hydrogen during the low-temperature transformation of small areas of residual austenite where the hydrogen had concentrated during the transformation of the greater portion of the heat-affected zone.

9. Restraint and thermal stresses in a weld are not primary causes of underbead cracks but are responsible for their propagation.

REFERENCES

1. W. Spraragen and G. E. Clausen: *The Welding Jnl.*, Research Supplement (1941) **20** (5).
2. C. B. Voldrich and R. D. Williams: *Ibid.* (1942) **21** (11), 540-S.
3. C. B. Voldrich and R. D. Williams: *Ibid.* (1943) **22** (11), 545-S.
4. S. A. Herres: *Ibid.* (1944) **23**, 43-S; *Trans. Amer. Soc. Metals* (1944) **33**, 535.

ADDENDUM

Since this work was completed and written up, several papers on underbead cracking have come to the authors'

attention. These appear in the *Transactions* of the Institute of Welding (July 1944), and have been published in the *Welding Journal* for December 1944. These papers show the effect of hydrogen in producing parent-metal cracking and also bring out the role played by stresses, particularly when the welding is done under restraint. Retained austenite is mentioned by Rollason, but only a summary of his paper is printed, and it is not clear how much weight is assigned to this constituent or just what role it has in the cracking phenomenon. These papers give a valuable and timely contribution to the welding of hardenable steels.



SYMPOSIA



Symposium on Determination of Hydrogen in Steel

(New York Meeting, February 1944)

CONTENTS

Introduction. By J. B. AUSTIN.....	353
Methods of Analyzing for Hydrogen in Iron and Iron Alloys. By T. D. YENSEN and R. K. McGEARY.....	355
Vacuum-fusion Analysis of Steel for Hydrogen. By G. DERGE, W. PEIFER and B. ALEXANDER.....	361
Discussion	367
Determination of Hydrogen in Iron and Steel by Vacuum Extraction at 800°C. By J. G. THOMPSON.....	369
Determination of Hydrogen in Steel Sampling and Analysis by Vacuum Extraction. By R. M. SCAFE.....	375
A Modified Vacuum Extraction Apparatus. By W. D. BROWN.....	381
Determination of Hydrogen by Vacuum Extraction and Tin Fusion. By JOHN NAUGHTON.....	385
Determining the Hydrogen Content of Molten Steel by Vacuum Extraction. By C. B. POST and D. G. SCHOFFSTALL.....	390
Discussion	395
Determination of Hydrogen in Molten Steel by the Gas-tube Method. By J. G. MRAVEC.....	398
Discussion	403
Preliminary Experiments on the Total Combustion Method for the Analysis of Hydrogen in Steel. By GEORGE A. MOORE.....	404
Discussion	411

THE meeting convened in the West York City, at 2.15 p.m., on February 22, 1944, Mr. J. B. Austin presiding.

Introduction

By J. B. AUSTIN,* MEMBER A.I.M.E.

The program is organized on the basis of short prepared discussions, which are divided into groups according to the nature of the method. Each person preparing one of these leading discussions was sent a statement defining the purpose of the symposium and suggesting certain topics that ought to be covered, as well as a few it was desired to avoid. Since this statement constitutes the ground rules for this meeting I should like to read it for the benefit of all who may wish to join the discussion.

"It is our desire to emphasize the hydrogen content of molten steel—that is, steel in the bath—even though it be determined on a solid sample, consequently it is thought advisable to avoid in the main any

discussion of flakes or of hydrogen absorbed during pickling. Discussion of any method of analysis, for whatever purpose developed, is however, proper to the Symposium."

It was further suggested that insofar as it was feasible each contributor should describe the following details of his method:

1. When, how and where the sample is taken.
2. The preparation and handling of the sample.
3. The time elapsing between sampling and analysis.
4. The method of calibration.
5. Any correlation of results with furnace practice or other operating variable.

The emphasis placed upon sampling is a direct reflection of my own view that

* Research Laboratory, U. S. Steel Corporation, Kearny, New Jersey.

proper sampling is likely to prove more difficult than proper analysis.

To these suggestions I should like to add two more: first, that every effort be made to separate inference from observation; that is, let us try at all times to distinguish what is actually observed from that which is deduction or opinion; second, that we keep in mind that there are in essence two types of analysis for hydrogen, the absolute methods that give an accurate measure of the hydrogen content of the sample and the relative methods, which, though they may not yield an absolute result, are nevertheless reproducible and may be extremely useful in characterizing a sample. This leads me to suggest further that we be careful to distinguish between accuracy and precision, since the relative methods may be precise and highly reproducible, even if somewhat inaccurate.

Anticipating that different sets of units may be used in the course of the discussion, and realizing that many of us are not fluently multilingual in these several systems, I have prepared the small conversion tables that have been distributed, and which I hope will prove useful as interpreters. I should like to call your attention particularly to the factor for converting weight per cent to atom per cent because I believe that in many cases we get a more accurate picture of what we are trying to do if we think in terms of the number of hydrogen atoms present rather than of the weight of hydrogen present. For instance, with 0.001 weight per cent of hydrogen, which may seem a mere trace, we have added about as many foreign atoms to the iron as if we had added 0.012 weight per cent carbon; 0.06 per cent manganese, 0.10 per cent molybdenum, or 0.184 per cent tungsten. Considered in these terms, 0.001 per cent hydrogen is far from being a trace.

The first subject on the program is that of vacuum fusion, under which is to be discussed first the original type of vacuum-fusion procedure in which oxygen, nitrogen

and hydrogen are determined in the same apparatus and on a single sample. In my experience this method does not yield a reliable value for hydrogen and in my opinion this method should not be given too much attention in view of the modified vacuum-fusion procedures designed primarily for the determination of hydrogen. Is there anyone here who disagrees with the statement that it is not desirable to determine hydrogen as a sort of by-product in the determination of oxygen?

J. G. THOMPSON.*—I do not entirely agree with you. I think there is more a question of the nature of the sample and of the character of the hydrogen in that sample. I do not think you are justified in damning the vacuum-fusion method categorically.

J. B. AUSTIN.—I am not damning it categorically because I think some of what I choose to call modified methods may well yield satisfactory results, but my own experience has been that hydrogen determinations that are a sort of afterthought to the analysis of oxygen and nitrogen are generally less reliable than the determinations of nitrogen and oxygen. Would you agree to that?

J. G. THOMPSON.—I think the precision of the vacuum-fusion method for hydrogen is as good as it is for oxygen or nitrogen but the amount of hydrogen that we are trying to determine is very small. In my opinion, if you have a high and stable content of hydrogen, your vacuum-fusion procedure is reliable. Many samples do not have that.

J. B. AUSTIN.—Perhaps we had better go on to the Modified Vacuum-fusion Procedures and give their protagonists a chance to give their stories. Dr. Yensen, would you care to tell us about your modifications of the vacuum-fusion method?

* National Bureau of Standards, Washington, D. C.

Methods of Analyzing for Hydrogen in Iron and Iron Alloys

BY T. D. YENSEN,* MEMBER A.I.M.E. AND R. K. McGEARY*

WHILE we have not been primarily interested in the determination of hydrogen in the alloys that we have been dealing with, we are very glad to cooperate in this symposium on sampling and analysis for hydrogen, as we can never tell when we may find it desirable to perform such analyses.

VACUUM-FUSION METHOD

Our primary interest has been oxygen and carbon, in the analysis of which we think we have become very proficient. Our oxygen-analyzing apparatus is of the vacuum-fusion type (Fig. 1). This employs Dr. Derge's type of graphite crucible and slit sleeve, with graphite powder between, for heat insulation (Fig. 2) supported in a clear quartz bulb connected to the Pyrex glass system by means of a carefully made ground joint. The latter is kept cool by means of an air blast from a circular copper tube surrounding the joint.

The crucible is heated by high-frequency induction and the 24 one-gram samples successively dropped in from the horizontal tube at the top by means of a magnet. The gases (H_2 , CO, N_2) are passed through the CuO catalyst held at $300^\circ C$. (converting CO to CO_2 , H_2 to H_2O) and the CO_2 and H_2O frozen out in the main liquid air trap, while N_2 is evacuated. At the end of the operation, shown by the thermocouple vacuum gauge indicating a pressure of 10^{-4} mm. Hg, the analyzing system is isolated

by means of the mercury cutoffs, and the CO_2 and H_2O are determined by transferring first the CO_2 and then the H_2O to the small trap at the right. This is done by placing liquid air on the small trap, then removing the liquid air from the large trap for one minute, which is sufficient to evaporate the CO_2 and transfer it to the small trap. The CO_2 is then measured by closing the mercury cutoff at the extreme right, removing the liquid air from the small trap, warming it up to room temperature, adjusting the mercury level to one of the three marks on the glass tube (corresponding to three volumes calibrated so that 1 mm. Hg of CO_2 corresponds to 0.001, 0.002 and 0.010 mg., respectively, of oxygen) and finally reading the pressure.

Liquid air is now replaced on the large trap, the mercury cutoff at the right opened, transferring the CO_2 back to the large trap. The cutoff to the pumps is then opened, the liquid air removed for one minute, thus evacuating the CO_2 , the pumps again cut off and the H_2O transferred to the small trap as before, except that it is now necessary to warm the large trap with a Bunsen burner in order to evaporate all the H_2O . This requires about three minutes, as the inner tube must be heated to at least $100^\circ C$.

In order to prevent H_2O from being adsorbed on the glass walls, the glass tubing beyond the catalyst (i.e., to the right in Figs. 1 and 3) is kept heated to about $150^\circ C$. by means of Nichrome ribbon as shown in Fig. 3.

For a 1-gram sample the above amounts of oxygen (0.001, 0.002 and 0.010 mg.)

Manuscript received at the office of the Institute April 17, 1944.

* Research Laboratories, Westinghouse Electric and Manufacturing Co., East Pittsburgh, Pennsylvania.

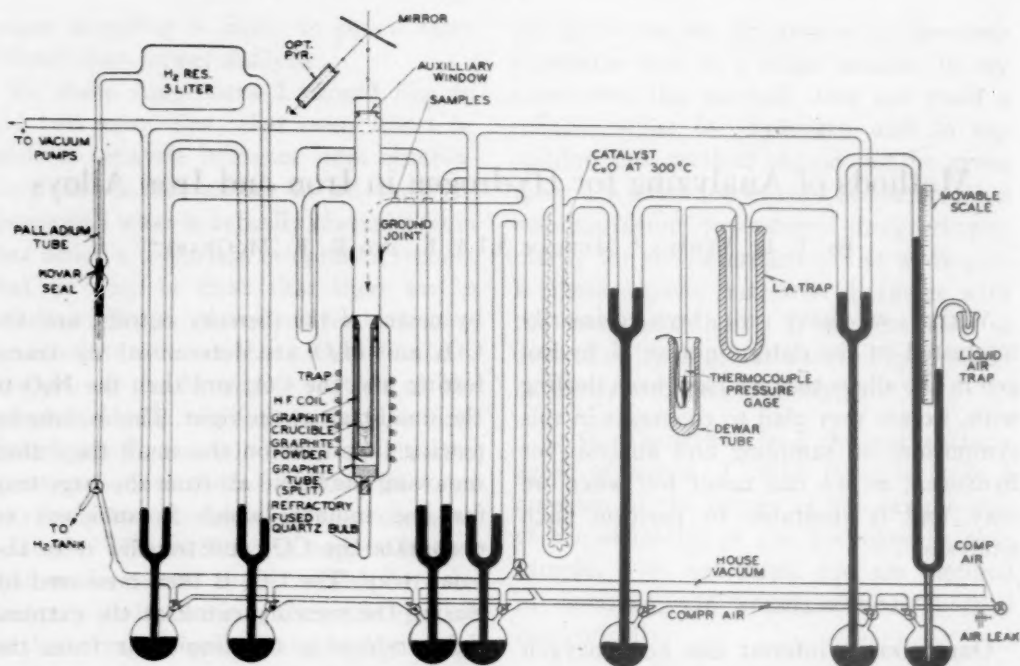


FIG. 1.—VACUUM-FUSION APPARATUS FOR OXYGEN ANALYSIS.

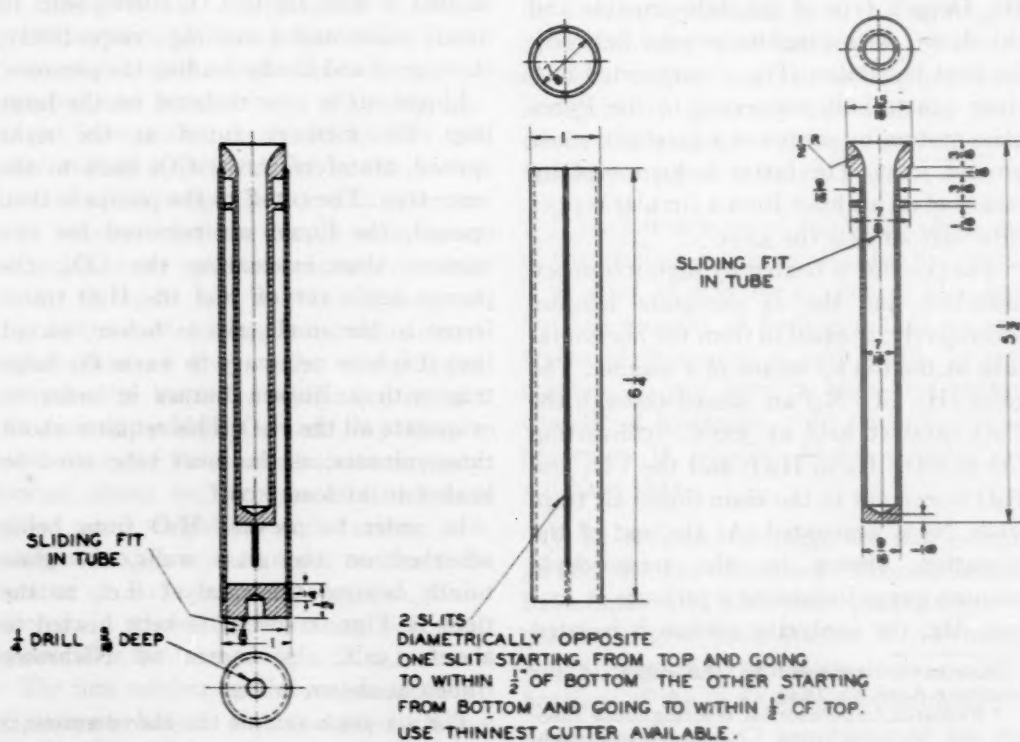


FIG. 2.—GRAPHITE TUBE AND CRUCIBLE FOR OXYGEN APPARATUS.

correspond to 0.0001 per cent, 0.0002 per cent, and 0.001 per cent O_2 as CO_2 , but as one-half of the oxygen comes from the catalyst these values must be divided by 2 in order to obtain the oxygen from the sample; i. e., 1 mm Hg for the three stations corresponds to 0.00005 per cent, 0.0001 per cent, and 0.0005 per cent O_2 in the sample. The sensitivity, therefore, is ample for all practical purposes.

To measure H_2 as H_2O , one mol of H_2O exerts the same pressure (up to 20 mm. at room temperature) as one mol of CO_2 , so that 1 mm. Hg of H_2O corresponds to $\frac{3}{32}$ (0.001, 0.002, and 0.01) mg. of H_2 ; i. e., 0.063×10^{-4} , 0.126×10^{-4} , and 0.63×10^{-4} per cent H_2 in a 1-gram sample. As 20 mm. is the limit to which we can go with H_2O at room temperature, this means that the maximum amount of H_2 we can measure in a 1-gram sample is 20×0.000063 , or 0.0013 per cent but this is more than is usually found in iron and iron alloys.* We can, of course use larger volumes and thus extend the range indefinitely.

Blanks and Reproducibility

For regular analysis the crucible is first heated for an hour at about $2200^\circ C$.† The temperature is then dropped to about $1300^\circ C$. and a blank obtained with the temperature gradually being raised to about $1600^\circ C$. and held there for 10 minutes.

The blank for oxygen is (4 ± 2) mm. of CO_2 at station No. 1, corresponding to (0.0002 ± 0.0001) per cent oxygen in a

* In the Bureau of Standards Cooperative Study. *Trans. A.I.M.E.* (1937) 125, 263. we find the maximum H_2 content (steel No. 2 Cooperator No. 24) to be 0.0008 per cent, while the maximum obtained by the Bureau of Standards (Cooperator No. 29) is only 0.0004 per cent (for steel No. 7).

† As measured with an optical pyrometer sighting down through the flat top and auxiliary window as shown in Fig. 1. The object of the auxiliary window is to prevent spattering on the inside of the flat top, which would be difficult to clean. The auxiliary window is removed and cleaned or replaced whenever necessary.

1-gram sample. The accuracy of analyzing the oxygen removed from the sample as CO and converted to CO_2 may, therefore, be regarded as ± 0.0001 per cent. This

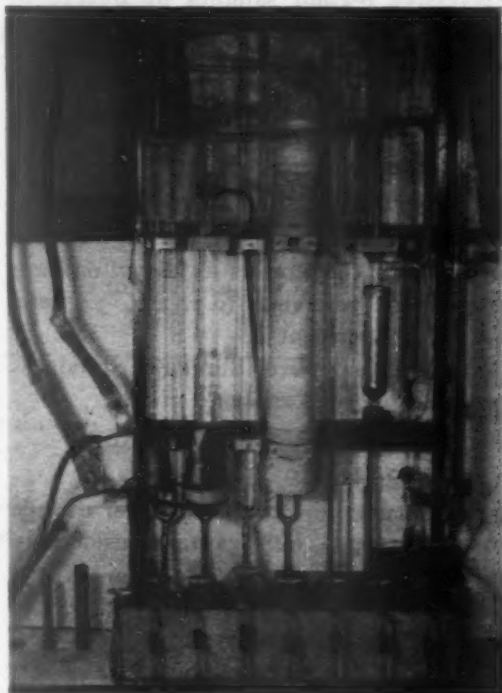


FIG. 3.—VACUUM-FUSION APPARATUS.

does not mean, however, that we can duplicate results with such accuracy, as variations in samples, in conversions and in operating techniques cannot be kept down to such values. Three successive analyses of Bureau of Standards sample No. 4 (Coop. anal.)* gave:

0.0028 per cent

0.0031 per cent

0.0024 per cent

Average, 0.00276 ± 0.00034 per cent

This is well within the "acceptable range" shown on page 256 of the reference given (0.001 to 0.004 per cent), the "best" value being regarded as 0.002 per cent.

The blank for hydrogen is (7 ± 1) mm. H_2O at station No. 1, corresponding to $(0.4 \pm 0.06) \times 10^{-4}$ per cent H_2 for a

* *Trans. A.I.M.E.* (1937) 125.

1-gram sample. As many samples of iron and iron alloys contain less than 0.4×10^{-4} per cent H_2 , it is necessary to use samples larger than 1 gram. For three successive 8-gram samples of Bureau of Standards No. 4 sample, we obtained, after deducting the blank correction,

$$0.39 \times 10^{-4} \text{ per cent } H_2$$

$$0.52 \times 10^{-4}$$

$$0.59 \times 10^{-4}$$

Average $(0.50 \pm 0.10) \times 10^{-4}$ per cent H_2

This is considerably less than was obtained by the four cooperators as shown on page 263 of the reference (0.7, 1.0, 3.0, and 2.0×10^{-4} per cent).

A 1-gram sample of Bureau of Standards sample No. 7 was analyzed giving:

$$0.116 \text{ per cent } O_2$$

$$0.22 \times 10^{-4} \text{ per cent } H_2$$

which checks the "best" value for oxygen (0.106 per cent), but again is considerably below the values for hydrogen in the reference given on page 357 (5.4, 3.0, 1.0 and 4.0×10^{-4} per cent).

In order to see whether we have difficulty in handling large amounts of H_2 , we analyzed two samples of electrolytic iron as deposited, with the following results:

No. 1. 0.032 per cent O_2

$$3.9 \times 10^{-4} \text{ per cent } H_2$$

No. 2. 0.034 per cent O_2

$$3.4 \times 10^{-4} \text{ per cent } H_2$$

While this is of the order of 10 times the amount we obtained with the Bureau of Standards samples, we should expect considerably more than that.

We next tried a slower rate of flow of the gas through the catalyst, but with negative results.

VACUUM-EXTRACTION METHOD

It has been suggested that hydrogen is all evolved in one hour at a temperature of $600^\circ\text{C}.$ * We have tried this many times,

* W. C. Newell: *Jnl. Iron and Steel Inst.*, (1940) 243.

W. C. Newell: Fourth Report of the Oxygen Subcommittee, Iron and Steel Inst., Advance Copy (July 1943) 48.

heating the samples in the quartz bulb by high-frequency induction without the graphite crucible. The results show that we obtain approximately the same amount of H_2 in one hour by this method that we obtain by the vacuum-fusion method in 10 min.; as the heating is continued more H_2 is given off, especially if the temperature is raised. Figs. 4 and 5 give the results obtained by analyzing a 6-gram piece, $\frac{1}{4}$ in. thick, of Bureau of Standards sample No. 4, the same for which we obtained 28×10^{-4} per cent O_2 and 0.5×10^{-4} per cent H_2 by the vacuum-fusion method.

In one hour at $680^\circ\text{C}.$, after deducting the blanks,* we obtained 6.5×10^{-4} per cent O_2 and 0.52×10^{-4} per cent H_2 ; i.e., about $\frac{1}{4}$ of the oxygen, but the same amount of hydrogen as obtained by vacuum fusion.

After 4 hr. at 680° , these values had increased to 8×10^{-4} per cent O_2 and 0.76×10^{-4} per cent H_2 .

By now raising the temperature to $780^\circ\text{C}.$ the rate of evolution was increased, particularly for oxygen, so that after 2 hr. at this temperature we had obtained 11.0×10^{-4} per cent O_2 and 0.85×10^{-4} per cent H_2 . After continuing all night at $780^\circ\text{C}.$ (22 hr.) we obtained a total of 32×10^{-4} per cent O_2 and 1.52×10^{-4} per cent H_2 .

Finally, by raising the temperature to $980^\circ\text{C}.$ we obtained in 35 min. an additional 3×10^{-4} per cent O_2 (making a total of 35×10^{-4} per cent O_2) and 0.2×10^{-4} per cent H_2 (making a total of 1.7×10^{-4} per cent H_2).

At this time a glow discharge began, which caused additional evolution of oxygen and hydrogen, undoubtedly due to bombardment of the glass walls of the tubing by electrons.

The question is: Where did these gases

* The blanks were found to come from the catalyst only. No measurable amount of gases (H_2 , CO , H_2O , CO_2) was obtained from the quartz bulb under any degree of heating, up to red.

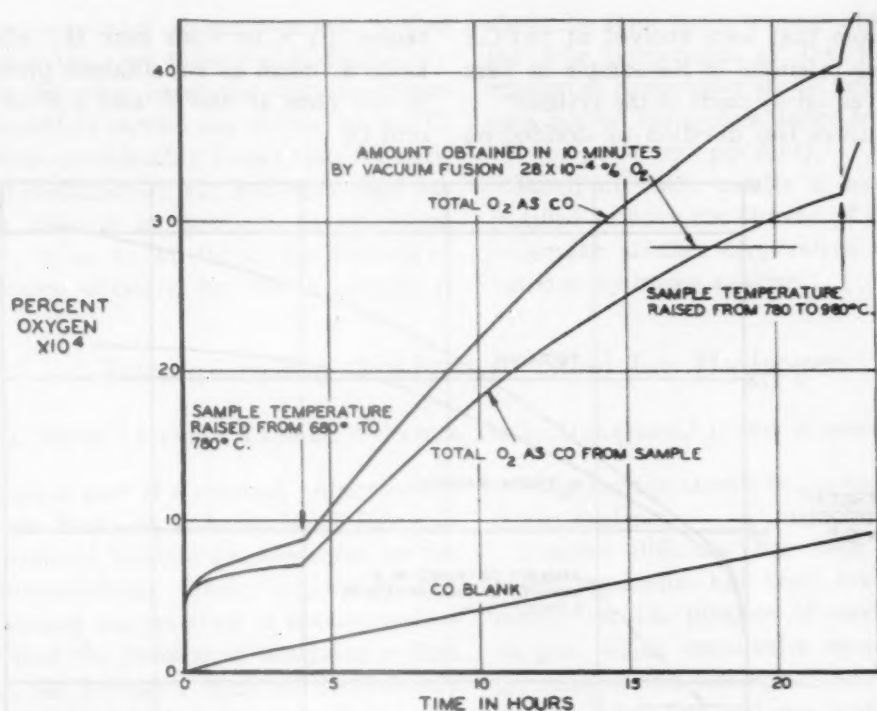


FIG. 4.—Oxygen evolution as carbon oxide gases. BUREAU OF STANDARDS No. 4 SAMPLE

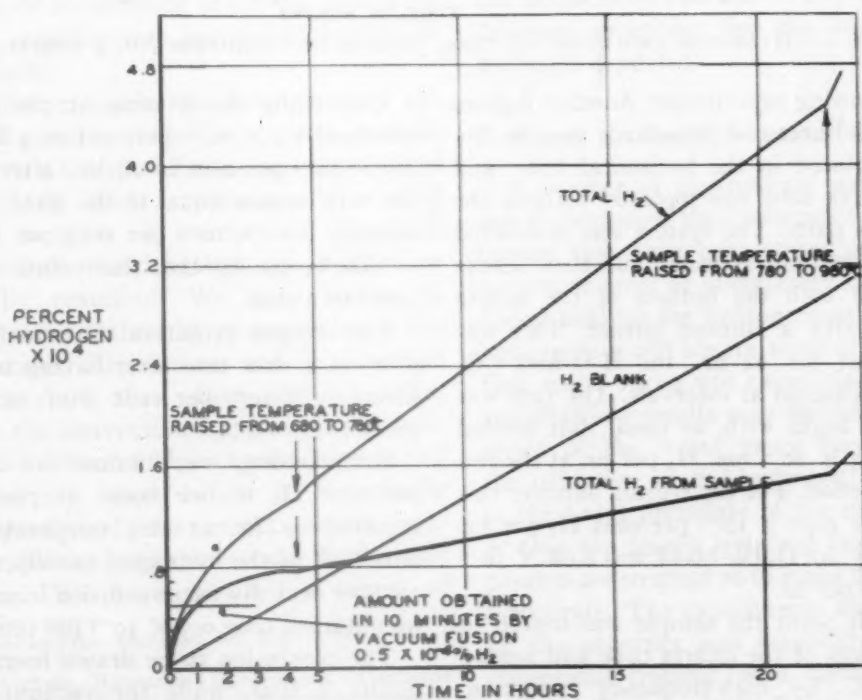


FIG. 5.—Hydrogen evolution, BUREAU OF STANDARDS No. 4 SAMPLE.

come from that were evolved at $780^{\circ}\text{C}.$? Did they originate in the sample or were they given off by parts of the system?

To answer this question we decided on

tained 1.1×10^{-4} per cent H_2 , which is twice as much as we obtained previously in one hour at $680^{\circ}\text{C}.$ and 9×10^{-4} per cent O_2 .

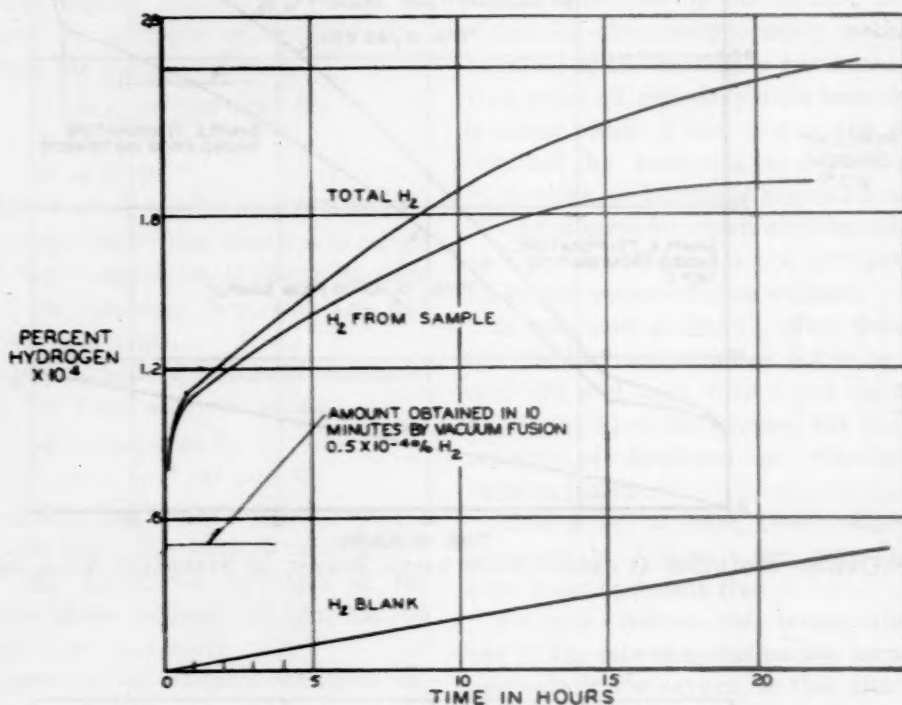


FIG. 6.—HYDROGEN EVOLUTION VS. TIME, BUREAU OF STANDARDS NO. 4 SAMPLE.

the following experiment: Another 6-gram piece of Bureau of Standards sample No. 4 was placed in the horizontal tube, and the quartz tube was replaced without the graphite parts. The system was evacuated and torched out as usual, and then blanks obtained with the bottom of the quartz heated with a Bunsen burner. This was continued for 24 hr., the H_2O and CO_2 being measured at intervals. The rate was large to begin with, as usual, but leveled off to 1.2×10^{-4} mg. H_2 per hr. at the end of the period. For the 6-gram sample, this would be 0.02×10^{-4} per cent H_2 per hr. Similarly, for O_2 the blank was 0.08×10^{-4} per cent per hr.

At this point the sample was moved to the bottom of the quartz tube and heated to $780^{\circ}\text{C}.$ by high-frequency induction. In one hour at this temperature we ob-

Continuing the heating at $780^{\circ}\text{C}.$, we obtained 1.3×10^{-4} per cent in 4 hr. and 1.9×10^{-4} per cent in 20 hr., after which the rate became equal to the blank rate—namely, 0.02×10^{-4} per cent per hour—so that we can say that the evolution of H_2 came to a stop.

The oxygen evolution continued, however, at a slow rate after having reached about 15×10^{-4} per cent after 20 hr. at $780^{\circ}\text{C}.$

Summarizing, we obtained 1.1×10^{-4} per cent H_2 in one hour, at $780^{\circ}\text{C}.$ It required 20 hr. at this temperature to obtain all of the hydrogen; namely, 1.9×10^{-4} per cent. By vacuum fusion in 10 min., we obtained only 0.5×10^{-4} per cent.

The conclusion to be drawn from these results is that, while the vacuum-fusion method, as carried out by us, gives the

correct amount of oxygen in 10 min., it does not give the total amount of hydrogen.

On the other hand, the vacuum-extraction method carried out at 700° to 800°C. requires considerably longer time for complete extraction of the hydrogen than has been claimed by previous investigators. In 15 to 20 hr. at 780°C. the amount of hydrogen obtained for No. 4 sample is

about the same as the average obtained by the four cooperators of the Bureau of Standards cooperative study (which, however, among themselves varied from 0.7×10^{-4} to 3.0×10^{-4} per cent).

Based on these results it would seem justified to have the Bureau of Standards undertake another cooperative study devoted to hydrogen analysis.

Vacuum-fusion Analysis of Steel for Hydrogen

By G. DERGE,* MEMBER A.I.M.E., W. PEIFER, AND B. ALEXANDER,* JUNIOR MEMBER A.I.M.E.

THIS is part of a research project in the Metals Research Laboratory of Carnegie Institute of Technology, sponsored by the Carnegie-Illinois Steel Corporation. In organizing our program it became apparent that the problem of analyzing molten steel for hydrogen must be divided into two parts: (1) the correct analysis of a given sample, and (2) the correct sampling of the bath. Emphasis has been placed upon these divisions in the order named because methods of sampling cannot be evaluated until a satisfactory method of analysis is available.

Vacuum fusion was selected from the list of possible analytical methods because it seemed to us to offer the best possibilities for giving rapid, accurate results on solid steel samples. A number of objections have been raised against this method as usually practiced. We have sought to meet some of these by proper design of the apparatus. Experiments will be described which show that others are not valid.

In the conventional apparatus the sample is held under high vacuum for a period of several hours before it is actually analyzed and one might expect considerable hydrogen to escape during this period. We have provided a means of

introducing the sample to the vacuum just before analysis.

Another difficulty has been that the entire apparatus has been designed primarily for the purpose of analyzing for oxygen, which constitutes upward of 90 per cent of the total gases evolved from the sample. The volume and pressure measurements have therefore been insensitive to the relatively small amounts of hydrogen present. This difficulty obviously can be taken into account in any apparatus designed especially for the amounts of hydrogen expected.

ANALYSIS IN VACUUM-FUSION APPARATUS

A number of experiments were carried out to determine the importance of several factors that have been stated as possible sources of error or uncertainty in vacuum-fusion analysis for hydrogen; namely, that hot graphite will absorb some of the gases, that metal vapor will cause discrepancies, and that low results may be obtained as a result of the water vapor (produced by the oxidation of the hydrogen) dissolving in the butyl phthalate of the manometer, or that the blanks obtained from the apparatus are so great as to make the method inaccurate. The experiments also checked on the accuracy and feasibility of using differential freezing as a method of gas analysis in a vacuum-fusion apparatus.

Manuscript received at the office of the Institute May 29, 1944.

* Metals Research Laboratory, Carnegie Institute of Technology, Pittsburgh, Pennsylvania.

These experiments were carried out in a conventional vacuum-fusion apparatus, where the gases (CO , H_2 and N_2) that are given off by the molten steel sample in

pure). The carbon monoxide was generated with formic and sulphuric acids, the gas being passed through two drying towers, a tower of soda lime, and finally through a

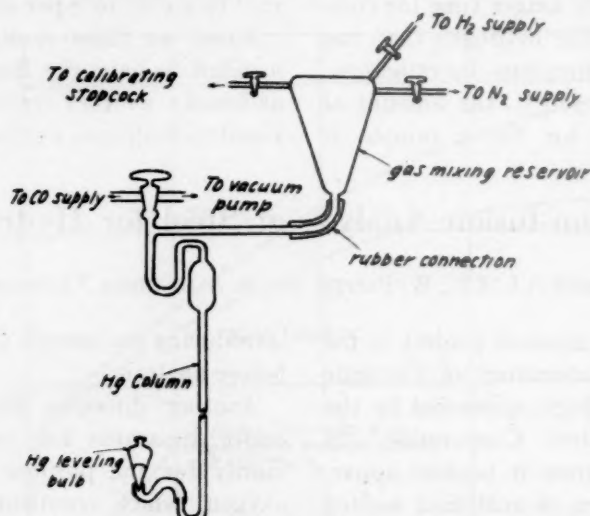


FIG. 1.—APPARATUS FOR MEASURING COMPOSITION AND PRESSURE OF GAS MIXTURE.

contact with graphite are collected in a known volume and the gas pressure measured with a butyl phthalate manometer. The gases are then circulated over heated CuO , which oxidizes the hydrogen to water vapor and the carbon monoxide to carbon dioxide. The water vapor (which ordinarily comprises about 5 per cent of the total gas after oxidation) can then be frozen out by passing the mixture through a freezing trap immersed in a slush of dry ice and acetone. After the loss in pressure has been measured, a measure of the hydrogen, the carbon dioxide is frozen out by passing the mixture through the freezing trap immersed in liquid nitrogen. The pressure is again measured to determine the amount of nitrogen in the gas mixture.

Method

An apparatus was constructed with which any desired mixture of gases (CO , H_2 and N_2) could be made at any desired pressure (Fig. 1). The hydrogen and nitrogen for this mixture were obtained from commercial tanks (99.5 per cent

freezing trap immersed in liquid nitrogen. The composition of the gas mixture was determined by measuring the partial pressures on a mercury column as the gases were introduced into a mixing reservoir. After mixing, the gas was passed into a calibrating stopcock, the volume of which had been accurately determined, and the pressure observed. This mixture of known composition was then analyzed in the vacuum-fusion apparatus.

A method of introducing the gas mixture into the hot crucible was devised (Fig. 2). The gas mixture was made to pass from the calibrating stopcock to a silica tube, which extended down to within $\frac{1}{2}$ in. of the crucible. A graphite nozzle on the end of this silica tube forced the gases to the bottom of the graphite crucible before they could be pumped out. Steel could also be introduced into the crucible at any time, so that the gases could be liberated over a molten steel bath.

The composition of the apparatus blank varies from time to time, but a typical analysis of the gases in the blank and their

rate of evolution at furnace temperatures of 1400° and 1700°C. are shown in Table 1. The blank with a cold furnace is zero. However, the hydrogen blank obtained during these experiments was only about

correction was made on the data as the correction for nitrogen and carbon monoxide would be negligible and for hydrogen would be less than 5 per cent of the hydrogen present.

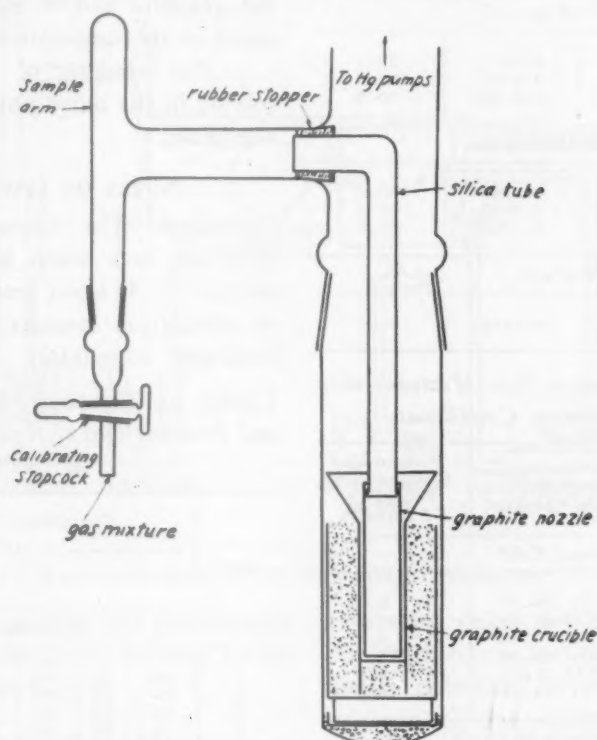


FIG. 2.—ARRANGEMENT OF FURNACE FOR INTRODUCING GAS SAMPLES TO HOT CRUCIBLE.

one third of the value shown in the table. This lower blank was probably due to the

TABLE 1.—Composition and Rate of Formation of Blank

Furnace Temperature, Deg. C.	Percentage Composition by			Rate of Formation, Millimols per Minute
	Gas	Volume	Weight	
1700	H ₂	60	9	0.00023
	N ₂	3	6	0.00001
	O ₂	37 as CO	85	0.00007
	Total			0.00031
1400	H ₂	49	6	0.00007
	N ₂	6	10	0.00001
	O ₂	45 as CO	84	0.00003
	Total			0.00011

particular graphite furnace components used during these experiments. No blank

DATA

The three gases (H₂, N₂, and CO) were first analyzed separately in the apparatus with the furnace cold. The results were satisfactory in each case and indicate the accuracy to be expected (see Table 2).

Mixtures of gas were then made which were approximately the same percentage composition by volume as that obtained in a vacuum-fusion analysis of steel. Various mixtures were analyzed in three ways: first, without graphite parts in the furnace; second, with empty crucible at 1700°C.; third, with crucible containing molten steel at 1700°C. Recovery was satisfactory under all conditions. Some typical results are given in Table 3.

TABLE 2.—*Separate Analyses of Hydrogen, Nitrogen and Carbon Monoxide*

Run	Gas Admitted, Millimols	Gas Frozen Out, Millimols	Percentage Recovered
Hydrogen			
1	0.0213	0.0211	99.1
2	0.0226	0.0226	100.0
3	0.0144	0.0139	96.6
Carbon Monoxide			
1	0.3295	0.3295	100.0
2	0.2305	0.2246	97.5
3	0.1290	0.1264	98.1
Nitrogen			
1	0.0514	0.0514	100.0

TABLE 3.—*Analyses of Gas Mixtures with Different Furnace Conditions*

Run	Gas Admitted, Millimols	Percentage Composition of Gas Admitted	Percentage Composition Found by Analysis
Furnace Cold			
1	0.2300	H ₂ 9.18 CO 90.82 N ₂ 0.00	H ₂ 9.64 CO 90.36 N ₂ 0.00
2	0.2781	H ₂ 13.09 CO 74.20 N ₂ 12.71	H ₂ 14.2 CO 72.0 N ₂ 13.8
Empty Furnace at 1700°C.			
1	0.1740	H ₂ 6.1 CO 93.9 N ₂ 5.55	H ₂ 8.2 CO 91.8 N ₂ 5.5
2	0.2000	H ₂ 5.55 CO 85.10 N ₂ 9.35	H ₂ 5.5 CO 85.2 N ₂ 9.3
3	0.2025	H ₂ 5.55 CO 85.10 N ₂ 9.35	H ₂ 5.0 CO 81.0 N ₂ 14.0
Molten Steel in Furnace at 1700°C.			
1	0.1611	H ₂ 11.3 CO 72.0 N ₂ 16.7	H ₂ 13.0 CO 67.2 N ₂ 19.8
2	0.1639	H ₂ 4.68 CO 85.99 N ₂ 9.33	H ₂ 4.1 CO 83.0 N ₂ 12.9
3	0.1620	H ₂ 4.68 CO 85.99 N ₂ 9.33	H ₂ 3.6 CO 84.0 N ₂ 12.4

DISCUSSION OF RESULTS

All of the results are within the limit of accuracy of the apparatus, and when the small amounts of gas present are considered the analyses appear satisfactory. The results show:

1. The differential freezing method of

gas analysis is accurate enough if the necessary precautions are taken. These will be described under Notes on Gas Analysis, below.

2. The contact of the gas mixture with hot graphite and/or metal vapors has no effect on its composition or volume.

3. The amount of water vapor dissolving in the butyl phthalate seems to be negligible.

NOTES ON GAS ANALYSIS

Catalyst.—The copper oxide catalyst functions best when kept between 300° and 310°C. At lower temperatures the time of circulation necessary to oxidize the hydrogen completely becomes excessive

TABLE 4.—*Combined Rates of Oxidation and Freezing Out of Hydrogen with Catalyst at 300°C.*

Run	Circulating Time, Minutes						
	1	2	3	4	5	6	7
	H ₂ Oxidized, Per Cent						
1	52	76	90	94	98	100	100
2	66	88	105	110	110		
3	54	85	99	99			
4	55	81	90	94	94		
5	67	81	93	98	98		
6	91	98	98				
7	71	81	91	95	99		

and at higher temperatures the catalyst blank becomes larger. At 300°C., all of the hydrogen in the mixture could be oxidized and frozen out after 3 to 5 min. of circulation, and all of the carbon monoxide after 10 min. See Table 4 for data on the combined rates of oxidation and freezing out of hydrogen.

FREEZING TRAP

The vapor pressure of ice at the temperature of dry ice (−78.5°C.) is 0.00052 mm. Hg, whereas the pressure inside the system is about 0.0003 mm. Hg. This indicates that the ice will be lost by evaporation from the freezing trap, and experiments show that approximately 10 to 20 per cent of the water is lost from the freezing trap after pumping for 10 min. This dif-

difficulty was overcome by using a mixture of dry ice and acetone that had been super-cooled to -90°C . by subjecting it to the reduced pressure of an aspirator for 5 min. At this temperature the vapor pressure of

analyzing the samples the conventional vacuum-fusion apparatus was used, so these results must be considered only as qualitative indications of what we may expect to find with more exhaustive study.

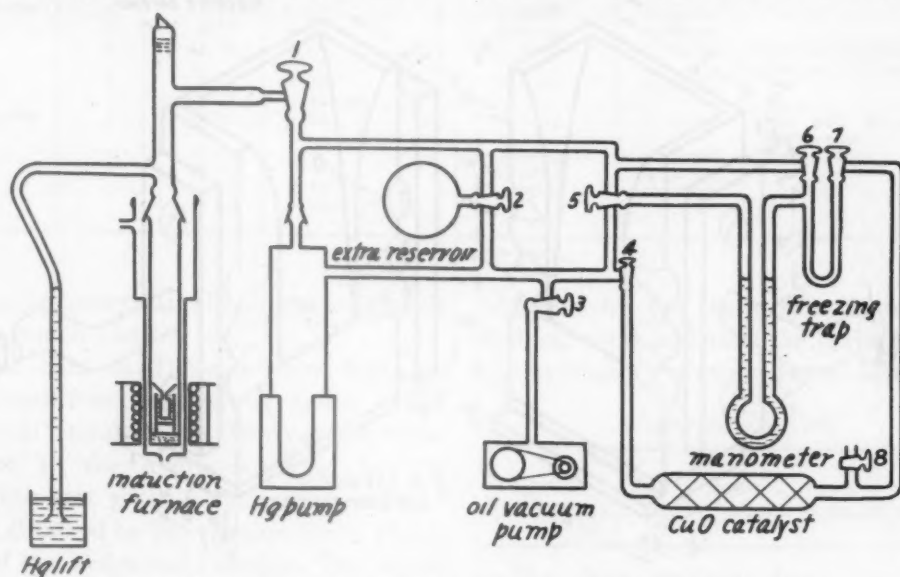


FIG. 3.—VACUUM-FUSION APPARATUS FOR DETERMINING HYDROGEN.

ice is 0.000070 mm. Hg, and experiments showed that by using this mixture no ice was lost by evaporation.

DESIGN OF HYDROGEN APPARATUS

The hydrogen apparatus was designed on the basis of the above discussion (Fig. 3).

The sample is introduced through the mercury lift after the apparatus has been evacuated and baked out. The gases are pumped off from the molten steel in the crucible and collected in the reservoir, of which the capacity is 56 c.c. When all the gas is removed from the metal, the collected gases are circulated over a copper-oxide catalyst, which oxidizes the hydrogen to water vapor that circulates through the freezing trap and is frozen out. The frozen water vapor is revaporized in the freezing trap and its pressure measured on the manometer.

SAMPLING

Some preliminary results have been obtained on methods of sampling. In

In two cases the results obtained by the Timken tube test can be compared with those obtained by the vacuum-fusion analysis of the wedge test, which was originally developed as an oxygen sample.*

Two heats of Ni-Cr-Mo acid open-hearth steels were sampled for hydrogen by taking simultaneous tests with the wedge mold (Fig. 4) and Timken tube. The results are indicated in Table 5. Two Timken tests (rods 2 and 16) were taken on the first heat and the gas evolved on solidification was analyzed for hydrogen. The results are indicated under Timken analyses in Table 5. Two wedge-mold tests were taken at the same time. The solid Timken-test rods were sampled at four equally spaced points along their length. The top sample was indicated as No. 1, the bottom as No. 4. These samples were analyzed by vacuum fusion, with the

* G. Derge: *Trans. A.I.M.E.* (1943) 154, 248.

results indicated. The same procedure was followed in the second heat.

In the vacuum-fusion analysis of the residual metal of the Timken test a con-

siderable amount of hydrogen was found, which seems to show that the Timken test does not give absolute values for hydrogen even though it may give a useful figure.

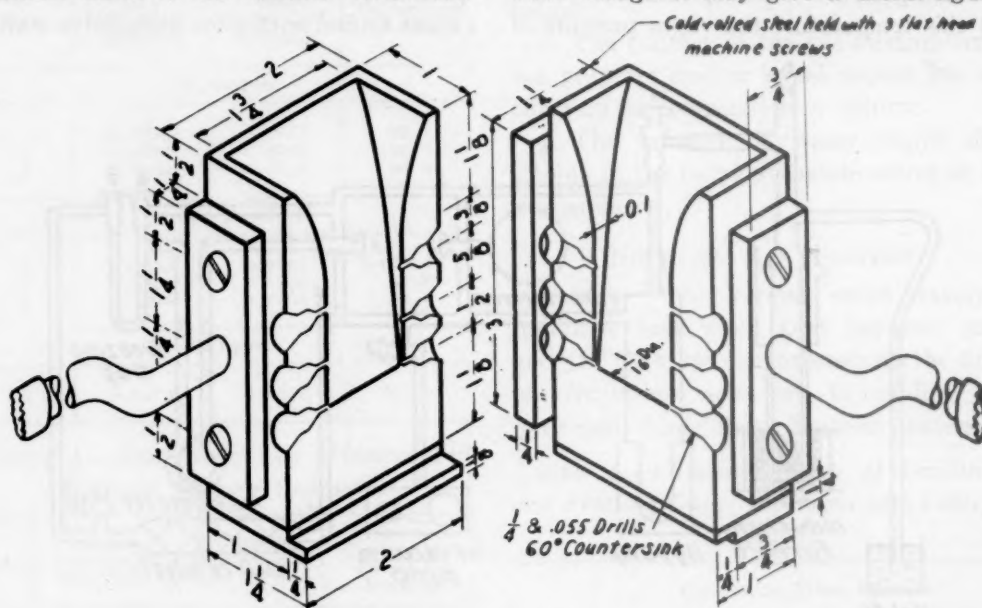


FIG. 4.—TAPERED COPPER MOLD.

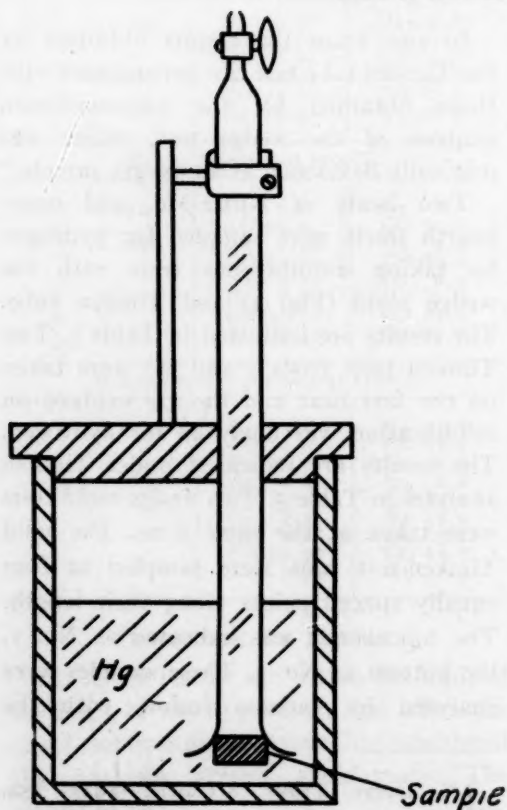


FIG. 5.—PORTABLE GAS BURETTE UNIT.

Many slag inclusions were found in the rods, so that there is no certainty that the samples used for analysis were free of slag. This would be an additional reason

TABLE 5.—Vacuum-fusion Analyses of Wedge-mold and Timken Tests for Hydrogen

Data No.	Test	Vacuum Fusion	Timken	Vacuum Fusion + Timken	Wedge-mold Furnace Tests
Heat 1					
Rod No. 10	1	0.00009	Test No. 1		0.0002
	2	0.0001	0.000171		0.0002
	3	0.0001			
	4	0.00009			
Averages..		0.0001	0.000171	0.00027	
Heat 2					
Rod No. 2	1	0.0002	Test No. 1		
	2	0.0001	0.000206		
	3	0.0001	Test No. 2		
	4	0.00007	0.000199		
Averages..		0.0001	0.000203	0.0003	
Rod No. 18	1	0.0001			0.0003
	2	0.00009			0.0003
	3	0.00007			
	4	0.00007			
Averages..		0.00008	0.000203	0.00028	

TABLE 6.—*Analysis of Open-hearth Furnace Samples in the Hydrogen Apparatus*

Heat No.	Sample No.	Time of Sampling	C, Per Cent	Oxygen,* Total Gas Calc. as O ₂ , Per Cent	Hydrogen* Per Cent	Furnace Additions
51L079	1	4:11	0.62	0.0263	0.00052	Lime 29 min. before test. Ore 14 min. before test
	2	4:11	0.62	0.0344	0.00082	
	3	4:44	0.46	0.0425	0.00079	
	4	4:44	0.46	0.0501	0.00101	
49L084		5-48	0.14 tap			Lime and ore 40 min. before test
	1	11:40	0.24	0.0485	0.00092	
	2	12:01		0.0689	0.00096	
	3	12:19		0.0804	0.00105	
	4	12:23	0.10	0.0723	0.00155	
		12:30	0.09-0.08 tap			

* Corrected for blank.

for being conservative in using quantitative data from a Timken test.

The data in Table 5 show that the hydrogen found by vacuum fusion in the residual metal of the Timken test when added to the hydrogen found by the Timken test gives a figure very close to that obtained by the vacuum-fusion analysis of the wedge-mold sample. This would indicate that wedge-mold method of sampling steel is satisfactory for hydrogen. The very rapid chilling of the wedge seems to effectively retain the hydrogen in the sample.

Our present technique in sampling molten steel for hydrogen with the wedge mold makes use of a special sampling burette (Fig. 5). This is simply an inverted burette with its open end placed under mercury, so that any gas evolved between the time the sample is taken and the time of the analysis can be collected. As used, this collecting device with the sample in it was placed on a hot plate, which maintained the mercury at 100°C., and the gas evolved was collected and analyzed.

A chilled wedge sample prepared in this way was analyzed in a conventional vacuum-fusion apparatus in such a way that the gas evolved below the melting point could be measured. The results that follow show that in this case a small amount of gas was collected in the gas burette at low temperature, that no hydrogen was

obtained by hot extraction below the melting point and that the major part of the hydrogen was evolved after fusion:

Hydrogen Per Cent

Sample . . .	100°C.	1100°C.	1700°C.	Total
No. 4-59492.	0.00011	0.0000	0.00087	0.00098

The data obtained from two open-hearth heats by this procedure are shown in Table 6. The hydrogen values are higher than normally shown for finished products and show the trends to be expected in the working of a heat.

On the basis of these experiments we are encouraged to believe that satisfactory hydrogen analyses can be made with a modified vacuum-fusion technique and that a chilled wedge sample will give useful results.

DISCUSSION

J. G. THOMPSON.—I still feel that the old, reliable vacuum-fusion method is a good analytical method for the determination of oxygen, nitrogen and hydrogen, if there are suitable amounts and suitable samples. The difficulties in the determination of hydrogen are twofold: (1) that the amount of hydrogen is so much less than that of the other gases and (2) that the hydrogen content is not as stable; it is hard to keep in the specimen. If you are concerned with hydrogen contents of a fraction of a thousandth of a per cent, out in the fourth or fifth decimal place, the ordinary vacuum-fusion procedure does need modifica-

tion, and if you are dealing with specimens in which the hydrogen content is unstable, tends to diffuse out in a vacuum at low temperatures, again you need some modification of the ordinary vacuum-fusion apparatus. I think that the modifications along those lines that have been discussed in the papers by Dr. Yensen and Dr. Derge are very well worth while, the quick sampling and a rapid analysis and the separation of the water vapor from the CO_2 and the other samples.

As to the matter of hydrogen content of standard sample steel No. 4, which Dr. Yensen brought up, I would like to point out that at the time of that cooperative analysis project—that was in 1937, and the determination of hydrogen was, as Dr. Austin said, a side line of the determination of oxygen and nitrogen—the values were obtained without attempting to utilize the special precautions, and the amounts were in general less than the precision of the different pieces of apparatus and methods that were used. At the Bureau we have since had occasion to run the cooperative steels again for hydrogen with apparatus with improved precision, and we get results that are in better agreement with Dr. Yensen's values than were the results that were reported in 1937.

Y. C. CHIU.*—I am very glad to hear the comments from Dr. Derge which agree very well with the work we did in Germany. Dr. Walter Eilender and Mr. Franz Willems and I were co-workers. The work was published in *Archiv für das Eisenhüttenwesen*, vol. 12 (1938/1939), pp. 485-498 and vol. 13, (1939/1940), 309-316. The first part of our work was to modify the gas-analysis apparatus used with high vacuum-fusion furnace and to work out a method for obtaining a blank so that hydrogen in steel can be determined together with oxygen and nitrogen in one sample to a reasonable accuracy. Hydrogen contents in commercial steel samples with flake-forming tendency and nonflake-forming tendency were determined. The results showed that the hydrogen contents of all the steels investigated were very low and lay in the range of 0.0001 to 0.0003 per cent by weight whether they are liable to flaking or not.

The second part of our work was to study the behavior of hydrogen in steels of various

compositions. Heats of about 200 lb. were made in a high-frequency furnace. After melting, hydrogen was bubbled through the metal. Samples were taken before and after passing hydrogen with a chill mold similar to that used for taking spectrographic pins. The chilled samples were put immediately under mercury in a gas-collecting apparatus. The hydrogen diffusing out of the sample was collected into the burette of the gas-collecting apparatus and the volume was read from time to time. When no appreciable amount of hydrogen diffused out, the residual hydrogen in the sample was determined by the vacuum-fusion method. By this procedure, the behavior of hydrogen in simple steels of various carbon contents and alloy steels of various compositions were systematically studied. The results showed that for plain carbon steels the higher the carbon content, the slower will be the rate of hydrogen diffusion out of the steel under mercury and at room temperature. For alloy steels, most of the alloying elements studied had the effect of retarding the process of hydrogen evolution.

After hydrogen had been passed through stainless steel of 18-8 type and manganese hard steel, it was noted that these steels retained 0.0015 and 0.0009 per cent by weight of hydrogen, respectively, but both of them did not give off any of the absorbed hydrogen even after being kept under mercury in the gas-collecting apparatus for a number of weeks.

G. DERGE.—I think those who are acquainted with trying to eliminate hydrogen in actual steelmaking processes all feel that an active bath is the best aid they have; as long as there is some CO bubbling, coming up through the metal, it will help get rid of hydrogen. The same thing helps in vacuum-fusion analysis. And in that respect the carbon in the steel and consequent evolution of oxygen as CO is a big help. We all recognize, however, that there are certain difficulties involved and we are merely looking for the most practical means of analysis. There will always remain certain inaccuracies.

J. B. AUSTIN.—I think we have to go on to the next paper, and I will call on Dr. Thompson to describe briefly the results that have been obtained at the Bureau of Standards.

* National Resources Commission, China.

Determinations of Hydrogen in Iron and Steel by Vacuum Extraction at 800°C.

By J. G. THOMPSON,* MEMBER A.I.M.E.

DETERMINATIONS of the hydrogen content of irons and steels invariably are subject to two serious difficulties: (1) the determination of amounts of 0.001 per cent or less of any constituent requires an analytical procedure of unusual precision and accuracy, and (2) the hydrogen content of many samples is decidedly not stable; i.e., there is no assurance that the content at the time the analysis is made is the same as it was when the sample was taken or at some previous time in the history of the piece. In respect to both the precision and speed of the determination, the vacuum-extraction procedure for the determination of hydrogen possesses advantages over the vacuum-fusion procedure, which has been the recognized standard for the determination of other gaseous elements in steel—oxygen and nitrogen for example.

The basic facts upon which the vacuum-extraction procedure is based—i.e., the evolution of gas from solid steel when it is heated in vacuum, and the fact that the evolved gas is rich in hydrogen—were observed by Graham¹ many years ago. Subsequent investigations have shown that hydrogen exists in steel chiefly as interstitial solid solution (i.e., in atomic dispersion) and perhaps to some extent as hydrides that are unstable and decompose to form atomic hydrogen. In either case practically all of the hydrogen in steel at elevated temperatures exists in the atomic condition and consequently is able to diffuse

readily through the metal. In contrast to this, other gaseous elements, such as oxygen and nitrogen, normally are present in steel chiefly in the form of relatively stable compounds such as oxides or silicates and nitrates; i.e., the oxygen and nitrogen atoms are fixed in stable combinations and are not free to migrate. The only oxygen or nitrogen that can diffuse in steel is the small amount in solution (atomically dispersed) and the rate of diffusion of these atoms is much less than that of hydrogen because of their greater atomic volume and lower mobility. Consequently, it is possible to extract most or all of the hydrogen from solid steel in a reasonable time at moderately elevated temperatures, but the procedure is not applicable to the determination of oxygen or nitrogen. It is only within the last decade that these observations have been developed into an analytical procedure for the determination of hydrogen.²⁻⁵

APPARATUS AND PROCEDURE

The apparatus used at the National Bureau of Standards,⁶ for the determination of hydrogen by the vacuum-extraction procedure, is shown schematically in Fig. 1. The specimen, freshly cleaned and dried,* is suspended on a fine wire within the quartz furnace tube that is connected to the reservoir system and analytical train.

* Samples usually are cleaned by lightly grinding but rough or irregular samples are conveniently cleaned by immersion for about 20 sec. in diluted hydrochloric acid, followed by a rinse in tap water. Cleaned specimens are rinsed with alcohol and dried with ether. The same results for hydrogen are obtained after cleaning by either method.

Manuscript received at the office of the Institute March 8, 1944.

* Principal Metallurgist, National Bureau of Standards, Washington, D. C.

¹ References are on page 374.

The apparatus is evacuated, by rotary and diffusion pumps, until the pressure is reduced to about 1×10^{-4} mm., which usually requires about 10 min. The speci-

The rate of evolution of gas from the heated specimen is rapid at first, when the hydrogen is coming from the surface or from the layers adjacent to the surface, and

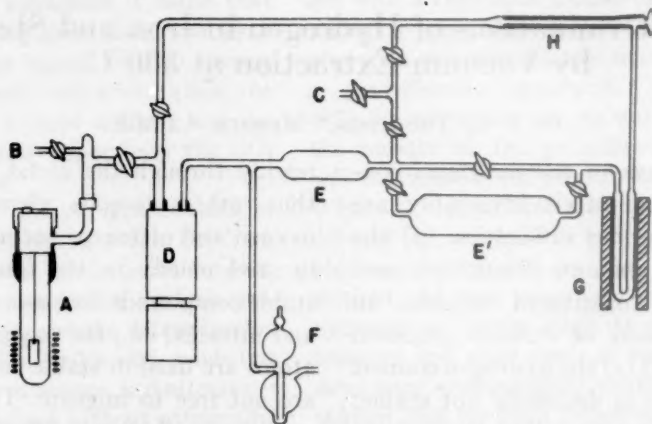


FIG. 1.—APPARATUS FOR DETERMINATION OF HYDROGEN BY VACUUM EXTRACTION AT 800°C.
 A, furnace tube.
 B, C, connections to oil pump or to air.
 D, mercury diffusion pump.
 E, E', reservoirs.
 F, McLeod gauge.
 G, copper oxide tube and furnace.
 H, absorption tube filled with anhydrous magnesium perchlorate.

men is then heated rapidly to about 800°C. and maintained at this temperature by means of a high-frequency induction coil activated by a 3-kva oscillator. The evolved volume of gas, which contains 50 to 90 per cent of hydrogen, is transferred to the reservoir system and subsequently circulated through hot copper oxide and an absorption tube, where the water vapor is absorbed by anhydrous magnesium perchlorate. The change in pressure in the system during the absorption of water vapor indicates the amount of hydrogen evolved from the sample.*

* The bulk of the hydrogen is evolved from the sample as molecular hydrogen, but it is possible that in special cases some of the evolved hydrogen might be present as water vapor or as methane. Water vapor could be formed by reaction of evolved hydrogen with oxides at the surface of the specimen or by vaporization of occluded moisture, and methane might be formed by combination of hydrogen with carbon from the specimen. Any hydrogen that exists as water vapor is determined by the absorption in magnesium perchlorate, regardless of whether the water vapor is formed in the furnace or by the oxidation of molecular hydrogen by hot copper oxide. Significant amounts of methane have not been encountered in our experience, but if methane was present it could be determined

subsequently tapers off as the surface concentration is exhausted and the hydrogen must diffuse from the interior. Pihlstrand's data⁷ show that the higher the temperature and the thinner the specimen, the less is the time required for complete extraction of hydrogen. In our apparatus, operating at 800°C., it was found that extraction should be continued 1 min. for each millimeter of thickness of the specimen. Most of the specimens were about 5 mm. thick, so that the extraction time was about 5 min. and the total time for placing the specimen, outgassing the apparatus, and completely extracting the hydrogen, was about 15 minutes.

The blank correction, determined with a previously outgassed specimen in the fur-

by raising the temperature of the copper oxide to about 600°C. Methane is not oxidized by copper oxide at 300°C. but is completely oxidized at higher temperatures. It appears therefore that the recommended procedure determines the hydrogen evolved from the sample as molecular hydrogen or as water vapor and would require only slight modification to include hydrogen combined as methane, if there was any indication of the presence of this compound.

nance, usually was about 7×10^{-6} grams of hydrogen for a 15-min. run, but varied from 5 to 10×10^{-6} with seasonal variations in temperature and humidity. This is equiva-

direct induction and the specimen within the hot thimble is brought to the desired temperature without loading the induction coil to its limit and without causing the

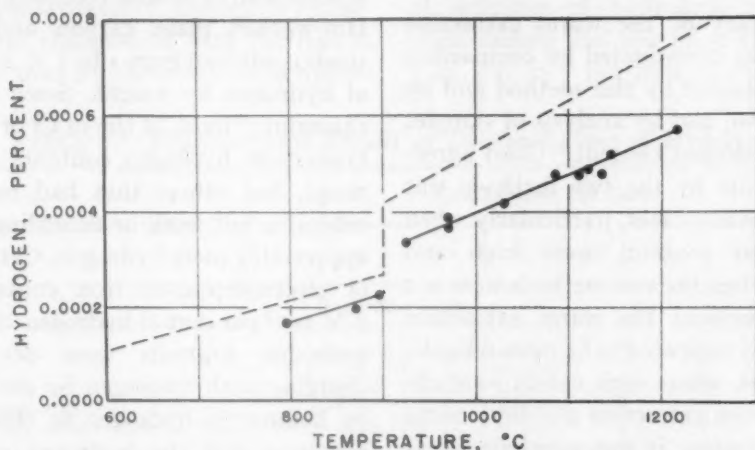


FIG. 2.—DETERMINATIONS OF HYDROGEN IN IRON QUENCHED AFTER SATURATION WITH HYDROGEN AT TEMPERATURES INDICATED.

Dashed line shows solubility of hydrogen in iron as reported in the literature.⁸⁻¹⁰

lent to 7×10^{-5} per cent of hydrogen if the sample weighed 10 grams. Several analyses showed that hydrogen constituted 25 to 35 per cent of the blank gases.

In the early stages of our investigation, the blank correction remained low and constant, but in subsequent work glow discharges or corona effects within the furnace tube sometimes made the blank correction high and erratic. This phenomenon was encountered principally with samples of metals such as stainless steel, the inductive heating of which is difficult, or with special samples that contained volatile metallic constituents. The trouble apparently is a result of ionization of the furnace atmosphere because of particular combinations of voltage, frequency, and atmospheric conditions within the furnace. In most cases of steels that are hard to heat inductively—i.e., that require full power on the induction coil to maintain them at the desired temperature—the difficulty can be overcome by suspending the sample in an iron thimble instead of on a wire. The thimble is readily heated by

glow discharge to occur. The use of the thimble, however, did not avoid the troubles when the sample contained volatile metals such as calcium and magnesium and the tendency for the glow discharge to occur was noticeable for some time after work with the special samples was discontinued.

These ionization troubles have not been encountered often enough in our experience to justify an extended investigation for their complete control. Many specimens have been run successfully, suspended from a fine wire and heated by direct induction, and a number of other specimens have been treated successfully in the iron thimble.

PRECISION AND ACCURACY OF METHOD

The precision of the method, judged by results obtained on duplicate samples usually is within $\pm 1 \times 10^{-5}$ per cent hydrogen. This is considerably better than the precision of other methods previously employed in these laboratories but there is

still room for improvement for the determination of hydrogen contents of the order of 1 to 5×10^{-5} per cent, values frequently encountered in samples that have been hot-worked.

The accuracy of the warm extraction procedure was investigated by comparison of results obtained by this method and by vacuum fusion, and by analysis of samples of known hydrogen content.⁶ Good agreement in results by the two methods was obtained in many cases, particularly when the hydrogen contents were high and stable, and when the two methods were not in good agreement the warm extraction results usually appeared to be more reliable. In some cases, where high values were obtained by warm extraction and low values by vacuum fusion, it was concluded that appreciable amounts of hydrogen were lost from the vacuum-fusion samples during the outgassing of the apparatus, and when the hydrogen content of the sample was low, the vacuum-fusion determinations were not precise enough to permit comparisons.

The preparation of samples of known hydrogen content was attempted by saturating a thin slab of remelted electrolytic iron with hydrogen at an elevated temperature, quenching the saturated specimen and then cleaning, drying, and analyzing it as rapidly as possible. Comparison of the experimental results with the solubility curve is shown in Fig. 2. Both curves show that the solubility increases with increasing temperature, and an abrupt change in solubility occurs at the alpha-gamma transformation. The analytical data lie consistently below the solubility values and the divergence increases with increasing temperature, probably because of losses of hydrogen during the quenching and cleaning operations. It is believed that recoveries of 75 per cent or more of the theoretical values represent full recovery of the hydrogen present in the samples at the time the analysis was made.

SOME EXPERIMENTAL RESULTS

Determinations of hydrogen have been made by this procedure on a variety of ferrous materials, as indicated by the representative results recorded in Table 1. Hot-worked plain carbon and low-alloy steels contained from 1 to 5×10^{-5} per cent of hydrogen by weight. Some samples of chromium steels, of the 14 Cr or 18:8 Cr-Ni types, had hydrogen contents within this range, but others that had received less extensive hot-work or annealing contained appreciably more hydrogen. Cathode plates of electrodeposited iron contained 2 or 3×10^{-3} per cent of hydrogen. Similar high hydrogen contents were developed by charging with hydrogen by electrolysis or by heating in hydrogen at elevated temperatures but the hydrogen content developed by either of these procedures is decidedly impermanent and will not withstand storage, even at room temperature. A specimen charged cathodically to a hydrogen content of 4×10^{-4} per cent lost more than half of its hydrogen in 2 days storage at room temperature and atmospheric pressure. Another specimen of cathodically charged iron dropped from 3×10^{-3} to 2×10^{-4} per cent of hydrogen during 11 days storage under the same conditions. Storage in a vacuum is even more efficient in removing this excess of hydrogen; rapid analyses of quenched samples, by the warm extraction method, yielded values of 2 to 6×10^{-4} per cent, depending upon the temperature at which the specimen had been saturated and quenched, but analyses of duplicate specimens by vacuum fusion consistently yielded 1×10^{-4} , regardless of the previous history of the specimen. Evidently most of the hydrogen of the latter specimens was lost during the extended outgassing of the vacuum-fusion apparatus, before the specimen was dropped for analysis.

The hydrogen content of most of these supersaturated steels rapidly approached the equilibrium value for room tempera-

ture, less than 1×10^{-4} , but this does not always occur. Plates of electrodeposited iron still contained more than 1×10^{-3} per cent of hydrogen after several years storage in the laboratory. Evidently hydrogen that was codeposited with the iron is more stable than similar amounts of hydro-

per cent of hydrogen after 10 years of storage in the laboratory.

Variations in composition of the steel may affect both the solubility and the rate of diffusion of hydrogen. Specimens of plain carbon and low alloy steels retained 3 or 4×10^{-4} per cent of hydrogen after

TABLE 1.—Representative Results of Determinations of Hydrogen

Sample No.	Description	Composition, Per Cent						Hydrogen, Per Cent
		C	Mn	Si	Ni	Cr	Mo	
Hot-rolled Rods								
1	Ingot iron.....	0.016	0.024	0.001				0.00001
2		0.03	0.31	0.002				0.00002
3		0.12	0.72	0.02				0.00004
4		0.17	0.65	0.09				0.00002
5		0.20	0.45	0.03				0.00004
6		0.22	0.45	0.14				0.00002
7	Plain carbon steel.....	0.42	1.15	0.26				0.00001
8		0.43	1.47	0.20				0.00002
9		0.34	1.60	0.26	3.5	0.09		0.00003
10		0.39	1.66	0.29			0.5	0.00002
11		0.36	1.58	0.16		0.82	0.2	0.00003
12		0.31	1.28	0.36		14.		0.00005
13	Alloy steel.....	0.06	1.56	0.76	8.4	17.6		0.00038
14		0.24	1.28		8	19.6		0.00010
Instable High-hydrogen Contents								
15	Cathodically charged iron.....							0.003
	After 11 days storage at room temperature.....							0.0002
16	Remelted electrolytic iron, saturated with H ₂ at 1100°C.....							0.00041
	After 2 days storage at room temperature.....							0.00015
	After 5 days storage at room temperature.....							0.00009
17	Ingot iron saturated with H ₂ at 1100°C.....							0.00049
	After 4 hours in vacuum at room temperature.....							0.00026
	After 6 hours in vacuum at room temperature.....							0.00010
Relatively Stable High-hydrogen Contents								
18	Electrolytic iron, cathode plates.....							0.002-0.003
19	Alloy steel No. 13 saturated with H ₂ at 1100°C.....							0.00071
	After 11 days storage at room temperature.....							0.00072
20	Electrolytic iron, cathode plate.....							0.0022
	After 7 months storage.....							0.0018
	After 1 years storage.....							0.0016
	After 15 months storage.....							0.0014
	After 2 years storage.....							0.0013

gen deposited cathodically on a solid surface or introduced by annealing in hydrogen at high temperature, and the rate of approach to equilibrium conditions, for specimens supersaturated with hydrogen, may be either fast or slow, depending upon the amount of hydrogen present and the way it was introduced. It is interesting to note that a sample of 18:8 Cr-Ni steel from a hot-worked billet contained 4×10^{-4}

annealing in hydrogen at 1100°C, whereas purer metal, i.e., remelted electrolytic iron, retained about 5×10^{-4} per cent. Variations in composition of the plain carbon and low-alloy steels investigated did not appreciably affect the amount of retained hydrogen, but steels that contained 14 to 18 per cent of chromium, quenched from 1100°C. in hydrogen, retained more than 7×10^{-4} per cent of hydrogen, which is

greater than the theoretical solubility of hydrogen in pure iron at 1100°C., and is approximately twice as much as the hydrogen retained by the simple steels under similar conditions.

SUMMARY

Vacuum extraction at 800°C. is preferred to the vacuum-fusion method for the determination of small amounts of hydrogen, on the grounds of greater speed and precision. The accuracy of the method appears to be satisfactory. Results obtained are believed to be reliable for the hydrogen content of the sample at the time of the analysis, but there is no guarantee that the hydrogen content of the sample at the time of the analysis is the same as it was when the sample was taken or at some previous time in the history of the metal. Because the hydrogen content of steel fre-

quently is unstable and fugitive it is essential that the sampling and analysis be conducted as expeditiously as possible.

REFERENCES

1. T. Graham: *Proc. Royal Soc. (London)* (1866) **15**, 502.
2. F. Körber and H. Ploum: *Mitt. K-W-I. Eisenforsch. Düsseldorf* (1932) **14**, 229.
3. P. Bardenheuer and H. Ploum: *Mitt. K-W-I. Eisenforsch. Düsseldorf* (1934) **16**, 129.
4. H. A. Sloman: 8th Rept. on Heterogeneity of Steel Ingots, 43 Iron and Steel Inst. (1939).
5. W. C. Newell: *Jnl. Iron and Steel Inst.* (1940) **141**, 243.
6. V. C. F. Holm and J. G. Thompson: *Jnl. of Research Nat. Bur. Stds.* (1941) **26**, 245.
7. F. Pihlstrand: *Jernkonterets Ann.* (1937) **121**, 219.
8. E. Martin: *Archiv Eisenhüttenwesen* (1929) **3**, 407.
9. L. Luckemeyer-Hasse and H. Schenck: *Archiv Eisenhüttenwesen* (1932) **6**, 209.
10. A. Sieverts, G. Zapf and H. Moritz: *Ztsch. physik. Chem.* (1938) **183**, 19.

Determination of Hydrogen in Steel Sampling and Analysis, by Vacuum Extraction

BY R. M. SCAFE*

ALTHOUGH hydrogen has been intensively studied in its relation to steel quality, the methods of sampling and determinations are still open to question. It is true that various procedures have been proposed but actually there has not been sufficient agreement to establish a common base from which to work. As a result, it is difficult, to say the least, to correlate the reported results of some of the investigators in this field. The present symposium, premised on methods rather than effects, should prove of considerable value.

For the purpose of this discussion two methods of sampling and analysis will be considered. First, sampling of molten steel in the ingot mold by use of an evacuated tube and cylinder using conventional methods of analysis for the gases collected; second, analysis by vacuum extraction involving the use of heating equipment and the determination of the amount of hydrogen evolved from solid steel samples by measurement at reduced pressures. Both methods have been used at Duquesne Steel Works and it is believed that either may be used with considerable benefit if the limitations of each method are recognized.

EVACUATED TUBE AND CYLINDER

Sampling devices for gases in molten steel suggested by various investigators range from very cumbersome and complicated devices to the relatively simple evacuated tube and cylinder used by Soler for deter-

mining the CO content of the bath. This latter device was adopted (Fig. 1) and modified to meet conditions at Duquesne Works. The principal modifications were in placing the cylinder at the side of the tube and the use of a sleeve on the immersion end of the tube. The first modification was made so that the cylinder could be readily detached and taken to the laboratory; the second, because of the difficulty encountered in obtaining an airtight seal after sampling and because of our practice of re-using the tube.

Rigid control of the method of sampling and of the handling of the sample according to plan are of primary importance in hydrogen determinations. This applies to both the sampling of molten steel and the determination of the hydrogen content of cold steel samples.

Except for a few preliminary samples taken from spoons, all work on molten steels using the evacuated tube was confined to the sampling and analysis of molten steel during the pour. As mentioned, uniformity of sampling was a basic consideration. As a result, every effort was made to follow definite sampling techniques and procedures. These included control of the depth below the surface from which the sample was taken, the timing between the shutoff and taking of the sample, as well as maintenance and care of the equipment. The distance below the surface at which the sample was taken was readily controlled by means of a crosspiece and centering device attached to the tube. The steel was poured into the mold to the hot-top junction, the tube was then lowered into the

Manuscript received at the office of the Institute March 22, 1944.

* Metallurgical Inspector, Duquesne Steel Works, Carnegie-Illinois Steel Corporation, Duquesne, Pennsylvania.



FIG. 1.—SAMPLING DEVICE BASED ON SOLER TECHNIQUE.

mold so that the sealed end entered to a depth of 3 to 4 in. in the molten metal.

After sampling, the entire unit was allowed to cool and then taken to the laboratory for gas analysis by the standard methods adopted by U. S. Steel Corporation chemists. Two samples were usually analyzed and a practice was adopted of discarding those samples showing the presence of a considerable amount of oxygen.

In order to check the reproducibility of results, a special unit was used, consisting of two tubes and containers attached together in such manner that they could be lowered into the mold simultaneously to the same depth and at the same distance from the respective mold walls. As an example of the reproducibility, the analysis of the two samples gave hydrogen values of 0.0016 per cent and 0.0018 per cent by weight.

Samples were taken from various grades of steel covering a range from low-carbon rimming grades to high-carbon killed and fine-grained steels. Hydrogen content varied from a 0.0008 per cent in a 0.08 per cent carbon rimmed steel to 0.0033 per cent in a fine-grained 0.52 per cent carbon open-hearth steel. Hydrogen content varied in killed steels between 0.0009 and 0.0033 per cent. These represent the relative hydrogen contents of the steels involved, in percentages by weight. The samples were taken during pouring and the hydrogen reported is the amount collected in a vacuum above the sample during solidification. The gas thus collected, however, does not contain all the hydrogen of the steel. There still remains a substantial percentage of gas in the solid steel sample in the tube. We did not know how much of the hydrogen collected in vacuum in this manner was the hydrogen that ordinarily would diffuse during solidification.

During our investigation of the hydrogen content of molten steel by the Soler method, efforts were also directed to

developing suitable equipment for determining the hydrogen content of cold steel samples, which would be dependable and at the same time sufficiently flexible to be

producing results. The apparatus consisted of a heat-resistant glass tube mounted vertically, a heating unit, potentiometer and a supporting frame. The tube was

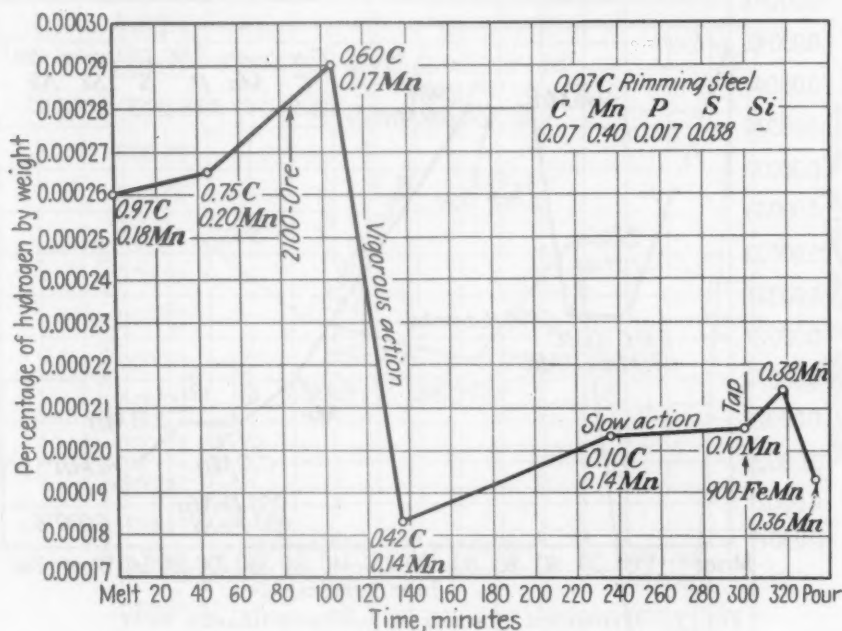


FIG. 2.—HYDROGEN CONTENT OF AN OPEN-HEARTH HEAT.

used during any phase of steelmaking operations. Various methods, including vacuum fusion and combustion, were considered. These were rejected in favor of a method requiring a minimum of equipment operating at a comparatively low temperature, largely based on the work of Newell and others as described in publications of the Iron and Steel Institute. Briefly, the apparatus was evacuated, the steel sample was heated to the desired temperature (approximately 600°C.) and the gas collected was removed from the vacuum system and suitably measured.

TORRICELLIAN VACUUM APPARATUS

It was suggested by Philip Schane, Jr., then Chief Metallurgist of the Duquesne Steel Works, that Torricellian vacuum should prove satisfactory. Experimental apparatus was built, which was as simple as possible consistent with reliable and re-

closed at the bottom with a rubber stopper into which was inserted a small-bore glass tube. To this tube was attached a rubber pressure tube attached to a pear-shaped leveling bulb containing a suitable amount of mercury. The upper end of the heat-resistant tube was drawn in, calibrated and closed with a glass stopcock. The sample was placed on a glass elevator and placed in the tube. The system was closed and the mercury was raised and lowered, forcing all air out of the tube. A scale was used to measure the various mercury levels to furnish barometer and pressure readings necessary for calculation of the results. The unit was heated by a Hevi-Duty hinged furnace, 9 in. high, with a maximum temperature of 1850°F.

This furnace was modified by attaching a permanent thermocouple through the furnace wall, the temperature at this point being calibrated to that determined by

the use of a standard thermocouple inserted in the glass tube directly opposite the permanent one.

A later and more satisfactory unit is

method is dependable and flexible. Numerous blanks were run with practically 100 per cent negative results with reference to hydrogen present, and duplicable results

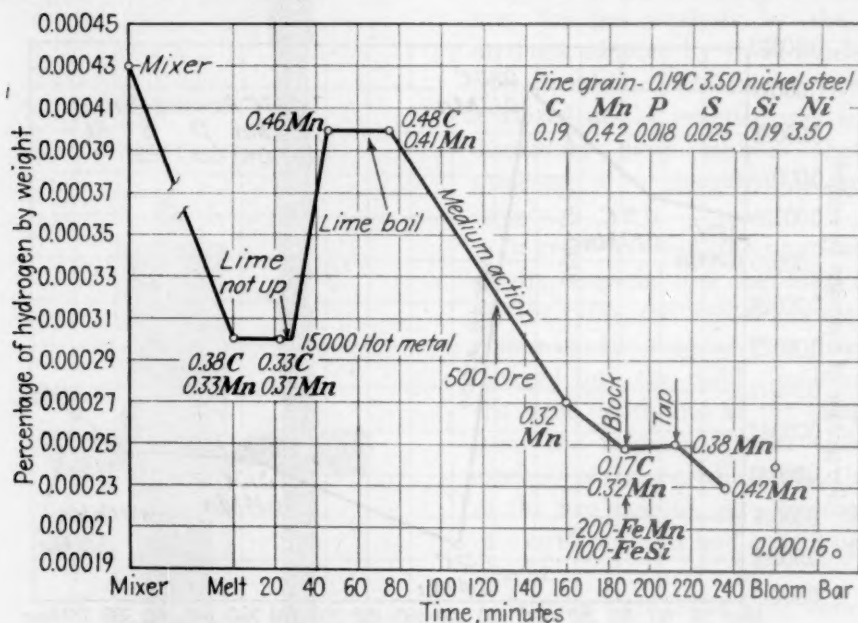


FIG. 3.—HYDROGEN CONTENT OF AN OPEN-HEARTH HEAT.

described by W. D. Brown, who designed it, on pages 381 to 384.

Samples were taken during the working of various open-hearth heats from melt-down to tap and again at the pouring platform. Several types of samples were taken before standardizing on a sample cut from a specimen cast in a standard carbometer test mold. Samples were carefully sawed to give a weight of approximately 30 grams. Surface defects and scale were removed by filing. The sample was weighed, washed in ether and then placed in a desiccator for later analysis. Samples were also taken from bloom and bar product during various stages of reduction by cutting a suitably sized sample. A canister-type desiccator for carrying samples from one point to another has been suggested as being advisable.

If it can be assumed that heating at approximately 1000°F. removed all the hydrogen, our results indicate that this

within 0.00001 per cent were obtained. However, it was found to be necessary to discard numerous samples because of the considerable difficulty encountered in maintaining leakproof conditions. Briefly, any sample showing signs of discoloration or any degree of oxidation after heating was discarded. Because of the difficulty of maintaining leakproof equipment, it was decided that it was necessary to construct new equipment (see page 381). Results from the new apparatus correspond closely with those from the equipment described in the foregoing paragraphs, with the added merit that the equipment is much more dependable in operation.

Validity of results obtained by this apparatus is demonstrated by the following data from five lots of samples from the same piece: (1) 0.00036 per cent H_2 ; (2) 0.00035 per cent H_2 ; (3) 0.00036 per cent H_2 ; (4) 0.00037 per cent H_2 ; (5) 0.00035 per cent H_2 .

HYDROGEN CONTENT

It is well to emphasize that in no case do we claim that the hydrogen value obtained is the absolute hydrogen. How-

steels, are generally recognized. It has been suggested that there is a relation between the hydrogen content of a steel and the surface conditions. A study of this possible

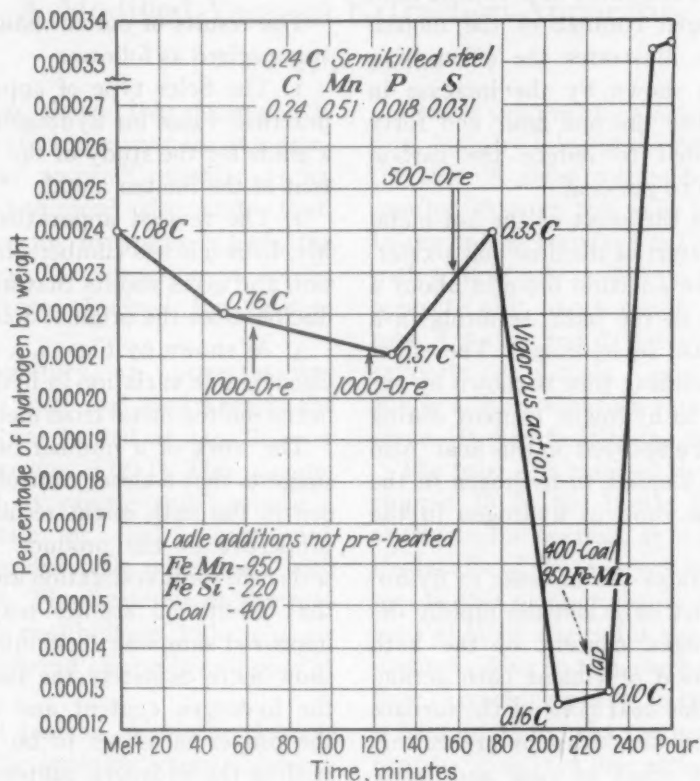


FIG. 4.—HYDROGEN CONTENT OF AN OPEN-HEARTH HEAT.

ever, we are convinced that the relative value obtained, which is reproducible, provides a practical means of indicating the hydrogen value for steel during various steps in processing.

Our investigation at Duquesne Works was inaugurated to determine the factors that influence hydrogen content of steel and its possible effect on surface quality. Everyone who has made any study of the factors affecting surface quality will recognize the inherent difficulty in allocating to any one factor its relative importance. The harmful effect of minute subsurface blowholes, the oxidizing action of particles or droplets of steel adhering to mold walls, the effect of high-sulphur fuels on surface quality of certain grades of

relation continues, but apart from some few confirmatory observations, much of the study has to be done and may be the subject of a future report.

We are often asked what can be done to eliminate or at least reduce the hydrogen that is present in steel. At the present time we know of no means of accomplishing this, although it is possible that some of the more reactive materials may be helpful. On the other hand, definite steps were taken during the course of this work to reduce the amount of hydrogen introduced into the steel by predrying of material in charge and in furnace and ladle additions.

The hydrogen values obtained during the various stages of processing are best illustrated by the three graphs showing the

hydrogen value plotted against time from melt to pour (Figs. 2 to 4). In Fig. 3 results of tests on the bloom and finished bar are given also.

Fig. 2 shows the effect of a violent bath on the hydrogen content of the molten metal. It also illustrates the effect of a quiet bath as shown by the increase in hydrogen during the one hour and forty minutes required to reduce the carbon from 0.42 to 0.10 per cent.

Fig. 3 shows the effect of the hot-metal addition. The start of the lime boil accelerated by the ore addition brought about a violent action in the bath, resulting in a decided decrease in hydrogen. The effect of increased blocking time is shown by the upward trend in hydrogen content during the short block employed on this heat. Also plotted is the increase in hydrogen in the bloom and the drop in hydrogen in the finished bar.

Fig. 4 illustrates the increase in hydrogen with a quiet bath and the rapidly decreasing hydrogen content of the bath during the period of violent bath action. Note that in this heat none of the furnace or ladle addition were dried by preheating. The combined effect of coal and ferro-

manganese in the ladle is well illustrated by the sharp increase in hydrogen from tap to pour.

SUMMARY

The results of our investigation may be summarized as follows:

1. The Soler type of apparatus gives a practical value for hydrogen and provides a guide for the study of the hydrogen content of the molten metal.

2. The revised apparatus described by Mr. Brown is less cumbersome in its operation and gives results that are more reproducible than the original Soler technique.

3. As shown by Figs. 2, 3 and 4, there is considerable variation in hydrogen content in the molten metal from melt down to tap.

The work of a number of investigators suggests that a closer control of the hydrogen in the bath might result in enhanced properties in the product. This offers a wide field for investigation and it is possible that additional studies may develop an improved sampling technique and thereby show more definitely the factors affecting the hydrogen content and thus point to the proper measures to be taken in controlling the hydrogen content of the steel.

A Modified Vacuum Extraction Apparatus

By W. D. BROWN*

NEWELL¹ has shown that hydrogen is removed from steel in a vacuum at a temperature of 500° to 900°C. within 1½ hr. Holm and Thompson² also state that, especially when the hydrogen is high, the results obtained by extraction at 800°C. agree with those obtained by vacuum fusion.

In this laboratory, an apparatus was designed (Oct. 1940) and used wherein the piece of steel was heated at 1100°F. in a Torricellian vacuum (Fig. 1). This vacuum was produced by raising and lowering a "leveling bottle or bulb" containing mercury. Extensive tests were made with this apparatus. The weakness of the procedure was the possibility of leakage of air into the tube around the rubber stopper at the bottom.

The present plan is to raise and lower the mercury by applying vacuum from a mechanical pump, to the top of the tube and then to a bottle of mercury in which the bottom of the tube is immersed.

THE APPARATUS

The extraction is made in a Pyrex tube *A*, 1 in. i.d. It is drawn down at the top at *N* and an 8-mm. i.d. tube is welded on it. To this a Pyrex stopcock *E*, 4-mm. bore, is welded. The tube between *N* and *E* is preferably 8 in. long and is graduated in milliliters. The total length of *A* to the stopcock is 28 inches.

Heat is supplied by a split-tube furnace, 9 in. long by 6 in. in diameter, hinged on the side. A short pyrometer couple *P* is inserted through the walls of the furnace. In use this is standardized by comparison with a standard couple in a 1-in. tube, just opposite this short couple. In the 1-in. tube *A* a glass rod *R*, flattened at one end, supports the sample *S* and the length of *R* is so adjusted that the sample is in proper place. (It may float in the mercury.)

The tube *A* is inserted in a large rubber stopper to fit the bottle *B* and extends nearly to the bottom. It is so placed that the handle of the stopcock faces the operator. In this stopper also is a short tube *D* bent at right angles for the application of vacuum. Also in this stopper is an 8-mm. tube *C* reaching nearly to the bottom; this is bent so as to miss the heater and again bent to bring it in line with and as near as possible to the upper and reduced part of tube *A*. On this tube *C* is welded a 4-mm.-bore stopcock *H*. In order that the two tubes may be as near as possible, the handle of stopcock *H* faces the back, or is the reverse of stopcock *E*. The total height of *H* above the bottom is 28 in. As explained later, this is the pressure-measuring tube *C*. The bottle *B* is about half full of mercury. The mercury must cover the ends of *A* and *C* by about 1 in. when they are evacuated. By tees *T* and rubber tubing *RT* the tubes *A*, *C* and *D*, the latter through the three-way stopcock *M*, are connected to the vacuum pump.

A sheet of asbestos at *K* prevents the stopcocks *E* and *H* from becoming so hot that they leak. A good grade of vacuum lubricant prevents leakage of *E* and *H*.

In order to measure the pressure of the

Manuscript received at the office of the Institute March 8, 1944.

* Chief Chemist, Duquesne Steel Works, Carnegie-Illinois Steel Corporation, Duquesne, Pennsylvania.

¹ *Jnl. Iron and Steel Inst.* (1940) 141, 243.

² *Jnl. of Research, Nat. Bur. Stds.* (1941) 26, 245.

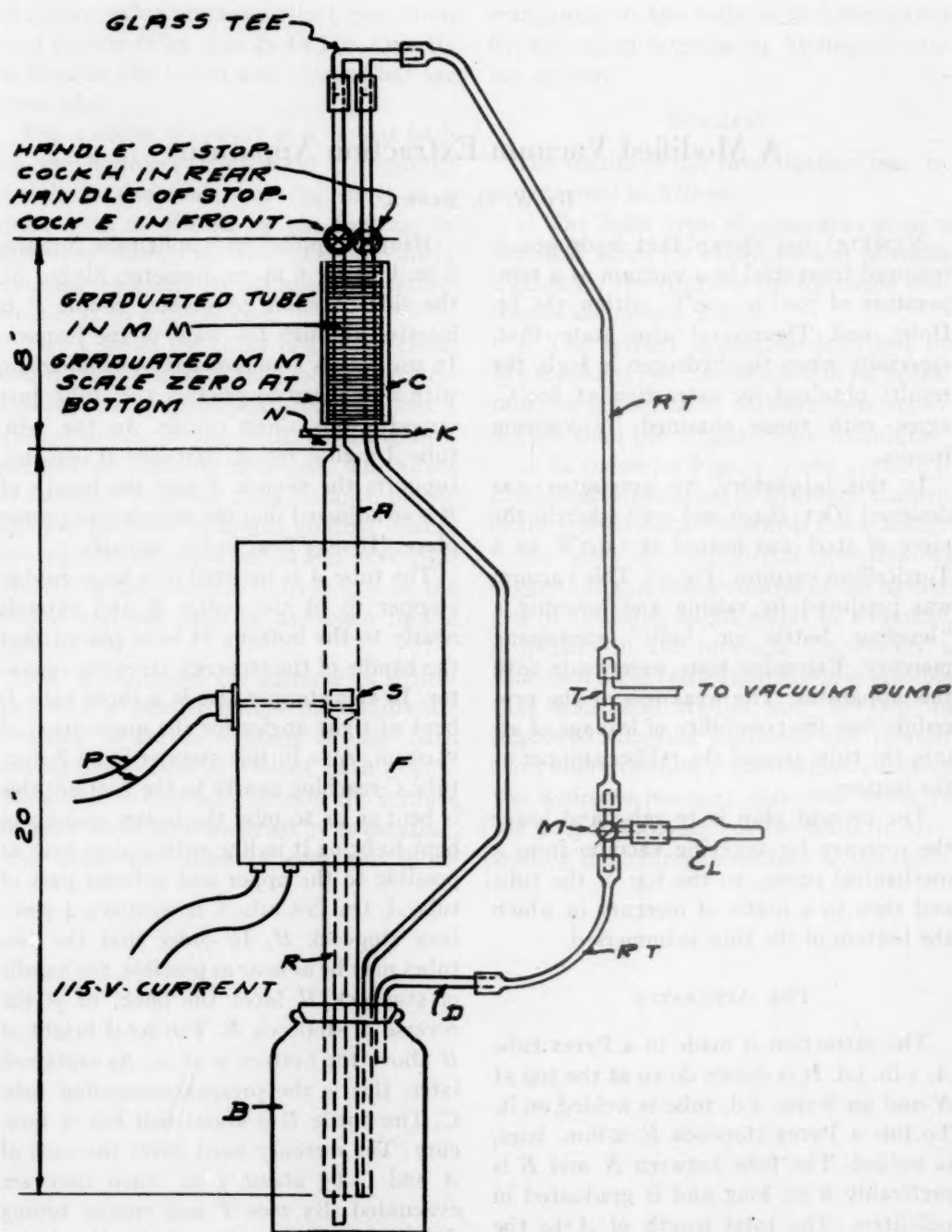


FIG. 1.—TORRICELLIAN VACUUM APPARATUS.
Developed by W. D. Brown, of Duquesne Works, Nov. 16, 1943.

gas extracted, use is made of a millimeter scale placed back of the tubes *A* and *C*.

THE PROCEDURE

Prepare the sample, a piece preferably $\frac{1}{2}$ -in. cube, by filing off sharp corners. Wash it in ether and, with tweezers, place it in desiccator until ready for use. Remove the 2-in. rubber stopper holding the extraction tube *A*, the measuring tube *C*, and the suction tube *D*. Using tweezers, place the sample *S* on the flattened end of the glass rod *R* and insert into the tube *A*. Insert the rubber stopper in the bottle. The sample should be opposite the pyrometer *P*, the rod possibly floating in the mercury. Change the length of the rod *R* until the sample is at *P*, if necessary.

Turn stopcock *M* to connect *D* through the calcium chloride tube *L* to the air and to shutoff vacuum. Open stopcock *E* and *H* and start the pump going. Mercury will be drawn up into tubes *A* and *C*. Care must be exercised that the sample *S* shall not rise too fast and break the tube *A* at *N*. This can be regulated by *E* or *M*. When the mercury has risen slightly above the stopcocks *E* and *H*, close the stopcocks.

Then turn *M* to connect *D* but not *L*. The mercury will be drawn down into the bottle *B*, leaving tubes *A* and *C* vacuum. However, there will be a small amount of air in *A*. To remove this, turn *M* slowly to close off vacuum and to connect *D* to *L*, thus allowing air to enter *B*. Mercury will rise in *A* and *C* (use care that it does not rise too fast) to or nearly to the stopcock. Open stopcocks *E* and *H* to evacuate any air. Then turn *M* to connect vacuum to bottle, thus drawing the mercury down. This should be repeated but tests have shown that one outgasing is sufficient.

Close the switch and heat the sample up to 950° to 1000° as shown by pyrometer *P*. By means of resistance not shown, keep the temperature at this point for 2 hours.

After this time open the switch, then open the furnace and move the bottle *B*

and tube *A* out of the groove. Place shields of asbestos between the tube *A* and the halves of the furnace. After the tube has cooled somewhat, air may be blown on it until it is cool to the hand.

Slowly turn stopcock *M* to connect with *L* and shut off the vacuum. The mercury will slowly rise in *A*. When the mercury rises to a definite point, say 6 ml., in the small part of *A*, turn *M* to hold it.

The mercury in tube *C* will be higher than that in *A*. On the millimeter scale back of *A* and *C*, read the difference in height between the mercury level of the two tubes. This is the pressure on the hydrogen gas in *A*.

CALCULATION OF RESULTS

Weight.—The weight of 1 liter of H_2 at 60°F. and 30 in. is given as 0.08526 gram, from which the weight at 80°F. and 760 mm. is 0.08188 gram and 1 ml. weighs 0.00008188 gram. From this, 1 ml. at 1 mm. pressure weighs 0.000000108 gram. At 70°F., 1 ml. weighs 0.00000011 gram. In our calculations, we use 0.00000011 gram.

In our calculation, multiply the number of milliliters of gas in *A* by the millimeters pressure and by 0.00000011, and divide by the weight of sample, and multiply by 100 to obtain percentage. Example: 6 ml. at 53 mm. pressure, weight of sample 16.5 grams H_2 in sample:

$$\frac{0.00000011 \times 6 \times 53 \times 100}{16.5} = 0.00021 \text{ per cent}$$

Capacity.—If the capacity of the small part of *A* is 6 ml. and the difference between the 6-ml. level and the height of stopcock *H* is 140 mm., the capacity with this method of measuring is 0.000092 gram H_2 , which is 0.00046 per cent on 20 grams. If the capacity is not sufficient, the small part of *A* may be lengthened to increase capacity, or by lowering *N* in reference to *H*, the possible difference in height between *N*

on *A* and *H* may be lengthened. There is always the alternative of permitting air to enter *B* freely and measuring the height of mercury in *A* above that in *B*, and comparing this with the barometer pressure.

Results obtained have been from 0.00007 to 0.00033 per cent. Duplicate samples check within 0.00001 per cent, or one point in the fifth decimal. While the usual practice is 2 hr. hot evacuation, some results on duplicate samples indicate that all the gas is evacuated in 1½ hr. On tests run without steel samples the gas obtained was from zero to 1 ml. at 2 mm. pressure, which would equal 0.000001 per cent.

It may be argued that after some gas comes off, the steel is not in a vacuum. For example, at the end of a determination the volume of gas is measured as 6 ml. at 40 mm. pressure (70°F.). Since the capacity of the tube is about 240 ml., the gas pressure in the tube when mercury is down is about 1 to 2 mm. To prove that this pres-

sure does not prevent the evacuation of the hydrogen, a sample was evacuated and cooled, the gas was expelled and the sample again evacuated at 1000°F. for 2 hr. No gas was obtained on this second evacuation.

CONCLUSION

As noted above, the steel is heated at 1000°F. (538°C.) for 2 hr. Newell shows the extraction practically complete in 1½ hr. even at 400°C. Best results were obtained 600°C. (1112°F.), but we found that 1100°F. is about the highest temperature that the Pyrex tubing will stand; at any increase or, possible, on repeated heatings at 1100°, the tube will collapse under vacuum. Apparently the tube will stand 1000°F., and we have shown by several tests that after heating for 2 hr., then cooling and measuring, and again heating, cooling and measuring, no increase in gas was obtained.

Determination of Hydrogen by Vacuum Extraction and Tin Fusion

BY JOHN NAUGHTON*

At the General Electric Research Laboratories, we have been interested in the iron-manganese system and the effect of hydrogen on the properties of these alloys.

The apparatus used is shown in Fig. 1. The design is a modification of the apparatus described by Holm and Thompson.²

To limit loss of hydrogen, samples are

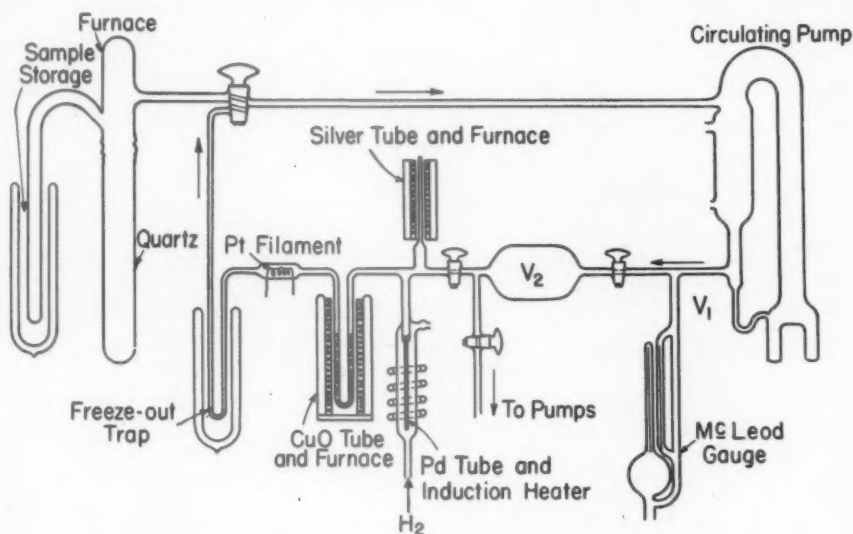


FIG. 1.—HOT EXTRACTION AND ANALYSIS SYSTEM.

Dr. H. H. Uhlig previously has presented some of these results.¹ We wish now to offer some other of the data that have a bearing on the subject of this symposium.

In the determination of hydrogen in the iron-manganese system by any heating method we are presented with the problem of the evaporation of volatile manganese and the consequent adsorption of hydrogen by this evaporated metal. It seems wise, therefore, to extract gas at as low a temperature as feasible. Consequently we chose the vacuum or hot extraction method for the analyses of these alloys.

Manuscript received at the office of the Institute Feb. 22, 1944.

* General Electric Research Laboratories, Schenectady, New York.

¹ References are on page 389.

stored in a chamber immersed in liquid air. We recommend this procedure whenever there is a question of loss of hydrogen at room temperature. Thence they are moved to the quartz furnace by means of a small magnet, where they are heated by induction to 700° to 800°C. The extracted gas is removed by the circulating pump and placed in the known volume V_1 (or V_2). The circulating pump has been described.³ It is so designed that in spite of the fact that the outlet portion of the pump is part of the known volume, this volume is affected neither by the speed of pumping nor by the pressure of stored gas. The pump also serves to circulate the gases for analysis.

The analytical system consists of a

quartz tube containing CuO, a platinum filament and a quartz freeze-out trap. The CuO tube may be heated by means of a

included are a silver tube, which, when heated to about 800°C., readily permits diffusion of oxygen from the air and admits

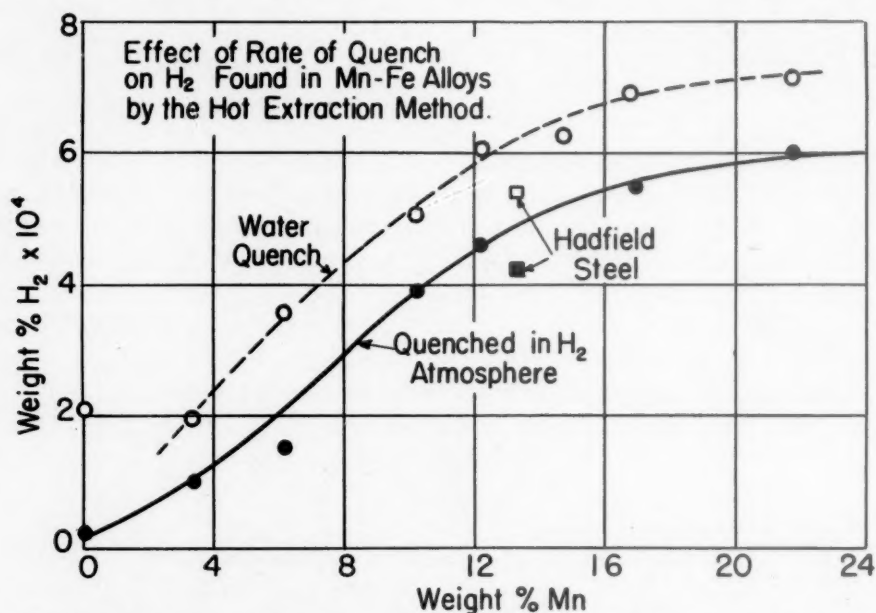


FIG. 2.—EFFECT OF RATE OF QUENCH ON HYDROGEN FOUND IN MANGANESE-IRON ALLOYS BY THE HOT EXTRACTION METHOD.

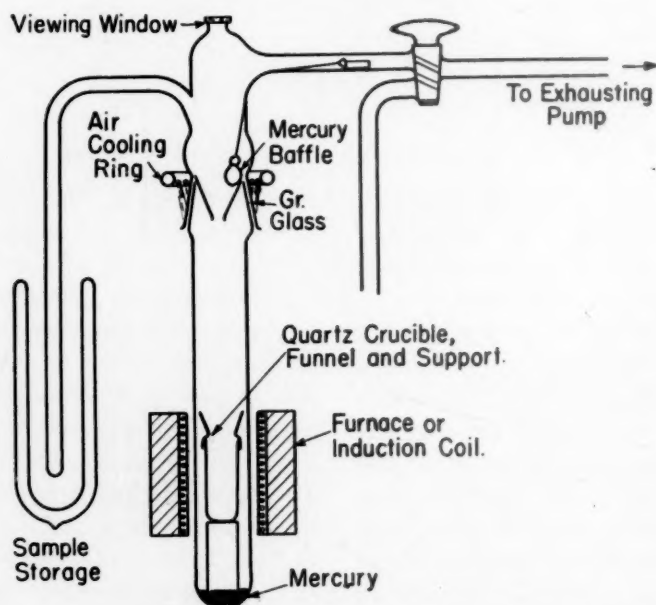


FIG. 3.—FURNACE FOR USE IN TIN-FUSION ANALYSIS FOR HYDROGEN.

furnace to any appropriate temperature for reaction, or cooled and rendered inactive by immersing in cold water. Also in-

it as pure gas to the system; and a palladium tube that acts in a similar way for the purification and admission of hydrogen.

Water vapor and CO_2 are frozen out in the trap by solid CO_2 -acetone and liquid nitrogen, respectively. We then analyze for hydrogen by oxidation in the CuO tube at 300°C . and subsequent freezing out of the resultant water vapor by means of solid CO_2 -acetone. The pressure decrease in the known volume gives a measure of the quantity of gas present. It has been suggested⁴ that quantities of hydrogen present in the samples might escape as methane. It has also been noted⁵ that analysis for methane in such a system as this, by combustion of the methane in the presence of excess oxygen, leads to inconclusive results because of oxidation of the platinum filaments used in the combustion. We have found, however, that the trouble was not platinum but the result of oxidation of mercury vapor present throughout the system. If this vapor was excluded from the vicinity of the hot platinum by low-temperature traps before and after the filament, no trouble was encountered and methane introduced into the system could be accounted for quantitatively. Methane was not found in the gases obtained by hot extraction.

The iron-manganese specimens were cylindrical in shape, 2 in. long and 150 mils in diameter. Hydrogen was introduced into the specimens by heating at 1000°C . for 2 hr. in a quartz tube through which a stream of purified hydrogen continuously passed. Quenching was accomplished in some cases (i.e., hydrogen quenched) by plunging the quartz tube containing the specimens into water. The hydrogen flow was maintained through the tube during the quench. Other specimens were quenched somewhat more rapidly by being dropped directly out of the hot quartz tube into the water (i.e., water quenched).

In Fig. 2 is plotted the hydrogen retained by iron-manganese alloys as a function of the manganese content. The effect of rate of quench on hydrogen retained is also shown. These curves well

illustrate the difference between ferrite and austenite with respect to the diffusion and solubility of hydrogen. In an alloy that retains its austenitic structure during

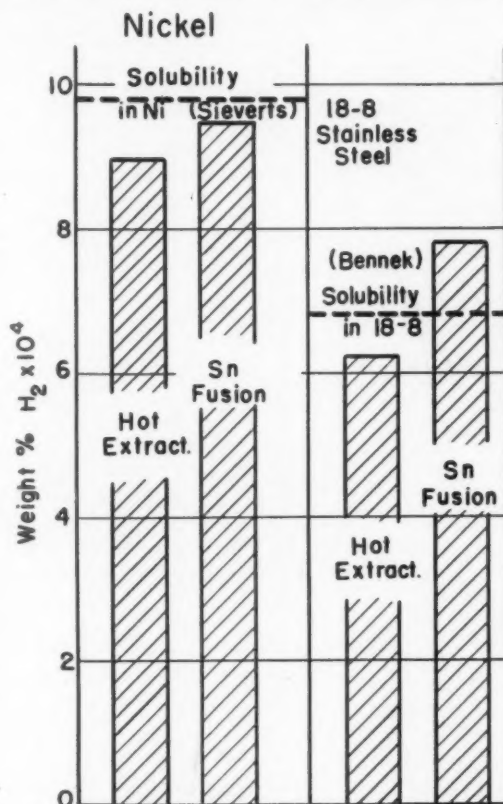


FIG. 4.—COMPARISON OF HYDROGEN FOUND BY TIN FUSION WITH AMOUNT FOUND BY HOT EXTRACTION FOR NICKEL AND 18-8 STAINLESS STEEL.

quenching until a low temperature is reached, one would expect a comparatively large amount of hydrogen retained, because of the high solubility of hydrogen and low rate of diffusion in the austenitic phase. This is illustrated by the alloys high in manganese content.

On the other hand, with an alloy that changes to the ferritic structure at a high temperature, we would expect greater loss and less retention of hydrogen when the specimen finally reaches room temperature, because of the comparatively lower solubility of hydrogen in this phase and greater rate of diffusion. This is, in turn, illustrated

by the alloys of lower manganese content. Both lattice types behave as would be expected.

It also follows from this that a more

X-ray. The hexagonal and face-centered cubic lattice make their appearance in alloys above 12 per cent in manganese content.

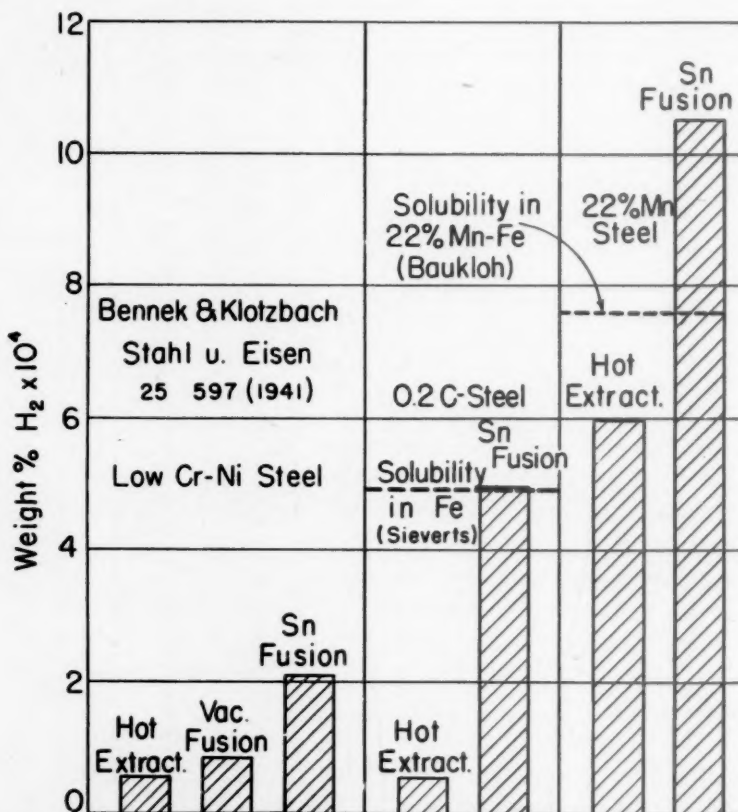


FIG. 5.—COMPARISON OF HYDROGEN FOUND BY TIN FUSION WITH AMOUNT FOUND BY HOT EXTRACTION FOR LOW-CARBON STEEL AND 22 PER CENT MANGANESE-IRON ALLOY. Results of Bennek and Klotzbach on low-chromium-nickel steel are also shown.

rapid rate of cooling should appreciably increase the hydrogen retained by these alloys. Such an increase in cooling rate is accomplished by the water quench outlined, and the consequent increase in hydrogen found in the samples is shown in the upper curve of Fig. 2.

Of great importance is the loss of hydrogen from samples on standing at room temperature and the effect of the relative proportions of austenite, ferrite and other phases. In this series of alloys those below 14 per cent manganese are found to contain mostly ferrite, whereas those above contain little if any of this phase as detected by

In conformity with what has been reported previously, it was found that alloys comparatively high in austenite (i.e., above 14 per cent manganese) tend to retain their hydrogen even after long periods, a fact also checked for Hadfield manganese steel, whereas alloys in which ferrite is present tend to lose hydrogen at a more rapid rate.

TIN-FUSION METHOD FOR DETERMINATION OF HYDROGEN

Aside from these few results with the hot extraction method for hydrogen determination, we also wish to present a few pre-

liminary results on a modified fusion method, which we shall call the "tin-fusion method."

Reeve,⁶ in his early work using tin as a flux in the fractional vacuum-fusion method for oxygen, noted that the hydrogen found by this method was higher than the values found by the conventional vacuum fusion. More recently Bennek and Klotzbach⁷ have claimed that the best method for removing all the hydrogen from a sample is by fusion with tin.

To further test these experiments we designed the furnace shown in Fig. 3. A silica crucible was used, and for degassing, a platinum-wound furnace could be placed around the large quartz tube of the furnace proper. This could, in turn, be replaced by the coil of the high-frequency generator. It is widely recognized that, in systems such as this, evaporation of metal (mostly tin) occurs, with condensation on cooler parts of the apparatus. In the course of condensation, the metal occludes within itself an appreciable portion of the gases present. A small amount of mercury placed in the bottom of the furnace was found to be helpful in that it condensed on the cooler parts of the walls of the furnace, amalgamated with and washed down the tin, and released any entrapped hydrogen. Any coating of metal not so affected could also be heated and the entrapped gas released, a method adopted by Bennek and Klotzbach.

COMPARISON OF METHODS

The comparison of the hydrogen content of metals by hot extraction with that found by tin fusion is shown in Figs. 4 and 5. These samples were subjected to the hydrogen treatment and quench described for the iron-manganese system. The results for nickel and 18-8 stainless steel (Fig. 4) show a slight increase in hydrogen as determined by tin fusion but nothing that is very startling. The results found by Bennek and Klotzbach are indicated in Fig. 5 along with some other of our results on low-car-

bon steel and high-manganese iron. Here the differences are of definite significance and, in conformity with the results of Bennek and Klotzbach, cast doubt on the reliability of results obtained by the hot extraction method.

We present the results of the tin-fusion method for hydrogen determination without any attempt at explanation. We believe that they indicate the basic need for further research to find the one simple method that will reveal the entire amount of hydrogen present in any sample of steel.

REFERENCES

1. H. H. Uhlig: *Trans. A.I.M.E.* (1944) **158**, 183.
2. V. C. F. Holm and J. G. Thompson: *Jnl. of Research, Nat. Bur. Stds.* (1941) **26**, 245.
3. J. J. Naughton and H. H. Uhlig: *Ind. and Eng. Chem., Anal. Ed.* (1943) **15**, 750.
4. F. Korber and H. Ploum: *Mitt. K-W-I. Eisenforschung* (1932) **14**, 229.
5. C. H. Prescott, Jr., and James Morrison: *Ind. and Eng. Chem., Anal. Ed.* (1939) **11**, 230.
6. L. Reeve: *Trans. A.I.M.E.* (1934) **113**, 82.
7. V. H. Bennek and G. Klotzbach: *Stahl und Eisen* (1941) **61**, 597.

DISCUSSION

B. M. LARSEN.*—The U. S. Steel Corporation Research Laboratory's work on the determination of hydrogen in samples taken from liquid steel in the furnace has been very preliminary in character, but a few remarks here may contribute a little to the developing picture of this yet unsolved problem. The sampling of liquid steel for H₂ analysis is uncertain because of the possible loss of gas by diffusion during sampling. Some small loss is probably inevitable with any method at present visualized. We have used mainly spoon sampling into carbometer molds (producing cast rods about 1/2-in. diameter), analyzing these by vacuum extraction at 500° to 650°C. The few results obtained vary in the range of about 4 to 10 c.c. H₂ per 100 grams Fe, which seems reasonable for metal in the open-hearth bath, but whether the sampling loss is consistent at around 3 to 8 per cent, or may run up to 20 to 30 per cent, we cannot be certain. We have developed a special "bomb" type

* Research Laboratory, U. S. Steel Corporation, Kearny, N. J.

mold to be immersed in the bath and plan to make a comparison of this with spoon sampling technique sometime in the future.

From experience in the laboratory we now believe that the most practical method for the open-hearth shop would be to obtain a small casting, a part of which is a $\frac{3}{8}$ to $\frac{1}{2}$ -in. cast rod, from the bath by one of the above methods, cooling the sample in ice water as quickly as possible and cleaning it with alcohol and ether. A piece of rod of around 30 to 50 grams in weight should then be broken off and quickly immersed under mercury in collecting tubes. By warming the mercury to about 175°C . overnight (10 to 15 hr.), practically all the hydrogen is removed, and may be measured very easily by observing its pressure and volume. Although the last traces of hydrogen may then be re-

moved by a vacuum extraction method, the results have indicated that this simple method yields 70 to 80 per cent H_2 on very low H_2 samples and about 95 per cent or more of the total on samples having the amounts usually found in liquid steel in the open-hearth bath.

It is important to begin collecting the gas as soon as possible, since an overnight period may lose around $\frac{1}{2}$ of the H_2 in such small pieces at room temperature and an appreciable percentage even in a freezing chamber. Also, pieces broken from a casting should not be allowed to stand in moist air; we have observed moisture evolution from such pieces, equivalent to much more than the original H_2 content, due to water vapor adsorbed in the tiny shrinkage cavities exposed on the broken surface of the cast metal.

Determining the Hydrogen Content of Molten Steel by Vacuum Extraction

BY C. B. POST* AND D. G. SCHOFFSTALL*

A determination of the hydrogen content of molten steel by means of the vacuum-extraction method, as reported here, consists in first casting a sample of the bath in a bomb, so that the gases evolved during solidification are trapped for analysis. A portion of the cast steel sample is then prepared and heated at a temperature of 600° to 800°C . under high vacuum, and the gases given off during this vacuum extraction (which are shown to be hydrogen), are collected and measured. Analysis of the gases evolved on solidification and the gases in the solid sample enables an accurate determination of hydrogen in the molten steel.

Fig. 1 shows the bomb and accessories that have been found suitable for trapping the gases evolved on solidification. The bomb is made of seamless steel pipe, approximately 7 in. long by $1\frac{1}{2}$ in. i.d., and welded at the bottom. An ordinary

pipe cap has a vacuum-type metal stop-cock threaded and brazed in its upper end. This pipe cap fits onto the bomb by means of machined threads. A flange is brazed to the pipe at the point where the cap starts to tighten up, and a rubber gasket is placed between the flange and cap. Heavy vacuum grease is used between the flange and gasket and the gasket and cap. The weight of the complete bomb and its interval volume is known before the sample is cast. In practice, a sample of about 400 grams of steel is poured into the bomb, the funnel quickly swung out of the way, the bomb cap spun down the threads and tightened against the gasket, and the bomb set in a pail of water to keep the gasket and vacuum grease cool. It is estimated that at least 80 per cent of the gases evolved from the liquid sample during solidification are trapped in the bomb.*

* Actually only a small percentage of hydrogen is evolved from stainless steels and high-alloy steels during solidification, the greater part of the hydrogen being retained in solid solution, or in solid solution and gas blowholes, depending on the magnitude of the hydrogen content.

Manuscript received at the office of the Institute March 8, 1944.

* Metallurgical Department, The Carpenter Steel Co., Reading, Pennsylvania.

After cooling to room temperature, the partial pressure of the gases in the bomb are measured by attaching the bomb to a capillary U-tube mercury manometer. The bomb is weighed and the increase in weight converted into volume occupied by the steel sample in the bomb. The gases are reduced to atmospheric pressure by inversion of the bomb over brine. After this, a portion of the gas is drawn into a Shepherd gas-analysis apparatus and the hydrogen content determined. These data yield the cubic centimeters of hydrogen at normal temperature and pressure per 100 grams of sample evolved during solidification.

Following this analysis, the steel sample is taken out, and a sample slug, approximately one cubic centimeter in volume, and weighing about 8 to 14 grams, is cut from the center of the slug.

The second step in the analysis is the determination of the hydrogen content of this sample specimen. If a sample of carefully cleaned steel is heated to approximately 600° to 800°C. in a high vacuum, and this high vacuum is maintained by pulling off the evolved gases, approximately 95 to 98 per cent of the evolved gas is hydrogen. The apparatus used in this step of the analysis is very similar to that described by W. C. Newell.¹

Fig. 2 shows a schematic drawing and Fig. 3 is a photograph of the apparatus in use in these laboratories. Note that the system has a mercury diffusion pump between the heating chamber and the calibrated bulbs. This enables a pressure of 10^{-4} mm. or less to be maintained in the heating chamber against a pressure of 5×10^{-2} mm. on the calibrated bulb side of the system. The mercury lift for transferring the samples into the heating chamber is convenient, since it enables about 15 samples to be run consecutively without breaking the vacuum of the system.

The leak rate for the system when the

main stopcock is closed is about 0.5 microns per minute when the heating chamber and small platform is at a temperature of about 600°C. This is frequently

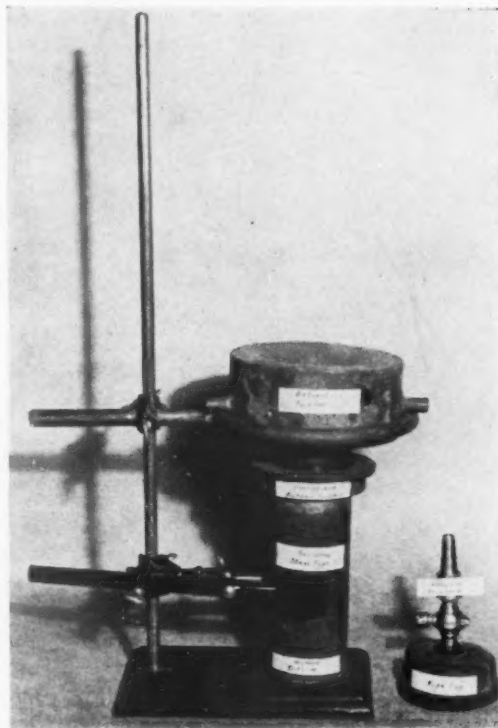


FIG. 1.—BOMB AND ACCESSORIES FOR CASTING SAMPLES FOR HYDROGEN DETERMINATION.

checked and is used to make an almost negligible correction to the amount of gas evolved from the samples.

The gases evolved are "pushed" to the left-hand side of the system by means of the mercury diffusion pump, and the gases are collected in the calibrated bulbs by flushing the 500 c.c. compression bulb with mercury. The gas-collection bulbs are calibrated so that by reading to the top of the arm of mercury the volume in cubic centimeters of gas at normal temperature and pressure is obtained.

At a temperature of 600°C. in the heating chamber, it has been found that about 30 min. of heating is required to extract the hydrogen from low-alloy steels and straight chromium-iron stainless steels, and about

¹ W. C. Newell: *Jnl. Iron and Steel Inst.* (1940) 141, 243-253.

40 min. to one hour for the chromium-nickel stainless and high-nickel steels, such as 36 to 80 per cent nickel.

A gas analysis is not performed on the

concerning a spectroscopic analysis of the gases evolved are submitted as verification of the fact that hydrogen is the principal gas extracted from clean steel and alloy

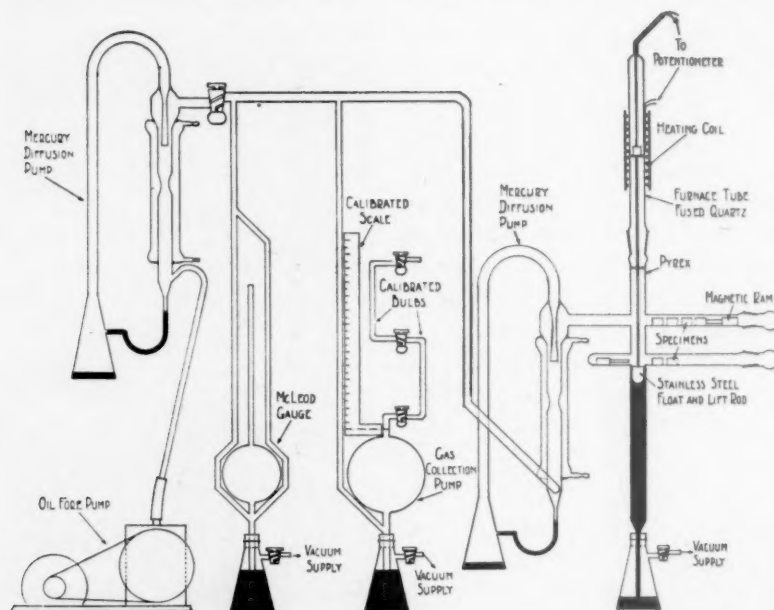


FIG. 2.—SCHEMATIC DRAWING OF VACUUM-EXTRACTION APPARATUS.

gases collected during vacuum heating. Certain experiments by Newell¹ and Herasymenko² lead to the conclusion that hydrogen is the only gas evolved from clean steels when baked in a vacuum at 600° to 800°C.* The following experiments

² P. Herasymenko and P. Bombrowski: *Archiv Eisenhüttenwesen* (1940) **14**, 109-115.

* Newell¹ inserted a bulb of activated charcoal into a system similar to the one described here. This bulb of activated charcoal was cooled to liquid oxygen temperatures, and all of the gas collected was passed through this bulb. Activated charcoal at this temperature has the property of absorbing all of the gases except hydrogen and the noble gases. The amount of gas collected was determined and then the activated charcoal allowed to warm up to room temperature. No measurable increase in the volume of collected gases was found by Newell, and it was concluded that hydrogen was the only gas extracted by vacuum heating in the temperature range of 600° to 800°C. Similarly, Herasymenko³ used large steel samples to obtain enough gas by the vacuum heating method, which could be analyzed by conventional gas-analysis methods. His conclusion was that hydrogen was the only gas evolved from clean steel samples at temperatures of 600° to 800°C. Above 800°C., small amounts of carbon monoxide and nitrogen make their appearance.

samples by vacuum heating in the range of 600° to 800°C. A quartz gas-discharge tube with aluminum anodes was attached to the system after the last stopcock on the calibrated bulbs. First the leak rate over an hour was determined when the empty platform was in the heating chamber at 600°C. This was 0.5 microns per minute, as read by the McLeod gauge. These gases were flushed into the bulbs until the McLeod-gauge reading was 10 microns, and were then let into the discharge tube. The gas spectra was excited by 5000-volt, 18-ma., 60-cycle alternating current. A photograph of the spectra, as recorded by a Zeiss hand spectroscope, model D, attached to a Leica camera, is shown in Fig. 4. The mercury discharge is present in addition to the pattern that is taken to be "air" under these conditions. Several samples of 18-8 stainless steels were then run in the conventional manner, and their gas spectra were photographed.

Standard discharge spectra of mercury and hydrogen were also photographed and appear in Fig. 4. Referring to the spectra of the samples, note that the only spectral

steel can be determined within ± 6 per cent by this method.

Table 2 shows a comparison of the hydrogen liberated during solidification and cool-

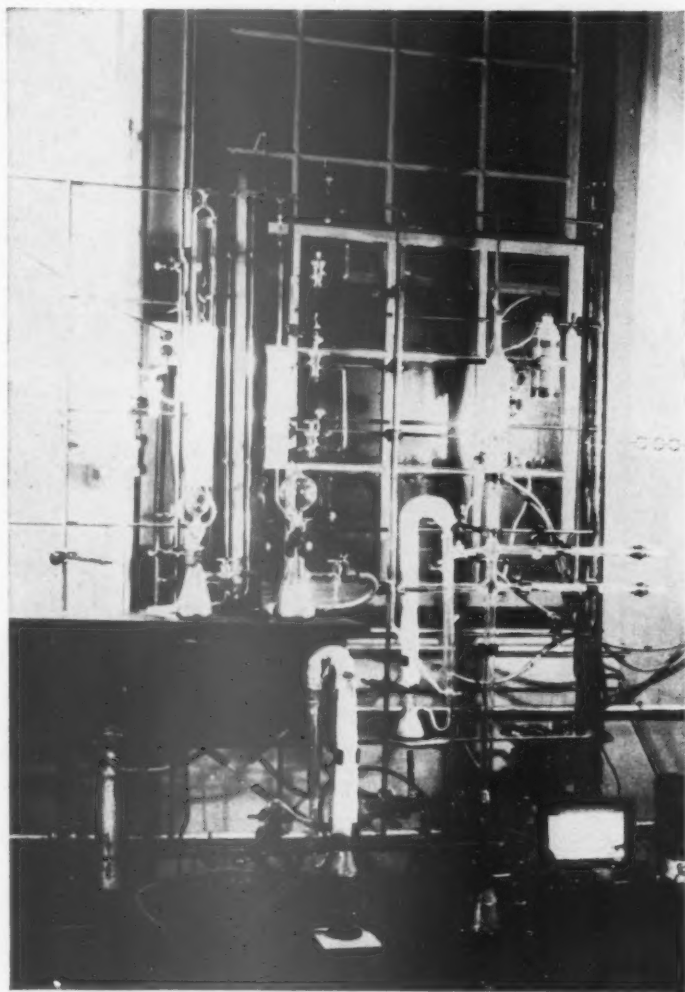


FIG. 3.—VACUUM EXTRACTION APPARATUS USED BY CARPENTER STEEL COMPANY.

lines excited, except those shown in the "leak-rate" spectra, are the lines that can be identified as hydrogen.

PRECISION OF THE METHOD

Duplicate specimens were cut from bomb samples for several types of alloys, and the hydrogen content of the samples was determined by the vacuum-extraction method. These results are summarized in Table 1. It is believed that the hydrogen content of a freshly prepared, clean specimen of

ing of the sample in the bomb, and the hydrogen retained in solution and evolved during vacuum extraction for several types of alloy steels. In general, the higher the nickel content, the more hydrogen is retained in solution. Straight chromium stainless steels show a slight tendency to retain more hydrogen in solution than do low-alloy steels.

Evidence has been obtained that small chill-cast specimens of molten steels retain almost all the hydrogen content in solu-

tion. For these experiments, the lower part of the bomb was made thicker and machined out so that a small portion of the test sample is in the form of a cylinder,

cylinder knocked off. Table 3 summarizes these experiments. The conclusion seems to be warranted that small chill-cast specimens of molten steel retain most of the

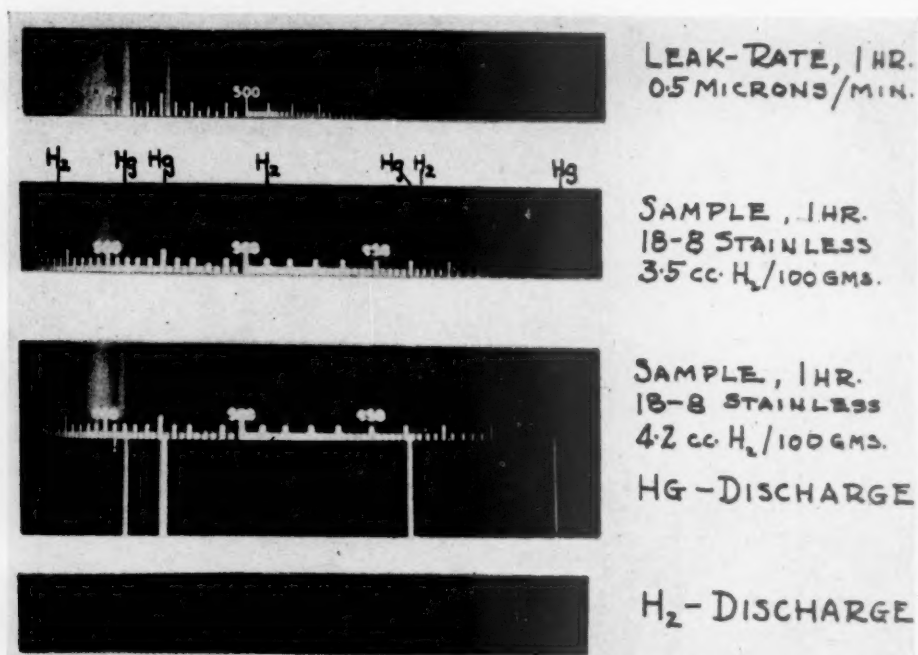


FIG. 4.—DISCHARGE SPECTRA OF GASES COLLECTED BY VACUUM HEATING AT 600°C.

measuring 1/2-in. round by 1/2-in. long. As before, the hydrogen content of the gases

TABLE 1.—*Reproducibility of Vacuum-heating Method for Determination of Hydrogen*

Type Steel	Sample No.	H ₂ at 600°C., C.C. per 100 Grams	H ₂ at 900°C., C.C. per 100 Grams
Cr-Ni stainless 18-8	1	10.5	11.2
	2	10.5	
	3		
Cr-Ni stainless 18-8	1	13.3	14.6
	2	14.0	
	3		
N.E.-8740	Top of cast slug	6.2	
	Bottom of cast slug	7.0	
N.E.-8740	Top of cast slug	3.55	
	Bottom of cast slug	3.00	

evolved from the complete cast sample was determined. A test specimen was cut from the large bulk of the sample, and the small

hydrogen in solution. In present and future tests we are using cast spectrographic

TABLE 2.—*Comparison of Hydrogen Evolved during Solidification and Hydrogen Retained in Solid Metal for Different Types of Alloys*

Type Steel	Sample No.	H ₂ in Gas, C.C. per 100 Grams	H ₂ in Metal, C.C. per 100 Grams	Total H ₂ , C.C. per 100 Grams	Percentage Evolved
Low-alloy S.A.E. 52100	1	4.60	6.50	11.10	41.5
	2	3.76	8.45	12.21	31.0
	3	2.10	8.10	10.20	19.6
Chrome-iron stainless	1	2.40	5.58	7.98	30.0
	2	.96	4.32	5.28	18.2
	3	2.12	4.34	6.46	33.0
Chrome-nickel stainless	1	3.20	12.76	15.96	20.0
	2	1.19	9.94	11.13	11.0
	3	1.00	10.8	11.80	8.5

electrodes for hydrogen determinations and dispensing with the bomb gas analysis.

Table 4 shows the hydrogen contents of

several common ferroalloys. With the exception of ferromanganese, the hydrogen contents are small, compared with 7.0 to

TABLE 3.—*Comparison of Hydrogen from Half-inch Round Chill-cast Specimens and Total Hydrogen by Bomb and Vacuum Heating Method*

Low Alloy Steels	Total H ₂ from Bomb and Vacuum Heating, C.C.			H ₂ from Small Chill-cast Specimen, C.C. per 100 Grams
	Evolved on Solidification	By Vacuum Extraction	Total, per 100 Grams	
S.A.E. 52100.	1.0	5.3	6.3	6.7
S.A.E. 52100.	0.9	4.8	5.7	6.1
S.A.E. 52100.	1.2	5.8	7.0	6.5
S.A.E. 52100.	1.0	5.0	6.0	5.4
S.A.E. 52100.	1.0	5.1	6.1	6.3

15.0 c.c. hydrogen per 100 grams metal commonly found for molten alloy steels in the basic electric-arc furnace.

TABLE 4.—*Hydrogen Content of Ferroalloys*
C.C.
H₂ PER
100
GRAMS

High-carbon ferromanganese (7 per cent C)...	27
Low-carbon ferromanganese (1.40 per cent C)	6
Low-carbon ferromanganese (0.04 per cent C)	22
Low-carbon ferrochromium.....	3.4
Low-carbon ferrosilicon.....	4.6
Low-carbon ferrotitanium.....	2.3
Low-carbon Cathode nickel- (5 samples)	5.2 cc.
	2.4 cc.
	3.4 cc.
	5.8 cc.
	3.1 cc.
	4.0

ACKNOWLEDGMENTS

The generous cooperation of the staff of the Metallurgical and Chemical Laboratories of The Carpenter Steel Co. in carrying out this investigation is gratefully acknowledged. The authors are especially grateful to G. V. Luerssen, Metallurgist, of The Carpenter Steel Co., for the helpful discussions and suggestions offered; and to J. H. Parker, President, and B. H. DeLong, Chief Metallurgist, of The Carpenter Steel Co., for permission to publish these results.

DISCUSSION

C. A. ZAPFFE.*—To find out how to get this gas out of steel, we should know something about its condition in the steel. So far this afternoon no point has been made of the fact that different types of steels respond differently to hydrogen analysis at any given temperature. The Europeans have shown that electrolytic iron and mild steels, for example, evolve most of their hydrogen during treatment at 400°C.; but that with higher carbon contents and with either alloying elements present in the steel, a higher temperature is often required because many of these elements reduce the fugacity, or "escaping tendency," of dissolved hydrogen.

Since the evolution of hydrogen from the sample depends upon diffusion of some sort or other, two simple factors, concentration and the diffusivity constant, in the diffusion equation:

$$\frac{dA}{dt} = K \frac{dc}{dx}$$

must govern the efficiency of the analysis. The *concentration* (activity) of hydrogen may be decreased by the formation of some type of compound:



and the diffusion coefficient may be lowered substantially by the presence of other elements, as is known to be true with chromium and carbon, to name but two. Obviously, a change in the temperature of A_c produced by alloying will affect hydrogen analysis.

Pursuing this reasoning further, I shall point out that there is no acceptable evidence for assuming that hydrogen exists in the iron as a true compound of iron, or iron hydride; and that most of the evidence points definitely instead to its existence as a separable gaseous phase within such tiny internal surfaces as those which can be associated with slip, cleavage, and general precipitation phenomena. Atomic diffusion through the iron lattice would require hundreds of years for the gas to travel a fraction of an inch, according to the best cal-

* Assistant Technical Director, Rustless Iron and Steel Corporation, Baltimore, Maryland.

culations.¹ This atomic picturization is therefore inconsistent with the known fact that the gas may actually travel as far in a few minutes. The picture of internal precipitation, akin to what is normally called "aging," of a separable gaseous phase is consistent with observed facts. For example, the repetitive isothermal evolutions at increasing temperatures, demonstrated so well by Moore and Smith,² points to the specimen as a safety valve set for a given pressure, which permits the excess occluded gas to "blow off" when its pressure is raised by increasing the temperature.

The reason I open this point is to suggest another technique for the analysis of hydrogen—a technique involving comminuting the steel to open these minute gas pockets in which the gas is trapped.

One of the first methods for analyzing for hydrogen was that which was used by F. C. G. Müller in Germany 65 years ago.³ Müller found that by drilling the steel gas was given off, and that the blunter the drill and the finer the drillings, the more gas he obtained. His values compare well with the best reported today.

In regard to the vacuum-fusion technique, one test of ours might be mentioned, in spite of the fact that it was not repeated. A steel specimen was carefully annealed to remove hydrogen and was then analyzed for hydrogen by vacuum fusion. A duplicate was cathodized until its impact value was reduced to only several-foot-pounds per square inch. This was similarly analyzed. Ten times as much hydrogen was found in the sample that had been treated to remove hydrogen. This result stands in qualitative agreement with Dr. Yensen's observation comparing vacuum fusion with vacuum heating.

Obviously there are vacuum-fusion techniques that differ from one another in important respects, and it is indeed gratifying to see Dr. Derge devising a method that eliminates

many previously objectionable features. One thing is particularly outstanding in his contribution, and that is the experiment showing that hydrogen is not absorbed or occluded by graphite to an extent that interferes measurably with his analytical procedure.

One further suggestion might be made regarding the vacuum-fusion method. There are two ways of removing hydrogen. One is to let it evaporate into a hydrogen-free atmosphere. The vacuum provides an approach to that condition; the bubbles from the C-O reaction do an especially good job. In fact, without a boil, vacuum fusion may be inferior as an analytical tool for hydrogen. As a second approach, a chemical reaction may be used to form an insoluble product with hydrogen, such as water vapor or hydrogen sulphide. Possibly the introduction of some form of carefully dried oxide would produce a boil in the vacuum-fusion crucible that would greatly improve the efficiency and the consistency of the technique for removing hydrogen.

G. A. MOORE.*—At the risk of having everyone tired out before I have a chance to present the last discussion on the program, I would like to take a moment to examine the monkey wrench in the works which is due to the difference between accuracy and precision. It appears to have been demonstrated that solid evolution is a precise method, but I am not at all sure that it is an accurate one. In some work presented to the Institute about five years ago² it was reported that at least six experimenters had found that the evolution does not go to completion. When you perform successive evolution experiments on the same sample at different temperatures, you usually find that each heating gives additional gas, although the evolution was apparently complete at lower temperatures. There have been certain objections to some of these experiments on grounds of blank troubles and impurities. Fig. 3 of the paper cited² shows an experiment free of these objections, since it represents a pure iron ribbon freely supported within a cool quartz tube, thus under conditions where the blank is completely unmeasurable.

The total gas accumulated is shown on the

¹ A. E. Stearn and H. Eyring: Absolute Rates of Solid Reaction: Diffusion. *Jnl. Phys. Chem.* (1940) **44**, 955-980. 72 references.

² G. A. Moore and D. P. Smith: Occlusion and Evolution of Hydrogen by Pure Iron. *Trans. A.I.M.E.* (1939) **135**, 255. 123 references.

³ F. C. G. Müller: New Experimental Investigations on the Gas Content of Iron and Steel. *Stahl und Eisen* (1883) **3**, 443-454; (1884) **4**, 69-80. Also, *Iron* (1883) **22**, 243-246; (1884) **23**, 137-139.

* Battelle Memorial Institute, Columbus, Ohio.

vertical scale, and the time of each run increases to the right on the horizontal scale. For 10 successive temperatures, each run gives additional gas on top of that given by the previous runs, after these were apparently complete. You will notice, at low temperatures, that the rates are rapid at the beginning, but fall off very sharply. In other words, low-temperature vacuum extraction is a suitable method for indicating the large differences in excess gas between greatly different conditions in the steel; for example, for distinguishing between an embrittled sample and a ductile one. There is not any good indication that low-temperature vacuum extraction is accurate in the sense of giving the actual amount present.

These curves were for pure iron, so the transition is sharp. When you go above the transition, the rate immediately becomes more or less rational, and evolution continues to apparent completion. The effect of the transition will naturally be different for different steels, as will the rates themselves. What I wish to point out is that the type and rate of evolution to be expected and the degree to which the precise and reproducible result approximates an accurate analysis, will depend both on the temperature and the type of steel. There have been some recent low-temperature vacuum evolution experiments run at Battelle. While I have not seen the complete results, it was immediately apparent that entirely different types of evolution were obtained on ferritic and austenitic compositions. If we are going to run ferritic steels, I think we can expect a perfectly good comparison of the different steels, so long as we do not try to compare them with the austenitic.

Comparing low and high temperatures in Fig. 3 of the paper cited,² or ferritic and austenitic steels at the same temperature, it will be noted that the rates at the start are *lower* in the austenitic condition than they are in the ferritic. When you carry on the evolution for a long time, the austenitic rate holds up where the ferritic does not, so that much more gas is finally evolved. Thus, it is only when you get up to the transition range that you can expect the result to be accurate as well as precise. Evolution at 800°C. may be expected to be satisfactory for some steels, but certainly not for all.

H. H. UHLIG.*—I should like to summarize the inherent difficulties, as I see them, in both the hot extraction and vacuum-fusion methods for the determination of hydrogen.

I think, first of all, that one difficulty with the vacuum-fusion method is the large quantities of other gases that come off with hydrogen. There may be a large volume of CO, as well as nitrogen, and the hydrogen is virtually lost in this large volume. This makes precise analysis somewhat difficult.

The second difficulty concerns itself with the high blank that usually accompanies the high temperatures of this method. The volume of incidental gases including hydrogen corrected for by the so-called blank may actually approach the total volume of hydrogen obtained from the sample.

A third difficulty is the large amount of vaporized metal that condenses on the colder parts of the furnace, which occludes and adsorbs the gases. Unless some method is used to get rid of the entrapped gas, there will be an appreciable error originating from this source. A good deal of the work that Dr. Naughton and others have done bears on this point and proves that the error exists.

In the hot extraction method there is also vaporized metal, but a smaller amount of it. In the analysis of high-manganese steels, there may be a manganese film that condenses on the cold parts of the furnace. This is not a serious problem, as with the fusion method, particularly if one is working with steels that do not contain volatile constituents.

A more serious difficulty with this particular method is that in many cases all of the hydrogen is not extracted. We tried to remove hydrogen from the sample by heating at 600° to 800°C. for periods of 1 to 2 hr., but for some alloys we did not succeed in getting out all of the gas. If we had heated for still longer periods, we might have succeeded, although this would have been an impractical time requirement.

The fusion method has the disadvantages that I enumerated before, but has the advantage that all the hydrogen apparently is released. By adding tin to the sample and fusing the tin alloy, one can extract the hydrogen at a

* Research Laboratory, General Electric Co., Schenectady, N. Y.

much lower temperature: for example, 1100° to 1150°C. The large volumes of CO and nitrogen do not at this temperature accompany the hydrogen, and, furthermore, the blank correction is smaller. The gases evolved from the sample are mostly hydrogen, so that it can be more easily analyzed.

The addition of tin, of course, does increase the amount of vaporized metal, but, as Dr. Naughton pointed out, this can be overcome by adding a bit of mercury to the quartz tube, which acts to wash down the tin and in so doing releases the hydrogen that is absorbed by the condensed metal.

Determination of Hydrogen in Molten Steel by the Gas-tube Method

By J. G. MRAVEC*

THE so-called gas-tube method as developed by Hare, Peterson and Soler for determining the type and content of gases in molten steel is particularly adapted for determining the hydrogen content in molten steel. The development of this method has been quite completely discussed in a paper published by these co-workers in 1937.¹ The purpose of this paper, therefore, is to familiarize with this method those who are not well acquainted with it.

The principle of the gas-tube method is as follows: One end of an evacuated gas tube is sealed with a very thin copper disk. When this end of the tube is immersed in a test spoonful of molten steel, the copper disk melts almost immediately, allowing a portion of the steel to be drawn up into the evacuated space. Any dissolved gases, and those produced by reactions between the components of the steel during freezing, are liberated into the unfilled portion of the sampling tube. A blob of steel that forms on the immersed end of the tube after the sample is drawn up seals up the end, making it airtight again. The evolved gases are subsequently drawn out of the gas tube through a suitable valve and analyzed by means of an Orsat apparatus. The volume of the sampling tube is sufficiently large so

that a pressure considerably below atmospheric is produced after the gas evolution. The low pressure is necessary to effect a nearly complete removal of gases from the steel.

CONSTRUCTION OF SAMPLING TUBE

The sampling gas-tube apparatus is illustrated in Fig. 1. Seamless S.A.E.-1015 tubing used for section *A* is first cut into 7-ft. lengths. Through experience it was found necessary to use two sizes of tubing for this part, $1\frac{1}{16}$ -in. and $\frac{3}{4}$ -in., respectively. The smaller tubing is generally used on the hotter or lower carbon steels. If the inside wall of the tube *A* is coated with grease or oil, it should be burned out before being machined as follows: One end is machined on the inside diameter to a depth of $\frac{1}{8}$ in., so as to form a seat for a $\frac{7}{8}$ -in. copper disk, which is stamped out from 0.005 to 0.007-in. thick copper sheet. The other end is machined on the outside diameter to a diameter of $1\frac{5}{16}$ in., to take a small reservoir or trap member *B*. About 4 in. below the same end, a $\frac{1}{2}$ -in. hole is drilled to receive the $\frac{1}{2}$ -in. copper tubing leading to the large reservoir *C*. The inside of tube *A* is then thoroughly cleaned with a round wire brush, such as is generally used to clean out shotgun barrels. It is very important that the surface be absolutely free of rust or any nonmetallic coating. Next, the thin copper disk is soldered in place with low-melting silver solder.

Manuscript received at the office of the Institute March 8, 1944.

* Research Metallurgist, Timken Roller Bearing Co., Canton, Ohio.

¹ W. Hare, L. Peterson and G. Soler: *Trans. Amer. Soc. for Metals* (1937) 25.

The small reservoir *B* is made from a 10-in. length of seamless tubing of $1\frac{5}{16}$ -in. inside diameter and $\frac{3}{16}$ -in. wall. One end is closed with a steel plug and silver-soldered. The other end is fitted over the machined end of tube *A* to a depth of 1 in. and then silver-soldered. The chief purpose of this small reservoir is to allow tube *A* to be opened at both ends for cleaning; also, it serves to entrap any steel that is splashed up during sampling.

The large reservoir *C* is made from a 30-in. length of steel tubing of 2-in. outside diameter and a $\frac{1}{8}$ -in. wall. Both ends are permanently closed by welded steel plates. Two holes, one $\frac{3}{8}$ in. in diameter and the other $\frac{1}{2}$ in. are drilled through the upper plate to take the valve and copper tubing connection to the tube *A*, respectively. The opening for the valve is tapped with a $\frac{3}{8}$ -in. pipe tap. The valve is then screwed in and soldered with lead to ensure a good tight seal. The valve is an ordinary pressure stopcock and is vacuum-tight when new, but may require regrinding after repeated use. Next, the $\frac{1}{2}$ -in. copper tubing, which is approximately 8 in. long, is fitted into the proper opening in reservoir *C* and silver-soldered. All reservoirs should be carefully made to size; their volume must be known because it enters into the calculation of the gas content. Their designed volume is approximately 1400 cubic centimeters.

The construction of the gas tube is completed by connecting reservoir *C* to tube *A*. This is done by silver-soldering to tube *A* the copper tubing that leads from the upper end of reservoir *C*. The lower end of *C* is attached to *A* by a clamp, as shown. The assembled gas-tube apparatus is then carefully tested for leaks by filling with air at about 35 lb. pressure and immersing under water. Any leaks will be revealed by bubbles of escaping air.

The detachable screen *E* serves as a safety shield against any possible spitting of the steel during sampling. It is clamped

to the bottom of the tube just before a sample is to be taken. There is, however, no hazard in sampling if the tube has been properly evacuated and is free of moisture.

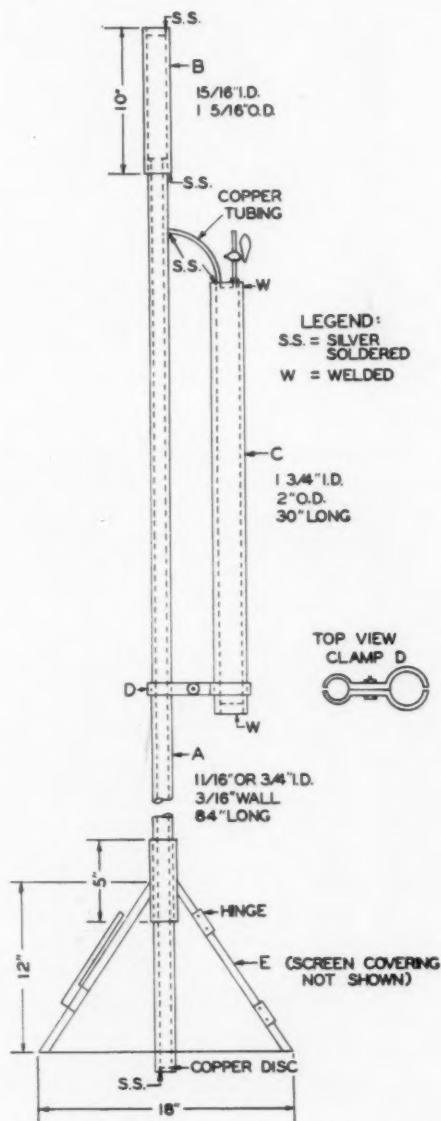


FIG. 1.—SAMPLE TUBE.

A photograph of a longitudinally split gas tube is shown in Fig. 2. The steel sample shown in the tube has been pulled out of a different gas tube. It serves, however, to illustrate the average height to which the molten steel is drawn up into the tube.

PREPARATION OF TUBE FOR SAMPLING

Using a Megavac pump and a mercury manometer, the sampling tube is evacuated through the valve to less than 1 mm. of

tion of the hydrogen content later, it is essential that the evacuated tube be weighed to an accuracy of one gram. The weighing may be done on a kilo-beam

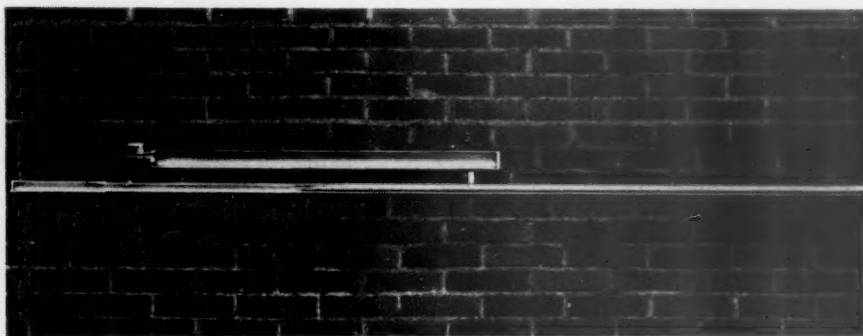


FIG. 2.—LONGITUDINAL SPLIT SECTION OF GAS TUBE, SHOWING POSITION OF STEEL SAMPLE.

mercury. After evacuation the tube is removed from the pump after the valve has been closed. It is allowed to stand for at least an hour, after which time its vacuum is checked by connecting again to the evacuated manometer system and opening

balance of 20 kilograms capacity. The weight is then recorded against the tube number whose identity is stamped on the valve. Also recorded against the valve number are the inside diameter and length of tube section A. A record of these data

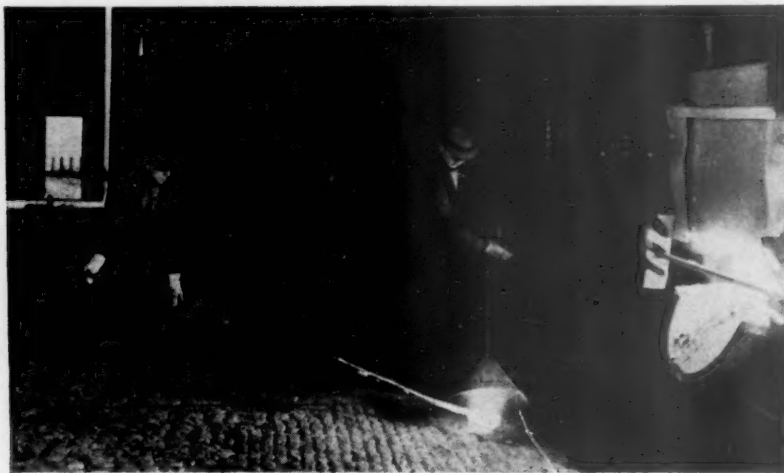


FIG. 3.—SAMPLING STEEL WITH A GAS TUBE.

the valve. If no leakage is noted, the tube is considered satisfactory for sampling. The outside surface of the end of the tube that will be immersed into the molten steel is then filed clean. This promotes a better weld between the tube and the blob of steel that seals the end after the sample has been drawn up. To enable the calcula-

tion is important, since it enters into the calculation of the gas content.

SAMPLING THE STEEL

Fig. 3 illustrates the gas-tube sampling operation. A suitable sampling spoon for dipping the molten steel from the furnace is one that can hold 8 or 9 lb. of steel after

it has been well "slagged up." The spoon handle preferably should be about 8 ft. long, so as to enable the dipping of a representative sample from well toward the center of the bath.

After the steel is drawn up, the bottom of the tube is moved in a circular motion in the remaining steel in the spoon. This aids in forming a "blob" of steel, which seals the end airtight. To assure the forma-



FIG. 4.—ARRANGEMENT OF SAMPLING AND ANALYTICAL EQUIPMENT.

Just prior to the taking of the gas-tube test, the safety wire screen is properly clamped to the tube and the copper sealed end is warmed up in front of a wicket hole, so as to assure the absence of any moisture. As soon as the spoonful of steel is withdrawn from the furnace and set on the floor, any slag that may be present on the surface of the sample is scraped off. The end of the sampling tube is then immediately immersed into the molten steel. Care should be taken at this point that the end of the tube does not hit the bottom of the spoon before the sample is drawn up, as this might loosen some of the slag and cause it to be drawn up into the tube. In immersing, the tube should be held at a slight angle and slipped into the steel with a side-wise motion, so as to avoid the possibility of an air bubble forming at the end of the tube. The copper disk melts almost immediately and a sample of molten steel is drawn into the tube.

tion of a nonporous "blob," and consequently a good seal, it is a good practice to deoxidize the steel remaining in the spoon with a few chips of aluminum. For added protection against air leakage, the bottom of the tube is pounded several times against a railroad track or some other solid object, while it is still white hot upon removal from the spoon.

On the average, the steel is drawn into the evacuated tube within 5 sec. after the sampling spoon is drawn out of the furnace and within 2 sec. after the slag is scraped off the sample in the spoon; an additional 15 to 30 sec. is required to form a good seal on the bottom of the tube. The weight of the steel drawn into the tube usually varies from 3 to 5 lb., depending on the steel and the size of the inside diameter of the tube.

ANALYTICAL PROCEDURE

Fig. 4 illustrates the arrangement of the sampling and analytical equipment. In

general, the analytical equipment consists of an all-Pyrex Toepler pump system and a Burrell gas-analysis apparatus. The Toepler pump arrangement is used as a

For such calculation the following factors are required:

1. *Weight of steel sample.* This is obtained by subtracting from the difference in tube

GAS ANALYSIS OF MOLTEN STEEL									
Heat No.	30347 X		Type	4615		Date	4-19-37		
Test No.	1		Time	7:18 PM					
Start	100.0	cc.	% CO	50.0		Wt. Tube After	12590 gr.		
KOH	99.8	cc.	% H ₂	48.8		Wt. Tube Before	10585 gr.		
OXS			CH ₄			Difference	2005 gr.		
COS	50.0	cc.	% CO ₂	0.2		Mass on Bottom	184 gr.		
O ₂	59.6	cc.				Total Weight	1821 gr.		
Total	109.6	cc.	Wt. %			Vol. of Apparatus	360 cc.		
H ₂ SO ₄	36.4	cc.	CO	.009		Res. No.	55	Vol.	1400 cc.
KOH	36.4	cc.	H ₂	.00064		Lgth. Tube	81"	Vol.	403 cc.
			Al ₂ O ₃			Small Res. Vol.	35 cc.		
Pressure (Inches of Hg.)			FeO	.023		Volume	2264 cc.		
Lt.	13.0	in.				Minus 1/4 Wgt. Steel	227 cc.		
Rt.	8.8	in.	Tubing I.D.	5/8"		Total Volume	2037 cc.		
Diff.	4.2	in.							
REMARKS: TEST TAKEN BEFORE AL AT TAP.									
Weimer Analyst									

FIG. 5.—RECORD OF DATA AND RESULTS OF TYPICAL GAS TEST.

means of transferring the gases from the gas tube to the gas-analysis apparatus. Two mercury manometers are a part of the Toepler pump system. One is used to check the vacuum of the system or of an evacuated tube. The other is used to measure the gas pressure after the gas from the tube is allowed to expand into the previously evacuated Toepler pump system, whose volume in this case is known to be 360 c.c. After the gas pressure is recorded, a 100-c.c. volume of the gas is drawn into the burette of the gas-analysis apparatus for analysis. The gas is then analyzed by standard procedures for CO₂, CO, and H₂.

The CO₂ and CO are determined by passing through potassium hydroxide and ammoniacal cuprous chloride solutions, respectively. The hydrogen is then slowly ignited with a known amount of oxygen. The hydrogen content is calculated from the loss in volume of gas and oxygen on ignition.

CALCULATION OF RESULTS

The gas results are calculated in terms of per cent by weight of the steel sample.

weight before and after sampling the weight of the blob of steel on the end of the tube, which presumably did not contribute to the trapped gas volume. The weight of the blob is calculated from its volume. This is determined by immersing 4 in. of the end of the tube in water in a graduated liter cylinder. The volume displaced, however, must be corrected for the normal displacement of 4 in. of the tube itself.

2. *Volume of entire apparatus when pressure is recorded.* This is the total volume of the gas tube and Toepler pump system less the volume of the steel sample.

3. *Pressure of gas at the total volume.* This is recorded directly from the mercury manometer.

4. *The percentage analysis (by volume) of the gas mixture.* This is the result of the gas analysis.

The actual calculation of the percentage by weight of hydrogen is simplified by the use of a nomograph, as shown at the right in Fig. 4. Once these factors on a test are known, the hydrogen content may be determined from the nomograph

within $\frac{1}{2}$ min. The normal over-all time from sampling of the molten steel through the calculation of its hydrogen content is approximately 15 to 20 min. A record of data and results of a typical gas test is shown in Fig. 5.

CONCLUSION

The gas tube as described in this paper has been found to be a practical tool for rapid determination of hydrogen in molten steel. As such, it is suitable for production control as well as for research work. An outstanding feature of this gas-tube method is that the results are based on a large steel sample (3 to 5 lb.).

DISCUSSION

H. K. WORK.—The method used by the Research and Development Division of the Jones and Laughlin Steel Corporation for the determination of hydrogen in steel is a modification of the familiar combustion procedure used extensively for carbon and sulphur. The apparatus consists of a furnace with a short heating zone, an oxygen purifying train, a porcelain combustion boat, and an absorption train for removing water vapor from the outgoing gases. The unit is assembled by means of gastight rubber stoppers and tubing. The only other equipment required is a standard analytical balance. The specimen used is a solid bar, $\frac{3}{8}$ in. in diameter and 3 in. long, weighing approximately 50 grams.

* Jones and Laughlin Steel Corporation, Pittsburgh, Pennsylvania.

The procedure adopted is as follows: The apparatus is completely assembled and prepared for use by raising the temperature of the furnace until the mid-point of the hot zone is at $1175^{\circ}\text{F.} \pm 25^{\circ}$. Oxygen is passed through the system until the absorption tube shows no significant change in weight during a one-hour interval. The specimen is then introduced into the boat and the system reclosed as quickly as possible. Oxygen is passed over the sample until the absorption tube again assumes a constant weight. The change in weight of the absorption tube represents the weight of water vapor corresponding to the hydrogen content of the sample. Experience has indicated that approximately one hour at temperature is necessary to attain a constant weight of the absorption tube with the given specimen and extraction apparatus.

A number of factors must be controlled in order to obtain reproducible results. The blank value must be small and reasonably constant at all times and a standard weighing routine established and rigidly adhered to if consistent results are to be obtained. The temperature of the furnace should be kept within the limits indicated. Variations in ambient temperature and humidity are objectionable both during the extraction of hydrogen in the furnace and during the subsequent weighing of the absorption tube.

With this equipment and procedure, the results have been consistent and reproducible. It is evident that, in the absence of standard samples for comparison, the absolute accuracy of the method cannot be checked and values obtained are relative.

Preliminary Experiments on the Total Combustion Method for the Analysis of Hydrogen in Steel

BY GEORGE A. MOORE,* MEMBER A.I.M.E.

A recent survey of existing analytical results, and an attempt to correlate them with each other and with the known history and behavior of the samples, indicated that none of the commonly applied methods could be considered established as intrinsically reliable. It was, therefore, desired to attempt to establish the reliability of some one method by external evidence. If this were to be accomplished, other methods could then be evaluated in terms of the method established. The correct method was accordingly to be chosen without regard for cost, speed, or convenience; with the requirements for routine application to be reserved for later consideration.

The method of total combustion was chosen and submitted to a limited number of tests against primary standard samples. Considerable experimental difficulty was encountered, indicating that additional work on the experimental arrangements is desirable. While the work to date by no means represents a completed investigation, it is believed that the combustion method is basically sound and that its development should be continued.

CHOICE OF METHOD

Of the several available methods, mechanical disintegration,¹ electrochemical methods^{2,3} modifications of the Sieverts experiment,⁴ and vacuum fusion,⁵ were all judged to contain one or more factors of un-

certainty not at present completely evaluated or subject to complete control. These methods, therefore, were considered currently unsuitable for referee purposes.

Solid evolution was considered to be of doubtful significance when conducted in the alpha range. A reasonable chance for a true analysis was found for evolution in the gamma range. Preliminary tests^{6,7} have indicated a very slow rate for evolution from gamma iron, indicating a running time of possibly 100 hr. for a one-centimeter sample. Difficulty in distinguishing such slow evolution from blank gas was anticipated, hence the method was not considered the most suitable for the present purpose.

The combustion method was evaluated as being most sound on fundamental principles. The only important unknown would be to determine that the iron oxide formed did not occlude water at the temperature of the combustion. With the obvious precautions of using a sound and clean specimen, providing a system sufficiently tight to give acceptable blanks in long-time runs, and providing a sufficiently sensitive measuring system, reasonable, precise, and truthful analytical results could be logically expected.

APPARATUS

The equipment as originally operated is shown in Fig. 1, and the glassware in its latest modification in Fig. 2. The sulphuric acid drier and small safety tube in the upper right of Fig. 1 were replaced by a KOH drier and combined manometer safety tube, to permit operation at reduced

Manuscript received at the office of the Institute July 10, 1944.

* Battelle Memorial Institute, Columbus, Ohio.

¹ References are at the end of the paper.

pressure. The extra waxed joints in the combustion tube were replaced by graded seals after clear quartz was adopted for this tube. Otherwise, the apparatus

operate the control bulbs of the Toeppler pump and compression bulb in the measuring system.

Oxygen is supplied through a regulator

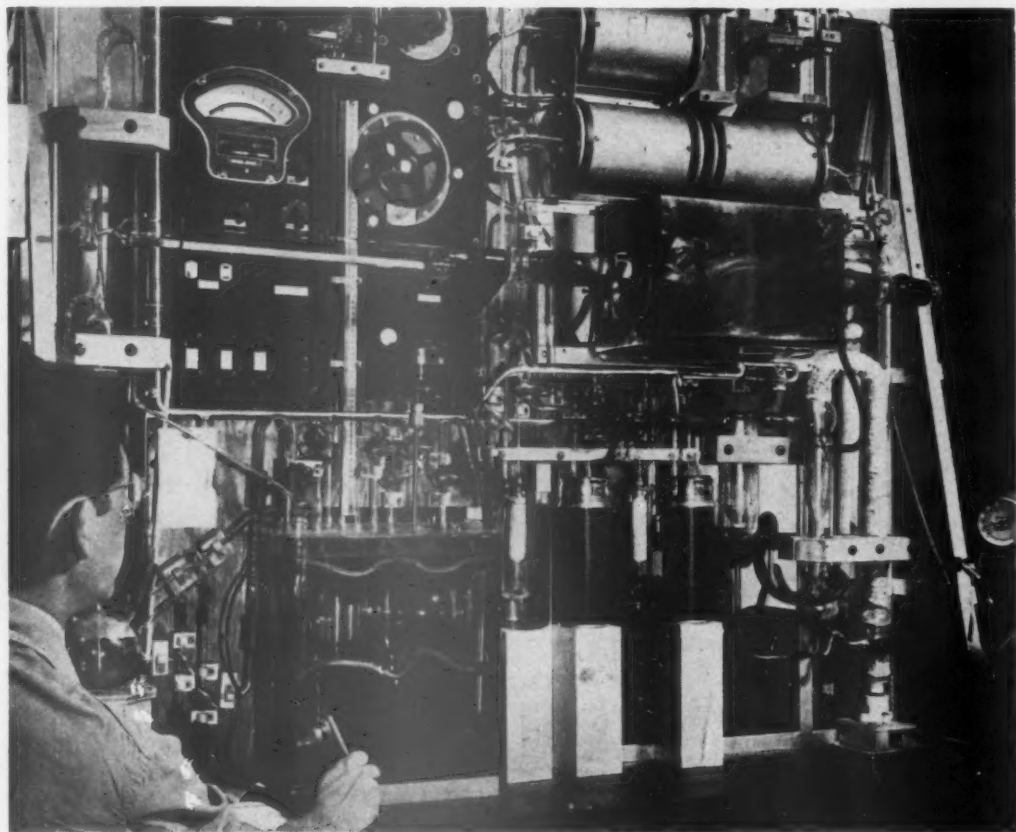


FIG. 1.—COMBUSTION APPARATUS AS ORIGINALLY OPERATED.

has remained unchanged throughout the experiments.

The requirement for a low blank dictated an entirely sealed system with fused joints. To prevent recurrent breakage, the entire apparatus is mounted on a rigid, welded frame as a portable unit, and has been proved to withstand transportation between buildings. Practically no leakage problems have been encountered.

For cleaning in advance of a run and for disposal of used gases, a two-stage mercury-diffusion pump, lower right, is so connected that it can evacuate the whole system or any part at will. A Hyvac oil pump serves both to back the diffusion pump and to

to the inlet at the upper right corner of the frame, whence it passes through the KOH preliminary drier, through furnace 1, where CuO at 700°C. catalyzes the removal of all combustible impurities, and thence down to trap T₄, where it is dried and purified by liquid air held in a Dewar flask. When desired, purified oxygen in liquid form is accumulated in this trap and admitted to the furnace as needed.

The combustion train consists of the extended tube in furnace 2, the CuO combustion completer in furnace 3, the lead chromate trap for sulphur in furnace 4, and one of the product-collecting traps, T₂ or T₃. Samples are first loaded in the

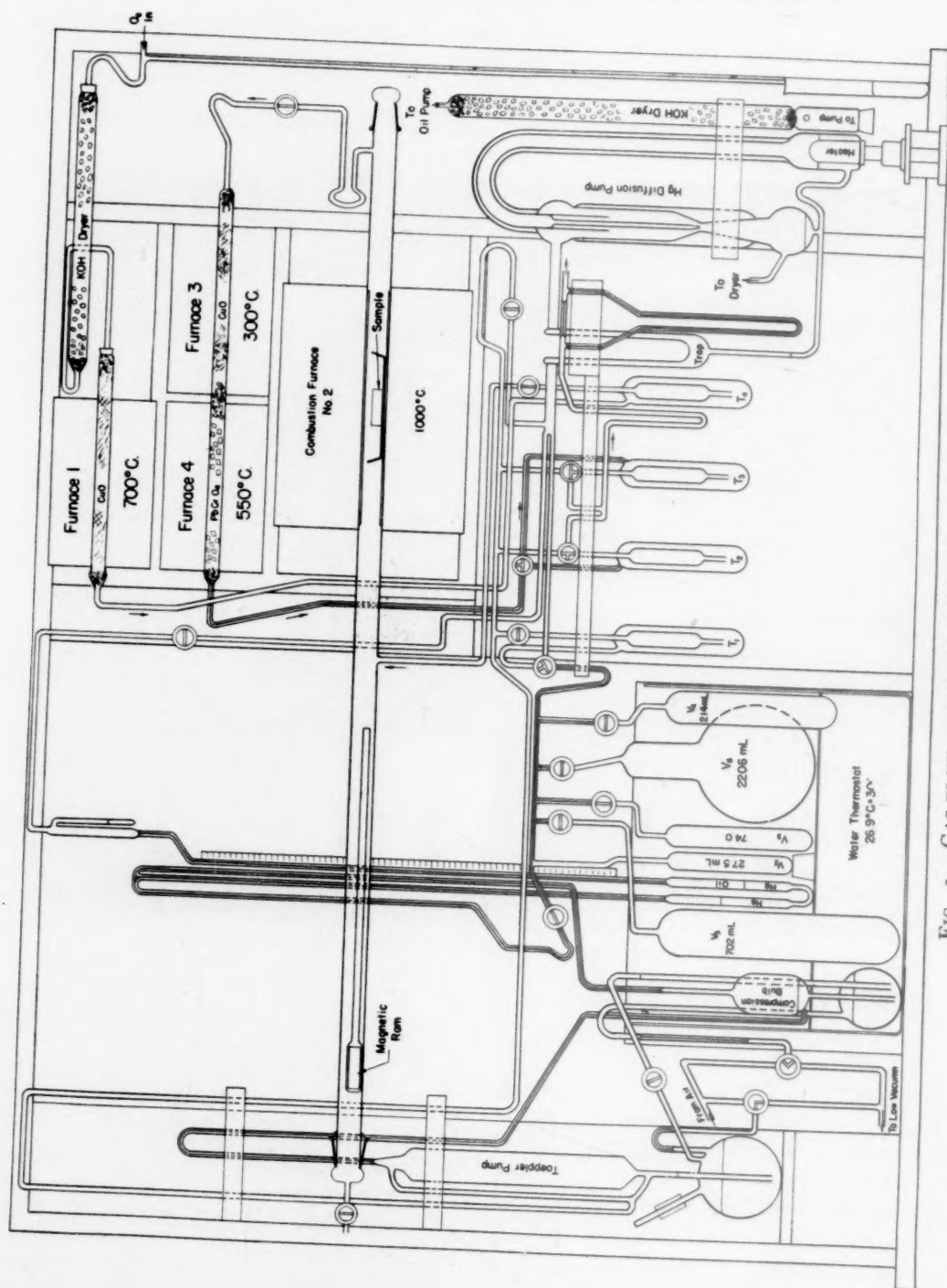


FIG. 2.—GAS-FLOW SYSTEM OF COMBUSTION APPARATUS.

cold extension of the combustion tube, ahead of the magnetic ram, then later pushed into the hot furnace after the system has been closed off and degassed. Combustion tubes of all apparently airtight ceramics available were tried and found in every case to evolve water at a rate too high to permit satisfactory use. Clear quartz was found to give the only satisfactory blanks. More choice can be permitted in the liner tube and boat, but quartz is generally used for its low water content.

In operation, the sample is pushed into the hot furnace under high vacuum; and oxygen is then admitted via the stopcock above trap T₄. Combustion may be run at normal or reduced pressure. Excess oxygen passes through furnaces 3 and 4, carrying the water and CO₂ into trap T₂ or T₃, where the products are frozen out by a second flask of liquid air. At low pressure, the stripped oxygen passes to the vacuum manifold where its pressure is determined by the outer leg of the Toepler pump acting as a manometer. Portions may be removed at intervals, via the diffusion pump, to maintain the flow of products in the right direction. At normal pressure, spare oxygen leaves T₂ or T₃ via the guard tube, which dips into the flask of T₄, thence through the flowmeter to the atmosphere. Successive fractions of a run may be accumulated alternately in T₂ and T₃, the contents of one being removed and analyzed while the other fills.

At temperatures varying from 1050° to 1150°C., depending on sample size, steel pieces catch fire in oxygen at one atmosphere, then burn freely and increase in temperature to about 1800°C. No satisfactory refractory for analytical work has been found that resists this free combustion, hence operation has so far been confined to the much slower solid combustion in the neighborhood of 1000°C.

For measurement, the sample is transferred to one or more of the calibrated volumes in the thermostat and its pressure

read on the oil-mercury combination manometer. This manometer gives about 10 times the deflection of mercury alone, reading to 0.01 millibars, and is a satisfactory substitute for a McLeod gauge, which cannot be used with water vapor. Six volumes logarithmically spaced from 5.16 to 3228 milliliters are provided. The range of useful pressure is from zero to 30 millibars for water and from zero to 60 millibars for CO₂. Least count is thus approximately 3×10^{-8} grams of hydrogen and 2×10^{-7} grams of carbon, being respectively 1×10^{-7} wt. per cent hydrogen and 5×10^{-7} wt. per cent carbon on a 40-gram sample. Maxima for a single fraction are similarly 6×10^{-3} wt. per cent (6 volumes) hydrogen and 0.04 wt. per cent carbon on the same sample. A precision of measurement of ± 1 per cent can be attained from amounts of 500 least counts upward.

FRACTIONATION AND MEASUREMENT

The sample collected in T₂ or T₃ is freed from residual oxygen by the diffusion pump while still at liquid-air temperature. For safety, it is customary to seal off and evaporate the sample, then to recondense and again clear occluded oxygen with the diffusion pump.

The water and CO₂ fractions are separated by distillation over dry ice, chloroform-carbon tetrachloride mixture at minus 80°C. The separation is free from measurable cross contamination except for cases of very wide difference in the amount of the two gases. Fractional distillation to T₁ can be used when desirable. Complete distillation to this trap frees the collecting trap for immediate re-use when collections are at short intervals.

Small samples of gas are transferred from traps T₁₋₂₋₃ to the calibrated bulbs by way of the Toepler pump, which is provided with a heating jacket to prevent condensation of water. The Toepler discharges into the compression bulb, which is operated with the mercury at the low

point as indicated in the diagram. When pumping is completed, the mercury is raised to a point level with the oil in the manometer, bringing the system to calibrated volume. For larger volumes, the sample fraction is distilled to T_1 and allowed to evaporate into the calibrated volumes. A beaker of water at thermostat temperature is placed around T_1 , which then becomes part of the calibrated system.

The CO_2 portion may be measured as indicated, or alternately discharged by the diffusion pump without measurement when hydrogen figures alone are desired. It has been customary to measure first the total fraction, then the water and CO_2 separately, giving both a check on measurement and on the progress of combustion.

STANDARD SAMPLES

Since our purpose has been primarily to determine whether combustion is a truthful method, we have analyzed principally standard samples whose hydrogen content was predetermined independently of analytical methods. Bars of 1010 steel, 1 cm. square, were decarburized in wet hydrogen at 1050°C . and then vacuum-annealed at the same temperature for 100 hr., until completely ductile. Pieces 55 mm. long were drilled centrally for most of their length and the hole threaded and provided with a conical valve seat. Threaded plugs with ends to fit the valve seat were made of the same material. Samples were degreased and stored in cleaned pure-iron baskets in desiccators. Samples were weighed accurately and small portions of lead formate or pure cane sugar were introduced. After sealing and cleaning the surface, the samples were reweighed and the amounts of hydrogen and carbon added were calculated. One sample of a set was treated in the same manner, but no organic matter was added. On heating, the organic matter decomposes, and both hydrogen and carbon enter the steel before combustion penetrates to the cavity, hence the

samples should behave similarly to uniform steels of the same total composition.

The cleaning of samples, as well as boats and other parts of the apparatus, is accomplished exclusively by the use of fully chlorinated hydrocarbons.

It is required that a satisfactory determination of carbon be obtained on a standard sample before hydrogen results may be considered acceptable.

REVISION OF EXPERIMENTAL ARRANGEMENT

Two important changes in the design of the apparatus have been indicated by the experiments already performed:

The furnace as used is incapable of handling free combustion, in which both the iron and iron oxide are in the liquid state. In addition, the amount of refractory raised to the combustion temperature is excessive, and, as a consequence, the blank values are higher than necessary. It appears desirable therefore to change to an induction-type furnace in which only a small crucible of yet-to-be-selected refractory will be heated to the reaction temperature. Incorporation of an arrangement to introduce the sample without breaking the vacuum also appears highly desirable.

The use of a water thermostat on the measuring volumes has been found to be unjustified for the accuracy attainable, as the room temperature may be held within 3°C . while measurements are being made. The stopcocks of the measuring system give occasional trouble. It would be desirable to substitute a vertical column of volume bulbs, arranged to be successively filled with mercury, for the present arrangement.

SCALES

Since the field of hydrogen analysis is already provided with an overabundance of scales of measurement, still another is suggested on the ground that it may be found more convenient. The scale of "Rela-

tive Volumes" (N.T.P.) already in use has been found convenient for many purposes, but somewhat artificial and cumbersome. Present results are given in a new unit which may be called a "Practical Volume." Measurements are made directly in millibar-liters of gas at 300°K., or 26.9°C. One millibar-liter equals 8.07×10^{-5} grams hydrogen. When divided by the volume of the sample, one relative volume (practical) equals 1.03×10^{-3} wt. per cent. With a reasonable allowance for error, one practical volume thus becomes 0.001 wt. per cent. The scale is convertible for variable pressure without involving fractional ratios, doubles for an even 300°C. rise in temperature, and indicates one sixth the true volume at the melting point of iron (1808°K).

OBSERVED FIGURES AND ACCURACY

It has been the practice, during the test experiments, to record all observations to the full capability of the scales. These observations appear in the next figure and in other places, and have been preserved in full in order that the errors may not be concealed. It is in no way implied that the analysis is good to such figures, as the accuracy of the analysis is to be evaluated in terms of the over-all results. Similarly, no claim is made that blank values have been established, but only that permissible estimations of the blanks give results varying only within certain limits.

TYPICAL ANALYSIS

The analysis of one standard sample in seven fractions over a period of 411 hr. is illustrated in Fig. 3. Previous experience estimated the basic C-H content of a 5.20-ml. sample (40.8574 grams) at 2.55 millibar-liters of methane (41.2×10^{-5} grams H_2 and 1.22×10^{-3} grams C). Artificial load was 31.3×10^{-3} grams of succrose, equal to 25.025 millibar-liters (2.02×10^{-3} grams) hydrogen and 27.500 millibar-liters carbon (13.2×10^{-3} grams).

It may be seen that while the rates of collection are near first order, the half time is several hours and the gas collected in the first run (4.25 hr.) is obviously less than the amount added. Some variation in interpretation of real and blank values may be applied to the later runs, of which the conceivable limits are expressed by the dotted lines. The most probable value for carbon is shown as 5 per cent above the known addition and 3 per cent below the load plus supposed original content. The supposed true hydrogen content falls almost exactly midway between the figures obtained using minimum and maximum blank allowances. Blank uncertainties allow several interpretations of the experimental result, varying about 10 per cent each way from the most probable value of hydrogen. An indicated result of 30.6 millibar liters would appear good to ± 3 per cent and agrees with the supposed hydrogen content of 30.15.

For purposes of illustration, a sample of higher than normal hydrogen content has been chosen in order that the details of the combustion may be shown with some accuracy.

COMPARATIVE RESULTS

As so far tested, the combustion method has given results that are very definitely higher than are commonly reported by other methods. A certain sample of mild steel, thought to be of low hydrogen content, had an indicated content by combustion of 0.7 to 0.9×10^{-3} wt. per cent (0.8 volume). The indicated base content of the standard purified iron was of the same order. These values correspond to points on the Sieverts curve in the gamma range. It is not, however, to be concluded that this gas was necessarily present as the occluded element, as all forms of hydrogen are included in the analysis by combustion.

One factor of the curve shown in Fig. 3 is enlightening with regard to solid evolution as well as the present method. It is a

logical certainty that all gas freely evolved from the iron at 1000°C. is included in the combustion result, and also that evolution into pure oxygen is no slower than into a vacuum. Thus, since the artificial load was not collected until after several hours, and since the supposed most probable content was not collected until nearly 100 hr., it is evident that neither solid evolution nor solid combustion are rapidly completed. While the evolution rate cannot be faster than the apparent combustion rate, there is so far no evidence to indicate that the combustion, as run, collects the gas appreciably faster than simple evolution.

CONCLUSIONS

Because of the known necessity of handling undivided solid samples of comparatively large size, coupled with inadequate refractories and other experimental difficulties, combustion analysis for hydrogen is not yet a rapid and convenient method of commercial applicability.

From the evidence so far available, controlled solid combustion near 1000°C. gives indication of being an accurate method useful in evaluating the truthfulness of other proposed methods. When operated on suitable samples in a clean and tight system provided with a sufficiently sensitive means of measurement, the method is free from logical objections. The apparent reliability of the method is shown by its ability to determine the hydrogen content of synthetically prepared standards within an acceptable limit of error.

From the limited experience so far obtained, it appears that the total hydrogen content of ordinary steels is of the order of the Sieverts solubility in the gamma range, often being nearly one relative volume or 1×10^{-3} wt. per cent. On this basis, it may be concluded that combustion analysis gives certain information not ordinarily given by other methods, and, therefore, that its further development is desirable.

REFERENCES

1. F. C. G. Müller: On the Gas Enclosed in Iron and Steel. *Ber. deut. Chem. Ges.* (1879) **12**, 93-95.
2. M. Thomas: *Ztsch. phys. Chem.* (1889) **3**, 69-102; *Centrallblatt Electrotechnik* (1889) **11**, 131.
3. T. Franzini: Occlusion of Hydrogen in Metals. *Pontifica Acad. Sci., Novi Lyncae, Sci. Nuncius Radiophonicus*, No. 4 (1931) 5; *Rend. Roy. Inst., Lombardo* 2, (1930) **63**, 465-482.
4. A. Sieverts, G. Zapf and H. Moritz: Solubility of Hydrogen, Deuterium, and Nitrogen in Iron. *Ztsch. phys. Chem.* (1938) **183-A**, 19-37 (other references herein).
5. V. C. F. Holm and J. G. Thompson: Determination of Hydrogen in Ferrous Materials by Vacuum Extraction at 800°C. and by Vacuum Fusion. *Jnl. of Research Nat. Bur. Stds.* (1941) **26**, 145-259.
6. G. A. Moore and D. P. Smith: Occlusion and Evolution of Hydrogen by Pure Iron. *Trans. A.I.M.E.* (1939) **135**, 255-292.
7. C. A. Zapffe and G. A. Moore: A Micrographic Study of the Cleavage of Hydrogenized Ferrite. *Trans. A.I.M.E.* (1943) **154**, 335-352 (see treatments on p. 336).
8. A. Müller: *Metallurgie* (1909) **6**, 145-160.
9. Gerke and Zolotareva: *Zavod. Lab.* (1935) **4**, 19.
10. H. A. Schwartz and G. M. Guiler: Hydrogen in Solid White Cast Iron. *Trans. Amer. Foundrymen's Assn.* (1939) **47**, 742-752.
11. H. A. Schwartz, G. M. Guiler and M. K. Barnett: Significance of Hydrogen in the Metallurgy of Malleable Cast Iron. *Trans. Amer. Soc. for Metals* (1940) **28**, 811-831.
12. W. L. Womochal: Progress Report on Hydrogen in Metals. *Proj. RP54*, Battelle Memorial Inst. (1937).
13. L. A. Wooten and W. G. Guldner: Determination of Carbon in Low-Carbon Iron and Steel—Low Pressure Combustion Method. *Ind. and Eng. Chem., Anal. Ed.* (1942) **14/10**, 835-838.
14. W. M. Murray, Jr., and S. E. Q. Ashley: Studies on the Determination of Carbon by the Low Pressure Combustion Method. General Electric Co. (Oct. 20, 1943).
15. W. M. Murray, Jr. and L. W. Niedrach: Determination of Carbon—Simplification of Low Pressure Combustion Apparatus. *Ind. and Eng. Chem., Anal. Ed.* (1944) **16**, 634-636.

DISCUSSION

H. H. UHLIG.—A suitable method for analysis of hydrogen in steels giving accurate results is an important problem of the moment. Dr. Moore's work in this field comes at an appropriate time. It would be helpful in interpreting Dr. Moore's results if answers were available to the following questions.

What was the maximum blank and also the average blank over the complete run in terms of percentage of hydrogen in the steel samples? In evaluating the method for accuracy it is important to know the answer to this question.

In separating CO_2 from water, how was correction made for water lost by evaporation along with the CO_2 ?

G. A. MOORE.—Stability of the blank value appears to be the final and most difficult step in establishing any of these analytical procedures. Our blanks were extremely variable in the few runs made and, moreover, were not constant throughout the run. Two high values are shown as B1 and B2 on Fig. 3, but the blank rate obviously dropped to lower values after baking out for 50 hr. Estimated total blank for the run shown was 3.67 ml. over 411 hr., or about 0.009 ml. per hour. This is 12 per cent of the hydrogen collected. This value is within the range of the Sieverts solubility at one atmosphere, hence values for many commercial steels may be very

uncertain until refinement of the method results in lower blank values.

The amount of H_2O included in the CO_2 analysis would be indeterminate for a continuous type of pump, but is a known value when a Toeppler is used.

Pressure H_2O at $-80^\circ\text{C} = 7.47 \times 10^{-4}$ millibar.

Volume taken in 10 strokes of Toeppler = 2910 milliliters.

Water evaporated = 0.00217 millibar liters.

Under average conditions, 10 or 20 strokes of the Toeppler are sufficient to collect the evaporated water, hence the correction is insignificant. A similar calculation with estimated solubility values shows the CO_2 retained in the water portion to be 0.12 per cent, approximately, of the water value. Calculation from the same figures will, however, show that a dry-ice trap is not sufficiently cold for use on a flowing oxygen stream or with a diffusion pump in operation.

Symposium on Segregation

(New York Meeting, February 1944)

CONTENTS

	PAGE
Fundamental Principles Involved in Segregation in Alloy Castings. By R. M. BRICK. (With discussion)	*
Review of Factors Underlying Segregation in Steel Ingots. By B. M. LARSEN. (With discussion)	414
Introduction to the Session on Segregation in Steel. By EARLE C. SMITH.	436
Relation of Open-hearth Practice to Segregation in Rimmed Steel. By J. W. HALLEY AND G. L. PLIMPTON, JR. (With discussion).	438
Segregation in a Large Alloy-steel Ingot. By S. W. POOLE AND J. A. ROSA. (With dis- cussion)	459

Issued as T.P. 1764 in METALS TECHNOLOGY, September 1944.

* The paper by R. M. Brick appears in Volume 161 of the TRANSACTIONS and is not included here.

A Review of Factors Underlying Segregation in Steel Ingots

By B. M. LARSEN,* MEMBER A.I.M.E.

ATTEMPTING to review the fundamental aspects of segregation in steel ingots of all types in a paper of reasonable length, we encounter two difficulties: (1) the fact that a large number of different physical and chemical effects are involved, and (2) rather incomplete and confusing evidence on certain aspects of detail and mechanism in the freezing process in which the segregation effect is involved. The best solution seemed to be to link together most of the underlying factors into a simplified theoretical picture that appears to the writer to explain most of the observed data, in the hope that this will serve as a reasonably good target for discussion and criticism.

Segregation effects, especially in steel ingots or castings, are often divided into "microscopic" and "macroscopic," depending on whether the variations in concentration of solutes† or dissolved elements in the iron occur as: (1) a periodic variation over the small distances between the nuclei and the surfaces of the primary grains, or (2) as a larger scale effect involving concentration gradients over distances of the order of several inches, more or less. The reason for this somewhat artificial division is, of course, that it is only the macroscopic scale effect that has much practical importance. About the only effect of practical importance that results from microscopic segregation is the banded structure often left in rolled sections, and

even this is relatively harmless in most cases. However, the causes of microscopic segregation also underly the larger scale effect, so we must first consider matters such as the formation and growth of crystal nuclei, selective freezing and diffusion, and others that are fundamental to all segregation effects.

UNDERCOOLING AND NUCLEI FORMATION

It is probable that although the degree of undercooling is small in iron, as in metals in general, a certain amount of it takes place, and also that the number of crystal nuclei increases very rapidly with increased undercooling below the liquidus temperature. In practical terms this means that the nuclei number increases very rapidly with increased cooling or freezing rate, thus being dependent on the rate of heat flow out from the zone of crystallization.

TEMPERATURE GRADIENTS AND HEAT DISSIPATION DURING FREEZING

Each pound of steel evolves about 100 B.t.u. when freezing. In addition to this, the temperature gradient in the solidified portion (required to dissipate the heat as freezing progresses into the axis) necessitates a loss of heat required to cool the solid metal below its freezing range, which is equivalent to an amount of not so much less in magnitude. In a 5-ton ingot, the total would include about one million B.t.u. for freezing alone and about 0.4 to 0.5 million B.t.u. for the gradient, up to the end of the freezing period. Thus the rate of freezing depends primarily on the rate of heat dissipation. In the ordinary ingot shapes, the axial rate of growth of the solid

Manuscript received at the office of the Institute June 1, 1944.

* Research Laboratory, U. S. Steel Corporation of Delaware, Kearny, N. J.

† This term is more exact and convenient to use than the more usual ones, such as "impurities" or "alloying elements."

skin drops off about as the square of time; the rate is initially very high for the extreme outer layer on the cold mold surface, but also drops off very rapidly as the skin

liquid zone will now, however, be almost zero, even at the beginning of freezing. The orientation of the crystals also will tend to be random throughout the mass

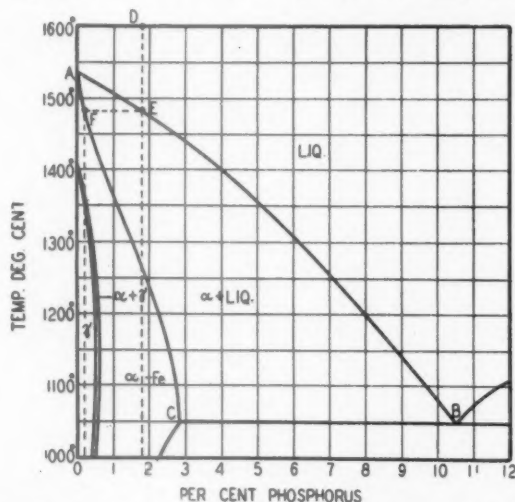


FIG. 1.—IRON-RICH PORTION OF Fe-P EQUILIBRIUM DIAGRAM.

thickens and shrinks away from the mold surface.

In the frozen skin, the temperature gradient is very steep at first, becoming flatter as the mold heats up and the solid skin thickens. At the solid-liquid boundary zone, the temperature is held constant at the freezing range by the heat of crystallization, so that the gradient in the remaining liquid between this zone and the ingot axis is small even at the beginning of freezing, and probably nearly approaches zero at an early stage. At the beginning, while the mold is being filled, it depends on pouring rate and on the superheat in the stream of metal. Since the metal stream presumably cools some 30° to 50°F. in the passage from ladle to liquid pool in the mold, if the superheat is less than this amount some crystal nuclei will be present throughout the liquid when the mold is being filled. Freezing must still progress from surface to center, since the only nuclei able to grow in size will be those at or near the mushy zone between solid and liquid, and thus able to dissipate their heat of crystallization; the gradient in the

because of the random orientation of the nuclei already present in the metal pouring in the mold.

This is not the normal mode of freezing, because apparently it is not practical to teem steel ingots with such a small margin of superheat in the ladle. With normal superheat the liquid portion probably remains at least slightly above the initial freezing temperature during at least the first 10 to 15 per cent of the whole freezing period, giving the requisite conditions for the formation of columnar crystals oriented nearly perpendicular to the cooling surface, as discussed later.

DIRECTIONAL GROWTH OF CRYSTALS

The cubic crystal nuclei of iron appear not to be able to grow with equal ease in all directions. Fastest rate of growth appears to be in one of the directions connecting the corners of the cube. Once a crystal starts to elongate in a given direction, it tends to continue in this original direction, or else at right angles to it, and this tendency would seem to be one factor in the mecha-

nism of growth of the common branching or treelike dendrites, as discussed later.

SELECTIVE FREEZING AND DIFFUSION

In pure metals with a sharp freezing point, the only factor limiting the growth of crystal nuclei is that of heat dissipation. With solute elements present and the

toward and phosphorus atoms diffuse away from the crystal surface, through the composition gradient in the adjacent layer of liquid metal.

DENDRITE FORMATION

These two diffusion processes plus the directional tendency in crystal growth

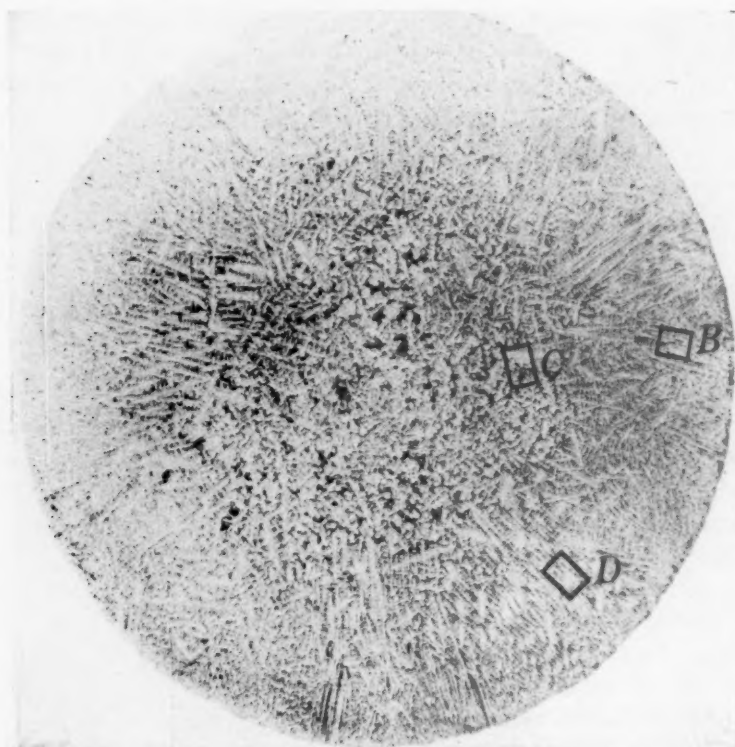


FIG. 2.—TRANSVERSE SECTION SAND-CAST BAR. $\times 2$. ETCHED WITH LE CHATELIER'S REAGENT. C, 0.15 per cent; Mn, 1.60 per cent. Annealed 6 hr. 1040°C ., furnace cooled.

freezing point widened to a range, we have the well-known condition illustrated by the iron-rich end of the Fe-P solubility diagram shown in Fig. 1. Metal of composition *D* starts to freeze at a temperature level of point *E*, but the first solid phase to crystallize has the composition *F*, which means that the adjacent liquid is enriched in whatever solute or solutes are present (in phosphorus in this case). This means that if the temperature remains at the level *EF*, further crystallization will be limited not only by the rate of heat dissipation but also by the rate at which iron atoms diffuse

probably combine to give the branching treelike forms we call dendrites, which characterize the solid crystals forming from the liquid steel. As a tiny crystal forms the liquid film around it is depleted in iron. Its points or edges are closer to a great volume of liquid than its flat surfaces and it seems to elongate first along one of the directions connecting two opposite cube corners and then send out branches perpendicular to the edges of this first or main axis of the dendrite. These branches may then also branch at right angles, but the inner branches quickly lower the iron

content of the remaining liquid between them. The outer branches (from which the heat of crystallization can also diffuse away most easily) continue to grow until they

slow cooling from the freezing range remain largely in the pattern of variable concentration caused by dendrite growth. This pattern apparently is revealed by

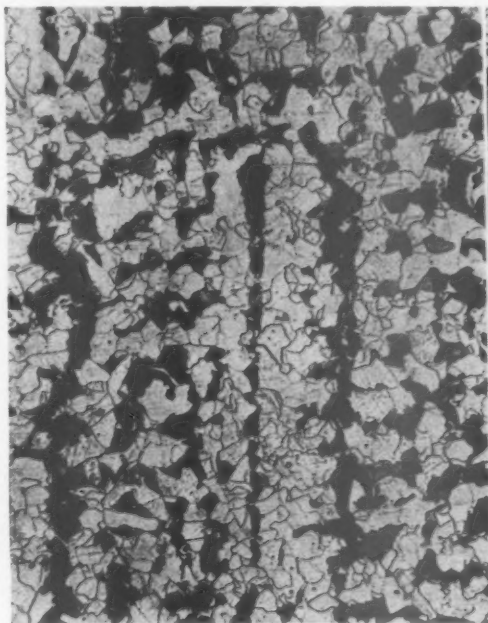


FIG. 3.

FIG. 3.—AREA MARKED *B* IN FIG. 2, REPOLISHED AND ETCHED WITH NITAL. $\times 40$. Shows dark or pearlite areas mainly in high-manganese fillings between dendrite axes.

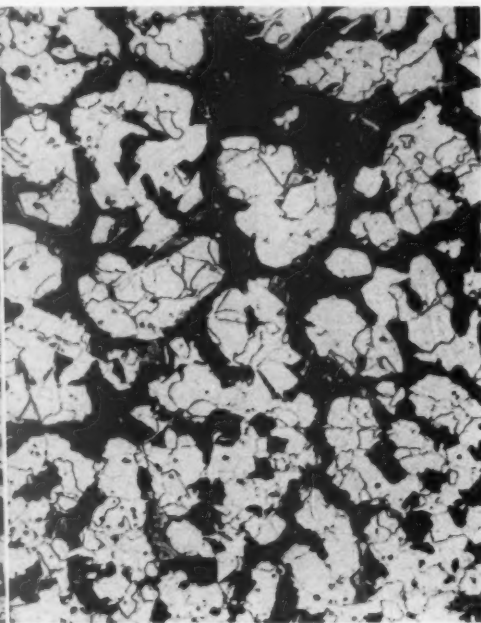


FIG. 4.

FIG. 4.—AREA MARKED *C* IN FIG. 2. $\times 40$.

Similar to Fig. 3, with dark or pearlite areas in high-manganese portions between dendrites, but with dendrites more rounded here nearer to center of casting.

approach neighboring dendrites, after which the liquid between freezes only as the temperature falls through the freezing range. The orientation between branches is related presumably to inherent growth habit of the crystal, but the essential point is that the dendrite in a sense "*reaches out*" its branches into the liquid in such manner as to minimize the limitation of the rate of supply by diffusion of extra iron atoms to the crystallizing surface.

Dendrites form in the freezing of pure iron-carbon alloys, but the resultant local segregation pattern tends to be quickly wiped out by the rapid rate of diffusion of carbon in the solid metal at temperatures slightly below the freezing range. Other common solutes, such as P, Mn, Cr, diffuse much more slowly, and even with

certain etching agents, as illustrated by Fig. 2, which is a transverse section of a small sand-cast bar of 0.15 per cent C steel, which is very low in other solutes except for 1.60 per cent Mn.¹ It is presumably the dendritic segregation of manganese that gives the etching pattern shown in this case. To confirm the validity of this inference, we may take advantage here of the fact that manganese lowers the critical points at which ferrite and pearlite form on cooling, so if we cool slowly through the critical range, ferrite grains should separate from austenite first along the dendrite axes, which are lowest in manganese. This effect is shown in Figs. 3 and 4, taken of the marked areas in Fig. 2 after repolishing

¹ References are at the end of the paper.

and etching to show the microstructure. Detailed examination showed much similarity in certain details of microstructure between dendrite and ferrite-pearlite pat-

GRAIN SIZE, ORIENTATION IN OUTER INGOT ZONES

During the first few seconds of rapid freezing on a cold mold surface, very many

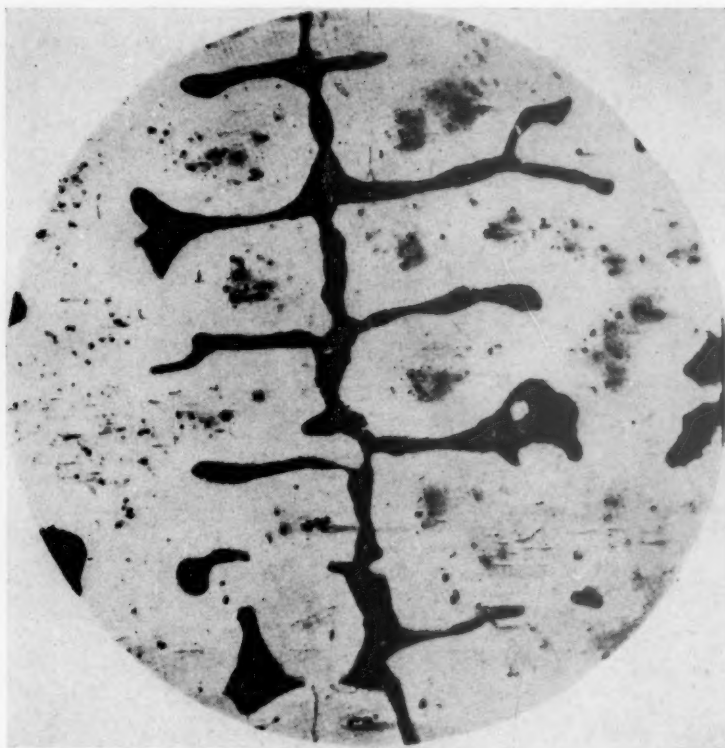


FIG. 5.—INGOT OF HIGH-PHOSPHORUS IRON. (After Sauveur and Krivobok.) $\times 50$. ETCHED WITH NITAL. C, 0.17 per cent; P, 0.39 per cent. Shows dark or pearlite areas in low-phosphorus dendrite axes.

terns, with elongated ferrite areas toward the outside (Fig. 3) and more round ones near the center (Fig. 4) as in the dendrite pattern, and left little doubt that the pearlite tended to concentrate in the manganese-rich fillings between the main dendrite axes. In a corresponding case, with phosphorus as the main solute, the fillings between dendrite axes should also be richer in phosphorus, but since phosphorus raises the critical point for ferrite separation, the pearlite should tend to be left in the phosphorus-low dendrite axes on slow cooling. This effect is shown by the microstructure in Fig. 5 of a 0.39 per cent P iron alloy with 0.17 per cent carbon, taken from a paper by Sauveur and Krivobok.²

nuclei form, and there is not time for any appreciable diffusion or resultant dendritic segregation, because the metal is chilled so quickly through its freezing range. Cooling rate then decreases rapidly, however, and the number of nuclei decreases; small dendrites form, but the temperature gradient is still so steep in the first minute or so that new nuclei form beyond those already forming and grain size remains small with random orientation. Very soon, with further decrease in cooling rate and slope of temperature gradient, if the liquid portion also has a normal superheat, relatively few or no more new nuclei form just beyond the less pure layer inside the already growing dendrites, so these tend to

keep on growing. Since freezing, controlled by heat loss, is in general perpendicular to the mold wall, those dendrites with main axes of growth at an angle to this wall run

increase in grain size and the elongated or columnar growth.

The typical columnar crystal zone involves a trapping of less pure liquid

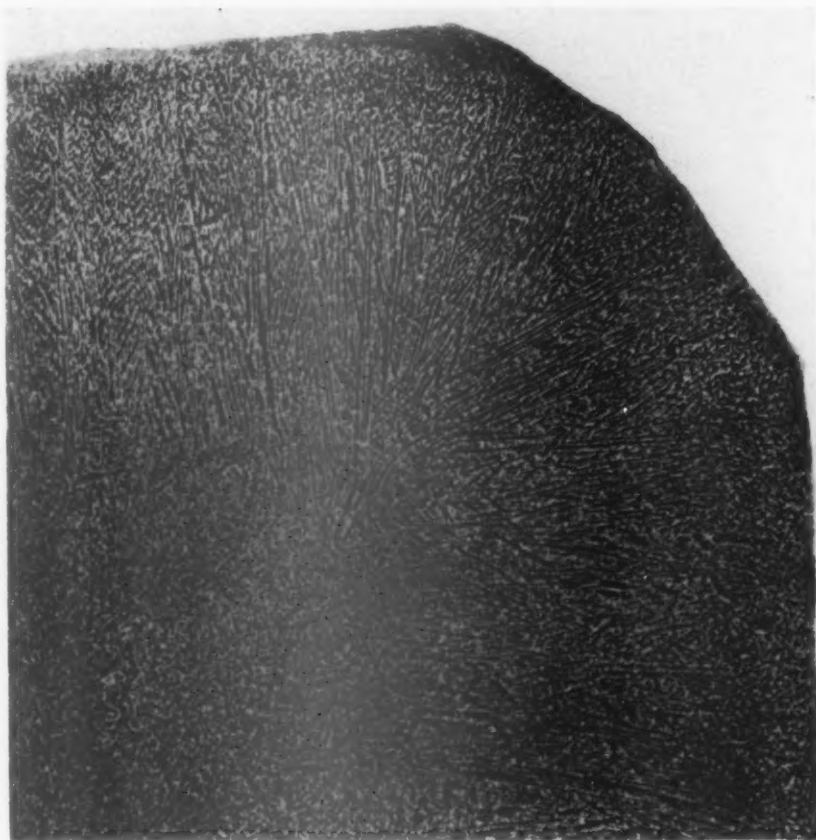


FIG. 6.—TRANSVERSE QUARTER SECTION, CHILL-CAST, 4-IN. INGOT (C, 0.35 per cent, Mn, 1.86 per cent). $\times 2$. ETCHED WITH LECHATelier REAGENT.

Shows dendrite forms in different ingot zones from surface to axis, with free-floating dendrites in central zone.

into adjacent ones, and those which are oriented so as to grow rapidly in a direction nearly perpendicular to the mold surface are the ones to survive.

These changes are illustrated by the dendrite pattern of a transverse cross-section of a small chill-cast ingot shown in Fig. 6. Beyond an outer skin of fine grains without appreciable dendritic outlines we have small dendrites of random orientation, gradually changing to elongated dendrites with predominantly radial orientation. The crystal structure in the axial cross section of Fig. 7 shows more clearly the

between attached, oriented dendrites reaching into the liquid and as regards segregation effects there are three essential factors involved here:

1. At least some small degree of superheat must exist in the main body of liquid inside the freezing zone. If the liquid entering the mold is already at its initial freezing temperature, it will contain some dendrites or crystal nuclei distributed throughout the liquid as the mold is filled. These, plus additional ones formed during freezing, will stop the growth of elongated dendrites, and most of the mass will freeze

from such nuclei oriented at random and, except in the outer chill zone, the dendrites will be "free floating" in the liquid for a variable time through the whole freezing

free-floating nuclei with random orientation, and freezing from such nuclei continues in to the center.

2. The presence of solutes, especially

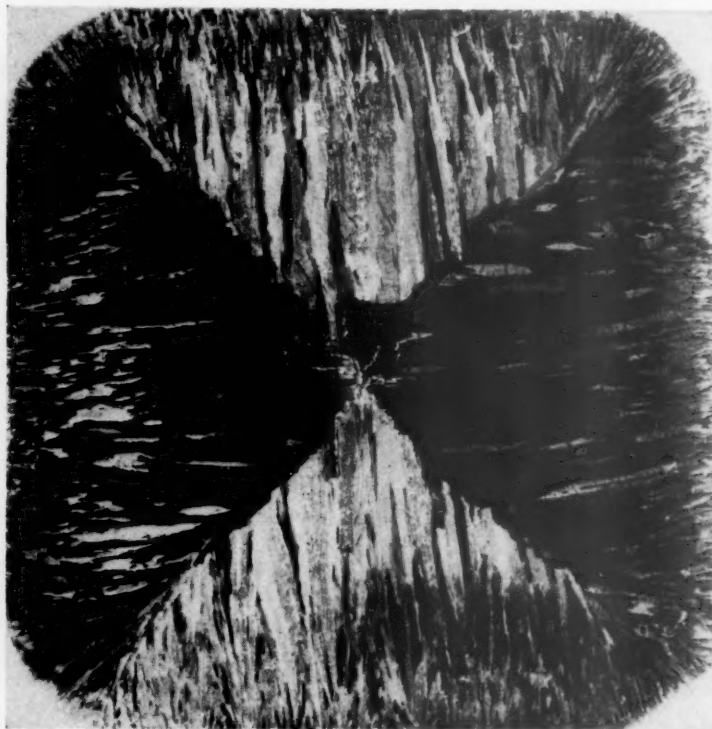


FIG. 7.—TRANSVERSE SECTION, CHILL-CAST 3.5-INCH INGOT OF PERMALLOY. $\times 100$. ETCHED WITH AQUA REGIA IN GLYCERINE.

Shows grain coarsening in from surface, with columnar crystallization persistent to end of freezing period.

period. Of course, even with some superheat in the steel as poured, at some stage during freezing the main body of remaining liquid will usually approach a zero temperature gradient, so that a zone of adjacent liquid inside is at the same temperature as the inner ends of the attached dendrites, and free-floating nuclei can form a little ahead of them. The liquid layer between is then impoverished in iron and the attached dendrites quickly stop growing. This change is shown in Fig. 6, when freezing had progressed a little over half way from surface to center. With the remaining liquid now all approaching a temperature level at or slightly below the liquidus (such as *AB* in Fig. 1), conditions now favor new

those with a low diffusion rate. In a pure metal, radial growth of crystals toward the axis would tend to be even more pronounced, but less pure liquid would not be enclosed between them. This sounds ridiculous in the sense that, of course, we cannot have segregation at all without solutes present, but the important point here is that these solutes and the resultant composition difference between crystals and adjacent liquid *introduce a rate of diffusion in the liquid metal* into the problem as mentioned above. In the pure metal, the crystals would advance almost as a solid wall perpendicular to the direction of heat flow, because any projecting crystal would lose heat less rapidly than its

adjacent liquid and the solid-liquid interface would tend to remain a plane surface with the rate of heat loss the single controlling factor. With solutes present, the liquid layer around and between any crystal projections is less pure and lower melting than the average, and dendrite elongation is dependent on a rate of counter-diffusion of iron and solute atoms (as discussed above in connection with dendrite growth) as well as upon the rate of heat dissipation. The projecting points and edges being favored in this diffusion, they can elongate into the liquid to give the condition illustrated crudely by the diagram of Fig. 8a, with dendrite axes *D* and less pure, later freezing portions *X*.

3. Closely related to factor 2 is the necessity for the absence of any marked stirring or convection in the liquid portion during the period of columnar crystal growth. The concentration gradient adjacent to freezing surfaces can exist only because interatomic diffusion in a quiet liquid is relatively slow even at the high temperatures in liquid steel. Vigorous stirring and flow of the liquid past the crystallizing surface will tend to wipe out such concentration gradients in the adjacent liquid. Projections from this surface are no longer favored by diffusion, and since they are farthest away from the cooling effect of the mold surface, if the stirring is vigorous, conditions tend to return to that in a pure metal, with freezing approaching a layerlike growth as in Fig. 8b. Such a stirring effect with relative motion between solid and liquid during freezing can in theory be produced artificially, though with obvious difficulties, especially in steel. A little experimental work along this line^{3,4} has been done but the practical importance of the effect in steel ingots arises from the fact that in a vigorously rimming ingot there is an approach to condition *b* in Fig. 8, owing to the natural rising tendency and associated stirring effect of the CO bubbles produced

by the carbon-oxygen reaction in the iron solution on or near the crystallizing surface, as discussed in a later section.

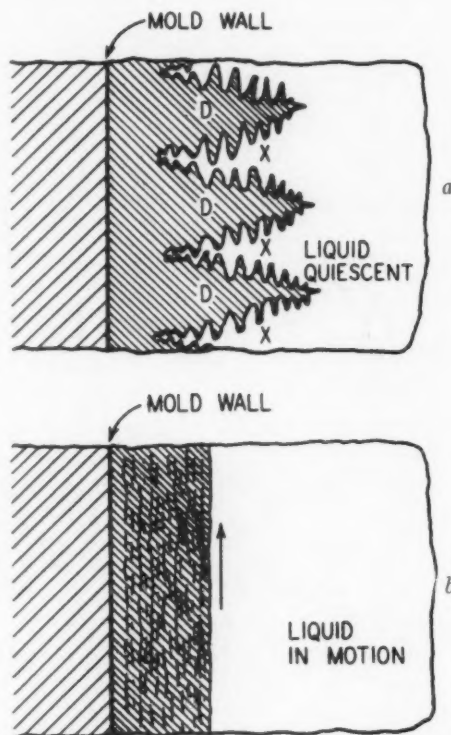


FIG. 8.—DIAGRAM TO ILLUSTRATE GROWTH OF CRYSTALLIZING SURFACE WITH (a) QUIET LIQUID AND (b) LIQUID IN RAPID MOTION PAST SURFACE OF CRYSTALLIZATION.

SETTLING OF FREE-FLOATING DENDRITES— VOLUME CHANGE IN FREEZING

These details involved in the process of radial columnar crystallization are not merely academic, because if we could freeze whole ingots in this manner, with the dendrites always attached to the solid portion and the less pure, last freezing liquid always subdivided into tiny zones between dendrite axes and trapped in position until frozen, macroscopic segregation would presumably be negligible in amount. In small castings and very small, 4 to 8-in. chill-cast ingots, this condition is approached. In the commercial ingot sizes, however, this mode of freezing probably occupies only about the first

5 to 15 min. out of a total freezing period of something like 2 hr. or more. Even with a reasonably large superheat in the metal as the mold is filled, the liquid inside the

ing liquid then freezes by the growth of such free-floating dendrites. This stage of solidification may represent only 40 to 60 per cent of the total ingot volume but it

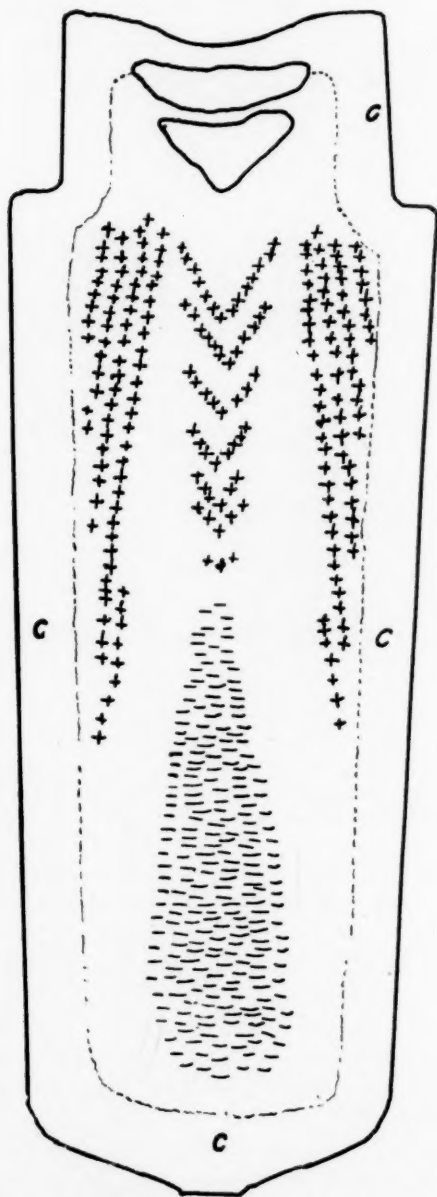


FIG. 9.—APPROXIMATE ZONES OF SEGREGATION AND CRYSTALLIZATION.
 ++ positive segregation.
 -- negative segregation.
 CC columnar crystallization.

freezing zone soon cools down to a point at which independent nuclei apparently form, floating free in the liquid, and the remain-

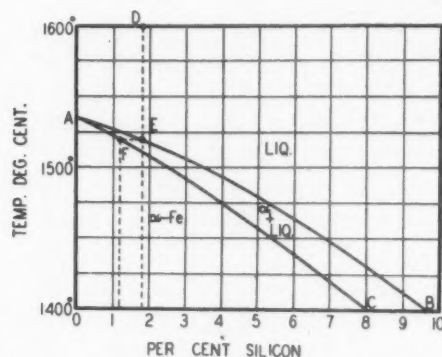


FIG. 10.—IRON-RICH PORTION OF IRON-SILICON EQUILIBRIUM DIAGRAM.

occupies perhaps 85 to 90 per cent or more of the total freezing time. The density change on freezing from roughly 7.0 in the liquid metal to 7.5 in the floating dendrites is only about 7 per cent in relative terms, but the absolute change is rather large, and these free-floating nuclei have a relatively slow growth and a long period to settle in the liquid toward the bottom central zone of the ingot, which in killed ingots is the main zone of negative segregation due to the concentration of the purer dendrite cores.

In general, positive segregation occurs in the upper central zone as the converse of this effect, but its local distribution is often more complex, as indicated by the diagram of Fig. 9, with so-called V-segregates near the axis and inverted A-segregates just inside the columnar zone. We probably do not understand the mechanisms here too well, but one factor involved is probably a consequence of the change in density; i.e., that liquid must flow in between the dendrites to make up for the shrinkage in volume.

The amount of segregation caused by these effects should in the main increase: (1) with factors increasing the length of the freezing period, such as ingot size, mode

of cooling, thermal conductivity, etc., and (2) with greater separation between the curves of liquid and solid compositions at equilibrium in the system of the solute element and iron. For example, Fig. 10 shows the iron-rich part of the silicon-iron system. The relative shift in composition between points *E* and *F* is here much less

on this reasoning. For example, in a study of 30 ingots reported mainly by the Committee on Heterogeneity of Steel Ingots of the Iron and Steel Institute, a tabulation was made (Table 1) of segregation ratios for the various elements; that is, the ratio between the highest and the lowest concentrations of a given element in a given

TABLE 1.—*Segregation Ratios in Steel Ingots*

Ingot No.	Weight of Ingot, Tons	Segregation Ratios							Remarks
		Ni	Cr	Mn	Si	C	P	S	
1	3 $\frac{3}{4}$	1.04				1.18	1.57	1.50	Killed steel, chill mold
2	1 $\frac{3}{4}$			1.08	1.24	1.24	1.23	1.32	Killed steel, bottom-cast
3	2 $\frac{3}{4}$	1.03	1.06			1.26			Killed steel, chill mold
4	2 $\frac{3}{4}$	1.03	1.05			1.36			Killed steel, chill mold
5	2 $\frac{3}{4}$			1.07	1.09	1.34	1.28	1.31	Killed steel, chill mold
6	2 $\frac{5}{8}$					1.14	1.45	1.92	Killed steel, chill mold
7	3 $\frac{1}{4}$			1.21		1.60	2.19	2.30	Killed steel, chill mold
8	8			1.11		1.43	1.26	1.81	Killed steel, chill mold
9	8 $\frac{1}{2}$					1.56	1.78	3.13	Killed steel, loam mold
10	10 $\frac{1}{4}$			1.16	1.15	1.73	1.33	3.87	Killed steel, chill mold
11	20			1.06	1.10	1.47	1.67	1.73	Killed steel, chill mold
12	25			1.17	1.16	1.59	1.92	2.43	Killed steel, chill mold
13	49	1.07	1.13	1.15	1.11	1.71	2.00	2.14	Killed steel, chill mold
14	50	1.11		1.13	1.23	1.50	1.60	1.83	Killed steel, chill mold
15	64			1.18	1.25	1.66	2.04	2.12	Killed steel, chill mold
16	110			1.25	1.17	3.07	2.52	3.48	Killed steel, chill mold
17	119	1.05	1.20	1.11		1.52	2.82	1.76	Killed steel, chill mold
18	172			1.27	1.43	3.14	4.00	4.53	Killed steel, chill mold
19	63 $\frac{3}{4}$			1.09		1.80	2.08	3.10	Semikilled plate steel
20	73 $\frac{3}{4}$			1.11		2.27	2.62	3.22	Semikilled plate steel
21	63 $\frac{3}{4}$			1.11		2.40	2.42	2.43	Semikilled plate steel
22	8			1.18		1.93	1.93	2.57	Semikilled plate steel
23	3 $\frac{1}{4}$			1.11		1.60	1.79	1.69	Free-cutting steel
24	73 $\frac{3}{4}$			1.09	1.21	1.60	1.64	1.70	Plate steel
25	3			1.07		2.73	3.20	5.43	Rimmed steel, chill mold
26	3			1.09		2.04	2.40	2.05	Rimmed steel, chill mold
27	3			1.13		1.80	2.60	2.60	Rimmed steel, chill mold
28	3			1.13		1.79		1.72	Rimmed steel, chill mold
29	3			1.13		2.34		2.05	Rimmed steel, chill mold
30	3 $\frac{1}{4}$			1.15		1.40	3.70	4.60	Rimmed steel, chill mold
Average		1.05	1.11	1.13	1.19	1.77	2.10	2.50	

than that between the corresponding points in the phosphorus-iron system of Fig. 1, so we should expect silicon to segregate much less than phosphorus. A comparison of existing phase diagrams of iron with the common "impurities" or alloying elements in steel from this standpoint indicates that Ni, Cr, Mn and Si should segregate about alike, with Ni perhaps a little less than Si. Carbon should show a big increase over this group, phosphorus somewhat more than carbon, and sulphur should show the greatest amount of segregation.

In a rough way, the available data on ingot segregation fulfill expectations based

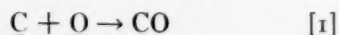
ingot cross section (except that in choosing highest values, extreme concentrations reported from hot-top feeder head zones or just at the base of the pipe were usually omitted and the next highest value was taken). Averages from all ingots for each impurity show that Ni, Cr, Mn and Si all grouped together with a small degree of segregating tendency, with a large increase to C and P, and with S the highest, just as indicated by the phase diagrams. Taking only the killed ingots in the ordinary chill molds, there is a general tendency for the ratios to increase with ingot size. For example, the ratios for carbon increase

from about 1.2 in 1-ton ingots to about 3.0 in those above 100 tons. In general, the values scatter about somewhat; such segregation surveys are of necessity rather crude, of course, since the difficulty of accurately mapping detailed composition variations in large steel masses is very great. Other complicating effects probably are involved; however, the factors mentioned above are very likely the main controlling effects.

EFFECTS OF LIQUID MOTION AND STIRRING CAUSED BY GAS EVOLUTION

Macroscopic or large-scale segregation must involve, in one way or another, some *relative motion of the less pure liquid portion relative to the dendritic crystals* during the freezing process, otherwise we should obtain only microscopic or dendritic segregation. Two common causes of such relative motion have been mentioned: (1) the stirring effect of expanding and rising CO bubbles formed by the carbon-oxygen reaction in the metal, and (2) the settling tendency of unattached dendrites in the less dense liquid in the central portion of the ingot. Returning now to the first effect, we find that although this is most pronounced in rimming ingots, it really occurs in gradually decreasing amount over a whole series of steel-ingot structures from very "wild" to almost "dead killed" and some attention to certain details of the gas-forming reaction will aid in understanding this gradually changing series of structures.

This reaction may be written



the underlined C and O indicating that these are in solution in iron, with the CO precipitated out of solution in the form of gas bubbles as the reaction proceeds. This reaction is thus retarded by increasing pressure. Since the ferrostatic pressure of a column of about 59 in. of liquid iron is

equal to one atmosphere, and since most ingot heights run around 65 to 75 in., the effective back pressure against this reaction is at least doubled between top and bottom ingot zones. Both carbon and oxygen contents tend to be lower in the solid crystals freezing out, so both are concentrated somewhat in the zone adjacent to the freezing surface. Also, these CO bubbles apparently start to form with some reluctance, somewhat like the bubbles of CO₂ in beer or soda water, and like the latter again, seem to start more easily on a more or less rough solid surface such as the surface of the freezing crystals. Both of these factors probably cooperate to favor bubble formation at the freezing surface.

If the steel entering the molds contains no other metals but very weak deoxidizers such as copper, nickel, molybdenum, or manganese in moderate amounts up to around 0.5 to 0.7 per cent, or silicon in amounts of not more than 0.01 to 0.02 per cent, the carbon concentration should then determine the oxygen concentration. Such steel should be "saturated" with respect to CO evolution and should start to evolve gas immediately as freezing commences, and one would expect that over at least a moderate range of carbon contents oxygen would decrease as carbon increased, with the product C times O and the gas-evolving tendency remaining about constant. Even in such simple, "open" steels without strong deoxidizers, the situation is not quite so simple, however. Apparently, as carbon increases from zero the gas-evolving tendency increases up to about 0.03 per cent C, but then begins to drop off again, until at around 0.25 to 0.30 per cent C gas evolution is relatively very sluggish. (This may be simply because at around 0.04 to 0.05 per cent C the equilibrium in reaction 1 is such that about equal numbers of C and O atoms are present in solution; at lower carbons the reaction may be starved for lack of carbon atoms, and at higher carbons for lack of oxygen atoms.)

If silicon or aluminum is added in appreciable amounts to the metal before it enters the molds, the oxygen content will be reduced below the equilibrium or "saturation" levels for reaction 1 and gas evolution usually will not start immediately upon entrance into the molds. If, however, the aluminum or silicon additions are small enough to reduce the oxygen content only moderately below the "saturation" value then, because of the concentration of C and O by selective freezing, after a moderately small thickness of metal has crystallized out, gas evolution can start at the solid-liquid interface, this being the condition in the typical low-carbon rimming ingot. With considerably more silicon or aluminum added, no gas evolution may occur until most of the ingot is frozen, but the concentration of carbon and oxygen and the low ferrostatic pressure may even then permit some gas evolution in the upper central zone, which freezes last, giving the typical semikilled ingot structure. After the top of the ingot has frozen over, gas evolution tends to be limited in amount to not much more than that which will fill up the normal 7 per cent volume shrinkage in freezing, since the "back pressure" then builds up rapidly to repress the gas-forming reaction. If silicon is present in excess to leave about 0.6 to 0.8 per cent or more in solution, or if enough aluminum is added to leave about 0.01 to 0.03 per cent or more of excess in solution, essentially all formation of gas bubbles will be prevented and the ingot will be "dead killed."

This gas-evolving tendency profoundly modifies both segregation and distribution of blowholes, as it decreases with increasing amounts of carbon or of other deoxidizing alloy additions. In the range of about 0.03 to 0.07 per cent C, if no strong deoxidizers are added, gas evolution is excessive. After a thin layer of chill crystals forms, gas bubbles start and appear to spread throughout the liquid metal, expanding and pushing up the liquid metal even before

the mold is filled, even pushing part of the metal out of the mold and then subsiding and leaving a thin, frozen shell above and a porous central mass in the bottom part, giving a so-called "wild" or "bootleg" ingot structure. With more carbon (above 0.10 per cent), or with a few ounces of aluminum added per ton, there is a vigorous gas evolution after some metal has frozen, but probably only at the liquid-crystal boundary, so that the liquid is not "wild" enough to boil up out of the mold but rises up in a zone around the outside and then flows down in the center zone, giving the typical "rimming action." With an increasing degree of deoxidation up to the semikilled and dead-killed stages we pass through a number of modifications in ingot structure, which will be treated later in some detail in the discussion of the series of ingot structures shown in Fig. 12.

FREEZING OF TYPICAL RIMMED INGOT

In a typical rimmed ingot the vigor of gas evolution is repressed just enough below that in a wild ingot to (1) allow a thin, practically solid skin to form before much gas evolution begins, and (2) to confine gas-bubble formation to an annular cylindrical zone just inside the freezing surface without spreading inward throughout the liquid volume to cause a wild, foaming rise of the gas-metal mixture. If these conditions are obtained, the metal is carried upward rapidly in this annular zone by the rising bubbles, the bubbles escape at the top surface and the metal flows down again in the center, the circulation preventing the top surface from freezing over. In the ideal case of an ingot that "rims in straight across" to form a flat top, there must be a rather delicate balance of gas formation and escape, so that the relative amount of gas present at any instant down in the liquid remains practically constant from the moment the mold is filled until the 10 to 20-min. period of rimming action is completed.

In this connection, it should be remembered that although liquid iron has a viscosity about like that of water, so that circulation can be maintained fairly easily

deoxidation must also be approximately correct.)

As noted above, in discussion of the diagrams of Fig. 8, such a rapid motion of the

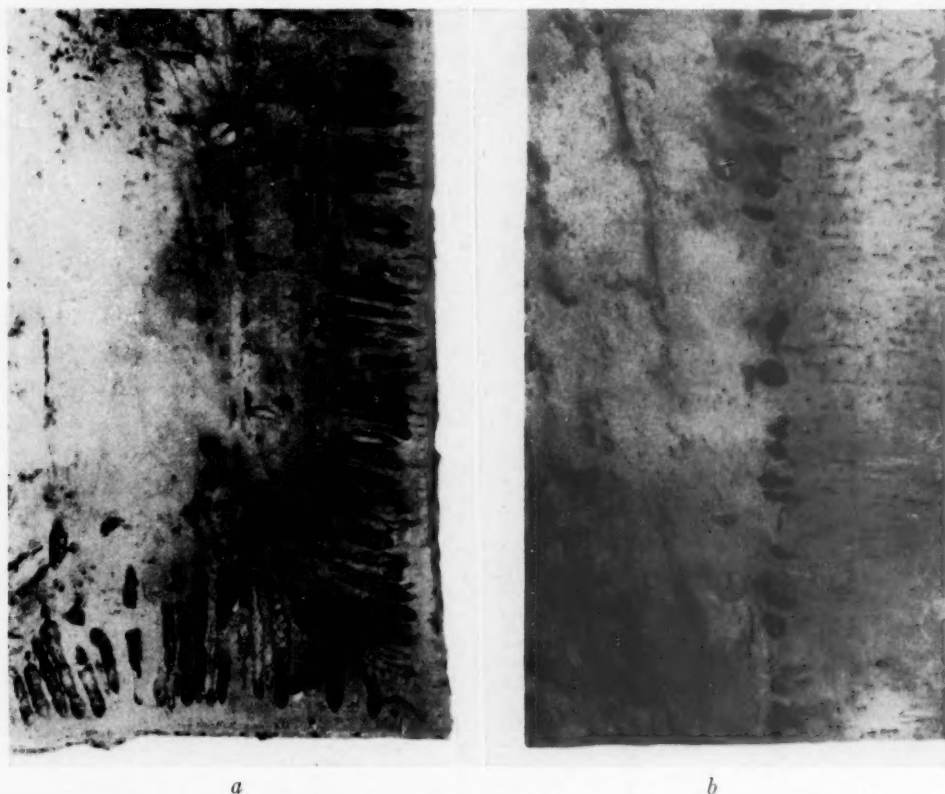


FIG. 11.—TWO PARTS OF AN AXIAL SECTION OF A TYPICAL RIMMED INGOT. $\times \frac{1}{3}$. Showing (a) skinholes in rim near bottom with greatest "ferrostatic" pressure, (b) nearly solid rim zone half way up, with lower pressure.

once it has been started, the liquid is heavy and to get several tons of it into such rapid motion requires a little time and the development of considerable kinetic energy. This is why a rimmed ingot should be filled rather slowly to allow the motion to develop in the bottom while only partly filled (with "ferrostatic" pressure low), so that by the time pouring is completed the whole liquid portion is in rapid motion and the proper balance between gas formation, rise and escape is established. Otherwise, the metal will either rise or drop or both in the early freezing period and excessive "skinhole" formation (see below) is likely to occur. (Of course, the degree of

liquid past the freezing surface will greatly modify the crystallization process. If the motion, mixing and sweeping away of less pure metal next to the solid surface is sufficiently vigorous, freezing is not limited by the rate of counter-diffusion of iron and solute atoms, but only by the rate of heat loss, and can occur at any point on the surface, so that it will tend to proceed in smooth layer fashion, as in Fig. 8b. If, however, the stirring and mixing is rather sluggish, dendrites probably start to grow out into the liquid; the liquid zones trapped between these will be highest in carbon and oxygen, so gas bubbles will form at such points (as X, in Fig. 8a). But these

bubbles will tend to be trapped in by the dendrite projections and all of them will not be swept upward to the top of the ingot; and the result is the familiar elongated skinholes in the outer zone of rimmed and other open steels. Much of the impure liquid portions will be pushed out from among the purer dendrites by these growing gas bubbles, however, so the negative segregation in such portions of the rim zone may be much the same as in the more solid portions of the rim where conditions approximate those of diagram *b*, Fig. 8.

Fig. 11 shows two parts of the cross section of rim and core zones of a typical rimmed ingot at about one third natural size; *a* is the bottom corner and *b* is about half way up on the side of the ingot, showing rim zone and nearly all the core to the ingot axis. In *a*, the outside layer of $\frac{1}{4}$ to $\frac{1}{2}$ in. thickness was quenched and frozen so rapidly that all but a few tiny bubbles were prevented from developing. (This zone will be of nearly the average composition, with practically no segregation permitted.) In this lower part, hydrostatic pressure was greatest and dendrite growth trapped in bubbles because of sluggishness in gas evolution and motion in the liquid. Farther up the pressure was less, metal movement built up more rapidly and swept away the bubbles as fast as they formed, giving a nearly solid rim zone and freezing conditions about as in *b*, Fig. 8. But as freezing continued, the rate of heat loss and freezing decreased and at the same time the vigorous up and down circulatory motion probably worked downward toward the bottom of the ingot, which may be the cause for the elimination of the projection of dendrites and the trapping of bubbles, first about a foot from the bottom (skinholes shortest here) and gradually clear down to the bottom layer, so that even here the inner part of the rim zone becomes solid. Another possible cause here is that the rate of dendrite growth became too low to trap the bubbles effectively. In this case,

of a typical rimmed ingot with vigorous gas-forming potential, the effects are essentially controlled by rate of pouring into the mold, the variable "ferrostatic" pressure or head at various levels and the energy input and time delay involved in getting a large weight of heavy liquid into rapid motion.

TRANSITION SERIES OF INGOT STRUCTURES WITH DECREASING GAS EVOLUTION

As the carbon content is increased or increasing amounts of aluminum and silicon are added to obtain a decreasing gas-forming tendency relative to the rimmed ingot just described, there is a continuous series of changing ingot forms. The series of diagrams shown in Fig. 12, which were derived by Belding* from an actual series of steel ingots of commercial size, gives an excellent illustration of certain stages in this continuous series of changing forms. (Comparison here is somewhat simplified by having all these ingots poured at the same rate and to about the same height in the same size bottle-top mold.) The typical rimming ingot just discussed corresponds to No. 7 in this series, while No. 8 (usually obtained in low-metalloid steel low in manganese and with 0.02 to 0.05 per cent carbon) is a slightly wild ingot, in which the gas evolution was so vigorous as to suppress dendrite growth and sweep away potential skinhole-forming bubbles even under the high pressure existing near the bottom of the ingot. This heavy gas evolution at the early freezing period also involved a *decrease* in the relative volume of gas existing in the liquid through the rimming period and a consequent fall of metal level at the top during this same period.

No. 6 shows a slightly rising steel, with stirring and gas evolution less vigorous than in ingot 7, so that skinholes could form higher up at lower pressure levels, and a resultant *increase* in the proportion of gas

* Communication from H. R. Belding, Chief Metallurgist, Farrell Works, Carnegie-Illinois Steel Corporation.

space present, so that the top metal level rises as freezing proceeds. Segregation between rim and core should be very

weaker here; the stirring effect is vigorous enough to suppress early skinhole formation only in the upper zones. The volume of

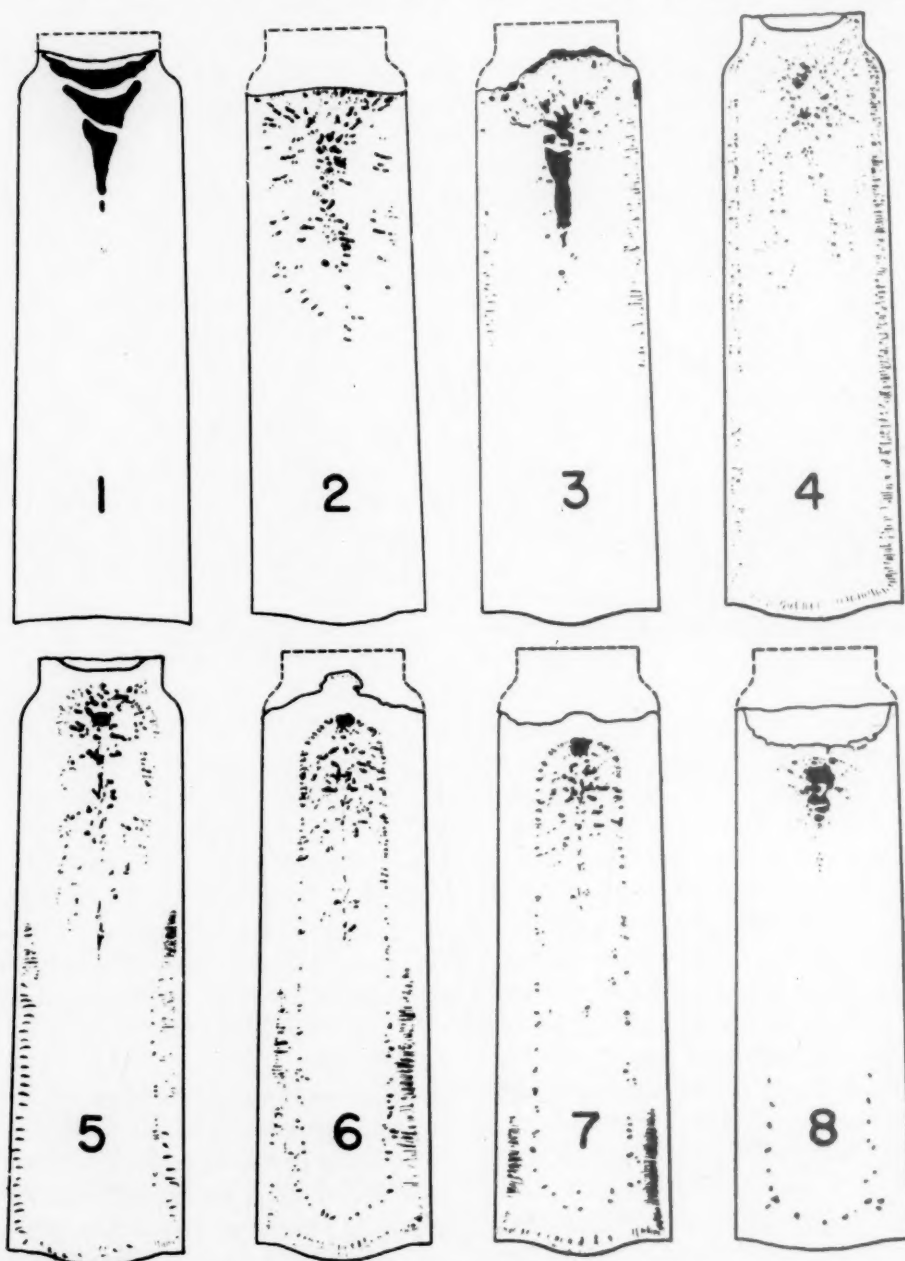


FIG. 12.—DIAGRAMMATIC AXIAL SECTIONS OF STEEL INGOT SERIES FROM DEAD-KILLED TO VIGOROUS RIMMING. (After Belding.)

pronounced in all of these last three ingots but with a moderate decrease in the order 8, 7, 6. No. 5 is a typical capped steel ingot structure. Gas evolution potential is still

trapped gas bubbles increases rapidly in the early freezing period, and the resultant rising tendency is enough greater so that the top level is pushed up into the bottle

neck, where it can freeze against a metal cap over the top of the mold and the rimming action is stopped usually in 1 to 5 min. after pouring is complete. Rim to core segregation should be less than in ingots 6 to 8 but segregation by falling dendrites in the core zone may now be more noticeable. No. 4 is a capped ingot, but with too much deoxidizer added. The gas evolution and stirring effect are not strong enough to sweep out much gas even in upper zones, but are enough to form bubbles near the surface, sometimes over the whole length of the ingot. The thin rim zone will show only moderate negative segregation. No. 3 usually is the result of trying to make a semikilled ingot but with too small an amount of effective deoxidation. Gas-evolving tendency is so weak that no bubbles are formed at the low levels where the ferrostatic pressure is high, but some skin blowholes can form at upper levels. Rimming action is nonexistent, or nearly so, and the top ingot surface soon freezes over. However, gas formation continues and breaks through this weak, thin, frozen top layer, pushing liquid metal out to form a spongy mass and increasing the shrinkage space below. Rim to core segregation should be almost nonexistent in 3.

No. 2 is a properly made semikilled ingot, with enough silicon or aluminum addition so that practically no blowholes can form in the outer layers. After enough freezing and positive segregation in the upper central zone has occurred, some gas bubbles can form in this upper zone, but by this time the frozen top layer is thick and strong enough to withstand the moderate pressure developed. At the same time the shrinkage volume will be well distributed in the gas pockets of the upper central zone, and the top surface will be flat or slightly bulged upward. No. 1 is a "dead-killed" or "piping" ingot, with sufficient aluminum, silicon, or other strong deoxidizing agent added so that the activity of oxygen in the iron solution was lower than

in CO at around one atmosphere pressure at any stage of the freezing process. Thus the shrinkage cavity will form with a pressure somewhat below one atmosphere (although some CO and H₂ will diffuse into it) and the ingot top will tend to be concave. Such an ingot, of course, would usually be poured in a hot-topped mold, usually big-end-up, and the shape of the shrinkage cavity and distribution of segregation would both be somewhat modified, but the form shown is better for comparison here. The top freezes over early and the shrinkage soon causes the metal below to separate from this crust in the center. This separation allows the crust here to cool more rapidly and the metal surface below the gas space later freezes, mainly by radiation across to the colder crust, forming a second frozen "bridge" over the growing shrinkage cavity, with a third or fourth bridge sometimes forming before freezing is complete. In ingots 1, 2 and 3 all macroscopic segregation is caused probably by the settling tendency of unattached dendrites in the central zones, with columnar crystallization and only microscopic or dendritic segregation in the outer zones.

HYDROGEN EVOLUTION DURING SOLIDIFICATION

In commercial steelmaking practice, H₂ probably has only a very minor effect on segregation, but its presence in solution in variable amounts in all ingots, and the frequent evolution of hydrogen as a gas during freezing, complicates the whole picture, and we tend to give the role of hydrogen more importance than it deserves. Liquid steel just above its melting range can dissolve roughly a little over twice its own volume (S.T.P.) of hydrogen at one atmosphere external hydrogen pressure; on freezing, the solubility drops to less than half this value, or roughly about one volume of hydrogen per volume of solid metal at its melting point. This causes hydrogen to segregate

like the other solutes; that is, it is concentrated microscopically between dendrites and macroscopically in the upper central part of the ingot. Methods of

builds up as the square of the amount in solution, such steel, after being dead killed, if poured directly into a mold would be likely to evolve bubbles of hydrogen in

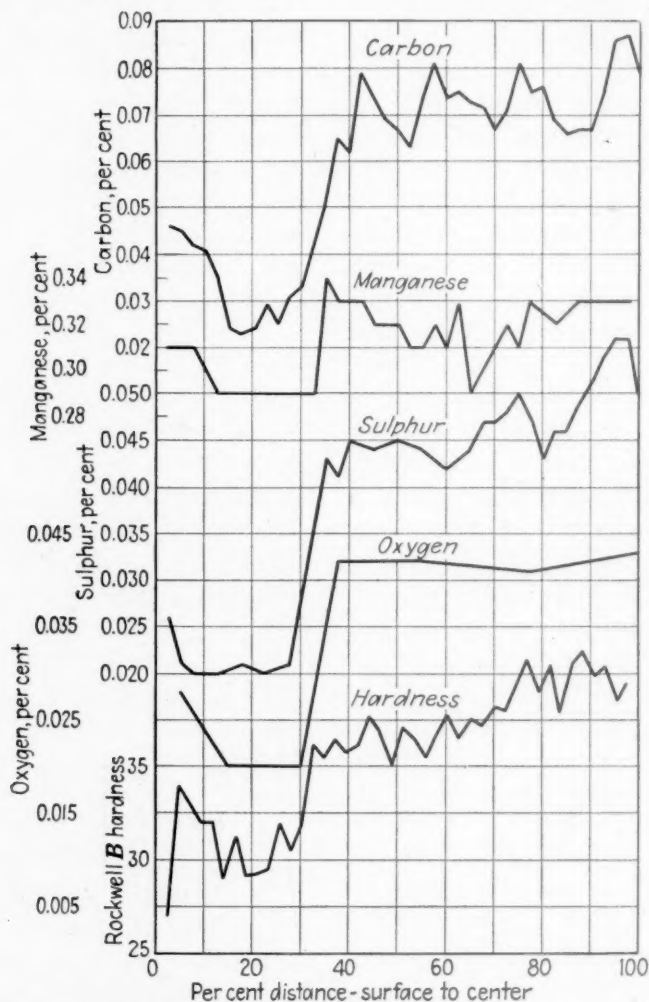


FIG. 13.—SEGREGATION CURVES, RADIAL TRANSVERSE AT 65 PER CENT LEVEL (SURFACE TO CENTER LINE). RIMMED INGOT.

C, 0.07 per cent; Mn, 0.45 per cent.

determination of hydrogen contents in liquid steel are still poorly developed, so the data are very scanty and somewhat uncertain, but we can give as a rough estimate that in the bath of the open hearth ready for tapping the contained hydrogen may be as high as 20 to 35 per cent of that required to saturate the liquid at its melting point and one atmosphere pressure. Since the equivalent pressure

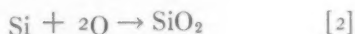
the upper part of the ingot at some stage of the freezing, and give an ingot structure like No. 2 in Fig. 12, or even a bleeding ingot top like No. 3.

Hydrogen also diffuses rapidly, however, and much of that present in the furnace bath is lost in the agitation and exposure to air incident to the operations of tapping and pouring. Thus, as it enters the mold, the metal probably is only about 10 to 15

per cent saturated with hydrogen, which is confirmed by the observations of about 1 to 3 per cent H_2 in the gases evolved during rimming at the beginning of the freezing of open steels. A few cases of bleeding ingots of dead-killed steels, probably caused by hydrogen, have been observed, often accompanied by skinholes in upper zones (as in No. 3 of Fig. 12). Rimmed ingots evolve around 1.5 to 2.5 times their own volume of gas, and since a steel saturated with hydrogen in the mold could evolve up to 1.0 times its volume in freezing, a moderate rimming action could in theory be produced in a dead-killed steel under these conditions. Such a condition is not normally even approached, however, so that though hydrogen is commonly found in pipe cavities and in blowholes, it has little part in the segregation or stirring effects that occur in the freezing of normal commercial ingots.

SEGREGATION OF OXYGEN AND NONMETALLICS

The segregation of oxygen (or oxides) in steel is somewhat complicated by the fact that in the average case the liquid metal entering the mold contains part of its oxygen in solution and part in the form of oxide particles suspended in the liquid metal. Furthermore, in semikilled steels, where silicon is usually the main deoxidizer, the amount of oxygen left in solution is controlled by the reaction



The equilibrium in this reaction shifts rather rapidly in the direction from left to right with falling temperature of the liquid metal, so that SiO_2 and silicate (the SiO_2 tends to take up FeO and MnO from solution) inclusions *will be formed during cooling* to the freezing point in the mold, *in addition to those already present in suspension* in the liquid entering from the ladle. Probably we still lack a clear understanding of many details in this rather

complex situation, but we can clarify it somewhat at least by keeping in mind the distinction between oxides suspended in the liquid metal at or above its freezing range and those precipitated from solution during the freezing.

In the ideal case of a rimmed steel to which no aluminum additions have been made, and containing no suspended oxides formed from erosion of refractories or other extraneous sources, the liquid metal entering the mold should have all its oxygen in solution (with no suspended oxides present). This dissolved oxygen is partly eliminated as CO in the rimming period, the rest being precipitated out as tiny FeO-MnO inclusions in the last portions of metal to freeze (mainly in the core zone). In such an ingot we should expect, therefore, that oxygen would segregate about the same as sulphur or carbon, and the little evidence that is available indicates this to be true; for example, Fig. 13 shows a radial traverse of an 0.07 per cent C rimmed ingot (ladle analysis) at the 65 per cent level from the bottom. The distribution of oxygen from the surface through the rim and the core zone to the ingot axis is very similar to that shown by the curves for sulphur and carbon.

In a dead-killed steel, we approach the other extreme of having all the oxygen present as suspended oxides in the liquid steel entering the mold. The larger oxide particles begin to rise to the surface even while the mold is only partly filled and by the time a crust forms on the top surface a fairly large amount of slag or scum is usually collected and trapped in this top crust. More of this material keeps floating up as freezing proceeds, however, and this may be largely trapped by the bridge across the pipe cavity (shown in No. 1, Fig. 11) or it may in part sink down again to the bottom of the pipe cavity and be found as slag near the center of the top portion of the top billet or slab if sufficient

top discard is not taken. In the useful portion of the ingot below the pipe cavity, we usually find that in the outer zone of columnar crystallization, where probably they are trapped by the growing dendrites, the oxide particles are rather uniformly distributed. In the central zone, however, there is usually a tendency for oxide inclusions to be larger and more numerous in the bottom 10 to 20 per cent portion as compared with the top central zone below the pipe. Probably this is caused by the tendency for the falling dendrites to catch and carry downward some of the rising oxide particles. In general, it seems as though the oxides either succeed in rising clear out of the liquid central zone (to be trapped by the top crust or to settle back a little way toward the base of the main pipe cavity) or are caught by falling dendrites and carried downward toward the bottom central zone.

Of course, in actual commercial ingots both dissolved oxygen and suspended oxides are present. In rimmed ingots, where most of the oxygen is dissolved (and separates as finely divided oxide sulphide particles with oxygen and sulphur segregation following similar patterns), we also have some suspended oxides from ladle aluminum additions, refractory erosion, etc. This in part rises into the top scum, but in part also is usually concentrated in the bottom zone, often in greater amount near the rim-core boundary or toward the ingot axis, and in these portions we are likely to find most of the larger oxide aggregates, usually containing some Al_2O_3 or SiO_2 , or both, but rich in FeO and MnO by reaction with dissolved oxygen and manganese.

In semikilled ingots deoxidized with silicon, there may be lesser amounts of suspended oxides in the metal entering the mold, but silicate inclusions should continue to separate in the liquid portion as it cools down to the freezing range (reaction 2). Less slag should collect on top in the early

freezing period but somewhat more silicate inclusions should be carried downward, toward lower central zones, by falling dendrites, as compared with dead-killed ingots deoxidized with aluminum or aluminum and silicon.

In dead-killed ingots, where much oxide material rises to the surface early during the filling of the mold, this top scum may be stirred back into the liquid by the force of the stream (or "folded in" near the mold walls). Such oxide aggregates tend to rise out again rapidly, but where they reach zones near the mold wall they can be caught by the dendrites growing inward rapidly from the ingot surface. This effect may thus be responsible for part of the surface or subsurface seams in killed steels.

SUMMARY

Summarizing some of the underlying factors, we may select the following as significant to the segregation effects that occur in the various types of steel ingots or other large castings:

1. The heat evolved in freezing, the outflow of which determines the rate and sometimes the direction of crystal growth.
2. The tendency of skeletal types of crystals, such as dendrites, to grow faster along the original axis of growth than in other directions.
3. The higher iron content of the crystal nuclei, thus leaving an adjacent layer higher in impurities and lower in freezing point.
4. The fact that as a result of these concentration gradients a rate of diffusion or mixing is introduced to limit the rate of freezing, thus favoring the dendritic form of crystal growth, which can, however, be suppressed or at least very much changed in character by such vigorous stirring as will practically eliminate these concentration gradients.
5. The high specific gravity of iron, involving a large kinetic energy storage in vigorous stirring and a large increase in

ferrostatic pressure between top and bottom ingot zones.

6. The very appreciable difference in specific gravity between liquid metal and the solid crystallites. This is not so large in terms of percentage (about 7 per cent) but the absolute difference is equal to about half the specific gravity of water, thus allowing for rather rapid settling of unattached dendrites.

7. Evolution of gas by the carbon-oxygen reaction in iron solution with the gas-bubble formation favored by a somewhat rough solid surface, its repression by increased ferrostatic pressure, the wide variation in the reaction tendency with variable oxygen content in the liquid steel, and the importance of the stirring and blowhole-forming effects of this reaction.

REFERENCES

1. B. M. Larsen: Effect of Mn on the Distribution of Carbon in Steel. U. S. Bur. Mines *Tech. Paper* 466 (1929).
2. A. Sauveur and V. U. Krivobok: Dendritic Segregation in Iron-carbon Alloys. *Jnl. Iron and Steel Inst.* (1925) **112**, 313.
3. A. Hultgren: Crystallization and Segregation Phenomena in 1.10 per cent C Steel Ingots of Smaller Sizes. *Jnl. Iron and Steel Inst.* (1929) **120**, 69-124.
4. H. M. Howe and E. C. Groesbeck: Prevention of Columnar Crystallization by Rotation during Crystallization. *Trans. A.I.M.E.* (1919) **62**, 341-346.

DISCUSSION

(T. S. Washburn presiding)

H. R. BELDING,* Farrell, Pa.—This discussion is in the nature of an extension of the ideas developed in Mr. Larsen's paper. An explanation is offered for the occasional erratic occurrence of a few badly piped ingots in heats of fully killed or semikilled steel poured in big-end-down, non-hot-topped molds, where the other ingots of the same heat, poured and deoxidized in the same manner, are free from pipe after rolling. Semikilled steel is a large-tonnage product, and the question of yield is important.

Some recent investigations have shown that this erratic segregation of nonmetallic matter

is not due to differences in the extent of the pipe cavity between the various ingots of a heat, but is due to the variations in the degree of nonmetallic contamination of the pipe cavities of the different ingots. This in turn is directly associated with the condition of the various "bridges" that form across the pipe cavity as this latter develops.

The interesting practical application of this aspect of the segregation of nonmetallic matter is that if you attempt to move in the opposite direction to keep these bridges continuous, or unperforated or unbroken, and especially if you endeavor at the same time to reduce the total amount of nonmetallic matter in the steel, you get, if successful, a considerable increase in yield.

If the bridges, especially the first one, are continuous or unbroken, they serve as barriers to trap the nonmetallic matter that separates out of the steel, and keep it from descending into the deeper portions of the pipe cavity. However, a puddle or "scab" of nonmetallic matter at the top of an ingot as poured will frequently prevent a continuous top crust from forming, because of its insulating action, and may repeat this effect again when the first bridge is forming. Nonmetallic matter and atmospheric oxygen, of course, will pass down through such incomplete bridges. For this reason, the removal of nonmetallic scabs from the tops of ingots after pouring may assist in securing a higher yield of sound steel.

Clean pipe cavities will weld during rolling, to produce a rolled product of sufficient soundness for most applications.

Many open-hearth superintendents and most metallurgists have probably reasoned, at one time or another, that piping in non-hot-topped ingots might be reduced by preventing the tops of the ingots from freezing over, or bridges from forming, by the use of brick dust, large blocks of wood, or other means, so that the remaining liquid steel might drain down into and fill up the pipe cavities as they formed. The invariable result of such an experiment, as may now be understood from the viewpoint just developed, is to have the product of every ingot badly piped.

J. W. HALLEY,* East Chicago, Ind.—Mr. Larsen has given an excellent exposition of the

* Chief Metallurgist, Farrell Works. Carnegie-Illinois Steel Corporation.

* Inland Steel Company.

theory of segregation in steel ingots. I would like to add an hypothesis of the formation of the inverted V (Λ) segregation.

These strings of positive segregation are usually irregular and occur in an area from just inside the columnar zone to just outside the central zone of positive segregation. It is suggested that they result from less pure liquid that has moved upward from the solidifying face. This upward movement would result from the settling of free crystals toward the bottom of the ingot . . . The liquid displaced by these settling crystals will rise and as it moves up along the solidifying surface will displace less pure liquid toward the top of the ingot. Since the friction of the liquid against the solid wall will tend to reduce this motion, the less pure liquid will move inward as it moves upward, to give a streak as found in the ingot.

The occurrence of more than one streak would indicate that this process is periodic. As the less pure liquid is moved away from the freezing wall the tendency to form free crystals will be greatly reduced and the motion consequently be decreased, which will cause the less pure liquid to accumulate along the freezing wall. The accumulation of less pure liquid will favor the formation of free crystals, which will again increase the motion and move the less pure liquid upward to form a second string of inverted-V segregate. It should be emphasized that these changes are slow and only in the largest ingots will more than two strings of segregate be found.

For rimmed steel, Mr. Larsen described the elongated blowholes in the rim as forming between columnar dendrites. The excellent photographs by Hultgren and Phragmén show no evidence of columnar dendrites associated with these blowholes. They attribute the elongated form of the blowholes to partial removal of bubbles by motion of the liquid, which is not great enough to completely wash away the bubbles. Their illustration of this theory is quite convincing and eliminates the necessity of columnar dendrites to account for the shape of the blowholes.

H. B. EMERICK,* Pittsburgh, Pa.—Mr. Larsen is to be commended for such a painstaking

* Metallurgical Department, Jones and Laughlin Steel Corporation.

analysis of the many factors involved in the phenomenon of segregation. He has made no attempt to assign a relative order of importance to his summary of factors influencing segregation. Differential freezing is commonly held to be the primary cause of major segregation of soluble impurities, being aided by movements in the liquid steel—chiefly by differences in specific gravity between the liquid highly concentrated in impurities (or solutes) and the purer molten metal. The second major factor in segregation appears to be the formation of an enriched film in the liquid adjacent to the solidifying interface and the entrapment of part of this film in the growing crystals.

It would be interesting to have Mr. Larsen comment on the theory advanced by Professor Andrew,* in England, to the effect that major segregation may occur while the metal is in the molten condition, resulting from the formation of an immiscible liquid phase high in impurities within the melt, and that this liquid complex, being of lower density than the metal surrounding it, tends to rise toward the surface while the steel is yet molten.

B. M. LARSEN (author's reply).—Mr. Belding's picture of the way in which lower or secondary portions of the shrinkage cavity or pipe sometimes get partly filled with slag perhaps contains some element of speculation (as, indeed, do most of our ideas about this general subject) but it agrees very well with the remarks on segregation of nonmetallics or oxides in the last section of the paper; and the writer feels that this is a brilliant elucidation of an effect usually overlooked, but often of much practical importance. Some secondary pipe presumably forms down toward the central and lower levels at or near the central axis in most ingots (probably even in hot-topped, but especially in big-end-down killed or semikilled steels) because in the "mushy" stage near the end of the freezing there are too many crystals present to allow feeding down of the remaining liquid. However, there is the tendency for such feeding down, and if an oxide scum is floating on the last portions of such liquid metal it will also fill into the

* J. H. Andrew et al.: Segregation in Steel. Eighth Report on the Heterogeneity of Steel Ingots, 1. Iron and Steel Inst. (1939).

central cavity, and the distance of its downward travel could well be irregular from one ingot to another. It is probably an undesirable effect, since if it is largely prevented there should be no larger nonmetallic agglomerations in the central shrinkage cavities and the metal should weld up in rolling to at least reasonably sound metal in the finished product. If any of the last remaining liquid below the main pipe cavity feeds down again very far, it will cause a "wet pipe" if some of the previously risen "scum" of oxides goes with it, and even if it is free of such "scum" it should tend to cause center segregation in such upper zones. Several bridges across the pipe cavity, therefore, should have a good effect, but, as Mr. Belding points out, the lower thermal conductivity of a small pool of floating oxides may keep the metal beneath it from freezing clear across to form a perfect bridge.

Mr. Halley's explanation of inverted or Λ -segregates seems to be in accord with the known facts at this time and is probably a substantially true picture. At least it seems the best explanation the writer has encountered regarding this effect. Concerning Hultgren and Phragmén's explanation of elongated rim-zone blowholes in rimmed ingots, there are two points which the writer would like to indicate here.

In the first place, close examination of the various rim-zone pictures in their paper will reveal that in several of them fairly distinct indications of a columnar crystal structure are apparent. Indeed, it is difficult to see how any other form than parallel, elongated crystals could be present here, since the direction of

movement of the solidifying surface remains perpendicular to the mold wall. The real difference between this rim zone and the columnar crystal zone of killed or semikilled ingots is that the rimming action sweeps away the less pure metal, the elongating crystals grow more closely together (as a solid wall in the limiting case?) and there is much less microsegregation, with its resultant less pure zones between adjacent crystals, so that the columnar structure cannot be brought out so clearly on etching.

Secondly, there is a certain lack of completeness in the picture outlined by Hultgren and Phragmén. If we postulate that a strong rimming action not only sweeps away the initial bubbles, but also prevents dendrites from extending appreciably into the liquid in advance of the freezing surface as a whole, then, whether or not these dendrite extensions help to trap the bubbles between them, there would seem to be a close relationship between the two phenomena, since the most natural place for bubbles to start would be from the less pure liquid that would tend to collect between adjacent dendrites.

Regarding the theory advanced by Professor Andrew and mentioned by Mr. Emerick, we do have a few cases of segregation in the liquid state, including the rising of nonmetallic particles and the rapid settling tendency of finely dispersed lead additions. However, as far as the writer is aware, there is an absence of positive evidence of such an effect for nearly all the common solutes present with iron in various commercial steels.

Segregation in Steel

(T. S. Washburn presiding)

THE CHAIRMAN.—Mr. Earle Smith has kindly offered to make some remarks in connection with segregation in the product, Mr. Smith:

E. C. SMITH,* Cleveland, Ohio—I will start this off by a story of the code days of the American Iron and Steel Institute. In those days, Republic did not have a big strip mill, and the question came up of the check analysis of rimmed steel. I suggested that they let me be the chairman of the Committee on Accumulating the Information on the Variation of the Composition of the Ingots of Rimmed Steel.

Somebody wanted to know why I wanted to be the chairman. I said, "We don't make any of the big ingots of rimmed steel, and no matter who makes them they are so bad that you don't dare publish the information. So if I collect it and hide it you can't charge me with having done anything that really disrupted the commercial situation." So, everybody furnished me with a rather complete story as to the horrible variations in big rimmed ingots. I took it out to my house and put it away, and it is still there.

Now, segregation in the big ingot is no longer an "academic" matter as far as I am concerned. I am in a situation like that of the German who was told in 1936 about the coming war. He said: "Until it is your throat that is going to be cut, you don't pay any attention to what is happening to the other man." That is the way with the problem that we have in front of us.

Recently I have been told that the comptroller was questioning the payment for certain articles of stamped steel that had been made from rimmed steel, because upon check analysis of the rimmed steel it had been determined that these stamped articles were not within the compositions that were included in the specification, and therefore he as the comptroller had no alternative. It was not meeting the specification; therefore, no payment.

So I would say to all of you: You can very

seriously consider this matter of segregation now and on into the future on the basis of the fact that it is actually going to cost your companies, which are making these products, money unless there is some new idea about the infallibility of quantitative chemists who analyze some of these products or lawyers who read specifications. I don't know which man is going to be the major factor in the future. If the National Bureau of Standards could in some way show the specification writers the variation between good chemists analyzing for what they expect to be umpire results, the writers would certainly realize that some of the specifications to which we have calmly signed our names as being O.K. are—well, as one man said to me, they might be filled by the devil, and they certainly could be filled by the Lord, but they could not be filled by mankind.

I would like to inject two or three things into a segregation study which I want you to think about, because I would be a little surprised if there is very much discussion of them.

In the first place, we generally make steel in the United States in the basic open hearth, and I do not think there has been nearly enough consideration given to segregation within the bath before it moves into the ladle. I am sure that any of the people who handled the 9400 series of the NE series when it contained the 0.60 per cent silicon have more respect than they had previously for the segregation that is within the ladle; that is, before the metal reaches the ingot mold, the frozen ingots and the segregation in them.

Another point to which I think we ought to give serious consideration is the segregation of iron oxide in the ingot-iron type of material, where the distinction between that and the steel segregation is that it is actually segregating iron oxide. Normally we are segregating some form of carbon or sulphur, or something like that, with the stamping steel industry now coming down into the ranges of chemistry, where the segregation of iron oxide will be just

* Republic Steel Corporation.

as pertinent as the segregation of phosphorus in the near future, in spite of American Rolling Mills' killed deep-stamping steel. That is a pertinent part of our business.

When we come to the types of products, only about half of the iron and steel products that we make, even in wartime, are produced to chemical specifications. In times of peace, it is certainly less than a third; I think hardly more than a fourth.

Why we put so much insistent emphasis on the determination of a quantitative chemist as acceptable or rejectable material has always been a mystery to me, because the great bulk of the steel we make goes into service without the aid of the clergy and performs a very creditable job. I think that at the present time we may be overstressing a little the need of serious attention to segregation. So, in your discussions this afternoon, while it is serious, I would not have you feel that the steel industry has to stop completely because we have now found out that there is segregation.

When we of the American Iron and Steel Institute were trying to work out standard ordering methods, one of the controversies developed arose from the request of the alloy steel people for a wider ordering range on the sections that were above 10 in. The rest of the steel industry looked at us in holy horror and said, "There is no difference, the analysis is just the same." We said, "When the chemist gets the sample of the material the analysis is the same, but the risk involved in making one of the big ingots means that the maker does need a wider ordering range when he starts out."

On these segregating types of steel, some day we are going to provide a wider ordering range. Look at the results given in Mr. Larsen's paper. On a 0.25 or 0.30 per cent spread of manganese at around 1.50 per cent manganese and 13 per cent variation for segregation, give the chemist a little chance to miss and you have a whole 0.30 per cent spread used up as a thing that ordinary horse sense would tell you that you can expect.

Now, if the man is going to order that kind of product, sooner or later we either have to agree that we are going to select it or we are going to make it. In your discussions, carry it on a little beyond the ingot, if you will.

B. M. LARSEN.—Some of Mr. Smith's remarks are well worth calling to the attention of many persons responsible for deciding upon steel specifications, at least for as long as most commercial steel is cast in ingot form. Even up to the beginning of the war period, it was often necessary to segregate certain portions of the ingot into separate lots in order to satisfy certain exacting requirements. It should be remembered that perhaps the biggest step toward lessening segregation is achieved at moderate cost by the use of big-end-up, hot-topped ingot molds, not because segregation is decreased in amount but simply by the localizing of most of the positive segregation in the discarded portion of the ingot. The effect can be largely eliminated by casting in small molds, and the most promising potential commercial possibility for certain types of steel is that of continuous casting in billet or thin slab form. However, segregation apparently remains as an inevitable commercial problem as long as steel is cast in larger masses.

THE CHAIRMAN.—I believe that there are two points that Mr. Smith discussed that certainly should be the basis for the study of the segregation problem. One is a better understanding of the normal range of segregation for different analysis ranges of the elements present in steel; in other words, a determination of the normal variation in composition, which is a function of the amount of the element present. With this information, we would have a better basis for establishing permissible variations in the check analysis on each specification. After having established normal variations in analysis, or segregation, for any given analysis range, the next problem is to determine the features in practice that control segregation within the desired limits. This is a problem for the open-hearth operators and metallurgists.

This afternoon we have two formal papers, one on rimmed steel and the other on killed steel. The paper on rimmed steel will be delivered first. This grade of steel is recognized as a type that is prone to much more variation in its composition than killed steel, and a large amount of data has already been published on this subject. Mr. Halley will now present his paper on The Relation of Open-hearth Practice to Segregation in Rimmed Steel.

The Relation of Open-hearth Practice to Segregation in Rimmed Steel

By J. W. HALLEY,* MEMBER, AND G. L. PLIMPTON, JR.,* JUNIOR MEMBER A.I.M.E.

BECAUSE of the two distinct stages in the solidification of rimmed steel, segregation in the rimmed ingot is more complex than that in the killed or semikilled ingot. In the earlier stage, chemical reactions, resulting in evolution of gas and vigorous stirring of the metal, effect a degree of negative segregation unique to rimmed steel. The composition of this zone constitutes the principal quality advantage of this type of steel. In the later stage of solidification, after the evolution of gas has ceased, the segregation follows the general pattern of a more completely deoxidized steel. However, the composition of the liquid remaining after the first solidification stage varies markedly from that of the original melt, some constituents having been partially removed as reaction products while the concentration of others has been intensified by rejection from the metal solidifying in the first zone.

The aim, from the standpoint of segregation, in rimmed steel of high quality is to effect a maximum negative segregation in the rim zone without excessive concentration of undesirable elements at the center of the ingot. To achieve this aim, the composition of the melt may be varied and the furnace and pouring practice may be adjusted within certain limits. It is the purpose of this study to discuss segregation in rimmed steel from the standpoint of the mechanisms that produce it and to survey

the phases of open-hearth practice that influence those mechanisms.

MECHANISMS PRODUCING SEGREGATION

The mechanisms that determine the degree of segregation in the rimmed ingot are closely interrelated, making it difficult to select the primary factors and to determine a satisfactory order for presenting them. For instance, the question of sulphur segregation is relatively simple, since sulphur is not directly involved in chemical reactions in the ingot; but its concentration in the rim zone is dependent not only on its original analysis in the melt, its segregation coefficient, and the freezing rate, but also on the rate of its removal from the impure film on the solidifying surface. This washing action involves all the factors (such as freezing rate, the carbon-oxygen product, pressure, etc.) that determine the rate of gas evolution and hence the efficiency of film removal. Sulphur distribution between the rim and core is affected by the volumetric ratio between the two zones, and its segregation in the core is a function not only of the freezing rate of the core but also of all the foregoing factors that determine its concentration in the metal when solidification of the core starts.

To simplify the presentation, it is proposed to treat the mechanisms affecting segregation independently in this section, reserving a discussion of their over-all effects for the section in which actual segregation data are given. The factors affecting segregation will be treated in the following order: (1) differential solidification, (2) removal of constituents as

This paper received the McKune Award (a certificate and one hundred dollars). Presentation was made at the Fellowship Dinner, Thursday, April 20, at Cleveland. Published also in *Open Hearth Proceedings*, 1944.

* Inland Steel Co., Indiana Harbor, Ind.

reaction products, (3) efficiency of film removal, (4) ratio of rim zone to core zone.

Differential Solidification

The theory of segregation in rimmed ingots has been developed most extensively by Hayes and Chipman.¹ They represent

negative segregation shown in Table 1 is obviously much greater than is ever obtained in actual ingots. This theoretical degree of segregation would be obtained if the impure liquid resulting from the freezing of purer crystals of iron was removed as fast as it formed and mixed

TABLE 1.—Segregation Coefficients and Composition of Rim Zone

Element	Segregation Coefficient, $1 - k$	Lowest Theoretical Composition in Rim by Negative Segregation for Ladle Analysis Shown, Per Cent									
		1		2		3		4		5	
		Ladle	Rim	Ladle	Rim	Ladle	Rim	Ladle	Rim	Ladle	Rim
Manganese.....	0.16	0.10	0.084	0.15	0.126	0.20	0.168	0.30	0.252	0.40	0.336
Copper.....	0.44	0.04	0.022	0.06	0.034	0.08	0.044	0.10	0.056	0.12	0.067
Phosphorus.....	0.87	0.005	0.0006	0.010	0.0013	0.020	0.0026	0.040	0.0052	0.080	0.014
Carbon.....	0.87	0.03	0.004	0.05	0.006	0.10	0.013	0.15	0.020	0.20	0.026
Oxygen.....	0.90	0.005	0.0005	0.01	0.001	0.015	0.0015	0.02	0.002	0.025	0.0025
Sulphur.....	0.95	0.015	0.00075	0.020	0.001	0.025	0.0012	0.030	0.0015	0.035	0.0017

the tendency of individual elements to segregate by the ratio of the concentration of the element in the liquid and the concentration of the element in the solid, in the delta region of the equilibrium diagram of the element and iron. They term this ratio the "distribution coefficient" and designate it as k . Since the tendency to segregate increases with increasing distance between the liquidus and solidus, the tendency of an element to segregate is given by $1 - k$, which they term the "segregation coefficient." Their values for segregation coefficients correlate well with the relative segregation of the elements. The segregation coefficient determines the greatest degree of negative segregation theoretically possible. It gives no measure of the extent of positive segregation, except the very general one that positive segregation will be greater when the negative segregation is greater. Table 1 shows values of segregation coefficients from Hayes and Chipman and the lowest possible composition in the rim zone for different ladle analyses. The degree of

with a liquid of infinite extent. Under these conditions crystallization would always be from liquid having the composition shown by the ladle analysis.

Removal of Constituents as Reaction Products

In addition to the rejection accompanying equilibrium solidification, carbon, oxygen and manganese are removed by chemical combination. The terms, "rejection" and "rejected," will be used in connection with the concentration of elements in the liquid resulting from selective solidification. These terms are strictly correct in the sense that whatever is not taken is rejected. They do, however, sound very much like "eject" and "ejected," which would indicate actual repulsion. There is, of course, no such process involved during the solidification of an alloy. Carbon and oxygen as carbon monoxide and carbon dioxide constitute most of the gas evolved during rimming. Manganese also combines with oxygen, and the manganese oxide, along with aluminum oxide and iron oxide, rises to accumulate as slag at the top of the ingot.

¹ References are on page 456.

Efficiency of Film Removal

Rimmed steels approach the condition of maximum possible segregation shown by the segregation coefficient because of the washing action of the liquid metal as it

been reported by McCutcheon and Chipman.² They found a rate of from 3 to 4 cu. ft. per min. shortly after finish of pour, which dropped to about 1 cu. ft. per min. by the normal capping time. On somewhat

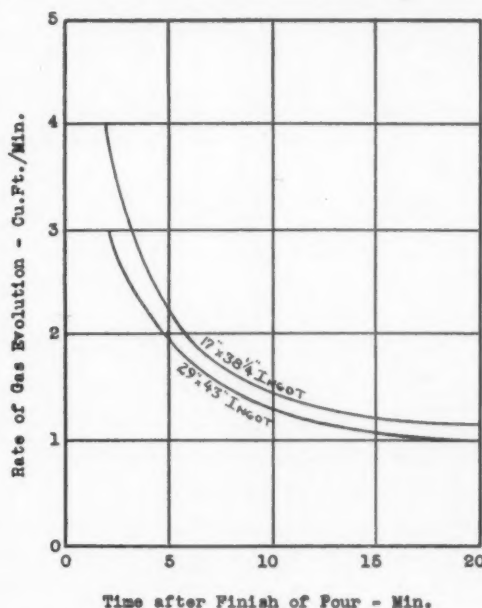
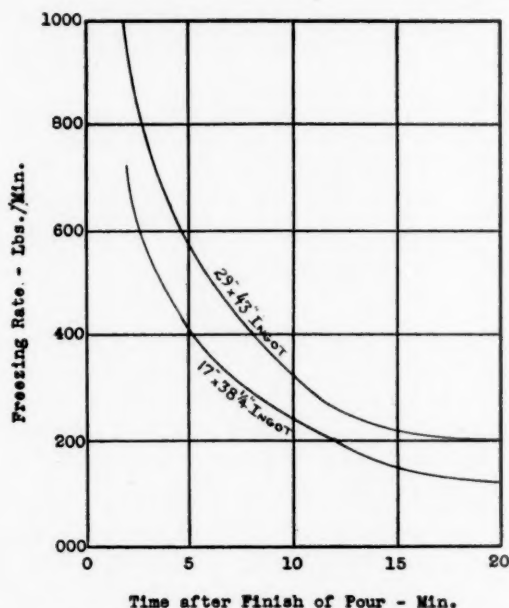


FIG. 1.—RELATION OF RIMMING TIME TO FREEZING RATE AND TO RATE OF GAS EVOLUTION IN INGOTS.

moves upward along the inside surface of the solidified metal. The less pure liquid is not completely removed but a certain portion of it is washed away and mixed with the body of the liquid. The degree to which actual segregation will approach the theoretically possible negative segregation will depend upon the efficiency of the washing action.

The movement of the liquid results from gas evolution caused primarily by the reaction between carbon and oxygen to form carbon monoxide and carbon dioxide. The more rapidly this reaction proceeds, the greater will be the gas evolution and the more efficient the washing. Since the reaction between carbon and oxygen is affected markedly by pressure, gas evolution will be much slower in the lower portion of the ingot.

Over-all rates of gas evolution from 18 by 39-in. ingots weighing 11,500 lb. have

larger ingots (29 by 43 in., weighing 18,000 lb.), the present authors found initial rates of $2\frac{1}{2}$ to 3 cu. ft. per min., decreasing to 1 cu. ft. per min. by normal capping time. Fig. 1 shows the rate of gas evolution and the rate of freezing in the authors' 18,000-lb. ingot and McCutcheon and Chipman's 11,500-lb. ingot. In both ingots the rate of gas evolution and the freezing rate change together. It will be noted that while the freezing rate is lower, the gas evolution is (contrary to expectation) greater in the small ingot throughout the rimming period.

The rate of removal of oxygen as gas was calculated from the gas analysis and rate of gas evolution, and is shown in Fig. 2. The rate of rejection of oxygen from the solid was calculated from the freezing rate, the oxygen content, and the distribution constant, and is also shown in Fig. 2. Similar curves for carbon are shown in Fig. 3. During the early part of rimming,

oxygen is rejected much faster than it is evolved. As rimming proceeds, the rate of oxygen rejection decreases very rapidly and approaches the rate of evolution.

rate of oxygen rejection, it must follow that oxygen from other sources enters the carbon-oxygen reactions. This oxygen must come from the body of liquid beyond the

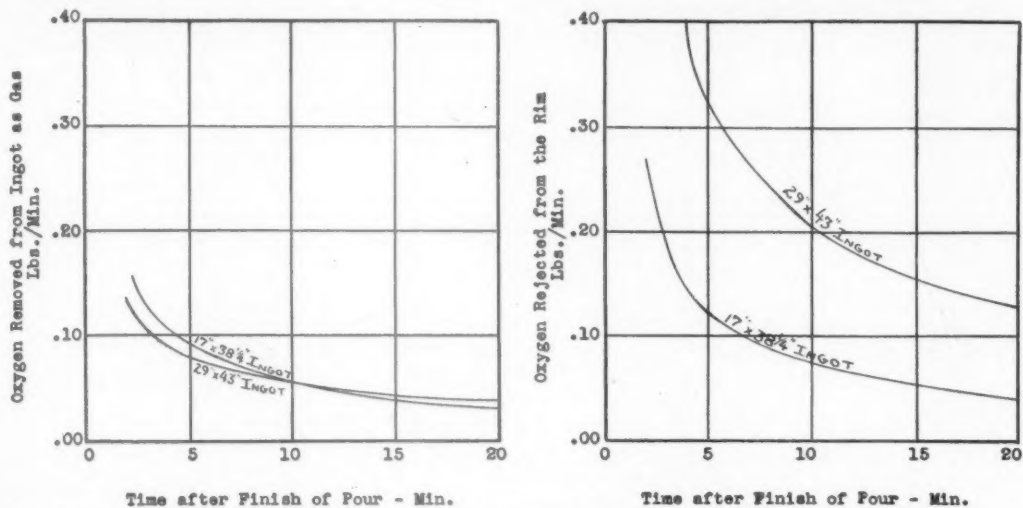


FIG. 2.—RELATION OF RIMMING TIME TO RATE OF OXYGEN REJECTION FROM THE RIM AND TO RATE OF OXYGEN REMOVAL FROM THE INGOT AS GAS.

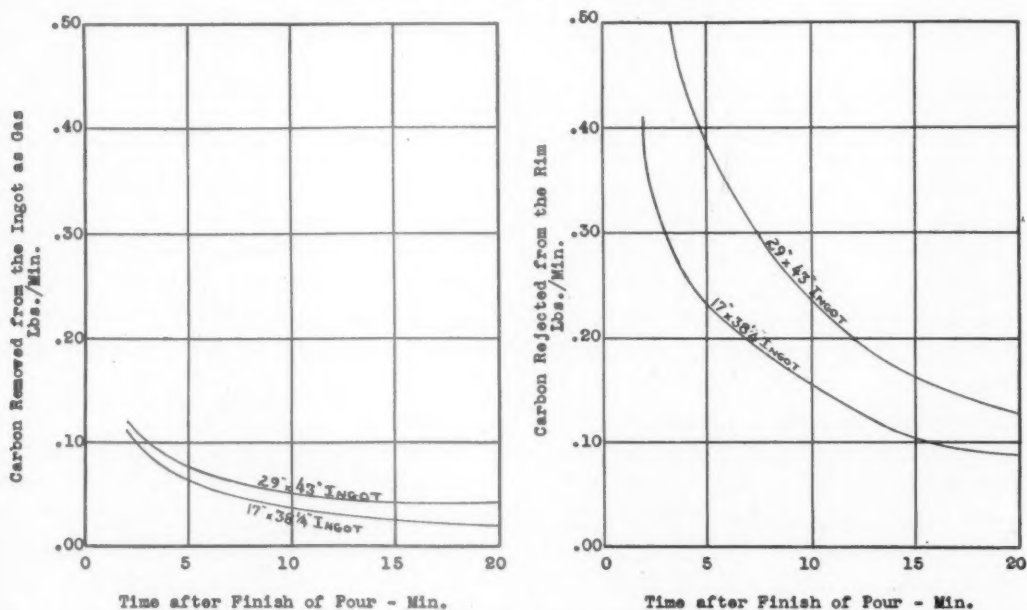


FIG. 3.—RELATION OF RIMMING TIME TO RATE OF CARBON REJECTION FROM THE RIM AND TO RATE OF CARBON REMOVAL FROM THE INGOT AS GAS.

Most of the oxygen is being evolved in the upper part of the ingot while rejection will be uniform over all the solidifying surface. Since the rate of oxygen evolution in the upper part of the ingot exceeds the

film of less pure liquid at the solidifying surface. Carbon, however, is rejected much faster than it is evolved throughout the rimming period. It is evident that in these steels (0.075 to 0.081 per cent carbon) oxy-

gen must be the controlling factor in gas evolution. This will also be true for higher carbon steels. With considerably lower carbon, in the neighborhood of 0.03 per cent, conditions would be reversed and the rate of gas evolution determined primarily by carbon.

Equilibrium conditions indicate that manganese must be in the order of 0.35 per cent to have a marked effect.

For sulphur, the efficiency of washing increases as the sulphur increases. This is the result of the immiscibility of iron-manganese-sulphide in liquid iron near the

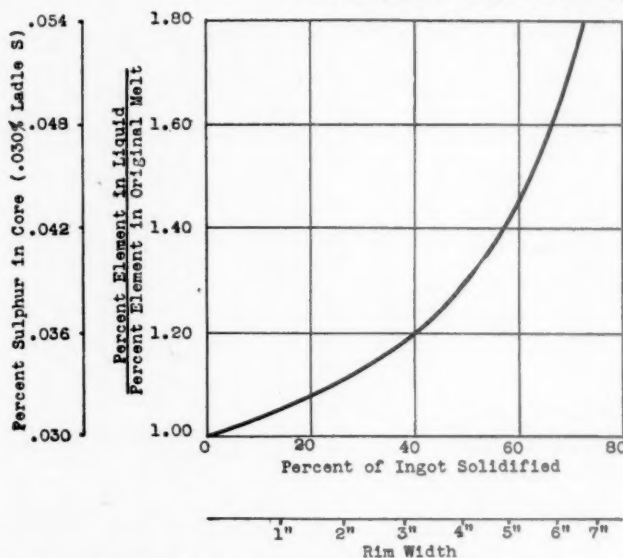


FIG. 4.—THEORETICAL INCREASE OF CONCENTRATION OF ELEMENT IN LIQUID PHASE AS SOLIDIFICATION IN INGOT PROGRESSES.

Concentration of element in solid assumed to be 70 per cent of that of original melt.

Manganese affects gas evolution much more in the lower part of the ingot than near the top. The reaction between oxygen and manganese to form manganese oxide is practically independent of pressure. In the lower part of a 72-in. ingot the pressure is between 2 and $2\frac{1}{2}$ times atmospheric, and the carbon-oxygen product must be more than twice as high as near the top, to evolve gas. As the oxygen in the liquid is increased by differential solidification, it will combine with both carbon and manganese. In the upper part of the ingot the amount combining with manganese will be so small as to have no appreciable effect on the rate of gas evolution. In the lower part of the ingot the carbon-oxygen reaction is so inhibited by pressure that enough oxygen combines with manganese for the manganese to have a noticeable inhibiting effect on the rate of gas evolu-

tion. The segregation of sulphur, therefore, is not directly proportional to the amount present, as would be anticipated from the segregation coefficient. The proportional segregation of sulphur actually increases as the sulphur increases.

Segregation within the Core Zone

After capping, the solidification of the core is usually considered to be the same as the solidification of a semikilled ingot. Though the mechanics of solidification are essentially the same in a semikilled ingot and the core of a rimmed ingot, there are a number of factors that make degrees of segregation different in the two cases.

A semikilled ingot at the start of solidification consists of a uniform liquid of the composition shown by the ladle analysis. The core of a rimmed ingot at the start of its solidification is higher in sulphur and

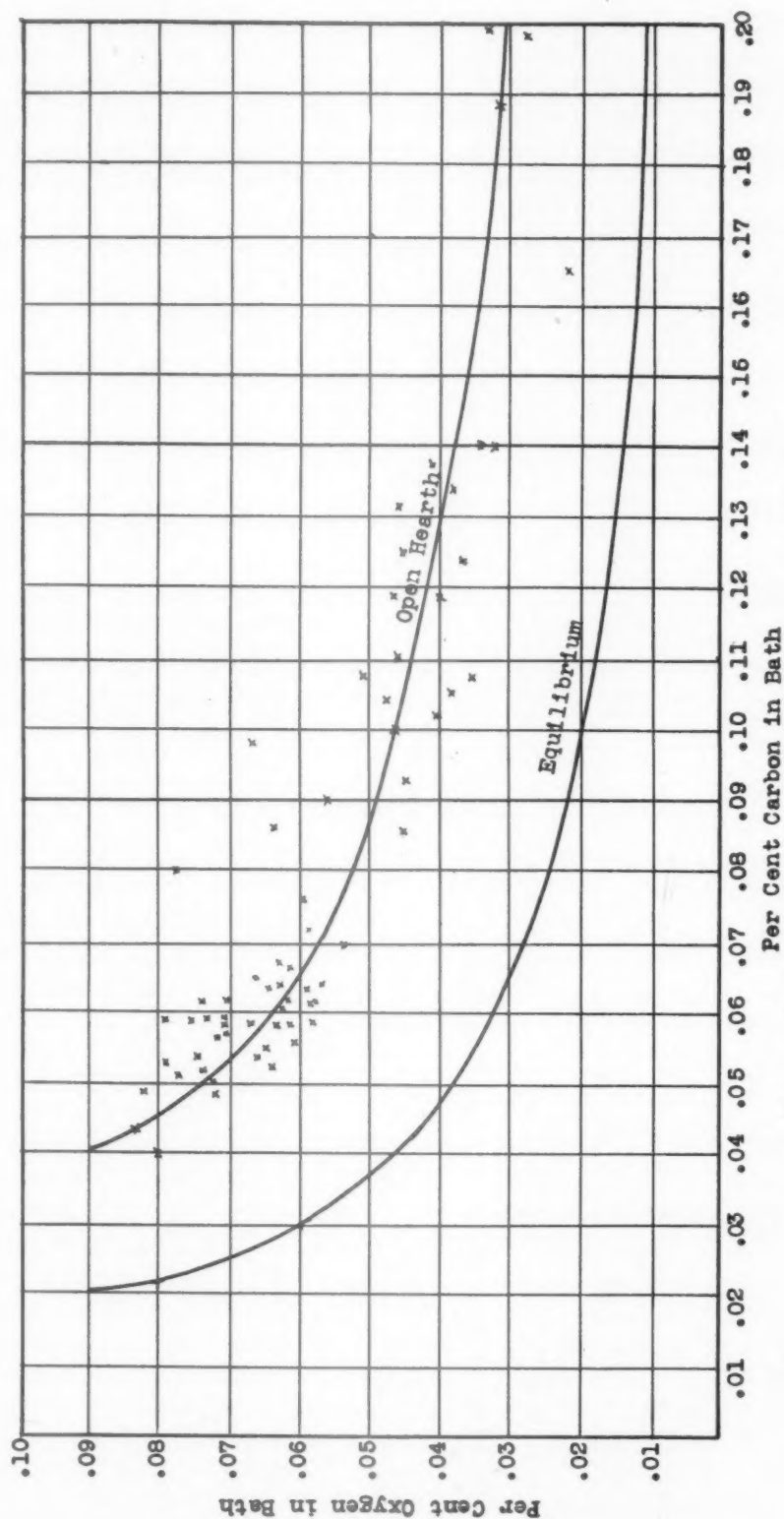


FIG. 5.—RELATION BETWEEN CARBON AND OXYGEN IN LIQUID IRON.

Equilibrium curve from Marshall and Chipman.³ Pressure, 1 atmosphere; temperature, 2805°F.
 Open-hearth curve: lime-silica ratio, 2.5 to 3.5. Slag FeO for C below 0.10 per cent, 15 to 25 per cent. Slag FeO for C above 0.10 per cent, 10 to 20 per cent.

carbon and lower in manganese and oxygen than the ladle analysis. In addition, the upper part of the core is richer in sulphur, manganese and carbon than the lower part of the core. This results from the more effective stirring action in the upper part of the ingot and the carrying up of rejected impurities along the freezing wall by the rimming action. An additional factor is the low temperature of the core of a rimmed ingot compared with that of a semikilled ingot at the beginning of solidification.

All of these factors tend to make positive segregation in the core of a rimmed ingot greater than in a semikilled ingot of the same ladle analysis.

Extent of Rim Zone

The importance of checking the rimming action before concentration of a segregating element has become excessively high in the core zone is apparent from a consideration of the increasing rate at which the composition of the liquid metal may change during solidification. To illustrate this relation, let it be assumed that the metal freezes at a uniform composition with respect to the original melt and that all the rejected portion of the element remains in the liquid. The composition of the liquid in the core at any time during the rimming period of the ingot may then be expressed as follows:

$$E_c = \frac{E_m(1 - SR)}{1 - S}$$

when

E_c = per cent of a given element in the liquid core.

E_m = per cent of a given element in the original melt.

S = fraction of the ingot solidified.

R = fraction of the concentration of the element in the original melt retained in the rim zone.

Fig. 4 shows the marked rate of increase of an element in the liquid core as solidification progresses, when the composition of

the rim is 70 per cent of that of the original melt. This relation is applied in the same figure to a hypothetical 24 by 43-in. ingot 70 in. high in which the ladle sulphur is 0.030 per cent, the percentage of sulphur in the liquid being shown as the ordinate and the width of rim as the abscissa. (It is assumed that solidification progresses from the mold walls and stool at a uniform rate.) Sulphur was used as an example because elements of this type (which have high segregation coefficients and which are not removed as reaction products) are most affected by an excessively high ratio of rim zone to core zone.

EFFECT OF PRACTICE ON SEGREGATION

Variations in furnace, ladle and pouring practice must be maintained within certain limits to control the mechanisms that produce segregation. From the foregoing discussion it is evident that the composition of the melt is an important factor in determining the degree of segregation in rimmed steel. Not only does the concentration of any element affect the segregation of that constituent, but the concentrations of C, O, and Mn affect the segregation of all elements. The steel temperature and mold conditions, which govern the freezing rate of the steel in the mold, and the capping practice, which determines the extent of the rim zone, also have an important influence on segregation. The following section will deal with such features of practice as have been shown to affect the segregation mechanisms in a major degree.

Carbon

The carbon content of the steel as it enters the mold is dependent on the bath carbon at tapping, loss of carbon during tapping (in the bath, runner, or ladle) and the introduction of carbon to the ladle by recarburizing materials or other alloying agents. In dealing with the low carbon values in rimmed steel, the accuracy of bath carbon determinations, in terms of

percentage of the carbon present, is limited on account of possible variations of ± 0.01 per cent C in standard mill analytical methods and by the varying amount of carbon lost during sampling. Comparison of

per cent of the carbon added. If it is assumed that all the carbon in the ferromanganese is recovered, the loss of residual carbon in the bath during tapping would be 0.015 per cent. The actual carbon loss,

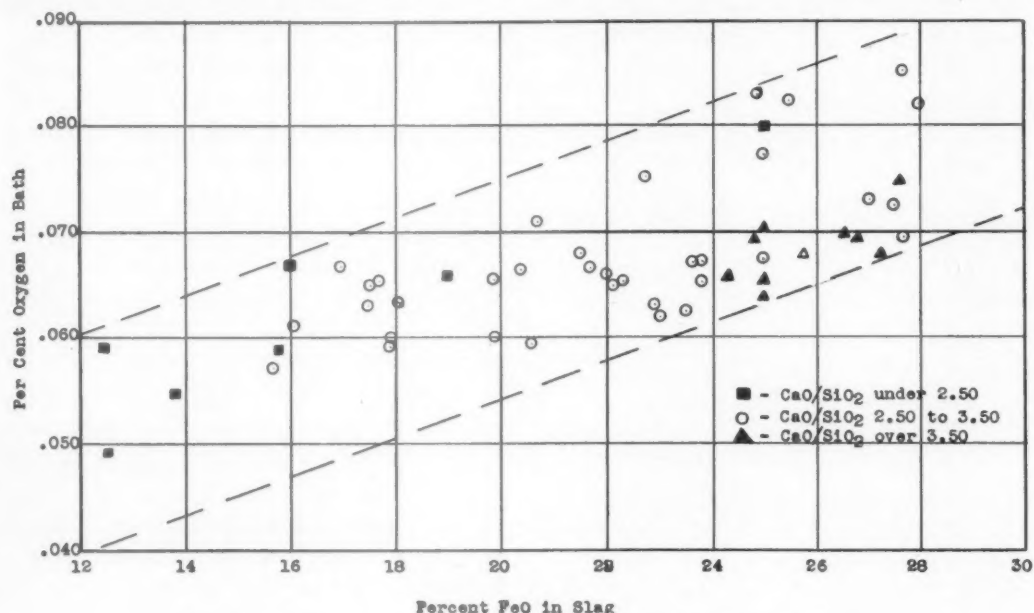


FIG. 6.—RELATION OF SLAG FeO AND BASICITY TO BATH OXYGEN.

the carbon content of McCutcheon-type bomb tests with the carbon in regular open-mold bath samples taken at the same time indicates that some loss of carbon by oxidation in the test spoon or test mold is generally present, under routine sampling conditions, and may be as high as 0.025 per cent. A determination on a low-carbon bath may thus be as much as 40 per cent in error.

The possible errors in determination of bath carbon combined with variations in recovery of carbon added to the ladle as ferromanganese makes it difficult to determine the loss in carbon through oxidation during tapping. In average low-carbon (0.10 per cent max. C) rimmed-steel practice, it has been observed that, disregarding loss of residual carbon in the steel by oxidation during tapping, when 0.035 per cent C is added as ferromanganese, about 0.020 per cent C is recovered, or about 60

then, probably lies between nil and 0.015 per cent. The carbon loss probably varies considerably with tapping conditions, the greater carbon loss being favored by a longer tapping time, which permits the furnace slag to oxidize the bath over a longer period and allows greater exposure of the metal in the runner and ladle to the oxygen in the atmosphere.

In all except the lowest carbon (ingot iron) rimmed steels it has been found desirable to increase the carbon through ladle additions by an increment that will produce a substantial departure from equilibrium conditions of carbon and oxygen. Consequently, the carbon in the bath is usually reduced below the desired ladle analysis, the difference being made up in the lower carbon (0.10 per cent max. C) grades by the additions of regular ferromanganese containing 7 per cent carbon; in the higher carbon grades (up to 0.30

per cent max. C) by recarburizing additions such as coke or coal to the ladle.

Oxygen

The oxygen content of the bath at tapping is largely dependent on the carbon content; to a lesser degree on the slag oxidation, slag basicity, and bath temperature. Shown on Fig. 5 is a curve for the carbon-oxygen relation under equilibrium conditions.³ Another curve in the same figure, plotted from experimental data, shows the relationship in the open-hearth bath. These curves indicate the marked increase in bath oxygen as the carbon decreases below 0.08 per cent and emphasizes the importance of taking the bath to as low a carbon as practicable before tapping to secure a high concentration of oxygen.

The effect of slag FeO and basicity on the oxygen in the bath are indicated on the curve in Fig. 6. The bath oxidation is shown to increase directly as the slag FeO. The practical effect of basicity is to increase bath oxidation, which it does indirectly by favoring higher slag oxidation. However, with a given bath carbon and slag FeO, the bath oxidation decreases with higher basicity, since a high basicity will render the slag less fluid and retard the rate of oxygen transfer from the slag to the bath. This relation is indicated by the grouping of high basicity points on the lower part of the band while the low basicity points tend to occupy the upper part of the band.

The effect of bath temperature on the solubility of the metal for oxygen is probably subordinate to its indirect effect on bath oxidation by increasing the slag fluidity and the rate of oxygen transfer from the slag to the bath. In any case, the effect of temperature variations (within the normal range of open-hearth tapping temperatures) on the bath oxygen has little weight as compared with the bath carbon and slag composition.

Some oxidation may take place as the

steel is exposed to the atmosphere during tapping. However, any such increase in oxygen is apparently counterbalanced by the deoxidizers added to the ladle. A few determinations have been made of oxygen in the steel as poured by submerging a bomb-type test box in the mold immediately after the mold is filled. The oxygen content shown in these tests has generally been lower than the oxygen in the bath.

Deoxidation schedules are designed to adjust the oxygen content from heat to heat at a level that will produce a uniform rimming action. The variables usually taken into account in such a schedule are the bath carbon and slag FeO. There is evidence that the rimming action may be stimulated by the addition of a small amount of aluminum or titanium to the ladle even when the oxygen content of the bath is below the desired value. This may be accounted for by the oxides of these elements forming nuclei for gas evolution in the ingot.

Manganese

The manganese content of rimmed steel (with the exception of the low-metalloid grades) is limited to a minimum of about 0.20 per cent Mn by the hot-short characteristics of lower Mn steel. The maximum of about 0.60 per cent Mn is determined by the inhibiting effect of manganese on rimming action, which was mentioned earlier. A higher manganese content of the bath at tapping is favored by a higher manganese input in the charge and a higher bath temperature. The addition of maniferous materials for reboiling may be a further source of manganese in the bath. A larger slag volume, higher slag and bath oxidation, and removal of manganese from the system in a runoff slag (if this practice is used) will produce a lower bath manganese content at tapping. While the manganese content of the bath will normally be low (below 0.20 per cent Mn) under the oxidizing conditions of rimmed-

steel manufacture, variations may be appreciable between heats from which some of the slag has been flushed and heats on which all the slag is retained. The principal importance of such variations in bath manganese lies in the variable amount of carbon introduced as ferromanganese. For example, a variation in residual manganese of 14 points (0.04 to 0.18 per cent Mn) would produce a variation of 0.015 per cent in carbon introduced as 7 per cent carbon ferromanganese. Consequently, it is necessary to work the low-manganese bath to a lower tapping carbon than the higher manganese bath.

When the specified ladle carbon is low (0.07 per cent max. or lower) some of the manganese added to the ladle may be in the form of low-carbon ferromanganese. However, the major part of the addition will be of the regular (7 per cent carbon) grade because of the desirability of adding some carbon to the ladle. A number of factors will affect the recovery of manganese from the ferromanganese during tapping. Some of these are the oxidation of the metal, the temperature, the tapping time, and the amount of manganese added.⁴ For a given grade of steel, these conditions ordinarily are sufficiently uniform to permit the use of a standard efficiency figure from heat to heat. For example, a recovery of about 70 per cent of the manganese added to a 0.07 to 0.09 per cent carbon, 0.30 to 0.40 per cent manganese rimmed heat is normally expected under the conditions prevailing in one open-hearth shop.

The addition of manganese and carbon to the ladle, the cooling of the steel, and the diffusion of oxygen from the ladle slag to the steel tend to raise the carbon-oxygen and manganese-oxygen products above equilibrium values while the steel is still in the ladle. The oxidation of manganese is particularly favored, since the oxide of manganese is not gaseous and its formation is not therefore inhibited by ferrostatic pressure. Also, the effect of oxidation on

manganese is more noticeable, since this element is present in greater proportion. Some loss of manganese to the ladle slag will normally be present, particularly during the pouring of the later ingots of the heat.⁵ A very rapid reversion of manganese to the ladle slag, a "ladle reaction," may take place under certain conditions such as low steel temperature, a large volume of highly oxidized slag on the ladle, or unusual agitation of the ladle. Such a reaction may be started by the temperature dropping to a point that permits the formation of a ladle skull that provides a solidifying surface on which a reaction similar to rimming in the ingot mold may take place. Rough handling of the ladle in transit may cause the mixing of the slag and steel, permitting the diffusion of oxygen from the slag to the steel. The ladle reaction, once started, tends to reinforce itself since, being endothermic, it tends to produce skulls, which, in turn, cause higher concentrations of the reacting elements in the liquid metal at the freezing surface, thereby favoring the reaction. As an example of an extreme case, a ladle reaction may significantly affect the composition of half the ingots of a heat, reducing the manganese content progressively until the last ingot of the heat may contain less than 0.20 per cent Mn as compared with a normal ladle manganese of 0.40 per cent.

Sulphur

On account of the marked tendency of sulphur to segregate in the rimmed ingot, the necessity for the bath to conform to a maximum specified sulphur is of particular importance in the case of rimmed steel. Darken and Larsen⁶ have shown the factors affecting good elimination of sulphur to be high concentrations of CaO and MnO, and low concentrations of FeO, SiO₂, and P₂O₅ in the slag, and a high slag volume. If the sulphur input (from hot metal, scrap, fuel, and fluxes) is controlled

within reasonable limits, if sufficient lime is charged to meet the basicity requirements, and the slag is rendered fluid early enough in the working period (before the

the bath at tapping and that in the ladle as the steel is poured, which may be the result of desulphurization in the ladle by ferromanganese.

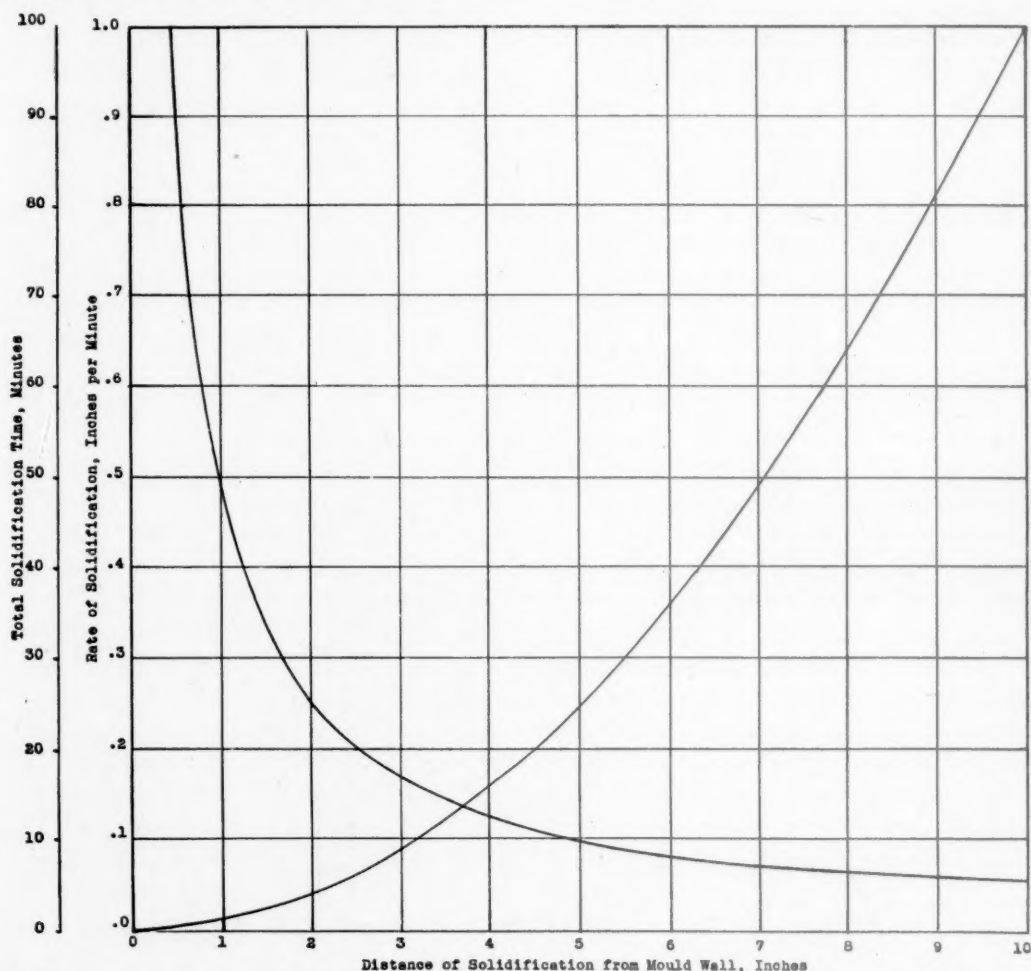


FIG. 7.—RELATION OF DISTANCE OF SOLIDIFICATION FROM MOLD WALL TO FREEZING RATE AND TIME OF SOLIDIFICATION.

FeO rises to high levels), desulphurization of the bath may be carried out to meet the maximum sulphur of 0.030 per cent or lower desirable for rimmed steel of deep-drawing quality. While desulphurization is carried out most effectively before the bath has reached a low carbon, it has been observed that the use of a spiegel reboil about 30 min. before tapping produces a lower ladle sulphur than heats without such a reboil. There is frequently a decrease in sulphur between the metal in

TEMPERATURE AND MOLD PRACTICE

A formula expressing the freezing rate of steel in a mold was developed by Feild⁷ from theoretical considerations and later verified experimentally by Nelson⁸ for killed steel and by Chipman and Fonder-Smith⁹ in its application to rimmed-steel ingots for times up to 30 min. after pouring. This formula, $D = K \sqrt{t}$, applies to liquid steel at its freezing temperature, when D represents the distance solidified from the mold wall; t , the time after

solidification starts; and K , a constant based on the characteristics of the mold and liquid metal. Assuming K to be unity (a representative value) a curve is shown (Fig. 7) indicating the parabolic relation-

tact with the mold wall was only 63 per cent of the distance that would be frozen if the liquid metal were at the freezing point.

For a maximum freezing rate, the opti-

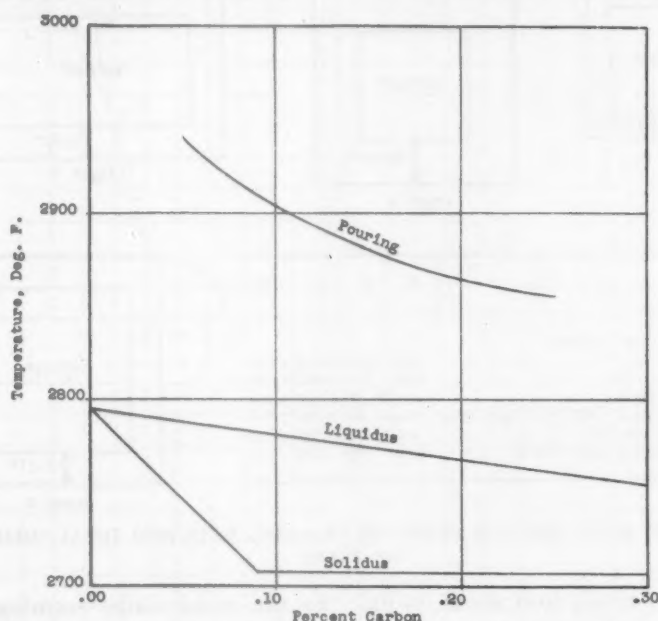


FIG. 8.—AVERAGE POURING TEMPERATURE FOR RIMMED HEATS COMPARED WITH LIQUIDUS AND SOLIDUS LINES FROM IRON-CARBON DIAGRAM.

ship between the distance frozen and the freezing time as solidification progresses. Some factors affecting the freezing rate other than the physical constants of the mold and liquid steel were pointed out by the investigators mentioned above. These factors are discussed below with regard to the degree of control to which they are subject through normal furnace and pouring practice.

Steel Temperature

In Feild's derivation of the formula, it was assumed that the temperature throughout the liquid was at the freezing point when solidification started. Calculations were made to show the effect of superheat on the freezing rate. At a temperature of liquid metal of 50°C . above the freezing point, it was shown that the distance solidified during the first minute after con-

tact with the mold wall was only 63 per cent of the distance that would be frozen if the liquid metal were at the freezing point. For a maximum freezing rate, the opti-

mum pouring temperature for rimmed steel is just above that at which a skull will form in the ladle. At higher temperatures, the freezing rate of the metal, and consequently the rate of gas evolution in the mold, is retarded. Lower temperatures involve the danger of ladle reactions and the pouring difficulties attendant on a heavily skulled ladle. Fig. 8 shows the average pouring temperature for the rimmed-steel range of ladle carbon that has been found satisfactory in one shop.

While instruments for measuring bath temperatures have been successfully developed, they are not currently available for general use, and the melter must depend on the rule-of-thumb methods for bath-temperature indication (erosion of a steel rod submerged in the bath, skulling of a test spoon, etc.), whose accuracy is based on the experience and judgment of the

furnace operator. Adjustment of combustion and the timing of ore additions are the principal means of temperature control in the furnace. In finishing the heat, an

is used for coating) a charred coating that will not be repellent to splashed steel. The lower limit is fixed largely by the tendency in cold molds for splashed metal to adhere

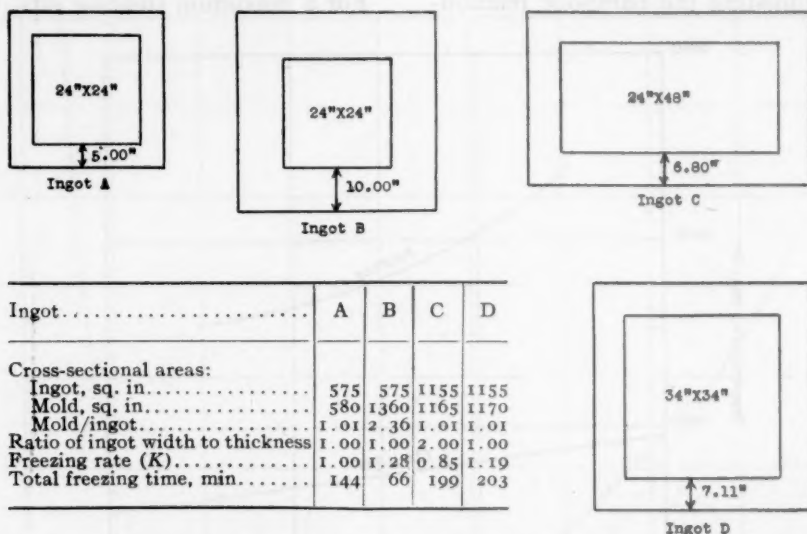


FIG. 9.—EFFECT OF MOLD SIZE AND SHAPE ON FREEZING RATE AND TOTAL SOLIDIFICATION TIME OF INGOT.

addition of spiegel or pig iron about $\frac{1}{2}$ hr. before tapping may be desirable to check the carbon drop momentarily, allowing the bath to pick up temperature, and to equalize the temperature throughout the bath by creating a stirring action. The first definite quantitative temperature determination may be made with the optical pyrometer during tapping. If this temperature is excessively high, pouring may be delayed to permit a cooling of the steel in the ladle.

Mold Temperature

Since the difference between the temperature of the steel and that of the mold is a controlling factor in the freezing rate, the use of excessively hot molds has the same effect on the rate of solidification as does excessive superheat of the steel. The upper temperature limit for molds for rimmed steel is established by the reduced freezing rate of the ingot poured in hot molds, the higher incidence of mold "stickers," and (if a material such as tar

is used for coating) a charred coating that will not be repellent to splashed steel. The lower limit is fixed largely by the tendency in cold molds for splashed metal to adhere

Mold Design

The effect of mold size and shape on the rate of solidification was calculated by Nelson. To demonstrate the effect of these factors, the solidification rate (K) for a hypothetical mold (ingot A in Fig. 9) was assumed to be 1.00 and calculations were made for other molds in which the dimensions are exaggerated for illustrative purposes. The formula used was a modification of the Feild equation in which the corrections for the ratio of length to width of the ingot cross section and for the ratio of mold-wall cross-sectional area to ingot cross-sectional area were introduced. The following effects of the dimensional properties of molds are illustrated in Fig. 9:

1. Comparing ingot A with ingot C: for ingots of the same cross-sectional width and the same ratio of mold-wall cross-
- creasing effect of heat transfer through the end walls.
2. Comparing ingot C with ingot D: for

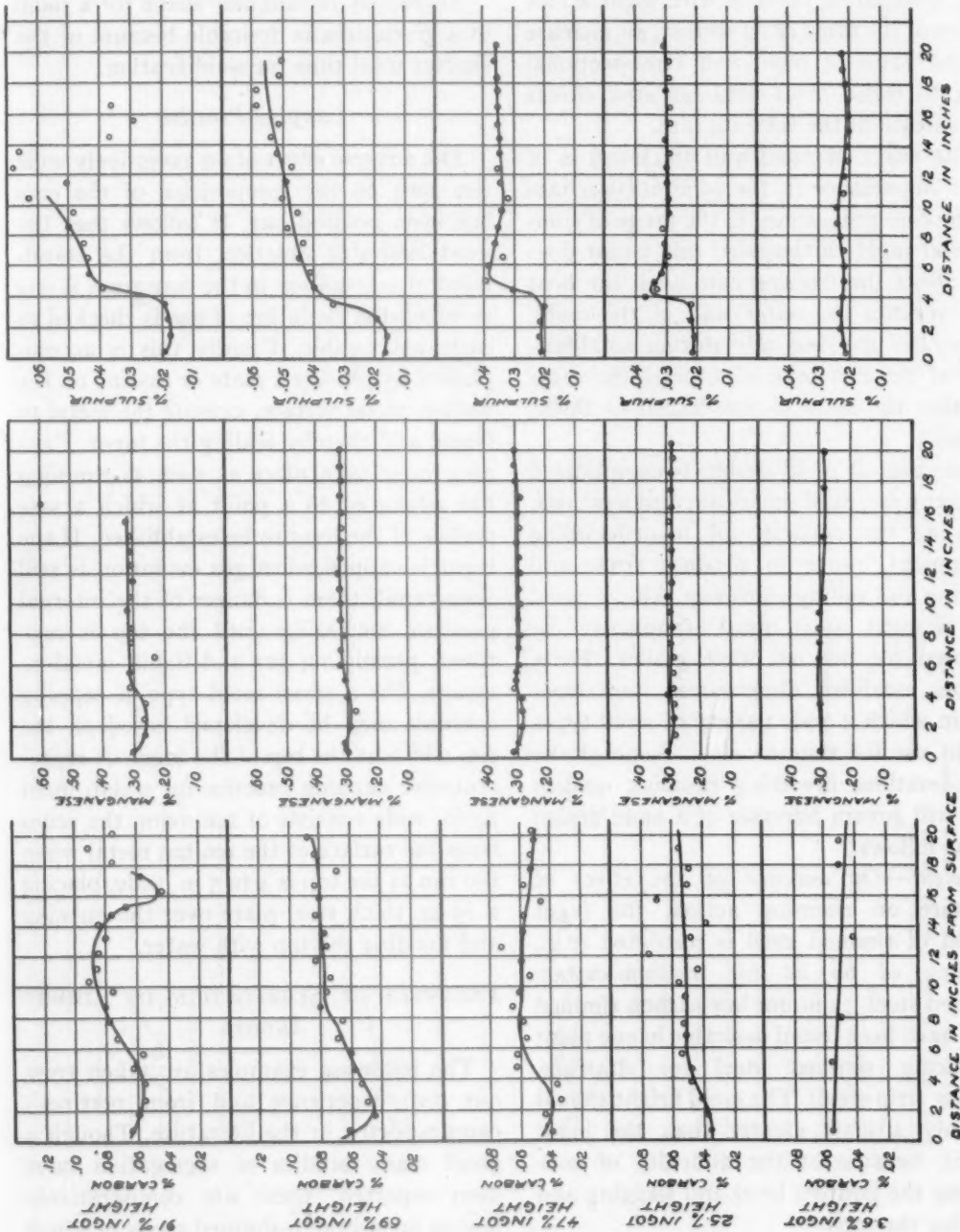


FIG. 10.—SPOT ANALYSES OF SLAB TESTS OF 18,000-LB. INGOT.
Ladle analysis: 0.06 per cent C; 0.35 Mn; 0.008 P; 0.027 S.

sectional area to ingot cross-sectional area, the freezing rate in a rectangular mold increases as the mold chamber approaches a square cross section, because of the in-

ingots of the same cross-sectional area and the same ratio of mold-wall cross-sectional area to ingot cross-sectional area, while the freezing rate is greater in a square ingot,

the total solidification time is greater because of the longer distance that must be frozen.

3. Comparing ingot *A* with ingot *B*: for ingots of the same cross section, an increase in the ratio of mold-wall cross-sectional area to ingot cross-sectional area effects an increase in the freezing rate.

The effect of mold-wall thickness is of most importance in the solidification rate of the core zone, since, in the range of commercial mold thicknesses, this factor does not affect the freezing rate until the heat flow reaches the outer wall of the mold. Thus, the freezing rate during solidification of the rim zone is actually the same whether the mold is thin-walled or thick-walled.

Selection of mold design is complicated by many essential practical considerations, such as the capacity of ingot-handling equipment, range of product sizes, and heating and rolling efficiency. Also, a mold for rimmed steel must frequently be adopted for use on other grades. These factors establish dimensional limitations within which a wide variety of mold types are in use for rimmed steel. Some of the considerations involving rimming quality that will govern selection of a mold design are as follows:

Height.—On account of the effect of pressure on rimming action, the ingot height of rimmed steel is restricted (e.g., maxima of 68 in. for medium-carbon rimmed steel, 75 in. for low-carbon rimmed steel have been found desirable in one plant producing rimmed steel for drawing-quality strip steel). The mold height should be only a little greater than the ingot height, because of the difficulty of controlling the pouring level and slagging and capping the tops.

Mold-wall Thickness.—Since mold-wall thickness becomes a factor in the freezing rate only after considerable solidification has taken place, thick walls are desirable in molds of large section, to produce rapid

freezing at the ingot center. In molds of small section, the mold-wall thickness has little effect on the freezing rate.

Shape.—A rectangular shape for a mold of a given area is desirable because of the shorter total time for solidification.

Capping Practice

The adverse effect of an excessively wide rim zone on the composition of the core has been pointed out. It follows that the most desirable practice, from the standpoint of segregation in the core zone, is one in which the evolution of gas is checked as early as possible. Usually this is accomplished by placing a plate or casting on the molten metal surface, causing the metal to freeze and thereby sealing the ingot. Capping may take place as soon as rimming has advanced to a point at which a safe sealing of the top can be established. If the ingot is capped when gas evolution is still very rapid, there is danger of the internal pressure increasing until the top is ruptured, permitting gas and liquid metal to escape. For a given mold type, a capping schedule may be developed based on the rim width at the top of the ingot. A representative capping practice for a slab mold 24 in. wide consists of removing the scum from the surface of the molten metal when the rim at the top is 4 to 5 in. wide, placing a $\frac{3}{8}$ -in. thick steel plate over the opening and flooding the top with water.

EXAMPLES OF SEGREGATION IN RIMMED INGOTS

The following examples are taken from our own experience and from pertinent cases reported in the literature. Though a great many studies of segregation have been reported, there are comparatively few on open-hearth rimmed steels in which the survey of the ingot has been detailed and complete. Edge to center analyses half way up the ingot and spot analyses from various parts of the ingot have been reported frequently, but there is only a

limited amount of data that present a comprehensive survey.

Fig. 10 shows the composition from

at $\frac{1}{2}$ -in. intervals from edge to center using a $\frac{3}{8}$ -in. drill. Manganese and sulphur were determined on samples that were an inch

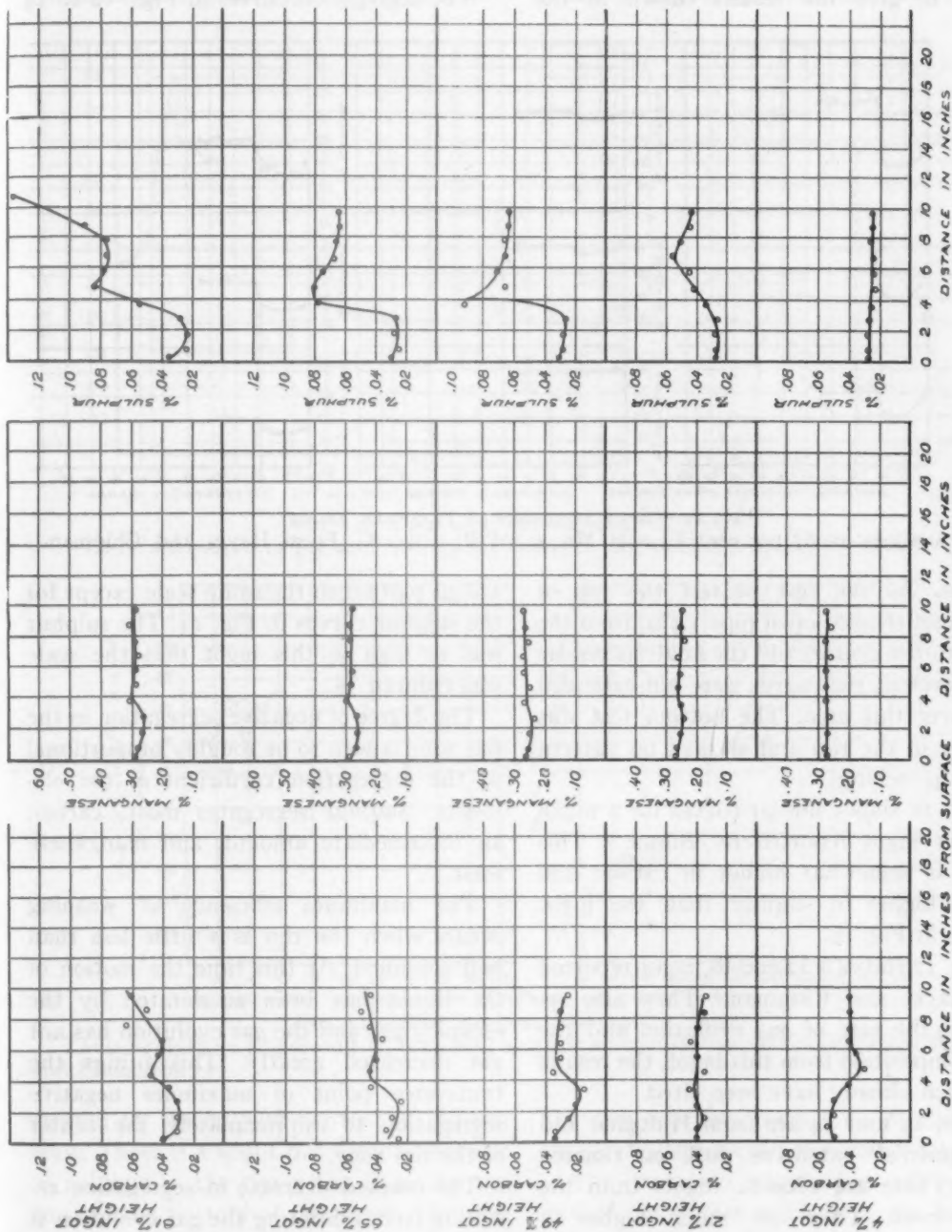


FIG. 11.—SPOT ANALYSES OF 6000-LB. INGOT.
Ladle analysis: 0.08 per cent C; 0.30 Mn; 0.041 S. (From Binnie.¹⁰)

edge to center at five different elevations of an 18,000-lb. rimmed ingot poured in a 24 by 43-in. mold. The analyses were made on drillings from slab tests sampled

apart except at the junction of the rim and core zones, where the samples were $\frac{1}{2}$ in. apart. Carbon was determined in duplicate on samples $\frac{1}{2}$ in. apart and the analyses

were checked by two different chemists. Even so, the carbon analyses showed wide scatter and adjacent positions were averaged to give the results shown in the

aluminum addition was enough to reduce the gas evolution greatly and cause the steel to rise in the mold.

The segregation curves in Figs. 10 to 14

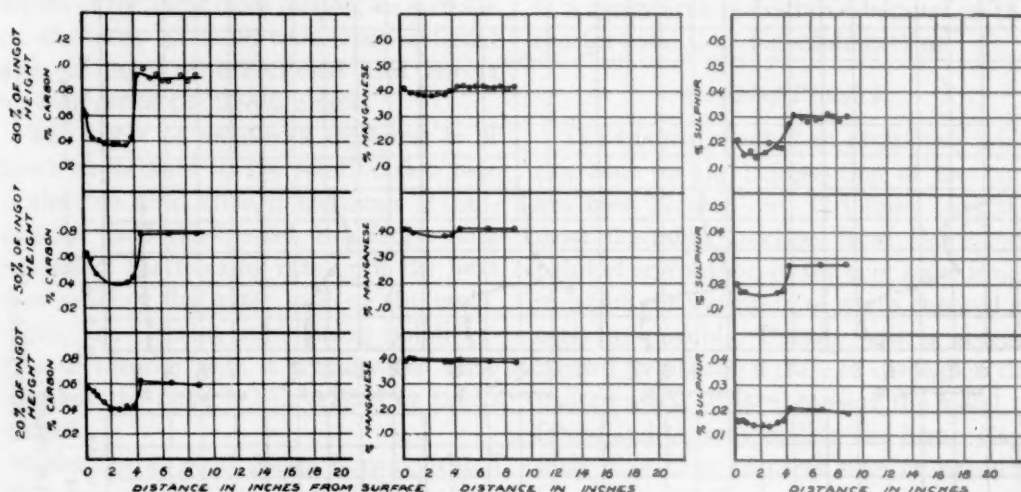


FIG. 12.—SPOT ANALYSES OF 12,000-LB. INGOT.

Ladle analysis: 0.087 per cent C; 0.41 Mn; 0.008 P; 0.019 S. (From Hayes and Chipman.¹)

curves. As the test nearest the top of the ingot showed open pipe 14 in. from the edge to the center, and the analysis results were erratic, the curves were not extended to cover this area. The bottom test was wholly in the rim and showed no pattern on deep etching.

Fig. 11 shows similar curves for a much smaller ingot reported by Binnie.¹⁰ This ingot is somewhat higher in carbon and much higher in sulphur than the ingot shown in Fig. 10.

Fig. 12 shows a 12,000-lb. ingot reported by Hayes and Chipman.¹ They also reported the rate of gas evolution and the gas composition from this ingot, the results of which already have been cited.

Figs. 13 and 14 are from Hultgren and Phragmén's¹¹ extensive work on rimmed steel. These are 1800-lb. ingots from the same heat. They are much higher in carbon than any of the other ingots shown. The ingot in Fig. 13 was permitted to rim normally, but 1¼ oz. of aluminum per ton was added to the ingot shown in Fig. 14. In steel containing so much carbon, this

are all plotted to the same scale except for the sulphur curves in Fig. 11. The sulphur was so high in this ingot that the scale was reduced ½.

The degree of negative segregation in the rim zone is seen to be roughly proportional to the segregation coefficient of the elements. Sulphur segregates most, carbon an intermediate amount, and manganese least.

The maximum efficiency of washing occurs when the rim is a little less than half solidified. At this time the motion of the liquid has been accelerated by the escaping gas and the gas evolution has not yet decreased greatly. This brings the transverse point of maximum negative segregation to approximately the center of the rim zone.

The marked decrease in segregation resulting from inhibiting the gas evolution is shown by comparing the ingots in Figs. 13 and 14. A very small aluminum addition was sufficient in this steel to cause an appreciable decrease in gas evolution. The ingot in Fig. 14, therefore, shows much less

segregation than the ingot in Fig. 13, to which no aluminum was added.

The decreasing efficiency of washing in the lower part of the ingot is best demon-

strated by the sulphur content of the rim zone. There is a slight but definite increase in sulphur in the rim going from the top toward the bottom of the ingot. The vertical segregation in the core is in the opposite direction, the sulphur content increasing markedly toward the top.

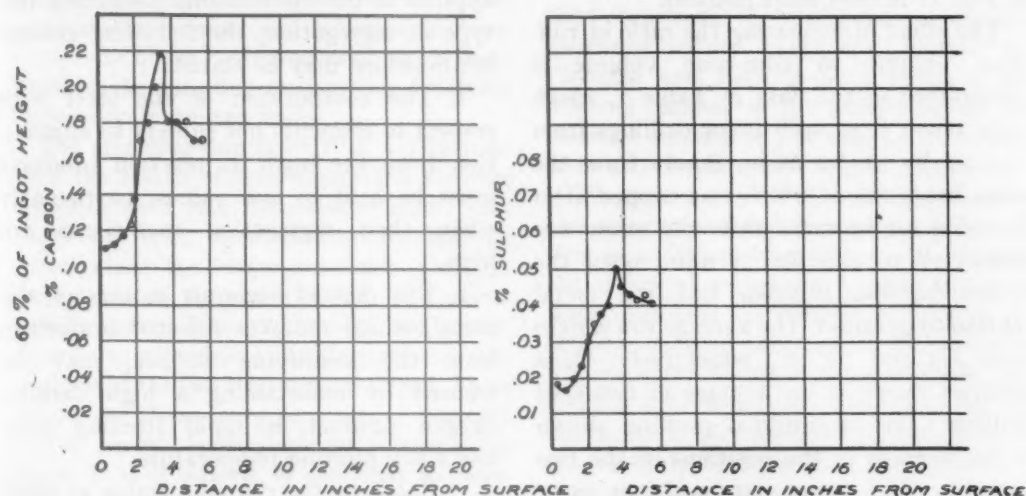


FIG. 13.—SPOT ANALYSES OF 1800-LB. INGOT.

Ladle analysis: 0.14 per cent C, 0.47 Mn, 0.035 S. (From Hultgren and Phragmén.¹¹)

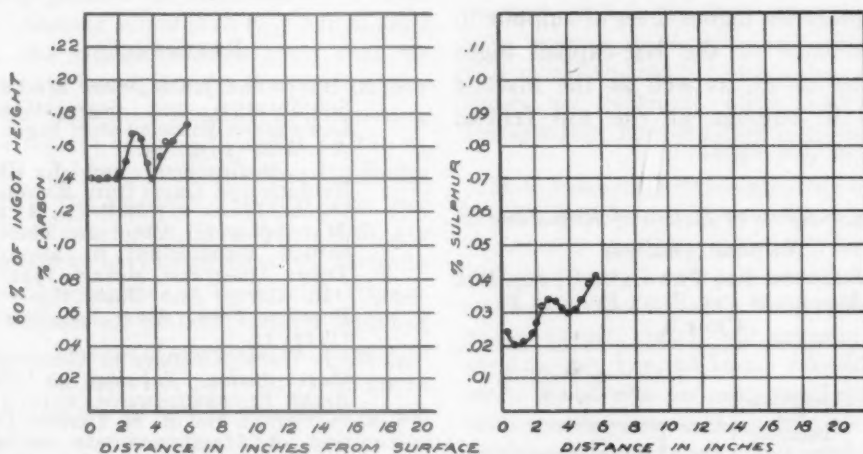


FIG. 14.—SPOT ANALYSES OF 1800-LB. INGOT.

Ladle analysis: 0.14 per cent C; 0.47 Mn; 0.035 S; 0.0037 per cent Al added. (From Hultgren and Phragmén.¹¹)

strated by the sulphur content of the rim zone. There is a slight but definite increase in sulphur in the rim going from the top toward the bottom of the ingot. The vertical segregation in the core is in the opposite direction, the sulphur content increasing markedly toward the top.

Though carbon has been removed from the ingot as gas, the core analyses in the

the core analyses average about the same or slightly lower than the ladle analysis.

The increased segregation of sulphur caused by higher sulphur in the ladle is shown by Figs. 10 and 11. The ingot in Fig. 10, with 0.027 per cent sulphur, shows a minimum of 0.017 per cent in the rim, or a maximum negative segregation of 37 per cent. The ingot in Fig. 11, with 0.041

per cent sulphur, shows a minimum of 0.022 per cent sulphur in the rim, or a maximum negative segregation of 46 per cent. The greater positive segregation in the ingot in Fig. 11 is even more marked.

The effect of increasing the ratio of rim-zone volume to core-zone volume is exemplified in the data in Table 2, which were taken from split ingot drillings from two 24 by 43 by 66-in. ingots from the same heat, one of which was capped after rimming for 17 min. while the other was permitted to rim for 34 min., until the action became sluggish and the metal started to pyramid. The average rim widths were 4.3 and 5.9 in., respectively. Each analysis shown is the average of two spot drillings; the longitudinal position shown is the average of the positions of the two samples. The transverse positions were selected with reference to the structure as shown in the table.

The generally higher level of sulphur in the core zone of the late-capped ingot should be noted, as well as the marked increase in sulphur at the top central position of this ingot.

TABLE 2.—Effect of Extent of Rim Zone on Sulphur Analysis

LADLE ANALYSIS: 0.09 PER CENT C; 0.40 PER CENT Mn; 0.008 PER CENT P; 0.027 PER CENT S

Practice	Longitudinal Position, Per Cent of Ingot Height	Transverse Position, Per Cent S			
		Out-side of Rim Zone	Inside of Rim Zone	Out-side of Core Zone	Center of Core Zone
Capped 17 min. after pouring.	93	0.021	0.020	0.040	0.076
	77	0.022	0.021	0.038	0.040
	52	0.020	0.022	0.033	0.023
	12	0.021	0.022	0.024	0.022
Capped 34 min. after pouring.	93	0.016	0.018	0.048	0.122
	77	0.018	0.022	0.042	0.040
	52	0.018	0.020	0.038	0.035
	12	0.021	0.022	0.022	0.026

It has been pointed out that the desirable type of segregation in the rimmed grade

of ingot consists of maximum negative segregation in the rim zone and minimum positive segregation in the core. To summarize the possible controls that may be applied to the mechanisms producing this type of segregation, the following general relationships may be stated:

1. The composition of the steel with respect to elements not subject to elimination from the ingot as reaction products must be held to low values, particularly when their segregation coefficients are high.

2. The desired vigorous motion of the metal, which removes rejected impurities from the solidifying surface, may be secured by maintaining a high carbon-oxygen product, a rapid freezing rate, and a low pouring temperature.

3. Checking the rimming action as early as possible by capping the ingot will reduce segregation in the core zone.

REFERENCES

1. A. Hayes and J. Chipman: Mechanism of Solidification and Segregation in a Low-carbon Rimmed-steel Ingot. *Trans. A.I.M.E.* (1939) 35.
2. K. C. McCutcheon and J. Chipman: Evolution of Gases from Rimming-steel Ingots. *Trans. A.I.M.E.* (1938) 131.
3. S. Marshall and J. Chipman: The Oxygen-carbon Equilibrium in Liquid Iron. *Trans. Amer. Soc. Metals* (1942) 30.
4. C. H. Hertzy, Jr.: Basic Open Hearth Practice. *Trans. Amer. Soc. Steel Treat.* (1927) 11.
5. N. J. Wark: Changes in Composition of Steel during Tapping or Teeming. *Archiv Eisenhüttenwesen* (1932) 15.
6. L. S. Darken and B. M. Larsen: Distribution of Manganese and of Sulphur between Slag and Metal in the Open-hearth Furnace. *Trans. A.I.M.E.* (1942) 150, 87.
7. A. L. Feild: Solidification of Steel in the Ingot Mould. *Trans. Amer. Soc. Steel Treat.* (1927) 11.
8. L. H. Nelson: Solidification of Steel in Ingot Moulds. *Trans. Amer. Soc. Metals* (1934) 22.
9. J. Chipman and C. R. FonDersmith: Rate of Solidification of Rimming Steel. *Trans. A.I.M.E.* (1937) 125.
10. D. Binnie: An Ingot of Rimmed Steel Made by the Basic Open Hearth Process. *Jnl. Iron and Steel Inst.* (1942) 146.
11. A. Hultgren and G. Phragmén: Solidification of Rimming-steel Ingots. *Trans. A.I.M.E.* (1939) 135.

DISCUSSION

(H. B. Emerick presiding)

K. L. FETTERS,* Youngstown, Ohio.—The authors have presented a paper that will arouse considerable interest, and which may bring forth some of the controversies of which Earle Smith spoke regarding specifications involving segregation in rimmed steels.

The accompanying figure (Fig. 15) summarizes the results of some segregation analyses we made on a slab rimmed-steel ingot. This ingot was split longitudinally through the center along the longer dimension. Drillings were taken at the center and at four points equally spaced between the edge and center. In order to minimize any microsegregation, the analyses of the two sides were averaged. These results are shown at 5 per cent, 40 per cent and 60 per cent levels above the bottom of the ingot. It is of interest to note that we show somewhat greater negative segregation of manganese than do Halley and Plimpton, and this may perhaps be attributed to a more intense rimming action than they had in their ingots. The sulphur curves confirm what the authors have found; namely, that the intensity of sulphur segregation increases with increasing sulphur content of the ladle metal. In Fig. 15 the ladle analyses are shown above the curves for each of the elements. This particular heat was somewhat higher in sulphur than our average and we have noted decreasing intensity of sulphur segregation in lower sulphur heats.

The authors are probably correct regarding the greater amount of segregation found nearer the top of the ingot but quantitative discussion of the degree should first be considered by the appropriate standardizing and specification committees before we discuss these data.

Mention is made of the variation in intensity of rimming action with mold size. We notice a better rimming action in certain sizes, with the best action in a mold that is more nearly square than in a narrow slab-type mold.

We can confirm the slightly greater degree of segregation that is to be found in an ingot with a thick primary skin.

The authors report that the oxygen content in the bath decreases with increasing basicity of the slag for a given oxide content of the slag

for any given carbon content of the bath. They attribute this decreasing oxidation of the bath to an increase in the viscosity of the slag and decrease in the rate of oxygen transfer. I believe it would be well to recognize the decrease in the FeO activity of the slag that accompanies increasing basicity. Taylor and Chipman* and Chipman and Fetters† have shown a pronounced decrease in the activity of the iron oxide in the slag as the basicity is increased from 2.2 lime-silica ratio to 3.0 or higher.

The authors speak of the oxidation of carbon and manganese that accompany a ladle reaction as endothermic reactions and postulate that if they occur the metal is chilled and a skull forms, and that the removal of heat by this skull causes more reaction to occur, and so on. The generally accepted thermodynamic data indicate these reactions to be exothermic and the equilibria are such that as the temperature is lowered the tendency is for the formation of more and more of the oxides. Thus if a heat is poured at a normal temperature any undue loss of temperature or chilling will favor a ladle reaction, so it is the skull that promotes the ladle reaction rather than the ladle reaction that causes the skull. Any freezing, of course, causes gas evolution, which, owing to the strong action, further favors ladle reactions.

H. B. EMERICK,‡ Pittsburgh, Pa.—At several points throughout the paper the authors have commented upon the desirability of reducing bath carbon to the lowest practical point in order to secure a high concentration of dissolved oxygen, which will promote vigorous mold action. For the higher carbon rimming steels (up to 0.30 per cent maximum carbon) ladle recarburizers such as coal or coke are recommended. Now, on the assumption that maximum homogeneity is sought after in any steel—even in an inherently heterogeneous product such as a rimmed ingot—it should be advantageous, from the standpoint of minimizing segregation, to tap the steel at the highest possible carbon content and the lowest possible oxygen content, consistent of course with the surface-quality requirements of the

* C. R. Taylor and J. Chipman: *Trans. A.I.M.E.* (1943) **154**, 228.

† J. Chipman and K. L. Fetters: *Trans. A.I.M.E.* (1941) **145**, 95.

‡ Metallurgical Department, Jones and Laughlin Steel Corporation.

* Youngstown Sheet and Tube Company.

grade. Over a number of years, our experience in the manufacture of 0.20 to 0.30 per cent carbon rimming steels has indicated that definitely less segregation occurs in heats that

to arrest rimming action as soon as 5 min. after topping off the ingot. Have the authors investigated the effects of earlier capping with cast-iron caps having greater chilling capacity

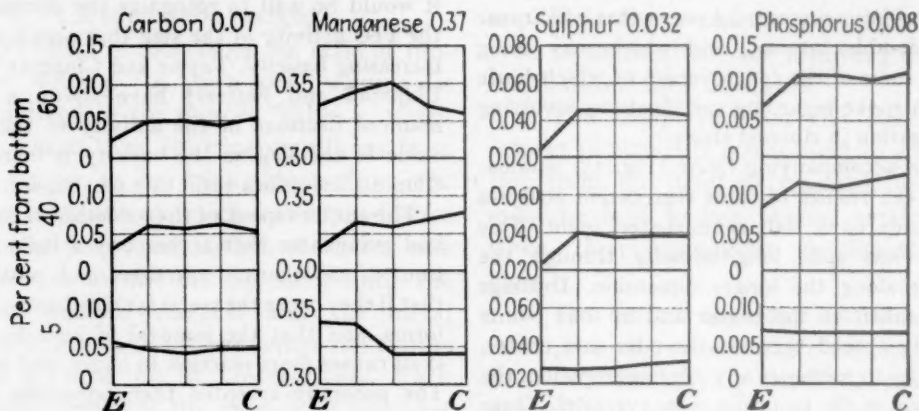


FIG. 15.

are tapped "straight" (without coal). This is particularly true of the element carbon, where the addition of any solid recarburizer to the ladle has been found to increase the non-uniformity of that element even in sound killed steels. Have the present authors accumulated any data on the comparative segregation tendencies of 0.20 to 0.30 per cent carbon rimming ingots produced with and without ladle recarburizers supplementary to the usual addition of ferromanganese?

The emphasis the authors have placed upon the severe segregation tendencies of the element sulphur is entirely warranted. In fabricating rimmed steels sulphur segregation has perhaps caused more processing difficulties than any other single factor. As noted by the authors, the principal means available to the steelmaker for limiting the objectionable positive segregation of sulphur are: (1) production of extremely low ladle sulphurs and (2) the early arrest of rimming action by means of capping. Extra heavy cast-iron caps are widely used for this purpose, as they permit the operator

than the $\frac{3}{8}$ -in. thick steel plates mentioned in the paper?

J. W. HALLEY.—I might say that Mr. Fetter's comment about the decreasing activity of the iron oxide in the slag with increasing basicity was very well taken. That is certainly as important, if not more important, than decreasing viscosity.

Mr. Larsen mentioned the humps and irregularities he found in his curves, which we also found. Our experience has been that drillings from slabs or ingots will give marked irregularities in the curves. Smooth curves are obtained from millings taken parallel to the surface of the ingot. Apparently the average analyses from zone to zone vary uniformly but there is erratic variation within each zone.

We have not done enough work on the 20 to 30 carbon range in comparing the difference between adding carbon and tapping on approximately the specified carbon, to have anything to offer on the relation of tapping practice to segregation.

Segregation in a Large Alloy-steel Ingot

By S. W. POOLE* AND J. A. ROSA*

THE object of this investigation was to determine the distribution of chemical elements within a large, killed alloy-steel ingot, by sulphur printing and quantitative chemical analysis.

With regard to segregation in steel ingots, the factors of melting practice, pouring temperatures, mold design, etc., and the mechanics of solidification and its attendant functions, have been the subject of intensive study over a period of years by many investigators. Notable among these is the Sub-Committee of the No. 5 Committee of the British Iron and Steel Institute. For an exposition of the many problems awaiting the researcher on the heterogeneity of steel ingots, the methods of attacking these problems, together with some of the answers, the reader is referred to the nine reports and numerous papers of that committee and its membership.

STEELMAKING DATA

Melt.—The heat was made in a 70-ton direct arc-type basic electric furnace. Furnace charge consisted of nickel-chromium-molybdenum steel, most of it in the form of heavy mill scrap. All of the scrap was charged cold.

The standard double-slag method was employed, the heat being finished under a strong carbide slag. Aluminum was used as the deoxidizing agent. Tapping tempera-

ture, as observed with an optical pyrometer, was 3000°F.

Detail of Mold and Ingot Size.—Details of the ingot mold and the ingot itself are given in Fig. 1.

Teeming.—Teeming temperature of the subject ingot as observed with an optical pyrometer was 2830°F. The ingot was top-poured directly through a 1½-in. nozzle and required 7 min., 44 sec. to fill up to the hot top. An additional 2 min., 30 sec. were required to fill the hot top.

The ingot was stripped hot and charged with the remainder of the heat into an annealing furnace. There it was given the standard annealing cycle used for these ingots. Subsequent heat-treatments are described elsewhere in this paper.

SECTIONING AND PREPARATION FOR SULPHUR PRINTING

Because of previous favorable experience in sectioning ingots up to 21½ in. square with an oxyacetylene torch, it was decided to use this method to section the subject ingot.

The ingot was preheated to 900°F. for 12 hr. It was then placed on a steel bed in a horizontal position so that the longitudinal axis was level and parallel to the track of the motor-driven torch carrier.

Two cuts were made, one 2 in. above the longitudinal axis and the other 2 in. below. The time required to make each cut was approximately 75 min. The cutting operation is shown in Figs. 2 and 3.

The 4-in. thick slab was immediately charged into a furnace standing at 1200°F.

Manuscript received at the office of the Institute Nov. 30, 1943. Preprinted in February 1944 as *Technical Publication* No. 1720.

* Supervisor Metallurgical Research and Research Metallurgist, respectively, Republic Steel Corporation, Canton Steel Division, Canton, Ohio.

This temperature was maintained for 12 hr., after which the slab was pulled and air-cooled to room temperature.

Final preparation of the ingot slice con-

Fifteen feet of 40-in. wide photographic silver bromide paper (Azo No. 3) was moistened in a 3 per cent solution of sulphuric acid. The moistened paper was

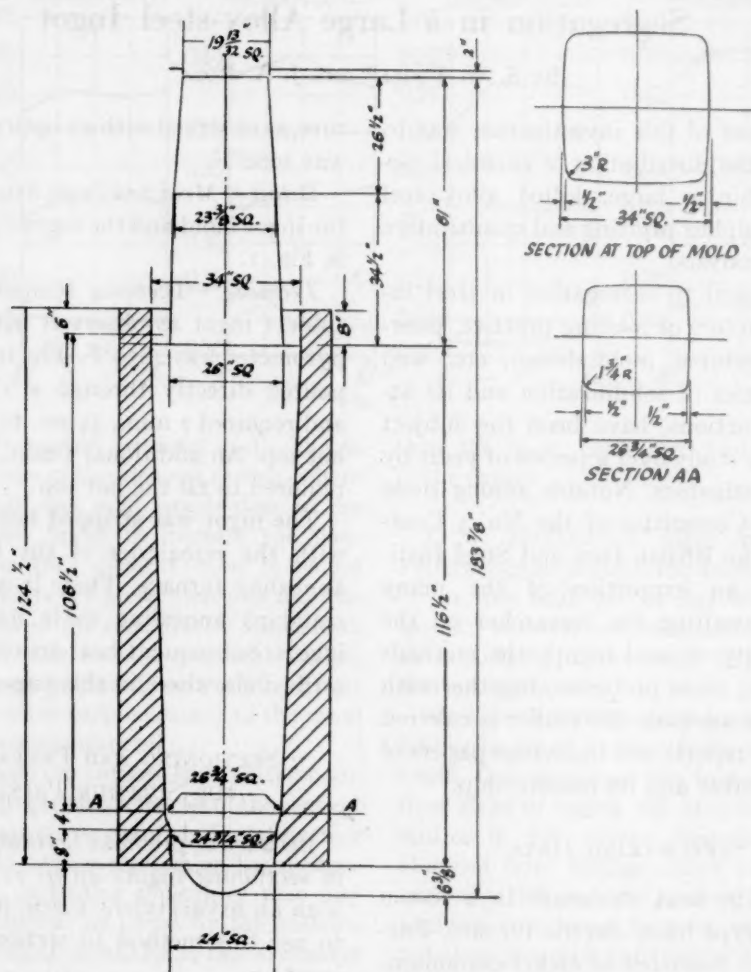


FIG. 1.—DETAIL OF MOLD AND INGOT.

Volume in hot top, 7400 lb.

" " body, 26,400 lb.

Total ingot, 34,000 lb.

Weight factor in ingot body

1 cu. in. = 0.262 lb.

sisted of planing off one surface to the exact longitudinal center. The last cut was made with a fine, light feed, so as to produce a reasonably smooth surface as free as possible from drag marks or smears.

The Baumann sulphur-printing method was employed to make a print of the ingot slice.

placed in contact with the freshly machined surface and held there for 4 min. Following this, the print was fixed and washed just as any other photographic print. The dried print was cut to outline and then pasted to a plywood pattern of the ingot slice. The whole of it was then covered with one application of a clear, waterproof, syn-

thetic coating. Fig. 4a illustrates the sulphur print.

revealing the general heterogeneity of an ingot, it is of unquestionable value; how-

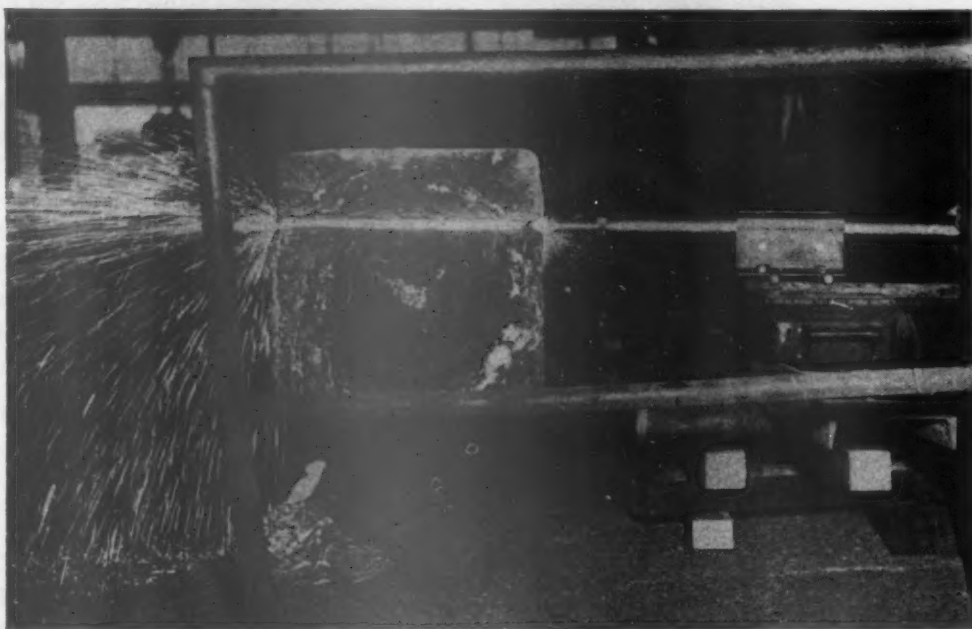


FIG. 2.—START OF TORCH CUT AT BOTTOM OF INGOT.

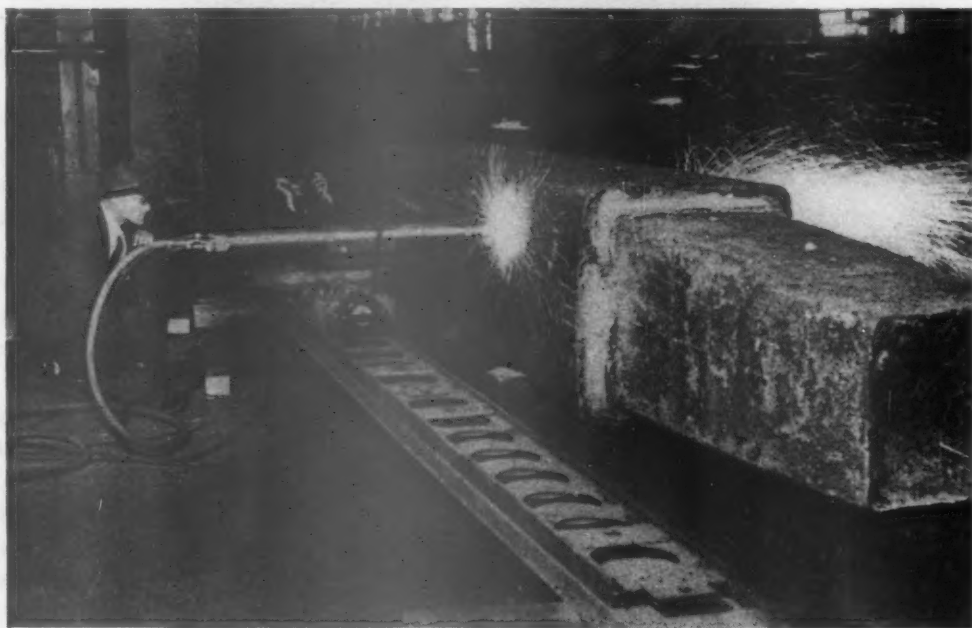


FIG. 3.—PROGRESS OF FIRST CUT.

The merits of sulphur printing as a means of studying segregation in ingots have been praised and disparaged.^{1,2} As a means of

ever, its value in disclosing sulphur segregation, particularly in the core area, is doubtful. Nevertheless, it appears that no better method—short of deep etching—has

¹ References are at the end of the paper.

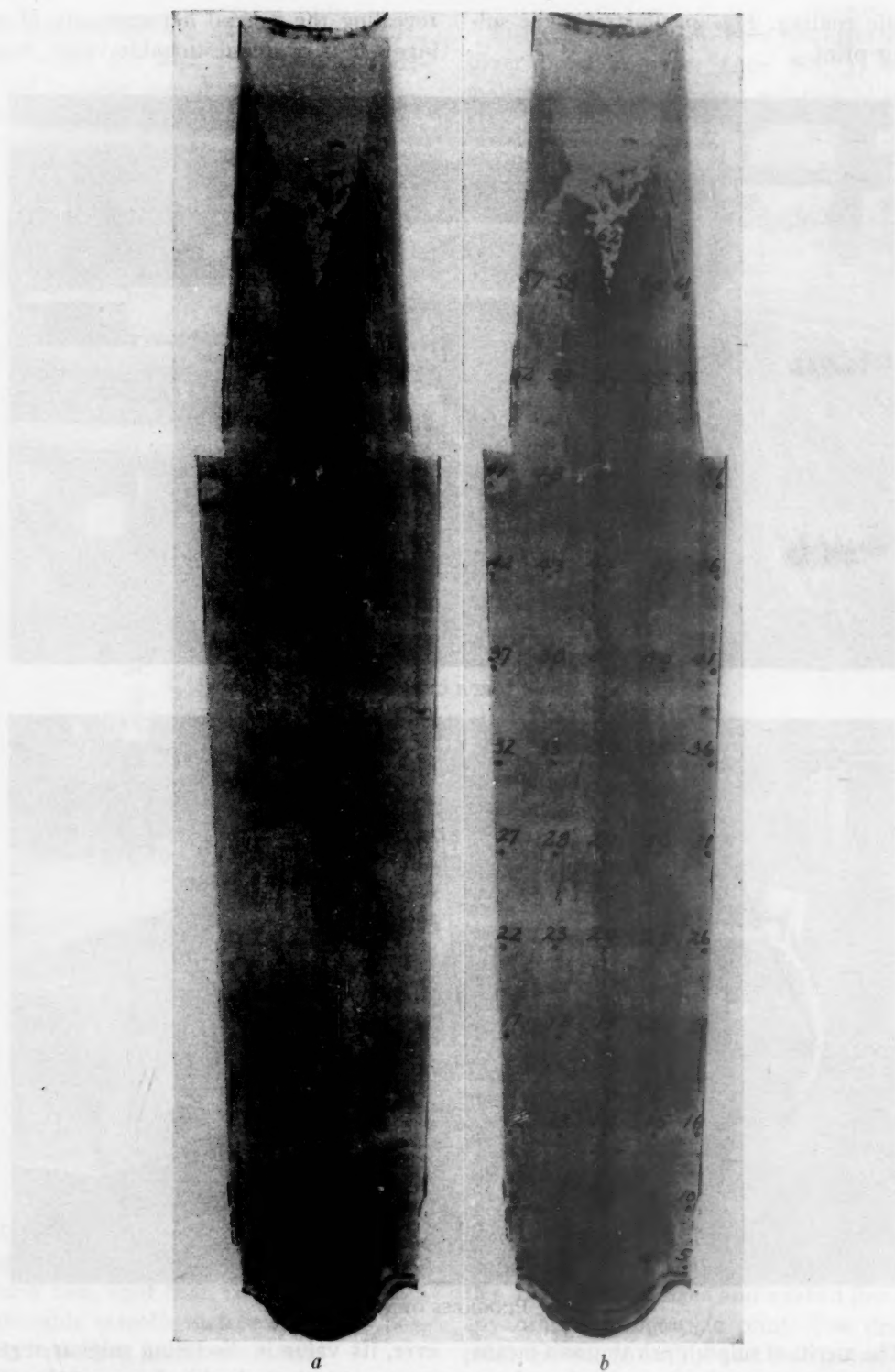
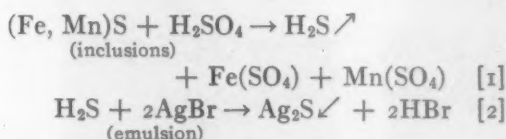


FIG. 4.—SULPHUR PRINT OF INGOT (*a*) AND POSITIONS OF DRILLINGS FOR CHEMICAL ANALYSES (*b*).

been devised to reveal physical discontinuities in an ingot structure.

In Fig. 4a it can be seen that the apparent high-sulphur areas are in the ∇ macroindications in the upper half of the ingot and in the \wedge indications in the bottom portion in the region of the apex of the so-called sedimentary cone. Sulphur analyses in these areas (Fig. 5), paradoxically, do not show any increase in sulphur.

A brief consideration of the probable chemical reactions occurring during sulphur printing will serve to explain the apparent paradox:



The principal reaction involves the liberation of hydrogen sulphide gas, which reacts with the silver bromide to form brown silver sulphide. The silver sulphide appears as a brown coloration on the photographic paper and ultimately is identified as representing a sulphur segregate in the steel. Assuming that each coloration on the paper resulted from contact with a sulphur compound, the interpretation is then correct.

At this point it must be considered that hydrogen sulphide is a gas and as such is capable of filling every void, cavity, or depression wherein it is generated. When a cavity at the machined surface of the ingot section is covered with photographic paper, the gas will react with every portion of the paper it contacts, and will, in consequence, leave its mark in the form of a uniform, dark brown coloration. Thus it becomes obvious that while the gas generated in a rupture may present a reasonably accurate picture of the physical discontinuity, it may at the same time give a gross exaggeration of the sulphur distribution.

It is not the authors' intention to dispute the oft-proven core segregation of non-metallic sulphide compounds. The sole

purpose of the foregoing is to point out the very real possibility of misinterpreting the sulphur print of an ingot.

The sulphur print in Fig. 4a does not display any pronounced segregation of sulphur. Primary sulphide segregation is evident in the form of thin threads somewhat removed from the core area. These threadlike segregates are in the form of discontinuous \wedge segregates inclined toward the central axis of the ingot and are not considered as excessive in amount.

Macroetching

Experience gained with previous ingot sections indicated that the liquor used for commercial pickling would give satisfactory results. For this reason, the 10 per cent sulphuric acid solution was chosen instead of the nitric acid reagents often used for this type of work.

The slice was immersed in a tub of fresh pickle liquor, which was maintained at 140° to 160°F. Etching progress was checked after 4, 8, 12, 16 and 18 hr. After 21 hr. the slice was removed from the tub, washed thoroughly with water, scrubbed with powdered pumice, rinsed and dried and then coated with a clear, waterproof synthetic lacquer.

Deep etching of the ingot slice did not reveal anything not already indicated by the sulphur print. Etching had progressed most rapidly in the ∇ and \wedge core "herring bone" and within the threadlike sulphide segregates adjacent to the core and within the hot top (Fig. 4a). The macrostructure otherwise was sound and dense throughout the ingot.

SAMPLING FOR CHEMICAL ANALYSIS

Drillings for chemical analysis were obtained from the reverse side of the macroetched 2-in. thick ingot slice.

Samples were taken with a 5/8-in. diameter drill. In each instance, drillings to a depth of 1/8 in. were discarded, to obviate the possibility of including decarburized

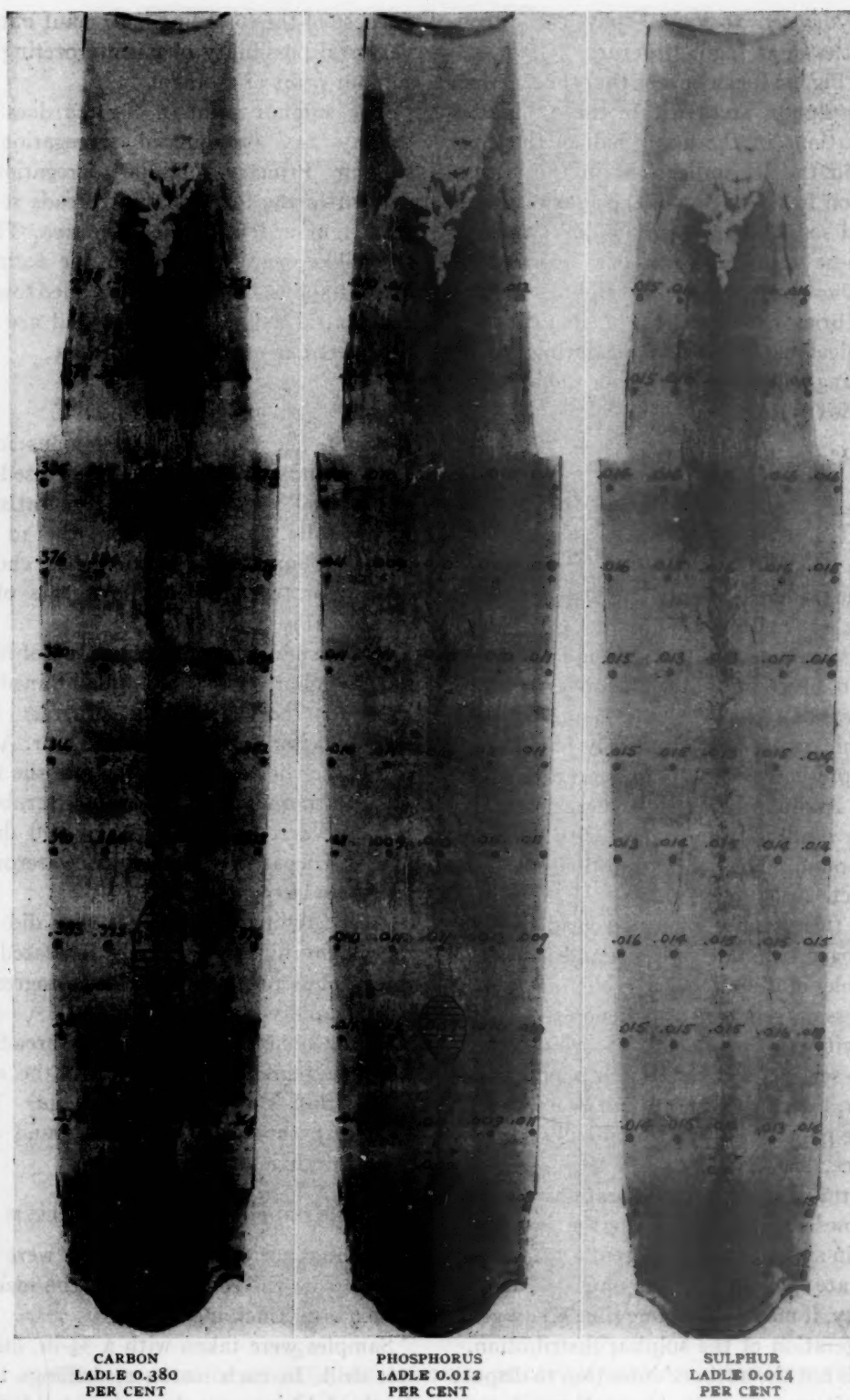


FIG. 5.—SEGREGATION OF ELEMENTS.

metal from the surface layer and of contamination by scale or foreign matter.

Sampling was begun at the extreme bottom left corner of the ingot, this being numbered position No. 1. The succeeding samples were numbered consecutively from left to right, as plotted in Fig. 4b.

The first row of drillings was taken on a line across the extreme bottom of the ingot.

The next row was 6 in. from the bottom. Position No. 11 (the single drilling in the bottom center) was 11 in. up from the bottom. The row third up (position 12 to 16) was 18 in. from the bottom. The fourth

TABLE 1.—Detailed Analyses of 62 Ingot Positions
PER CENT

	C	Mn	S	P	Si	Ni	Cr	V	Mo
Ladle.....	0.380	0.65	0.014	0.012	0.30	1.86	0.81	0.07	0.34
Position No. 1.....	0.381	0.65	0.013	0.010	0.32	1.85	0.82	0.07	0.35
2.....	0.381	0.66	0.013	0.010	0.32	1.85	0.81	0.06	0.36
3.....	0.375	0.65	0.013	0.010	0.32	1.85	0.81	0.06	0.35
4.....	0.383	0.65	0.013	0.011	0.33	1.88	0.81	0.07	0.35
5.....	0.400	0.65	0.022	0.011	0.33	1.87	0.84	0.07	0.36
6.....	0.366	0.66	0.015	0.010	0.32	1.88	0.83	0.06	0.34
7.....	0.352	0.66	0.014	0.008	0.32	1.85	0.82	0.06	0.34
8.....	0.344	0.65	0.014	0.010	0.32	1.84	0.82	0.06	0.34
9.....	0.376	0.65	0.014	0.009	0.32	1.84	0.82	0.06	0.34
10.....	0.379	0.65	0.015	0.008	0.32	1.85	0.82	0.07	0.34
11.....	0.364	0.64	0.014	0.009	0.31	1.85	0.82	0.07	0.34
12.....	0.374	0.67	0.014	0.010	0.29	1.85	0.83	0.06	0.38
13.....	0.332	0.66	0.015	0.011	0.29	1.84	0.82	0.06	0.36
14.....	0.328	0.63	0.014	0.011	0.29	1.83	0.83	0.06	0.34
15.....	0.378	0.66	0.013	0.009	0.31	1.85	0.83	0.06	0.34
16.....	0.364	0.64	0.014	0.011	0.32	1.86	0.83	0.06	0.36
17.....	0.385	0.66	0.015	0.011	0.31	1.86	0.83	0.06	0.34
18.....	0.368	0.66	0.015	0.012	0.29	1.86	0.84	0.06	0.34
19.....	0.330	0.63	0.015	0.007	0.29	1.83	0.79	0.06	0.32
20.....	0.384	0.67	0.016	0.010	0.31	1.88	0.81	0.07	0.33
21.....	0.378	0.67	0.018	0.010	0.31	1.88	0.81	0.06	0.33
22.....	0.383	0.66	0.016	0.010	0.31	1.85	0.83	0.07	0.34
23.....	0.395	0.66	0.014	0.011	0.32	1.85	0.83	0.07	0.34
24.....	0.345	0.65	0.015	0.011	0.31	1.84	0.83	0.07	0.33
25.....	0.384	0.66	0.015	0.012	0.30	1.87	0.82	0.07	0.35
26.....	0.376	0.65	0.015	0.009	0.31	1.87	0.82	0.06	0.35
27.....	0.390	0.66	0.013	0.011	0.31	1.86	0.81	0.08	0.34
28.....	0.384	0.65	0.014	0.009	0.31	1.84	0.81	0.07	0.34
29.....	0.365	0.64	0.015	0.010	0.30	1.84	0.82	0.07	0.34
30.....	0.390	0.66	0.014	0.011	0.31	1.85	0.82	0.07	0.35
31.....	0.378	0.65	0.014	0.011	0.31	1.86	0.83	0.07	0.35
32.....	0.366	0.65	0.015	0.010	0.31	1.87	0.83	0.07	0.35
33.....	0.380	0.66	0.015	0.011	0.31	1.84	0.82	0.07	0.35
34.....	0.370	0.66	0.013	0.010	0.31	1.85	0.82	0.07	0.34
35.....	0.388	0.66	0.015	0.011	0.31	1.86	0.82	0.07	0.35
36.....	0.382	0.66	0.014	0.011	0.32	1.87	0.83	0.07	0.34
37.....	0.380	0.65	0.015	0.011	0.29	1.86	0.83	0.07	0.34
38.....	0.382	0.65	0.013	0.011	0.30	1.87	0.83	0.07	0.35
39.....	0.364	0.65	0.013	0.010	0.29	1.86	0.83	0.07	0.34
40.....	0.380	0.65	0.017	0.010	0.30	1.87	0.83	0.07	0.35
41.....	0.384	0.64	0.016	0.011	0.30	1.87	0.83	0.07	0.35
42.....	0.376	0.66	0.016	0.011	0.32	1.87	0.84	0.07	0.35
43.....	0.384	0.66	0.015	0.009	0.32	1.87	0.83	0.07	0.34
44.....	0.374	0.66	0.016	0.010	0.32	1.84	0.84	0.07	0.35
45.....	0.384	0.66	0.016	0.009	0.32	1.87	0.83	0.07	0.34
46.....	0.376	0.65	0.015	0.010	0.32	1.86	0.83	0.06	0.34
47.....	0.385	0.66	0.014	0.010	0.33	1.85	0.81	0.06	0.34
48.....	0.369	0.67	0.014	0.010	0.32	1.85	0.78	0.07	0.35
49.....	0.379	0.69	0.016	0.010	0.32	1.87	0.81	0.07	0.36
50.....	0.382	0.67	0.016	0.010	0.32	1.86	0.81	0.07	0.35
51.....	0.378	0.67	0.016	0.011	0.32	1.86	0.84	0.07	0.36
52.....	0.379	0.66	0.015	0.011	0.32	1.87	0.84	0.07	0.35
53.....	0.388	0.66	0.016	0.008	0.32	1.85	0.81	0.07	0.35
54.....	0.389	0.67	0.018	0.011	0.32	1.89	0.84	0.07	0.35
55.....	0.379	0.66	0.016	0.011	0.32	1.87	0.84	0.07	0.36
56.....	0.386	0.65	0.014	0.011	0.32	1.86	0.83	0.07	0.35
57.....	0.375	0.68	0.015	0.010	0.33	1.83	0.84	0.07	0.35
58.....	0.390	0.66	0.014	0.010	0.33	1.84	0.85	0.07	0.35
59.....	0.454	0.70	0.019	0.013	0.33	1.90	0.84	0.07	0.36
60.....	0.384	0.68	0.016	0.010	0.33	1.86	0.84	0.07	0.36
61.....	0.352	0.64	0.016	0.012	0.33	1.86	0.83	0.07	0.35
62*.....	0.494	0.74	0.026	0.014	0.35	1.91	0.90	0.07	0.36
Average of 51 positions in ingot body..	0.374	0.66	0.015	0.010	0.31	1.86	0.82	0.07	0.35

* Six inches above shrinkage cavity in hot top.

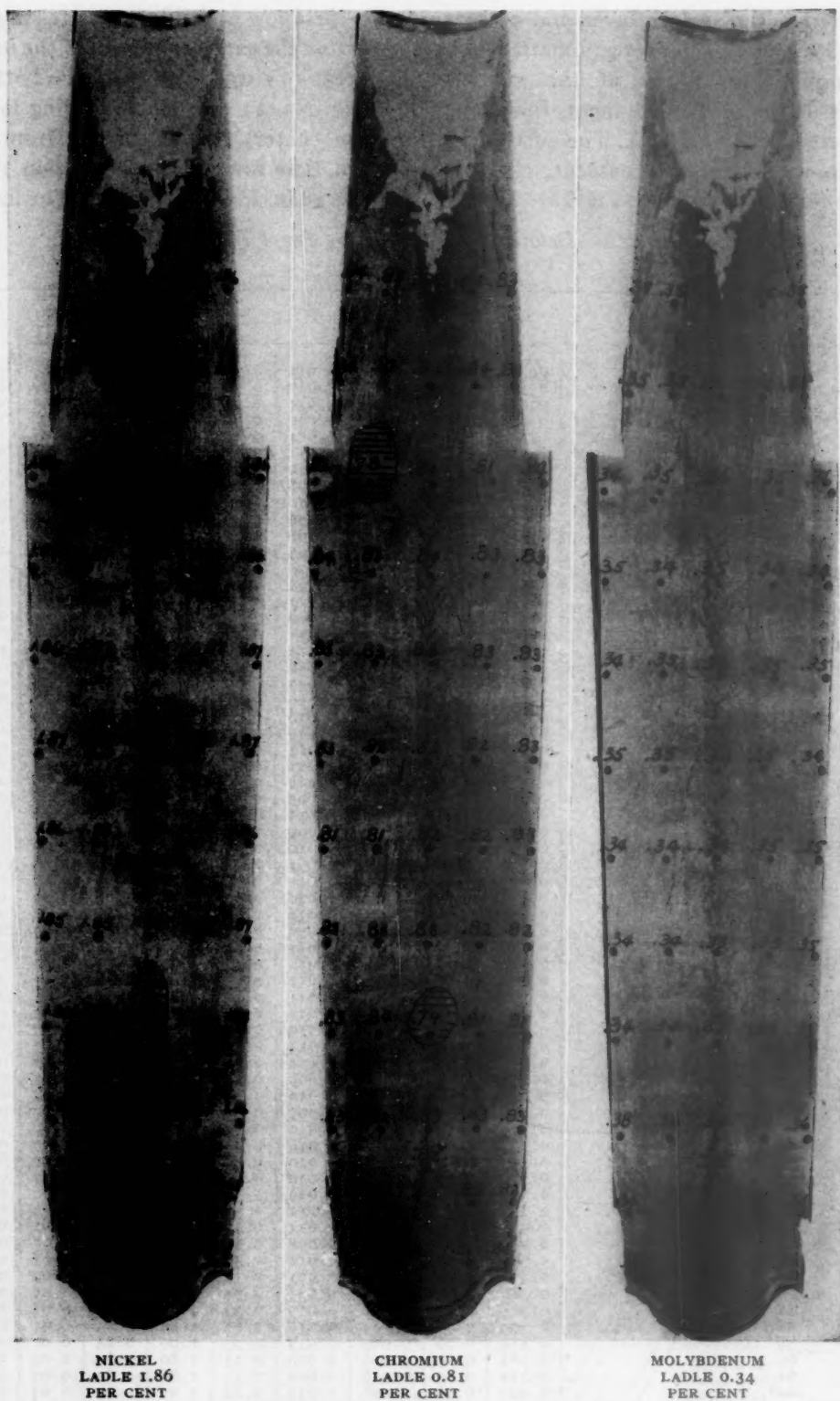


FIG. 6.—SEGREGATION OF ELEMENTS.

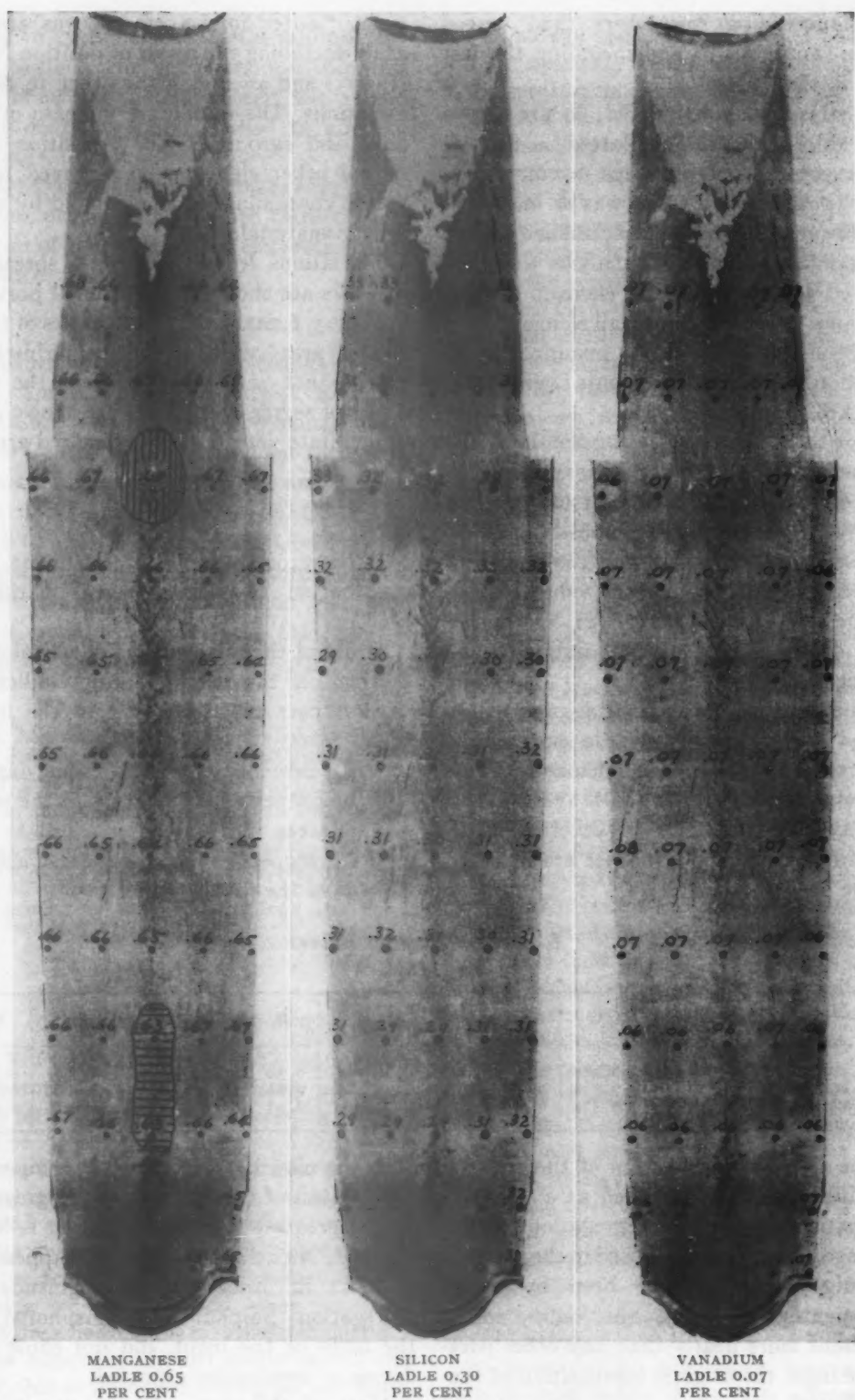


FIG. 7.—SEGREGATION OF ELEMENTS.

and succeeding rows were then spaced 12 in. apart up to and including the last row in the hot top.

Analyses of position No. 62 are shown in Table 1 but are not plotted on the sulphur print shown in Figs. 5, 6, and 7. This position (No. 62) was 6 in. above the lower terminus of the shrinkage cavity.

Standard methods of analysis were employed to determine the element concentrations. All positions and all elements were double checked. In a few instances, some positions and some elements were triple checked.

For the sake of evaluating the data, it is assumed that a variation, plus or minus, of 0.02 or 0.002 actual per cent (as the case may be), of calculated composition, is not excessive and will adequately cover analytical error. Assuming this, any values outside of the 0.04 or 0.004 actual per cent spread are considered as being indicative of segregation.

The calculated composition was established by averaging the 20 outer zone determinations of each element. These values, together with the ladle analyses and the average values of 51 determinations within the ingot body proper are listed in Table 2.

under "outer zone average" was arrived at by excluding the result of position No. 5 (Fig. 5) and averaging the other 19 determinations. The inordinate increase of sulphur and carbon in No. 5 position—but not of other elements—is believed to be due to contamination in the mold by some foreign material.

Deviations from the normal spread in analyses are shown in the shaded portions of Figs. 5, 6, and 7. The boundaries of these shaded areas were established arbitrarily and do not necessarily indicate the true limits of segregation. They are shown only to facilitate detection of segregated areas.

DISCUSSION

In view of the mass of the ingot, the distribution of elements is remarkably uniform.

Study of the quantitative chemical data plotted on the sulphur prints indicates, with respect to segregation in the ingot body, that:

1. All elements segregate to some degree.
2. Major segregation occurs in the same general areas.
3. All segregation in these areas apparently is of the inverse order.

TABLE 2.—Average Values
PER CENT

Sample Position	C	Mn	P	S	Si	Ni	Cr	V	Mo
Ladle.....	0.380	0.65	0.012	0.014	0.30	1.86	0.81	0.07	0.34
Outer zone, average.....	0.379	0.655	0.0103	0.0149	0.313	1.86	0.826	0.066	0.347
Ingot average (51 positions)...	0.374	0.66	0.010	0.015	0.31	1.86	0.82	0.07	0.35

The average composition of the rapidly solidified outer zone is used as a basis of comparison of element segregation within the ingot. This method is used in the present investigation—as it has been by other investigators³—because the outer zones represent more nearly than any other part of the ingot the original composition of the liquid steel.

The value for sulphur shown in Table 2

Of the nine alloying elements composing the analysis of this steel, carbon segregates to the greatest degree. Vanadium is least affected. Nickel and manganese appear to be next in order in the magnitude of segregation. Sulphur and phosphorus, in the body of the ingot, did not show the degree of segregation expected.

Most of the segregation occurs in the lower third of the ingot in the area re-

ferred to by Benedicks⁴ as the sedimentary cone region. The segregation within this area is of the inverse order, the region being definitely impoverished in alloying elements.

Slight enrichment of manganese and sulphur occurs in the upper third central portion of the ingot; other elements do not appear to be affected.

ACKNOWLEDGMENT

The writers express their thanks to Mr. E. C. Smith, Chief Metallurgist, Republic Steel Corporation, and to the management of the Central Alloy District for their help in making it possible to obtain and publish these data; likewise to Mr. E. O. Waltz, Chief Chemist, Canton Steel Division, for carrying out the chemical determinations.

The cooperation of the Linde Air Products Company in sectioning the ingot is gratefully acknowledged.

REFERENCES

1. H. Moore: Report on the Heterogeneity of Steel Ingots. Iron and Steel Inst. (1926) **113**, 158.
2. W. H. Hatfield: Report on the Heterogeneity of Steel Ingots. Iron and Steel Inst. (1926) **113**, 167.
3. Report on the Heterogeneity of Steel Ingots. Iron and Steel Inst. (1926) **113**, 77.
4. C. Benedicks: Second Report on the Heterogeneity of Steel Ingots. Iron and Steel Inst. (1928) **118**, 557.

DISCUSSION

(T. S. Washburn presiding)

C. R. FUNK,* Latrobe, Pa.—The authors are to be complimented for so clearly and concisely presenting some very interesting work. I have no particular comments to make except that we have done somewhat similar work on ingots ranging from 8400 up to 36,000 lb. We find a more marked increase of negative segregation in the cross section of ingot. Basing this on actual chemical determinations, not allowing for any chemical error, we have found, by averaging the carbon determinations at the edge, midway and center axis of the ingot, that at the center it is 8.5 per cent lower than at the edge and 7.4 per cent lower than

at the midway point. These figures, I believe, will be somewhat higher than those shown in the paper under discussion.

Our steel runs considerably higher in phosphorus and sulphur, as would be expected in acid steel, but the percentage of segregation on actual determinations, not allowing for any chemical error, has been fairly low. Again the segregation is negative. The phosphorus through the center axis of the ingot is 11 per cent lower than at the edge, and 9 per cent lower than midway; the sulphur through the center axis is 8 per cent lower than at the edge, and 4.5 per cent lower than midway. The sulphur shows somewhat higher segregation than that of the Republic ingot.

The figures given have been taken from a somewhat smaller ingot than was used by the authors but results have been similar on a comparative weight.

The ladle analysis of ingot was: 0.31 per cent C; 0.70 Mn; 0.28 Si; 0.033 P; 0.027 S; 0.75 Ni; 0.32 Mo; 0.05 Va. To express comparisons, a table similar to Table 2 is given here (Table 3).

We have studied numerous sulphur prints but do not rely on them too greatly to show chemical segregation. We enjoy using them to study ingot structure. For some reason, our sulphur prints have never shown the so-called sulphur streaks just beyond the center zone of the ingot. Actual chemical analysis has not shown any segregation in this area. Possibly our method of testing may have had something to do with this failure to show the streaks.

We have tried extreme pouring rates on a 36,000-lb. ingot, ranging from 5 to 12 min., in pouring the body of the ingot, but have found no appreciable differences in segregation. We do not like to fast-pour the larger ingots and believe the smaller ingots are less critical to pouring rate. We have had ingots of 8400 lb., 15,000 lb. and 36,000 lb. show the same percentage of segregation.

We have never checked the ingot for Cr, Ni, Mo, Si, and Va. These elements show such a small amount of segregation that we have never considered it worth while to study them. As a matter of record, possibly this should have been done.

We wonder if the mold shown here would show as good results or as little segregation if the phosphorus and sulphur were two to three times as high as in the ingot studied.

* American Locomotive Company.

M. METZGER,* Harrison, N. J.—I should like to ask some questions regarding the interpretation of the sulphur print. We did some work on ingots of comparable analysis, although much smaller size, more from the point of view of a microstudy than a chemical-analysis study. We found that the distribution of sulphur indicated in the sulphur print was pretty well checked by the microstudy, but that where a streak representing a V-segrega-

chill zone and the columnar zone. We did not, as I recall, observe more than very infrequently the threads of primary sulphides, as you call them.

J. A. ROSA.—The single spots I am not familiar with. I do not believe we have ever seen them.

M. METZGER.—They do not occur frequently, but we have observed them.

TABLE 3
PER CENT

Sample Position	C	Mn	P	S	Si ^a	Ni ^a	Cr ^a	Mo ^a	Va ^a
Ladle analysis.....	0.31	0.70	0.033	0.027	0.28	1.75	0.75	0.32	0.05
Outer zone, average.....	0.315	0.691	0.0367	0.0261					
Midway zone, average.....	0.311	0.686	0.036	0.0251					
Ingot, average.....	0.308	0.685	0.0356	0.0253					

^a Not checked in ingot.

tion on the sulphur print was associated with concentration of sulphides the steel immediately adjacent was fairly free of sulphide. If the drill sample were fairly large, the over-all sulphur content at the V-segregation might show no increase over that at the edge. We had intended to try to obtain small samples directly in the V-segregation, but never did so.

Also, in some sulphur prints we have seen, directly below the rim, in the chill zone, concentrations of sulphide that show as isolated dark spots. I do not see any in the sulphur print shown here, and I should like to ask whether the authors have observed this condition.

J. A. ROSA (author's reply).—As we state in the paper, and as Mr. Funk also has stated, we do not like to take a too literal interpretation of the sulphur print, particularly of the cast structure. As you know, the core of an ingot is the last part to freeze, and it is, consequently, porous to some degree, of either a macroscopic or submacroscopic nature. There is porosity there; and the very nature of the sulphur print itself—the mechanism of the sulphur printing, which introduces the gas into the cavities—will, of course, leave its mark on the sulphur print.

Did I answer your question, Mr. Metzger?

M. METZGER.—The spots of sulphide to which I referred were directly between the

J. A. ROSA.—The inverted threads leaning toward the central axis of the ingot we have found, but as to the single spots I do not recall ever seeing anything like that.

M. METZGER.—Toward the bottom of Fig. 4 there is a dark streak running vertically. Does this represent primarily voids, or what does it represent?

J. A. ROSA.—That is a zone of low density where we actually have a very coarsely porous condition. On the actual sulphur print on exhibition in our laboratory, that appears as a very dark stain—one big spot and several smaller spots and some streaks. But actually they are the result of a coarsely porous condition of steel rather than of sulphur.

R. S. BABCOCK,* Newark, N. J.—In connection with the cutting that was done on this ingot it is worth noting that the oxygen used in cutting was only 8 lb. per sq. in. at the blowpipe. This feature has been the result of some work which has been done in the past couple of years in which we have found that we can get better results in cutting by the use of lower oxygen pressures than have been heretofore used.

Also, as the cutting progressed we noticed that small segregations, or imperfections, showed up as bright spots in the reaction zone. They were of minute size and rapidly disap-

* Crucible Steel Company of America.

* The Linde Air Products Company.

peared as the cut progressed. We have in the past noticed larger segregations in cutting armor plate steel, which we had considered as segregations of nickel, or something of that kind. I wonder if anybody here could give us any more light on that subject?

S. W. POOLE.—I have some remarks on the use of the spectrograph in studying segregated areas, which I think may be of interest.

In 1939 F. G. Barker* did some rather interesting work with the spectrograph in determining the analysis of segregate spots in deep-etched forgings of nickel-chrome-molybdenum steel, which, on transverse deep etching and longitudinal etching, also, showed very definite segregated areas. When these segregated areas in the transverse deep-etch section were measured they were found to be of the order of about 2 mm. in diameter. He applied spectroscopic methods, using a carbon electrode with a point that would produce a crater on sparking of 1 mm. in diameter, which would arc well within the segregated area.

He analyzed a series of these segregated spots and obtained figures that are of considerable interest with respect to some of the segregations noted. His average segregate analysis on the basis of about five different spots, which he analyzed, showed 0.23 per cent Si, 0.64 Mn, 2.84 Ni, 0.72 Cr and 0.78 Mo.

For the unsegregated metal around these spots, he had an average of 23 analyses, many more analyses to be sure, but the unsegregated analyses showed 0.19 per cent Si as against 0.23 in the segregated areas; 0.43 Mn as against 0.64 in the segregated areas; 2.65 Ni as against 2.84 in the segregated areas; and 0.59 Cr as against 0.72 for the segregated areas. With molybdenum the unsegregated metal showed 0.44 per cent whereas the segregated spots went as high as 0.78; i.e., almost a twofold increase in molybdenum segregation in these areas.

The average chemical analysis of the forging checked very closely with the spectrographic analysis of the unsegregated metal, there being very little difference in results obtained. Carbon and sulphur also were present in the segregates but these elements cannot be determined by spectrographic methods.

* F. G. Barker: *Jnl. Iron and Steel Inst.* (1939) 139, 211-255.

It was thought that this material represented some interesting information with regard to spot-testing of segregated areas in alloy forgings, which could be readily applied by the use of spectroscopic methods of analysis.

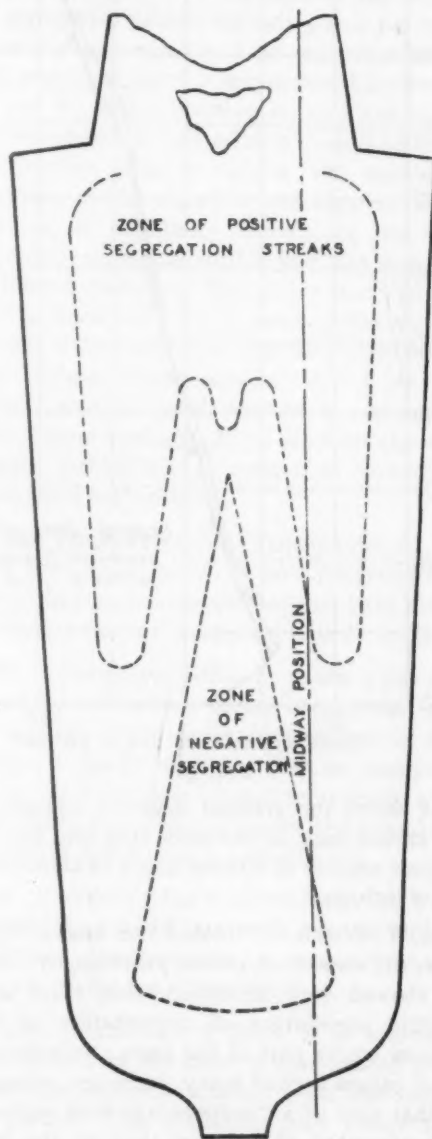


FIG. 8.

R. K. KULP,* Washington, Pa.—I wonder if Mr. Poole plans to do any work on cleanliness or on inclusion content in that large section? There has been some discussion on negative segregation in the bottom central section of the ingot. A number of papers and discussers over

* Jessop Steel Company.

past years have indicated that it is at that point that the highest content of such non-metals as silica and alumina may be found, and it is my belief that the part of the ingot

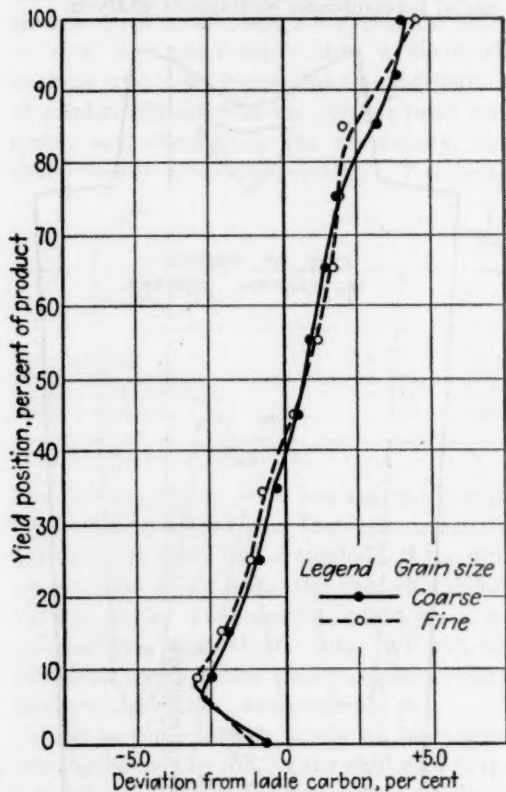


FIG. 9.

that shows the greatest negative segregation for carbon may be the point that also has the highest content of minute clouds of alumina or other inclusions.

S. W. POOLE.—I think I can answer that. Soler did some work several years ago by which he showed very accurately that there is a definite segregation of nonmetallics in the bottom center part of the ingot. Benedict, in some papers a good many years ago, referred to that area as a "sedimentary cone region," and advanced the theory that in the last remaining liquid area there is a formation of relatively pure small metallic dendrites, which can nucleate on nonmetallic particles and settle in this sedimentary cone area. This behavior, of course, would produce a segregation of nonmetallics in this area.

Probably we will conduct some further investigations along that line, as it is a very interesting subject.

M. TENENBAUM,* East Chicago, Ind.—The accompanying illustrations are not intended as a presentation of any novel segregation data. They do, however, illustrate an effective

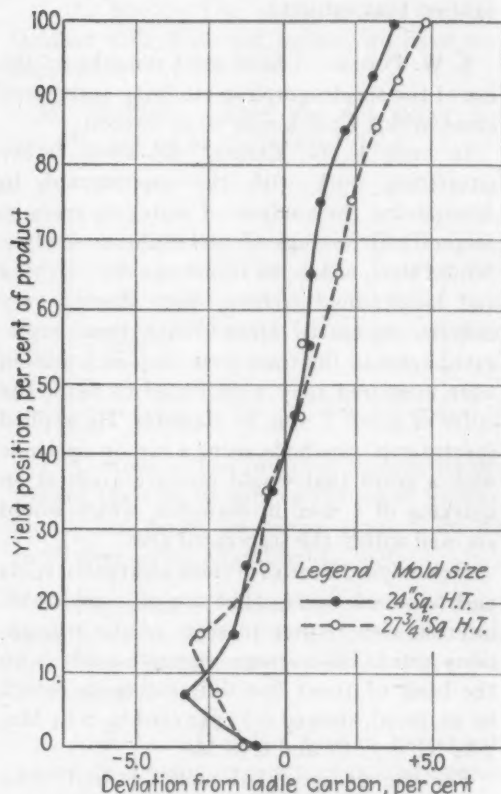


FIG. 10.

method for evaluating segregation in ingots. In this method curves are drawn representing the percentage of deviation from the ladle analysis at all levels along the height of the semifinished product of an ingot. In order to construct these curves, samples from the midway position in the top of each product cut on a selected ingot are analyzed. At some steel mills routine tests of this type are taken to assist in the identification and application of the product cuts. In such plants, this method of evaluating segregation would entail no additional testing. An evaluation of the segregation characteristics of a complete heat can thus be obtained by plotting such curves for two ingots, one from the beginning and one from the end of the pour.

* Inland Steel Company.

The position of the tests with respect to the original ingot can be seen in Fig. 8. From the approximate location of the segregation zones indicated very schematically, the general distribution of values that can be expected from midway-position samples becomes apparent. The analyses would range from positive segregation values near the top of the ingot to negative values in the lower half. If the bottom test is taken below the negative segregation zone, a decrease in the absolute percentage segregation would be expected. A similar decrease can occur near the top of the ingot. The position and degree of the variations depend to some extent on the number and location of the tests taken.

Figs. 9 and 10 illustrate the application of this method of evaluating carbon segregation in high-carbon spring steel. Fig. 9 compares the carbon segregation of fine-grained and coarse-grained steels of similar analysis. The curves represent the percentage deviation from ladle carbon at all product yield positions. Each point shown represents average values from corresponding positions in about 40 ingots. The full line represents the percentage segregation in coarse-grained steel while the broken line indicates the same information for the fine-grained steel. Very little separation of the curves can be noted, indicating that the extra deoxidation required to obtain fine-grained steel had little apparent effect on the segregation characteristics of the steel.

Another application is shown in Fig. 10. Here the segregation curves for two different mold sizes are compared. The full line represents the segregation in 24-in. square hot-top molds (ingot weight 9300 lb.) while the broken line indicates the segregation in steel of the same analysis poured into 27 $\frac{3}{4}$ -in. square hot-top molds (ingot weight 12,400 lb.). Little difference can be observed in the negative segregation zone. In the upper half of the ingot, however, there is definitely a greater tendency for positive segregation in the large-sized mold.

Further application of segregation curves can be made to observe the effect of variations in open-hearth practice on segregation. One example would be the study of the effect of ingot pouring temperature on segregation. While no data of this type have been prepared for this symposium, previous studies using these curves have clearly demonstrated that,

for any given mold size, temperature is the most important single variable influencing segregation.

J. R. ROSA.—One thing that stands out in Mr. Tenenbaum's curves is that the degree of segregation seldom exceeds 3 or 4 per cent, plus or minus, which is of the order of what we call analytical error. It is questionable whether it can be called positive or negative segregation when it is only of such a small order.

However, Fig. 8, giving the schematic diagram of the negative and positive segregations, is essentially correct, as we have learned from actual studies and also from the published literature. We believe that you will find a deviation from a norm, either plus or minus, depending upon the zone from which you obtain your samples. But I do not believe that the small amount of segregation Mr. Tenenbaum has shown is of an alarming nature. I think it is no more than normally is found in a cast product.

THE CHAIRMAN.—Mr. Tenenbaum, do you care to comment on Mr. Rosa's statement that the variations in analysis that you have shown are in the range of analytical error?

M. TENENBAUM.—Plus or minus 5 per cent on, say, 100 carbon spring steel would give a variation of 0.10 per cent carbon in that range. I hardly consider that an analytical error. Since the data plotted represented averages taken from some 40 ingots, this would also eliminate any tendency toward error.

R. F. VINES,* Long Island City, N. Y.—I wonder if we could have some discussion of the practical disadvantages of segregation with respect to the use of the steel?

THE CHAIRMAN.—I think it is somewhat self-evident in the case of heat-treated steels that there will be a variation in the heat-treated properties. This variation may result both from heat-treating variables and from deviations in the analysis of the product as compared with the average analysis represented by the ladle test. This variation in the analysis of the product from the average is present to a certain degree in all steel, and the effect that it may have on the final properties must be taken into consideration by the consumer.

* Ford Instrument Company.

An Investigation of the Technical Cohesive Strength of Metals*

By D. J. McADAM, JR.,† MEMBER A.I.M.E., AND R. W. MEBS‡

(New York Meeting, February 1943)

THE technical cohesive strength of a metal means, not the interatomic forces, but the technically estimated resistance to fracture. An example of such resistance to fracture is the so-called "true" breaking stress of a tension-test specimen, the breaking load divided by the sectional area at fracture. According to the prevalent view,⁸ the technical cohesive strength of a metal, in any particular state as regards prior mechanical treatment and heat-treatment, is determined by a limiting value of the algebraically greatest principal stress.§ In two previous papers by one of the authors,^{14,15} evidence was presented to indicate that the technical cohesive strength of a metal cannot be represented by a single stress value, but that it comprises an infinite number of values corresponding to the infinite number of possible combinations of the principal stresses. The *technical cohesive strength* thus comprises an infinite number of *technical cohesion limits*, each representing a specific stress combination at fracture. In the same papers, evidence

was presented that plastic extension causes a continuous increase in the technical cohesive strength. Such a variation is not in accordance with the prevalent view that plastic extension first increases, then decreases, the technical cohesive strength.⁸

In this paper, as in the previous papers,^{14,15} the *algebraically* greatest principal stress will be designated S_1 , the least principal stress will be designated S_3 , and the intermediate principal stress will be designated S_2 . The technical cohesion limit under polarsymmetric tension ($S_1 = S_2 = S_3$) will be termed the "disruptive stress," and the cohesion limit under unidirectional tension (S_2 and $S_3 = 0$) will be termed the "severing stress."^{14,15}

The yield strength of a metal, according to the generally accepted theory, may be represented by a constant value of the shearing-strain energy, and hence by a constant value of the sum of the squares of the three principal stress differences. In the second of the previous papers,¹⁵ however, evidence was presented that the limiting yield stress decreases with increase in the volume stress, the algebraic average of the three principal stresses.* This influence of the volume stress becomes prominent only in the field of triaxial tension.

In the two previous papers,^{14,15} diagrams were presented to show the variation of the technical cohesion limit, yield stress, and ultimate stress with the combination of principal stresses and with plastic extension. Those diagrams and the resultant

* This paper, although not a part of the Symposium on Cohesive Strength (beginning on p. 538) is so closely connected with it that it is placed here instead of in the preceding section of the book.

Manuscript received at the office of the Institute Dec. 1, 1942. Issued as T.P. 1615 in METALS TECHNOLOGY, August 1943.

† Chief of Section, Thermal Metallurgy, National Bureau of Standards, Washington, D. C.

‡ Associate Metallurgist, National Bureau of Standards.

§ References are on page 501.

§ Any stress system may be resolved into three principal stresses normal to three mutually perpendicular planes, known as "principal planes," on which there is no shearing stress. Tensile stresses are viewed as positive and compressive stresses as negative.

* Any stress system may be resolved into a polarsymmetric stress causing pure volume strain and a combination of pure shearing stresses, which cause no change of volume.

conclusions are derived from experimental data obtained by other investigators. They are based chiefly on results of tension tests of notched specimens by Ludwick and Scheu¹⁰ and by Kuntze,⁷ and partly on results of compression tests reported by Bridgman.¹⁻⁴ The diagrams are believed to be qualitatively correct, except possibly in some minor details. The available data, however, permitted the construction of only a few such diagrams, which are confined to several carbon steels. There was need for additional data to be used in deriving diagrams for other steels and for nonferrous metals. There was also need for further investigation of the influence of the depth, angle, and root radius of the notch on the tensile properties. Moreover, there was need for further study of the relative effects of the transverse radial stress and the stress concentration induced by notches. For these reasons, the authors have made an experimental investigation of the tensile properties of notched specimens of some ferrous and nonferrous metals, and have thus studied the influence of the combination of principal stresses and of plastic extension on the technical cohesion limit, ultimate stress, yield stress, and ductility. The results are presented in this paper.

Neither the technical cohesive strength, the yield strength,* nor the ultimate strength can be adequately represented by a single stress value; complete representation would require a three-dimensional diagram with values of the three principal stresses as coordinates.¹⁵ A three-dimensional diagram would also be required for complete representation of ductility. A simpler representation is possible, however, when two of the principal stresses are kept equal (with the intermediate principal stress equal either to S_2 or S_1). Such stress

combinations would be produced by subjecting a cylinder to various combinations of axial and uniform radial stress. The uniform radial stress may be resolved into two equal principal stresses, whose mutually perpendicular directions are rotatable around the specimen axis. In such a system, the stress is the same in any direction in a plane perpendicular to the axis. When two of the principal stresses are kept equal, the influence of the combination of principal stresses on the technical cohesion limit, yield stress, ultimate stress, and work-hardening capacity can be represented by a two-dimensional diagram, whose coordinates represent the axial and radial stresses. Two-dimensional diagrams were so used in the previous papers.^{14,16} In this paper, attention will be confined to stress combinations with two of the principal stresses equal, and with the axial stress algebraically greater than the radial stress. The axial stress, therefore, will be designated S_1 and the radial stress will be designated S_2 .

With an unnotched specimen, such a stress system cannot readily be obtained experimentally. When a notched cylindrical specimen is subjected to longitudinal tension, however, the minimum section is under radial tension. The ratio of S_2 to S_1 increases with the depth and sharpness of the notch, but cannot become actually equal to 1.0. The use of notched specimens in an investigation of the influence of the combination of principal stresses on the technical cohesion limit and yield stress has certain disadvantages due to the influence of the stress gradient induced by a notch. A stress gradient tends to make the estimated mean stress at any strength limit somewhat too low.^{14,16} Even slight plastic extension, however, greatly reduces the stress gradient. At maximum load or at fracture, under favorable conditions, the original stress gradient is practically removed and only a deformation gradient remains. Under such conditions, the mean

* In this paper, a distinction is made between the term "yield strength" and the term "yield stress," which is used to indicate a value corresponding to a specific stress combination. A similar distinction is made between "ultimate strength" and "ultimate stress."

stress is a satisfactory criterion of the ultimate stress and breaking stress. By suitable tension tests of notched specimens, it is thus possible to study the influence of the combination of principal stresses on the technical cohesion limit. Results so obtained are presented in this paper. The diagrams are believed to be qualitatively, and not far from quantitatively, correct.

In the following study, attention is given first to the influence of the notch angle, notch depth, and root radius on the strength and ductility. From the diagrams representing these relations other diagrams have been derived to represent the influence of the combination of principal stresses on the *technical cohesion limit* and the influence of plastic extension on the *technical cohesive strength*. The metals studied can be classified in two groups in accordance with the forms of some of the curves.

MATERIALS AND METHODS

Materials and Specimens

The materials included in this investigation were oxygen-free copper, Monel metal, 13-2 chromium-nickel steel, a 0.2 per cent carbon steel (S.A.E. 1020), and a 0.04 per cent carbon steel.

The oxygen-free high-purity copper was supplied by the Scomet Engineering Co. through the cooperation of Mr. Sidney Rolle, assistant manager. It had been given a reduction of 75 per cent by cold rolling without intermediate anneal. Some of this material was tested in that condition, and some was annealed at 800°F. Some of the annealed material was given a further reduction in area of about 23 per cent, by tensile extension. Hereafter the three hardness grades of copper will be termed "annealed," "half-hard" and "hard."

The Monel metal was supplied by the International Nickel Co. through the cooperation of Mr. A. J. Wadhams, director of research. It had been given a reduction of 40 per cent by cold drawing without

intermediate anneal. Some of this material was tested in that condition; some was annealed at 1400°F. to place it in its softest condition.

The 13-2 Cr-Ni steel was obtained from the Carpenter Steel Co. through the cooperation of Mr. G. V. Luerssen. It was in its softest condition, which is obtained by heating to 1240°F. and cooling slowly in the furnace. This material was tested as received.

The 0.2 per cent carbon steel, which was obtained from the laboratory stock room, was originally in the hot-rolled condition. Before test, however, it was heated to 1625°F., quenched in water, and tempered at 900°F.

The 0.04 per cent carbon steel, purchased in the open market, had been cold-drawn to a reduction of 12 per cent without intermediate anneal; in this laboratory it was cold-drawn further to a total reduction of 33 per cent. Before test, it was heated to 1750°F. and cooled in the furnace.

All the metals were in the form of round rods. A description of the metals is given in Table 1 and details of the heat-treatments and mechanical treatments applied in the laboratory in Table 2. (See p. 502.)

Most of the notched specimens were approximately 6 in. long; those having deep notches and large angles were necessarily somewhat longer. The ends of all specimens were threaded to $\frac{3}{4}$ -in. diameter. Between the threaded ends, each specimen was machined to a selected uniform diameter and a circumferential vee notch of suitable angle, depth, and root radius was made at the mid section. The notch radius was carefully machined so that the conical sides of the notch were tangent to the arc at the root. Care was taken also to avoid heating, bending, or appreciable cold-working during the machining.

Before testing, each specimen was carefully calibrated as follows: The maximum diameter was measured by micrometer

calipers; the diameter of the minimum section, at positions 90° apart circumferentially, was determined by means of a measuring microscope. The root radius

When using the pendulum-hydraulic machine, a Baldwin-Southward stress-strain recorder was employed. With this apparatus it was possible to record auto-

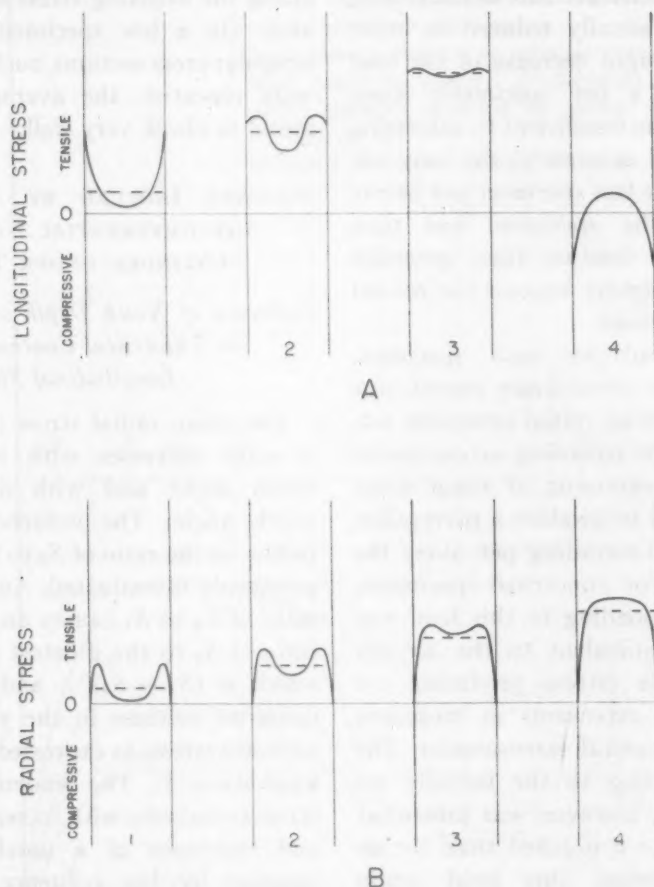


FIG. 1.—VARIOUS DISTRIBUTIONS OF LONGITUDINAL AND RADIAL STRESS ACROSS THE MINIMUM SECTION OF A NOTCHED SPECIMEN.

was measured by the use of a graduated set of wires of various diameters, and the notch angle was measured on a magnified photograph of the notched specimen.

Part of this material was also machined to the form of unnotched specimens.

Apparatus

A pendulum-hydraulic testing machine of 50,000 lb. capacity was used for most of these tests. In a few early tests, a Riehle beam-and-poise screw-type machine was used. The specimens were held in grips with spherical seats.

matically on a chart, during a test, the variations of the load with extension even to fracture. The yield load, maximum load, and breaking load could be determined from the chart, and the values of maximum load and breaking load could be compared with the values read directly from the dial gauge of the testing machine.

In the few experiments made with the beam-and-poise type of machine, no load-extension record was obtained; the maximum load and breaking load were obtained by reading the scale, keeping the beam balanced throughout the test.

Method of Test

The specimens were loaded at a slow uniform rate up to the maximum load, after which the extension rate of the testing machine was gradually reduced in order to prevent too rapid decrease of the load to fracture. In a few specimens, when this procedure was insufficient to determine the fracture load accurately, the load was removed from the test specimen just before fracture, and the specimen was then reloaded slowly; fracture then generally occurred at or slightly beyond the second maximum of the load.

The yield load for each specimen, selected from the stress-strain record, was the load at which an initial extension was indicated. For the recording extensometer used, an initial extension of about 0.002 in. was necessary to produce a perceptible movement of the recording pen along the extension axis. For unnotched specimens, the stress corresponding to this load was approximately equivalent to the 0.1 per cent proof stress (stress producing 0.1 per cent plastic extension) as measured with a sensitive optical extensometer. The strain corresponding to the initially recorded extension, however, was somewhat greater locally for a notched than for an unnotched specimen; this local strain increased with decreasing notch angle, and was not directly determinable. An estimate of this value of strain for the notched specimens can be obtained, however, by extrapolating the yield-stress values obtained on the notched specimens to the condition of uniaxial stress (by the method indicated on page 497), and selecting the strain corresponding to this extrapolated stress value from the ordinary stress-strain curve of an unnotched specimen. For the metals tested, the stress values so obtained correspond roughly to a strain of 3 per cent.

After test, the diameter at fracture was obtained with a measuring microscope for

six positions spaced uniformly around the circumference of the specimen. An average of these values was used in computing the fracture area, which was used in calculating the breaking stress and reduction of area. On a few specimens having quite irregular cross sections, such measurements were repeated; the average values were found to check very well.

STRESSES INDUCED BY A TRANSVERSE CIRCUMFERENTIAL NOTCH IN A CYLINDER UNDER TENSION

Influence of Notch Depth and Root Radius on Theoretical Concentration of Longitudinal Stress

The mean radial stress (S_2) induced by a notch increases with increase in the notch depth and with decrease in the notch angle. The influence of the root radius on the ratio of S_2 to S_1 has not been previously investigated. An increase in the ratio of S_2 to S_1 causes an increase in the ratio of S_1 to the greatest shearing stress, which is $(S_1 - S_2)/2$, and thus tends to cause an increase in the yield stress and ultimate stress, as expressed in terms of the axial stress S_1 . The tendency of the yield stress to increase with increase in the depth and sharpness of a notch, however, is opposed by the influence of the other important effect of a notch, stress concentration. The distribution of longitudinal stress across the minimum section of a notched specimen is illustrated by diagram A-1 of Fig. 1. The stress concentration at the circumference causes the mean stress at yield to be lower than if the stress were uniform. With increase in the plastic deformation, however, the stress concentration decreases as illustrated by diagrams A-2 and A-3 of the same figure. The original stress gradient thus is practically removed and only a deformation gradient remains. The contour of the deformation gradient is qualitatively similar to that of the original stress gradient (diagram A-1).

Consequently, removal of the load after the stress distribution has become nearly uniform (as in diagram A-3) would cause

of a ductile metal, much (if not all) of the initial stress concentration has been eliminated. Nevertheless, even a small fraction

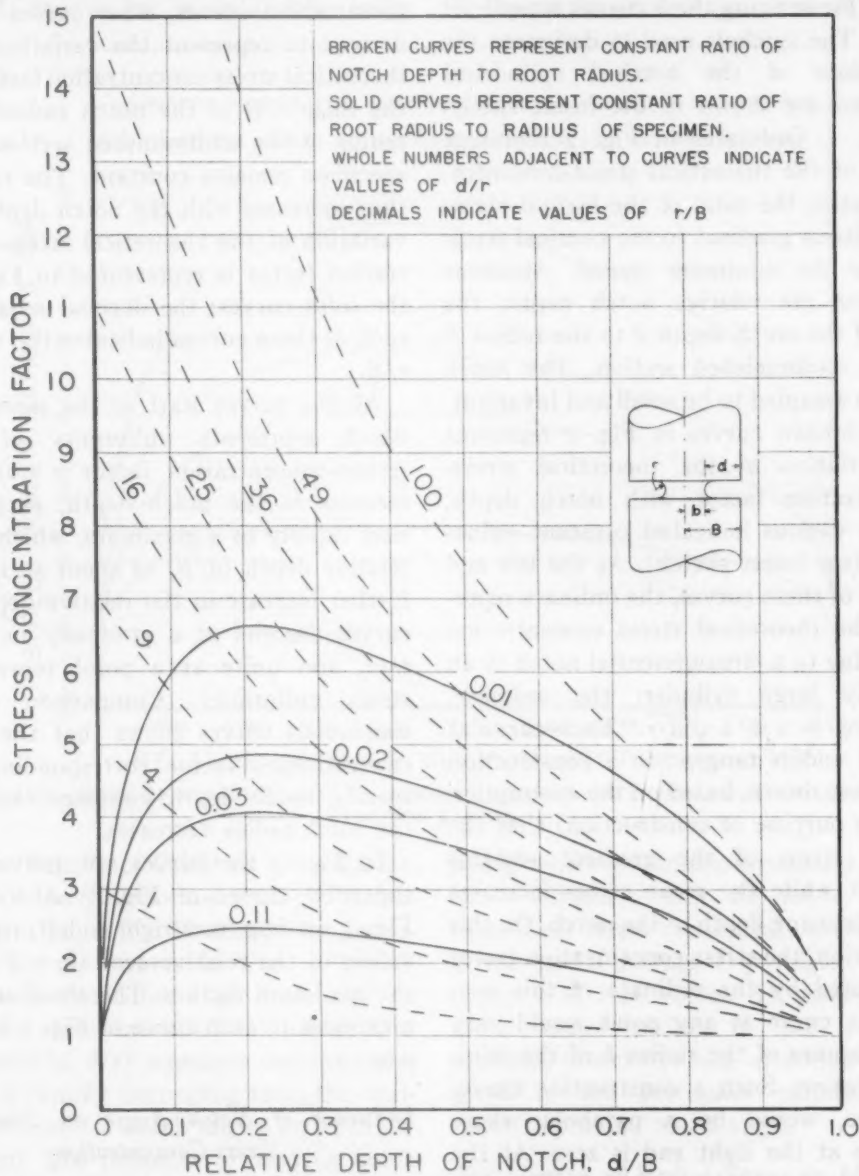


FIG. 2.—INFLUENCE OF NOTCH DEPTH AND ROOT RADIUS ON THEORETICAL STRESS CONCENTRATION FACTOR.

the internal stress distribution illustrated by diagram A-4.*

At the ultimate stress and at fracture

* In the diagrams of Fig. 1, distances from the center line represent squares of the radial distances from the specimen axis. This method of plotting simplifies the location of lines representing mean stresses.

of an initially high stress concentration might have a considerable effect on the mean ultimate stress and breaking stress. In considering the influence of notches on the various indices of strength, therefore, careful consideration must be given to stress concentration.

The variation of the theoretical stress concentration with notch depth and root radius is illustrated in Fig. 2. The procedure for deriving these curves is outlined below. The symbols used to designate the dimensions of the notched cylindrical specimen are shown in the insert sketch of Fig. 2. Ordinates in Fig. 2 represent values of the theoretical stress-concentration factor, the ratio of the highest stress in the stress gradient to the nominal stress (not to the minimum stress). Abscissas represent the relative notch depth, the ratio of the notch depth d to the radius B of the undiminished section. The notch angle is assumed to be small and invariant.

The broken curves in Fig. 2 represent the variation of the theoretical stress-concentration factor with notch depth, for the various indicated constant values of d/r (see insert sketch). At the left end of each of these curves, the ordinate represents the theoretical stress concentration factor due to a circumferential notch in an infinitely large cylinder; the ordinate, therefore, is $1 + 2\sqrt{d/r}$.⁵ Each curve at the left end is tangent to a construction curve, not shown, based on the assumption (for the purpose of construction) that the highest stress of the gradient remains constant while the mean stress increases with increasing depth of the notch. On this assumption, the stress-concentration factor represented by the ordinate of this construction curve at any point would vary as the square of the radius b of the minimum section. Such a construction curve, therefore, would be a parabola whose ordinate at the right end is zero. At the right end each broken curve in Fig. 2 is tangent to another construction curve (not shown) based on an investigation by Neuber^{16,17} of the theoretical stress concentration induced by hyperbolic grooves. The Neuber curves are qualitatively similar to the descending portions of the solid curves in Fig. 2. Each broken curve, drawn tangent to the two construction curves at

the ends, can be considered not far from quantitatively correct.

From the broken curves and the Neuber construction curves, other curves may be derived to represent the variation of the theoretical stress-concentration factor when the ratio r/B of the notch radius to the radius of the undiminished section of the specimen remains constant. The ratio d/r thus increases with the notch depth. This variation of the theoretical stress-concentration factor is represented in Fig. 2 by the solid curves; the decimal adjacent to each of these curves indicates the value of r/B .

All the curves start at the same point, which represents uniformity of stress (stress-concentration factor = 1.0). With increase in the notch depth, each curve rises rapidly to a maximum, which is at a relative depth (d/B) of about 0.22.* With further increase in the relative depth, the curves descend at a gradually increasing rate, and unite at a point representing stress uniformity. Comparison of the continuous curves shows that the stress-concentration factor corresponding to a specific notch depth increases rapidly as the notch radius decreases.

In Fig. 3 the curves are derived from the solid curves of Fig. 2. Abscissas in Fig. 3, reading from right to left, represent values of the relative area ($k = b^2/B^2$) of the minimum section. The abscissa of the maximum in each curve of Fig. 3 is about 0.61.

Influence of Notch Angle on Theoretical Stress Concentration

The influence of the notch angle on the theoretical stress concentration due to a notch at the edge of an otherwise infinite plate has been studied mathematically by Inglis.⁶ He found that the theoretical stress-concentration factor is influenced only slightly by an increase of the notch angle

* This value applies only to a notched cylindrical specimen under tension.

from zero to about 60° . A similar conclusion was reached by Griffith⁵ with regard to the stress concentration induced by a circumferential groove in a relatively large

cylinder is infinitely large, they show qualitatively the influence of the angle for notches of any constant relative depth. By the combination of the curves in Figs. 3

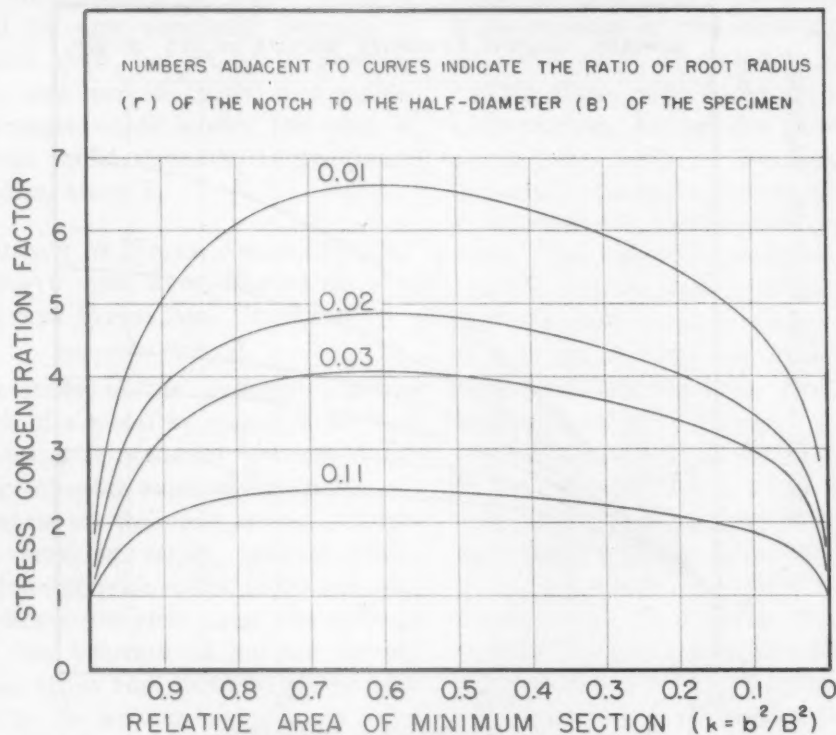


FIG. 3.—INFLUENCE OF RELATIVE AREA AT MINIMUM SECTION ON THEORETICAL STRESS CONCENTRATION FACTOR.

cylinder. Results of Griffith's investigation by use of the "membrane analogy," tabulated in a paper by Thomas,¹⁸ are represented by the curves in Fig. 4.* With decrease in the notch angle from 180° to zero, the stress-concentration factor (for any value of d/r) increases continuously, but at a rapidly decreasing rate; the variation is small for notch angles between 60° and zero. The influence of varying notch angle thus is qualitatively very different from the influence of varying notch depth (solid curves of Figs. 2 and 3).

Although the curves in Fig. 4 represent the influence of the notch angle when the

and 4, moreover, an approximately quantitative estimate may be made of the theoretical stress concentration factor for a vee notch having any angle, relative depth, and root radius. In discussion of stress concentration in the following sections, however, chief attention will be given to the qualitative variation with notch depth and notch angle.

Distribution of Radial Stress in Minimum Cross Section of Notched Cylindrical Specimen

In considering the distribution of the radial tensile stress throughout the minimum section, attention will be given first to the theoretical stress distribution, the distribution existing prior to any plastic deformation induced by the longitudinal

* These curves have been drawn so as to obtain a consistent series based on all the experimental points (not shown here). The curve for d/r value of 2 has been added by interpolation.

tension. The radial stress is zero at the boundary of the minimum section, but increases rapidly from the boundary inward. When the relative depth of the

The effect of plastic deformation on the distribution of radial stress probably would be qualitatively similar to the effect of an increase in the initial relative notch depth.

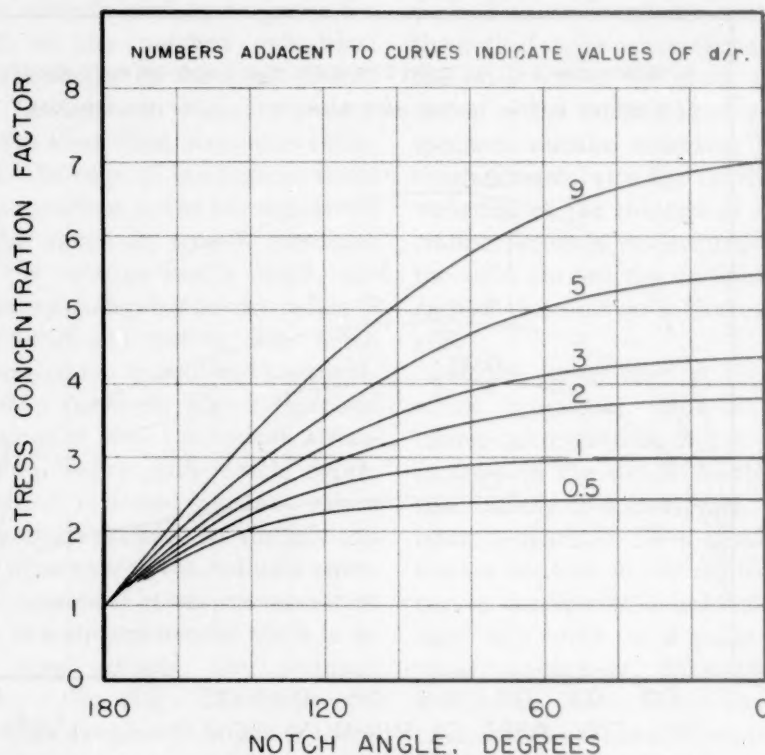


FIG. 4.—INFLUENCE OF NOTCH ANGLE AND ROOT RADIUS ON THEORETICAL STRESS CONCENTRATION FACTOR.

notch is small, the theoretical radial stress reaches a maximum close to the section boundary and decreases rapidly from this point inward, as illustrated in diagram B-1 of Fig. 1. The greater the relative depth, however, the less is the distance between any two diametrically opposite points of maximum stress, and the less is the decrease of radial stress from the circular locus of maxima to the center of the cross section (diagrams B-2 and B-3). With a relatively deep notch, the maximum radial stress theoretically would be at or near the axis, and would not vary greatly throughout most of the cross section (diagram B-4). Whether the notch were shallow or deep, however, the radial stress would rise rapidly from zero at the boundary.

The change of the distribution would thus be represented by a sequence of diagrams similar to those in Fig. 1-B. At the boundary of the minimum section the radial stress would remain zero.

Longitudinal Distribution of Radial Stress

In studying the strength and ductility of notched specimens, attention should be given to the longitudinal gradient, especially that of the radial stress. In the minimum section the radial stress is at a maximum. The gradient tends to increase with decrease in the notch angle. For a constant root radius, the gradient also tends to increase with the notch depth (at least to a certain depth, which depends on the root radius). Plastic extension of a

notched specimen would tend to decrease the longitudinal gradient. This tendency, however, would be opposed by the increase in the notch depth associated with the plastic deformation; it would also be opposed by any associated decrease in the notch angle, but would be accentuated by any increase in the root radius. Such changes would modify the ratio of the mean radial stress S_3 to the mean longitudinal stress S_1 .

INFLUENCE OF NOTCH ANGLE, NOTCH DEPTH, AND ROOT RADIUS ON YIELD STRESS AND ULTIMATE STRESS

In a study of the technical cohesive strength of a metal by means of notched specimens, it is necessary to consider the influence of notch angle, notch depth, and root radius on the yield stress, ultimate stress, breaking stress, and ductility. Attention will be given first to the influence of notches on the yield stress and ultimate stress; the influence of notches on the breaking stress and ductility will be considered in the sections beginning on pages 13 and 20. The specimens used had notch angles (ω) ranging from 180° (unnotched specimen) to very small angles, in some instances less than 20° . The values of k (see p. 7) ranged from 1.0 (unnotched specimen) to 0.09. The root radius r for most of the specimens was about 0.01 in.; for some specimens, however, the root radius was much smaller, ranging from 0.001 to 0.004 inch.

Influence of Notch Angle on Yield Stress and Ultimate Stress

The influence of the notch angle on the yield stress and ultimate stress* is represented by two families of curves in each of Figs. 6, 8, 10, 12, 14, 16, 18, 20, and 22.

* The plotted values of ultimate stress are based, as usual, on the initial area of cross section, not on the area at maximum load. The values of breaking stress are based on the cross-sectional area measured after fracture.

Each of these curves shows the influence of varying notch angle, with the indicated approximately constant values of k and r .

The effect of varying the notch angle on either the yield stress or the ultimate stress is the resultant of two variables: (a) The ratio of S_3 to S_1 , which will be termed the "radial stress ratio;" and (b) the stress concentration. An increase in the radial-stress ratio tends to increase, and an increase in the stress concentration tends to decrease the yield stress and ultimate stress. The radial-stress ratio tends to increase with decrease in the notch angle, and thus tends to cause a continuous rise of a curve of variation of the ultimate stress with the notch angle. The theoretical stress-concentration factor, however, also increases continuously with decrease in the notch angle (Fig. 4). Any stress concentration remaining at yield or at maximum load, therefore, would tend to depress the corresponding curve of ultimate stress. Consequently, in studying the curves of variation of these properties with the notch angle, attention must be given not only to the influence of the varying radial-stress ratio, but also to a possible depressing influence of stress concentration.

Some of the yield-stress values in Figs. 6, 8, 10, 12, 14, 16, 18, and 20 show considerable scatter, especially those obtained with shallow notches (large values of k). The yield-stress values obtained with deep notches, and nearly all the values of the ultimate stress, show very little scatter. For an example of concordance of ultimate-stress values, reference may be made to the results obtained with cold-drawn Monel metal specimens having notches with k values of about 0.25 (Fig. 12); nearly all these experiments were made in triplicate. Reference may also be made to the results obtained with copper specimens having deep notches (Figs. 6 and 10). Such concordant results indicate that there was no important eccentricity of the tensile loading.

All the curves of yield stress and ultimate stress have an initial rise. Some of the curves representing shallow notches, however, become nearly horizontal as the notch angle is decreased below about 120° , and a few eventually turn downward. With these exceptions, all the curves rise continuously at a decreasing rate, because of the dominant influence of the increasing radial-stress ratio. Generally, the deeper the notch and the smaller the root radius, the higher is the course of the curve. The curvature is less for radii of 0.004 and 0.001 than for radii of 0.01 in., but a linear relationship was not found for any notch depth or radius. The results, therefore, do not support the validity of Kuntze's method of determining the disruptive stress by linear extrapolation.^{14,15}

An interruption to the rise of a curve of ultimate stress or yield stress must be attributed to the depressing influence of increasing stress concentration. To this cause is due final descent of some of the curves for shallow notches. An uninterrupted rise of a curve of ultimate stress, however, does not necessarily mean that stress concentration has not affected the course of the curve. Nevertheless, evidence yet to be presented indicates that stress concentration is not sufficient to have important influence on the curves representing deep notches ($k = 0.18$ or less).

Influence of Notch Depth on Ultimate Stress

The influence of notch depth on the ultimate stress, for six of the metals already considered, is shown in Figs. 23, 24, and 25. Abscissas, reading from right to left, represent values of k and ordinates represent values of the ultimate stress. Each curve shows the effect of varying k , with approximately constant notch angle ω and root radius r .

For each metal represented in Figs. 23, 24, and 25, there are two sets of curves. One of these comprises the solid curves;

the other the broken curves and the portions of the solid curves to the right of their junction with the broken curves. At their right ends, the two sets of curves coincide. The curves consisting entirely of solid lines represent the actual variations of the ultimate stress; the broken curves show qualitatively the way the ultimate stress would vary if stress concentration at maximum load were absent.* The vertical distance between corresponding broken and solid curves at any abscissa, therefore, represents the depressing influence of stress concentration.

In each set of solid curves, there is a crowding together in the regions representing shallow notches. The crowding is greatest for the curves representing small notch angles; these curves almost coincide at values of k greater than about 65 per cent.† The curves representing notch angles greater than about 120° show no crowding other than the normal crowding near their origin at the left. (At very small notch depths, however, these curves possibly would join or even cross the curves representing small notch angles.) This distribution of the crowding of the curves suggests that the crowding is due to the depressing influence of stress concentration. In the absence of this influence, the entire set of curves probably would be a logical amplification of the uncrowded portion, and thus would have the form indicated by the broken curves.

With increase in the notch depth from zero, the depressing influence of stress concentration evidently first increases rapidly to a maximum, and then decreases. This variation is qualitatively similar to the variation of the theoretical stress

* Each family of broken curves was constructed by prolonging the solid curves from the right end toward their common origin, starting with one of the best established of the lower curves.

† The crowding of these curves corresponds with the nearly horizontal course of the curves representing shallow notches in diagrams of the previously described type (Figs. 6, 10, 12, 14, 16, and 18).

concentration (Fig. 3). The influence of the notch angle on the depressing effect is also qualitatively similar to the influence of the notch angle on theoretical stress concentration (Fig. 4). The depressing influence is most prominent in the curves for work-hardened metals or metals that have a hard microconstituent. In the diagrams for cold-rolled copper (Fig. 23A), cold-drawn Monel metal (Fig. 24A), 13-2 chromium-nickel steel (Fig. 25A), and heat-treated 0.2 per cent carbon steel (Fig. 25B), the depressing influence is great enough to change not only the position but also the form of some of the curves throughout the abscissa range representing shallow notches. In the diagrams representing annealed copper (Fig. 23B) and annealed Monel metal (Fig. 24B), however, this influence is not sufficient to change the form of the curves, but merely causes crowding and decreased curvature in the portion representing shallow notches. The notch depth at which the depressing influence vanishes, moreover, is much less for annealed copper and annealed Monel metal than for the other four metals.

For notch depths greater than a certain value, which varies with the notch angle, the influence of stress concentration evidently is negligible (provided that the ductility is sufficient to permit the load to reach a true maximum). For any of the metals considered, stress concentration at maximum load evidently is slight when k is less than 25 per cent, and is negligible when k is less than about 15 per cent. For the annealed copper and annealed Monel metal, stress concentration evidently is negligible when k is less than 25 per cent; that is, when the radial depth of the notch is greater than 0.5.

Three-dimensional Diagrams Representing Influence of Both Notch Angle and Notch Depth on Ultimate Stress

Each family of curves in Figs. 23, 24, and 25 may be pictured as a side view

of a three-dimensional diagram representing the influence of notch angle and notch depth on the ultimate stress. The front view of the three-dimensional diagram is the corresponding family of curves in a diagram of the previously discussed type, in which abscissas represent notch angles (Figs. 6, 10, 12, 14, 16 or 18). By correlating the two views, it is possible to obtain by extrapolation a curve representing the influence of varying notch depth with notch-angle zero. Such a relationship, in absence of stress concentration, would be represented by the dotted curves in Figs. 23, 24, and 25. Each of these curves should be viewed as the uppermost of a family of curves representing results obtained with a root radius of the indicated value, either 0.01, 0.004, or 0.001 in. The right end of each of these dotted curves is the highest point on the surface in a three-dimensional diagram. Its ordinate represents the (imaginary) ultimate stress for zero values of both ω and k , and for the indicated value of r . For r values of 0.01, 0.004, and 0.001 in., the uppermost points in the three-dimensional diagrams are designated E , E' , and E'' , respectively.

Corresponding curves could be drawn in the front views of the three-dimensional diagrams (Figs. 6, 10, 12, 14, 16 and 18) to represent the influence of varying notch angle, with a zero value of k . Such curves have not been drawn, but the uppermost points (E , E' or E'') of the three-dimensional diagrams have been indicated.

The form of the surface in a three-dimensional diagram evidently disproves the general validity of the linear extrapolation used by Kuntze to determine the disruptive stress.^{14,15} An approximately correct value of the disruptive stress might be obtained by linear extrapolation, when the notch angle is about 60° and the root radius about 0.001 in. (Figs. 23, 24, and 25). The method of linear extrapolation, however, evidently is not generally valid for the variation of either ω or k . A correct value of the ultimate

stress corresponding to zero values of ω and k can be obtained only by the indicated curvilinear extrapolation.

According to Kuntze's views, based on his experiments, the approach of ω and k to zero causes the ductility to approach zero and the ultimate stress to approach the breaking stress. The ultimate stress corresponding to zero values of ω and k , consequently, would be identical with the disruptive stress. This view, however, takes no account of the influence of the root radius. As shown in Figs. 23, 24, and 25, the ultimate-stress value obtained by the curvilinear extrapolation increases as the root radius is decreased from 0.01 to 0.001 in. With further decrease in r , however, the extrapolated value of the ultimate stress probably would increase very little. Evidence for this statement will appear in the next two sections, in the study of the influence of notches on the breaking stress and ductility.

The disruptive stress cannot be less than the highest extrapolated value obtained for the ultimate stress, the value represented in Figs. 23, 24, and 25, by the ordinate of either E , E' , or E'' . That the disruptive stress is little, if any, greater than this value is indicated by evidence yet to be studied. Probable approximate values of the disruptive stress are indicated by the points designated T_1 .

INFLUENCE OF NOTCHES ON BREAKING STRESS AND DUCTILITY OF COPPER AND MONEL METAL

In each of Figs. 6, 8, 10, 12, 14, 16, 18, 20, and 22, there is a family of curves representing the influence of the notch angle on the breaking stress, which is the load at fracture divided by the corresponding sectional area measured after fracture. Facing each of these figures except the last, on the opposite page, is a corresponding figure representing the relation between

breaking stress and ductility.* By studying each of these pairs of diagrams it is possible to obtain a complete picture of the influence of notches on the breaking stress and ductility. Attention will be given first to the influence of notches on the breaking stress of copper and Monel metal.

Influence of Notch Angle, Notch Depth, and Root Radius on Breaking Stress of Copper and Monel Metal

In studying the influence of notch angle, notch depth, and root radius on the breaking stress, it is most convenient to represent directly the relation between the breaking stress and the notch angle. For copper, such a representation is given in a family of curves in each of Figs. 6, 8, and 10. Each curve in these three diagrams shows the influence of varying the notch angle, with the notch depth and root radius held at the indicated approximately constant values. Moreover, a comparison of the curves in a diagram gives information about the influence of the notch depth and root radius. The three diagrams of this type (Figs. 6, 8, and 10) show the influence of notches on copper in three different degrees of hardness, due to different degrees of prior plastic deformation.

None of the curves of breaking stress (Figs. 6, 8, and 10) rises continuously with decrease in the notch angle. In this respect, the curves representing deep notches differ from the corresponding curves of ultimate stress. The variation of the breaking stress with the notch angle is the resultant of three factors dependent on the notch angle. Two of these factors, radial-stress ratio and stress concentration, are the same that influence the course of a curve of yield stress or ultimate stress (Figs. 6, 8, and 10); the third factor is the continuous decrease of the total deformation at frac-

* The relation between the abscissa scale in these figures and ductility is explained on page 488.

ture, shown in the diagrams of ductility in the same figures. The initial rise in a curve of breaking stress is due to dominant influence of the increasing radial-stress ratio; the eventual descent of the curve is due to one or both of the other two factors. The descent of some of the curves representing shallow notches (Fig. 6) may be due largely to the depressing influence of increasing stress concentration. Stress concentration, however, has little influence on the curves representing deep notches ($k < 25$ per cent). The descent of the curves representing deep notches, and even of some of the curves representing shallow notches (Fig. 10), is due to eventual dominance of the third factor, the continuous decrease in ductility. As shown in previous papers,^{14,15} plastic extension causes continuous increase in the technical cohesive strength, and hence *tends* to cause increase in any specific technical cohesion limit. Consequently, the continuous *decrease* in total plastic deformation (ductility) with decrease in the notch angle *tends* to cause a continuous descent in the curve of breaking stress. This tendency eventually becomes dominant.

For annealed copper (Fig. 10), the variable plastic deformation has relatively great influence on the curve of breaking stress. At 180° , this curve is much higher in relation to the curve of ultimate stress than is the curve for cold-rolled copper (Fig. 6). This difference is due to the greater work-hardening capacity and greater ductility of the annealed copper. For the same reason the breaking stress of an unnotched specimen of annealed copper, represented by point P in Fig. 10, is greater than the disruptive stress T_1 . For cold-rolled copper (Fig. 6), however, the influence of the radial-stress ratio predominates, and the disruptive stress is greater than the breaking stress of an unnotched specimen. This relationship is in spite of the fact that the disruptive stress represents fracture without plastic deformation, whereas fracture

of an "unnotched specimen represents fracture after considerable work-hardening.

Points P_0 represent the hypothetical stress at fracture under unidirectional tension, the "severing stress." They can be established only indirectly. On the curves drawn to points P_0 , points P are placed at the proper heights.

The breaking-stress curves obtained with root radius 0.004 and 0.001 in., unlike the corresponding curves of ultimate stress, generally are below the corresponding curves obtained with root radius 0.01 in. If extended to zero notch angle, each of these curves would be not far above the corresponding curve of ultimate stress, and would be not far from the point E'' representing the summit of the surface in the three-dimensional diagram for ultimate stresses (p. 485). Point T_1 for cold-rolled copper evidently should not be far from point E'' ; the two points have been placed so as to coincide in Fig. 6. For annealed copper (Fig. 10), T_1 has been placed about midway between E'' and the lowest curve of breaking stress (extended to zero notch angle). It is possible, however, that even for the annealed metal T_1 should coincide with E'' .

The influence of notches on the breaking stress of Monel metal is represented by a family of curves in each of Figs. 12 and 14. The metal represented in Fig. 12 had been cold-drawn to 40 per cent reduction in sectional area; the metal represented in Fig. 14 was in the fully annealed condition.

The scatter of experimental points is considerably greater in the diagrams for Monel metal than in those for the copper. The greater scatter probably is due to slight local variations in composition. The effects of such unavoidable variations might not be apparent in tests with unnotched specimens, but might become apparent in tests with notched specimens. These diagrams for Monel metal are generally similar to those for copper, therefore they will not be discussed in detail.

Flow Stress, Breaking Stress, and Ductility of Initially Unnotched Specimens

In Figs. 7, 9, 11, 13, and 15 are diagrams representing the relation between breaking stress and ductility, for both notched and unnotched specimens of copper and Monel metal. In these diagrams, ductility is not represented by reduction of area, as it is in diagrams of Figs. 6, 8, 10, 12, and 14, and in the two previous papers.^{14,15} An abscissa scale based on reductions of area has the disadvantage that the same difference in abscissa does not always represent the same difference in plastic deformation. At high percentages of decrease in sectional area, a small change in abscissa represents a large change in plastic deformation. In Figs. 7, 9, 11, 13, and 15, deformations are represented logarithmically in such a way that the same difference in abscissa always represents the same percentage of plastic deformation. This method, suggested and used by MacGregor,¹¹⁻¹³ consists essentially in a logarithmic representation of values of A_0/A , in which A_0 and A are the initial and current areas of minimum cross section. In the diagrams, this ratio is designated as the "effective length ratio." By subtracting 1.0 from this ratio, a value is obtained for the "effective extension." The origin of abscissas in such a diagram, therefore, is 1.0.

Curve F in each of these diagrams represents the variation of the flow stress* with plastic extension of an initially unnotched specimen. By this method of plotting, the line of flow stresses is practically straight between the point M , representing maximum load, and the point P , representing fracture. Because of the notch effect, curve F rises more rapidly than it would if the specimen could be kept cylindrical. As shown by Kuntze,⁷ this notch effect may be minimized by repeatedly interrupt-

ing the tension test and machining the specimen to cylindrical form. A study of the brief description of his experiments, however, shows that when the test was resumed after an interruption, the local contraction began at a new place, where the metal had received less reduction and consequently less strengthening. His results, therefore, do not show quantitatively the influence of the notch effect of the local contraction on the breaking stress and ductility. A different procedure, therefore, was adopted in the experiments whose results are shown in Figs. 7, 9, 11, 13, and 15. After each interruption of the local contraction, the specimen was machined so as to increase the angle of the notch formed by the contraction, but the diameter on each side of the contracted region was not reduced enough to allow local contraction to start in a new place. It was possible thus to eliminate much of the notch effect, and to obtain some breaking-stress values that probably differ little from those corresponding to unidirectional tension.

In the diagrams, the effects of this procedure are revealed by the changes in the course of the curves of flow stress. After each machining during the progress of local contraction, the initial flow stress on retest was lower than the flow stress at interruption. This lowering must be attributed to a decrease in the radial-stress ratio due to the increased angle of the notch. After resumption of the loading, the line of flow stresses generally was roughly parallel to its course before the interruption. The abrupt drop was greater at the first interruption than at any later interruption, except some interruptions that occurred after copper specimens had begun to fracture internally.

With the Monel-metal specimens (Figs. 13 and 15), the interrupted tension tests were continued until the specimens fractured completely, and the breaking stresses were calculated in the usual way. The

* By "flow stress" is meant the yield stress based on the corresponding sectional area, not on the original area.

results are indicated in the diagrams. With the copper, however, the usual procedure did not give even an approximately correct value of the breaking stress. When an originally unnotched specimen of this oxygen-free copper is completely fractured, by either continuous or interrupted tension, the breaking stress based on measurement of the sectional area after fracture is too high. Values as high as 130,000 lb. per sq. in. are thus obtained, although similar tests with electrolytic copper give values around 75,000 or 80,000 lb. per sq. in. The high values obtained with the oxygen-free copper, however, are illusory. After fracture starts near the axis of the specimen, the surrounding metal continues its plastic extension, and the load thus may drop to a very low value while the total cross section continues to contract. An example of this rim effect is seen in Fig. 37*a*, which is a photograph of a longitudinal section through an originally unnotched specimen of cold-rolled copper after fracture by continuous tensile loading. The values of breaking stress and ductility based on the sectional area of such a specimen are much too high. Moreover, as will be shown later, this rim effect is not confined to originally unnotched specimens or to any one metal, but manifests itself in varying degree as a cause of error in the determination of breaking stress and ductility.

The breaking stress and ductility of the initially unnotched specimens of copper can be determined approximately by means of the lines representing the variations of the flow stress in the interrupted tension tests, and by examination of longitudinal sections made prior to complete fracture. The flow-stress curves representing the interrupted tension tests of copper (Figs. 7 and 11) first take a generally upward course parallel to the original trend, except for the abrupt drops at interruptions. Eventually, however, the upward trend ceases rather abruptly, and the flow stress apparently

takes a generally downward course. This downward trend does not mean that the local flow stress is actually decreasing; it means that the specimen has begun to fracture internally. Longitudinal sections of outwardly sound specimens, after discontinuation of the tension tests at stages represented by P_s , showed that this interpretation is correct. Internal fractures had started near the axis of each of these specimens.

The true values of breaking stress and ductility of initially unnotched specimens, therefore, are the values corresponding to the beginning of a generally downward trend in a flow-stress curve. This point evidently can be determined only approximately. After such a determination for the cold-rolled copper (Fig. 7), however, a check test was made by continuous loading of another specimen to the point P_s to which no line has been drawn. As a section through this specimen showed a small internal fracture, the breaking-stress value represented by this point is too low and the ductility too high. Point P has been selected to represent the average breaking stress and ductility of initially unnotched specimens of this metal, and a similar procedure has been used in Figs. 9 and 11.

In the diagram for half-hard copper (Fig. 9), the lines of flow stress and the points representing fracture of initially unnotched specimens are merely reproductions of the corresponding lines and points for fully annealed copper, with proper adjustment of the abscissas to allow for the prior tensile extension of the half-hard copper.

Points P_0 in Figs. 7, 9, 11, 13, and 15 represent estimated approximate values for the severing stress, the unidirectional tensile stress necessary to cause fracture. Each of these points would be the terminus of a curve representing the course that the flow-stress curve would take if the specimen could be kept cylindrical. Such a flow-stress curve is not shown in these diagrams,

but is shown in derived diagrams to be discussed in detail later (Figs. 33 and 34). As shown in the derived diagrams, this flow-stress curve (F_0) diverges from curve F at the point M representing the beginning of local contraction. As this curve is tangent to F , it cannot be straight between M and P_0 , but must be curved as indicated. If curve F_0 were drawn in each of the diagrams of Figs. 7, 9, 11, 13, and 15, it would pass slightly below the points representing initial flow on reloading. The terminus (P_0) of such a curve must be lower than P unless the ductility is greatly increased because of the removal of the notch effect of the local contraction. With the copper and Monel metal, the ductility evidently is not greatly increased by the removal of this notch effect, and hence P_0 is lower than P . With some metals, as will be shown later (Fig. 21), the relative heights of P and P_0 appear to be reversed.

Influence of Notches on Relation between Breaking Stress and Ductility of Copper and Monel Metal

Consideration has already been given to diagrams representing the influence of notch angle, notch depth, and root radius on the breaking stress of copper and Monel metal. Following each of these diagrams is a corresponding diagram representing the influence of the same three notch variables on the relation between the breaking stress and ductility.

The curves representing this relationship (Figs. 7, 9, 11, 13 and 15) are qualitatively similar to the curves in the diagrams of Figs. 6, 8, 10, 12 and 14 in that each curve rises from point P_0 , traverses a maximum, and descends. The rise of each curve is due to the dominant influence of increasing radial-stress ratio. Evidence for this is found in the associated increase of slope of the broken lines of flow stress drawn between experimental points representing yield and fracture. Moreover, during the descent of the curves representing deep

notches, the slope of the line of flow stress generally continues to increase. The descent of these curves, therefore, must be attributed chiefly to a dominant influence of the continuous decrease in ductility. The rise and descent of each curve, consequently, are due chiefly to the successive dominance of the influences of increasing radial-stress ratio and decreasing ductility.

In the absence of the influence of stress concentration, the course of a curve of this type would depend on only one variable, the radial-stress ratio. The relation between the breaking stress and ductility, as affected by variations in the notch, would then be represented by a single curve. In the diagram for severely cold-rolled copper (Fig. 7), consequently, the differences in height of the curves must be attributed chiefly to differences in the stress concentration remaining at fracture. In the uppermost curve, representing deep notches, the depressing influence of stress concentration probably is negligible.* In the diagram for fully annealed copper (Fig. 11), the scatter of experimental points is generally small, and the relation between breaking stress and ductility may be represented by a single curve. At fracture of this metal, therefore, the influence of stress concentration evidently is negligible, even for shallow notches. Even at maximum load, as shown in Fig. 23B, stress concentration is small.

In the diagram for cold-drawn Monel metal (Fig. 13), the vertical range of experimental points is considerably smaller than in the diagram for the more severely cold-worked copper (Fig. 7). The experimental points representing shallow notches (k values ranging between 65 and 82 per cent) are not far from the point of divergence of the two continuous curves in Fig. 13. The vertical range of scatter,

* Even at maximum load, as shown in the section beginning on page 483 and Fig. 23A, stress concentration probably is negligible when the value of k is less than about 15 per cent.

however, increases as the curves extend to the left. The wider range of the experimental points representing the deepest notches ($k = 11$ to 13 per cent) may be attributed to the increased difficulty of obtaining accurate values of the breaking stress and ductility of specimens so greatly reduced in section. Stress concentration probably has negligible influence on the uppermost curve, and little influence on the lower curve.

In the diagram for annealed Monel metal (Fig. 15), with due allowance for the wide scatter of experimental points, a single curve may be used to represent the influence of all the notches except those having a range of k between 64 and 67 per cent. The upper curve evidently is practically free from the influence of stress concentration. A decrease of the root radius r from 0.01 to 0.001 in. has a great effect in extending this curve, as it does in extending the curve in the diagram for annealed copper (Fig. 11).

Nominal Ductility and True Ductility

Although the uppermost curve in each of the diagrams of Figs. 7, 9, 11, 13 and 15 is practically free from the influence of stress concentration, evidently it does not represent the influence of the radial-stress ratio on the relation between the true breaking stress and true ductility. The correct relationship would be represented by a curve extending from P_0 to the point (T_1) representing the disruptive stress. If the solid curves as drawn were extended to abscissa 1.0 (representing zero ductility), however, they would be below T_1 ; the curves for annealed copper (Fig. 11) and annealed Monel metal (Fig. 15) would be far below this point. Moreover, each of these curves would be below E'' , which represents the highest point on the surface in a three-dimensional diagram of ultimate stresses (p. 485). As previously shown, however, the disruptive stress, the only technical cohesion limit corresponding to

zero plastic deformation of a naturally ductile metal, cannot be less than the highest extrapolated value of the ultimate stress.

The evidence, therefore, indicates that the ductility values plotted in these diagrams are generally too high, that the nominal values for ductility are higher than the true values. If the true values could be plotted, each of these curves would be tilted to the left so as to bring the left end closer to the vertical line representing zero ductility, and so that the curve would not point below T_1 and E'' . The abscissa range should also be increased; the need for this change is most apparent in the diagrams for annealed copper (Fig. 11) and annealed Monel metal (Fig. 15). For reasons now to be given, moreover, these changes in ductility will involve a decrease in the maximum height of the curve. The "ideal locus of fractures" in each diagram thus would be represented, at least qualitatively, by the dotted curve. Each dotted curve shows the influence of the radial-stress ratio on the relation between true breaking stress and true ductility.

There are two distinct factors tending to make the nominal ductility differ from the true ductility. One of these is the previously mentioned "rim effect," the continued plastic deformation of the rim of the minimum cross section after fracture has started near the center. With the oxygen-free copper, this effect is prominent. Attention has been called previously to a longitudinal section through an initially unnotched specimen of this metal after fracture (Fig. 37a). The rim effect, however, is not confined to initially unnotched specimens. With specimens having shallow, wide-angled notches (Fig. 38, *a* and *b*), the effect is so great that values of the breaking stress obtained by the usual procedure are much too high. With deeper notches or with acute-angled shallow notches, the rim effect is less, but is not

negligible (Fig. 37, *b, c, d*, and Fig. 38, *c, d*). Moreover, the rim effect is not confined to copper. As shown in Fig. 39, this type of fracture is found in specimens of Monel metal. The evidence, therefore, suggests that the effect is not uncommon, and must be viewed as a general cause of error in the determination of breaking stress and ductility.

After fracture starts near the specimen axis, the rim of the cross section not only extends but is pulled inward, thus causing the sectional area after complete fracture to be less than the area at the beginning of fracture. The calculated value of the stress necessary to cause fracture, therefore, is too high. The rim effect, consequently, is a cause of error in the determination of both ductility and breaking stress.

The second factor now to be considered affects the calculated value of the ductility, but not the value of the breaking stress. This factor is the deformation gradient. During the plastic extension of a notched specimen, the gradient of longitudinal stress (diagram A-1 of Fig. 1) is leveled out and only a qualitatively similar deformation gradient remains. At fracture of a notched specimen of a ductile metal, the ratio between the greatest and least plastic deformation probably is greater than the initial ratio between the greatest and least values of the longitudinal stress. A similar deformation gradient develops during the local contraction of an initially unnotched specimen. Because of the deformation gradient, the reduction of the area of cross section is merely a measure of the mean ductility. It is not a measure of the true ductility, which would be represented by the *local* reduction of cross section in the metal at the origin of fracture.

The relation between the true ductility and the nominal ductility depends on the location of the origin of fracture. If fracture of a notched specimen starts near the center of the cross section, where the plastic deformation is least, the true

ductility is *less* than the nominal ductility. If fracture starts near the circumference, where the plastic deformation is greatest, the true ductility is *greater* than the nominal ductility. The relation between the true ductility and the nominal ductility varies with the deformation gradient, and thus varies with the characteristics of the notch.

The location of the origin of fracture depends not only on the distribution of the longitudinal stress, but also on the distribution of the radial stress and on the deformation gradient. The conditions determining the location of the origin of fracture, therefore, are much more complex than is generally supposed. The technical cohesive strength of the metal is not constant throughout the cross section; it is greatest at the circumference of the cross section, where the plastic deformation is greatest, and is least at the center. Some phases of this subject are represented in Fig. 5, which shows conditions that would cause fracture to start at the center, and also conditions that theoretically would cause simultaneous fracture throughout the entire cross section. This figure is discussed in detail in the appendix.

The curves representing the ideal locus of fractures in Figs. 7, 9, 11, 13, and 15, are intended to represent only qualitatively the variations of the true ductility and true breaking stress with the radial-stress ratio. At no point on such a curve, not even at point *P*, does the abscissa represent a value of the true ductility. The curve is intended to represent merely relative variations of the ductility.

The varying relation between the true ductility and the nominal ductility probably accounts for some of the variations of nominal ductility with notch depth as represented in Figs. 26 and 27. The apparent increase in ductility with the decrease in *k* below a certain value could be due partly to an increase in the relative magnitude of the rim effect, but could be due

partly to variations in the deformation gradient and in the position of the origin of fracture. This increase in the nominal ductility with the notch depth, therefore, does not necessarily represent an increase in the true ductility.

INFLUENCE OF NOTCHES ON BREAKING STRESS AND DUCTILITY OF TYPICAL FERRITIC STEELS

The group of metals now to be studied differs from copper and monel metal in the type of space lattice. The three steels comprising this group are termed "ferritic steels" to distinguish them from austenitic steels. Two of these ferritic steels have as their chief constituent alpha iron, the other contains also delta iron. The space lattice of each of these steels, therefore, is predominantly body-centered cubic, whereas the space lattice of the metals considered in the previous section is face-centered cubic.

13-2 Chromium-nickel Steel and 0.2 Per Cent Carbon Steel

The influence of notches on the breaking stress and ductility of 13-2 chromium-nickel steel is illustrated by a pair of correlated diagrams (Figs. 16 and 17) of the same two types that have been used for copper and Monel metal. The breaking-stress curves in these two diagrams differ greatly in form from the corresponding curves obtained with copper and Monel metal. Whereas the curves for copper and Monel metal have a single rise and descent, the curves in Figs. 16 and 17 have two reversals. In each of these diagrams, all the curves of breaking stress rise from P_0 through P , traverse a maximum, and descend. The curve representing shallow notches ($k = 63$ to 66 per cent) continues its descent, first at a decreasing rate, then at an increasing rate. A curve drawn to represent shallower notches ($k = 79$ per cent) would take a still lower course. The curves representing deeper notches ($k = 24$

to 27 per cent, and $k = 10$ to 18 per cent), however, diverge from the curves representing shallow notches. They traverse a minimum, which evidently is the same for all values of k between 10 and at least 27 per cent, then reascend, traverse a second maximum, and probably redescend. To the right of the minimum in Fig. 16 these curves are qualitatively similar to the curves for Monel metal and copper.

The rise from P_0 to the first maximum and the redescend are within a narrow range of notch angles (180° to about 150°), and the greater part of the descent is within a range of not more than 5° (Fig. 16). The rise from P_0 to the first maximum cannot be much less, and may even be somewhat greater, than the rise in the curve as drawn. The position of P_0 in Fig. 17 was established approximately by means of the previously discussed interrupted tension tests. A curve representing the variation of the flow stress under unidirectional tension would diverge from curve F at M , and would pass below the points designated "initial flow in retest." The terminus of such a curve evidently would be at about the position designated P_0 . The course of the experimentally determined curve drawn between P_0 and the minimum in Figs. 16 and 17, therefore, is well established.

The complex form of the curves in Figs. 16 and 17 cannot be attributed to variable stress concentration. The variation of theoretical stress concentration with the notch angle is represented by a continuously rising curve without reversal (Fig. 4). Moreover, by plastic deformation to maximum load, stress concentration evidently is practically eliminated when k is less than about 25 per cent (Fig. 25A). Furthermore, the minimum of the curves in Figs. 16 and 17 evidently is unaffected by a decrease in k from about 27 to 10 per cent. The evidence, therefore, indicates that the course of the curve between P_0 and the minimum is practically unaffected by stress concentration, and that this

course is due entirely to variation of the radial-stress ratio.

During the reascent from this minimum, however, the curve representing k values of 24 to 27 per cent probably is somewhat affected by stress concentration. In the absence of stress concentration, this curve and the curve representing deep notches should coincide in a diagram of the type shown in Fig. 17. In the absence of stress concentration, therefore, the curve representing k values of 24 to 27 per cent possibly would take a higher course. It is also possible, however, that the curve representing deep notches ($k = 10$ to 18 per cent) may be slightly too high because of the previously discussed "rim effect." On account of the difficulty of fitting together the fractured ends of specimens of this steel, the presence or absence of the rim effect could not be determined.

There is additional evidence, however, that the curve representing k values of 24 to 27 per cent is too low at its second maximum in Fig. 16. This maximum is lower than E' , which represents the highest point on the surface in a three-dimensional diagram of ultimate stress (Fig. 25A). Point T_1 , representing the disruptive stress, has been placed slightly higher than E' , it is in about the right position with reference to the uppermost curve of breaking stresses.

The dotted curve in Fig. 17 represents qualitatively the influence of the radial-stress ratio on the relation between the true breaking stress and true ductility. It is possible, however, that the first maximum in this curve should be somewhat higher and the minimum somewhat lower.

The influence of notches on the breaking stress and ductility of 0.2 per cent carbon steel is illustrated by a pair of correlated diagrams (Figs. 18 and 19) of the same two types that have been used for the 13-2 chromium-nickel steel. The corresponding diagrams for both these steels are so similar that there is no need for a detailed dis-

cussion of the diagrams in Figs. 18 and 19. In Fig. 19, however, a single curve apparently may be used to represent values of k ranging between about 14 and 26 per cent, whereas two curves are necessary for the 13-2 chromium-nickel steel (Fig. 17). Stress concentration apparently has a negligible effect at fracture of the 0.2 per cent carbon steel when k is less than about 26 per cent. At about this value of k , as shown in Fig. 25B, stress concentration has been practically eliminated even at maximum load.

Influence of Notches on Breaking Stress and Ductility of 0.04 Per Cent Carbon Steel

Experiments were made with 0.04 per cent carbon steel in the cold-drawn condition and after annealing (Table 2). Because not much of this metal was available, attention was confined to deeply notched specimens ($k = 12$ to 17 per cent). Figs. 20 and 21A show the influence of notches on the breaking stress and ductility of the annealed metal.

The breaking-stress curves representing notches with root radius 0.002 to 0.004 in. diverge from the curve representing notches with root radius 0.01 in., and take a lower course, as they generally do in the previously described diagrams for other metals. The lower course of these curves for annealed 0.04 per cent carbon steel, however, is not associated with an elevation of the corresponding curves of ultimate stress. With decrease in the notch angle below about 60°, the breaking stress, apparent ultimate stress, and ductility drop rapidly, and the surfaces of fracture of some of these specimens have a crystalline appearance. The evidence, consequently, indicates that "premature" fracture occurs when the root radius is 0.004 in. or less, and the notch angle is less than about 60°.

At zero notch angle (Fig. 20), the curve of breaking stresses for notches with root

radius 0.01 in. is not far above the highest point on the corresponding curve of ultimate stresses, and would be only slightly above the highest point on the surface in a three-dimensional diagram for ultimate stress (a diagram not determined for this metal). The end of the uppermost curve of breaking stress in Figs. 20 and 21A has been selected as the position for point T_1 , representing approximately the disruptive stress. The uppermost curve thus serves the same purpose as the dotted curves designated "ideal locus of fractures" in previously described diagrams of the same type as Fig. 21.

The course of this curve between T_1 and P in Fig. 21A suggests that it would continue to rise at a decreasing rate if extended beyond P . It was not found feasible to determine experimentally the approximate position of P_0 in this figure. Because the contraction of an initially unnotched specimen of this metal during a tension test is not abruptly localized, it would be difficult to increase the effective notch angle by the previously described method involving interruption of a tension test and remachining of the specimen. The notch effect of the local contraction, however, probably is so slight that the stress at fracture is not far from unidirectional. Consequently, a curve of unidirectional flow stress (if drawn in Fig. 21A) would not diverge greatly from curve F . The terminus of such a curve has been represented arbitrarily by P_0 .^{*} If extended to the right of P_0 in Fig. 21A, the curve probably would traverse a maximum and then descend at an increasing rate, as do the corresponding curves in the previously described diagrams of this type. This maximum in the curve for annealed 0.04 per cent carbon steel, however, evidently is in the field of negative values of S_3/S_1 , whereas the corresponding maxima in

the diagrams for the 13-2 chromium-nickel steel (Fig. 17) and 0.2 per cent carbon steel (Fig. 19) are in the field of positive values.

The uppermost curves in Figs. 20 and 21A are qualitatively similar to the corresponding curves for 13-2 chromium-nickel steel and 0.2 per cent carbon steel, except in the relative heights of T_1 and P_0 . For annealed 0.04 per cent carbon steel, the disruptive stress evidently is less than the unidirectional stress at fracture; the strengthening effect of the plastic deformation during unidirectional loading to fracture evidently more than counterbalances the effect of the great difference in the radial-stress ratios corresponding to P_0 and T_1 .

Figs. 22 and 21B show the influence of notches on the breaking stress and ductility of cold-drawn 0.04 per cent carbon steel. Attention has been confined to deep notches with root radius 0.01 inch.

Initially unnotched specimens showed good ductility. The introduction of even a wide-angled notch, however, caused considerable decrease in ductility, and an increase in the ultimate stress and breaking stress. With a notch angle of 120° , the ductility was small, but the ultimate stress and breaking stress were higher. With a notch angle of 85° , the ultimate stress and breaking stress were still higher. With a 58° notch angle, however, both the apparent ultimate stress and the breaking stress were *considerably lower*. The load evidently did not reach a true maximum.

By prolongation of the curves in Fig. 22, a position was arbitrarily selected to represent T_1 . As illustrated in Fig. 21B, point P_0 evidently would be below P . Its position has been arbitrarily selected to complete the diagram, and so that it can be used in deriving the diagrams in Figs. 32B and 36B, to be discussed in following sections.

The locus of fractures (Figs. 21B and 22) is qualitatively similar to the corresponding curves for the ferritic steels previously

^{*} Use has been made of this point in constructing derived diagrams to be discussed in following sections (Figs. 32A and 36A).

described, in that it has two reversals of curvature. The locus of fractures of the cold-drawn 0.04 per cent carbon steel, however, has no minimum. The cold drawing evidently has caused a great increase in the disruptive stress, but has had relatively little effect on the stress at fracture under unidirectional loading (P_0).^{*} The effect of prior work-hardening on the relative heights of T_1 and P_0 is qualitatively the same for the 0.04 per cent carbon steel (Fig. 21) as for copper (Figs. 7, 9, and 11) and Monel metal (Figs. 13 and 15). The influence of prior work-hardening is discussed further in the section that begins on page 498.

INFLUENCE OF COMBINATION OF AXIAL AND RADIAL UNIFORM STRESSES ON TECHNICAL COHESION LIMIT, YIELD STRESS AND ULTIMATE STRESS

Derivation of Diagrams

Although the previously described diagrams show the influence of the radial-stress ratio, they do not show the quantitative variation of this ratio. It is desirable, therefore, to develop diagrams in which the variations of both S_3 and S_1 are represented directly. Diagrams of this type, which have been used in the two previous papers,^{14,15} are shown in Figs. 28 to 32 inclusive.

Abscissas represent radial stresses and ordinates represent axial stresses. The axis of ordinates is the locus of all points representing unidirectional tensile stress ($S_3 = S_2 = 0$). Line H making an angle of 45° with the axes of coordinates, is the locus of all points representing polarsymmetric stress ($S_1 = S_2 = S_3$). Each of the radiating broken lines is the locus of all points representing the indicated value of the radial-stress ratio (S_3/S_1). The field representing combinations of axial tension with radial tension, (that is, the field

derived from the tension tests of notched specimens) is included between the axis of ordinates and line H . The field to the left of the axis of ordinates and above the axis of abscissas represents combinations of axial tension with radial compression; the field to the left of the axis of ordinates and below the axis of abscissas represents combinations of both axial and radial compression. These two fields have been studied by Bridgman.¹⁻⁴

In deriving the curves in each diagram of Figs. 28 to 32, the position of T_1 on line H can be established directly by reference to the corresponding basic diagram. Similarly P_0 and the intersection of curve U can be established on the axis of ordinates. The course of each curve between its intersection with the axis of ordinates and its junction with the other curves at T_1 was established by making an arbitrary assumption as to the variation of the ultimate stress with the radial-stress ratio. As the evidence already presented has shown that Kuntze's method of determining S_3/S_1 from the form characteristics of a notched specimen is not valid, this method was not used. The method used, however, was similar in one respect to Kuntze's method. It involves the empirical assumption that S_3/S_1 varies linearly with the ultimate stress from zero for an unnotched specimen to 1.0 for the disruptive stress. This assumption is the basis for the location of the small circles traversed by curves U in Figs. 28 to 31, which are derived from the corresponding positions on curves U for deep notches in Figs. 6, 10, 12, 14, 16, and 18. It is also assumed that the radial-stress ratio does not change during the plastic deformation between maximum load and fracture.* This assump-

* Some age-hardening probably has occurred in the cold-drawn 0.04 per cent carbon steel.

* Between maximum load and fracture, the notch depth increases and thus tends to increase S_3/S_1 . The root radius, however, increases, and thus tends to decrease S_3/S_1 . With a wide-angled notch, the angle decreases, and thus tends to increase S_3/S_1 . With a deep, acute-angled notch, the dominant change probably is an increase of the root radius and

tion leads to the location of the small circles traversed by the solid curves of breaking stress (Figs. 28 to 31), which are derived from corresponding positions in curves of breaking stresses of deeply notched specimens in Figs. 6, 10, 12, 14, 16, and 18. For reasons given in the discussions of the basic diagrams, the ideal locus of fractures must reach line H at point T_1 . The ideal locus of fractures is represented by curve L in each diagram of Figs. 28 to 32. This curve represents the course that the locus of fractures would take if the specimens could be subjected to uniform axial and radial stresses.

The intersection of the curve of yield stress with the axis of ordinates cannot be established directly because the plastic deformation at the observed yield was less for an unnotched than for a notched specimen. A curve of yield strength, therefore, was established by means of experimental points (not shown) representing yield of notched specimens, and was prolonged across the axis of ordinates so that at the intersection it is nearly parallel to line H .¹⁵ The curves of yield strength represent stresses corresponding to plastic deformation of about 3 per cent (p. 478).

In these derived diagrams, as in the basic diagrams, the locus of fractures L is of two different forms. For the copper and Monel metal, the locus is a simple curve (Figs. 28 and 29); for the three ferritic steels, the locus has two reversals of curvature (Figs. 30, 31, and 32). With prior plastic deformation, the distance between the locus of fractures and the curve of ultimate strength decreases. (Compare diagrams A , B , and C of Fig. 28; A and B of Fig. 29, and A and B of Fig. 32.) With prior plastic deformation, moreover, the distinction between the two forms of the locus of fractures becomes less prominent (Fig. 32B). With sufficient prior plastic

deformation, the locus of fractures and the curve of yield strength would coincide with the curve of ultimate strength. Practical coincidence of these three curves is shown in diagrams for a brittle steel in the two previous papers;^{14,15} those diagrams are based on data published by Kuntze.

The locus of fractures of a brittle metal, therefore, is similar in form to the curves of ultimate strength in Figs. 28 to 32. As variable plastic deformation is not a factor affecting the curve for a brittle metal, such a curve represents the influence of the radial-stress ratio alone on the technical cohesion limit. The technical cohesive strength of a brittle metal, therefore, is represented by a curve of the same form as the curve of ultimate strength of a ductile metal. The *initial* technical cohesive strength of a ductile metal is represented by a curve similar in form to the curve for a brittle metal. Curves T in Figs. 28 to 32 represent approximately the initial technical cohesive strength of these more or less ductile metals. The method of establishing the approximate position of such a curve is discussed in detail in the two previous papers.^{14,15} The point T_0 generally is near the intersection of the curve of ultimate strength U with the axis of ordinates.

In the field of negative values of S_3 (Figs. 29 to 32), the extension of curve T has been determined by establishing approximately points T_{c2} (Figs. 30, 31, and 32) in accordance with Bridgman's statement (1-4) that the pure radial compressive stress ($S_1 = 0$, $S_3 = S_2$ negative) necessary to cause a tensile type of fracture is a little greater than the unidirectional tensile stress that would cause unidirectional fracture (T_0). Curve U also has been extended so as to diverge slightly outward from line H , in accordance with a similar statement by Bridgman¹⁻⁴ with regard to the ultimate strength of a ductile metal under pure radial compression.

a consequent tendency to a decrease in S_3/S_1 . This accounts for the decidedly higher ultimate stress values sometimes obtained with the smaller root radii.

*Variation of Technical Cohesive Strength,
Work-hardening Capacity, and
Ductility, Represented by Locus
of Fractures of Ductile Metal*

Curve T in each of the diagrams represents initial *technical cohesive strength*, the cohesive strength of unaltered metal. The curve represents an infinite number of *technical cohesion limits* corresponding to the infinite number of possible values of the radial-stress ratio. Any specific technical cohesion limit must be designated with reference to the corresponding value of S_3/S_1 . The cohesion limits for unidirectional and polarsymmetric tension have been designated T_0 and T_1 , respectively, and the cohesion limit corresponding to any other value of S_3/S_1 has been designated by T with that value as a subscript.

No point on curve T (for a ductile metal) except T_1 could conceivably be attained by experiment. Under any other stress combination except polarsymmetric tension, the yield stress corresponding to that combination would be exceeded before the initial cohesion limit; the metal would thus be plastically deformed, and its technical cohesive strength would be increased. The curve representing the technical cohesive strength, consequently, would be moved outward and the point representing the disruptive stress would be moved upward along line H . (Such an effect is illustrated qualitatively by the relative positions of curves T in diagrams A , B , and C of Fig. 28.) The curve representing the yield strength would also be moved outward, and more rapidly than the curve of technical cohesive strength. Eventually the curve of yield strength would touch the curve of cohesive strength and the metal would fracture without further plastic deformation. The total plastic deformation up to this point would depend on the radial-stress ratio existing during the deformation.¹⁵

Although no point on curve T except T_1 can be attained directly by experiment,

the position of the entire curve with reference to curves U and Y is of practical as well as theoretical importance. As pointed out by Ludwik years ago,⁹ the ductility of a metal and the energy that it will absorb before fracture depend on the difference between the flow stress and an initial technical cohesion limit. In accordance with the prevalent view, however, Ludwik erroneously assumed that there is only one technical cohesion limit for a metal, in any specific state of heat-treatment and plastic deformation. He assumed that the ductility and total work under *any* stress combination depend on the difference between the flow stress for that combination and the calculated value of the breaking stress under polarsymmetric tension. As illustrated in Figs. 28 to 32, however, that view is incorrect. The ductility and total work would depend primarily on the generally much smaller difference between the flow stress and the technical cohesion limit *for that stress combination*, a stress difference represented by the distance between two corresponding points on curves Y and T .

The locus of fractures (L) does not represent constant technical cohesive strength. Through any point on curve L , a curve similar to T could be drawn to represent the technical cohesive strength corresponding to that point. This curve would be outside curve T , thus representing increased technical cohesive strength due to the plastic deformation that occurred under the stress combination represented by the mentioned point on curve L .

INFLUENCE OF PLASTIC EXTENSION ON TECHNICAL COHESIVE STRENGTH

Diagrams of the type now to be considered show directly the influence of plastic deformation on the technical cohesive strength. In these diagrams abscissas represent plastic deformations and ordinates represent breaking stresses. Coordinates in these diagrams, therefore,

are the same as in the diagrams from which they are derived (Figs. 7, 9, 11, 13, 15, 17, 19, and 21). The locus of fractures (L) in each derived diagram, moreover, is identical with the ideal locus of fractures in the corresponding basic diagram. Curve F , and points M , P , and P_0 , have also been reproduced in each derived diagram.

Curve F_0 represents the approximate course of a curve of flow stress in the absence of the radial stress induced by the notch effect of local contraction. It thus represents the approximate variation of the flow stress under unidirectional tension.

The locus of fractures shows the combined influence of plastic deformation and the radial-stress ratio on the breaking stress. Any point on the locus of fractures could be made the terminus of a curve representing the influence of plastic deformation on the cohesion limit corresponding to a single value of S_3/S_1 . A single curve of this kind, however, cannot represent the influence of plastic deformation on the technical cohesive strength. A complete view of the influence of plastic deformation upon the technical cohesive strength would comprise a series of curves, each representing a typical value of S_3/S_1 . Such a series of curves is shown in each diagram in Figs. 33 to 36.

As shown in the two previous papers,^{14,15} a curve representing the influence of plastic deformation on a single cohesion limit rises continuously at a decreasing rate. It thus resembles qualitatively flow-stress curve F_0 or any other curve of flow stress corresponding to a single value of S_3/S_1 . The greater the rate of hardening of a metal with plastic deformation, the more rapid is the rise of a curve of either flow stress or cohesion. A curve of flow stress, however, rises more rapidly than the corresponding curve of cohesion. Although these curves may be far apart at the origin, they converge and eventually intersect at a small angle, at a point on the locus of fractures. This relation is

illustrated by curves F_0 and T_0 . Other curves of flow stress could be constructed, as in the two previous papers,^{14,15} for comparison with the other curves of technical cohesion. The rapidity of the rise of a curve of either flow stress or cohesion increases with increase of S_3/S_1 .

The vertical distribution of the left ends of the cohesion curves in each of these diagrams is in accordance with the relative heights of the intersections of curve T with the radiating broken lines in the corresponding diagram of the previously described type (Figs. 28 to 32).

The effect of *prior* plastic extension on an entire diagram of technical cohesive strength may be studied by comparing the diagrams representing annealed metal with those representing metal that has received various degrees of cold-work. Comparison may thus be made between diagrams A , B , and C of Fig. 33, between diagrams A and B of Fig. 34, and between diagrams A and B of Fig. 36. The evidence indicates that prior plastic deformation has very little effect on the locus of fractures at P_0 , because this point represents fracture after about the same amount of total plastic deformation whether the metal before test was in the annealed or cold-worked condition. Prior plastic extension, however, elevates the locus of fractures near the left end; the greater the amount of prior plastic extension, the greater is the elevation of the left end and of much of this curve.

When the typical curves of technical cohesion are correctly drawn for an annealed metal and are sufficiently extended, it is possible to derive another diagram to represent the technical cohesive strength after any specified equivalent* reduction of sectional area (any given value of A_0/A). As the cold-drawn Monel metal had been reduced 40 per cent in

* Evidence indicates that reduction of sectional area by rolling is not equivalent in effect to reduction by tensile extension or by cold-drawing.

sectional area by cold-drawing, the origins of the cohesion curves in diagram *B* of Fig. 34 should correspond theoretically to points on the curves in diagram *A* at abscissa 1.67. Similarly the origins of the cohesion curves in diagram *B* of Fig. 33 should correspond theoretically to points on the curves in diagram *A* at abscissa 1.3. Such a relationship has been kept in mind in constructing the cohesion curves in Figs. 33, 34, and 36. When ductilities are represented by the method used in these diagrams, a curve of cohesion in a diagram for previously cold-worked metal should be merely an extension of the corresponding curve beyond the proper abscissa in diagram *A*. The 75 per cent reduction of area of copper by cold-rolling evidently was not equivalent to the same amount of deformation by tensile extension. Otherwise the cohesion curves in Fig. 33C would start at points corresponding to points in diagram *A* at abscissa 4.

FORM OF LOCUS OF FRACTURES AS RELATED TO DIFFERENTIAL EFFECT OF S_3/S_1 AND TEMPERATURE ON CURVES OF FLOW STRESS AND COHESION

Because the corresponding curves of flow stress and cohesion (Figs. 33 to 36) intersect at a small angle, any variable that has even a slight differential effect on the height of these two curves may have a great effect on the ductility. An increase of S_3/S_1 causes an elevation of both curves, but the effect on the curve of flow stress is the greater; for this reason an increase in S_3/S_1 causes a decrease in ductility. Comparison of Figs. 33 to 36, moreover, shows that the differential effect of an increase of S_3/S_1 varies greatly with the metal and with the prior plastic extension.

The difference in form between the locus of fractures for copper or Monel metal (Figs. 33 and 34) and the locus of fractures for a ferritic steel (Figs. 35 and 36) may be attributed to a difference in the differential effect of variation of S_3/S_1 on

corresponding curves of flow stress and cohesion. This difference in the differential effect manifests itself most clearly when S_3/S_1 is between about 0.1 and 0.3. Variation of S_3/S_1 within this range causes little change in the ductility of copper or Monel metal (Figs. 33 and 34), but an abrupt change in the ductility of the ferritic steels (Figs. 35 and 36). The differential effect of a variation of S_3/S_1 , therefore, evidently is greater for the ferritic steels than for the face-centered cubic metals. In spite of the relatively high differential effect for the ferritic steels, however, the ductility may change rather slowly with increase of S_3/S_1 above the value corresponding to the minimum in the locus of fractures (Figs. 35 and 36). This irregular variation of the ductility is associated with the influence of another variable, the *slope* of the cohesion curve. As shown in these figures, the slope increases with increase in S_3/S_1 . At high values of S_3/S_1 , the slope is so steep that even a large differential effect of variation of S_3/S_1 on the heights of the curves of flow stress and cohesion may have little effect on the ductility. The effect on the ductility is greatest when the curves of flow stress and cohesion are not steep, and when an increase of S_3/S_1 causes a relatively large change of slope.

It appears possible that the steep drop in the impact value for steels within a narrow temperature range, therefore, may be related to the abrupt decrease in ductility within a narrow range of S_3/S_1 .

APPENDIX

The location of the origin of fracture in the cross section of a notched specimen, as affected by the gradients of longitudinal and radial stress and by the deformation gradient, was discussed briefly on page 492. Reference was made to Fig. 5, which illustrates some phases of the subject.

Diagrams *A* and *B* of Fig. 5 may be viewed as longitudinal sections of

cylindrical diagrams representing stress distributions over the minimum cross section of a notched cylindrical specimen. Diagram *C* represents a cross section of diagram *B* at the indicated position. Abscissas in each of these diagrams represent squares of radial distances. By this method of plotting, the curves in diagrams *A* and *B* are made less abrupt, and the circles in diagram *C* are less closely crowded near the circumference, than they would be if radial distances were plotted directly.

The influence of the deformation gradient (p. 492) on the technical cohesive strength is illustrated by the series of curves in diagram *B*. Because of the deformation gradient, the technical cohesive strength increases with distance from the center of the cross section. The technical cohesive strength cannot be represented by a single curve, but may be illustrated by the series of curves in diagram *B*, each curve representing the variation of a specific technical cohesion limit, in terms of the longitudinal stress component. To illustrate the influence of this gradient of technical cohesive strength together with the influence of the distribution of the applied longitudinal and radial stresses on the origin of fracture, it will be assumed that all concentration of longitudinal stress has been eliminated during the plastic deformation to fracture, that the amount and distribution of the longitudinal stress at fracture are represented by line *MM'* of diagram *B*, and that the variation of the radial-stress ratio is represented by curve *R* of diagram *A*.

At the axis of the specimen, the conditions then would be represented by point *F* of diagram *B*. At this point, line *MM'* touches the curve representing $T_{0.6}$. As shown in diagram *A*, the radial-stress ratio at point *F* of diagram *B* is 0.6. The stress conditions represented by point *F*, therefore, would cause fracture. At any other point on the cross section, however,

the longitudinal stress would be below the cohesion limit for the corresponding radial-stress ratio. Fracture, therefore, would start at the center of the cross section. This relationship is illustrated also by the cross section of the cylindrical diagram represented by diagram *C*. The circles representing values of S_3/S_1 are larger than the corresponding circles representing values of specific technical cohesion limits.

Curve *W* in diagram *B* represents the distribution of longitudinal stress that would theoretically cause simultaneous fracture throughout the cross section. Curve *W* has been drawn through the intersections of the curves of technical cohesion limits with the broken vertical lines representing corresponding values of S_3/S_1 . If the distribution of longitudinal stress be represented by any curve between curve *W* and line *MM'*, fracture would start at the center of the cross section.

ACKNOWLEDGMENTS

The authors are indebted to P. Devaney, National Bureau of Standards, for the development of the technique and the precise machining of the deeply notched specimens, especially those having small notch angles and root radii.

REFERENCES

1. P. W. Bridgman: Breaking Tests under Hydrostatic Pressure, and Conditions of Rupture. *Phil. Mag.* (July 1912) 24, 63-80.
2. P. W. Bridgman: Theoretically Interesting Aspects of High-Pressure Phenomena. *Reviews of Modern Physics* (1935) 7, 1-35.
3. P. W. Bridgman: Reflections on Rupture. *Jnl. Appl. Physics* (1938) 9, 517-528.
4. P. W. Bridgman: Considerations on Rupture under Triaxial Stress. *Mech. Eng.* (Feb. 1939) 61, 107-111.
5. A. A. Griffith: The Effect of Surface Scratches on the Strength of Shafts and other Members. Advisory Comm. for Aeronautics Report T. 1275 (Dec. 1918).
6. C. E. Inglis: Stresses in a Plate due to the Presence of Cracks and Sharp Corners. *Trans. Inst. Nav. Arch.* (1913) 55, 219-230.
7. W. Kuntze: Der Material Verfestigung im Fließkegel. *Mitt. Mat. Prüf. K. W. I. für Metallforschung* (1924) 42, 31-32.
8. W. Kuntze: Kohäsionsfestigkeit. *Mitt. Mat. Prüf. Anstalten* (1932) 20, 1-61.

9. P. Ludwik: Über die Bedeutung der Elastizitätsgrenze, Bruchdehnung und Kerbzähigkeit. *Ztsch. Metallkunde* (1924) **16**, 207-212.
10. P. Ludwik and R. Scheu: Über Kerbwirkungen bei Flusseisen. *Stahl und Eisen* (1923) **43**, 999-1001.
11. C. W. MacGregor: Relations between Stress and Reduction in Area for Tensile Tests of Metals. *Trans. A. I. M. E.* (1937) **124**, 208-226.
12. C. W. MacGregor: A Two-Load Method of Determining the Average True Stress-Strain Curve in Tension. *Trans. Amer. Soc. Mech. Engrs.* (1939) **61**; *Jnl. Appl. Mech.* (1939) **6**, A156-158.
13. C. W. MacGregor: The Tension Test. *Proc. Amer. Soc. Test Mat.* (1940) **40**, 508-531.
14. D. J. McAdam, Jr.: The Technical Cohesive Strength of Metals. *Trans. Amer. Soc. Mech. Engrs.* (1941) **63**, *Jnl. Appl. Mechanics* (Dec. 1941) **8**, A155-165.
15. D. J. McAdam, Jr.: The Technical Cohesive Strength and Yield Strength of Metals. *A. I. M. E. Tech. Pub.* 1414 (*Metals Tech.*, Jan. 1942).
16. H. Neuber: Elastisch Strenge Lösungen Zur Kerbwirkung bei Scheiben und Umdrehungs-Körpern. *Ztsch. Angew. Math u. Mech* (1933) **13**, 439-442.
17. H. Neuber: Kerbspannungslehre. Berlin, 1937. J. Springer.
18. W. N. Thomas: The Effect of Scratches and of Various Workshop Finishes upon the Fatigue Strength of Steel. *Aero. Res. Comm. R. and M. No. 860* (March 1923).

TABLE 1.—Mechanical Treatment and Chemical Composition

Metal	Designation	Mechanical Treatment		Rod Diameter, In.	Composition, Per Cent									
		Method	Reduction in Area, Per Cent		C	Fe	Ni	Cu	Cr	Mn	P	S	Si	
Oxygen-free copper...	N	Cold-rolled	75	0.875				99.97						
Monel metal.....	G	Cold-drawn	40	0.875	0.18	1.24	diff.	28.46		0.94			0.10	
13-2 Cr-Ni steel.....	E	Hot-rolled		0.875	0.09	diff.	2.06		13.3	0.48			0.26	
0.20 % carbon steel...	T	Hot-rolled		1.125	0.20	diff.				0.60	0.033	0.05	0.20	
0.04 % carbon steel...	Q	Cold-drawn	33	0.937	0.045	diff.				0.31	0.019	0.017	0.24	

TABLE 2.—Heat-treatments

Material	Designation	Temperature, Deg. F.	Time Held, Hr.	Cooled in	Temperature	Time Held, Hr.	Cooled in
Copper.....	N-8	800	5	Air			
Monel metal.....	G-14	1400	1	Air			
13-2 Cr-Ni steel.....	E	1240		Furnace			
0.2 per cent carbon steel.....	T-W-9	1625	1	Water	900	2	Air
0.04 per cent carbon steel.....	Q-17.5	1750	1	Furnace			

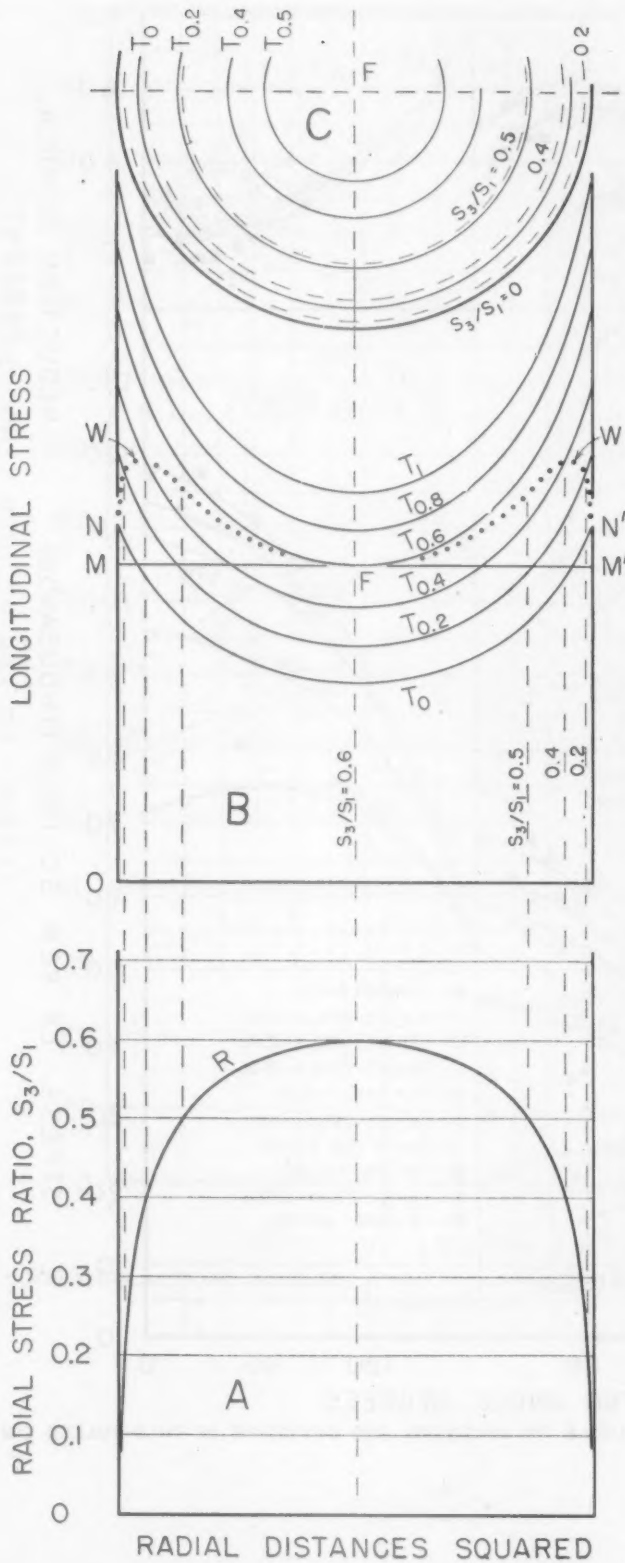


DIAGRAM A--LONGITUDINAL SECTION OF CYLINDRICAL DIAGRAM REPRESENTING AN ASSUMED VARIATION OF S_3/S_1 WITH SQUARE OF DISTANCE FROM SPECIMEN AXIS.
 DIAGRAM B--LONGITUDINAL SECTION OF CYLINDRICAL DIAGRAM ILLUSTRATING THE RELATION BETWEEN STRESS DISTRIBUTION, TECHNICAL COHESIVE STRENGTH, AND ORIGIN OF FRACTURE.
 DIAGRAM C--CROSS SECTION OF DIAGRAM B THROUGH MM'.

R-- VARIATION OF RADIAL STRESS RATIO.
 MM'--ASSUMED UNIFORM LONGITUDINAL STRESS AT FRACTURE.
 F--ORIGIN OF FRACTURE.
 W--DISTRIBUTION OF LONGITUDINAL STRESS AT SIMULTANEOUS FRACTURE THROUGHOUT CROSS SECTION.

FIG. 5.--INFLUENCE OF GRADIENT OF RADIAL STRESS, AND OF DEFORMATION GRADIENT, ON POSITION OF ORIGIN OF FRACTURE.

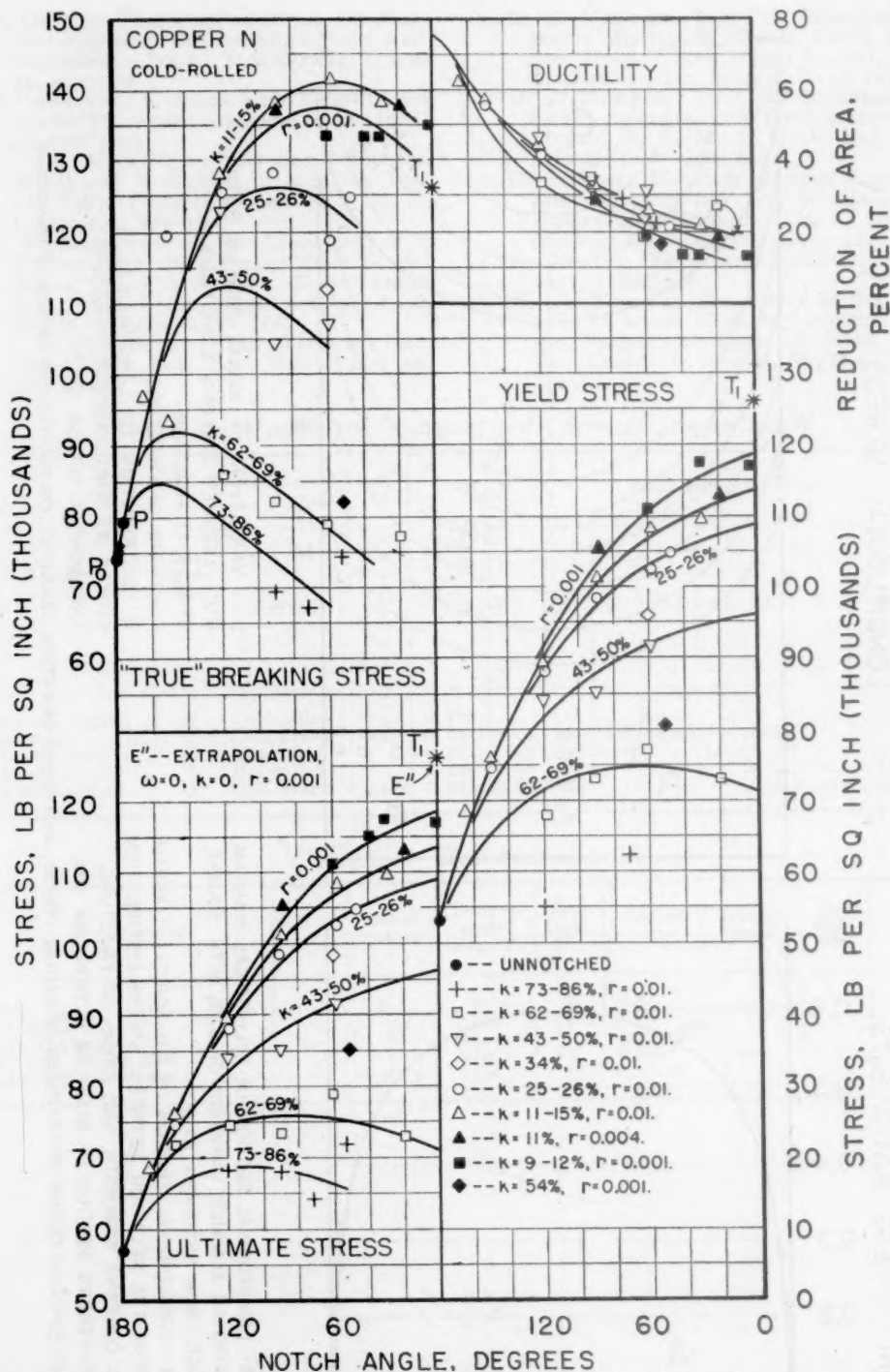


FIG. 6.—INFLUENCE OF NOTCH ANGLE ON STRENGTH AND DUCTILITY OF COLD-ROLLED COPPER.

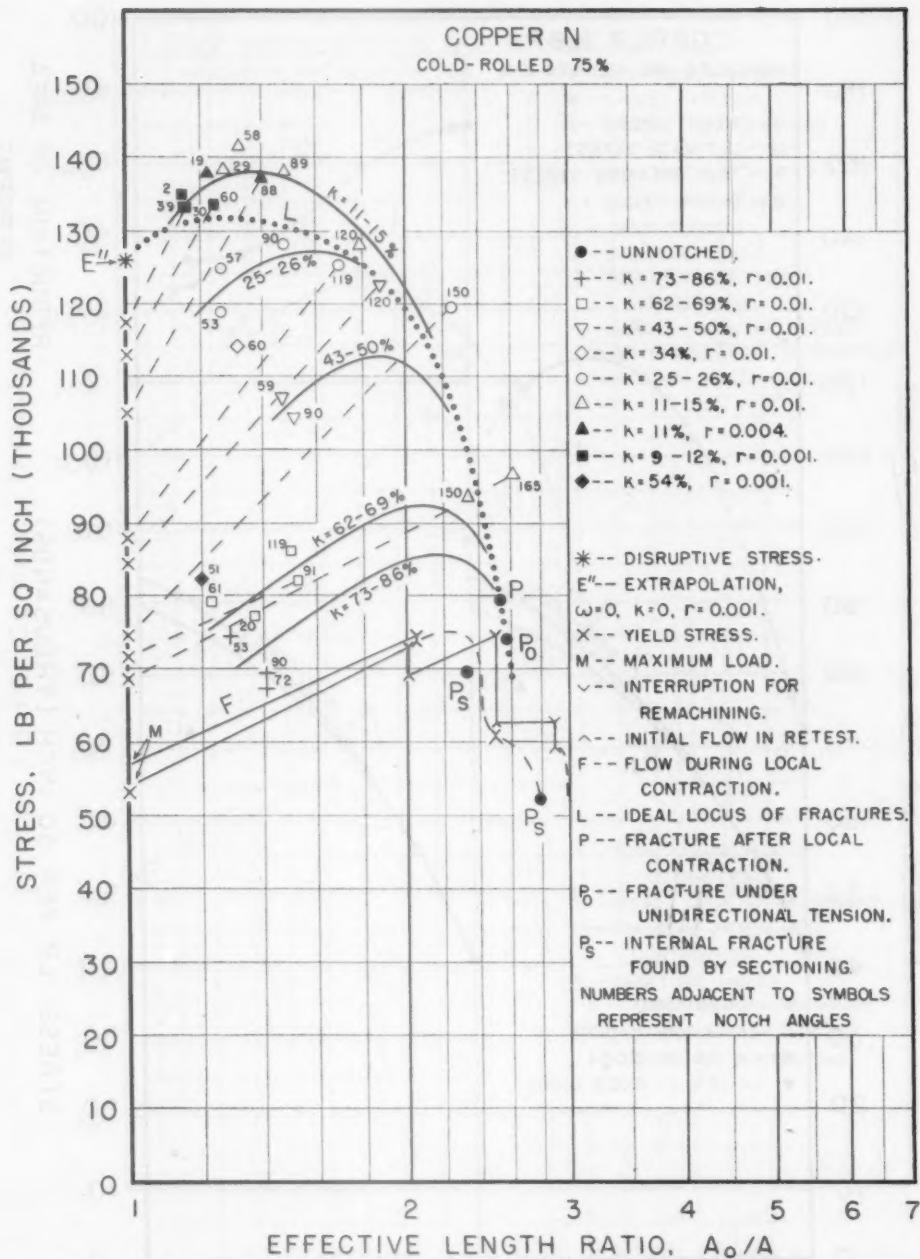


FIG. 7.—RELATION BETWEEN BREAKING STRESS AND DUCTILITY AS AFFECTED BY NOTCHES, COLD-ROLLED COPPER.

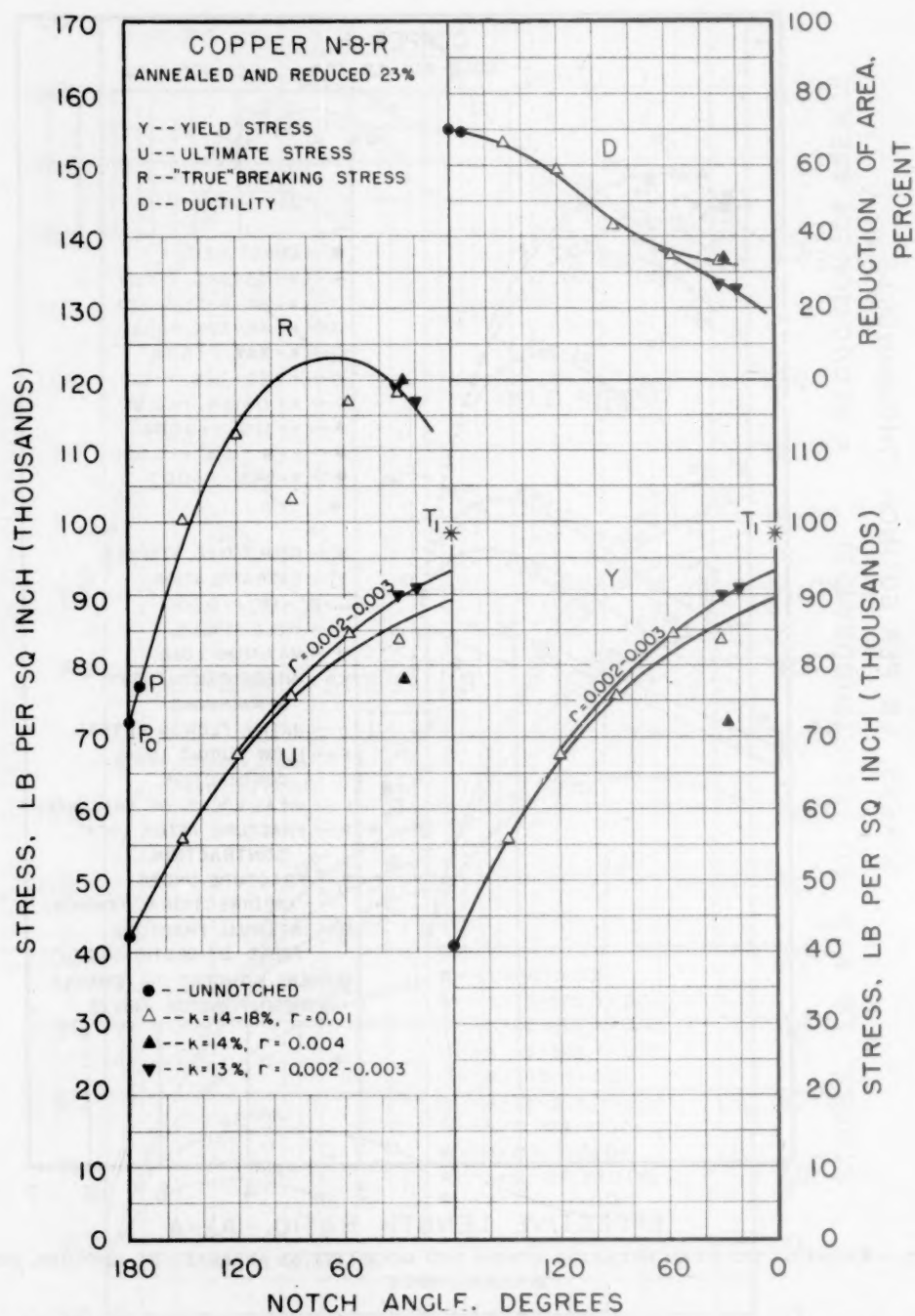


FIG. 8.—INFLUENCE OF NOTCH ANGLE ON STRENGTH AND DUCTILITY OF HALF-HARD COPPER.

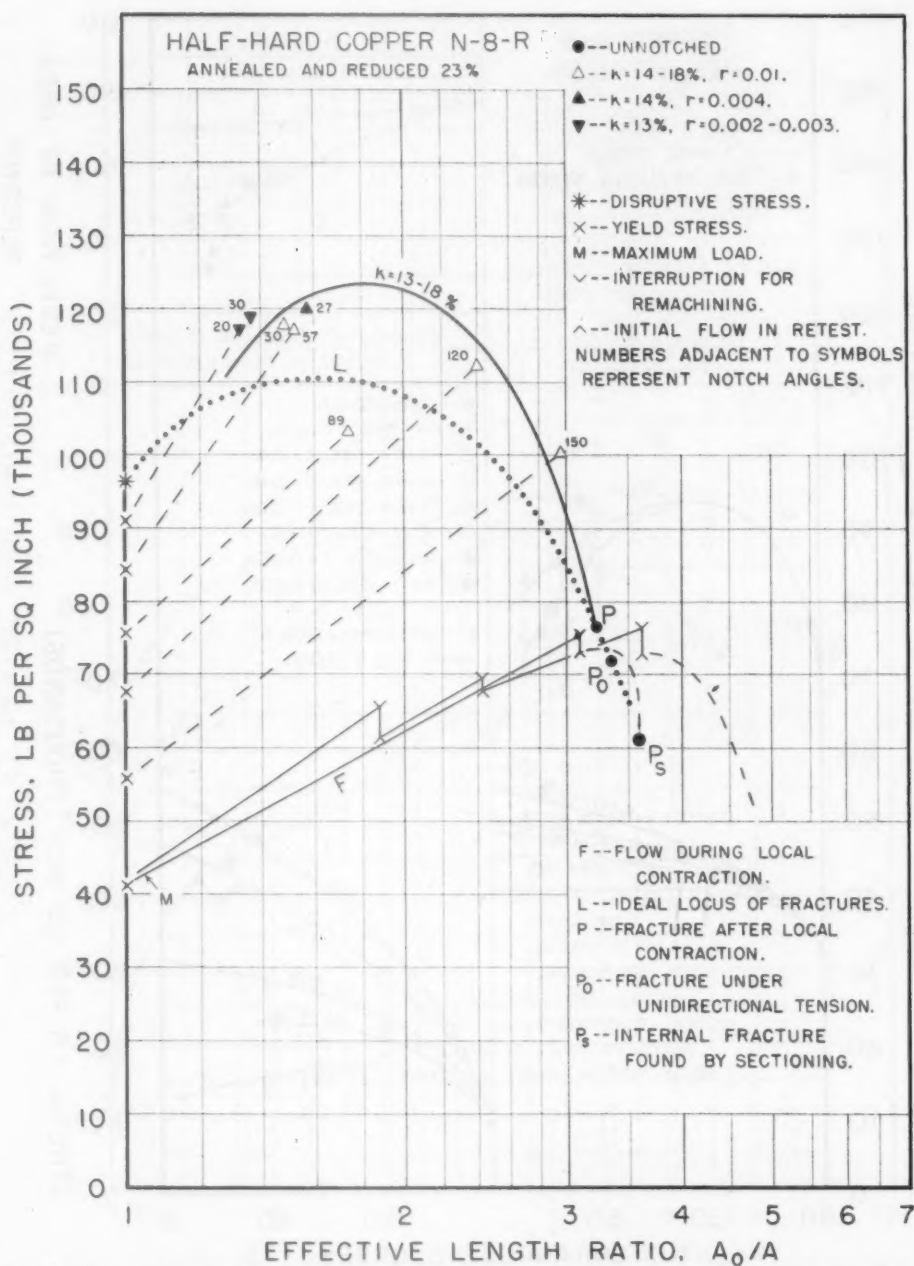


FIG. 9.—RELATION BETWEEN BREAKING STRESS AND DUCTILITY AS AFFECTED BY NOTCHED, HALF-HARD COPPER.

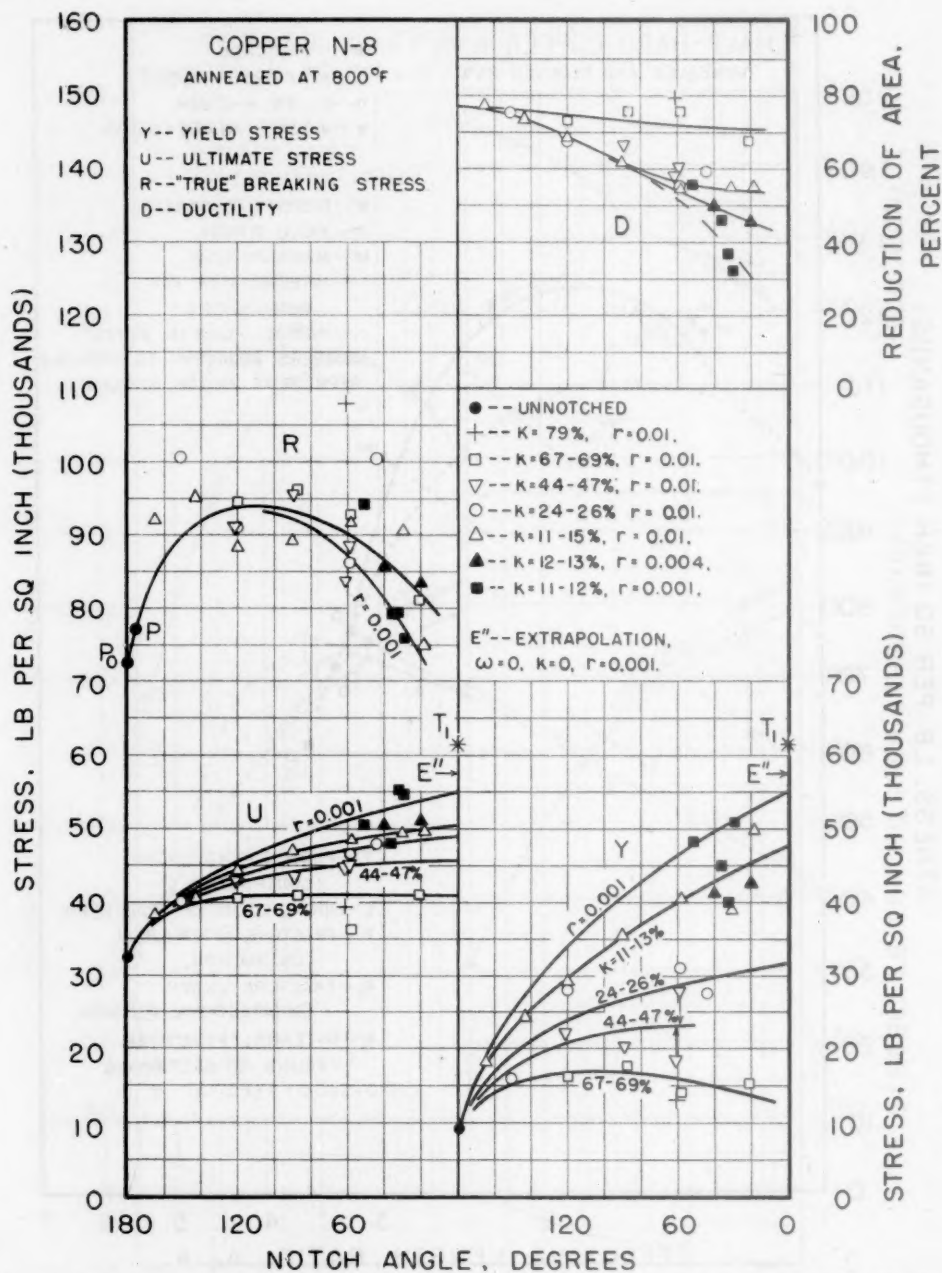


FIG. 10.—INFLUENCE OF NOTCH ANGLE ON STRENGTH AND DUCTILITY OF ANNEALED COPPER.

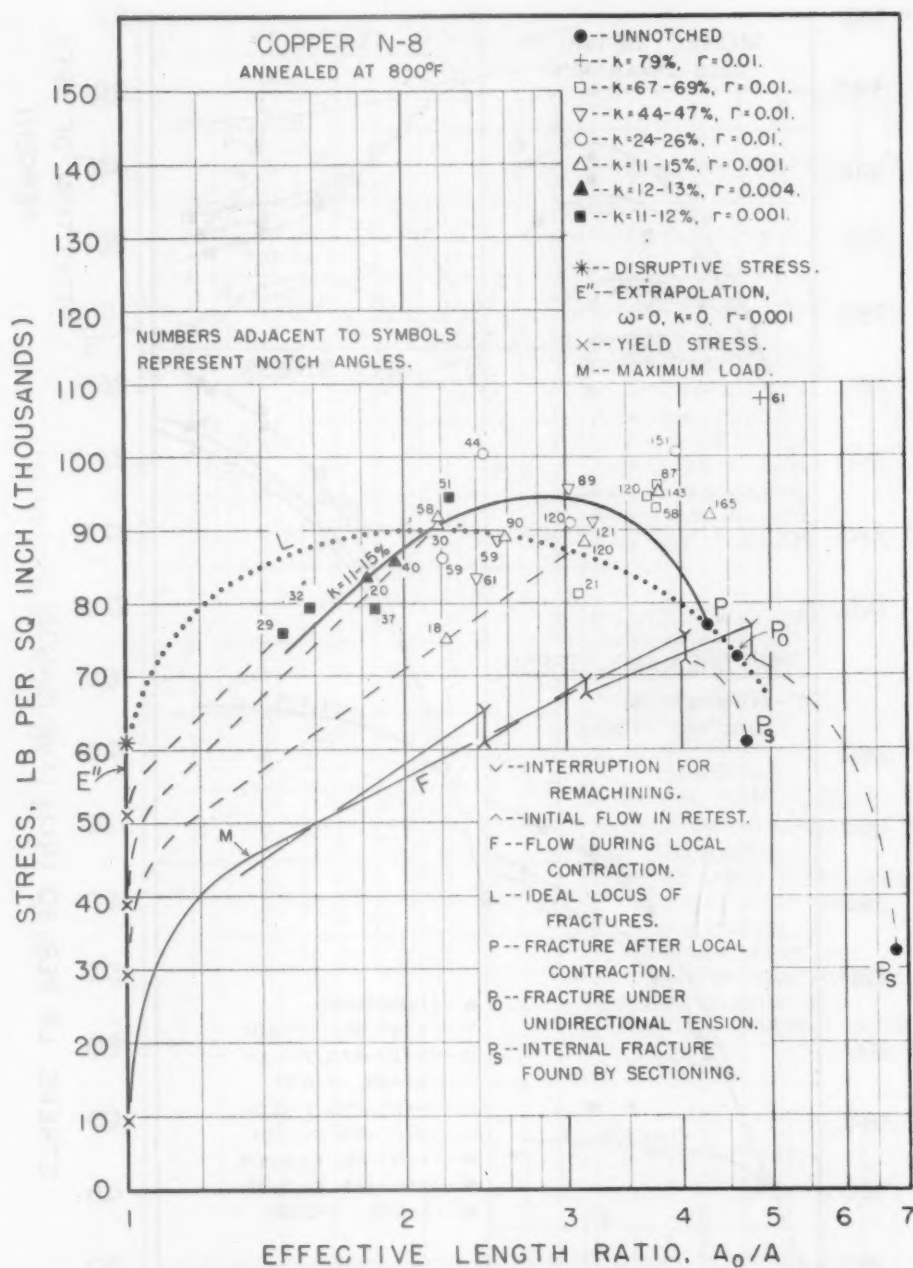


FIG. 11.—Relation between breaking stress and ductility as affected by notches, ANNEALED COPPER

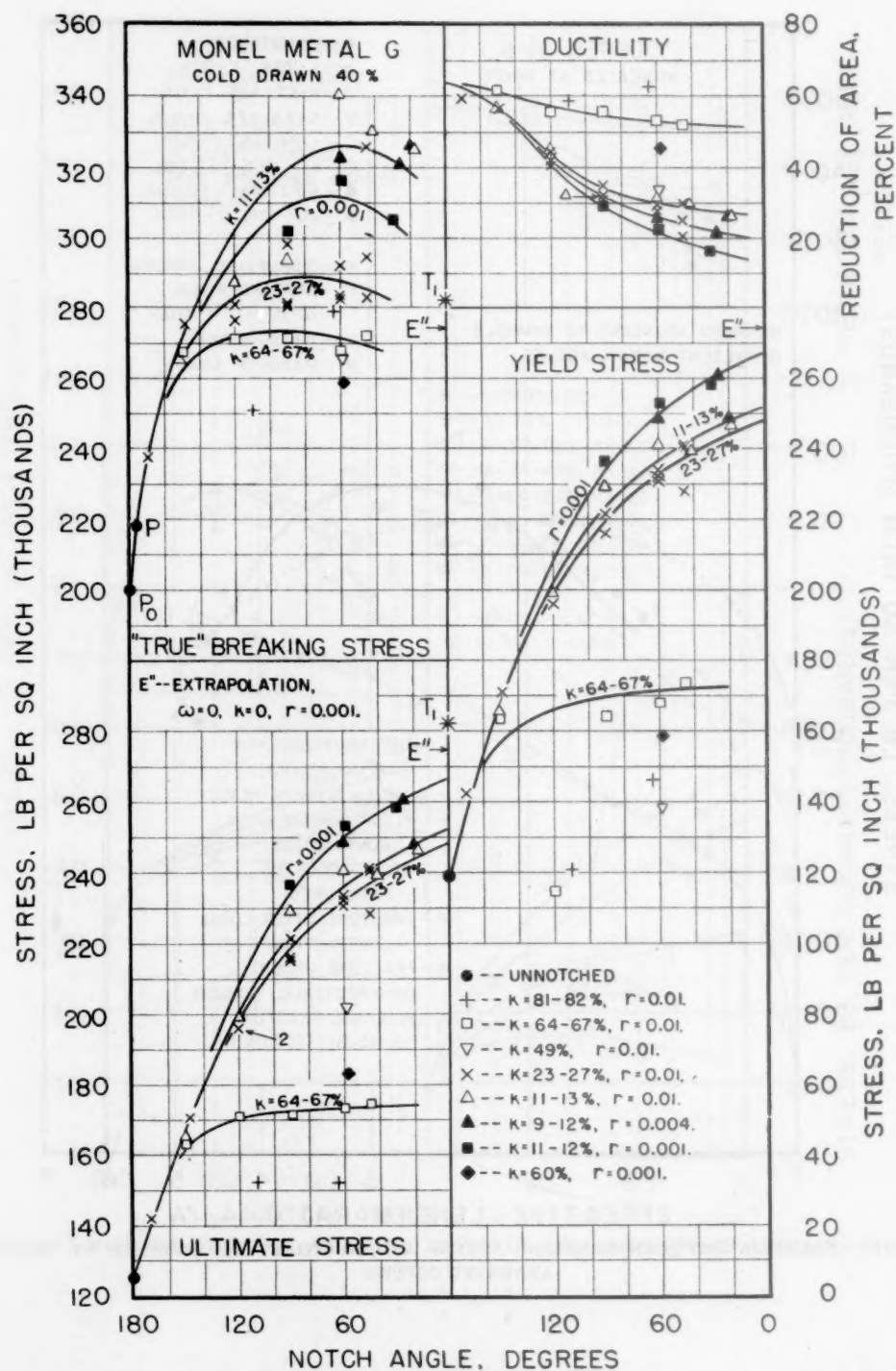


FIG. 12.—INFLUENCE OF NOTCH ANGLE ON STRENGTH AND DUCTILITY OF COLD-DRAWN MONEL METAL.

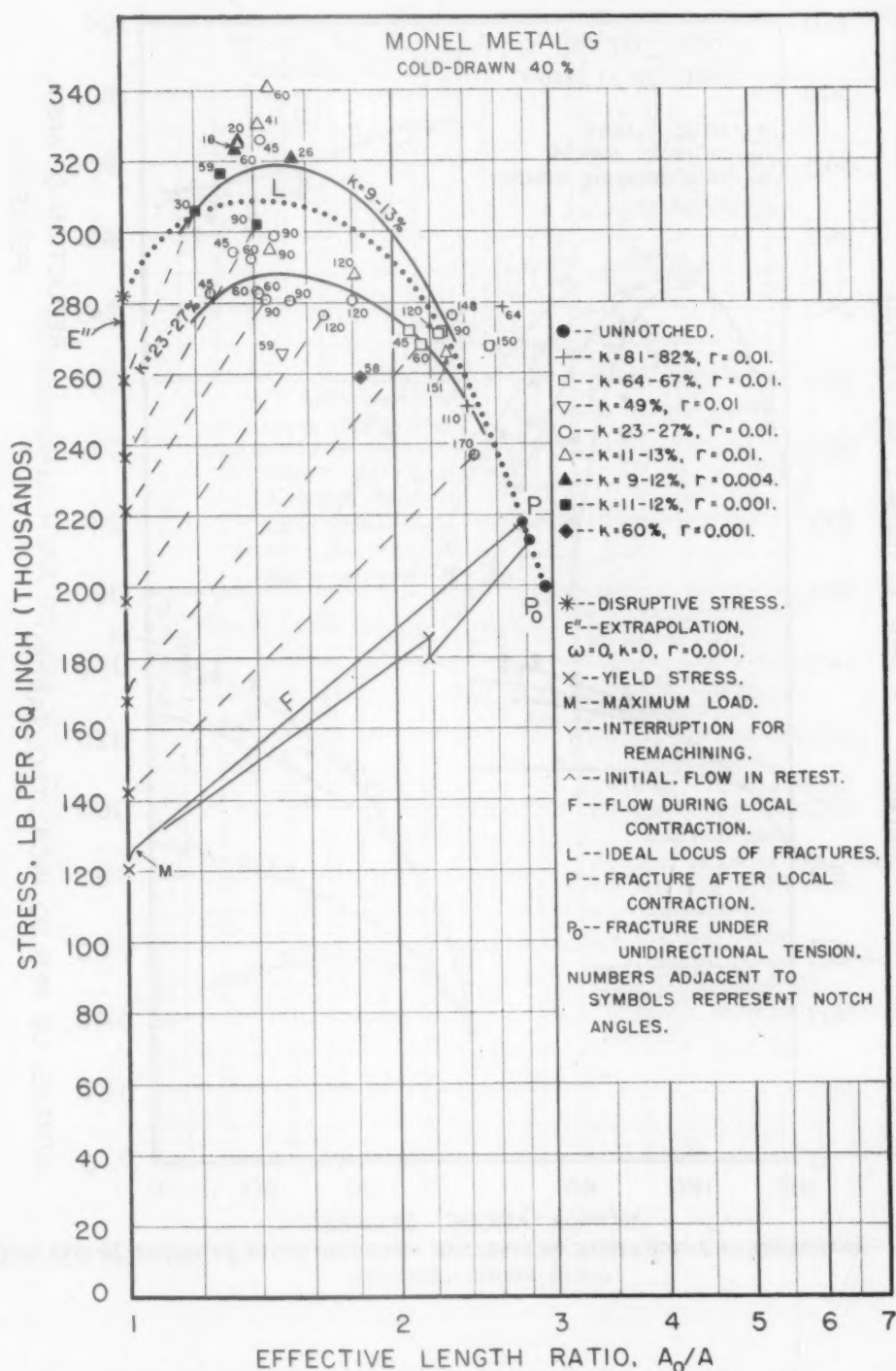
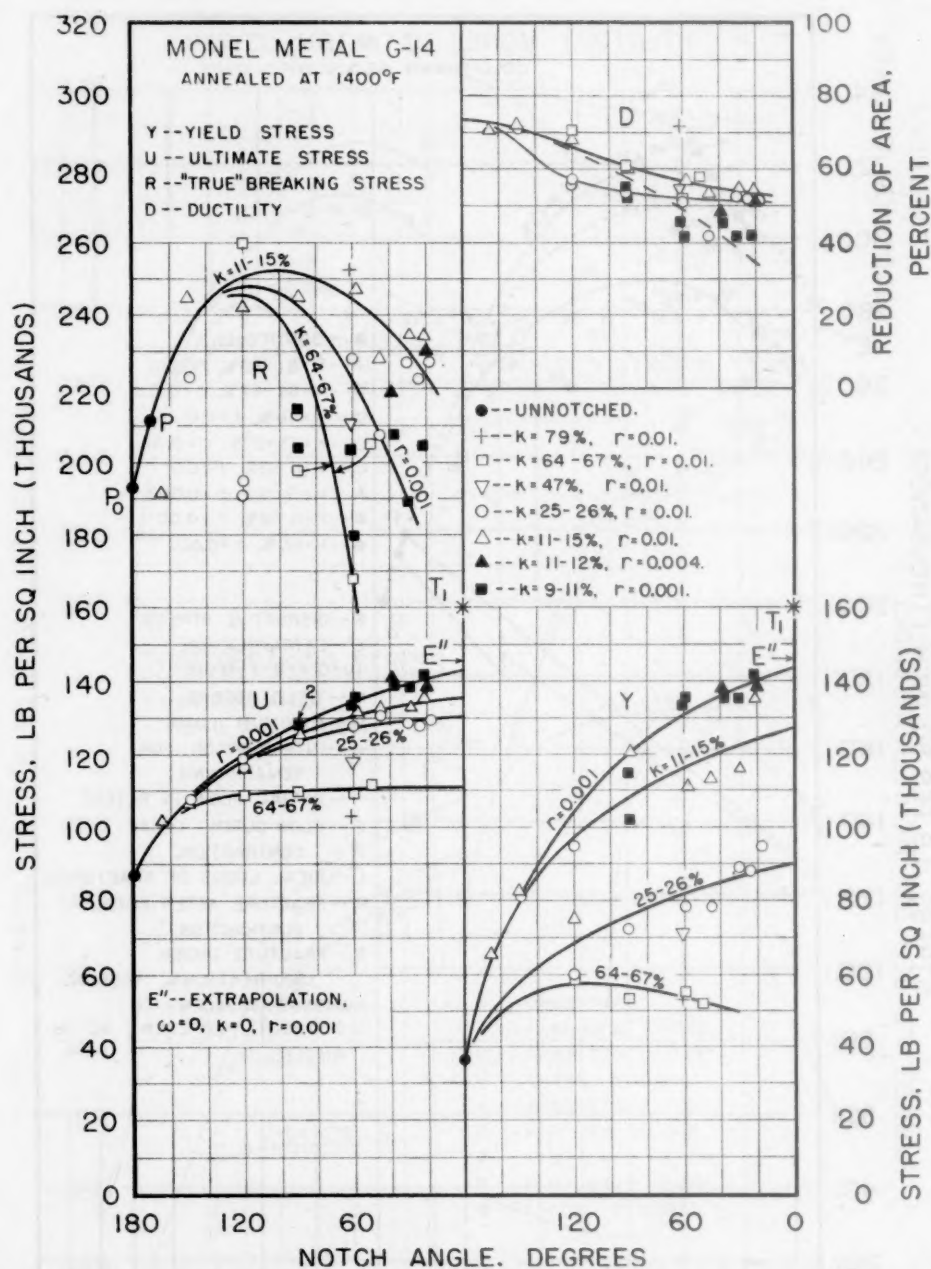


FIG. 13.—RELATION BETWEEN BREAKING STRESS AND DUCTILITY AS AFFECTED BY NOTCHES, COLD-DRAWN MONEL METAL.



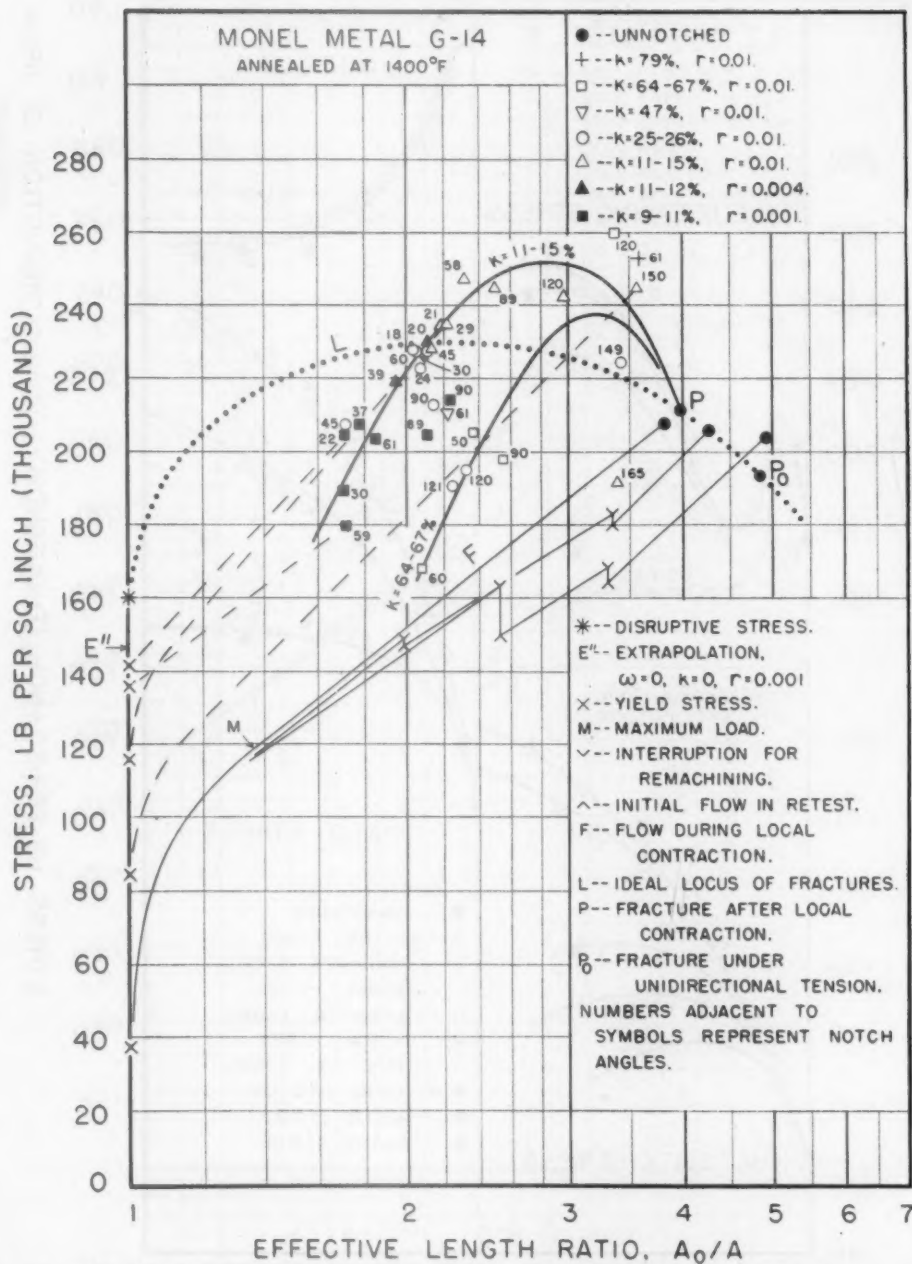


FIG. 15.—RELATION BETWEEN BREAKING STRESS AND DUCTILITY AS AFFECTED BY NOTCHES, ANNEALED MONEL METAL.

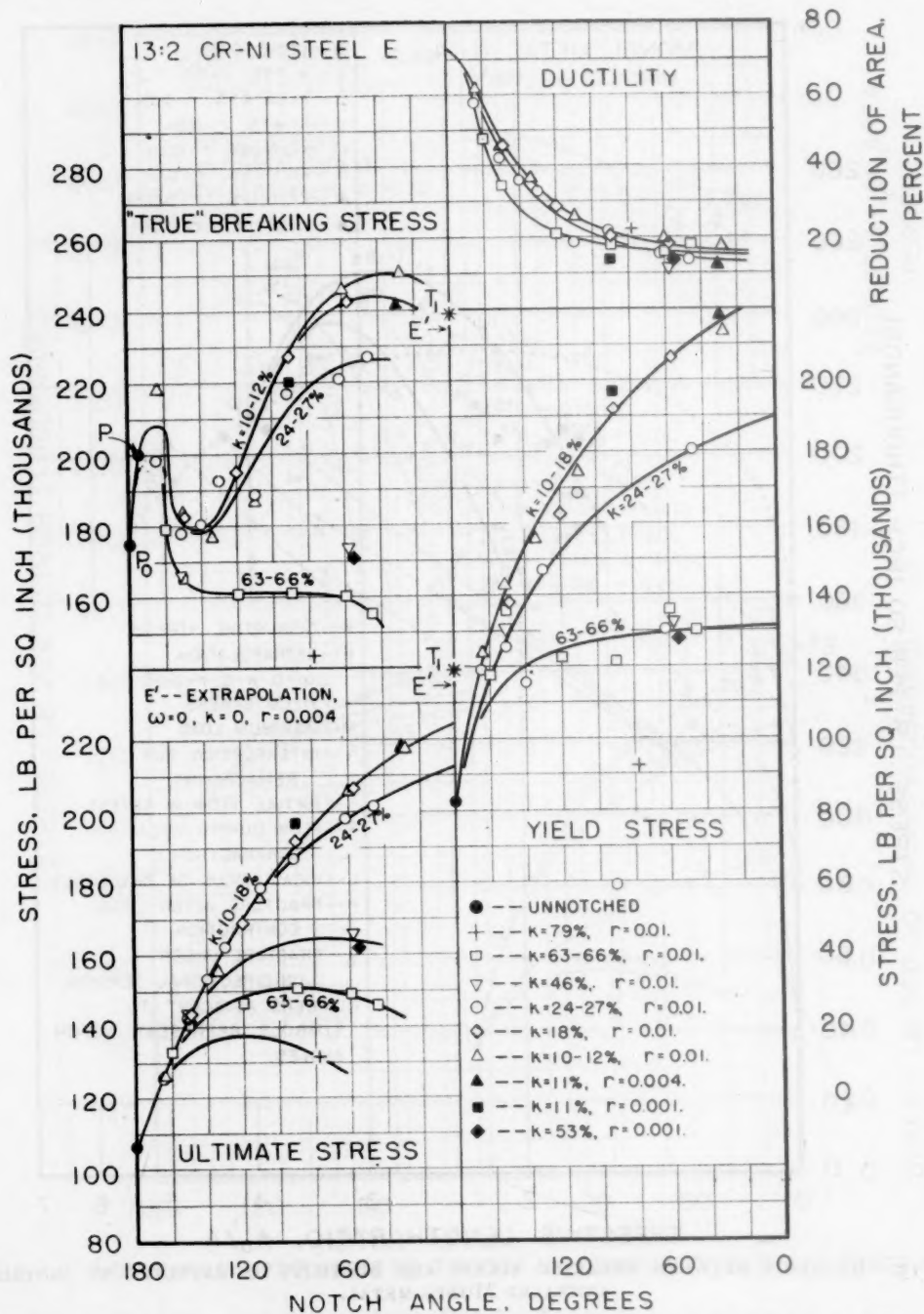


FIG. 16.—INFLUENCE OF NOTCH ANGLE ON STRENGTH AND DUCTILITY OF ANNEALED 13-2 CHROMIUM-NICKEL STEEL.

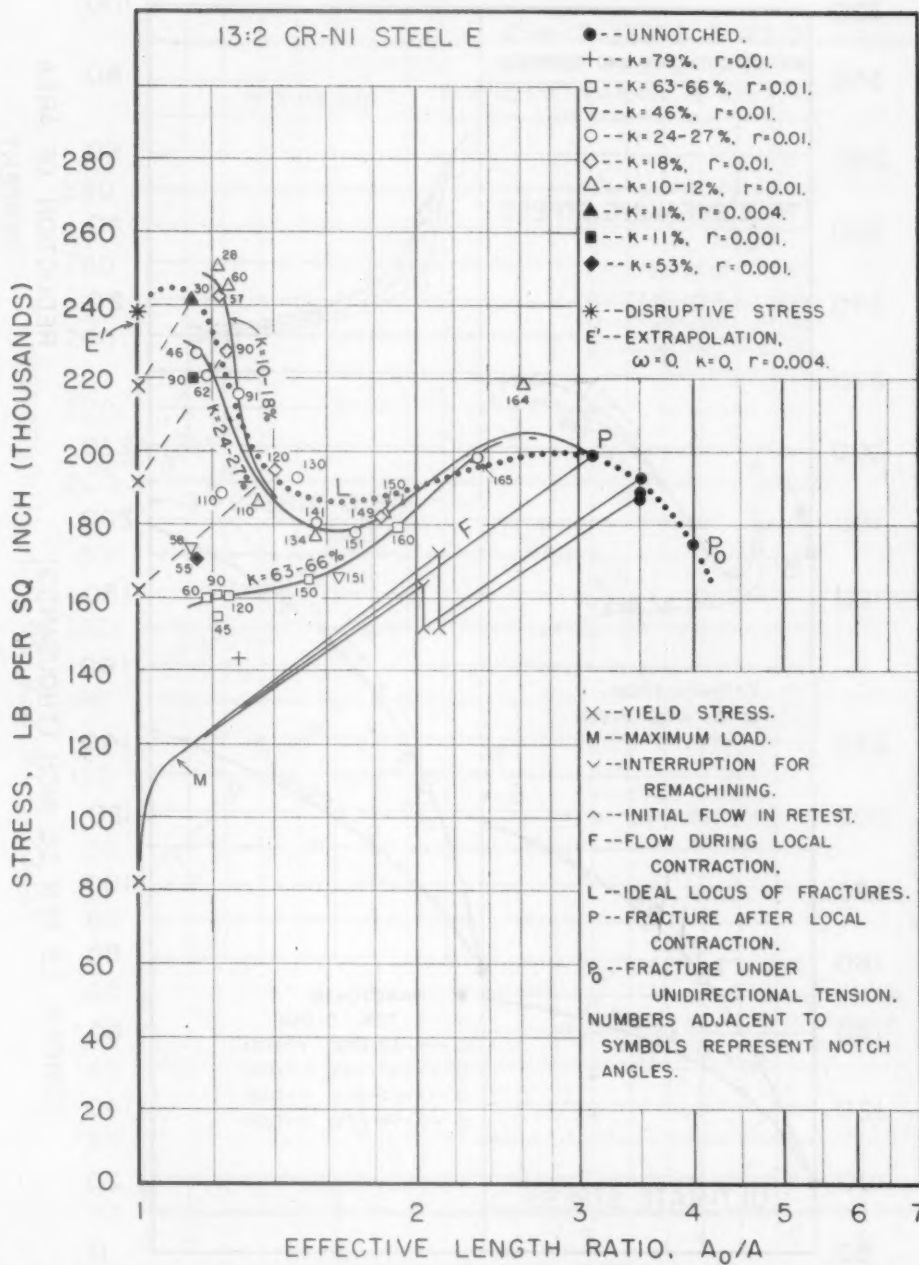


FIG. 17.—RELATION BETWEEN BREAKING STRESS AND DUCTILITY AS AFFECTED BY NOTCHES, ANNEALED 13-2 CHROMIUM-NICKEL STEEL.

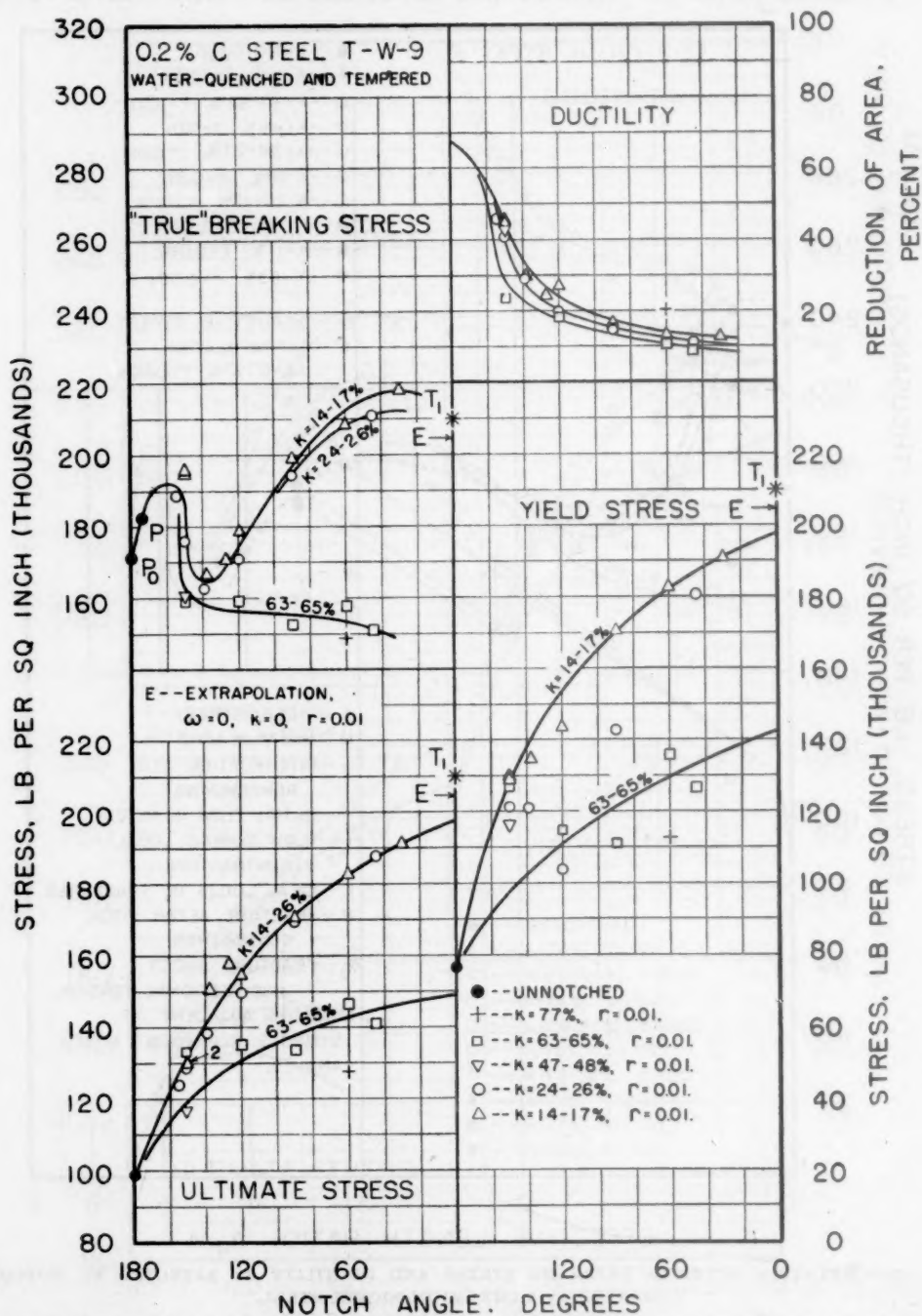


FIG. 18.—INFLUENCE OF NOTCH ANGLE ON STRENGTH AND DUCTILITY OF QUENCHED AND TEMPERED 0.2 PER CENT CARBON STEEL.

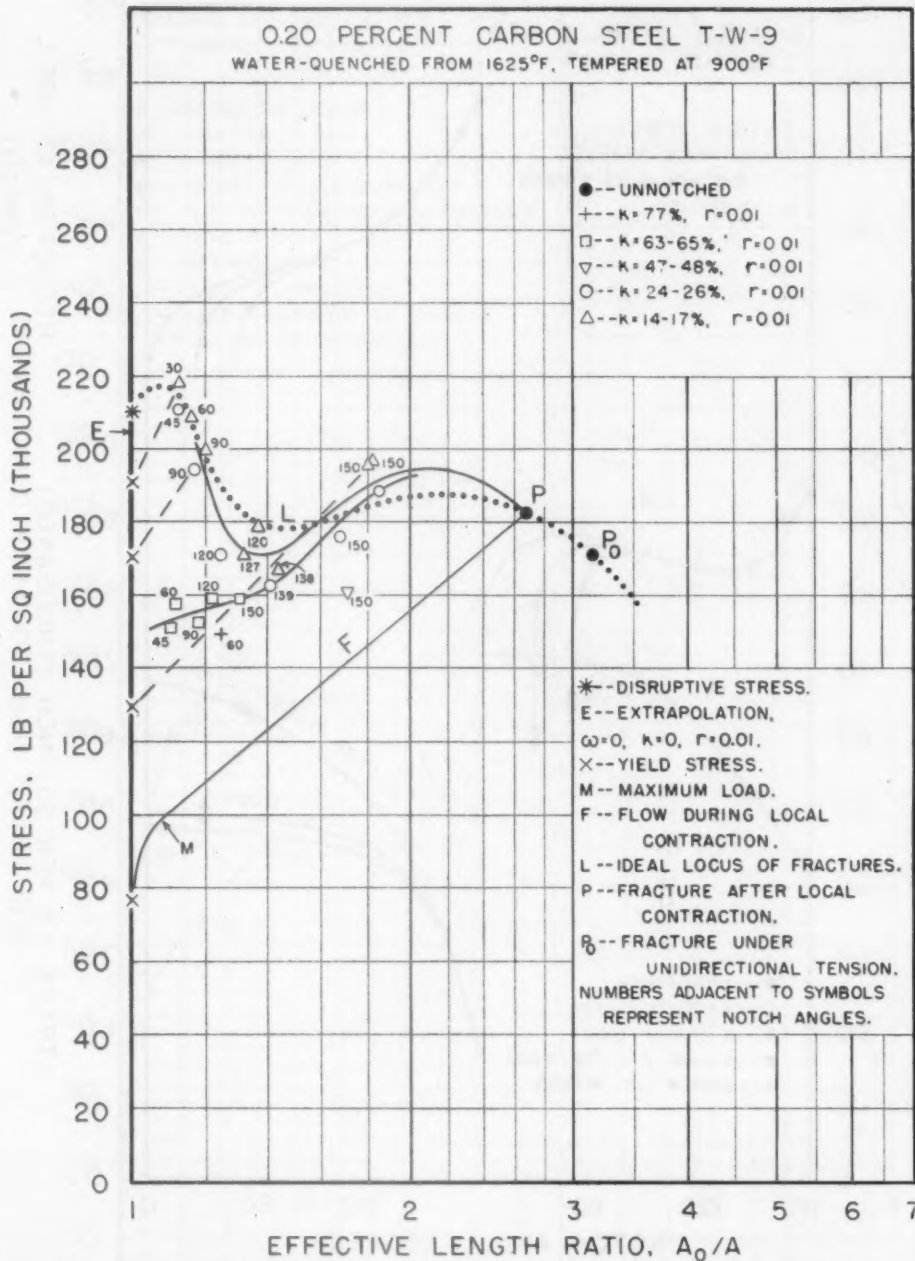


FIG. 19.—RELATION BETWEEN BREAKING STRESS AND DUCTILITY AS AFFECTED BY NOTCHES
QUENCHED AND TEMPERED 0.2 PER CENT CARBON STEEL.

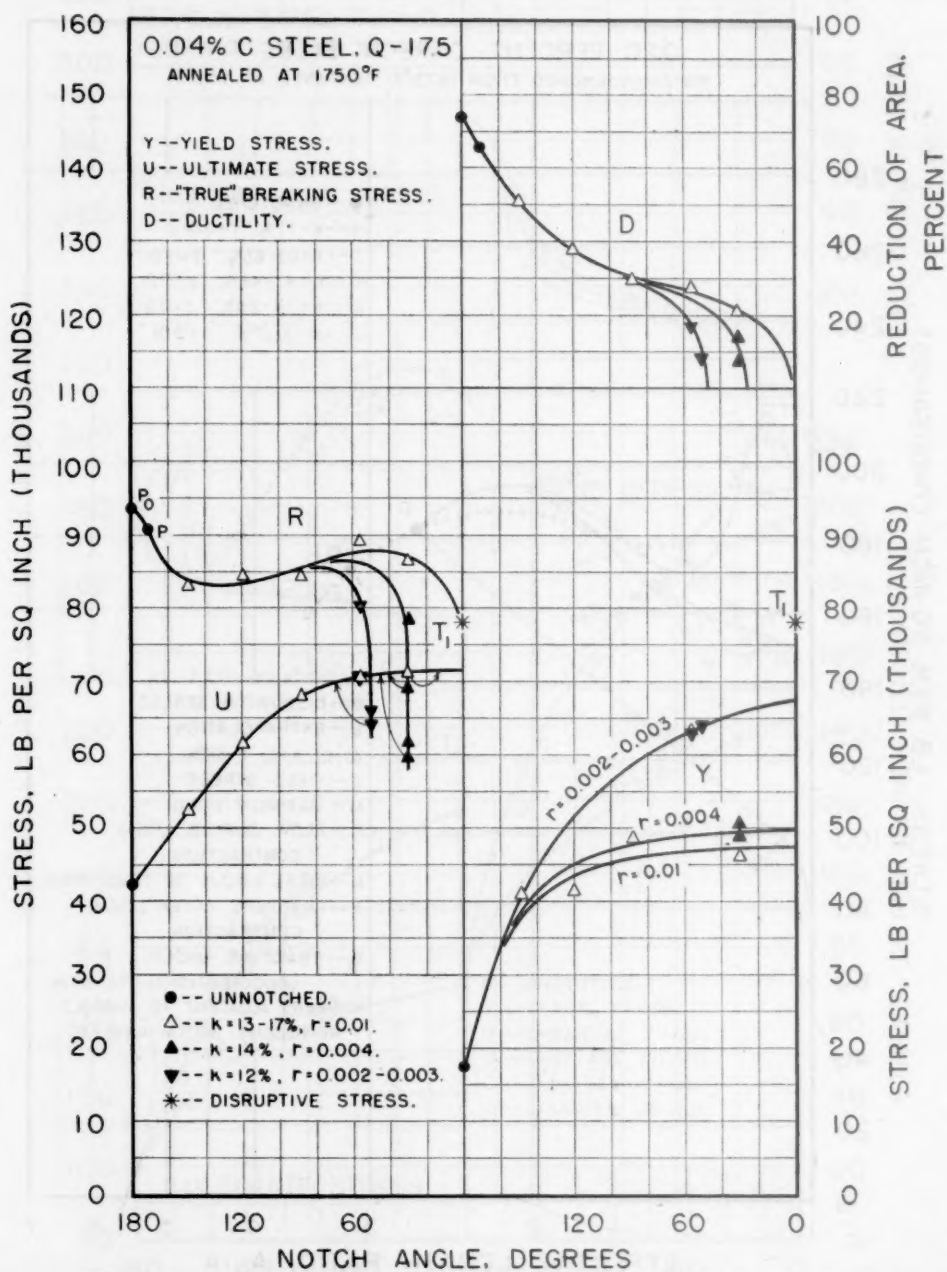


FIG. 20.—INFLUENCE OF NOTCH ANGLE ON STRENGTH AND DUCTILITY OF ANNEALED 0.04 PER CENT CARBON STEEL.

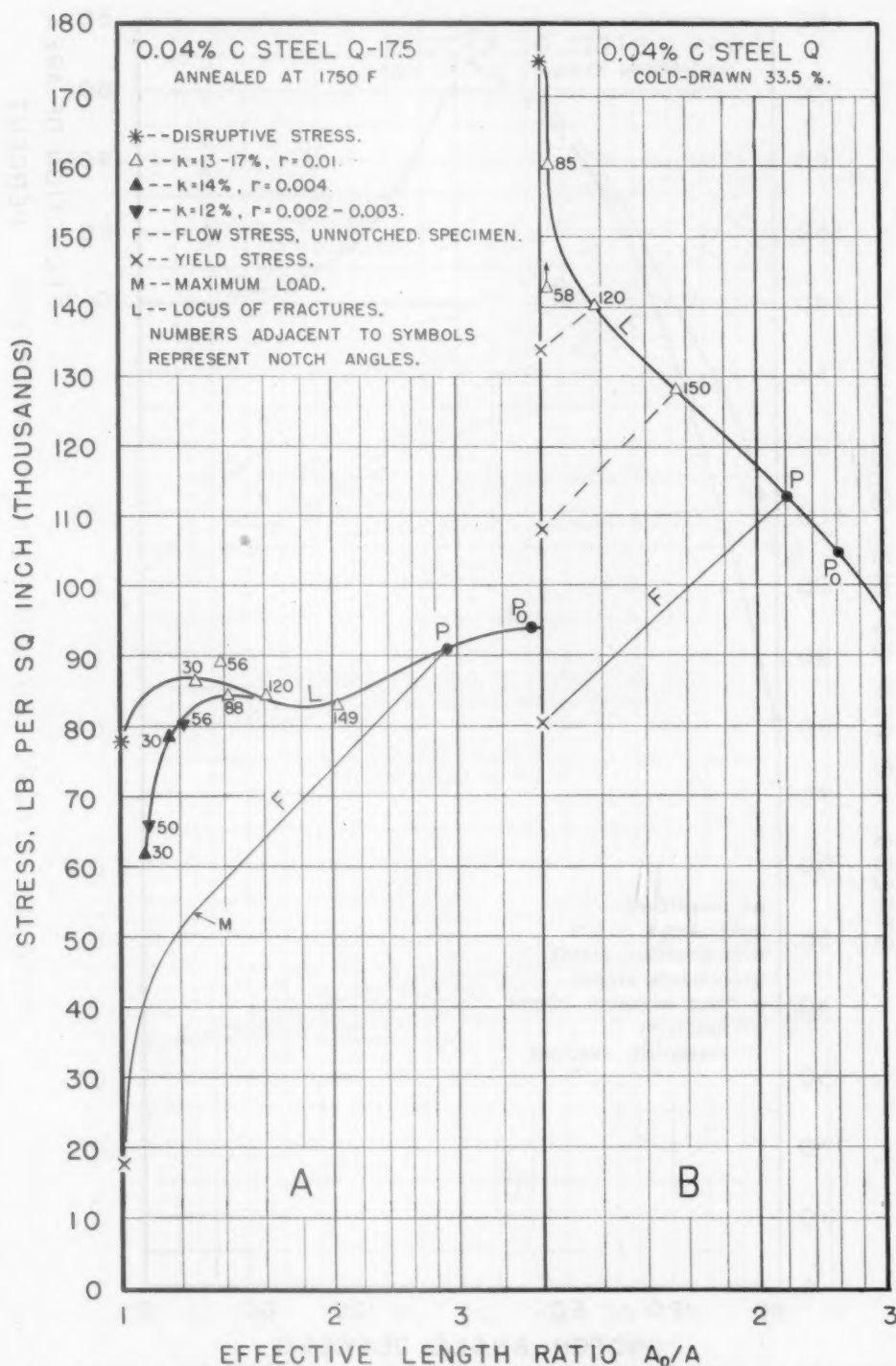


FIG. 21.—RELATION BETWEEN BREAKING STRESS AND DUCTILITY AS AFFECTED BY NOTCHES, ANNEALED AND COLD-DRAWN 0.04 PER CENT CARBON STEEL.

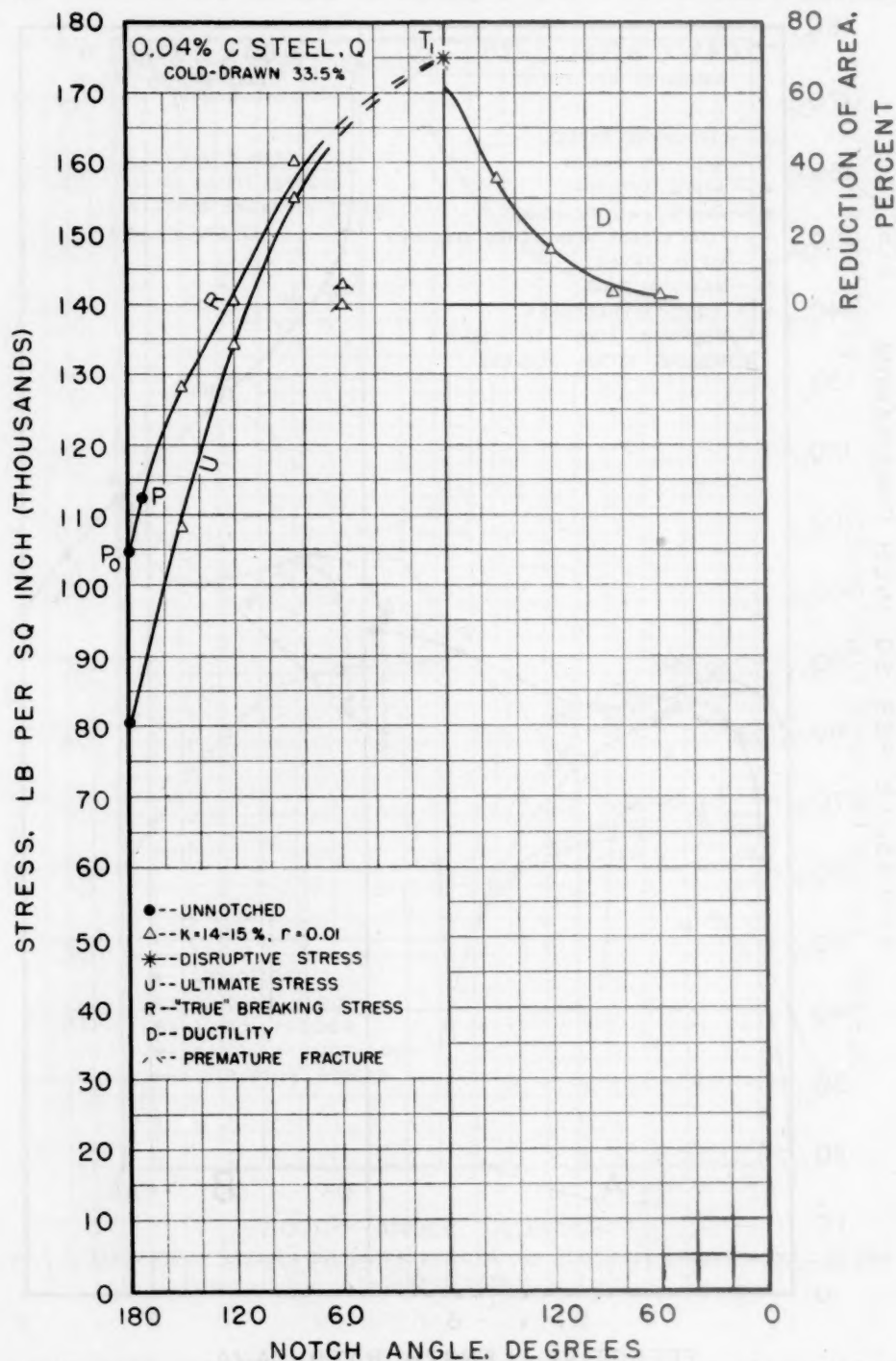
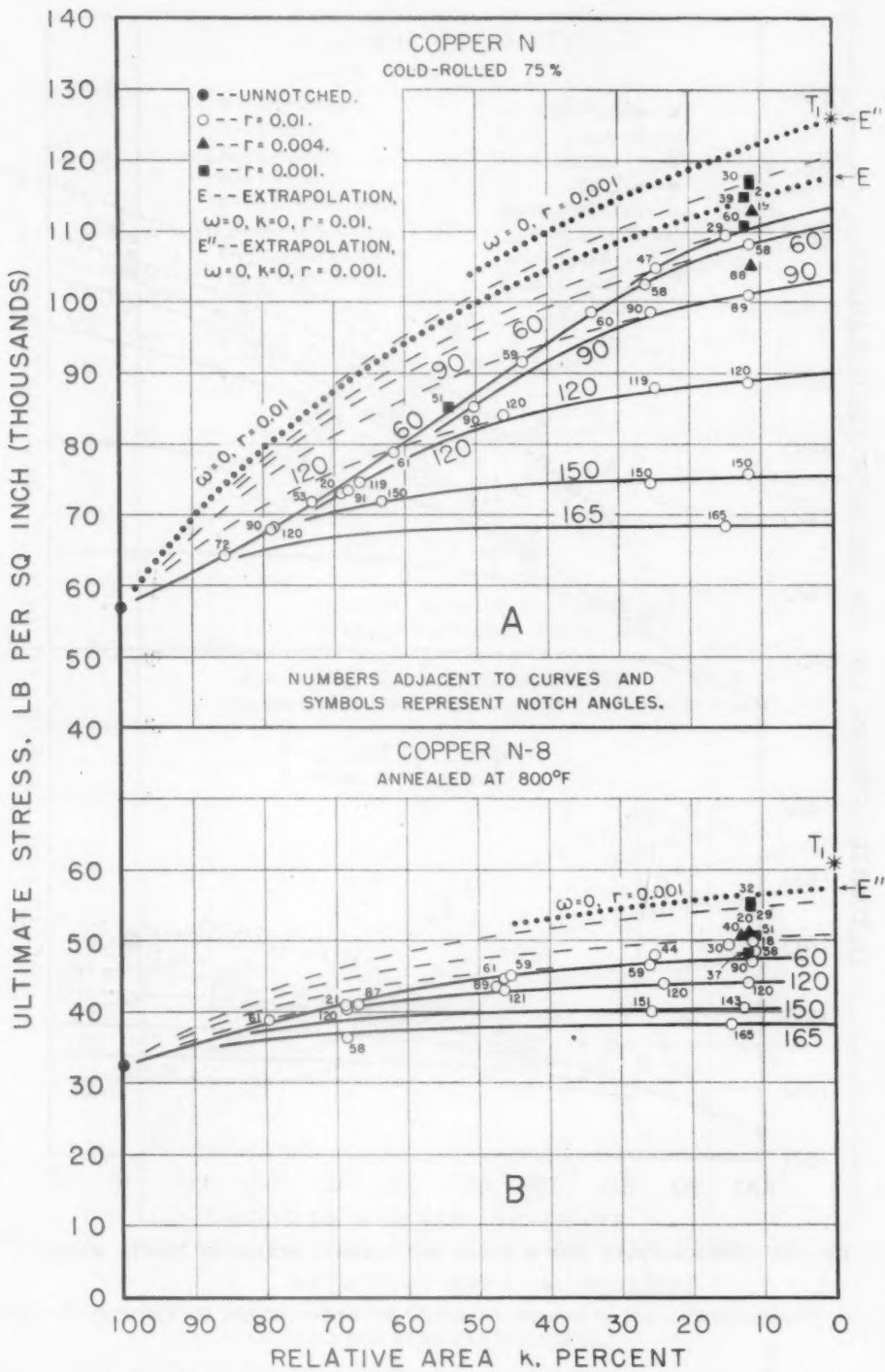


FIG. 22.—INFLUENCE OF NOTCH ANGLE ON STRENGTH AND DUCTILITY OF COLD-DRAWN 0.04 PER CENT CARBON STEEL.



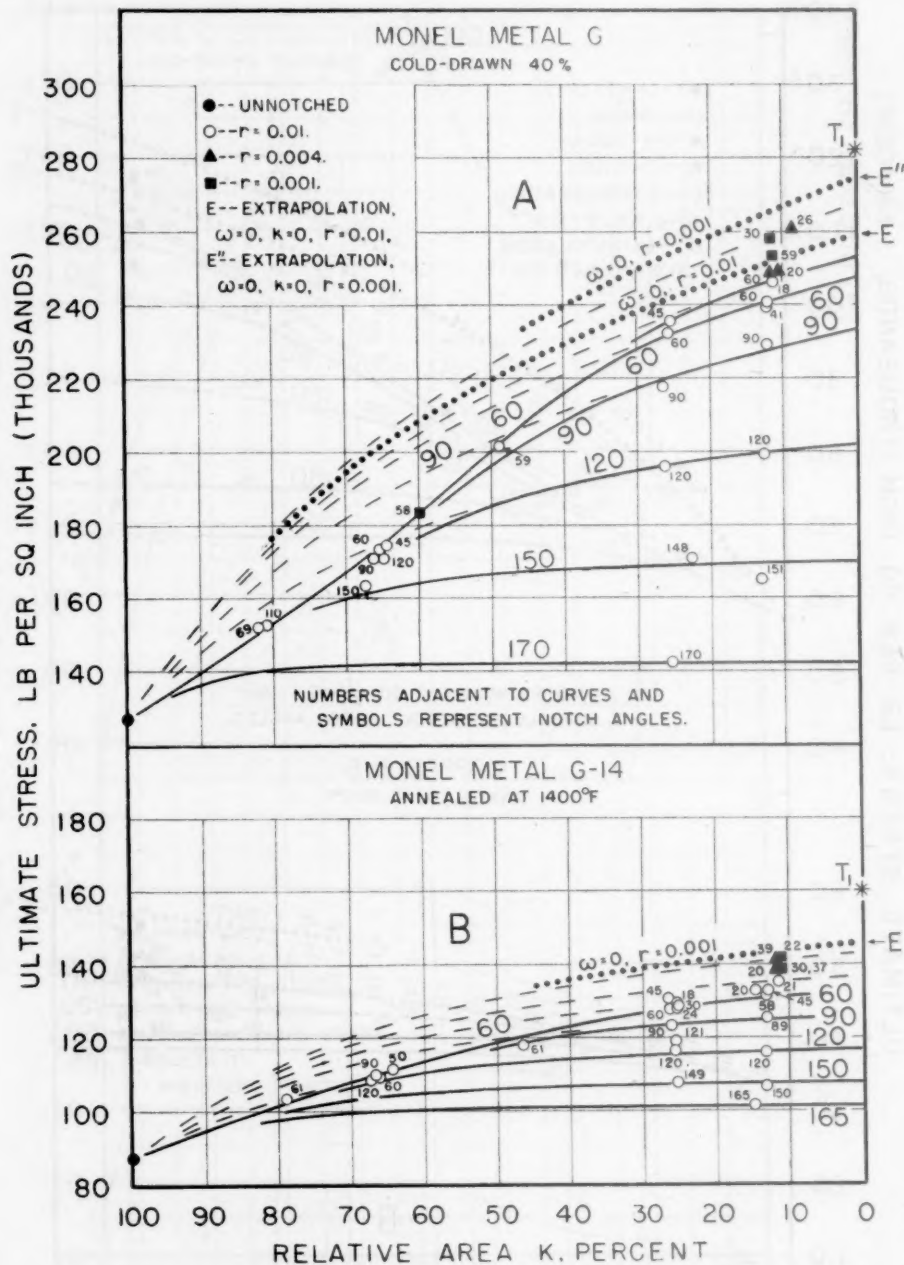


FIG. 24.—INFLUENCE OF NOTCH DEPTH ON ULTIMATE STRESS OF MONEL METAL.

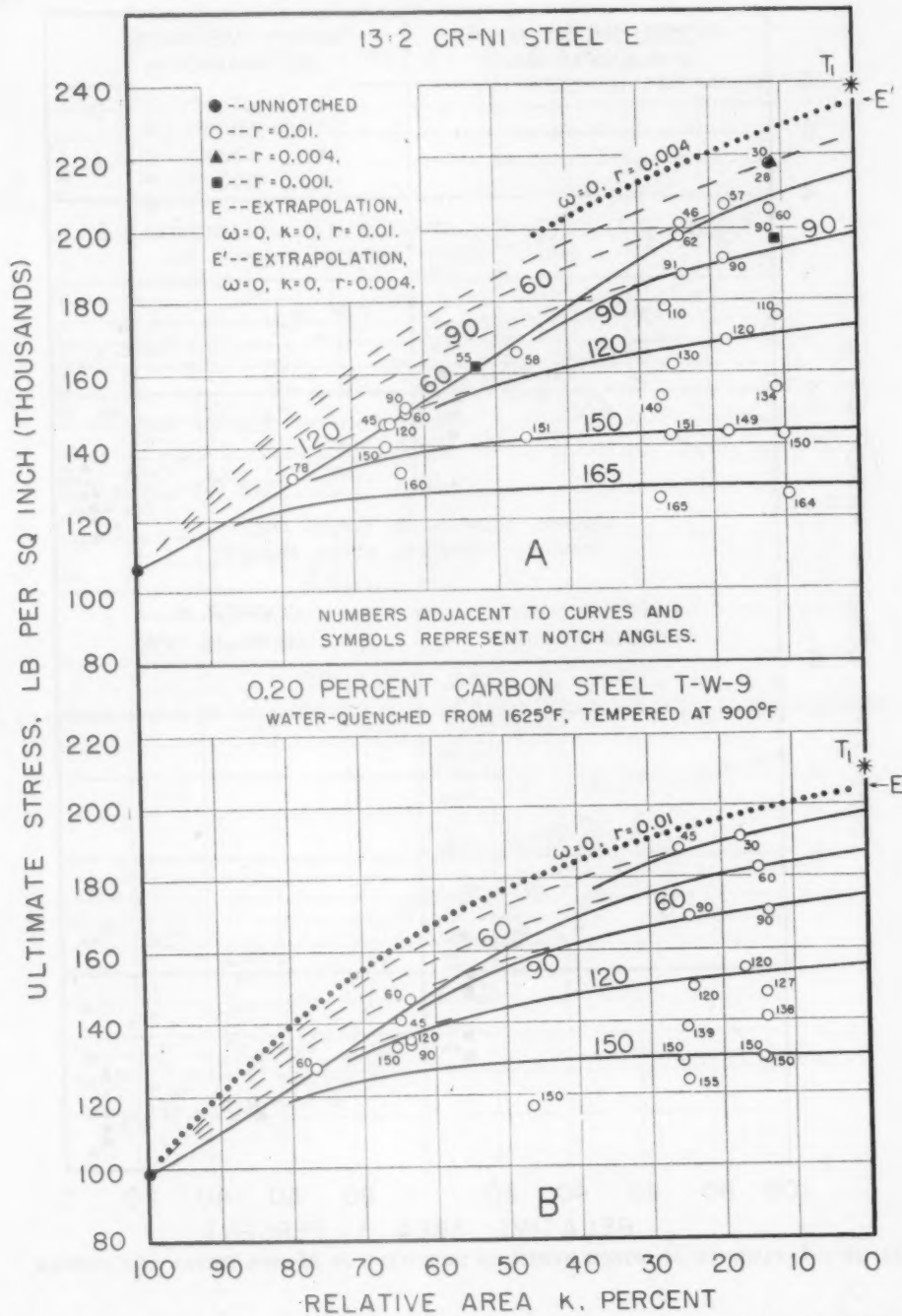


FIG. 25.—INFLUENCE OF NOTCH DEPTH ON ULTIMATE STRESS OF 13-2 CHROMIUM-NICKEL AND OF 0.2 PERCENT CARBON STEEL.

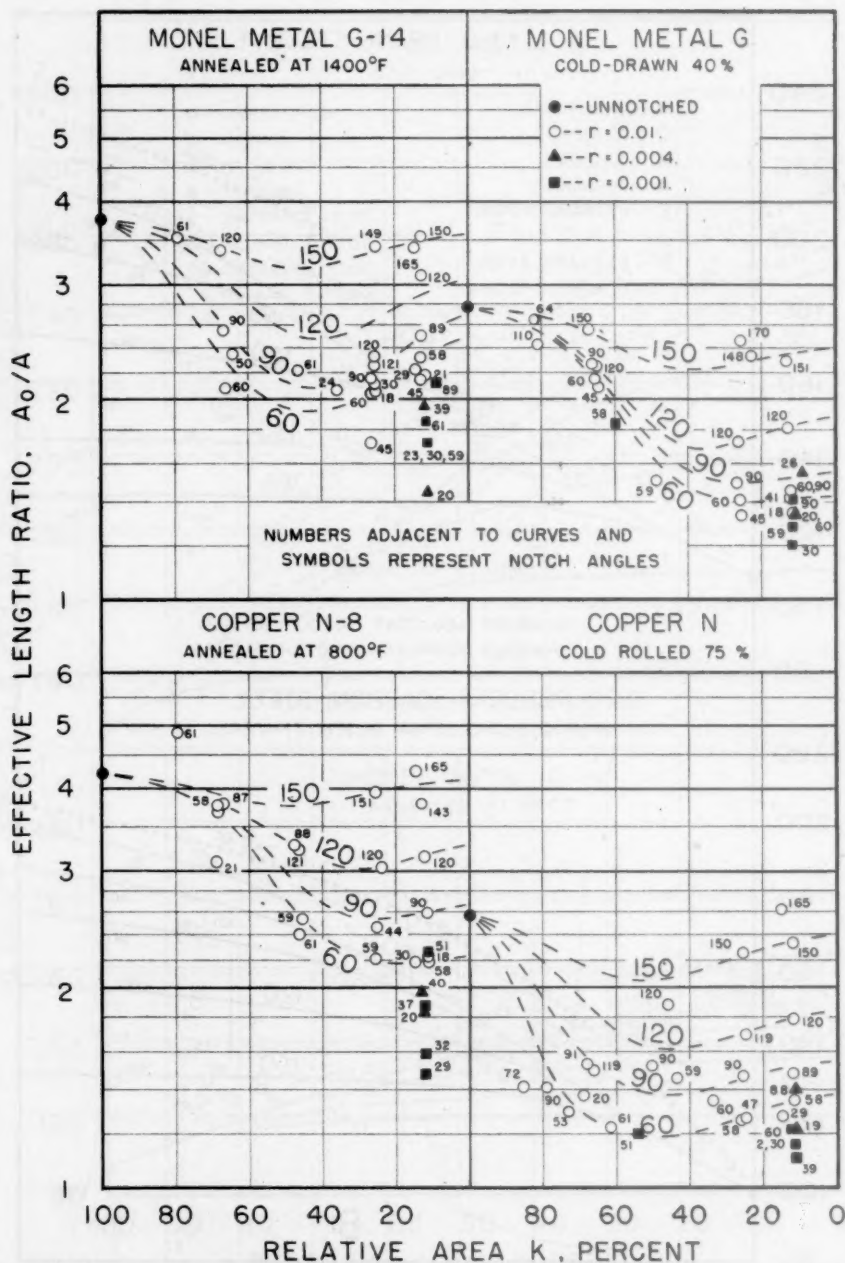


FIG. 26.—INFLUENCE OF NOTCH DEPTH ON DUCTILITY OF MONEL METAL AND COPPER.

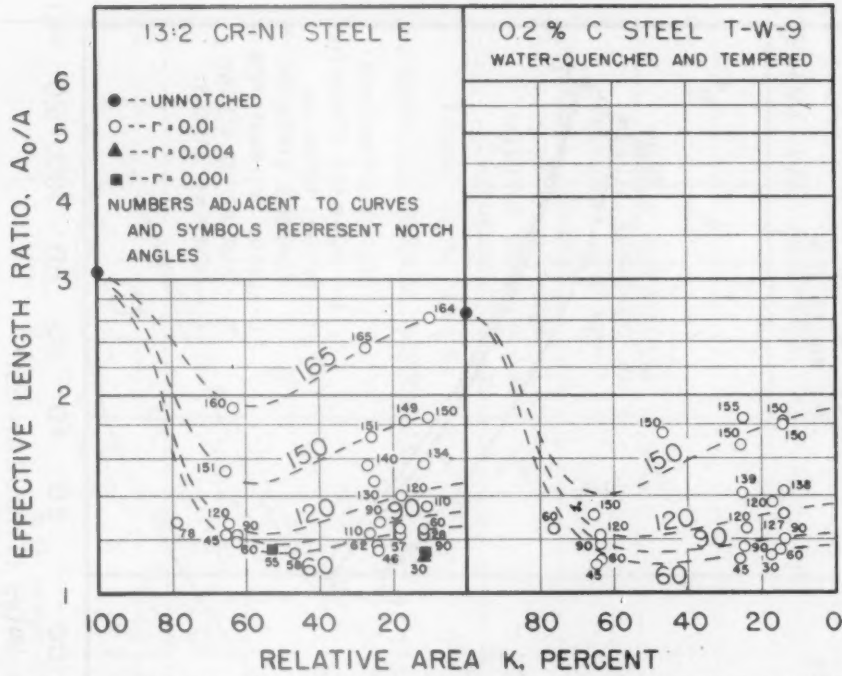


FIG. 27.—INFLUENCE OF NOTCH DEPTH ON DUCTILITY OF 13-2 CHROMIUM-NICKEL AND OF 0.2 PER CENT CARBON STEEL.

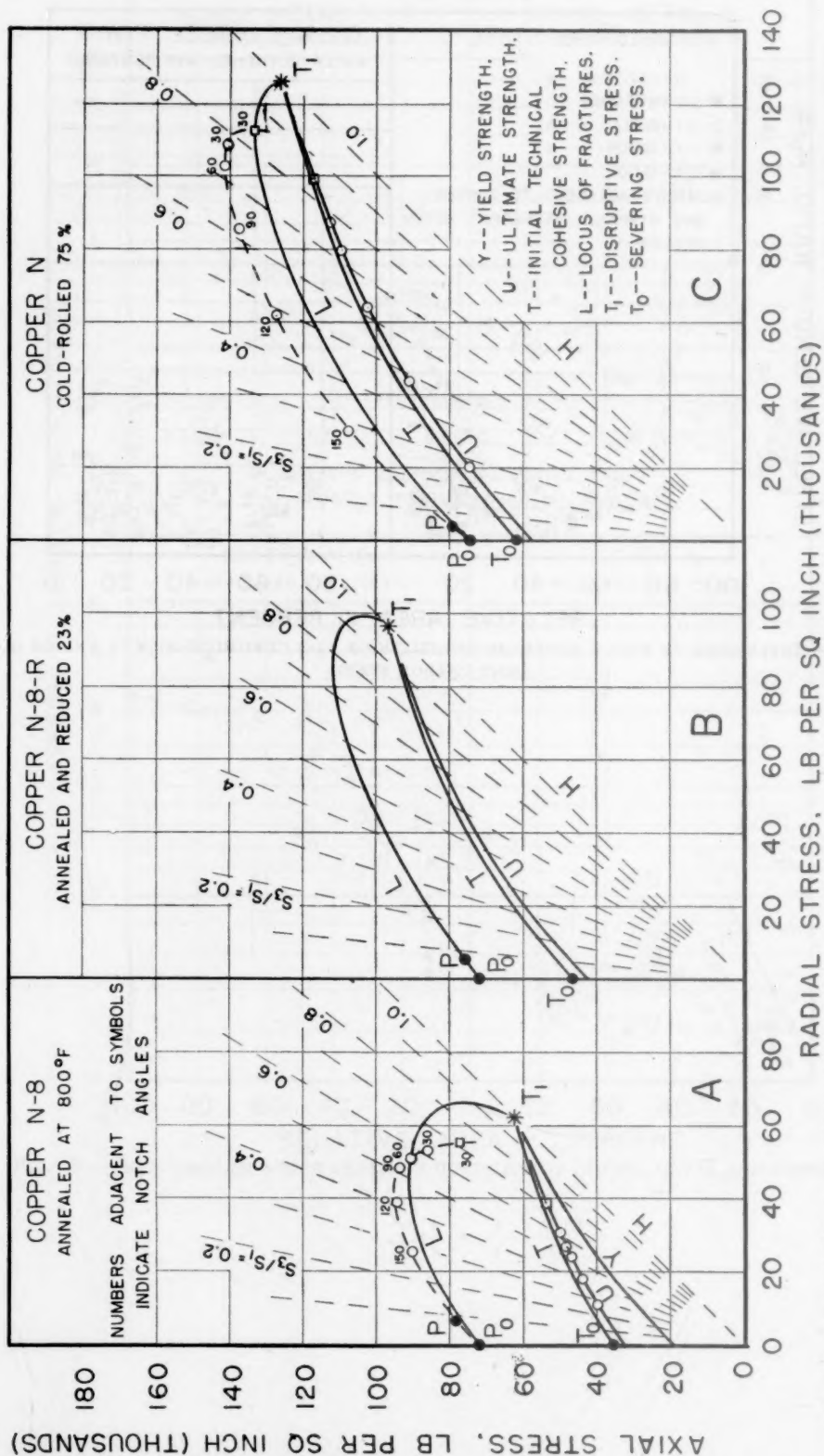
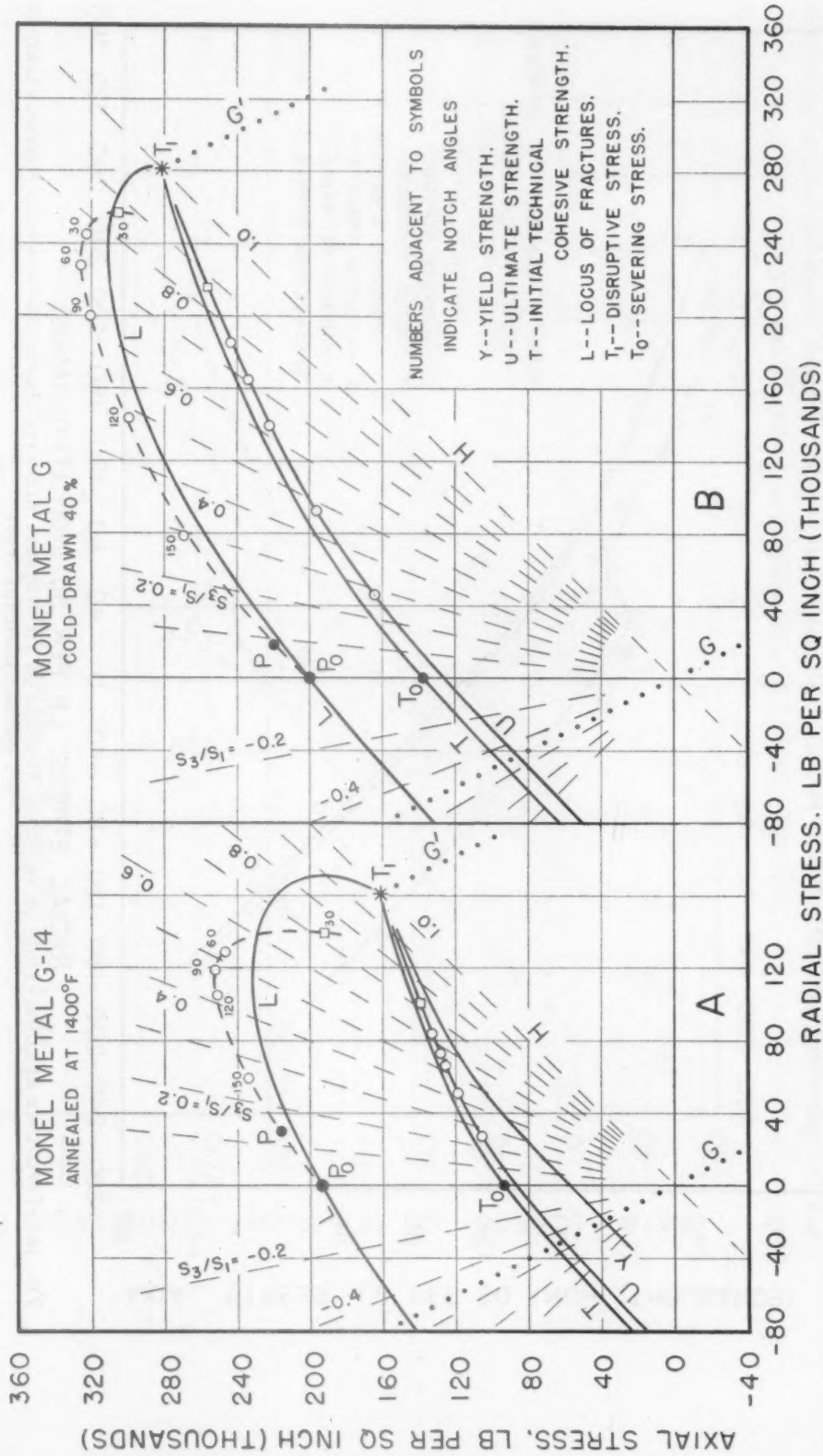


FIG. 28.—INFLUENCE OF COMBINATION OF PRINCIPAL STRESSES ON YIELD STRESS, ULTIMATE STRESS AND TECHNICAL COHESION LIMIT OF COPPER.



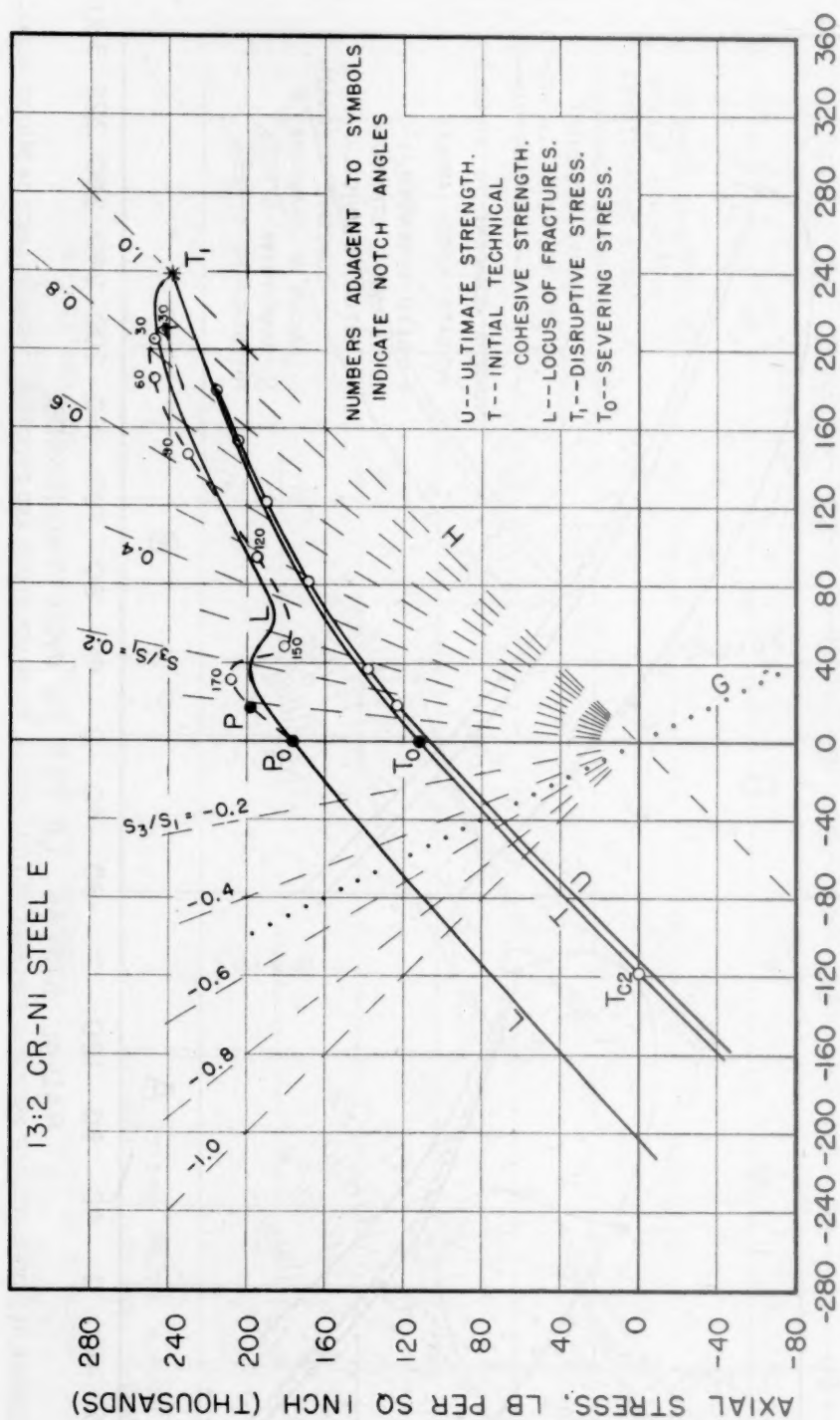


FIG. 30.—INFLUENCE OF COMBINATION OF PRINCIPAL STRESSES ON YIELD STRESS, ULTIMATE STRESS AND TECHNICAL COHESION LIMIT OF 13-2 CHROMIUM-NICKEL STEEL.

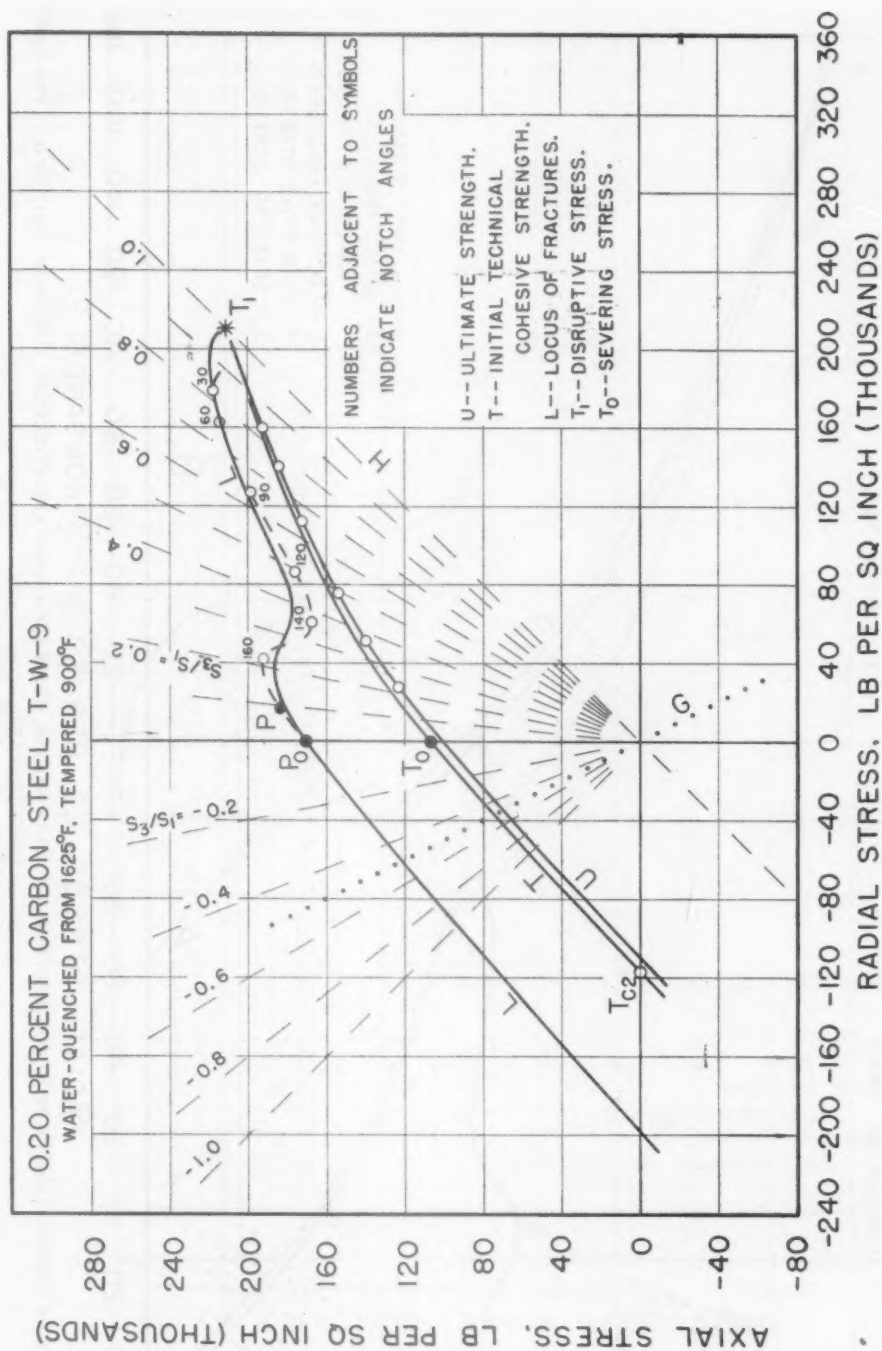
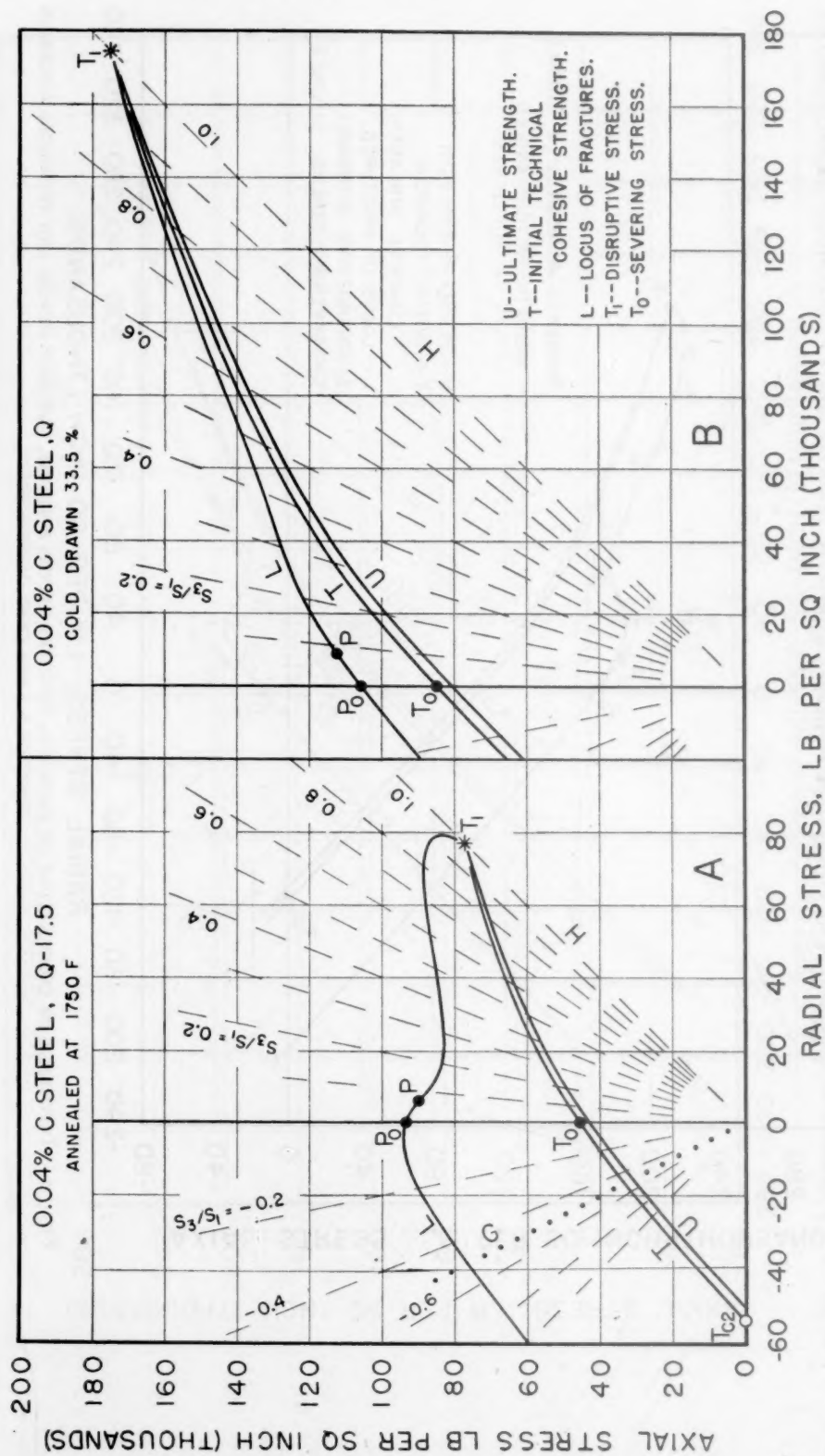


FIG. 31.—INFLUENCE OF COMBINATION OF PRINCIPAL STRESSES ON YIELD STRESS, ULTIMATE STRESS AND TECHNICAL COHESION LIMIT OF 0.2 PER CENT CARBON STEEL.



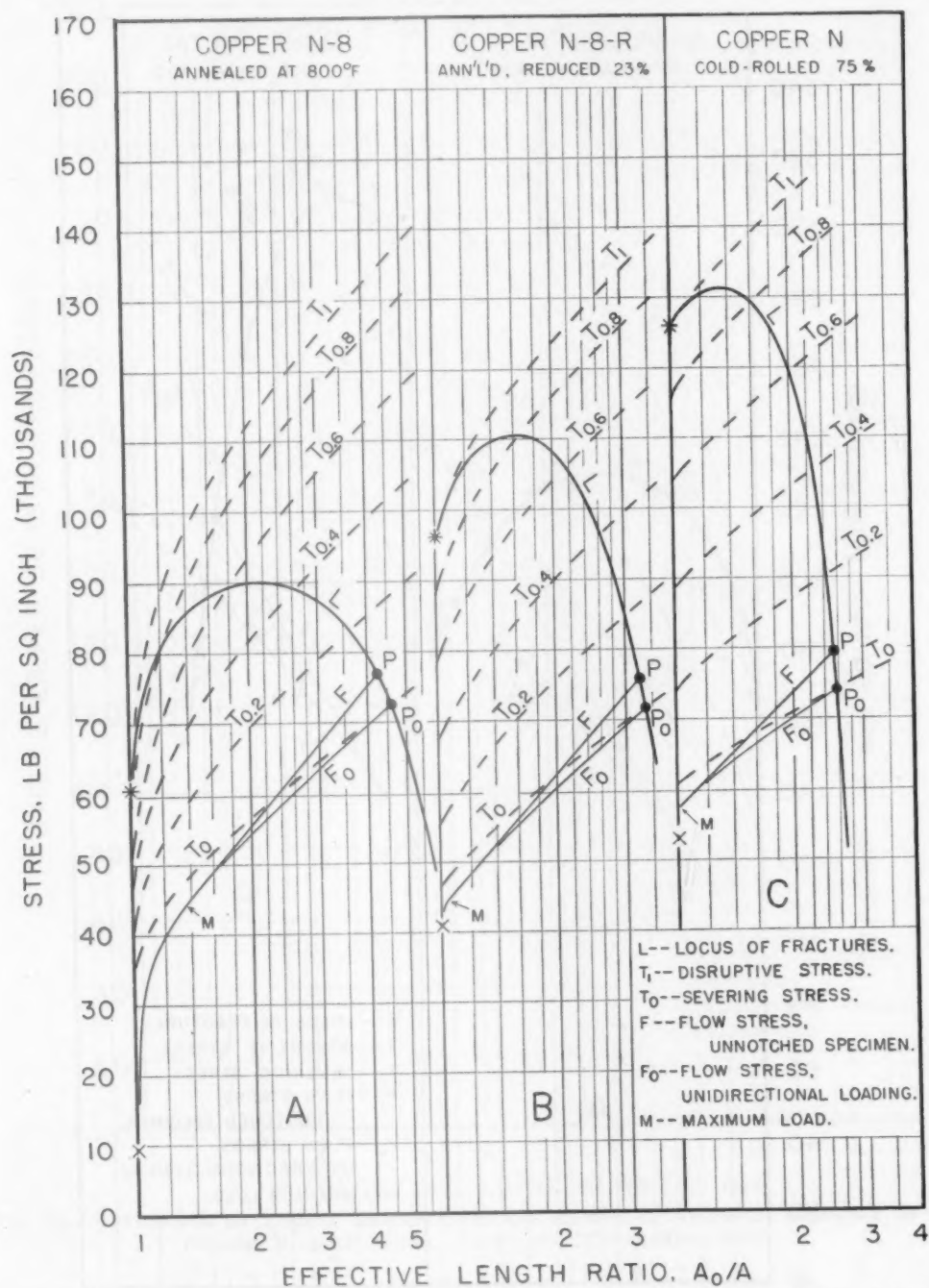


FIG. 33.—INFLUENCE OF PLASTIC DEFORMATION ON TECHNICAL COHESIVE STRENGTH OF COPPER.

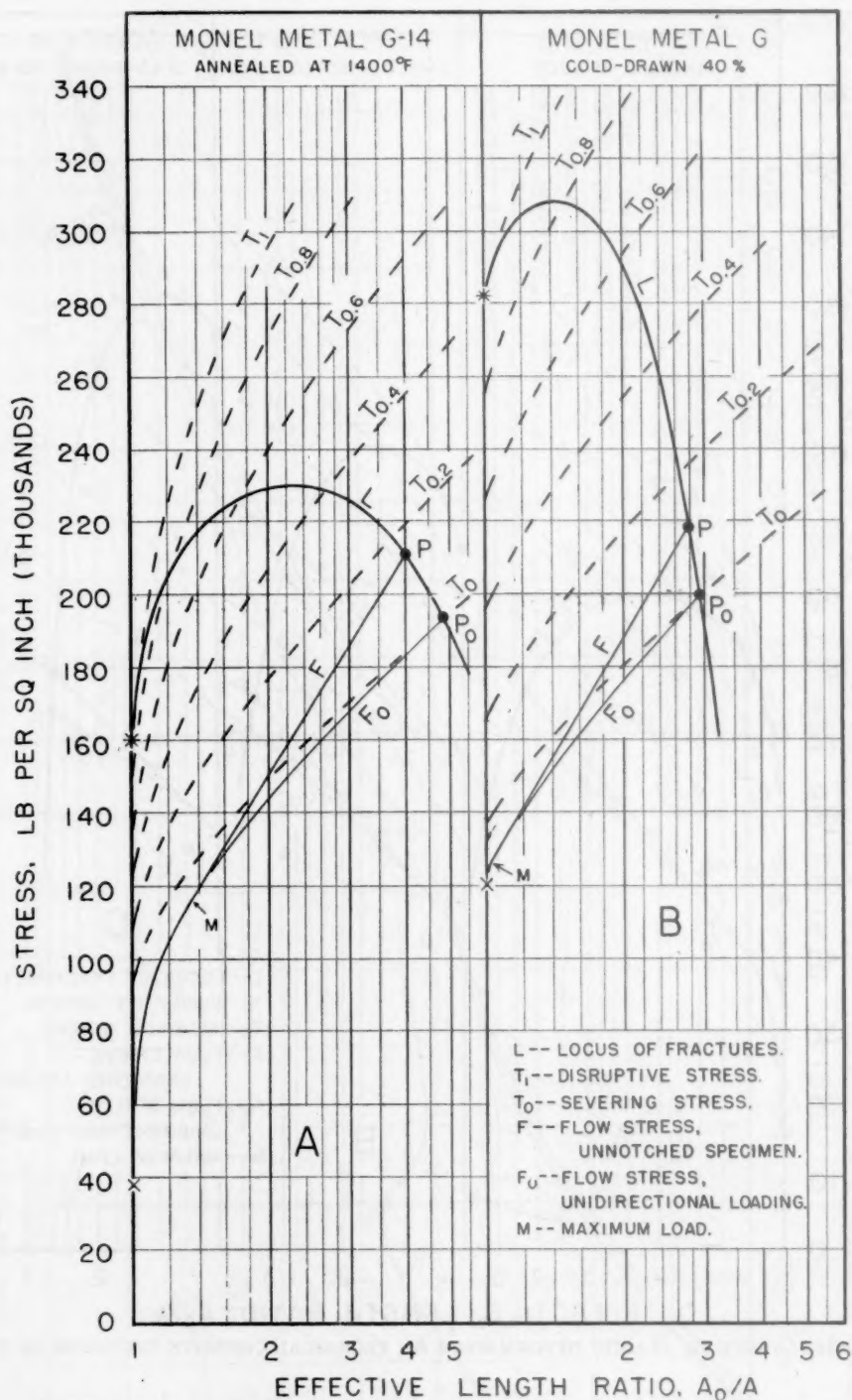


FIG. 34.—INFLUENCE OF PLASTIC DEFORMATION ON TECHNICAL COHESIVE STRENGTH OF MONEL METAL.

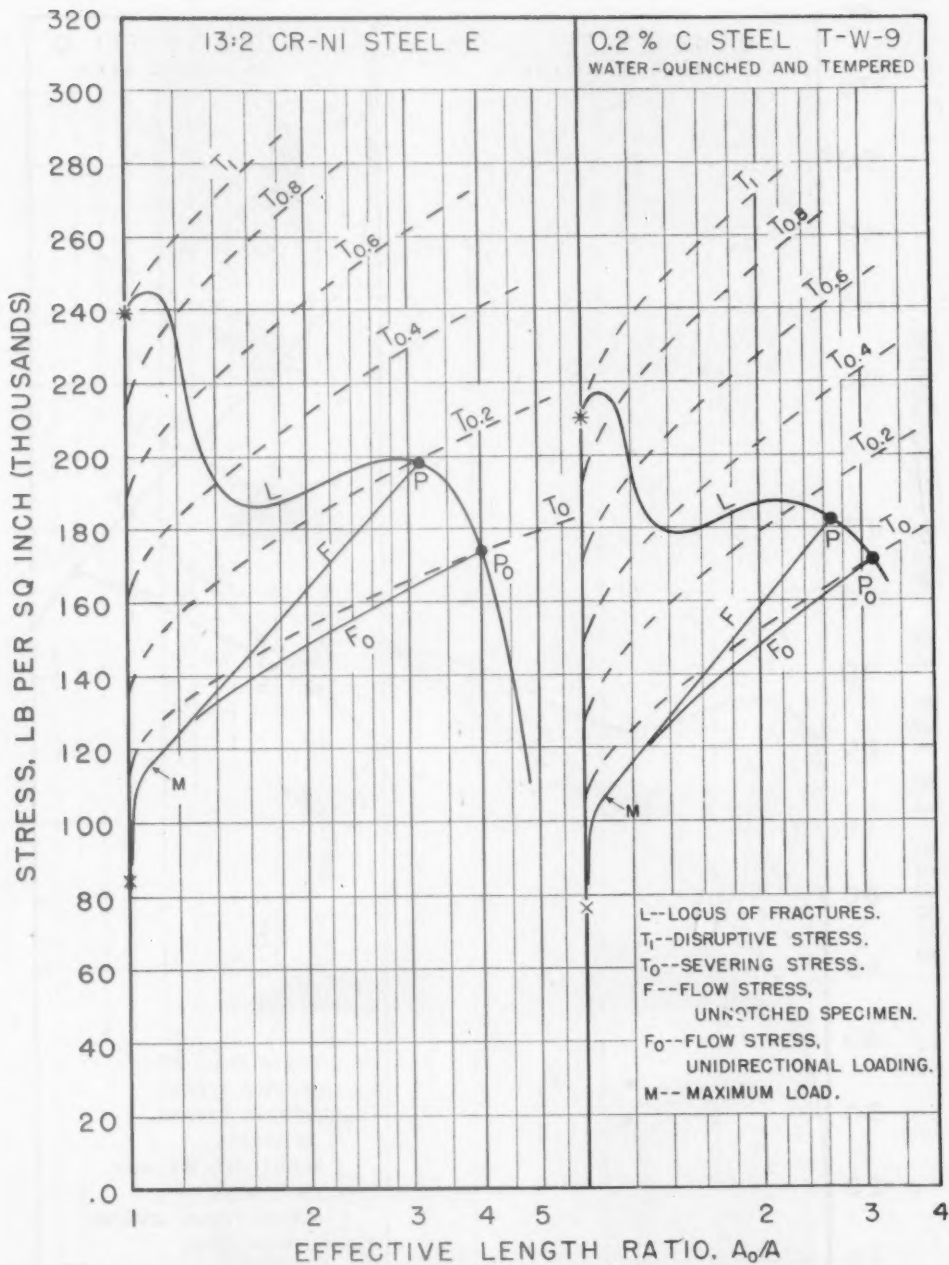


FIG. 35.—INFLUENCE OF PLASTIC DEFORMATION ON TECHNICAL COHESIVE STRENGTH OF 13-2 CHROMIUM-NICKEL STEEL AND 0.2 PER CENT CARBON STEEL.

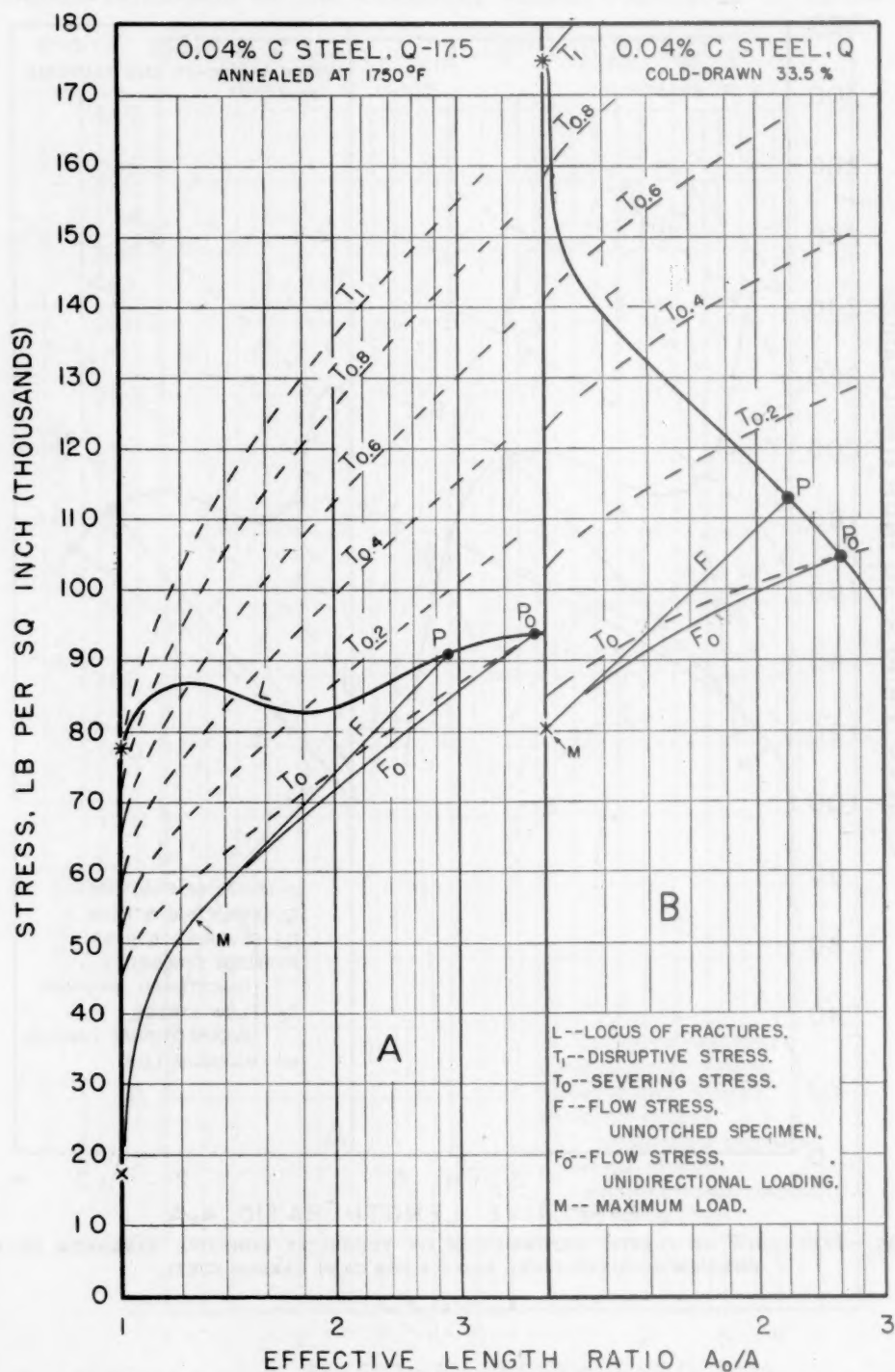


FIG. 36.—INFLUENCE OF PLASTIC DEFORMATION ON TECHNICAL COHESIVE STRENGTH OF 0.04 PER CENT CARBON STEEL.

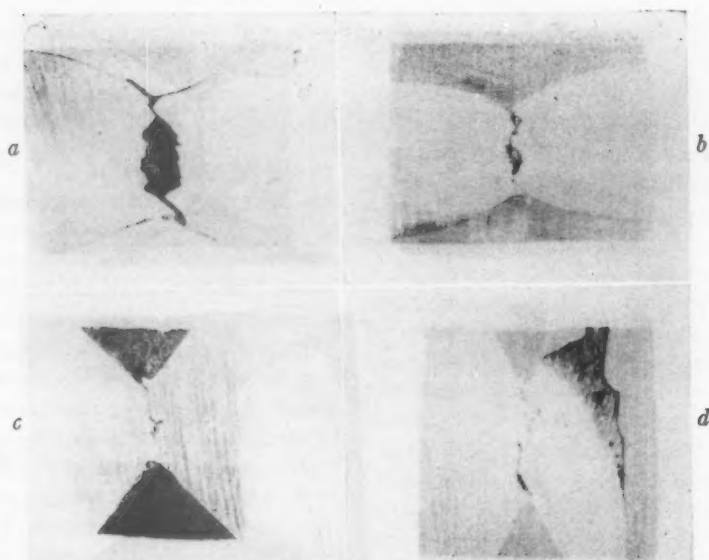


FIG. 37.—LONGITUDINAL SECTIONS OF FRACTURED COPPER SPECIMENS.

- a. Cold-rolled copper, unnotched specimen.
- b. Cold-rolled copper, $k = 0.15$, $\omega = 165^\circ$.
- c. Cold-rolled copper, $k = 0.12$, $\omega = 120^\circ$.
- d. Cold-rolled copper, $k = 0.11$, $\omega = 50^\circ$.

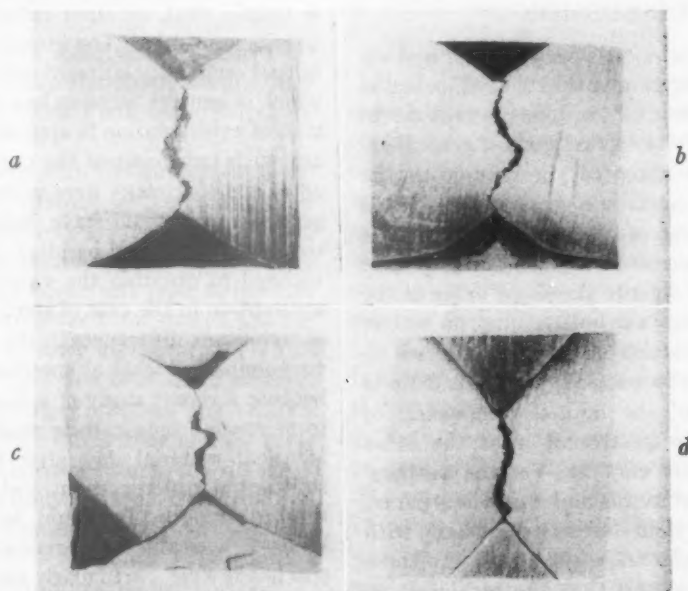


FIG. 38.—LONGITUDINAL SECTIONS OF FRACTURED COPPER SPECIMENS.

- a. Cold-rolled copper, $k = 0.79$, $\omega = 150^\circ$.
- b. Cold-rolled copper, $k = 0.79$, $\omega = 120^\circ$.
- c. Annealed copper, $k = 0.12$, $\omega = 120^\circ$.
- d. Annealed copper, $k = 0.12$, $\omega = 90^\circ$.

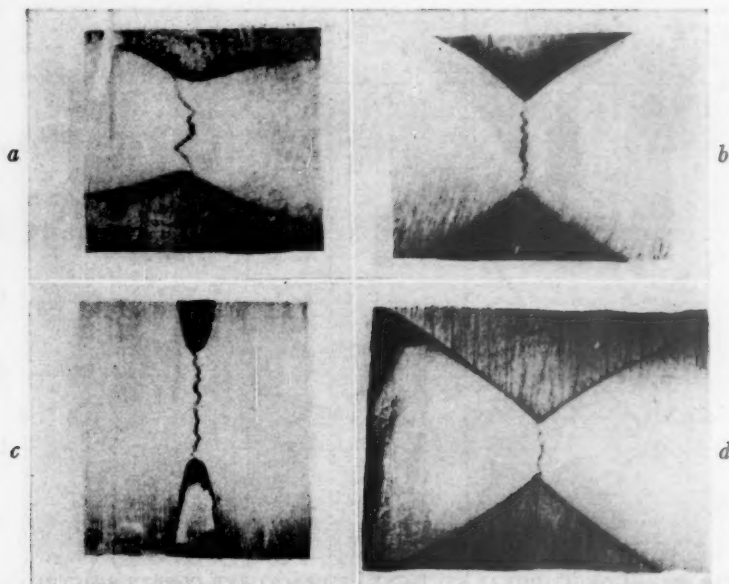


FIG. 39.—LONGITUDINAL SECTION OF FRACTURED MONEL-METAL SPECIMENS.

- a. Cold-drawn Monel metal, $k = 0.26$, $\omega = 170^\circ$.
- b. Cold-drawn Monel metal, $k = 0.13$, $\omega = 120^\circ$.
- c. Cold-drawn Monel metal, $k = 0.11$, $\omega = 18^\circ$.
- d. Annealed Monel metal, $k = 0.13$, $\omega = 120^\circ$.

DISCUSSION

K. HEINDLHOFFER.*—The wealth of new experimental material in this extensive paper, as interpreted by the authors, tends to raise doubt as to the validity of two important generalizations, currently accepted, pertaining to the behavior of a metal subjected to combined stresses. The first of these states that, in a polycrystalline metal in a given state, plastic flow begins at a definite threshold value of the elastic shear energy per unit volume, no matter what the combination of principal stresses is; the second, that the metal ruptures at a definite limiting value of the normal component of tensile stress, irrespective of what the other stress components may be. Yet the authors' results, presented in this and a previous paper, indicate that yield stress decreases with increase of the algebraic average of the three principal stresses, and that the technical cohesive limit does depend upon the stress combination. These generalizations have been so useful to engineers as a basis of design that it would seem unwise, as a practical matter, to discard them, on the basis of the authors' measurements on notched specimens, until it

is certain that no other interpretation of the data is admissible. The interpretation is based in part on extrapolation of curves the course of which in general becomes less certain as the region of extrapolation is approached; moreover, any such treatment of the curves implies that all of the specimens were isotropic and homogeneous and would have behaved alike had they been made and handled identically. I am inclined to question the validity of this tacit assumption in the case of steel, in part because of significant differences in the authors' results on nominally identical specimens, but mainly because a recent study of a large mass of data from routine tensile tests made on nominally identical material day after day showed up substantial differences in yield strength and tensile strength. It would be interesting to know how really homogeneous the authors' specimens were, particularly those tested under the more extreme conditions (e.g., a sharp notch) where any lack of isotropy would be expected to exert the largest effect on the result of the test. In any case it is probable that any lack of validity there may be in the two generalizations above is of little consequence to the designing engineer because he is dealing with materials whose tensile properties are not

* Research Laboratory, U. S. Steel Corporation, Kearny, N. J.

the same from one piece to another, but vary over a range the width of which cannot safely be assumed to be less than 10 per cent of the value of the property.

R. C. STURM.*—The authors have presented some very interesting data from several points of view. The actual data on ultimate strength and breaking strength appear to be quite definite values, whereas the values of yield stress and ductility may be questioned. The use of a constant elongation of specimen for determining the yield stress of both notched and unnotched specimens leads to radically different amounts of strain to which the so-called yield stress corresponds. It is altogether possible that the strain corresponding to the so-called yield stress for deeply notched specimens will be many times that for unnotched specimens.

Recognition of the effects of biaxial stress upon the breaking strength, technical cohesive strength, yield strength and ductility of metals, as considered by the authors, is a most important factor. Stress concentration at the bases of notches are consequently of great importance but the nature of these stress concentrations for large amounts of local plastic strain may be quite different than for elastic strains, and any similarity between them may be purely coincidental.

The writer agrees with the authors that for elastic strains the contour of the deformation gradient is qualitatively similar to that of the original stress gradient but with the large plastic strains that occur just prior to fracture all similarity between the total strains and the elastic stresses may have disappeared, for two reasons; (1) the presence of a large uniform over-all strain certainly changes the relative aspects of local strain differences, and (2) these large uniform strains cause transverse deformations, which materially change the distribution and relative magnitudes of biaxial stresses. The authors quite ably describe the redistribution of stress resulting from plastic deformation.

The fact that residual stresses result from unequal elastic recoveries of the stresses existent in the strained material suggests that the

stress distribution, after removal of a load near the ultimate, would be more nearly uniform than that shown by the authors' diagram A-4 in Fig. 1. Of course the elastic recovery of varying biaxial stresses may cause some variation in residual stress but the relation between such residual stresses and static breaking loads is not clear.

In view of the relatively great significance that the authors place on stress concentration factors for elastic stresses, it would seem highly desirable to obtain an experimental check on the strain characteristics of the surface of the notches for loads ranging from those producing purely elastic stresses to those causing appreciable permanent set. By means of biaxial stress measurements a direct indication of the biaxial and triaxial stress distribution during loading could be obtained. It is altogether possible that the strains so measured would indicate biaxial stress relationships quite different from those assumed by the authors. While the actual test data for ultimate stress or true breaking stress will not change, the interpretation of the effects of biaxial stress upon the technical cohesive strength might be significantly changed.

D. J. McADAM, JR. (author's reply).—The evidence presented in the paper that two currently accepted generalizations are incorrect cannot be avoided by a surmise about the homogeneity of the metals used. Moreover, the evidence presented by the authors in several more recent papers clearly establishes the conclusion that the breaking stress tends to increase with increase in the radial stress ratio (S_2/S_1), and does so increase except when the influence of the associated decrease in ductility is dominant.

The authors have not investigated the effects of "biaxial" stress, mentioned by Mr. Sturm. The results of their investigation of the effects of triaxial stress, however, have led them to the conclusion that the technical cohesion limit varies with the stress combination in the indicated manner. This conclusion must be considered proved unless one is willing to assert that the actual longitudinal stress at fracture of a notched specimen may be much less than the mean stress at fracture, and sometimes even less than the mean stress at yield.

* Research Engineer Physicist, Aluminum Research Laboratories, New Kensington, Pennsylvania.

Symposium on Cohesive Strength

(Chicago Meeting, October 1943)

CONTENTS

	PAGE
Summary of the Symposium. By M. GENSAMER	538
Opening Remarks.	540
The Technical Cohesive Strength of Metals in Terms of the Principal Stresses. By D. J. McADAM, JR.	542
Fracture and Flow in Metals. By P. W. BRIDGMAN.	569
Discussion.	576
Conditions of Fracture in Steel. By J. H. HOLLOMON and CLARENCE ZENER.	*
Some Speculations Regarding the Plastic Flow and Rupture of Metals under Complex Stresses. By L. R. JACKSON	584
Discussion.	595

Summary

By M. GENSAMER†

It has been suggested by a number of people that it would be worth while for some one to attempt to summarize or condense the proceedings of this symposium. This task has fallen to me as organizer and co-chairman. Its difficulty will be appreciated by anyone who attempts to read the whole proceedings. It is therefore with trepidation that I offer the following digest.

In recent years there has been a renewal of interest in America on this subject of the cohesive strength of materials, and a growing appreciation of the need for a better theory of cohesion failure. The theories of elastic action and plastic action are well developed, particularly the former. The theory of plastic action is still in the course of development, but it is well along. Plastic action is terminated by cohesion failure and what is needed is a theory that will tell us when to expect the cohesion

failure. In the past it has generally been assumed that cohesion failure will occur when a critical value of the maximum tensile stress has been reached. Many experiments have shown that this is not strictly true, and this symposium concerns itself with the failures of this simple hypothesis, and with the efforts that have been made to devise a more satisfactory theory.

The most active contributor in recent years to knowledge in this field is Dr. McAdam, and he was asked to open the symposium with a summary or condensation of his papers and views. Undoubtedly it is presumptuous to attempt a still greater condensation, but perhaps it will be useful, because even his contribution to this symposium contains no summary, no concise statement of just what his contribution has been.

Dr. McAdam makes two main points. The first is that the cohesive strength is not a single valued quantity, but that it is a function of all three principal stresses and hence must be represented diagrammatically by a surface in a three-dimensional figure. Dr. McAdam has attempted so to delineate the cohesion limit, basing his

Issued as T.P. 1782 in METALS TECHNOLOGY, December 1944.

* This paper appeared in Volume 158 of the TRANSACTIONS, pp. 283-297, therefore is not repeated here.

† Co-Chairman of the Symposium; Professor of Metallurgical Engineering, Carnegie Institute of Technology, Pittsburgh, Pennsylvania.

diagrams on his own experiments as well as on the researches of others, prominent among whom are Kuntze, Bridgman and Tuckerman. His conclusion that the cohesion limit increases with increasing triaxiality is most interesting.

The second main point made by Dr. McAdam is that the cohesion limit depends upon the previous mechanical history of the material. One may represent the cohesion limit as a surface in three-dimensional principal stress space only for a single set of values of all the other variables, prominent among which are temperature, the whole complex of previous deformations, and the rates at which these deformations were produced. This has been emphasized by Dr. Bridgman in his discussion. Dr. McAdam has investigated and elucidated the behavior of the cohesion limit as a function of the amount of previous simple stretching, but the validity of his conclusions is still a matter of debate.

Dr. Bridgman has attacked the validity of Dr. McAdam's conclusions on the basis that the stress in a notched bar is probably far from as uniform as assumed by Dr. McAdam. On the other hand, Dr. McAdam has ably defended himself in this respect, abetted by Professor MacGregor, so that one is now inclined to the opinion that Dr. McAdam's assumption of a fairly uniformly distributed stress probably introduces little error.

Perhaps a more serious error is introduced by the assumption that very little deformation occurs in the testing of deeply notched bars, or that the amount of this deformation is about the same, one material to another. This assumption is mentioned in Mr. Morkovin's discussion. That this deformation may be considerable has been revealed by the recent researches of Dr. George Sachs and his collaborators. Unfortunately, Dr. Sachs could not be prevailed upon to take part in this symposium. Until a method is devised that enables one to measure the stress at fracture in a test that really involves no plastic

deformation of the specimen, the extent to which this plastic deformation influences the measured cohesive strength must remain uncertain.

Mr. Morkovin, in his closing discussion, suggests that more confidence be placed in the observations of several investigators which lead to the conclusion that the cohesion limit changes very little with temperature. Because the resistance to deformation increases markedly as the temperature is lowered, it is generally possible, using notched bars, to suppress plastic deformation and thus bring about a brittle failure. Neuber has calculated the stress distribution for all three principal stresses in notched bars of certain shapes, so that the stresses at *brittle* fracture could be known. This would not be a general solution of the problem for it would apply only to those materials that have a high dependence on temperature for the flow stress, and it would also be limited to cohesion limits at high degrees of triaxiality.

Just what is meant by the degree of triaxiality is clarified in the paper by Mr. Jackson, who has extended Neuber's analysis of the stress distribution in notched bars and reanalyzed the existing data on the basis of this analysis. He has used the relationship between the maximum strain to fracture and the triaxial stress ratio as a quality index, a procedure that seems to me should be very practical and useful. His approximations of the stress distributions and triaxiality ratio in simple V-notches with definite bottom curvatures should also be very useful.

Methods for determining the effects of temperature and strain rate, two of the variables that must be taken into account in the description of cohesion limits, are discussed by Messrs. Hollomon and Zener, who give examples of the dependence of the flow stress and fracture stress on these two variables. Their thesis that there are unique relationships between the effects of strain rate and temperature has aroused much interest and may give us a simple

way to study the effects of wide variations in strain rate, through the simple technique of controlling the temperature of the test. Their observations on the superiority of tempered martensite over pearlite, with respect to fracture strength at low temperatures and equivalent high strain rates, are interesting from both the practical and theoretical points of view.

None of the participants in the symposium have mentioned one important aspect of this problem, which is the development of anisotropy as deformation proceeds. It is gradually becoming known that transverse ductility, by which we mean either stress at fracture or strain at fracture, gradually diminishes as a metal is elongated. For instance, in rolled plates the ductility measured in tensile tests taken in the direction perpendicular to the surface of the plate may be very much less than in the directions lying in the plane of the plate, and gets worse as rolling proceeds. This anisotropy greatly complicates the description of the cohesive strength of a metal, introducing orientation variables that have not been considered in this symposium.

The symposium has focused attention on so many variables that metallurgists might well be dismayed at the complexity

of the problem. Some will be disappointed by the discovery that cohesion failure cannot be treated in a very simple way, and some will continue to try to treat it simply in spite of its complexity. Perhaps the most useful outcome of the symposium will be to discourage the latter, thus leading to more conservatism where low temperatures and fast rates of loading are involved, and to greater caution in design, more attention being given to the elimination of the features of design that introduce triaxiality of stress and stress concentration. The best design is still the one that permits some plastic deformation for redistribution of stress, and apparently, in the light of the statements in this symposium, for the improvement of cohesive strength by moderate amounts of deformation. A high degree of triaxiality acts to help us by increasing cohesive strength, but to hurt us by preventing plastic deformation at points of stress concentration.

Perhaps another useful outcome will be that the complexity of the problem revealed here will serve as a challenge and result in an increased activity in this field of research. Obviously, much remains to be done.

The Symposium

THE Symposium on Cohesive Strength, held in connection with the Regional Meeting and the Annual Fall Meeting of the Institute of Metals Division and the Iron and Steel Division of the American Institute of Mining and Metallurgical Engineers, at the Sherman Hotel, Chicago, Illinois, October 16-20, 1943, convened at 2:10 o'clock on Oct. 19, Dr. S. L. Hoyt, co-chairman, presiding.

INTRODUCTION

THE CHAIRMAN.—This session has to do with what has come to be known as cohesive strength. This morning I sat in on a session over at the Welding Society which had to do with the so-called brittle ship

situation. The discussion was predominantly on the effect of internal stresses on the behavior of ships. This session differs from the Welding Society session this morning, because here we are interested in cohesive strength in all of its aspects, including the scientific study of the thing that we used to call notch brittleness.

Dr. Gensamer, of the Carnegie Institute of Technology, is one of the leading lights in this field, and he has done a splendid job in getting these various discussions together and organizing the program. Full credit for this goes to him. The program will be opened by him.

M. GENSAMER.—Dr. Hoyt, in view of the length of the papers that we have received and the amount of discussion that seems likely from the people to whom I have talked, and also in view of the fact that some of the comment that I had intended to make has been made in the other papers that are to follow, I am going to make these introductory remarks of mine very brief.

I wish to define the objectives of the symposium and to say what I think we should try to accomplish here this afternoon. The need for a symposium on this subject has been growing for some time and has been intensified in recent years by the papers of Dr. McAdam and his associates. Dr. McAdam's somewhat lengthy papers have been hard to read and to understand, and one of the foremost objectives of this symposium is to give him an opportunity to condense and summarize his papers, to clarify his concepts, definitions, and procedures for us. I think a good many of us feel some need for this. For instance, I find myself in a state of utter confusion as a result of his abandonment of Kuntze's old technical cohesive strength, which Dr. McAdam I believe now calls the disruptive strength. Dr. McAdam evidently now applies this term "technical cohesive strength" to some other property and has it vary with the geometry and dimensions of the notched tensile bars, but he has not made it clear to me yet just how this quantity is determined, and I am sure he will clear this up this afternoon.

Our first concern here is to define our terms, and I hope each speaker will do this very carefully. As I understand it, Kuntze's technical cohesive strength is the value to which all measures of resistance to flow and fracture extrapolate as the state of stress approaches balanced triaxial tension; that is, all three principal stresses equal and positive. With sharp notches, disturbances enter which cause fracture to occur at low values of the average stress. Extreme localization of the high stress region at the

base of a notch would do this sort of thing. So the technical cohesive strength of Kuntze was obtained by extrapolation to the extreme notch, very sharp and very deep, from tests made with less severe notches, but of varying degrees of severity.

Basic to Kuntze's method is the assumption that the fracture stress and the tensile strength extrapolate to the same value. I personally am not convinced that this assumption is valid, in spite of Kuntze's efforts to prove it experimentally. If it were so, it would be very surprising to me, for it can be shown quite easily that the tensile strength is determined entirely by the shape of the stress-strain curve even under the action of unbalanced triaxial stresses. The tensile strength is just the point on the curve where the rate of strain-hardening falls below the rate of increase of stress resulting from reduction of area, which leads to necking down and deformation under decreasing load. This establishes the maximum load, which, when divided by the original area, is the tensile strength. What the resistance to plastic deformation has to do with resistance to fracture, I do not know. Kuntze's technical strength to me may be all right as a value to which the tensile strengths of notched bars extrapolate as the notch is made more severe, but I fail to see what this has to do with cohesive strength, which I take to mean resistance to coming apart or fracture. Perhaps this afternoon someone will enlighten me on this point.

I am sure everyone in the audience wants to have something explained to him, something clarified about this subject, and I think that with Dr. McAdam's summary and the discussions of the papers that follow, we should have a good opportunity to iron out a number of these points that bother us.

THE CHAIRMAN.—Thank you, Dr. Gensamer. We will now have Dr. McAdam's paper, "The Technical Cohesive Strength of Metals in Terms of the Principal Stresses."

The Technical Cohesive Strength of Metals in Terms of the Principal Stresses

BY D. J. McADAM, JR.,* MEMBER A.I.M.E.

As shown in three recent papers by the author,^{6,7,8} in two papers by McAdam and Mebs,^{9,10} and in a paper by McAdam, Mebs, and Geil,¹¹ the technical cohesive strength of a metal, in any particular state as regards mechanical treatment and heat-treatment, cannot be represented by a single stress value, but must be represented by a diagram with the principal stresses† as coordinates. Each point on the boundary of such a diagram represents a technical cohesion limit. The *technical cohesive strength* thus comprises an infinite number of *technical cohesion limits*, each representing fracture under a specific stress combination. Moreover, neither the yield strength‡ nor the ultimate strength can be represented completely by a single stress value, but must be represented by a diagram with the principal stresses as coordinates.

All combinations of the principal stresses may be classified in three groups as illustrated by Fig. 1. Fig. 1a shows three typical

stress combinations with no two principal stresses equal. The magnitude of each principal stress is indicated qualitatively by the length of the arrow. Arrows pointing away from the cube indicate tensile stresses; arrows pointing toward the cube indicate compressive stresses. Typical stress combinations with two principal stresses equal are illustrated in Figs. 1b and 1c. Such stress combinations would be produced by subjecting a cylinder to combinations of uniform axial and radial stresses. The uniform radial stress may be resolved into two equal principal stresses, with the mutually perpendicular directions rotatable around the axis of the cylinder. Fig. 1b shows stress combinations with S_2 equal to S_3 . The greatest principal stress is in the axial direction, and the stress combination tends to cause either absolute or relative increase in length.* Fig. 1c shows stress combinations with S_2 equal to S_1 . The greatest principal stress is in the radial direction, and the combination tends to cause either absolute or relative decrease in length.

The complete representation of either technical cohesive strength, yield strength, or ultimate strength generally requires a three-dimensional diagram. When two of the principal stresses are kept equal, however, the strength of a metal may be represented by a two-dimensional diagram with the coordinates representing the axial and radial stresses.⁶⁻¹¹ In this paper, attention will be confined almost entirely to stress combinations with two of the prin-

* Chief of Section on Thermal Metallurgy, National Bureau of Standards, Washington, D. C.

† References are on page 567.

‡ Any stress system may be resolved into three principal stresses normal to three mutually perpendicular planes, known as the "principal planes," on which there is no shearing stress. Tensile stresses are viewed as positive and compressive stresses as negative. In this paper, as in the previous papers,⁶⁻¹¹ the algebraically greatest principal stress will be designated S_1 , the least principal stress will be designated S_3 , and the intermediate principal stress will be designated S_2 .

§ A distinction is made between the term "yield strength" and the term "yield stress," which is used to indicate a value corresponding to a specific stress combination. A similar distinction is made between "ultimate strength" and "ultimate stress."

* By "relative" increase in length is meant an increase in the ratio of length to diameter.

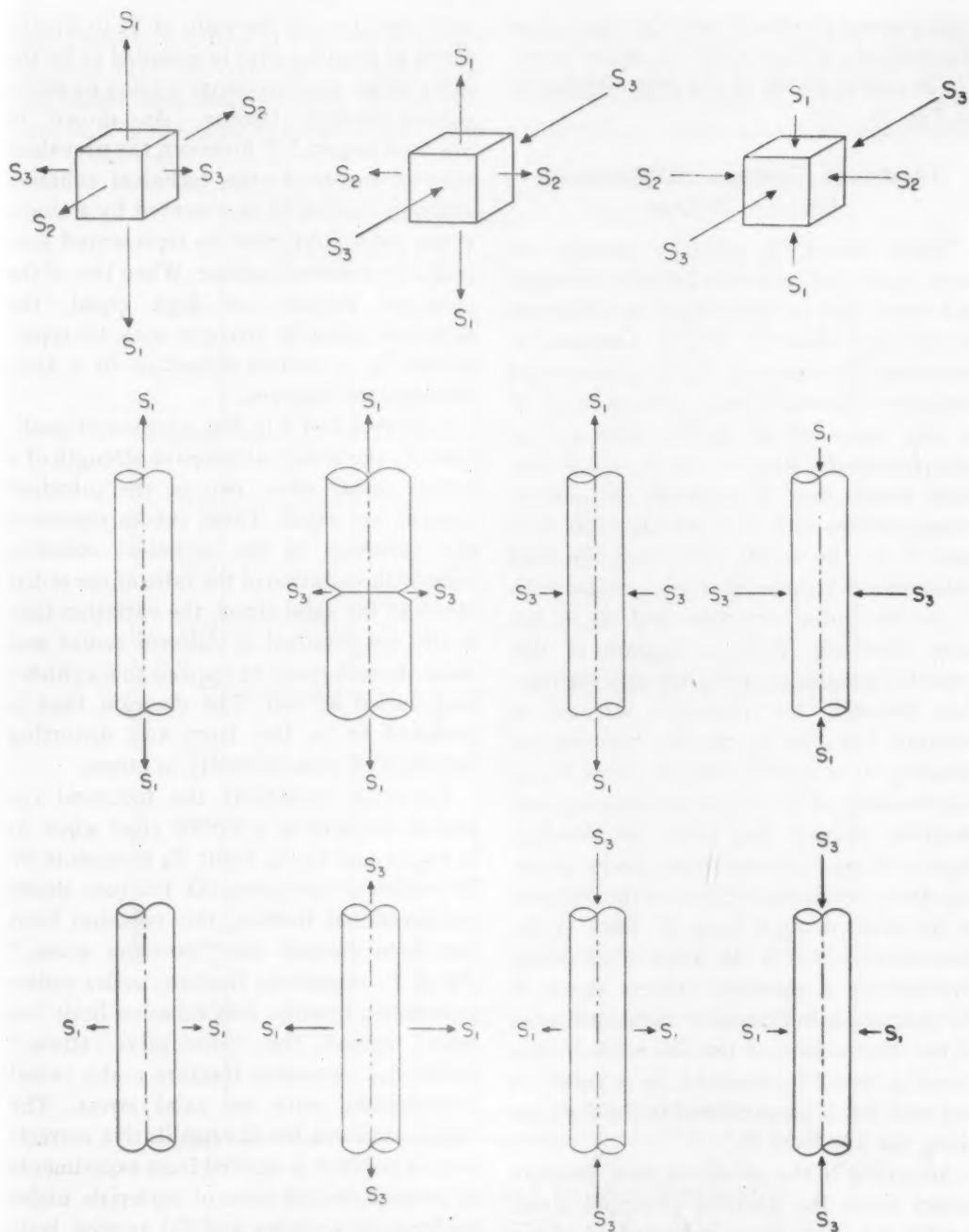


FIG. 1.—THREE CLASSES OF STRESS COMBINATIONS.
a. No two principal stresses equal. *b.* $S_2 = S_3$. *c.* $S_2 = S_1$.

principal stresses equal and with the axial stress algebraically greater than the radial stress, stress combinations of the type illustrated in Fig. 1b.

TECHNICAL COHESIVE STRENGTH OF BRITTLE METALS

When two of the principal stresses are kept equal, the technical cohesive strength of a metal may be represented by a diagram of the type shown in Fig. 2. Abscissas in this diagram represent radial stresses and ordinates represent axial stresses. Line *H* is the locus of all points representing polarsymmetric stress ($S_1 = S_2 = S_3$). The field above line *H* evidently represents stress systems with S_1 in the axial direction and S_3 in the radial direction; the field below line *H* represents stress systems with S_1 in the radial direction and S_3 in the axial direction. With a diagram of this type it is possible to study not only the relation between the principal stresses at fracture, but also the relation between the shearing stress and the volume stress.* Line *G* is the locus of all points representing pure shearing stresses. Any point on this line represents zero volume stress, and a shearing stress value proportional to the distance of the point along *G* from *H*. Each of the lines parallel to *G* is the locus of all points representing a constant volume stress of the magnitude indicated by the coordinates of the intersection of the line with *H*; the shearing stress represented by a point on any such line is proportional to the distance along the line from *H*.

According to the prevalent view, fracture occurs when the greatest principal stress reaches a critical value independent of the other two principal stresses. This view is illustrated by lines *L* in Fig. 2. These lines imply that S_1 at fracture does not change

with variation of the ratio of S_2 to S_1 ; the stress at fracture thus is assumed to be the same under unidirectional tension as under polarsymmetric tension. As shown in previous papers,⁶⁻¹¹ however, the prevalent view is incorrect; the technical cohesive strength cannot be represented by a single stress value, but must be represented generally by a curved surface. When two of the principal stresses are kept equal, the technical cohesive strength may be represented by a curved boundary in a two-dimensional diagram.

Curves *A* and *R* in Fig. 2 represent qualitatively the technical cohesive strength of a brittle metal when two of the principal stresses are equal. These curves represent the variation of the technical cohesion limit with variation of the ratio of the radial stress to the axial stress, the variation that would be obtained if uniform radial and axial stresses could be applied to a cylinder and varied at will. The diagram thus is assumed to be free from any distorting influence of nonuniformity of stress.

Curve *A* represents the technical cohesive strength of a brittle steel when S_2 is kept equal to S_3 . Point T_0 represents by its ordinate the stress at fracture under unidirectional tension; this cohesion limit has been termed the "severing stress." Point T_1 represents fracture under polarsymmetric tension; this cohesion limit has been termed the "disruptive stress." Point T_2 represents fracture under radial compression, with no axial stress. The ample evidence for the qualitative correctness of curve *A* is derived from experiments of two kinds: (1) tests of materials under hydrostatic pressure and (2) tension tests of notched specimens. The compression tests give evidence for the course of curve *A* to the left of T_0 ; the tension tests of notched specimens give evidence for the course of the curve to the right of T_0 . Compression tests reported by Bridgman give evidence that the curve of technical cohesion crosses the axis of abscissas at the

* Any stress system may be resolved into a polarsymmetric stress causing pure volume strain and a combination of shearing stresses, which cause no change of volume. The volume stress is one third the algebraic sum of the principal stresses.

approximate position of T_{C2} and descends into the field representing combined axial and radial compressive stresses. In compression tests of one type, cylindrical specimens

fractured transversely as if it had been broken by tension, and the broken pieces were projected violently from the vessel. Ductile materials contracted locally before

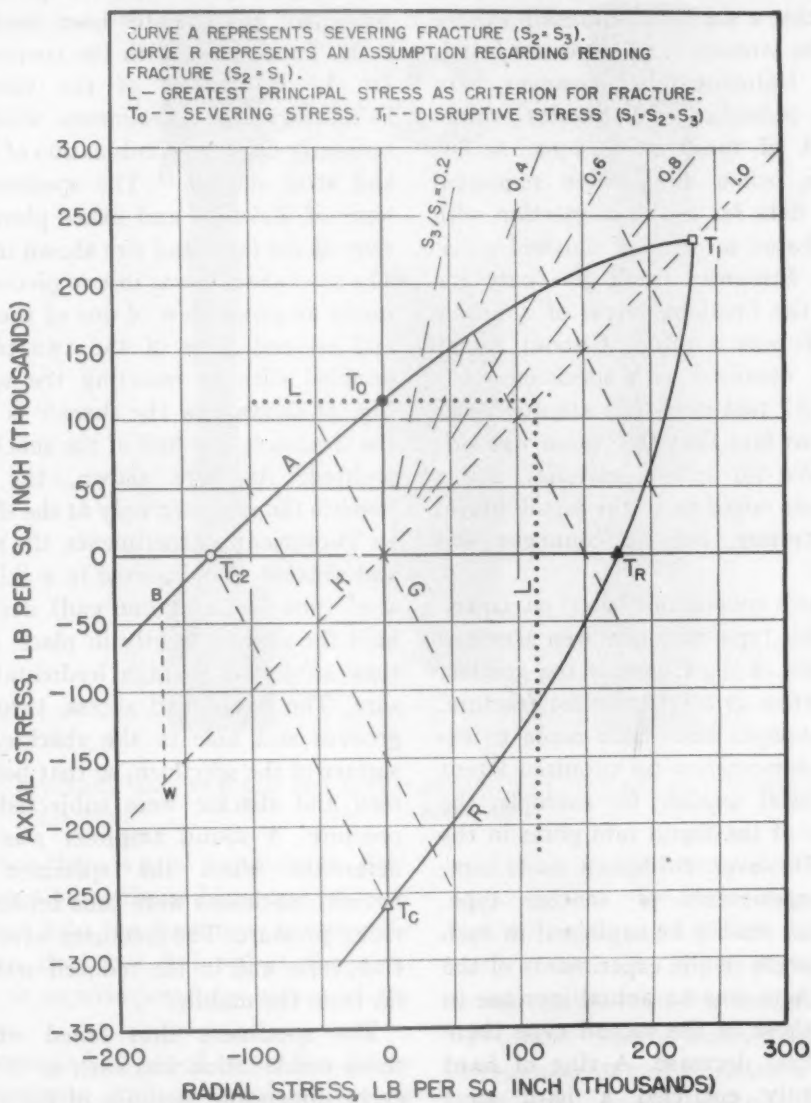


FIG. 2.—TECHNICAL COHESIVE STRENGTH OF A BRITTLE METAL.

were subjected to hydrostatic pressure on the cylindrical surface, while the ends of the cylinder projected through the sides of the pressure vessel; the ends of the specimen thus were subjected only to atmospheric pressure. When the hydrostatic pressure reached a certain value, depending on the material, the specimen

fracture; brittle materials, such as hard tool steel or glass, did not contract locally, but broke with clean, exactly transverse fractures. In a brittle material, therefore, there was said to be no stress normal to the plane of fracture, except the small axial compressive stress induced by the atmospheric pressure and by the frictional re-

sistance of the packing. Bridgman reported that the lateral compressive stress necessary to cause necking of ductile metals was slightly greater than the stress necessary to cause necking in an ordinary tension test, and that a similar relationship existed between the stresses at fracture of a brittle material. Unfortunately, however, Dr. Bridgman published no numerical values in support of these conclusions. A few years ago, when the writer requested numerical data for use in connection with diagrams based on tests of notched specimens, Dr. Bridgman could give only one value for the breaking stress of a brittle metal. This was a value of about 72,000 lb. per in. obtained with specimens of a "glass hard" tool steel. His attention was called to the fact that this value was surprisingly low for such a material, and a question was raised as to the possibility of bending stresses, but no comment was received.

Bridgman's conclusions based on experiments of this type have not been accepted by adherents of the theory of the greatest principal stress as a criterion for fracture. Various attempts have been made to explain the phenomenon by surmised latent causes of axial tension; for example, the penetration of the liquid into pores in the specimen. However, Bridgman made compression experiments of another type, which cannot readily be explained in such a way. Whereas in the experiments of the first type there was an actual increase in length, in those of the second type there was an actual decrease. A ring of hard rubber tightly encircled a hard steel cylinder. When the entire ring and cylinder were subjected to hydrostatic pressure, the rubber ring broke as though it had been stretched by an expansion of the cylinder, although every dimension of both cylinder and ring was decreased by the hydrostatic pressure. The fracture, therefore, cannot be attributed to a tensile stress or to an extension, but may be attributed to increase

in one dimension relative to another. The radial dimensions of the rubber ring were decreased less than in the absence of restraint by the relatively rigid steel cylinder.

The principle of this experiment by Bridgman has recently been used by Dr. L. B. Tuckerman, with the cooperation of Dr. L. H. Adams of the Geophysical Laboratory, in experiments with an ingeniously designed combination of specimen and steel shackle.¹² The specimens used were of Bakelite and other plastics, and were of the form and size shown in Fig. 3a. The steel shackle was in two pieces. Fig. 3b shows an inner view of one of these pieces and an end view of the two pieces assembled without inserting the specimen. Fig. 3c shows how the shackle is fitted to the specimen, one half of the shackle being omitted. As here shown, the shackle touches the specimen only at the shoulders. In Tuckerman's experiments, the specimen and shackle were inserted in a thin-walled steel tube (open at one end) designed to hold the shackle lightly in place, and was then subjected to high hydrostatic pressure. The liquid had access, through the grooves and hole in the shackle, to the surface of the specimen, so that both specimen and shackle were subjected to full pressure. A sound amplifier was used to determine when the specimen broke. Several specimens were thus broken under rising pressure. The fractures were exactly transverse and in the reduced section not far from the middle.

The specimens thus failed when the stress combination was such as to shorten every dimension. Because of the restraint of the shackle, however, the percentage decrease was less in length than in diameter. The stress combination may be represented by a point, such as *B*, to the left of Tc_2 on a curve of the form of curve *A* of Fig. 2. The combination may be resolved into a hydrostatic pressure, represented by point *W* on line *H*, plus an axial tensile stress represented by distance *WB*. The

results of these experiments seem to give conclusive evidence that these materials will fail under sufficient radial compressive stress, when there is no axial tension or

curve of technical cohesion for a brittle metal rises between T_{c2} and T_0 as indicated in Fig. 2. If so, the rise would be expected to continue to the right of T_0

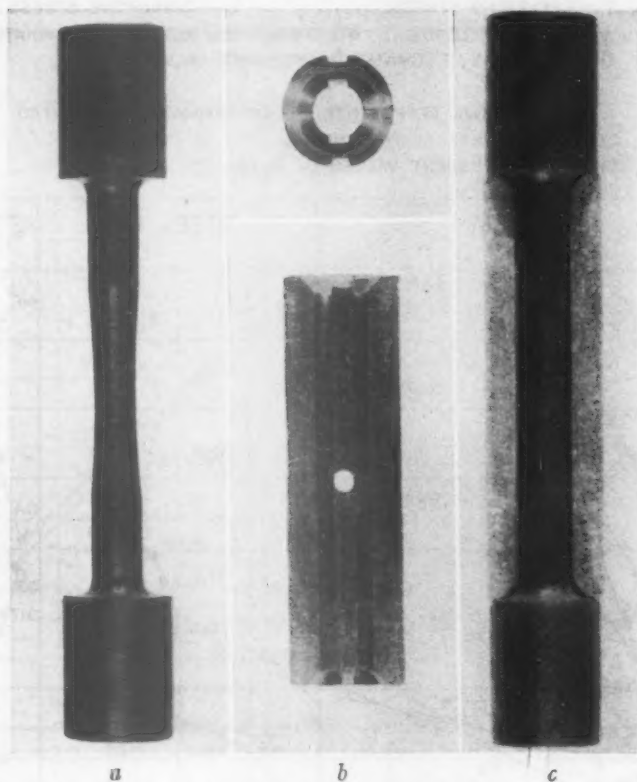


FIG. 3.—SPECIMEN AND SHACKLE FOR INVESTIGATING FAILURE UNDER HYDROSTATIC PRESSURE (L. B. Tuckerman).

even when there is axial compression. Failure cannot be attributed to penetration of the liquid into the specimen, because the specimen does not fail unless the axial tension is superimposed by means of the shackle.

Tuckerman had hoped to use this device to investigate various combinations of axial compression and superimposed tension. This could be readily done by starting with various initial tensile stresses induced by the reaction between specimen and shackle. It should thus be possible to determine the curve between T_{c2} and T_0 . Unfortunately, these experiments had to be deferred.

The evidence seems to indicate that the

until the curve intersects H at a point representing the disruptive stress. Irrespective of the course to the left of T_0 , however, curve A between T_0 and T_1 is well established qualitatively by evidence obtained by tension tests of notched specimens.⁶⁻¹¹ An example of this evidence is seen in Fig. 4, which is reproduced with some modifications from previous papers.^{6,7} The diagrams are based on data published by Kuntze.

Abscissas in Fig. 4 represent values of ductility, and ordinates represent breaking stresses. In each diagram, a curve is drawn through the points representing fracture of notched and unnotched specimens, and is prolonged to a point representing fracture

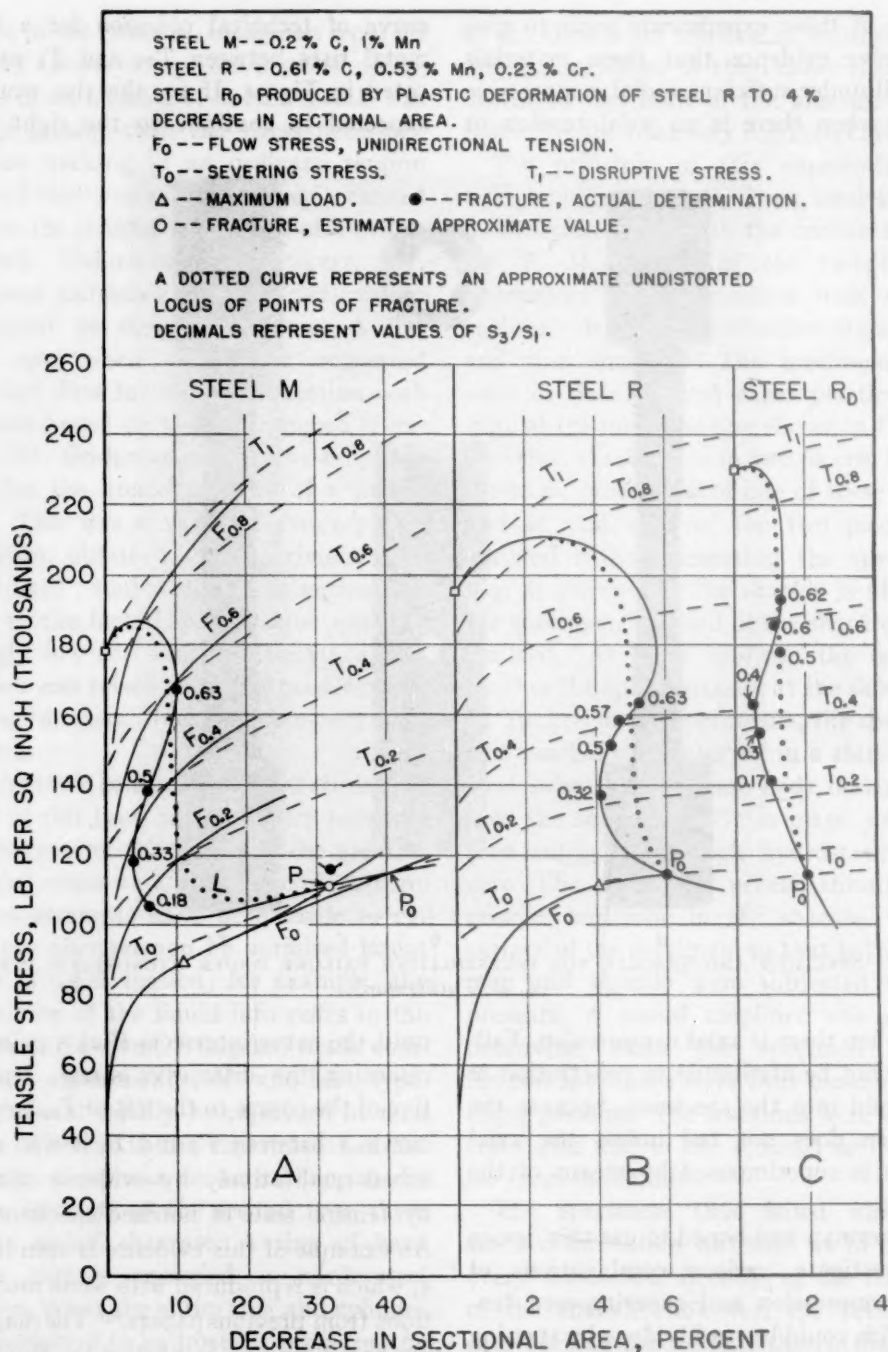


FIG. 4.—VARIATION OF TECHNICAL COHESION LIMIT AND DUCTILITY OF STEELS WITH S_3/S_1 .

under polarsymmetric tension.* The course of this curve of fracture depends on the variable plastic deformation before fracture, and on the variable radial stress ratio

stress ratio.* Any stress concentration remaining at fracture would tend to make the actual stress at fracture *greater* than the mean stress. The evidence thus shows that

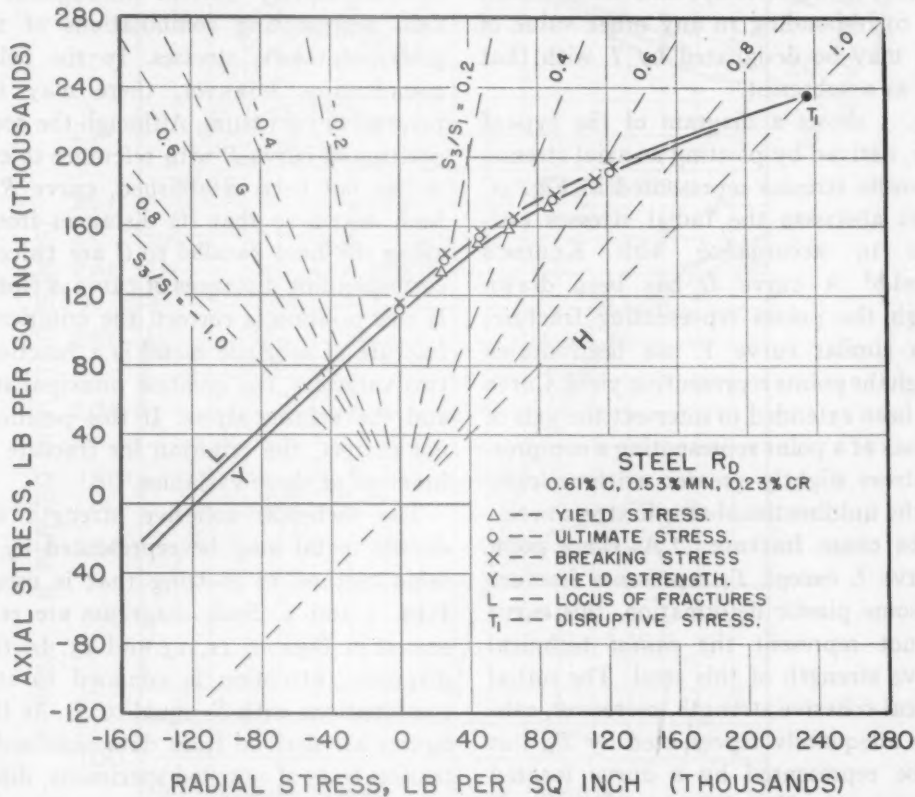


FIG. 5.—TECHNICAL COHESIVE STRENGTH, ULTIMATE STRENGTH AND YIELD STRENGTH OF SLIGHTLY DUCTILE METAL.

(ratio of S_3 to S_1). For the slightly ductile steels R and R_D (diagrams B and C), the variable ductility is a minor factor and the course of the locus of fractures depends chiefly on the variable radial stress ratio. At fracture of the unnotched specimens of these two steels, the stress was practically unidirectional, because the local contraction was so small. At fracture of the notched specimens the mean stress was greater and increased with the depth of the notch. This increase of the breaking stress can be attributed only to the increase in the radial

an increase in the radial stress ratio tends to cause an increase in the technical cohesion limit. This conclusion must be considered as proved unless one wishes to assert that the actual stress at the origin of fracture of a notched specimen may be much less than the mean stress at fracture, and even much less than the mean stress at maximum load or at yield.

The locus of fractures in such a diagram represents an infinite number of technical cohesion limits corresponding to the infinite number of possible values of the radial stress ratio. Any specific technical cohesion

* Although Kuntze's method of extrapolation probably is not correct,* the error will not affect the conclusions to be derived from the data.

* Numbers adjacent to symbols represent radial stress ratios estimated by Kuntze's method.

limit must be designated with reference to the corresponding value of S_2/S_1 . The cohesion limits for unidirectional and polar-symmetric tension have been designated T_0 and T_1 , respectively, and the cohesion limit corresponding to any other value of S_2/S_1 may be designated by T with that value as a subscript.

Fig. 5 shows a diagram of the type of Fig. 2, derived by plotting as axial stresses the tensile stresses represented in Fig. 4C and as abscissas the radial stresses estimated in accordance with Kuntze's method.^{6,7} A curve L has been drawn through the points representing fracture, and a similar curve Y has been drawn through the points representing yield. Curve L has been extended to intersect the axis of abscissas at a point representing a compressive stress slightly greater arithmetically than the unidirectional tensile stress necessary to cause fracture.¹⁻⁴ As every point on curve L except T_1 represents fracture after some plastic deformation, this curve does not represent the *initial* technical cohesive strength of this steel. The initial technical cohesive strength, moreover, cannot be adequately represented by T_1 , but may be represented by a curve located between curves Y and L . An approximate curve for this purpose would pass through the points representing values of the ultimate stress. A curve representing the *initial* technical cohesive strength of a slightly ductile metal is qualitatively similar to a curve representing the technical cohesive strength of a brittle metal (Fig. 2).

A curve of initial technical cohesive strength does not imply that any point on the curve except T_1 can be actually attained by increasing the stress beyond the yield value for that stress combination. Plastic deformation would increase the technical cohesive strength and thus elevate the curve representing the *initial* technical cohesive strength. Nevertheless, a curve of initial technical cohesive strength is of much more than academic importance.

Brief consideration will now be given to curve R of Fig. 2. This curve, which is intended to represent the technical cohesive strength when S_2 is equal to S_1 , probably is qualitatively correct throughout the field representing combinations of three principal tensile stresses. In the field of compression, however, there may be a reversal of curvature. Although the correct position of curve R with reference to curve A has not been established, curve R has been drawn so that its distances from H along the lines parallel to G are twice the corresponding distances of curve A from H . If this position is correct, the criterion for fracture of a brittle metal is a function of two variables, the greatest principal stress and the volume stress. If this position is not correct, the criterion for fracture is a function of three variables.⁷

The technical cohesive strength of a ductile metal may be represented by the same method of plotting that is used in Figs. 2 and 5. Such diagrams are represented in Figs. 9, 11, 13 and 15. In these diagrams, attention is confined to stress combinations with S_2 equal to S_3 . As these figures are derived from data obtained by tension tests of notched specimens, discussion of the diagram will follow a discussion of the influence of notches on the strength and ductility of metals.

INFLUENCE OF NOTCH ANGLE, NOTCH DEPTH, AND ROOT RADIUS ON STRENGTH AND DUCTILITY OF METALS

Influence of Notch Angle, Notch Depth, and Root Radius on Yield Stress and Ultimate Stress

In Fig. 6 are curves representing the variation of the yield stress, ultimate stress, breaking stress and ductility of Monel metal with the notch angle. Comparison of these curves shows qualitatively the influence of notch depth and root radius. Attention will be given first to the curves

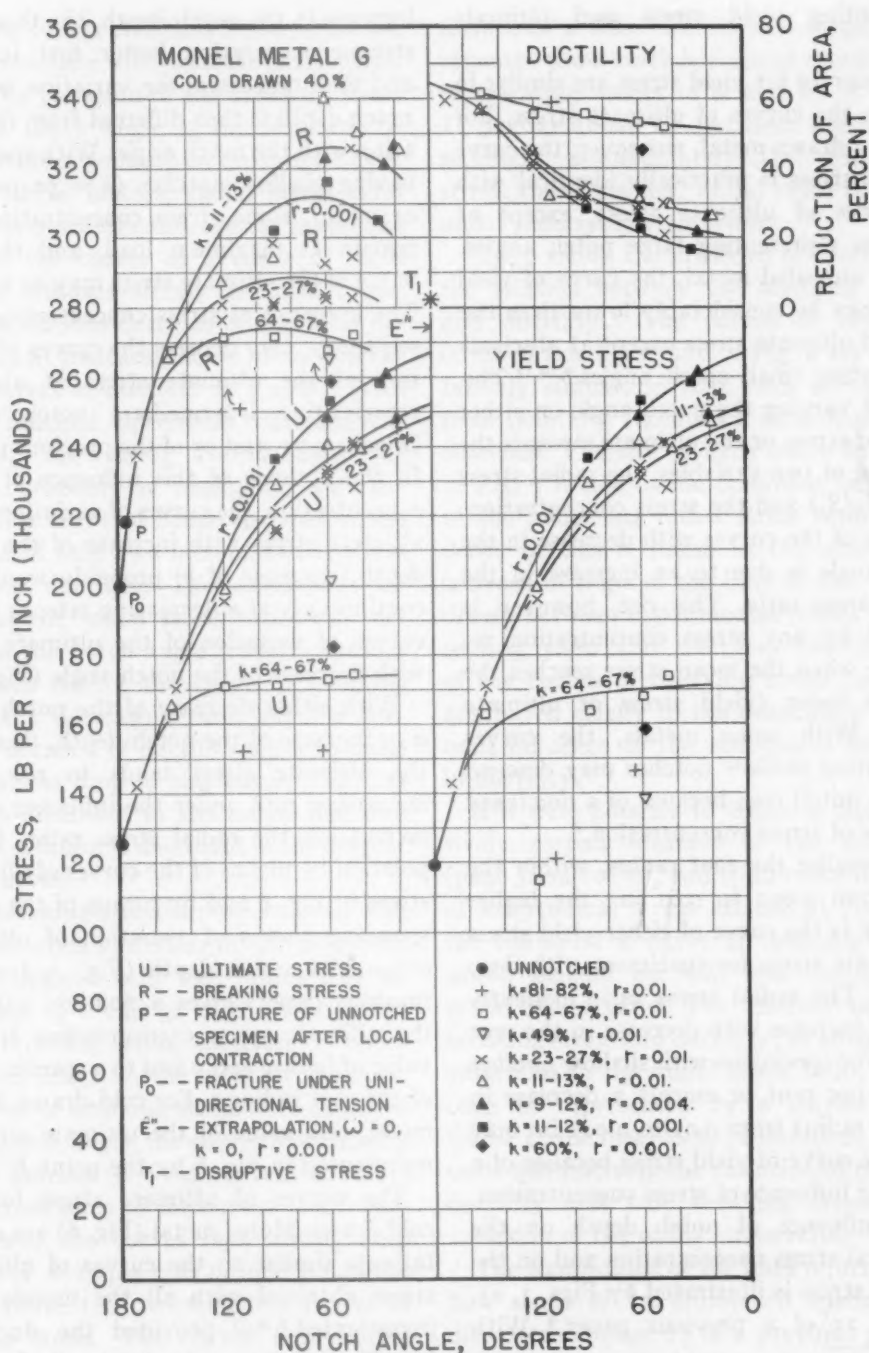


FIG. 6.—INFLUENCE OF NOTCH ANGLE, NOTCH DEPTH AND ROOT RADIUS ON STRENGTH AND DUCTILITY OF COLD-DRAWN MONEL METAL.

representing yield stress and ultimate stress.

The curves for yield stress are similar in form to the curves of ultimate stress. For this cold-drawn metal, moreover, the curve of yield stress is practically identical with the curve of ultimate stress, except at abscissas representing large notch angles. For an annealed metal, the curve of yield stress may be considerably lower than the curve of ultimate stress except at abscissas representing small notch angles.^{9,10,11} The effect of varying the notch angle on either the yield stress or the ultimate stress is the resultant of two variables, the radial stress ratio (S_2/S_1) and the stress concentration. The rise of the curves with decrease in the notch angle is due to an increase in the radial stress ratio. This rise, however, is opposed by any stress concentration remaining when the mean stress reaches the strength index (yield stress or ultimate stress). With some metals, the curves representing shallow notches may descend after an initial rise, because of a dominant influence of stress concentration.*

The smaller the root radius, within the range from 0.001 to 0.01 in., the higher generally is the curve of either yield stress or ultimate stress for specimens with deep notches. The radial stress ratio evidently tends to increase with decrease in the root radius. For specimens with shallow notches ($k = 60$ per cent or more)[†] a decrease in the root radius from 0.01 to 0.001 in. may lower the curve of yield stress because of a dominant influence of stress concentration.

The influence of notch depth on the theoretical stress concentration and on the ultimate stress is illustrated by Figs. 3, 23, 24, and 25 of a previous paper.⁹ With

* As shown in Fig. 4 of a previous paper,⁹ the theoretical stress concentration rises at a decreasing rate with decrease in the notch angle.

† Notch depth is expressed in terms of the relative area ($k = b^2/B^2$) of the minimum cross section of the specimen, where b and B represent the minimum and maximum radii of the section, respectively. Thus the greater the notch depth, the smaller is the value of k .

increase in the notch depth, the theoretical stress-concentration factor first increases and then decreases; the variation with the notch depth is thus different from the variation with the notch angle. With specimens having shallow notches ($k = 50$ per cent or more), some stress concentration may remain at maximum load, and thus the value of the ultimate stress may be too low. The influence of stress concentration, consequently, may depress the curves of variation of the ultimate stress at abscissas representing intermediate notch depths (Figs. 23, 24, and 25 of the previous paper). In the absence of this influence of stress concentration, the curves of variation of the ultimate stress with increase of the notch depth (decrease of k) probably would rise continuously at a decreasing rate, as do the curves of variation of the ultimate stress with decrease of the notch angle (Fig. 6).

With either decrease of the notch angle ω or increase of the notch depth, therefore, the ultimate stress tends to rise at a decreasing rate under the influence of the increase in the radial stress ratio. Extrapolation by means of the curves of ultimate stress in Fig. 6 and by means of the corresponding curves of variation of ultimate stress with notch depth (Fig. 24A of the previous paper) gives a nominal value of the ultimate stress corresponding to zero value of both ω and k and to a specific value of the root radius r . For cold-drawn Monel metal, this value of the ultimate stress is represented in Fig. 6 by the point E'' .

The curves of ultimate stress for the cold-drawn Monel metal (Fig. 6) are qualitatively similar to the curves of ultimate stress obtained with all the metals thus investigated,^{9,10,11} provided the ductility is sufficient to permit the tensile load to reach a maximum.¹¹

Influence of Notches on the Breaking Stress

The influence of the notch angle on the breaking stress is represented in Fig. 6 by the curves designated R . These curves,

unlike the curves of ultimate stress, do not rise continuously with decrease in the notch angle. The variation of the breaking stress with the notch angle is the resultant of three factors dependent on the notch angle. Two of these factors, radial stress ratio and stress concentration, are the same that influence the course of a curve of yield stress or ultimate stress; the third factor is the continuous decrease of the total deformation at fracture, shown in the descent of the curves of ductility in Fig. 6.* With deeply notched specimens of sufficient ductility, the stress concentration at fracture probably is negligible, and the course of a curve of breaking stress is the resultant of only two factors, radial stress ratio and ductility. The continuous increase of the radial stress ratio with decrease in the notch angle tends to cause a continuous rise of the curve of breaking stress at a decreasing rate, but the continuous decrease of ductility tends to cause a continuous drop of this curve. The first factor is dominant in the initial rise, and the second factor is dominant in the descent of the curves.

The breaking-stress curves obtained with root radii 0.004 and 0.001 in. are below the curves obtained with root radius 0.01 in. The effect of a change of the root radius on the breaking stress, therefore, is opposite to its effect on the ultimate stress. If the curves of breaking stress were extended to zero notch angle, the curves representing shallow notches ($k = 60$ per cent or more) would cross some of the curves of ultimate stress, and the curves representing deep notches ($k = 25$ per cent or less) would not be far above the corresponding curves of ultimate stress. The curves representing deep notches would be not far from point E'' , which represents the summit of the

surface in a three-dimensional diagram of ultimate stress (with horizontal coordinates representing values of ω and k). A point T_1 not far above E'' has been selected to represent approximately the disruptive stress, the stress that would cause fracture under polarsymmetric tension.

Fig. 7 shows the influence of notches on the relation between the breaking stress and ductility.* The curves of breaking stress in this figure and in Fig. 6 are qualitatively similar, in that each curve rises from point P_0 , traverses a maximum, and descends. The rise of each curve from P_0 in Fig. 7 is due to the dominant influence of the increasing radial stress ratio. Evidence of this is found in the associated increase of slope of the lines of flow stress drawn between experimental points representing yield and fracture. The descent of the curves of breaking stress must be attributed chiefly to the eventually dominant influence of the continuous decrease in ductility.

If it were possible to obtain a quantitatively correct measure of the ductility (page 18 of ref. 9), and if no concentration of longitudinal stress existed at fracture, the course of a curve of breaking stress would depend on only one factor, the radial stress ratio. The relation between breaking stress and ductility, as affected by variations in the radial stress ratio, would then be represented by a single curve. Curve L , the ideal locus of fractures; represents qualitatively the variation of the true ductility and true breaking stress with variation of the radial stress ratio.

The significance of the lines representing flow stress of an unnotched specimen is discussed on page 15 of a previous paper.⁹

Curves of breaking stress qualitatively similar to those in Fig. 6 and 7 have been obtained with annealed Monel metal and with annealed and cold-rolled copper.^{9,10}

* As shown in previous papers, ^{6,7,9,10,11} plastic extension causes a continuous increase in the technical cohesive strength, and hence tends to cause increase in any specific technical cohesion limit. A decrease in the total deformation at fracture would have the opposite effect.

* This method (suggested by MacGregor) of representing ductility is discussed on page 15 of a previous paper.⁹

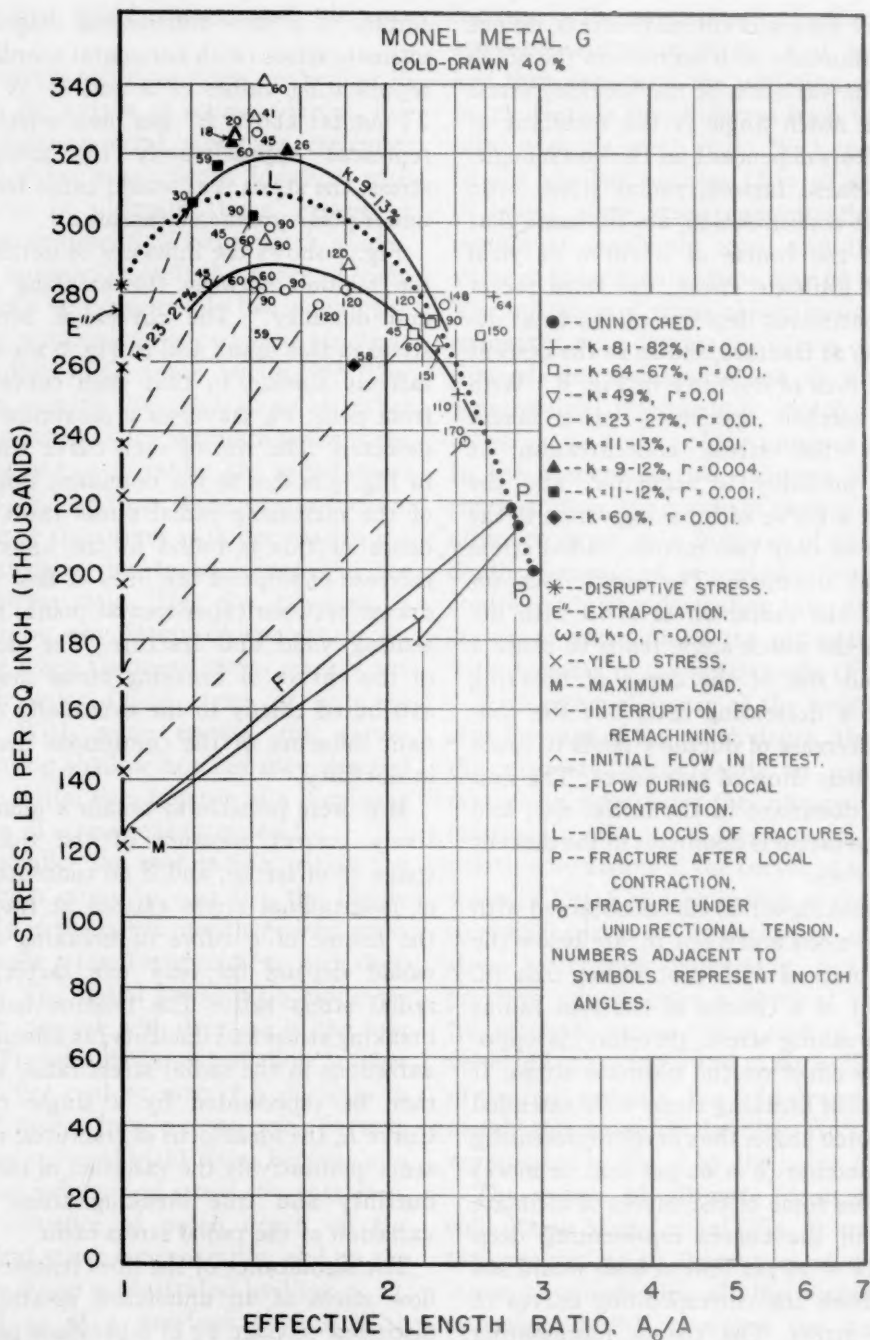


FIG. 7.—INFLUENCE OF NOTCHES ON RELATION BETWEEN BREAKING STRESS AND DUCTILITY OF COLD-DRAWN MONEL METAL.

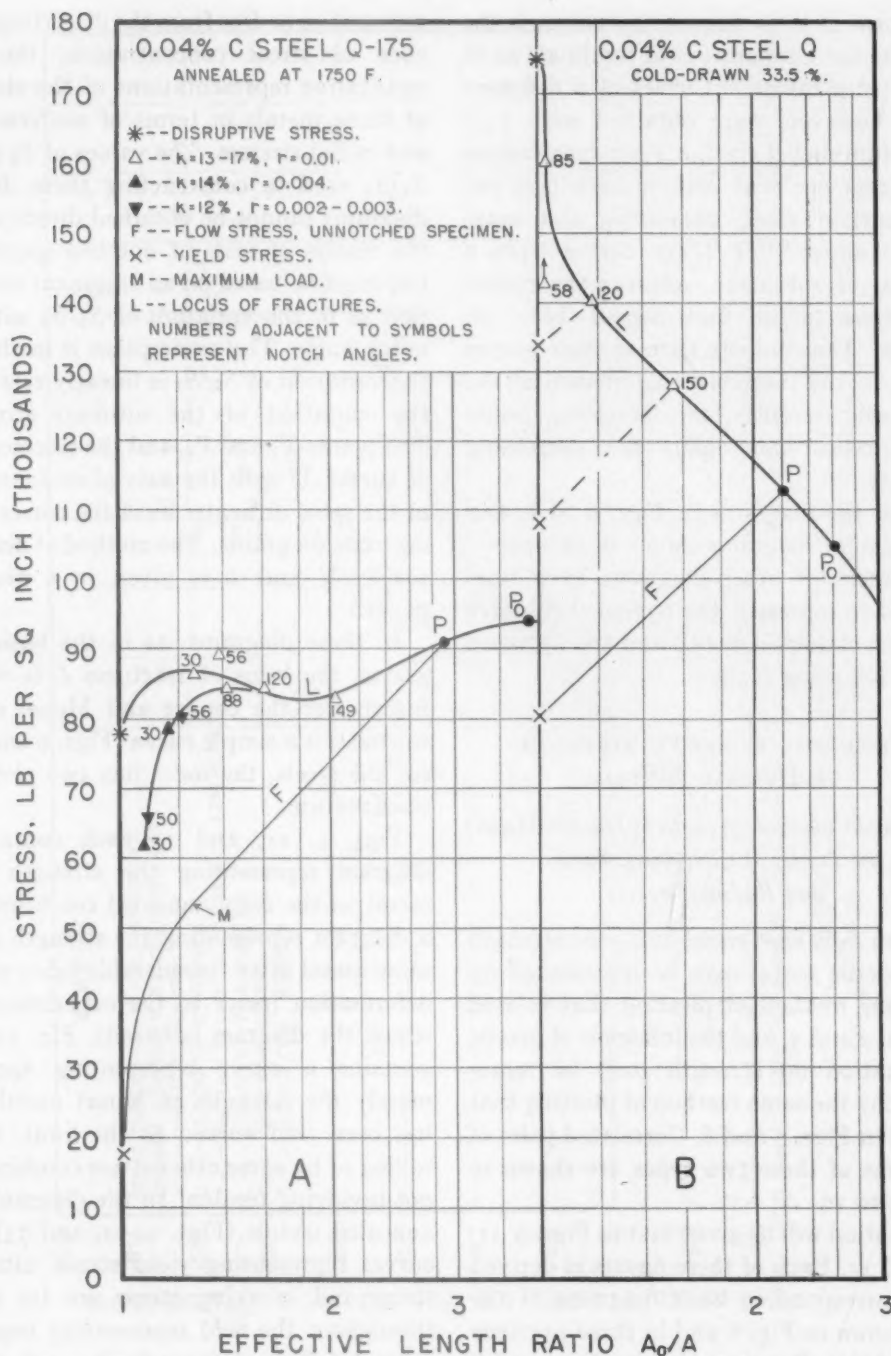


FIG. 8.—INFLUENCE OF NOTCHES ON RELATION BETWEEN BREAKING STRESS AND DUCTILITY OF 0.04 PER CENT CARBON STEEL.

The form of these curves, moreover, is the same at the temperature of liquid air as at room temperature.¹⁰ Curves of a different form, however, were obtained with 13:2 chromium-nickel steel, 0.2 per cent carbon steel, 0.73 per cent carbon steel, 0.04 per cent carbon steel, duralumin and magnesium alloys.^{9,10,11} These curves have a reversal of curvature, whereas the curves for Monel metal and copper have no reversal. The complex form of these curves is due to the successive dominance of the decreasing ductility, the increasing radial stress ratio, and again the decreasing ductility.

From the diagrams in Figs. 6 to 8, and from similar diagrams shown in two previous papers,^{9,10} other diagrams have been derived to represent the technical cohesive strength of ductile metals and are discussed in the following section.

TECHNICAL COHESIVE STRENGTH OF DUCTILE METALS

Technical Cohesive Strength of Ductile Metals in Terms of Combined Axial and Radial Stresses

When S_2 is kept equal to S_3 , the strength of a ductile metal may be represented by the same method of plotting that is used in Figs. 2 and 5, and the influence of plastic deformation on strength may be represented by the same method of plotting that is used in Figs. 7 and 8. Correlated pairs of diagrams of these two types are shown in Figs. 9 to 16.

Attention will be given first to Figs. 9, 11, 13, and 15. Each of these figures is derived from corresponding basic diagrams of the kind shown in Fig. 6 and in three previous papers.^{9,10,11} For example, the diagram for cold-drawn Monel metal G in Fig. 11 is derived from the diagrams in Fig. 6, and the diagram for annealed Monel metal G-14 in Fig. 11 is derived from the corresponding diagrams in Fig. 14 of a previous paper.⁹ The diagrams in Figs. 9, 11, 13, and 15 are

assumed to be free from the distorting influence of stress concentration; they are qualitative representations of the strength of these metals in terms of *uniform* axial and radial stresses. The values of S_3 and of S_3/S_1 used in constructing these derived diagrams cannot be obtained directly from the results of tests of notched specimens, but must be based on an empirical assumption as to the variation of S_3/S_1 with the notch angle. The assumption is made that the variation of S_3/S_1 is linearly related to the variation of the ultimate stress.^{9,10} The points T_1 and P_0 , and the intersections of curves U with the axis of ordinates are at the same ordinates as in the corresponding basic diagrams. The method of deriving curves U and L is given in a previous paper.⁹

In these diagrams, as in the basic diagrams, the locus of fractures L is of two forms. For the copper and Monel metal, the locus is a simple curve (Figs. 9 and 11); for the steels, the locus has two reversals of curvature.

Figs. 9, 11, and 13 each contains a diagram representing the strength of a metal in the fully annealed condition and a diagram representing the strength of the same metal after considerable prior plastic deformation (prior to the experiments on which the diagram is based). Fig. 11 also contains a curve representing approximately the strength of Monel metal that has been cold-worked to the limit, as by rolling or by some other stress combination not involving tension. In the diagrams for annealed metals (Figs. 9, 11, and 13), the curves representing yield stress, ultimate stress and breaking stress are far apart throughout the field representing negative values of S_3 , and throughout much of the field representing positive values of S_3 . In the diagrams representing cold-worked metals, these three curves are much closer together; a curve of yield stress (not shown) would almost coincide with the curve of ultimate stress. The greater the amount of

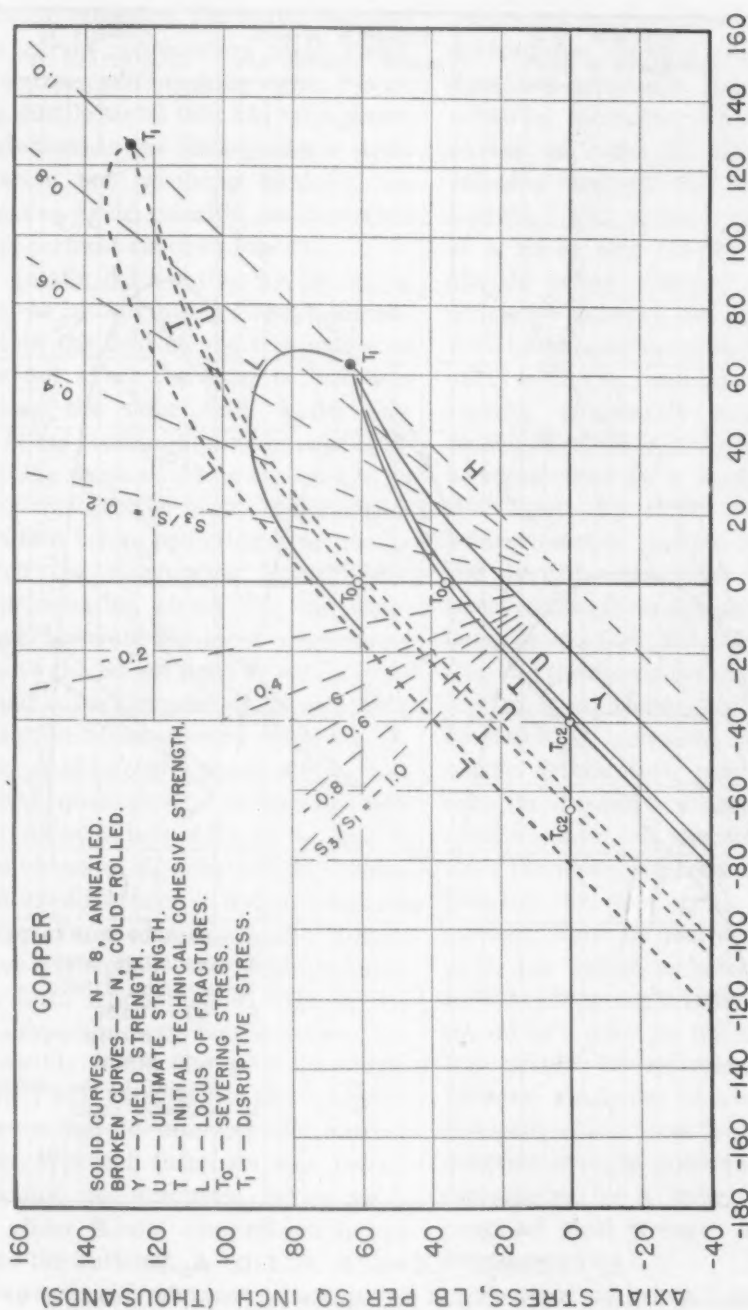


FIG. 9.—STRENGTH DIAGRAMS FOR ANNEALED AND COLD-ROLLED COPPER.

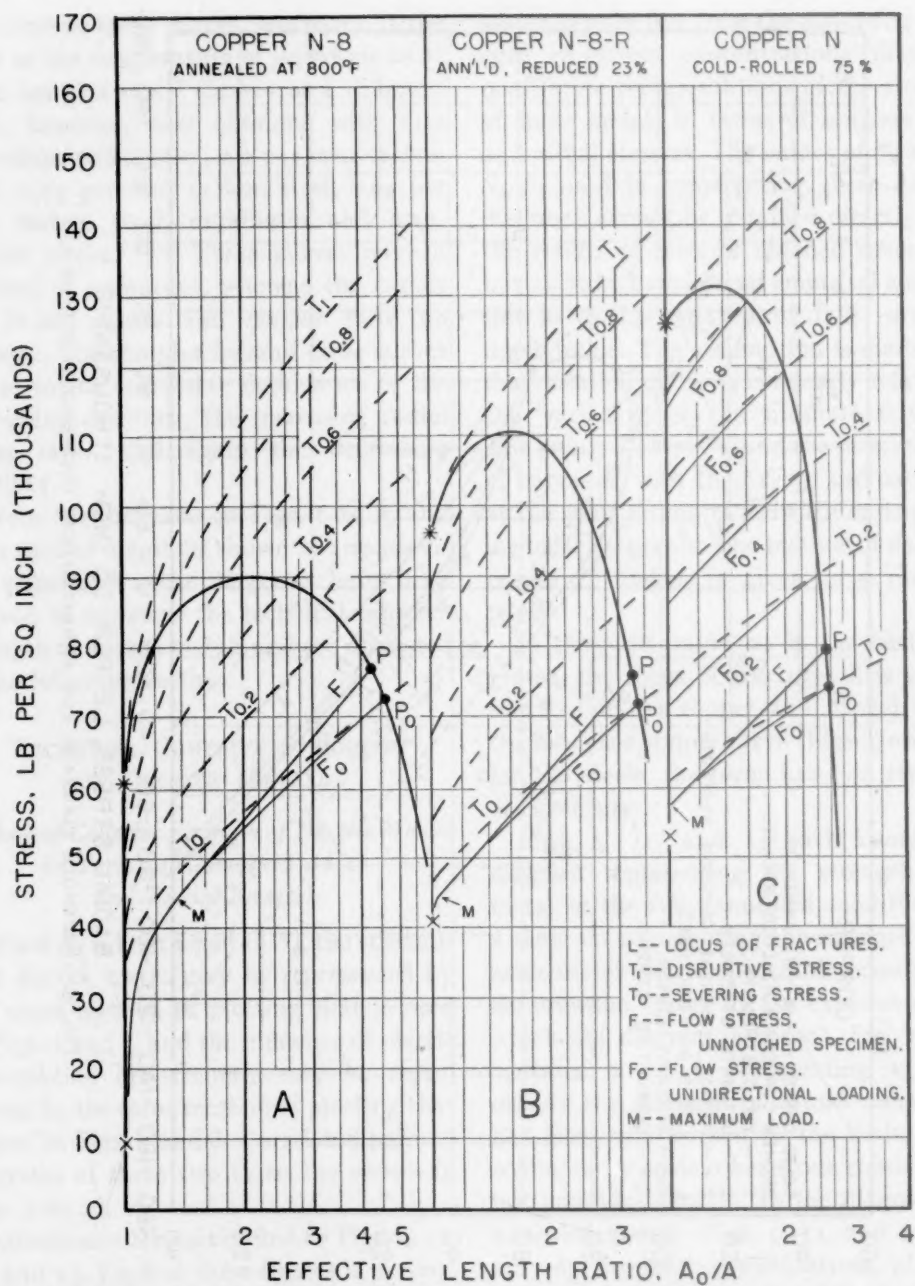


FIG. 10.—INFLUENCE OF PLASTIC DEFORMATION ON TECHNICAL COHESIVE STRENGTH OF COPPER

prior plastic extension, the nearer together are the curves representing yield stress, ultimate stress, and breaking stress. For an initially ductile metal that has been plastically deformed to the limit (under a stress combination not involving tension), the three curves would coincide, as illustrated by the uppermost curve in Fig. 11.

Prior plastic deformation by rolling or drawing, or by any other stress combination within the field of negative values of S_3 , does not affect the locus of fractures throughout the same field. Under any specific stress combination within the field, the breaking stress would be expected to be the same whether the plastic deformation had occurred before or during experiments on which the diagram is based. Prior plastic deformation within this field, however, would elevate the locus of fractures throughout the field of positive values of S_3 and would move the point T_1 representing the disruptive stress upward along line H .

The locus of fractures appears to be well established qualitatively throughout the field of positive values of S_3 . In the field of negative values of S_3 , however, the course of the locus of fractures is not so definitely established. For moderately ductile metals, the curve throughout this field probably has the form represented in Figs. 9, 11, and 13. For some very ductile metals, the curve possibly would diverge more widely from line H as it extends into this field, and might even fail to intersect the axis of abscissas. Whether there are any metals that cannot be fractured when cold-worked under biaxial compression is not known to the author.*

In the previous discussion of Figs. 9, 11, and 13, no mention has been made of curve T , which represents the *initial* technical cohesive strength, the technical cohesive strength of the metal unaltered by any except "*prior*" plastic deformation. As any point on the locus of fractures except T_1

represents fracture after *additional* plastic deformation, curve L for a ductile metal does not represent the initial technical cohesive strength. The desirability of having an index of the initial technical cohesive strength was first discussed by Ludwik,⁶ who showed that the ductility of a metal and the energy that it will absorb before fracture depend on the difference between the flow stress and an initial technical cohesion limit. In accordance with the prevalent view, however, Ludwik erroneously assumed that the technical cohesive strength of a metal can be represented by a single technical cohesion limit, the stress at fracture under polarsymmetric tension. He assumed that the ductility and total work under *any* stress combination depend on the difference between the flow stress for that combination and the disruptive stress. As illustrated in Figs. 9, 11, and 13, however, this view is incorrect. A cohesion limit, even after plastic deformation, may be much lower than the disruptive stress. The ductility of a metal under any specific stress combination, therefore, depends on the difference between the flow stress and a technical cohesion limit *for that combination*. Moreover, the *initial* technical cohesion limit for that stress combination cannot be represented by a point on the locus of fractures, but should be represented by a point between the curve of yield strength and the locus of fractures. The initial technical cohesive *strength*, consequently, should be represented by a *curve* (T) between the curve of yield strength and the locus of fractures.

No point on curve T (except T_1) can be established directly because the yield stress for that stress combination would be exceeded before fracture and the technical cohesive strength would increase. Nevertheless, a suitable curve to represent the initial technical cohesive strength can be established approximately by correlating each diagram of Figs. 9, 11, and 13 with the

* Under unidirectional compression, very ductile metals cannot be fractured.⁷

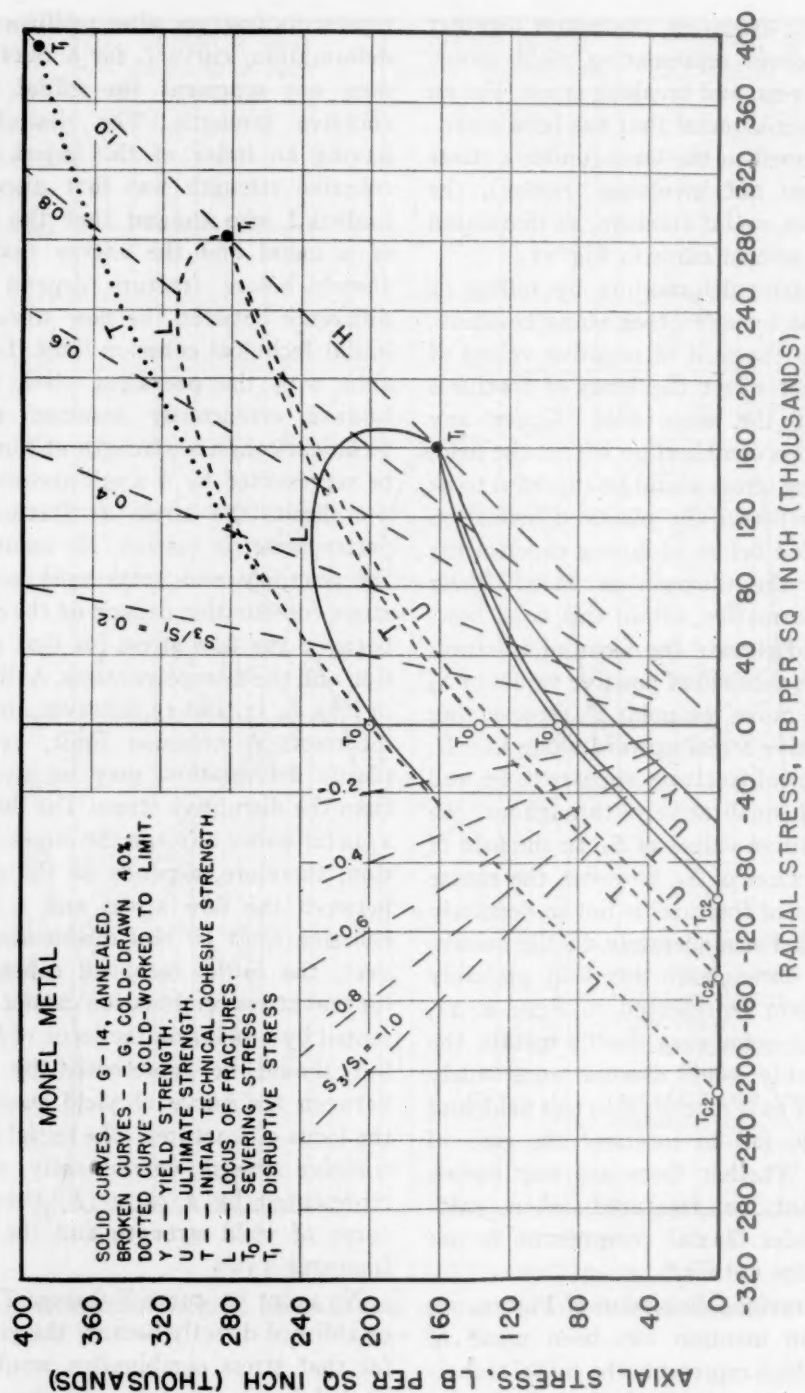


FIG. 11.—STRENGTH DIAGRAMS FOR ANNEALED AND COLD-DRAWN MONEL METAL.

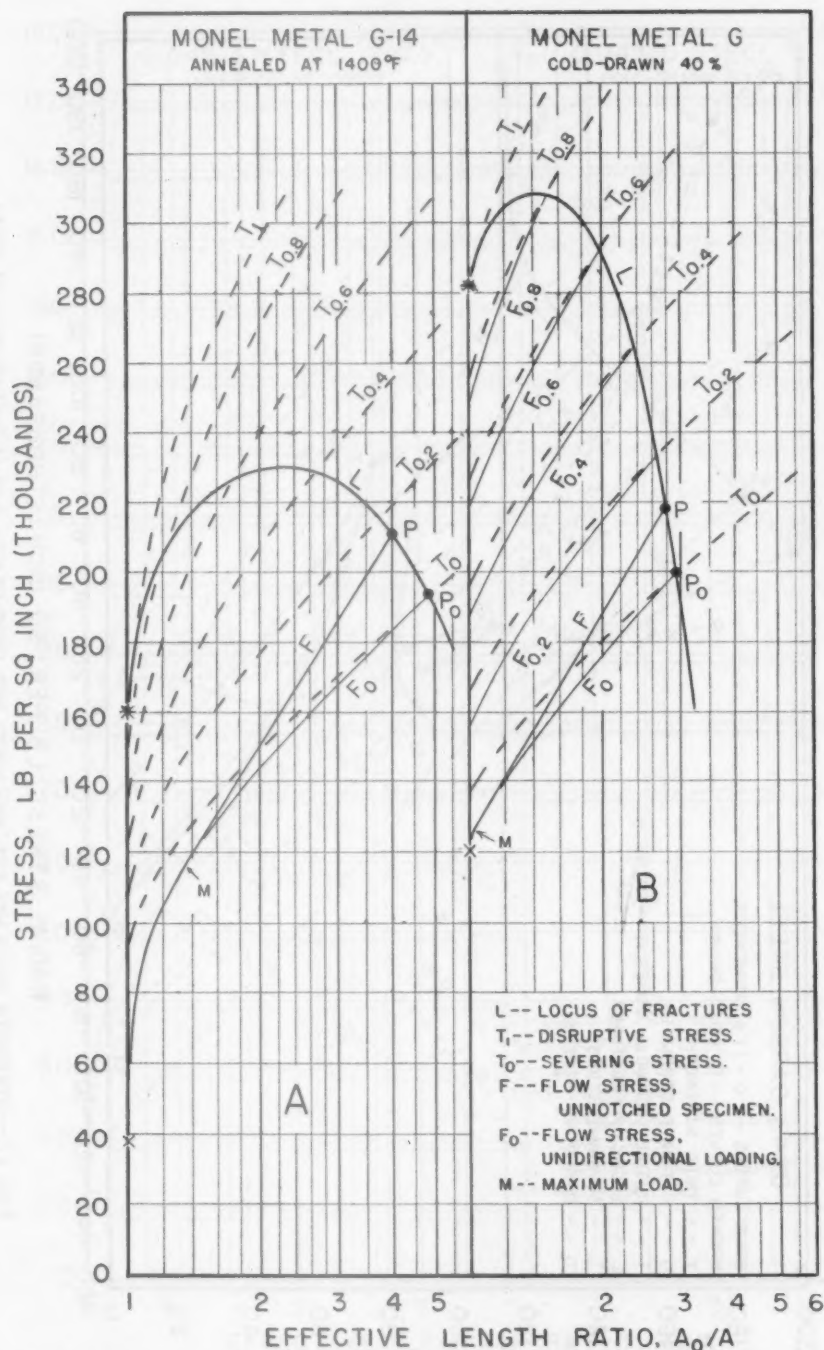


FIG. 12.—INFLUENCE OF PLASTIC DEFORMATION ON TECHNICAL COHESIVE STRENGTH OF MONEL METAL.

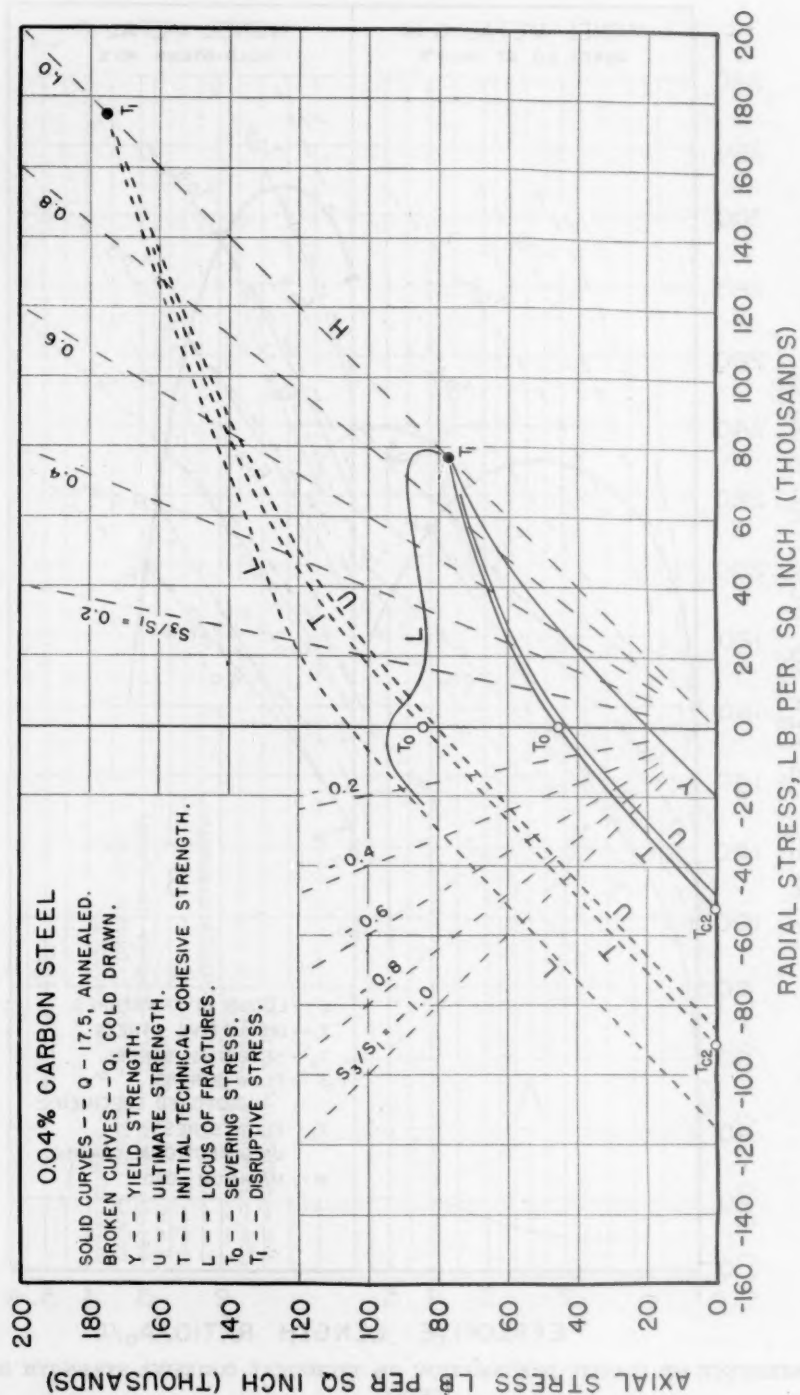


FIG. 13.—STRENGTH DIAGRAMS FOR ANNEALED AND COLD-DRAWN 0.04 PER CENT CARBON STEEL.

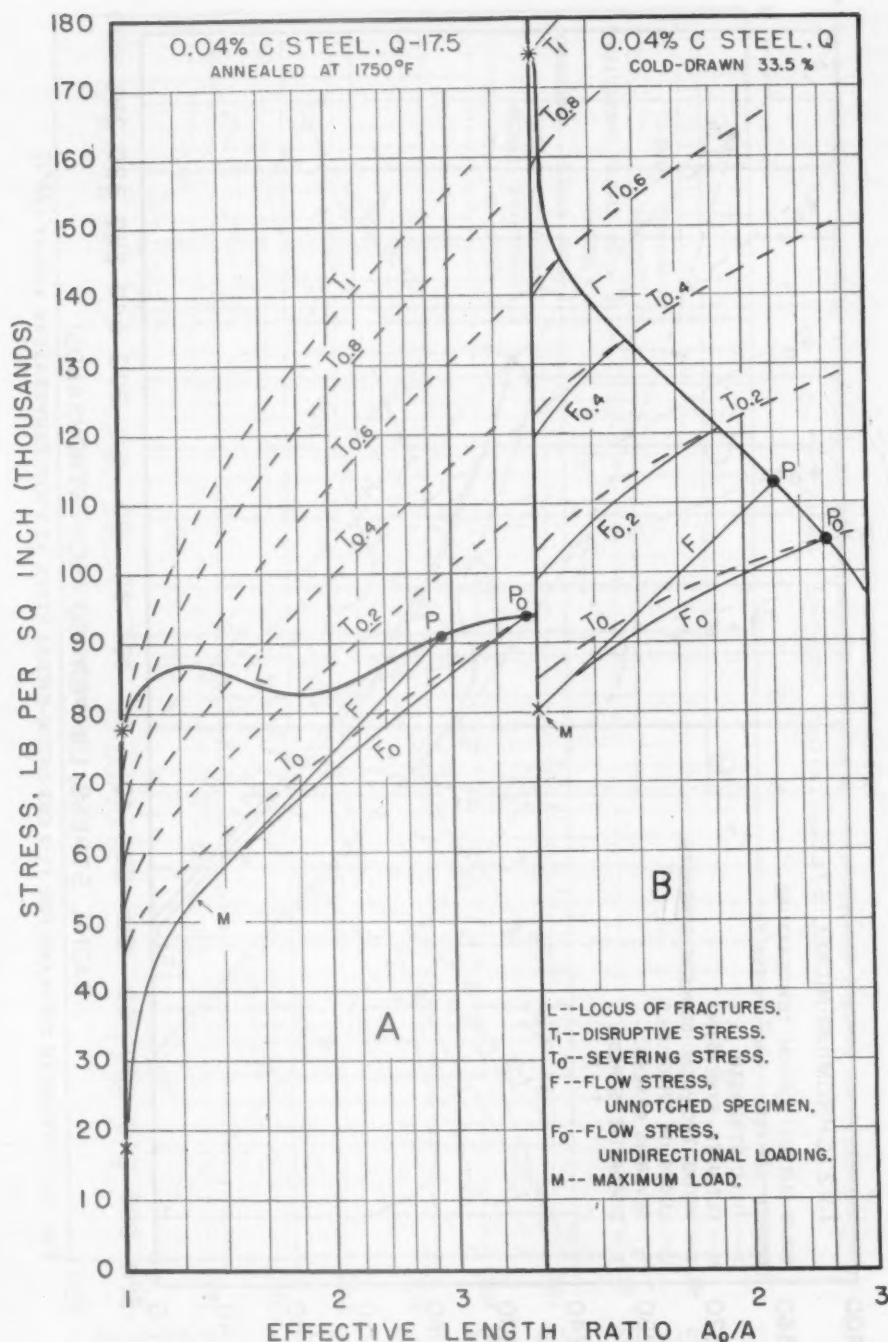
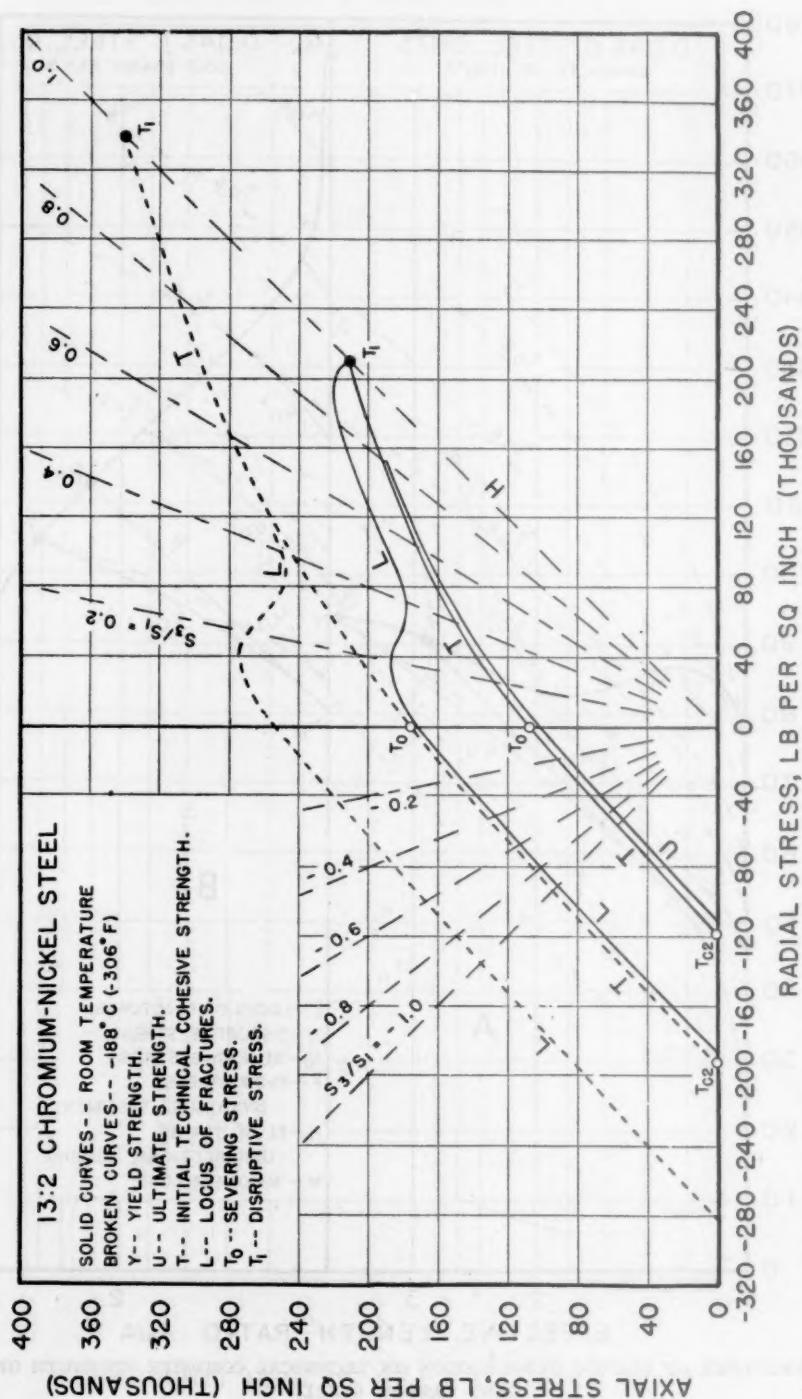


FIG. 14.—INFLUENCE OF PLASTIC DEFORMATION ON TECHNICAL COHESIVE STRENGTH OF 0.04 PER CENT CARBON STEEL.



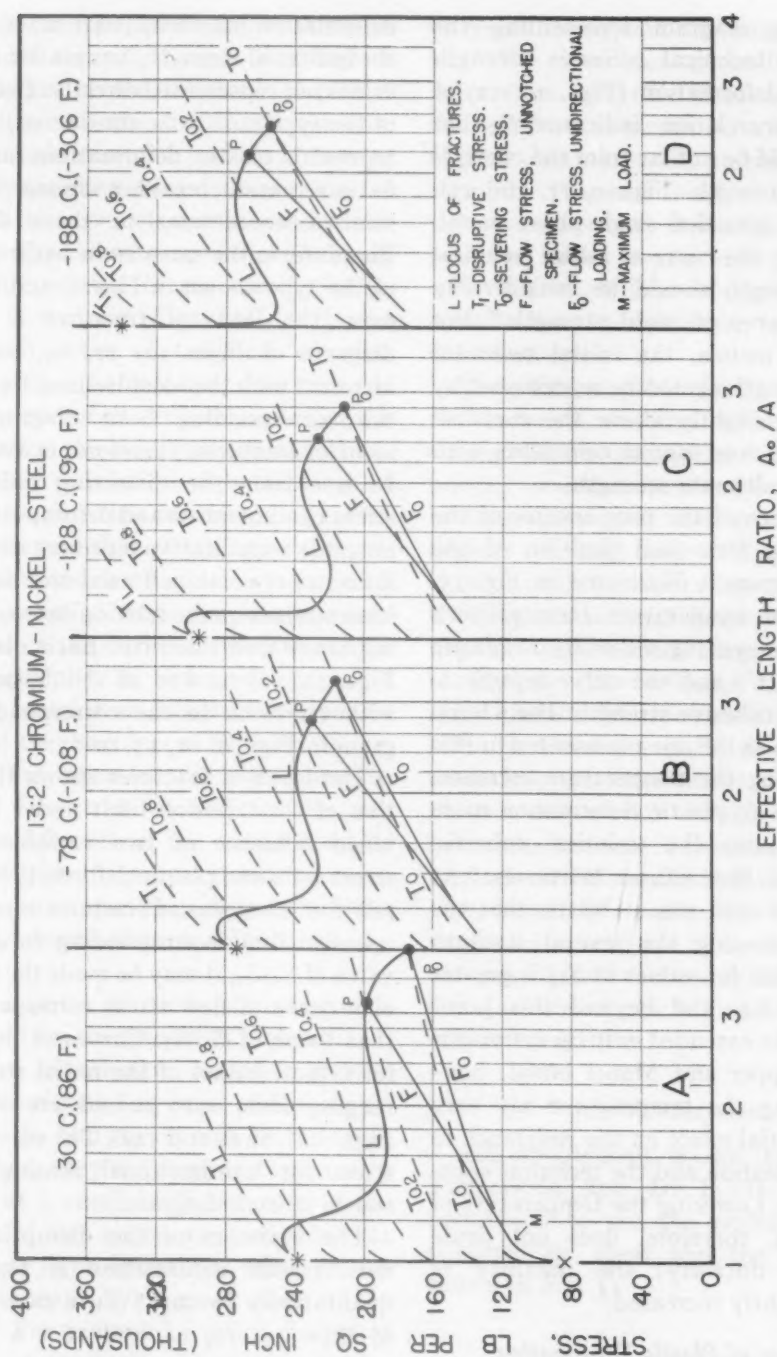


FIG. 16.—INFLUENCE OF PLASTIC DEFORMATION AT VARIOUS TEMPERATURES ON TECHNICAL COHESIVE STRENGTH OF 13:2 CHROMIUM-NICKEL STEEL.

corresponding diagram representing the variation of technical cohesive strength with plastic deformation (Figs. 10, 12, or 14). Such correlation indicates⁶⁻¹¹ that curve T should be not far from the curve U of ultimate strength (Figs. 9, 11, and 13). For a fully annealed single-phase metal, consequently, the curve of initial technical cohesive strength should be considerably above the curve of yield strength.* For cold-worked metals, the initial technical cohesive strength should be represented by a curve only slightly above the curve of yield strength, and almost coinciding with the curve of ultimate strength.

The influence of the temperature of the metal on the form and position of the strength diagram is illustrated in Fig. 15. A decrease of temperature elevates both the curve representing resistance to plastic deformation (U) and the curve representing technical cohesive strength. For a ferritic steel, such as the one represented in this figure, lowering the temperature increases the resistance to plastic deformation more than it increases the technical cohesive strength, and thus causes brittleness. At -188°C . this steel was so brittle that the curves representing the several strength indices coincide for values of S_2/S_1 greater than about 0.4, and beyond this point curve T can be extended only by extrapolation. For copper and Monel metal, however, lowering the temperature has very little differential effect on the resistance to plastic deformation and the technical cohesive strength. Lowering the temperature of these metals, therefore, does not cause decrease of ductility; the ductility of copper is slightly increased.

Influence of Plastic Deformation on Technical Cohesive Strength

In the diagrams just discussed (Figs. 9, 11, 13, and 15), the influence of plastic

* Although curve T for the annealed metals has been drawn slightly above curve U , it is possible that for some annealed metals curve T should be between curve Y and curve U .

deformation manifests itself in its effect on the indices of strength, but plastic deformation is not represented directly. In diagrams of the type now to be considered, abscissas represent plastic deformations and ordinates represent breaking stresses. The system of coordinates in these diagrams, therefore, is the same as in basic diagrams of the type shown in Figs. 7 and 8. Moreover, the locus of fractures L in each diagram of Figs. 10, 12, 14, and 16 is identical with the ideal locus of fractures in the corresponding basic diagram. Each locus of fractures, therefore, is assumed to be free from the distorting influence of stress concentration and deformation gradient; it is a qualitative representation of the influence of combined axial and radial uniform stresses on the relation between breaking stress and ductility. Each diagram in Figs. 10, 12, 14, and 16 should be studied with reference to the corresponding diagram in Figs. 9, 11, 13, or 15.

The locus of fractures shows the variation of the cohesion limit under the combined influence of two variables, radial stress ratio and plastic deformation. As any point on the locus of fractures represents a cohesion limit corresponding to a specific value of S_2/S_1 , it may be made the terminus of a curve of flow stress corresponding to that value of S_2/S_1 . Curves of flow stress for typical values of the radial stress ratio ranging from zero to 0.8 are shown in Figs. 10C, 12B, and 14B. The curve of flow stress for unidirectional tension (F_0) is shown in each diagram.

The variation of the disruptive stress with plastic deformation is represented qualitatively by curve T_1 in each diagram of Figs. 10, 12, 14, and 16.* A curve of variation of a single *technical cohesion limit*, however, is not an adequate representation

* In previous papers,^{6,7} reasons are given for the view that plastic extension causes the disruptive stress to increase continuously at a decreasing rate. The effect of plastic deformation on the disruptive stress is qualitatively similar to its effect on the flow stress.

of the influence of plastic deformation on the *technical cohesive strength*. A complete representation of the influence of plastic deformation on the technical cohesive strength would comprise a series of curves, each corresponding to a typical value of S_2/S_1 . Each curve of a series should be qualitatively similar to curve T_1 and should be properly related to the corresponding curve of flow stress (Figs. 10C, 12B, and 14B). Each curve of technical cohesion must be above the corresponding curve of flow stress except at the intersection of the two curves on the locus of fractures. Moreover, proper correlation with the locus of fractures requires that corresponding curves of cohesion and flow stress have approximately the indicated relationship; each curve of cohesion must rise continuously and intersect the curve of flow stress at a small angle.^{6-11*} A series of curves of technical cohesion so constructed is shown in each of the diagrams of Figs. 10, 12, 14, and 16, but some of the corresponding curves of flow stress are omitted. In each series, the left ends of the curves must be correlated with the proper points on curve T in the corresponding diagram of the previously described type (Figs. 9, 11, 13, or 15).

When a series of curves of cohesion is constructed on the principles just outlined, each curve of cohesion rises less rapidly than the corresponding curve of flow stress. Although the two curves may be far apart at the origin, they converge and eventually intersect at a small angle. Because of the acuteness of this angle, any variable that has even as light differential effect on the two curves may have a great effect on the ductility. For example, a small change of S_2/S_1 or a small change of temperature may have a great effect on the ductility (Figs. 14A and 16). The evidence thus indicates that the difference between the technical cohesive strength of a metal and

its resistance to plastic deformation is much less than has been generally supposed. After even moderate plastic deformation, the resistance to plastic deformation is only slightly less than the technical cohesive strength. The additional plastic deformation to overcome this slight difference, however, varies greatly with the metal and with the conditions of stressing (stress combination, temperature, and rate of deformation).

The effect of *prior* plastic extension on the technical cohesive strength may be studied by comparing the diagrams representing annealed metal with those representing metal that has received various degrees of cold-work. Comparison may thus be made between diagrams A , B , and C of Fig. 10, between diagrams A and B of Fig. 12, and between diagrams A and B of Fig. 14. The evidence indicates that prior plastic deformation has very little effect on the stress at P_0 ; this point represents fracture after about the same total plastic deformation whether the metal before the test was in the annealed or cold-worked condition. Prior plastic deformation, however, elevates the locus of fractures at and near the left end; the greater the prior plastic extension, the greater is the elevation of the left end and of much of this curve.^{7,9}

Acknowledgment

Acknowledgment is due to Dr. L. B. Tuckerman and Dr. L. H. Adams for permission to use the evidence that was obtained by them and the photographs shown in Fig. 3.

REFERENCES

1. P. W. Bridgman: Breaking Tests under Hydrostatic Pressure, and Conditions of Rupture. *Phil. Mag.* (July 1912) **24**, 63-80.
2. P. W. Bridgman: Theoretically Interesting Aspects of High Pressure Phenomena. *Reviews of Modern Physics* (1935) **7**, 1-35.
3. P. W. Bridgman: Reflections on Rupture. *Jnl. Applied Physics* (1938) **9**, 517-528.

* For a fuller discussion of this subject see page A164 of Ref. 6.

4. P. W. Bridgman: Considerations on Rupture under Triaxial Stress. *Mech. Eng.* (Feb. 1939) **61**, 107-111.
5. P. Ludwik: Über die Bedeutung der Elastizitätsgrenze, Bruchdehnung und Kerbzähigkeit. *Ztsch. Metallkunde* (1924) **16**, 207-212.
6. D. J. McAdam, Jr.: The Technical Cohesive Strength of Metals. *Trans. Amer. Soc. Mech. Engrs.* (1941) **63**; *Jnl. Applied Mechanics* (Dec. 1941) **3**, A156-165.
7. D. J. McAdam, Jr.: The Technical Cohesive Strength and Yield Strength of Metals. *Trans. A.I.M.E.* (1942) **150**, 311-357.
8. D. J. McAdam, Jr.: The Influence of the Combination of Principal Stresses on Fatigue of Metals. *Proc. Amer. Soc. Test. Mat.* (1942) **42**, 576-592.
9. D. J. McAdam, Jr. and R. W. Mebs: An Investigation of the Technical Cohesive Strength of Metals. This volume, p. 474.
10. D. J. McAdam, Jr. and R. W. Mebs: The Technical Cohesive Strength and Other Mechanical Properties of Metals at Low Temperatures. *Proc. Amer. Soc. Test. Mat.* (1943) **43**, 661-703.
11. D. J. McAdam, Jr., R. W. Mebs and G. W. Geil: The Technical Cohesive Strength of Some Steels and Light Alloys at Low Temperatures. Preprint No. 27, Amer. Soc. Test. Mat. Annual Meeting, June 1944.
12. L. B. Tuckerman: Oral communication to Philosophical Society of Washington, mentioned in *Jnl. Wash. Acad. Sci.* (1935) **25**, 463.

Flow and Fracture

By P. W. BRIDGMAN*

Flow and fracture are admittedly complicated phenomena of which we are yet only partially masters. There is not even universal agreement as to the details of the language best adapted merely to describe the phenomena, to say nothing of any theory. Certain points of view, however, are widely held, and there are certain general expectations as to what sort of procedures will prove permissible.

A complete description of any situation involving fracture would demand a complete history of all the variables in the control of the experimenter. The experimenter endeavors so to choose his independent variables that they are adequate to determine completely the situation in the sense that when an experiment is repeated on the same initial material and with the independent variables running through the same sequence, all the other measurable properties of the system will also run through the same course.

It is, I think, the universal conviction that when we are dealing with phenomena of flow and fracture, the most important of the necessary variables are the external forces acting on the various parts of the body; when the force history repeats, with certain obvious restrictions such as that temperature must be constant and non-mechanical forces, such as magnetic field, must be small enough to be ineffective, then the history of all measurable properties will repeat; in particular the alteration of geometrical shape due to flow will run through the same course, and

when fracture comes, the character of the fracture will be reproduced.

Complete mastery of merely the descriptive aspects of flow and fracture would demand the ability to predict the entire course of flow and complete characterization of the final fracture for every possible combination of forces, varying in time in all possible ways, when applied to bodies of all possible shapes. This full situation is obviously of prohibitive complexity.

The first stage in reduction to manageable simplicity is to resolve the total situation into the sum of contributions made by small elements. Our thesis is that if each of the elements is adequately characterized, the behavior of the whole system is fixed. The element is usually taken of a simple geometrical shape, suggested by the mathematics best adapted to the particular situation. The forces acting across the faces of the elements are ultimately determined by the forces acting across the free faces of the whole system.

The detailed process of finding the precise forces on the faces of all the elements in terms of the external forces involves the use of a special mathematical invention, the stress, a constructional quantity consisting of six components. The stress at any point in the body is determined by both the external force system and by the physical properties of the body at all points; quite different stresses prevail at the interior of bodies of the same shape under the same external forces in the elastic and plastic ranges. The forces on the faces of any element are, however, uniquely determined by the stress system at the element. Our fundamental thesis

*Hollis Professor of Mathematics and Natural Philosophy, Harvard University, Cambridge, Massachusetts.

now demands that the physical properties of the elements are completely determined by the stress history at the corresponding elements. This means in particular that when the stress history of the element repeats, the entire course of the distortion, that is, the entire flow history, repeats.

This minimum of assumption—that is, description in terms of stresses, application to elements—and the assumption that if the stress history repeats the flow history repeats, is, I believe, implicit in the thinking of most people who have concerned themselves with questions of flow and fracture. It is, I believe, customary to go a step further than this and to expect that rupture will always occur at the same stage in the stress history of the elements, no matter where the elements are situated. That is, it is common to suppose that fracture is a point phenomenon, determined only by conditions at the point. This, it seems to me, is a much more questionable assumption; fracture may well demand the cooperation of a number of elements, and may not occur unless neighboring elements are so mutually conditioned as to permit a propagation. A necessary condition for the possibility of such a propagation is set by the requirement that the total energy of the whole system must decrease in consequence of the fracture. In practice, however, it would appear that the conditions for propagation are usually present, so that in a great many situations fracture as well as flow may be handled as a point phenomenon.

STRESS HISTORY

The problem, with the minimum of assumption outlined above, is still of baffling complexity. A great simplification would obviously be achieved if it were possible to neglect the effect of the stress history, for then the distortion of an element under any system of stresses would be completely determined by the instantaneous stress alone. This is known to be

the case within the elastic range; in fact this is involved in the definition of elastic range. Under suitable conditions it may also hold in the plastic range; it is a matter of experience that the conditions so demanded are liberal enough to permit application to many important practical situations. If the stress system has only one component, this implies that the final distortion or fracture is independent of the rate of application of the stress; or if the stress system has more than one component, it may imply that the stress builds up from zero in such a way that the components always bear the same ratio to each other. At the same time it is easy to give examples in which the stress history is of vital importance. For example, under a hydrostatic pressure no plastic flow occurs, but if the final state of hydrostatic stress is reached by increasing in succession the three components of stress from zero to their maximum value, evidently very large plastic deformations in the final state may be expected for high pressures. This situation is accentuated with regard to fracture.

A great deal of work has been done on situations subject to the restrictions just described, that is, in which the state of flow or fracture in any element is determined by the complete stress system at the element, and it would, I believe, be easy to obtain agreement in most special cases as to whether the conditions justified a specification in such simple terms. The relations in such systems may be represented in different ways. Thus fracture may be represented by a surface in three dimensions, using the three principal stresses as coordinates. If the stress on an element is represented by a point on the surface, then the element is in a state of fracture. If the stress point lies within the surface, the material has flowed without fracture, and points outside the surface represent systems of stress impossible of attainment in the specified material. The

flow cannot be so adequately represented by simple geometrical construction; to specify it completely the six components of the strain tensor must be given at every point of the triply infinite stress manifold. This representation has to be done in general by systems of equations. It is to be remarked that in particular the flow is determined at fracture, or infinitesimally below fracture, so that a complete specification of the phenomena at fracture demands not only giving the fracture surface but also the complete strain tensor at every point on the fracture surface.

INTERCONNECTION OF FLOW AND STRESS

In the region in which we are interested not only is the flow a function of the stress, but the stress is also a function of the flow, that is, either the stress or the distortion may be taken as the independent variable (we neglect here questions arising from multiple values). We might, therefore, construct a surface for fracture in a space in which the components of flow are taken as the coordinates instead of the components of stress. This representation, however, is not very common; perhaps the reason is that it is more natural to regard the stress as the independent variable because it is the stress which is usually subject to independent control in any experimental setup.

Situations are easy to construct in which neither of these geometrical methods of representing fracture is obviously general enough, as when the stress has passed through wide cycles. Many such situations may be treated by special devices; thus for some purposes it is possible to discuss the behavior of a material which has been prestrained by treating the prestrained material like a virgin material with initial properties altered by the prestrain.

A corollary of the fact that stress and flow are interconnected and either may be taken as the independent variable is that we cannot isolate the effects of stress

and strain. Taken at their face value questions like: "How would the properties of a body be changed if a stress were applied to it without producing distortion?" or, "At what stress would a body fracture if the stress were applied without producing flow?" are meaningless, because the stress distorts the body along with changing its other properties. Questions like these can be given only a conventionalized meaning, which has to be set up by definition for every specific situation. Whether it is profitable to set up such conventionalized meanings will be to a large extent determined by the fruitfulness of the theoretical background which suggests the convention.

The actual construction of the surface of fracture and the complete mathematical specification of flow in terms of stress is something which has been hardly touched in practice, but at present it is almost entirely a program for the future. The principal reason is doubtless the experimental difficulty of independently controlling the principal stress components. By far the larger part of routine testing is tensile testing, in which a bar is subject to a controlled force along one axis. With more difficulty it is possible to control more complicated situations, in which the force has two degrees of freedom. The simplest cases of two degrees of freedom are probably those with rotational symmetry, in which one principal stress component may be given one value and the two other principal components the same different value. Even here the practical possibilities are much limited; the axially symmetric external force that gives rise to two equal stress components may be readily applied if the desired stresses are compressive by means of a fluid under pressure, but there seems to be no simple direct way of applying an axially symmetric tension, and indirect methods have to be used. In spite, however, of the experimental awkwardness, there is now a considerable body of experimental material for stress

systems with two degrees of freedom. Such experiments give the intersection of the complete three-dimensional fracture surface with certain planes, and give enough information to make possible at least plausible guesses as to the shape of the complete fracture surface. But because the methods of attack are often indirect and because of the general experimental difficulty, it is just here that difference of opinion begins to arise, and we approach the field of controversy.

I think a large part of the lack of agreement here arises from the projection, into the unexplored three-dimensional domain, of expectations and theories extrapolated from experience in one or two dimensions. This is particularly true with regard to phenomena of fracture; the phenomena of flow are so much more complicated that there is less temptation to treat them intuitively. For example, in a tensile test, fracture occurs when a critical tensile force is applied, and one speaks of the tensile strength, a thing which is characterized by giving a single number. There is a temptation to carry this point of view over to the general situation and to think of fracture in general as determined by some single parameter reaching a critical value, as in the maximum principal stress criterion of fracture or the maximum principal extension criterion. In general the "strength" is not a single simple thing, but is a complex aggregate. It would be well to recognize this explicitly in the nomenclature; I think it would lessen confusion if, instead of using such terms as "cohesive strength," we used the expanded term "the cohesive strength tensor."

STRESSES WITH TWO DEGREES OF FREEDOM

Recently a large amount of work in the field of stresses with two degrees of freedom has been done by McAdam. His earlier papers were largely a discussion and recalculation of experimental material of others, but in his last two papers a large

mass of new experimental material has been presented. The experimental material comprises almost entirely tensile tests on notched bars; here the longitudinal tensile force is capable of independent variation, but the radially symmetric stress at the notch has to be controlled indirectly by varying the geometry of the notch and calculating with the use of special formulas. This extensive work is, it seems to me, of undoubted and great value, both for its experimental material and for its often stimulating discussion. Thus, it is emphasized that the strength of a material is not determined by a single parameter but demands, for example, that the maximum principal stress be given and the ratio to it of the other principal stresses. I would, nevertheless, like to make two criticisms. The first is more or less formal and superficial. I think the term "technical cohesive strength" is used in a way which is often obscure and which demands close analysis by the reader to find exactly what is meant. If one examines what McAdam does, I think it will be found that in a large part of his work his "technical cohesive strength" is merely the algebraically greatest principal stress at fracture. He does, nevertheless, speak, in closely juxtaposed parts of his exposition, of the effect of stress ratio and of flow on the technical cohesive strength in such a way as to give the impression that these are two independent things. He speaks of *curves* of "initial cohesive strength of unaltered material" for varying ratios of the principal stresses, and he says that no point of this curve, except one, could conceivably be attained by experiment. In most of the usages of McAdam, clarity can be attained by the reader if he will paraphrase his "technical cohesive strength" by "the entire stress complex at fracture," but even this is not always enough, for there are situations in which the meaning can be found only with the assumption of a background of theory and presupposition

which is not explicitly stated, and which I personally am unable to reconstruct.

The second criticism is more serious and is concerned with the technical details of the work. It is necessary for McAdam to evaluate by some method the radially symmetric stress field at the notch of the tension specimen. The actual field varies from zero at the outer surface of the notch, where it is fixed by the boundary conditions, to some maximum value at an interior point. In his analysis, McAdam uses the average radial stress; to find the average, the distribution must be known. The problem of the exact distribution of stress in the plastically strained notch has never been solved; McAdam has to use an approximate solution obtained by a qualitative argument, based on graphical constructions and the known solution in the elastic case. His final result is a longitudinal stress component approximately constant across the entire section, and a radial component approximately constant across all the section except in a thin outer skin, where it drops rapidly to zero. The strain, on the other hand, is recognized to vary importantly across the section. McAdam recognizes the approximation and speculates on corrections arising from gradients of stress and strain. The criticism which I offer here is that it appears to me that McAdam's picture is not qualitatively adequate; I believe that the longitudinal and radial stresses depart much more from constancy than McAdam assumes, and that this departure from constancy is important, particularly in determining fracture.

The basis of this criticism is contained in a paper given at another session of this same meeting.* The results of ordinary tensile tests are usually given in terms of the average stress across the neck, and the conditions at fracture of a tensile

specimen are given in terms of this single parameter. It has been recognized, however, that stress is not uniform across the neck, and that on the axis there is a radial component of stress, but there has been no method of evaluating numerically how large these effects are. The paper to which I refer presents a solution for the distribution of stress at the neck of an ordinary tension specimen which is mathematically rigorous on the assumption of a certain simple form for the equations of plasticity, and which should approximate closely enough to actual plastic materials to give a qualitatively adequate picture. It turns out that under ordinary conditions of testing, when the specimen breaks with a reduction of area up to 70 per cent, the coordinates of the flow and strain-hardening curves are not too greatly different from those obtained by the ordinary procedure, neglecting the variation of stress across the neck. Even in the ordinary case, however, the conditions of fracture are materially altered by the radial stresses. Under more extreme conditions of necking, the corrections, both for flow and for fracture, become more important. Since a notch constitutes an extreme case of a neck, it is to be presumed that McAdam's results may require essential modification.

STRESS DISTRIBUTION AT NECK

I have collected and reviewed a large mass of new experimental data in the light of the correction for the effect of stress distribution at the neck, and certain simple features in the situation begin to stand out; I shall give a brief account of them now. It will pay first to describe more fully the stress distribution at the neck. Under ordinary conditions of testing the stress at the neck of a tension specimen may be analyzed into the sum of two stress systems. The first is a tension along the axis constant across the section, and the second is a superposed hydrostatic tension (what McAdam calls a polar symmetric

* Stress Distribution at the Neck of a Tension Specimen. *Trans. Amer. Soc. Metals* (1944) 32, 553.

stress), varying from zero at the outside surface to a maximum on the axis. The average tensile stress at the neck, that is, the total load divided by the cross section of the neck, which alone is given in reporting conventional tensile tests, is an average of the constant component and the contribution arising from the component of the hydrostatic tension in the direction of the axis. Flow at the neck of the conventional tension specimen, which starts with a cylindrical figure and necks down during the progress of the test, is uniform across the section of the neck. This is obvious from geometrical considerations of symmetry.* In this respect an ordinary necked specimen is much simpler than a notched specimen, in which flow may be far from uniform across the section, and the results therefore less capable of unambiguous interpretation. Since the flow is uniform and the stress not uniform, it follows that the same flow may occur under different stress systems. It is tacitly assumed in constructing curves of tensile flow or strain-hardening curves

for tension that the stress is of a specified simple type; that is, there is one principal stress component in the direction of tensile flow, with the other two components vanishing. This is the condition at the outer surface of the neck of a tension specimen. It follows that in deducing a strain-hardening or flow curve from the results of a tensile test one should plot strain at the neck against the first of the two stress systems above; that is, against the constant stress component or the stress at the outside surface. This is less than the average stress obtained by dividing the total load by the neck area. The factor by which it is less depends on the degree of necking; if the reduction of area is 37 per cent, the flow stress at the edge is approximately 0.9 of the average stress. For a 73 per cent reduction, it is 0.80, and for a 95 per cent reduction 0.75.

The mathematical solution demands that the flow be unaffected by a superposed hydrostatic stress. This may be checked experimentally by repeating the tensile test in a medium under hydrostatic pressure. It is found that if the average tensile stress is corrected to give the flow stress, all the extension versus flow stress points lie on a single curve, irrespective of the hydrostatic pressure at which the experiment is performed. This holds for pressures up to 30,000 kg. per sq. cm. (If we call the flow stress F , taken along the Z axis, and conduct the experiment in a medium under hydrostatic pressure P , then in conventional cylindrical coordinates the three principal stresses at the outer surface of the neck are: $rr = \theta\theta = -P$; $zz = F - P$.)

By performing the experiment under different hydrostatic pressures, instructive results may be obtained. The use of pressure not only affords a method of varying the ratio of the axial to the radial components of stress, but drastic changes are produced in the physical properties of the material. Under high hydrostatic pressure the ductility of ordinary steels or other

* Note added on reading proof, Nov. 11, 1944.—A direct experimental investigation has now been made of the validity of the assumption that the strain is uniform across the neck of a tension specimen. The method is to core the tension specimen by silver-soldering into it a solid core. After pulling, and on making a longitudinal section of the specimen, the very thin film of silver solder affords a means of identifying internal points and so finding the strain at internal points. The complete phenomena were mapped out by varying the core diameter and by pulling to different reductions of area, employing the cooperation of high hydrostatic pressure to permit large reductions of area. A small but measurable deviation of strain from uniformity was found, the longitudinal strain at the axis being somewhat greater than at the periphery. Numerically, for the extreme conditions realized, corresponding to a reduction of area of 92 per cent and the inner 12 per cent of the cross-sectional area, this would mean a flow stress greater by 5 per cent than that calculated by the mathematical formulas based on the assumption of uniform flow. When integrated over the entire area and when applied to specimens with a reduction of area in the normal range, any corrections for the effect of nonuniformity of flow turn out to be entirely negligible.

These experiments are described in detail in a nonrestricted report to the Watertown Arsenal, No. WAL 111/7-6.

metals is enormously increased, and at pressures of the order just mentioned reductions of area of nearly 100 per cent may be obtained without fracture. In one case an elongation at the neck of 300 fold was obtained in a steel that normally breaks with a reduction of area of 60 per cent. The increased ductility manifests itself not only in a greatly increased elongation without fracture, but also in a radical change in the qualitative character of the fracture, the normal cup and cone fracture, which is part shear and part tensile, giving way to a type of break entirely shear.

By conducting experiments under different hydrostatic pressures and taking advantage of the great increase of ductility under pressure, it is possible to extend the strain-hardening or flow curves to much greater strains than are ordinarily attainable. A large number of such curves have been determined for a number of different steels out to natural strains of 3; that is, to extensions of 20 fold. It is the universal result of all these experiments that the stress-strain curve—that is, flow stress against natural strain—is linear beyond the low natural strain (about 0.1) at which necking starts. On occasion points have been located on the line as far out as natural strains of 5 (extensions of 150 fold), but at such large strains the experimental accuracy becomes unduly diminished because of excessive reduction of cross section and hence of the total load.

FRACTURE

So much for flow at the neck; it is a phenomenon occurring uniformly across the neck, and may be specified indifferently by giving the stress components at any point of the neck. Fracture, however, is a different sort of thing; it is initiated at a definite point, and to characterize it the stress components at this point must be given. The evidence from ordinary tensile tests seems to be that fracture is initiated

on the axis. This is consistent with the results of the mathematical analysis for stress distribution, and in fact the whole picture with regard to fracture is clarified by considering the effect of the stress distribution. Fracture starts because of the presence of a hydrostatic tension superposed on the uniform tension. The general effect of a hydrostatic tension is to make the substance more brittle so that it will break with less plastic flow. In fact, if sufficient hydrostatic tension were applied to any substance, without any other stress component, it would eventually break brittly without any flow. Fracture in the tensile specimen starts on the axis because the hydrostatic tension is a maximum on the axis. The mathematics indicates that this hydrostatic tension on the axis is more important than one would perhaps guess from the magnitude of the correction factor by which average stress is converted into flow stress. Thus for reductions of area of respectively 37, 73, and 95 per cent, the hydrostatic tension on the axis is 0.21, 0.47 and 0.62 of the flow stress. This hydrostatic tension vitally determines fracture, and is large enough so that it should be reported as part of the fracture data. This demands a reformation of the technique of reporting tensile fracture. Thus suppose that a certain steel breaks with a reduction of area of 73 per cent at a "true stress" (total load divided by area of neck at the moment of fracture) of 10,000 kg. per sq. cm. The corresponding point on the fracture surface is not to be located at the coordinates (0, 0, 10,000), but is rather to be situated at the point (3800, 3800, 8000 + 3800).^{*} The difference in the character of the resulting fracture surface will obviously be very material. It seems to me that at the very minimum both the reduction of area at fracture and the "true stress" should be reported for a tensile test. It would be better if the

^{*} $8000 = 10,000 \times 0.8$; $3800 = 8000 \times 0.47$.

radius of curvature of the contour of the neck at fracture were also determined.

With regard to the effect of hydrostatic pressure on fracture, certain regularities are beginning to emerge. In the first place, the natural strain at which tensile fracture occurs is a linear function of the hydrostatic pressure in the medium in which the experiment is conducted. This holds up to strains so high that the actual loads and consequent flow stress can be determined only with materially diminished accuracy. A second generalization is that fracture under the conditions of these experiments seems to be determined by a single parameter. If the sum of the three principal stresses reaches a critical value, then fracture occurs. This holds for a wide range of material (the critical value may vary from material to material), for a wide range of strain, for a wide range of hydrostatic pressure, and independent of whether the material has been prestrained or whether its geometrical configuration has been altered by machining in the middle of the experiment.* The principal stresses just mentioned comprise the total stress system, consisting of the tension applied to the system, the hydrostatic tension generated by the combination of necking and tension, and the external applied hydrostatic pressure. The physical meaning is that fracture occurs when the volume has been distended to a critical amount, independent of the concomitant alteration of shape. It may be mentioned incidentally that the mean hydrostatic tension at fracture is materially less than would be deduced from extrapolations from the results of experiments on notched bars in which the stress distribution is assumed to be approximately uniform. It now becomes a problem for experiment to investigate to how wide a range of circumstances this criterion of fracture applies. Probably it

does not apply to all classes of materials, for it demands some paradoxical results, such as that fracture can never occur in simple compression or in shear. Probably it does not apply to brittle materials like glass, but it is certain that it does apply approximately over a wide range to ordinary ductile steels.

MCADAM'S METHOD

Returning to McAdam's data, I think one may have certain misgivings as to the justification of pushing his method of analysis too far, in view of the importance of the role that appears to be played by the hydrostatic tension generated by the geometry of necked or notched specimens, and of the difficulty of satisfactorily evaluating the hydrostatic tension component under the conditions of McAdam's experiments. I think our misgivings should be more serious in the case of fracture than of flow phenomena. A rough inspection shows that many of McAdam's results for flow fall approximately in line with the suggestions above. In many of his diagrams it will be found that flow curves that he plots as different for different values of the ratio of the principal stresses may be brought into approximate coincidence if the strain is plotted against the maximum tensile-stress component diminished by the hydrostatic tension (or the flow stress as defined above) instead of the unmodified tensile-stress component (that is, if $S_1 - S_3$ is plotted instead of S_1).

DISCUSSION

(*S. L. Hoyt presiding*)

D. J. MCADAM, JR.—Several of the assumptions in Dr. Bridgman's mathematical analysis are questionable. One of these is the assumption that the stress at the periphery of the minimum section is unidirectional; as MacGregor suggests, tangential (hoop) tension probably exists at the periphery. Another dubious assump-

* Later work has indicated that the condition does not hold for certain conditions of prestraining—Nov. 11, 1944.

tion is that there is no deformation gradient, and hence no hardness gradient, across the minimum section. Another is that the von Mises theory governs flow at the axis, where the stress system is well within the field of positive values of all three principal stresses. As illustrated in Fig. 5 of my paper in this symposium, the locus of yields is not parallel to line H , as is required by either the von Mises theory or the theory of maximum shear stress. If any or all of these three assumptions are incorrect, the stress gradient is considerably less than that reported by Bridgman.

There is much experimental evidence that the local contraction of an unnotched tension test specimen causes considerable transverse radial tensile stress, and thus elevates the mean flow stress above the flow stress for unidirectional tension.* Quantitative information about this elevation of the flow stress may be obtained by comparing a curve of flow stress for a tension test specimen with a curve of variation of the tensile strength of rod or wire that has been cold-drawn varying amounts, both curves being plotted with abscissas representing true plastic strains. Beyond the point representing the beginning of local contraction, the curve of tensile strength becomes essentially a curve of unidirectional flow stress, and consequently drops below the straight line of variation of the mean flow stress in a tension test specimen. Results of a number of such comparisons show that the percentages of elevation of the mean flow stress differ little from values that Bridgman cites as percentage differences between the mean flow stress and the flow stress at the periphery of the minimum section of the specimens.

This agreement, however, does not confirm Bridgman's assumption that the stress at the periphery is unidirectional,

* The term "flow stress" here means, as usual, the greatest principal stress during flow under any stress combination.

and does not indicate that the actual differences between the peripheral stress and the mean stress are as great as those reported by Bridgman. Moreover, even if Bridgman's values for this stress difference are correct, I should hesitate to accept his values for the differences between the mean stress and the stress at the axis. Bridgman's values for the mean flow stress are almost exactly half way between his values for the flow stress at the periphery and at the axis. Consideration of the curvilinear variation of the transverse radial stress over the cross section leads to the view that the mean longitudinal stress is much nearer to the longitudinal stress at the axis than to the longitudinal stress at the periphery. If the mean flow stress were half way between the maximum and minimum flow stresses, the curve representing the flow-stress-variation over the diameter of the cross section would be a parabola with its vertex in line with the axis. Such a curve does not rise rapidly enough from the periphery, and is not flat enough near the axis to represent the probable variation of the transverse radial stress. The actual stress at fracture of an unnotched specimen, therefore, may differ much less from the mean stress than in accordance with Bridgman's views.

However, even if we should apply the full corrections that Bridgman suggests to the results of our tension tests of unnotched specimens, the evidence would still show that the technical cohesion limit tends to rise with increase in the radial stress ratio, as our diagrams indicate. The corrections to be added, ranging from 18 per cent to 0 for specimens of widely ranging ductility, would not obscure the influence of the varying radial stress ratio. We are interested much less in obtaining absolute values of the breaking stress than in comparing values for unnotched and variously notched specimens.

In a notched specimen, the longitudinal stress is initially highest at the periphery.

The first effect of plastic deformation, therefore, is to decrease this gradient until the stress is practically uniform, and any accumulation of stress at the axis would appear later. In our experiments, the root radius was varied so as to permit varying amounts of plastic deformation before fracture. Some specimens broke before the initial stress concentration was fully relieved. With increase in the root radius, the breaking stress was first raised then lowered. The final lowering, however, must be attributed partly to the decrease in the radial stress ratio. Qualitatively correct pictures were thus obtained of the influence of the radial stress ratio on the technical cohesion limit. These pictures would be confirmed rather than invalidated, if it were assumed that axial stress concentration generally exists in a notched specimen at fracture.

When ductility is a minor factor, as shown in Fig. 4 of my paper, the breaking stress of notched specimens may be much higher than that of an unnotched specimen. As the unnotched specimen of this steel did not contract locally, the stress at fracture was unidirectional, and the higher breaking stress of the notched specimens can be attributed only to the influence of the radial stress. Similar examples may be found in other papers. A striking example is given in Fig. 10 of reference 11 of my paper. The breaking stress of a notched specimen of duralumin is there shown to be 50 per cent higher than that of an unnotched specimen, which broke with practically no local contraction. If axial stress concentration existed in the notched specimen, the actual elevation of the breaking stress was *greater* than 50 per cent.

The evidence that increase in the radial stress ratio tends to cause increase in the technical cohesion limit stands in the way of the new theory of Dr. Bridgman that fracture occurs when the volume stress, $\frac{1}{3}(S_1 + S_2 + S_3)$, reaches a critical value independent of associated variations in ductility. This theory implies that the

technical cohesion limit *decreases* with increase in the radial stress ratio. In a diagram of the type shown in Fig. 2 of my paper, the locus of fractures according to Bridgman's theory would be a line passing through point T_0 and parallel to line G . The disruptive stress ($S_1 = S_2 = S_3$) would be one third the cohesion limit for unidirectional tension, instead of about twice the latter cohesion limit as indicated by our experiments. As the corresponding locus of yields would be approximately parallel to line H , this locus would intersect the locus of fractures in such a way as to imply that brittle fracture of most metals would occur when the radial stress exceeds a very small value, and that even a wide-angled notch in a ductile metal would make the specimen as brittle as glass. It is indeed fortunate that this theory does not govern the mechanical properties of metals.

The evidence indicates that no single parameter can be used as an index of the breaking stress of a brittle metal under various combinations of the principal stresses, and that a single parameter cannot be obtained by introducing plastic deformation as a fourth variable.

THE CHAIRMAN.—Dr. McAdam's paper is now open for general discussion.

C. W. MACGREGOR.*—Some difference of opinion seems to have arisen relating to the possible stress conditions existing in the necked region of a tension test bar. The present discussion refers only to the stress conditions present in the necked region of an initially unnotched tension specimen. We have made certain tests that lend support to some of the concepts presented by Dr. McAdam in this connection.

Dr. Bridgman has given an interesting analytical attack on the problem. It is an admittedly difficult question and certain simplifying assumptions were made. His solution thus contains two relations that

* Massachusetts Institute of Technology, Cambridge, Massachusetts.

need further examination: (1) that the axial strain is constant across the section and, (2) that the tangential stress on the outside of the necked section is zero.

The first of these relations—namely, that the axial strain is constant across the neck—mathematically is an assumption of plane strain. Normally this is considered to apply to the case of a long cylinder of uniform cross section. Such conditions are not present in the case of a necked tension test bar. In addition, experiments we have made on steel bars of rectangular cross section show that the axial strain distribution across the neck is indeed not uniform. Measurements of scribed networks in the necked region have shown that the axial strain at the center of the bar may be 25 per cent greater than that at the edges. Comparisons of axial surface strains and average axial strains, the latter being determined from diameter measurements on large test cylinders during necking, have indicated similar conditions maintaining for round bars.

The second relation that follows—namely, that the tangential stress is zero on the outside of the bar in the necked region—is rather difficult to visualize mechanically. Observation of various types of tensile fractures leads one to the conclusion that a substantial tangential stress is very likely present on the outside of the bar. The Mohr explanation of tensile fractures—whether they are cup and cone, rosette, or of the spiral cup and cone type—is predicated on the condition that a tangential stress is present on the outside of the bar. Experience seems to bear out the validity of Mohr's explanation.

It thus appears advisable, until more information becomes available concerning the stress distribution in the neck of a tension specimen, to plot the average of the axial true stresses determined by dividing the load by the instantaneous area when constructing true stress-strain diagrams.

P. W. BRIDGMAN.*—Both Dr. McAdam and Dr. MacGregor speak of my analysis for the stress distribution at the neck of a tension specimen as containing several assumptions; in particular, that the strain is uniform across the section of the neck, that there is no hoop tension at the periphery, and that the plasticity conditions of von Mises hold. As far as the mathematics goes, the situation is no different in this problem of plastic flow than in a conventional problem of elasticity. That solution is unique which satisfies the boundary conditions on the stresses, the stress equations of equilibrium, and in addition the constitutive equations connecting stress and strain in the elastic case, or a corresponding set of equations, of which the von Mises relations are a special form, in the plastic case. In the particular case of the necked tension specimen I have found that there is a solution satisfying the boundary conditions, the stress equations of equilibrium, and the von Mises plasticity conditions in which the strain is uniform across the section, and there is no hoop tension at the periphery. This is therefore *the* solution, and the uniformity of strain and vanishing of hoop tension at the periphery are to be described as discoveries, over which the operator has no control, rather than as assumptions.

The only part of the solution that can properly be described as an assumption is the von Mises plasticity condition. With regard to this it is to be noted that the condition is needed only in a much weakened form, for the analysis uses the condition only at the neck, where the strain is approximately constant. Thus, in the extreme case referred to in a footnote of my paper (p. 574, this volume) the actually measured strain across the section varies from 2.4 to 2.6. Obviously it is a much weaker assumption to postulate that the von Mises condition holds

* Supplement issued in METALS TECHNOLOGY, April 1945.

in the strain range 2.4 to 2.6 than to assume it to hold for the entire range of strain from 0 up to 2.6, which would be necessary if the solution applied to the entire tension specimen rather than to the immediate region of the neck only. Furthermore, it is to be commented that under the special conditions of this problem the von Mises condition becomes identical with the maximum shearing-stress criterion of plastic flow; this amounts also to a weakening of the restrictions imposed by the von Mises condition.

Dr. MacGregor refers to actual experiments of his own in which the strain was found not to be uniform across the neck. It is to be emphasized, however, that these were experiments on bars of rectangular section, and that the nonuniformity established was a nonuniformity around the perimeter, not a nonuniformity from the surface toward the axis. My method of solution applies only to a circular cross section. It can be said that the solution that satisfies the boundary conditions, etc., would definitely not be expected to demand a uniform strain for noncircular sections.

In discussing my results, Dr. McAdam uses a definition of "flow stress" different from mine, so that the immediate application of his remarks requires interpretation. He defines flow stress (p. 577) as: "the greatest principal stress during flow under any stress combination." I apply the term flow stress only when the stress system is equivalent to a hydrostatic pressure or tension plus a single other non-vanishing component of principal stress. The justification of my usage is the experimental fact that a superposed hydrostatic stress has little effect on flow under a single stress component. Furthermore, the full situation with three different stress components is too complicated to be described adequately in terms of any single parameter such as "flow stress."

The difference between the two definitions may be great, as appears in the

following example: Imagine a tension bar one square inch in section, supporting a weight of 100,000 lb. at atmospheric pressure, under which it just starts to stretch plastically. We would both say that the flow stress is 100,000 lb. per sq. in. in this situation. Imagine now the same bar with the same weight in a fluid medium supporting a hydrostatic pressure of 200,000 lb. per sq. in. Neglecting the small specific effect of hydrostatic pressure, the bar is again on the verge of flow and the numerically greatest component of flow is still an extension. Dr. McAdam, according to his definition, would now have to say that the flow stress for *extension* is *minus* 100,000 lb. per sq. in. (or perhaps minus 200,000 lb. per sq. in.?), while my definition would report the flow stress as still plus 100,000 lb. per sq. in. It seems to me that there can be no question which is the more desirable method of description.

In general comment on Dr. McAdam's rebuttal, the examples he adduces to show that my conclusions are not acceptable are examples quoted from his own papers and calculated by his own method of analysis. But it was exactly the validity of this method of analysis that I was calling in question; it would seem to be not legitimate to assume the analysis in making the rebuttal.

In conclusion, it must, of course, be recognized that my solution for the neck of a tension specimen is not exact, but nothing has appeared in the discussion to alter my opinion that it is very much better to apply the corrections indicated by the mathematical analysis than to neglect them, particularly when analyzing phenomena of fracture. If this result is accepted, one effect must be to render insecure certain of Dr. McAdam's conclusions, which rest on experiments on notched specimens, where the effects I have been discussing for necked specimens must be present in much greater degree.

D. J. McADAM, JR. (author's reply to Dr. Bridgman's supplement).—Dr. Bridgman's symposium paper comprises three topics: (1) a mathematical analysis of the stress distribution in the neck of a locally contracting tension-test specimen, (2) the presentation of a theory that fracture is determined by a limiting value of the expansion under stress, and (3) a criticism of the papers on technical cohesion presented by myself and associates. In my discussion on p. 576 I criticized the mathematical analysis, showed that the theory of the limiting expansion is untenable, and replied to the criticism of our papers. Dr. Bridgman has replied to my criticism of his mathematical analysis, but has made no reply to my criticism of his new theory of the limiting expansion. However, he resumed his criticism of the papers of myself and associates. As his reply to my criticism of his mathematical analysis should be viewed as the "author's closure," I shall not continue the discussion of that subject, but merely say that I still doubt the validity of his analytical method, and the accuracy of his results. As shown in my discussion, however, the results of his mathematical analysis do not affect the validity of our results and conclusions.

In Dr. Bridgman's renewal of his discussion of our papers, he criticizes our use of the term "flow stress." We have used this term, however, in its generally accepted significance. In the literature of technical cohesion, the prevalent view has been that fracture is determined by a limiting value of the greatest principal stress, and that fracture of a ductile metal under any stress combination occurs when the "flow stress" reaches that limiting value. Moreover, in tension tests of notched and unnotched specimens the yield stress is generally expressed in terms of the greatest principal stress, and the stress during flow is generally expressed in the same terms and called the "flow stress." Under some stress combinations, the flow stress is negative,

and is sometimes called the "compressive flow stress." Sachs and others have investigated the variation of the compressive flow stress during compressive tests of notched and unnotched specimens. In tests of notched specimens, resistance to flow must be expressed in terms of the longitudinal flow stress until the stress distribution is known during the flow to fracture of variously notched specimens of metals varying widely in mechanical properties.

In the basic diagrams of our papers, the recorded breaking stresses are the mean "true" stresses and the ductilities are mean true strains. As our papers were under discussion, and as the discussion consisted of unsupported general assertions, it seemed to me proper to cite several specific examples to show that these assertions are without foundation. The numerical values were calculated by dividing the breaking load by the corresponding cross-sectional area so as to obtain the mean breaking stresses. The remainder of the "analysis" consisted in comparing the mean breaking stresses for notched and unnotched specimens, and drawing an axiomatic conclusion. The argument has not been answered.

In the cited examples, the mean breaking stresses of notched specimens were about 50 per cent greater than the mean breaking stresses of unnotched specimens. Even the mean yield stresses of some notched specimens were higher than the mean breaking stresses of the unnotched specimens. As these unnotched specimens broke with practically no local contraction, the stress was practically unidirectional and hence practically uniform. The higher mean breaking stresses of the notched specimens, therefore, can be attributed only to the higher radial stress ratio (S_3/S_1). If there was concentration of longitudinal stress near the axis of the notched specimens, the actual breaking stress would be *higher* than the mean breaking stress, and thus would be *more* than 50 per cent higher than the

mean breaking stress for unidirectional tension.

The evidence based on these examples and on many experimental results pointing

might consider to be a measure of cohesive strength dependent on the amount of preceding plastic deformation, i.e., on the degree of cold-work). Kuntze postulated

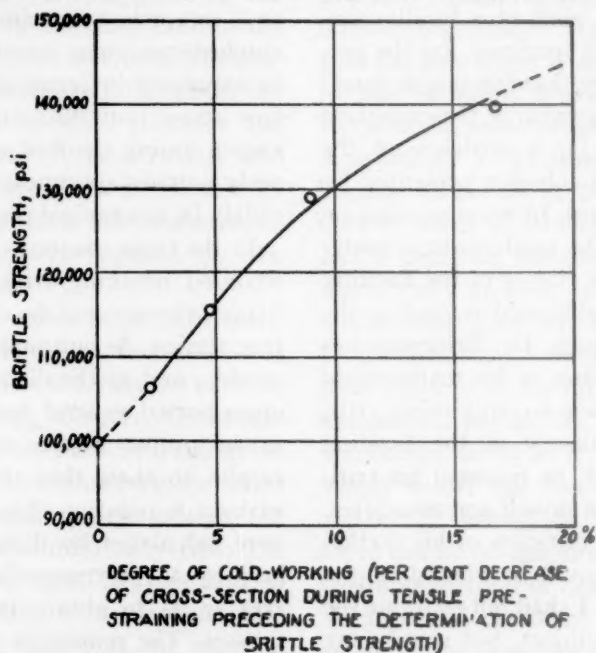


FIG. 1.—DEPENDENCE OF BRITTLE STRENGTH ON AMOUNT OF PRECEDING PLASTIC DEFORMATION IN TENSION (Sakharov).

in the same direction shows that the breaking stress, like the flow stress, tends to increase with increase in the radial stress ratio, and does so increase except when the influence of the associated decrease of ductility is dominant.

D. MORKOVIN.*—I am supposed to have some discussion later on, but now I will say a few words about Dr. McAdam's paper.

I understand that Dr. McAdam admits that plastic flow increases cohesive limit or cohesive strength. Fig. 1 herewith shows results of work by a Russian, Sakharov.† Similar work has been done by Captain Hollomon and Dr. Zener, and shows the same thing. The figure shows a rise in "completely brittle strength" (which you

the same thing—that with an increasing amount of plastic deformation cohesive strength rises. Although one may criticize Kuntze's method, it predicted this phenomenon correctly. Of course Kuntze also shows that if the plastic deformation exceeds a certain amount the cohesive strength falls. Sakharov's work does not extend to such large amounts of cold-work. Trouble with notched specimens is the nonuniform stress distribution across the critical (minimum) cross section.

The axial stress and the tangential stress are a maximum at the surface while the radial stress is zero at the surface at the bottom of the notch. That leaves the maximum shearing stress, also a maximum on the surface at the bottom of the notch. I think it becomes apparent that to obtain a measure of strength across a cross section over which the stress varies in such a manner is rather hopeless. Besides that, as

* Cook County Hospital, Chicago, Illinois.

† P. S. Sakharov: Determination of Brittle Strength. *Jnl. for Technical Physics* (Russian) (1936) 6 (8), 1381. (See footnote on p. 595.)

shown in Sakharov's figure, the cohesive strength, or cohesive limit—I do not know which Dr. McAdam would call it—increases with the amount of preceding plastic flow. A notched specimen, before it breaks in tension test, undergoes a lot of flow in the surface layers at the bottom of the notch where there is no radial stress.

At the middle of the minimum cross section, on the other hand, the amount of plastic flow is much smaller.

After the stresses exceed the yield point in the surface layers at the bottom of the notch and flow takes place in this region, the cohesive strength of the metal thus cold-worked will increase. As flow takes place closer and closer to the center, the original or initial technical cohesive

strength of the metal in the critical region of the notched specimen will have been to a large extent changed. If failure occurs after some flow has taken place, we are not getting the initial cohesive strength of the material but a changed cohesive strength, and that change is dependent upon the amount of previous plastic flow. The amount of previous plastic flow varies across the critical cross section of the notched specimen and, therefore, we have again a very complicated situation. I believe that the peculiar forms of many of Dr. McAdam's curves are largely because he had varying amounts of plastic flow, and the initial cohesive strength has been altered by different amounts in specimens of different notch depths and radii.

Some Speculations Regarding the Plastic Flow and Rupture of Metals under Complex Stresses

By L. R. JACKSON*

THE idea presented in this paper is that the capacity of a metal for plastic flow before rupture is dependent on the type of stress system applied—that is, the absolute magnitude of the stresses are unimportant provided that they are large enough to produce continued flow; the important factor is the “type” of stress system. A term called the “triaxial stress ratio” is defined in such a way that this ratio can be used to characterize the “type” of system.

The paper is divided into three sections. The first section discusses means of representing the effect of complex stresses on plastic flow and defines “triaxial stress ratio”; the second section discusses various methods of obtaining complex stress distribution. The third section gives some experimental results showing the effect of types of complex stress on the capacity of various metals for flow. An appendix discusses some details on methods of obtaining complex stresses.

REPRESENTATION OF COMPLEX STRESS SYSTEMS AND THEIR EFFECT ON PLASTIC FLOW

Representation of Stresses

It is convenient to have a consistent system of notation that will allow the representation of the entire range of complex stresses from hydrostatic compression to hydrostatic tension on plastic flow in a single diagram.

Such a system is provided by making

use of the fact that any complex stress system can be resolved into a hydrostatic tension or compression and a pure shear.

Consider a stress system having the principal stresses $S_1 \geq S_2 \geq S_3$. This system can be resolved into a new system consisting of the three components

$$S_1' = S_2' = S_3' = Sm = \frac{S_1 + S_2 + S_3}{3} \quad [1]$$

and three pure shears.

If Sm is positive, the net stress effect is hydrostatic tension; if it is negative, the effect is hydrostatic compression.

In order to produce a systematic notation, a quantity that will be referred to as the “triaxial ratio” will be defined by the equation

$$Tr = \frac{Sm}{S_1} \quad [2]$$

Sm is given by Eq. 1 and S_1 is the absolute magnitude of the largest principal stress without regard to sign.

Table 1 lists the triaxial ratios for various common systems.

TABLE 1.—*Triaxial Ratios for Various Common Systems*

STRESS SYSTEM	TRIAXIAL RATIO Tr
Hydrostatic compression $-S_1 = -S_2 = -S_3$	-1
Torsion or shear $-S_1 = S_2, S_3 = 0$	0
Simple tension $S_1, S_2 = S_3 = 0$	+0.33
Biaxial tension $S_1 = S_2, S_3 = 0$	+0.66
Hydrostatic tension $+S_1 = +S_2 = +S_3$	+1.00

Representation of Strains

Strains will be plotted as “true” strains according to the system proposed by Ludwik.¹

*Battelle Memorial Institute, Columbus, Ohio.

¹ References are on page 595.

This system will be used because it is valid not only for small strains but also for large amounts of plastic flow. In this system, the three principal strains are defined by the equations

$$\left. \begin{aligned} E_1 &= \ln(1 + e_1) = \ln \frac{A_0}{A_1} = \ln \frac{l_1}{l_0} \\ E_2 &= \ln(1 + e_2) = \ln \frac{A_0}{A_2} = \ln \frac{l_2}{l_0} \\ E_3 &= \ln(1 + e_3) = \ln \frac{A_0}{A_3} = \ln \frac{l_3}{l_0} \end{aligned} \right\} [3]$$

In Eq. 3, the areas A_0 , A_1 , A_2 and A_3 are those perpendicular to the strains along the directions 0, 1, 2, and 3 and the quantities e_1 , e_2 and e_3 are the conventional elongations or reductions in area as

$$e_1 = \frac{l_1 - l_0}{l_0} = \frac{A_0 - A_1}{A_1}, \text{ etc.}$$

When "true" strains are used, the relation

$$E_1 + E_2 + E_3 = 0 \quad [4]$$

is valid.

The maximum strain is given by the relation

$$E_m = \frac{1}{2}[(E_1) + (E_2) + (E_3)] \quad [5]$$

where the symbol (||) indicates that the value is the absolute magnitude of the strain disregarding sign.

In the representation of experimental work to follow in the third section, the two quantities used will be those defined in Eqs. 2 and 5.

METHODS OF OBTAINING TRIAXIAL STRESSES

Combinations Involving Hydrostatic Compression

This case needs no discussion since, experimentally, the problem of superimposing hydrostatic compression on other stresses is not difficult.

Pure Shear ($T_r = 0$)

The condition of pure shear is attained most easily by means of the torsion test piece. The torsion stress T_s is equivalent to the two principal stresses S_1 and S_2 , making an angle of 45° with the axis of torsion.

The two principal stresses are equal in magnitude but opposite in sign; S_1 is tension, and S_2 is compression. The relation between these two stresses and the conventional torsion shear stress T_s is

$$T_s = \frac{S_1 - (-S_2)}{2} = S_1 = -S_2 \quad [6]$$

The torsion shear stress varies from zero at the center of the test piece to a maximum at the outside surface. This variation in stress across the cross section is a complicating factor; however, experimentally, its effect can be much reduced by running the test on hollow test pieces. In the case of a hollow test piece, the torsion stress (and thereby the two principal stresses $S_1 + S_2$) can be computed by the relation suggested by Bridgman:²

$$T_s = \frac{3x_3 (\text{torque})}{4\pi(r_o - r_i)} \quad [7]$$

where r_o and r_i are, respectively, the outside and inside radii of the cylinder and the torque is in inch-pounds.

Conventionally, in torsion, the maximum strain is measured by the relation $\gamma = \frac{r_o\theta}{l}$ where θ is the angle of twist in radians and l is the length of the test piece. This measure of strain is related to the "true" strains associated with the principal stresses S_1 and S_2 by the equations:³

$$\left. \begin{aligned} E_1 &= \frac{1}{2} \ln \left[1 + \frac{\gamma^2}{2} + \gamma \left(1 + \frac{\gamma^2}{4} \right)^{1/2} \right] \\ E_2 &= \frac{1}{2} \ln \left[1 + \frac{\gamma^2}{2} - \gamma \left(1 + \frac{\gamma^2}{4} \right)^{1/2} \right] \end{aligned} \right\} [8]$$

The relation $E_1 + E_2 = 0$ holds

and

$$E_{\max.} = E_1 \quad [9]$$

defines the maximum strain in torsion in a notation consistent with section 1.

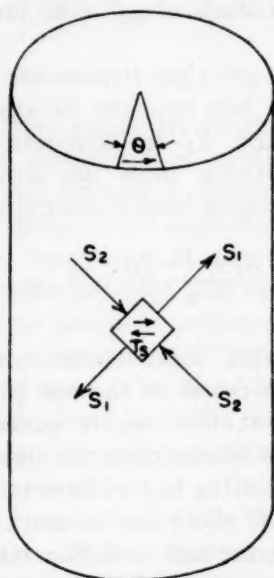


FIG. 1.—STRESSES IN TORSION TEST.

Thus, Eqs. 6 and 9 allow the results of torsion tests on hollow cylinders to be plotted on the same type of diagram as conventional tension or compression tests.

Stress Systems Involving Hydrostatic Tension

As noted in Table 1, simple tension produces a triaxial ratio of +0.33, and biaxial tension produces a ratio of +0.66. Both of these conditions are experimentally reasonable. It is more difficult, however, to produce known triaxial ratios greater than 0.66. Usually attempts to produce those high ratios have been made by means of notches. While properly shaped notches do produce high triaxial ratios, the effect is complicated by stress concentrations which are difficult to describe accurately.

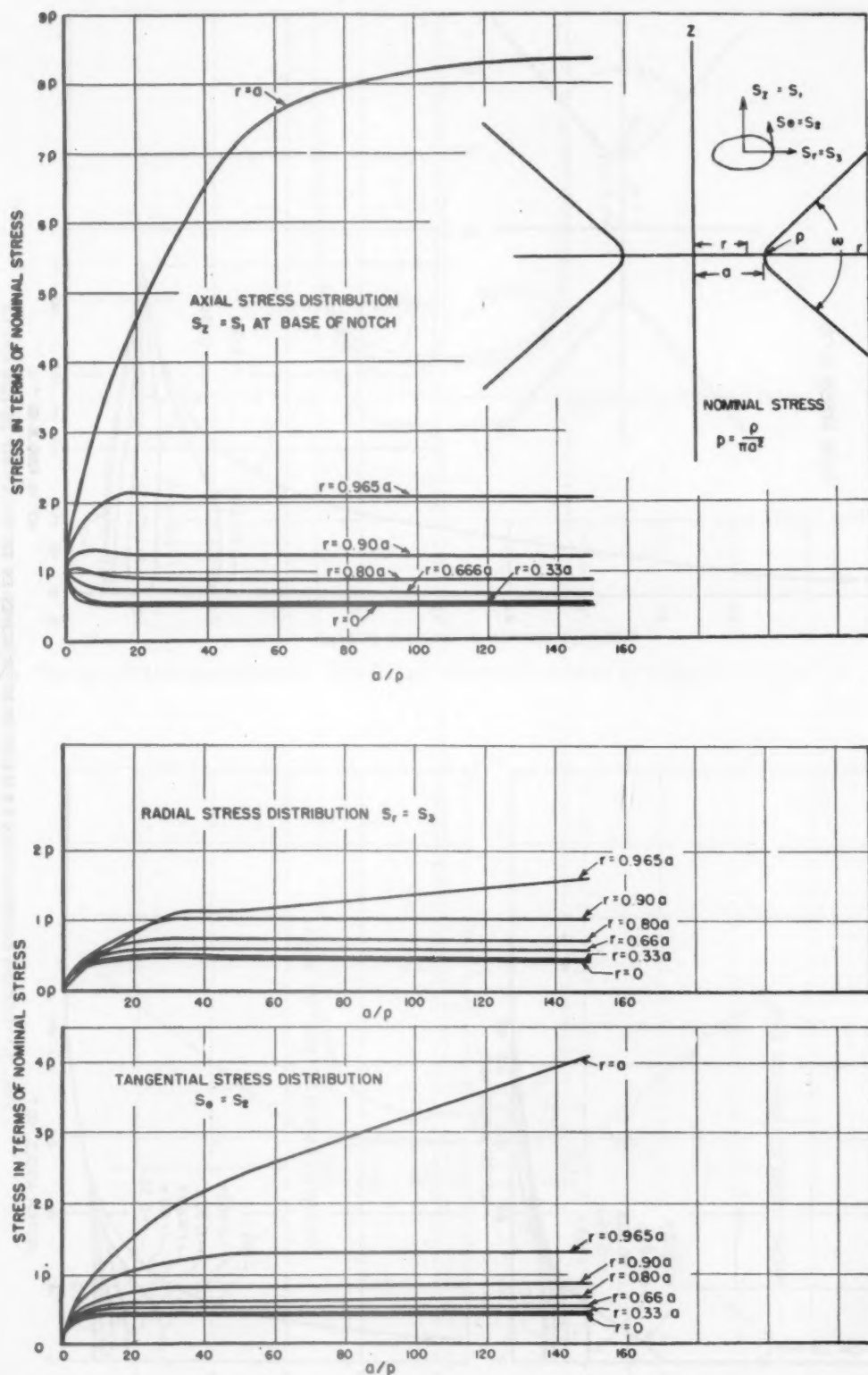
The most satisfying theoretical analysis of the stress distribution in the vicinity of notches has been accomplished by Neuber.⁴ His method applies only to very deep

notches of hyperbolic contour, but it does provide an accurate description of this type of notch, involving only the assumptions that the medium is elastic, isotropic, and homogeneous. Figs. 2 and 3 are plotted from Neuber's equations.* These figures can be used to plot the stress distribution across the base of any specific notch. In Fig. 3, the notch angle ω used as the abscissa is the average angle of the hyperbola in the region up to $r = 2a$ where a is the radius at the root of the notch. In both Figs. 2 and 3, the ordinates are given in terms of the nominal stress $\left(\frac{\text{load}}{\pi a^2}\right)$ at the root of a notch. Fig. 3 is convenient because it covers the entire range of a/ρ , since the value $a/\rho = 0$ corresponds to $\omega = 180^\circ$, and the value $a/\rho = \infty$ corresponds to $\omega = 0^\circ$.

Figs. 4, 5, and 6 show stress distributions for some specific notches. Fig. 4 shows the distribution for an infinitely sharp notch ($a/\rho = \infty$, $\omega = 0$) in a bar 0.3-in. diameter at the root of the notch; Figs. 5 and 6 show, respectively, the distributions for $a/\rho = 2.4$, $\omega = 90^\circ$ and $a/\rho = 15$, $\omega = 43^\circ$. Fig. 6 also shows how the stress distribution varies along the axis in planes 0.03 and 0.067 in. from the root of the notch. From Fig. 6, it is to be noted that, while the effects of stress concentration disappear rapidly, the triaxial character of the stresses is preserved for some distance.

Fig. 7, plotted from the results in Figs. 2 and 3, shows how the triaxial ratio T_r varies over the cross section of the plane through the root of the notch. This figure brings out several interesting features of notches. First, note that the triaxial ratio rises rapidly even for very blunt notches and that, after this initial sharp rise has been achieved, the remainder of the increase is achieved only by making notches very sharp. Second, it is to be noted that.

* A more detailed discussion of Neuber's equations is given in the Appendix.

FIG. 2.—STRESS DISTRIBUTION AT BASE OF DEEP NOTCHES IN TERMS OF RATIO a/p .

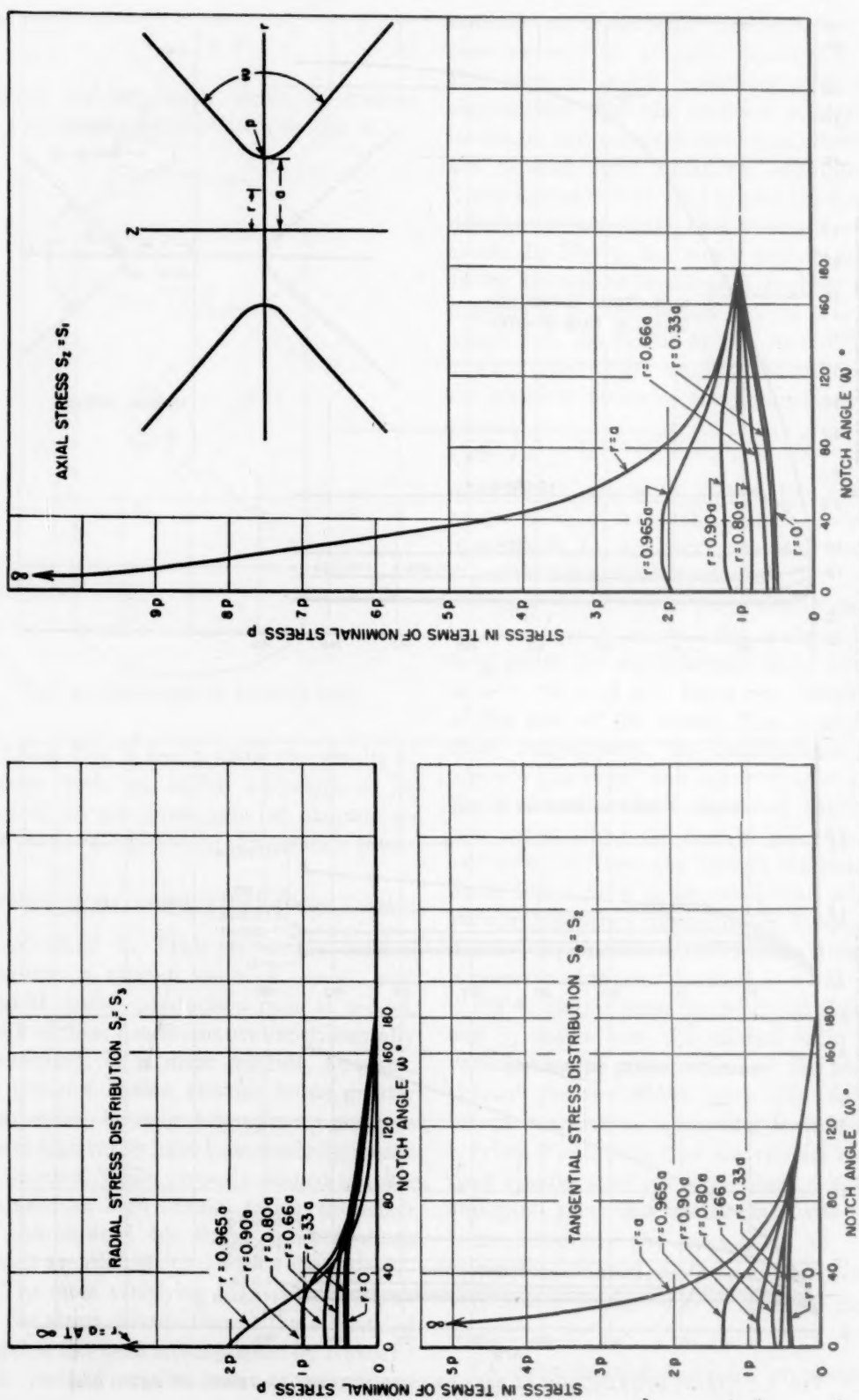
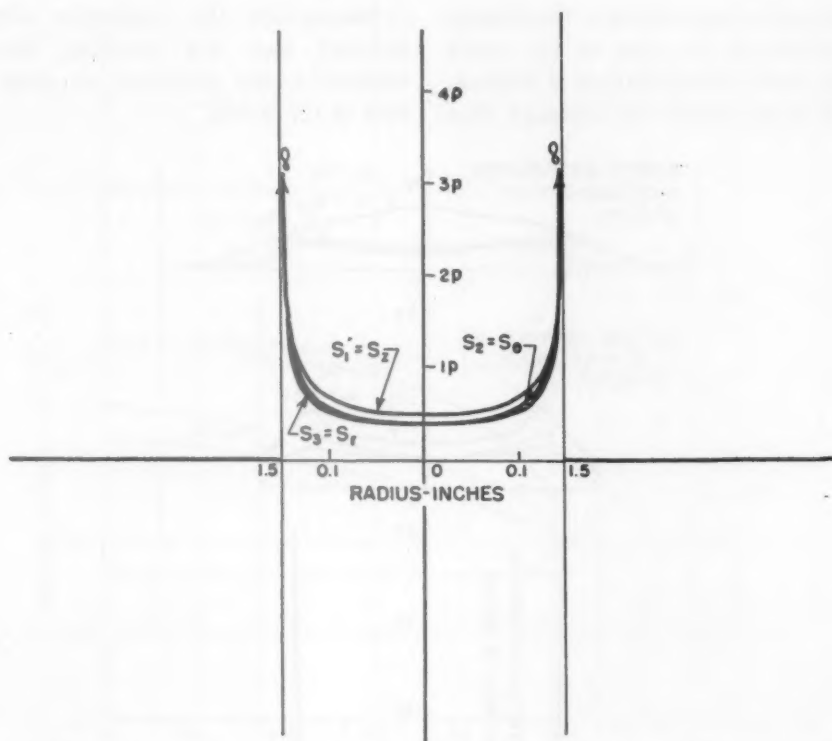
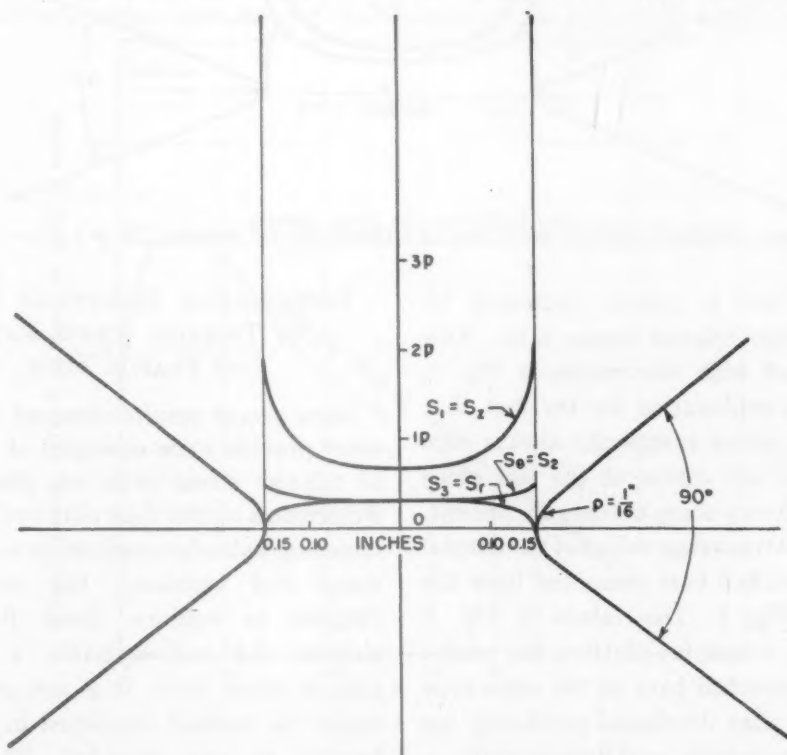


FIG. 3.—STRESS DISTRIBUTION AT BASE OF DEEP NOTCHES IN TERMS OF NOTCH ANGLE.


 FIG. 4.—STRESS DISTRIBUTION AT ROOT OF INFINITELY SHARP NOTCH; $a/\rho = \infty$, $\omega = 0$.

 FIG. 5.—STRESS DISTRIBUTION AT ROOT OF 90° NOTCH; $a/\rho = 2.4$, $\rho = 1/16$ INCH

except for very sharp notches, the triaxial ratio is lowest at the root of the notch where the stress concentration is highest. As will be shown later, the capacity of a

Values for the maximum strains in notched bars are obtained simply by measuring the reduction in area at the root of the notch.

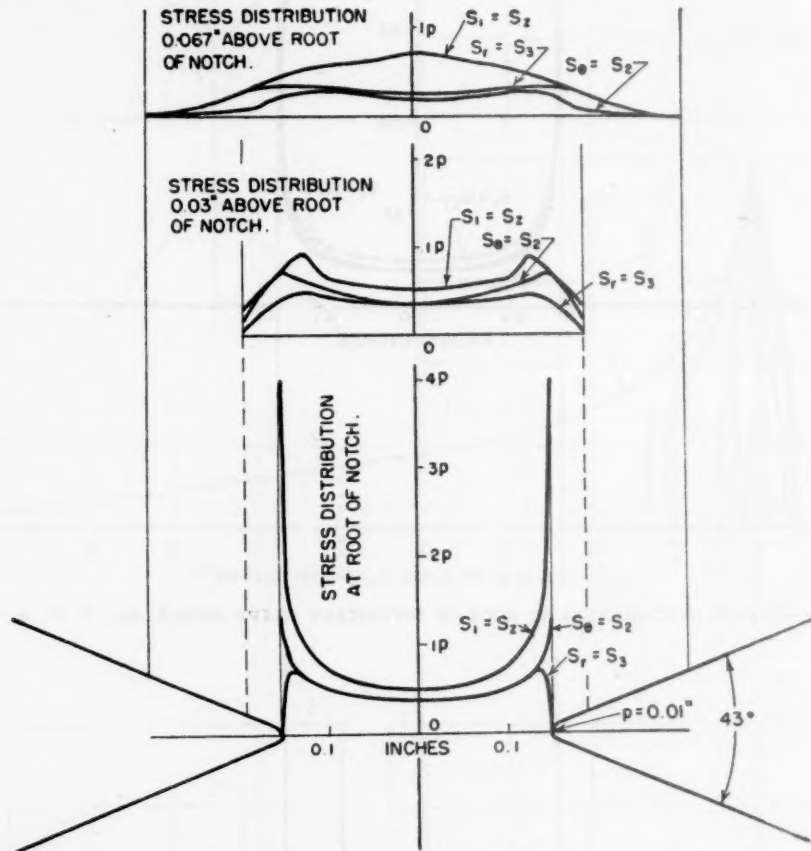


FIG. 6.—STRESS DISTRIBUTION AT ROOT AND IN VICINITY OF 43° NOTCH; $a/\rho = 15$, $\rho = 0.01$ INCH.

metal for flow is greatly decreased by increasing the triaxial stress ratio. This fact, coupled with the results in Fig. 7, suggests an explanation for the fact that tensile test pieces practically always rupture first at the center of the test piece except when very sharp notches are present.

Fig. 8 shows average values of the triaxial ratio for notched bars computed from the curves in Fig. 7. The values in Fig. 8 provide the means for plotting the results of tests on notched bars on the same type of chart as that developed previously for tension, compression, and torsion tests.

EXPERIMENTAL RESULTS ON EFFECT OF TRIAXIAL STRESS RATIO ON PLASTIC FLOW

Some recent results obtained by Bridgman² provide some examples of the effect of triaxial stress ratio on plastic flow. Bridgman's results were obtained by superimposing a steady compression on a torsion stress and obtaining the stress-strain diagram to rupture. Since Bridgman's method did not maintain a constant triaxial stress ratio, it is not possible to apply the method developed in section 2 exactly as was intended. The results

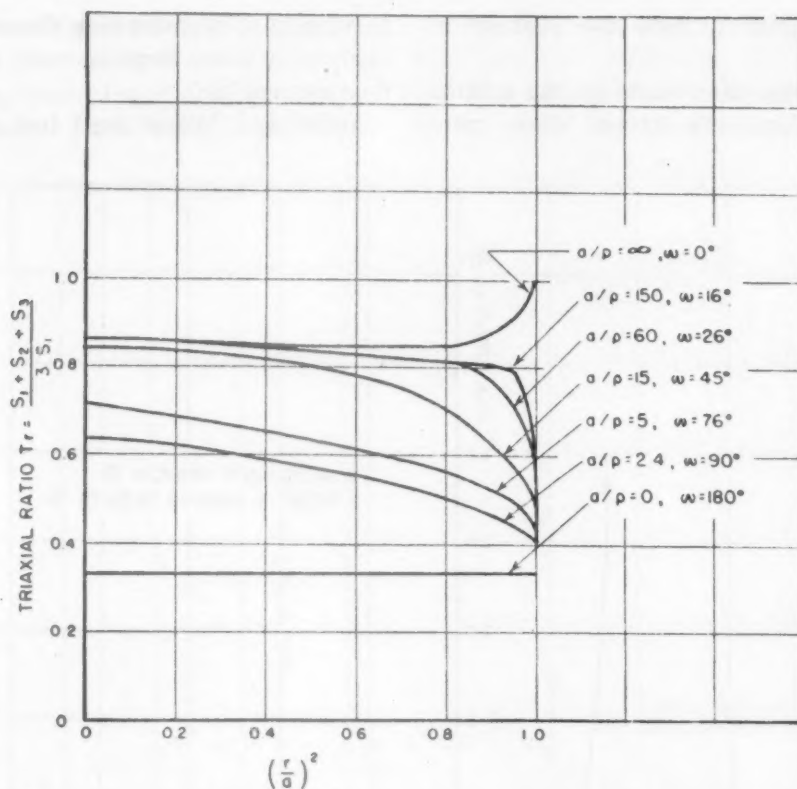
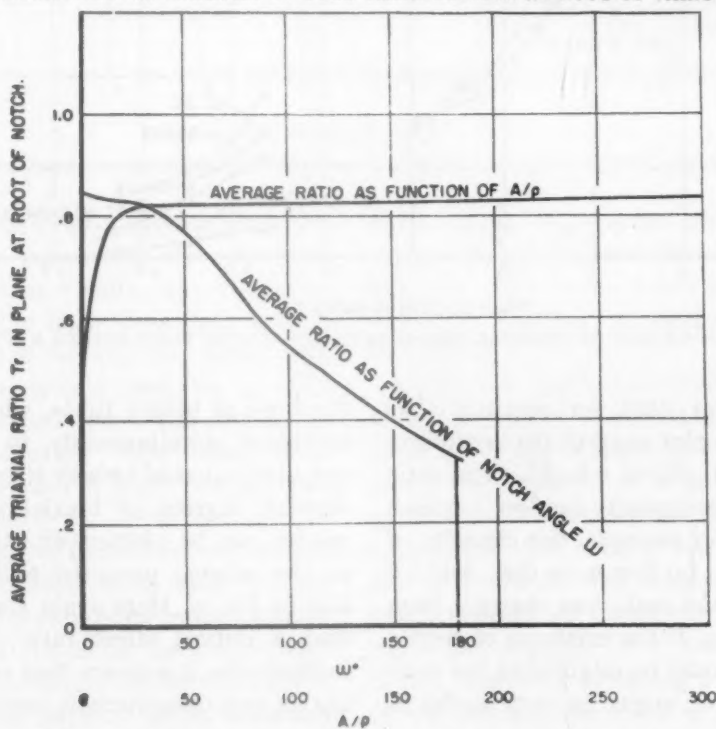

 FIG. 7.—DISTRIBUTION OF TRIAXIAL T_r OVER CROSS SECTION AT ROOT OF VARIOUS NOTCHES.


FIG. 8 —AVERAGE TRIAXIAL RATIO FOR DEEP NOTCHED BARS

from Bridgman's tests are plotted in Fig. 9.

In reducing his results to the scheme proposed here, the triaxial stress ratio

the design of deep-drawing dies and other equipment where large amounts of plastic flow are required.

Siebel and Maier⁵ used test pieces in

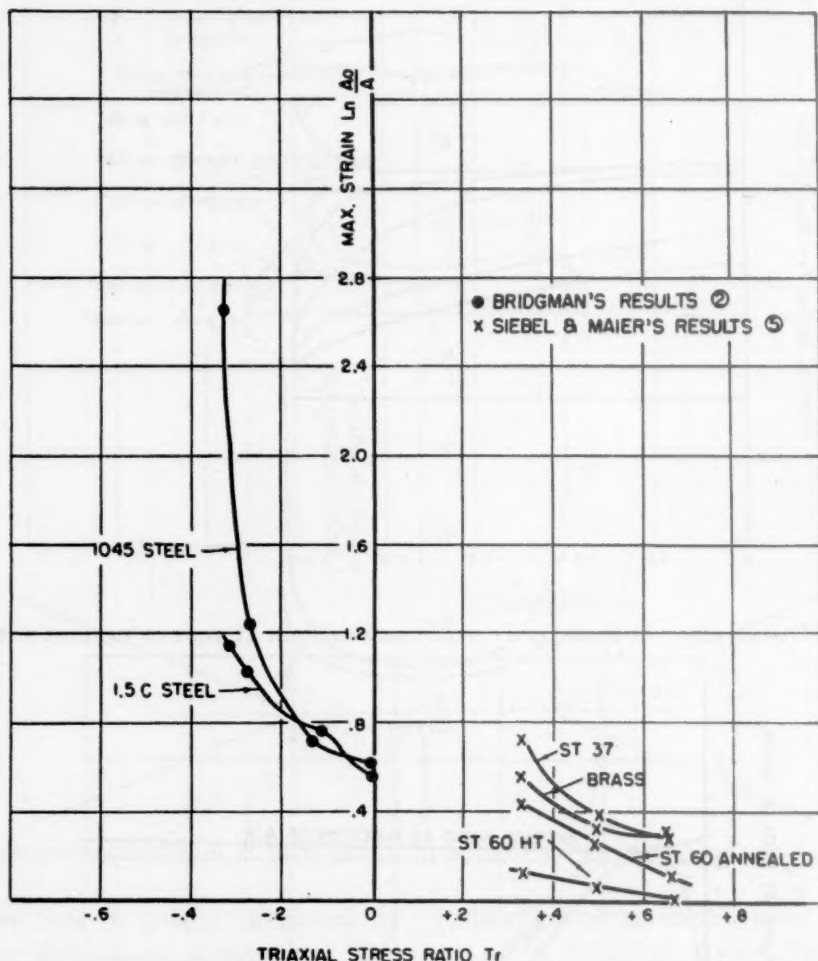


FIG. 9.—EFFECT OF TRIAXIAL STRESS RATIO ON PLASTIC FLOW BEFORE RUPTURE.

at rupture was used for plotting. The results of this plot suggest the possibility that there is a critical triaxial stress ratio below which the capacity for flow increases enormously. For example, the capacity of the S.A.E. 1045 for flow more than doubled when the triaxial ratio was changed from -0.3 to -0.33 . If the existence of such a critical ratio could be established for various materials, it might be very useful in

the form of hollow tubes, which could be subjected simultaneously to internal oil pressure and axial tension stress to produce varying degrees of biaxial stress. Their results can be plotted directly according to the scheme proposed and are shown also in Fig. 9. Here again there is a hint that a critical stress ratio might exist; furthermore, it appears that each material has its own characteristic response.

Triaxial Stress Ratios Obtained by Notched Bars

No data were found to which the average curves for triaxial stress ratio

by the analysis was the fact that the notch angle was not consistent with the a/ρ ratio. In computing the triaxial stress ratio, the a/ρ ratio was used instead of the

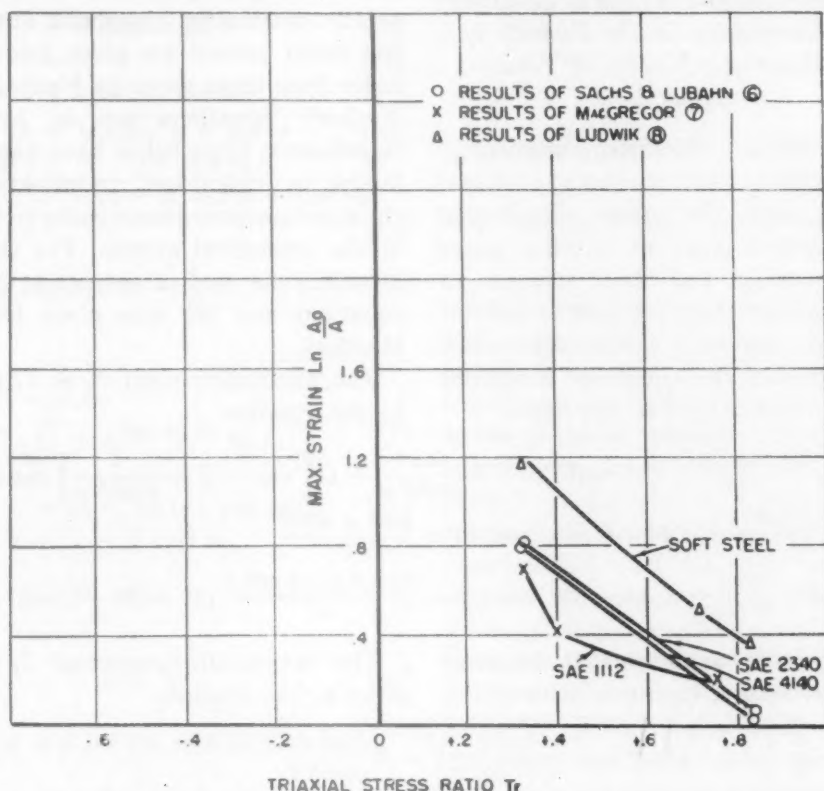


FIG. 10.—EFFECT OF TRIAXIAL STRESS RATIO ON PLASTIC FLOW FROM NOTCHED TENSION TESTS.

in Fig. 8 could be strictly applied; however, three sets were found that serve to illustrate the type of results that might be expected. Results from these three sets of data are plotted in Fig. 10. Sachs and Lubahn⁶ made tensile tests on a wide variety of notched bars. The curves in Fig. 10, illustrating their data, were selected on the basis of depth of notch—in the tests selected for these curves, the notch used removed 65 per cent of the cross section. The triaxial stress ratio for the notched bars was computed on the assumption that the notch radius used was about 0.0004 in. as measured from the photograph in Fig. 6 of their paper. Another deviation of their test bars from the shape required

notch angle. This same procedure was used on the results taken from MacGregor⁷ and the ones from Ludwik.⁸ Thus, a consistent method of choice was used throughout.

While the applicable experimental results are scanty, there do appear to be some advantages gained by attempting to relate the capacity of a metal for flow to the type of stress applied. If it could be established that such a relation existed, and this relation was independent of the exact method of obtaining the type of stress (for example, if it could be shown that a biaxial stress having a triaxial ratio of 0.6 was equivalent to a triaxial stress having the same ratio), curves of this

type would be very useful in the design of equipment for plastic flow and in predicting the relative behavior of various materials.

APPENDIX.—*Neuber's Method of Computing Stress Distribution in the Vicinity of Deep Hyperbolic Notches in Tensile Bars*

In his book, "Kerbspannungslehre," H. Neuber has solved a number of problems concerned with the stress distribution around various types of notches under tension, bending, and shear stresses. In view of the fact that this book is difficult to obtain at present, it was thought worth while to record the equations developed by Neuber that pertain to this paper.

$$S_z = \frac{\cosh u \cos v}{h^3} \left\{ A \tanh^2 u + B \frac{\cos v}{\cosh^2 u} + C \left[-2 - \alpha + \frac{1}{\cosh^2 u} \right] \cos v \right\} \\ + \frac{\cosh u \cos^2 v}{h^5} \{ -A + B + C \cos^2 v \} - \frac{\sinh u \sin v}{h^3} \\ \left\{ -A \frac{\cos v}{1 + \cos v} + (\alpha - 1)C \cos v \right\} - \frac{\sinh u \sin v \cos v}{h^5} \{ A - B - C \cos^2 v \} \quad [11]$$

A. E. H. Love has shown that the stress distribution accompanying a deformation

$$S_\theta = S_z = \frac{1}{h^2} \left\{ A \left(-\tanh^2 u + \frac{\cos v}{1 + \cos v} \right) - B \frac{\cos v}{\cosh^2 u} \right.$$

The tangential component $S_\theta = S_z$ is given by the relation

$$\left. + C \left[\alpha - 1 - \frac{1}{\cosh^2 u} \right] \cos v \right\} \quad [12]$$

can be represented by a single function ϕ where ϕ satisfies the equation (in cylindrical

The radial component $S_r = S_\theta$ is given by

$$S_r = S_\theta = \frac{\sinh u \sin v}{h^3} \left\{ A \tanh u + \frac{B \cos v}{\cosh^2 u} + C \left[-2 - \alpha + \frac{1}{\cosh^2 u} \right] \cos v \right\} \\ + \frac{\sinh u \sin v \cos v}{h^5} \{ -A + B + C \cos^2 v \} \\ + \frac{\cosh u \cos v}{h^3} \left\{ -A \frac{\cos v}{1 + \cos v} + (\alpha - 1)C \cos v \right\} \\ + \frac{\cosh u \cos^2 v}{h^5} \{ A - B - C \cos^2 v \} \quad [13]$$

coordinates)

$$\left(\frac{\partial^2}{\partial r^2} + \frac{1}{r} \frac{\partial}{\partial r} + \frac{\partial^2}{\partial z^2} \right) \\ \left(\frac{\partial^2 \phi}{\gamma r^2} + \frac{1}{r} \frac{\partial \phi}{\partial r} + \frac{\partial^2 \phi}{\partial z^2} \right) = 0 \quad [10]$$

Neuber's contribution is that he has

The various quantities in the three equations above are given by the following relations:

The equation for the notch is

$$\frac{r^2}{\sin^2 v_0} - \frac{x^2}{\cos^2 v_0} = k^2 \quad [14]$$

and from Eq. 14, $\tan^2 v_0 = \frac{a}{\rho}$ when a is the radius of the bar at the root of the notch and ρ is the radius of curvature at the root of the notch.

$$r = k \cosh u \sin v \quad [15]$$

$$\theta = \theta \quad [16]$$

$$z = k \sinh u \cos v \quad [17]$$

$$h = \sqrt{\sinh^2 u + \cos^2 v} \quad [18]$$

$$C = -\frac{P}{2} \left(\frac{1 + \cos v_0}{1 + (2 - \alpha) \cos v_0 + \cos^2 v_0} \right) \quad [19]$$

from Eq. 14, $\tan^2 v_0 = \frac{a}{\rho}$

and

$$\cos v_0 = \frac{1}{\sqrt{\frac{a}{\rho} + 1}} \sin v_0 = \sqrt{\frac{\frac{a}{\rho}}{\frac{a}{\rho} + 1}} \quad [20]$$

$$A = (\alpha - 1)(1 + \cos v_0)C \quad [21]$$

$$B = A - C \cos^2 v_0 \quad [22]$$

From Eq. 6 when $u = 0$ and $v = v_0$ when $r = a$,

$$k = \frac{a}{\sin v_0} \quad [23]$$

and for $u = 0$ (at the root of the notch),

$$\sin v = \frac{r}{k} \quad [24]$$

$$\alpha = 2(1 - \mu) \quad [25]$$

where μ = Poisson's ratio.

The curves in Figs. 2, 3, 4, 5 and 6 were obtained from Eqs. 11, 12 and 13 and the relations 14 to 25.

REFERENCES

1. P. Ludwik: *Elemente der technologischen Mechanik*. 1909.
2. P. W. Bridgman: On Torsion Combined with Compression. *Int. Applied Physics* (1943) 14, 273-283.
3. A. Nadai: Plastic Behavior of Metals in the Strain-hardening Range. *Int. Applied Physics* (1937) 8, 205-213.
4. H. Neuber: *Kerbspannungslehre*. Germany, 1937. Julius Springer.
5. E. Siebel and A. Maier: Der Einfluss Mehrachsigen Spannungszustande auf das Formänderungsvermögen Metallischer Werkstoffe. *Ztschr. Ver. deut. Ing.* (1933) 77, 1345-1349.
6. G. Sachs and J. D. Lubahn: Notched Bar Tensile Tests on Heat Treated Low Alloy Steels. *Trans. Amer. Soc. Metals* (1942) 31.
7. C. W. MacGregor: The Tension Test. *Proc. Amer. Soc. Test. Mat.* (1940) 40, 508-534.
8. P. Ludwik: Über Kerbwirkungen bei Flusseisen. *Stahl und Eisen* (1923) 43, 999-1001.
9. A. E. H. Love: *Theory of Elasticity*, Ed. 4. 274. 1927.

DISCUSSION

(M. Gensamer presiding)

THE CHAIRMAN.—Dr. Morkovin will now complete the presentation of his paper.

D. MORKOVIN.—Several of the things that I was going to speak about have already been said. I have not done the experimental work to prove the postulates I am going to mention. They are just speculations. I am afraid that with my present duties and the outlook for the future I will not have a chance to do the experimental work required to prove or disprove these postulates. Therefore, if anybody finds anything that appeals to him, please try to test it and tell us about it.

Fig. 2* shows some results of work done by Joffé† on rock-salt crystals. The material tested was not a metal, and objection may be raised that the conclusions drawn from this will not apply to metals. That may be so, but there should be no objection against using the conclusions obtained from the work on nonmetals as working hypotheses whose validity for metals is to be tested.

Fig. 2 represents tensile tests performed on rock-salt crystals at a number of different testing temperatures. At the melting point M , the yield strength is equal to zero, and as the temperature decreases the yield stress increases. At about 400°F.,

* The figures with Dr. Morkovin's remarks are taken from his thesis (D. Morkovin: Completely Brittle Failure and the Technical Cohesive Strength. Ph. D. Thesis, University of Illinois, 1944), but have been renumbered here in the order of presentation.—EDITOR.

† A. F. Joffé, M. W. Kirpitschewa and M. A. Lewitsky: *Ztsch. Physik* (1924) 22, 286.

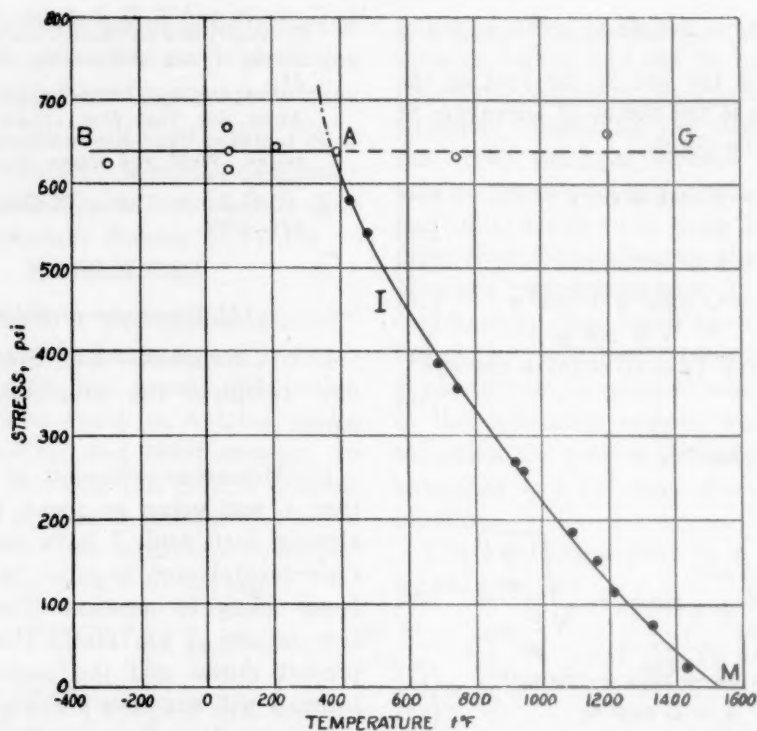


FIG. 2.—VARIATION OF YIELD STRENGTH AND BRITTLE STRENGTH OF ROCK SALT WITH TEMPERATURE (Joffe).

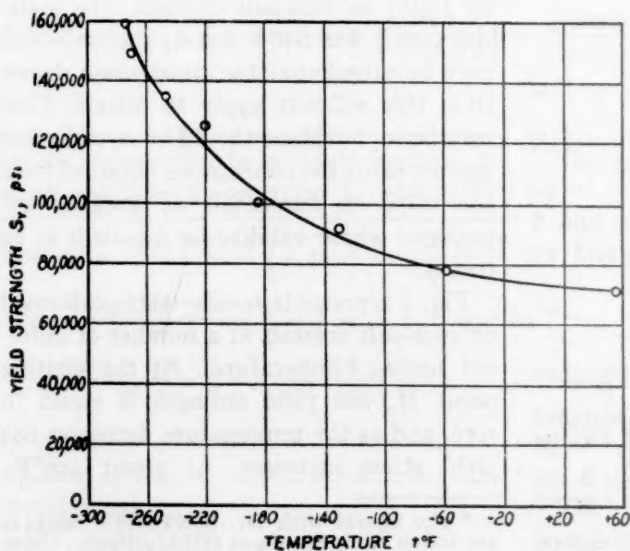


FIG. 3.

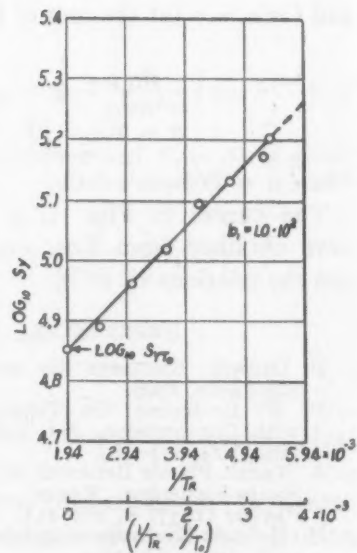


FIG. 4.

FIGS. 3 AND 4.—VARIATION OF YIELD STRENGTH WITH TEMPERATURE (Wilman and Stepanov).

the critical temperatures of brittleness is reached. Below the critical temperature of brittleness, the mode of failure is sudden brittle fracture. Below the critical temperature, from plus 400° to minus 290°F., the fracture stress does not vary with temperature.

If a tensile test is performed at 1000°F., a yield point of about 225 lb. per sq. in. is obtained. After yield point is reached, there follows ductile flow in rock salt; and finally, at a true breaking stress entirely too high to appear in the figure shown—i.e., out of range of its scale—the specimen breaks. This rise in the true breaking stress of the material is due to the cold strengthening or work-hardening of the material. Cohesive strength is increased by plastic flow. The points along the line AG were obtained at high rates of straining, which increased the yield point sufficiently so that no yielding took place before brittle fracture occurred. The points on line AG represent completely brittle fractures at sufficiently high rates of straining to prevent any yielding. Thus, with a variation less than about ± 5 per cent, the brittle strength of rock salt remains constant and does not change with temperature over a temperature range from minus 290°F. to at least 1200°F.

Figs. 3 and 4 represent some experimental work on steel.* Again, with decreasing temperatures, there is increase in yield point (Fig. 3). If we plot this on a logarithmic scale, yield point against the reciprocal of the absolute temperature, we get a straight line of Fig. 4. On account of this straight-line characteristic, the variation of yield strength with temperature for a given material may be possible to obtain from only two tests, possibly from only a room-temperature test and one other test at low temperature.

Figs. 5, 6, 7 and 8 represent some experimental work on high-phosphorus steel* and its interpretation.

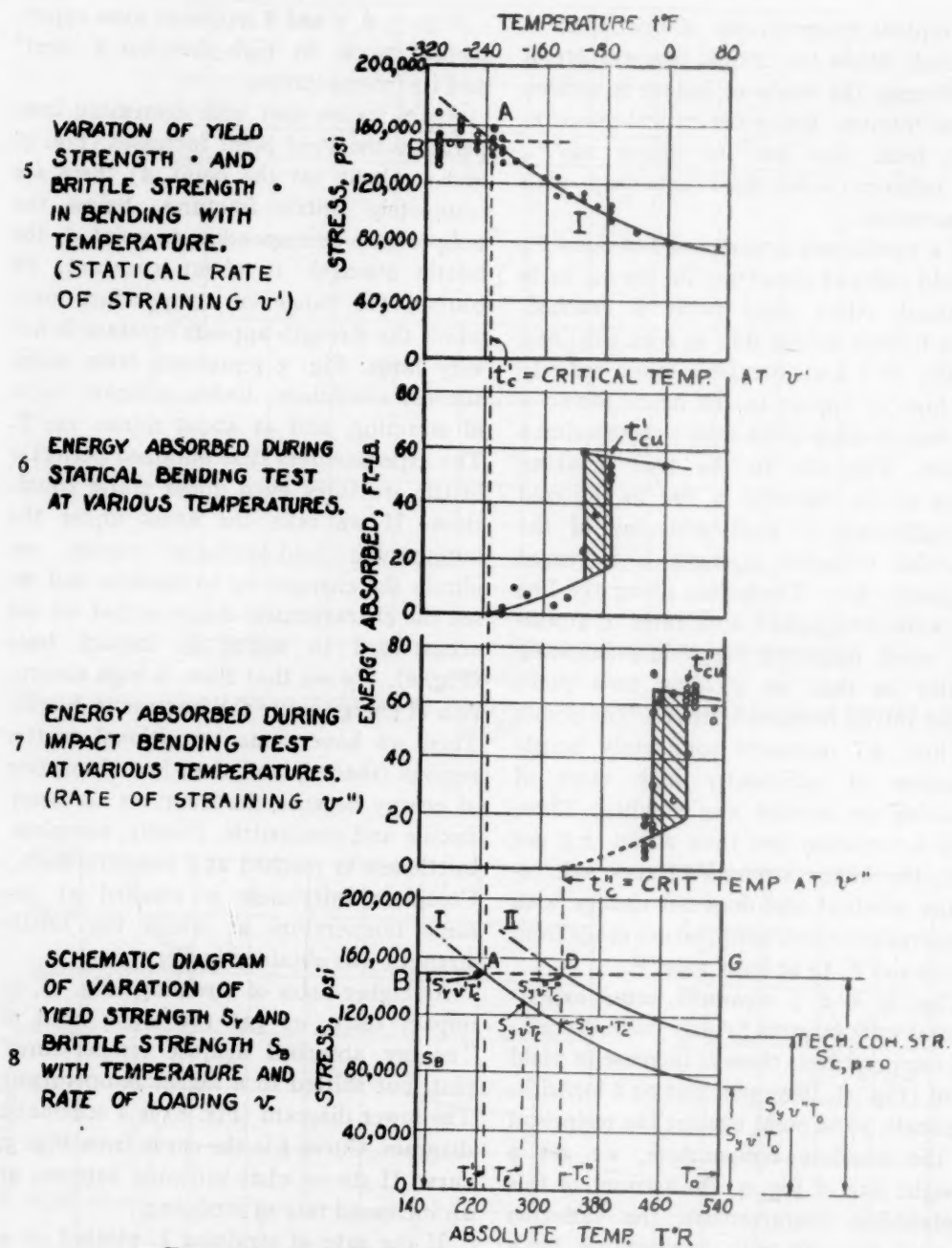
Again we see that with decreasing temperature the yield point increases (Fig. 5) and suddenly (at the point A) there are completely brittle fractures. Below the temperature corresponding to point A, the brittle strength is about constant. Of course, the range of temperature over which the strength appears constant is not very large. Fig. 5 represents tests under static conditions, under ordinary rates of straining, and at about minus 240°F. The experimenters thus obtained perfectly brittle fractures even under static conditions. If we take the areas under the autographic load-extension curves, we obtain the energies up to fracture and we see the characteristic diagram that we are accustomed to seeing in impact tests (Fig. 6). We see that there is high absorption of energy while the fracture is ductile. Then we have some transitional scatter regions (shaded) and then low absorption of energy because the fractures are semiductile and semibrittle. Finally, complete brittleness is reached at a temperature t_b' . Complete brittleness is reached at the same temperature at which the brittle strength was obtained in Fig. 5.

At higher rates of straining (Fig. 7), in impact tests, we get this same kind of "energy absorbed against temperature" plot, but shifted to a higher temperature. The lower diagram (Fig. 8) is a schematic diagram. Curve I is the curve from Fig. 5; curve II shows what probably happens at an increased rate of straining.

If the rate of straining is plotted on a logarithmic scale against the reciprocal of the absolute temperature at which completely brittle fractures were obtained in bending (using the result of Witman and Stepanov, *loc. cit.*) the result is a straight-

*F. F. Witman and V. A. Stepanov: Influence of Rate of Deformation upon Brittleness of Steel. *Jnl. of Technical Physics* (Russian) (1939) 9 (12), 1070.

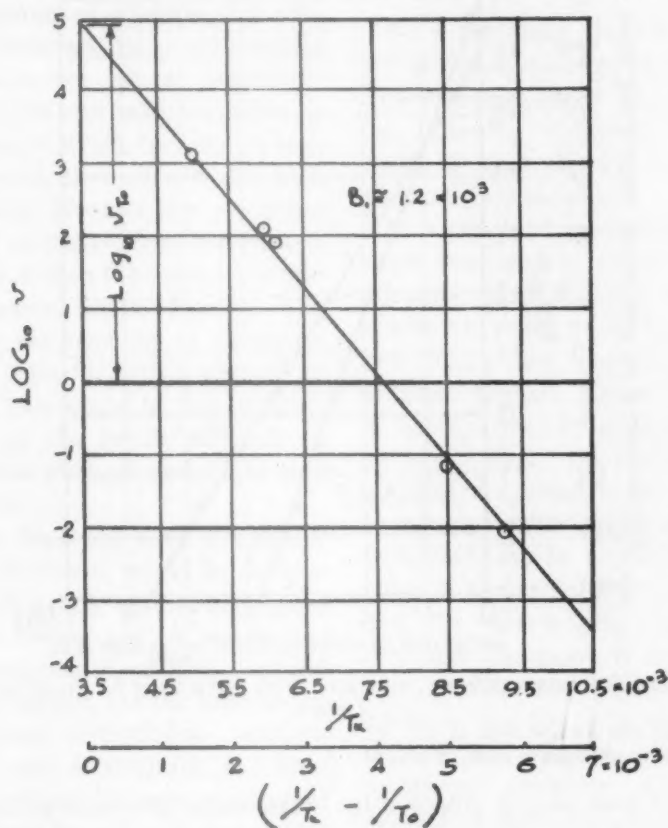
*F. Shevandin and I. Kisin: Cold Brittleness of a High-phosphorus Iron. *Jnl. of Technical Physics*. (Russian) (1939) 9 (11), 958.



FIGS. 5 TO 8.—HIGH-PHOSPHORUS STEEL (Shevandin and Kisin).

line plot (Fig. 9). This is rather interesting because Hollomon and Zener have proposed the same relationship between rate of straining and temperature. This is

Winlock and Leiter* have performed many experiments at different straining rates and obtained higher yield points at higher straining rates. If some of their



T_0 = DEGREES KELVIN.

v = INCHES PER INCH PER SEC.

FIG. 9.—VARIATION OF UPPER CRITICAL TEMPERATURE OF BRITTLNESS WITH RATE OF STRAINING (Witman and Stepanov).

showing that certain change in rate of straining is equivalent to a certain change in temperature. The equivalence is clearer if plotted in this manner.

It appears that the high-phosphorus steel used by Shevandin and Kisin must have had a value of Q (to use Hollomon's term), which is the heat of activation, of about 5000 cal. per gram mol. On a different basis, I have obtained from those same data approximately the same heat of activation.

results are plotted as shown in Fig. 10, straight lines again occur. This type of plotting was suggested in the discussion of Winlock and Leiter's paper, by Mr. Kanter, of Crane Company of Chicago.

The technical cohesive strength, which Kuntze first proposed to find, was defined

* J. Winlock and R. Leiter: Some Observations on the Yield Point of Low-carbon Steel. *Trans. Amer. Soc. Mech. Engrs.* (1939) 63, 581.

Some Factors Affecting the Plastic Deformation of Sheet and Strip Steel. *Trans. Amer. Soc. Metals* (1937) 25, 163.

as that normal stress at which separation fracture occurs with no previous yielding. I believe that Dr. McAdam is right in criticizing Kuntze's method. Kuntze's

If a material is completely brittle at room temperature in a statical tension test, its ultimate strength is equal to the technical cohesive strength, because no flow

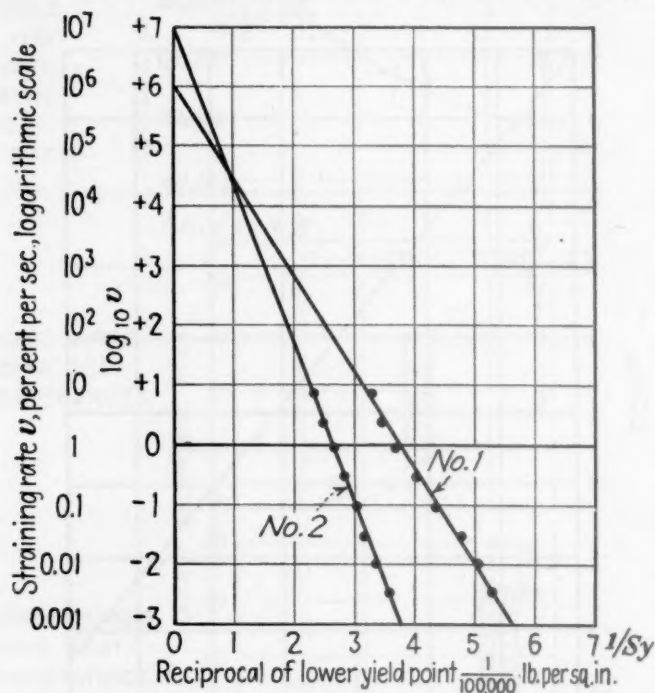


FIG. 10.—VARIATION OF YIELD POINT S_y OF MILD STEEL WITH RATE OF STRAINING v (Winlock and Leiter).

No. 1, 20 grains per square inch at 100 X.
No. 2, 200 grains per square inch at 100 X.

method does not give what it proposed to give. However, as I tried to show before, I believe that Dr. McAdam's method does not eliminate all plastic yielding. According to Kuntze's definition, therefore, Dr. McAdam is not getting the cohesive strength. Of course, the term can be defined differently. Cohesive strength can be obtained by a different approach; that is, from tests with completely brittle fractures. All we have to do is to cause completely brittle fracture with no previous flow, then we have something useful for design, whatever you wish to call it, brittle strength or technical cohesive strength. It is useful for design because the thing we are afraid of is a completely brittle fracture. If there is any yielding, there is higher strength.

takes place. If a material is ductile at room temperature in statical tension tests of unnotched specimens, but at a lowered temperature exhibits completely brittle fractures, what is more reasonable than to say that the ultimate strength of a well-centered unnotched specimen at a sufficiently low temperature (say at liquid-air temperature), at which the fracture is perfectly brittle, is the cohesive strength. Call it what you like, it is the thing we are interested in in design.

Finally, there are, of course, metals that will not be completely brittle in statical tests of unnotched specimens at even very low temperatures. Then we must go to high rates of straining, as Captain Hollomon showed, and I propose to perform a direct experiment this way:

On an unnotched specimen put one of the new strain-measuring gauges, say a Baldwin-Southwark metallic wire resistance gauge or a carbon resistance gauge, and break the specimen in impact at a sufficiently high rate of straining and at a sufficiently low temperature to get a brittle fracture. Because we get a completely brittle fracture, we can say that stress is still proportional to strain, by Hooke's law. It has been found that even under high rates of straining, Hooke's law, or rather the modulus of elasticity, does not change. Why not measure then the breaking strain at the completely brittle fracture and multiply it by the modulus of elasticity, and in that way get the brittle strength of the specimen? This would be then a direct determination of the brittle strength or technical cohesive strength and might give something useful.

Suppose one does not have the equipment, which, of course, would be complicated—an oscillograph and a high-speed motion picture camera and, of course, the strain gauge equipment, control box and so on would be needed. On the basis of the previously shown straight-line relationships between rate of straining and temperature (Fig. 9) and between yield point and temperature (Fig. 4), and postulating that, as was shown in Joffé's diagram for rock salt (Fig. 2), the brittle strength is independent of temperature also in metals, we can get an estimation of brittle strength or technical cohesive strength from the results of a few conventional tests. A number of proposed methods of estimating the cohesive strength from the results of a few rather simple tests is given in my University of Illinois thesis.* Time does not permit going into details here.

I should like to say that I do not presume to question at all the work of Dr. McAdam and the work of the men who talked here before me. I do not know as

much as they do, and I recognize the great importance of Dr. McAdam's theoretical relations. What I have tried to present is a way in which to obtain a useful design value.

D. J. MCADAM, JR.—Although I have not had an opportunity to read the paper by Hollomon and Zener, in this symposium,* the following comments probably will apply to that paper as well as to Dr. Morkovin's discussion.

It is generally recognized that the flow stress expressed in terms of the greatest principal stress depends on five variables in addition to the variable plastic deformation. These five variables are the three principal stresses, temperature, and speed of deformation. It is generally assumed, however, that the technical cohesive strength of a metal, in any particular state as regards mechanical treatment and heat-treatment, can be represented by a single value of the greatest principal stress, and that this value is independent of temperature and the speed of deformation. This view persists in spite of ample irrefutable evidence that the technical cohesion limit† depends on all five of the previously mentioned variables, and also on the amount of plastic deformation. Moreover, the combination of principal stresses affects the technical cohesion limit only slightly less than it affects the flow stress; temperature and speed of deformation affect the technical cohesion limit about as much as they affect the flow stress.

A single technical cohesion limit, therefore, cannot completely represent the technical cohesive strength of a metal, whether or not the fracture is preceded by plastic deformation. Consequently, the *initial* technical cohesive strength, the strength prior to plastic deformation, can-

* See note on page 538.

† By "technical cohesion limit" is here meant the greatest principal stress at fracture under a specific combination of the five variables.

* See footnote on page 595.

not be completely represented by the stress at a brittle* fracture, whether the brittle fracture be obtained by adjusting the combination of principal stresses, or by adjusting the temperature and speed of deformation. For a specific temperature and speed of deformation, however, the technical cohesive strength of a brittle metal may be represented by a curved surface in a diagram with the three principal stresses as coordinates, and the initial technical cohesive strength of a ductile metal may be pictured approximately by a similar curved surface inside the surface representing fracture after the varying plastic deformation, and outside the surface representing yield.

Plastic deformation increases the technical cohesive strength continuously, at a decreasing rate, and only slightly less rapidly than it increases the flow stress. As shown in references 6 and 7 of my paper, Kuntze's idea that plastic deformation eventually decreases the technical cohesive strength is incorrect.

Evidence that temperature greatly affects the technical cohesive strength of metals is given in two of our papers (references 10 and 11). The evidence is especially clear in Figs. 19, 20, 22, and 23 of reference 10. Lowering the temperature of unnotched and notched specimens of the ductile nonferrous metals there represented raises the breaking stress about as rapidly as it raises the yield stress or ultimate stress, but causes little or no change in the ductility. The rapid rise of the breaking stress with fall of temperature, therefore, must be attributed almost entirely to the influence of the variable temperature. Moreover, the rapid increase of these specific cohesion limits denotes a correspondingly rapid increase in the size of the diagram that may be used to represent the technical cohesive strength.

Scattered evidence of a similar type

* Such a fracture generally is not microscopically brittle.

shows that the *technical* cohesive strength increases with the speed of deformation, and that this increase is about as rapid as the increase of the flow stress. The effect of an increase of speed on the technical cohesive strength, therefore, is qualitatively similar to the effect of a decrease of temperature. The tacit incorrect assumption that the technical cohesive strength is practically unaffected by speed leads naturally to the incorrect view that cohesive strength is little affected by temperature, because the latter incorrect view is based on experiments in which both temperature and speed were changed simultaneously. Such procedure may account for the constancy of the stress at brittle fracture of rock salt, illustrated by Fig. 2 of Dr. Morkovin's discussion, although it is possible that the behaviour of rock salt differs in this respect from the behaviour of metals.

If an attempt were made to obtain a brittle fracture of copper by testing at high speed at room temperature, as Dr. Morkovin suggests, the ductility might prove to be as great as it is at minus 188°C. when tested at low speed. Even if a brittle fracture should be obtained, however, the breaking stress would merely represent the cohesion limit corresponding to that set of conditions. It would give no information about the cohesion limit that would be obtained by subjecting copper to polar-symmetric stress at low speed at room temperature, or at any other speed and temperature, and would give no information about the variation of the cohesion limit with the combination of principal stresses.

C. ZENER.*—I should like to point out a difficulty in Professor Morkovin's method. In trying to obtain the technical cohesive strength at a low temperature of a substance that is not brittle at low temper-

* State College of Washington, Pullman, Washington.

ature, he proposes that we go to a high strain rate at a low temperature. A possible difficulty is that at high strain rates the deformation is adiabatic, and at low temperatures adiabatic strain has a negative slope in the plastic region. Such a negative slope will give rise to localized necking before any uniform plastic deformation has occurred.

D. MORKOVIN.—That cannot happen with completely brittle fractures. That was the thing I tried to bring out. With low enough temperatures at high enough rate of straining, we get completely brittle fracture. That means elastic deformation up to fracture. As there is no yielding, there is virtually no increase in temperature, because during the elastic deformation the heat generated is very small.

Probably this method will not apply to all materials. There may be some materials in which, even under extremely low temperatures and high rates of straining, it will not be possible to get a brittle fracture, but the indications are that the embrittling action of high speed and low temperature is universal for metals as well as other materials. For the steels tested and reported on by Zener and Hollomon (tempered pearlite and tempered martensite), the tests showed an example of simultaneous action of high rate of straining and low temperature in causing a completely brittle fracture. Completely brittle fracture was obtained by them with tempered pearlitic steel. Their curves for tempered martensitic steel show a tendency to complete brittleness at testing conditions still more drastic than those they used.

S. L. HOYT.*—As a metallurgist, I have considerable interest in these deliberations, but possibly we should consider some of the more practical aspects of this general problem. I think it is important to bear in

mind that what has been done—does not as yet bring any direct evidence on the technical problem of notch brittleness, and that is what this thing is all about.

The problem that the metallurgist is concerned with is why is it that steels—and this behavior is limited to steels—sometimes break as perfectly brittle material and sometimes as rather ductile or tough material? I should like to propose taking two steels, one of which is notch brittle and one of which is not, and putting them through their performance. Let us have the curves and see what those points look like and how they plot out. Some of the data that we have seen here might apply either to a face-centered cubic metal or body-centered cubic metal. The face-centered cubic metals do not show the peculiar, abnormal or eccentric notch effects. They respond to the notch effect, and no doubt they could be made to break in a brittle fashion. But it is the body-centered cubic metals that show marked eccentricity of behavior. I should like to propose testing samples that will show a very marked contrast, like a low-carbon, open-hearth steel, and a strain-aged and brittle bessemer steel with a lot of nitrogen in it, but both of which are ductile in the tension test. These steels may have the same properties in the tension test and yet behave quite differently when notched.

C. ZENER.—The questions raised by Dr. Hoyt have already been covered in our paper. In particular, the general brittle behavior of pearlitic steels in the notched-bar impact test, as contrasted with the behavior of tempered martensitic steels in this test, has been interpreted in terms of a fundamental concept. This concept relates to the variation of the fracture strength with deformation.

S. L. HOYT.—Do they have the same tensile properties?

C. ZENER.—A pearlitic and a tempered martensitic steel that behave quite differ-

* Battelle Memorial Institute, Columbus, Ohio.

ently under a complex stress pattern may have identical tensile properties as measured under the usual test conditions. If, however, the rate of strain is increased greatly, or if the temperature is lowered, the tensile properties will become quite different. Such a change of conditions will often embrittle the pearlitic steel, but not the tempered martensitic steel.

S. L. HOYT.—I am thinking again of a symposium in the Welding Society this morning on brittle ships. There the assumption is that these internal stresses, by setting up a severe condition of three-dimensional stresses, produce brittle fracture. Your statement leads me to suspect that this cannot be the complete explanation. The explanation must have something to do with the character or the quality of the metal, and not solely with the condition of the stress system that was imposed upon those ships by design that introduces notches, and by welding.

C. ZENER.—I believe it is perfectly clear from Captain Hollomon's presentation of our paper why welded ship steel is apt to be brittle. The structural steel used in ships is the type known as mild steel and consists of proeutectoid ferrite and pearlite. The fracture strength of the undeformed metal of such steels is generally only about 10

per cent above the yield strength. A single transverse stress, which can raise the yield strength by about 15 per cent, while leaving the fracture strength unaltered may therefore cause the ship steel to break brittly (with no prior plastic deformation). A tempered martensitic steel with a moderate yield strength has an initial fracture strength considerably above the yield strength, and cannot thus be embrittled by a single transverse stress.

S. L. HOYT.—Will notch tough open-hearth steel behave like fully quenched and tempered steel?

C. ZENER.—It appeared from the results reported in our paper and other unpublished work that the most important variable affecting the notched-bar impact testing properties of steel is its metallurgical structure. In general, tempered martensitic steels have a greater toughness and maintain this toughness to lower temperature than do pearlitic materials. For steels of a given structure, the steelmaking practice, the cleanliness of the steel and the amount and the direction of hot-working will, of course, affect the impact properties. Such changes, however, are small compared with those that can be brought about by changes in metallurgical structure.

(The meeting adjourned at 5.45 p.m.)

Symposium on Recent Developments in Dilatometric Analysis

(Cleveland Meeting, October 1944)

CONTENTS

	PAGE
A High-speed Dilatometer and the Transformational Behavior of Six Steels in Cooling. By ARTHUR L. CHRISTENSON, EDWARD C. NELSON and CLARENCE E. JACKSON. (With discussion)	606
Dilatometric Studies of the Graphitization of Cast Iron. By N. A. ZIEGLER. (With discussion)	627
An Interferometer Type of Dilatometer and Some Typical Results. By L. A. WILLEY and W. L. FINK. (With discussion).	642

THE meeting was held in the Pine Room of the Statler Hotel, Cleveland, Ohio, on Tuesday afternoon, October 17, 1944. The chairmen were F. M. Walters, Jr. and Howard Scott.

INTRODUCTION

F. M. WALTERS, JR.—The principal advantages of the dilatometric method perhaps are two, as compared with the method of thermal analysis. One is that the dilatometric method can be applied with a large variety of rates of heating and cooling, whereas thermal analysis—that is, the

study of the transformational characteristics by means of heat evolution—is limited to the rates of heating and cooling that reveal the evolution of heat. The dilatometer can be used for the study of reactions at zero rates of heating and cooling; that is, isothermal reactions. As you will hear this afternoon, the rates have been pushed up as far as 500°C. a second.

The other advantage is that the dilatometric method shows that a two-phase region is a two-phase region, whereas the thermal analysis merely reveals the temperature at which the rates of heat evolution are greatest.

A High-speed Dilatometer and the Transformational Behavior of Six Steels in Cooling

BY ARTHUR L. CHRISTENSON,* JUNIOR MEMBER A.I.M.E., EDWARD C. NELSON,*
AND CLARENCE E. JACKSON,* MEMBER A.I.M.E.

(Cleveland Meeting, October 1944)

MUCH information regarding the transformational characteristics of a steel as it cools in a known manner from the austenitic state can be obtained from dilatometric studies. This method has received more and more attention because of its great flexibility, accuracy, and ease of interpretation. The method is entirely applicable to any rate of heating and cooling although the experimental procedures for high rates of cooling have offered some difficulties. This paper presents a description of equipment employing cooling rates up to 500°C. per second and the results of dilatometric observations on six commercial steels are included.

French and Klopsch¹ studied the cooling transformations of a series of carbon steels using the thermal arrest method. This was followed by the systematic investigation of Esser and co-workers on the effect of carbon² and other alloying additions³, in which the transformation temperatures were determined by magnetic induction measurements indicated by a string galvanometer. Emphasis was placed on determining Ar' transformations and the critical cooling rates for these steels. The magnetic

measurements were used in an effort to obtain more accurate data at higher cooling rates. Measurements of thermal arrest were made also to check the validity of the magnetic indications, and good correlation was found between the two, although Esser's Ar'' temperature measurements on iron-carbon alloys were about 200°F. lower than the measurements made by French and Klopsch. A notable contribution by Esser was the introduction of gas quenching.

Wever and Rose⁴ used a moving-coil galvanometer in the study of the Ar' and Ar'' of iron-carbon alloys by the thermal arrest method and obtained somewhat lower Ar'' temperatures than those observed by Esser below 1 per cent carbon and considerably higher above. They concluded that the cooling rate had little influence on the Ar'' temperatures above 0.4 per cent carbon, although Esser had observed a decrease in the Ar'' temperature with increasing cooling rate with similar steels.

Digges⁵⁻⁷ determined the Ar'' temperatures for a series of high-purity iron-carbon alloys, and close agreement with his results was obtained by Greninger.⁸ The thermal arrest method, together with metallographic observation used in both these studies, represents the latest investigations of this type. Any investigation by thermal analyses is dependent on the heat of reaction and the specific heat of the

This paper represents only the personal opinions of the authors and in no way reflects the official attitude of the U. S. Navy. Published by permission of the Navy Department. Manuscript received at the office of the Institute July 12, 1944. Listed as T. P. 1768.

* Division of Physical Metallurgy, Naval Research Laboratory, Anacostia Station, Washington, D. C.

¹ References are at the end of the paper.

reaction products. In many instances this method does not yield satisfactory data. It is not only desirable to measure the temperature ranges during which the

products, and such extraneous effects on magnetic induction as may be produced by stresses set up during the transformation. Neither the magnetic nor thermal

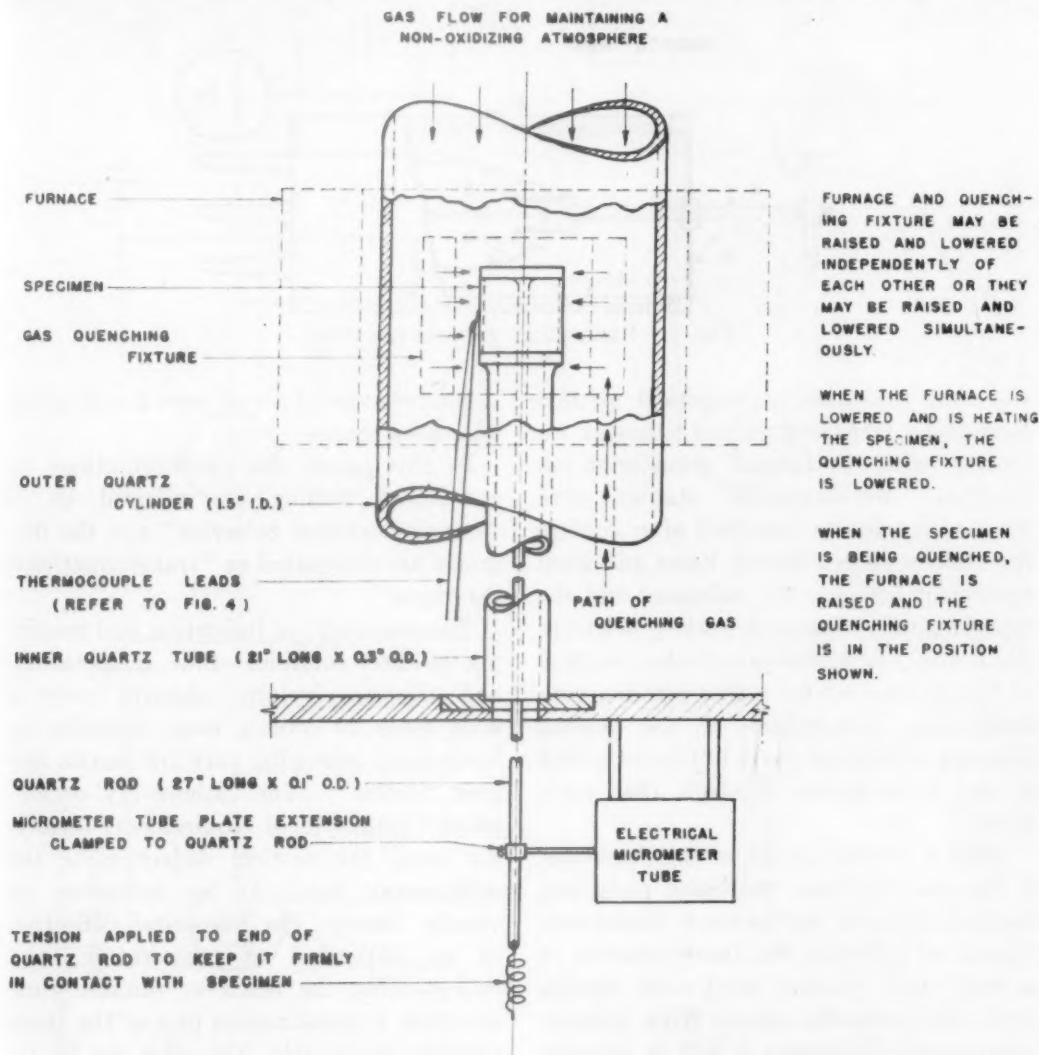


FIG. 1.—SPECIMEN ASSEMBLY.

austenite transformation takes place when cooled in a known manner but also to obtain a good indication of the amount of austenite that has transformed. Any investigation of cooling transformation behavior by magnetic induction measurements is necessarily dependent on the magnetic properties of the transformation

arrest method lends itself readily to obtaining quantitative information regarding transformational behavior on cooling

While studies have been made on a variety of steels, data are yet lacking for construction of complete diagrams of transformations on cooling. Grange and Kiefer⁹ pointed out the experimental diffi-

FURNACE AND QUENCHING FIXTURE MAY BE RAISED AND LOWERED INDEPENDENTLY OF EACH OTHER OR THEY MAY BE RAISED AND LOWERED SIMULTANEOUSLY.

WHEN THE FURNACE IS LOWERED AND IS HEATING THE SPECIMEN, THE QUENCHING FIXTURE IS LOWERED.

WHEN THE SPECIMEN IS BEING QUENCHED, THE FURNACE IS RAISED AND THE QUENCHING FIXTURE IS IN THE POSITION SHOWN.

culties to be encountered in the study of the transformations of any but the most sluggish alloys and suggested that cooling diagrams be derived from isothermal data,

are important in the study of transformation stresses and their effect on cracking tendencies. The equipment described herein is suitable for investigating the transforma-

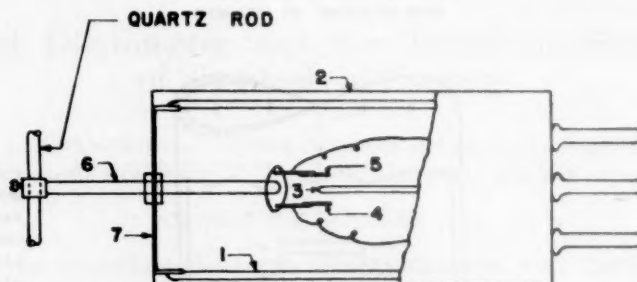


FIG. 2.—ELECTRICAL MICROMETER TUBE.

and they presented an empirical method correlating transformational behavior on cooling with isothermal transformation behavior. Metallographic studies were made of specimens quenched after cooling for various predetermined times and good agreement between the estimated and the experimentally observed cooling behavior was found. The interrupted cooling method of Grange and Kiefer makes possible very satisfactory observation of the cooling behavior of sluggish steels but is not suited to the investigation of steels that react faster.

After a careful survey of the literature, it was decided that the most promising method of attack was to use a dilatometer capable of following the transformation of a small steel specimen as it cools rapidly from the austenitic state. With suitable dilatometric equipment it will be possible to obtain the information required for the construction of a diagram indicating transformations on continuous cooling. If the temperature ranges in which the various transformation products are formed can be determined for a series of different cooling rates, the problem of interpreting the microstructures will be very much simplified. The dilatometric method is of particular advantage in the field of welding, where the actual dilation characteristics

tional behavior of a steel over a wide range of cooling rates.

In this paper, the transformations on continuous cooling are referred to as "transformational behavior" and the diagrams are designated as "transformational diagrams."

The necessity for indicating and recording the three variables—time, temperature, and dilation (volume change)—over a wide range of cooling rates demands an instrument possessing very low inertia and good flexibility. The cathode-ray oscillograph¹⁰ fulfills these requirements ideally. By using the vertical deflection of the cathode-ray beam as an indication of volume change, the horizontal deflection as an indication of temperature, and extinguishing the beam at suitable time intervals, a simultaneous plot of the three variables is possible. This plot can be recorded photographically.

From a functional standpoint, the equipment is best considered in four parts:

1. The mechanical arrangement of specimen, furnace, and cooling device.
2. The measurement of dilation.
3. The measurement of temperature.
4. The measurement of time.

The mechanical construction of the dilatometer is similar to many of those now in use (Fig. 1). A quartz rod with a quartz

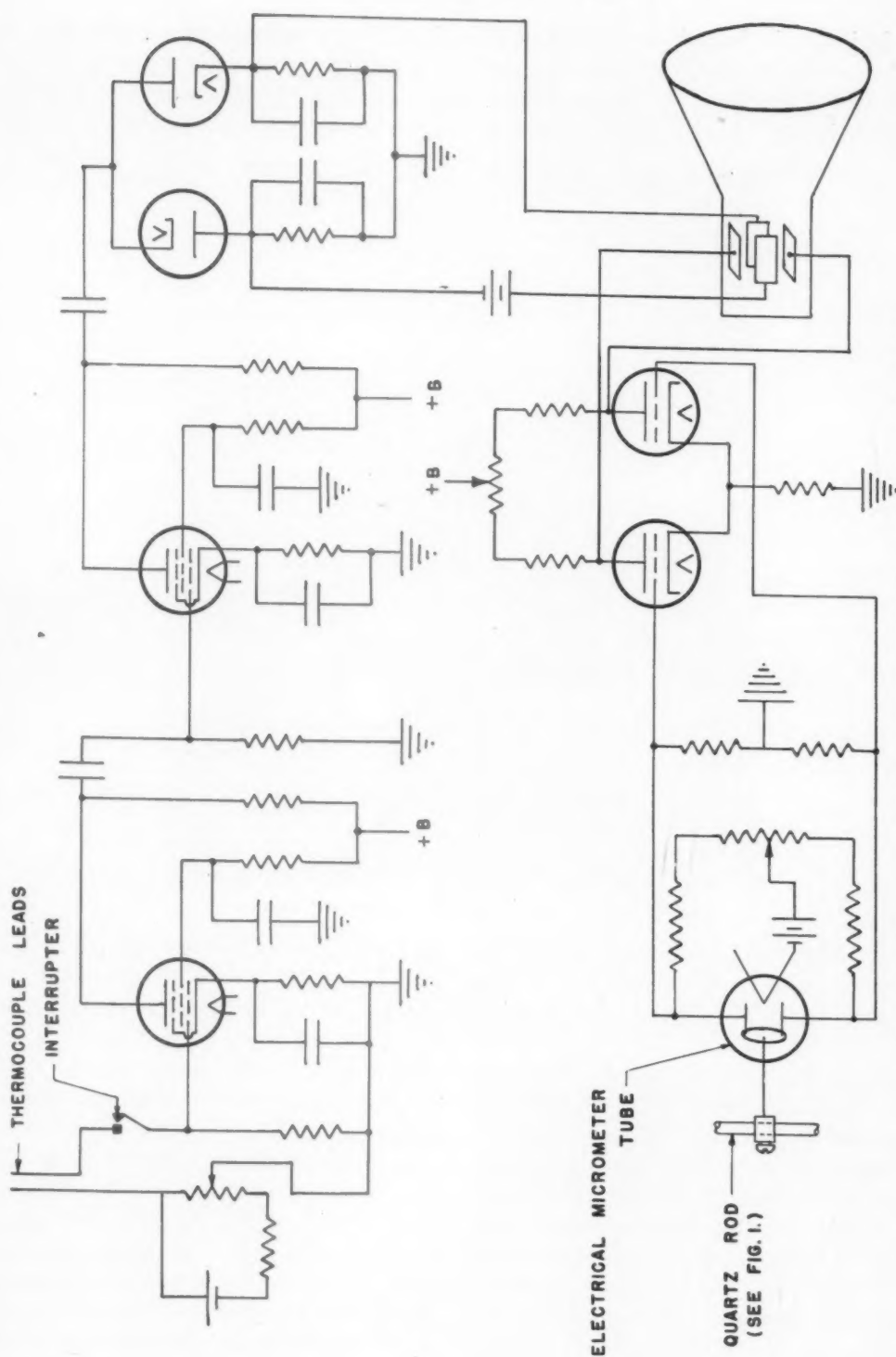


FIG. 3.—CIRCUIT DIAGRAM FOR TEMPERATURE AND VOLUME MEASUREMENT.

cap is inserted through a tubular steel specimen with the cap in contact with the upper end of the specimen. (The specimen is approximately $\frac{3}{8}$ in. inside diameter,

sists of an evacuated glass bulb¹ (Fig. 2), enclosed by a metal shell,² containing a hot electron emissive filament³ and two insulated plates^{4,5} mounted on a tube arm⁶

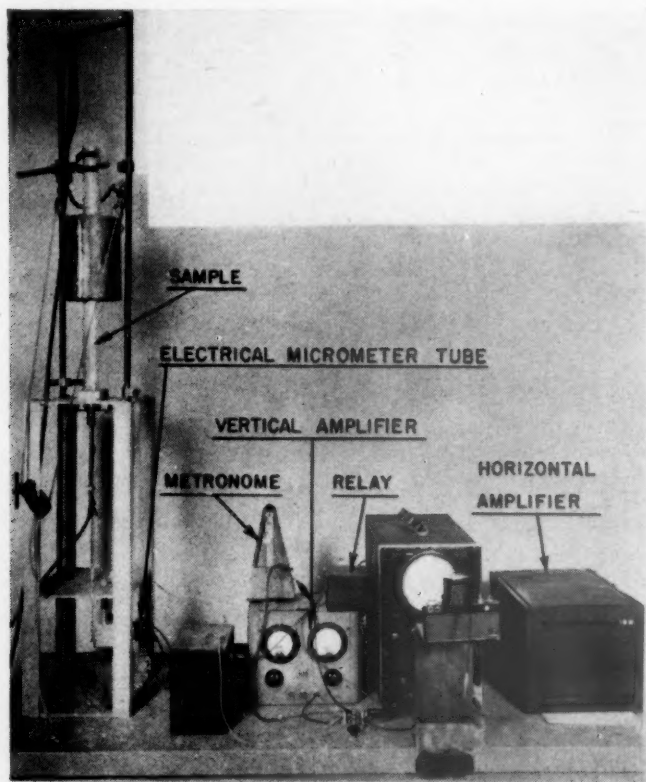


FIG. 4.—THE DILATOMETER ASSEMBLY.

$\frac{7}{10}$ in. long and $\frac{1}{32}$ -in. wall thickness.) A quartz tube is then slipped over the quartz rod until the upper end of the tube is in contact with the lower end of the specimen. Positive contact between the quartz and the specimen is assured by means of a small spring. Any volume change of the steel thus causes a relative displacement between the quartz tube and the quartz rod. The quartz tube is supported in a fixed position and the quartz rod is attached to the movable element of an electrical micrometer tube. Any expansion or contraction of the metal specimen thus produces a proportional displacement of the movable element of the tube.

The electrical micrometer tube¹¹ con-

that extends outside the tube. The tube arm is carried by an elastic metal diaphragm⁷ sealed to the glass envelope. By this construction the plates may be moved with respect to the filament from outside the tube. Two fixed resistances and an adjustable resistance complete a bridge circuit with the plate resistance of the tube (Fig. 3).

Any movement of the tube arm moves one plate closer to the filament and the other farther from the filament, changes the electrical balance of the bridge and causes a voltage to develop across the bridge. Within the limits specified for the tube (approximately 0.012 in. from the point of zero displacement), the voltage developed across the bridge is directly

proportional to the displacement of the tube arm. This allowable displacement is within the limits of expansion of a one-inch specimen heated from room temperature to 1600°F.

gen-hydrogen mixture, may be used satisfactorily.

The specimen and quenching-fixture assembly is placed within a quartz cylinder through which a small flow of helium is

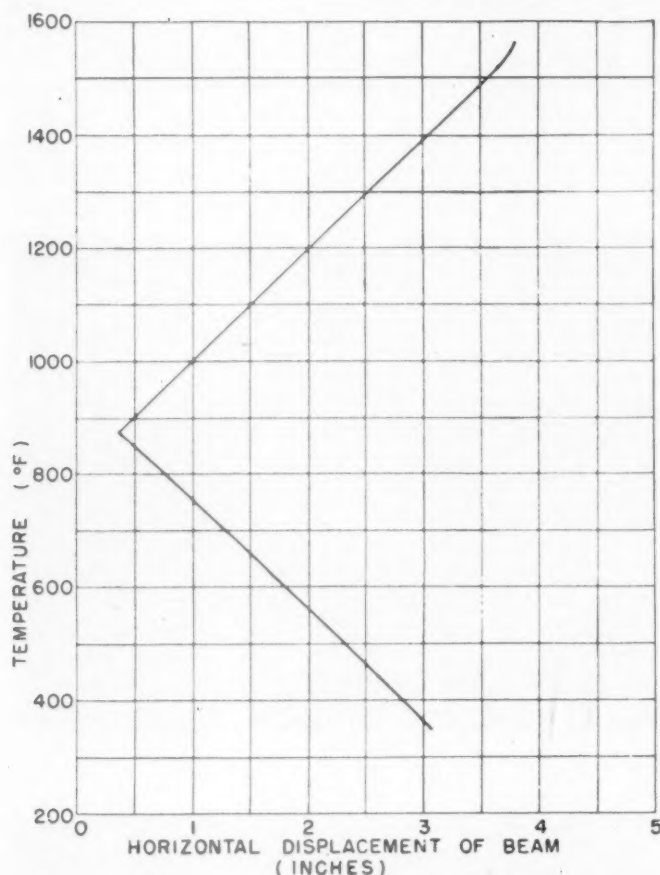


FIG. 5.—TEMPERATURE CALIBRATION OF DILATOMETER.

A gas quenching fixture is mounted concentrically with the specimen and allowed to move freely in the axial direction, so that it may be moved down away from the specimen while the latter is being heated and moved up around it to cool the specimen. Rubber tubing is used to provide a flexible coupling between the quenching fixture and the pressure regulator of the supply tank. The pressure adjustment of the tank regulator establishes the severity of quench. Helium gas is used as the cooling medium, although other gases or mixture of gases, such as hydrogen or nitro-

introduced from the top, to maintain an inert atmosphere. A resistance-type heating coil is suspended around the outer quartz cylinder, mechanically arranged so that it may be raised away from the specimen when the specimen is being cooled. The dilatometer assembly is shown in Fig. 4.

The output of the micrometer bridge is about 1.5 volts and is amplified to approximately 200 volts by means of a direct coupled single-stage push-pull amplifier to give full-scale deflection of the cathode-ray beam. The 5-in. DuMont cathode-ray

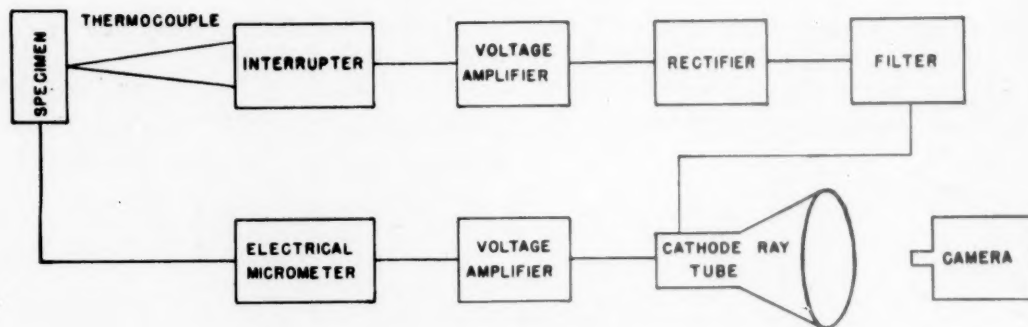


FIG. 6.—SCHEMATIC ARRANGEMENT OF DILATOMETER COMPONENTS.

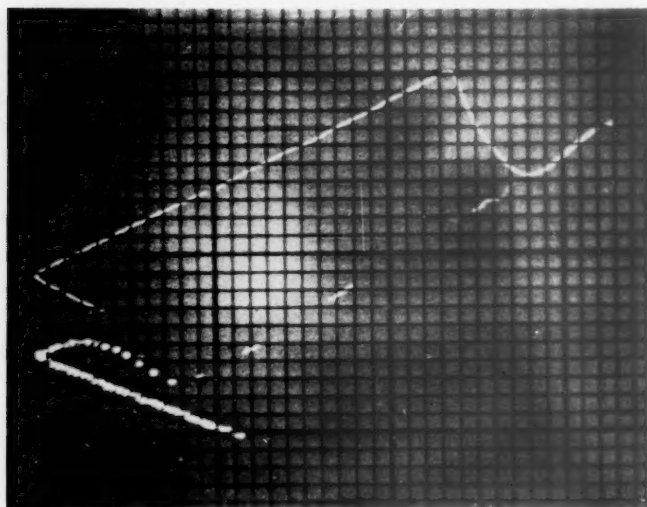
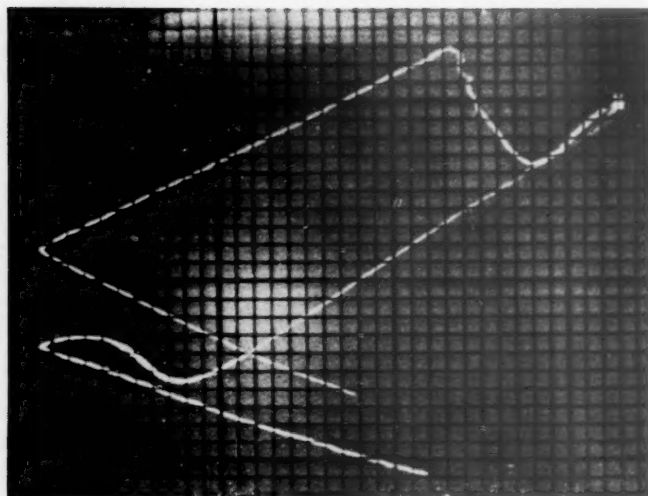
*a**b*

FIG. 7.—PHOTOGRAPHIC RECORD OF A DILATION CURVE. THE COOLING CYCLE OF THE UPPER CURVE HAS BEEN TIMED.

oscillograph, type 208, with a deflection sensitivity of approximately 50 volts per inch, is used with the output of the amplifier directly coupled to the vertical

gauge Chromel-Alumel thermocouple spot-welded to its surface. The output of the thermocouple is about 40 millivolts at 1700°F. To make possible a more accurate

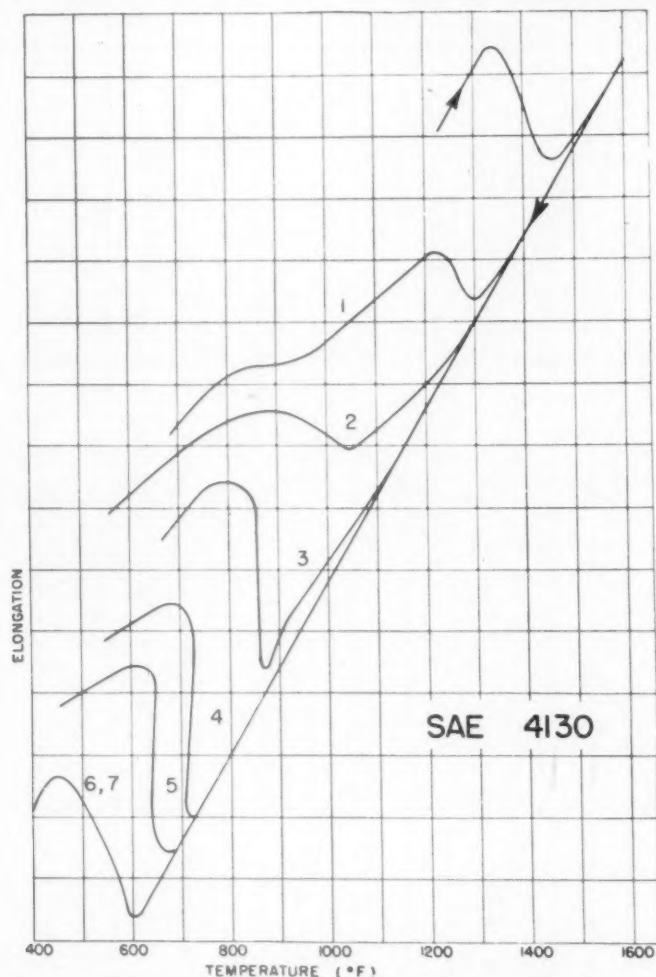


FIG. 8.—FAMILY OF DILATION CURVES OBTAINED FOR A MODIFIED S.A.E. STEEL 4130 AT RATES SHOWN ON FIG. 9.

deflector plates of the cathode-ray tube. By operating the amplifier tubes on the linear portion of their characteristics curves, the deflection of the cathode-ray beam will be for all practical purposes directly proportional to the dilation of the specimen. The adjustable resistance of the micrometer bridge provides a means of vertical positioning of the cathode-ray beam.

The temperature of the specimen is measured by means of a No. 28 B. and S.

temperature measurement on the oscillograph, the temperature scale has been doubled by using the full viewing-screen width to indicate the temperature range from 0 to 20 mv. At 20 mv., the trace then reverses in direction to indicate the temperature range from 20 to 40 mv. To do this it is necessary that the 20 mv. be amplified to approximately 200 volts, to give the full-scale deflection on the screen. This would not be difficult if a resistance coupled amplifier could be satisfactorily

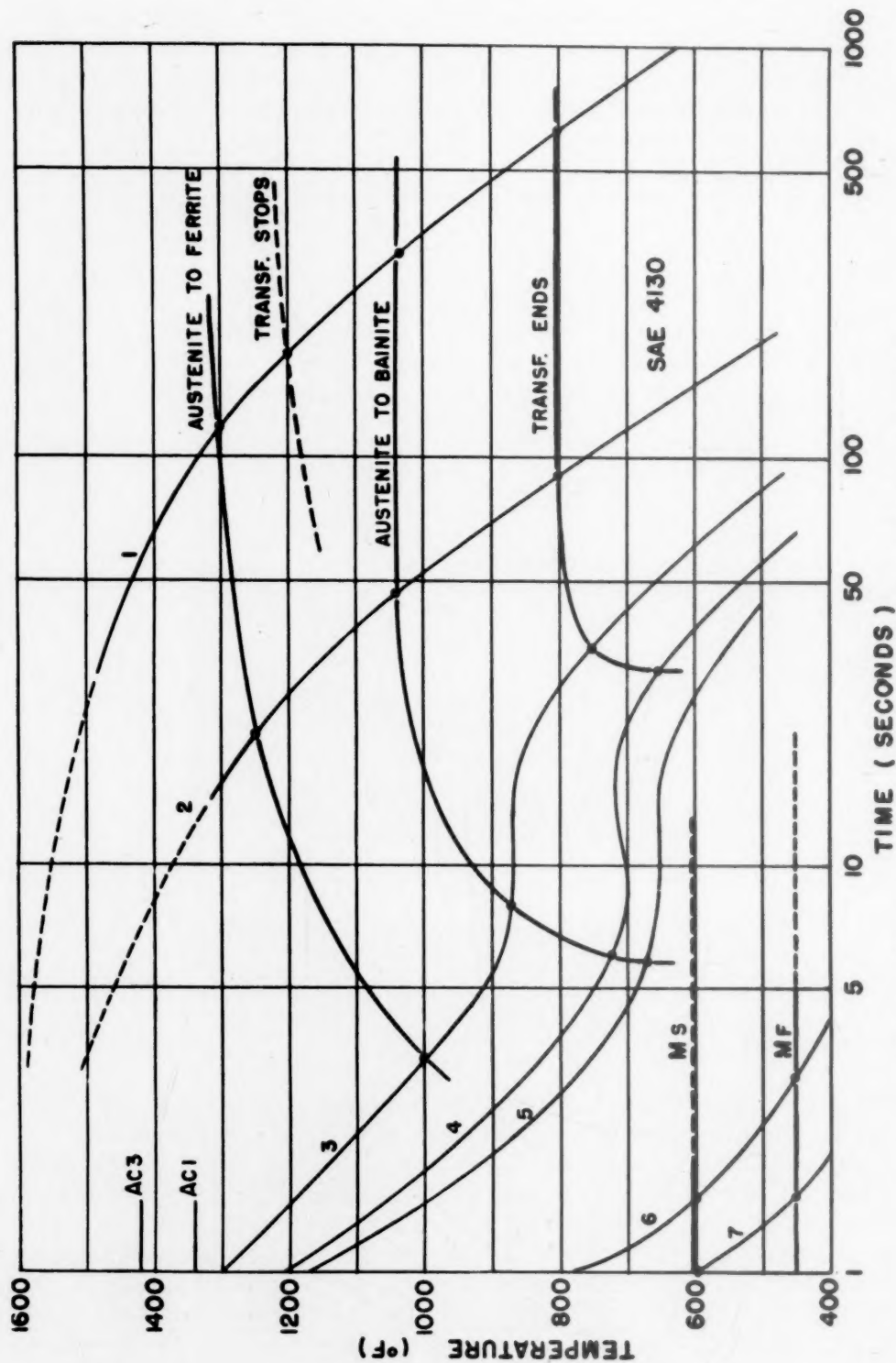


FIG. 9.—TRANSFORMATIONAL DIAGRAM FOR A MODIFIED S.A.E. STEEL 4130.
Composition: 0.29 C., 0.77 Mn., 0.30 Si., 0.021 S., 0.012 P., 0.20 Mo., 0.68 Cr., 0.02 Al.

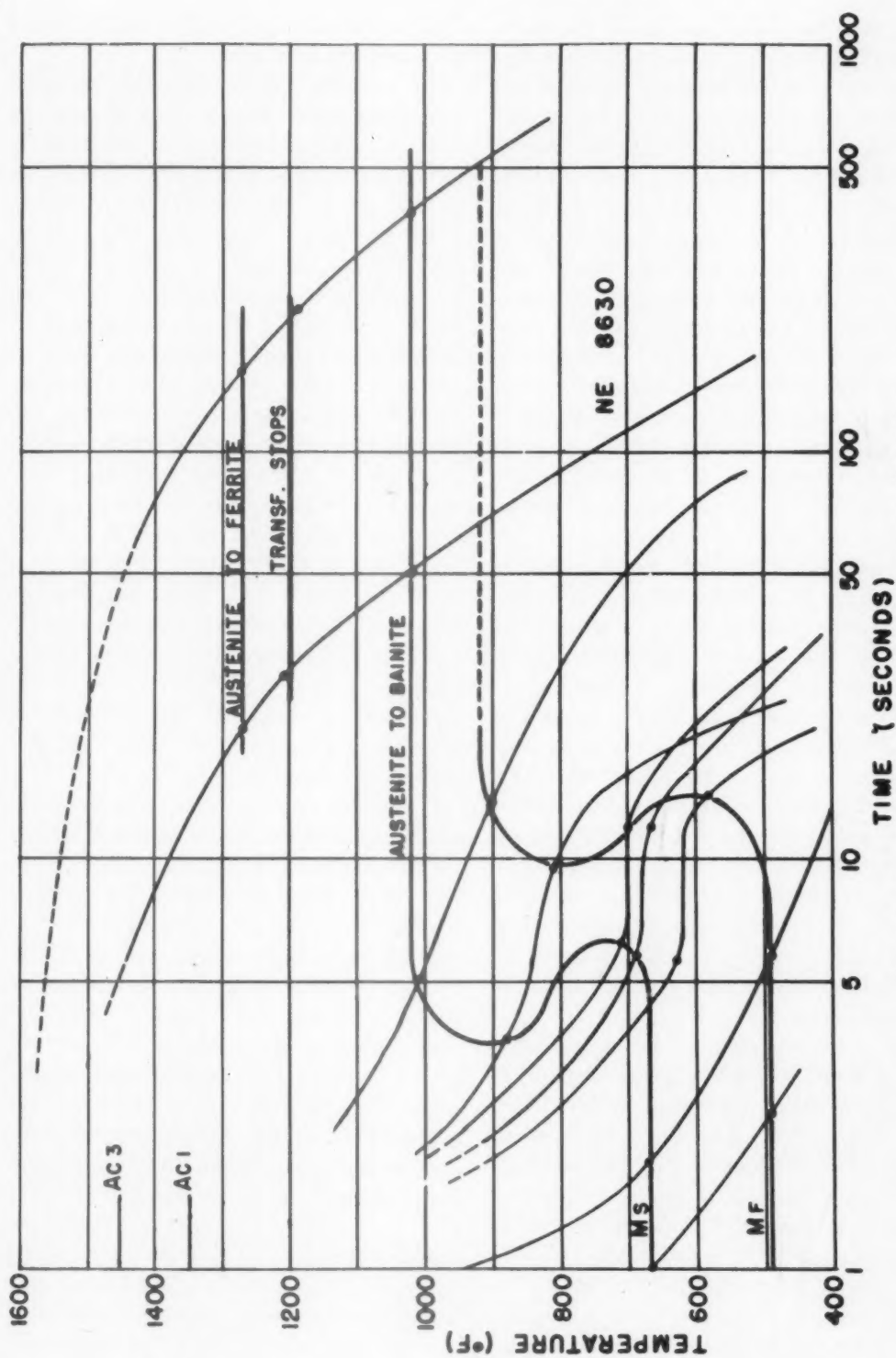


FIG. 10.—TRANSFORMATIONAL DIAGRAM FOR STEEL NE 8630.
Composition: 0.30 C., 0.91 Mn., 0.32 Si., 0.016 S., 0.017 P., 0.61 Ni., 0.06 Cu., 0.17 Mo., 0.52 Cr.

used, but the drift inherent in resistance coupled amplifiers demanded constant recalibration of the temperature scale and for this reason was unsatisfactory. In order that a resistance-capacitance coupled amplifier may be used, the thermocouple current is interrupted by an electrical vibrator having make-and-break contacts that operate at a repetition rate of 500 cycles.* This supplies a square wave signal, the amplitude of which is alternately zero and the full thermocouple voltage; this can be amplified by a standard two-stage resistance-capacitance coupled amplifier. The amplified signal is then full wave rectified, filtered free of undesired ripple and applied to the horizontal deflector plates of the cathode-ray tube.

A bucking potential of 20 mv. is put in series with the thermocouple, with the result that as the specimen is heated the potential applied to the amplifier starts at minus 20 mv., gradually becomes zero, and then assumes a positive value as the thermocouple voltage rises above 20 mv. The reversal of the trace occurs when the potential is zero. Adjustment of the bucking potential can be used to compensate for the cold-junction temperature. Satisfactory horizontal positioning of the cathode-ray beam is obtained by placing two 45-volt dry cells in series with one of the leads from the amplifier to the horizontal deflector plates.

The viewing screen of the cathode-ray tube is provided with a transparent face cover upon which uniform grid lines have been ruled. The grid lines have been calibrated with respect to temperature and a calibration curve is shown on Fig. 5. No calibration was made of the electrical micrometer, since it is necessary to know only the relative dilation; although, a

calibration could easily be made by means of a micrometer screw.

An indication of the time rate at which the temperature and volume changes of the steel are taking place is obtained by extinguishing the beam that traces the pattern at preestablished time intervals. The oscillograph is provided with a beam switch that operates to increase the modulating electrode to cathode bias to beyond cutoff. By replacing the switch with a small magnetic relay and exciting the relay by means of a metronome in series with a dry cell, the beam can be momentarily extinguished at rates from every 0.3 sec. to every 3.0 sec., depending upon the adjustment of the metronome. Slower cooling rates are timed by manual operation of the beam switch but this can be done electrically if desired. It is important that the relay be carefully shielded to prevent disturbance of the cathode-ray beam by the magnetic field of the relay.

A block diagram of the dilatometer assembly is shown in Fig. 6 and examples of photographic records in Fig. 7.

It has been found desirable first to obtain a continuous record of the transformational characteristics of a sample and then to follow this with a time interrupted record, in order to adjust the cooling rate and to provide an accurate interpretation of the transformational behavior. A replot of the observations can be made from the photographic records giving a family of curves similar to that shown for a modified S.A.E. 4130 steel (Fig. 8). From the time-temperature cooling curves plotted from the photographic record, the transformation diagram (Fig. 9) may be constructed. The interpretation of these curves will be assisted by supplementing the dilatometric study with microscopic observations and hardness measurements. Details, especially in the complex "split transformation" range, will be clarified by skillful interpretation of the dilatometric observations. The equipment herein described is a tool that

* A converter tube from a Brown potentiometer pyrometer, although designed for 60-cycle operation, gave fair operation on 500 cycles. A change in the circuit so that the vibrator could be operated at 60 cycles would be desirable.

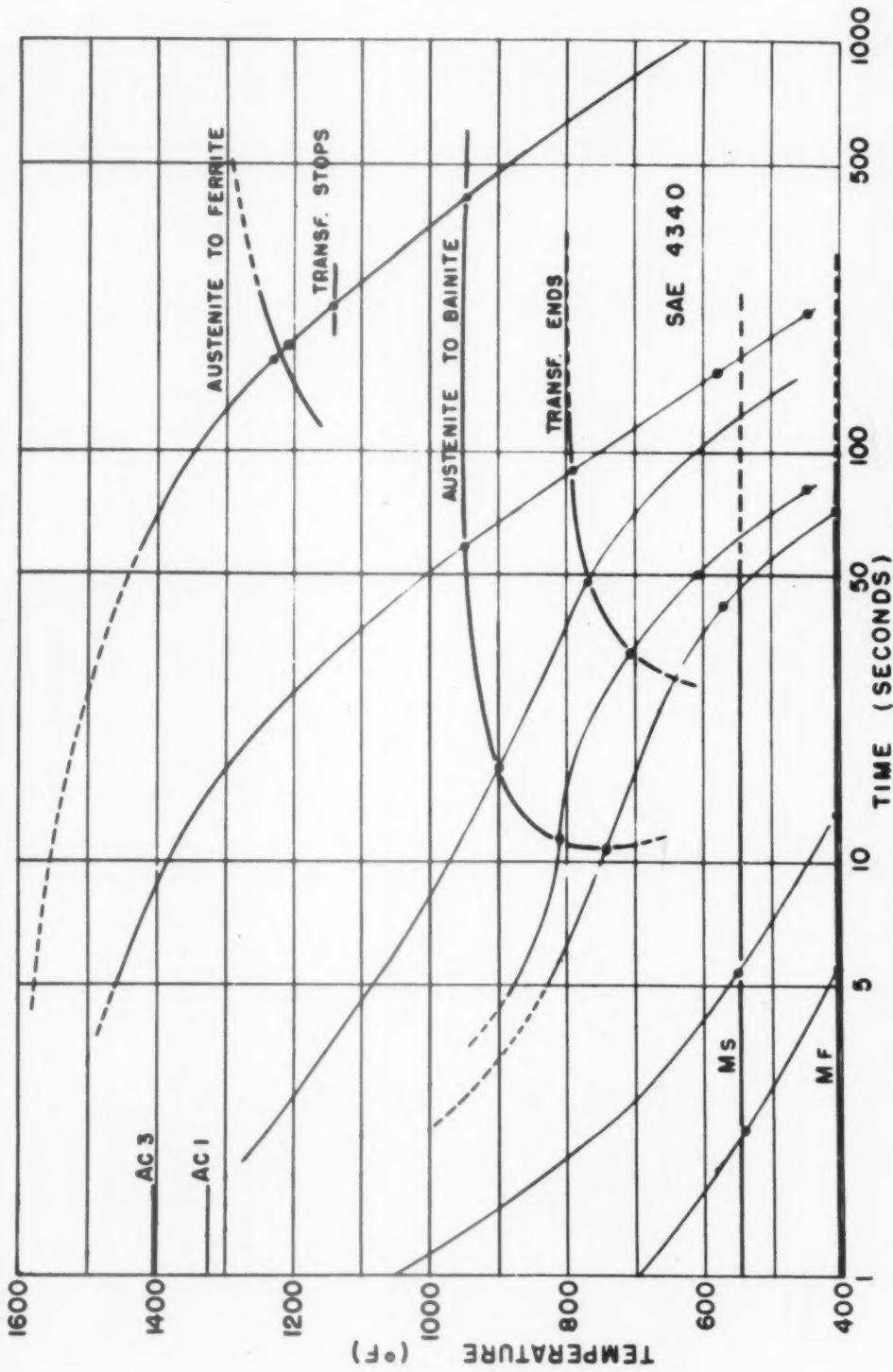


FIG. 11.—TRANSFORMATIONAL DIAGRAM FOR S.A.E. STEEL 4340.
Composition: 0.41 C, 0.73 Mn, 0.30 Si, 0.015 S, 0.018 P, 1.79 Ni, 0.25 Mo, 0.82 Cr.

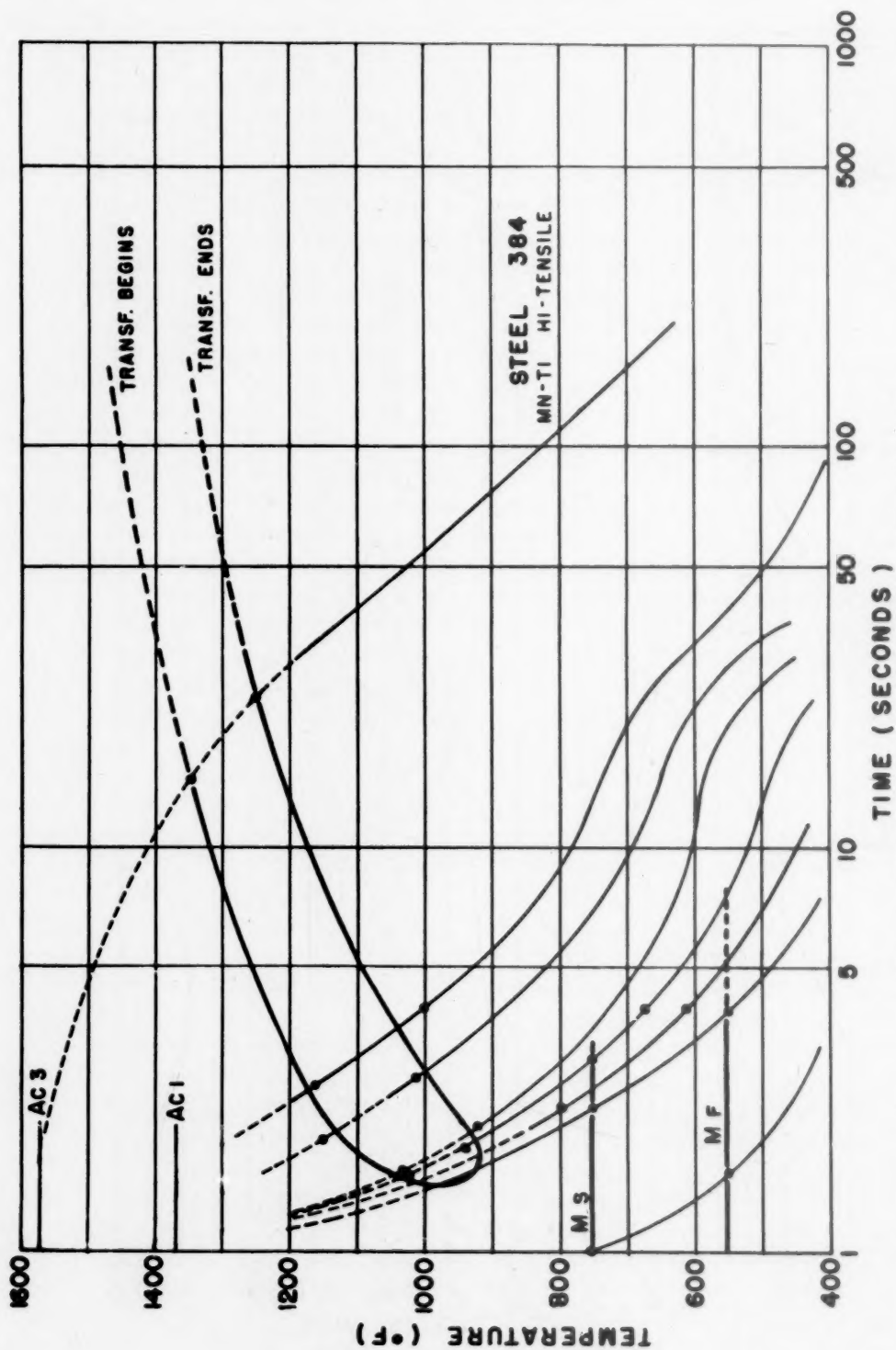


FIG. 12.—TRANSFORMATIONAL DIAGRAM FOR STEEL NO. 386.
Composition: 0.17 C., 1.21 Mn., 0.27 Si., 0.020 S., 0.021 P., 0.13 Ni., 0.25 Cu., 0.04 Mo., 0.05 Cr., 0.005 V., 0.008 Ti., 0.010 Al.

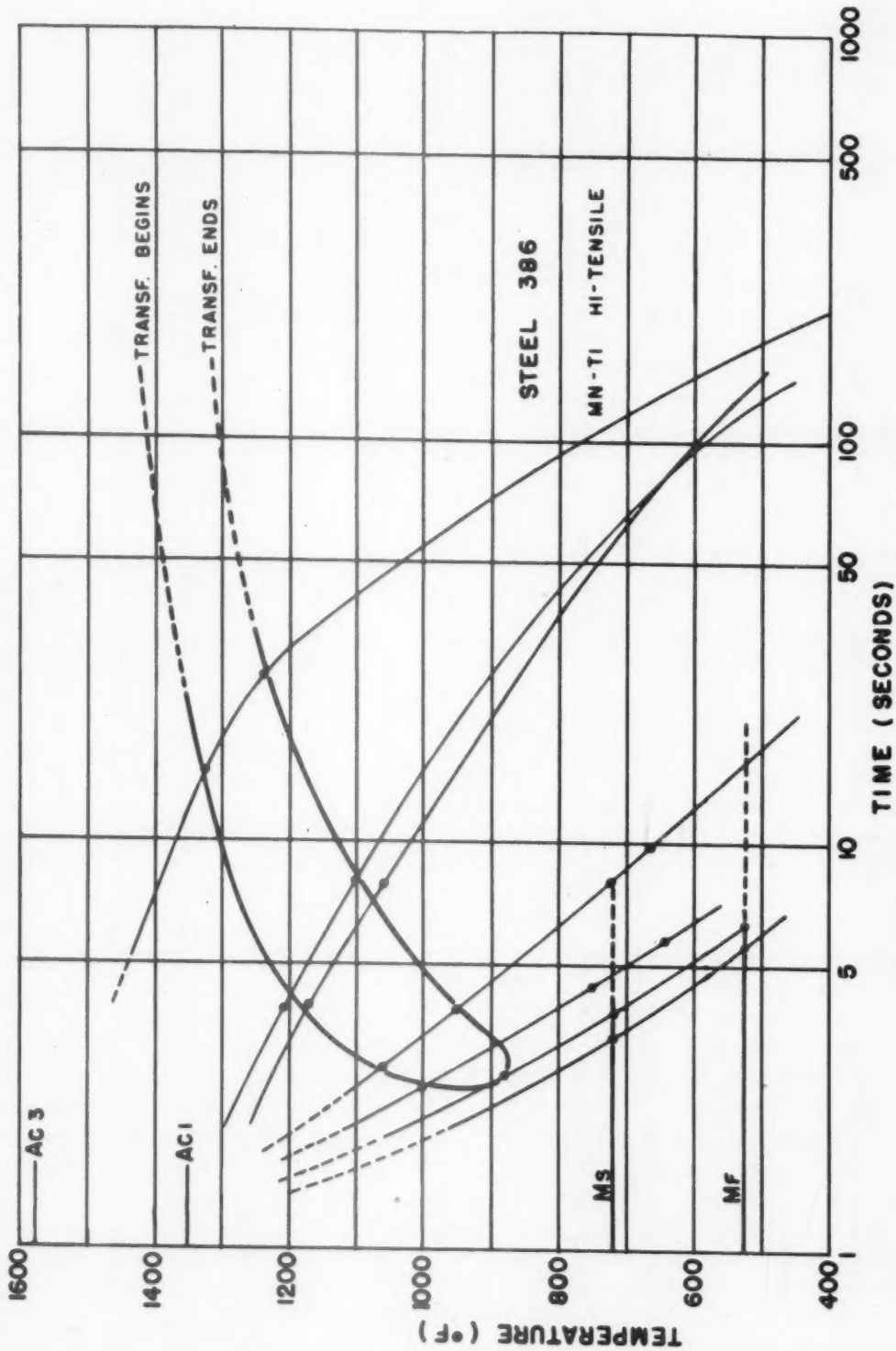


FIG. 13.—TRANSFORMATIONAL DIAGRAM FOR STEEL No. 384.
Composition: 0.17 C., 1.19 Mn., 0.24 Si., 0.032 S., 0.021 P., 0.10 Ni., 0.20 Cu., 0.03 Mo., 0.05 Cr., 0.002 V., 0.007 Ti., 0.020 Al.

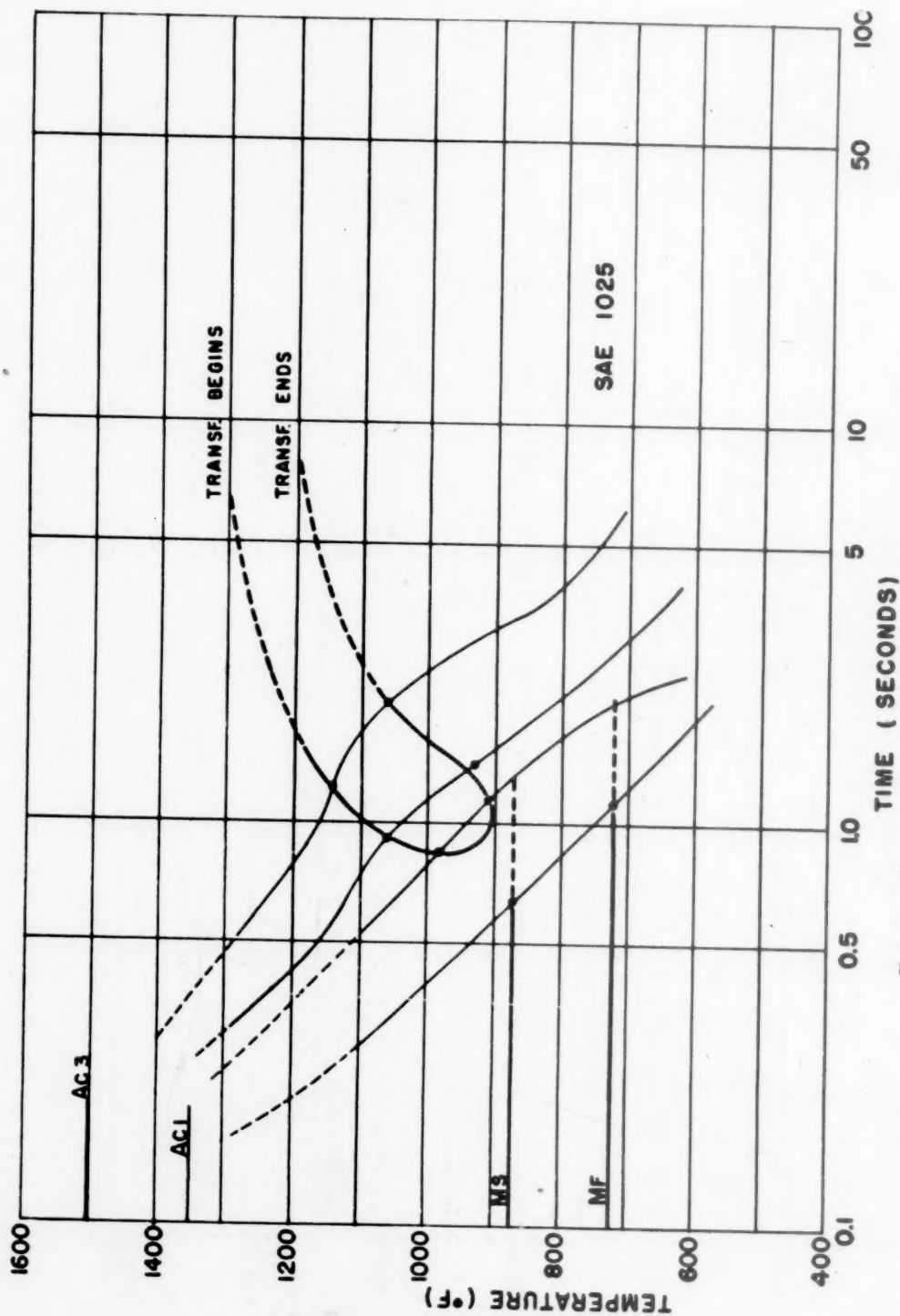


FIG. 14.—TRANSFORMATION DIAGRAM FOR S.A.E. STEEL 1025.
Composition: 0.25 C., 0.54 Mn., 0.14 Si., 0.035 S., 0.022 P.

will enable the metallurgist to obtain direct fundamental data regarding the transformational behavior, which up to this time has been available only through cumbersome

or less similar type of transformation for the whole range of thickness in the continuous air-cooled or normalized condition. The information obtained from a study

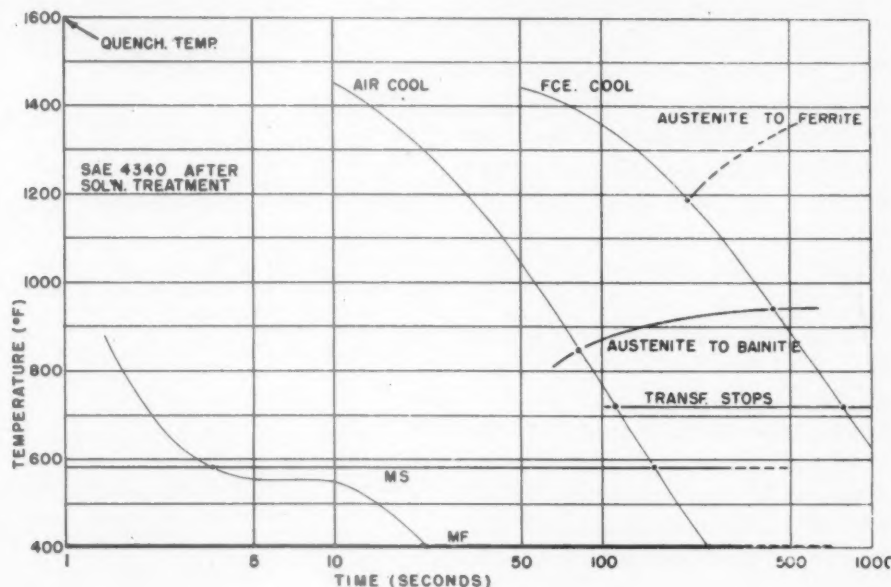


FIG. 15.

some indirect methods that can be handled only by skillful and experienced workers in the field.

The cooling curves show a diminishing cooling rate as the temperature is lowered. This may be objectionable for some fundamental studies, although it more nearly approaches cooling conditions in actual practice. No difficulty was encountered in obtaining the desired range in cooling velocity by means of the gas quench, although care had to be taken to prevent decarburization of the thin specimens from the oxygen present as an impurity in the quenching gas.

Of practical interest in connection with the transformations on continuous cooling are the cooling curves for normalized sheet steel of S.A.E. X4130 composition ranging in thickness from 0.020 to 0.250 in. The time to cool from 1600° to 400°F. in these tests ranged from 60 to 600 sec. The preliminary observation of the transformation of this steel (Fig. 9) would indicate a more

of a sample of NE 8630 (Fig. 10) indicates that the transformational characteristics are much more complicated than those observed for the S.A.E. 4130 type of steel. The completion of the austenite to bainite transformation is not clearly defined. Here again nearly isothermal transformations are encountered just preceding the martensitic type of reaction. The opportunity of observing the finish of the martensitic reaction as well as the start of this reaction will be useful in practical heat-treatment.

A study of a highly alloyed steel such as S.A.E. 4340 (Fig. 11) indicates a similarity between the transformational diagram and the isothermal diagram presented by Davenport.¹² In the present studies, however, the start and finish of the martensitic reaction can be determined. The constancy of the start and finish of the martensitic reaction is to be noted. After the diagram for S.A.E. 4340 steel was completed, it was noted from a microstructure of one of the dilatometer specimens that the carbon was

not entirely in solution. Therefore the steel was given a 30-min. solution treatment at 1650°F. The results are shown in Fig. 15. The specimens were quenched from 1600°F. as were all the steels in these experiments.

The transformational diagrams were determined for two samples of treated manganese-titanium high-tensile steels whose weldability was being studied. In these diagrams (Figs. 12 and 13) it is shown that steel 386 has a higher hardenability than steel 384. This is supported by the fact that the ductility of the heat-affected zone under bead welds was lower for steel 386 than for steel 384. The maximum Vickers hardness in the heat-affected zone was 322 for steel 386 compared with 277 for steel 384. The hardenability for steel 386 was slightly higher than for steel 384 as measured by the end-quench hardenability test. The chemical compositions of the two steels, however, were almost identical. Additional information regarding the transformational characteristics of steels of this type will be highly desirable in the evaluation of the effect of minor constituents on any such property as weldability.

The transformational diagram presented in Fig. 14 for an S.A.E. 1025 steel illustrates the range of measurements made possible by the use of the present equipment. The time ordinate has been expanded as the information given is that which occurs within two seconds after quenching.

SUMMARY

A high-speed dilatometer has been described which has sufficient range and accuracy so that it will be useful in many metallurgical problems that depend upon continuous cooling behavior. A limited number of observations are presented showing the wide range and flexibility of the method. It is hoped that such measurements will prove directly applicable to heat-treatment studies and will be useful in a fundamental interpretation of the behavior of steels as affected by such proc-

esses as welding. The information may be useful also in other metallurgical studies of quenching stresses and properties of structures that undergo nonuniform cooling.

REFERENCES

1. H. J. French and O. Z. Klopsch: Quenching Diagrams for Carbon Steels in Relation to some Quenching Media for Heat Treatment. *Trans. Amer. Soc. Steel Treat.* (1924) **6**, 251-294.
2. H. Esser, W. Eilender and Spenle: Das Härtungsschaubild der Eisen-Kohlenstoff-Legierungen. *Archiv Eisenhüttenwesen* (1933) **6**, 389-393.
3. H. Esser, W. Eilender and U. H. Majert: Der Einfluss Verschiedener Legierungselementen auf die Abschreckhärbarkeit von Stahl. *Archiv Eisenhüttenwesen* (1933) **7**, 367-370.
4. F. Wever and A. Rose: Ueber den Einfluss der Abkühlungsgeschwindigkeit auf die Umwandlungen der Stähle. *Mitt. Kaiser Wilhelm Inst. Eisenforschung* (1930) **20**, 93-114.
5. T. Digges: Effect of Carbon on the Hardenability of High Purity Iron-Carbon Alloys. *Trans. Amer. Soc. Metals* (1938) **26**, 408-424.
6. T. Digges: Transformation of Austenite on Quenching High Purity Iron-Carbon Alloys. *Trans. Amer. Soc. Metals* (1940) **28**, 575-600.
7. T. Digges: Influence of Austenitic Grain Size on the Critical Cooling Rate of High Purity Iron-Carbon Alloys. *Trans. Amer. Soc. Metals* (1941) **29**, 285-316.
8. A. B. Greninger: The Martensite Thermal Arrest in Iron Carbon Alloys and Plain Carbon Steels. *Trans. Amer. Soc. Metals* (1942) **30**, 1-26.
9. R. A. Grange and J. M. Kiefer: Transformation of Austenite on Continuous Cooling and Its Relation to Transformation at Constant Temperature. *Trans. Amer. Soc. Metals* (1941) **29**, 85-116.
10. C. Austin, R. Allen and W. VanNote: Application of Oscillograph to Determination of Cooling Rates of Quenched Steels. *Trans. Amer. Soc. Metals* (1942) **30**, 747-772.
11. R. Gunn: A Convenient Electrical Micrometer and Its Use in Mechanical Measurements. *Jnl. Applied Mechanics* (1940) **7**, 49-52.
12. E. S. Davenport and E. C. Bain: The Transformation of Austenite at Constant Subcritical Temperatures. *Trans. A.I.M.E.* (1930) **90**, 117-144.

DISCUSSION

(Howard Scott presiding)

HOWARD SCOTT.—Gentlemen, you have heard a very interesting paper on the high-speed dilatometer. I am sure a number of

questions have occurred to you, that Mr. Nelson will be glad to answer.

E. P. KLIER.*—In the case at hand transformation of the austenite is accompanied by an expansion while the cooling leads to a contraction of the specimen. How does the overlapping of these effects affect the determination of initial transformation?

E. C. NELSON.—I see what you mean. In that first family of curves, we showed a straight line going down, and the other curves growing, as it were, out of it. In some cases there was a slight deviation at the start, before there was a marked upswing. We took the first point at which we could see a deviation from what should be a straight line of length versus temperature on cooling.

E. P. KLIER.—Were the points determined by any other method, so that the amount of transformation products present at the point, indicated as initial transformation, could be evaluated? With reference to determinations made such as to invalue mixed structures—i.e., austenite plus ferrite and pearlite—the prior transformation must considerably affect the subsequent contraction of the specimen on cooling, so that determinations made from such curves should be checked by some other method.

E. C. NELSON.—We have been interested in the possibility of mixed structures that will arise from such a cause. There is metallographic work going on at present in regard to that. At present, though, we can only say that we take as our point the first noticeable deviation.

R. A. GRANGE.†—Measurement of volume change has long been one of the basic methods for determining the progress of austenite transformation, particularly as it occurs during continuous heating or cooling. In convenience and flexibility the high-speed dilatometer developed by Messrs. Christenson, Nelson and Jackson seems to surpass any such dilatometric apparatus previously employed for this purpose. Because dilatometric measurements fail

to reveal the character of the transformation product, interpretation of dilatometric data is not always easy; but with the aid of microscopic observations and a background of knowledge of the isothermal transformation behavior of low-alloy steels, the authors seem to have made a very satisfactory interpretation of their dilatometric data.

The "transformational diagrams" presented are of great practical interest, but they do have the limitation that they quantitatively apply only to cooling that follows, throughout the transformation temperature range, the pattern of cooling obtained by gas-quenching small cylinders. The time plotted on the diagram is obviously the *total* cooling time commencing at 1600°F.; therefore the location of the curves on the time axis is affected, apart from grain size, composition and homogeneity of austenite, by the heating temperature. Incidentally, some of the cooling curves obtained are rather surprising in that they indicate an appreciable time interval during which approximately constant temperature was maintained. For example, in Fig. 9, cooling curves 3, 4 and 5 are nearly horizontal between about 8 and 20 sec.; if this horizontal portion of the cooling curve was due to recalescence accompanying transformation of austenite to bainite, it is surprising that at least some recalescence was not registered in curves 6 and 7 of Fig. 9, both of which represent faster cooling and include the temperature range in which austenite transformed very rapidly to martensite. Perhaps the authors might comment regarding the reason for the shape of cooling curves such as 3, 4 and 5 in Fig. 9.

It is to be regretted that the authors fail to discuss more specifically the reproducibility of their dilatometric measurements. However, some indication of the reproducibility may be gained by comparing Fig. 11 with Fig. 15. Both of these diagrams represent the same S.A.E. 4340 steel; in connection with the former the authors say that "the carbon was not entirely in solution," while in the latter it presumably was in solution. In these two diagrams, there is no great difference in the location of the curves representing the beginning of ferrite on continuous cooling, but a surprisingly large difference exists in the bainite region. This difference is not entirely consistent with what must have been only a small differ-

* School of Mineral Industries, The Pennsylvania State College, State College, Pennsylvania.

† U. S. Steel Corporation Research Laboratory, Kearny, N. J.

ence in austenite composition in the two cases, especially since a corresponding difference in ferrite transformation was not observed. Complete solution of carbon and alloying elements might be expected to lower the M_s temperature; thus, it would seem logical to assume that M_s in Fig. 15 should, if anything, be lower than in Fig. 11, yet, according to the diagrams, M_s turns out to be about 30°F. higher when the carbides are all in solution. These seeming discrepancies raise some doubt as to the reproducibility of these dilatometric measurements.

The high-speed dilatometer permits such a convenient and rapid determination of the temperature range in which martensite forms ($M_s - M_f$) that it is interesting to compare the authors' results with the M_s temperature obtained by the more tedious and indirect metallographic method described by Greninger.⁸ We have measured M_s by the metallographic method for their identical S.A.E. 4130 and NE 8630 steels and for an S.A.E. 4340 steel almost identical in composition to that studied by the authors. For several years we have used an empirical formula to calculate the approximate M_s from the chemical composition of any given steel; as more experimental data became available, the formula has been revised and, in its present form, is as follows:

$$M_s (^\circ\text{F.}) = 1000 - 645 \times \%C - 70 \times \%Mn - 0 \times \%Si - 30 \times \%Ni - 60 \times \%Cr - 30 \times \%Mo$$

Our measured M_s values as well as those calculated using this empirical formula are listed in the following table, for comparison with the authors' results.

Steel	Deg. F.		
	Dilatometric (Figs. 9-15)	Metallo- graphic Method	Calcu- lated
S.A.E. 4130.....	600	710	710
NE 8630.....	670	680	690
S.A.E. 4340 (Fig. 11)	540		
S.A.E. 4340 (Fig. 15)	580	540	570
Steel 386 (Mn-Ti)...	720		800
Steel 384 (Mn-Ti)...	750		800
S.A.E. 1025.....	870		800

For the NE 8630, the M_s determined with the dilatometer agrees with that determined ex-

perimentally by the metallographic method and with that calculated from chemical composition using the empirical formula. In the other steels there is not always satisfactory agreement; it should not be concluded, however, that the dilatometric M_s is necessarily any less accurate than M_s determined metallographically.

Obviously, the high-speed dilatometer developed by the authors offers great promise as a "tool" for studying transformation; the seeming discrepancies that may exist in some of the results obtained in this early stage of its development will doubtless be cleared up as more experience is gained in its use.

A. L. CHRISTENSON (author's reply).—I wish to thank Mr. Grange for his cooperation in preparing such a comprehensive discussion. The points that he has raised are ones that have concerned us also; and, in fact, are still concerning us. As to the evidence of recalescence at some cooling rates and its absence at others, I believe this is due to the position of the thermocouple (on the outer surface of the specimen) and on the rate of heat removal from the surface of the specimen as compared with the heat liberated within the specimen during the transformation. It is entirely possible, I think, to obtain recalescence at some intermediate cooling rate and not obtain it at either very rapid or very slow rates.

The reproducibility of the indicating instrument appeared very good when synthetic conditions simulating an actual experimental run were imposed on it (by means of oscillators). It is true, however, as has been mentioned several times in the discussion, that many variables such as grain size, homogeneity, and solution temperature will have a definite effect on the experimental results, and these must be carefully controlled if uniform results are to be obtained.

The apparent discrepancy existing in either Fig. 11 or Fig. 15 on the value of the M_s temperature for S.A.E. 4340 was recognized by the authors, but as yet cannot be explained. The equipment is being redesigned and rechecked in order that a more systematic investigation can be made in the hope of explaining many of the points now under question.

HOWARD SCOTT.—I have a question of my own. I am in the unfortunate position of having

to deal with coarse grain materials more often than fine grain. What would be the effect of a really coarse-grained steel in here, steels being normally fairly fine grained? Roughening of the surface then may produce an abnormally high expansion.

E. C. NELSON.—Our principal work has been routine checking of inherently fine-grained tensile steels. We have run some coarse-grained steels and have not noticed anything like that.

J. V. RUSSELL.*—A point was raised of recalescence. Does that mean thermal arrest as well? In other words, was the thermal arrest absent as well as recalescence?

E. C. NELSON.—You mean on hardening?

J. V. RUSSELL.—Changing from slow to faster cooling rates.

E. C. NELSON.—That was due to heat coming out under cooling conditions under which it would be apparent. The heat has to come out some place, and with other cooling rates it does not show on our curve.

J. V. RUSSELL.—I believe Dr. Greninger's work is quite similar to this, in that he also used gas quenching. At rates as high as 4000°C. per second he had a thermal arrest. I would like to know whether you have any comments on that.

E. C. NELSON.—Our technique and Dr. Greninger's differed in that we were not precisely looking for thermal arrest. If we were very careful to obtain a simple time versus temperature plot we might be able to find a thermal arrest. I believe the location of Dr. Greninger's thermocouple had quite an effect. Our thermocouple is out on the surface. We consider our steel being cooled uniformly from all sides, and the consequence is that the conditions are about as poor as possible for picking up recalescence inside the steel.

I should like also to thank Dr. Grange for his cooperation in trying to find some tangible, well-recognized methods to check our data.

We are in a unique spot, in that it is difficult to prove whether or not our data are valid.

C. E. SIMS.*—I should like to congratulate the authors on their extremely ingenious and effective means of studying the transformation in steel at these high speeds. I have long felt the need of something like this, and it has been my belief for many years that the transformations as determined by the ordinary dilatometer at some slow speed have very little meaning. They are practically valueless, except for determining heat-treating temperatures. For too long we have considered transformations from the standpoint of equilibrium conditions, and we seldom get true equilibrium.

The transformation temperatures are by no means fixed points, and they do vary, depending on the previous history of the steel and the time at which it has been held at temperature, as well as the rate at which it is cooled or heated. By the use of dilatometric readings at different heating and cooling rates, we have been able to explain some phenomena in steel that previously were obscure.

There were two steels of almost identical composition, one of which gave very poor performance by cracking in welding and the other gave very good performance and did not crack at all. These two steels, when given a thermal treatment to obtain the critical temperatures, by the usual method, gave results that were as identical as their composition, but when we speeded up the whole cycle, we found one was depressed more than the other. We have been able to produce that difference in the same steel by different pretreatments.

There is a considerable amount of information to be gained in such studies, and this seems to be an excellent apparatus for the work.

E. C. NELSON.—I want to thank Mr. Sims for pointing out that in considering points as fixed we do so without any particular right. The martensite point seems to be an experimentally elusive value, and we probably would not be too sure whether what we are talking about is a martensite point until thermal, magnetic, microscopic, and dilatometric measurements can pin it down as a certain value.

* Republic Steel Corporation, Chicago, Illinois.

* Battelle Memorial Institute, Columbus, Ohio.

Perhaps Mr. Jackson might like to comment on our use of the instrument for welding research, for which it was developed.

C. E. JACKSON.—The equipment that we are presenting was developed in the Welding Section, and we were mainly interested in being able to follow some of the things that happen adjacent to welds in steels. In other words, the equipment that was available up to

the time of this instrument would in no way give us information that we could use in actually telling what is happening in the heat-affected zone.

We have used the new equipment on a number of steels, including the welding steels, the fast-transforming steels, and it has given us information that we have wanted. We look to a bright future for this type of equipment in the welding field.

Dilatometric Studies of the Graphitization of Cast Iron

By N. A. ZIEGLER,* MEMBER A.I.M.E.

(Cleveland Meeting, October 1944)

GRAPHITIZATION phenomena occurring in solid cast iron have principally been studied from the angle of the reactions taking place during annealing of white castings in the manufacturing of malleable iron. The selected bibliography at the end of this paper presents the high spots of the published information in this field. Graphitization of gray iron upon reheating has received much less attention, primarily because only on rare occasions is this material subjected to any kind of industrial heat-treating. Moreover, articles made from gray iron are seldom used commercially at temperatures when any graphitization can take place. When used in such conditions, it is assumed that the articles can be replaced at frequent intervals, which can be afforded because of the low cost of gray iron.

However, there is at least one commercial process in which articles made from gray iron, during their manufacturing processing, are subjected to rather high temperatures; that is, manufacturing of cast-iron enamelware, which is glazed at about 1600° to 1700°F. (870° to 930°C.)

From practical experience, it has been found that one of the convenient and economical compositions of gray iron suitable for enameling is, in round figures, as follows: Si, 2.50 per cent; Mn, 0.35; S, 0.07; P, 0.80; T.C., 3.35; C.C., 0.70.

Since this iron usually is cast into thin-walled sections, the percentage of com-

bined carbon in it is relatively high. Upon heating in the enameling furnaces, this combined carbon graphitizes, which causes permanent dimensional changes of the articles. Obviously, from practical considerations, it is desirable to maintain these dimensional changes as constant as possible.

In the course of experimentation with this iron, two series of experimental heats were prepared in which the manganese to sulphur ratio of the standard cupola metal was offset by ladle additions of: (1) progressively larger amounts of sulphur, and (2) progressively larger amounts of manganese. Each one of these ladle charges was cast into experimental plates 8 by 4 in. and about $\frac{5}{16}$ in. thick. All told, 13 ladle charges were thus treated. All of them are listed in Table 1, together with their chemical analyses. It may be noted that the manganese to sulphur ratio in these samples ranges between 1.2 and 30.2.

Every one of these compositions was subjected to thermal analysis, using an automatic, self-recording differential dilatometer. The specimens used in this instrument are 50 mm. long and 4 mm. in diameter. During the dilatometer cycle they are kept under a vacuum of about 3 microns. Each one of them was subjected to a thermal cycle by heating it to 1830°F. (1000°C.) in 2 hr. and cooling to room temperature in 5 hr. Figs. 1, 2 and 3 present three automatically recorded dilatometer curves for irons: Serial No. 1 (normal composition), Serial No. 6 (high sulphur), and Serial No. 13 (high manganese). All three of these figures are

Manuscript received at the office of the Institute Nov. 24, 1944. Listed as T. P. 1874.

* Research Metallurgist, Crane Co., Chicago, Illinois.

tracings of the original photographically recorded dilatometer curves.

It may be observed that the expansion branch of each of these curves forms nearly

two extremes. The increasing percentages of manganese (Serial Nos. 7 to 13) do not affect the temperature of the beginning of the rapid growth, so that in Fig. 3

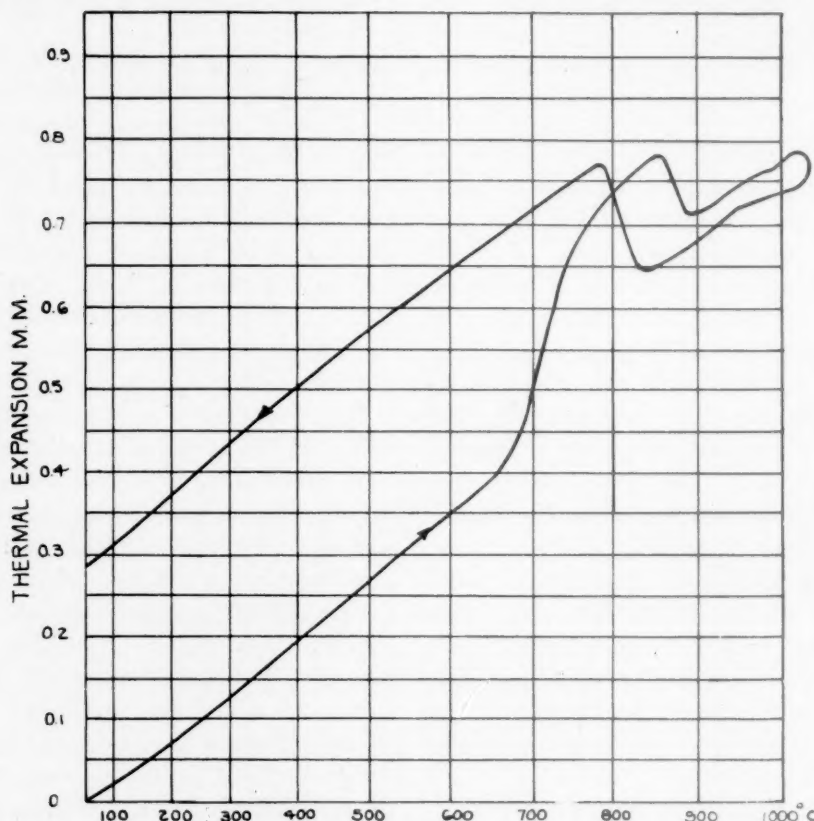


FIG. 1.—AUTOMATICALLY RECORDED DILATOMETER CURVE FOR IRON, NORMAL COMPOSITION. Si, 2.51 per cent; Mn, 0.33; S, 0.063–0.060; P, 0.80; graphitic C, 2.51; total C, 3.25. Mn/S ratio, 5.4.

a straight line up to about 1200° to 1300°F. (650° to 700°C.), and that at this temperature the iron begins to grow very rapidly.* The temperature at which this rapid growth commences is raised by the sulphur content: in Fig. 1 (0.06 per cent S) it starts at 1200°F. (650°C.), while in Fig. 2 (0.25 per cent S) at 1380°F. (750°C.). With the intermediate sulphur contents (Serial Nos. 2 to 5, curves not presented) the beginning of the growth occurs at progressively higher temperatures between the

(1.45 per cent Mn) it occurs at 1250°F. (650°C.), which is the same as in Fig. 1 (0.33 per cent Mn). At about 1560° to 1650°F. (850° to 900°C.) the transformation on heating comes to completion in all of these compositions.

Transformation on cooling in the high-sulphur compositions (Figs. 1 and 2) occur at 1530° to 1420°F. (830° to 770°C.) and are not affected by progressively higher sulphur contents. Increasing manganese, on the other hand, tends to suppress transformation on cooling to somewhat lower temperatures, so that in Fig. 3 (1.45 per cent Mn) they occur at 1420° to 1290°F. (770° to 700°C.). After the trans-

* In some of the original photographically recorded curves the portions of the heating branches between 1200°F. (650°C.) and 1560°F. (850°C.) were hardly visible, thus indicating a very rapid movement of the light beam.

formations on cooling are completed, the rest of the cooling branch is practically a straight line. Upon cooling to room temperature, the curve does not come back

due to graphitization alone and not to oxidation. It is difficult to interpret these dilatometer curves in terms of conventional, constitutional diagrams, because of

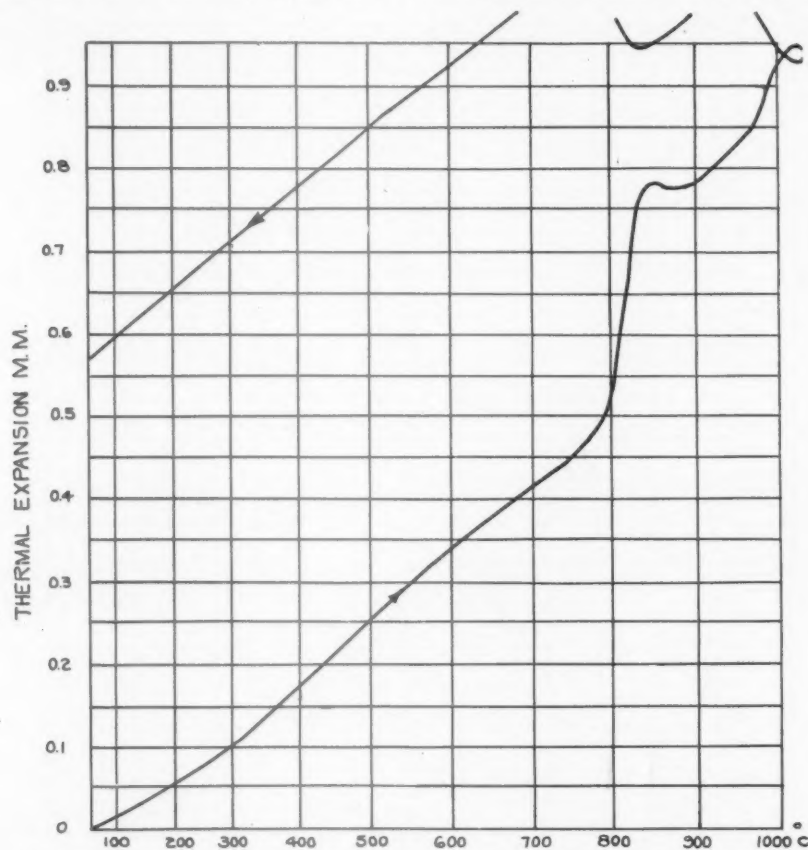


FIG. 2.—AUTOMATICALLY RECORDED DILATOMETER CURVE FOR IRON, HIGH SULPHUR. Si, 2.50 per cent; Mn, 0.30; S, 0.247–0.250; P, 0.80; graphitic C, 2.03–2.08; total C, 3.32. Mn/S ratio 1.2.

to the original starting point, but, because of the permanent growth during the dilatometer cycle, it assumes a position on the ordinate, higher than the original starting point. By measuring along the ordinate, the distance between the initial and final points, the total permanent linear growth of the metal can be determined. It checks quite well with the micrometer measurements of the length of the sample before and after the dilatometer runs. All of these dilatometer runs were performed while the dilatometer samples were under vacuum of about 3 microns, which means that the total growth of the metal was

very complex basic compositions of the alloys and because of the additional factor of graphitization and permanent growth.

The history of each sample, including its chemical analysis, manganese to sulphur ratio, Brinell hardness (before the dilatometer run) and the dilatometer data, is summarized in Table 1. Using these data, total growth during the dilatometer runs, percentage of the original combined carbon and Brinell hardness (before the dilatometer runs) were plotted in Fig. 4: (1) against percentage sulphur (manganese content being constant at 0.30 to 0.36 per cent) for high-sulphur irons, and (2)

against percentage manganese (sulphur content being constant at 0.05 to 0.09 per cent) for high-manganese irons.

Increasing sulphur (the right-hand side

sulphur on stabilizing of the original combined carbon, and consequently on the increase of the original hardness, is stronger than that of manganese. On the other

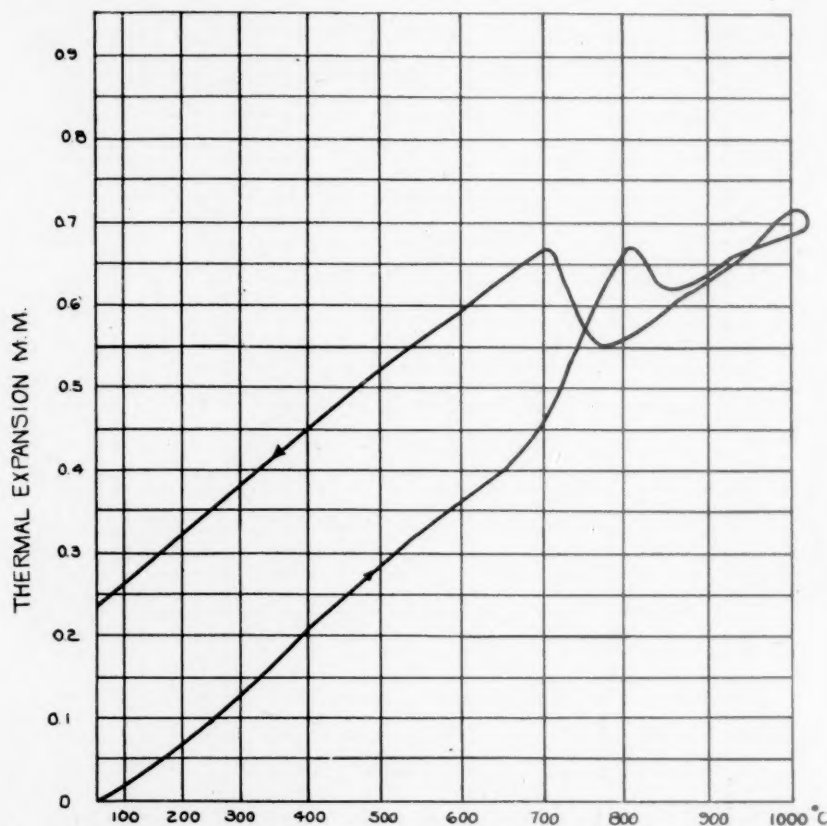


FIG. 3.—AUTOMATICALLY RECORDED DILATOMETER CURVE FOR IRON, HIGH MANGANESE. Si, 2.44 per cent; Mn, 1.42–1.45; S, 0.050–0.045; P, 0.82; graphitic C, 2.72; total C, 3.42. Mn/S ratio, 30.2.

of the diagram) causes the amount of the original combined carbon, permanent growth and the original hardness to increase. This increase is more rapid with the early sulphur additions; i.e., up to about 0.10 to 0.12 per cent. The increasing manganese (the left-hand side of the diagram) also causes the original hardness and the amount of combined carbon to increase. The latter, however, is not as pronounced as that caused by the increasing sulphur.

The permanent growth, on the other hand, decreases with increasing manganese. It thus appears that the effect of

hand, the original carbides in the high-sulphur irons are less stable than those in the high-manganese irons. This is the reason why in the high-sulphur irons the amount of the original combined carbon as well as the permanent growth during the dilatometer cycle increase with progressive increase in the sulphur content. The increasing percentages of manganese also cause the amount of the original combined carbon to increase, but the subsequent permanent growth not only does not increase but even has a tendency to decrease, because of the stability of carbides due to manganese and their reluc-

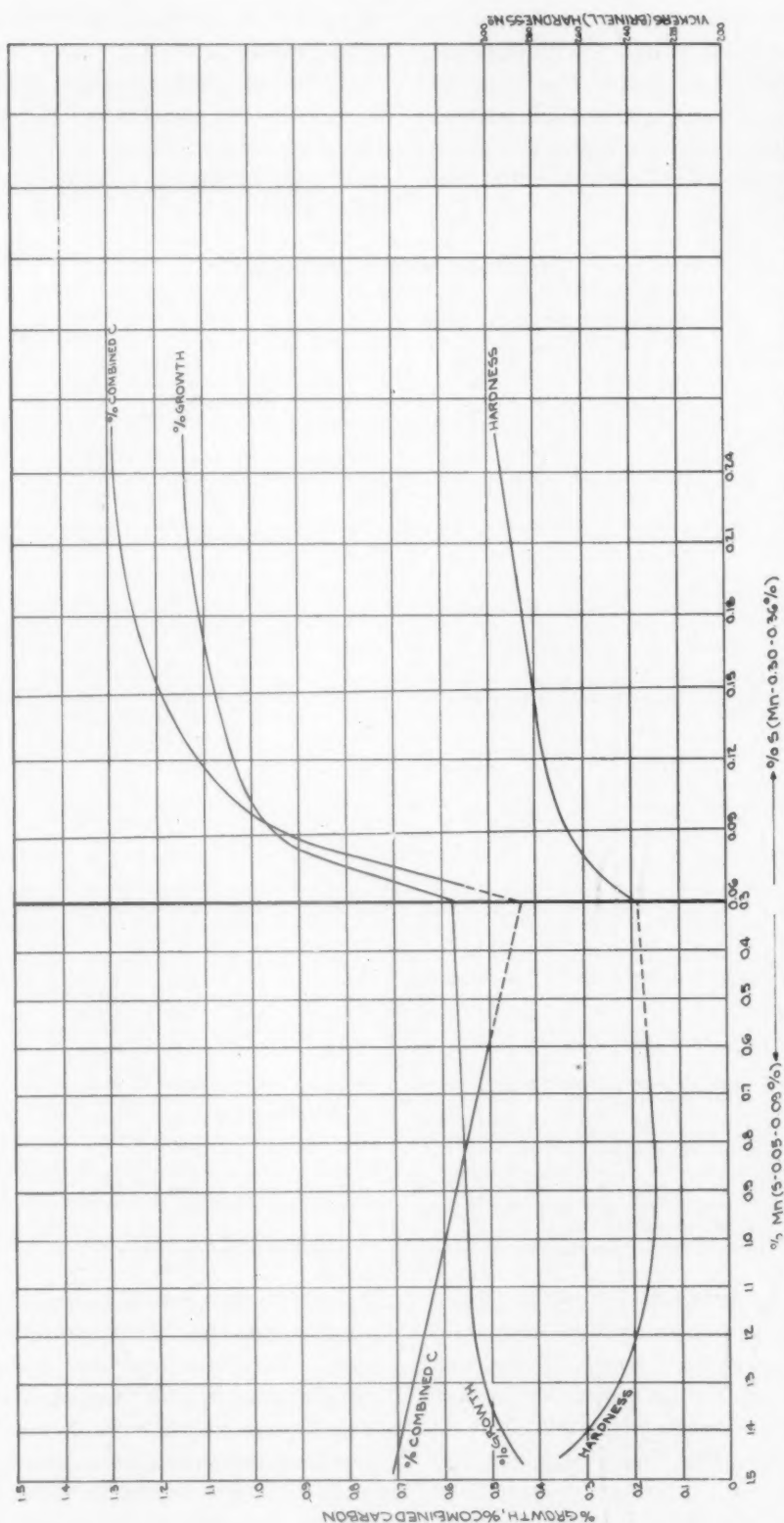


FIG. 4.—INFLUENCE OF SULPHUR AND MANGANESE CONTENT ON AMOUNT OF COMBINED CARBON, GROWTH AND HARDNESS OF GRAY IRON.

tance to graphitize during the dilatometer cycle. It appears that the increase in sulphur content promotes the formation of cementite (Fe_3C), upon solidification of the metal in the molds, whereas manganese forms a carbide of its own, which is more stable than Fe_3C .

of combined carbon but also of the nature of the carbides.

All the original cast irons (i.e., as cast) as well as the dilatometer samples, after the runs, were subjected to microexamination. Fig. 6 represents the structure of the original Serial No. 12; i.e., one containing

TABLE 1.—History of Samples

Serial No.	Chemical Analysis, Per Cent							Mn/S Ratio	Hardness V.P.N. Origin	Dilatometer Data, Growth		Additions
	Si	Mn	S	P	C Total	C Graphitic	C Combined, by Difference			Millimeters in 0.50-mm. Sample	Per Cent	
1	2.51	0.33	0.060	0.80	3.25	2.51	0.74	5.4	259	0.29	0.58	Sulphur added to ladle
			0.063									
2	2.48	0.34	0.065	0.76	3.27	2.72	0.55	5.0	249	0.41	0.81	
			0.070									
3	2.55	0.31	0.084	0.83	3.27	2.54	0.73	3.7	249	0.33	0.66	
4	2.50	0.32	0.100	0.74	3.37	2.36	1.01	3.2	272	0.49	0.98	
5	2.62	0.32	0.158	0.82	3.26	2.01	1.24	2.0	283	0.54	1.08	Sulphur added to ladle
						2.03						
6	2.50	0.30	0.250	0.80	3.32	2.08	1.26	1.2	295	0.57	1.14	
			0.247			2.03						
7	2.67	0.36	0.090	0.80	3.32	2.59	0.73	4.0	265	0.48	0.94	Manganese added to ladle
	2.76											
8	2.71	0.62	0.085	0.85	3.27	2.83	0.44	7.3	233	0.28	0.56	
9	2.59	0.68	0.080	0.79	3.35	2.87	0.46	8.5	238	0.28	0.56	
10	2.57	0.83	0.070	0.83	3.32	2.69	0.63	11.9	230	0.26	0.52	
11	2.59	0.96	0.070	0.80	3.33	2.74	0.59	13.7	230	0.29	0.58	
12	2.57	1.30	0.055	0.80	3.39	2.72	0.67	24.8	248	0.26	0.52	Manganese added to ladle
		1.30	0.050									
13	2.44	1.45	0.045	0.82	3.42	2.72	0.70	30.2	266	0.23	0.46	
		1.42	0.050									

In Fig. 5, percentage of total growth is plotted against the amount of combined carbon in the original metal. There is a general tendency for the growth to increase with increasing combined carbon. Nevertheless, considerable scattering of the points indicates that total growth is a function not only of the absolute amount

1.3 per cent manganese. It is composed of graphitic rosettes and pearlitic background. Free carbides are present in limited amounts. This structure is typical of this kind of iron and of all compositions containing increasing amounts of manganese. In other words, increase in manganese content has only a slight effect on

the structural characteristics of the metal. On the other hand, with increasing sulphur content, free carbides are beginning to appear in abundance. Fig. 7 is the structure

indicating a greater completeness of graphitization. This structure is typical of the iron of this type subjected to enameling, as well as of all dilatometer

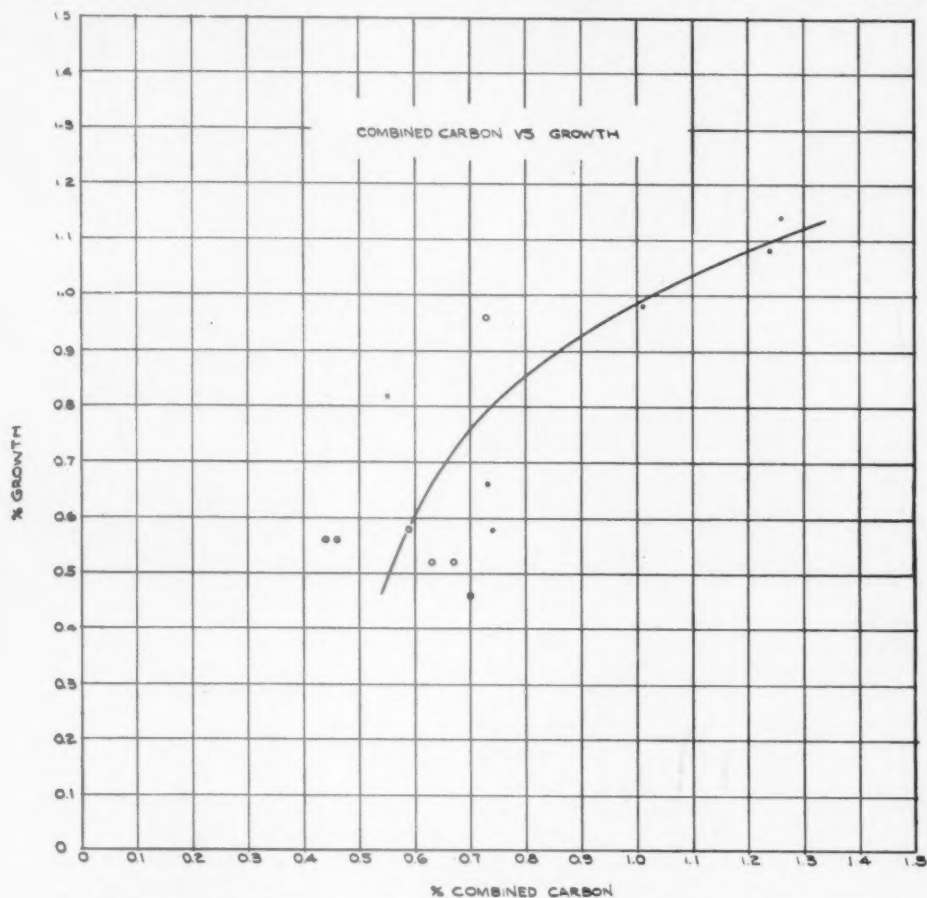


FIG. 5.—PERCENTAGE OF TOTAL GROWTH VS. AMOUNT OF COMBINED CARBON IN ORIGINAL METAL.

of the iron, Serial No. 6, containing 0.25 per cent sulphur, in which considerable amounts of carbide can be observed in the pearlite background.

Fig. 8 is the structure of the iron Serial No. 12 (containing 1.30 per cent manganese) after the dilatometer run. Some pearlite can still be seen in the ferritic background, which is an indication of incompleteness of graphitization. The amount of this residual pearlite increases with increasing manganese content. Fig. 9 is the structure of the iron Serial No. 6; i.e., one containing 0.25 per cent sulphur. No residual pearlite can be observed,

specimens of irons to which sulphur was added.

These observations are in line with the information obtained by the hardness measurements, chemical analysis and dilatometer studies. It may be noted that structures of all these irons show rather appreciable amounts of steadite (phosphorus eutectic), which apparently is not affected by the dilatometric cycles.

SUMMARY

1. Growth of gray iron is due primarily to graphitization of combined carbon.

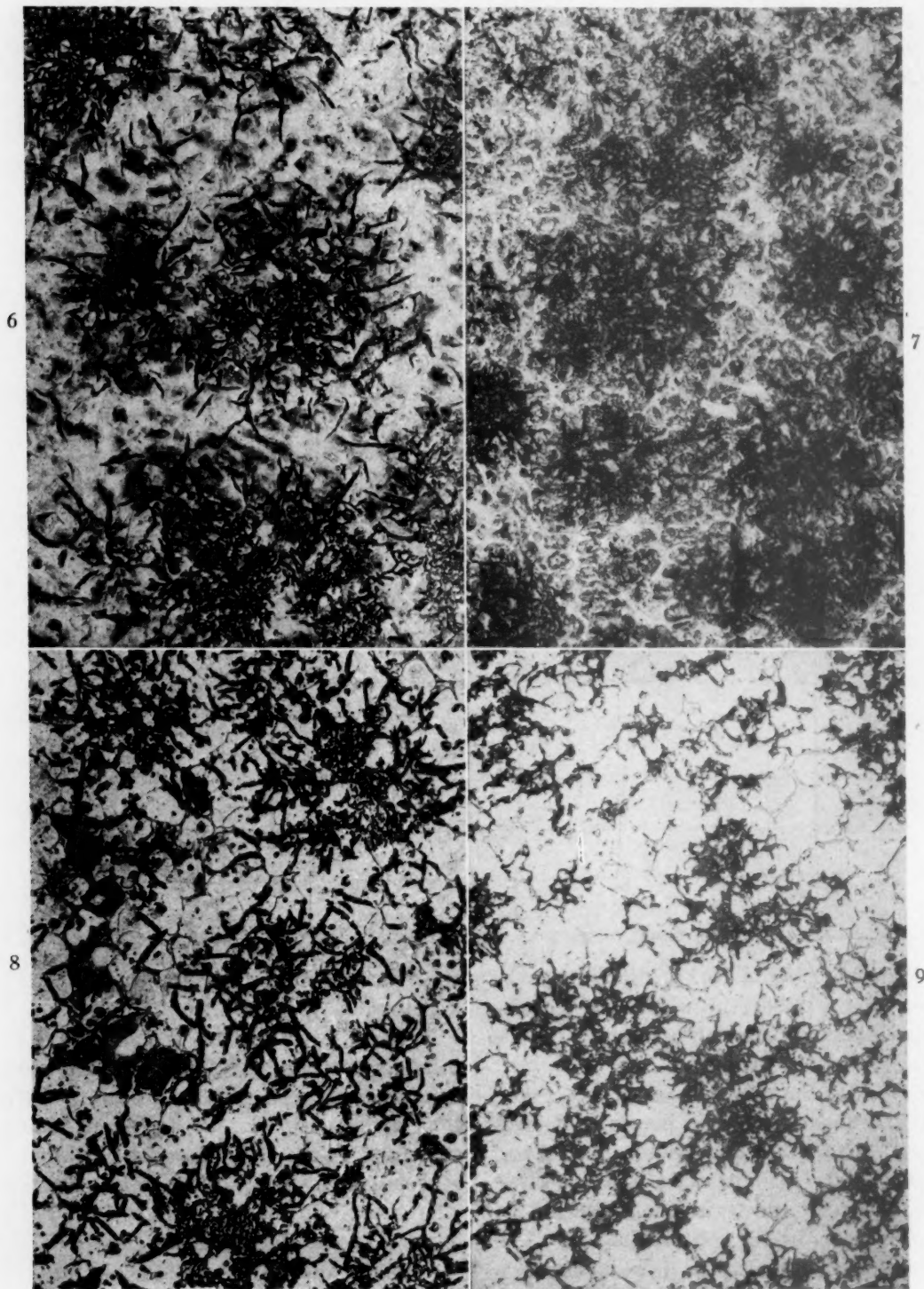


FIG. 6.—SERIAL NO. 12. AS CAST.

Mn, 1.30 per cent; S, 0.053; T.C., 3.39; C.C., 0.67.

FIG. 7.—SERIAL NO. 6. AS CAST.

Mn, 0.30; S, 0.249; T.C., 3.32; C.C., 1.26.

FIG. 8.—SERIAL NO. 12. AFTER THE DILATOMETER RUN.

Mn, 1.30; S, 0.053; T.C., 3.39.

FIG. 9.—SERIAL NO. 6. AFTER THE DILATOMETER RUN.

Mn, 0.30; S, 0.249; T.C., 3.32.

All $\times 150$. Etched in nital.

2. Major part of the growth occurs in the temperature range of 1200° to 1550°F. (650° to 850°C.).

3. The rate of growth is very rapid.

4. The total permanent growth is affected by both manganese and sulphur.

5. The amount of the original combined carbon and the hardness of the iron are likewise affected by sulphur and manganese contents.

6. The effect of sulphur on formation of combined carbon upon solidification of the metal is stronger than that of manganese.

7. Carbides due to manganese upon subsequent reheating of the metal are more stable than those due to sulphur, and graphitize with greater difficulty.

8. Although the total growth of iron is a function of the amount of combined carbon, it is not a direct function; the nature of carbides—i.e., whether due to sulphur or to manganese—determines their stability, and consequently the growth of metal.

SELECTED BIBLIOGRAPHY

1. A. Portevin and P. Chevenard: Influence of Fineness of Structure on Annealing of Gray Cast Iron. *Compt. rend. Acad. des. Sci.* (1929) **189**, 759.
2. R. S. MacPherran and R. H. Krueger: Effect on Cast Iron of Prolonged Heating at 800°–1100°F. *Trans. Amer. Foundrymen's Assn.* (Feb. 1931) **2**, 826.
3. E. Scheil et al.: Formation of Graphite Nuclei in Cast Iron. *Archiv Eisenhüttenwesen* (Dec. 1933) **7**, 333.
4. E. K. Klein: The Rate of Cementite Decomposition in Cast Iron. *Stahl und Eisen* (1934) **54**, 827.
5. O. v. Keil et al.: The Influence of Non-metallic Nuclei on Graphite Formation in Cast Iron. *Archiv Eisenhüttenwesen* (Apr. 1934) **7**, 579.
6. W. A. Pennington and W. K. Jennings: The Determination of the Rates of Graphitization at 925°C. in W-Mn White Cast Iron. *Trans. Amer. Soc. Metals* (Aug. 1934) **22**, 751.
7. H. Nipper: Graphite Formation in Gray Iron. *Giesserei* (1935) **22**, 280.
8. H. A. Schwartz and W. Ruff: Origin and Growth of Graphite Nuclei in Solid and Liquid Iron Solutions. *Trans. A.I.M.E.* (1936) **120**, 217.
9. H. A. Schwartz, H. H. Johnson and C. H. Junge: Some Transient Phase Changes during the Graphitization Reaction. *Trans. Amer. Soc. Metals* (Sept. 1936) **24**, 551.
10. R. Schneidewind and A. E. White: Properties of Fully Annealed and Heat Treated Malleable Irons. *Trans. Amer. Foundrymen's Assn.* (May–June 1937) **8**, 1.
11. W. B. Sallitt: Copper in Cast Iron and Malleable Iron. *Fdry. Tr. Jnl.* (Nov. 4, 1937) **57**, 354.
12. J. W. Bolton: Graphitization and Inclusions in Gray Iron. *Trans. Amer. Foundrymen's Assn.* (Dec. 1937) **8**, 467.
13. H. A. Schwartz: The Conversion of Solid Cementite into Iron and Graphite. *Jnl. Iron and Steel Inst.* (1938) **138**, 205.
14. P. G. Bastien and L. Guillet: The Influence of Some Special Additions of Certain Properties of Cast Iron. *Jnl. Iron and Steel Inst., Carnegie Schol. Mem.* (1938) **27**, 77.
15. R. M. Parke, V. A. Crosby and A. J. Herzig: Notes on the Graphitization of Gray Cast Iron. *Metals and Alloys*, (Jan. 1938) **9**, 9.
16. H. A. Schwartz and M. K. Barnett: The Initial Stages of Graphitization. *Trans. Amer. Soc. Metals* (June 1938) **26**, 358.
17. E. Piwowarsky: The Graphitization of Cast Iron. *Giesserei* (Oct. 24, 1938) **25**, 523.
18. A. L. Boegehold: Some Unusual Aspects of Malleable Iron Melting. *Trans. Amer. Soc. Metals* (Dec. 1938) **26**, 1084.
19. A. Boyles: The Formation of Graphite in Gray Iron. *Trans. Amer. Foundrymen's Assn.* (Dec. 1938) **46**, 297.
20. R. G. McElwee: Deoxidation and Graphitization of Cast Iron. *Trans. Amer. Foundrymen's Assn.* (Dec. 1938) **46**, 341.
21. A. L. Boegehold: Factors Influencing Annealing Malleable Irons. *Trans. Amer. Foundrymen's Assn.* (Dec. 1938) **46**, 449.
22. H. A. Schwartz and M. K. Barnett: Graphitization Rate and Nodule Number. *Trans. Amer. Soc. Metals* (June 1939) **27**, 570.
23. H. A. Schwartz, H. J. Schindler and J. F. Elliott: Nodule Size and Tensile Properties of Malleable Cast Irons. *Amer. Soc. Test. Mat. Preprint* 35 (1939) **1**.
24. H. A. Schwartz, V. Fiordalis, J. L. Fisher, J. F. Shumar and M. J. Trinter: The Accelerating Effect of Certain Metallic Elements on Graphitization. *Trans. Amer. Soc. Metals* (March 1940) **28**, 143.
25. H. G. Hall: Malleable Cast Iron. *Fdry. Tr. Jnl.* (March 31, 1940) **62**, 223.
26. R. Schneidewind and C. D. d'Amico: The Influence of Undercooling on the Graphite Pattern of Gray Cast Iron. *Trans. Amer. Foundrymen's Assn.* (June 1940) **47**, 831.
27. R. J. Cowan: Heat Treatment of Malleable Iron. *Fdry. Tr. Jnl.* (Sept. 5, 1940) **153**.
28. H. A. Schwartz, G. M. Guiler and M. K. Barnett: The Significance of Hydrogen in the Metallurgy of Malleable Cast Iron. *Trans. Amer. Soc. Metals* (Dec. 1940) **28**, 811.
29. C. D. d'Amico and R. Schneidewind: The Solidification and Graphitization of Gray Iron. *Trans. Amer. Foundrymen's Assn.* (June 1941) **48**, 775.
30. N. A. Ziegler, W. L. Meinhardt, and A. J. Deacon: Graphitization of Cementite in Cupola White Iron. *Trans. Amer. Foundrymen's Assn.* (June 1942) **49**, 449.

31. S. C. Massari and R. W. Lindsay: Some Factors Influencing the Graphitizing Behavior of Cast Iron. *Trans. Amer. Foundrymen's Assn.* (June 1942) **49**, 953.
32. Symposium on Graphitization of White Cast Iron. *Trans. Amer. Foundrymen's Assn.* (July 1942) **50** (1), 1.
33. H. A. Schwartz: The Kinetics of Graphitization in White Cast Iron. *Trans. Amer. Foundrymen's Assn.* (Dec. 1942) **30**, 1328.
34. A. Elsea and C. H. Lorig: The Effect of Copper Content at Low Temperature Pretreatment of Some White Irons in Malleabilization. *Trans. Amer. Foundrymen's Assn.* (June 1943) **50**, 1032.
35. Symposium on Malleable Iron. *Trans. Amer. Foundrymen's Assn.* (Dec. 1943) **51**, 261.
36. O. W. Simmons: Quenching Rate vs. Graphite Formation in Prequenched White Cast Iron. *Trans. Amer. Soc. Metals* (1944) **32**, 255.
37. C. H. Lorig: Graphitization of Malleable Iron. *Foundry* (May 1944) **72**, 61.
38. C. T. Eakin and H. W. Lownie: A Metallographic Quality Tests for Malleable Iron. *Trans. Amer. Foundrymen's Assn.* (Sept. 1944) **52**, 261.

DISCUSSION

(Howard Scott presiding)

W. R. FERGUSON.*—Is it not true that most of the transformation that takes place in cast iron is a form of growth, when changing from pearlite to graphite, irrespective of manganese and sulphur?

N. A. ZIEGLER (author's reply).—The dilations of the presented dilatometer curves are combinations of the allotropic transformations of the metal plus graphitization of combined carbon, which is present in the original metal.

The first part of it is reversible. For a steel, dilations are due to allotropic transformations only, so that upon completion of a heating-cooling cycle, the dilatometer curve returns to its starting point. In cast iron, this does not occur, because heating to above the critical temperature results in a permanent increase in volume, due to graphitization, in addition to the normal allotropic transformations.

W. R. FERGUSON.—How about the graphite size change due to heating?

N. A. ZIEGLER.—I do not think the shape of the original graphite flakes formed in the mold is changed, although a slight increase in

size may occur. Perhaps Dr. MacKenzie will say whether I am right or wrong.

J. T. MACKENZIE.*—I do not know. If you have time, and the graphite is formed from the decomposition of pearlite and/or carbide, probably it will eventually migrate to the primary graphite flakes. As a matter of fact, though, the primary graphite formed during the freezing of the metal is very little affected by ordinary heat-treatment.

C. H. LORIG.†—Was the change in combined carbon obtained through the addition of manganese to the iron in the charge or as a late addition? If the latter, I would suspect some difference between the combined carbon obtained that way and the combined carbon obtained if the manganese is in the iron at meltdown.

I might comment a little on the variation in growth with manganese. Your data seem to confirm some work Mr. Forbes did some years ago with malleable iron, in which he added increased amounts of manganese and found that when the manganese went beyond 0.7 per cent the structures were quite stable, and could not be decomposed very readily on annealing.

N. A. ZIEGLER.—I would prefer not to introduce the subject of malleable iron, because that is a very involved subject by itself. It is perfectly true that the nature of the iron is affected not only by the percentage of manganese, but also the way in which it is introduced in the metal.

J. T. MACKENZIE.—That is true not only of manganese; it is even more true of the sulphur. If you melt, say, 0.20 per cent sulphur in the cupola, the irons in all probability would be all white. You can add up to about 0.25 or 0.30 per cent, even 0.35 sulphur in the ladle without getting white iron. That is even more peculiar to me than the manganese.

N. A. ZIEGLER.—That is true.

J. S. VANICK.‡—There is no criticism possible of the result reported in Mr. Ziegler's paper

* American Cast Iron Pipe Co., Birmingham, Alabama.

† Battelle Memorial Institute, Columbus, Ohio.

‡ Metallurgist, International Nickel Co., Inc., New York, N. Y.

* Battelle Memorial Institute, Columbus, Ohio.

within the scope indicated by the title and the excellent research methods that accompanied the work. The work makes a substantial contribution to the much discussed problem of manganese-sulphur ratios in cast iron that is to be used for enamelware. It points out that growth due to graphitization in the high-sulphur iron is high, and in the high-manganese iron it is low. From an idealistic standpoint as related to enameling, it would appear that a desirable product should combine these divergent results. The product would be one that did not grow and yet became annealed to the ferritic condition free of combined carbon in the enameling process. In some respects this objective closely resembles the end product sought in malleable iron production where a ferritic structure is the desired end product. Malleable producers are keenly conscious of the importance of the manganese-sulphur ratio and are equally alert to any contamination of their product that will deflect them from obtaining the desired ferritic end structure. They are conscious of the importance of cooling rates in producing this structure. The same problems would exist in the production of enamelware where the abrupt dimensional changes that occur in the transformation ranges may be displaced by changes in cooling rate. Most of the difficulties related to differences in expansivity of enamel and metal are actually associated with differences in rates of contraction during cooling below 700°C . when the enamel has lost its plasticity, and stresses between the metal and ceramic interfaces will develop. The author knows that the break in contraction on cooling cast iron is retarded with faster cooling rates. It is doubtful whether similar information on the enamels is available. Because manganese may depress the temperature range of the dimensional change in enameling irons, the amount of manganese present must be held down to quantities that will not become troublesome for the rate of cooling of the castings. For this reason, manganese contents are kept very low and its contribution toward increasing the combined carbon content or the stability of the carbides is correspondingly low.

Manufacturers of enamelware have adhered closely to established compositions, and for apparently good reasons, fearful that any departure from established practice invites

economic disaster. High-phosphorus irons are commonly used to obtain fluidity and smooth surfaces. The author's study concludes that the growth is due primarily to the graphitization of combined carbon. He reports that the irons show appreciable amounts of steadite that is not affected by the annealing treatment. Steadite is not a pure iron-phosphorus compound, but is contaminated by carbon in considerable amounts, so that the desirable end product of a carbide-free structure might be altered for these manganese-sulphur ratios if lesser amounts of phosphorus were present. In making malleable iron, a low-phosphorus product is maintained, presumably for the reason that high physical properties are necessary. The effect that phosphorus might exert upon the persistence of carbide after annealing is a less critical problem in malleable production because the total amount is usually very small. Producers of enamelware know that carbide residues in the microstructure of cast iron may lead to blistering, arising from the presence of microchill. They are also aware that the cracking of the castings during cleaning, enameling and handling invites the production of tougher irons. Contaminants in the iron, arising from the presence of embrittling elements in the enamel itself, that is charged back into the cupola with enameled scrap present prospects for introducing difficulties that may be more disturbing than the composition of the base metal itself. Modern research tools such as the spectroscope might assist in tracking down their presence and evaluating their good or bad influences.

As mentioned before, Mr. Ziegler has presented an "open and shut" case concerning the effects of manganese and sulphur on the graphitization. The debatable elements of the metallurgy of the problem, as distinct from the ceramic problem concerning the enamel, might include further studies, some of which are: (1) the phosphorus effect, (2) can steadite be alloyed or inoculated to completely graphitize its carbon content? (3) does one type of graphite provide better anchorage for enamel and thus better adherence than another? (4) cooling-rate effects, (5) rate of graphitization for different types of primary graphite structure.

It has been impossible for me to shut out of my mind the application for which the iron

described in these tests was intended. The process of producing enamelware is as complicated as the process of producing castings, and these comments are intended to bring attention to a few important details related to the study of manganese-sulphur vs. graphitization reported upon in this paper. The results offer some inducement toward modifying enamelware processes moderately with a view toward improving the product or its production and without appreciably altering the general practice.

R. M. PARKE.*—The data presented by Mr. Ziegler are of interest in connection with attempts to describe the causes of growth in cast iron, since it seems that by performing the heat-treatment in vacuum he has eliminated oxidation as one of the causes. He shows also that the order of magnitude of growth for the single heat-treating cycle used is the same as that generally reported for the growth of iron in air.

I have sought to compute the growth of the cast irons of Mr. Ziegler's investigation by assuming that all of the combined carbon graphitizes during the heating cycle and that on so doing the irons grow equally in all directions. In these computations I have used the following data:

Density of cast iron.....	7	grams per c.c.
Density of graphite.....	2.2	grams per c.c.
Density of cementite.....	7.7	grams per c.c.
Carbon in cementite.....	6.66	per cent

The computed changes in length are as follows, along with the values determined experimentally:

Serial No.	Combined Carbon, Per Cent	Growth, Per Cent	
		By Experiment	By Computation
1	0.74	0.58	0.50
2	0.55	0.81	0.34
3	0.73	0.66	0.49
4	1.01	0.98	0.67
5	1.24	1.08	0.82
6	1.26	1.14	0.82
7	0.73	0.94	0.49
8	0.44	0.56	0.29
9	0.46	0.56	0.30
10	0.63	0.52	0.41
11	0.59	0.58	0.35
12	0.67	0.52	0.39
13	0.70	0.46	0.44

* Research Metallurgist, Climax Molybdenum Co., Detroit, Michigan.

For most of the irons, appreciably more growth occurred than can be accounted for by graphitization, even assuming that all of the combined carbon graphitized—which undoubtedly it did not. Furthermore, no reasonable change in the density values employed or in the carbon content of the cementite will make up the difference, therefore it appears that while graphitization accounts for the largest part of the growth of cast iron in a single heating cycle, a considerable portion of growth yet remains unexplained.

R. SCHNEIDEWIND.*—The author presents some very interesting data on the growth of cast iron when heated in vacuum. It is good that vacuum heating was used in order to prevent possible growth through oxidation or other gas reactions.

From the data presented, it is not possible to speculate at length on the reason for the expansion. The results of the tests are presented in percentage of linear growth; when converted to percentage of expansion by volume, the amount of expansion found is considerably greater than would be expected from the reaction $\text{Fe}_3\text{C} \rightarrow 3\text{Fe} + \text{C}$ and assuming the usual density values for carbide, ferrite, and graphite.

It is unfortunate that the author did not include: (1) the combined carbon analysis after heating and (2) the densities of the samples prior to and after heating. More valuable deductions might have been derived from this carefully conducted series of tests.

If growth under the conditions of test is due to decomposition of cementite, the theoretical relationship between growth and combined carbon (Fig. 5) should be a straight line intersecting the abscissa at about 0.1 per cent C, which probably is the solubility of carbon in silicoferrite in commercial irons. Deviations from the theoretical would be due to the different stabilities of the carbides in different samples as affected by sulphur and manganese, as the author says.

Although there are insufficient data to draw the theoretical line with accuracy, it is possible to derive a function of the carbide stability by dividing the expansion by the graphitizable carbon (per cent combined carbon - 0.1).

* Professor of Metallurgy, University of Michigan, Ann Arbor, Michigan.

This has been done in the following table and the results are compared with the respective Mn/S ratios,

Serial No.	Ratio Mn/S	% Growth % C.C. - 0.1 Per Cent
1	5.4	0.905
2	5.0	1.800
3	3.7	1.048
4	3.2	1.079
5	2.0	0.948
6	1.2	0.985
7	4.0	1.490
8	7.3	1.649
9	8.5	1.556
10	11.9	0.983
11	13.7	1.182
12	24.8	0.914
13	30.2	0.768

When these values are plotted as in Fig. 10, the curve passes through a maximum at Mn/S = 5, indicating that carbide stability is minimum at that point. Both manganese and sulphur are carbide stabilizers, but in the proper proportions neutralize each other's stabilizing effect. This proportion is not exactly what would be computed from the formula MnS. It is significant that in the malleable industry, where least carbide stability is demanded, the Mn/S ratio is maintained between 3 and 5. The higher silicon content of the irons of this research may account for the higher Mn/S ratio at the maximum point.

H. A. SCHWARTZ.*—This commentator has always held certain reservations with regard to the application of the dilatometer to the study of graphitization. Here he agrees with the author's phrase, "It is difficult to interpret these dilatometer curves," not only in terms of constitutional diagrams, but also in terms of reaction velocities. For example, we recognize the beginning of graphitization in such a diagram as Fig. 1 by a departure from the initial direction of the temperature thermal expansion line. We can only recognize a departure when this has become some detectable amount. If we run through a given temperature cycle slowly, the time, counting from the beginning of graphite formation to the precipitation of that amount of graphite that we can measure, in terms of thermal expansion, will involve a smaller change of temperature than

had we run the dilatometer cycle more rapidly. Therefore, in connection with such slow reactions as graphitization, the dilatometer curve is largely a function of heating rate.

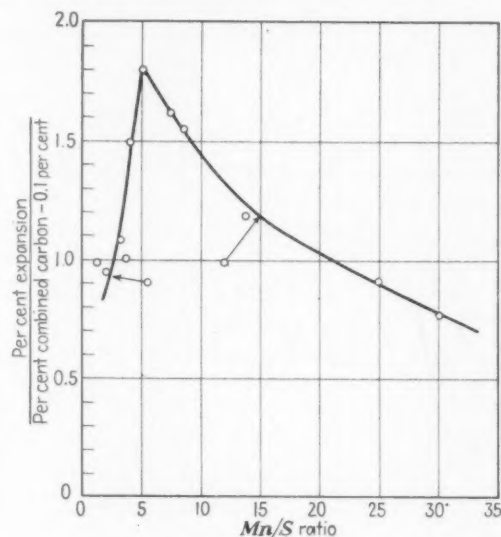


FIG. 10.

The author has not given us any details as to the heating rates he employed. It may be that the cycles he chose were sufficiently related to the commercial cycles, producing the expansion in which he is practically interested, as to give quite useful results. The commentator's point is merely that such a point as that on the heating line of Fig. 1, representing the intersection of that line with an expansion of 0.4 at approximately 650°F., has no theoretical significance. The author apparently is disturbed by the considerable scatter of the points in his Fig. 5. Could not these be explained by the fact that with the time-temperature cycles upon which he standardized, the degree of completion of graphitization of the originally existing combined carbon differed with the composition of the metal? There seems to be some internal evidence in Fig. 5 that this is so.

Alloys high in combined carbon, and therefore initially presumably those high in alloys, certainly those of slow graphitizing rate, have grown less in proportion to their combined carbon content than the alloys initially low in combined carbon, and therefore rather graphitizable. Since it is well known that alloys high in manganese and otherwise of such composition as used for the manufacture of pearlitic

* Manager of Research, National Malleable and Steel Castings Co., Cleveland, Ohio.

malleable, graphitize below the critical point much more slowly than alloys lower in manganese, it would seem quite likely that metals starting at some high temperature and some-

it was prepared in response to an invitation to participate in a symposium on dilatometry from some data already on hand.

Mr. Vanick's remarks are well received.

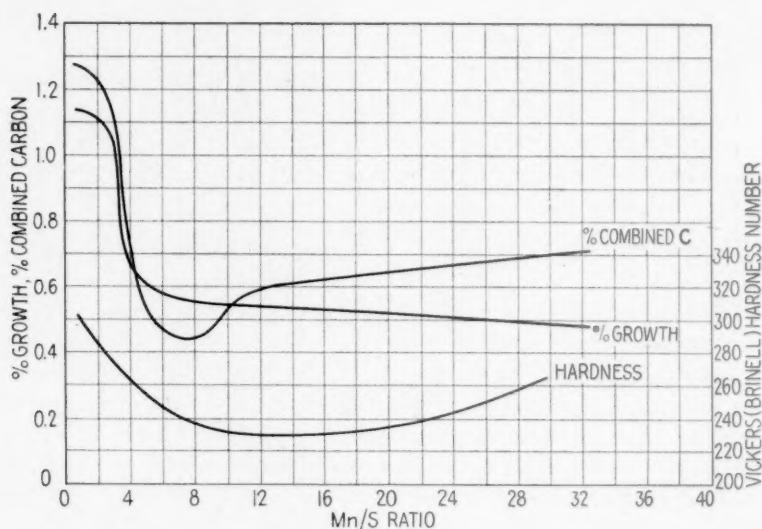


FIG. 11.

what constant combined carbon, should, with a constant dilatometer cycle, arrive at room temperature with higher combined carbon, the higher the manganese.

This commentator has the feeling that if the object of an investigation is primarily to study the graphitizing phenomenon, the dilatometer is a less useful tool than is the analytical attack by the determination of either combined carbon or graphite. The dilatometer is an elegant piece of equipment and of undisputed value in other fields, such as the determination of the alpha-gamma transformation, which is of great rapidity. It does not seem to the writer to be of much use in the study of graphitization unless it is used as a constant-temperature instrument for the study of an isothermal reaction.

These comments are made entirely without reference to Mr. Ziegler's observations. They refer entirely and only to the general question of the use of dilatometer studies in the particular field of graphitization.

N. A. ZIEGLER (author's reply).—It is gratifying to receive so many constructive remarks and to realize that the discussers have found enough interest and time for a careful study of the present paper. As previously pointed out,

They are a very interesting and valuable addition to this presentation.

Messrs. Parke and Schneidewind bring out a very interesting point; namely, that the linear growth observed in many cases is higher than one that should be expected from decomposition of "cementite." Two explanations may be suggested as a hypothetical possibility:

1. It may be possible that "cementite" in cast iron is different in composition from Fe_3C , and that its density and carbon content are different from those cited by Mr. Parke. Likewise, there is a possibility that the resultant "graphite" is not pure carbon, but contains other elements such as, say, silicon. Since the reported linear changes due to the dilatometric cycle are quite accurate, it may be possible for someone to work backward, and from the data available (perhaps with some additional experiments); to figure out the composition of the original "cementite" and of the resultant "graphite" necessary to produce the observed dimensional changes.

2. It may be that the total growth is partly due to minute submicroscopic permanent separations within the metal, caused by the combined effect of graphitization and anisotropic expansion-contraction of the individual metallic crystals.

These two suggestions may be rather promising lines of attack for future experimentation.

Mr. Schneidewind's curve is very interesting and checks rather well with our curves that were omitted from the paper but which, for the sake of completeness of the record, are now presented in Fig. 11. It seems that the maximum of Mr. Schneidewind's curve is not exactly at 5, but closer to 6, Mn/S ratio.

To answer the question raised by Dr. Schwartz, the dilatometric cycle used in this particular set of experiments was as follows: 2 hr. to heat to 1000°C. and 5 hr. to cool to room temperature. The rate was uniform in both cases, which is about 8.3°C. per min. for heating and about 3.2° per min. for cooling. This was a purely arbitrarily selected cycle, and no claims are being made that it approximates conditions existing in enameling or malleablizing furnaces.

The author cannot agree with Dr. Schwartz that the dilatometer is not well adapted to the

study of graphitization. The remark that the dilatometer curves presented in the paper are "difficult to interpret" was made in the sense that they are different from those usually obtained with steels to which we are accustomed. Nevertheless, every discontinuity of cast-iron dilatometer curves shown in this paper is real and significant. Their full significance will be revealed by future research. It was not the object of the present paper to go into any great lengths discussing the mechanism of graphitization. It merely presents a few observations in connection with the behavior of enameling iron. We have, however, a considerable amount of dilatometric data on graphitization of malleablizing irons of different compositions based on isothermal reactions, as suggested by Dr. Schwartz. In conjunction with metallographic studies and chemical analyses, they make a very interesting study and it is hoped that some day they will be available for publication.

An Interferometer Type of Dilatometer, and Some Typical Results

BY L. A. WILLEY* AND W. L. FINK,* MEMBERS A.I.M.E.

(Cleveland Meeting, October 1944)

ALTHOUGH the interferometric method for the determination of length changes was devised by Fizeau more than three quarters of a century ago, it has not achieved the widespread use in the metallurgical field that its precision and simplicity would seem to warrant.

The interferometer and the basic principle are both very simple. When optically plane surfaces held at a very slight angle to each other are illuminated by monochromatic light, rectilinear, equally spaced interference fringes are formed. Each fringe corresponds to a definite thickness of the wedge formed by the optical flats. The difference in wedge thickness between two consecutive fringes is equal to one half the wave length of the illuminating light.

Instruments for viewing the interferometer have passed through a number of modifications. Outstanding among the improvements were those contributed by Abbé in 1884. His improved instrument permitted micrometric measurements to the order of one-hundredth of the width of an interference fringe (i.e., lengths were measured to the order of one two-hundredth of the wave length of light). It also permitted the consecutive use of light of several wave lengths, which made possible the determination of the order number of any fringe and therefore the absolute thickness of the wedge at any point. The Abbé dilatometer and methods of measurement,

including corrections to be applied for the change of index of refraction with change in temperature and barometric pressure in an air wedge, have been thoroughly described by Pulfrich.¹

Pulfrich² made further improvements in the interference measuring apparatus. His instrument embodied all the features of the Abbé dilatometer but was made more versatile by its complete mechanical separation from the interferometer. The introduction of an Amici prism in the eyepiece permitted the *simultaneous* observation of the whole set of fringe systems developed in the interferometer from the visible light of a Geisler tube. Also, the introduction of a direct-vision, reflecting prism made it possible to set the fringes parallel to the two vertical fiducial lines of the instrument without the necessity of rotating the interferometer.

Interferometric methods employed in this country have been developed and described by Priest,³ Peters and Cragoe,⁴ Austin,⁵ Merritt,⁶ Saunders,⁷ and Nix and MacNair.⁸ Since none of these authors used the type of instrument that was employed in the present investigation, they will not be discussed here. This paper will be limited to the description of the interferometric apparatus and method used at the Aluminum Research Laboratories and to the presentation of data so obtained.

APPARATUS AND PROCEDURE

A general view of the dilatometer, not including equipment for controlling and

Manuscript received at the office of the Institute Oct. 14, 1944. Listed as T. P. 1859.

* Aluminum Research Laboratories, Aluminum Company of America, New Kensington, Pennsylvania.

¹ References are at the end of the paper.

measuring the temperature, is shown in Fig. 1. It consists of a Zeiss (Pulfrich) interference-measuring apparatus, a furnace, and an adjusting stand on which the inter-

shell and the refractory core, the thermal capacity of the furnace was low, permitting quick thermal response. An insulating block that extended for a distance of 5 cm.

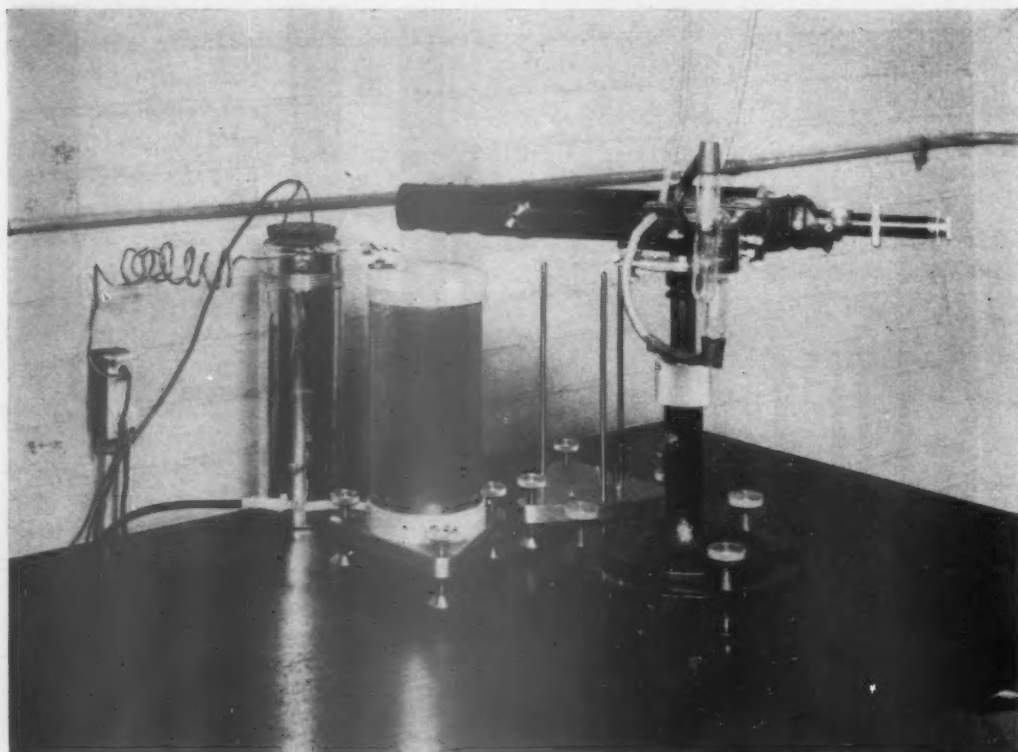


FIG. 1.—THE DILATOMETER.

ferometer is assembled and adjusted before it is placed in the furnace. The helium Geisler tube on the arm of the Pulfrich apparatus was used for illuminating the interferometer. This was energized by a 110 to 7500-volt transformer. The intensity of the light was controlled with an autotransformer placed between the energizing transformer and the power source.

Furnace

The furnace was of simple construction. A refractory core, 8.6 cm. o.d. by 6 cm. i.d. by 20 cm., threaded with coiled resistance wire, was encased within a sheet-metal shell of 11.4-cm. diameter. It was held in place with end blocks of Transite. Since no insulation was placed between the

into the core was fastened to the Transite base. The entire furnace was mounted on a triangular steel base supplied with three screws for optical alignment.

The lid of the furnace, shown on the adjusting stand in Fig. 2, was made to serve as a support for the interferometer and its casing. This provided a means of maintaining alignment when transferring the interferometer from the adjusting stand to the furnace. The interferometer casing, which was used to reduce temperature fluctuations and gradients in the interferometer, consisted of an aluminum base, 3-mm. thick, and a cylinder with a 3-mm. wall, provided with a quartz window at the top. The aluminum base was fastened rigidly to a nichrome stirrup, which served

also to hold the insulating end core to the cap of the cover and to hold in a fixed position two thermocouples which extended through the lid.

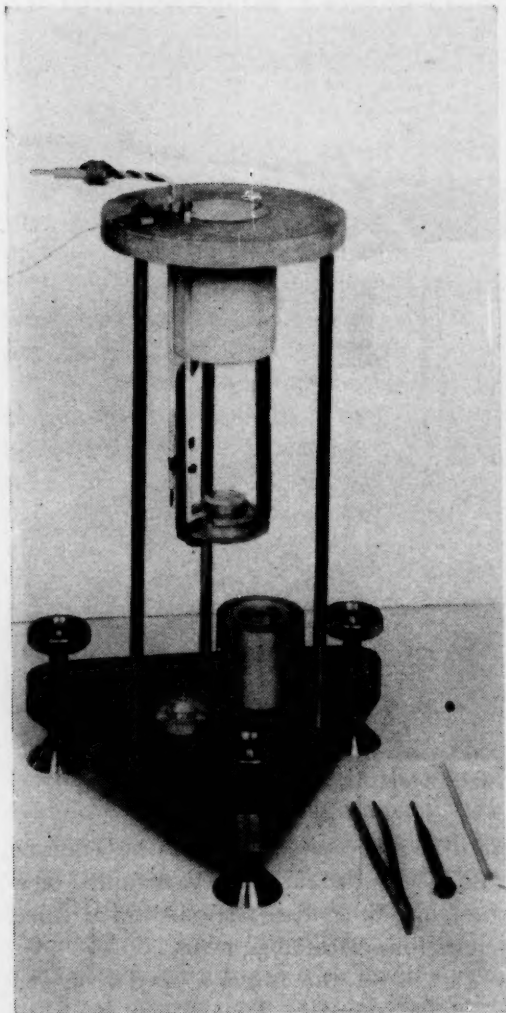


FIG. 2.—ADJUSTING STAND IN USE.

Shows furnace lid and method of supporting interferometer. The cylinder of the casing and the silver weight used to stabilize the interferometer are shown on the base of the stand.

The temperature of the furnace was controlled by an indicating potentiometer controller of the photoelectric type, in connection with an iron-constantan thermocouple which was placed approximately midway between the furnace wall and the interferometer case. A rheostat in series with the furnace element was used for

adjusting the current to prevent wide fluctuations in furnace temperature. The controller was operated either by turning the current on and off or by shorting out a

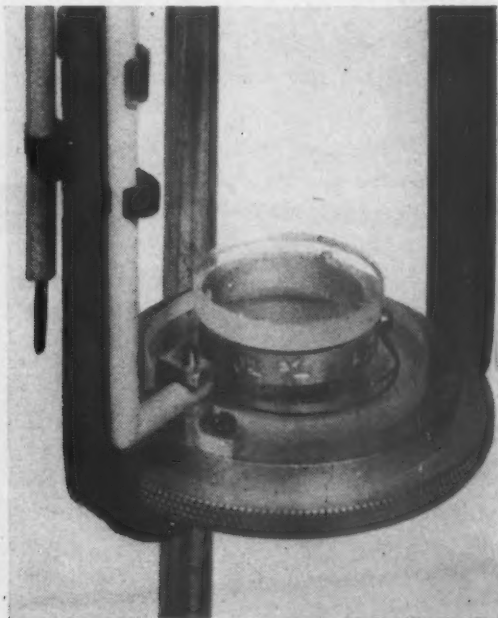


FIG. 3.—THE INTERFEROMETER—NATURAL SIZE.

Shows quartz base and cover plates and specimen of interferometer in place on base of aluminum casing. Also shows thermocouple attached to specimen.

second rheostat, which was in series with the one just mentioned.

For obtaining temperatures down to minus 65°C. , the furnace shell was replaced by a larger insulated shell. The space (approximately 50 mm.) between it and the refractory core was packed with crushed dry ice. At these temperatures a precooled stream of dry air was used to prevent fogging and to avoid contamination of the air wedge with CO_2 .

Interferometer

The interferometer, shown at approximately natural size in Fig. 3, consisted of a fused quartz base plate, 30-mm. diameter by 6 mm. thick; a fused quartz cover plate, 20-mm. diameter by 3 mm. thick and a specimen serving as the spacer. The sur-

faces of the plates did not depart from optical planeness by more than 0.1 the wave length of yellow light. The lower surface of the cover plate was supplied with an index circle 0.4 mm. in. diameter at its center.

Several types of test specimens were employed for the determination of thermal expansion. These usually comprised rings of metal approximately 19 mm. o.d. by 16 mm. i.d. by approximately 5 mm. in height. Metal was filed from the ring, leaving three equally spaced 1-mm. diameter pins which extended about 1 mm. from the body of the ring in each direction. The various types are shown in Fig. 4. The type obtained by machining a ring from heavy sections is shown at *a*. With sheet samples, blanks were cut and tapered at the ends as shown at *b* and then bent, riveted, and filed to form the type shown at *c*. In some cases three individual legs were prepared to the form shown at *d* and these were fastened rigidly to a narrow ring of aluminum or quartz of somewhat larger diameter as shown at *e*. With all three types of specimens, the pins were carefully worked down on fine metallographic emery paper to a height between 5.0 and 5.1 mm., one of the three approximately 0.003 mm. longer than the other two. The operation usually had to be completed by using the interferometer to measure this difference. With this difference in height, a section of a wedge having an angle of between 30" and 40" was obtained between the quartz plates, giving from 10 to 14 interference fringes under yellow light.

Temperature Measurement

The temperature of the specimen was measured with a Leeds and Northrup type K potentiometer and a thermocouple was attached to it with a small machine screw at a point directly opposite one of the pins. Two types of thermocouples were employed. For tests in which the expansion was determined in the range from room

temperature up to 500°C., a platinum-platinum + 13 per cent rhodium thermocouple was used. This couple was calibrated against the melting points of tin, zinc and

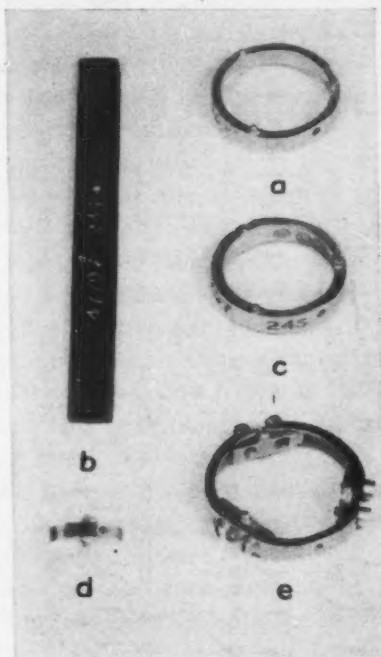


FIG. 4.—TYPICAL SPECIMENS.

the aluminum-copper eutectic and was found not to deviate from the standard calibration by more than 0.5°C. For tests in which the expansion was determined in the range from minus 65° to plus 120°C., a copper-constantan thermocouple was used. This couple was calibrated against the sublimation temperature of CO₂ using the method described by Scott⁹ and against the melting points of mercury and tin. It was found not to deviate more than 0.7°C. from the standard calibration in the range employed.

Since the thermocouple was attached directly to the specimen, it was necessary to guard against its disturbance of the interferometer. This was accomplished by using fine thermocouple wire, by providing a substantial loop between the point at which the element was attached to the specimen and that at which it was rigidly

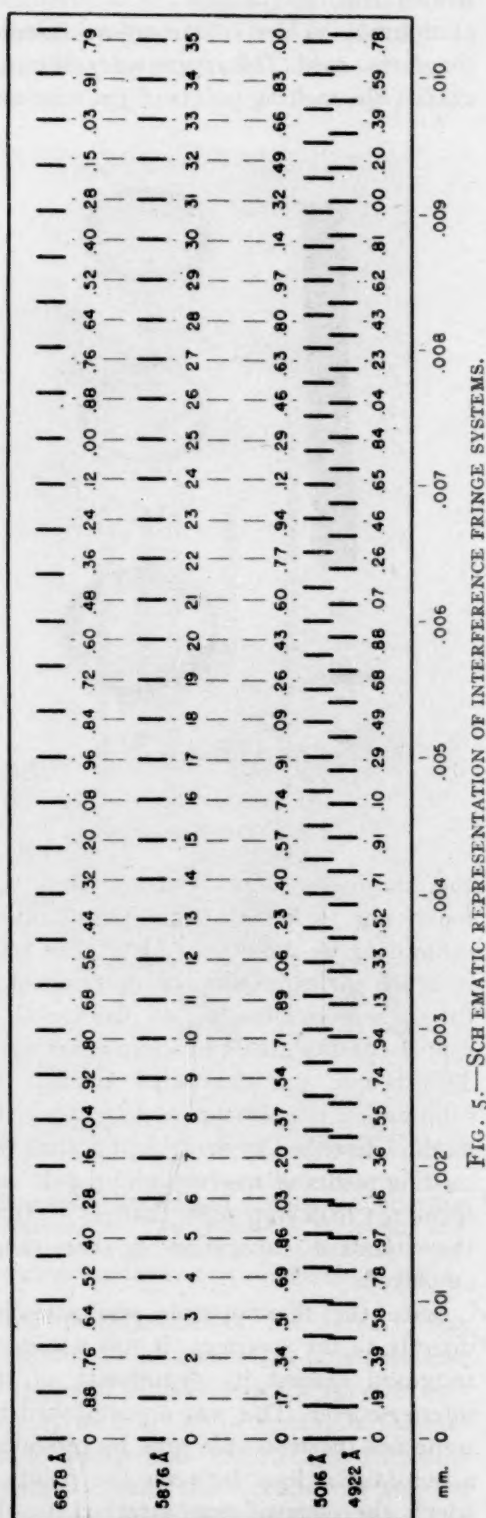


FIG. 5.—SCHEMATIC REPRESENTATION OF INTERFERENCE FRINGE SYSTEMS.

attached to the interferometer case, and by using a 25-gram silver weight (shown on the base of the adjusting stand in Fig. 2) on the cover plate of the interferometer. This weight was 30 mm. o.d. by 16.5 mm. i.d. and approximately 5 mm. thick, and was provided with three equally spaced feet. It was placed so that the feet were directly over the pins of the specimen. These feet were shaped like small steps to prevent lateral movement of the weight with respect to the cover plate. It was found that the weight not only made possible the attachment of the thermocouple to the specimen but also provided a more stable interferometer.

Determination of the Order Number of the Fringe

One of the principal advantages of the Abbé or Pulfrich type of interference measuring apparatus is that it permits the identification of the order number of a given fringe. This eliminates the necessity of counting the fringes as they pass the reference point and it also makes possible the absolute measurement of lengths rather than merely the measurement of change in length. This identification is accomplished by using simultaneously two or more different fringe systems. The method will be illustrated for a case in which are used four of the fringe systems produced by light from a helium Geisler tube. The four fringe systems are related to each other as shown in Fig. 5, which covers wedge thicknesses from 0 to 0.010 mm. For simplicity, the fringe systems will be designated as red (6678 Å.), yellow (5876 Å.), green (5016 Å.), and blue (4922 Å.), although the last named is really blue-green rather than blue. Since the yellow system is used as the reference and therefore for calculating distances, order numbers are given below the lines representing the yellow fringes in Fig. 5. In general, the red, green and blue fringes do not coincide with the yellow fringes. For example, the tenth yellow fringe is 0.80

of a red fringe beyond the eighth red fringe, 0.71 of a green fringe beyond the eleventh green fringe and 0.94 of a blue fringe beyond the eleventh blue fringe. The decimal

TABLE 1.—*Table for Determination of Fringe Number*

Thickness of Air Space, Mm.	Fringe No. in Yellow System ($\lambda = 5875.630\text{\AA}$)	Fraction of Fringes Coincident with Fringe in Yellow System		
		Red ($\lambda = 6678.062\text{\AA}$)	Green ($\lambda = 5015.613\text{\AA}$)	Blue ($\lambda = 4921.9\text{\AA}$)
4.9943	17000	0.29	0.96	0.06
4.9946	17001	0.17	0.13	0.25
4.9949	17002	0.05	0.30	0.45
4.9952	17003	0.93	0.47	0.64
4.9955	17004	0.81	0.64	0.83
4.9958	17005	0.69	0.81	0.03
4.9960	17006	0.57	0.98	0.22
4.9963	17007	0.45	0.16	0.41
4.9966	17008	0.33	0.33	0.61
4.9969	17009	0.21	0.50	0.80
4.9972	17010	0.09	0.67	0.00
4.9975	17011	0.97	0.84	0.19
4.9978	17012	0.85	0.01	0.38
4.9981	17013	0.73	0.19	0.58
4.9984	17014	0.61	0.36	0.77
4.9987	17015	0.49	0.53	0.96
4.9990	17016	0.37	0.70	0.16
4.9993	17017	0.25	0.87	0.35
4.9996	17018	0.13	0.04	0.55
4.9999	17019	0.01	0.21	0.74
5.0002	17020	0.89	0.39	0.93
5.0005	17021	0.77	0.56	0.13
5.0007	17022	0.65	0.73	0.32
5.0010	17023	0.53	0.90	0.51
5.0013	17024	0.41	0.07	0.71
5.0016	17025	0.29	0.24	0.90
5.0019	17026	0.17	0.41	0.10
5.0022	17027	0.05	0.59	0.29
5.0025	17028	0.93	0.76	0.48
5.0028	17029	0.81	0.93	0.68
5.0031	17030	0.69	0.10	0.87
5.0034	17031	0.57	0.27	0.06
5.0037	17032	0.45	0.44	0.26
5.0040	17033	0.32	0.61	0.45
5.0043	17034	0.20	0.79	0.65
5.0046	17035	0.08	0.96	0.84
5.0049	17036	0.96	0.13	0.03
5.0052	17037	0.84	0.30	0.23
5.0054	17038	0.72	0.47	0.42
5.0057	17039	0.60	0.64	0.61

parts (fringe fractions) of the red, green and blue fringes are indicated for each yellow fringe. It is evident that Fig. 5 would have to be extended many fold to show the

recurrence of the same combination of fractions. In other words, if the distance between the quartz plates is known approximately, the order number of the yellow fringe can be identified quickly by reference to the proper section of a table giving the fringe fractions.

An example will be given for the region in the vicinity of 5 mm., the length of specimen most frequently used in this work. If it is known that the specimen is approximately 5 mm. high, and observation shows that the yellow fringe nearest the index circle coincides with 0.65 of a red fringe, 0.73 of a green fringe and 0.32 of a blue fringe, reference to Table 1 shows that the number of the yellow fringe in question is 17,022. This corresponds to an air space of 5.0007 mm. (wave length being 5875.63\AA). If this yellow fringe coincided with the index circle on the plate, this would be the length of the specimen.

Although the measurement of fringe fractions can be made with the micrometer on the telescope of the instrument as described by Pulfrich, the procedure is rather time consuming, since it is based on the accurate measurement of three to five fringes in two to four fringe systems. A much quicker method, and one that can be used even when the fringes are in motion,* is illustrated by Fig. 6. This figure shows the fringe systems for the illustration given in the last paragraph. In this figure the dotted lines show the nearest coincidence between yellow fringes and fringes in the other systems within the field of view. The first yellow fringe to the left of the index circle is taken as the reference fringe. (The viewing instrument is always adjusted so that the narrowest part of the wedge appears to the left of the index circle with the consequence that the order numbers of the fringes progressively increase from

* In some cases such as the measurement of length changes occurring during aging, it is imperative to have a method which will identify the fringes when they are in motion.

left to right.) It will be noted that the third yellow fringe to the left of the reference fringe coincides very closely with a red fringe. In the green fringe system, the best

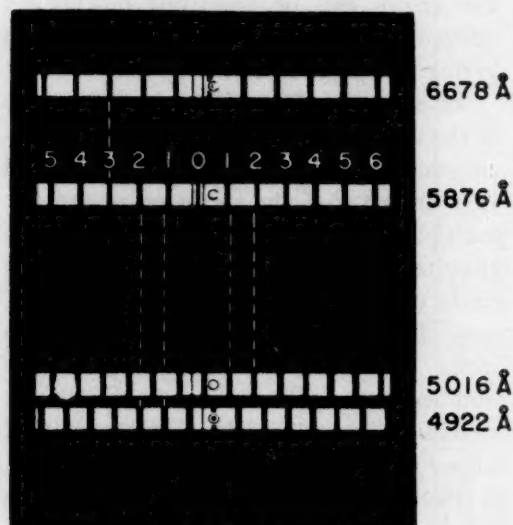


FIG. 6.—SCHEMATIC REPRESENTATION OF A PART OF THE FRINGE SYSTEMS AS VIEWED THROUGH THE INTERFERENCE MEASURING APPARATUS. ILLUSTRATES THE METHOD FOR DETERMINING FRINGE FRACTIONS.

coincidences are with the first and second yellow fringes to the right of the reference fringe. Since the coincidence is equally good for the two fringes in question, the number of fringes to coincidence is taken as one and a half. In the blue fringe system, the best coincidences are with the first and second yellow fringe to the left of the reference fringe. In this case, however, the second yellow fringe gives a better coincidence than the first so that the number of fringes to coincidence is taken as $1\frac{3}{4}$. In Table 2 the fringe fractions can be read directly from the number of yellow fringes to coincidence. The values read from this table (0.64, 0.75 and 0.34) vary one or two-hundredths of a fringe from the accurate values given in Table 1. However, these values are sufficiently close to identify the fringes with certainty.

An understanding of this method can be gained by referring again to Fig. 5. There is a near coincidence between red and

yellow fringes at approximately every eighth yellow fringe, between green and yellow fringes at approximately every sixth yellow fringe and between blue and yellow fringes at approximately every fifth yellow fringe. In other words, the yellow fringe system can be used as a vernier in which each yellow fringe to coincidence indicates approximately 0.12 part of a red fringe, 0.17 part of a green fringe, and 0.195 part of a blue fringe. The fractional part thus

TABLE 2.—Table for Determination of Fringe Fractions

Number of Yellow Fringes to Coincidence between Systems	Fringe Fractions					
	Red		Green		Blue	
	Left	Right	Left	Right	Left	Right
0	0	0	0	0	0	0
$\frac{1}{4}$	0.97	0.03	0.04	0.96	0.05	0.95
$\frac{1}{2}$	0.94	0.06	0.09	0.91	0.10	0.90
$\frac{3}{4}$	0.91	0.09	0.13	0.87	0.15	0.85
1	0.88	0.12	0.17	0.83	0.19	0.81
$1\frac{1}{4}$	0.85	0.15	0.21	0.79	0.24	0.76
$1\frac{1}{2}$	0.82	0.18	0.26	0.74	0.29	0.71
$1\frac{3}{4}$	0.79	0.21	0.30	0.70	0.34	0.66
2	0.76	0.24	0.34	0.66	0.39	0.61
$2\frac{1}{4}$	0.73	0.27	0.39	0.61	0.44	0.56
$2\frac{1}{2}$	0.70	0.30	0.43	0.57	0.48	0.52
$2\frac{3}{4}$	0.67	0.33	0.47	0.53	0.53	0.47
3	0.64	0.36	0.51	0.49	0.58	0.42
$3\frac{1}{4}$	0.61	0.39	0.56	0.44		
$3\frac{1}{2}$	0.58	0.42	0.60	0.40		
$3\frac{3}{4}$	0.55	0.45				
4	0.52	0.48				
$4\frac{1}{4}$	0.49	0.51				
$4\frac{1}{2}$	0.46	0.54				
$4\frac{3}{4}$	0.43	0.57				
5	0.40	0.60				

obtained may be either the actual fraction or one minus the fraction, depending upon the system under consideration and whether the coincidence occurs to the right or left of the reference fringe. There is a slight error caused by the fact that coincidences are determined only to the nearest quarter of a fringe. However, the maximum error from this source is 0.03 of a fringe—an error too small to cause any uncertainty in the identification of the fringe.

Determination of Specimen Length

In order to determine the length of the specimen accurately it is necessary to

TABLE 3.—Table of Wave Lengths
WAVE LENGTHS OF HELIUM YELLOW LIGHT IN ÅNGSTRÖM UNITS

t°C.	0	1	2	3	4	5	6	7	8	9	Correction Barometric Pressure for Each Mm. Hg below 760 Add
-70	5874.950	.938	.927	.915	.904	.892	.881	.869	.858	.846	0.00304
-60	5875.058	.048	.037	.026	.016	.005	.994*	.983*	.972*	.961*	0.00292
-50	.157	.147	.137	.128	.118	.108	.098	.088	.078	.068	0.00281
-40	.247	.238	.229	.221	.211	.202	.193	.184	.175	.166	0.00270
-30	.329	.321	.313	.305	.297	.289	.280	.272	.264	.255	0.00260
-20	.405	.398	.391	.383	.376	.368	.360	.353	.345	.337	0.00250
-10	.476	.469	.462	.455	.448	.441	.434	.427	.420	.413	0.00240
-0	.541	.534	.528	.522	.515	.509	.502	.496	.489	.482	0.00231
0	.541	.547	.553	.559	.566	.572	.578	.584	.590	.596	0.00222
10	.601	.607	.613	.619	.624	.630	.636	.641	.647	.652	0.00214
20	.658	.663	.669	.674	.679	.685	.690	.695	.700	.705	0.00206
30	.710	.716	.721	.726	.731	.736	.740	.745	.750	.755	0.00200
40	.760	.765	.769	.774	.779	.783	.788	.793	.797	.802	0.00193
50	.806	.811	.815	.819	.824	.828	.833	.837	.841	.845	0.00187
60	.850	.854	.860	.862	.866	.870	.874	.879	.883	.887	0.00182
70	.891	.895	.898	.902	.906	.910	.914	.918	.922	.925	0.00177
80	.929	.933	.937	.940	.944	.948	.951	.955	.959	.962	0.00172
90	.966	.969	.973	.976	.980	.983	.987	.990	.994	.997	0.00167
100	5876.000	.004	.007	.010	.014	.017	.020	.023	.027	.030	0.00163
110	.033	.036	.039	.043	.046	.049	.052	.055	.058	.061	0.00159
120	.064	.067	.070	.073	.076	.079	.082	.085	.088	.091	0.00155
130	.094	.097	.099	.102	.105	.108	.111	.113	.116	.119	0.00151
140	.122	.124	.127	.130	.133	.135	.138	.141	.143	.146	0.00147
150	.148	.151	.154	.156	.159	.161	.164	.167	.169	.172	0.00143
160	.174	.177	.179	.182	.184	.186	.189	.191	.194	.196	0.00140
170	.198	.201	.203	.206	.208	.210	.213	.215	.217	.219	0.00137
180	.222	.224	.226	.229	.231	.233	.235	.238	.240	.242	0.00134
190	.244	.246	.248	.251	.253	.255	.257	.259	.261	.263	0.00131
200	.265	.268	.270	.272	.274	.276	.278	.280	.282	.284	0.00128
210	.286	.288	.290	.292	.294	.296	.298	.300	.302	.304	0.00126
220	.306	.308	.309	.311	.313	.315	.317	.319	.321	.323	0.00124
230	.324	.326	.328	.330	.332	.334	.335	.337	.339	.341	0.00122
240	.343	.344	.346	.348	.350	.351	.353	.355	.357	.358	0.00120
250	.360	.362	.363	.365	.367	.368	.370	.372	.373	.375	0.00118
260	.377	.378	.380	.382	.383	.385	.387	.388	.390	.391	0.00116
270	.393	.395	.396	.398	.399	.401	.402	.404	.406	.407	0.00114
280	.409	.410	.412	.413	.415	.416	.418	.419	.421	.422	0.00112
290	.424	.425	.427	.428	.429	.431	.432	.434	.435	.437	0.00111
300	.438	.440	.441	.442	.444	.445	.447	.448	.449	.451	0.00109
310	.452	.453	.455	.456	.458	.459	.460	.462	.463	.464	0.00108
320	.466	.467	.468	.470	.471	.472	.474	.475	.476	.477	0.00106
330	.479	.480	.481	.483	.484	.485	.486	.488	.489	.490	0.00105
340	.491	.493	.494	.495	.496	.498	.499	.500	.501	.502	0.00103
350	.504	.505	.506	.507	.508	.510	.511	.512	.513	.514	0.00102
360	.516	.517	.518	.519	.520	.521	.522	.524	.525	.526	0.00100
370	.527	.528	.529	.530	.531	.533	.534	.535	.536	.537	0.00099
380	.538	.539	.540	.541	.542	.544	.545	.546	.547	.548	0.00097
390	.549	.550	.551	.552	.553	.554	.555	.556	.557	.558	0.00096
400	.559	.561	.562	.563	.564	.565	.566	.567	.568	.569	0.00095
410	.570	.571	.572	.573	.574	.575	.576	.577	.578	.578	0.00094
420	.579	.580	.581	.582	.583	.584	.585	.586	.587	.588	0.00093
430	.589	.590	.591	.592	.593	.594	.595	.596	.597	.598	0.00092
440	.598	.599	.600	.601	.602	.603	.604	.605	.606	.607	0.00091
450	.608	.608	.609	.610	.611	.612	.613	.614	.615	.615	0.00090
460	.616	.617	.618	.619	.620	.621	.622	.622	.623	.624	0.00089
470	.625	.626	.627	.627	.628	.629	.630	.631	.632	.632	0.00088
480	.633	.634	.635	.636	.637	.637	.638	.639	.640	.641	0.00086
490	.641	.642	.643	.644	.645	.645	.646	.647	.648	.649	0.00085

TABLE 3.—(Continued)

t°C.	0	1	2	3	4	5	6	7	8	9	Correction Barometric Pressure for Each Mm. Hg below 760 Add
500	5876.649	.650	.651	.652	.652	.653	.654	.655	.656	.656	0.00084
510	.657	.658	.659	.659	.660	.661	.662	.662	.663	.664	0.00083
520	.665	.665	.666	.667	.668	.668	.669	.670	.671	.671	0.00082
530	.672	.673	.673	.674	.675	.676	.676	.677	.678	.678	0.00081
540	.679	.680	.681	.681	.682	.683	.683	.684	.685	.685	0.00080
550	.686	.687	.688	.688	.689	.690	.690	.691	.692	.692	0.00079
560	.693	.694	.694	.695	.696	.696	.697	.698	.698	.699	0.00078
570	.700	.700	.701	.702	.702	.703	.704	.704	.705	.705	0.00076
580	.706	.707	.707	.708	.709	.709	.710	.711	.711	.712	0.00075
590	.713	.713	.714	.714	.715	.716	.716	.717	.717	.718	0.00074
600	.719	.719	.720	.721	.721	.722	.722	.723	.724	.724	0.00073
610	.725	.725	.726	.727	.727	.728	.728	.729	.730	.730	0.00072
620	.731	.731	.732	.732	.733	.734	.734	.735	.735	.736	0.00071
630	.737	.737	.738	.738	.739	.739	.740	.740	.741	.742	0.00070
640	.742	.743	.743	.744	.744	.745	.746	.746	.747	.747	0.00069
650	.748	.748	.749	.749	.750	.751	.751	.752	.752	.753	0.00068
660	.753	.754	.754	.755	.755	.756	.756	.757	.757	.758	0.00067
670	.759	.759	.760	.760	.761	.762	.762	.763	.764	.764	0.00066

determine also the fraction of a yellow fringe from the reference fringe to the index circle. This is accomplished by using the micrometer on the telescope of the measuring apparatus. Three readings are taken: (1) on the reference fringe, (2) on the index circle, and (3) on the first fringe to the right of the index circle. The difference between the first and second readings divided by the difference between the first and the third readings will give the fringe fraction.* The fringe fraction so obtained is added to the order number of the reference fringe, of course. Since each fringe corresponds to a difference in wedge thickness of one half a wave length, the number of yellow fringes plus the fraction multiplied by one half of the corrected wave length gives the length of the specimen. The wave lengths of the helium yellow light in air for various temperatures and pressures are given in Table 3. The table is based on the value of 5875.63 Å. as the wave length of helium yellow light in

dry air at 15°C. and one atmosphere pressure.¹⁰

Program

After the length of the specimen pins had been adjusted, the thermocouple attached, the interferometer and its silver weight assembled and the cylindrical part of the aluminum casing put in place, the whole assembly was transferred from the adjusting stand to the furnace. The length of the specimen was determined first at room temperature and then at various other temperatures over the range to be investigated. For each measurement the temperature was held constant long enough to ensure thermal equilibrium (i.e., until no change in temperature could be detected by the type K potentiometer and no movement of the fringes could be detected by the micrometer of the measuring apparatus). This procedure eliminated temperature gradients that would have existed throughout the interferometer if the temperature were changing rapidly.

After the first series of measurements, the length of the specimen was checked again at room temperature. A difference

* The accuracy can be increased by measuring several fringes but this refinement is not justified by the accuracy of other factors involved in the determination.

TABLE 4.—Coefficients of Thermal Expansion of Some Wrought Aluminum Alloys

Specimen No.	Alloy No.	Nominal Composition, ^a Per Cent							Wrought Form ^b	Temper ^c	Average Coefficients of Thermal Expansion per Deg. Centigrade $\times 10^6$						Per Cent Change after Heating and Cooling ^d
		Cu	Si	Mn	Mg	Zn	Ni	Cr			-60° to 20°C.	20° to 100°C.	20° to 200°C.	20° to 300°C.	20° to 400°C.	20° to 500°C.	
59410	Alcoa 2S								Sheet	As rolled	23.0	23.9	24.3	25.5	26.6	-0.054	
59411	Alcoa 3S								Sheet	O	21.7	24.6	25.6	26.5	27.5	-0.001	
70596	Alcoa 14S	4.4	0.8	0.8	0.4				Bar	As rolled	23.4	23.8	24.2	25.3	26.3	-0.049	
70528	Alcoa 17S	4.0		0.5	0.5				Rod	O	21.4	24.2	25.1	26.0	27.1	-0.001	
70529	Alcoa A17S	2.5							Rod	As forged	23.1	23.8	25.8			+0.037	
70597	Alcoa 18S	4.0		0.5			2.0		Bar	O	21.6	24.0	25.0			-0.001	
47797	Alcoa 24S	4.5		0.6	1.5				Sheet	T	21.7	23.3	24.8			0.000	
70599	Alcoa 25S	4.5	0.8	0.8					Bar	As rolled	20.9	23.3	23.6	25.7		+0.012	
70600	Alcoa 32S	0.9	12.5		1.0		0.9		Bar	O	21.5	23.9	24.7	25.9		-0.001	
70601	Alcoa A51S		1.0		0.6			0.25	Bar	As forged	22.8	23.3	23.6	25.9		-0.048	
33613	Alcoa 52S			2.5				0.25	Sheet	T	21.6	24.2	25.0	27.0		-0.003	
70530	Alcoa 53S		0.7	1.3				0.25	Rod	O	21.6	24.4	25.1	26.1	27.0	-0.001	
59416	Alcoa 61S	0.25	0.6	1.0				0.25	Sheet	As rolled	22.0	24.9	25.8	26.7	27.9	-0.007	
63001	Alcoa 75S ^e	1.6	0.15	2.5	5.75			0.25	Sheet	O	21.7	24.1	25.1			-0.001	
									Sheet	As rolled	23.5	23.7	24.5			0.000	
									Sheet	T	22.8	24.3	25.4			-0.024	
									Sheet	As rolled	23.5	24.3	25.4			-0.002	
									Sheet	O	21.6	22.8	24.5			0.000	
									Sheet	T	23.6	24.2	26.0			-0.049	
									Sheet	O	23.2	24.2	26.0			0.000	
									Sheet	T	21.6	23.6	26.0			-0.001	

^a Percentage of alloying elements, aluminum, and normal impurities constitute the remainder.^b Sheet, 14-gauge (0.064-in.) cold-rolled; rod, 3/4-in. diameter rolled and drawn; bar, 1-in. square forged. Expansion was measured transverse to the direction of rolling in sheet and parallel to the axis in rod and bar.^c O means annealed (in this case, annealed through the heating of the as-wrought specimens to temperature of 350°C. or above and slow cooling in the initial test); T, heat-treated and aged according to standard practice.^d Determined from expansion curve on heating and the final length after cooling to room temperature. A plus sign indicates a growth, and a minus sign a shrinkage.^e 75S is a standard alloy for extrusions and as the core alloy of Alclad 75S sheet.

between the two readings may be caused by changes in the specimen or errors in the method, such as films between specimen

Although the results in this table are largely self-explanatory, it seems advisable to discuss briefly a few of the features.

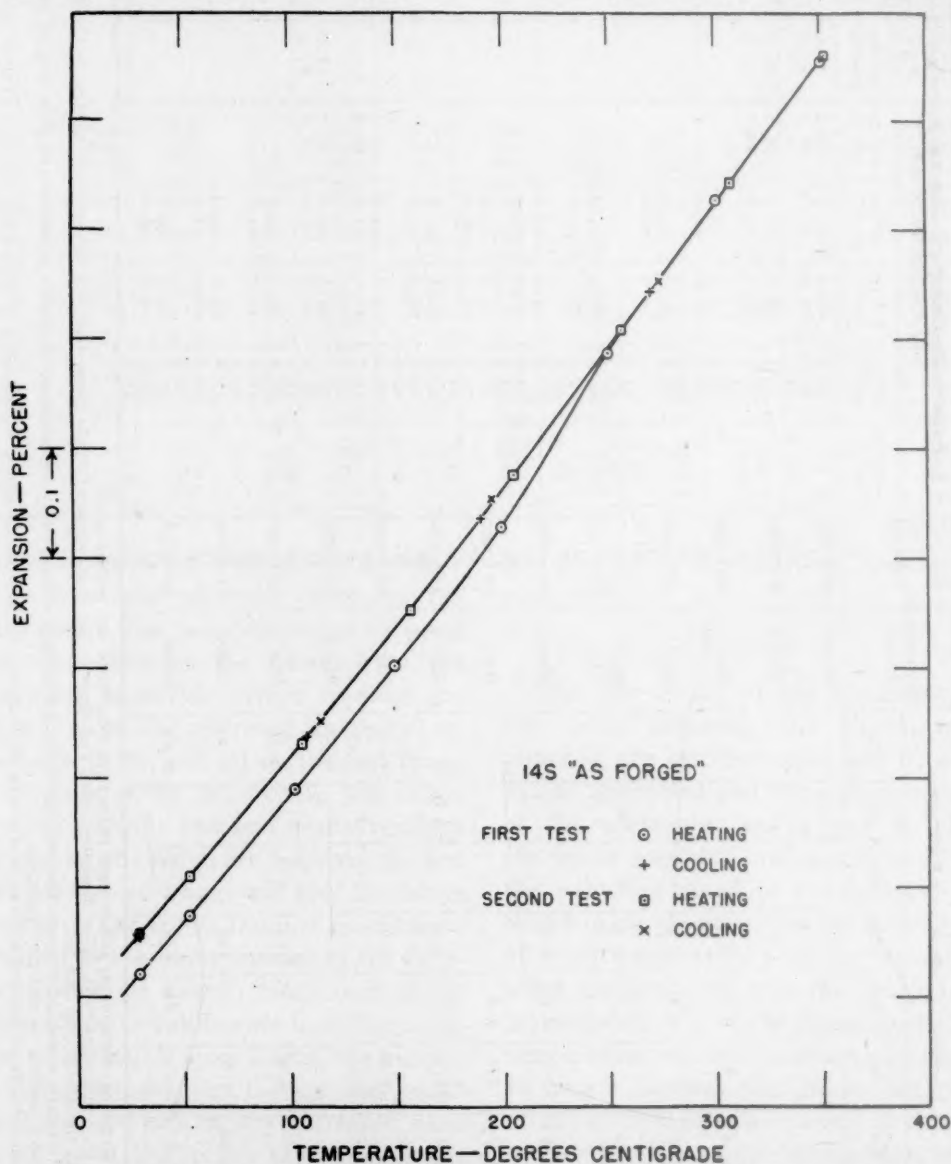


FIG. 7.—LINEAR THERMAL EXPANSION OF ALCOA 14S IN THE RANGE 20° TO 350°C.

or plate or lateral movement of the cover plate.

RESULTS

To illustrate the results obtained by the method described, coefficients of thermal expansion of some wrought aluminum alloys have been assembled in Table 4.

Although the table includes a wide variety of alloys—in fact, all of the wrought aluminum alloys commonly used in the construction of aircraft (except composite materials)—there is a rather small difference between the coefficients of expansion of the different alloys except for Alcoa 32S, which was developed especially to obtain

as low a coefficient of expansion as possible consistent with the other properties required of piston alloys.

Invariably there is a "permanent change"

The permanent length changes that occur when as-wrought material is heated are clearly illustrated in the curve for the first heating of as-forged 14S in Fig. 7.

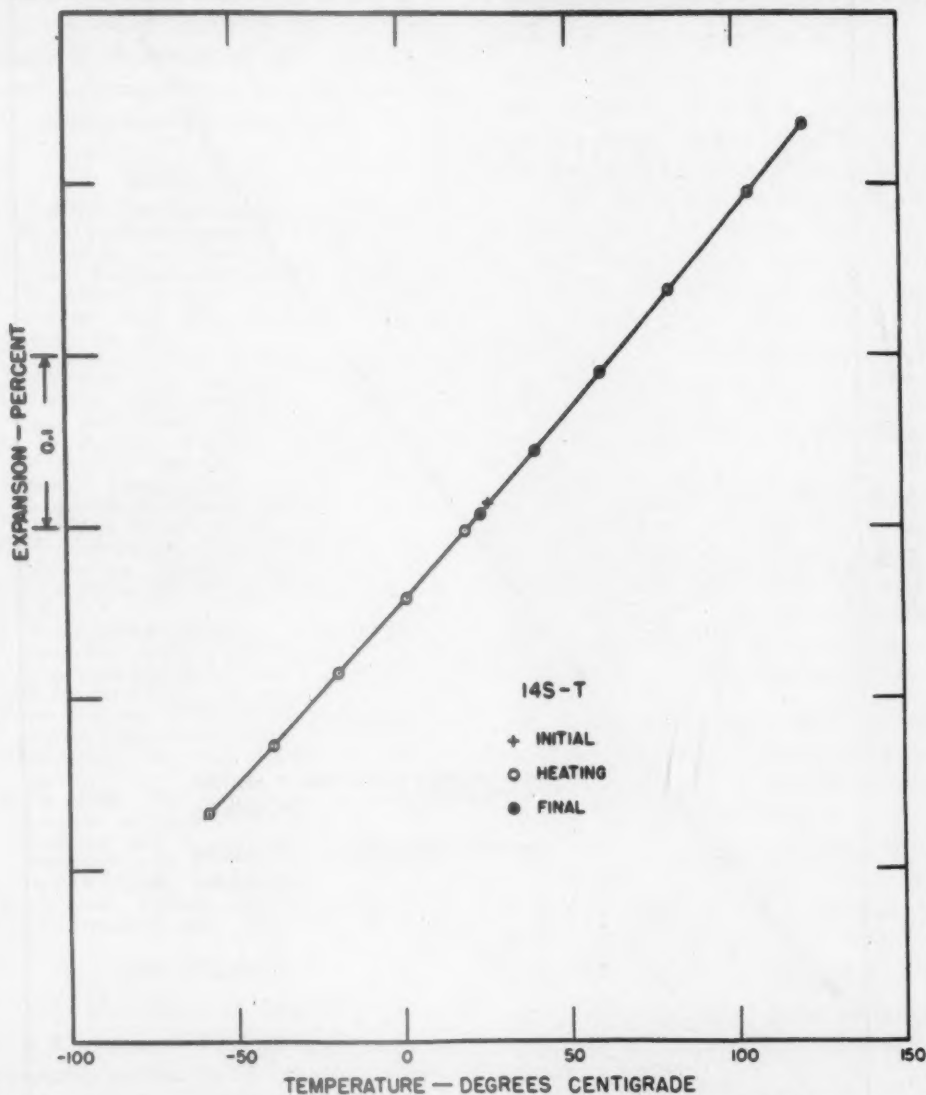


FIG. 8.—LINEAR THERMAL EXPANSION OF ALCOA 14S-T IN THE RANGE MINUS 60° TO PLUS 120°C.

in length when as-wrought material is heated for the first time to 350°C. or above. This is caused principally by changes within the specimens, such as relief of stresses, recrystallization, and precipitation or solution of soluble constituents. As a result, the coefficients of expansion given for as-wrought material are not precisely coefficients of thermal expansion.

Thereafter the material was in the annealed temper, and the length of the specimen at a given temperature was reproducible. Fig. 8 shows the absence of permanent changes when 14S-T was measured over the range minus 60° to plus 120°C.

Specimens in the heat-treated temper were not heated above 120°C. in order to avoid permanent length changes that would

occur at higher temperatures as a result of changes in the state of the precipitated constituents.

weight on the cover plate; a single curve can be drawn through the points. There was no indication of creep even at 500°C.

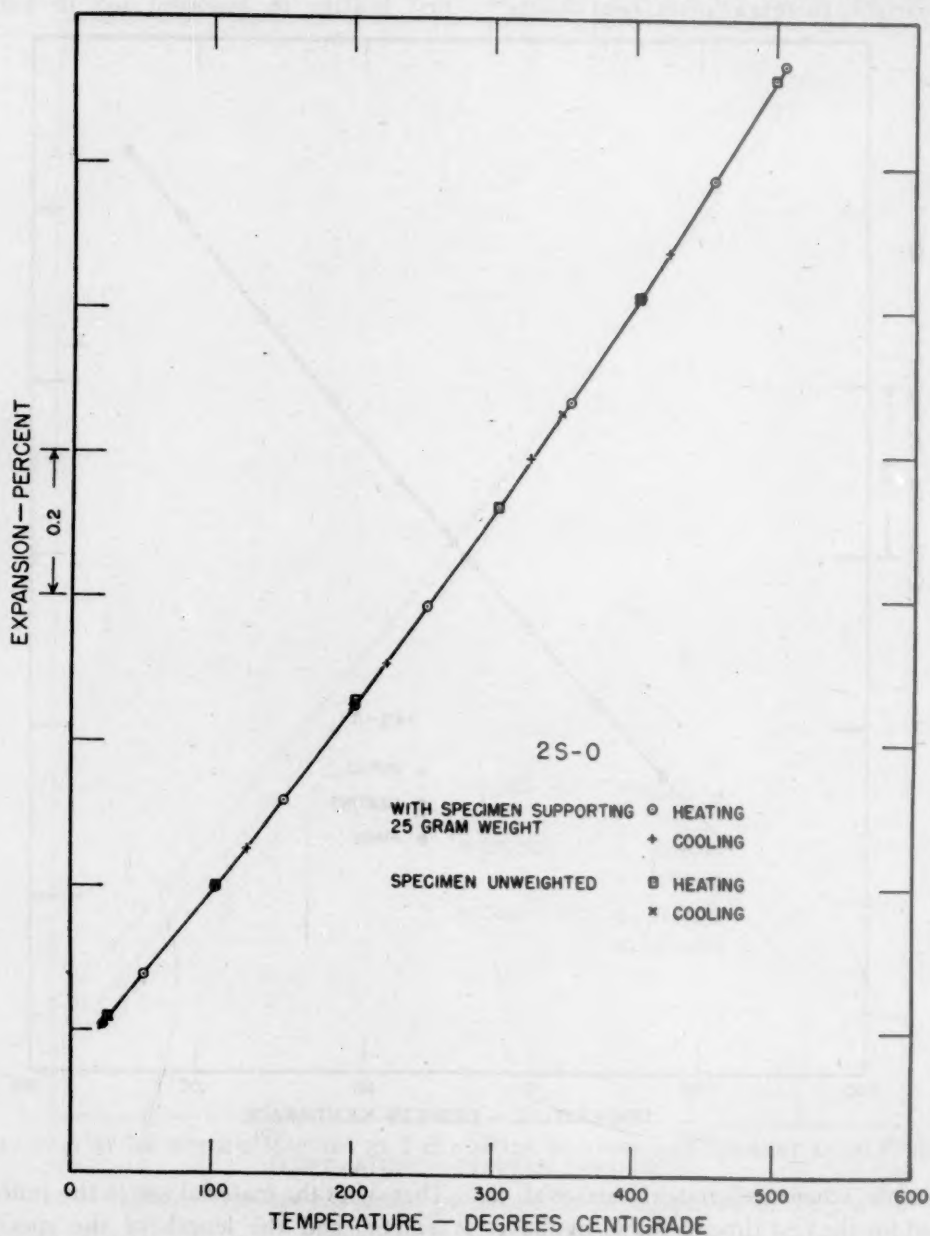


FIG. 9.—LINEAR THERMAL EXPANSION OF ALCOA 2S-O IN THE RANGE 20° TO 400°C.

The expansion curve of Alcoa 2S-O is of interest as a proof that the silver weight on the interferometer cover plate does not introduce an error. In Fig. 9 are plotted points that were obtained on both heating and cooling with and without the 25-gram

CONCLUSION

The interferometric method described in this paper has been used in the Aluminum Research Laboratories for several years and has proved to be accurate and convenient.

ACKNOWLEDGMENT

The authors desire to express their appreciation to Betty L. Magealson for her most careful work in connection with the thermal expansivity determinations and to other members of the staff of the Aluminum Research Laboratories at New Kensington and Cleveland for their assistance.

REFERENCES

1. C. Pulfrich: The Abbé-Fizeau Dilatometer. *Ztsch. Instrumentenkunde* (1893) 13, 366.
2. C. Pulfrich: An Interference Apparatus. *Ztsch. Instrumentenkunde* (1898) 18, 18.
3. I. G. Priest: A New Interferential Dilatometer. *Nat. Bur. Stds. Sci. Papers*, (1919) 15, 669.
4. C. G. Peters and C. H. Cragoe: Measurements of the Thermal Dilatation of Glass at High Temperature. *Nat. Bur. Stds. Sci. Papers* (1920) 16, 449.
5. J. B. Austin: Vacuum Apparatus for Measuring Thermal Expansion at Elevated Temperatures, with Measurements on Platinum, Gold, Magnesium and Zinc. *Physics* (1932) 3, 240.
6. G. E. Merritt: The Interference Method of Measuring Thermal Expansion. *Nat. Bur. Stds. Jnl. of Research* (1933) 10, 59.
7. J. B. Saunders: Improved Interferometric Procedure with Application to Expansion Measurements. *Nat. Bur. Stds. Jnl. of Research* (1939) 23, 179.
8. T. C. Nix and D. MacNair: An Interferometric-Dilatometer with Photographic Recording. *Rev. Sci. Instruments* (1941) 12, 66.
9. R. B. Scott: The Calibration of Thermocouples at Low Temperatures. Temperature—Its Measurement and Control in Science and Industry. American Institute of Physics (1941) 206.
10. H. Kayser: Tabelle der Hauptlinien der Linienspektren aller Elemente, 37. 1926.

DISCUSSION

(F. M. Walters, Jr., presiding)

W. E. KINGSTON.*—It might be brought out that probably the limiting factor is the accuracy of measuring the temperature of the specimen. I know we found that true, and I am sure that this is a characteristic limitation of such equipment.

W. L. FINK.—That is right.

W. E. KINGSTON.—The over-all accuracy is limited by the best calibration you can get on the thermocouple and the temperature measuring equipment.

I want to ask one more question; that is, do you cover the specimens with a protective

atmosphere? I should think, with your very precise method, and since most oxide coatings are at least on the order of 50 Ångströms thick, that the formation of oxide layers during measurement might introduce serious errors.

W. L. FINK.—There are really two major errors in this method. One is the inaccuracy of the temperature measurement and the other is the uncertainty of the position of the index point with respect to the specimen. If you use the ring-shaped aluminum specimen I showed, that ring expands and contracts at a different rate than the quartz plate so there is necessarily a relative movement. That may cause a slight permanent lateral displacement of the cover plate. We are doing some work now with a new specimen that permits the index point to be on the specimen in order to eliminate this source of error.

In regard to protecting the specimen, we found that an inert atmosphere was not necessary. It is true that the thickness of the oxide coating, even the thin coating on aluminum, could be measured by this method, but we find that the thickness of the aluminum oxide remains constant during measurement.

W. E. KINGSTON.—That might be particularly true with aluminum, whose oxide coating is comparatively thin, but with oxides of other materials it would not be true.

W. L. FINK.—Oh, that is right. With ferrous alloys or pure iron, or many other metals, it would be necessary to employ an inert atmosphere or, better yet, a vacuum. That is what Austin did in his well-known work on steels.

F. M. WALTERS, JR.—There was a question implied in Mr. Kingston's question, which you did not answer.

W. E. KINGSTON.—With the interferometer, you were interested primarily in the changes associated with precipitation-hardening, and those changes are usually so minute that it takes a particularly sensitive instrument to detect them.

W. L. FINK.—Yes. We got the instrument initially for studying the age-hardening of aluminum alloys, which produces very small length changes. As a matter of fact, we used a somewhat different specimen for that work—a specimen 5 cm. meters long instead of 5 millimeters.

*Sylvania Electric Products Inc., Bayside N. Y.

Symposium on Deoxidation

CONTENTS

	PAGE
Introduction. By GILBERT SOLER	657
Deoxidation of Basic Open-hearth Steel. By T. S. WASHBURN	658
Slag-metal-oxygen Relationships in the Basic Open-hearth and Electric Processes. By J. S. MARSH. (With discussion)	672
The Total Oxygen Content of Plain Carbon Open-hearth Steel during Deoxidation and Teeming. By MICHAEL TENENBAUM and C. C. BROWN. (With discussion)	685
The Occurrence of Oxygen in Liquid Open-hearth Steel—Sampling Methods. By T. E. BROWER and B. M. LARSEN	712
Effect of Deoxidation on the Strain-sensitivity of Low-carbon Steels. By H. K. WORK and G. H. ENZIAN. (With discussion)	723
The Relation among Aluminum, Sulphur, and Grain Size. By C. E. SIMS	734

SOME of the papers and discussions that appear on the following pages were presented at the meeting of the Iron and Steel Division in Cleveland, Ohio, on Wednesday, October 18, 1944,

with L. F. Reinartz and H. K. Work as Chairmen; the remainder were scheduled for the New York Meeting of the Institute in February 1945, which was canceled.

Introduction

By GILBERT SOLER,* Member A.I.M.E.

DURING the working and finishing periods of an open-hearth heat, oxygen is always being transferred from the slag to the metal. Much of this oxygen is consumed in the elimination of metalloids and by the oxidation of iron. However, from the time the heat is melted, the oxygen content of the bath increases and the carbon content decreases. Carbon content may thus be considered a fair index of oxygen content.

Since the metal and the slag in actual open-hearth operations never reach full equilibrium, and since wholly satisfactory methods of determining the temperature and the oxygen content of the metal are yet to be developed, a plot of actual experimental data must be shown as a band. There is a divergence between actual open-hearth values and equilibrium values, and various reasons have been advanced to explain this excess of oxygen in the metal.

The relation of carbon and oxygen is of primary importance in steelmaking because it is one of the principal reasons for the different methods used in finishing

heats. For example, in the manufacture of rimmed steels, carbon is usually reduced below 0.15 per cent, so that the metal contains enough oxygen to provide a rimming action in the molds. When a steel to be fully killed is tapped at less than 0.15 per cent carbon, the amount of oxygen and the resulting deoxidation products to be disposed of present a difficult problem in the economical production of clean steel.

Proper deoxidation practice and control are essential in any steelmaking process. Unquestionably steelmaking is more of an art than a science. It has been said that science will advance the art of steelmaking but will never supplant it. A great deal of valuable work has been published based on theoretical calculations and experiments backed up by careful studies of actual open-hearth operations. These studies have been concerned largely with the carbon-oxygen relation before final deoxidizers are added to the furnace, ladle, or molds. It is encouraging to note the interest in the actual deoxidation phase of steelmaking as evidenced by the excellent papers listed on our program.

* Timken Roller Bearing Co., Canton, Ohio.

Deoxidation of Basic Open-hearth Steel

By T. S. WASHBURN,* MEMBER A.I.M.E.

(Cleveland Meeting, October 1944)

DEOXIDATION is one of the most complex metallurgical operations in the basic open-hearth process. The necessity for deoxidation arises from the fact that the refining operations that precede it require the oxidation of the steel bath. When the refining is completed and the desired composition of the bath has been obtained with respect to the elements subject to control by oxidation, there is usually an excess of oxygen present in the bath from the standpoint of the amount desired in the finished steel. The primary objectives of deoxidation are to control the amount and type of oxides and, although not directly implied by the term or always considered as a part of the process, to control the amounts of gases such as hydrogen or nitrogen that will be present in the finished steel.

There are other aspects to be considered in connection with deoxidizing procedures. In addition to the primary objectives of oxide and gas control, the composition of the steel is affected by the elements introduced during the deoxidizing process. Factors in furnace operations are likewise involved, such as slag composition, temperature control, and heat time. All of these should be considered in establishing the most satisfactory deoxidizing procedure for each grade of steel. The purpose of this paper is to outline the objectives of deoxidation as related to steel characteristics, and to summarize the factors in furnace practice and the economic aspects

to be considered in connection with deoxidation procedures.

OBJECTIVES OF DEOXIDATION

The primary objectives of deoxidation are the formation and elimination of oxides. The amount of oxygen present in the bath prior to deoxidation is an important factor, since it is the basis of any deoxidation procedure. The oxygen content of the bath is primarily a function of the carbon content, although it is affected also by the temperature, the oxidation of the slag, and transient conditions within the furnace. The relation of oxygen to carbon in the bath is shown in Table 1.

TABLE 1.—*Relation of Oxygen to Carbon Content of Bath*

Carbon, Per Cent	Oxygen, Per Cent	
	Actual	At Equilibrium (1 Atm.)
0.05	0.069	0.036
0.10	0.044	0.019
0.15	0.033	0.013
0.20	0.027	0.011
0.25	0.023	0.009
0.30	0.020	0.008
0.40	0.018	0.006
0.60	0.015	0.005
0.80	0.014	0.004
1.00	0.014	0.004

Table 1 shows that under actual operating conditions, the amount of oxygen present in the bath is higher than the theoretical amount. This relation would be expected, since the bath is in a state of metastable equilibrium during the period that the carbon is being eliminated. The most important feature demonstrated by this table, however, is the rapid increase

Manuscript received at the office of the Institute Feb. 19, 1945. Listed as T.P. 1903.

* Inland Steel Co., Indiana Harbor, Indiana.

in oxygen as the carbon content decreases below 0.25 per cent. Since deoxidation involves the formation and removal of oxides, it is apparent that it can have the

relation to the oxygen in the bath has already been shown in Table I. It should also be noted that the first element in this series, manganese, is a relatively weak

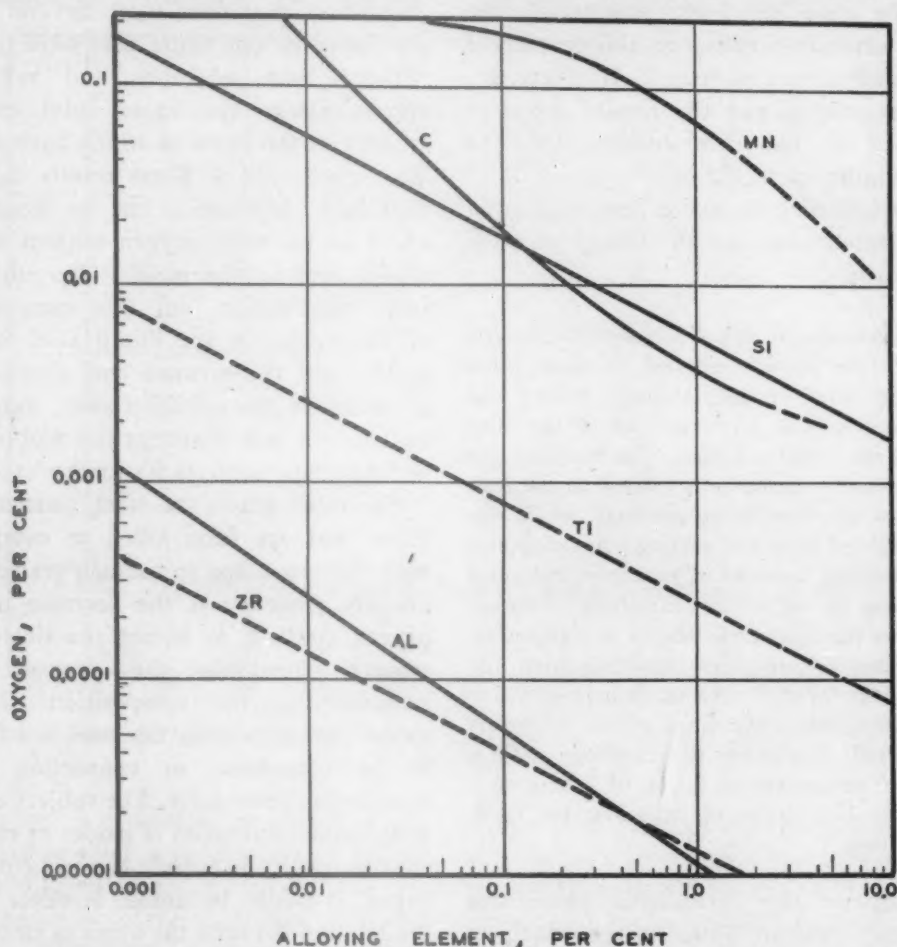


FIG. 1.—EQUILIBRIUM RELATION BETWEEN RESIDUAL DEOXIDIZING ELEMENT AND RESIDUAL OXYGEN IN STEEL.

greatest effect in the low-carbon ranges, and also that the degree of deoxidation will be more critical in these ranges.

The first step in deoxidation is the formation of oxides, which can be achieved by the addition of any element to the steel that has a greater affinity for oxygen than iron. The elements normally used for this purpose are manganese, silicon, titanium, aluminum, and zirconium—listed in the order of increasing deoxidizing power. Carbon also belongs in this series, but its

deoxidizer as compared with the other elements listed. The final deoxidizing effect, with respect to the amount of oxygen remaining dissolved in the iron at any given temperature, is determined principally by the amount of deoxidizing elements present that are not combined with oxygen. The relation of the excess of these elements present to the percentage of oxygen in the metal as demonstrated by Chipman¹ is shown in Fig. 1.

¹ References are at the end of the paper.

Since an important objective of deoxidation is the removal of oxygen from the steel by the formation of insoluble oxides, it is necessary to form the type of oxides that will be most effectively eliminated. The most extensive studies of this feature of deoxidation were made by C. H. Herty, Jr., and associates, and the results are summarized in the final bulletin on *The Deoxidation of Steel*.²

The following quotation from page 55 of that bulletin outlines the theory of oxide elimination:

The general principle of inclusion elimination is that the particles formed on deoxidation shall be large enough, through fluxing and coalescence, that they rise out of the steel before the metal solidifies. The tendency for fluxing and coalescence is related to the fusibility of the deoxidation products, which can be predicted from the melting point diagrams of the oxides involved. The largest inclusions and those having the lowest melting points are found in the manganese silicate or manganese-aluminum silicate slags, resulting from the deoxidation of steel with manganese-silicon or manganese-silicon-aluminum alloys. All factors considered, manganese-silicon alloys with a ratio of manganese to silicon of 4 or 5 to 1 give the best types of inclusions for rapid elimination.

Many of the deoxidizing procedures currently used are based on the principles developed by Herty. However, the use of single deoxidizing additions containing manganese and silicon or aluminum in the same alloy is not considered essential to obtain satisfactory results. Alternative methods involving the addition of several alloys are based usually on the principle of adding the weaker deoxidizing alloys first in the sequence of additions so as to facilitate the formation of fusible inclusions.

A recent investigation by Tenenbaum and Brown³ of the relation of deoxidizing methods to the oxygen content after bath deoxidation and during teeming developed some interesting conclusions.

The results of their investigation indicated, as shown in Fig. 2, that the oxygen content of the steel in the molds after teeming was not affected by the types of bath deoxidizers that were used. Several heats are shown in this figure that were tapped without bath additions and yet had approximately the same total oxygen content as the heats to which bath deoxidizers were added. These results indicate that bath deoxidation has no significant effect on the total oxygen content of the liquid steel in the molds. The effect of bath deoxidation on the composition of the oxides in the liquid steel in the molds, and the amount and distribution of oxides in the solidified steel, were not included in this investigation and would be interesting subjects for further study.

For most grades of steel, particularly those that are fully killed as compared with the semikilled or rimmed grades, the primary objective is the decrease of the oxygen content. It is not practicable to remove completely the oxygen, and, consequently, the composition of the oxides that remain in the steel is a factor to be considered in connection with deoxidation procedures. The subject of the distribution and types of oxides as related to steel quality is outside the scope of this paper. It might be noted, however, that the relation between the types of deoxidizing additions and the inclusion content of the solidified steel has not been thoroughly investigated. The composition of the inclusions obviously is affected by the type of deoxidizing alloy used; for instance, the formation of silicates from silicon additions. It is probable, however, that other factors associated with the deoxidizing procedure, such as temperature, slag activity, time, teeming practice, and final steel analysis have as much effect on the amount and distribution of inclusions as the types of deoxidizers used.

One relation between deoxidizing practice and steel characteristics that has

been developed in recent years is the control of austenitic grain size. Usually this is measured by the McQuaid-Ehn test, and the control by deoxidation has been per-

shows the amounts of these gases normally present in liquid and solid steel and indicates the importance that the gas content may have during the solidification period.

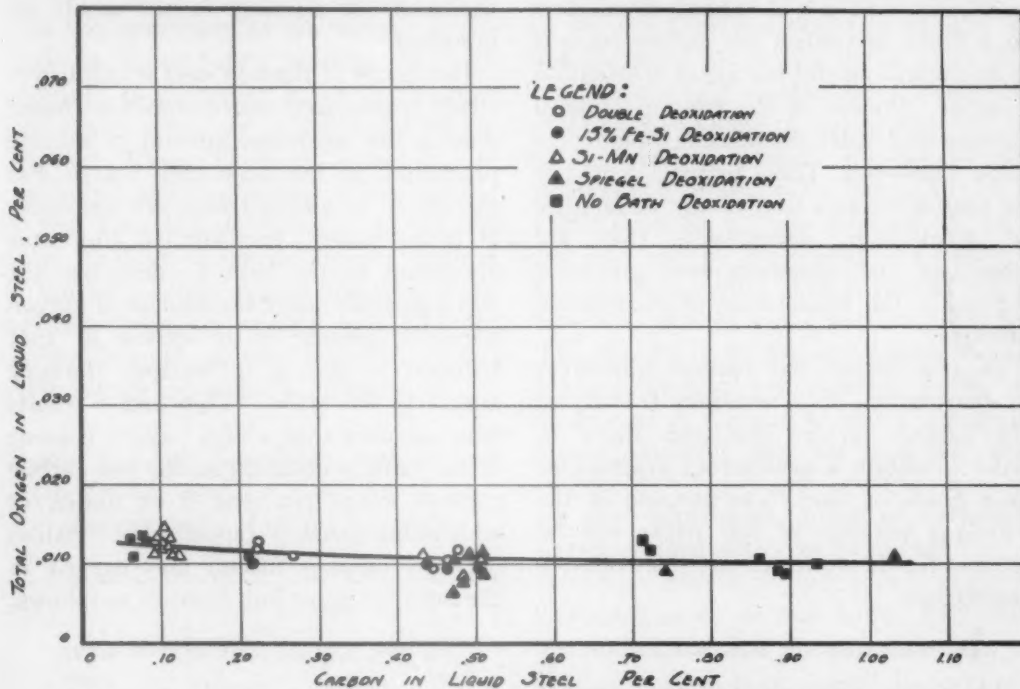


FIG. 2.—RELATIONSHIP BETWEEN CARBON AND TOTAL OXYGEN IN FULLY KILLED LIQUID STEEL IN THE INGOT MOLD.

fected and is considered as a part of the standard practice in most plants producing the fully killed grades of steel.

In addition to the objectives discussed above and implied by the term deoxidation, a secondary but important feature involved is the effect of deoxidation on the gases in the steel. The principal ones to be considered are hydrogen and nitrogen. Table 2

TABLE 2.—Hydrogen and Nitrogen Solubility in Iron at Various Temperatures*

Temperature, Deg. F.	Phase	Hydrogen, Per Cent	Nitrogen, Per Cent
2950	Liquid	0.0027	0.040
2600	Delta	0.0007	0.010
2100	Gamma	0.0007	0.023
600	Alpha	0.0001	0.001

* The data in this table were taken from Fig. 123, Chap. 16, of Basic Open Hearth Steelmaking. New York, 1944. A.I.M.E.

There is a pronounced decrease in the solubility of these gases in passing from the liquid to the solid phase. If these gases are evolved during solidification, they may be as significant as carbon monoxide and dioxide from the standpoint of the ingot structure, since they can also form blowholes. Just as the elements added to the steel in the deoxidation processes combine with oxygen and prevent the carbon-oxygen reaction and the consequent formation of gas, some of these elements combine with nitrogen or affect the solubility of both gases. As a consequence, deoxidation has an important function in controlling the effects of hydrogen and nitrogen both during solidification and also as related to their effect on the properties of the solid steel.

An important aspect of deoxidation is the relation of various deoxidation processes to the control of steel composition with respect to elements other than oxides and gases. The use of furnace deoxidizers as a block to control the carbon content is an example of this feature of deoxidation practice. Another is the relation of both furnace and ladle deoxidation practice to alloy recoveries. These features may not be considered as a part of the metallurgy of deoxidation, nevertheless they are important and sometimes even governing factors in the establishing of deoxidation practice.

In considering the various objectives of deoxidation, it is necessary to balance the various factors discussed above in order to obtain a satisfactory practice for each grade of steel. The purpose of the following portions of this paper will be to consider these factors and their relative importance.

DEOXIDATION OF RIMMED STEEL

The degree of deoxidation is the principal factor governing the type of ingot structure. These structures vary from the type characteristic of rimmed steel through a progressively changing series ending with the fully killed structure. The intermediate types between the rimmed and fully killed are termed semikilled.

Rimmed steel may be considered as a grade that is produced by allowing the refining action to continue after teeming into the molds and during the first stages of solidification. This is a valid concept, since the reactions that occur in the molds are similar to those that take place during the refining period in the furnace. From this viewpoint, it is obvious that rimmed steel is produced with the minimum amount of deoxidation, since an adequate amount of oxygen must be present in the steel after teeming to support the carbon-oxygen reaction, which is the basis of the rimming action. The oxygen present in

iron must also be free to react with carbon. If too large a proportion of the oxygen is combined with silicon or aluminum in the form of more stable oxides, the reactions necessary for rimming in the molds are inhibited.

One grade of rimmed steel is ingot iron, which is produced under conditions representing the maximum amount of refining practicable in the basic open hearth. For this grade, no alloying additions are made. It is customary, however, to add some aluminum to the ladle to deoxidize the metal partially, since the amount of oxygen normally present is in excess of that required to give a satisfactory rimming action in the molds. This excess results from the fact that a high oxygen content of the bath is obtained at the low carbon content, 0.040 per cent C or under, at which this grade is tapped. The relation between tapping carbon and oxygen in the bath for ingot-iron heats is as follows:

Carbon, 0.03 per cent; oxygen, 0.107	
0.04	0.087
0.05	0.069

It is desirable to maintain a balanced relation between the oxygen and carbon when the steel is poured into the molds. The ideal ratio is one that results in there being just enough oxygen to react with and remove carbon from the solidifying interface at the same rate that it is being concentrated in the liquid at the interface during the rimming period of solidification. If there is a deficiency of oxygen during this period, the carbon concentration of the core zone will increase, whereas if there is an excess, the oxygen content of the core zone will increase. In the former case, undesirable amounts of carbon may segregate in the upper central portion of the core zone; in the latter, there is an excessive amount of oxides in the core-zone portion of the product.

The principal tonnage of rimmed steel is produced to analysis ranges that require

alloying additions to meet the required composition. Ferromanganese is the principal alloy used, but other alloys, such as ferrophosphorus, copper, and nickel, may be used in the production of special grades. It is not customary to use furnace deoxidizers in rimmed-steel practice, although additions of spiegel or 10 to 15 per cent ferrosilicon often are incorporated in the practice. These additions, however, are normally made long enough before tapping so that their full reboil occurs in the furnace. Table 3 shows the oxygen content of the bath before spiegel additions made 30 min. prior to tapping and also the oxygen content at tap. Included in this table are the calculated temperatures.

TABLE 3.—*Bath Conditions with Spiegel (10 Pounds per Net Ton) Added 30 Minutes before Tapping (Average 10 Heats)*

Time	Bath Analysis, Per Cent		Bath Temperature, Deg. F.
	Carbon	Oxygen	
At spiegel.....	0.056	0.072	2902
At tap.....	0.050	0.076	2951

Table 3 shows that after the use of spiegel there was an increase in the final oxygen content before tapping, associated with a decrease in carbon content, and that the temperatures increased approximately 50°F. during this period. The purpose of the spiegel reboil is not to deoxidize the steel but to raise the temperatures before tapping. The merit of this practice is that the heats can be worked down at a lower temperature and brought up to the desired tapping temperature with a spiegel reboil. As noted above, 10 to 15 per cent ferrosilicon can also be used for the same purpose. At some shops, the lower working temperature is considered advantageous from the standpoint of bank and roof conditions, and the reboil also

ensures uniformity of bath temperature when the heat is tapped.

Since a certain amount of oxygen is necessary in rimmed steel when it is poured, to obtain the necessary reactions in the mold, only a moderate amount of deoxidation is permissible in the ladle. The reaction can be considered from the standpoint of the product of carbon and oxygen in the steel as poured, relative to the product at equilibrium. In rimmed steel, for example, with a ladle analysis of 0.08 per cent carbon, the equilibrium product at 2900°F. is 0.0020. This is equivalent to $0.0020 \div 0.08$, or 0.025 per cent oxygen. The changes in oxygen and carbon values between tapping and pouring should be considered in relation to this equilibrium value. Assuming that the 0.08 per cent carbon steel has a ladle analysis of 0.36 per cent manganese, it will be necessary to add approximately 10 lb. per net ton of the 80 per cent Mn, 7 per cent C grade of ferromanganese to the ladle. This will introduce 0.7 lb. per net ton of carbon to the ladle, which is equivalent to 0.035 per cent C added. It is necessary to tap steel of this analysis at approximately 0.055 per cent carbon in the bath. This assumes that 0.01 per cent C is lost. With an oxygen content of 0.065 per cent in the bath at 0.055 per cent C, the heat when tapped has an excess of oxygen over the equilibrium value during the pouring of 0.065 to 0.025 per cent, or 0.040 per cent O. The actual excess is less than this value, since some oxygen is eliminated in the ladle. These figures give a general concept of the oxygen-carbon relations in rimmed steel, and the sequence of changes should be considered in connection with the deoxidation.

When the 7 per cent carbon grade of ferromanganese is used, there is normally an excess of oxygen present when the steel is poured. Consequently, it is necessary to add some aluminum to the ladle to correct the excess of oxygen. The amount

of aluminum may be varied with the iron oxide of the slag or the carbon content of the bath, in order to adjust it as closely as possible to the variations in oxygen content of the steel. Even when there is not an excess of oxygen, however, it is desirable to add some aluminum, since, in addition to its deoxidation effect, the formation of some aluminum oxide is advantageous from the standpoint of developing the desired rimming action. This is probably caused by the Al_2O_3 particles serving as nuclei for gas formation and thus favoring the development of rimming action during and immediately after the ingot is poured.

As an alternative to aluminum, titanium may be used and is considered advantageous by some metallurgists. In high-carbon grades of rimmed steel, ferro-carbon-titanium seems to develop a more satisfactory rimming action than aluminum. It is usually necessary to add some aluminum in the molds during pouring (irrespective of the ladle additions of aluminum or titanium) as a final means of controlling the action in the molds. The customary practice is to schedule an aluminum or titanium ladle addition, which is less than the full amount of deoxidation required, and to provide for the additional deoxidation with an aluminum addition to the molds. The aluminum addition can then be adjusted to take care of the particular conditions on each heat. The general considerations discussed above cover the principles of deoxidation practice for rimmed steel. Other combinations are used occasionally in the production of rimmed steel. For example, sodium fluoride may be added to the molds to stimulate rimming action. In general, however, the basic relation is that of carbon to oxygen when the steel is poured, and this should be considered in establishing the bath condition at tap and the type of ladle and mold additions for all grades of rimmed steel.

DEOXIDATION OF KILLED STEEL

The objectives of deoxidation of killed steel are to remove as much oxygen as possible and to have the remaining oxygen present in the form of stable oxides. Under these conditions, no reaction takes place between carbon and oxygen after the steel is poured into the molds, as described for rimmed steel. Consequently, the steel solidifies without the formation of carbon monoxide or dioxide gas. A further objective is to render hydrogen and nitrogen inert in order to prevent the formation of gas by these elements.

The complete deoxidation of killed steel is achieved usually by the use of silicon, although often aluminum is added in conjunction with silicon, or even as the only deoxidizer if a low-silicon steel is desired. Other special deoxidizing alloys that are used contain elements such as titanium, calcium, zirconium, which have a strong affinity for oxygen. The relative deoxidizing power of these alloys has been discussed in the foregoing pages. The relation between their concentration and the residual oxygen content is shown in Fig. 1.

Many of the deoxidizing additions are made both to obtain the deoxidizing effect of their alloys and also because the presence of certain amounts of the alloys are a part of the requirements for the finished steel. Alloys such as silicon and manganese normally function in this dual role, whereas alloys such as aluminum and titanium are more often added only for the deoxidizing effect. If a sufficient amount of these alloys is added, however, to provide an excess over that combined with the oxygen, the excess functions as an alloy and affects the physical properties of the steel.

Other alloys, such as chromium and vanadium, could function as deoxidizers, since they have a stronger affinity for oxygen than iron. These alloys are always used in conjunction with stronger deoxidizers, however—for instance, silicon with

chromium, and silicon and aluminum with vanadium—so that they are not combined with oxygen and consequently are free to function according to their alloying effect. There is another series of alloys, represented by nickel, copper, molybdenum, and cobalt, which do not combine with oxygen in steel, and consequently are always used for their alloying effect.

For killed steel, the deoxidizing and alloying additions may be added to the furnace or ladle, or at both points. The wide variety of practice with respect to the bath additions is demonstrated by a questionnaire sent to a number of steel producers to determine the types of practice used for different grades of steel.⁴ An example of the variety of practices in use for only one grade of steel is shown in Table 4.

TABLE 4.—*Types of Bath Deoxidation for Killed Steel*

ANALYSIS RANGE: C = 0.40–0.50;

MN = 0.60–0.90; SI = 0.10–0.25

BATH ADDITIONS	NUMBER OF PLANTS USING PRACTICE
Silicon pig and ferromanganese..	4
Spiegel, silicon pig and ferromanganese.....	2
Spiegel and ferromanganese.....	2
Silicomanganese.....	1
Spiegel, silicomanganese and ferromanganese.....	1
Silicospiegel.....	1
Ferromanganese.....	1

It can be assumed that with seven different types of bath-deoxidation practice used for the same grade, this feature of deoxidation cannot be particularly critical from the standpoint of the quality of the finished product. These different practices presumably have been established by the various plants for analysis control and economic reasons as well as for their merits as deoxidizers.

Under satisfactory conditions, it is

probable that all of the standard ferroalloys used as furnace additions can function adequately as deoxidizers. The effect of the carbon content on the percentage of oxygen in the bath prior to deoxidation should always be considered in connection with deoxidation procedures. The weaker deoxidizers, such as spiegel or ferromanganese, will not decrease the oxygen content of the steel to as low a percentage as would be obtained with the silicon-bearing alloys. Under certain operating conditions, especially in the presence of appreciable percentages of carbon, the situation may arise where small additions of manganese and even silicon-bearing deoxidizers do not effect any appreciable oxygen elimination.

The relation of the various furnace-deoxidation practices to the type and distribution of inclusions is not well established, and would justify further investigation. It is a difficult relation to study, for the effects of other variables, such as temperature, reoxidation during tapping and pouring, pouring practice and ingot size, are all factors that influence the inclusion content, and in the correct combinations probably have more influence than does the furnace deoxidation.

The furnace deoxidation practice must be properly controlled in order to obtain satisfactory deoxidation and alloy recoveries. Irrespective of the merits of furnace deoxidation as related to the final inclusion content, it serves a useful function by increasing the alloy recoveries from subsequent additions to the furnace and ladle. The effect of two types of furnace deoxidizers are shown in Fig. 3 and 4. In Fig. 3 it is shown that the maximum deoxidizing effect occurs 15 minutes after the addition, and the maximum manganese recovery is obtained at about the same time. The tapping time should be considered in conjunction with the deoxidation period, however, and assuming that this may take from 5 to 10 min., it would be

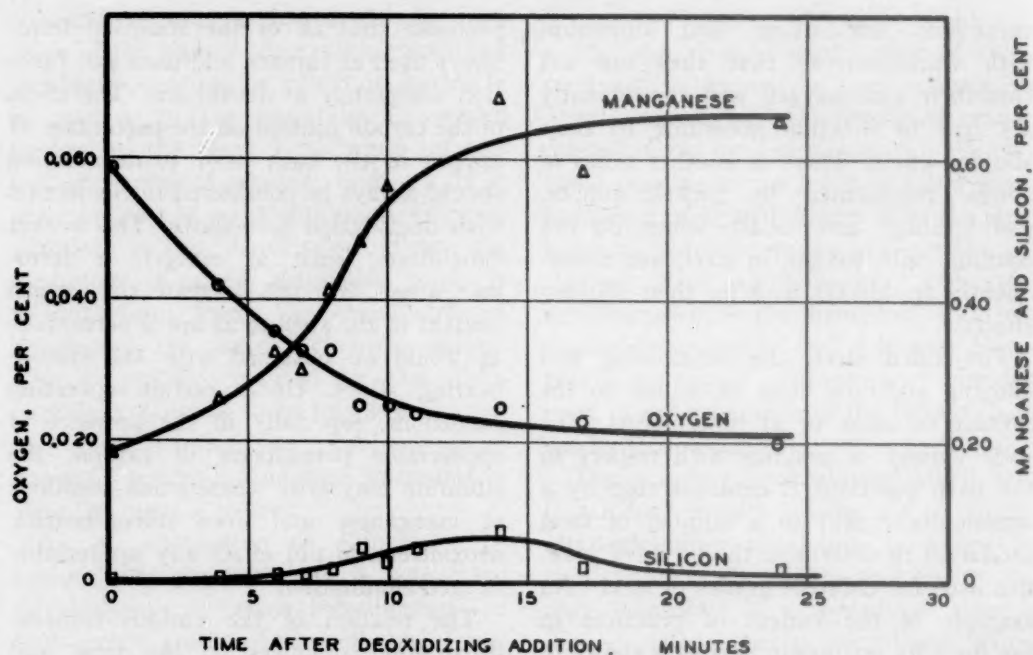


FIG. 3.—CHANGES IN BATH ANALYSIS AFTER DEOXIDATION WITH SILICOMANGANESE (20 POUNDS PER NET TON OF INGOTS).
Bath carbon 0.09 per cent at 0 minutes.

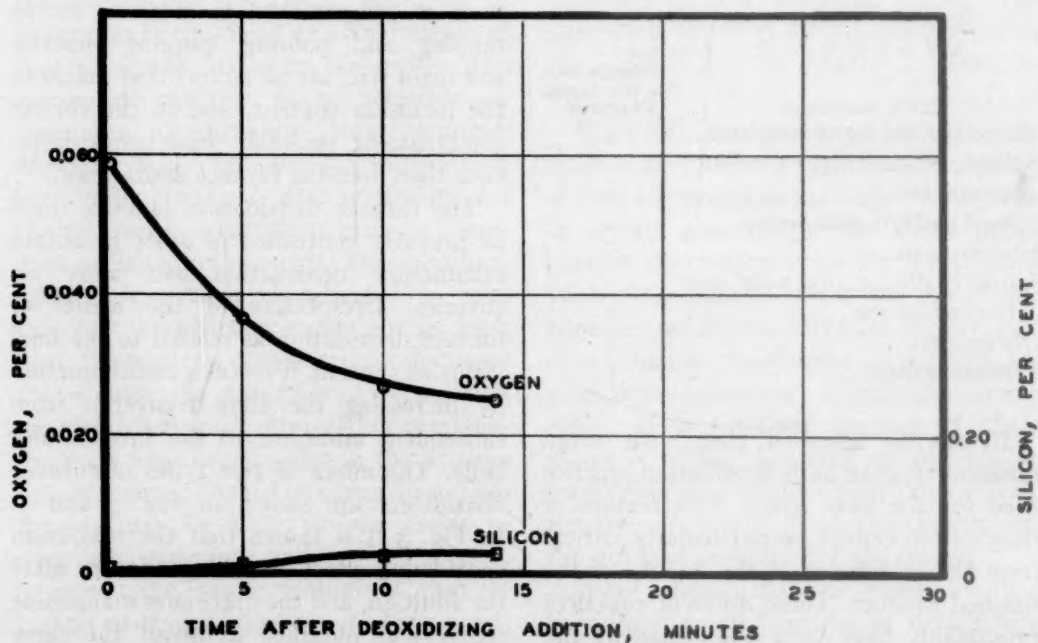


FIG. 4.—CHANGES IN BATH ANALYSIS AFTER DEOXIDATION WITH 15 PER CENT FERROSILICON (20 POUNDS PER NET TON OF INGOTS).
Bath carbon 0.06 per cent at 0 minutes.

desirable to tap this type of heat 10 min. after the silicomanganese addition.

The effect of a 15 per cent ferrosilicon addition on the bath composition is shown in Fig. 4. The time for deoxidation is approximately the same as with silicomanganese. There are also maximum time limits, which should be considered in connection with furnace deoxidation practice, since the bath is subject to reoxidation by the slag. It is customary to cut off the fuel for an interval when making the furnace additions, so as to chill the slag, as the increase in viscosity of the slag when it is cooled tends to prevent the transfer of oxygen to the bath. The temperature effect may be supplemented by adding burnt lime, coke, or graphite to the slag.

DEOXIDATION OF SEMIKILLED STEEL

The term semikilled is used to classify steel with characteristics intermediate between the rimmed and killed types. The ingot structure of semikilled steel has a certain similarity to that of rimmed steel, since it is poured in open-top molds and usually has blowholes or gas pockets near the surface and in the upper central part of the ingot. The absence of rimming action, however, prevents the formation of the rim and core zones that are characteristic of rimmed-steel ingots, and consequently the general structure is similar to that of killed steel. The well-defined segregation pattern of rimmed steel is not present in semikilled steel, but usually a greater degree of segregation is shown than in the killed type.

The objective of deoxidation of semikilled steel is to decrease the oxygen content below the point where rimming action will occur in the molds, but to allow enough to remain in the steel to permit the formation of some gas during solidification. The evolution of gas, which forms internal blowholes and gas pockets, partly compensates for the shrinkage

during solidification, and consequently reduces the volume of the pipe cavity. This is a similar condition relative to the pipe cavity that occurs in rimmed steel. In killed steel, in which the evolution of gas is usually suppressed, the full shrinkage resulting from solidification is present, but the pipe cavity is limited to the hot top portion of the ingot.

It should be noted that there is a considerable variety of ingot structures that can be classified as being of the semikilled type, according to the definition given above. The structure depends on the steel composition and the degree of deoxidation. In some grades, particularly those in the lower carbon range of which the deoxidation is completed in the molds, the ingot structure verges on the rimmed type. At the other extreme, characterized by the higher carbon grades and more completely deoxidized low-carbon grades, the ingot structure may have characteristics similar to those of killed steel. In such grades, the pipe cavity is welded during rolling, so that usually a relatively sound product can be obtained without the use of a hot top. There will normally be more segregation in these grades, however, as compared with killed and hot-topped steel.

The deoxidation of semikilled steel is done usually in the ladle and molds, although furnace additions may be made for some grades. The common deoxidizing alloys are silicon, aluminum, and titanium. The amounts added depend on the carbon and manganese content of the steel and the ingot structure that is desired. If silicon is used as the principal deoxidizer, it may be added as a scheduled addition or to meet a certain ladle analysis. The silicon content of the steel usually is specified to ranges lower than the 0.10 to 0.20 per cent or 0.15 to 0.30 per cent silicon ranges characteristic of killed steel. As an example, semikilled structural steel deoxidized with silicon may finish

within the range of 0.03 to 0.08 per cent Si. For aluminum or titanium deoxidation, these additions usually are made to the ladle according to established schedules. The practice with all of these alloys may also involve final deoxidizing additions to the molds, and in this case aluminum is usually added, although ferrosilicon fines may also be used.

RELATION OF SEGREGATION TO DEOXIDATION

The relation of deoxidation to ingot segregation should first be considered from the standpoint of the three general types of steel—rimmed, semikilled, and killed. In this series the greatest amount of segregation occurs in the rimmed type of steel, and the minimum amount in the killed type, the semikilled showing intermediate characteristics. Since the type of steel is determined by the degree of deoxidation, these three types demonstrate that the general relation between the degree of deoxidation and segregation in the ingot is an inverse one. In other words, an increase in the degree of deoxidation leads to a decrease in the amount of ingot segregation. This relation is true when considering the three types, but is not always valid when considering any one type.

The solidification characteristics of rimmed steel, with the resultant ingot structure of the rim and core zone favor segregation. During the formation of the rim zone, the higher-melting-point constituent, iron, solidifies in preference to the lower-melting-point constituents, which are concentrated in the liquid adjacent to the solidifying metal. During the rimming period, there is a continuous movement of the liquid metal, which removes the low-melting-point constituents from the liquid-solid interface, and this action causes the rim zone to be higher in iron content than the melt.

In the discussion of deoxidation of rimmed steel, it was pointed out that an

increasing degree of deoxidation was associated with a decrease in the rate of gas formation, and consequently there would be less action or movement of the liquid metal along the solidifying wall during the rimming period. Since the composition of the rim zone is related to the movement of metal at the solid-liquid interface, the decrease in this movement associated with an increase in deoxidation would be expected to decrease the amount of segregation. In general, this relation is confirmed by studies of rimmed steel. If heats with the same carbon are considered, the heats that have a strong rimming action will generally have a lower sulphur analysis in the rim zone, with a resultant higher analysis in the core zone, than heats with weak rimming action. Another consideration is the ratio of rim to core-zone thickness, since, with an increase in the volume of the rim zone relative to the core zone, there will be a greater amount of low-melting-point constituents concentrated in the reduced core zone.

The killed type of steel, as previously defined, is almost completely deoxidized and the action of the metal resulting from the formation of gas does not occur in the molds. Consequently, the amount of segregation is not affected by this factor and is considerably less in killed steel than in rimmed steel. The segregation that does occur may vary slightly with the degree of deoxidation, but probably this is a minor variable as compared with steel temperature and ingot size and type. An example of the segregation characteristics of fine-grained as compared with coarse-grained steel, the former representing a higher degree of deoxidation with aluminum, was cited by Tenenbaum⁵ as showing no significant differences in the amount of segregation. A study of the segregation characteristics of 2.00 per cent silicon spring steel as compared with the 0.25 per cent silicon grade has likewise shown that the difference in silicon content has

no appreciable effect on the amount of ingot segregation.

The segregation characteristics of semi-killed steel have a greater similarity to the killed than the rimmed type. The amount of segregation in semikilled steel, however, may be much greater than in killed steel. In general, the amount of segregation decreases with increasing deoxidation, but the variables of steel temperature and mold size and type are major factors, so that it is difficult to evaluate the deoxidation factor.

RELATION OF DEOXIDATION TO AUSTENITIC GRAIN SIZE

In the discussion of objectives, it was pointed out that the austenitic grain size, which is usually measured by the McQuaid-Ehn test, is controlled by the deoxidation practice. The control of grain size usually is accomplished by the use of aluminum, either alone or in conjunction with other deoxidizing alloys. The grain size is related to the amount of aluminum present in the steel after solidification, as shown in Table 5. The tests in this table

TABLE 5.—*Relation of Total Aluminum Content to McQuaid-Ehn Grain Size*

Group	Number of Tests in Group	Total Aluminum, Per Cent	Fine Grain Tests, Per Cent
A	7	Under 0.005	14
B	68	0.005-0.010	29
C	42	0.010-0.014	52
D	58	0.015-0.030	100

were classified as fine (5-8) or coarse (1-5) in accordance with the standard McQuaid-Ehn procedure. There are usually more than one test per heat and in some cases both coarse and fine grain tests occur in the same heat. In such cases, the coarse-grained tests usually come from the latter part of the heat. The results of this tabulation show that if the aluminum content is over 0.015 per cent, the tests were always fine grained and that the percentage of

fine-grain tests decreased rapidly as the aluminum dropped below this figure. In group A, the 14 per cent figure probably is not representative of the grain size normally obtained with aluminum contents under 0.005 per cent, and more data probably would show a lower percentage of fine-grain tests. The value of 0.015 per cent aluminum appears to be almost independent of the carbon content or the amount of other deoxidizers present, although there is some evidence that the probability of obtaining fine-grained steel when the aluminum content is less than 0.015 per cent increases with increasing carbon content or when the steel is fully killed with silicon.

The aluminum values given above are based on the analysis of the finished steel, and the aluminum additions made to the ladle are variable and depend on the deoxidation practice. In Table 6 are shown representative values for the aluminum efficiency, or recovery under different

TABLE 6.—*Effect of the Weight of the Addition and the Carbon Content on Aluminum Recoveries*

Group	Carbon, Per Cent	Weight of Aluminum Added, Lb. per Net Ton Ingots	Aluminum Recovery, Per Cent
I	0.09	2.4	30
	0.09	5.1	58
II	0.16	0.9	26
	0.46	0.5	34
	0.90	0.8	44

conditions. This table shows that the amount of aluminum recovered in the finished steel increases with the amount added and with the carbon content of the steel. This relation would be expected, since a larger proportion of the aluminum is lost in smaller additions, and the higher oxygen content of steel in lower carbon ranges will always result in a greater loss of aluminum. In establishing a deoxidation practice for the control of grain size, it is thus necessary to consider both the final

aluminum content and the aluminum efficiency, in order to determine the amount of aluminum to be added.

minum had grain-coarsening temperatures under 1650°F. The next test, with 0.008 per cent aluminum, had a grain-coarsening

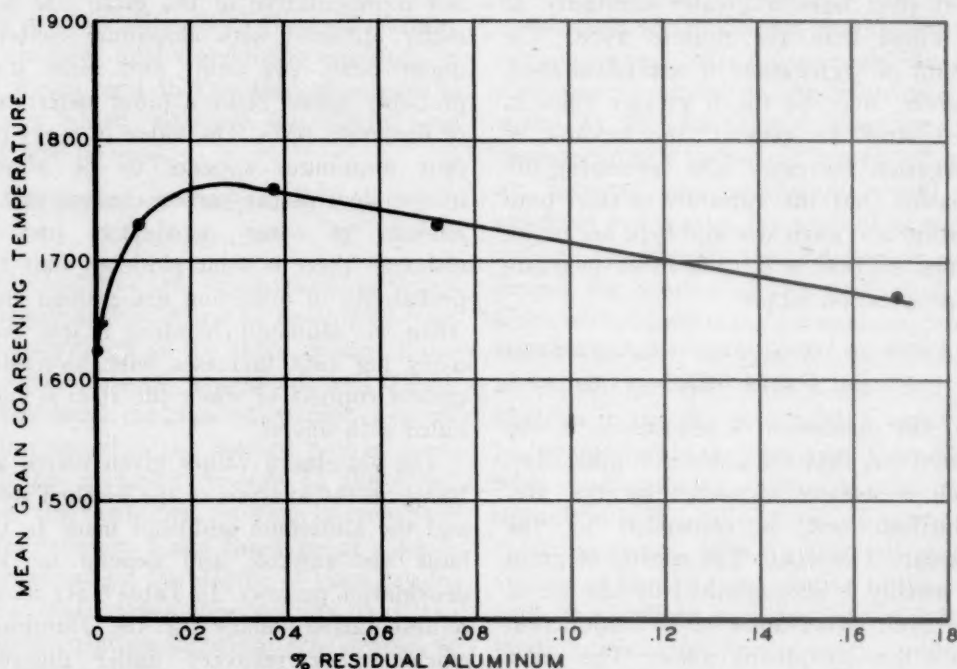


FIG. 5.—EFFECT OF RESIDUAL ALUMINUM ON GRAIN-COARSENING TEMPERATURE OF S.A.E. 1030 STEEL.

Another feature that should be considered in connection with the use of aluminum to control grain size is the relation between the amount of aluminum and the grain-coarsening temperature. As noted, the grain size usually reported is the one determined by the McQuaid-Ehn test, which represents the austenitic grain size of the steel carburized for 8 hr. at 1700°F. The basic relation, however, is that between the aluminum content and the grain-coarsening temperature. In Fig. 5 an example is given of the change in grain-coarsening temperature with the aluminum content. The tests shown in this figure were obtained by adding progressively larger additions of aluminum to the molds when pouring a heat to which no aluminum was added in the ladle. The tests that contained less than 0.003 per cent alu-

minum had grain-coarsening temperatures under 1650°F. A maximum grain-coarsening temperature was reached with 0.025 per cent residual aluminum. Further increases in aluminum resulted in a downward trend in the grain-coarsening temperature, so that the tests with aluminum content of 0.170 per cent had a grain-coarsening temperature of 1670°F. and consequently would be classified as a coarse-grained steel by the McQuaid-Ehn test. Only a limited amount of work has been done on the relation of grain-coarsening temperature to deoxidation practice, but this relation is probably more significant than that obtained by making the McQuaid-Ehn test. There is also evidence that the grain-coarsening temperature and the aluminum content should both be considered when studying the difference in physical properties of coarse-grained and fine-grained steel.

SUMMARY

This paper has surveyed some of the more obvious factors involved in the deoxidation of basic open-hearth steel. It was the purpose of this survey to review some of the objectives of deoxidation, to present some of the considerations that determine the selection of any specific deoxidation practice, and to relate these practices with the characteristics and properties of the final steel product. The data available on many of the more important features of deoxidation are regrettably inadequate. It is hoped that this survey will stimulate further studies of the fundamental problems associated with deoxidation.

ACKNOWLEDGMENTS

The writer wishes to express his appreciation to Messrs. M. Tenenbaum, J. W. Halley, and C. C. Brown, for their assistance in assembling many of the data and preparing the figures for this report.

REFERENCES

1. Basic Open Hearth Steelmaking, Chap. 16. New York 1944, A.I.M.E.
2. C. H. Herty, Jr.: The Deoxidation of Steel. *Coop. Bull.* 69, Carnegie Inst. of Tech., 1934.
3. M. Tenenbaum and C. C. Brown: Total Oxygen Content of Plain Carbon Open-hearth Steel during Deoxidation and Teeming. This volume, page 685.
4. Summary of Questionnaire on Deoxidation Practice. *Open Hearth Proc.*, 1944. A.I.M.E.
5. M. Tenenbaum: Discussion of Segregation in a Large Alloy-steel Ingot. This volume, page 472.

Slag-metal-oxygen Relationships in the Basic Open-hearth and Electric Processes

By J. S. MARSH,* MEMBER A.I.M.E.

(Cleveland Meeting, October 1944)

THE student of steelmaking is all too well acquainted with the fact that in many instances he must deal with data that in graphical representation exhibit the property most desirable in bird shot. This is scarcely mystifying, since the effort to establish one variable as a function of another is usually hampered by the simultaneous operativeness of two or three other factors that may be important. A large part of arriving at relationships that have the pleasing self-consistency of, say, precise measurements of thermal expansion, consists of determining what factors must be held constant—an even larger part usually consists of collecting data for which those factors have been so maintained.

It is not intended to imply that functional relationships in the physical chemistry of steelmaking are hopelessly obscure; on the contrary, it is merely necessary to be undisturbed by marked deviation of some points from a curve that otherwise makes sense. A reaction mechanism suggested by such a curve may call attention to hitherto unsuspected factors operative in the origin of the deviating points, and thus permit another step to be taken in the direction of fuller understanding. It is proposed, therefore, to suggest several empirical relationships. Even though the approach is not always rigorous, deviations caused by simplifying assumptions appear to be too small to obscure a provisional

working picture of the general behavior of oxygen in slag-metal reactions.

CARBON-OXYGEN EQUILIBRIUM

It has been appreciated for some time that the carbon-oxygen reaction in liquid steel is highly important. For example, Körber et al.,¹ in introducing a summary of their extensive work on steelmaking reactions, said: "... the far-reaching and truly dominating action of carbon upon the metallurgical reactions will be especially stressed . . ." In "Basic Open Hearth Steelmaking"* (hereafter BOHS, for simplicity), it is accepted repeatedly that the various slag-metal interactions are nearly always controlled by the carbon-oxygen reaction. Before further discussion of this reaction, however, it will be worth while to consider briefly the carbon-oxygen equilibrium.

In BOHS (p. 483) it is stated that:

When liquid iron is brought into contact with gases containing carbon monoxide it absorbs carbon and oxygen. Conversely the carbon and oxygen in the metal unite to form carbon monoxide which is evolved from the bath during the open-hearth boil or while rimming ingots are solidifying. . . . When the equilibrium pressure is one atmosphere the equilibrium-constant equation simplifies, on the assumption that the activity of each element is equal to its percentage, to a constant which has been so much used that it has acquired a special symbol m .

where

$$m = \%C \times \%O$$

¹ References are at the end of the paper.

Reprinted from *Proc. Elec. Furnace Steel Conference*, 1944. Manuscript received at the office of the Institute Aug. 8, 1944. Listed as T.P. 1921.

* Engineer, Development and Research Department, Bethlehem Steel Co., Bethlehem, Pennsylvania.

This, of course, is the equation of a hyperbola. In terms of the iron-carbon-oxygen phase diagram, it is represented schematically as the curve op in Fig. 1. Point o' is the intersection of the plane of the isothermic section with the liquid-metal plus liquid-oxide gap of the iron-oxygen diagram (about 0.23 per cent oxygen at 1600°C.); point p' is its intersection with the solubility curve of carbon in iron (about 7 per cent carbon at the same temperature). Fig. 1, although schematic, is of construction dictated by fundamental thermodynamics; therefore it is possible to predict with perfect assurance, as is implied by the location of points o and p , that the carbon cannot be removed entirely from homogeneous liquid steel by oxidation and that the oxygen cannot be removed entirely by carburization. As a first approximation, use can be made of the value of m selected on p. 534 of BOHS—viz., $m = 0.0028$, in terms of percentage oxygen—and the saturation values already cited for oxygen and carbon. Thus, minimum carbon would be

$$0.0028/0.23 = 0.012 \text{ per cent.}$$

Cleaves and Thompson³ quoted a value of 0.013 per cent carbon for a standard sample of basic-open-hearth ingot iron, but this analysis may be doubted. The agreement is probably too good to be true anyway, for the computation assumed a temperature of 1600°C., unchanged saturation oxygen in the ternary space, and precise substitutability of weight percentages for activities.

Several aspects of the matter of saturation oxygen are to be considered. In the first place, under ordinary open-hearth conditions, oxygen exceeds the equilibrium value for a given carbon content. This fact has been variously interpreted; for example, some metallurgists have felt that varying carbon monoxide pressure is responsible; others have called upon deviation from unity of the activity coeffi-

cient of carbon and/or oxygen, and so on. However, at minimum carbon content, conditions are not ordinary, because the carbon reaction can proceed no longer. In

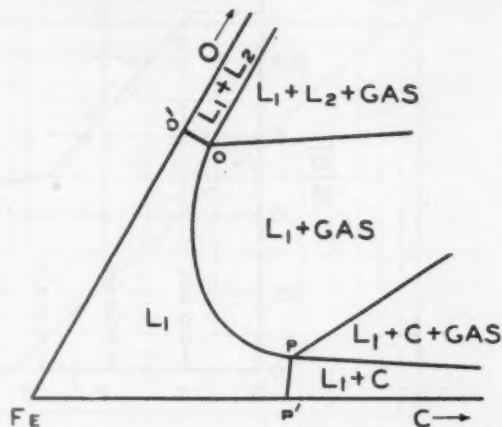


FIG. 1.—SCHEMATIC PARTIAL ISOTHERMIC (1600°C.), ISOBARIC (1 ATM.), SECTION OF THE IRON-CARBON-OXYGEN DIAGRAM.

the second place, basicity of lime-silica-iron oxide slags has an effect on metal oxygen content in the absence of carbon reaction; this is demonstrated clearly by Fig. 2, which was plotted from data of Fetters and Chipman,⁴ on heat E15, and which shows oxygen content of low-carbon iron as a function of lime-silica ratio. Assuming a lime-silica ratio of 2.3, a metal oxygen content of about 0.15 per cent is indicated or

$$0.0028/0.15 = \text{about } 0.02 \text{ per cent carbon.}$$

This value is altogether consistent with open-hearth experience. The lower value of 0.012 probably is more nearly correct for iron in contact with pure iron oxide, however. Incidentally, an implication of Fig. 2 is that lower minimum carbons should be possible in both the acid open hearth and bessemer than in the basic process.

Another possible way of arriving at minimum carbon is through extrapolation of rate of carbon drop ($d[C]/dt$) as a function of carbon content $[C]$ to $d[C]/dt = 0$. To test this, and to exclude as many disturbing factors as possible, logs for four consecutive 135-ton heats on the same

furnace with identical scrap and hot-metal charges were selected. Carbon-drop curves were drawn, then tangents at various

in Fig. 3. The values for two heats were identical at 0.20 and 0.30 per cent carbon and further appeared to lie on a smooth

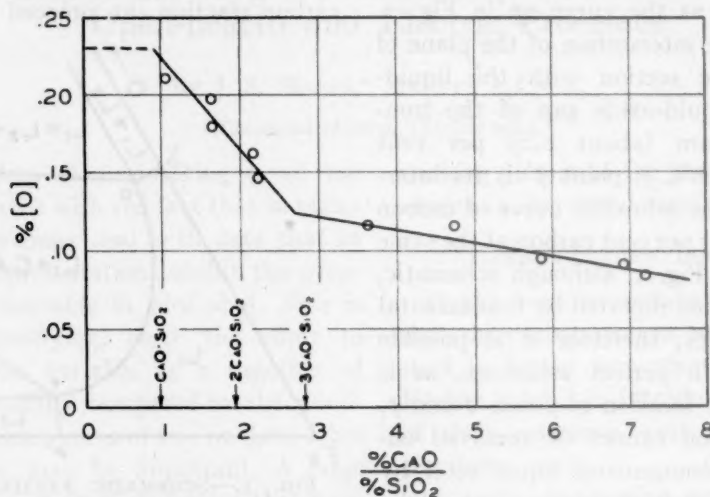


FIG. 2.—OXYGEN CONTENT OF LOW-CARBON IRON AS A FUNCTION OF BASICITY OF LIME-SILICA-IRON OXIDE SLAGS.

Plotted from data of Fetters and Chipman.⁴

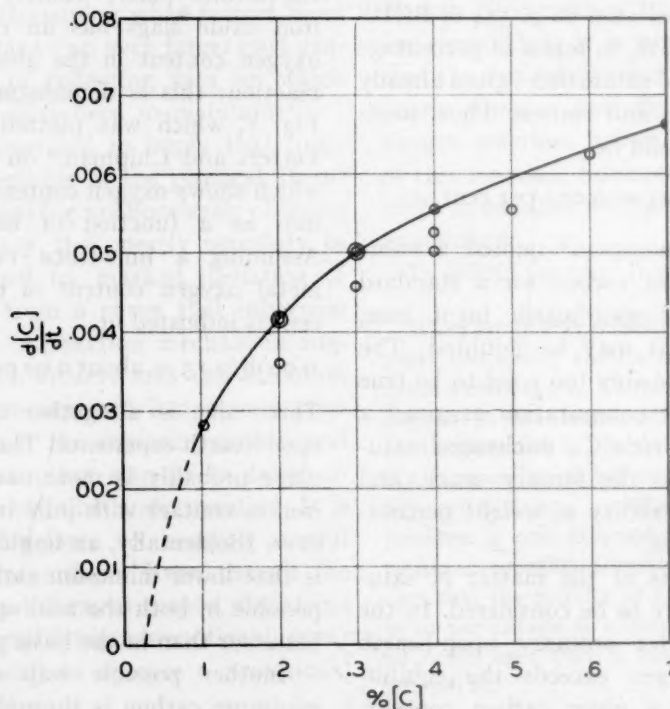


FIG. 3.—RATE OF CARBON DROP AS A FUNCTION OF CARBON CONTENT.
Data from four consecutive open-hearth heats.

points were determined and expressed as percentage carbon per minute. These were plotted against carbon content, as shown

curve connecting the uppermost points; consequently, such a curve was drawn from 0.10 to 0.70 per cent carbon. An additional

reason for selecting the uppermost points is that it may be assumed provisionally that the highest rates of carbon drop so indicated are consistent with more efficient

would be proportional to the amount of carbon present; i.e.,

$$\frac{d[C]}{dt} = k[C]$$

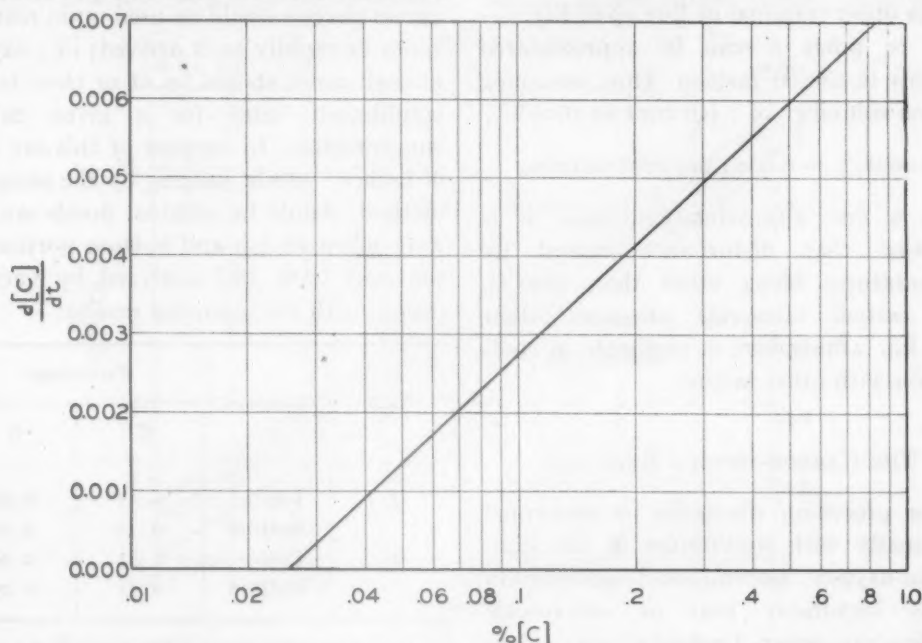


FIG. 4.—RATE OF CARBON DROP AS A FUNCTION OF LOGARITHMIC CARBON CONTENT.

working of the heats by the furnace operators. The form of the curve immediately suggests a logarithmic relationship; consequently, the curve is so replotted in Fig. 4. There is no doubt, at least for the selected heats, that rate of carbon drop was a linear function of the logarithm of the carbon content. This makes it possible to extrapolate to zero carbon drop with some confidence. The minimum carbon content so found is 0.025 per cent—a value gratifyingly consistent with the others, considering the fact that the open-hearth process is not isothermic. It is well known that increasing temperature increases the rate of carbon drop* and it may be this fact that caused the rate of carbon drop observed to be a logarithmic function. By analogy, it seems reasonable to suppose that, at constant temperature, and other things being constant, the rate of carbon drop

where k is the velocity constant of the reaction and t is time. The isothermic carbon-drop curve is given by the integrated form

$$\ln[C] = kt$$

This curve seems to be close enough to the truth for the low-carbon range in which bath temperature is often substantially constant, although it indicates too rapid drop in the high-carbon range. But the temperatures of the bath during passage through the high-carbon range is usually lower than through the low-carbon range; hence, the velocity constant is smaller. The effect of temperature on such constants is given by an equation of the form

$$k = k_0 e^{-\frac{A}{T}}$$

which implies that $\log k$ is proportional to reciprocal absolute temperature. This is the origin of the suggestion that temperature change in the course of a heat is the

* See, for example, Oelsen's discussion in reference 1.

cause of the experimentally found dependence of $d[C]/dt$ upon $\log [C]$.

Before proceeding to other aspects of the matter of carbon drop, the coordinates of the other terminal of line op of Fig. 1—that is, point p —can be approximated roughly in similar fashion. Thus, assuming carbon solubility of 7 per cent at 1600°C ,

$$0.0028/7 = 0.0004 \text{ per cent oxygen.}$$

As a first approximation, then, it is assumed that disturbance caused by temperatures being other than 1600°C . and carbon monoxide pressures other than one atmosphere is negligible in comparison with other factors.

THE CARBON-OXYGEN REACTION

The preceding discussion is concerned principally with *equilibrium* in the iron-carbon-oxygen system, and equilibrium means inexorably that no macroscale reaction can occur. Under ordinary open-hearth conditions, however, the fact that the carbon-oxygen reaction does proceed is sufficient proof that the system is not in equilibrium; consequently—even in the absence of oxygen analyses—it would be proper to conclude that, at a given carbon content, oxygen must be present in excess of the equilibrium value. That this is true has been shown repeatedly by experiment; furthermore, the excess oxygen tends to be constant for a given set of conditions, such as type of charge, and absence of bottom or lime boils, or recent ore additions. These matters were discussed and demonstrated by Larsen,⁵ who stated that:

The usual zone in which the carbon reaction proceeds toward completion by evolution of CO is not the slag-metal interface (as for the other reactions) but the surface of the bubbles, which begin to form only at the surface of the solid bottom or hearth. The reaction can proceed only as fast as carbon and oxygen move to these surface zones by diffusion or convection.

There is ample evidence that the carbon reaction is virtually instantaneous as compared with, say, the diffusion of oxygen. It may be concluded, then, that excess oxygen would be used up in reaction zones as rapidly as it arrived; i.e., oxygen in such zones should be at or close to the equilibrium value for a given carbon concentration. In support of this are data of Leiber,⁶ which, judging by the sampling method, should be reliable. Bomb samples were taken at top and bottom portions of the steel bath and analyzed by vacuum fusion, with the following results:

Heat	Location	Percentage	
		C	O
J	Top	0.31	0.013
	Bottom	0.31	0.008
K	Top	0.51	0.009
	Bottom	0.51	0.005

Oxygen contents at the bottom of the bath agree with computed equilibrium values well within the precision of measurement, whereas those at the top are materially in excess. The notion that the carbon reaction is ordinarily initiated on solid surfaces thus gains weight and it follows that the oxygen content found for a given carbon content depends upon the depth at which the sample is taken. (The interesting laboratory-crucible experiments of Körber and Oelsen⁷ are described briefly in the aforementioned paper of Larsen.⁵ Another interesting statement was made by Schwarz in discussion of the previously cited summarizing paper of Körber et al.:¹

The crucible experiments of Oelsen may be traceable to the same phenomenon which we observe in practice when stirring heats with slagged and unslagged rabbles. The former do not cause the heat to boil, whereas the latter produce a vigorous reaction.

The foregoing prompts some additional remarks on the carbon reaction. The form

of the equation for rate of carbon drop ($d[C]/dt$) found for *one* furnace, admittedly, is $d[C]/dt = a \log [C] - b$, where a is the slope of the line and b is the intercept.

driving the carbon reaction forward is worth still further examination. Some investigators feel that the constancy of excess oxygen is no longer valid in the

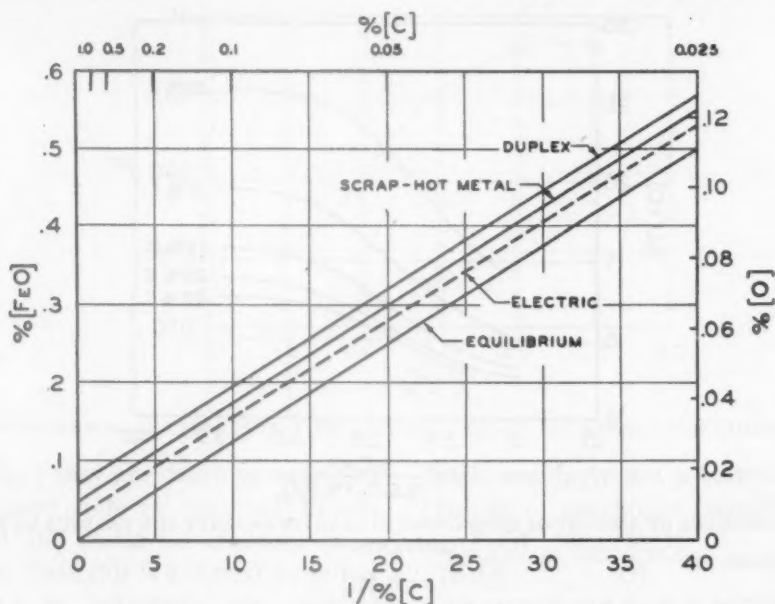


FIG. 5.—METAL OXYGEN COMPUTED TO FERROUS OXIDE AS A FUNCTION OF RECIPROCAL CARBON CONTENT FOR SEVERAL CONDITIONS.

The intercept is the carbon value of point a of Fig. 1, which, though not constant except for constant conditions, is sufficiently so (say 0.02 per cent carbon on the average) to be ignored. The factor of interest then becomes the slope a and it is suggested that in this term are lumped all such items as physical characteristics of the furnace (such as depth of bath and thermal efficiency), type of charge, presence or absence of unreacted ore, presence or absence of lime or bottom boils, and so forth. In other words, slope a includes all items that affect the rate of supply of oxygen. More data are needed to be sure that even the form of the carbon-drop equation is correct; however, it is difficult to avoid the conclusion that the mechanism of the carbon reaction is simple and that the necessary information is separable from the disturbing factors.

In concluding this part of the discussion, the matter of excess oxygen necessary for

low-carbon ranges—say under 0.10 per cent. It is suggested that this feeling arose in part over the increasing effect of analytic error as carbon decreases toward the lower limit and that the data are satisfied equally well by assuming no changed behavior in the low-carbon ranges. This assumption is illustrated graphically in Fig. 5, in which oxygen (in terms of FeO) is plotted against reciprocal carbon concentration. Strictly speaking, of course, these lines terminate in points corresponding to a and b of Fig. 1; however, inasmuch as there is little interest in limiting cases, the fictitious terminals seem permissible. The lowermost line, representing equilibrium, assumes ideal behavior—i.e., activity coefficients of unity—and substitutability of weight percentages for mol fractions. The upper lines are averages, taken from the literature, for several standard processes, and arise, it is assumed here, entirely out of the fact that they are able to supply oxygen to the metal

at different rates. Variations for a given process are possible; for example, the broken line shown for the electric process under oxidizing conditions might be repre-

CARBON REACTION AND SLAG IRON OXIDE

It is widely recognized that bath carbon content and slag basicity affect iron-oxide content of the slag. An empirical attempt

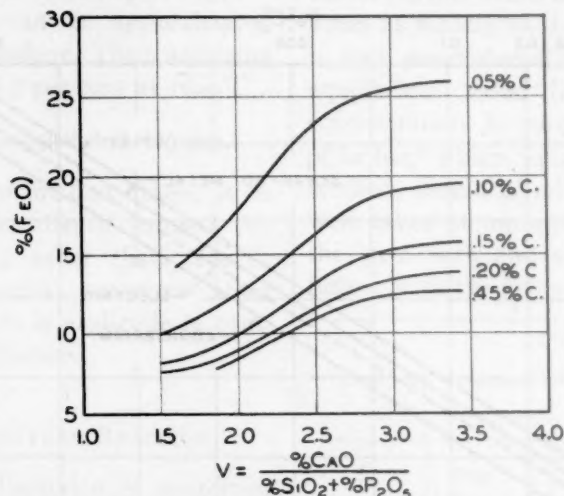


FIG. 6.—DEPENDENCE OF AMOUNT OF IRON OXIDE IN SLAG ON BASICITY FOR VARIOUS METAL-CARBON CONTENTS.²

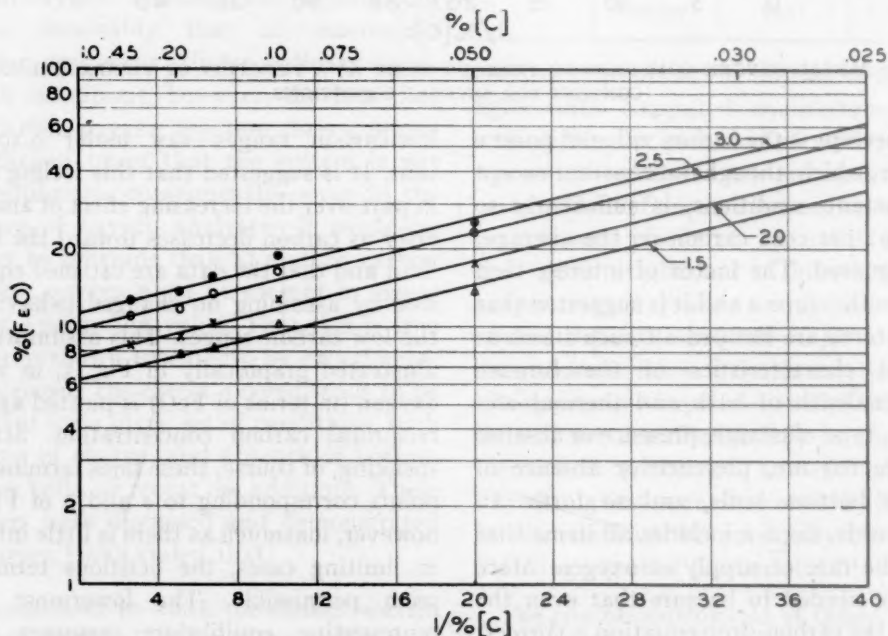


FIG. 7.—LOGARITHMIC SLAG IRON OXIDE AS A FUNCTION OF RECIPROCAL CARBON CONTENT OF THE METAL FOR SEVERAL LIME-SILICA RATIOS.

sentative for a shop whose aim is close melt carbon, whereas the line for a shop charging excess carbon and ore might approach that for the conventional scrap-hot metal open-hearth charge.

to summarize this fact is made in BOHS, p. 509, and reproduced in Fig. 6; slag ferrous oxide is plotted against lime-silica ratio in a family of constant-carbon curves. Repeated comparison of our data with these

curves confirmed their essential correctness; consequently, they are accepted here. However, it is felt that their story is more illuminating if presented in another way;

Repeated attempts have been made to establish distribution ratios of slag iron oxide (FeO) and metal oxygen [O] or [FeO], such as $[O]/(FeO)$ or $(FeO)/[FeO]$, but

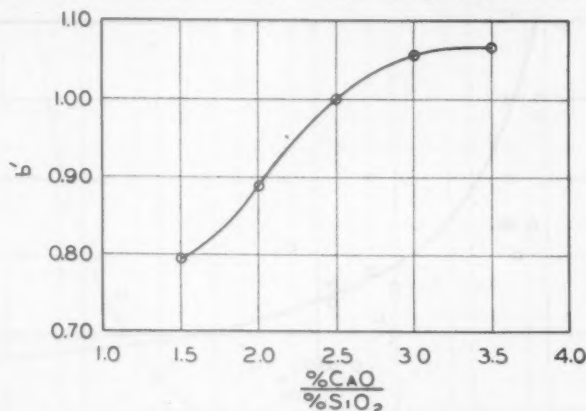


FIG. 8.—DEPENDENCE OF INTERCEPT b' OF SLAG-IRON-OXIDE EQUATION UPON LIME-SILICA RATIO.

thus, in Fig. 7 they are shown as logarithm of slag ferrous oxide vs. reciprocal carbon content of the metal for constant lime-silica ratio. That this is a correct empirical relationship is indicated; the greatest deviation shown is at 0.10 per cent carbon. Even these points, however, would lie on the straight lines if they really represent 0.09 per cent carbon; considering the nature of the data upon which the original curves are based, it must be concluded that they are remarkably self-consistent. (The terminals of the lines are again fictitious.) In this connection, entirely self-consistent ferrous oxide values can result only as averages of a large number of values, since there is an oxygen gradient through the slag, as was proved by Herty et al.⁸

The form of the equation of the family of straight lines is

$$\log (FeO) = \frac{a'}{[C]} + b'$$

The slope a' in this instance is 0.0185. It will be recognized at once that, excepting the logarithm, the form of the equation is identical with that for the reaction of carbon and oxygen (or, its noncommittal equivalent, FeO), in liquid iron, viz.,

$$[FeO] = \frac{a''}{[C]} + b''$$

this is seemingly not a correct procedure. The only conclusion possible is that $\frac{\log (FeO)}{[FeO]}$ or $\frac{\log (FeO)}{[O]}$ is constant for the same process and slags of constant basicity. It may be assumed that the slopes a' and a'' are constant and that determining factors are the intercepts b' and b'' . Intercept b'' is intimately connected with the process and with those other items that are lumped in the slope of general carbon-drop equation. Intercept b' is a function of slag basicity—or, in other words, of slag constitution. Since the intimate details of constitution have not yet been worked out, the variation of b' with lime-silica ratio as determined empirically is shown in Fig. 8 without comment.

The implication of the $\frac{\log (FeO)}{[FeO]}$ relationship is that there is no distribution of oxygen between slag and metal under working conditions in the sense that is true of other substances such as manganese (or manganese oxide); it arises out of the fact that carbon is such a potent controller of oxygen. It is this fact, as has been recognized by others, that is responsible for the very definite approach to equilibrium distribution of those other

substances in the later stages of an open-hearth heat.

Another implication is that, for a given set of conditions, slag ferrous oxide is

factors. In this instance, the marked negative deviation of the points from the curve is interpreted to mean merely that these heats were so worked, or the furnace

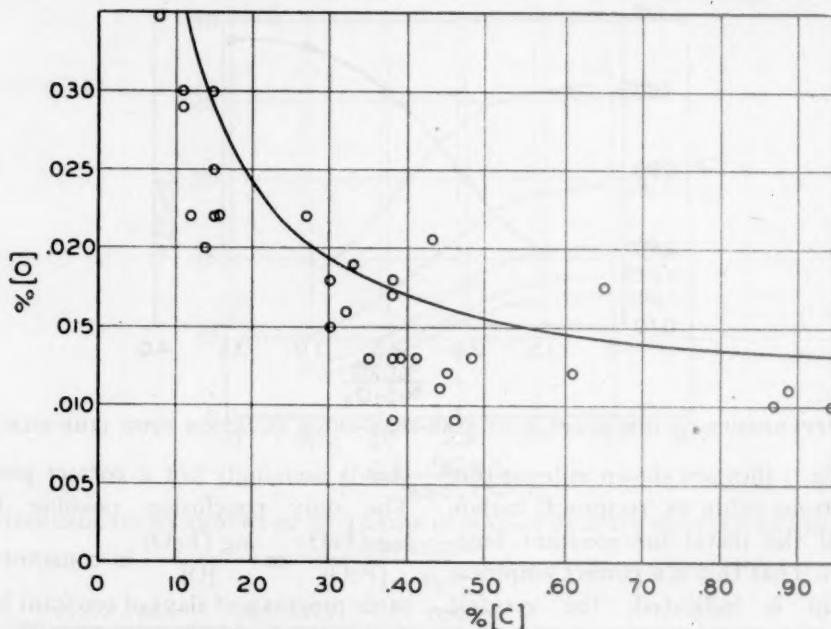


FIG. 9.—OXYGEN-CARBON DATA FOR ELECTRIC-FURNACE OXIDIZING PERIOD COMPARED WITH OPEN-HEARTH AVERAGE CURVE.

least for the greatest rate of carbon drop, since the oxygen is then consumed fastest. This is equivalent to the electrical analogy of the largest potential drop for the greatest flow of current through a given resistance.

BEHAVIOR OF OXYGEN IN THE BASIC ELECTRIC FURNACE

In the conventional two-slag process there is no essential difference of behavior of oxygen during the oxidizing period from that in the open hearth. Oxygen as a function of carbon concentration for a number of electric heats is shown in Fig. 9, with the average open-hearth curve for comparison. Although not intended to represent the electric-furnace data, it appears that the curve approximates the upper limit of the oxygen range. The scatter is of no consequence, since the amount by which oxygen exceeds the equilibrium value depends on a number of

characteristics were such, that the rate of carbon drop was less than that obtaining on the average in the open hearth. As is true of the open hearth, it is futile to seek an equilibrium distribution of oxygen between slag and metal, because the carbon reaction is the controller.

Under the finishing slag, however, conditions differ from those existing under oxidizing slags, in that there is insufficient oxygen potential to cause the transfer of oxygen from slag to metal. In the absence of addition of a deoxidizer such as silicon or aluminum, it appears that oxygen in excess of equilibrium is consumed by reaction with carbon (to the extent of a loss of carbon of the order of 0.01 per cent or less) and that equilibrium is attained or approached closely. Experimental data are given in Fig. 10; on the whole, the points agree with the selected equilibrium curve within the precision of measurement

(vacuum fusion of aluminum-killed bomb samples) and considering the fact that no effort has been made to correct for such factors as content of other elements and temperature.

A further word on finishing slags may be in order, however. Iron oxide content is often used as a criterion of maturity of such slags and an indication of degree of oxidation of the metal; the latter cannot

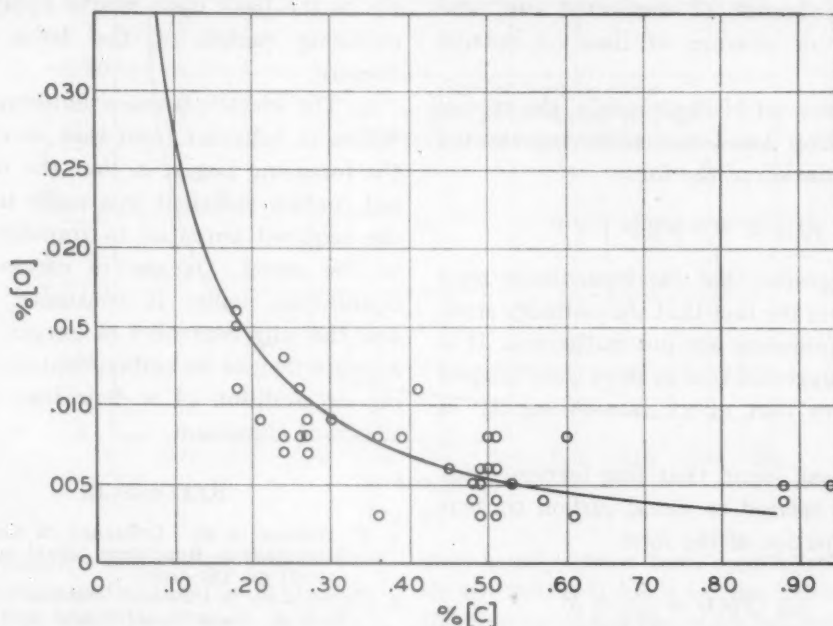


FIG. 10.—OXYGEN-CARBON DATA FOR THE ELECTRIC FURNACE FINISHING PERIOD COMPARED WITH EQUILIBRIUM CURVE.

Assuming, provisionally at least, that equilibrium is attained, the matter of rate of approach arises. Although incomplete, available data indicate that the drop is accomplished ordinarily in a matter of a few minutes. The problem is somewhat obscure, because it takes time to get the metal under cover of a shaped-up slag. Furthermore, the oxygen will sometimes refuse to fall for a considerable time. The explanation for this might be that unusual amounts of iron oxide are sometimes absorbed by the furnace bottom during the oxidizing period, then returned to the bath during the finishing period.

As implied already, all knowledge of the behavior of oxygen in the open hearth is applicable to its behavior in the electric furnace; there appears to be no need to have one set of data for the open hearth and another for the electric furnace.

follow, according to the iron oxide-oxygen-carbon relationship already discussed. The deduction that high slag iron oxide does not mean high metal oxygen, and vice versa, is substantiated by practical experience.

SUMMARY AND CONCLUSIONS

1. In this study of slag-metal-oxygen relations it is assumed that the carbon-oxygen product in the metal is exceeded, on the average, only when the carbon reaction is in progress (One exception is supersaturation, which can be effected in smooth-walled containers, such as were used in the crucible experiments of Körber et al. Such a condition must be rare in a large basic furnace, however.) The carbon reaction is inherently very rapid; consequently, its controlling factor is rate of supply of oxygen. The extent of departure

found by experiment depends upon the depth of bath at which the bath is sampled, and upon other factors, such as the type of process. For a given process, the extent of departure depends principally upon presence or absence of unreacted ore, and presence or absence of lime or bottom boils.

2. In one set of experiments, the rate of carbon drop was found to be represented by an equation of the form

$$d[C]/dt = a \log [C] - b.$$

It is suggested that the logarithmic term arises from the fact that the ordinary steel-making processes are not isothermic. It is further suggested that in slope a are lumped all factors that affect rate of supply of oxygen.

3. It was found that slag ferrous oxide could be related to metal carbon content by an equation of the form

$$\log (\text{FeO}) = \frac{a'}{[C]} + b'$$

where b' depends principally upon slag basicity for a given process. It is seemingly dependent also upon those factors that affect rate of supply of oxygen to the metal.

4. Since metal iron oxide (or oxygen) is related to metal carbon by the equation

$$[\text{FeO}] = \frac{a''}{[C]} + b''$$

it follows that slag and metal are related, while the carbon reaction is in progress by

$$\frac{\log (\text{FeO})}{[\text{FeO}]} = a''' + b'''$$

where a''' is constant and b''' depends upon slag basicity and the factors that affect rate of supply of oxygen to the metal. There is thus no distribution of iron oxide between an oxidizing slag and metal in the sense that would be true of slag and metal in equilibrium. A true distribution in the latter sense could exist, for example, at the composition represented by point o

of Fig. 1. The distribution ratio then depends only on slag basicity, being greatest for a pure iron oxide slag, and increasingly less for slags of increasing basicity.

5. Slag-metal-oxygen relations applicable to the basic open hearth apply to the oxidizing period of the basic electric furnace.

6. The electric-furnace finishing period differs in behavior from that described in the foregoing pages, in that the slag does not contain sufficient iron oxide to supply the required potential to transfer oxygen to the metal. Oxygen in excess of the equilibrium value is consumed quickly and the only controller of oxygen content appears then to be carbon content, assuming no addition of a deoxidizer such as silicon or aluminum.

REFERENCES

1. F. Körber et al.: Influence of Carbon on Steelmaking Reactions. *Stahl und Eisen* (1936) 56, 181-208.
2. Committee on Physical Chemistry of Steelmaking: Basic Open-Hearth Steelmaking. A.I.M.E. 1944.
3. H. E. Cleaves and J. G. Thompson: The Metal Iron, 78. New York, 1935. McGraw-Hill Book Co.
4. K. L. Fetters and J. Chipman: Equilibria of Liquid Iron and Slags of the System CaO-MgO-FeO-SiO_2 . *Trans. A.I.M.E.* (1941) 145, 95-112.
5. B. M. Larsen: Controlling Reactions in the Open-hearth Process. *Trans. A.I.M.E.* (1941) 145, 67-83.
6. G. Leiber: Reactions in the Basic Open Hearth. *Mitt. K. W. Inst. Eisenforschung* (1936) 18, 135-147.
7. F. Körber and W. Oelsen: Reaction of Carbon in Molten Iron with Oxides. *Naturwiss.* (1935) 23, 462-465.
8. C. H. Herty, Jr., et al: The Control of Iron Oxide in the Basic Open-hearth Process. Min. and Met. Advisory Boards, *Bull.* 68 (1934) 19-24.

DISCUSSION

N. J. GRANT.*—What I have to say is in no way going to change what Mr. Marsh said in his paper. I merely want to bring out a few points with which perhaps I was slightly more familiar than he was at the time he had the information available to him.

* Massachusetts Institute of Technology, Cambridge, Massachusetts.

Particularly, I want to direct attention to Fig. 2. This was in connection with heat E-15, which was made by Dr. Fethers and Dr. Chipman. I realize that Mr. Marsh did not

tion with Fig. 2, that acid open-hearth and bessemer steels would be capable of having lower final carbons than the basic open-hearth. I think that is a very good comparison for acid

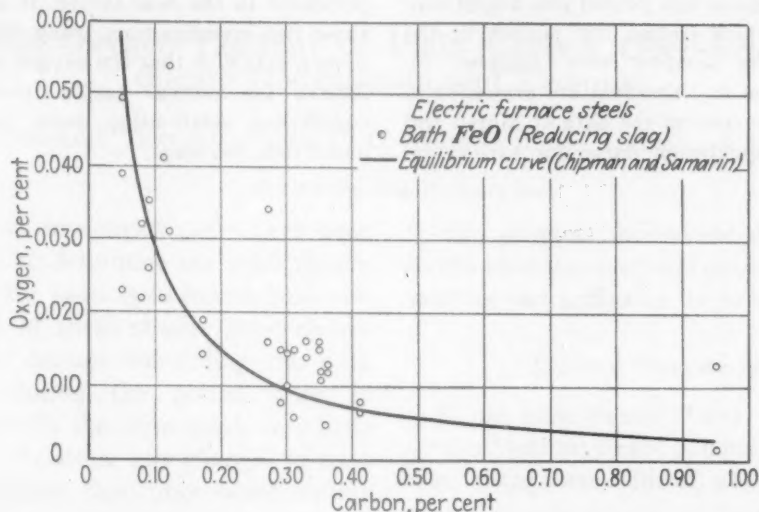


FIG. 11.

have the complete information, and for that reason I want to caution that the results shown should not be taken too literally. It looks a little too good, actually. All the points that are included in the particular plot run anywhere from 1600° to 1678°, which is quite a temperature spread; and of course that temperature spread has a strong effect on the sweep of the curve. Correcting the points for temperature by the method Dr. Fethers used, and listed in his paper, would lower the curve appreciably. It doesn't change the actual trend of the curve; that is, the more acid slags would sustain a higher oxygen content in the metal. I took several other heats in that same study, E12 and E11 and E16, and in general all I have to say concerning this is that the curve is considerably flatter, that the upsweep on the acid side is not nearly so great as is shown in Fig. 2.

One other point: Concerning the figure 0.0028 used for m , which is the product of percentage of carbon times percentage of oxygen, I think it is well known that the m figure changes with increasing carbon; that is, m increases with increasing carbon; yet I notice in one section of the paper that "7 per cent carbon" is used with that figure 0.0028. I should like to ask whether that seems proper or not.

Finally, one statement was made in connec-

open-hearth against basic open-hearth, but I do not believe it holds for the bessemer, for the bessemer is just that much further from an equilibrium process. The oxygen is not obtained from the slag, as in the open-hearth furnace. For that reason the bessemer actually should not be in there as a comparative, because there is a totally different condition. You can pile in oxygen to a greater extent there than in the open-hearth processes.

S. F. URBAN* and GERHARD DERGE.*—Mr. Marsh has presented many interesting ideas in his paper. The features of immediate interest to electric-furnace operators are the data shown in the last two figures, especially in Fig. 10. It has been generally believed that one of the advantages of electric steelmaking practice has been that the reducing slags bring the oxygen below the equilibrium levels normally obtained in other steelmaking practices. Fig. 10 shows that this is not true and such a radical departure from conventional beliefs should be substantiated by independent measurements.

Mr. Marsh's data were obtained by the conventional aluminum-killed bomb sample analyzed by vacuum fusion. Comparable data

* Carnegie Institute of Technology, Pittsburgh, Pennsylvania.

have been obtained at the South Works of the Carnegie-Illinois Steel Corporation by the chilled-wedge method of sampling. In this method the sample is dipped from the furnace in a slagged spoon and poured into a split copper mold, which freezes the oxygen in the sample. These samples were analyzed by vacuum fusion and the data are presented in Fig. 11. They confirm the data of Marsh and follow the equilibrium curve for carbon vs.

oxygen very closely. This figure also extends the data to as low as 0.05 per cent carbon. These data and their significance will be discussed more extensively in a formal paper to be presented in the near future. It appears that these two investigations, using different techniques, establish that the oxygen in the metal follows the normal carbon versus oxygen equilibrium relationship quite closely, even under reducing slags.

The Total Oxygen Content of Plain Carbon Open-hearth Steel during Deoxidation and Teeming

BY MICHAEL TENENBAUM* AND C. C. BROWN,* JUNIOR MEMBERS A.I.M.E.

(New York Meeting, February 1944)

NUMEROUS investigations¹⁻⁴ have been carried out to determine the total oxygen present in the basic open-hearth bath and the results of these studies have clearly defined the factors controlling the bath oxidation during the period prior to deoxidation. On the other hand, very little is known concerning any changes in total oxygen content that may occur during deoxidation, tapping and teeming. The need for such additional data is continually becoming more apparent, since there is no strict technical basis for selecting any particular deoxidation practice. Many steels are made for the same purposes and to the same chemical analyses by widely differing practices.

Apparently, each practice is satisfactory. However, it would be desirable to establish more definitely the effects and relative merits of the individual practices. Such information could be used to give a definite foundation for evaluating various types of deoxidation. In order to approach this problem, a study was made of the changes effected in the total oxygen content of several grades of steel by representative open-hearth deoxidation practices.

To carry out such studies, it was necessary that a reliable testing procedure for determining the oxygen content of the steel bath and the ingot mold be established. Before entering on any extensive

testing program, consideration was given to the available methods of obtaining steel samples and analyzing for oxygen.

TESTING PROCEDURES

It has been shown⁵⁻⁹ that in solidified steel oxygen may exist in combination with iron, manganese, silicon, aluminum, titanium, chromium and carbon, depending upon the amount of these elements in the sample. In molten steel, however, there has been no direct distinction of the various oxides. Accordingly, the total active oxygen in the molten steel bath is designated by the symbol *O*. During deoxidation, various oxides may be present either in solution in the molten steel or as solid or liquid inclusions. Any sample taken from the molten steel for oxygen analysis will include both the dissolved and the mechanically included oxygen. Similarly, samples of the solid steel product will also include the two forms of oxygen.

Methods of Sampling the Molten Steel Bath

In order to obtain a true oxygen analysis from liquid steel, this element must be completely retained in the solidified sample. Several methods have been proposed whereby this stabilization can be effected. As early as 1915, Kichline¹⁰ proposed a method for testing molten steel, in which the oxygen combined with some added aluminum. The concentration of the resultant aluminum oxide was determined by chemical analysis. This method was

Manuscript received at the office of the Institute Dec. 15, 1943. Listed as T.P. 1699.

* Inland Steel Co., East Chicago, Indiana.

¹ References are at the end of the paper.

modified by Kinzel¹¹ and later by Herty and his associates.¹² A distinct improvement in sampling technique for the aluminum oxide method was effected with the introduction of the McCutcheon and Rautio³ bomb test. This type of test proved very satisfactory for sampling the open-hearth bath, since it minimized atmospheric oxidation and slag contamination and at the same time retained all of the alumina in the final sample. Further changes in the design of the sampling bomb were described by Swinden and Stevenson.¹³ However, in principle, this mold is identical with that introduced by McCutcheon.

Probably the most universally accepted method for oxygen analysis has been by means of the vacuum-fusion apparatus. The technique has been reviewed in numerous publications.^{5,14-16} Recent work¹³ has demonstrated that with careful sampling technique the total oxygen content as determined by vacuum fusion agrees very well with the results of direct chemical analysis of an aluminum-killed sample. In this same work it was shown that the more tedious gravimetric analysis for Al_2O_3 can be replaced by more rapid nephelometric measurements without impairing the accuracy of the results.

Derge¹⁷ has recently reported on the use of a rapidly cooled sample for oxygen analysis of steel to which no aluminum has been added. A modified vacuum-fusion apparatus was used to make the actual oxygen determination. During pouring, however, Derge's sample is exposed to atmospheric oxidation. Compensating for this oxidation is the rimming action that takes place on pouring open bath tests. The discrepancies between the results obtained by the chilled sample and those of the bomb test reported in Derge's paper may be partly due to these effects.

Other methods for oxygen and oxide analysis have been used with varying degrees of success in other investigations.

In general, however, these methods involve complex analytical techniques and would not be satisfactory for routine analysis of large numbers of tests.

Both the vacuum-fusion analysis and the chemical analysis for Al_2O_3 yield the total oxygen content of the sample. A modification of the vacuum-fusion method¹⁸ is also used, in which each oxide is removed fractionally at a selected temperature. In the bomb-type sample, essentially all of the oxides present in the sample are reduced by the added aluminum. Accordingly, in these samples it is no longer possible to distinguish the various oxides that may have been present in the original liquid steel. The type of sample proposed by Derge would be amenable to oxide analysis by either the fractional vacuum-fusion or by various extraction and electrolytic methods. However, no data distinguishing between the forms of the oxide in the chilled sample have been published.

For this investigation it was decided to use the standard McCutcheon bomb test to sample the liquid steel during the deoxidation and teeming periods. This type of sample can be obtained easily and gives reproducible results. In addition, the widespread application of this testing technique in other investigations provides a background for comparison with the results of the present study. Before entering on any extensive testing program, however, it was necessary to establish a method for analysis of the product of the bomb test for total oxygen content. Three methods were considered; namely, vacuum fusion, gravimetric chemical analysis, and turbidity comparison.

To compare the merits of the last two named, a series of bomb tests was first analyzed gravimetrically for Al_2O_3 . Samples from these same tests were dissolved and the turbidity of the resultant solution was measured by means of a standard Cenco photometer. The results of the turbidity measurements were plotted against

the gravimetric Al_2O_3 . While a fair correlation was obtained, the relationship was not sufficiently exact to justify the replacement of the tedious gravimetric analysis by the rapid turbidity measurement. In order to illustrate these results, the line was drawn that best fitted the data relating the turbidity with the gravimetrically determined Al_2O_3 . The Al_2O_3 content indicated by this line for each turbidity measurement was then recorded. A comparison of the oxygen contents of the various samples obtained by these two methods is made in the third and fourth columns of Table I.

TABLE I.—Total Oxygen in Steel Samples as Determined by Gravimetric Analysis, Turbidity Measurements, and Vacuum Fusion

Sample No.	Origin of Sample	Oxygen, Per Cent		
		Gravimetric	Turbidity	Vacuum Fusion
1	Bath	0.011	0.016	0.014
2	Bath	0.021	0.023	0.023
3	Bath	0.037	0.046	0.034
4	Bath	0.056	0.055	0.039
5	Bath	0.061	0.055	0.044
6	Special melt	0.106	0.103	0.061
7	Bath	0.016	0.011	0.008
8	Ingot mold	0.006	0.005	0.005
9	Ingot mold	0.009	0.006	0.002
10	Ingot mold	0.010	0.003	0.005
11	Ingot mold	0.007	0.006	0.006
12	Bath	0.009	0.012	
13	Bath	0.012	0.015	
14	Bath	0.013	0.010	
15	Bath	0.015	0.032	
16	Bath	0.018	0.018	
17	Bath	0.021	0.021	
18	Bath	0.021	0.028	
19	Bath	0.025	0.027	
20	Bath	0.026	0.033	
21	Bath	0.026	0.025	
22	Bath	0.029	0.031	
23	Bath	0.038	0.037	
24	Bath	0.043	0.043	
25	Bath	0.054	0.062	
26	Bath	0.055	0.062	

Since vacuum-fusion equipment was not available at the plant where this investigation was carried out, it was not feasible to make a comprehensive comparison of the results of this type of oxygen analysis with those previously

discussed. However, 11 representative samples were sent to an independent research laboratory for vacuum-fusion analyses for total oxygen. Considerable difficulty¹⁹ was reported in making these determinations. Under the conditions existing in the vacuum-fusion furnace, apparently it was not possible always to reduce the Al_2O_3 completely. The error from this source became most evident on samples that contained high concentrations of this compound. In three instances, nonmetallic material removed from the vacuum-fusion sample after the completion of the determination was identified as Al_2O_3 by X-ray diffraction. The presence of excess aluminum was shown to exert a marked retarding effect on the rate of gas evolution, thus considerably impairing the accuracy of the over-all results. Observations made during the vacuum-fusion extraction indicated, however, that all the oxygen was present as Al_2O_3 . The results of the vacuum-fusion analysis are tabulated in the fifth column of Table I. Only the first 11 samples were analyzed by this method. With the exception of samples 1 and 2 all the vacuum-fusion analyses indicated a lower oxygen content than did the gravimetric analysis. In these samples it was reported that there was a possibility of high results due to picking up of oxygen present in the system from previous analysis.

Table I indicates that there is considerable discrepancy between the results of the three methods of total oxygen analysis. These findings do not agree with results obtained by Swinden and Stevenson.¹³ Since the development of analytical techniques for oxygen determinations was only a secondary consideration in this investigation, it was decided that results obtained by gravimetric analysis were the most dependable. Accordingly, all values for total oxygen given in the succeeding part of this paper were determined by this method.

A modified type of handle for the bomb test was used in this investigation to take liquid steel tests from the ingot mold. The arrangement of the handle and bomb are

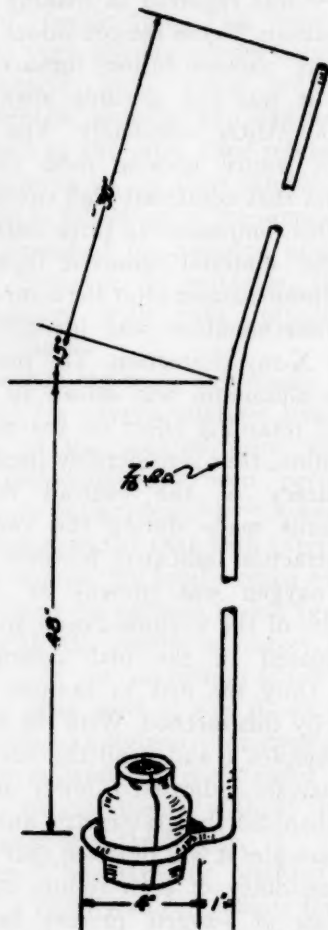


FIG. 1.—ARRANGEMENT OF HANDLE AND BOMB USED FOR SAMPLING LIQUID STEEL IN INGOT MOLD.

sketched in Fig. 1. In taking the sample from the ingot mold, the bomb was dipped into the molten steel at the time when the body of the ingot mold was filled. The bomb was lowered rapidly about 3 ft. below the surface, held in that position for about 4 sec. and then withdrawn from the ingot mold. On removal, the outer surface of the bomb mold was coated with metal. This outer layer of metal was peeled from the sample mold either by burning with an acetylene torch or by

pounding the hot sample until the outer shell separated from the bomb. Since the technique of sampling the molten steel ingot was essentially the same as that used in the open-hearth bath, the results obtained were directly comparable.

The time allowed for immersing the bomb-test mold in the liquid steel ingot was relatively short. Accordingly, an investigation was made of the possibility that all the available oxygen would not have time to react with the aluminum. It was not considered practical to increase the time of immersion in the ingot, since such practice might cause the mold to burn off and contaminate 6 tons of steel with a cast-iron inclusion. Accordingly, successive melts were made under duplicate conditions in a 300-lb. induction furnace. In each melt the steel was highly oxidized and low in carbon. The melts were similar in chemical analysis but differed somewhat in temperature at the time of sampling. The first and third tests were obtained by immersing the bomb for the customary 4 sec., while the second test remained in the molten metal for 10 sec. The results are listed in Table 2.

TABLE 2.—Effect of Immersion Time on Total Oxygen Obtained by Chemical Analysis of Bomb Test 300-pound Induction Furnace

Test No.	Immersion Time, Sec.	Bomb-test Analysis, Per Cent						Metal Temperature, Deg. F.
		C	Mn	P	S	Si	O	
1	4	0.05	0.06	0.012	0.028	0.005	0.081	2990
2	10	0.05	0.04	0.013	0.025	0.005	0.088	3040
3	4	0.045	0.04	0.012	0.028	0.005	0.106	3060

The relatively high oxygen concentrations present in tests 1 and 3 indicate that essentially all of the oxygen present in the liquid steel combines with the added aluminum in 4 sec. The differences noted can be attributed probably to slight

variations in meltdown conditions and the increase in oxygen solubility with increased temperature. Since the steels studied for this table were far more highly oxidized than those that will be discussed later, little error could be anticipated from variations in the time of immersion.

Another feature that was considered was the possibility of certain more or less stable oxides that are present after the addition of deoxidizing elements to the liquid steel not being reduced by the added aluminum. It was not known whether the rate of reduction of any such oxide particles would be sufficiently rapid for the oxygen to be entirely converted to Al_2O_3 in the few seconds that the test was molten. It should be remembered, however, that in order for such oxides to remain in the liquid steel bath they must be very finely distributed. Such a condition would be conducive to a rapid reduction rate even though the reaction is heterogeneous. If the reduction were not complete, the total oxygen content of the sample would be greater than the oxygen present as Al_2O_3 . Samples 8, 9, 10 and 11 of Table I were taken from the ingot mold. In these samples, therefore, there was a possibility of some other oxides existing in the solidified bomb test. If this were true the total oxygen as indicated by the vacuum-fusion method should exceed the gravimetric results. While these results are of limited value, it can be seen that in no case did the vacuum-fusion total oxygen exceed the gravimetric results. In these few samples the vacuum-fusion findings approached the gravimetric results as a limiting value, indicating that essentially all the oxygen was present as Al_2O_3 . Samples 8, 9, 10 and 11 were examined in the metallographic microscope also, to observe whether any silica or silicate inclusions could be detected. The individual inclusions were very small in size, hence it was not possible to identify positively either silicate or alumina in-

clusions. The small particle size of the inclusions would favor a rapid reaction rate with aluminum. Finally, observations¹⁹ made during vacuum-fusion analysis indicated that all the oxygen was combined as Al_2O_3 .

Later work on killed bath tests demonstrates that in these samples, also, essentially all of the oxygen must be converted to Al_2O_3 . Samples that were taken before and at successive intervals after the addition of bath deoxidizers showed little change in total oxygen content, despite the fact that more stable oxides obviously were present.

CHANGES IN TOTAL OXYGEN CONTENT DURING DEOXIDATION

In order to operate the open-hearth furnace economically, it is desirable that during the refining period a considerable excess of oxygen be present in the liquid metal over that which would be in equilibrium with the carbon in the bath. When the specified bath carbon is reached, it is desirable to remove the bulk of this oxygen from the metal to prevent further reaction and to minimize the oxides present in the final product. Two alternative general methods are available to remove the excess oxygen. The oxygen removal may be effected partly in the bath and partly in the ladle and molds. The second alternative is to accomplish all the deoxidation outside of the furnace after the heat has been tapped.

When an addition is made to the liquid steel bath, the actual time required after melting for the deoxidizing element to combine with oxygen is relatively small.²⁰ However, appreciable time is required for the products of deoxidation to agglomerate and rise to the liquid steel surface. Since the bath action ceases during the normal deoxidation period, the oxide particles must rise to the surface according to Stokes' law, therefore it might be expected that the changes in total oxygen content

take place rather slowly unless considerable percentages are present, depending not on the rate of deoxidation but on the slower process whereby the oxide products rise to the surface of the bath.

In the following section of this paper a study is made of the changes in total oxygen as well as of the bath and slag analysis when various deoxidation practices are used on standard grades of steel. All tests were made in 145 or 175-net-ton basic open-hearth furnaces. The various deoxidation practices tried on each grade of steel are tabulated separately. For the most part, the analyses shown in these tables are averages of at least three heats. In order to obtain a representative value for the ingot analysis on each heat, three tests were taken—near the start, in the middle, and toward the end of the pour. The average value of these three tests was considered as the ingot analysis for each heat. This study includes the results of more than 50 heats.

Effect of Five Deoxidation Practices on Changes in Analysis of Liquid 0.40 to 0.50 Per Cent Carbon Steel

In order to survey the effect of various finishing practices on the changes in analysis of liquid steel, five different deoxidation procedures were used on standard 0.40 to 0.50 per cent carbon forging grades of steel. Each practice was used on at least three heats. All heats were made to a 4 to 7 McQuaid-Ehn grain size. The specified additions and timing for the five types of deoxidation can be outlined briefly, as follows:

1. *Double deoxidation:*

- a. 20 lb. per net ton of ingots of 20 per cent spiegel followed in 10 min. by
- b. 24 lb. per net ton of ingots of 15 per cent ferrosilicon followed in 12 min. by
- c. 16 lb. per net ton of ingots of 80 per cent ferromanganese and tapped in 10 min.

- d. 4.4 lb. Si, 0.75 lb. Al, and 0.60 lb. Ti per net ton of ingots were added to the ladle.

2. *Single 15 per cent ferrosilicon deoxidation:*

- a. 24 lb. per net ton of ingots of 15 per cent ferrosilicon followed in 12 min. by
- b. 18 lb. per net ton of ingots of 80 per cent ferromanganese and tapped in 10 min.
- c. 4.4 lb. Si, 0.75 lb. Al and 0.60 lb. Ti per net ton of ingots were added to the ladle.

3. *Spiegel deoxidation with burnt lime added to slag:*

- a. 14 lb. per net ton of ingots of burnt lime followed in 20 to 30 min. by
- b. 24 lb. per net ton of ingots of 20 per cent spiegel followed in 6 min. by
- c. 16 lb. per net ton of ingots of 80 per cent ferromanganese and tapped in 9 min.
- d. 6.4 lb. Si, 0.75 lb. Al, and 0.60 lb. Ti per net ton of ingots were added to the ladle.

4. *Spiegel deoxidation with graphite added to slag:*

- a. 1.5 lb. per net ton of ingots of graphite shoveled onto slag followed in 5 min. by
- b. 24 lb. per net ton of ingots of 20 per cent spiegel followed in 6 min. by
- c. 16 lb. per net ton of ingots of 80 per cent ferromanganese and tapped in 9 min.
- d. 6.5 lb. Si, 0.75 lb. Al and 0.60 lb. Ti per net ton of ingots were added to the ladle.

5. *Silicomanganese deoxidation with burnt lime added to slag:*

- a. 14 lb. per net ton of ingots of burnt lime followed in 20 to 30 min. by
- b. 20 lb. per net ton of ingots of silicomanganese and tapped in 8 min.
- c. 1.9 lb. Mn, 4.0 lb. Si, 0.75 lb. Al and 0.60 lb. Ti per net ton of ingots were added to the ladle.

These five practices constitute a cross section of the type of deoxidation currently being used by the plants producing the greatest tonnage of plain carbon basic

the general results of this survey. The use of 15 per cent ferrosilicon (or 10 per cent ferrosilicon) to deoxidize a basic open-hearth heat, as in practices 1 and 2, has

TABLE 3.—*Effect of Five Practices on Analysis of Liquid Steel during Deoxidation and Pouring*
0.40 TO 0.50 PER CENT CARBON

Sampling Time	Bath Analysis, Per Cent						Slag Analysis, Per Cent									
	C	Mn	P	S	Si	Total Oxy- gen	FeO	Fe ₂ O ₃	SiO ₂	Al ₂ O ₃	CaO	MgO	MnO	P ₂ O ₅	S	
1. DOUBLE DEOXIDATION ^a (AVERAGE DATA FROM 3 HEATS)																
Before 20 per cent spiegel.....	0.41	0.18	0.010	0.028	0.003	0.017	11.56	2.77	16.69	3.42	46.47	9.19	6.00	2.05	0.17	
Before 15 per cent Fe-Si.....	0.42	0.30	0.010	0.027	0.003	0.018										
Before 80 per cent Fe-Mn.....	0.41	0.29	0.015	0.028	0.13	0.018										
At tap.....	0.47	0.76	0.016	0.027	0.10	0.018	9.03	4.05	17.90	3.41	45.50	9.49	7.89	1.89	0.15	
Average in molds..	0.46	0.74	0.019	0.027	0.24	0.011										
2. SINGLE 15 PER CENT FERROSILICON DEOXIDATION ^a (AVERAGE DATA FROM 3 HEATS)																
Before 15 per cent Fe-Si.....	0.46	0.21	0.014	0.030	0.003	0.014	9.51	3.81	17.38	3.51	45.23	10.03	6.59	2.64	0.15	
Before 80 per cent Fe-Mn.....	0.43	0.22	0.015	0.029	0.11	0.017										
At tap.....	0.47	0.70	0.018	0.030	0.10	0.017	8.43	3.43	18.75	3.35	45.13	10.75	6.68	2.44	0.12	
Average in molds..	0.47	0.81	0.023	0.030	0.24	0.010										
3. SPIEGEL DEOXIDATION WITH LIME ^a (AVERAGE DATA FROM 3 HEATS)																
Before CaO.....	0.51	0.14	0.009	0.027	0.003	0.013	12.35	3.64	14.61	4.35	46.75	7.51	5.29	2.62	0.20	
Before 20 per cent spiegel.....	0.41	0.14	0.011	0.027	0.003	0.013										
Before 80 per cent Fe-Mn.....	0.42	0.27	0.012	0.026	0.01	0.014										
At tap.....	0.46	0.75	0.013	0.026	0.01	0.013	11.42	5.00	13.07	3.46	49.20	8.25	5.82	2.14	0.15	
Average in molds..	0.50	0.75	0.014	0.026	0.25	0.012										
4. SPIEGEL DEOXIDATION WITH GRAPHITE ^a (AVERAGE DATA FROM 3 HEATS)																
Before graphite..	0.45	0.19	0.012	0.029	0.003	0.017	10.82	4.17	16.01	3.74	45.86	9.16	6.00	2.71	0.18	
Before 20 per cent spiegel.....	0.42	0.19	0.013	0.028	0.004	0.017										
Before 80 per cent Fe-Mn.....	0.45	0.33	0.014	0.028	0.01	0.016										
At tap.....	0.49	0.82	0.015	0.027	0.01	0.014	8.05	6.22	16.03	3.42	45.80	9.51	7.26	2.61	0.15	
Average in molds..	0.48	0.74	0.017	0.027	0.25	0.010										
5. SILICOMANGANESE DEOXIDATION WITH LIME ^a (AVERAGE DATA FROM 3 HEATS)																
Before CaO.....	0.49	0.15	0.008	0.026	0.004	0.014	14.32	4.28	14.07	3.90	44.63	9.04	5.96	2.23	0.20	
Before Si-Mn....	0.45	0.14	0.009	0.026	0.004	0.015										
At tap.....	0.46	0.63	0.012	0.025	0.11	0.014	11.06	5.69	12.70	3.21	48.20	8.81	6.75	2.06	0.18	
Average in molds..	0.48	0.76	0.015	0.025	0.27	0.010										

* The weights and timing of the additions for each practice are given on the opposite page.

open-hearth steel. While obviously there are some differences between the preceding deoxidation schedules and those used in individual plants, these are of a minor nature and would not seriously affect

long been standard practice in the steel industry. While spiegel is not generally considered as a bath deoxidizer, the use of adequate amounts of this material in closely timed finishing practice has given

good results in some plants. To increase the efficiency of the spiegel addition, some preliminary treatment of the slag to reduce its ability to transfer oxygen to the bath

the start of deoxidation and tap, the changes in the total oxygen of the bath are relatively small. The values plotted in Fig. 2, however, give no definite clue

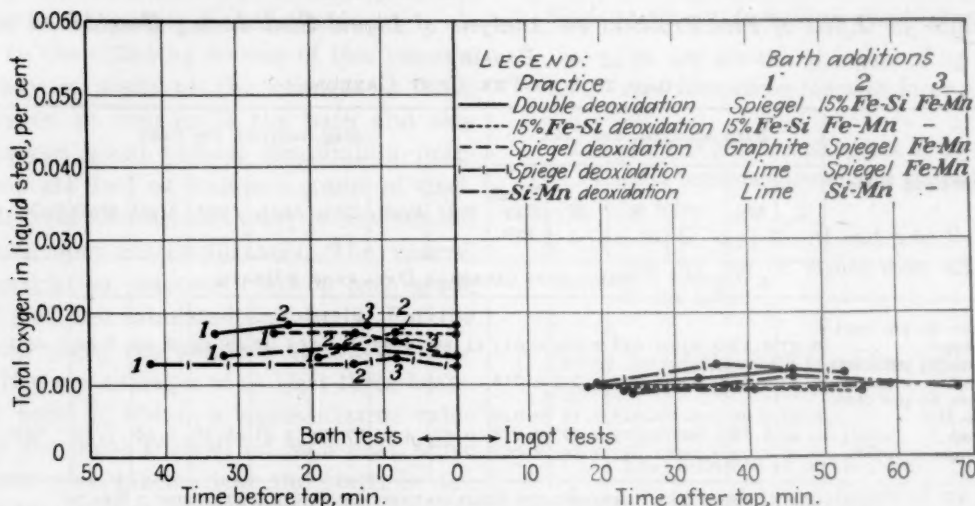


FIG. 2.—CHANGES IN TOTAL OXYGEN CONTENT OF LIQUID 0.40 TO 0.50 PER CENT CARBON STEEL FOR FIVE DEOXIDATION PRACTICES.

is used ordinarily. In practice 3, burnt lime was added to thicken the slag before the spiegel was added. In order to avoid the difficulties in draining furnaces and maintaining bottoms that normally are associated with late lime additions, practice 4 was used; i.e., graphite was shoveled over the slag, causing it to become foamy and thick and thus reducing its ability to transfer oxygen. The use of silicomanganese for deoxidation is standard practice for many grades of steel and was included as practice 5 in this study. The average changes in bath and slag analysis during deoxidation, tapping and teeming for each of these practices are shown in Table 3.

From this table, it can be seen that essentially the same final analysis was made despite the differences in deoxidation practices and the changes taking place during the finishing period. The average changes in the total oxygen content of the liquid from the start of deoxidation through the tapping and pouring periods are shown graphically in Fig. 2. This figure shows that during the period between

as to changes in the form in which the oxygen exists. The differences in the changes in total oxygen brought about by the various deoxidations are very slight. The highest and lowest total oxygen contents of the bath at tap are associated with the highest and lowest predeoxidation values, respectively. These differences in total oxygen content, however, are largely eliminated by the time the steel is in the ingot mold. At that time the average values are essentially the same for all practices. As would be expected, the largest and most positive decrease in total oxygen of the liquid steel takes place during tapping and pouring.

Effect of Two Deoxidation Practices on Changes in Analysis of Liquid 0.20 to 0.25 Per Cent Carbon Steel

Practices 1 and 2 that were used on the 0.40 to 0.50 per cent carbon steel were repeated on a 0.20 to 0.25 per cent carbon steel to see whether the characteristics noted would persist in steel of different analysis. The general details of the prac-

tice were the same as on the higher carbon heats. Again, all heats were made to a 4 to 7 McQuaid-Ehn grain size. The specified timing and the bath additions

tapping and teeming are given in Table 4. The average changes in total oxygen content of the steel are illustrated in Fig. 3. No marked differences in the final average

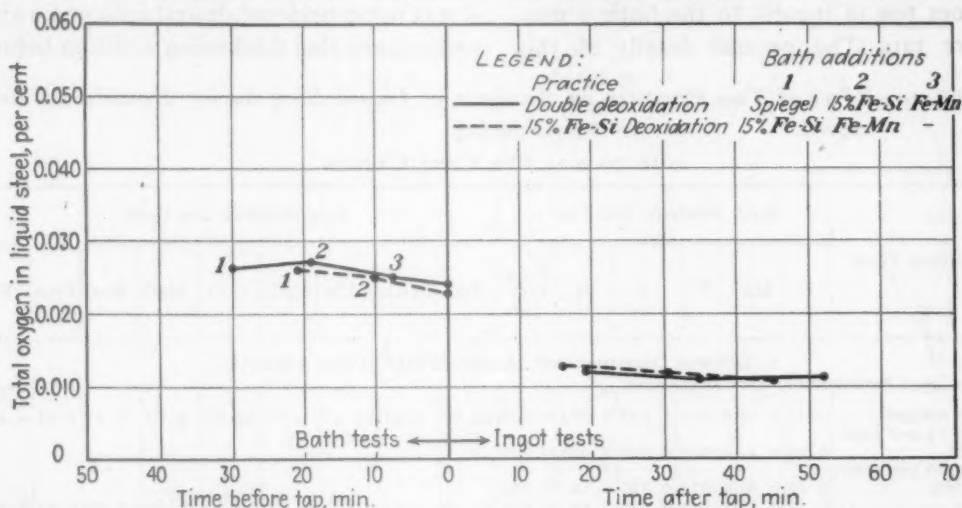


FIG. 3.—CHANGES IN TOTAL OXYGEN CONTENT OF LIQUID 0.20 TO 0.25 PER CENT CARBON STEEL FOR TWO DEOXIDATION PRACTICES.

made on the two practices are listed, as follows:

1. *Double deoxidation:*

- a. 20 lb. per net ton of ingots of 20 per cent spiegel followed in 10 min. by
- b. 24 lb. per net ton of ingots of 15 per cent ferrosilicon followed in 12 min. by
- c. 8 lb. per net ton of ingots of 80 per cent ferromanganese and tapped in 10 min.
- d. 1.6 lb. Mn, 3.7 lb. Si, 0.95 lb. Al and 0.60 lb. Ti per net ton of ingots were added to the ladle.

2. *Single 15 per cent ferrosilicon deoxidation:*

- a. 24 lb. per net ton of ingots of 15 per cent ferrosilicon followed in 12 min. by
- b. 8 lb. per net ton of ingots of 80 per cent ferromanganese and tapped in 10 min.
- c. 2.1 lb. Mn, 3.6 lb. Si, 0.95 lb. Al, and 0.60 lb. Ti per net ton of ingots were added to the ladle.

The average changes in analysis of liquid steel during deoxidation and in

analysis resulted. A slightly higher final phosphorus content in the 15 per cent ferrosilicon-deoxidized steel can be attributed entirely to the combined effects of the lower slag basicity, the lower slag oxidation, and the higher P_2O_5 content in the heats made by that practice.

The changes in the total oxygen content of the liquid steel were almost identical for the two practices. In both practices a small drop in total oxygen took place between the start of deoxidation and tap. A much more marked decrease occurred during the tapping and pouring of the steel. The average total oxygen in the molds was the same for both practices.

Effect of Two Deoxidation Practices on Changes in Analysis of Liquid 0.80 to 0.95 Per Cent Carbon Steel

For this study two finishing practices were used in the manufacture of plain carbon spring steel containing 0.80 to 0.95 per cent carbon. The first practice involved no bath deoxidation whatsoever, the heat being tapped on an open bath.

In this practice all deoxidizing additions were made to the ladle during the tap. The second deoxidation practice consisted of a heavy spiegel addition (24 lb. per net ton of ingots) to the bath 9 min. before tap. The general details of this

practice were the same as for practices 3 and 4 that were used on the 0.45 per cent carbon steel. Since slags on this grade of steel are inherently heavy and foamy, it was not considered desirable to make any preliminary slag thickening addition before

TABLE 4.—*Effect of Two Practices on Analysis of Liquid Steel during Deoxidation and Pouring*

0.20 TO 0.25 PER CENT CARBON

Sampling Time	Bath Analysis, Per Cent						Slag Analysis, Per Cent								
	C	Mn	P	S	Si	Total Oxy- gen	FeO	Fe ₂ O ₃	SiO ₂	Al ₂ O ₃	CaO	MgO	MnO	P ₂ O ₅	S
1. DOUBLE DEOXIDATION ^a (AVERAGE DATA FROM 3 HEATS)															
Before spiegel.....	0.21	0.17	0.010	0.028	0.003	0.026	14.66	4.97	14.53	3.85	42.60	9.25	6.87	2.01	0.15
Before 15 per cent Fe-Si.....	0.20	0.27	0.011	0.026	0.003	0.027									
Before 80 per cent Fe-Mn.....	0.20	0.26	0.013	0.027	0.11	0.025									
At tap.....	0.20	0.32	0.014	0.026	0.10	0.024	11.40	7.05	14.96	3.46	41.10	10.84	7.91	1.95	0.15
Average in molds..	0.24	0.48	0.016	0.026	0.20	0.012									
2. 15 PER CENT FERROSILICON DEOXIDATION ^a (AVERAGE DATA FROM 3 HEATS)															
Before 15 per cent Fe-Si.....	0.20	0.23	0.016	0.026	0.003	0.026	9.51	3.81	17.38	3.51	45.23	10.03	6.59	2.64	0.15
Before 80 per cent Fe-Mn.....	0.21	0.23	0.017	0.026	0.13	0.025									
At tap.....	0.21	0.30	0.018	0.026	0.13	0.023	8.43	3.43	18.71	3.35	45.13	10.75	6.68	2.44	0.12
Average in molds..	0.22	0.47	0.023	0.026	0.20	0.012									

^a The weights and timing of the additions for both practices are given on page 693.

TABLE 5.—*Effect of Two Practices on Analysis of Liquid Steel during Deoxidation and Pouring*

0.80 TO 0.95 PER CENT CARBON

Sampling Time	Steel Analysis, Per Cent						Slag Analysis, Per Cent									
	C	Mn	P	S	Si	Total Oxy- gen	FeO	Fe ₂ O ₃	SiO ₂	Al ₂ O ₃	CaO	MgO	MnO	P ₂ O ₅	S	
1. TAPPING ON OPEN BATH (AVERAGE DATA FROM 6 HEATS)																
At tap ^a	0.83	0.27	0.016	0.028	0.003	0.014	9.08	4.41	18.77	3.30	42.43	8.25	9.90	2.59	0.14	
Average in molds ^b ..	0.84	0.69	0.019	0.027	0.15	0.010										
2. SPIEGEL DEOXIDATION (AVERAGE DATA FROM 2 HEATS)																
Before 20 per cent spiegel ^c	0.93	0.24	0.015	0.031	0.004	0.014	10.20	4.37	16.55	3.55	45.85	7.94	7.57	3.07	0.18	
At tap ^d	0.95	0.40	0.015	0.030	0.005	0.014	10.45	3.15	16.15	3.29	47.35	7.77	7.79	2.89	0.17	
Average in molds ^b ..	0.95	0.60	0.019	0.030	0.19	0.010										

^a 9.8 lb. Mn and 3.9 lb. Si per net ton of ingots were added to the ladle.

^b On fine-grained heats 0.75 lb. Al per net ton of ingots were added to the ladle.

^c 24 lb. spiegel per net ton of ingots added 9 min. before tap.

^d 4.8 lb. Mn and 4.4 lb. Si per net ton of ingots were added to the ladle.

addition of the spiegel. In contrast with the practice at the lower carbon, no ferromanganese was added in the furnace. Both fine and coarse-grained steel were

oxidizers. The addition of any great quantity of that element would require that the heat be worked down to excessively low carbon content prior to de-

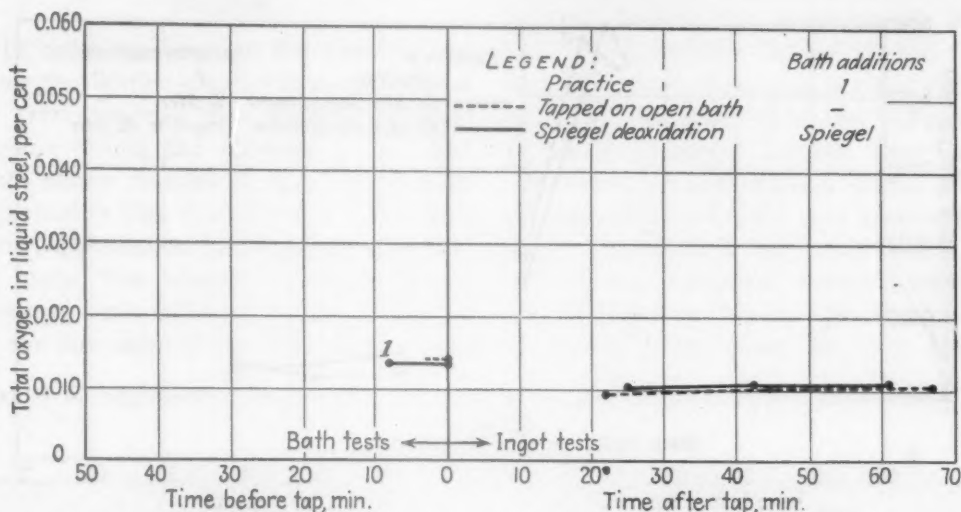


FIG. 4.—CHANGES IN TOTAL OXYGEN CONTENT OF LIQUID 0.80 TO 0.95 PER CENT CARBON STEEL FOR TWO DEOXIDATION PRACTICES.

made by these practices. The resultant average changes in bath and slag analysis are given in Table 5.

The changes in the total oxygen content of the liquid steel are shown graphically in Fig. 4. The total oxygen in the bath at tap was the same in both practices. In the heats made by the spiegel practice, the bath was absolutely dead at tap. Accordingly, it is evident that the form in which the oxygen exists must differ in the two practices. Only a small drop in the total oxygen of the liquid steel takes place during the time that the heat is tapped and poured. There was practically no difference in the total oxygen of the liquid steel in the ingot mold.

Effect of Two Deoxidation Practices on Changes in Analysis of Liquid 0.10 Per Cent Carbon Steel

In the manufacture of low-carbon killed steels, it is not practical to add large quantities of carbon-bearing de-

oxidation, in order that the specified analysis should not be exceeded in the product. Accordingly, in studying the changes in total oxygen of 0.10 per cent carbon heats, only the silicomanganese deoxidation was considered. Two modifications of this practice were used. In the first practice 20 lb. of silicomanganese per net ton of ingots was added 10 min. before tapping, without any preliminary slag treatment. In the second modification of this practice, one pound of graphite per net ton of ingots was shoveled over the slag 5 min. before the addition of the deoxidizer. The purpose of the graphite addition again was to thicken the slag and decrease the rate of oxygen transfer to the bath after the deoxidizer had been added.

The changes in the analysis of the liquid steel during the finishing period for the two modifications of the silicomanganese deoxidation are given in Table 6. The steels were made to a 5 to 7 McQuaid-Ehn grain size.

Since the particular grade of steel being considered was rephosphorized, the final phosphorus analysis was omitted from Table 6. Despite the fact that the average

oxygen occurred between the time of the silicomanganese addition and tap, despite the fact that this period was only about 10 min. long. The lines representing the

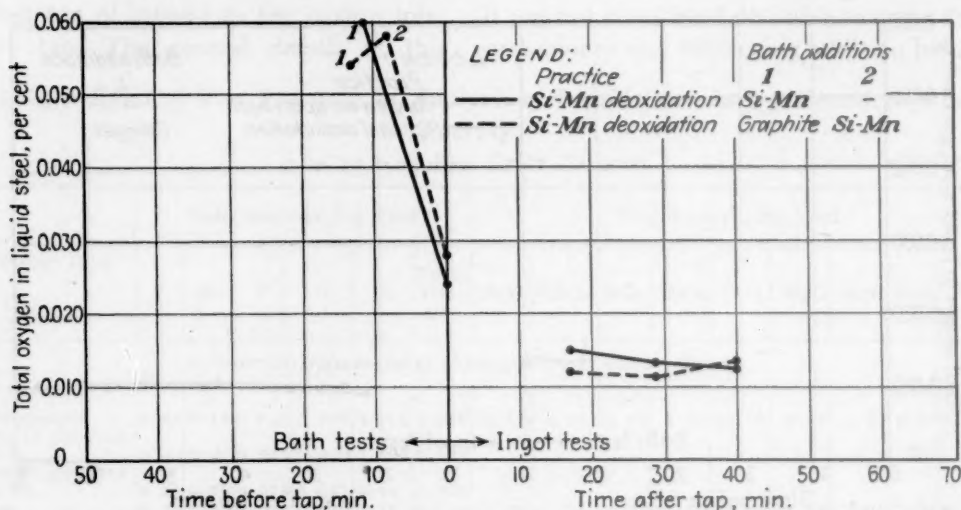


FIG. 5.—CHANGES IN TOTAL OXYGEN CONTENT OF LIQUID 0.10 PER CENT CARBON STEEL FOR TWO DEOXIDATION PRACTICES.

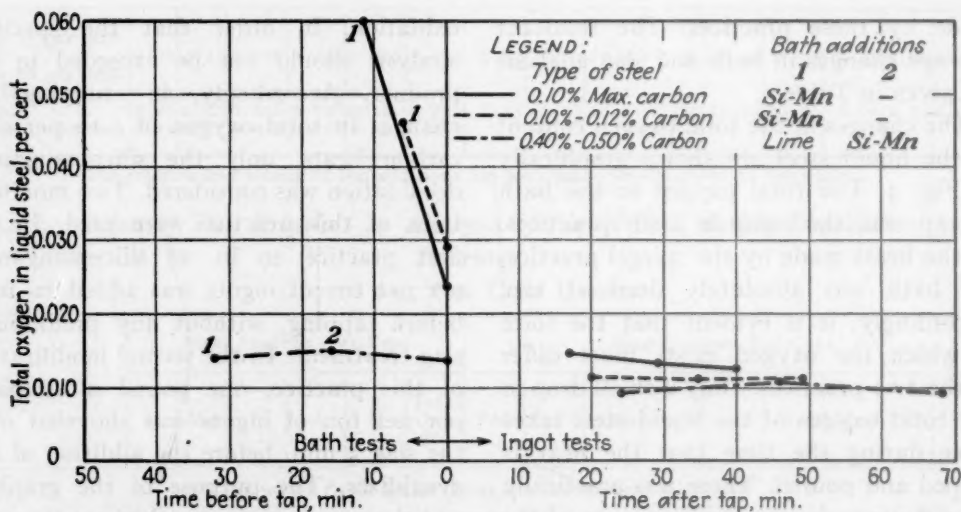


FIG. 6.—CHANGES IN TOTAL OXYGEN CONTENT OF THREE GRADES OF LIQUID STEEL USING SILICO-MANGANESE DEOXIDATION.

carbon content of the heats treated with graphite was two points lower than in the other practice, the total bath oxygen before deoxidation was essentially the same. The changes in total oxygen content can be seen in Fig. 5. The changes in bath oxygen were also similar. A marked drop in total

decrease in total oxygen between the addition of silicomanganese and tap parallel each other. Another marked drop in total oxygen resulted during tapping and pouring the heat. As in all other practices, there was very little difference in the average total oxygen in the ingot mold.

*Effect of Steel Analysis on Changes in
Oxygen of Liquid Metal Resulting
from Various Deoxidation
Practices*

In order to illustrate the effect of the same deoxidation practice in several ranges of steel analysis, the changes in total oxygen during the finishing period that were shown in Figs. 2, 3, 4 and 5 were replotted in Figs. 6, 7, 8 and 9. These data were supplemented by two additional series of heats. The practice on these supplementary heats will be described more fully in the discussion of the individual graphs.

oxygen of the liquid steel are shown in Fig. 6. The drop in total oxygen for the two low-carbon grades paralleled each other during the deoxidation period in the furnace. During this same period, there was no appreciable change in the total oxygen content of the 0.45 per cent carbon heat. In the ingot mold the differences in the total oxygen content were small. The 0.45 per cent carbon heats, which averaged only 0.015 per cent total oxygen before deoxidation, had only 0.010 per cent in the ingot—the lowest oxygen of the three grades. The 0.10 per cent carbon heat, which had 0.060 per cent oxygen

TABLE 6.—*Effect of Two Practices on Analysis of Liquid Steel during Deoxidation and Pouring*

0.10 PER CENT CARBON

Sampling Time	Steel Analysis, Per Cent						Slag Analysis, Per Cent									
	C	Mn	P	S	Si	Total Oxy- gen	FeO	Fe ₂ O ₃	SiO ₂	Al ₂ O ₃	CaO	MgO	MnO	P ₂ O ₅	S	
1. SILICOMANGANESE DEOXIDATION (AVERAGE DATA FROM 3 HEATS)																
Before Si-Mn ^a . . .	0.10	0.20	0.012	0.024	0.003	0.060	15.43	5.05	14.20	2.97	38.46	10.62	9.14	2.47	0.09	
At tap ^b	0.10	0.70	0.020	0.023	0.08	0.024	11.69	8.06	15.89	2.95	40.86	7.49	9.00	2.59	0.09	
Average in molds. .	0.10	0.64		0.022	0.06	0.013										
2. SILICOMANGANESE DEOXIDATION WITH GRAPHITE (AVERAGE DATA FROM 3 HEATS)																
Before graphite ^c . .	0.08	0.18	0.012	0.024	0.004	0.054	14.21	5.98	15.56	3.10	38.47	9.32	9.48	2.50	0.11	
Before Si-Mn ^a . . .	0.08	0.18	0.013	0.024	0.003	0.058										
At tap ^d	0.09	0.43	0.017	0.025	0.03	0.028	13.29	5.48	17.17	3.23	39.28	7.58	9.89	2.48	0.11	
Average in molds. .	0.10	0.62		0.024	0.04	0.012										

^a 20 lb. per net ton of ingots added 10 min. before tap.

^b 2.5 lb. Al and 0.60 lb. Ti per net ton of ingots were added to the ladle.

^c 1 lb. per net ton of ingots shoveled onto slag 5 min. before silicomanganese.

^d 2.9 lb. Mn, 2.6 lb. Al and 0.60 lb. Ti per net ton of ingots were added to the ladle.

Silicomanganese Deoxidation.—The silicomanganese deoxidation was used in making three grades of steel containing 0.10 per cent carbon, 0.12 per cent carbon, and 0.45 per cent carbon. The specified practice on the 0.12 carbon heats was the same as that described for 0.10 per cent carbon steel (p. 11). Owing to conditions that could not be controlled, the average time from the addition of silicomanganese to tap was only 6 min. instead of the specified 10 min. The changes in total

before deoxidation, averaged 0.013 per cent in the ingot—the highest value of the series.

Double Deoxidation.—The double deoxidation, which consists of consecutive bath additions of 20 per cent spiegel, 15 per cent ferrosilicon and ferromanganese, was used on a 0.20 and 0.45 per cent carbon grade of steel. The changes in total oxygen are shown in Fig. 7. Again, the drop in total oxygen during the period from the addition of the deoxidizer (15 per cent Fe-Si) to

tap was greater for the lower carbon steel. No definite change in total oxygen was effected in the furnace on the 0.45 per cent carbon grade. A comparatively large drop

Single 15 Per Cent Ferrosilicon Deoxidation.—As shown in Fig. 8, the changes in total oxygen during the 15 per cent silicon deoxidation on the 0.20 per cent carbon

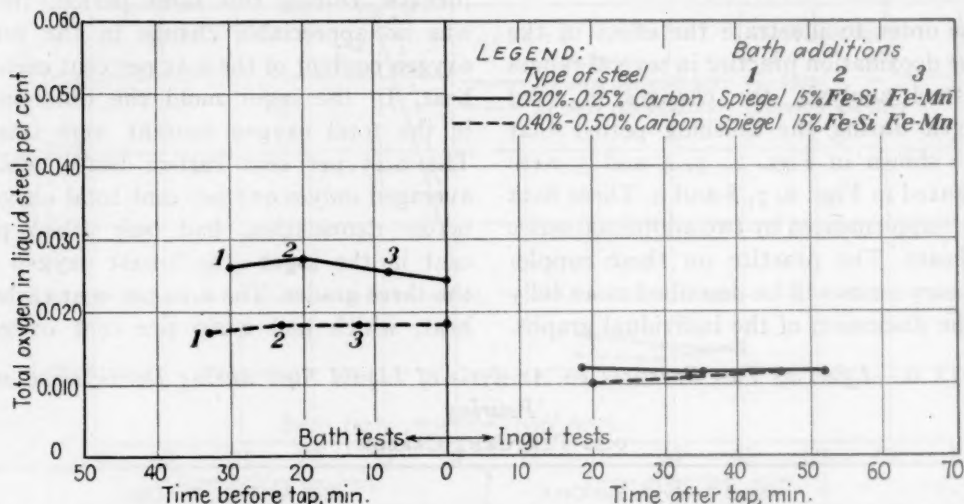


FIG. 7.—CHANGES IN TOTAL OXYGEN CONTENT OF TWO GRADES OF LIQUID STEEL USING DOUBLE DEOXIDATION.

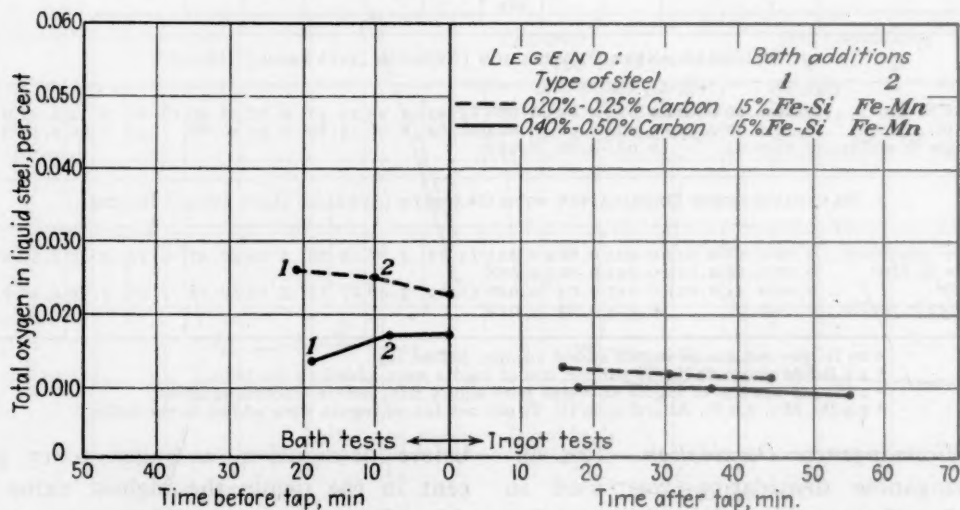


FIG. 8.—CHANGES IN TOTAL OXYGEN CONTENT OF TWO GRADES OF LIQUID STEEL USING 15 PER CENT FERROSILICON DEOXIDATION.

in total oxygen resulted during tapping and pouring for both specifications, the more highly oxidized grade having the larger decrease. In the mold, the difference between the average total oxygen content of the two grades of steel was small. The lower carbon heats again had the higher total oxygen in the ingot mold.

and the 0.45 per cent carbon steels were similar to those from the double deoxidation. A small drop in the total bath oxygen took place on the 0.20 per cent carbon steel whereas a slight increase was obtained on the 0.45 per cent carbon grade. In the molds the difference in the average total oxygen content for the two grades was

slight. Again, the lower carbon steel had a slightly greater total oxygen content.

Spiegel Deoxidation.—The over-all changes in total oxygen content resulting

higher carbon heats in the period preceding the spiegel addition, were similar in many physical respects to the treated slags of the 0.45 per cent carbon heats. The changes

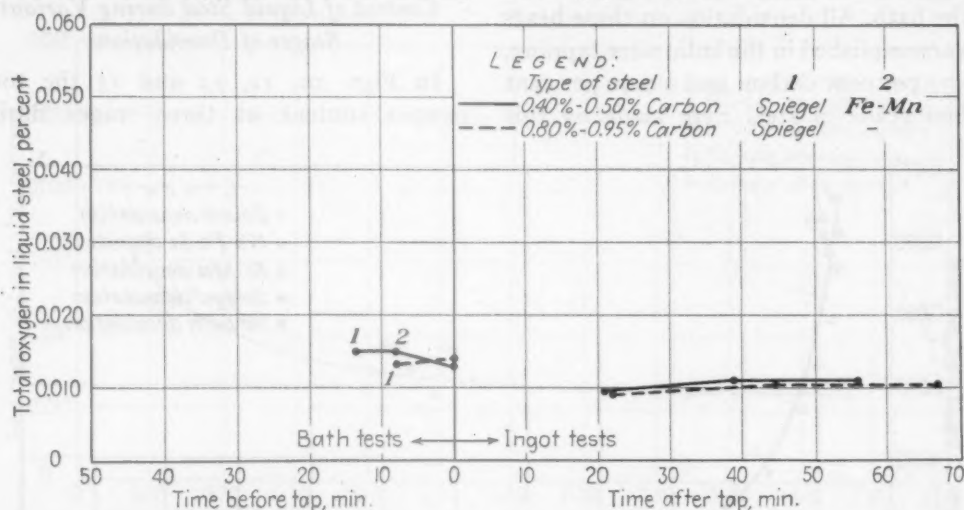


FIG. 9.—CHANGES IN TOTAL OXYGEN CONTENT OF TWO GRADES OF LIQUID STEEL USING SPIEGEL DEOXIDATION.

from the use of the spiegel deoxidation practice on the 0.45 and the 0.90 per cent carbon grades of steel were comparatively small. In the 0.45 per cent carbon heats, the spiegel was preceded by an addition to thicken the slag. Also, the spiegel addition to the bath on the lower carbon grade was followed by ferromanganese. The heavy, foamy slags, which characterized the

in total oxygen for the two grades are compared in Fig. 9. Neither grade of steel shows any marked change in the total oxygen content of the bath. A comparatively small decrease takes place during tapping and pouring. Again, the difference in total oxygen content in the molds is small, the lower carbon heat having a slightly higher total oxygen value.

TABLE 7.—Changes in Analysis during Finishing of Two Grades of Steel without Any Bath Deoxidation
0.07 AND 0.90 PER CENT CARBON

Sampling Time	Steel Analysis, Per Cent						Slag Analysis, Per Cent									
	C	Mn	P	S	Si	Total Oxy- gen	FeO	Fe ₂ O ₃	SiO ₂	Al ₂ O ₃	CaO	MgO	MnO	P ₂ O ₅	S	
1. 0.07 PER CENT CARBON STEEL (AVERAGE DATA FROM 4 HEATS)																
At tap ^a	0.07	0.13	0.009	0.025	0.005	0.059	18.03	6.04	14.83	2.78	37.63	9.52	7.63	1.85	0.13	
Average in molds..	0.07	0.34	0.009	0.025	0.005	0.013										
2. 0.80 TO 0.95 PER CENT CARBON STEEL (AVERAGE DATA FROM 3 HEATS)																
At tap ^b	0.88	0.29	0.018	0.028	0.005	0.013	8.77	3.43	19.74	3.53	42.03	7.13	11.05	2.74	0.15	
Average in molds..	0.90	0.65	0.021	0.027	0.15	0.009										

^a 5.9 lb. Mn and 3.3 lb. Al per net ton of ingots were added to the ladle.

^b 8.8 lb. Mn, 4.0 lb. Si, and 0.75 lb. Al per net ton of ingots were added to the ladle.

Tapping on an Open Bath.—Two grades of fine-grained killed steel were made by tapping directly from the furnace without the addition of any deoxidizing elements to the bath. All deoxidation on these heats was accomplished in the ladle after tapping. A 0.07 per cent carbon and a 0.90 per cent carbon grade of steel were made by this

cent, as compared with 0.009 per cent for the 0.90 carbon steel.

Effect of Carbon Content on Total Oxygen Content of Liquid Steel during Various Stages of Deoxidation

In Figs. 10, 11, 12 and 13 the total oxygen content at three stages during

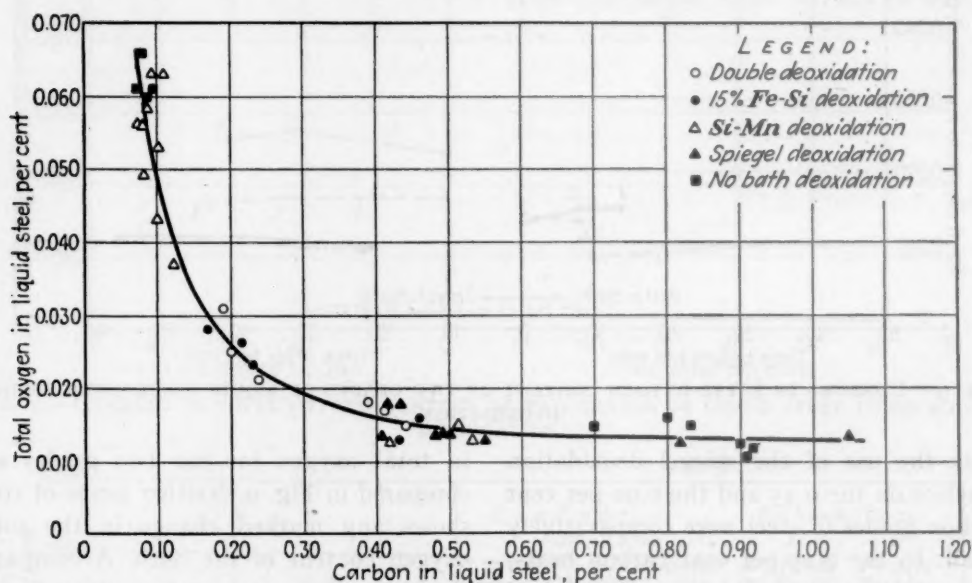


FIG. 10.—RELATIONSHIP BETWEEN CARBON AND TOTAL OXYGEN IN LIQUID STEEL BEFORE ADDITION OF BATH DEOXIDIZERS.

practice. Since the results on these grades cannot be depicted effectively in graphic form, the changes in analysis are presented only in Table 7.

Both grades were fully killed when poured into the ingot molds. As would be expected, a large decrease in total oxygen content occurred during the tapping and pouring periods on the low-carbon heats. The total drop was much larger than that caused by adding deoxidizer to the bath. The decrease during the same period on the high-carbon heat was comparatively small. Despite the extreme difference in steel analyses, the difference between the average total oxygen content of the liquid steel in the ingot mold was small. The average total oxygen in the ingot mold on the low-carbon heat was 0.013 per

cent, as compared with 0.009 per cent for the 0.90 carbon steel. The relationship, as would be expected, is a fairly good one especially since all heats were fully killed and therefore worked in a similar manner.

The curve in Fig. 11 represents the total oxygen content in all heats deoxidized in the bath to the extent that all action apparently has ceased. The bath samples were all taken at the start of

tap. The timing for each practice was specified in such a way as to obtain the optimum effect from the bath additions. The curve relating the total oxygen at

sampling time and diversions from the specified timing for the finishing practice, the relationship is not as good as that shown in Fig. 10 for open bath conditions.

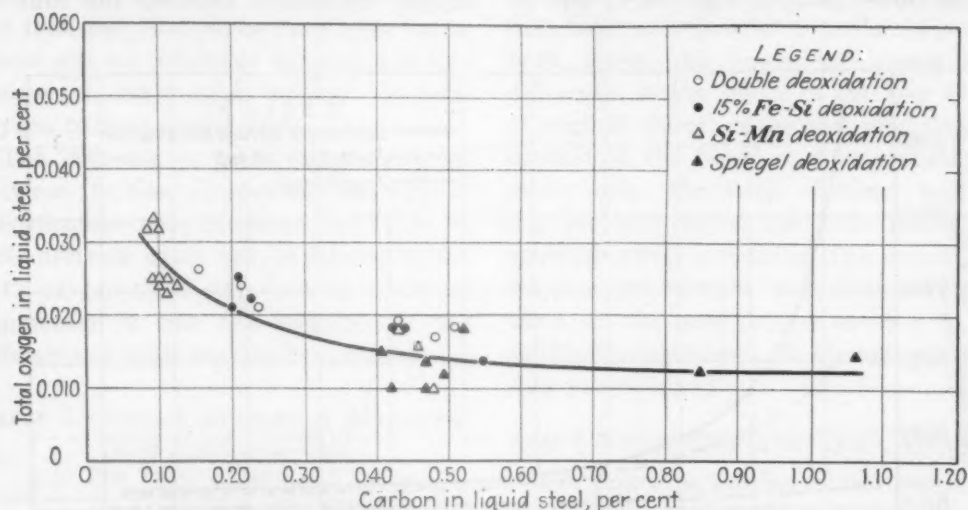


FIG. 11.—RELATIONSHIP BETWEEN CARBON AND TOTAL OXYGEN IN LIQUID STEEL AT TIME OF TAP AFTER ADDITION BATH DEOXIDIZERS.

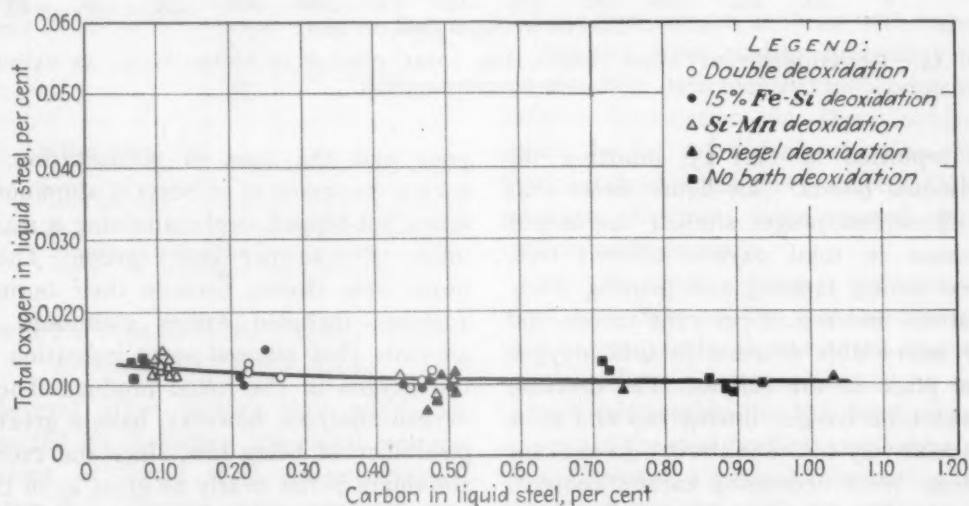


FIG. 12.—RELATIONSHIP BETWEEN CARBON AND TOTAL OXYGEN IN FULLY KILLED LIQUID STEEL IN THE INGOT MOLD.

tap with the carbon content has the same general appearance as that showing the open bath relationship. However, for the tapping tests the increase in total oxygen content with decreasing carbon is much less rapid below 0.30 per cent carbon. Because of the indefinite nature of the

The relation between the total oxygen and the carbon content of fully killed liquid steel in the ingot mold is shown in Fig. 12. The increase of total oxygen content with decreasing carbon was very small, even in the low-carbon range. Each practice contributed points both

above and below the curve, indicating again that there is little difference in the total oxygen resulting from the various deoxidations.

The three curves of Figs. 10, 11 and 12

OXYGEN ANALYSIS OF LOW-CARBON ALUMINUM-KILLED STEEL AFTER SOLIDIFICATION

In order to obtain some measure of the oxygen elimination between the time of

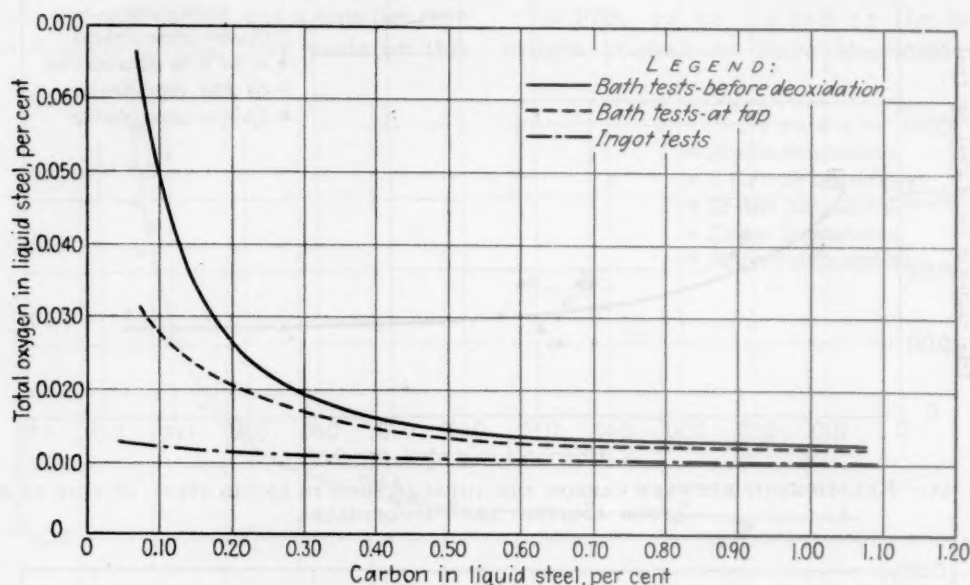


FIG. 13.—RELATIONSHIP BETWEEN CARBON AND TOTAL OXYGEN IN LIQUID STEEL AT VARIOUS STAGES OF DEOXIDATION.

are replotted in Fig. 13, omitting the individual points. This figure shows that in all carbon ranges studied the largest decrease in total oxygen content took place during tapping and pouring. Only in steels under 0.25 per cent carbon did any appreciable decrease in total oxygen take place in the furnace. The decrease in the total oxygen during tap and pour was relatively constant above 0.30 per cent carbon. With decreasing carbon content, this drop in total oxygen increased rapidly.

During the time that the heat remained in the furnace after the start of deoxidation, very little elimination of total oxygen took place in heats above 0.30 per cent carbon. Below this carbon, a definite elimination of total oxygen was effected while the heat was in the furnace. This elimination of oxygen increased markedly with decreasing carbon.

pour and the time of solidification, a review was made of 10 heats of aluminum-killed hot-topped steel containing a maximum of 0.10 per cent carbon. These heats were chosen because their normal analyses included excess aluminum in amounts that allowed some indication of the oxygen in the rolled product. These oxygen analyses, however, have a greater possibility of being low, since the excess aluminum is not nearly as great as in the bath and ingot tests. All the oxygen contents are based on Al_2O_3 analyses. Accordingly, the greater the excess aluminum present, the more efficiently the aluminum should have reduced other oxides and combined with the total oxygen.

Six of the heats were deoxidized in the furnace with silicomanganese and four were tapped with virtually an open bath (scrap reboil used ahead of tap). The

remaining amounts of deoxidizers and alloys including the aluminum were added to the ladle. Table 8 shows that the heats deoxidized with silicomanganese tapped with an average bath oxygen content of less than half that of the open bath heats. There was no difference between the two groups of heats with respect to total oxygen content during pour.

The decrease in total oxygen content between the time of pour and the time of solidification also is shown in Table 8. This decrease could not be related to the bath oxygen or to slag FeO. In addition, apparently it was not affected by the difference in bath-deoxidation practice.

TABLE 8.—*Oxygen Analyses of Aluminum-killed Hot-topped Steel*
0.10 PER CENT MAXIMUM CARBON

Number of Heats	Furnace Practice	Average Total Oxygen Analysis, Per Cent			
		Liquid Steel			Rolled Product
		Before Bath Deoxidation	At Tap	In-gots	
6	SiMn deox. 8 min. pre tap....	0.059	0.026	0.013	0.009 ^a
4	Scrap reboil 8 min. pre tap....	0.060	0.059	0.013	0.008 ^b

^a Aluminum in product 0.051 per cent.

^b Aluminum in product 0.034 per cent.

OTHER FACTORS AFFECTING TOTAL OXYGEN CONTENT OF LIQUID STEEL

Several other factors that might be expected to influence the total oxygen content of liquid steel were surveyed. Three that deserve some mention are: (1) the metal temperature, (2) the type of open-hearth charge and open-hearth practice, and (3) the actual equilibrium conditions for the particular steel analysis being considered. The last factor cannot be approached in the present paper, since the method by which the oxygen was determined gives no positive indication of the form in which the oxygen existed

in the liquid steel. The relations between carbon and total oxygen shown in Figs. 10, 11, 12 and 13 include heats made with hot metal and scrap charges, using both the flush and nonflush open-hearth practice. Since each practice contributed points both above and below the curve, any difference in the effect of the two types of original charge on the final total oxygen content of the liquid steel is probably a minor one. The data obtained on the 0.45 per cent carbon steel were studied to establish whether pouring time or pouring temperature exerted any distinguishable effect on the total oxygen content of the steel in the ingot mold. No obvious relationship was obtained.

ALLOY RECOVERIES AND STEEL QUALITY

The preceding portion of this paper has dealt with variations in total oxygen content of steel. Other observations were made to determine the possible significance of these total oxygen analyses with respect to finished steel quality and alloy recoveries. The data required to develop any definite information on these subjects should be far more comprehensive than that contained in this survey of deoxidation practices. However, some general observations could be made.

Alloy Recoveries.—From a study of the alloy recoveries on the 0.40 to 0.50 per cent carbon steels, it was noted that the over-all silicon recoveries showed no consistent relationship to the total oxygen content of the steel preliminary to deoxidation. However, a general relationship was found between the total iron oxide in the slag ($\text{FeO} + 1.35 \text{Fe}_2\text{O}_3$) and the over-all silicon recovery. The heats having finishing slags with high iron oxide had lower silicon recoveries than heats with slags low in iron oxide. The data indicated that for the same iron oxide content of the slag the average over-all silicon recovery on the heats deoxidized with silicomanganese or spiegel were 15 to 20 per cent

higher than on the practices in which 15 per cent ferrosilicon was used. The manganese recoveries could not be related to either the slag FeO or the bath total oxygen.

Soundness of Product.—It was found that samples of the rolled product submitted on each heat for deep-etch tests were generally sound internally on heats having slags low in total iron oxide. The heats with high iron oxide in the slag gave poor deep-etch ratings. The total oxygen in the bath before deoxidation showed no relationship to the etch ratings. Again, the available data were limited.

These remarks do not in any way preclude the possibility of further investigation into the composition and form of oxides revealing trends that are not measurable by the total oxygen analyses employed in the present work. The determination of the effect of different deoxidation practices on steel quality would require extensive studies specifically directed toward this problem. Such studies would be of definite value to the industry.

SUMMARY

The current study was carried out in order to survey the changes in total oxygen content that take place in deoxidizing, tapping and pouring basic open-hearth steel. No attempt was made to identify the form in which the oxygen existed in the liquid steel during the various stages of the finishing period. The results of this survey are summarized in the following statements:

1. For a given final analysis, the total oxygen content of liquid steel during the various stages of the finishing, tapping and pouring periods was not affected appreciably by the specific type of bath deoxidation practice used.
2. The average total oxygen content of the liquid steel in the ingot mold for the various series of steel specifications and practices surveyed ranged only from 0.009 to 0.014 per cent.

3. The carbon content had a more direct effect in determining the total oxygen content of the liquid steel in the bath and in the mold than did the specific deoxidation practice. These relations are summarized graphically in Fig. 13.

4. The maximum decrease in the total oxygen content of the liquid steel occurred during tapping and pouring of the heat. Except on heats under 0.30 per cent carbon, any changes in total oxygen taking place while the steel is still in the furnace were relatively small.

5. The total oxygen content of the liquid metal could not be directly related to such features as alloy recoveries or the internal soundness of the finished product. A general relationship existed between these features and the total available oxygen in the slag. The available data were too limited to make anything more than general observations.

The data on the total oxygen content of liquid steel indicate that there is little difference between various deoxidation practices. It should be noted, however, that other features—such as the form of the oxides, the security of the furnace block, the recovery of alloying additions—as well as local economic conditions must be considered before a comparison of the merits of individual deoxidation practices would be justified. The present study merely points out some of these variables. Considerable further work must be done on this problem before a satisfactory basis for selecting any individual deoxidation practice is established.

ACKNOWLEDGMENTS

The data for this paper are from a general investigation of deoxidation practices in progress at the Inland Steel Company's plant. The authors desire to express their appreciation for the assistance and cooperation they received from the personnel associated with open-hearth operations at Inland Steel Co. They are especially

indebted to Mr. T. S. Washburn, Assistant Chief Metallurgist, under whose guidance the work was carried out and without whose advice and suggestions the investigation could not have been completed. They wish to thank Mr. J. H. Nead, Chief Metallurgist, who made this investigation possible.

Acknowledgment is due Messrs. C. O. Geyer, Chief Chemist, and R. L. Harbaugh, Assistant Chief Chemist, who were responsible for all chemical analyses.

The vacuum-fusion determinations were made by the staff of Battelle Memorial Institute.

Finally, the authors wish to express their gratitude to the management of Inland Steel Co. for permission to publish the data presented in this paper.

REFERENCES

1. K. C. Feters and J. Chipman: Slag-metal Relationships in the Basic Open Hearth. *Trans. A.I.M.E.* (1940) **140**, 170-198.
2. C. H. Herty, Jr., H. Freeman and M. W. Lightner: U. S. Bur. Mines R. I. 3166 (1932).
3. K. C. McCutcheon and L. J. Rautio: Oxygen Samples from the Open-hearth Bath. *Trans. A.I.M.E.* (1940) **140**, 133-135.
4. W. O. Philbrook: Discussion. *Trans. A.I.M.E.* (1940) **140**, 136-137.
5. J. G. Thompson, H. C. Vacher and H. A. Bright: Cooperative Study of Methods for Determination of Oxygen in Steel, and Discussion. *Trans. A.I.M.E.* (1937) **125**, 246-312.
6. F. W. Scott: Extraction of Slag and Oxide Inclusions in Iron and Steel. *Ind. and Eng. Chem., Anal. Ed.* (1932) **4**, 121.
7. T. L. Joseph: Oxides in Basic Pig Iron and in Basic Open-hearth Steel. *Trans. A.I.M.E.* (1937) **125**, 204-243.
8. S. Marshall and J. Chipman: The Carbon-oxygen Equilibrium in Liquid Steel. *Trans. Amer. Soc. Metals* (1942) **30**, 695-739.
9. T. E. Rooney and A. G. Stapleton: The Iodine Method for the Determination of the Oxides in Steel. *Jnl. Iron and Steel Inst.* (1935) **131**, 249-254.
10. F. O. Kichline: Estimation of Aluminum in Steel. *Ind. and Eng. Chem.* (1915) **7**, 806-807.
11. A. B. Kinzel, J. J. Egan and R. J. Price: Rapid Determination of Oxide in Molten Metal. *Metals and Alloys* (May 1934) **5**, 96.
12. C. H. Herty, Jr., J. M. Gaines, H. Freeman and M. W. Lightner: A New Method for Determining Iron Oxide in Liquid Steel. *Trans. A.I.M.E.* (1930) **90**, 28.
13. T. Swinden and W. W. Stevenson: The Determination of Oxygen in Liquid Steel. Fourth Report of the Oxygen Sub-Committee. *Jnl. Iron and Steel Inst.* (July 1943) 167-177.
14. H. A. Sloman: The Vacuum-fusion Method for the Determination of Oxygen. Fourth Report of the Oxygen Sub-Committee. *Jnl. Iron and Steel Inst.* (July 1943) 5-8.
15. S. Marshall and J. Chipman: Improvements in the Accuracy of the Vacuum-fusion Method for the Determination of Oxygen in Steel. *Trans. A.I.M.E.* (1940) **140**, 127-131.
16. W. W. Stevenson and G. E. Speight: The Vacuum Fusion Method for the Determination of Total Oxygen in Steel. Seventh Report on Heterogeneity of Steel Ingots, Iron and Steel Inst. (1937) Special Report No. 16, 65.
17. G. Derge: Rapid Analysis of Oxygen in Molten Iron and Steel. *Trans. A.I.M.E.* (1943) **154**, 248.
18. S. L. Hoyt and M. A. Scheil: Fractional Vacuum-fusion Analysis for the Determination of Oxygen in Steel. *Trans. A.I.M.E.* (1937) **125**, 313-327.
19. H. R. Nelson, Battelle Memorial Institute. Private communication.
20. B. M. Larsen: Controlling Reactions in the Open-hearth Process. *Trans. A.I.M.E.* (1941) **145**, 67-78.

DISCUSSION

K. L. FETERS.*—I have no prepared discussion of the paper by Tenenbaum and Brown. I have just a few general remarks, mostly things that occurred during the delivery of the paper.

There is one question I would like to ask: What size of wire was used in the bomb test? I think we are going to have some later discussion perhaps comparing the bomb test with other methods of oxygen determination. Perhaps this point will be brought out at that time. The wire size has been found to be quite significant in determining the accuracy of the oxygen value obtained by the gravimetric method.

This paper brings together some things we have noted for quite a while. Those of us who have had to do with plant deoxidation have noticed that probably it does not make too much difference in the final quality of material as long as we remain within reasonable limits of deoxidation practice. For instance, in plant A a certain deoxidation practice has been set up and the men at that plant swear by it; if you were to change the order of the additions

* Youngstown Sheet and Tube Co., Youngstown, Ohio.

by the least bit or change the amount they would be horrified and expect to have very poor quality steel. At another plant, quite different results are being obtained. Then, if we try to take the practice from one plant into another, we again find that sometimes it appears to make a difference but more often it does not.

We can all cite examples, I think, from our practice of trouble at a plant on a given product as to the quality of material being produced, yield, or some other factor. So we decide to improve that practice and change the deoxidation. We find out what our competitor is doing, and we try that. Immediately we find that we have had a great improvement in quality of the material. So we decide that was a pretty good practice, and we sit down contentedly with it for 4 or 5 months, and then we get into exactly the same trouble we had before. We change back to the original deoxidation and find the same improvement taking place, and we are completely at sea. Most of us have noted that happening time and time again.

I think that the authors tend to confirm these occurrences with some scientific proof in that it does not seem to make a great deal of difference what the order of additions is or what the final oxygen content is but we should relate the final deoxidation of the ingot to the steel quality. There must be a pretty good relation there.

Another point is brought out by the paper—that apparently in most cases the authors must have shown some residual aluminum, since in the analysis below the last table they show that to be of the order of 0.03 per cent. This variation was 0.03 to 0.05, perhaps a little greater. The final oxygen that would be expected at equilibrium with that amount of aluminum would not be greatly different. It would probably be less than the experimental error in determining oxygen. Therefore it seems not at all unreasonable that the findings reported by the authors, of virtually constant oxygen, have occurred, since they are ending their deoxidation practice in most cases with an amount of aluminum in the neighborhood of 0.03 to 0.05 per cent, and, therefore, they find the amount of oxygen that would be in equilibrium with that percentage of aluminum.

The authors state that they find little or no

relation between the soundness of the product as viewed by a macroetch test and the amount of oxygen in the ingot, but that they do find some relation between the FeO content of slag and the soundness of product. That might bring to mind the practice that is followed in a number of plants, where, in addition to varying the amount of aluminum or other deoxidizers added for deoxidation, there is some compensation made in the amount of the addition to take care of unusually high or unusually low slag FeO. It might be that a correction of that sort would bring a little bit better relation into deoxidation and would tend to decrease the relation found between the slag FeO and the soundness.

GERHARD DERGE.*—The data presented in this paper are extremely interesting, as they add considerably to our knowledge of the oxygen levels existing in the basic open-hearth process.

In order to complete the references on methods of sampling, note should be taken of a patent granted to C. B. Francis,²¹ of Carnegie-Illinois Steel Corporation, in 1934. This describes a method of bomb sampling of the open-hearth bath that includes the essential features of the McCutcheon and Rautic method, which has come into vogue more recently. The Francis bomb is essentially simpler than the later types and may offer some advantages for that reason.

Tenenbaum and Brown have discussed a number of the difficulties encountered in oxygen sampling and some of the merits and demerits of the various methods. Their discussion shows that we will not have a complete understanding of these phenomena until data such as theirs have been collected by several different techniques. We are glad, therefore, that preliminary results from a comparable study using the chilled-wedge method of sampling²² can be reported at the present time, although it is expected that a detailed and complete paper will be presented later. These

* A joint contribution from the metallurgical staff of the Homestead Works of the Carnegie-Illinois Steel Corporation and the Research Project sponsored by that Corporation in the Metals Research Laboratory of the Carnegie Institute of Technology.

²¹ C. B. Francis: U. S. Patent 1979737 (1934).

²² G. Derge: *Trans. A.I.M.E.* (1943) 154, 248.

particular results are of interest now because they offer a comparison of bomb tests and the chilled-wedge test on similar grades of steel. Both methods of sampling show the same

ent heats. These are superposed (Fig. 14) on Fig. 3 of the authors, which is for 0.20 to 0.25 per cent carbon steels. The data from the wedge tests taken prior to tap are somewhat

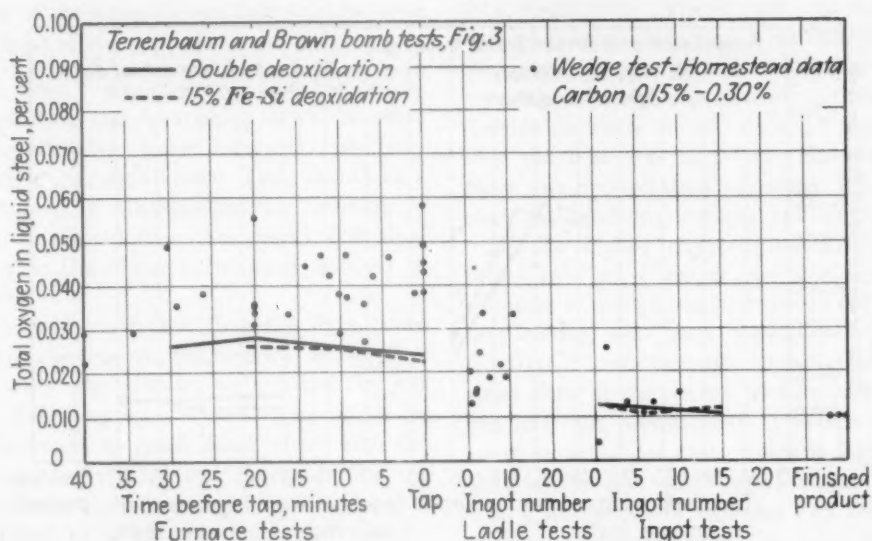


FIG. 14.—HOMESTEAD DATA SUPERPOSED ON TENENBAUM AND BROWN'S FIGURE 3.

general trends although there are numerous differences in detail.

The steels studied at Homestead were all semikilled grades. No special additions were made to the slag immediately prior to the time of tap. Some of these heats were blocked in the furnace and some were not. The data are insufficient to indicate specific effects of such practice. The samples designated as ladle samples were taken by fastening the same kind of mold to a long handle so that it could be placed immediately under the ladle nozzle, which was then partly opened. The samples taken from the bath prior to tap were poured into the copper mold from a slag spoon, as described in reference 22. The ingot tests were taken by the glass-tube method recently described by Motok. These were taken from the top of the ingot before any aluminum had been added. The finished product samples were cut from the hot-rolled product. All samples were analyzed for oxygen by vacuum fusion. In order to provide as direct a comparison as possible, these data were divided into two carbon ranges and superposed on the corresponding data of Tenenbaum and Brown.

The higher range includes 0.15 to 0.30 per cent carbon and includes data from eight differ-

ent heats. These are superposed (Fig. 14) on Fig. 3 of the authors, which is for 0.20 to 0.25 per cent carbon steels. The data from the wedge tests taken prior to tap are somewhat

higher than those from the bomb tests. The differences between the two sets of data may be attributed to differences in types of steel. The ladle oxygens are intermediate between the bath and ingot values, as might be expected. The lower range includes 0.08 to 0.14 per cent carbon and also includes data from eight different heats. These are superposed (Fig. 15) on Fig. 5 of the authors, which is for 0.10 per cent carbon steels. The furnace tests agree well with those of the authors taken before deoxidation. The other remarks on the author's Fig. 3 (Fig. 14) also apply here.

One conclusion to be drawn from this comparison is that essentially the same data are obtained by either method of sampling and analysis. It is our opinion that the chilled-wedge sample and vacuum-fusion analysis combination is far simpler, but this of course is determined by the facilities and experience available.

It is also our feeling that the range of oxygens shown by the data from eight heats is characteristic of any grade of steel, and that a knowledge of this range is more important than any particular average.

This statement is based on the fact that at the present time rapid oxygen analysis of

wedge samples is being used to determine the ladle deoxidation of semikilled steels. The results to date include 20 heats (certainly too few for final conclusions) and the rejections on

by manganese and chromium to specification. Ladle deoxidizers consist of Alsifer and silicon for grain-size control, and final adjustments of manganese and chrome to specification.

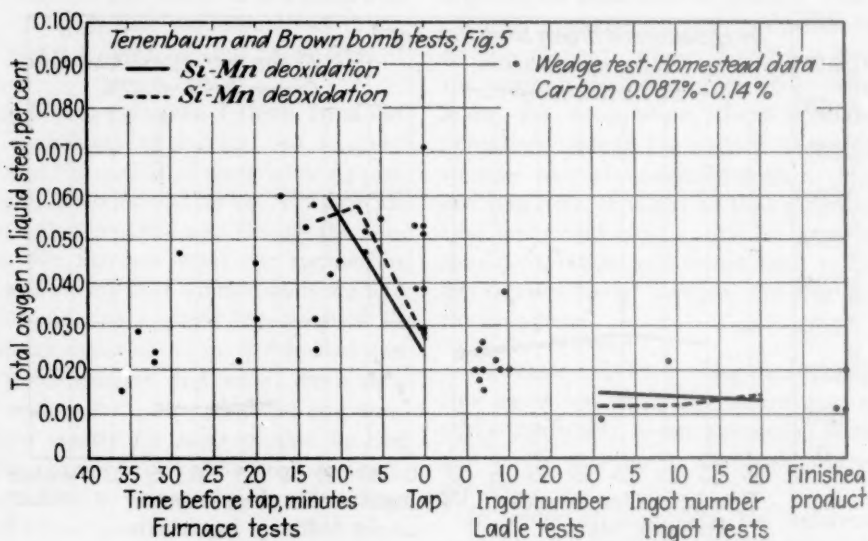


FIG. 15.—HOMESTEAD DATA SUPERPOSED ON TENENBAUM AND BROWN'S FIGURE 5.

finished products from these heats have been reduced from a normal range of 2.5 to 3 per cent to a range of 1 to 1.5 per cent. The reduction in rejections may be attributed to the fact that by knowing the true FeO in the metal before tapping the proper deoxidation practice can be carried out. Proper deoxidation reduces defects due to overdeoxidation or underdeoxidation.

CHAIRMAN SOLER.—I should like to hear from one of the dyed-in-the wool steelmakers. Mr. Ramsey.

E. L. RAMSEY.*—We all get good results when using our own individual deoxidation practices, whereas using some other plant's practice might cause us trouble.

At our plant, furnace deoxidation follows good open-hearth melt-carbon practice, slag control, and control of temperature.

We use spiegel as our principal furnace deoxidizer. We also use a little 15 per cent silicon to supplement the spiegel. With 10-minute final preliminary analyses, we get very good results from a straight spiegel block followed

J. A. ROSA.*—I should like to ask the authors to explain the marked decrease in oxygen content, which occurs, they say, during the tapping point of 8.

C. H. HERTY, JR.†—I should like to ask one question of the authors in connection with these five practices, arriving at essentially the same total oxygen content. They have certain time intervals in each practice between the spiegel and the silicon and other additions. Are these practices as they are set up those that have given the best results for each type? In other words, does the 20-minute interval between spiegel and silicon, in their opinion, represent the best practice for that grade of steel?

I should also like to point out one other thing. A glance at this paper indicates that all that is needed for a good heat is a first helper and a man that can weigh up materials. But many other things are mentioned in the latter part of the paper that may vary a practice; that is, whether there is temperature control at all times, what the carbon practice is, how

* Wisconsin Steel Works, South Chicago, Illinois.

* Republic Steel Corporation, Canton, Ohio.
† Bethlehem Steel Co., Bethlehem, Pennsylvania.

close the limits are on other alloys, and a number of other factors. I think that we ought to remember in connection with deoxidation that to get the oxygen down to a certain value is just one of the many things that must be done with a heat of steel.

C. E. SIMS.*—It is believed that the importance of these enlightening data will be more appreciated when fuller interpretation indicates their true significance. They should be a distinct help in rationalizing our thinking in respect to deoxidation phenomena and their relation to the ultimate inclusion content of the steel.

There is some doubt that the data given represent the true oxygen contents of the bath at the time the samples were taken, for the reason that it appears virtually impossible for the aluminum to reach equilibrium with the dissolved oxygen in the very short time that the steel remains molten in the bomb. The precautions taken to avoid this unfinished reaction, however, have probably reduced the discrepancy to a constant error, which gives the data a very practical value. The beautiful consistency that runs through them must have some significance.

On the premise that the oxide inclusions of solid steel bear a direct relation to the oxygen content of the steel when liquid, the data of this paper can be checked qualitatively by microscopic examination. In a paper²³ presented before this body in 1932, evidence was given that, except for the extraneous inclusions picked up during pouring, all the oxide inclusions found in solid steel were in chemical solution while the steel was molten. About the only exception to this occurs when steel is deoxidized in the mold.

The oxygen in the liquid steel is that which is in equilibrium with the other elements present. This equilibrium is upset during cooling to the freezing temperature and by segregation during freezing, with the result that oxides are precipitated at this time. Oxides that are precipitated as a result of the addition of deoxidizers float out quickly and enter the slag.

The results of the present paper were pre-

dicted and can be explained by the conclusions of the earlier paper. In the first nine heats, the manganese and silicon added did not introduce contents higher than 0.82 per cent and 0.13 per cent, respectively. The oxygen contents at the time of the first bath tests were established by the carbon content as is shown in Fig. 10. The quantity of manganese or silicon added to the furnace in these heats, although enough to stop the boil, was apparently insufficient to cause any precipitation of oxides. The oxygen content, therefore, remained stationary.

In the higher oxygen, low-carbon heats shown in Figs. 5 and 6, however, equivalent amounts of manganese and silicon did precipitate oxides, and these oxides were quickly eliminated from the bath, as indicated by the steep slope of the curves. The amount of oxygen left (not precipitated) is in the range of 0.023 to 0.029 per cent, which is higher than that of the first nine heats, except those in Fig. 3, and probably explains why the oxygen content was not lowered in those heats. In the 0.20 per cent C heats of Fig. 3, where the oxygen was in the same range, there was a drop from 0.026 to 0.023 per cent.

It has already been noted that all heats, regardless of previous conditions, lost oxygen between the tap test and the first ingot test; that the oxygen in all heats was brought close to a common level, and that there was practically no change after the first ingot test. This is contrary to the often expressed opinion that contact of the steel with the air and slag during tapping is bound to increase the oxide content. Two things were common to all these heats during this period, which can explain this phenomenon.

In the first place, all the heats lost temperature (from 100° to 150°F.) during tapping. This alone should cause some oxide precipitation, but this effect probably is unimportant in view of the fact that all heats were deoxidized with ladle additions of silicon, aluminum and titanium. Because of the relative amounts added, aluminum undoubtedly dominated the deoxidation and established the new equilibrium conditions. Oxides were precipitated down to a new level, in equilibrium with the aluminum, and the precipitated oxides floated out quickly, as per custom, and were eliminated. The data of this paper are clearly in

* Battelle Memorial Institute, Columbus, Ohio.

²³ C. E. Sims and G. A. Lillieqvist: Inclusions—Their Effect, Solubility, and Control in Cast Steel. *Trans. A.I.M.E.* (1932) 100, 154.

accord with what can be seen in a comprehensive study of inclusions.

W.O. PHILBROOK.*—I should like to add a few qualifying observations, some of which confirm Tenenbaum and Brown's work and some of which are at slight variance.

Some years ago we changed from a spiegel and pig-silicon deoxidation to a straight spiegel block. At the time of changeover we found that there was a tendency for the steel leaving the furnace to have a somewhat higher oxygen content as determined by the bomb test in the case of the spiegel block than for the dual block. That oxygen content is also dependent on the carbon content of the steel. At the pouring platform, however, the oxygen levels in the steel coming from the ladle were substantially the same, regardless of which deoxidation practice was used.

I would also like to place a qualification on Mr. Sims' statement with regard to the effect of temperature. I think that his thesis probably is true in the higher temperature range, but there is a practical limitation that we all know, as, for example an alloy heat that is teemed cold, with a heavy skull, is a dirty heat. In other words, probably there is a decrease in solubility of oxygen and precipitation of oxides occurring with falling temperature. But if the temperature level is too low the inclusions are not floated out. There must be a practical balance maintained between the fluidity of the steel and the precipitation of inclusions as affected by temperature.

We also have some indication from electrolytic extraction work for silica and aluminum inclusions that there is an elimination of silica and alumina in the ladle and possibly even in the molds.

N. C. FICK.†—Several years ago an article appeared in one of the German journals in which the authors claimed that much oxygen was carried into the steel through the stream as it was coming out of the furnace into the ladle, and they advocated tipping the ladle and pouring down the side of it in order to avoid contaminating the steel with an excess of oxygen.

* Wisconsin Steel Works, International Harvester Co., S. Chicago, Illinois.

† Battelle Memorial Institute, Columbus, Ohio.

M. TENENBAUM.—Dr. Feters' question on the size of the wire used is very well taken, because unless very fine carbometer wire is used (18 gauge pure aluminum wire was used in the study) the results that are obtained are not dependable. To ensure more accurate results it was necessary to distribute the wire throughout the bomb mold.

The actual residual aluminum that was shown for the rolled product was not the residual aluminum that is obtained in a bomb test. Ordinarily, in a bomb test, residual aluminum is in the order of 0.5 per cent.

Dr. Derge pointed out that the total oxygen content as obtained in their work was higher than that obtained by the bomb test. However, in his original work he also showed such a discrepancy between the two methods of oxygen sampling and oxygen analysis. Whether the difference shown in Figs. 14 and 15 can be attributed to the same causes is something that he probably can answer better than I can.

Mr. Rosa's question on the decrease of oxygen during pouring has come up several times, and I think Mr. Sims provided an adequate and plausible answer to his question.

One other point might be mentioned, and that is the fact that during tapping and pouring we do have considerable stirring action of the molten metal. In a bath that is perfectly dead while it is in the furnace, all oxide or slag particles must rise according to Stokes' law. In tapping and pouring the stirring action possibly assists in the elimination of the oxides.

As to Dr. Herty's question on the timing we selected, several of the practices are regular practice at our plant. We have considerable experience with respect to these practices. I do not recall that we showed any practice in which 20 min. elapsed between the spiegel and silicon additions. However, there were times when conditions did get a little out of control, and we were not able to follow the specified practice. It is possible and very probable that with some of the practices on which we had very little experience the timing selected for these curves was not the best one.

Dr. Herty's remarks on the precautions that should be used in interpreting these data are very well taken, and I think they should be emphasized here.

K. L. FETTERS.—I referred not to the amount of residual in the bomb test but rather the amount of residual aluminum in the metal being poured in the molds.

There is evidence to indicate that in the authors' test in practically every case they must have had an appreciable content of residual aluminum. In every case they report a fine-grained steel, and although they do not show this residual aluminum content in all cases there seems to be a reasonable suspicion that there is an appreciable aluminum content.

If we take the ordinary aluminum deoxidation diagram, in accord with the diagrams that Dr. Chipman has published, we plot our aluminum at 2912°F., or some such temperature. We have found that if the aluminum is around

0.03 to 0.05 per cent the portion of the curve is fairly flat. Therefore, if we have an amount of residual aluminum in the metal as it goes into the mold that is sufficient to bring us up into this range, if we merely retain the equilibrium we expect to have a constant aluminum in the metal and the mold, as reported by the authors.

M. TENENBAUM.—The aluminum in most of the steels surveyed was much lower than that of the grade mentioned in Table 8. The residual content of the higher carbon grades was well below 0.020 per cent. Since the deoxidation curves referred to are fairly flat even down to 0.010 per cent aluminum, Dr. Fetter's explanation for the constancy of the mold oxygen appears plausible.

The Occurrence of Oxygen in Liquid Open-hearth Steel— Sampling Methods

BY T. E. BROWER* AND B. M. LARSEN,* MEMBER A.I.M.E.

FOR some years we have been carrying on a rather comprehensive investigation of the occurrence of oxygen in liquid open-hearth steel. This investigation was interrupted by the war emergency and is therefore incomplete, with many questions still answered only partially, if at all; yet it seemed worth while to present a report of progress on this difficult field of research, if for no other reason than to promote discussion and further investigation of this important problem.

The significance of such studies depends in large measure upon the accuracy of measurements of oxygen content in liquid steel while it is still in the furnace or as it flows into the ladle, or thence into the mold and there is, as we shall show, good reason for believing that the main source of uncertainty is in the sampling, not in the analytical method as such. The difficulty arises from the fact that any method of sampling is of itself apt to alter the amount of oxygen in solution in the liquid steel, because this oxygen is in a readily reactive condition. On the one hand, being usually present at a concentration appreciably in excess of that corresponding to equilibrium with the carbon then present, it may decrease rapidly in percentage by reaction with carbon and evolution of CO, especially if the liquid metal is in any way shaken or brought in contact with a cooler solid surface. On the other hand, it may increase rapidly by ab-

sorption of oxygen from a slag, a furnace atmosphere, or from air.

These circumstances, which are inherent in the problem, as well as our conclusion that, despite the considerable amount of careful work already done, there is still no method of sampling liquid steel acceptable as an unquestioned standard, led us to undertake systematic comparisons of oxygen content of large numbers of samples taken: (1) by a single method at different positions and levels in the bath; (2) at the same place by different sampling methods; and (3) from bath, tapping stream and pouring stream. The different sampling methods yield somewhat different values and there is as yet no way to tell with certainty which is the most accurate. But the general reproducibility and consistency of the results give us some confidence in certain inferences we draw from them: namely, that the "spoon" method of sampling, properly carried out, gives somewhat more consistent results than the "bomb" method, as it has usually been practiced; that, in the bomb method, an aluminum cap is preferable to a steel cap; that the oxygen content of liquid steel in a finished heat is substantially the same all over the bath at the same level, and tends to decrease at lower levels further from the slag interface; also that it tends to decrease, and to decrease erratically, from furnace bath to tapping stream entering the ladle. Accordingly it seemed desirable to report these observations in detail as a first step, so that the reader may judge their significance as a contribution towards solution of the main problem, which is to find a means of pre-

Manuscript received at the office of the Institute Jan. 22, 1945. Listed as T.P. 1868.

* Research Laboratory, U.S. Steel Corporation, Kearny, N. J.

cise control of both the amount of oxygen and of the modes of its occurrence in the finished steel product.

METHOD OF ANALYSIS

This problem, which proved to be somewhat easier than that of sampling tech-

method is indicated by the frequency curve of Fig. 2, in which, out of 88 determinations on one standard sample (0.048 per cent [O]) made over a period of about a year, 84, or 95 per cent, gave values within a range of 0.002 per cent oxygen (equivalent to 0.01 per cent FeO).

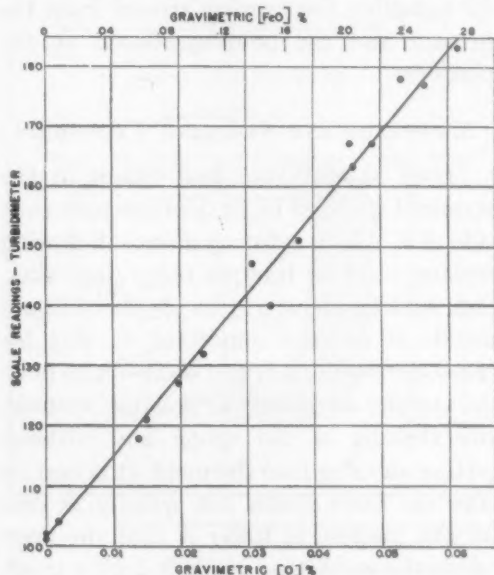


FIG. 1.—TURBIDIMETER CALIBRATION AGAINST GRAVIMETRIC [O] VALUES.

nique, can be disposed of first. We used the well known method of running the liquid steel into a small mold containing aluminum wire to the amount of about 1 per cent of the sample weight; drillings from this tiny ingot were dissolved in nitric acid, the solution brought to standard volume, and the turbidity caused by the very fine suspended particles of alumina was measured. This was done by a sensitive turbidimeter (or colorimeter) in which the output of the two matched photocells illuminated from a common light source is balanced to a null reading on a galvanometer in a bridge circuit. Details of the procedure are given in the appendix. The calibration curve of the instrument, shown in Fig. 1, was made against a series of standard samples that had been analyzed carefully for alumina content by a gravimetric procedure. The precision of the

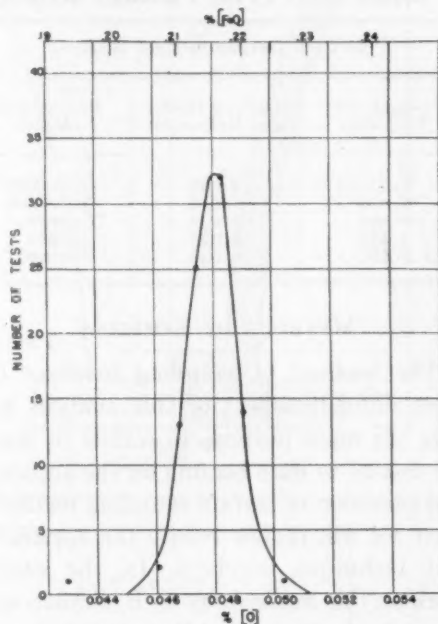


FIG. 2.—FREQUENCY DISTRIBUTION OF RESULTS OF ANALYSIS OF 0.048 PER CENT [O] STANDARD BY TURBIDIMETER.

This analysis can be made within 15 to 20 min. after the furnace sample is received. It is thus about fast enough for routine testing of the condition of the bath, although we have not used it extensively for this purpose. Even for research studies on open-hearth problems, it is almost necessary to have a quick, inexpensive method of this kind, since certain effects can often be detected only by statistical comparisons among large groups of data.

Table 1 contains a few comparisons of results by this turbidity method on samples of liquid steel taken at the pouring platform, with values on the same steel after casting, reheating and rolling, analyzed by the hydrogen reduction method.¹ The good

¹ T. E. Brower, B. M. Larsen and W. E. Shenk: *Trans. A.I.M.E.* (1934) **113**, 61-81.

agreement in the quiet steels lends support to the general reliability of both methods on simple steels, and the differences in the others are in accord with the obvious loss of oxygen as CO during freezing.

TABLE 1.—*Results Obtained on Samples of Liquid Steels by the Turbidity Method*

Per Cent Oxygen in Steel When—		
Liquid, by Turbidity	Solid, by Hydrogen Reduction	Behavior in Mold
0.006	0.006	No action
0.018	0.018	No action
0.049	0.032	Capped
0.049	0.037	Capped
0.066	0.046	Rimmed

METHODS OF SAMPLING

The method of sampling involves the most difficult aspect of this analysis and it is our main purpose to review in detail the results to date bearing on the accuracy and precision of certain sampling methods. First we will review briefly the apparatus and technique involved. In the earlier work on this method, by C. B. Francis and others in the U. S. Steel Corporation, spoon sampling was mainly used. It was found necessary to obtain a good slag coating on the spoon and it appeared better to put the aluminum in the mold, or in both mold and spoon, rather than in the spoon alone. A block-shaped mold welded on a long rod, with the aluminum wire inside and its top opening closed by a thin layer of sheet steel, was also tried; this mold was dipped into the slag to coat it, then directly into the liquid steel and held there until the steel melted through the thin cover and filled the mold. With the somewhat lower degree of precision in sampling and analysis characterizing this earlier work, no definite difference was found between this sampling method (which for convenience we call the "bomb") and that using the spoon. A somewhat more convenient design of bomb, developed by the American Rolling Mill Co., has become popular. We have found

that the bomb sample tends to give consistently lower results than the spoon sample; this difference has also been reported by others, but no data have been published that show definitely better absolute accuracy for either of these methods. We have also evolved a third type of mold for sampling the tapping stream from the furnace and the pouring stream at the platform.

APPARATUS AND SAMPLING TECHNIQUE

Spoon samples are best taken in the standard spoon (a lip or depression on each side of it aids in securing a smooth flowing stream) used for fracture tests, slag cakes, etc., holding about $2\frac{1}{2}$ to $3\frac{1}{2}$ lb. of liquid metal. It is very important to *slag the spoon thoroughly*; it is also necessary to pour the samples as quickly as possible, without any shaking of the spoon and without getting any slag into the mold. It is best to take the filled spoon out quickly in one smooth motion, to lower it near the floor beside the mold, then to tip it until a small stream starts to flow on the floor. As soon as slag stops breaking away, the spoon is moved over the mold and emptied quickly. In using this method (with the usual mold design), we have standardized on putting the aluminum only in the mold, about 30 ft. of No. 20 (B and S) gauge (0.032-in. dia.) pure aluminum wire (about 1.0 per cent of the weight of the ingot) being crumpled into a loose ball and jammed into the mold so that it fills most of the space to be occupied by the sample ingot. Putting aluminum in the spoon as well as in the mold sometimes gives the same result, but there is usually the danger of too high a result by reaction of the aluminum with slag; therefore we prefer using aluminum in the mold only, although with this procedure there is the danger of low results due to boiling in the spoon.

With a fairly fluid slag the spoon may be slagged to a very smooth surface in which case this boiling rarely occurs unless the

spoon is held until the metal starts to freeze. With a heavy slag or with ore in the slag, however, the slag coating may be

may be eliminated by quick pouring and by taking duplicate samples whenever a heavy slag is present, discarding all sam-

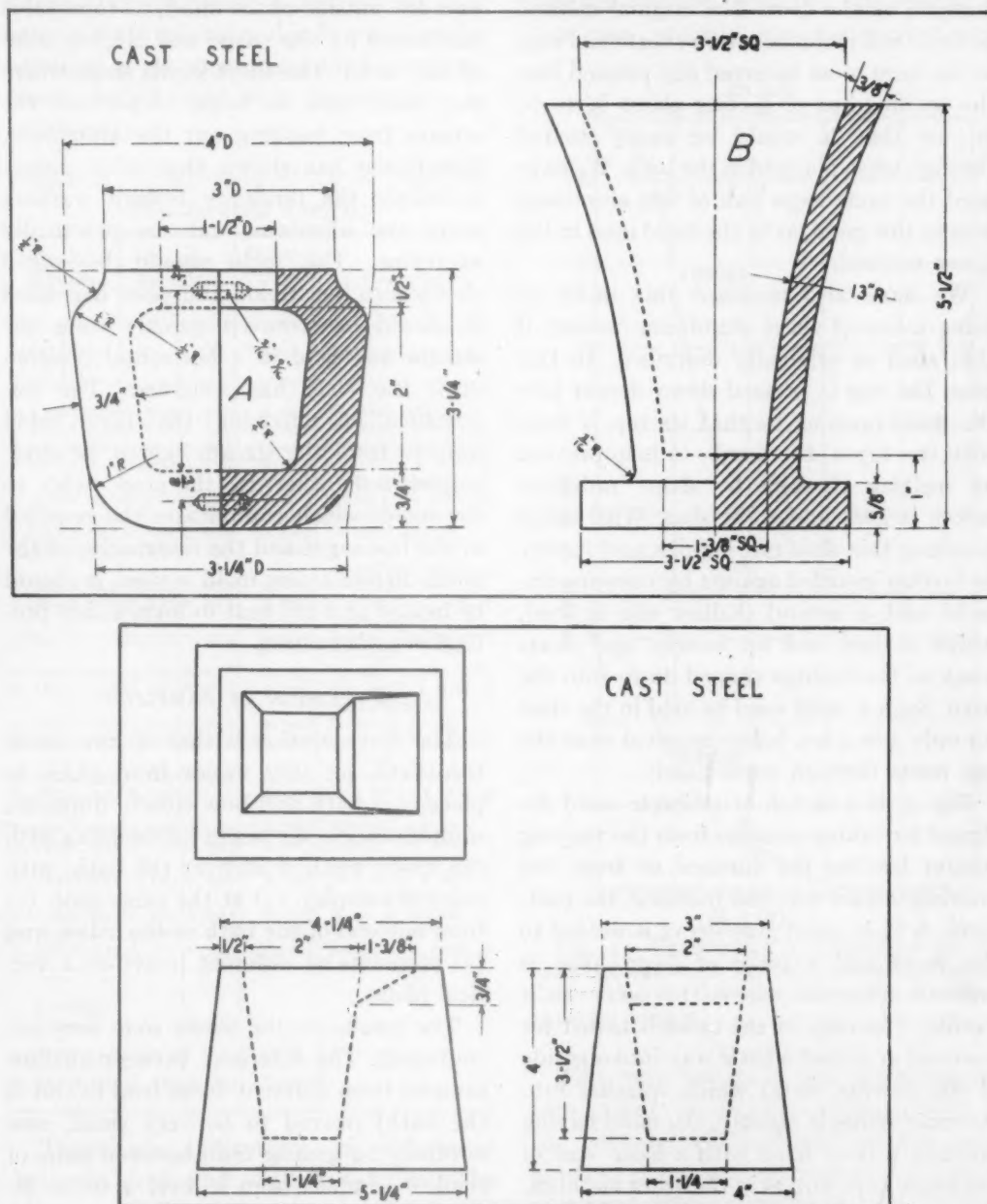


FIG. 3.—MOLDS.

- a. Bomb mold for submersion in bath.
- b. Mold used when bath samples are taken with spoon.
- c. Mold used in tapping and pouring streams.

rough or porous in spots, and boiling may occur and yet not be observed. Something like 80 to 90 per cent of such bad samples

ples that give appreciably lower values for both carbon and oxygen than the other member of the same pair. We also used the

usual bomb-sample mold, closed with loose dowels and held in position in a deep spoon by wedges so that it will fall apart when dumped on the floor. The original method as described included a thin sheet-steel cap, in the form of an inverted cup pressed into the opening but projecting about $\frac{3}{8}$ to $\frac{5}{8}$ in., so that it would be easily melted through when plunged in the bath. We have used the same loose ball of fine aluminum wire in this mold, as in the mold used in the spoon method.

We have also modified this mold by using a cap of sheet aluminum instead of thin steel as originally described. In this case, the cap is pressed down deeper into the mold opening so that its top is flush with the top of the bomb, to help prevent its melting through by flame radiation before it goes under the slag. With quick handling this does not happen and it may be further guarded against by covering the mold with a second shallow cap of steel, which is just laid on loosely and floats away as the mold is dipped down into the bath. Such a mold need be held in the steel for only 3 or 4 sec. before removal since the cap melts through immediately.

Fig. 3c is a sketch of a simple mold designed for taking samples from the tapping stream leaving the furnace or from the pouring stream into the molds at the platform. A $\frac{3}{4}$ -in. steel pipe sleeve is welded to the mold and a piece of $\frac{3}{4}$ -in. pipe is screwed into this sleeve to serve as a handle. The edge of the mold is thrust for a second or so just a little way into one side of the flowing metal which splashes into the mold filling it quickly, the mold having previously been filled with a loose wad of fine aluminum wire as in the other methods. For sampling the tapping stream a pipe handle 15 to 20 ft. long may be required, depending on the layout of the platform back of the furnace. On the pouring plat-

form a shorter handle 5 to 6 ft. long may be used.

The metal sometimes splashes badly over the outside of the mold; its removal is facilitated by the shape and sloping sides of this mold. The short inside slope where the metal runs in helps to prevent the stream from washing out the aluminum. Experience has shown that with proper technique the tendency toward washing away the aluminum can be practically overcome. The mold should be edged slowly into the stream and when it is filled it should be removed quickly from the stream and held in a horizontal position until the steel has solidified. The importance of removing the filled mold quickly from the stream cannot be over-emphasized; otherwise the steel welds to the mold, which complicates the removal of the test ingot and the resurfacing of the mold. Before a new mold is used, it should be heated to a red heat to form a thin protective scale coating.

PRECISION OF SAMPLING

The first question is that of how much the [FeO] (or [O]) varies from place to place in a bath and how closely duplicate samples check. We began by sampling with the spoon method all over the bath, with pairs of samples: (1) at the same spot, (2) from one end of the bath to the other, and (3) at points at different levels on a vertical plane.

The results on the whole were very encouraging. The difference between shallow samples from different doors (end to end of the bath) proved to be very small, and normally no greater than between pairs of shallow samples from a level 4 to 10 in. deep in the metal, at the same spot. Therefore, we have lumped together all these pairs of duplicate and "door-to-door" samples, and have plotted the difference between members of each pair as a frequency curve in Fig. 4, curve A, according to which about 72 per cent of all such

* These various sampling molds should all be made of cast steel, preferably not less than about 0.3 to 0.4 per cent C.

pairs check to within 0.002 per cent oxygen and about 88 per cent to within 0.003 per cent oxygen (or 0.015 per cent FeO). This shows that the point of dipping out of a sample is not critical and indicates that the precision of the spoon method of sampling, when carried out with proper care, is satisfactory.

TABLE 2.—Comparison of [O] in Deep and Shallow Bath Samples

Deep Samples, Per Cent		Shallow Samples, Per Cent		Difference, Per Cent	Remarks
[C]	[O]	[C]	[O]	[O]	Conditions in bath
0.110	0.046	0.110	0.053	0.007	Normal action
0.110	0.036	0.120	0.046	0.010	Normal action
0.070	0.050	0.063	0.055	0.005	Strong bottom boil
0.080	0.048	0.083	0.058	0.010	Stir with 2 rods 9 min. before
0.310	0.022	0.310	0.027	0.005	Small lime boil at sampling point
0.073	0.047	0.090	0.053	0.006	Normal action
0.080	0.049	0.080	0.051	0.002	Bottom boil at sampling point
0.080	0.045	0.063	0.053	0.008	Normal action
0.063	0.051	0.070	0.057	0.006	Stir with 1 rod 2 min. before
0.130	0.042	0.100	0.045	0.003	Bottom boil at end of bath
0.070	0.053	0.080	0.056	0.003	Small bottom boil
0.180	0.048	0.150	0.047	-0.001	Stir with 3 rods 3 min. before
0.117	0.047	0.123	0.045	0.002	Normal action
0.070	0.066	0.070	0.058	-0.008	Very little bath action
0.170	0.039	0.170	0.044	0.005	Normal action
0.080	0.043	0.090	0.050	0.007	Stir with 1 rod 4 min. before
0.090	0.047	0.090	0.053	0.006	Normal action
0.120	0.032	0.130	0.043	0.011	Small ore feed 8 min. before
0.147	0.032	0.143	0.037	0.005	Stir with 1 rod 6 min. before
0.143	0.024	0.150	0.044	0.020	Normal action
0.183	0.028	0.190	0.031	0.003	Normal action
0.200	0.027	0.220	0.033	0.006	Small ore feed 7 min. before
Average Values					
0.121	0.042	0.122	0.047	0.005	

There are indications of differences between deep and shallow samples. The latter were from near the slag level; the deep samples were taken with a long-handled spoon which was slagged, slid down inverted to the bottom center portion of the bath, inverted there, removed and poured as quickly as possible. Table 2 gives a number of such pairs. In a normal

bath with moderate or quiet boil some deep samples were lower by 0.005 to 0.010 per cent oxygen than the shallow, but with a vigorous boil the difference was smaller in some cases, or about 0.002 to 0.004 per cent.

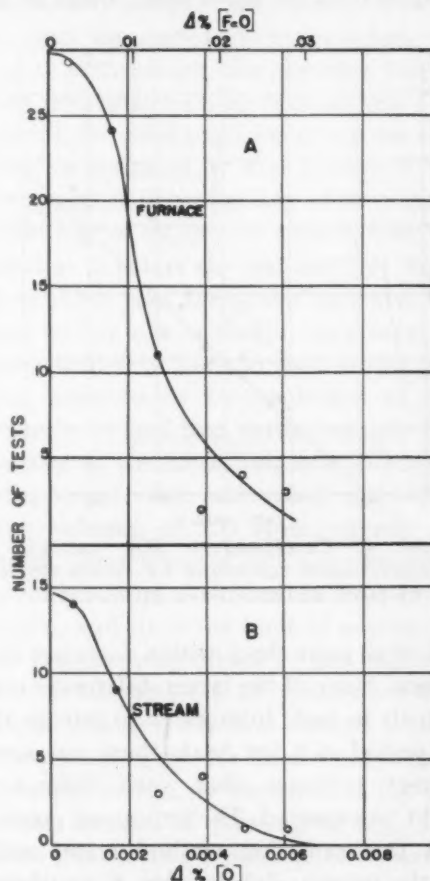


FIG. 4.—FREQUENCY DISTRIBUTION OF DIFFERENCE BETWEEN DUPLICATE SAMPLES TAKEN: CURVE A, IN FURNACE BATH; CURVE B, IN TAPPING STREAM.

This may well be a real difference, because most CO bubbles start to form on the bottom, which should produce some gradient of oxygen concentration, since all of it must diffuse downward from the slag.²

We were also interested in the precision of sampling of the tapping stream, since this operation would seem to be difficult

² B. M. Larsen: Controlling Reactions in the Open Hearth Process. *Trans. A.I.M.E.* (1941) 145, 67-83.

and somewhat haphazard. In many cases it was possible to take 2 or 3 samples from the stream during tap before slag started to come. Fig. 4, curve B, is a frequency curve of the difference between duplicate samples from the same heat. About 72 per

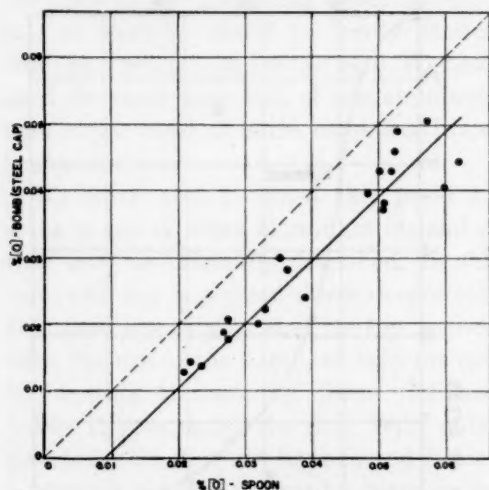


FIG. 5.—COMPARATIVE [O] VALUES OF SAMPLES TAKEN TOGETHER BY SPOON METHOD AND BY BOMB METHOD USING STEEL CAPS.

cent of all pairs check within 0.002 per cent oxygen. Some of the larger differences may be real; in fact, from early to late in the tap period of a few heats there was some indirect evidence that such differences might be expected. The important point is that this sampling method seems sufficiently precise: (1) to give a significant comparison with furnace samples as to changes in [O] during tapping and (2) to serve as a means of measuring the [O] entering the ladle in different heats.

We do not have sufficient data to show the precision of furnace samples taken by the bomb method. Present indications are that with the original sheet-steel cap the precision is not as good as that of the other two methods, as shown in Fig. 4. Results to date with an aluminum cap are not conclusive: this method may prove to be about as precise as the spoon method with which it seems to correlate well, as shown below.

COMPARISON OF SPOON WITH BOMB SAMPLING

The spoon method of sampling the bath has the apparent advantages of (1) using only the ordinary open-hearth sampling technique, with a little extra care, and (2)

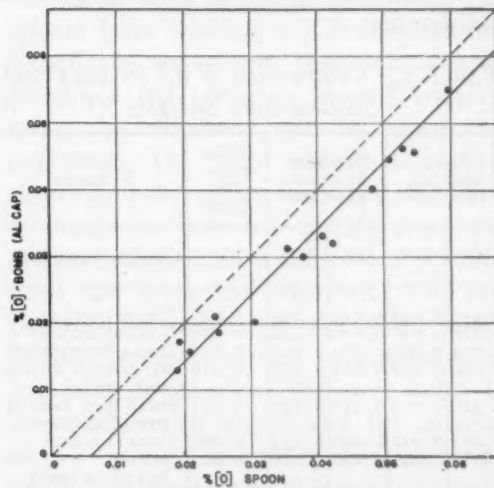


FIG. 6.—COMPARATIVE [O] VALUES OF SAMPLES TAKEN TOGETHER BY SPOON METHOD AND BY BOMB METHOD USING ALUMINUM CAPS.

keeping the steel enclosed in an envelope of liquid slag much the same as in the furnace, and usually with no boiling before it mixes with aluminum in the test mold.

Since several observers have found that the spoon method gives higher [O] values than the bomb method, it has been argued that this extra oxygen was probably absorbed from air or slag or both during the spoon sampling operation, and therefore that the bomb method should give a sample more closely representing the bath. We have no data which definitely establish the absolute accuracy of either method, in spite of repeated efforts to find some basis for a decision. For example, in spoon sampling, the metal was held in the spoon 8 to 10 sec. extra before pouring into the mold, and these samples were compared with others where the total time between bath and mold was about 3 to 4 sec., or about a threefold change in this critical sampling period. In some cases the differ-

ence was negligible; in a few cases carbon was lost by boiling; in others the increase was as much as 0.009 to 0.011 per cent [O]. These results, although not conclusive, indicate that with normally quick sampling, the "high" error in the spoon method should be less than 0.002 per cent oxygen, with possibly as much as 0.004 per cent only exceptionally.

Figs. 5 and 6 show comparative [O] values of samples taken together by the spoon method and the bomb method using a steel and an aluminum cap respectively. With a steel cap, the bomb values average 0.010 per cent oxygen lower than the spoon; with an aluminum cap, the bomb is again lower but the average difference is less, only 0.006 per cent oxygen. The correlation with the spoon is better with the aluminum cap; that is, the points show less average deviation from the straight line in Fig. 6 than in Fig. 5. These results, combined with the known tendency of steel rods or billets to start a boil, lead us to the conclusion that the values from the bomb with steel cap are probably low and somewhat erratic. From what is known about the carbon reaction, in presence of the usual excess of [O], and of the stimulation of bubble formation by any solid surface immersed in the liquid steel, one would expect at least some small loss of oxygen as CO from the metal before it melts through the steel cap and reaches the aluminum wire inside; the results in Fig. 5 indicate that this loss may be appreciable in some cases.

With an aluminum cap, however, this obvious source of error on the low side has been removed, yet the values are still a little lower than in spoon samples, and the average carbon content of the groups compared in Fig. 6 is not definitely lower in the bomb samples than in the corresponding spoon samples. This evidence favors the conclusion that the spoon-test values tend to be somewhat higher than the percentage actually present in the bath.

Comparing spoon samples taken in the furnace just at tap with samples from the stream of metal entering the ladle (on heats with no block or other alloy additions in the furnace near tap time), we find that the stream samples are usually lower in [O] than the furnace samples taken only 2 to 3 min. earlier, the decrease varying from zero up to 0.02 per cent oxygen. Considering the good precision of stream sampling, as indicated by Fig. 4 curve B, and the apparent improbability of any appreciable loss of oxygen or carbon from the metal as it enters the test mold, it would seem either that the spoon values at tap must be too high or that in such heats the metal definitely loses oxygen during tapping, presumably by evolution of CO. Actually we find that carbon usually does decrease at the same time and this agrees with visual observations of apparently large volumes of CO from taphole and stream. Since a loss of only 0.01 per cent of carbon is needed to eliminate 0.013 per cent oxygen, and since the limit of accuracy of the carbon determination (as ordinarily done) is not better than ± 0.005 per cent, a small change in carbon content is not a very accurate guide for the present purpose. However, we can see the trend of the data by the method of plotting in Fig. 7, in which the abscissa represents the observed difference in [O] between spoon samples from the bath and stream samples during tap, and the ordinate the oxygen equivalent of the corresponding change in carbon, that is, the per cent change in carbon multiplied by 1.33. If the metal was absolutely uniform in composition, if both bath and stream sampling and the analyses for both [C] and [O] were accurate, and if the metal picked up no oxygen from air or slag during these few minutes between bath and stream samples, the points in Fig. 7 should all fall on the 45° straight line. Since extra oxygen may very possibly be absorbed rapidly from the slag or gas phases by the stirring action of the tap, some points might fall

above the line, representing cases where the loss in carbon is greater than the loss in oxygen because part of the latter is replaced by oxygen absorbed during tapping. If the

bath samples at tap gives correct [O] values, and therefore that the bomb samples are too low. On the other hand, one might argue that the absorption of oxygen

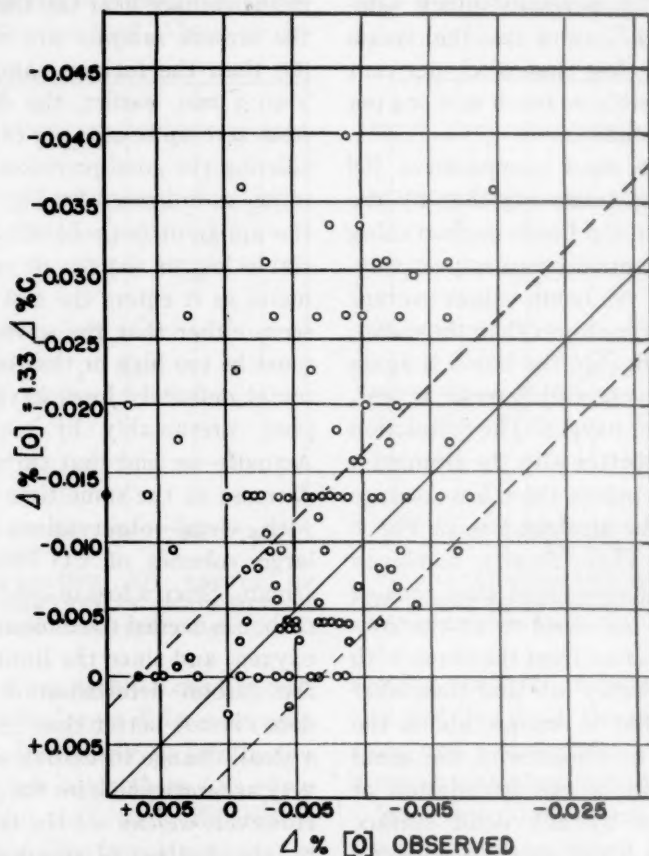


FIG. 7.—OBSERVED CHANGE IN [O] VERSUS CALCULATED [O] DIFFERENCE EQUIVALENT TO C CHANGE —BETWEEN BATH AT TAP AND TAPPING STREAM.

spoon sample in the furnace gives the correct [O] value, no point should fall below the line since there is no available source of extra carbon, except that because of inaccuracies in carbon analysis, points would be expected to scatter both above and below the line within a range of about 0 to 0.005 [O] (or 0 to 0.03 per cent FeO) as indicated by the dashed lines.

This is precisely the trend of distribution of the points in Fig. 7 indicating variable absorption of from 0 to 0.02 per cent oxygen during tap. Making this rather reasonable assumption, we would then infer that the spoon method used for the

is never close to zero, as would be indicated by Fig. 7, but that it always amounts to at least 0.006 to 0.009 per cent, consequently that the spoon values in the furnace are high by the amount of this minimum absorption; this interpretation seems rather less reasonable, but there is no really definite basis for a choice.

The foregoing discussion shows how, in spite of all our efforts, we are left with a small range of uncertainty in [O] values for the bath. Because of the reasonable nature of the values and of the inferences from the data given by the spoon method, and because of its good precision when samples

are taken carefully (as shown by Fig. 4a), we favor this method as the best but cannot be certain that the slightly lower values by the aluminum-cap-bomb sampling are not closer to the true values. The difference is small, however, and the two methods correlate so well that the choice between them will probably not appreciably affect conclusions as to the effect of residual [O] in open-hearth operation.

Of the two, the spoon method is more convenient and less time-consuming since it requires fewer special gadgets and less preparation before and after sampling. However, the spoon method requires that the spoon be well slagged and the metal quickly poured; additional care must be exercised when there is a heavy slag on the bath. We believe that the use of a steel cap with the bomb may often give a low result and that an aluminum cap is preferable. With reasonable care, sampling of the stream at tap or at the pouring platform by the method described seems satisfactory. In general, with due care in sampling and analysis, the deviation from proportionality for 80 to 90 per cent of all samples should not exceed the overall limits ± 0.002 per cent oxygen, (or ± 0.01 per cent FeO).

ACKNOWLEDGMENTS

The results given above should really be credited very largely to the excellent cooperative efforts of various members of the staff in the Chemical Laboratory and in the Open Hearth Department of the Donora Steel Works, American Steel & Wire Co. We are especially indebted to Mr. V. C. Boucek for his excellent work in developing sampling technique and to Mr. Russell Ruff and Mr. J. R. Carson for painstaking work in analytical procedures.

APPENDIX

Method of Analysis

Two grams of steel turnings are weighed into a 250 ml. beaker with cover and put

into solution with 30 ml. of dissolving acid, using little heat until foam subsides, then boiling for about 3 minutes.

Ten milliliters of ammonium persulphate solution (12.5 per cent) are now added and the boiling continued for another 3 min. By this time all persulphate should be decomposed, and it is important that this should be the case, else the undecomposed persulphate will form bubbles later on and lead to high results.

The beaker contents are removed to an 8 by 1 in. test tube, using the washing solution to effect the transfer and to bring the volume up to the 50-ml. mark. The temperature of the solution is brought to between 80° and 90°F. and its volume then adjusted to exactly 50 ml. This done, the tube is closed with a rubber stopper and its contents thoroughly mixed by inverting several times, but never so violently as to cause undue bubble formation.

Some of this solution is now transferred to the turbidimeter cell (which must be kept very clean or carefully wiped) and placed in the instrument for reading; (it is best to first fill the cell about half full and empty this out, then fill up for the measurement).

The solutions required are:

Dissolving acid:	165 ml. H_3PO_4 (85 per cent)
	335 ml. HNO_3 (1.42 sp. gr.)
	500 ml. H_2O
Washing solution:	250 ml. HNO_3 (1.42 sp. gr.)
	750 ml. H_2O

The phosphoric acid used in the foregoing method may cause difficulty by precipitating ferric phosphate over test tubes and beakers. This will happen whenever the acid concentration is reduced, but is usually encountered in rinsing the tubes and beakers if sufficiently acid wash water is not used, so that extra care in cleaning is required. More serious, unless this precipitation be guarded against, it may persist through the analysis and raise the readings given by the turbidimeter.

The following modification of the method

might give a somewhat simpler and more foolproof procedure; we mention it for this reason, although we have not yet had an opportunity to make sure that it would be as generally satisfactory as the one given above:

Dissolve the sample in straight nitric acid solution (about 1.20 sp. gr.). Use a dilute potassium permanganate solution in place of the ammonium persulphate, remove from hot plate and add a slight excess of sodium nitrite solution to reduce any unused permanganate as well as any manganese dioxide resulting from the carbon oxidation. Transfer and cool to 80° to 90°F. as above for the rest of the procedure.

Fig. 1 shows the comparison with tur-

bidimeter readings of a set of carefully conducted gravimetric analyses for Al_2O_3 , expressed as equivalent [O] contents.

The blank reading on the turbidimeter is determined by identical procedure on a companion sample ingot poured slowly without any deoxidizer addition in spoon or mold. In the practice of any one shop, such blanks usually give a very nearly constant value on bath or stream samples taken before deoxidation so that only an occasional one for a check is needed. After furnace block or at the pouring platform, however, the blank values may show some little variation, and more frequent blanks, even to the point of taking one with each [O] sample, may be required if maximum precision is desired.

Effect of Deoxidation on the Strain-sensitivity of Low-carbon Steels

By H. K. WORK,* MEMBER AND G. H. ENZIAN,† JUNIOR MEMBER A.I.M.E.

IN the manufacture of steel for commercial purposes, the deoxidation practice used, i.e., the method and degree of deoxidation, is an important factor affecting the structure and mechanical properties of the finished steel. Deoxidation practice exerts a pronounced influence not only on the soundness of the ingots but also on the reaction of the steel to a number of mechanical and thermal treatments. The first mentioned effect of deoxidation is more or less obvious and was first demonstrated, though perhaps not fully appreciated, by Robert Mushet when, in 1856, he added speigelleisen to low-carbon bessemer blown metal. In 1861, Bessemer patented the addition of one pound per ton of silicon to his blown metal to "cause the metal to lie quietly in the mold." The second effect of deoxidation—that is, the effect on the properties and behavior of the steel—is, one might say, more subtle, and certainly not as well understood as the first, although in many cases it is the more important consideration. This paper is limited to a discussion of only the second effect of deoxidation and, in particular, to the effect on the strain-sensitivity of low-carbon steels.

GENERAL DISCUSSION

Originally it was thought that the function of a deoxidizer was to combine with

the oxygen present in the steel as iron oxide and prevent its subsequent evolution as a gas. More recently it has been realized that a deoxidizer does more than this. Frequent reference has been made to the effect of deoxidizers on the nitrogen in the steel, and some attention has also been paid to hydrogen. As a consequence of the above situation any study of deoxidation must be concerned with the gas content of the steel and the effect of the deoxidizer on the gases involved. The term "gas content" as used here refers to gases extracted from steel during melting in vacuum rather than to elements present in steel in the gaseous state. The extracted gases, at least in the case of oxygen and nitrogen, are generally accepted to be products of decomposition of oxides, nitrides, or other more complex compounds.

The manner in which deoxidation affects the gas content of steel and the significance of gases in steel have been and still are subjects of considerable speculation. No attempt will be made here to give a complete discussion of the literature on this subject but a few references will be cited for purposes of illustration. N. Hamilton¹ found a correlation between the oxygen content of alloy steel and the behavior of the steel during tube piercing. Davenport, Bain, and others²⁻⁴ associated oxygen with aging properties of steel while Köster⁵ and a number of others⁶⁻¹⁰ made similar claims for nitrogen. Daniloff, Mehl, and Herty¹¹ stated that "deoxidation decreases the susceptibility of steels to aging directly

Manuscript received at the office of the Institute Dec. 1, 1944. Listed as T.P. 1835.

* Manager of Research and Development, Jones and Laughlin Steel Corporation, Pittsburgh, Pennsylvania.

† Research Engineer, Jones and Laughlin Steel Corporation.

¹ References are at the end of the paper.

through the decrease in dissolved oxygen content." Graham and Case¹² attributed the effect of aluminum deoxidation on strain-sensitivity to the formation of aluminum nitride and thus indicated that nitrogen is the principal factor involved. Recent work by Low and Gensamer¹³ virtually eliminated oxygen, *per se*, as a cause of strain-aging although they believed that it may have a minor influence on the effects of carbon and nitrogen. Epstein¹⁴ also attributed aging to nitrogen and has proposed a nonaging rimmed steel, which is made by using "substances which combine readily with nitrogen but which do not act as strong deoxidizers." In spite of the disagreement among the various investigators as to whether oxygen or nitrogen is the major contributing element, all seem to agree that deoxidation generally decreases susceptibility to aging. It is also indicated that deoxidation affects the strain-sensitivity of the steel although little has been published on this subject until quite recently.^{12,15,16} While this paper is concerned primarily with strain-sensitivity, the references on strain-aging were included because it is believed that the main factor that causes strain-aging is also one of the important factors in causing the type of strain-sensitivity that is most affected by deoxidation.

It has been pointed out that the process of deoxidizing steel is not a simple operation of reducing the iron oxide present to other, more stable oxides which are eliminated into the slag or remain entrapped in the solid metal. As a consequence it seems desirable to consider briefly some of the factors involved in deoxidation.

For purposes of this discussion it will be considered that the more important effects of the deoxidizers have to do with their effects on both oxygen and nitrogen, and, even though an attempt will be made later to show that nitrogen is the more important of the two in its effect

on strain-sensitivity, the presence of oxygen cannot be disregarded. This is because the deoxidizers commonly used vary considerably in the ease with which they combine with oxygen and nitrogen. Furthermore, most of the deoxidizers appear to combine more readily with oxygen than they do with nitrogen. Consequently, in order to secure the effect of a suitable deoxidizer on the nitrogen, it is frequently necessary to be certain that sufficient deoxidizer has been added to combine with all of the oxygen present as well as the nitrogen. It is further to be noted that even when deoxidizers are present in sufficient quantity to combine with both oxygen and nitrogen their effectiveness may vary greatly.

As a further complication to this subject, many deoxidizers or deoxidation practices involve the use of more than one deoxidizer. Hence it is easy to see that a theoretical study of the deoxidation operation is quite difficult and involved, and this paper will deal only with a few common deoxidation practices. Furthermore the evaluation of the effect of the deoxidation practice on the strain-sensitivity will be based on special but nevertheless very simple mechanical tests.

In a paper presented in 1932 before the American Iron and Steel Institute, H. W. Graham¹⁷ reported some results of strain-sensitivity measurement and submitted evidence indicating that this behavior serves as a useful measure of steel quality. The purpose of the present paper is to present some results taken from a number of laboratory investigations made in a study of factors affecting the strain-sensitivity of steel. The study of this fundamental characteristic has extended over a period of years and some of the data so gathered provide pertinent information regarding the role of deoxidizers in control of steel quality. Strain-sensitivity has been selected as a measure of quality because it has been found that this be-

havior is more valuable than conventional mechanical properties in predicting the probable behavior of the steel in many important types of fabrication and service. In addition, strain-sensitivity is closely associated with the strain-aging phenomenon, about which so much has already been written.

MATERIALS AND METHODS

Strain-sensitivity studies have been made in our laboratory on hundreds of steels during the past 10 or 15 years and a selected group of these steels was also analyzed for oxygen and nitrogen contents by fractional vacuum-fusion analysis at the University of Michigan. The selection of the steels analyzed was based on the fact that they were typical and covered a range of properties and behavior. It is felt that these selected heats serve particularly well to establish the relationships between deoxidation, gas content, and strain-sensitivity.

As a matter of interest most of the heats involved were made in our experimental open-hearth furnace.¹⁸ These heats were chosen because they represent closely results obtained in mill operations yet the heats were made under more strict observation and with greater control over the raw materials than is practical with mill heats. In addition a few mill heats and laboratory induction furnace heats were employed to round out the picture.

Method of Analysis

The method of analysis used by D. W. Murphy at the University of Michigan was essentially similar to the procedure used by Hoyt and Scheil¹⁹ and is based on the generally accepted assumption that FeO and MnO are completely reduced at 2140°F., SiO₂ at 2400°F., and Al₂O₃ at 2800° to 2900°F. Also, according to Hoyt and Scheil,¹⁹ the nitrogen content determined in each of these fractions indicates

the form in which it was present in the steel. Thus the 2140°F. fraction should result from the disintegration of iron and manganese nitrides, silicon nitride in the 2400°F. fraction and aluminum nitride at 2800° to 2900°F. While various investigators seem to be in substantial agreement on the oxide fractions, the identities of the nitride fractions are more of a conjecture and have no foundation of an accepted analytical background.

The Work-brittleness Test

It is now common knowledge that steels differ in their reaction to cold-work and that some steels harden and embrittle during cold-working to a greater extent

TABLE I.—*Steelmaking Practice and Chemical Composition*

Heat	Practice	Composition, Per Cent				
		C	Mn	P	S	Si
A	Rimmed	0.07	0.50	0.009	0.014	
B	Rimmed	0.06	0.37	0.014	0.024	
C	Rimmed	0.07	0.37	0.012	0.035	
D	Rimmed	0.11	0.44	0.039	0.016	
E	Al-killed (4 lb. per ton)	0.07	0.47	0.012	0.018	0.02
F	Si-killed	0.11	0.50	0.019	0.023	0.11
G	Si-capped	0.12	0.33	0.009	0.019	0.04
H	Semikilled	0.07	0.32	0.014	0.016	0.03

and at faster rates than others. The work-brittleness test, described by Graham and Work,²⁰ has been found to be a convenient measure of "strain-sensitivity," or the intensity of the reaction of the steel to cold-working. Briefly, this test consists in drawing a round specimen, usually tapered from 0.450 to 0.475 in. diameter, through a 0.450-in. die in order to obtain a reduction in area varying along the length of the bar from 0 to approximately 10 per cent. The specimen is then notched in the standard round Izod manner at regular intervals and thus the effect of increasing amounts of cold-work on the Izod impact toughness can readily be determined. In order to

minimize variations due to differences in strain-aging rates in different steels, and because aging generally becomes a factor in actual service, it is usually found desirable to test the steel in the fully aged condition; this can be accomplished by heating the bars to 450°F. for one hour after cold-drawing. The test therefore indicates the result of strain-aging embrittlement brought about by different amounts of straining and provides a useful measure for comparing the strain-sensitivity of steels.

TEST RESULTS

Compositions of Steels Used

From the many steels tested, several have been selected for purposes of illus-

The oxygen contents of these steels are fairly uniform and range from 0.012 to 0.026 per cent. The average total oxygen content of the rimmed heats was somewhat higher than for the killed heats but the values overlap; this has been found to be the general rule in additional studies involving approximately 60 heats of various grades. The nitrogen contents vary appreciably, ranging from 0.003 to 0.022 per cent. The higher contents were obtained by ladle additions of nitrogen-bearing materials in order to obtain a wider range of values than is possible with any normal steel-making operation. The steels used in this paper furnish a representative cross section of the many heats, varying in oxygen and nitrogen contents

TABLE 2.—*Vacuum-fusion Gas Analyses Data*

Heat	Practice	Total		Fractions, Deg. F.					
		O ₂	N ₂	Oxygen			Nitrogen		
				2140	2400	2820	2140	2400	2820
A	Rimmed	0.022	0.003	0.021	0.001	0.000	0.001	0.001	0.001
B	Rimmed	0.017	0.005	0.009	0.006	0.002	0.003	0.002	0.000
C	Rimmed	0.026	0.010	0.012	0.009	0.005	0.005	0.005	0.000
D	Rimmed	0.012	0.015	0.009	0.003	0.000	0.012	0.003	0.000
E	Al-killed	0.012	0.022	0.008	0.001	0.003	0.017	0.004	0.001
F	Si-killed	0.015	0.003	0.008	0.005	0.002	0.002	0.001	0.000
G	Si-capped	0.023	0.003	0.017	0.004	0.002	0.002	0.001	0.000
H	Semikilled	0.016	0.019	0.013	0.002	0.001	0.014	0.004	0.001

tration. The practices used in making these heats and the chemical compositions are listed in Table 1. Results of fractional vacuum-fusion gas analyses are shown in Table 2; each value reported is the average of two and often three determinations. The gas analyses presented here were made with the hope that they would provide additional information which would be useful in explaining the effect of deoxidation on strain-sensitivity and other properties of steel. However, any interpretation of vacuum-fusion results should take into account the recognized limitations of this method of analysis.²¹

and deoxidation practices, which have been tested at one time or another.

Gas Content and Strain-sensitivity

The conflict in views, among the many investigators, on the relationship between oxygen and nitrogen contents and aging behavior is largely attributable to the fact that both elements are present in varying amounts in steel and it is thus difficult to isolate the effect of one or the other. Furthermore, since oxygen and nitrogen can each form stable compounds with the same elements, both nitrides and

oxides of iron, manganese, silicon, aluminum, etc., may be present in a steel at the same time. Based on a wide experience with this subject, however, it seems prob-

nitrogen content, heat A, is the least sensitive to cold-work; heat D has the highest total nitrogen and is the most sensitive although it contains the lowest

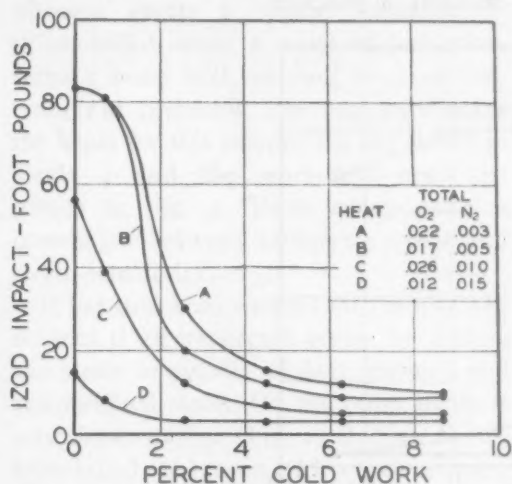


FIG. 1.—WORK-BRITTLENESS CURVES FOR RIMMED STEELS.

Note that heats show increased strain-sensitivity with increasing nitrogen contents.

able that the form in which oxygen or nitrogen is present in the steel has a greater bearing on the properties than the total content of either element. As indicated earlier, some investigators feel that the dissolved oxygen content is the principal factor involved. However, this theory is difficult to substantiate with factual data chiefly because there is no recognized method for determining accurately the amount of oxygen dissolved in the steel as opposed to that which is not in solution.

In the series of heats used in this investigation, oxygen and nitrogen were present in varying quantities and it was felt that these heats might point to definite trends from which conclusions might be drawn with regard to the effects of oxygen and nitrogen on strain-sensitivity. Figs. 1 and 2 show a representative number of work-brittleness curves on some of the steels on which gas analyses were made. The four steels shown in Fig. 1 were rimming heats and have varying oxygen and nitrogen contents. The steel with the lowest total

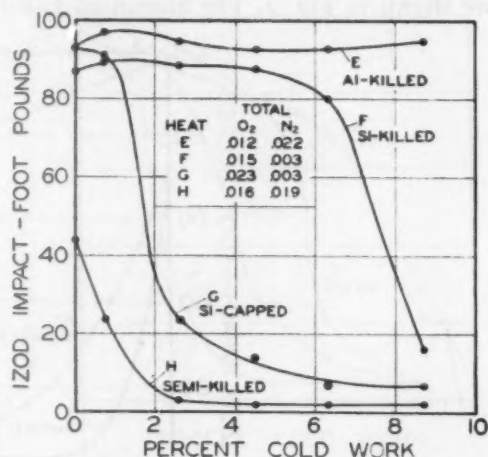


FIG. 2.—WORK-BRITTLENESS CURVES OF KILLED AND SEMIKILLED STEELS.

Variation in strain-sensitivity of these heats cannot be explained on the basis of gas content but must be associated with the deoxidation practice.

amount of oxygen of the four heats. The work-brittleness curves for the two other heats lie between heats A and D roughly in proportion to the nitrogen contents but with no apparent relation to the total oxygen. The results of fractional vacuum-fusion analyses on these steels, summarized in Table 2, also fail to show a relationship between sensitivity and the various oxide fractions. It is seen, therefore, that although no definite trend can be drawn between sensitivity and oxygen content, the curves show that increasing nitrogen contents result in increased strain-sensitivity.

Deoxidation and Strain-sensitivity

It was shown that the sensitivity of rimmed steels was essentially independent of oxygen content but apparently was related to nitrogen. However, these steels did not provide information regarding the effect of more thorough deoxidation. In order to show the relationship between

deoxidation, gas content, and strain-sensitivity, four killed and semikilled experimental open-hearth steels were selected. Work-brittleness curves for these heats are shown in Fig. 2. The aluminum-killed

sensitivity cannot be completely explained on the basis of gas content alone, and it is obvious that the difference in the results obtained must be associated with the deoxidation practice.

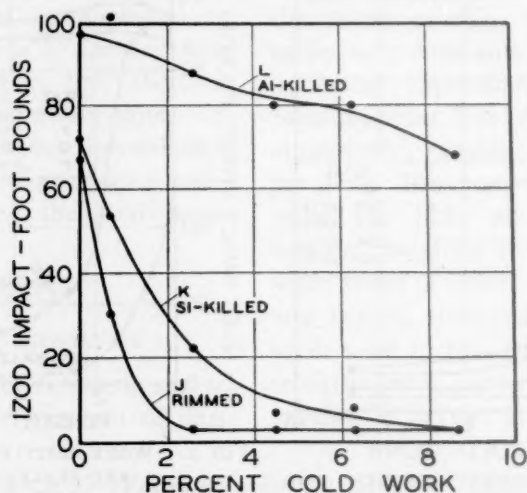


FIG. 3.—EFFECT OF DEOXIDATION ON STRAIN-SENSITIVITY.

These curves show the comparative effectiveness of silicon and aluminum deoxidation in reducing the strain-sensitivity of a normally sensitive steel.

steel, heat E, had the lowest total oxygen and highest total nitrogen contents, and was the least sensitive to cold-work, although it was previously shown that in the rimmed steels the highest nitrogen heat was the most sensitive. Heat F was silicon-killed, contained approximately the same total oxygen but considerably less total nitrogen than the aluminum-killed steel, and was somewhat more strain-sensitive. Evidently, then, silicon deoxidation is not as effective as aluminum in promoting insensitivity. The silicon-capped steel, heat C, had a slightly higher oxygen content than the silicon-killed heat and was more strain-sensitive; the sensitivity of this latter heat was similar to that of rimmed heat A (Fig. 1), which had approximately the same oxygen and nitrogen contents. Heat H was semikilled, and has a lower oxygen and higher nitrogen content and is more strain-sensitive than heat G. It is apparent, therefore, that in these four steels the variation in strain-

To illustrate the relative effects of silicon and aluminum deoxidation on the strain-sensitivity of a normally sensitive steel, the three heats shown in Fig. 3 were selected. The chemical compositions of the three heats tested are listed in Table 3; with the exception that the rimmed heat was low in silicon, all were of approximately the same chemical composition. The work-brittleness curves for these steels show that the silicon-killed heat is only slightly less sensitive than the rimmed heat but the aluminum-killed steel shows little sensitivity to cold-work. Thus it is again seen that aluminum has a much greater effect than silicon on the factors that contribute to strain-sensitivity.

THEORETICAL CONSIDERATIONS

From the foregoing results, it is apparent that the total oxygen content of the steel, as determined by vacuum-fusion analysis, has little if any bearing on the strain-sensitivity of rimmed, killed, or semikilled

steels. However, the data in Fig. 1 provided some indication that the nitrogen content affects strain-sensitivity in rimmed steels, and in order to determine whether nitrogen exerts a similar influence on silicon-killed steels a series of induction-furnace heats with varying nitrogen contents was prepared. The compositions of the heats for this comparison are shown in Table 4 and the work-brittleness test results in Fig. 4. These curves show a correlation between nitrogen content and strain-sensitivity.

It has thus been shown that the nitrogen content is an important factor controlling the strain-sensitivity of both rimmed and silicon-killed steels. On the other hand, it was shown earlier (Fig. 2) that an aluminum-killed steel, even with a high nitrogen content, may be appreciably less sensitive than a silicon-killed steel with low nitrogen, although both, to all practical intents, are considered completely deoxidized in that the heats were "dead" in the molds.

whereby deoxidation affects strain-sensitivity is associated with nitride formation.

To pursue the question of the mechanism of strain-sensitivity further, heats D and

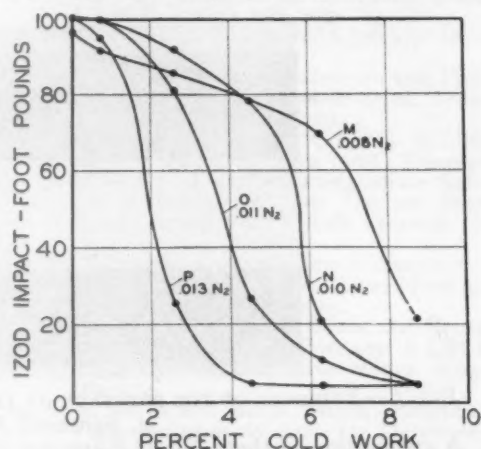


FIG. 4.—EFFECT OF NITROGEN ON THE STRAIN-SENSITIVITY OF SILICON-KILLED STEELS.

These work-brittleness curves show a relationship between nitrogen content and strain-sensitivity.

E represent the extremes in strain-sensitivity noted in this investigation. Both

TABLE 3.—Effect of Deoxidation on Strain-sensitivity of a Normally Sensitive Steel

Heat	Practice	Chemical Composition, Per Cent					Sensitivity
		C	Mn	P	Si	N ₂	
J	Rimmed	0.11	0.53	0.105	0.01	0.006	Very sensitive
K	Si-killed	0.14	0.51	0.096	0.14	0.006	Sensitive
L	Al-killed (2½ lb. per ton)	0.15	0.59	0.100	0.18	0.006	Insensitive

Since it has been brought out that sensitivity to cold-work is largely influenced by the nitrogen content of the steel, it seems probable that an important mechanism

TABLE 4.—Effect of Nitrogen Content on Strain-sensitivity

Heat	Practice	Chemical Composition, Per Cent				
		C	Mn	P	Si	N ₂
M	Si-killed	0.13	0.49	0.013	0.13	0.008
N	Si-killed	0.13	0.56	0.012	0.12	0.010
O	Si-killed	0.15	0.57	0.019	0.13	0.011
P	Si-killed	0.15	0.58	0.018	0.10	0.013

heats have low oxygen and high nitrogen contents but the insensitive heat was killed with aluminum and the sensitive heat was a rimmed steel. If nitrogen is actually a factor that controls sensitivity, it is evident that the nitrogen must be present in these two steels in different forms, and it would seem logical to suspect that a large percentage of the nitrogen in heat E must be in the form of aluminum nitride. An X-ray diffraction study was made of nonmetallic material obtained from heat E by a new method (which is still in its developmental stages and not

yet ready for open discussion). The diffraction pattern so obtained was compared with a similar one made from synthetic aluminum nitride; the results are shown

carbon and phosphorus affect strain-sensitivity; other elements probably also affect this behavior under certain conditions. However, most of these would not

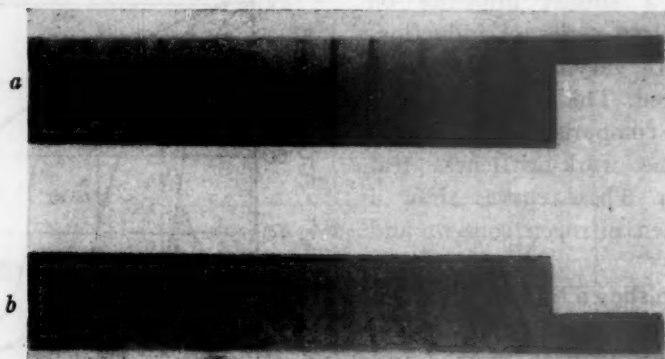


FIG. 5.—EVIDENCE OF THE PRESENCE OF ALUMINUM NITRIDE IN ALUMINUM-KILLED STEEL.
a. Synthetic Al N. *b.* Heat E.

A comparison of these X-ray diffraction photograms indicates the presence of aluminum-nitride in aluminum-killed heat E.

in Fig. 5. These photograms show that aluminum nitride is present in the aluminum-killed heat E.

The existence of aluminum nitride in aluminum-treated steels has been verified by examination of a number of heats. It is possible that silicon nitride may be formed in silicon-killed steels, but this has not as yet been definitely determined. In any event the results seem to show that aluminum nitride is extremely effective in contributing to insensitivity and that silicon nitride, if it is actually present, is evidently less effective. Whether the aluminum nitride contributes to insensitivity merely by rendering the nitrogen "inactive" or whether the presence of the aluminum nitride is actually beneficial may be a matter for some conjecture at this time, although other studies have indicated that in some cases the presence of the nitride seems to have a beneficial effect.

In closing it seems proper to mention that there are factors other than nitrogen that also influence the strain-sensitivity of steel. It is known, for example, that

be expected to take part in the reactions of deoxidation. Hence it is felt that in considering the subject of strain-sensitivity there is sufficient evidence to support the view that nitrogen is one of the more important factors involved.

While only two deoxidizers are considered in this paper, it should be kept in mind that many simple and complex deoxidizers are available on the market. Such deoxidizers show quite a wide range of effectiveness in changing strain-sensitivity, but it is beyond the scope of this paper to cover the whole field in detail.

SUMMARY AND CONCLUSIONS

Fractional vacuum-fusion gas analyses and work-brittleness tests were used for a number of steels to show the relationship between deoxidation practice, gas content, and strain-sensitivity. The results of this investigation may be summarized as follows:

1. Neither total oxygen nor its fractions as determined by vacuum-fusion analysis shows a relationship to the strain-sensitivity of steel.

2. Total nitrogen content seems to bear a direct relationship to the strain-sensitivity of undeoxidized steel. From this it is believed that the principal effect of at least some deoxidizers on strain-sensitivity results from the reaction of the deoxidizer with the nitrogen of the steel. In this respect aluminum is more effective than silicon.

3. X-ray diffraction data, obtained on steels killed with aluminum that showed a marked reduction in sensitivity to cold-work, have indicated the presence of aluminum nitride.

ACKNOWLEDGMENT

The authors gratefully acknowledge the help and cooperation of their associates in the preparation of the material used in this paper.

REFERENCES

1. N. Hamilton: Determination of Oxygen in Alloy Steels and Its Effect Upon Tube Piercing. *Trans. A.I.M.E.* (1934) **113**, 110-125.
2. E. S. Davenport and E. C. Bain: The Aging of Steel. *Trans. Amer. Soc. Metals* (1935) **23**, 1047-1093.
3. C. H. Herty, Jr. and B. N. Daniloff: The Effect of Deoxidation on The Aging of Mild Steels. Mining and Metallurgical Investigations, Cooperative Bull. 66.
4. M. A. Grossman: Oxygen in Steel. *Trans. Amer. Soc. Steel Treat.* (1930) **18**, 601-631.
5. W. Köster: Nitrogen in Commercial Iron. *Archiv Eisenhüttenwesen* (1930) **3**, 637-658.
6. W. Eilender, H. Cornelius and P. Menzen: Effect of Impurities in Iron on Changes in Mechanical Properties at Blue Heat. *Archiv Eisenhüttenwesen* (1940) **14**, 217-221.
7. W. Eilender, H. Cornelius and H. Knuppel: Influence of Nitrogen and Oxygen Upon Mechanical Aging of Steel. *Archiv Eisenhüttenwesen* (1936) **8**, 507-509.
8. R. S. Dean, R. O. Day and J. L. Gregg: Relation of Nitrogen to Blue Heat Phenomena in Iron and Dispersion Hardening in the System Iron-nitrogen. *Trans. A.I.M.E.* (1929) **84**, 446-453.
9. G. Schmidt: Influence of Impurities in Commercial Iron on Impact. *Archiv Eisenhüttenwesen* (1934) **8**, 263-267.
10. W. Eilender, A. Fry and A. Gottwald: Influence of Different Elements on Precipitation Phenomena Occurring in Steel During Low Temperature Annealing. *Stahl und Eisen* (1934) **54**, 554-564.
11. B. N. Daniloff, R. F. Mehl and C. H. Herty, Jr.: The Influence of Deoxidation

- on the Aging of Mild Steels. *Trans. Amer. Soc. Metals* (1936) **24**, 595-634.
12. H. W. Graham and S. L. Case: U. S. Patent 2,174,740 (Oct. 1939).
13. J. R. Low, Jr. and M. Gensamer: Aging and the Yield Point in Steel. *Trans. A.I.M.E.* (1944) **158**, 207.
14. S. Epstein: U. S. Patent 2,356,450 (Aug. 1944).
15. E. C. Wright: The Manufacture and Properties of Killed Bessemer Steel. *Trans. A.I.M.E.* (1944) **158**, 107.
16. G. F. Comstock and J. R. Lewis: A Comparison of Aluminum and Titanium Deoxidation for Preventing Strain Aging Embrittlement in Low Carbon Steel. (1944) Amer. Soc. Metals Preprint No. 24.
17. H. W. Graham: A Modern Conception of Steel Quality. Yearbook Amer. Iron and Steel Inst. (1932) 59-102.
18. H. K. Work and M. H. Banta, An Experimental Open-hearth Furnace. *A.I.M.E.* 22nd Open-hearth Proceedings (1939) 161-174.
19. S. L. Hoyt and M. A. Scheil: Fractional Vacuum-fusion Analysis for Determination of Oxygen in Steel. *Trans. A.I.M.E.* (1937) **125**, 313-328.
20. H. W. Graham and H. K. Work: A Work-brittleness Test for Steel. *Proc. Amer. Soc. Test. Mat.* (1939) **39**, 571-580.
21. J. G. Thompson, H. C. Vacher and H. A. Bright: Cooperative Study of Methods for the Determination of Oxygen in Steel. *Trans. A.I.M.E.*, (1937) **125**, 246-291.

DISCUSSION

G. F. COMSTOCK.*—This paper is of special interest to the writer because of a study of the same subject made several years ago in an effort to determine the effect of nitrogen in steel on strain aging. In that work, the results of which were published in the *Proceedings* of the American Society for Testing Materials [(1943) **43**, 521], the conclusion was reached that nitrogen up to 0.02 per cent has a negligible effect on any kind of strain-aging in killed steel.

The work now reported by the authors supports quite definitely the conclusions of other investigators that strain-aging embrittlement, which I believe is what they mean by "strain sensitivity," is controlled by deoxidation, in spite of the fact that the results of their oxygen determinations are not in line with the work-brittleness curves of Fig. 1. Although the nitrogen contents are in line with those curves, they are out of line with those of Fig. 2, so that the same correlation of work-brittleness results

* Titanium Alloy Manufacturing Co., Niagara Falls, N. Y.

with nitrogen contents, especially in the killed steels, may not always be found.

Our own experience with nitrogen was confined to killed steel, and was not reported in full detail in the A.S.T.M. paper referred to, so that a further report may be in order in this discussion. Work-brittleness tests of our steels killed with silicon and 0 to 0.15 per cent aluminum, but without titanium, gave no impact values below 114 ft-lb. after aging three weeks at room temperature subsequent to straining as much as 8 per cent, with nitrogen

ent with normalized and annealed specimens, respectively. It would therefore be of interest if the authors would report how their specimens were heat-treated.

As a result of this work it appeared to us that nitrogen had no effect on the strain-aging embrittlement of killed steels, and the authors' data on killed steels do not seem to be sufficient to change this decision. It is commendable that they avoid a direct conclusion regarding killed steel. While their conclusion regarding nitrogen in "undeoxygenized steel" appears to

TABLE 5

Normalized and Aged			Normalized, Annealed and Aged		
Steel No., from A.S.T.M. Paper	Nitrogen, Per Cent		Steel No., from A.S.T.M. Paper	Nitrogen, Per Cent	
	Soluble	Total		Soluble	Total
26 (highest curve).....	0.0000	0.0052	23 (highest curve).....	0.0011	0.0046
23.....	0.0011	0.0046	22.....	0.0097	0.0103
22.....	0.0097	0.0103	24.....	0.0014	0.0137
27.....	0.0029	0.0054	27.....	0.0029	0.0054
30.....	0.0000	0.0043	25.....	0.0002	0.0108
24.....	0.0014	0.0137	26.....	0.0000	0.0052
28.....	0.0012	0.0055	30.....	0.0000	0.0043
25.....	0.0002	0.0108	28.....	0.0012	0.0055
29.....	0.0009	0.0060	31.....	0.0019	0.0099
31 (lowest curve).....	0.0019	0.0099	29 (lowest curve).....	0.0009	0.0060

contents varying between 0.004 and 0.015 per cent. This applied to both normalized and annealed specimens, but aging at 450°F. was not used. We felt that room-temperature aging was sufficient for steels with less than 0.10 per cent carbon; would the authors agree with this?

Thus in our nontitanium steels we did not obtain any such correlation of impact resistance with nitrogen as is indicated in the authors' Fig. 4. In our titanium steels there was a similar lack of correlation with nitrogen, as was demonstrated in Table 2 and Fig. 1 of the A.S.T.M. paper. This can be appreciated from Table 5, in which the soluble and total nitrogen contents of the titanium steels of my Fig. 1 are given with the steels arranged in the order of the work-brittleness curves, the highest curves being at the top of the list and the lowest curves at the bottom.

It is obviously very difficult to find any correlation of the work-brittleness curves with the nitrogen contents of these titanium steels, even when the soluble nitrogen, instead of total, is considered. The results are seen to be differ-

be sound, the evidence that nitrogen has any similar effect in killed steel remains far from clear, and strong deoxidation still seems to be important for the control of strain-aging embrittlement.

H. K. WORK AND G. H. ENZIAN (authors' reply).—We have followed Mr. Comstock's studies on the effect of titanium additions on strain-aging behavior quite closely, and whereas his interest in this subject has been largely from the point of view of deoxidizers, ours has been mainly concerned with steelmaking. For this reason it is probable that our experience has covered a somewhat wider range of steels than Mr. Comstock has had available for study.

Mr. Comstock mentions a disagreement between the results reported in the present paper and a conclusion he reached in his A.S.T.M. paper. However, certain testing conditions were used in his work which lead us to believe that this conclusion was too broad. It has been our experience that aging for three weeks at room temperature is not sufficient to

indicate the probable full extent of strain-aging embrittlement with the work-brittleness test except in cases of sensitive and rapidly aging steels. Test results have shown that even a moderately sensitive capped steel may show no loss in impact toughness on the work-brittleness test after aging one month at room temperature; after six months the curve begins to approach that found on aging one hour at 450°F.

This behavior is shown graphically in Fig. 6 for a silicon-capped steel whose composition is shown in Table 6. This steel is similar to heat G in Fig. 2.

TABLE 6.—*Steelmaking Practice and Chemical Composition*

Heat	Practice	Composition, Per Cent					
		C	Mn	P	S	Si	N ₂
Q	Si-capped	0.08	0.44	0.039	0.012		0.003

For fully skilled steels, a change in impact properties with room-temperature aging may take place at an even slower rate than that shown for the capped heat Q. Therefore we feel that Mr. Comstock's conclusion that nitrogen up to 0.02 per cent has a negligible effect on strain-aging in killed steels was based on tests that had not aged sufficiently.

Developing this point further: Fig. 4 shows a relationship between nitrogen content and strain-sensitivity of silicon-killed steels; this relationship might not have been apparent had an aging treatment of three weeks at room temperature been used. For aluminum-killed steels, however, the situation is somewhat different, and our results agree with Mr. Comstock's in that such steel with as much as 0.022 per cent nitrogen (heat E, Fig. 2) shows insensitive characteristics. Here, however, since the steel is substantially nonaging, it

makes little difference whether the material is tested in the aged or partially aged condition.

The present paper has attempted to show that nitrogen affects strain-sensitivity and that

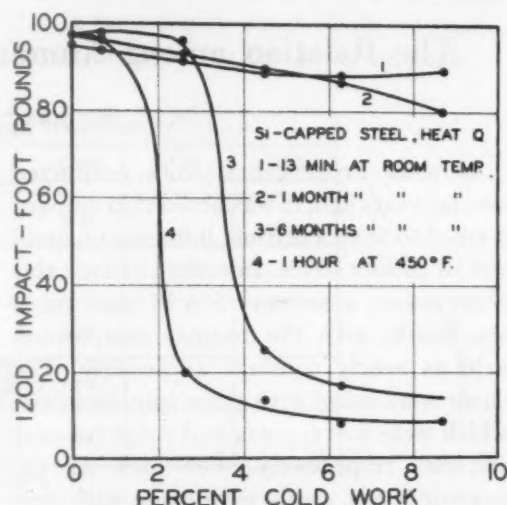


FIG. 6.—EFFECT OF AGING TREATMENTS ON RESULTS OF WORK-BRITTLENESS TEST.

These work-brittleness curves show that no appreciable change in strain-sensitivity due to aging at room temperature took place in this steel until more than one month had elapsed after cold drawing.

different deoxidizers affect the influence of nitrogen on this behavior in different ways. Conclusion 2 of the paper covers our thoughts on this subject and, although we agree that strong deoxidation is important for the control of strain-sensitivity, it is our belief that the important consideration in this respect is the reaction of the deoxidizer with the nitrogen in the steel.

All tests were made on normalized material; this has been our usual practice, unless otherwise stated, and was not mentioned in the present paper. The reasons for such heat-treating were covered in the original paper on the work-brittleness test.²⁰

The Relation among Aluminum, Sulphur, and Grain Size

By C. E. SIMS,* MEMBER A.I.M.E.

IN some experimental work conducted several years ago, it was noted that sulphur seemed to have a distinct influence on grain size of carbon steels. In order to check this observation, a series of S.A.E. 1040 steels was made with the normal composition held as nearly constant as possible. The steels were made with three sulphur levels, which were 0.012, 0.024 and 0.038 per cent sulphur, respectively. For each of the sulphur levels, steels were made with only silicon deoxidization and with aluminum additions of 0.015, 0.025, 0.050 and 0.10 per cent. The melting medium was an acid-lined high-frequency induction furnace. These steels were forged and rolled and differentially quenched from temperatures in the range of 1500° to 1800°F. After this, the A.S.T.M. grain size was determined and plotted as in Fig. 1.

It will be noted, first of all, that the aluminum-free steels had finer grain size with higher sulphur when heated to 1500°, but that this condition was reversed at 1700°. When aluminum was added to produce fine grain size, the steels in the lowest sulphur level were fine-grained only to 1600°, and then only with an addition of one pound of aluminum per ton. The medium sulphur steels were fine-grained to 1600° with a wider range of aluminum addition. The steels in the highest sulphur level were fine-grained at 1600° over a still wider range of aluminum additions and fine-

grained at 1700° with an addition of one pound per ton.

Fig. 2 shows curves of the grain-coarsening temperature for these steels and illustrates how sulphur and aluminum combine to give greater inhibition to grain growth than aluminum alone. Only the highest sulphur steels have a grain-coarsening temperature above 1700°. At 1650°, the low sulphur steel is fine-grained only at its peak, while the highest sulphur steel is fine-grained over a wide range. In these tests, one pound of aluminum per ton gave the best results; this is equivalent to about 1½ lb. per ton for commercial condition. McQuaid-Ehn tests made on these steels showed the same trend but to a lesser degree.

The tests were repeated on a series of S.A.E. 1015 steels with sulphur levels of 0.02 and 0.035 per cent. Aluminum additions were made in the range from 0.025 to 0.15 per cent. These steels were forged and rolled, normalized at 2000°F. to put them all in the same starting condition, then reheated to various temperatures from 1600° to 1800° and cooled at rates that would allow ferrite precipitation in the austenitic grain boundaries. The results of these tests are shown in Fig. 3.

It will be noted that, up to the temperature of 1650°, there is very little difference in the grain size obtained from the two levels of sulphur. At temperatures of 1700° and 1750°, however, the lower sulphur steel was fine-grained only with an aluminum addition of 1½ lb. per ton;

Manuscript received at the office of the Institute Jan. 15, 1945. Listed as T.P. 1867.

*Supervising Metallurgist, Battelle Memorial Institute, Columbus, Ohio.

whereas, the higher sulphur steel was fine-grained throughout the range from one to three pounds per ton. Both steels were coarse-grained at 1800°. The higher aluminum addition required to give the peak result in these steels is probably related to

the lower carbon content which would, in turn, mean a higher oxygen content to be neutralized.

This information is given in the hope that it may clarify some of the inconsistencies in obtaining fine grain in steels.

HEAT NO.	AL ADDED %	QUENCHING TEMPERATURE—DEG. F.				
		1500	1600	1700	1750	1800
4102	0	2-4	2-3	2-3		
4103	.015	3-4	2-4	2-3		
4104	.025	5-6	2-3	2-3		
4105	.050	7	5-6	106	1	
4106	.10	6-7	107	1-3		

0.012% SULPHUR

4142	0	3-5	2-4	1-3		
4108	.015	4-5	2-4	2-4		
4109	.025	6	107	1-2	2	
4110	.050	6-7	7	106	105	2
4111	.10	7	6-7	1-4	1-2	

0.024% SULPHUR

4143	0	5	105	1		
4113	.015	5-6	105	2-4		
4114	.025	6-7	6-7	107	2-3	2
3920	.050	7	6-7	6-7	107	2-4
4119	.10	6-7	6-7	106	2-4	1

0.038% SULPHUR

FIG. 1.—GRAIN SIZE OF S.A.E. 1040 STEELS WITH THREE LEVELS OF SULPHUR, DEOXIDIZED WITH VARIOUS ALUMINUM ADDITIONS AND HEAT-TREATED AT DIFFERENT TEMPERATURES.

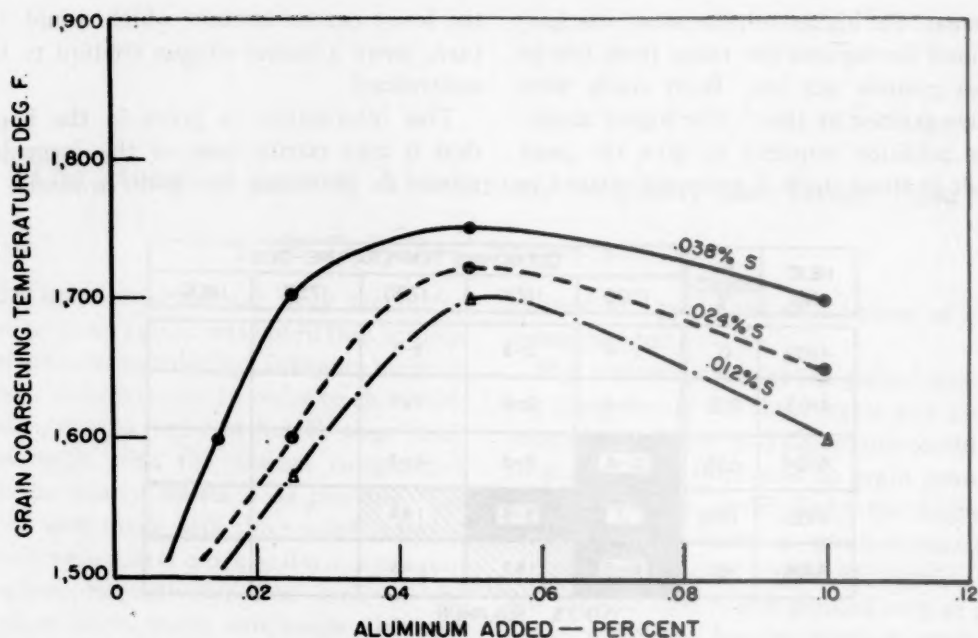


FIG. 2.—GRAPHIC REPRESENTATION OF GRAIN-COARSENING TEMPERATURE OF STEELS SHOWN IN FIG. 1.

Note that at 1700°F. the aluminum addition to retain fine grain is very critical in the 0.012 per cent sulphur level, but that with 0.038 per cent sulphur, it can be varied considerably.

HEAT NO	AL ADD'D %	QUENCHING TEMP. DEG F				
		1600	1650	1700	1750	1800
4470	.025	3&8	1&7	1	1	1
4471	.05	8	7	1&6	5	1
4472	.075	8	8	7	6	1
4473	.10	8	8	2&8	5-6	1
4474	.15	8	7-8	1	3-6	1

0.02 % SULPHUR

4475	.025	4&7	1&6	1	1	1
4476	.05	8	7-8	7	6-7	1
4477	.075	8	8	8	6-7	1
4478	.10	8	8	8	6	1
4479	.15	8	8	8	6	1

0.035 % SULPHUR

FIG. 3.—EFFECT OF ALUMINUM AND SULPHUR ON GRAIN SIZE OF S.A.E. 1015 STEEL. Similar to Fig. 1 but for two sulphur levels in a low-carbon steel.

Institute of Metals Division, Volume 161 Transactions A.I.M.E., 1945

TECHNICAL PAPERS AND DISCUSSIONS

Institute of Metals Division Lecture

A New Microscopy and Its Potentialities. By Charles S. Barrett. (*Metals Technology*, April 1945)

Physical Metallurgy

Fundamental Principles Involved in Segregation in Alloy Castings. By R. M. Brick. (*Metals Technology*, Sept. 1944)

A Study of Age-hardening Using the Electron Microscope and Formvar Replicas. By D. Harker and M. J. Murphy. (*Metals Technology*, June 1945)

Standards for Identifying Complex Twin Relationships in Cubic Crystals. By C. G. Dunn. (*Metals Technology*, April 1945)

Orientation Changes during Recrystallization in Silicon Ferrite. By C. G. Dunn. (*Metals Technology*, April 1945)

The Orientation Texture at the Surface of Cast Metals. By Gerald Edmunds. (*Metals Technology*, Jan. 1945) (With discussion)

Internal Friction of Single Crystals of Brass, Copper and Aluminum. By George H. Found. (*Metals Technology*, June 1945) (With discussion)

Recrystallization of Aluminum in Terms of the Rate of Nucleation and the Rate of Growth. By W. A. Anderson and R. F. Mehl (*Metals Technology*, Feb. 1945) (With discussion)

Copper and Copper-rich Alloys

Textures, Anisotropy and Earing Behavior of Brass. By F. H. Wilson and R. M. Brick. (*Metals Technology*, June 1945) (With discussion)

Phantom Laminations in Brass. By Daniel R. Hull, H. F. Silliman and John R. Freeman, Jr. (*Metals Technology*, Jan. 1945) (With discussion)

Corrosion of Yellow Brass Pipes in Domestic Hot-water Systems—a Metallographic Study. By E. P. Polushkin and Henry L. Shuldener. (*Metals Technology*, Oct. 1944) (With discussion)

The Alpha Solid Solution Field of the Copper-manganese-zinc system. By R. S. Dean, J. R. Long, T. R. Graham and A. H. Roberson. (*Metals Technology*, June 1945)

A White High-manganese Brass. By R. S. Dean, J. R. Long, T. R. Graham and C. W. Matthews. (*Metals Technology*, June 1945)

Magnesium Alloys

Oxidation Inhibitors in Core-sand Mixtures for Magnesium Castings. By O. Jay Myers. (*Metals Technology*, Feb. 1945) (With discussion)

Grain Size and Properties of Sand-cast Magnesium Alloys. By R. S. Busk and C. W. Phillips. (*Metals Technology*, Feb. 1945) (With discussion)

Water Quenching of Some Typical Magnesium Casting Alloys. By R. S. Busk and R. E. Anderson (With discussion)

- Factors Affecting Abnormal Grain Growth in Magnesium-alloy Castings. By A. T. Peters, R. S. Busk, and H. E. Elliott. (*Metals Technology*, June 1945) (With discussion)
- Grain Refinement of a Carbothermic Magnesium Alloy by Superheating. By Ralph Hultgren, David W. Mitchell and Bernard York. (*Metals Technology*, June 1945)
- Grain Refinement of Magnesium Alloys without Superheating. By Ralph Hultgren and David W. Mitchell. (*Metals Technology*, June 1945)
- A Study of Factors Influencing Grain Size in Magnesium Alloys and a Carbon Inoculation Method for Grain Refinement. By C. H. Mahoney, A. L. Tarr and P. E. Le Grand (*Metals Technology*, June 1945) (With discussion)
- Solubility of Manganese in Liquid Magnesium. By N. Tiner. (*Metals Technology*, June 1945) (With discussion)

Miscellaneous Metals and Alloys

- The Hardness of Silver-antimony Solid Solutions. By R. M. Treco and J. H. Frye, Jr. (*Metals Technology*, Oct. 1944)
- The Constitution of the Gold-germanium System. By Robert I. Jaffee, Eugene M. Smith and Bruce W. Gonser. (*Metals Technology*, June 1945)
- Hydrogen Content of Electrolytic Manganese and Its Removal. By E. V. Potter, E. T. Hayes and H. C. Lukens. (*Metals Technology*, June 1945)
- Substitute Solders of the 15-85 Tin-lead Type. By J. B. Russell and J. O. Mack. (*Metals Technology*, Oct. 1944) (With discussion)

Symposia

Symposium on Creep of Nonferrous Metals and Alloys

- Application of Nonferrous Alloys in Stress Design. By J. J. Kanter. (With discussion)
- Creep Characteristics of a Phosphorized Copper. By H. L. Burghoff and A. I. Blank. (With discussion)
- Creep Properties of Cold-drawn Annealed Monel and Inconel. By B. B. Betty, H. L. Eiselstein and F. P. Huston, Jr. (With discussion)
- Properties of Some Cast Copper-base Alloys at Elevated Temperatures. By H. E. Montgomery. (With discussion)
- Creep Data on Die-cast Zinc Alloy. By E. H. Kelton and B. D. Grissinger. (With discussion)
- Creep Properties of Some Rolled Lead-antimony Alloys. By A. A. Smith, Jr. and H. E. Howe. (With discussion)

Symposium on Continuous Casting (*Metals Technology*, February 1945)

- Opening Remarks. By Carl E. Swartz
- Continuous Casting Yesterday and Today. By T. W. Lippert
- Continuous Casting of Molten Metals—History, Requirements, Metallurgy, and Economics. By Norman P. Goss. (With discussion)
- Improvements in the Direct Rolling of Strip Metal. By C. W. Hazelett
- The Soro Process. By E. J. Valyi
- The Williams Process of Casting Metals. By E. R. Williams

Conference on Production and Design Limitations and Possibilities for Powder Metallurgy Parts (*Metals Technology*, January 1945)

Foreword. By F. N. Rhines

Design Factors for the Metal Forms with Which Powder Metallurgy May Compete. By Fred P. Peters. (With discussion)

Powder Metallurgy as Applied to Machine Parts. By A. J. Langhammer. (With discussion)

Pole Pieces for Electric Motors Made from Iron Powder. By F. V. Lenel. (With discussion)

Bearings from Metal Powders. By W. R. Toeplitz. (With discussion)

Brushes and Allied Powder-metal Parts. By R. R. Hoffman

Electrical Contacts Manufactured from Metal Powders. By E. I. Larsen

Sintered Magnets. By C. R. Fulton

Friction Articles from Metal Powders. By C. T. Cox. (With discussion)

Certain Characteristics of Silver-base Powder Metallurgical Products. By F. R. Hensel and E. I. Larsen. (With discussion)

Some Properties of Sintered and Hot-pressed Copper-tin Powder Compacts. By C. G. Goetzel. (With discussion)

The Sintering of Metal Powders—Copper. By C. J. Bier and J. F. O'Keefe. (*Metals Technology*, October 1944)

Some Experiments on the Effect of Pressure on Metal-powder Compacts. By Jerome F. Kuzmick. (With discussion)

INDEX

(NOTE: In this index the names of authors of papers and discussions and of men referred to are printed in SMALL CAPITALS, and the titles of papers in *italics*.)

A

- ALEXANDER, B., DERGE, G. AND PEIFER, W.: *Vacuum Fusion Analysis of Steel for Hydrogen*, 361
- Aluminum iron: cold-worked: recovery: detected by changes in magnetic properties, 106
- Aluminum Research Laboratories: an interferometer type of dilatometer, 642
- ANDERSON, W. A.: *Discussion on Effect of Variables on the Recrystallization of Silicon Ferrite in Terms of Rates of Nucleation and Growth*, 139
- AUSTIN, C. H., ST. JOHN, C. R. AND LINDSAY, R. W.: *Creep Properties of Some Binary Solid Solutions of Ferrite*, 84
- AUSTIN, J. B.: *Introduction to Symposium on Methods of Sampling and Analysis of Steel for Hydrogen*, 353
- Discussion on Determination of Hydrogen in Steel*, 353, 354, 368

B

- BABCOCK, R. S.: *Discussion on Segregation in Steel Ingots*, 470
- BANTA, H. M., HOYT, S. L. AND SIMS, C. E.: *Metallurgical Factors of Underbead Cracking*, 326
- Battelle Memorial Institute: preliminary experiments on total combustion method for analysis of hydrogen in steel, 404
- some speculations regarding the plastic flow and rupture of metals under complex stresses, 584
- study of liquidus-solidus temperatures and emissivities of some commercial heat-resistant alloys, 156
- study of metallurgical factors of underbead cracking, 326
- study of relation among aluminum, sulphur and grain size in steel, 734
- BELDING, H. R.: *Discussion on Segregation in Steel Ingots*, 433
- Bessemer steel: quality: effect of ingot delivery time, 73
- significance of steel manganese, mixer silicon and steel sulphur, 73
- Bethlehem Steel Co.: slag-metal-oxygen relationships in the basic open-hearth and electric processes, 672
- Brass: tensile deformation: stress-strain curves: initial yielding and plastic flow, 268, 273, 289

- BRASUNAS, A. DE S., GOW, J. T. AND HARDER, O. E.: *The Liquidus-solidus Temperatures and Emissivities of Some Commercial Heat-resistant Alloys*, 156
- BRICK, R. M.: *Fundamental Principles Involved in Segregation in Alloy Castings*. See Contents.
- BRIDGMAN, P. W.: *Flow and Fracture*, 569; discussion, 579
- BROWER, T. E. AND LARSEN, B. M.: *The Occurrence of Oxygen in Liquid Open-Hearth Steel—Sampling Methods*, 712
- BROWN, C. C. AND TENENBAUM, M.: *Application of pH Slag-basicity Measurements to Basic Open-hearth Phosphorus Control*, 60
- The Total Oxygen Content of Plain Carbon Open Hearth Steel during Deoxidation and Teeming*, 685
- BROWN, W. D.: *A Modified Vacuum Extraction Apparatus*, 381

C

- Carnegie-Illinois Steel Corporation, Duquesne Steel Works: determination of hydrogen in steel sampling and analysis, by vacuum extraction, 375
- a modified vacuum extraction apparatus, 381
- Carnegie Institute of Technology: vacuum-fusion analysis of steel for hydrogen, 361
- Carpenter Steel Co.: determination of hydrogen content of molten steel by vacuum extraction, 390
- Cast iron: for enamelware: manganese and sulphur contents, 627
- graphitization: bibliography, 635
- dilatometric studies, 627
- have doubtful value, 639, 641
- effects of manganese and sulphur, 627
- growth: dimensional changes caused by graphitization: dilatometric studies, 627
- unknown causes, 638
- Cast steel: Nos. 1030, 2330, 4130 and 4330: hardenability curves, 250
- heat-treatment: time-temperature transformation curves, 250
- S-curves, 250
- CHIU, Y. C.: *Discussion on Determination of Hydrogen in Steel*, 368
- CHRISTENSON, A. L.: *Discussion on Recent Developments in Dilatometric Analysis*, 624

CHRISTENSON, A. L., NELSON, E. C. AND JACKSON, C. E.: *A High-speed Dilatometer and Transformational Behavior of Six Steels in Cooling*, 606

Cohesive strength of metals: complex stress systems:
 effect on plastic flow, 584
 representation, 584
 triaxial stress ratio: definition, 584
 effect on plastic flow, 590
 triaxial stresses: methods of obtaining, 585
 computing stress distribution in vicinity of deep hyperbolic notches in tensile bars, 594
 effect of temperature on yield point, 597
 flow and fracture, 474, 542, 569
 flow and stress: interconnection, 571
 fracture, 575
 influence of combination of principal stresses and of plastic extension on technical cohesion limit, ultimate stress, yield stress and ductility, 474, 583
 stress distribution at neck of test specimen, 573, 578 et seq.
 stresses with two degrees of freedom, 572
 symposium, 538
 technical: brief bibliography, 501, 567
 brittle fracture a measure, 600
 definition, 474, 541, 572, 599
 experimental investigation of tensile properties of notched specimens, 474
 in terms of principal stresses, 542
 tests with rock-salt crystals, 595
 Coke ovens: heat flow: electrical analogue. *See* Heat Flow.
 COMSTOCK, G. F.: *Discussion on Deoxidation*, 731
 Copper: oxygen-free: technical cohesive strength, 474
 tensile deformation: stress-strain curves: initial yielding and plastic flow, 268, 273
 Crane Co.: dilatometric studies of the graphitization of cast iron, 627
 Creep of metals: ferrite: binary solid solutions: properties, 84

D

Deoxidation. *See* Open-hearth Steel.
 DERGE, G.: *Discussions: on Deoxidation*, 706
 on Determination of Hydrogen in Steel, 368
 DERGE, G., PEIFER, W. AND ALEXANDER, B.: *Vacuum Fusion Analysis of Steel for Hydrogen*, 361
 DERGE, G., AND URBAN, S. F.: *Discussion on Deoxidation*, 683
 Dilatometer: high-speed, 606
 interferometer type: apparatus and procedure, 642
 Dilatometric analysis: advantages, 605
 doubtful value in study of graphitization, 639, 641
 graphitization of cast iron, 627
 interferometer method: results of tests, 652
 recent developments: symposium, 605
 transformational behavior of six steels in cooling, 606
 DUNKLE, H. C.: *Effect of Ingot Delivery Time as a Factor in Quality of Bessemer Steel*, 73; discussion, 83

DUNN, C. G. AND WARD, R.: *Discussion on Effect of Variables on the Recrystallization of Silicon Ferrite in Terms of Rates of Nucleation and Growth*, 138

E

EDDY, C. T., MARCOTTE, R. J. AND SMITH, R. J.: *Time-temperature Transformation Curves for Use in the Heat-treatment of Cast Steel*, 250
 Electric-furnace steel: slag-metal-oxygen relationships, 672
 Electricity: analogue of heat flow. *See* Heat Flow.
 EMERICK, H. B.: *Discussions: on Effect of Ingot Delivery Time as a Factor in Quality of Bessemer Steel*, 82
 on Segregation in Steel Ingots, 457
 ENZIAN, G. H. AND WORK, H. K.: *The Effect of Deoxidation on the Strain-sensitivity of Low-carbon Steels*, 723; discussion, 732

F

FERGUSON, W. R.: *Discussion on Recent Developments in Dilatometric Analysis*, 636
 Ferrite: binary solid solutions: creep properties, 84
 silicon: recrystallization. *See* Recrystallization.
 FETTERS, K. L.: *Discussions: on Application of pH Slag-basicity Measurements to Basic Open-hearth Phosphorus Control*, 70
 on Deoxidation, 705, 711
 on Segregation in Rimmed Steel, 457
 FICK, N. C.: *Discussion on Deoxidation*, 710
 FINK, W. L.: *Discussion on Recent Developments in Dilatometric Analysis*, 655
 FINK, W. L. AND WILLEY, L. A.: *An Interferometer Type of Dilatometer, and Some Typical Results*, 642
 FISHEL, W. P.: *Discussion on Distribution of Carbon between Titanium and Iron in Steel*, 314
 FISHEL, W. P. AND ROBERTSON, B.: *Distribution of Carbon between Titanium and Iron in Steels*, 310
 Flow. *See* Cohesive Strength of Metals.
 FUNK, C. R.: *Discussion on Segregation in Steel Ingots*, 469

G

General Electric Co.: determination of hydrogen by vacuum extraction and tin fusion, 385
 study of oxide-metal layers formed on commercial iron-silicon alloys exposed to high temperatures, 141
 GENSAMER, M.: *Summary of Symposium on Cohesive Strength*, 538
 GOLLER, G. N.: *Discussion on The Liquidus-solidus Temperatures and Emissivities of Some Commercial Heat-resistant Alloys*, 173
 GOW, J. T.: *Discussion on The Liquidus-solidus Temperatures and Emissivities of Some Commercial Heat-resistant Alloys*, 174
 GOW, J. T., BRASUNAS, A. DE S. AND HARDER, O. E.: *The Liquidus-solidus Temperatures and Emissivities of Some Commercial Heat-resistant Alloys*, 156

- GRANGE, R. A.: *Discussion on Recent Developments in Dilatometric Analysis*, 623
- GRANT, N. J.: *Discussions: on Application of pH Slag-basicity Measurements to Basic Open-hearth Phosphorus Control*, 70
on Deoxidation, 682
- H
- HALLEY, J. W.: *Discussion on Segregation in Steel Ingots*, 433, 458
- HALLEY, J. W. AND PLIMPTON, G. L., JR.: *Relation of Open-hearth Practice to Segregation in Rimmed Steel*, 438
- HARDER, O. E., GOW, J. T. AND BRASUNAS, A. DE S.: *The Liquidus-solidus Temperatures and Emissivities of Some Commercial Heat-resistant Alloys*, 156
- Harvard University: study of flow and fracture, 569
- Heat flow: electrical analogue in a regenerator system: calculation of proper size of condenser and resistor units, 28, 33, 35
construction, 22
operation, 26
theory, 15
heat and mass flow analyzer: operation and results, 33
- Heat-resistant alloys: commercial: HH and HT types: liquidus and solidus temperatures and emissivities, 156
- HEINDLHOFFER, K.: *Discussions: on An Electrical Analogue of the Flow of Heat in a Regenerator System*, 35
on An Investigation of the Technical Cohesive Strength of Metals, 536
- HEINDLHOFFER, K. AND LARSEN, B. M.: *An Electrical Analogue of the Flow of Heat in a Regenerator System*, 15
- HENRY, T. P., PHILBROOK, W. O. AND JOLLY, A. H. JR.: *A Rapid Laboratory Method for Estimating the Basicity of Open-hearth Slags*, 49
- HERRES, S. A.: *Discussion on Effect of Time of Storage on Ductility of Welded Test Specimens*, 322
- HERTY, C. H. JR.: *Discussion on Deoxidation*, 708
- HH and HT alloys: liquidus and solidus temperatures and emissivities, 156
- HOLLOMON, J. H.: *Tensile Deformation*, 268; discussion, 290
Discussion on Isothermal Transformation of Austenite in One Per Cent Carbon, High-chromium Steels, 220
- HOLLOMON, J. H. AND JAFFE, L. D.: *Time-temperature Relations in Tempering Steel*, 223; discussion, 249
- HOLLOMON, J. H. AND ZENER, C.: *Condition of Fracture in Steel*. See Contents.
- HOYT, S. L.: *Discussion on Cohesive Strength of Metals*, 603, 604
- HOYT, S. L., SIMS, C. E. AND BANTA, H. M.: *Metallurgical Factors of Underbead Cracking*, 326
- Hydrogen in steel: determination: accuracy vs. precision of methods, 396
bomb-mold sampling, 389, 390
condition of gas in steel must be known, 395
gas-tube method, 375, 398, 403
- Hydrogen in steel: determination: Jones and Laughlin Steel Corporation, 403
symposium, 353
Timken Roller Bearing Co., 398
tin-fusion analysis, 388
total combustion method: accuracy, 409, 412
apparatus, 404, 408
fractionation and measurement, 407
scale of measurement, 408
stability of blank value, 412
vacuum-extraction method, 358
apparatus at Bureau of Standards, 369
Carpenter Steel Co., 390
Duquesne Steel Works, 375, 381
inherent difficulties, 397
iron-manganese system, 385
precision, 393
precision and accuracy, 371
results at 800°C., Bureau of Standards, 372
sampling molten steel in ingot mold, 375
solid steel samples, 375, 377
Torricellian apparatus, 377, 381
vacuum-fusion method: dried oxide suggested to improve process, 396
inherent difficulties, 397
modification at Metals Research Laboratory, 361
modification at Westinghouse Laboratory, 355
some work in Germany, 368
value, 354, 367
vs. vacuum heating, 358, 396
- I
- Inland Steel Co.: application of pH slag-basicity measurements to basic open-hearth phosphorus control, 60
study of relation of open-hearth practice to segregation in rimmed steel, 438
study of total oxygen content of plain carbon open-hearth steel during deoxidation and teeming, 685
- Interferometer. See Dilatometer.
- Iron: aluminum. See Aluminum Iron.
hydrogen content: determination. See Hydrogen in Steel.
- Iron alloys: binary: ferrite solid solutions: creep properties, 84
- Iron-chromium alloys: Ar': determinations on 17 steels, 175
Ar': point defined, 176
austenite to martensite transformation: X-ray studies, 176
stabilization: effect on determination of Ar', 182
- Iron-chromium-nickel alloys: HH and HT types: liquidus and solidus temperatures and emissivities, 156
- Iron-silicon alloys: commercial: oxidation: rate: effect of composition, temperature, time, and atmosphere, 141
oxide-metal layers: effect of composition, temperature, time and atmosphere on type of scale, 141

J

- JACKSON, C. E.: Discussions: on Effect of Time of Storage on Ductility of Welded Test Specimens, 324
on Recent Developments in Dilatometric Analysis, 626
- JACKSON, C. E., CHRISTENSEN, A. L. AND NELSON, E. C.: A High-speed Dilatometer and Transformational Behavior of Six Steels in Cooling, 606
- JACKSON, C. E. AND LUTHER, G. G.: Effect of Time of Storage on Ductility of Welded Test Specimens, 315
- JACKSON, L. R.: Some Speculations Regarding the Plastic Flow and Rupture of Metals under Complex Stresses, 584
- JAFFE, L. D.: Discussions: on Distribution of Carbon between Titanium and Iron in Steels, 313
on Isothermal Transformation of Austenite in One Per Cent Carbon, High-chromium Steels, 220
- JAFFE, L. D. AND HOLLOMON, J. H.: Time-temperature Relations in Tempering Steel, 223; discussion, 249
- JOLLY, A. H., JR., PHILBROOK, W. O. AND HENRY, T. R.: A Rapid Laboratory Method for Estimating the Basicity of Open-hearth Slags, 49

K

- KLIER, E. P.: Transformation of Austenite in a Steel Containing 3 Per Cent Chromium and 1 Per Cent Carbon, 186
Discussion on Recent Developments in Dilatometric Analysis, 623
- KLIER, E. P. AND TROIANO, A. R.: $A_{r''}$ in Chromium Steels, 175
- KINGSTON, W. E.: Discussion on Recent Developments in Dilatometric Analysis, 655
- KRAMER, I. R.: Discussion on Distribution of Carbon between Titanium and Iron in Steel, 314
- KULP, R. K.: Discussion on Segregation in Steel Ingots, 471

L

- LARSEN, B. M.: Review of Factors Underlying Segregation in Steel Ingots, 414
Discussions: on An Electrical Analogue of the Flow in a Regenerator System, 35
on Determination of Hydrogen in Steel, 389
on Segregation in Steel Ingots, 434, 437
- LARSEN, B. M. AND BROWER, T. E.: The Occurrence of Oxygen in Liquid Open-Hearth Steel—Sampling Methods, 712
- LARSEN, B. M. AND HEINDLHOFFER, K.: An Electrical Analogue of the Flow of Heat in a Regenerator System, 15
- LARSEN, B. M. AND SHENK, W. E.: A Completely Automatic Control of Open-hearth Reversal, 37
- LINDSAY, R. W., AUSTIN, C. R. AND ST. JOHN, C. R.: Creep Properties of Some Binary Solid Solutions of Ferrite, 84

- LORIG, C. H.: Discussion on Recent Developments in Dilatometric Analysis, 636
- LOW, J. R., JR.: Discussion on Tensile Deformation, 289
- LUTHER, G. G. AND JACKSON, C. E.: Effect of Time of Storage on Ductility of Welded Test Specimens, 315
- LYMAN, T. AND TROIANO, A. R.: Isothermal Transformation of Austenite in One Per Cent Carbon, High-chromium Steels, 196; discussion, 221

M

- MACGREGOR, C. W.: Discussion on Cohesive Strength of Metals, 578
- MACGREGOR, C. W. AND MEHRINGER, F. J.: Effects of Cold-rolling on the True Stress-strain Properties of a Low-carbon Steel, 291
- MACKENZIE, J. T.: Discussion on Recent Developments in Dilatometric Analysis, 636
- Magnetic terminology, 106
- MARCOTTE, R. J., EDDY, C. T. AND SMITH, R. J.: Time-temperature Transformation Curves for Use in the Heat-treatment of Cast Steel, 250
- MARSH, J. S.: Slag-metal-oxygen Relationships in the Basic Open-hearth and Electric Processes, 672
- Massachusetts Institute of Technology: study of effects of cold-rolling on true stress-strain properties of a low-carbon steel, 291
- MCADAM, D. J., JR.: The Technical Cohesive Strength of Metals in Terms of the Principal Stresses, 542
Discussion on Cohesive Strength of Metals, 537, 576, 581, 601
- MCADAMS, D. J., JR. AND MEBS, R. W.: An Investigation of the Technical Cohesive Strength of Metals, 474
- MCGEARY, R. K. AND YENSEN, T. D.: Methods of Analysing for Hydrogen in Iron and Iron Alloys, 355
- MEBS, R. W. AND MCADAM, D. J., JR.: An Investigation of the Technical Cohesive Strength of Metals, 474
- MEHRINGER, F. J. AND MACGREGOR, C. W.: Effects of Cold-rolling on the True Stress-strain Properties of a Low-carbon Steel, 291
- METCALF, N.: Discussion on Application of pH Slag-basidity Measurements to Basic Open-hearth Phosphorus Control, 71
- METZGER, M.: Discussion on Segregation in Steel Ingots, 470
- Michigan College of Mining and Technology: study of time-temperature transformation curves for use in heat-treatment of cast steel, 250
- Monel metal: technical cohesive strength, 474
- MOORE, G. A.: Preliminary Experiments on the Total Combustion Methods for the Analysis of Hydrogen in Steel, 404
Discussion on Determination of Hydrogen in Steel, 396, 412
- MORKOVIN, D.: Discussion on Cohesive Strength of Metals, 582, 595, 603

- MRAVEC, J. G.: *Determination of Hydrogen in Molten Steel by the Gas-tube Method*, 398
Discussion on Application of pH Slag-basicity Measurements to Basic Open-hearth Phosphorus Control, 69

N

- National Bureau of Standards: an investigation of the technical cohesive strength of metals, 474, 542
 determinations of hydrogen in iron and steel by vacuum extraction at 800°C., 369
 NAUGHTON, J.: *Determination of Hydrogen by Vacuum Extraction and Tin Fusion*, 385
 Naval Research Laboratory: a high-speed dilatometer and the transformational behavior of six steels in cooling, 606
 study of effect of time of storage on ductility of welded test specimens, 315
 NELSON, E. C.: *Discussion on Recent Developments in Dilatometric Analysis*, 623, 625
 NELSON, E. C., CHRISTENSEN, A. L. AND JACKSON, C. E.: *A High-speed Dilatometer and Transformational Behavior of Six Steels in Cooling*, 606

O

- Office of Production Research and Development: research project on factors affecting cracking tendency of hardenable steels, 326
 Open-hearth furnaces: regenerators: heat flow: electrical analogue. *See* Heat Flow.
 reversal: automatic control: apparatus, 42
 automatic control: control circuit, 46,
 control settings, 41
 operating results, 42
 principle, 38
 Open-hearth slags: basicity: estimating: pH measurements: principle of method, 49
 technique and procedure, 53
 pH method vs. pancake method: accuracy, 51
 rapid laboratory method, 49
 pH measurements: application to phosphorus control, 60
 relation to free lime, 72
 Open-hearth steel: basic: deoxidation: effect on strain-sensitivity of low-carbon steels, 723
 objectives, 658
 oxygen content during, 685
 relation among aluminum, sulphur and grain size, 734
 relation to austenitic grain size, 669
 relation to segregation, 668
 rimmed steel, 662
 semikilled steel, 667
 summary of furnace practice and economic aspects, 658
 oxygen content: after solidification, 702
 brief bibliography, 705, 731
 during deoxidation and teeming, 685
 Open-hearth steel: basic: oxygen content: relation to alloy recoveries and soundness of product, 703
 sampling methods, 712
 slag-metal-oxygen relationships, 672
 Oxygen in iron and iron alloys: analysis: Westinghouse apparatus, 355
 Oxygen in steel: sampling: bomb method, 714
 spoon method, 714

P

- PARKE, R. M.: *Discussion on Recent Developments in Dilatometric Analysis*, 638
 PASCHKIS, V.: *Discussion on An Electrical Analogue of the Flow in a Regenerator System*, 33
 PEIFER, W., DERGE, G. AND ALEXANDER, B.: *Vacuum Fusion Analysis of Steel for Hydrogen*, 361
 Pennsylvania State College: study of creep properties of some binary solid solutions of ferrite, 84
 pH measurements. *See* Open-hearth Slags.
 PHILBROOK, W. O.: *Discussion on Deoxidation*, 710
 PHILBROOK, W. O., JOLLY, A. H., JR. AND HENRY, T. R.: *A Rapid Laboratory Method for Estimating the Basicity of Open-hearth Slags*, 49
 Plastic deformation. *See* Tensile Deformation.
 PLIMPTON, G. L., JR. AND HALLEY, J. W.: *Relation of Open-hearth Practice to Segregation in Rimmed Steel*, 438
 POOLE, S. W. AND ROSA, J. A.: *Segregation in a Large Alloy-steel Ingot*, 459; discussion, 470 et seq.
 POST, C. B. AND SCHOFFSTALL, D. G.: *The Hydrogen Content of Molten Steel by Vacuum Extraction*, 390
 Pyrometers: discussion of Pyro, Leeds and Northrup and Rustless Corporation instruments, 173

R

- RAMSEY, E. L.: *Discussion on Deoxidation*, 708
 REAGAN, W. J.: *Discussion on Application of pH Slag-basicity Measurements to Basic Open-hearth Phosphorus Control*, 71
 Recrystallization: silicon ferrite: rate: effect of deformation, 116
 effect of grain size, 116, 138, 139
 effect of recovery, 116, 138
 effect of temperature, 116, 140
 in terms of rates of nucleation and growth, 116, 138
 Regenerator: heat flow: electrical analogue. *See* Heat Flow.
 Republic Steel Corporation: effect of ingot delivery time as a factor in quality of bessemer steel, 73
 study of segregation in a large alloy-steel ingot, 459
 ROBERTSON, B. AND FISHEL, W. P.: *Distribution of Carbon between Titanium and Iron in Steels*, 310
 Rock salt: tensile tests, 595
 ROSA, J. A.: *Discussion on Deoxidation*, 708

- ROSA, J. A. AND POOLE, S. W.: *Segregation in a Large Alloy-steel Ingot*, 459; discussion, 470 et seq.
- RUSSELL, J. V.: *Discussion on Recent Developments in Dilatometric Analysis*, 625
- S
- S-curves: cast steels 1030, 2330, 4130 and 4330, 250
- ST. JOHN, C. R., LINDSAY, R. W. AND AUSTIN, C. R.: *Creep Properties of Some Binary Solid Solutions of Ferrite*, 84
- SCAFE, R. M.: *Determination of Hydrogen in Steel Sampling and Analysis*, 375
- SCHWARTZ, H. A.: *Discussion on Recent Developments in Dilatometric Analysis*, 639
- SCHNEIDEWIND, R.: *Discussion on Recent Developments in Dilatometric Analysis*, 638
- SCHOFFSTALL, D. G. AND POST, C. B.: *The Hydrogen Content of Molten Steel by Vacuum Extraction*, 390
- SCOTT, H.: *Discussion on Recent Developments in Dilatometric Analysis*, 622, 624
- Segregation in steel: relation to deoxidation, 668
- in steel ingots: alloy steel: cutting ingot for inspection with low oxygen pressure, 470
- distribution of chemical elements, 459
- sulphur prints: interpretation, 470
- curves for evaluating, 472
- factors underlying: dendrite formation, 416
- directional growth of crystals, 415
- effects of liquid motion, 424
- grain size orientation in outer zones, 418
- heat evolved in freezing, 414
- stirring by gas evolution, 424
- volume change in freezing, 421
- hydrogen effect minor, 429
- inverted V: hypothesis of formation, 434, 435
- nonmetallic matter, segregation erratic, 433, 434
- oxygen and nonmetallics, 431
- rimmed steel: effect of composition of melt, 444, 457
- effect of temperature and mold practice, 448
- examples, 452
- mechanisms producing, 438
- relation of open-hearth practice, 438
- specifications: wider ordering range needed, 437
- spectrographic analysis, 471
- transition series of structures with decreasing gas evolution, 427
- iron oxide in ingot iron, 436
- within steel bath, 436
- SHENK, W. E. AND LARSEN, B. M.: *A Completely Automatic Control of Open-hearth Reversal*, 37
- SIMS, C. E.: *The Relation Among Aluminum, Sulphur and Grain Size*, 734
- Discussions: on Deoxidation*, 709
- on Effect of Ingot Delivery Time as a Factor in Quality of Bessemer Steel*, 82
- on Recent Developments in Dilatometric Analysis*, 625
- SIMS, C. E., HOYT, S. L. AND BANTA, H. M.: *Metallurgical Factors of Underhead Cracking*, 326
- Slag control: open-hearth. *See* Open-hearth Slags.
- Slag pancakes. *See* Open-hearth Slags.
- SMITH, E. C.: *Discussion on Segregation in Steel*, 436
- SMITH, R. J., EDDY, C. T. AND MARCOTTE, R. J.: *Time-temperature Transformation Curves for Use in the Heat-treatment of Cast Steel*, 250
- SOLER, G.: *Discussion on Effect of Ingot Delivery Time as a Factor in Quality of Bessemer Steel*, 82
- Introduction to Symposium on Deoxidation*, 657
- STANLEY, J. K.: *Effect of Variables on the Recrystallization of Silicon Ferrite in Terms of Rates of Nucleation and Growth*, 116; discussion, 139
- Recovery of Cold-worked Aluminum Iron as Detected by Changes in Magnetic Properties*, 106
- Steel (*see also* Electric Furnace, Open Hearth, etc.): cast. *See* Cast Steel.
- chromium (*see also* Iron-chromium Alloys): ductility: effect of welding: nick-bend test, 315
- T-bend test, 315
- 0.04 per cent carbon: technical cohesive strength, 474
- grain size: relation of aluminum and sulphur, 734
- hydrogen content: determining. *See* Hydrogen in Steel.
- iron-titanium-carbon: distribution of carbon between titanium and iron, 310
- low-carbon: properties: true stress-strain: effect of aging, 291
- effects of cold-rolling, 291, 299
- low-carbon, aluminum-killed: oxygen analysis after solidification, 702
- 1 per cent C, high-chromium: austenite: bainite formation, 213, 217, 220, 222
- isothermal transformation: microscopic, X-ray and dilatometric investigation, 196
- open-hearth. *See* Open-hearth Steel.
- rimmed: definition, 662
- S.A.E. 1020: technical cohesive strength, 474
- S.A.E. 4130: welded: crack sensitivity: effect of aluminum and titanium, 333
- relation to strength, 343
- technical control, 348
- underhead cracking: metallurgical factors responsible, 326
- segregation. *See* Segregation.
- semikilled: definition, 667
- silicon. *See* Iron-silicon Alloys.
- tempering: hardness obtained: calculations: by time-temperature relations, 238
- charts for finding time-temperature combinations, 245, 246, 248
- steels varying in carbon content: effect of temperature and time, 223
- structure obtained: effects of carbon content, temperature and time, 223
- time-temperature relations with structure obtained, 223
- tensile deformation: relation of fracture and yield strengths of tempered martensitic steels, 285

- Steel: tensile deformation: stress-strain curves initial yielding and plastic flow, 268
- 13-2 chromium-nickel: technical cohesive strength, 474
- 3 per cent Cr, 1 per cent C: austenite transformation: metallographic examination, 186
- X-ray analysis, 186
- bainite formation, 187, 194
- welded: crack sensitivity: effect of structure and thermal history, 333
- metallurgical factors responsible, 326
- underbead cracking: effect of postheating, 344
- welded test specimens: ductility: effect of hydrogen, 318, 322
- effect of time of storage, 315
- underbead cracking: crack-sensitivity test, 328
- effect of hydrogen, 349
- explanation of the phenomenon, 345
- extent: dilatometric determination, 331
- yield point: effect of temperature, 597
- Steel Founders' Society of America: research on time-temperature transformation curves for use in heat-treatment of cast steel, 250
- Steelmaking: deoxidation. *See* Open-hearth Steel.
- slag-metal-oxygen relationships in basic open-hearth and electric processes, 672
- Strain-sensitivity: steels: effect of deoxidation on low-carbon metal, 723
- effect of titanium additions, 732
- work-brittleness test, 725
- STURM, R. C.: *Discussion on An Investigation of the Technical Cohesive Strength of Metals*, 537
- T
- TENENBAUM, M.: *Discussions: on Deoxidation*, 710, 711
- on Segregation in Steel Ingots*, 472, 473
- TENENBAUM, M. AND BROWN, C. C.: *Application of Ph Slag-basicity Measurements to Basic Open-hearth Phosphorus Control*, 60; *discussion*, 71
- The Total Oxygen Content of Plain Carbon Open-hearth Steel during Deoxidation and Tempering*, 685
- Tensile deformation of metals (*see also* Cohesive Strength of Metals):
- brief bibliography, 288
- brass: stress-strain curves, 268, 273, 289
- copper: stress-strain curves, 268, 273
- steel: low-carbon: true stress-strain properties: effect of cold-rolling, 291
- stress-strain curves, 268
- stress-strain curves: elastic, 269
- initial yielding and plastic flow, 268
- THOMPSON, J. G.: *Determination of Hydrogen in Iron and Steel by Vacuum Extraction at 800°C.*, 369
- Discussion on Determination of Hydrogen in Steel*, 354, 367
- Timken Roller Bearing Co.: determination of hydrogen in molten steel by the gas-tube method, 398
- Tin-fusion analysis for hydrogen. *See* Hydrogen in Steel.
- TROIANO, A. R. AND Klier, E. P.: *Ar'' in Chromium Steels*, 175
- TROIANO, A. R. AND LYMAN, T.: *Isothermal Transformation of Austenite in One Per Cent Carbon, High-chromium Steels*, 196; *discussion*, 221
- U
- UHLIG, H. H.: *Discussion on Determination of Hydrogen in Steel*, 397, 411
- University of Notre Dame: study of Ar'' in chromium steels, 175
- study of isothermal transformation of austenite in one per cent carbon, high-chromium steels, 196
- URBAN, S. F. AND DERGE, G.: *Discussion on Deoxidation*, 683
- U. S. Steel Corporation: completely automatic control of open-hearth reversal, 37
- review of factors underlying segregation in steel ingots, 414
- study of an electrical analogue of the flow of heat in a regenerator system, 15
- study of sampling methods for oxygen in liquid open-hearth steel, 712
- V
- Vanderbilt University: study of distribution of carbon between titanium and iron, 310
- VANICK, J. S.: *Discussion on Recent Developments in Dilatometric Analysis*, 636
- VINES, R. F.: *Discussion on Segregation in Steel Ingots*, 473
- W
- WALTERS, F. M., JR.: *Discussion on Recent Developments in Dilatometric Analysis*, 655
- War Production Board. *See* O. P. R. D.
- WARD, R.: *Oxide-metal Layers Formed on Commercial Iron-silicon Alloys Exposed to High Temperatures*, 141
- WARD, R. AND DUNN, C. G.: *Discussion on Effect of Variables on the Recrystallization of Silicon Ferrite in Terms of Rates of Nucleation and Growth*, 138
- WASHBURN, T. S.: *Deoxidation of Basic Open Hearth Steel*, 658
- Watertown Arsenal: study of tensile deformation, 268
- study of time-temperature relations in tempering steel, 223
- Welding: effect on properties of steel. *See* Steel.
- Westinghouse Electric and Manufacturing Co.: methods of analyzing for hydrogen in iron and iron alloys, 355
- study of effect of variables on recrystallization of silicon ferrite in terms of rates of nucleation and growth, 116
- study of recovery of cold-worked aluminum iron as detected by changes in magnetic properties, 106
- WHITE, A. M.: *Discussion on Time-temperature Relations in Tempering Steel*, 248

WILLEY, L. A. AND FINK, W. L.: *An Interferometer Type of Dilatometer, and Some Typical Results*, 642

Wisconsin Steel Works: a rapid laboratory method for estimating the basicity of open-hearth slags, 49

WORK, H. K.: *Discussion on Determination of Hydrogen in Steel*, 403

WORK, H. K. AND ENZIAN, G. H.: *The Effect of Deoxidation on the Strain-sensitivity of Low-carbon Steels*, 923; discussion, 732

Y

YENSEN, T. D. AND MCGEARY, R. K.: *Methods of Analyzing for Hydrogen in Iron and Iron Alloys*, 355

Z

ZAPFFE, C. A.: *Discussions: on Determination of Hydrogen in Steel*, 395

on Effect of Time of Storage on Ductility of Welded Test Specimens, 322

ZENER, C.: *Discussions: on Ar¹¹ in Chromium Steels*, 185

on Cohesive Strength of Metals, 602, 603, 604
on Isothermal Transformation of Austenite in One Per Cent Carbon, High-chromium Steels, 220

on Tensile Deformation, 289

ZENER, C. AND HOLLOMON, J. H.: *Conditions of Fracture in Steel*. See Contents.

ZIEGLER, N. A.: *Dilatometric Studies of the Graphitisation of Cast Iron*, 627; discussion, 636, 640

